

# Graphical Models

Michael I. Jordan

Computer Science Division and Department of Statistics  
University of California, Berkeley

## 1. Introduction

The fields of Statistics and Computer Science have generally followed separate paths for the past several decades, which each field providing useful services to the other, but with the core concerns of the two fields rarely appearing to intersect. In recent years, however, it has become increasingly evident that the long-term goals of the two fields are closely aligned. Statisticians are increasingly concerned with the computational aspects, both theoretical and practical, of models and inference procedures. Computer scientists are increasingly concerned with systems that interact with the external world and interpret uncertain data in terms of underlying probabilistic models. One area in which these trends are most evident is that of probabilistic graphical models.

 A graphical model is a family of probability distributions defined in terms of a directed or undirected graph. The nodes in the graph are identified with random variables, and joint probability distributions are defined by taking products over functions defined on connected subsets of nodes. By exploiting the graph-theoretic representation, the formalism provides general algorithms for computing marginal and conditional probabilities of interest. Moreover, the formalism provides control over the computational complexity associated with these operations.

The graphical model formalism is agnostic to the distinction between frequentist and Bayesian statistics. However, by providing general machinery for manipulating joint probability distributions, and in particular by making hierarchical latent variable models easy to represent and manipulate, the formalism has proved to be particularly popular within the Bayesian paradigm. Viewing Bayesian statistics as the systematic application of probability theory to statistics, and viewing graphical models as a systematic application of graph-theoretic algorithms to probability theory, it should not be surprising that many authors have viewed graphical models as a general Bayesian “inference engine” (Cowell et al., 1999).

What is perhaps most distinctive about the graphical model approach is its naturalness in formulating probabilistic models of complex phenomena in applied fields, while maintaining control over the computational cost associated with these models. Accordingly, in this article our principal focus is on the presentation of graphical models that have proved useful in applied domains, and on ways in which the formalism encourages the exploration of extensions of classical methods. Before turning to these examples, however, we begin with an overview of basic concepts.

## 2. Representation

The two most common forms of graphical model are *directed graphical models* and *undirected graphical models*, based on directed acyclic graphs and undirected graphs, respectively.

Let us begin with the directed case. Let  $\mathcal{G}(\mathcal{V}, \mathcal{E})$  be a directed acyclic graph, where  $\mathcal{V}$  are the nodes and  $\mathcal{E}$  are the edges of the graph. Let  $\{X_v : v \in \mathcal{V}\}$  be a collection of random variables indexed by the nodes of the graph. To each node  $v \in \mathcal{V}$ , let  $\pi_v$  denote the subset of indices of its parents. We allow sets of indices to appear wherever a single index appears, thus  $X_{\pi_v}$  denotes the vector of random variables indexed by the parents of  $v$ . Given a collection of kernels,  $\{k(x_v | x_{\pi_v}) : v \in \mathcal{V}\}$ , that sum (in the discrete case) or integrate (in the continuous case) to one (with respect to  $x_v$ ),

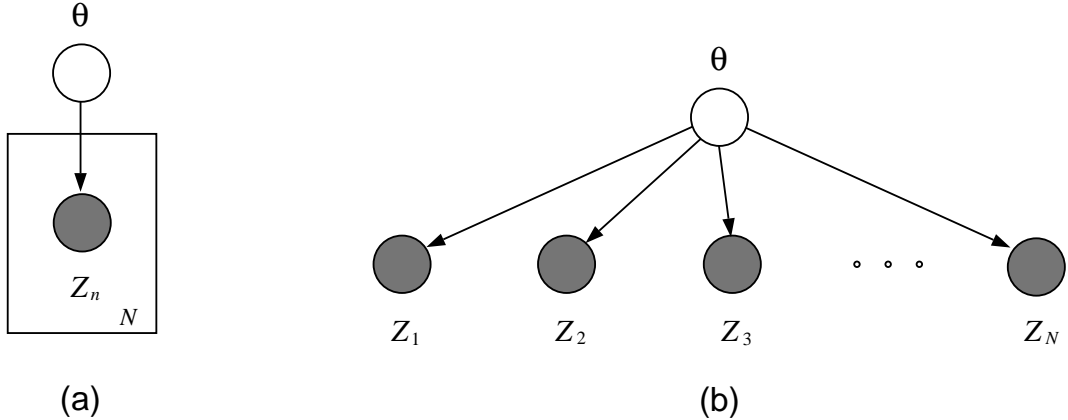


Figure 1: The diagram in (a) is a shorthand for the graphical model in (b). This model asserts that the variables  $Z_n$  are conditionally independent and identically distributed given  $\theta$ , and can be viewed as a graphical model representation of the De Finetti theorem. Note that shading, here and elsewhere in the paper, denotes observed variables.

we define a joint probability distribution (a probability mass function or probability density as appropriate) as follows:

$$p(x_{\mathcal{V}}) = \prod_{v \in \mathcal{V}} k(x_v | x_{\pi_v}). \quad (1)$$

It is easy to verify that this joint probability distribution has  $\{k(x_v | x_{\pi_v})\}$  as its conditionals; thus, henceforth, we write  $k(x_v | x_{\pi_v}) = p(x_v | x_{\pi_v})$ .

Note that we have made no distinction between data and parameters, and indeed it is natural to include parameters among the nodes in the graph.

A plate is a useful device for capturing replication in graphical models, including the factorial and nested structures that occur in experimental designs. A simple example of a plate is shown in Figure 1; this figure can be viewed as a graphical model representation of the **de Finetti exchangeability theorem**.



Directed graphical models are familiar as representations of hierarchical Bayesian models. An example is given in Figure 2.

The graph provides an appealing visual representation of a joint probability distribution, but it also provides a great deal more. First, whatever the functional forms of the kernels  $p(x_v | x_{\pi_v})$ , the factorization in Eq. (1) implies a set of conditional independence statements among the variables  $X_v$ , and the entire set of conditional independence statements can be obtained from a polynomial time *reachability algorithm* based on the graph (Pearl, 1988). Second, as we discuss in the following section, the graphical structure can be exploited by algorithms for probabilistic inference.

Let us now consider the undirected case. Given an undirected graph  $\mathcal{G}(\mathcal{V}, \mathcal{E})$ , we again let  $\{X_v : v \in \mathcal{V}\}$  be a collection of random variables indexed by the nodes of the graph, and let  $\mathcal{C}$  denote a collection of cliques of the graph (i.e., fully connected subsets of nodes). Associated with each clique  $C \in \mathcal{C}$ , let  $\psi_C(x_C)$  denote a nonnegative potential function. We define the joint probability  $p(x_{\mathcal{V}})$  by taking the product over these potential functions and normalizing:

$$p(x_{\mathcal{V}}) = \frac{1}{Z} \prod_{C \in \mathcal{C}} \psi_C(x_C), \quad (2)$$

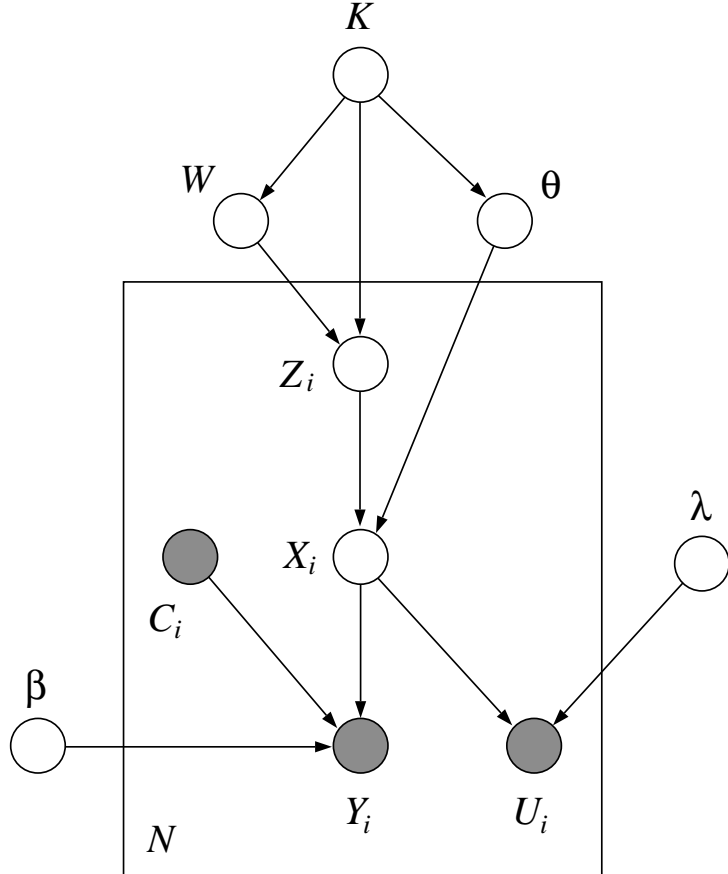


Figure 2: An example of a hierarchical Bayesian model represented as a directed graphical model. This is the “errors-in-covariates” logistic regression model of Richardson et al. (2002). The core of this model is a logistic regression of  $Y_i$  on  $X_i$ . The covariate  $X_i$  is not observed (in general), but noisy measurements  $U_i$  of  $X_i$  are available, as are additional observed covariates  $C_i$ . The density model for  $X_i$  is taken to be a mixture model, where  $K$  is the number of components,  $W$  are the mixing proportions,  $Z_i$  are the allocations and  $\theta$  parameterizes the mixture components.

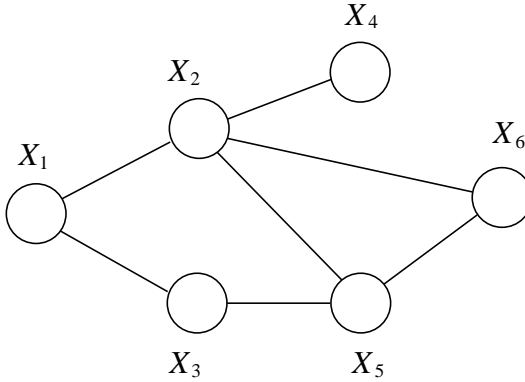


Figure 3: An example of an undirected graphical model. Probability distributions associated with this graph can be factorized as  $p(x_{\mathcal{V}}) = \frac{1}{Z} \psi(x_1, x_2) \psi(x_1, x_3) \psi(x_2, x_4) \psi(x_3, x_5) \psi(x_2, x_5, x_6)$ .

where  $Z$  is a normalization factor, obtained by integrating or summing the product with respect to  $x_{\mathcal{V}}$ . See Figure 3 for an example of an undirected graphical model.

Undirected graphs are often used in problems in areas such as spatial statistics, statistical natural language processing and communication networks—problems in which there is little causal structure to guide the construction of a directed graph. However, there is no need to restrict undirected models to such domains, and in particular it is possible to include parameters among the nodes of an undirected graph to yield an alternative general tool for Bayesian modeling. It is also possible to work with hybrids that include both directed and undirected edges (Lauritzen, 1996).

In general, directed graphs and undirected graphs make different assertions of conditional independence. Thus, there are families of probability distributions that are captured by a directed graph and are not captured by any undirected graph, and vice versa (Pearl, 1988).

The representations shown in Eq. (1) and Eq. (2) can be overly coarse for some purposes. In particular, in the undirected formalism the cliques  $C$  may be quite large, and it is often useful to consider potential functions that are themselves factorized, in ways that need not be equated with conditional independencies. Thus, in general, we consider a set of “factors,”  $\{f_i(x_{C_i}) : i \in \mathcal{I}\}$ , for some index set  $\mathcal{I}$ , where  $C_i$  is the subset of nodes associated with the  $i$ th factor. Note in particular that the same subset can be repeated multiple times (i.e., we allow  $C_i = C_j$  for  $i \neq j$ ). We define a joint probability by taking the product across these factors:

$$p(x_{\mathcal{V}}) = \frac{1}{Z} \prod_{i \in \mathcal{I}} f_i(x_{C_i}). \quad (3)$$

As shown in Figure 4, this definition is associated with a graphical representation—the *factor graph* (Kschischang et al., 2001). A factor graph is a bipartite graph in which the random variables are round nodes and the factors appear as square nodes. There is an edge between the factor node  $f_i$  and the variable node  $X_v$  if and only if  $v \in C_i$ .

Factor graphs provide a more fine-grained representation of the factors making up a joint probability, and are useful in defining inference algorithms that exploit this structure (the topic of the following section). Note also that the factor  $f_i(x_{C_i})$  can often be written as  $\exp(\theta_i \chi_i(x_{C_i}))$ , for a parameter  $\theta_i$  and a fixed function  $\chi_i$ , in which case the representation in Eq. (3) is nothing but the canonical form of the exponential family. Thus factor graphs are widely used as graph-theoretic representations of exponential family distributions.

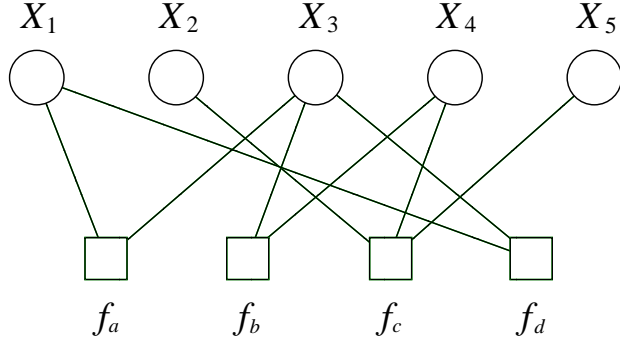


Figure 4: An example of a factor graph. Probability distributions associated with this graph can be factorized as  $p(x_{\mathcal{V}}) = \frac{1}{Z} f_a(x_1, x_3) f_b(x_3, x_4) f_c(x_2, x_4, x_5) f_d(x_1, x_3)$ .

### 3. Algorithms for probabilistic inference

The general problem of probabilistic inference is that of computing conditional probabilities  $p(x_F | x_E)$ , where  $\mathcal{V} = E \cup F \cup H$  for given subsets  $E$ ,  $F$  and  $H$ . In this section we are concerned with algorithms for performing such computations, and the role that graphical structure can play in making such computations efficient.

In discussing inference algorithms, it proves useful to treat directed graphs and undirected graphs on an equal footing. This is done by converting the former to the latter. Note in particular that Eq. (1) could be treated as a special case of Eq. (2) if it were the case that each factor  $p(x_i | x_{\pi_i})$  were a function on a clique. In general, however, the parents  $\pi_i$  of a given node  $i$  are not connected, and so the set  $\pi_i \cup \{i\}$  is not a clique. We can force this set to be a clique by adding (undirected) edges between all of the parents  $\pi_i$ , essentially constructing a new graph that is a *graphical cover* of the original graph. If we also convert the directed edges (from parents to children) to undirected edges, the result is an undirected graphical cover—the so-called *moral graph*—in which all of the arguments of the function  $p(x_i | x_{\pi_i})$  are contained in a clique. That is, in the moral graph, the factorization in Eq. (1) is a special case of Eq. (2). Thus we can proceed by working exclusively within the undirected formalism.

It is also useful to note that from a computational point of view the conditioning plays little essential role in the problem. Indeed, to condition on the event  $\{X_E = x_E\}$ , it suffices to redefine the original clique potentials. Thus, for  $i \in \mathcal{E}$ , we multiply the potential  $\psi_C(x_C)$  by the Kronecker delta function  $\delta(x_i)$ , for any  $C$  such that  $\{i\} \in C \cap E$ . The result is an unnormalized representation of the conditional probability that has the factorized form in Eq. (2). Thus, from a computational point of view, it suffices to focus on the problem of marginalization of the general factorized expression in Eq. (2). We are interested in controlling the growth in computational complexity of performing such marginalization, as a function of the cardinality of  $\mathcal{V}$ . In the following three sections, we describe the three principal classes of methods that attempt to deal with this computational issue—*exact* algorithms, *sampling* algorithms, and *variational* algorithms. Our presentation will be brief; for a fuller presentation see Cowell et al. (1999) and Jordan (1999).

#### 3.1 Exact algorithms

We begin with an example. Consider the graphical model shown in Figure 3 and suppose that we wish to compute the marginal probability  $p(x_1)$ . We obtain this marginal by summing (assuming

discrete random variables) over the remaining variables:

$$p(x_1) = \sum_{x_2} \sum_{x_3} \sum_{x_4} \sum_{x_5} \sum_{x_6} \frac{1}{Z} \psi(x_1, x_2) \psi(x_1, x_3) \psi(x_2, x_4) \psi(x_3, x_5) \psi(x_2, x_5, x_6). \quad (4)$$

Naively, each of these sums is applied to a summand involving six variables, and thus the computational complexity scales as  $r^6$  (assuming for simplicity that each variable has cardinality  $r$ ). We can obtain a smaller complexity, however, by exploiting the distributive law:

$$\begin{aligned} p(x_1) &= \frac{1}{Z} \sum_{x_2} \psi(x_1, x_2) \sum_{x_3} \psi(x_1, x_3) \sum_{x_4} \psi(x_2, x_4) \sum_{x_5} \psi(x_3, x_5) \sum_{x_6} \psi(x_2, x_5, x_6) \\ &= \frac{1}{Z} \sum_{x_2} \psi(x_1, x_2) \sum_{x_3} \psi(x_1, x_3) \sum_{x_4} \psi(x_2, x_4) \sum_{x_5} \psi(x_3, x_5) m_6(x_2, x_5) \\ &= \frac{1}{Z} \sum_{x_2} \psi(x_1, x_2) \sum_{x_3} \psi(x_1, x_3) m_5(x_2, x_3) \sum_{x_4} \psi(x_2, x_4) \\ &= \frac{1}{Z} \sum_{x_2} \psi(x_1, x_2) m_4(x_2) \sum_{x_3} \psi(x_1, x_3) m_5(x_2, x_3) \\ &= \frac{1}{Z} \sum_{x_2} \psi(x_1, x_2) m_4(x_2) m_3(x_1, x_2) \\ &= \frac{1}{Z} m_2(x_1), \end{aligned} \quad (5)$$

where we have defined intermediate factors  $m_i$  in an obvious notation. We obtain the value of  $Z$ , and hence the marginal, by summing the final expression with respect to  $x_1$ . Note that no more than three variables appear together in any summand, and thus the computational complexity is reduced to  $r^3$ , a notable improvement.

We can also perform this summation in a different order. In general we would like to choose an order—an *elimination order*—so that the worst-case summation is as small as possible (in terms of the number of arguments in the summand).

This problem can be reduced to a graph-theoretic problem. Note in particular that each summation creates an intermediate factor that is a function of all of the variables in the summand, other than the variable being summed over. This functional dependence can be captured graphically. In particular, we define a *triangulation algorithm* by sequentially (1) choosing the next node in the elimination order, (2) linking all remaining nodes that are neighbors of the node, and (3) removing the node from the graph. This defines a sequence of graphs. The largest clique that arises in this sequence characterizes the complexity of the worst-case summation (the complexity is exponential in the size of this clique).

The minimum (over elimination orders) of the size of the maximal clique is known as the *treewidth* of the graph.<sup>1</sup> To minimize the computational complexity of inference, we wish to choose an elimination ordering that achieves the treewidth. This is a graph-theoretic problem—it is independent of the numerical values of the potentials<sup>2</sup>

The problem of finding an elimination ordering that achieves the treewidth turns out to be NP-hard (Arnborg et al., 1987). It is often possible in practice, however, to find good or even optimal orderings for specific graphs, and a variety of inference algorithms in specific fields (e.g., the algorithms for inference on phylogenies and pedigrees in Section 4.1) have been based on specific

---

1. By convention the treewidth is actually one less than this maximal size.

2. Moreover, it is also directly applicable to continuous variables. Replacing sums with integrals, and taking care with regularity conditions, our characterization of computational complexity in graphical terms still applies. There is of course the issue of computing individual integrals, which introduces additional computational considerations.

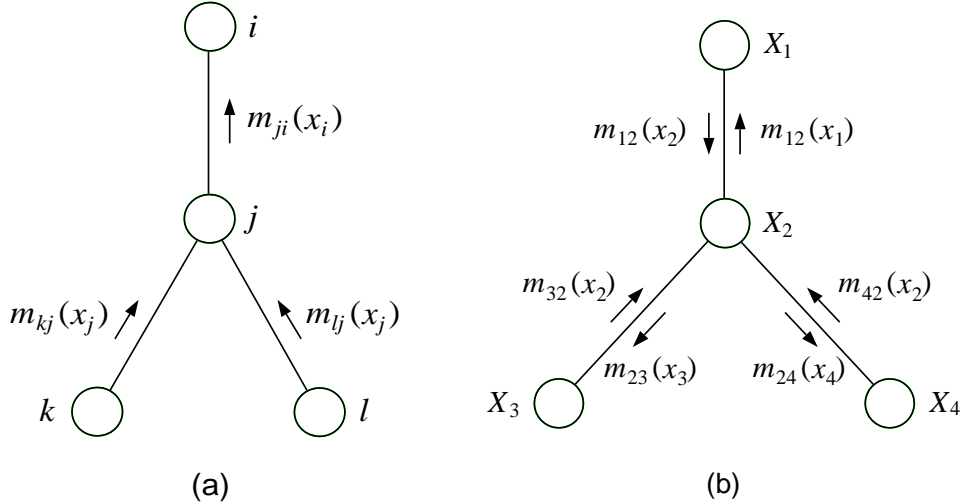


Figure 5: (a) The intermediate terms that are created by the elimination algorithm when nodes  $k, l$  and  $j$  are eliminated in a fragment of an undirected tree. (b) The set of all messages that are created by the sum-product algorithm in a tree with four nodes.

choices of elimination orderings in problems of interest. In general this class of algorithms is known as *probabilistic elimination*, and it forms an important class of exact inference algorithms.

A limitation of the elimination approach to inference is that it yields only a single marginal probability. We often require more than one marginal probability, and we wish to avoid the inefficiency of requiring multiple runs of an elimination algorithm.

To see how to compute general marginal probabilities, let us first restrict ourselves to the special case in which the graph is a tree. In an undirected tree, the cliques are pairs of nodes and singleton nodes, and thus the probability distribution is parameterized with potentials  $\{\psi(x_i, x_j) : (i, j) \in \mathcal{E}\}$  and  $\{\psi(x_i) : i \in \mathcal{V}\}$ . To compute a specific marginal,  $p(x_f)$ , consider a rooted tree in which node  $f$  is taken to be the root of the tree, and choose an elimination order in which all children of any node are eliminated before the node itself is eliminated. Given this choice, the steps of the elimination algorithm can be written in the following general way (see Figure 5(a)):

$$m_{ji}(x_i) = \sum_{x_j} \left( \psi(x_j) \psi(x_i, x_j) \prod_{k \in \mathcal{N}(j) \setminus i} m_{kj}(x_j) \right), \quad (6)$$

where  $\mathcal{N}(j)$  is the set of neighbors of node  $j$ , and where  $m_{ji}(x_i)$  is the intermediate term that is created when node  $j$  is eliminated (note that we have added the subscript  $i$  to the notation for intermediate terms; the reason will become clear shortly). The desired marginal is obtained as follows:

$$p(x_f) \propto \psi(x_f) \prod_{e \in \mathcal{N}(f)} m_{ef}(x_f), \quad (7)$$

where the proportionality constant is obtained by summing the right-hand side with respect to  $x_f$ .

If we now consider the problem of computing the marginals  $p(x_i)$  for *all* of the nodes in the graph, it turns out that we already have the solution at hand. Dropping the notion of “elimination order,” we define an asynchronous algorithm in which any “message”  $m_{ji}(x_i)$  is computed via Eq. (6) whenever the “messages”  $m_{kj}(x_j)$  on the right-hand side of the equation have already been computed. (See Figure 5(b) for an example on a tree with four nodes). It can be shown that this

algorithm will compute all of the  $2|\mathcal{E}|$  possible messages associated with the tree in a number of operations proportional to the diameter of the graph. (That is, for any  $(i, j) \in \mathcal{E}$ , both  $m_{ij}(x_j)$  and  $m_{ji}(x_i)$  will both be computed, and all such messages will be computed in time proportional to the length of the longest path in the graph). Once all messages have been computed, we compute the marginal for any node via Eq. (7).

This algorithm is known as the *sum-product algorithm*. It is essentially a dynamic-programming-like algorithm that achieves the effect of multiple elimination orders by computing the intermediate terms that are needed for any given marginal only once, reusing these intermediate terms for other marginals. In the case of discrete nodes with cardinality  $r$ , the algorithm has a computational complexity of  $O(|\mathcal{E}|r^2)$ .

The sum-product algorithm can be generalized in a number of ways. First, a variant of the algorithm can be defined on factor graphs. In this case two kinds of messages are defined, in accordance with the bipartite structure of factor graphs. Second, the algebraic operations that underly the sum-product algorithm are justified by the fact that sums and products form a *commutative semiring*, and the algorithm generalizes immediately to any other commutative semiring (Aji and McEliece, 2000, Shenoy and Shafer, 1990). In particular, “maximization” and “product” form a commutative semiring, and a “max-product” variant of the sum-product algorithm can be used for computing modes of posterior distributions. Finally, as we now describe, a generalization of the sum-product algorithm known as *junction tree algorithm* can be used for computing marginals in general graphs.

The *junction tree algorithm* can be viewed as combining the ideas of the elimination algorithm and the sum-product algorithm. The basic idea is to work with a tree-like data structure in which the nodes are cliques rather than single nodes. (Such a graph is known as a *hypergraph*). A variant of the sum-product algorithm is defined that defines messages that pass between cliques rather than single nodes, and this algorithm is run on a tree of cliques. Which cliques do we use in forming this tree? It turns out that it is not possible (in general) to use the cliques from the original graph, but rather we must use the cliques from an augmented graph obtained by triangulating the original graph. Conceptually we go through the operations associated with the elimination algorithm, using a specific elimination ordering. Rather than actually performing these operations, however, we perform only the graph-theoretic triangulation process. This defines a set of cliques, which are formed into a tree. The sum-product algorithm running on this tree yields not only a single marginal, but all marginals, where by “marginal” we now mean the marginal probability of all variables in each clique. The computational complexity of the algorithm is determined by the size of the largest clique, which is lower bounded by the treewidth of the graph.

In summary, exact inference algorithms such as the elimination algorithm, the sum-product algorithm, and the junction tree algorithm compute marginal probabilities by systematically exploiting the graphical structure; in essence exploiting the conditional independencies encoded in the pattern of edges in the graph. In the best case, the treewidth of the graph is small, and an elimination order that achieves the treewidth can be found easily. Many classical graphical models, including hidden Markov models, trees, and the state-space models associated with Kalman filtering, are of this kind. In general, however, the treewidth can be overly large, and in such cases exact algorithms are not viable.

To see how to proceed in the case of more complex models, note that large treewidth heuristically implies that the intermediate terms that are computed by the exact algorithms are sums of many terms. This provides hope that there might be concentration phenomena that can be exploited by approximate inference methods. These concentrations (if they exist) are necessarily dependent on the specific numerical values of the potentials. In the next two sections, we overview some of the algorithms that aim to exploit both the numerical and the graph-theoretic properties of graphical models.

### 3.2 Sampling algorithms

Sampling algorithms such as *importance sampling* and *Markov chain Monte Carlo (MCMC)* provide a general methodology for probabilistic inference (Green and Richardson, this volume). The graphical model setting provides an opportunity for graph-theoretic structure to be exploited in the design, analysis and implementation of sampling algorithms.

Note in particular that the class of MCMC algorithms known as Gibbs sampling requires the computation of the probability of individual variables conditioned on all of the remaining variables. The Markov properties of graphical models are useful here; conditioning on the so-called *Markov blanket* of a given node renders the node independent of all other variables. In directed graphical models, the Markov blanket is the set of parents, children and co-parents of a given node (“co-parents” are nodes which have a child in common with the node). In the undirected case, the Markov blanket is simply the set of neighbors of a given node. Using these definitions, Gibbs samplers can be set up automatically from the graphical model specification, a fact that is exploited in the BUGS software for Gibbs sampling in graphical models Gilks et al. (1994). Similar automation is possible for Metropolis-based algorithms.

The graphical representation can also be useful in importance sampling. In particular, the key goal of choosing an importance sampling distribution that is both tractable and yet close to target distribution can often be achieved by considering distributions defined on simplified graphs in which edges have been removed.

Finally, a variety of hybrid algorithms can be defined in which exact inference algorithms are used locally within an overall sampling framework (Jensen et al., 1995, Murphy, 2002).

### 3.3 Variational algorithms

The basic idea of variational inference is to characterize a probability distribution as the solution to an optimization problem, and then to solve this optimization problem approximately. (Alternatively, one can attempt to solve exactly an approximation to the optimization problem). While these methods are applicable in principle to general probabilistic inference, thus far their main domain of application has been to graphical models.

To characterize the joint probability  $p(x)$  variationally, define  $E(x) = -\log p(x) - \log Z$ , and define the following *variational free energy*:

$$\begin{aligned} F(q) &= \sum_x q(x)E(x) + \sum_x q(x) \log q(x) \\ &= -\sum_x q(x) \log p(x) + \sum_x q(x) \log q(x) - \log Z, \end{aligned} \tag{8}$$

where  $q(x)$  is a free parameter. When  $q(x)$  is a probability distribution we see that the variational free energy is equal (up to an additive constant) to the Kullback-Leibler divergence between  $q(x)$  and  $p(x)$ . It is therefore minimized when  $q(x) = p(x)$  and attains the value of  $-\log Z$  at the minimum.

Approximate inference algorithms can be obtained by optimizing over simplified families of distributions  $q(x)$ . In the context of graphical models, these families are generally obtained by omitting some of the edges in the graph and endowing the potentials in the resulting simplified graph with free parameters. This provides a flexible, yet tractable, family of distributions for computing the averages in Eq. (8). Minimizing the variational free energy with respect to these parameters yields a *variational inference algorithm* (Jordan, 1999, Yedidia et al., 2001).

Approximate inference algorithms can also be obtained by approximating the terms in the variational free energy. In particular, approximating the second term (the entropy) with an expression that depends only on pairs of variables and single variables (and is thus exact for trees) yields an expression known as the *Bethe free energy*. Adding Lagrange multipliers to the free energy (to enforce marginalization constraints between pairs of variables and singletons) and differentiating

we obtain a set of fixed point equations. Surprisingly, these equations end up being equivalent to the “sum-product” algorithm for trees in Eq. (6). The messages  $m_{ij}(x_j)$  are simply exponentiated Lagrange multipliers. Thus the Bethe approximation is equivalent to applying the local message-passing scheme developed for trees to graphs that have loops (Yedidia et al., 2001). The algorithm has been surprisingly successful in practice, and in particular has been the algorithm of choice in the applications to error-control codes discussed in Section 5.

The area of variational inference has been quite active in recent years. Algorithms known as “cluster variation methods” have been proposed that extend the Bethe approximation to clusters larger than two (Yedidia et al., 2001). Other papers on higher-order variational methods include Leisink and Kappen (2002) and Minka (2002). Wainwright (2002) has presented general variational methods that provide both lower and upper bounds on marginal probabilities. For papers devoted specifically to Bayesian applications of variational inference, see Attias (2000) and Ghahramani and Beal (2001).

## 4. Bioinformatics

The field of bioinformatics is a fertile ground for the application of graphical models. Many of the classical probabilistic models in the field can be viewed as instances of graphical models, and variations on these models are readily handled within the formalism. Moreover, graphical models naturally accommodate the need to fuse multiple sources of information, a characteristic feature of modern bioinformatics.

### 4.1 Phylogenetic trees

Phylogenetic trees are graphical models. Let us briefly outline the key ideas and then consider some extensions. We assume that we are given a set of homologous biological sequences, one from each member of a set of species, where “homologous” means that the sequences are assumed to derive from a common ancestor. We focus on DNA or protein sequences, in which the individual elements in the sequences are referred to as “sites,” but phylogenetic trees are also often based on sequences of other “characters” such as morphological traits.

Essentially all current methods for inferring phylogenetic trees assume that the sites are independent, and let us begin by making that assumption. We represent a phylogeny as a binary tree in which the leaves of the tree are the observed values of a given site in the different species and the nonterminals are the values of the site for putative ancestral species (see Figure 6). Thus, in the case of DNA, all of the nodes in the tree are multinomial random variables with four states, and in the case of proteins, all nodes are multinomial with twenty states. Treating the tree as a directed graphical model, we parameterize the tree by following the recipe in Eq. (1) and annotating each edge with the conditional probability of a state given its ancestral state.<sup>3</sup> These conditional probabilities are generally parameterized in terms of an “evolutionary distance” parameter that is to be estimated, and their parametric form is an exponential decay to an equilibrium distribution across the four nucleotides or twenty amino acids (Felsenstein, 1981).

Taking the product of the local parameterizations, we obtain the joint probability of the states of a given site, and taking a further product over sites (the plate in Figure 6), we obtain the joint probability across all sites. The likelihood is easily computed via the elimination algorithm—indeed the “pruning” algorithm of Felsenstein (1981) was an early instance of a graphical model elimination algorithm. The conditional probabilities of ancestral states can be computed by the sum-product algorithm. Finally, while classical methods for fitting phylogenetic trees rely on the EM algorithm for parameter estimation (in which the E step is computed via the sum-product algorithm), and search across tree topologies to find the maximum likelihood tree, it is also possible to use MCMC methods within a Bayesian framework (Huelsenbeck and Bollback, 2001).

---

3. In fact, the likelihood of a phylogenetic tree is generally independent of the choice of root, and the undirected formalism is often more appropriate.

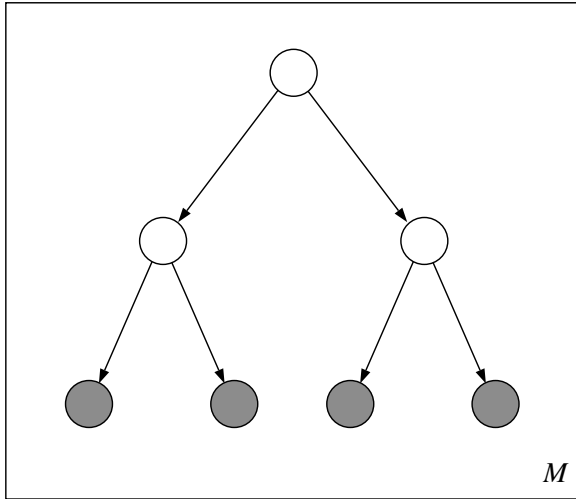


Figure 6: A simple example of a phylogeny on four extant organisms and  $M$  sites. The tree encodes the assumption that there is a first speciation event and then two further speciation events that lead to the four extant organisms. The plate represents the assumption that the  $M$  sites evolve independently. Note that classical phylogenies are generally drawn with varying edges lengths to denote the evolutionary distance, but in the graphical model formalism this distance is simply a parameter in the conditional distribution  $p(x_v | x_{\pi_v})$ , and is left implicit in the figure.

The assumptions leading to the classical phylogenetic tree model are wanting in several respects. First, the assumption of site independence is generally incorrect. There are biochemical interactions that affect mutation probabilities at neighboring sites, and there are global constraints that alter mutation rates in conserved regions of DNA and proteins. Second, genes do not necessarily evolve according to tree topologies—for example, in bacteria there are several mechanisms for “lateral gene transfer” between species.

The graphical model formalism provides a natural upgrade path for considering more realistic phylogenetic models that capture these phenomena. Lateral gene transfer is readily accommodated by simply removing the restriction to a tree topology. Lack of independence between sites is captured by replacing the plate in Figure 6 with an explicit array of graphs, one for each site, with horizontal edges capturing interactions. For example, one could consider Markovian models in which there are edges between ancestral nodes in neighboring sites. In general, such models create loops in the underlying graph and approximate inference methods will generally be required.

#### 4.2 Pedigrees and multilocus linkage analysis

While phylogenies attempt to model relationships among the instances of a single gene as found in different species in evolutionary time, pedigrees are aimed at a finer level of granularity. A *pedigree* displays the parent-child relationships within a group of organisms in a single species, and attempts to account for the presence of variants of a gene as they flow through the population. A *multilocus pedigree* is a pedigree which accounts for the flow of multiple genes. Multilocus pedigrees turn out to be a special case of a graphical model known as a *factorial hidden Markov model*.

Let us briefly review the relevant genetic terminology. Arrayed along each *chromosome* are a set of *loci*, which correspond to *genes* or other markers. Chromosomes occur in pairs, and thus there

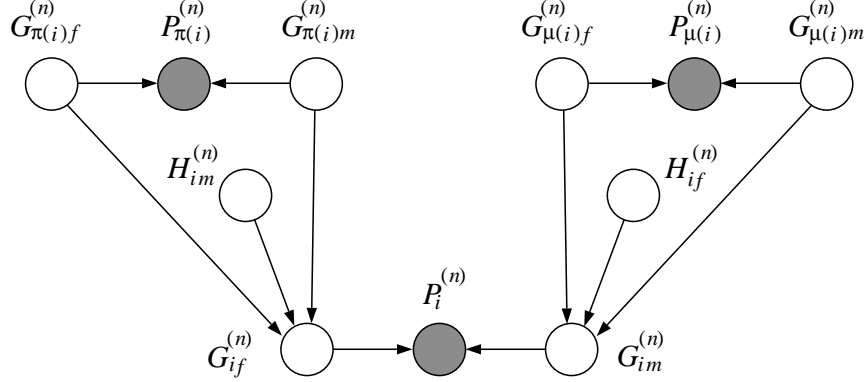


Figure 7: A pedigree on three organisms—a child  $i$ , the father  $\pi(i)$  and the mother  $\mu(i)$ . The variables  $G^{(n)}$ ,  $H^{(n)}$  and  $P^{(n)}$  encode the values of the genotype, haplotype and phenotype, respectively, at locus  $n$ , for each of the three organisms.

are a pair of genes at each locus.<sup>4</sup> Each gene occurs in one of several variant forms—*alleles*—in the population. Thus at each locus, there is a pair of alleles. The full set of all such pairs for a given individual is referred to as the *genotype* of that individual. Given the genotype, there is a (generally stochastic) mapping to the *phenotype*—a set of observable traits. One often makes the simplifying assumption that each trait is determined by a single pair of alleles, but as will be seen our modeling formalism does not require this (generally inaccurate) assumption.

In the process of *meiosis*, one of the alleles in the pair at each locus is selected and transmitted to the offspring. The offspring receives one allele at each locus from his or her father, and the other allele at that locus from his or her mother.

Define genotype variables  $G_{if}^{(n)}$  for the paternal allele at the  $n$ th locus in the  $i$ th organism, and  $G_{im}^{(n)}$  for the maternal allele at that locus. Also let  $P_i^{(n)}$  denote the corresponding phenotype variables. Finally, let  $H_{if}^{(n)}$  denote a binary “haplotype variable.” This variable is equal to one if organism  $i$  receives the father’s paternal allele (i.e., the grandfather’s allele), and is equal to zero if organism  $i$  receives the father’s maternal allele (i.e., the grandmother’s allele). Similarly, let  $H_{im}^{(n)}$  denote the corresponding binary haplotype variable on the mother’s side.

The relationships between these variables are summarized in the graphical model in Figure 7. Letting the haplotype variables take on their two values with probability 0.5, the probability of an offspring’s genotype given the parental genotypes is simply given by Mendel’s laws.

The graph in Figure 7 is a simple example of a *pedigree*. In general, pedigrees involve many organisms. The graphical topology is a tree only in the simplest cases. In general, there are large numbers of loops in pedigrees of sufficient size.

The final issue to consider is the relationship between the haplotype variables at different loci. The key biological fact is that pairs of chromosomes *cross over* during meiosis, so that alleles that were on different chromosomes in the parent may be on the same chromosome in the child. Crossover can be modeled by treating the haplotype variables as a Markov chain. Thus,  $H_{if}^{(n)}$  and  $H_{if}^{(n+1)}$  are equal if no crossover occurs between locus  $n$  and locus  $n+1$ , and are unequal otherwise. The probability of crossover is a parameter of the model. Estimating these parameters from data yields an estimate of *genetic distance* between loci, and yields *genetic maps* of the chromosomes.

4. This is true for humans (for all but the X and Y chromosomes), but not for all organisms. The models that we discuss can easily be specialized to organisms in which chromosomes are not paired, and in particular can accommodate the X and Y chromosomes in humans.

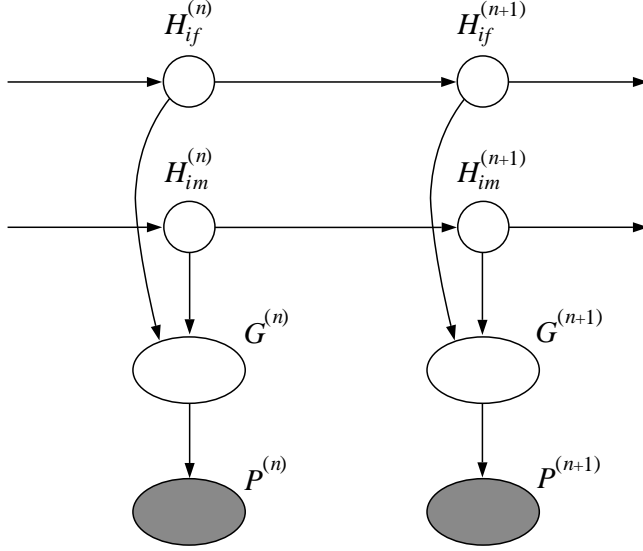


Figure 8: A representation of a multilocus pedigree for one organism and two loci. The figure is obtained from the pedigree diagram in Figure 7 by grouping all of the genotype variables at locus  $n$  into a single oval denoted  $G^{(n)}$ , grouping all of the phenotype variables into a single oval denoted  $P^{(n)}$ , and connecting the haplotype variables horizontally between loci.

Connecting the haplotype variables according to the Markovian assumption yields the graphical model shown in Figure 8. Note that the horizontal dimension of this graph corresponds to layout along the chromosome, whereas the vertical dimension corresponds to individuals. The fact that the haplotype variables in different individuals are independent is captured in the graphical structure.

The model in Figure 8 is an instance of a graphical model family known as a *factorial hidden Markov model (fHMM)* (Ghahramani and Jordan, 1996); see Figure 10(c) for a generic example. Classical algorithms for inference on multilocus pedigrees are variants of the elimination algorithm on this fHMM, and correspond to different choices of elimination order (Lander and Green, 1987, Elston and Stewart, 1971). While these algorithms are viable for small problems, exact inference is intractable for general multilocus pedigrees. Indeed, focusing only on the haplotype variables, it can be verified that the treewidth is bounded below by the number of organisms, and thus the computational complexity is exponential in the number of organisms. More recently, Gibbs sampling methods have been studied; in particular, Thomas et al. (2000) have proposed a *blocking Gibbs sampler* that takes advantage of the graphical structure in Figure 8. Ghahramani and Jordan (1996) presented a suite of variational and Gibbs sampling algorithms for fHMMs, and further developments are presented by Murphy (2002).

## 5. Error-control codes

Graphical models play an important role in the modern theory of error-control coding. Ties between graphs and codes were explored in the early sixties by Gallager (1963), but this seminal line of research was largely forgotten, due at least in part to a lack of sufficiently powerful computational tools. A flurry of recent work, however, has built on Gallager's work and shown that surprisingly effective codes can be built from graphical models. Codes based on graphical models are now the most effective codes known for many channels, achieving rates near the Shannon capacity.

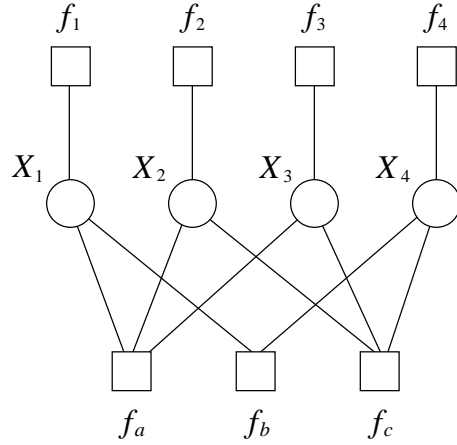


Figure 9: A factor graph representation of an LDPC code. The code has  $N = 4$  message bits and  $K = 3$  parity checks. The factor nodes below the message bits represent the parity checks while the factor nodes above the message bits represent the channel.

The basic problem of error-control coding is that of transmitting a message (a sequence of bits) through a noisy channel, in such a way that a receiver can recover the original message despite the noise. In general, this is achieved by transmitting additional (redundant) bits in addition to the original message sequence. The receiver uses the redundancy to detect, and possibly correct, any corruption of the message due to the noise. The key problems are that of deciding the overall mapping between messages and the redundant bits (the problem of *code design*), that of computing the redundant bits for any given message (the *encoding problem*), and that of estimating the original message based on a transmitted message (the *decoding problem*).

There are three ways in which probability enters into the problem. First, the set of possible messages (the *source*) is given a prior distribution. We will treat this distribution as uniform, assuming in essence that a *source code* has been developed that extracts the statistical redundancy from the source (this redundancy is distinct from the redundancy that we wish to impose on the message, a redundancy which is designed to be appropriate for a given channel). Second, the channel is noisy. A simple example of a channel model is a binary symmetric channel (BSC), in which each message bit is transmitted correctly (with probability  $\alpha$ ) or flipped (with probability  $1 - \alpha$ ). These transmission events are often assumed IID across the bits in a message sequence; that is, the channel is often assumed to be *memoryless*. We make that assumption here for simplicity, but it will be clear that the graphical model formalism can readily cope with non-memoryless channels.

Finally, the code itself is often taken to be random. In the graphical model setting, in which an instance of a code is identified with a graph, this means that we are considering random ensembles of graphs. This assumption is not an inherent feature of the problem; rather it is imposed to allow probabilistic tools to be applied to theoretical analysis of the properties of a code (see below).

In Figure 9, we show a specific example of a graph from an ensemble known as a *low-density parity check (LDPC) code*. The variable nodes in the graph are binary-valued, and represent the message bits; a *message* is a specific instance of the  $2^N$  possible states of these nodes. The factor nodes above the message nodes represent the channel. Thus, for the message variable  $X_i$ , the factor node  $f_i$  represents the likelihood  $p(y_i | x_i)$ , where  $y_i$  is the observed value of the transmitted message. The factor nodes below the message nodes are *parity-check nodes*; these are equal to one only if and only if an even number of the nodes that they are connected to are equal to one. The prior probability distribution on messages is obtained as an instance of Eq. (3) based on the parity check factors.

This distribution assigns zero probability to any message that violates one of the parity checks, and uniform probability to any message that satisfies all of the parity checks.<sup>5</sup>

If we now impose an upper bound on the degree of the message nodes (i.e., the number of parity check nodes that a message node is connected to) and an upper bound on the degree of the parity check nodes (the number of message nodes that a parity check node is connected to), we obtain the family of graphs referred to as a low-density parity check code.<sup>6</sup>

The graphical model in Figure 9 provides a representation of both the uniform prior on messages and the likelihood of transmitted bits given original message bits. We thus have a well-formed inference problem—the goal is that of computing the posterior probability distribution of the original message bits given the transmitted bits. The mean or mode of this distribution can be used as an estimate of the original message.

While in principle any of the inference algorithms associated with general graphical models could be used for LDPC codes, the presence of loops in the graph, and the large scale of graphs that are used (in which  $N$  may be as large as many tens of thousands) rules out exact inference. Moreover, MCMC algorithms do not appear to be viable in this domain. The algorithm that is used in practice is the sum-product algorithm. The algorithm is quite successful in practice for large block lengths (large values of  $N$ ). Moreover, theoretical convergence results are available for the sum-product algorithm in this setting (Richardson et al., 2001). Averaging over the ensemble of graphs, it can be shown that the average error probability goes to zero over the iterations of the sum-product algorithm, given conditions on the channel, the degree distributions, the block length and the code rate. Also, a martingale argument can be invoked to show that almost all codes behave like the average code, which justifies the random selection of a specific code from the ensemble for use in practice.

Graphical models continue to play a central role in the development of error-control codes. New codes are designed by proposing alternative graphical structures, and the analysis of decoding performance makes direct use of the graphical structure. The graphical framework allows the exploration of more complex channel models (for example, the factor nodes representing the channel can connect to multiple message nodes in Figure 9 in the case of channels with memory).

## 6. Speech, language and information retrieval

The fields of speech recognition, natural language processing and information retrieval involve complex phenomena with many kinds of structural relationships. Graphical models play an increasingly important role in attempts to model these phenomena and extract information that is needed in a given problem domain.

### 6.1 Markov and hidden Markov models

Markov models and hidden Markov models are graphical models that attempt to capture some of the simplest sequential structure inherent in speech and language. In both cases the graphical model is a chain of multinomial “state” nodes  $X_t$ , with links between these nodes parameterized by a state transition matrix. In the case of a first-order Markov model, there is an edge between state  $X_{t-1}$  and state  $X_t$ , for  $t \in \{1, \dots, T\}$ , while in higher-order Markov models there are edges from earlier states  $X_{t-\tau}$ . Hidden Markov models (HMMs) have an additional set of “output” nodes  $Y_t$ , with edges between  $X_t$  and  $Y_t$ .

A simple yet important application of HMMs arises in the *part-of-speech problem*. In this problem, the data are word sequences, and the goal is to tag the words according to their part of speech (*noun*,

---

5. If there are  $K$  factor nodes, and each node imposes an independent constraint on the message sequences, then there are  $2^{N-K}$  possible message sequences. The ratio  $(N - K)/N$  is known as the *rate* of the code.

6. Actually, in both practice and theory, LDPC codes incorporate an additional level of randomness; the degrees of the nodes are selected from a distribution.

*verb, preposition, etc.*). Thus the states  $X_t$  take as many values as there are parts of speech (typically several dozen), and the outputs  $Y_t$  take as many values as there are words in the vocabulary (typically many tens of thousands). Training data generally consist of “tagged data”— $(X_t, Y_t)$  pairs—and the subsequent inference problem is that of inferring a sequence of  $X_t$  values given a sequence of  $Y_t$  values.

*Speech recognition* provides a wide-ranging set of examples of the application of HMMs. In this setting, the observables  $Y_t$  are generally short-term acoustic spectra, either continuous-valued or discretized. A single HMM is often designed to cover a small phonetic unit of speech such as a syllable or diphone, and the states  $X_t$  are generally treated as unobserved (latent) variables. A library of such HMMs is created based on a corpus of training data. The HMMs in this library are then assembled into a lattice, which is itself a large graphical model that has edges between each of the elemental HMMs. The inference problem in this lattice of HMMs is generally that of finding the mode of the posterior distribution on state sequences, a computation which effectively segments a long observation sequence into its component speech units.

The elemental HMMs in this lattice are often trained based on “segmented data,” in which the portion of the speech sequence appropriate to each HMM is known in advance. It is also necessary to estimate the parameters associated with the transitions between the speech units, a problem known as *language modeling*. In this setting, Markov models are widely used. In particular, it is generally necessary to provide an estimate of the probability of a given word based on the previous two words (a “trigram model”). Given the large number of words in the vocabulary, this involves a large number of parameters relative to the amount of available data, and fully Bayesian methods (or adhoc “smoothing” techniques) are generally necessary for parameter estimation.

Finally, returning briefly to bioinformatics, it is worth noting that HMMs have a large number of applications in bioinformatics, including the problems of gene-finding in DNA and domain modeling in proteins. See Durbin et al. (1998) for a discussion of these applications.

## 6.2 Variations on Markovian models

A large number of variations on Markovian models are currently being explored in the fields of speech and language processing, and also in bioinformatics. Many of these models are readily seen to be members of the larger family of graphical models.

In speech recognition models, the state-to-output distribution,  $p(y_t | x_t)$ , is commonly taken to be a mixture of Gaussians, reflecting the multimodality that is commonly observed in practice. As shown in Figure 10(a), this can be represented as a graphical model in which additional (multinomial) variables are introduced to encode the allocations of the mixture components. The model remains eminently tractable for exact inference.

A more serious departure is the *coupled hidden Markov model* shown in Figure 10(b) (Saul and Jordan, 1995). This model involves two chains of state variables which are coupled via links between the chains.<sup>7</sup> Triangulating this graph yields cliques of size three, and the model remains tractable for exact inference.

More generally, the *factorial hidden Markov model* shown in Figure 10(c) is an instance of model involving multiple chains (Ghahramani and Jordan, 1996). In this particular model the states are coupled only via their connection to a common set of output variables (but variations can also be considered in which there are links among the chains). The factorial HMM allows large state spaces to be represented with a small number of parameters. Note that triangulation of this model yields cliques of size  $M + 1$ , where  $M$  is the number of chains, and thus for even moderate values of  $M$  this model is intractable. MCMC and variational methods have been employed successfully in this setting (Ghahramani and Jordan, 1996).

---

7. The model is a hybrid of the directed and undirected formalisms; an instance of the family of *chain graphs* (Lauritzen, 1996).

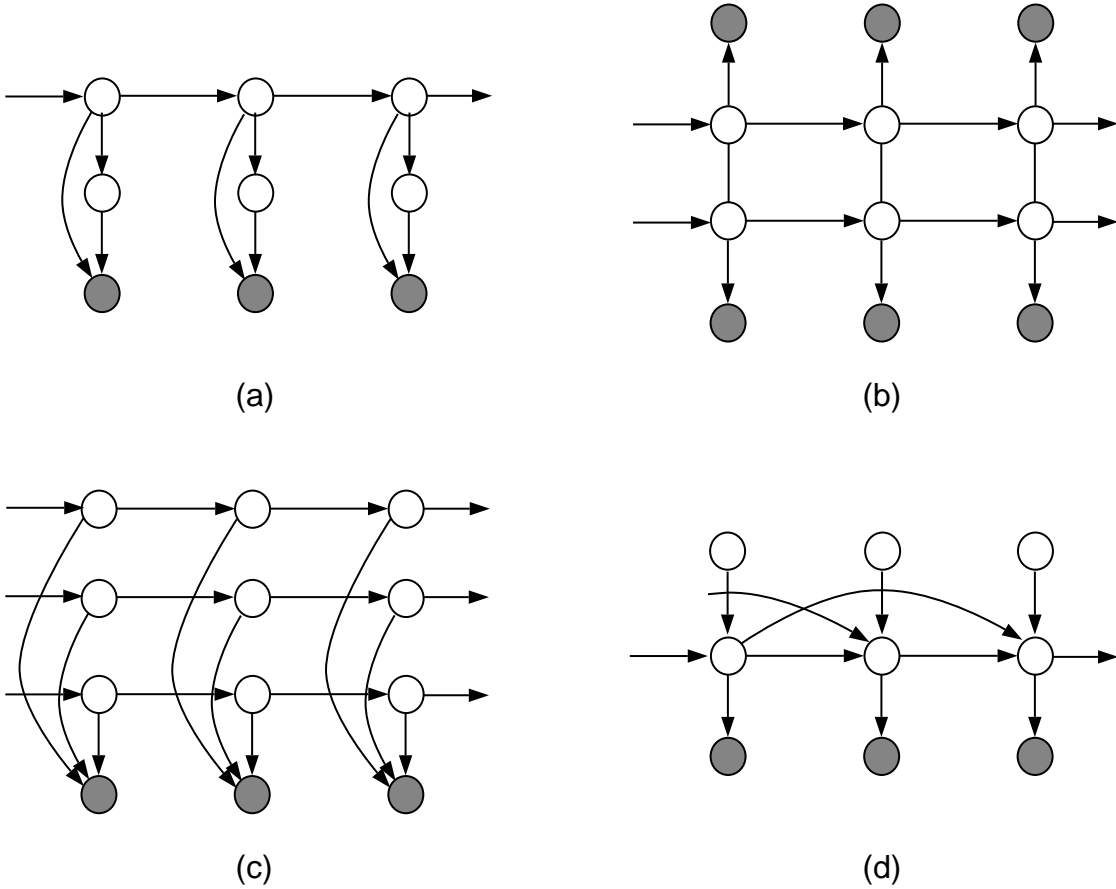


Figure 10: Variations on the hidden Markov model theme. (a) A model in which the emissions are mixture models. (b) A coupled HMM. (c) A factorial HMM. (d) A model in which the transition distribution is a mixture model.

Finally, in the *mixed memory Markov model* shown in Figure 10(d), the transition distribution is a mixture over pairwise transitions (Saul and Jordan, 1999). This model makes it possible to approximate high-order Markov models with a small number of parameters.

Further examples of variations of Markovian models include hierarchical HMMs (Murphy and Paskin, 2002), variable length HMMs (Ron et al., 1996), and buried HMMs (Bilmes, 2003). For a recent overview of these models in the context of applications to speech and language problems, see Bilmes (2003).

### 6.3 A hierarchical Bayesian model for document collections

For large-scale collections of documents (such as the World Wide Web), it is generally computationally infeasible to attempt to model the sequential structure of individual documents, and the field of *information retrieval* is generally built on the “bag-of-words” assumption—the assumption that word order within a document can be neglected for the purposes of indexing and retrieving documents. This is simply an assumption of exchangeability, and leads (via the de Finetti theorem) to the consideration of latent variable models for documents.

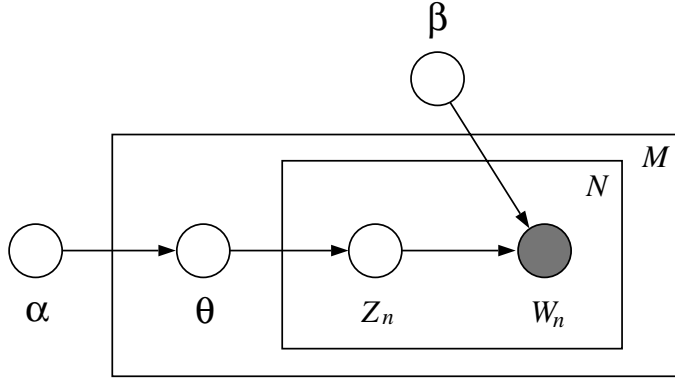


Figure 11: The *latent Dirichlet allocation model* for document collections. The outer plate represents a corpus containing  $M$  documents, while the inner plate represents an  $N$ -word document within that corpus.

While neglecting sequential structure, it may be desirable to attempt to capture other kinds of statistical structure in document collections, in particular the notion that documents are characterized by *topics*. Blei et al. (2002) have proposed a hierarchical latent variable model that has explicit representations for documents, topics and words. The model is shown in Figure 11. Words are represented by a multinomial variable  $W$  and topics are represented by a multinomial variable  $Z$ . Generally the cardinality of  $Z$  is significantly smaller than that of  $W$ . As shown by the innermost plate, the  $M$  words in a document are generated by repeatedly choosing a topic variable and then choosing a word corresponding to that topic. The probabilities of the topics are document-specific, and they are assigned via the value of a Dirichlet random variable  $\theta$ . As shown by the outermost plate, this variable is sampled once for each of the  $N$  documents in the corpus.

## 7. Discussion

Let us close with a few remarks on the present and future of graphical models in statistics. Until very recently, graphical models have been relegated to the periphery in statistics, viewed as useful in specialized situations but not a central theme. Several factors are responsible for their increasing prominence. First, hierarchical Bayesian models are naturally specified as directed graphical models, and the ongoing interest in the former has raised the visibility of the latter. Second, graph-theoretic concepts are key in recent attempts to provide theoretical guarantees for MCMC algorithms. Third, a increasing awareness of the importance of graph-theoretic representations of probability distributions in fields such as statistical and quantum physics, bioinformatics, signal processing, econometrics and information theory has accompanied a general increase in interest in applications of statistics. Finally, the realization that seemingly specialized methods developed in these disciplines are instances of a general class of inference algorithms has led to an increasing awareness that there may be alternatives to MCMC for general statistical inference that are worth exploring.

While the links to graph theory and thence to computational issues are a major virtue of the graphical model formalism, there is much that is still lacking. In the setting of large-scale graphical models, one would like to have some general notion of a tradeoff between computation and accuracy on which to base choices in model specification and the design of inference algorithms. Such a tradeoff is of course missing not only in the graphical model formalism but in statistics at large. Taking a decision-theoretic perspective, we should ask that our loss functions reflect computational complexity as well as statistical fidelity. By having a foot in both graph theory and probability

theory, graphical models may provide hints as to how to proceed if we wish to aim at a further and significantly deeper linkage of statistical science and computational science.

## References

- S. M. Aji and R. J. McEliece. The generalized distributive law. *IEEE Transactions on Information Theory*, 46:325–343, 2000.
- S. Arnborg, D. G. Corneil, and A. Proskurowski. Complexity of finding embeddings in a  $k$ -tree. *SIAM Journal on Algebraic and Discrete Methods*, 8:277–284, 1987.
- H. Attias. A variational Bayesian framework for graphical models. In *Advances in Neural Information Processing Systems 12*, 2000.
- J. Bilmes. Graphical models and automatic speech recognition. In Springer-Verlag, editor, *Mathematical Foundations of Speech and Language Processing*, 2003.
- D. M. Blei, M. I. Jordan, and A. Y. Ng. Hierarchical Bayesian models for applications in information retrieval. In *Bayesian Statistics 7*, 2002.
- R. G. Cowell, A. P. Dawid, S. L. Lauritzen, and D. J. Spiegelhalter. *Probabilistic Networks and Expert Systems*. Springer, New York, NY, 1999.
- R. Durbin, S. Eddy, A. Krogh, and G. Mitchison, editors. *Biological Sequence Analysis*. Cambridge University Press, Cambridge, 1998.
- R. C. Elston and J. Stewart. A general model for the genetic analysis of pedigree data. *Human Heredity*, 21:523–542, 1971.
- J. Felsenstein. Evolutionary trees from DNA sequences: a maximum likelihood approach. *Journal of Molecular Evolution*, 17:368–376, 1981.
- R. G. Gallager. *Low-Density Parity Check Codes*. MIT Press, Cambridge, MA, 1963.
- Z. Ghahramani and M.J. Beal. Propagation algorithms for variational Bayesian learning. In *Advances in Neural Information Processing Systems 13*, 2001.
- Z. Ghahramani and M. I. Jordan. Factorial hidden Markov models. *Machine Learning*, 37:183–233, 1996.
- W. Gilks, A. Thomas, and D. Spiegelhalter. A language and a program for complex Bayesian modelling. *The Statistician*, 43:169–178, 1994.
- J. P. Huelsenbeck and J. P. Bollback. Empirical and hierarchical Bayesian estimation of ancestral states. *Systematic Biology*, 50:351–366, 2001.
- C. S. Jensen, A. Kong, and U. Kjaerulff. Blocking-Gibbs sampling in very large probabilistic expert systems. *International Journal of Human-Computer Studies*, 42:647–666, 1995.
- M. I. Jordan, editor. *Learning in Graphical Models*. MIT Press, Cambridge, MA, 1999.
- F. Kschischang, B. J. Frey, and H.-A. Loeliger. Factor graphs and the sum-product algorithm. *IEEE Transactions on Information Theory*, 47:498–519, 2001.
- E. S. Lander and P. Green. Construction of multilocus genetic maps in humans. *Proceedings of the National Academy of Sciences*, 84:2363–2367, 1987.

- S. L. Lauritzen. *Graphical Models*. Clarendon Press, Oxford, 1996.
- M. A. R Leisink and H. J. Kappen. General lower bounds based on computer generated higher order expansions. In *Uncertainty in Artificial Intelligence, Proceedings of the Eighteenth Conference*, 2002.
- T. Minka. *A family of algorithms for approximate Bayesian inference*. PhD thesis, Massachusetts Institute of Technology, 2002.
- K. Murphy. *Dynamic Bayesian Networks: Representation, Inference and Learning*. PhD thesis, University of California, Berkeley, 2002.
- K. Murphy and M. Paskin. Linear time inference in hierarchical HMMs. In *Advances in Neural Information Processing Systems 13*, 2002.
- J. Pearl. *Probabilistic Reasoning in Intelligent Systems: Networks of Plausible Inference*. Morgan Kaufmann, San Mateo, CA, 1988.
- S. Richardson, L. Leblond, I. Jaussent, and P. J. Green. Mixture models in measurement error problems, with reference to epidemiological studies. *Biostatistics (submitted)*, 2002.
- T. Richardson, A. Shokrollahi, and R. Urbanke. Design of provably good low-density parity check codes. *IEEE Transactions on Information Theory*, 47:619–637, 2001.
- D. Ron, Y. Singer, and N. Tishby. The power of amnesia: Learning probabilistic automata with variable memory length. *Machine Learning*, 25:117–149, 1996.
- L. K. Saul and M. I. Jordan. Boltzmann chains and hidden Markov models. In *Advances in Neural Information Processing Systems 7*. MIT Press, Cambridge, MA, 1995.
- L. K. Saul and M. I. Jordan. Mixed memory Markov models: Decomposing complex stochastic processes as mixture of simpler ones. *Machine Learning*, 37:75–87, 1999.
- P. Shenoy and G. Shafer. Axioms for probability and belief-function propagation. In North-Holland, editor, *Uncertainty in Artificial Intelligence*, pages 169–198, 1990.
- A. Thomas, A. Gutin, V. Abkevich, and A. Bansal. Multilocus linkage analysis by blocked Gibbs sampling. *Statistics and Computing*, 10:259–269, 2000.
- M. J. Wainwright. *Stochastic processes on graphs with cycles: geometric and variational approaches*. PhD thesis, Massachusetts Institute of Technology, 2002.
- J.S. Yedidia, W.T. Freeman, and Y. Weiss. Generalized belief propagation. In *Advances in Neural Information Processing Systems 13*, 2001.

# An Introduction to Probabilistic Graphical Models

Michael I. Jordan  
*University of California, Berkeley*

June 30, 2003



# **Chapter 1**

## **Introduction**

Chapter 1 isn't written yet, but an effective substitute is the article entitled "Graphical Models" at:

[www.cs.berkeley.edu/~jordan/publications.html](http://www.cs.berkeley.edu/~jordan/publications.html)

That article overviews the basic graphical model framework and basic inference algorithms, and provides several examples of real-life graphical models. If you are new to graphical models, I'd recommend starting there.

# An Introduction to Probabilistic Graphical Models

Michael I. Jordan  
*University of California, Berkeley*

June 30, 2003



## Chapter 2

# Conditional Independence and Factorization

A graphical model can be thought of as a probabilistic database, a machine that can answer “queries” regarding the values of sets of random variables. We build up the database in pieces, using probability theory to ensure that the pieces have a consistent overall interpretation. Probability theory also justifies the inferential machinery that allows the pieces to be put together “on the fly” to answer queries.

Consider a set of random variables  $\{X_1, X_2, \dots, X_n\}$  and let  $x_i$  represent the realization of random variable  $X_i$ . Each random variable may be scalar-valued or vector-valued. Thus  $x_i$  is in general a vector in a vector space. In this section, for concreteness, we assume that the random variables are discrete; in general, however, we make no such restriction. There are several kinds of query that we might be interested in making regarding such an ensemble. We might, for example, be interested in knowing whether one subset of variables is independent of another, or whether one subset of variables is conditionally independent of another subset of variables given a third subset. Or we might be interested in calculating conditional probabilities—the probabilities of one subset of variables given the values of another subset of variables. Still other kinds of queries will be described in later chapters. In principle all such queries can be answered if we have in hand the joint probability distribution, written  $P(X_1 = x_1, X_2 = x_2, \dots, X_n = x_n)$ . Questions regarding independence can be answered by factoring the joint probability distribution, and questions regarding conditional probabilities can be answered by appropriate marginalization and normalization operations.

To simplify our notation, we will generally express discrete probability distributions in terms of the probability mass function  $p(x_1, x_2, \dots, x_n)$ , defined as  $p(x_1, x_2, \dots, x_n) \triangleq P(X_1 = x_1, X_2 = x_2, \dots, X_n = x_n)$ . We also will often use  $X$  to stand for  $\{X_1, \dots, X_n\}$ , and  $x$  to stand for  $\{x_1, \dots, x_n\}$ , so that  $P(X_1 = x_1, X_2 = x_2, \dots, X_n = x_n)$  can be written more succinctly as  $P(X = x)$ , or, more succinctly still, as  $p(x)$ . Note also that subsets of indices are allowed wherever single indices appear. Thus if  $A = \{2, 4\}$  and  $B = \{3\}$ , then  $X_A$  is shorthand for  $\{X_2, X_4\}$ ,  $X_B$  is shorthand for  $\{X_3\}$ , and  $P(X_A = x_A | X_B = x_B)$  is shorthand for  $P(X_2 = x_2, X_4 = x_4 | X_3 = x_3)$ .

While it is in fact our goal to maintain and manipulate representations of joint probabilities, we must not be naive regarding the size of the representations. In the case of discrete random

variables, one way to represent the joint probability distribution is as an  $n$ -dimensional table, in which each cell contains the probability  $p(x_1, x_2, \dots, x_n)$  for a specific setting of the variables  $\{x_1, x_2, \dots, x_n\}$ . If each variable  $x_i$  ranges over  $r$  values, we must store and manipulate  $r^n$  numbers, a quantity exponential in  $n$ . Given that we wish to consider models in which  $n$  is in the hundreds or thousands, such a naive tabular representation is out.

Graphical models represent joint probability distributions more economically, using a set of “local” relationships among variables. To define what we mean by “local” we avail ourselves of graph theory.

## 2.1 Directed graphs and joint probabilities

Let us begin by considering directed graphical representations. A directed graph is a pair  $\mathcal{G}(\mathcal{V}, \mathcal{E})$ , where  $\mathcal{V}$  is a set of nodes and  $\mathcal{E}$  a set of (oriented) edges. We will assume that  $\mathcal{G}$  is acyclic.

Each node in the graph is associated with a random variable. Formally, we assume that there is a one-to-one mapping from nodes to random variables, and we say that the random variables are *indexed* by the nodes in the graph. Thus, for each  $i \in \mathcal{V}$ , there is an associated random variable  $X_i$ . Letting  $\mathcal{V} = \{1, 2, \dots, n\}$ , as we often do for convenience, the set of random variables associated with the graph is given by  $\{X_1, X_2, \dots, X_n\}$ .

Although nodes and random variables are rather different formal objects, we will find it convenient to ignore the distinction, letting the symbol “ $X_i$ ” refer both to a node and to its associated random variable. Indeed, we will often gloss over the distinction between nodes and random variables altogether, using language such as “the marginal probability of node  $X_i$ .”

Note that we will also sometimes use lower-case letters—that is, the realization variables  $x_i$ —to label nodes, further blurring distinctions. Given the strict one-to-one correspondence that we enforce between the notation for random variables ( $X_i$ ) and their realizations ( $x_i$ ), however, this is unlikely to lead to confusion.

It would be rather inconvenient to be restricted to the symbol “ $X$ ” for random variables, and we often use other symbols as well. Thus, we may consider examples in which sets such as  $\{W, X, Y, Z\}$  or  $\{X_1, X_2, X_3, Y_1, Y_2, Y_3\}$  denote the set of random variables associated with a graph. As long as it is clear which random variable is associated with which node, then formally the random variables are “indexed” by the nodes in the graph as required, even though the indexing is not necessarily made explicit in the notation.

Each node has a set of *parent nodes*, which can be the empty set. For each node  $i \in \mathcal{V}$ , we let  $\pi_i$  denote the set of parents of node  $i$ . We also refer to the set of random variables  $X_{\pi_i}$  as the “parents” of the random variable  $X_i$ , exploiting the one-to-one relationship between nodes and random variables.

We use the locality defined by the parent-child relationship to construct economical representations of joint probability distributions. To each node  $i \in \mathcal{V}$  we associate a function  $f_i(x_i, x_{\pi_i})$ . These functions are assumed to have the properties of conditional probability distributions: that is,  $f_i(x_i, x_{\pi_i})$  is nonnegative and sums to one with respect to  $x_i$  for each value of  $x_{\pi_i}$ . We impose no additional constraint on these functions; in particular, there is no assumption of any relationship between the functions at different nodes.

Let  $\mathcal{V} = \{1, 2, \dots, n\}$ . Given a set of functions  $\{f_i(x_i, x_{\pi_i}) : i \in \mathcal{V}\}$ , we define a joint probability distribution as follows:

$$p(x_1, x_2, \dots, x_n) \triangleq \prod_{i=1}^n f_i(x_i, x_{\pi_i}). \quad (2.1)$$

That is, we define the joint probability as a product of the local functions at the nodes of the graph. To verify that the definition obeys the constraints on a joint probability, we check: (1) the right-hand side is clearly nonnegative; and (2) the assumption that each factor  $f_i(x_i, x_{\pi_i})$  sums to one with respect to  $x_i$ , together with the assumption that the graph is acyclic, implies that the right-hand side sums to one with respect to  $\{x_1, x_2, \dots, x_n\}$ . In particular, we can sum “backward” from the leaves of the graph, summing over the values of leaf nodes and removing the nodes from the graph, obtaining a value of one at each step.<sup>1</sup>

By choosing specific numerical values for the functions  $f_i(x_i, x_{\pi_i})$ , we generate a specific joint probability distribution. Ranging over all possible numerical choices for these functions, we define a *family of joint probability distributions associated with the graph  $\mathcal{G}$* . It will turn out that this family is a natural mathematical object. In particular, as we will see later in this chapter, this family can be characterized not only in terms of products of local functions, but also more “graph-theoretically” in terms of the patterns of edges in the graph. It is this relationship between the different ways to characterize the family of probability distributions associated with a graph that is the key to the underlying theory of probabilistic graphical models.

With a definition of joint probability in hand, we can begin to address the problem of calculating conditional probabilities under this joint. Suppose in particular that we calculate  $p(x_i | x_{\pi_i})$  under the joint probability in Eq. (2.1). What, if any, is the relationship between this conditional probability and  $f_i(x_i, x_{\pi_i})$ , a function which has the properties of a conditional probability but is otherwise arbitrary? As we ask the reader to verify in Exercise ??, these functions are in fact one and the same. That is, under the definition of joint probability in Eq. (2.1), the function  $f_i(x_i, x_{\pi_i})$  is necessarily the conditional probability of  $x_i$  given  $x_{\pi_i}$ . Put differently, we see that the functions  $f_i(x_i, x_{\pi_i})$  must form a consistent set of conditional probabilities under a single joint probability. This is a pleasant and somewhat surprising fact given that we can define the functions  $f_i(x_i, x_{\pi_i})$  arbitrarily.

Given that functions  $f_i(x_i, x_{\pi_i})$  are in fact conditional probabilities, we henceforth drop the  $f_i$  notation and write the definition in terms of  $p(x_i | x_{\pi_i})$ :<sup>2</sup>

$$p(x_1, x_2, \dots, x_n) = \prod_{i=1}^n p(x_i | x_{\pi_i}). \quad (2.2)$$

---

<sup>1</sup>If this point is not clear now, it will be clear later when we discuss inference algorithms.

<sup>2</sup>Eq. (2.2) is often used as the definition of the joint probability for a directed graphical model. Such a definition risks circularity, however, because it is not clear in advance that an arbitrary collection of conditional probabilities,  $\{p(x_i | x_{\pi_i})\}$ , are necessarily conditionals under the same joint probability. Moreover, it is not clear in advance that an arbitrary collection of conditional probabilities is internally consistent. We thus prefer to treat Eq. (2.1) as the definition and view Eq. (2.2) as a consequence. Having made this cautionary note, however, for simplicity we refer to Eq. (2.2) as the “definition” of joint probability in the remainder of the chapter.

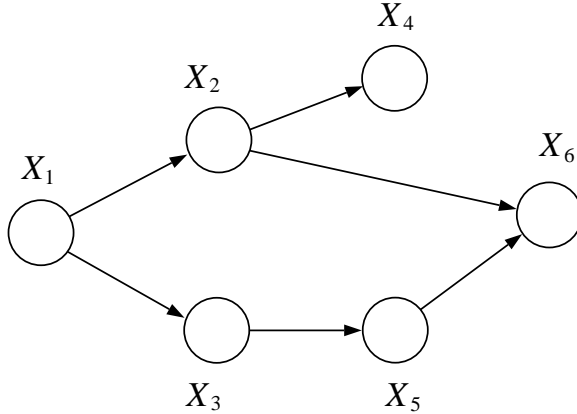


Figure 2.1: An example of a directed graphical model.

We refer to the conditional probabilities  $p(x_i | x_{\pi_i})$  as the *local conditional probabilities* associated with the graph  $\mathcal{G}$ . These functions are the building blocks whereby we synthesize a joint distribution associated with the graph  $\mathcal{G}$ .

Figure 2.1 shows an example on six nodes. According to the definition, we obtain the joint probability as follows:

$$p(x_1, x_2, x_3, x_4, x_5, x_6) = p(x_1)p(x_2 | x_1)p(x_3 | x_1)p(x_4 | x_2)p(x_5 | x_3)p(x_6 | x_2, x_5), \quad (2.3)$$

by taking the product of the local conditional distributions.

Let us now return to the problem of representational economy. Are there computational advantages to representing a joint probability as a set of local conditional probabilities?

Each of the local conditional probabilities must be represented in some manner. In later chapters we will consider a number of possible representations for these probabilities; indeed, this representational issue is one of the principal topics of the book. For concreteness, however, let us make a simple choice here. For a discrete node  $X_i$ , we must represent the probability that node  $X_i$  takes on one of its possible values, for each combination of values for its parents. This can be done using a table. Thus, for example, the probability  $p(x_1)$  can be represented using a one-dimensional table, and the probability  $p(x_6 | x_2, x_5)$  can be represented using a three-dimensional table, one dimension for each of  $x_2, x_5$  and  $x_6$ . The entire set of tables for our example is shown in Figure 2.2, where for simplicity we have assumed that the nodes are binary-valued. Filling these tables with specific numerical values picks out a specific distribution in the family of distributions defined by Eq. (2.3).

In general, if  $m_i$  is the number of parents of node  $X_i$ , we can represent the conditional probability associated with node  $X_i$  with an  $(m_i + 1)$ -dimensional table. If each node takes on  $r$  values, then we require a table of size  $r^{m_i+1}$ .

We have exchanged exponential growth in  $n$ , the number of variables in the domain, for exponential growth in  $m_i$ , the number of parents of individual nodes  $X_i$  (the “fan-in”). This is very often a happy exchange. Indeed, in many situations the maximum fan-in in a graphical model is relatively small and the reduction in complexity can be enormous. For example, in hidden Markov

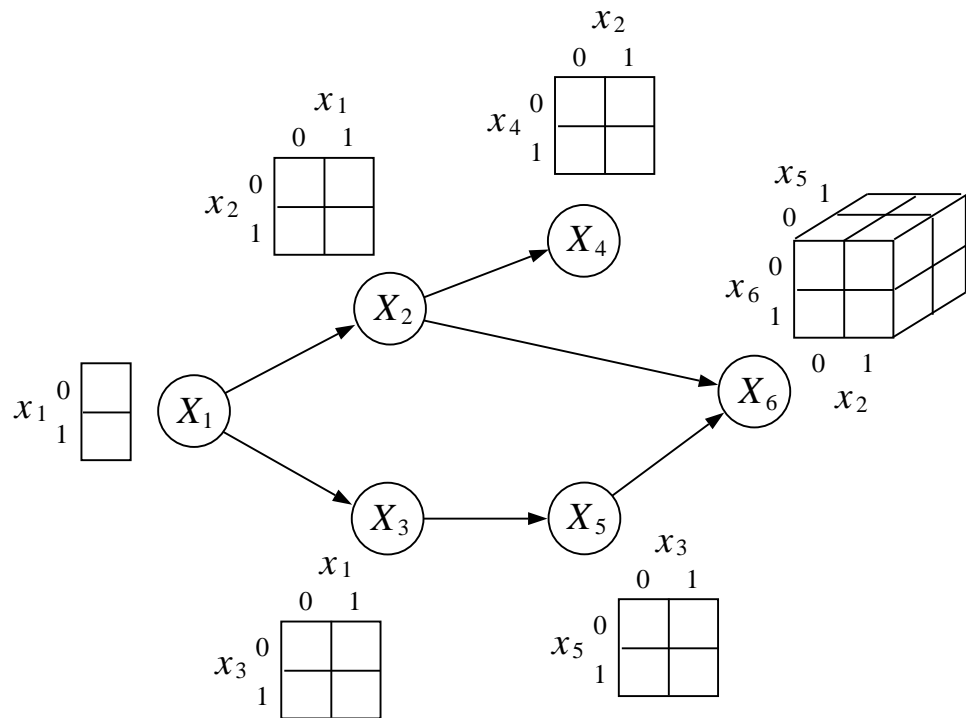


Figure 2.2: The local conditional probabilities represented as tables. Each of the nodes is assumed to be binary-valued. Each of these tables can be filled with arbitrary nonnegative numerical values, subject to the constraint that they sum to one for given fixed values of the parents of a node. Thus, each column in each table must sum to one.

models (see Chapter 12), each node has at most a single parent, while the number of nodes  $n$  can be in the thousands.

The fact that graphs provide economical representations of joint probability distributions is important, but it is only a first hint of the profound relationship between graphs and probabilities. As we show in the remainder of this chapter and in the following chapter, graphs provide much more than a data structure; in particular, they provide *inferential* machinery for answering questions about probability distributions.

### 2.1.1 Conditional independence

An important class of questions regarding probability distributions has to do with conditional independence relationships among random variables. We often want to know whether a set of variables is independent of another set, or perhaps conditionally independent of that set given a third set. Independence and conditional independence are important qualitative aspects of probability theory.

By definition,  $X_A$  and  $X_B$  are *independent*, written  $X_A \perp\!\!\!\perp X_B$ , if:

$$p(x_A, x_B) = p(x_A)p(x_B), \quad (2.4)$$

and  $X_A$  and  $X_C$  are *conditionally independent given  $X_B$* , written  $X_A \perp\!\!\!\perp X_C | X_B$ , if:

$$p(x_A, x_C | x_B) = p(x_A | x_B)p(x_C | x_B), \quad (2.5)$$

or, alternatively,

$$p(x_A | x_B, x_C) = p(x_A | x_B), \quad (2.6)$$

for all  $x_B$  such that  $p(x_B) > 0$ . Thus, to establish independence or conditional independence we need to factor the joint probability distribution.

Graphical models provide an intuitively appealing, symbolic approach to factoring joint probability distributions. The basic idea is that representing a probability distribution within the graphical model formalism involves making certain independence assumptions, assumptions which are embedded in the structure of the graph. From the graphical structure other independence relations can be derived, reflecting the fact that certain factorizations of joint probability distributions imply other factorizations. The key advantage of the graphical approach is that such factorizations can be read off from the graph via simple graph search algorithms. We will describe such an algorithm in Section 2.1.2; for now let us try to see in general terms why graphical structure should encode conditional independence.

The *chain rule of probability theory* allows a probability mass function to be written in a general factored form, once a particular ordering for the variables is chosen. For example, a distribution on the variables  $\{X_1, X_2, \dots, X_6\}$  can be written as:

$$\begin{aligned} & p(x_1, x_2, x_3, x_4, x_5, x_6) \\ &= p(x_1)p(x_2 | x_1)p(x_3 | x_1, x_2)p(x_4 | x_1, x_2, x_3)p(x_5 | x_1, x_2, x_3, x_4)p(x_6 | x_1, x_2, x_3, x_4, x_5), \end{aligned}$$

where we have chosen the usual arithmetic ordering of the nodes. In general, we have:

$$p(x_1, x_2, \dots, x_n) = \prod_{i=1}^n p(x_i | x_1, \dots, x_{i-1}). \quad (2.7)$$

Comparing this expansion, which is true for an arbitrary probability distribution, with the definition in Eq. (2.2), we see that our definition of joint probability involves dropping some of the conditioning variables in the chain rule. Inspecting Eq. (2.6), it seems natural to try to interpret these missing variables in terms of conditional independence. For example, the fact that  $p(x_4 | x_2)$  appears in Eq. (2.3) in the place of  $p(x_4 | x_1, x_2, x_3)$  suggests that we should expect to find that  $X_4$  is independent of  $X_1$  and  $X_3$  given  $X_2$ .

Taking this idea a step further, we might posit that *missing variables in the local conditional probability functions correspond to missing edges in the underlying graph*. Thus,  $p(x_4 | x_2)$  appears as a factor in Eq. (2.3) because there are no edges from  $X_1$  and  $X_3$  to  $X_4$ . Transferring the interpretation from missing variables to missing edges we obtain a probabilistic interpretation for the missing edges in the graph in terms of conditional independence. Let us formalize this interpretation.

Define an ordering  $I$  of the nodes in a graph  $\mathcal{G}$  to be *topological* if for every node  $i \in \mathcal{V}$  the nodes in  $\pi_i$  appear before  $i$  in the ordering. For example, the ordering  $I = (1, 2, 3, 4, 5, 6)$  is a topological ordering for the graph in Figure 2.1. Let  $\nu_i$  denote the set of all nodes that appear earlier than  $i$  in the ordering  $I$ , excluding the parent nodes  $\pi_i$ . For example,  $\nu_5 = \{1, 2, 4\}$  for the graph in Figure 2.1.

As we ask the reader to verify in Exercise ??, the set  $\nu_i$  necessarily contains all *ancestors* of node  $i$  (excluding the parents  $\pi_i$ ), and may contain other *nondescendant* nodes as well.

Given a topological ordering  $I$  for a graph  $\mathcal{G}$  we associate to the graph the following set of *basic conditional independence statements*:

$$\{X_i \perp\!\!\!\perp X_{\nu_i} | X_{\pi_i}\} \quad (2.8)$$

for  $i \in \mathcal{V}$ . Given the parents of a node, the node is independent of all earlier nodes in the ordering.

For example, for the graph in Figure 2.1 we have the following set of basic conditional independencies:

$$X_1 \perp\!\!\!\perp \emptyset \quad | \quad \emptyset \quad (2.9)$$

$$X_2 \perp\!\!\!\perp \emptyset \quad | \quad X_1 \quad (2.10)$$

$$X_3 \perp\!\!\!\perp X_2 \quad | \quad X_1 \quad (2.11)$$

$$X_4 \perp\!\!\!\perp \{X_1, X_3\} \quad | \quad X_2 \quad (2.12)$$

$$X_5 \perp\!\!\!\perp \{X_1, X_2, X_4\} \quad | \quad X_3 \quad (2.13)$$

$$X_6 \perp\!\!\!\perp \{X_1, X_3, X_4\} \quad | \quad \{X_2, X_5\}, \quad (2.14)$$

where the first two statements are vacuous.

Is this interpretation of the missing edges in terms of conditional independence consistent with our definition of the joint probability in Eq. (2.2)? The answer to this important question is “yes,” although proof will be again postponed until later. Let us refer to our example, however, to provide a first indication of the basic issues.

Let us verify that  $X_1$  and  $X_3$  are independent of  $X_4$  given  $X_2$  by direct calculation from the

joint probability in Eq. (2.3). We first compute the marginal probability of  $\{X_1, X_2, X_3, X_4\}$ :

$$p(x_1, x_2, x_3, x_4) = \sum_{x_5} \sum_{x_6} p(x_1, x_2, x_3, x_4, x_5, x_6) \quad (2.15)$$

$$= \sum_{x_5} \sum_{x_6} p(x_1)p(x_2 | x_1)p(x_3 | x_1)p(x_4 | x_2)p(x_5 | x_3)p(x_6 | x_2, x_5) \quad (2.16)$$

$$= p(x_1)p(x_2 | x_1)p(x_3 | x_1)p(x_4 | x_2) \sum_{x_5} p(x_5 | x_3) \sum_{x_6} p(x_6 | x_2, x_5) \quad (2.17)$$

$$= p(x_1)p(x_2 | x_1)p(x_3 | x_1)p(x_4 | x_2), \quad (2.18)$$

and also compute the marginal probability of  $\{X_1, X_2, X_3\}$ :

$$p(x_1, x_2, x_3) = \sum_{x_4} p(x_1)p(x_2 | x_1)p(x_3 | x_1)p(x_4 | x_2) \quad (2.19)$$

$$= p(x_1)p(x_2 | x_1)p(x_3 | x_1). \quad (2.20)$$

Dividing these two marginals yields the desired conditional:

$$p(x_4 | x_1, x_2, x_3) = p(x_4 | x_2), \quad (2.21)$$

which demonstrates the conditional independence relationship  $X_4 \perp\!\!\!\perp \{X_1, X_3\} | X_2$ .

We can readily verify the other conditional independencies in Eq. (2.14), and indeed it is not hard to follow along the lines of the example to prove in general that the conditional independence statements in Eq. (2.8) follow from the definition of joint probability in Eq. (2.2). Thus we are licensed to interpret the missing edges in the graph in terms of a basic set of conditional independencies.

More interestingly, we might ask whether there are other conditional independence statements that are true of such joint probability distributions, and whether these statements also have a graphical interpretation.

For example, for the graph in Figure 2.1 it turns out that  $X_1$  is independent of  $X_6$  given  $\{X_2, X_3\}$ . This is not one of the basic conditional independencies in the list in Eq. (2.14), but it is *implied* by that list. We can verify this conditional independence by algebra. In general, however, such algebraic calculations can be tedious and it would be appealing to find a simpler method for checking conditional independencies. Moreover, we might wish to write down *all* of the conditional independencies that are implied by our basic set. Is there any way to do this other than by trying to factorize the joint distribution with respect to all possible triples of subsets of the variables?

A solution to the problem is suggested by examining the graph in Figure 2.3. We see that the nodes  $X_2$  and  $X_3$  *separate*  $X_1$  from  $X_6$ , in the sense that all paths between  $X_1$  and  $X_6$  pass through  $X_2$  or  $X_3$ . Moreover, returning to the list of basic conditional independencies in Eq. (2.14), we see that the parents  $X_{\pi_i}$  block all paths from the node  $X_i$  to the earlier nodes in a topological ordering. This suggests that the notion of *graph separation* can be used to derive a graphical algorithm for inferring conditional independence.

We will have to take some care, however, to make the notion of “blocking” precise. For example,  $X_2$  is *not* necessarily independent of  $X_3$  given  $X_1$  and  $X_6$ , as would be suggested by a naive interpretation of “blocking” in terms of graph separation.

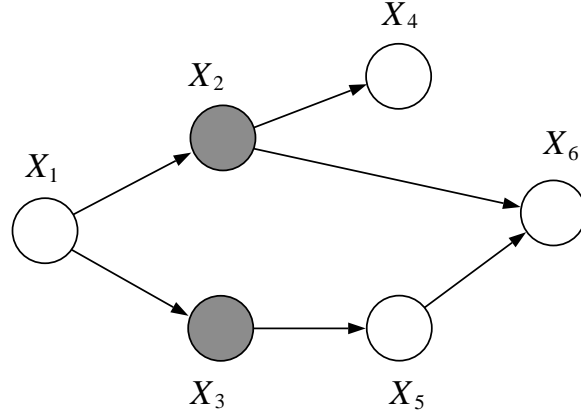


Figure 2.3: The nodes  $X_2$  and  $X_3$  separate  $X_1$  from  $X_6$ .

We will pursue the analysis of blocking and conditional independence in the following section, where we provide a general graph search algorithm to solve the problem of finding implied independencies.

Let us make a final remark on the definition of the set of basic conditional independence statements in Eq. (2.8). Note that this set is dependent on both the graph  $\mathcal{G}$  and on an ordering  $I$ . It is also possible to make an equivalent definition that is defined only in terms of the graph  $\mathcal{G}$ . In particular, recall that the set  $\nu_i$  necessarily includes all ancestors of  $i$  (excluding the parents  $\pi_i$ ). Note that the set of ancestors is independent of the ordering  $I$ . We thus might consider defining a basic set of independence statements that assert the conditional independence of a node from its ancestors, conditional on its parents. It turns out that the independence statements in this set hold if and only if the independence statements in Eq. (2.8) hold. As we ask the reader to verify in Exercise ??, this equivalence follows easily from the “Bayes ball” algorithm that we present in the following section.

The definition in Eq. (2.8) was chosen so as to be able to contrast the definition of the joint probability in Eq. (2.2) with the general chain rule in Eq. (2.7). An order-independent definition of the basic set of conditional independencies is, however, an arguably more elegant characterization of conditional independence in a graph, and it will take center stage in our more formal treatment of conditional independence and Markov properties in Chapter 16.

### 2.1.2 Conditional independence and the Bayes ball algorithm

The algorithm that we describe is called the *Bayes ball algorithm*, and it has the colorful interpretation of a ball bouncing around a graph. In essence it is a “reachability” algorithm, under a particular definition of “separation.”

Our approach will be to first discuss the conditional independence properties of three canonical, three-node graphs. We then embed these properties in a protocol for the bouncing ball; these are the local rules for a graph-search algorithm.

Two final remarks before we describe the algorithm. In our earlier discussion in Section 2.1.1,

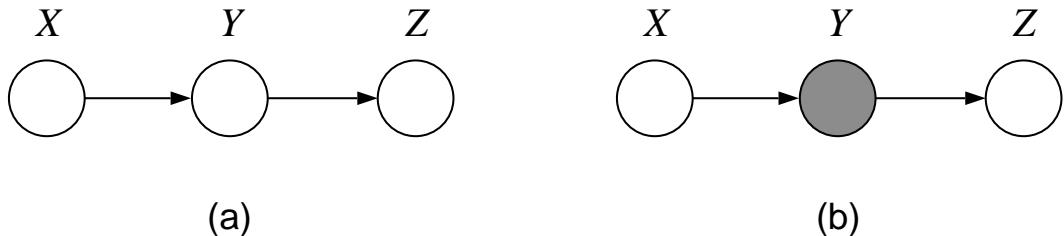


Figure 2.4: (a) The missing edge in this graph corresponds to the conditional independence statement  $X \perp\!\!\!\perp Z | Y$ . As suggested in (b), conditioning on  $Y$  has the graphical interpretation of blocking the path between  $X$  and  $Z$ .

and also in the current section, we presented conditional independence as being subservient to the basic definition in Eq. (2.2) of the joint probability. That is, we justified an assertion of conditional independence by factorizing Eq. (2.2) or one of its marginals. This is not the only point of view that we can take, however. Indeed it turns out that this relationship can be reversed, with Eq. (2.2) being derived from a characterization of conditional independence, and we will also introduce this point of view in this section. By the end of the current section we hope to have clarified what is meant by a “characterization of conditional independence.”

On a related note, let us recall a remark that was made earlier, which is that to each graph we associate a *family of joint probability distributions*. In terms of the definition of joint probability in Eq. (2.2), this family arises as we range over different choices of the numerical values of the local conditional probabilities  $p(x_i | x_{\pi_i})$ . Our work in the current section can be viewed as providing an alternative, more qualitative, characterization of a family of probability distributions associated to a given graph. In particular we can view the conditional independence statements generated by the Bayes ball algorithm as generating a list of constraints on probability distributions. Those joint probabilities that meet all of the constraints in this list are in the family, and those that fail to meet one or more constraints are out. It is then an interesting question as to the relationship between this characterization of a family of probability distributions in terms of conditional independence and the more numerical characterization of a family in terms of local conditional probabilities. This is the topic of Section 2.1.3.

## Three canonical graphs

As we discussed in Section 2.1.1, the missing edges in a directed graphical model can be interpreted in terms of conditional independence. In this section, we flesh out this interpretation for three simple graphs.

Consider first the graph shown in Figure 2.4, in which  $X$ ,  $Y$ , and  $Z$  are connected in a chain. There is a missing edge between  $X$  and  $Z$ , and we interpret this missing edge to mean that  $X$  and  $Z$  are conditionally independent given  $Y$ ; thus:

$$X \perp\!\!\!\perp Z \mid Y. \quad (2.22)$$

Moreover, we assert that there are no other conditional independencies associated with this graph.

Let us justify the first assertion, showing that  $X \perp\!\!\!\perp Z | Y$  can be derived from the assumed form of the joint distribution for directed models Eq. (2.2). We have:

$$p(x, y, z) = p(x)p(y|x)p(z|y), \quad (2.23)$$

which implies:

$$p(z|x, y) = \frac{p(x, y, z)}{p(x, y)} \quad (2.24)$$

$$= \frac{p(x)p(y|x)p(z|y)}{p(x)p(y|x)} \quad (2.25)$$

$$= p(z|y), \quad (2.26)$$

which establishes the independence.

The second assertion needs some explanation. What do we mean when we say that “there are no other conditional independencies associated with this graph”? It is important to understand that this does *not* mean that no further conditional independencies can arise in any of the distributions in the family associated with this graph (that is, distributions that have the factorized form in Eq. (2.23)). There are certainly some distributions which exhibit additional independencies. For example, we are free to choose any local conditional probability  $p(y|x)$ ; suppose that we choose a distribution in which the probability of  $y$  happens to be the same no matter the value of  $x$ . We can readily verify that with this particular choice of  $p(y|x)$ , we obtain  $X \perp\!\!\!\perp Y$ .

The key point, then, is that Figure 2.4 does not assert that  $X$  and  $Y$  are necessarily dependent (i.e., not independent). That is, edges that are present in a graph do not necessarily imply dependence (whereas edges that are missing do necessarily imply independence). But the “lack of independence” does have a specific interpretation: the general theory that we present in Chapter 16 will imply that if a statement of independence is not made, then there exists at least one distribution for which that independence relation does not hold. For example, it is easy to find distributions that factorize as in Eq. (2.23) and in which  $X$  is not independent of  $Y$ .

In essence, the issue comes down to a difference between universally quantified statements and existentially quantified statements, with respect to the family of distributions associated with a given graph. Asserted conditional independencies *always* hold for these distributions. Non-asserted conditional independencies *sometimes* fail to hold for the distributions associated with a given graph, but sometimes they do hold. This of course has important consequences for algorithm design. In particular, if we build an algorithm that is based on conditional independencies, the algorithm will be correct for *all* of the distributions associated with the graph. An algorithm based on the absence of conditional independencies will *sometimes* be correct, sometimes not.

For an intuitive interpretation of the graph in Figure 2.4, let  $X$  be the “past,”  $Y$  be the “present,” and  $Z$  be the “future.” Thus our conditional independence statement  $X \perp\!\!\!\perp Z | Y$  translates into the statement that the past is independent of the future given the present, and we can interpret the graph as a simple classical Markov chain.

Our second canonical graph is shown in Figure 2.5. We associate to this graph the conditional independence statement:

$$X \perp\!\!\!\perp Z | Y, \quad (2.27)$$

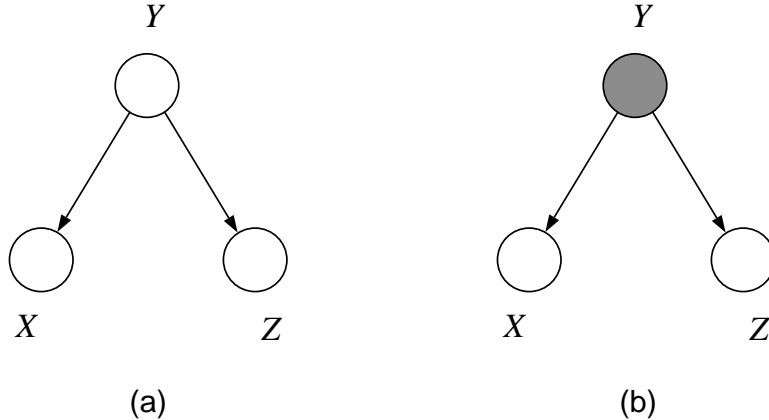


Figure 2.5: (a) The missing edge in this graph corresponds to the conditional independence statement  $X \perp\!\!\!\perp Z | Y$ . As suggested in (b), conditioning on  $Y$  has the graphical interpretation of blocking the path between  $X$  and  $Z$ .

and once again we assert that no other conditional independencies associated with this graph.

A justification of the conditional independence statement follows from the factorization rule. Thus:

$$p(x, y, z) = p(y)p(x | y)p(z | y) \quad (2.28)$$

implies:

$$p(x, z | y) = \frac{p(y)p(x | y)p(z | y)}{p(y)} \quad (2.29)$$

$$= p(x | y)p(z | y), \quad (2.30)$$

which means that  $X$  and  $Z$  are independent given  $Y$ .

An intuitive interpretation for this graph can be given in terms of a “hidden variable” scenario. Let  $X$  be the variable “shoe size,” and let  $Z$  be the variable “amount of gray hair.” In the general population, these variables are strongly dependent, because children tend to have small feet and no gray hair. But if we let  $Y$  be “chronological age,” then we might be willing to assert that  $X \perp\!\!\!\perp Z | Y$ ; that is, given the age of a person, there is no further relationship between the size of their feet and the amount of gray hair that they have. The hidden variable  $Y$  “explains” all of the observed dependence between  $X$  and  $Z$ .

Note once again we are making no assertions of dependence based on Figure 2.5. In particular, we do not necessarily assume that  $X$  and  $Z$  are dependent because they both “depend” on the variable  $Y$ . (But we can assert that there are at least some distributions in which such dependencies are to be found).

Finally, the most interesting canonical graph is that shown in Figure 2.6. Here the conditional independence statement that we associate with the graph is actually a statement of marginal independence:

$$X \perp\!\!\!\perp Z, \quad (2.31)$$

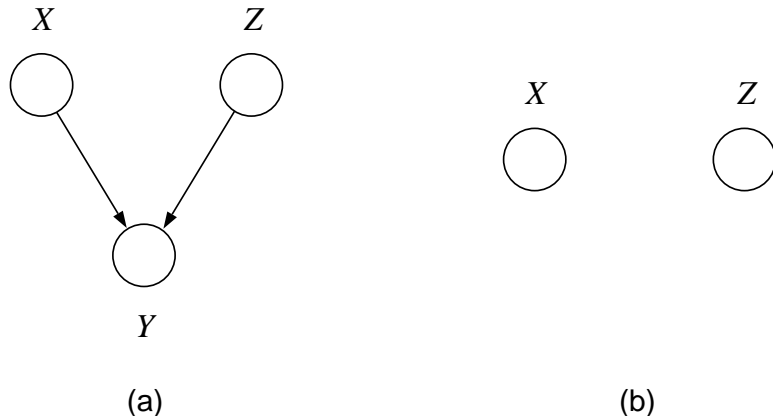


Figure 2.6: (a) The missing edge in this graph corresponds to the marginal independence statement  $X \perp\!\!\!\perp Z$ . As shown in (b), this is a statement about the subgraph defined on  $X$  and  $Z$ . Note moreover that conditioning on  $Y$  does not render  $X$  and  $Z$  independent, as would be expected from a naive characterization of conditional independence in terms of graph separation.

which we leave to the reader to verify in terms of the form of the joint probability. Once again, we assert that no other conditional independencies hold. In particular, note that we do not assert any conditional independence involving all three of the variables.

The fact that we do not assert that  $X$  is independent of  $Z$  given  $Y$  in Figure 2.6 is an important fact that is worthy of some discussion. Based on our earlier discussion, we should expect to be able to find scenarios in which a variable  $X$  is independent of another variable  $Z$ , given no other information, but once a third variable  $Y$  is observed these variables become dependent. Indeed, such a scenario is provided by a “multiple, competing explanation” interpretation of Figure 2.6.

Suppose that Bob is waiting for Alice for their noontime lunch date, and let  $\{\text{late} = \text{"yes"}\}$  be the event that Alice does not arrive on time. One explanation of this event is that Alice has been abducted by aliens, which we encode as  $\{\text{aliens} = \text{"yes"}\}$  (see Figure 2.7). Bob uses Bayes' theorem to calculate the probability  $P(\text{aliens} = \text{"yes"} | \text{late} = \text{"yes"})$  and is dismayed to find that it is larger than the base rate  $P(\text{aliens} = \text{"yes"})$ . Alice has perhaps been abducted by aliens. Now let  $\{\text{watch} = \text{"no"}\}$  denote the event that Bob forgot to set his watch to reflect daylight savings time. Bob now calculates  $P(\text{aliens} = \text{"yes"} | \text{late} = \text{"yes"}, \text{watch} = \text{"no"})$  and is relieved to find that the probability of  $\{\text{aliens} = \text{"yes"}\}$  has gone down again. The key point is that  $P(\text{aliens} = \text{"yes"} | \text{late} = \text{"yes"}) \neq P(\text{aliens} = \text{"yes"} | \text{late} = \text{"yes"}, \text{watch} = \text{"no"})$ , and thus **aliens** is not independent of **watch** given **late**.

On the other hand, it is reasonable to assume that **aliens** is *marginally* independent of **watch**; that is, Bob's watch-setting behavior and Alice's experiences with aliens are presumably unrelated and we would evaluate their probabilities independently, outside of the context of the missed lunch date.

This kind of scenario is known as “explaining-away” and it is commonplace in real-life situations. Moreover, there are other such scenarios (e.g., those involving multiple, synergistic explanations)

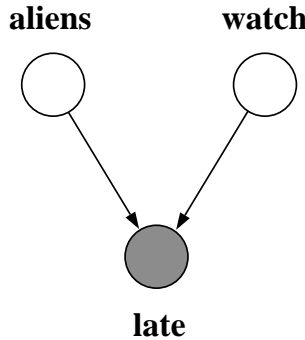


Figure 2.7: A graph representing the fact that Alice is late for lunch with Bob, with two possible explanations—that she has been abducted by aliens and that Bob has forgotten to set his watch to reflect daylight savings time.

in which variables that are marginally independent become dependent when a third variable is observed. We clearly do not want to assume in general that  $X$  is independent of  $Z$  given  $Y$  in Figure 2.6.

### Graph separation

We would like to forge a general link between graph separation and assertions of conditional independence. Doing so would allow us to use a graph-search algorithm to answer queries regarding conditional independence.

Happily, the graphs in Figure 2.4 and Figure 2.5 exhibit situations in which naive graph separation corresponds directly to conditional independence. Thus, as shown in Figure 2.4(b), shading the  $Y$  node blocks the path from  $X$  to  $Z$ , and this can be interpreted in terms of the conditional independence of  $X$  and  $Z$  given  $Y$ . Similarly, in Figure 2.5(b), the shaded  $Y$  node blocks the path from  $X$  to  $Z$ , and this can be interpreted in terms of the conditional independence of  $X$  and  $Z$  given  $Y$ .

On the other hand, the graph in Figure 2.6 involves a case in which naive graph separation and conditional independence are opposed. It is when the node  $Y$  is unshaded that  $X$  and  $Z$  are independent; when  $Y$  is shaded they become dependent. If we are going to use graph-theoretic ideas to answer queries about conditional independence, we need to pay particular attention to this case.

The solution is straightforward. Rather than relying on “naive” separation, we define a new notion of separation that is more appropriate to our purposes. This notion is known as *d-separation*, for “directed separation.” We provide a formal discussion of d-separation in Chapter 16; in the current chapter we provide a simple operational definition of d-separation in terms of the Bayes ball algorithm.

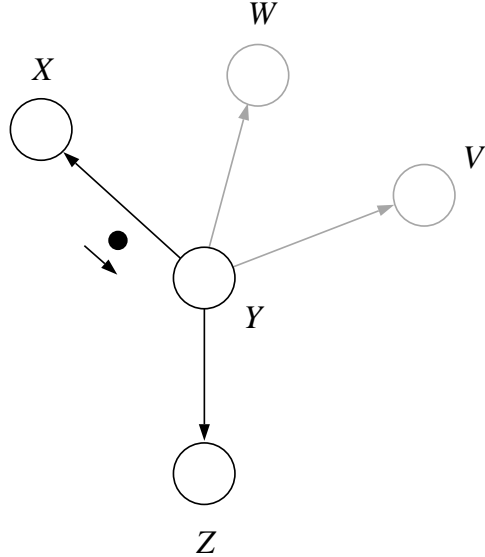


Figure 2.8: We develop a set of rules to specify what happens when a ball arrives from a node  $X$  at a node  $Y$ , en route to a node  $Z$ .

### The Bayes ball algorithm

The problem that we wish to solve is to decide whether a given conditional independence statement,  $X_A \perp\!\!\!\perp X_B | X_C$ , is true for a directed graph  $\mathcal{G}$ . Formally this means that the statement holds for every distribution that factors according to  $\mathcal{G}$ , but let us not worry about formal issues for now, and let our intuition—aided by the three canonical graphs that we have already studied—help us to define an algorithm to decide the question.

The algorithm is a “reachability” algorithm: we shade the nodes  $X_C$ , place a ball at each of the nodes  $X_A$ , let the balls bounce around the graph according to a set of rules, and ask whether any of the balls reach one of the nodes in  $X_B$ . If none of the balls reach  $X_B$ , then we assert that  $X_A \perp\!\!\!\perp X_B | X_C$  is true. If a ball reaches  $X_B$  then we assert that  $X_A \perp\!\!\!\perp X_B | X_C$  is not true.

The basic problem is to specify what happens when a ball arrives at a node  $Y$  from a node  $X$ , en route to a node  $Z$  (see Figure 2.8). Note that we focus on a particular candidate destination node  $Z$ , ignoring the other neighbors that  $Y$  may have. (We will be trying all possible neighbors, but we focus on one at a time). Note also that the balls are allowed to travel in either direction along the edges of the graph.

We specify these rules by making reference to our three canonical graphs. In particular, referring to Figure 2.4, suppose that ball arrives at  $Y$  from  $X$  along an arrow oriented from  $X$  to  $Y$ , and we are considering whether to allow the ball to proceed to  $Z$  along an arrow oriented from  $Y$  to  $Z$ . Clearly, if the node  $Y$  is shaded, we do not want the ball to be able to reach  $Z$ , because  $X \perp\!\!\!\perp Z | Y$  for this graph. Thus we require the ball to be “blocked” in this case. Similarly, if a ball arrives at  $Y$  from  $Z$ , we do not allow the ball to proceed to  $X$ ; again the ball is blocked. We summarize these rules with the diagram in Figure 2.9(a).

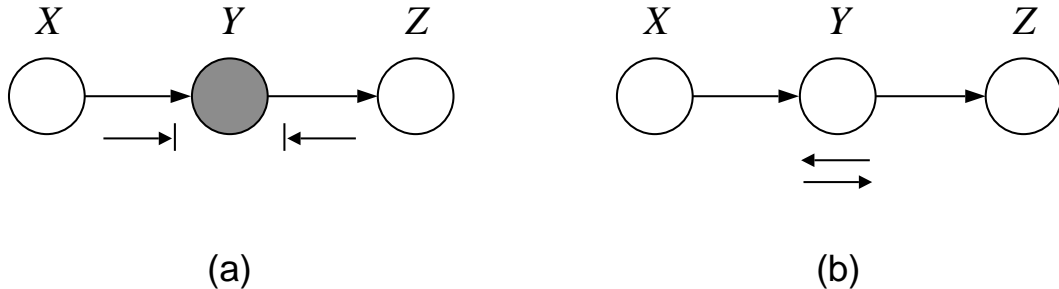


Figure 2.9: The rules for the case of one incoming arrow and one outgoing arrow. (a) When the middle node is shaded, the ball is blocked. (b) When the middle node is unshaded, the ball passes through.

On the other hand, if  $Y$  is not shaded, then we want to allow the ball to reach  $Z$  from  $X$  (and similarly  $X$  from  $Z$ ), because we do not want to assert conditional independence in this case. Thus we have the diagram in Figure 2.9(b), which shows the ball “passing through” when  $Y$  is not shaded.

Similar considerations apply to the graph in Figure 2.5, where the arrows are oriented outward from the node  $Y$ . Once again, if  $Y$  is shaded we do not want the ball to pass between  $X$  and  $Z$ , thus we require it to be blocked at  $Y$ . On the other hand, if  $Y$  is unshaded we allow the ball to pass through. These rules are summarized in Figure 2.10.

Finally, we consider the graph in Figure 2.6 in which both of the arrows are oriented towards node  $Y$  (this is often referred to as a “v-structure”). Here we simply reverse the rules. Thus, if  $Y$  is not shaded we require the ball to be blocked, reflecting the fact that  $X$  and  $Z$  are marginally independent. On the other hand, if  $Y$  is shaded we allow the ball to pass through, reflecting the fact that we do not assert that  $X$  and  $Z$  are conditionally independent given  $Y$ . The rules for this graph are given in Figure 2.11.

We also intend for these rules to apply to the case in which the source node and the destination node ( $X$  and  $Z$ , respectively) are the same. That is, when a ball arrives at a node, we consider each possible outgoing edge in turn, including the edge the ball arrives on.

Consider first the case in which the ball arrives along an edge that is oriented from  $X$  to  $Y$ . In this case, the situation is effectively one in which a ball arrives on the head of an arrow and departs on the head of an arrow. This situation is covered by Figure 2.11. We see that the ball should be blocked if the node is unshaded and should “pass through” if the node is shaded, a result that is summarized in Figure 2.12. Note that the action of “passing through” is better described in this case as “bouncing back.”

The remaining situation is the one in which the ball arrives along an edge that is oriented from  $Y$  to  $X$ . The ball arrives on the tail of an arrow and departs on the tail of an arrow, a situation which is covered by Figure 2.10. We see that the ball should be blocked if the node is shaded and should bounce back if the node is unshaded, a result that is summarized in Figure 2.13.

Let us consider some examples. Figure 2.14 shows a chain-structured graphical model (a Markov chain) on a set of nodes  $\{X_1, X_2, \dots, X_n\}$ . The basic conditional independencies for this graph (cf.

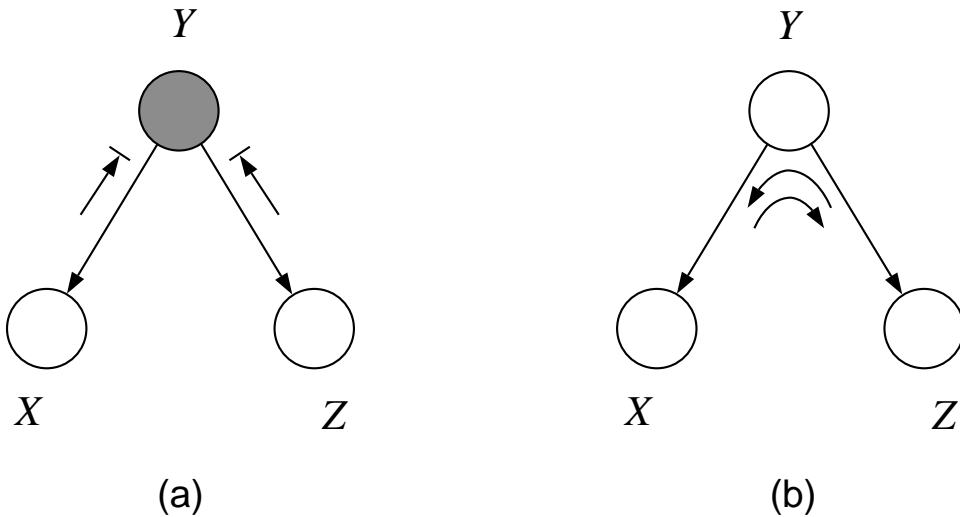


Figure 2.10: The rules for the case of two outgoing arrows. (a) When the middle node is shaded, the ball is blocked. (b) When the middle node is unshaded, the ball passes through.

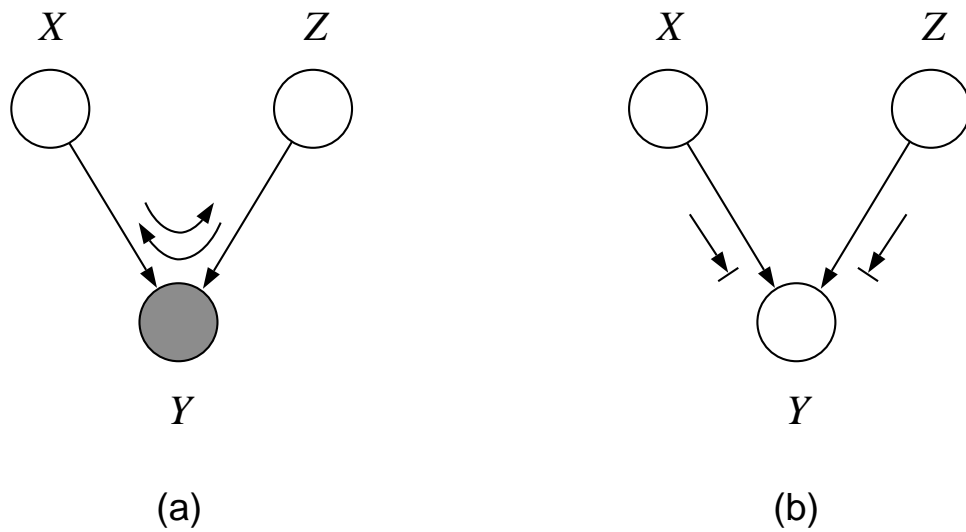


Figure 2.11: The rules for the case of two outgoing arrows. (a) When the middle node is shaded, the ball passes through. (b) When the middle node is unshaded, the ball is blocked.



Figure 2.12: The rules for this case follow from the rules in Figure 2.11. (a) When the ball arrives at an unshaded node, the ball is blocked. (b) When the ball arrives at a shaded node, the ball “passes through,” which effectively means that it bounces back.



Figure 2.13: The rules for this case follow from the rules in Figure 2.10. (a) When the ball arrives at an unshaded node, the ball “passes through,” which effectively means that it bounces back. (b) When the ball arrives at a shaded node, the ball is blocked.

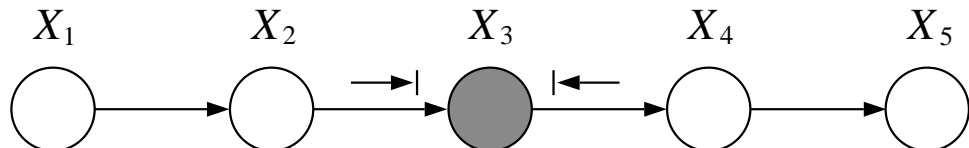


Figure 2.14: The separation of  $X_3$  from  $X_1$ , given its parent,  $X_2$ , is a basic independence statement for this graph. But conditioning on  $X_3$  also separates any subset of  $X_1, X_2$  from any subset of  $X_4, X_5$ , and all of these separations also correspond to conditional independencies.

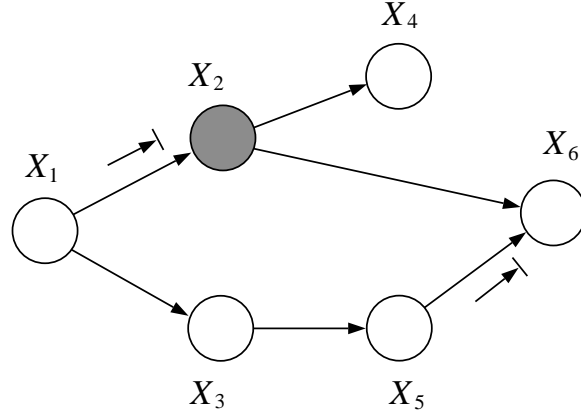


Figure 2.15: A ball arriving at  $X_2$  from  $X_1$  is blocked from continuing on to  $X_4$ . Also, a ball arriving at  $X_6$  from  $X_5$  is blocked from continuing on to  $X_2$ .

Eq. (2.8)) are the conditional independencies:

$$X_{i+1} \perp\!\!\!\perp \{X_1, X_2, \dots, X_{i-1}\} \mid X_i. \quad (2.32)$$

There are, however, many other conditional independencies that are implied by this basic set, such as:

$$X_1 \perp\!\!\!\perp X_5 \mid X_4, \quad X_1 \perp\!\!\!\perp X_5 \mid X_2, \quad X_1 \perp\!\!\!\perp X_5 \mid \{X_2, X_4\}, \quad (2.33)$$

each of which can be established from algebraic manipulations starting from the definition of the joint probability. Indeed, in general we can obtain the conditional independence of any subset of “future” nodes from any subset of “past” nodes given any subset of nodes that separates these subsets. This is clearly the set of conditional independence statements picked out by the Bayes ball algorithm; the ball is blocked when it arrives at  $X_3$  from either the left or the right.

Consider the graph in Figure 2.1 and consider the conditional independence  $X_4 \perp\!\!\!\perp \{X_1, X_3\} \mid X_2$  which we demonstrated to hold for this graph (this is one of the basic set of conditional independencies for this graph; recall Eqs. 2.9 through eq:example-set-of-basic-CI). Using the Bayes ball approach, let us consider whether it is possible for a ball to arrive at node  $X_4$  from either node  $X_1$  or node  $X_3$ , given that  $X_2$  is shaded (see Figure 2.15). To arrive at  $X_4$ , the ball must pass through  $X_2$ . One possibility is to arrive at  $X_2$  from  $X_1$ , but the path through to  $X_4$  is blocked because of Figure 2.9(a). The other possibility is to arrive at  $X_2$  via  $X_6$ . However, any ball arriving at  $X_6$  must do so via  $X_5$ , and such a ball is blocked at  $X_6$  because of Figure 2.11(b).

Note that balls can also bounce back at  $X_2$  and  $X_6$ , but this provides no help with respect to arriving at  $X_4$ .

We claimed in Section 2.1.1 that  $X_1 \perp\!\!\!\perp X_6 \mid \{X_2, X_3\}$ , a conditional independence that is not in the basic set. Consider a ball starting at  $X_1$  and traveling to  $X_3$  (see Figure 2.16). Such a ball cannot pass through to  $X_5$  because of Figure 2.9(a). Similarly, a ball cannot pass from  $X_1$  through  $X_2$  (to either  $X_4$  or  $X_6$ ) because of Figure 2.9(a).

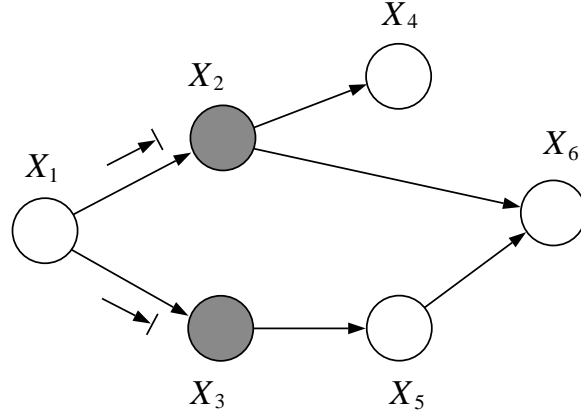


Figure 2.16: A ball cannot pass through  $X_2$  to  $X_6$  nor through  $X_3$ .

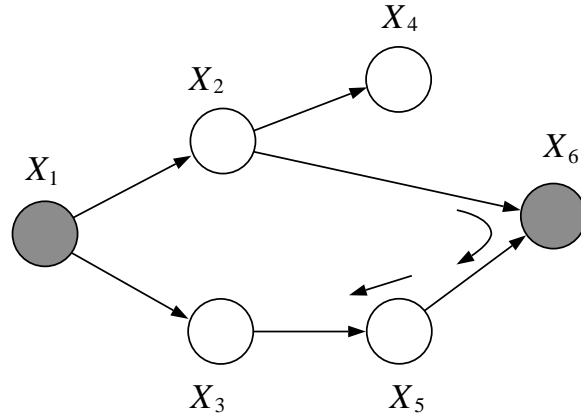


Figure 2.17: A ball can pass from  $X_2$  through  $X_6$  to  $X_5$ , and thence to  $X_3$ .

We also claimed in Section 2.1.1 that it is not the case that  $X_2 \perp\!\!\!\perp X_3 \mid \{X_1, X_6\}$ . To establish this claim we note that a ball can pass through  $X_2$  to  $X_6$  because of Figure 2.9(b), and (see Figure 2.17) can then pass from through  $X_6$  to  $X_5$ , on the basis of Figure 2.11(a). The ball then passes through  $X_5$  and arrives at  $X_3$ . Intuitively (and loosely), the observation of  $X_6$  implies the possibility of an “explaining-away” dependency between  $X_2$  and  $X_5$ . Clearly  $X_5$  and  $X_3$  are dependent, and thus  $X_2$  and  $X_3$  are dependent.

Finally, consider again the scenario with Alice and Bob, and suppose that Bob does not actually observe that Alice fails to show at the hour that he expects her. Suppose instead that Bob is an important executive and there is a security guard for Bob’s building who reports to Bob whether a guest has arrived or not. We augment the model to include a node **report** for the security guard’s report and, as shown in Figure 2.18, we hang this node off of the node **late**. Now observation of **report** is essentially as good as observation of **late**, particularly if we believe that the security guard is reliable. That is, we should still have **aliens**  $\perp\!\!\!\perp$  **watch**, and moreover we should not assert

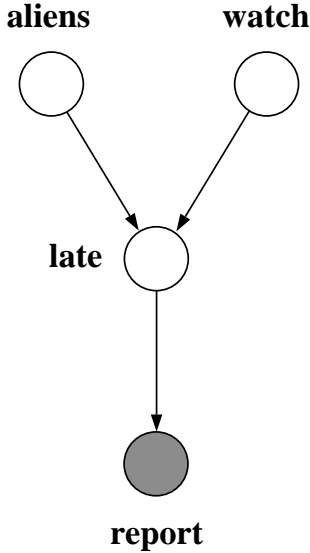


Figure 2.18: An extended graphical model for the Bob-Alice scenario, including a node **report** for the security guard’s report.

**aliens  $\perp\!\!\!\perp$  watch | report.** That is, if the security guard reports that Alice has not arrived, then Bob worries about aliens and subsequently has his worries alleviated when he realizes that he has forgotten about daylight savings time.

This pattern is what the Bayes ball algorithm delivers. Consider first the marginal independence **aliens  $\perp\!\!\!\perp$  watch**. As can be verified from Figure 2.19(a), a ball that starts at **aliens** is blocked from passing through **late** directly to **watch**. Moreover, although a ball can pass through **late** to **report**, such a ball dies at **report**. Thus the ball cannot arrive at **watch**.

Consider now the situation when **report** is observed (Figure 2.19(b)). As before a ball that starts at **aliens** is blocked from passing through **late** directly to **watch**; however, a ball can pass through **late** to **report**. At this point Figure 2.12(b) implies that the ball bounces back at **report**. The ball can then pass through **late** on the path from **report** to **watch**. Thus we cannot conclude independence of **aliens** and **watch** in the case that **report** is observed.

Some further thought will show that it suffices for any descendant of **late** to be observed in order to enable the explaining-away mechanism and render **aliens** and **watch** dependent.

### Remarks

We hope that the reader agrees that the Bayes ball algorithm is a simple, intuitively-appealing algorithm for answering conditional independence queries. Of course, we have not yet provided a fully-specified algorithm, because there are many implementational details to work out, including how to represent multiple balls when  $X_A$  and  $X_B$  are not singleton sets, how to make sure that the algorithm considers all possible paths in an efficient way, how to make sure that the algorithm doesn’t loop, etc. But these details are just that—details—and with a modicum of effort the reader

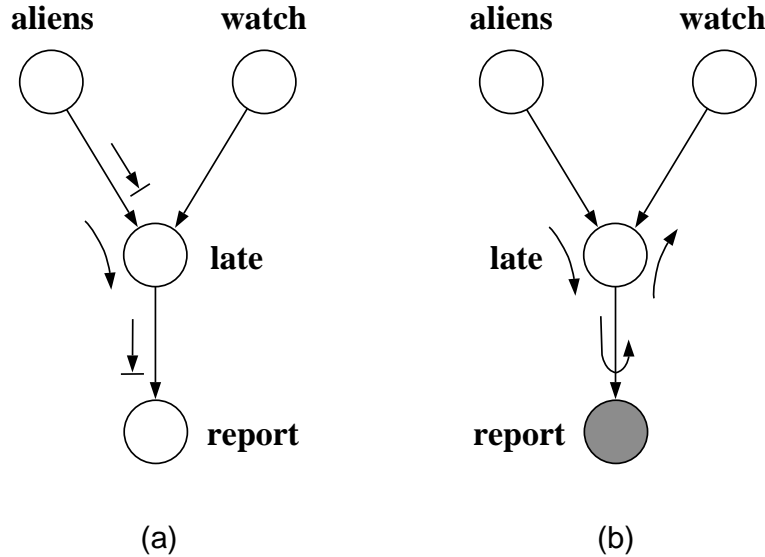


Figure 2.19: (a) A ball cannot pass from **aliens** to **watch** when no observations are made on **late** or **report**. (b) A ball can pass from **aliens** to **watch** when **report** is observed.

can work out such an implementation. Our main interest in the Bayes ball algorithm is to provide a handy tool for quick evaluation of conditional independence queries, and to provide concrete support for the more formal discussion of conditional independence that we undertake in the next section.

### 2.1.3 Characterization of directed graphical models

A key idea that has emerged in this chapter is that a graphical model is associated with a *family* of probability distributions. Moreover, as we now discuss, this family can be characterized in two equivalent ways.

Let us define two families and then show that they are equivalent. Actually we defer the proof of equivalence until Chapter 16, but we state the theorem here and discuss its consequences.

The first family is defined via the definition of joint probability for directed graphs, which we repeat here for convenience. Thus for a directed graph  $\mathcal{G}$ , we have:

$$p(x_1, x_2, \dots, x_n) \triangleq \prod_{i=1}^n p(x_i \mid x_{\pi_i}). \quad (2.34)$$

Let us now consider ranging over all possible numerical values for the local conditional probabilities  $\{p(x_i | x_{\pi_i})\}$ , imposing only the restriction that these functions are nonnegative and normalized. For discrete variables this would involve ranging over all possible real-valued tables on nodes  $x_i$  and their parents. While in practice, we often want to choose simplified parameterizations instead of these tables, for the general theory we must range over all possible tables.

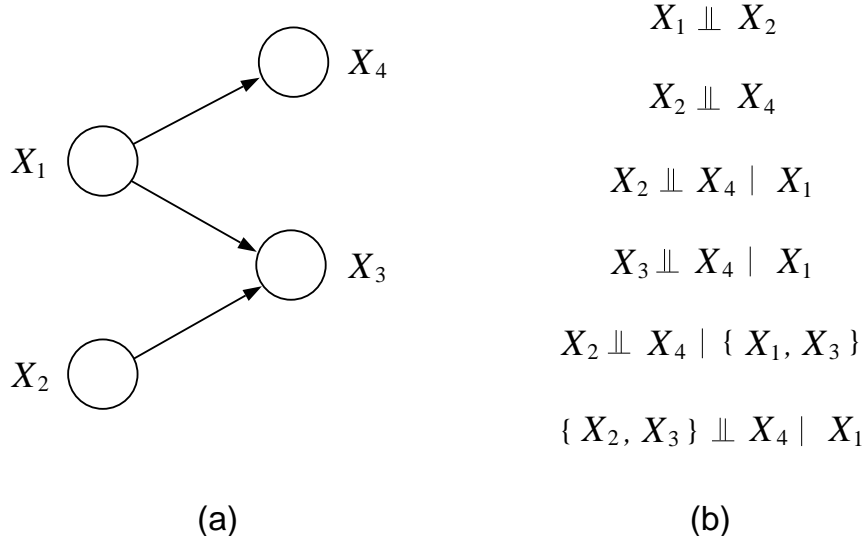


Figure 2.20: The list in (b) shows all of the conditional independencies that hold for the graph in (a).

For each choice of numerical values for the local conditional probabilities we obtain a particular probability distribution  $p(x_1, \dots, x_n)$ . Ranging over all such choices we obtain a family of distributions that we refer to as  $\mathcal{D}_1$ .

Let us now consider an alternative way to generate a family of probability distributions associated with a graph  $\mathcal{G}$ . In this approach we will make no use of the numerical parameterization of the joint probability in Eq. (2.34)—this approach will be more “qualitative.”

Given a graph  $\mathcal{G}$  we can imagine making a list of all of the conditional independence statements that characterize the graph. To do this, imagine running the Bayes ball algorithm for all triples of subsets of nodes in the graph. For any given triple  $X_A$ ,  $X_B$  and  $X_C$ , the Bayes ball algorithm tells us whether or not  $X_A \perp\!\!\!\perp X_B \mid X_C$  should be included in the list associated with the graph.

For example, Figure 2.20 shows a graph, and all of its associated conditional independence statements. In general such lists can be significantly longer than the list in this example, but they are always finite.

Now consider all possible joint probability distributions  $p(x_1, \dots, x_n)$ , where we make no restrictions at all. Thus, for discrete variables, we consider all possible  $n$ -dimensional tables. For each such distribution, imagine testing the distribution against the list of conditional independencies associated with the graph  $\mathcal{G}$ . Thus, for each conditional independence statement in the list, we test whether the distribution factorizes as required. If it does, move to the next statement. If it does not, throw out this distribution and try a new distribution. If a distribution passes all of the tests in the list, we include that distribution in a family that we denote as  $\mathcal{D}_2$ .

In Chapter 16, we state and prove a theorem that shows that the two families  $\mathcal{D}_1$  and  $\mathcal{D}_2$  are the same family. This theorem, and an analogous theorem for undirected graphs, provide a strong and important link between graph theory and probability theory and are at the core of the graphical

model formalism. They show that the characterizations of probability distributions via numerical parameterization and conditional independence statements are one and the same, and allow us to use these characterizations interchangeably in analyzing models and defining algorithms.

## 2.2 Undirected graphical models

The world of graphical models divides into two major classes—those based on directed graphs and those based on undirected graphs.<sup>3</sup> In this section we discuss undirected graphical models, also known as *Markov random fields*, and carry out a development that parallels our discussion of the directed case. Thus we will present a factorized parameterization for undirected graphs, a conditional independence semantics, and an algorithm for answering conditional independence queries. There are many similarities to the directed case—and much of our earlier work on directed graphs carries over—but there are interesting and important differences as well.

An undirected graphical model is a graph  $\mathcal{G}(\mathcal{V}, \mathcal{E})$ , where  $\mathcal{V}$  is a set of nodes that are in one-to-one correspondence with a set of random variables, and where  $\mathcal{E}$  is a set of undirected edges. The random variables can be scalar-valued or vector-valued, discrete or continuous. Thus we will be concerned with graphical representations of a joint probability distribution,  $p(x_1, x_2, \dots, x_n)$ —a mass function in the discrete case and a density function in the continuous case.

### 2.2.1 Conditional independence

As we saw in Section 2.1.3, there are two equivalent characterizations of the class of joint probability distributions associated with a directed graph. Our presentation of directed graphical models began (in Section 2.1) with the factorized parameterization and subsequently motivated the conditional independence characterization. We could, however, have turned this discussion around and started with a set of conditional independence axioms, subsequently deriving the parameterization. In the case of undirected graphs, indeed, this latter approach is the one that we will take. For undirected graphs, the conditional independence semantics is the more intuitive and straightforward of the two (equivalent) characterizations.

To specify the conditional independence properties of a graph, we must be able to say whether  $X_A \perp\!\!\!\perp X_C | X_B$  is true for the graph, for arbitrary index subsets  $A$ ,  $B$ , and  $C$ . For directed graphs we defined the conditional independence properties operationally, via the Bayes ball algorithm (we provide a corresponding declarative definition in Chapter 16). For undirected graphs we go straight to the declarative definition.

We say that  $X_A$  is independent of  $X_C$  given  $X_B$  if the set of nodes  $X_B$  separates the nodes  $X_A$  from the nodes  $X_C$ , where by “separation” we mean naive graph-theoretic separation (see Figure 2.21). Thus, if every path from a node in  $X_A$  to a node in  $X_C$  includes at least one node in  $X_B$ , then we assert that  $X_A \perp\!\!\!\perp X_C | X_B$  holds; otherwise we assert that  $X_A \perp\!\!\!\perp X_C | X_B$  does not hold.

---

<sup>3</sup>There is also a generalization known as *chain graphs* that subsumes both classes. We will discuss chain graphs in Chapter ??.

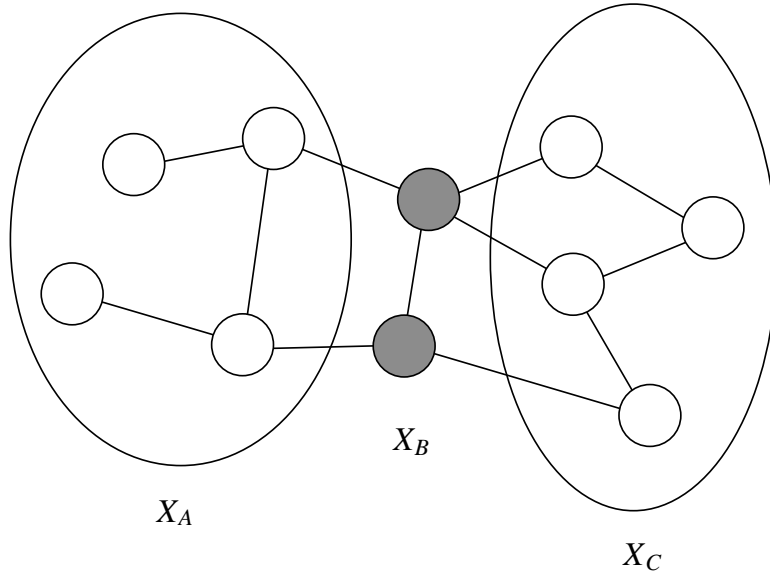


Figure 2.21: The set  $X_B$  separates  $X_A$  from  $X_C$ . All paths from  $X_A$  to  $X_C$  pass through  $X_B$ .

As before, the meaning of the statement “ $X_A \perp\!\!\!\perp X_C | X_B$  holds for a graph  $\mathcal{G}$ ” is that every member of the family of probability distributions associated with  $\mathcal{G}$  exhibits that conditional independence. On the other hand, the statement “ $X_A \perp\!\!\!\perp X_C | X_B$  does not hold for a graph  $\mathcal{G}$ ” means—in its strong form—that some distributions in the family associated with  $\mathcal{G}$  do not exhibit that conditional independence.

Given this definition, it is straightforward to develop an algorithm for answering conditional independence queries for undirected graphs. We simply remove the nodes  $X_B$  from the graph and ask whether there are any paths from  $X_A$  to  $X_C$ . This is a “reachability” problem in graph theory, for which standard search algorithms provide a solution.

### Comparative semantics

Is it possible to reduce undirected models to directed models, or vice versa? To see that this is not possible in general, consider Figure 2.22.

In Figure 2.22(a) we have an undirected model that is characterized by the conditional independence statements  $X \perp\!\!\!\perp Y | \{W, Z\}$  and  $W \perp\!\!\!\perp Z | \{X, Y\}$ . If we try to represent this model in a directed graph on the same four nodes, we find that we must have at least one node in which the arrows are inward-pointing (a “v-structure”). (Recall that our graphs are acyclic). Suppose without loss of generality that this node is  $Z$ , and that this is the only v-structure. By the conditional independence semantics of directed graphs, we have  $X \perp\!\!\!\perp Y | W$ , and we do not have  $X \perp\!\!\!\perp Y | \{W, Z\}$ . We are unable to represent both conditional independence statements,  $X \perp\!\!\!\perp Y | \{W, Z\}$  and  $W \perp\!\!\!\perp Z | \{X, Y\}$ , in the directed formalism.

On the other hand, in Figure 2.22(b) we have a directed graph characterized by the singleton

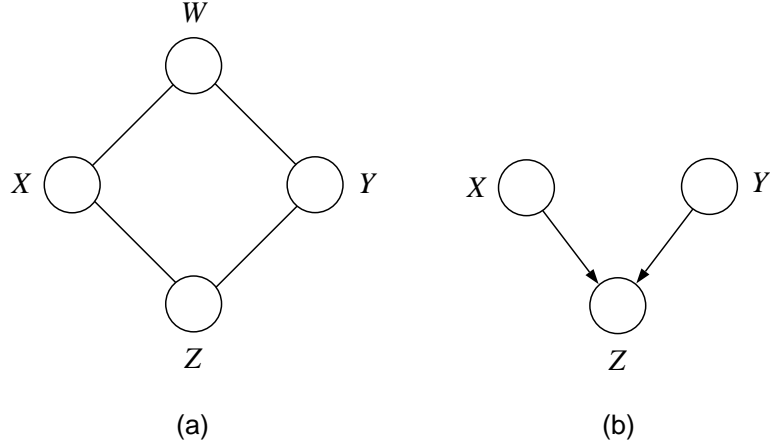


Figure 2.22: (a) An undirected graph whose conditional independence semantics cannot be captured by a directed graph on the same nodes. (b) A directed graph whose conditional independence semantics cannot be captured by an undirected graph on the same nodes.

independence statement  $X \perp\!\!\!\perp Y$ . No undirected graph on three nodes is characterized by this singleton set. A missing edge in an undirected graph only between  $X$  and  $Y$  captures  $X \perp\!\!\!\perp Y | Z$ , not  $X \perp\!\!\!\perp Y$ . An additional missing edge between  $X$  and  $Z$  captures  $X \perp\!\!\!\perp Y$ , but implies  $X \perp\!\!\!\perp Z$ .

We will show in Chapter 16 that there are some families of probability distributions that can be represented with either directed or undirected graphs. There is no good reason to restrict ourselves to these families, however. In general, directed models and undirected models are different modeling tools, and have different strengths and weaknesses. The two together provide modeling power beyond that which could be provided by either alone.

### 2.2.2 Parameterization

As in the case of directed graphs, we would like to obtain a “local” parameterization for undirected graphical models. For directed graphs the parameterization was based on local conditional probabilities, where “local” had the interpretation of a set  $\{i, \pi_i\}$  consisting of a node and its parents. The definition of the joint probability as a product of such local probabilities was motivated via the chain rule of probability theory.

In the undirected case it is rather more difficult to utilize conditional probabilities to represent the joint. One possibility would be to associate to each node the conditional probability of the node given its neighbors. This approach falls prey to a major consistency problem, however—it is hard to ensure that the conditional probabilities at different nodes are consistent with each other and thus with a single joint distribution. We are not able to choose these functions independently and arbitrarily, and this poses problems both in theory and in practice.

A better approach turns out to be to abandon conditional probabilities altogether. By so doing we will lose the ability to give a local probabilistic interpretation to the functions used to represent the joint probability, but we will retain the ability to choose these functions independently and

arbitrarily, and we will retain the all-important representation of the joint as a *product* of local functions.

A key problem is to decide the domain of the local functions; in essence, to decide the meaning of “local” for undirected graphs. It is here that the discussion of conditional independence in the previous section is helpful. In particular, consider a pair of nodes  $X_i$  and  $X_j$  that are not linked in the graph. The conditional independence semantics imply that these two nodes are conditionally independent given all of the other nodes in the graph (because upon removing this latter set there can be no paths from  $X_i$  to  $X_j$ ). Thus it must be possible to obtain a factorization of the joint probability that places  $x_i$  and  $x_j$  in different factors. This implies that we can have no local function that depends on both  $x_i$  and  $x_j$  in our representation of the joint. Such a local function, say  $\psi(x_i, x_j, x_k)$ , would not factorize with respect to  $x_i$  and  $x_j$  in general—recall that we are assuming that the local functions can be chosen arbitrarily.

Recall that a *clique* of a graph is a fully-connected subset of nodes. Our argument thus far has suggested that the local functions should not be defined on domains of nodes that extend beyond the boundaries of cliques. That is, if  $X_i$  and  $X_j$  are not directly connected, they do not appear together in any clique, and correspondingly there should be no local function that refers to both nodes. We now consider the flip side of the coin. Should we allow arbitrary functions that are defined on all of the cliques? Indeed, an interpretation of the edges that are present in the graph in terms of “dependence” suggests that we should. We have not defined dependence, but heuristically, dependence is the “absence of independence” in one or more of the distributions associated with a graph. If  $X_i$  and  $X_j$  are linked, and thus appear together in a clique, we can achieve dependence between them by defining a function on that clique.

The *maximal cliques* of a graph are the cliques that cannot be extended to include additional nodes without losing the property of being fully connected. Given that all cliques are subsets of one or more maximal cliques, we can restrict ourselves to maximal cliques without loss of generality. Thus, if  $X_1$ ,  $X_2$ , and  $X_3$  form a maximal clique, then an arbitrary function  $\psi(x_1, x_2, x_3)$  already captures all possible dependencies on these three nodes; we gain no generality by also defining functions on sub-cliques such as  $\{X_1, X_2\}$  or  $\{X_2, X_3\}$ .<sup>4</sup>

In summary, our arguments suggest that the meaning of “local” for undirected graphs should be “maximal clique.” More precisely, the conditional independence properties of undirected graphs imply a representation of the joint probability as a product of local functions defined on the maximal cliques of the graph. This argument is in fact correct, and we will establish it rigorously in Chapter 16. Let us proceed to make the definition and explore some of its consequences.

Let  $C$  be a set of indices of a maximal clique in an undirected graph  $G$ , and let  $\mathcal{C}$  be the set of all such  $C$ . A *potential function*,  $\psi_{X_C}(x_C)$ , is a function on the possible realizations  $x_C$  of the maximal clique  $X_C$ .

Potential functions are assumed to be nonnegative, real-valued functions, but are otherwise arbitrary. This arbitrariness is convenient, indeed necessary, for our general theory to go through,

---

<sup>4</sup>While there is no need to consider non-maximal cliques in developing the general theory relating conditional independence and factorization—our topic in this section—in practice it is often convenient to work with potentials on non-maximal cliques. This issue will return in Section 2.3 and in later chapters. Let us define joint probabilities in terms of maximal cliques for now, but let us be prepared to relax this definition later.

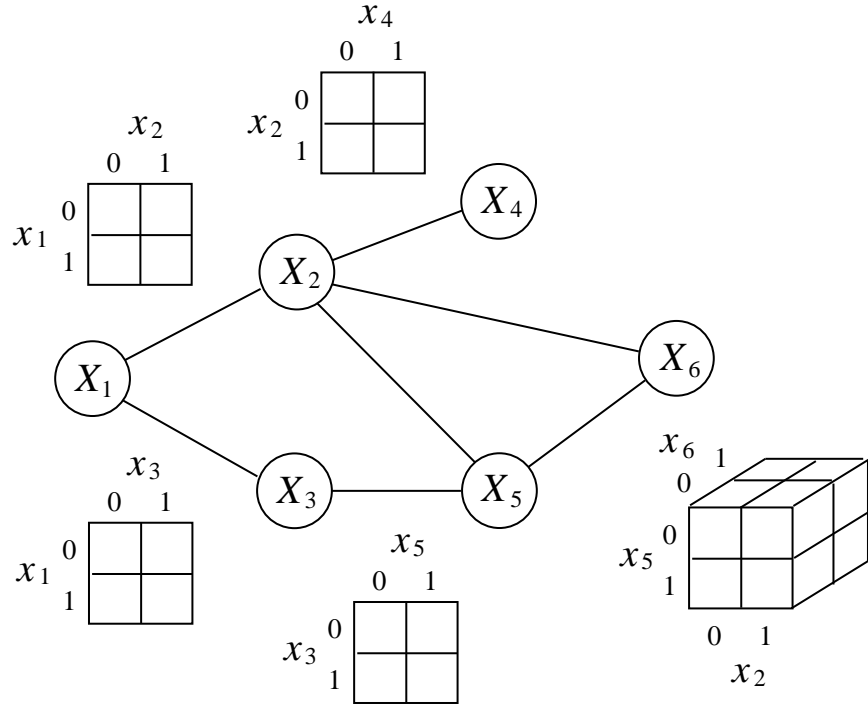


Figure 2.23: The maximal cliques in this graph are  $\{X_1, X_2\}$ ,  $\{X_1, X_3\}$ ,  $\{X_2, X_4\}$ ,  $\{X_3, X_5\}$ , and  $\{X_2, X_5, X_6\}$ . Letting all nodes be binary, we represent a joint distribution on the graph via the potential tables that are displayed.

but it also presents a problem. There is no reason for a product of arbitrary functions to be normalized and thus define a joint probability distribution. This is a bullet which we simply have to bite if we are to achieve the desired properties of arbitrary, independent potentials and a product representation for the joint.

Thus we define:

$$p(x) \triangleq \frac{1}{Z} \prod_{C \in \mathcal{C}} \psi_{X_C}(x_C), \quad (2.35)$$

where  $Z$  is the normalization factor:

$$Z \triangleq \sum_x \prod_{C \in \mathcal{C}} \psi_{X_C}(x_C), \quad (2.36)$$

obtained by summing the product in Eq. (2.35) over all assignments of values to the nodes  $X$ .

An example is shown in Figure 2.23. The nodes in this example are assumed discrete, and thus tables can be used to represent the potential functions. An overall configuration  $x$  picks out subvectors  $x_C$ , which determine particular cells in each of the potential tables. Taking the product of the numbers in these cells yields an unnormalized representation of the joint probability  $p(x)$ .

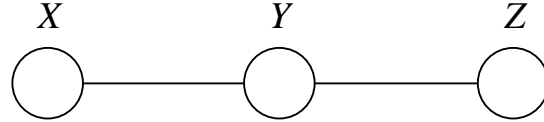


Figure 2.24: An undirected representation of a three-node Markov chain. The conditional independence associated with this graph is  $X \perp\!\!\!\perp Z | Y$ .

The normalization factor  $Z$  is obtained by summing over all configurations  $x$ . There are an exponential number of such configurations and it is unrealistic to try to perform such a sum by naively enumerating all of the summands. Note, however, that the expression being summed over is a factored expression, in which each factor refers to a local set of variables, and thus we can exploit the distributive law. This is an issue that is best discussed in the context of the more general discussion of probabilistic inference, and we return to it in Chapter 3.

Note, however, that we do not necessarily have to calculate  $Z$ . In particular, recall that a conditional probability is a ratio of two marginal probabilities. The factor  $Z$  appears in both of the marginal probabilities, and cancels when we take the ratio. Thus we calculate conditionals by summing across unnormalized probabilities—the numerator in Eq. (2.35)—and taking the ratio of these sums.

### The interpretation of potential functions

Although local conditional probabilities do not provide a satisfactory approach to the parameterization of undirected models, it might be thought that marginal probabilities could be used instead. Thus, why not replace the potential functions  $\psi_{X_C}(x_C)$  in Eq. (2.35) with marginal probabilities  $p(x_C)$ ?

An example will readily show that this approach is infeasible. Consider the model shown in Figure 2.24. The conditional independence that is associated with this graph is  $X \perp\!\!\!\perp Z | Y$ . This independence statement implies (by definition) that the joint must factorize as:

$$p(x, y, z) = p(y)p(x | y)p(z | y). \quad (2.37)$$

The cliques in Figure 2.24 are  $\{X, Y\}$  and  $\{Y, Z\}$ . We can multiply the first two factors in Eq. (2.37) together to obtain a potential function  $p(x, y)$  on the first clique, leaving  $p(z | y)$  as the potential function on the second clique. Alternatively, we can multiply  $p(z | y)$  by  $p(y)$  to yield a potential  $p(y, z)$  on the second clique, leaving  $p(x | y)$  as the potential on the first clique. Thus we can obtain a factorization in which one of the potentials is a marginal probability, and the other is a conditional probability. But we are unable to obtain a representation in which both potentials are marginal probabilities. That is:

$$p(x, y, z) \neq p(x, y)p(y, z). \quad (2.38)$$

In fact, it is not hard to see that  $p(x, y, z) = p(x, y)p(y, z)$  implies  $p(y) = 0$  or  $p(y) = 1$ , and that this representation is thus a rather limited and unnatural one.

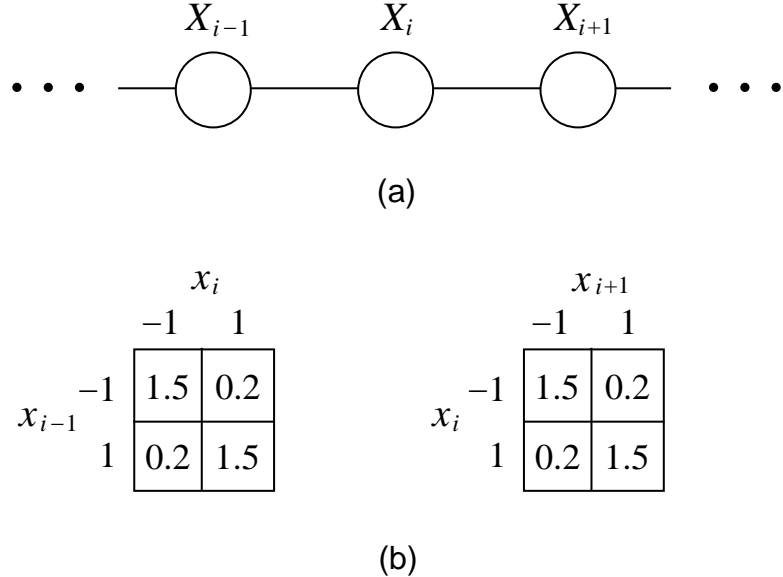


Figure 2.25: (a) A chain of binary random variables  $X_i$ , where  $X_i \in \{-1, 1\}$ . (b) A set of potential tables that encode a preference for neighboring variables to have the same values.

In general, potential functions are neither conditional probabilities nor marginal probabilities, and in this sense they do not have a local probabilistic interpretation. On the other hand, potential functions do often have a natural interpretation in terms of pre-probabilistic notions such as “agreement,” “constraint,” or “energy,” and such interpretations are often useful in choosing an undirected model to represent a real-life domain. The basic idea is that a potential function favors certain local configurations of variables by assigning them a larger value. The global configurations that have high probability are, roughly, those that satisfy as many of the favored local configurations as possible.

Consider a set of binary random variables,  $X_i \in \{-1, 1\}, i = 0, \dots, n$ , arrayed on a one-dimensional lattice as shown in Figure 2.25(a). In physics, such lattices are used to model magnetic behavior of crystals, where the binary variables have an interpretation as magnetic “spins.” All else being equal, if a given spin  $X_i$  is “up”; that is, if  $X_i = 1$ , then its neighbors  $X_{i-1}$  and  $X_{i+1}$  are likely to be “up” as well. We can easily encode this in a potential function, as shown in Figure 2.25(b). Thus, if two neighboring spins agree, that is, if  $X_i = 1$  and  $X_{i-1} = 1$ , or if  $X_i = -1$  and  $X_{i-1} = -1$ , we obtain a large value for the potential on the clique  $\{X_{i-1}, X_i\}$ . If the spins disagree we obtain a small value.

The fact that potentials must be nonnegative can be inconvenient, and it is common to exploit the fact that the exponential function,  $f(x) = \exp(x)$ , is a nonnegative function, to represent potentials in an unconstrained form. We let:

$$\psi_{X_C}(x_C) = \exp\{-H_C(x_C)\}, \quad (2.39)$$

for a real-valued function  $H_C(x_C)$ , where the negative sign is a standard convention. Thus if we

range over arbitrary  $H_C(x_C)$ , we can range over legal potentials.

The exponential representation has another useful feature. In particular, products of exponentials behave nicely, and from Eq. (2.35) we obtain:

$$p(x) = \frac{1}{Z} \prod_{C \in \mathcal{C}} \exp\{-H_C(x_C)\} \quad (2.40)$$

$$= \frac{1}{Z} \exp\left\{-\sum_{C \in \mathcal{C}} H_C(x_C)\right\} \quad (2.41)$$

as an equivalent representation of the joint probability for undirected models. The sum in the latter expression is generally referred to as the “energy”:

$$H(x) \triangleq \sum_{C \in \mathcal{C}} H_C(x_C) \quad (2.42)$$

and we have represented the joint probability of an undirected graphical model as a *Boltzmann distribution*:

$$p(x) = \frac{1}{Z} \exp\{-H(x)\}. \quad (2.43)$$

Without going too far astray into the origins of the Boltzmann representation in statistical physics, let us nonetheless note that the representation of a model in terms of energy, and in particular the representation of the total energy as a sum over local contributions to the energy, is exceedingly useful. Many physical theories are specified in terms of energy, and the Boltzmann distribution provides a translation from energies into probabilities.

Quite apart from any connection to physics, the undirected graphical model formalism is often quite useful in domains in which global constraints on probabilities are naturally decomposable into sets of local constraints, and the undirected representation is apt at capturing such situations.

### 2.2.3 Characterization of undirected graphical models

In Section 2.1.3 we discussed a theorem that shows that the two different characterizations of the family of probability distributions associated with a directed graphical model—one based on local conditional probabilities and the other based on conditional independence assertions—were the same. A formally identical theorem holds for undirected graphs.

For a given undirected graph  $\mathcal{G}$ , we define a family of probability distributions,  $\mathcal{U}_1$ , by ranging over all possible choices of positive potential functions on the maximal cliques of the graph.

We define a second family of probability distributions,  $\mathcal{U}_2$ , via the conditional independence assertions associated with  $\mathcal{G}$ . Concretely, we make a list of all of the conditional independence statements,  $X_A \perp\!\!\!\perp X_B | X_C$ , asserted by the graph, by assessing whether the subset of nodes  $X_A$  is separated from  $X_B$  when the nodes  $X_C$  are removed from the graph. A probability distribution is in  $\mathcal{U}_2$  if it satisfies all such conditional independence statements, otherwise it is not.

In Chapter 16 we state and prove a theorem, the Hammersley-Clifford theorem, that shows that  $\mathcal{U}_1$  and  $\mathcal{U}_2$  are identical. Thus the characterization of probability distributions in terms of potentials on cliques and conditional independence are equivalent. As in the directed case, this is an important and profound link between probability theory and graph theory.

## 2.3 Parameterizations

We have introduced two kinds of graphical model representations in this chapter—directed graphical models and undirected graphical models. In each of these cases we have defined conditional independence semantics and corresponding parameterizations. Thus, in the directed case, we have:

$$p(x) \triangleq \prod_{i=1}^n p(x_i | x_{\pi_i}), \quad (2.44)$$

and in the undirected case, we have:

$$p(x) \triangleq \frac{1}{Z} \prod_{C \in \mathcal{C}} \psi_{X_C}(x_C). \quad (2.45)$$

By ranging over all possible conditional probabilities in Eq. (2.44) or all possible potential functions in Eq. (2.45) we obtain certain families of probability distributions, in particular exactly those distributions which respect the conditional independence statements associated with a given graph.

Conditional independence is an exceedingly useful constraint to impose on a joint probability distribution. In practical settings conditional independence can sometimes be assessed by domain experts, and in such cases it provides a powerful way to embed qualitative knowledge about the relationships among random variables into a model. Moreover, as we will discuss in the following chapter, the relationship between conditional independence and factorization allows the development of powerful general inference algorithms that use graph-theoretic ideas to compute marginal probabilities of interest. We often impose conditional independence as a rough, tentative assumption in a domain so as to be able to exploit the efficient inference algorithms and begin to learn something about the domain.

On the other hand, conditional independence is by no means the only kind of constraint that one can impose on a probabilistic model. Another large class of constraints arise from assumptions about the algebraic structure of the conditional probabilities or potential functions that define a model. In particular, rather than ranging over all possible conditional probabilities or potential functions, we may wish to range over a proper subset of these functions, thus defining a proper subset of the family of probability distributions associated with a graph. Thus, in practice we often work with *reduced parameterizations* that impose constraints on probability distributions beyond the structural constraints imposed by conditional independence.

We will present many examples of reduced parameterizations in later chapters. Let us briefly consider two such examples in the remainder of this section to obtain a basic appreciation of some of the issues that arise.

Directed graphical models require conditional probabilities, and if the number of parents of a given node is large, then the specification of the conditional probability can be problematic. Consider in particular the graph shown in Figure 2.26(a), where all of the variables are assumed binary (for simplicity), and where the number of parents of  $Y$  is assumed large. In particular, if  $Y$  has 50 parents, then ranging over “all possible conditional probabilities” means specifying  $2^{50}$  numbers, one probability for each configuration of the parents. Clearly such a specification cannot

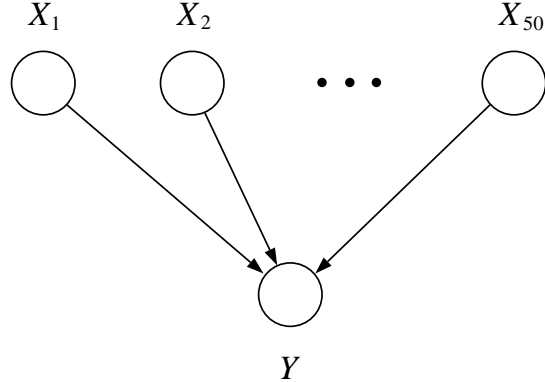


Figure 2.26: An example in which a node has many parents. In such a graph, a general specification of the local conditional probability distribution requires an impractically large number of parameters.

be stored on a computer, and, equally problematically, it would be impossible to collect enough data to be able to estimate these numbers with any degree of precision. We are forced to consider “reduced parameterizations.” One such parameterization, discussed in detail in Chapter 8, is the following:

$$p(Y = 1 | x) = f(\theta_1 x_1 + \theta_2 x_2 + \cdots + \theta_m x_m), \quad (2.46)$$

for a given function  $f(\cdot)$  whose range is the interval  $(0, 1)$  (we will provide examples of such functions in Chapter 8). Here, we need only specify the 50 numbers  $\theta_i$  to specify a distribution.

In general, we can consider directed graphical models in which each node is parameterized as shown in Eq. (2.46). The family of probability distributions associated with the model as a whole is that obtained by ranging over all possible values of  $\theta_i$  in the defining conditional probabilities. This is a proper sub-family of the family of distributions associated with the graph.

If practical considerations often force us to work with reduced parameterizations, of what value is the general definition of “the family of distributions associated with a graph”? As we will see in Chapter 4 and Chapter 17, given a graph, efficient probabilistic inference algorithms can be defined that operate on the graph. These algorithms are based solely on the graph structure and are correct for any distribution that respects the conditional independencies encoded by the graph. Thus such algorithms are correct for any distribution in the family of distributions associated with a graph, including those in any proper sub-family associated with a reduced parameterization.

Similar issues arise in undirected models. Consider in particular the graph shown in Figure 2.27(a). From the point of view of independence, there is little to say—there are no independence assertions associated with this graph. Equivalently, the family of probability distributions associated with the graph is the set of all possible probability distributions on the three variables, obtained by ranging over all possible potential functions  $\psi(x_1, x_2, x_3)$ . Suppose, however, that we are interested in models in which the potential function is defined algebraically as a product of

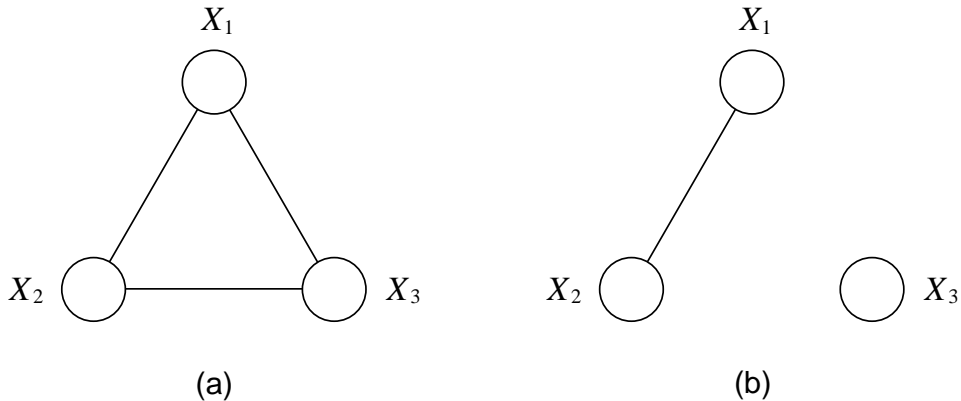


Figure 2.27: (a) An undirected graph which makes no independence assertions. (b) An undirected graph which asserts  $X_3 \perp\!\!\!\perp \{X_1, X_2\}$ .

factors on smaller subsets of variables. Thus, we might let:

$$\psi(x_1, x_2, x_3) = f(x_1, x_2)g(x_3), \quad (2.47)$$

or let:

$$\psi(x_1, x_2, x_3) = r(x_1, x_2)s(x_2, x_3)t(x_1, x_3), \quad (2.48)$$

for given functions  $f$ ,  $g$ ,  $r$ ,  $s$  and  $t$ . Ranging over all possible choices of these functions, we obtain potentials that are necessarily members of the family associated with the graph in Figure 2.27(a)—because all such potentials respect the (vacuous) conditional independence requirement. The potential in Eq. (2.47), however, also respects the (non-vacuous) conditional independence requirement of the graph in Figure 2.27(b). We would normally use this latter graph if we decide (a priori) to restrict our parameterization to the form given in Eq. (2.47). On the other hand, the potential given in Eq. (2.48) is problematic in this regard—there is no smaller graph that represents this class of potentials. Any graph with a missing edge makes an independence assertion regarding one or more pairs of variables, and  $\psi(x_1, x_2, x_3) = r(x_1, x_2)s(x_2, x_3)t(x_1, x_3)$  does not respect such an assertion, when we range over all functions  $r$ ,  $s$  and  $t$ .

Thus we see that “factorization” is a richer concept than “conditional independence.” There are families of probability distributions that can be defined in terms of certain factorizations of the joint probability that cannot be captured solely within the undirected or directed graphical model formalism. From the point of view of designing inference algorithms, this might not be viewed as a problem, because an algorithm that is correct for the graph is correct for a distribution in any sub-family defined on the graph. However, by ignoring the algebraic structure of the potential, we may be missing opportunities for simplifying the algebraic operations of inference.

In Chapter 4 we introduce *factor graphs*, a graphical representation of probability distributions in which such reduced parameterizations are made explicit. Factor graphs allow a more fine-grained representation of probability distributions than is provided by either the directed or the undirected graphical formalism, and in particular allow the factorization of the potential in Eq. (2.48) to be

represented explicitly in the graph. While factor graphs provide nothing new in terms of representing and exploiting conditional independence relationships—the main theme of the current chapter—they do provide a way to represent and exploit algebraic relationships, an issue that will return in Chapter 4.

## 2.4 Summary

In this chapter we have presented some of the basic definitions and basic issues that arise when one associates probability distributions with graphs. A key idea that we have emphasized is that a graphical model is a representation of a *family* of probability distributions. This family is characterized in one of two equivalent ways—either in terms of a numerical parameterization or in terms of a set of conditional independencies. Both of these characterizations are important and useful, and it is the interplay between these characterizations that gives the graphical models formalism much of its distinctive flavor.

Directed graphs and undirected graphs have different parameterizations and different conditional independence semantics, but the key concept of using graph theory to capture the notion of a joint probability distribution being constructed from a set of “local” pieces is the same in the two cases.

We have also introduced simple algorithms that help make the problem of understanding conditional independence in graphical models more concrete. The reader should be able to utilize the Bayes ball algorithm to read off conditional independence statements from directed graphs. Similarly, for undirected graphs the reader should understand that naive graph separation encodes conditional independence. Conditional independence assertions in undirected graphs can be assessed via a graph reachability algorithm.

## 2.5 Historical remarks and bibliography

# An Introduction to Probabilistic Graphical Models

Michael I. Jordan  
*University of California, Berkeley*

June 30, 2003



## Chapter 3

# The Elimination Algorithm

In this chapter we discuss the problem of computing conditional and marginal probabilities in graphical models—the problem of *probabilistic inference*. Building on the ideas in Chapter 2, we show how the conditional independencies encoded in a graph can be exploited for efficient computation of conditional and marginal probabilities.

We take a very concrete approach in the current chapter, basing the presentation on a simple “elimination algorithm” for probabilistic inference. This algorithm applies equally well to directed and undirected graphs. It requires little formal machinery to describe and to analyze. On the other hand, the algorithm has its limitations, and is not our final word on the inference problem. But it is a good place to start.

### 3.1 Probabilistic inference

Let  $E$  and  $F$  be disjoint subsets of the node indices of a graphical model, such that  $X_E$  and  $X_F$  are disjoint subsets of the random variables in the domain. Our goal is to calculate  $p(x_F | x_E)$  for arbitrary subsets  $E$  and  $F$ . This is the general *probabilistic inference problem* for graphical models (directed or undirected).

We begin by focusing on directed graphs. Almost all of our work, however, will transfer to undirected graphs with little or no change. Our subsequent treatment of undirected models in Section 3.1.3 will be short and sweet.

Throughout the chapter we limit ourselves to the probability of calculating the conditional probability of a single node  $X_F$ —which we refer to as the “query node”—given an arbitrary set of nodes  $X_E$ . This is a limitation of the simple elimination algorithm that we discuss in this chapter, and is not a limitation of the more general algorithms that we discuss in later chapters.

Graphically we indicate the set of conditioning variables by shading the corresponding nodes in the graph. Thus, the dark shading in Figure 3.1 indicates the nodes (indexed by  $E$ ) on which we condition. We will often refer to these nodes as the *evidence nodes*. The unshaded nodes (indexed by  $F$ ) are the nodes for which we wish to compute conditional probabilities. Finally, the lightly shaded nodes, indexed by  $R = V \setminus (E \cup F)$ , are the nodes that must be marginalized out of the joint probability so that we can focus on the conditional,  $p(x_F | x_E)$ , of interest. Thus, symbolically, we

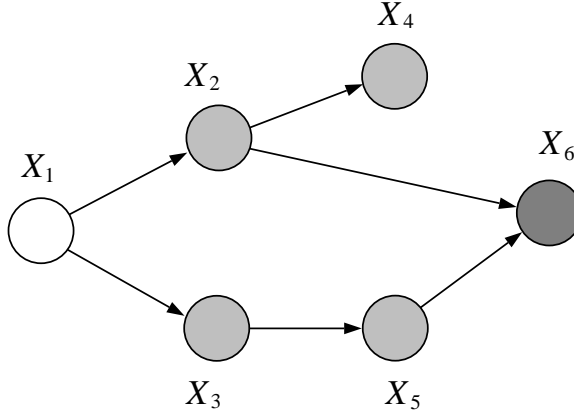


Figure 3.1: The dark shaded node,  $X_6$ , is the node on which we condition, the lightly shaded nodes,  $\{X_2, X_3, X_4, X_5\}$ , are nodes that are marginalized over, and the unshaded node,  $X_1$  is the node for which we wish to calculate conditional probabilities. Thus, for this example, we have  $E = \{6\}$ ,  $F = \{1\}$ , and  $R = \{2, 3, 4, 5\}$ .

must compute the marginal:

$$p(x_E, x_F) = \sum_{x_R} p(x_E, x_F, x_R), \quad (3.1)$$

which can be further marginalized to yield  $p(E)$ :

$$p(x_E) = \sum_{x_F} p(x_E, x_F), \quad (3.2)$$

from which we obtain the conditional probability:

$$p(x_F | x_E) = \frac{p(x_E, x_F)}{p(x_E)}. \quad (3.3)$$

We will be interested in finding effective computational methods for making these calculations.

A special case of the general problem is worth noting. Consider the case of just two nodes,  $X$  and  $Y$ , as shown in Figure 3.2(a). This model is specified in terms of the distributions  $p(x)$  and  $p(y|x)$ , reflecting the arrow from  $X$  to  $Y$ . Suppose that we condition on  $X$ , as shown in Figure 3.2(b), and wish to calculate the probability of  $Y$ . This “calculation” is simply a table lookup using  $p(y|x)$ . On the other hand, suppose that we condition on  $Y$  and wish to calculate the probability of  $X$ , as indicated in Figure 3.2(c). This is achieved via an application of Bayes rule:

$$p(x|y) = \frac{p(y|x)p(x)}{p(y)}. \quad (3.4)$$

where the denominator is calculated as follows:

$$p(y) = \sum_x p(y|x)p(x). \quad (3.5)$$

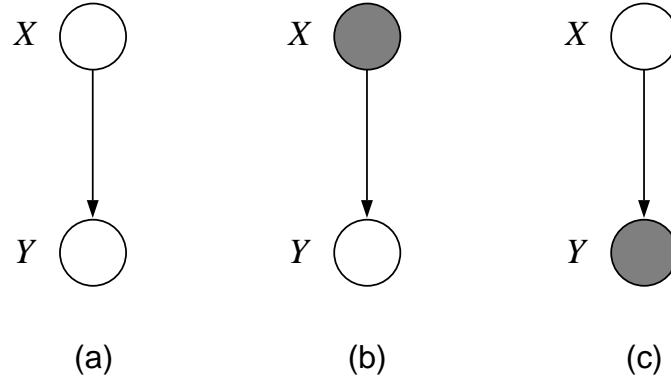


Figure 3.2: (a) A two-node model. (b) Conditioning on  $X$  involves a simple evaluation of  $p(y|x)$ . (c) Conditioning on  $Y$  requires the use of Bayes rule.

Can we find an efficient extension of these familiar ideas to general graphs?

The summations in Eq. (3.1) and Eq. (3.2) should give us pause. The summation  $\sum_{x_R}$  expands into a sequence of summations, one for each of the random variables indexed by  $R$ . If each such random variable can take on  $k$  values, and there are  $|R|$  variables, we obtain  $k^{|R|}$  terms in our summation. A similar statement applies to the summation  $\sum_{x_F}$ . With  $|F|$  and  $|R|$  in the dozens or hundreds in typical cases, naive summation is infeasible.

We need to take advantage of the factorization offered by the definition of the joint probability. If we do not take advantage of the factorization we will be in trouble performing even a single summation, much less a sequence of summations. Consider summing  $p(x_1, x_2, \dots, x_6)$  with respect to  $x_6$ , where we naively represent the joint probability as a table of size  $k^6$ . (Recall that  $k$  is the number of values that each variable  $x_i$  can take on, assumed independent of  $i$  for simplicity.) Given that we must perform the sum for each value of the variables  $\{x_1, x_2, \dots, x_5\}$ , we see that we must perform  $O(k^6)$  operations to do a single sum (essentially, we must touch each entry in the table). To reduce the computational complexity let us instead represent the joint probability in its factored form (cf. Eq. (2.3)) and exploit the distributive law:

$$p(x_1, x_2, \dots, x_5) = \sum_{x_6} p(x_1)p(x_2|x_1)p(x_3|x_1)p(x_4|x_2)p(x_5|x_3)p(x_6|x_2, x_5) \quad (3.6)$$

$$= p(x_1)p(x_2|x_1)p(x_3|x_1)p(x_4|x_2)p(x_5|x_3)\sum_{x_6} p(x_6|x_2, x_5). \quad (3.7)$$

The summation over  $x_6$  is now applied to  $p(x_6|x_2, x_5)$ , a table of size  $k^3$ . We have reduced the operation count from  $O(k^6)$  to  $O(k^3)$ , a significant improvement.<sup>1</sup>

Successive summations also take advantage of the factorization. A summation over, say,  $x_5$ , can also be moved along the chain of factors until it encounters a factor involving  $x_5$ . If each such summation is of reduced complexity, say  $O(k^r)$  for some  $r$ , then the result is an algorithm that

---

<sup>1</sup>Of course this sum is unity by the definition of conditional probability, and thus we don't actually have to perform any operations at all, but let us pretend not to know that.

scales as  $O(nk^r)$  instead of  $O(k^n)$ . Of course, the summations create intermediate factors that may link variables, making it not entirely clear whether or not we can keep  $r$  small. It is here that graphical methods are helpful. We can determine the parameter  $r$  by a graph-theoretic algorithm.

Let us introduce the basic ideas in the context of an example. Referring to the graph in Figure 3.1, let us condition on the event  $\{X_6 = x_6\}$  and calculate the conditional probability  $p(x_1 | x_6)$ .

A point to note at the outset is that  $x_6$  is a fixed constant in this calculation and does not contribute to the computational complexity of the calculation. Thus, while the table representing  $p(x_6 | x_2, x_5)$  is nominally a three-dimensional table, the observation of  $X_6$  involves taking a two-dimensional slice of this table. Unfortunately our notation is ambiguous in this regard; we have been using “ $x_6$ ” as a variable that ranges over the possible values of  $X_6$ . In particular it is meaningful to sum over “ $x_6$ .” In the remainder of this section, to avoid confusion, we refer to a particular fixed value of  $X_6$  as “ $\bar{x}_6$ .” Thus, we wish to compute  $p(x_1 | \bar{x}_6)$ , for any  $x_1$  and for a particular  $\bar{x}_6$ .

We begin by computing the probability  $p(x_1, \bar{x}_6)$  by summing over  $\{x_2, x_3, x_4, x_5\}$ . We introduce some notation to refer to intermediate factors that arise when performing these sums. In particular, let  $m_i(x_{S_i})$  denote the expression that arises from performing the sum  $\sum_{x_i}$ , where  $x_{S_i}$  are the variables, other than  $x_i$ , that appear in the summand. Thus we have:

$$p(x_1, \bar{x}_6) = \sum_{x_2} \sum_{x_3} \sum_{x_4} \sum_{x_5} p(x_1) p(x_2 | x_1) p(x_3 | x_1) p(x_4 | x_2) p(x_5 | x_3) p(\bar{x}_6 | x_2, x_5) \quad (3.8)$$

$$= p(x_1) \sum_{x_2} p(x_2 | x_1) \sum_{x_3} p(x_3 | x_1) \sum_{x_4} p(x_4 | x_2) \sum_{x_5} p(x_5 | x_3) p(\bar{x}_6 | x_2, x_5) \quad (3.9)$$

$$= p(x_1) \sum_{x_2} p(x_2 | x_1) \sum_{x_3} p(x_3 | x_1) \sum_{x_4} p(x_4 | x_2) m_5(x_2, x_3) \quad (3.10)$$

where we define  $m_5(x_2, x_3) \triangleq \sum_{x_5} p(x_5 | x_3) p(\bar{x}_6 | x_2, x_5)$ . (Note that to simplify notation we do not indicate explicitly the dependence of this term on the constant  $\bar{x}_6$ ). Computing  $m_5(x_2, x_3)$  has eliminated  $X_5$  from further consideration in the computation. As we will see later, this algebraic notion of “elimination” corresponds to a graphical notion of elimination in which the node  $X_5$  is removed from the graph. We continue the derivation:

$$p(x_1, \bar{x}_6) = p(x_1) \sum_{x_2} p(x_2 | x_1) \sum_{x_3} p(x_3 | x_1) m_5(x_2, x_3) \sum_{x_4} p(x_4 | x_2) \quad (3.11)$$

$$= p(x_1) \sum_{x_2} p(x_2 | x_1) m_4(x_2) \sum_{x_3} p(x_3 | x_1) m_5(x_2, x_3). \quad (3.12)$$

Of course,  $m_4(x_2) \triangleq \sum_{x_4} p(x_4 | x_2)$  is equal to one by definition, and in practice we would not do this sum, but let us be systematic and keep the term in our calculations. Finally, we have:

$$p(x_1, \bar{x}_6) = p(x_1) \sum_{x_2} p(x_2 | x_1) m_4(x_2) m_3(x_1, x_2) \quad (3.13)$$

$$= p(x_1) m_2(x_1). \quad (3.14)$$

From this result we can also obtain the probability  $p(\bar{x}_6)$  by taking an additional sum over  $x_1$ :

$$p(\bar{x}_6) = \sum_{x_1} p(x_1)m_2(x_1), \quad (3.15)$$

and the desired conditional is obtained by dividing Eq. (3.14) into Eq. (3.15):

$$p(x_1 | \bar{x}_6) = \frac{p(x_1)m_2(x_1)}{\sum_{x_1} p(x_1)m_2(x_1)}. \quad (3.16)$$

Alternatively we can view  $p(x_1, \bar{x}_6)$  in Eq. (3.14) as an unnormalized representation of the conditional probability  $p(x_1 | \bar{x}_6)$ —recall once again that  $\bar{x}_6$  is a fixed constant. Thus we obtain the conditional by normalization, where the normalization constant is given by Eq. (3.15).

Lying behind this flurry of algebra is a simple general algorithm for computing marginal probabilities. We present this algorithm in Section 3.1.2. First, however, we set the stage for the general algorithm with some preparatory remarks on conditioning.

### 3.1.1 Conditioning

To provide a simple exposition of the general elimination algorithm in Section 3.1.2, and also to simplify our exposition of inference algorithms presented in later chapters, it is useful to make use of a notational trick in which conditioning is viewed as a summation. This trick will allow us to treat marginalization and conditioning as formally equivalent, and will make it easier to bring the key operations of the inference algorithms into focus.

Let  $X_i$  be an evidence node whose observed value is  $\bar{x}_i$ . To capture the fact that  $X_i$  is fixed at the value  $\bar{x}_i$ , we define an *evidence potential*,  $\delta(x_i, \bar{x}_i)$ , a function whose value is one if  $x_i = \bar{x}_i$  and zero otherwise. The evidence potential allows us to turn evaluations into sums: To evaluate a function  $g(x_i)$  at  $\bar{x}_i$  we multiply  $g(x_i)$  by  $\delta(x_i, \bar{x}_i)$  and sum over  $x_i$ :

$$g(\bar{x}_i) = \sum_{x_i} g(x_i)\delta(x_i, \bar{x}_i), \quad (3.17)$$

a trick that also extends to multivariate functions with  $x_i$  as one of the arguments. In particular, returning to the example from the previous section, we can express the evaluation of  $p(x_6 | x_2, x_5)$  at  $\bar{x}_6$  as follows:

$$m_6(x_2, x_5) = \sum_{x_6} p(x_6 | x_2, x_5)\delta(x_6, \bar{x}_6), \quad (3.18)$$

where  $m_6(x_2, x_5)$  is nothing but  $p(\bar{x}_6 | x_2, x_5)$ .

In general, let  $E$  be the set of nodes whose values are to be conditioned on. That is, for a specific configuration  $\bar{x}_E$ , we wish to compute  $p(x_F | \bar{x}_E)$ . Formally, we achieve this as follows. Define the *total evidence potential*:

$$\delta(x_E, \bar{x}_E) \triangleq \prod_{i \in E} \delta(x_i, \bar{x}_i), \quad (3.19)$$

a function that is equal to one if  $x_E = \bar{x}_E$  and is equal to zero otherwise. Using this potential, we can obtain both the numerator and the denominator of the conditional probability  $p(x_F | \bar{x}_E)$  by summation. Thus:

$$p(x_F, \bar{x}_E) = \sum_{x_E} p(x_F, x_E) \delta(x_E, \bar{x}_E) \quad (3.20)$$

and:

$$p(\bar{x}_E) = \sum_{x_F} \sum_{x_E} p(x_F, x_E) \delta(x_E, \bar{x}_E). \quad (3.21)$$

This suggests that it may be useful to define:

$$p^E(x) \triangleq p(x) \delta(x_E, \bar{x}_E) \quad (3.22)$$

as a generalized measure that represents conditional probability with respect to  $E$ . By formally “marginalizing” this measure with respect to  $x_E$ , we evaluate  $p(x)$  at  $X_E = \bar{x}_E$ , and obtain  $p(x_F, \bar{x}_E)$ , an unnormalized version of the conditional probability  $p(x_F | \bar{x}_E)$ . Moreover, by marginalizing over  $x$ , we obtain the total “mass”  $p(\bar{x}_E)$ .

This tactic is particularly natural in the case of undirected graphs, where multiplication by an evidence potential  $\delta(x_i, \bar{x}_i)$  can be implemented by simply redefining the local potentials  $\psi(x_i)$  for  $i \in E$ . Thus, we define:

$$\psi_i^E(x_i) \triangleq \psi_i(x_i) \delta(x_i, \bar{x}_i), \quad (3.23)$$

for  $i \in E$ . Leaving all other clique potentials unchanged, that is, letting  $\psi_C^E(x_C) \triangleq \psi_C(x_C)$ , for  $C \notin \{\{i\} : i \in E\}$ , we obtain the desired unnormalized representation:

$$p^E(x) \triangleq \frac{1}{Z} \prod_{C \in \mathcal{C}} \psi_{X_C}^E(x_C). \quad (3.24)$$

Moreover, since we are working with an unnormalized representation, we may as well drop the  $1/Z$  factor, and simply work with  $\prod_{C \in \mathcal{C}} \psi_{X_C}^E(x_C)$  as an unnormalized representation of conditional probability.

It should be clear that the use of evidence potentials is merely a piece of formal trickery that will (turn out to) simplify our description of various inference algorithms. In practice we would not actually perform the sum over a function that we know to be zero over most of the sample space, but rather we would take “slices” of the appropriate probabilities or potentials. Thus, in evaluating  $p(x_6 | x_2, x_5)$  at  $X_6 = \bar{x}_6$ , while formally we can view ourselves as multiplying by  $\delta(x_6, \bar{x}_6)$  and summing over  $x_6$ , algorithmically we would simply take the appropriate two-dimensional slice of the three-dimensional table representing  $p(x_6 | x_2, x_5)$ .

### 3.1.2 Elimination and directed graphs

In this section we describe a general algorithm for performing probabilistic inference in directed graphical models.

At each step of the algorithm, we perform a sum over a product of functions. The functions that can appear in such sums include the original local conditional probabilities,  $p(x_i | x_{\pi_i})$ , the

evidence potentials,  $\delta(x_i, \bar{x}_i)$ , and the intermediate factors,  $m_i(x_{S_i})$ , generated by previous sums. All of these functions are defined on local subsets of nodes, and we use the generic term “potential” to refer to all of them.<sup>2</sup> Thus our algorithm will involve taking sums over products of potential functions.

The algorithm works as follows (see Figure 3.3 for a summary). Given a graph  $\mathcal{G} = (\mathcal{V}, \mathcal{E})$ , an evidence set  $E$ , and a query node  $F$ , we first choose an elimination ordering  $I$  such that  $F$  appears last in the ordering.<sup>3</sup> Throughout the algorithm we maintain an *active list* of potential functions. The active list is initialized to hold the local conditional probabilities,  $p(x_i | x_{\pi_i})$ , for  $i \in \mathcal{V}$ , and the evidence potentials,  $\delta(x_i, \bar{x}_i)$ , for  $i \in E$ . At each step of the algorithm, we find all those potentials on the active list that reference the next node (call it  $X_i$ ) in the elimination ordering  $I$ . These potential functions are removed from the active list. We take the product of these functions and sum this product with respect to  $x_i$ . This defines a new intermediate factor,  $m_i(x_{S_i})$ , where  $x_{S_i}$  are the variables (other than  $x_i$ ) that appear in the summand. This intermediate factor is added to the active list. We then proceed to the next node in the elimination ordering.

Note that we have introduced the notation  $T_i = \{i\} \cup S_i$  in the description of the algorithm in Figure 3.3. The subset  $T_i$  indexes the set of all variables that appear in the summand of the operator  $\sum_{x_i}$ . We give a graph-theoretic interpretation of  $T_i$  later in the chapter.

The algorithm terminates when we arrive at the final node in the elimination ordering, the query node  $X_F$ . The product of potentials on the active list at this point defines the (unnormalized) conditional probability,  $p(x_F, \bar{x}_E)$ . Summing this product over  $x_F$  yields the normalization factor  $p(\bar{x}_E)$ .

Let us now return to the example in Section 3.1 and show how the steps of ELIMINATE correspond to the steps in the algebraic calculation in that section. The evidence node in this example is  $X_6$  and the query node is  $X_1$ . We choose the elimination ordering  $I = (6, 5, 4, 3, 2, 1)$ , in which the query node appears last.

We begin by placing the local conditional probabilities,  $\{p(x_1), \dots, p(x_6 | x_2, x_5)\}$ , on the active list. We also place  $\delta(x_6, \bar{x}_6)$  on the active list.

We first eliminate node  $X_6$ . The potential functions on the active list that reference  $x_6$  are  $p(x_6 | x_2, x_5)$  and  $\delta(x_6, \bar{x}_6)$ . Thus we have  $\phi_6(x_2, x_5, x_6) = p(x_6 | x_2, x_5)\delta(x_6, \bar{x}_6)$ . Summing this expression with respect to  $x_6$  yields  $m_6(x_2, x_5) = p(\bar{x}_6 | x_2, x_5)$ . We place this potential on the active list, having removed  $p(x_6 | x_2, x_5)$  and  $\delta(x_6, \bar{x}_6)$ . We have simply evaluated  $p(x_6 | x_2, x_5)$  at  $\bar{x}_6$ .

We now eliminate  $X_5$ . The potentials on the active list that reference  $x_5$  are  $p(x_5 | x_3)$

---

<sup>2</sup>The reader may be concerned that we are using the term “potential” somewhat loosely here. In particular we are using it in the context of directed graphs and in the context of subsets that may not be cliques; this usage clashes with the definition of “potential” in Chapter ???. We hope that the reader will forgive the seeming abuse of terminology. It is worth noting, however, that the “potentials” discussed in this section are in fact honest-to-goodness potentials, but not with respect to  $G$ . Rather they are potentials on the cliques of a different graph, a graph known as the *moral graph*  $G^m$ . This point will be clarified in Section ?? below.

<sup>3</sup>We will not discuss the choice of elimination ordering in this chapter, but instead will defer this (non-trivial) problem until Chapter 17, where it will arise in a more general way in the context of the junction tree algorithm. For now, let the ordering  $I$  be arbitrary, under the constraint that  $F$  appears last. We might encourage the reader, however, to start to ponder how to characterize good elimination orderings. Some useful food for thought in this regard will be provided in Section ?? below.

```

ELIMINATE( $\mathcal{G}, E, F$ )
  INITIALIZE( $\mathcal{G}, F$ )
  EVIDENCE( $E$ )
  UPDATE( $\mathcal{G}$ )
  NORMALIZE( $F$ )

INITIALIZE( $\mathcal{G}, F$ )
  choose an ordering  $I$  such that  $F$  appears last
  for each node  $X_i$  in  $\mathcal{V}$ 
    place  $p(x_i | x_{\pi_i})$  on the active list
  end

EVIDENCE( $E$ )
  for each  $i$  in  $E$ 
    place  $\delta(x_i, \bar{x}_i)$  on the active list
  end

UPDATE( $\mathcal{G}$ )
  for each  $i$  in  $I$ 
    find all potentials from the active list that reference  $x_i$  and remove them from the active list
    let  $\phi_i(x_{T_i})$  denote the product of these potentials
    let  $m_i(x_{S_i}) = \sum_{x_i} \phi_i(x_{T_i})$ 
    place  $m_i(x_{S_i})$  on the active list
  end

NORMALIZE( $F$ )
   $p(x_F | \bar{x}_E) \leftarrow \phi_F(x_F) / \sum_{x_F} \phi_F(x_F)$ 

```

Figure 3.3: The ELIMINATE algorithm for probabilistic inference on directed graphs.

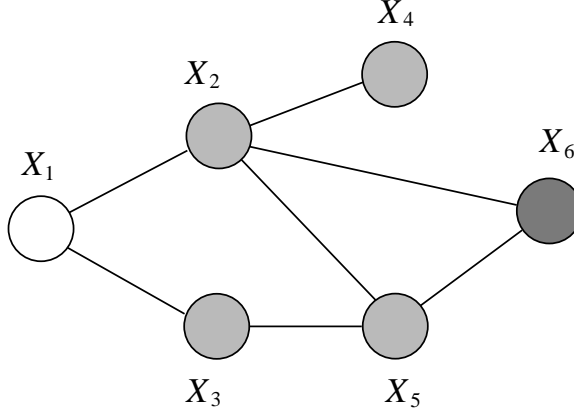


Figure 3.4: The dark shaded node,  $X_6$ , is the node on which we condition, the lightly shaded nodes,  $\{X_2, X_3, X_4, X_5\}$ , are the nodes that are marginalized over, and the unshaded node,  $X_1$ , is the node for which we wish to calculate conditional probabilities.

and  $m_6(x_2, x_5)$ . We remove them, and define the product  $\phi_5(x_2, x_3, x_5)$ . Summing over  $x_5$  yields  $m_5(x_2, x_3)$  (cf. Eq. (3.11)).

The only potential that references  $X_4$  is  $p(x_4 | x_2)$ . The elimination of  $X_4$  thus involves summing  $p(x_4 | x_2)$  with respect to  $x_4$  to obtain the factor  $m_4(x_2)$ . This factor is identically one and in practice we would not bother computing it.

Eliminating  $X_3$  involves taking the sum over  $\phi_3(x_1, x_2, x_3) = p(x_3 | x_1)m_5(x_2, x_3)$  to yield  $m_3(x_1, x_2)$  and we are now at Eq. (3.13) in the earlier derivation.

We now eliminate  $X_2$  to obtain  $\phi_1(x_1) = p(x_1)m_2(x_1)$ , which is the “unnormalized conditional probability,”  $p(x_1, \bar{x}_6)$ . Eliminating  $X_1$  yields  $m_1 = \sum_{x_1} \phi_1(x_1)$ , which is the normalization factor,  $p(\bar{x}_6)$ .

### 3.1.3 Elimination and undirected graphs

In the case of directed models, we have shown that the problem of calculating conditional probabilities can be usefully viewed in terms of a simple elimination algorithm. The same perspective applies to undirected models, and indeed the entire ELIMINATE algorithm from Figure 3.3 goes through without essential change to the undirected case.

The only change needed to handle the undirected case occurs in the INITIALIZE procedure, where instead of using local conditional probabilities we initialize the active list to contain the potentials  $\{\psi_{X_C}(x_C)\}$ .

Let us briefly consider an example. Paralleling the example from Section 3.1.2 we calculate the probability  $p(x_1 | \bar{x}_6)$  for the graph in Figure 3.4. We represent the joint probability on the graph via potential functions on the cliques  $\{X_1, X_2\}$ ,  $\{X_1, X_3\}$ ,  $\{X_2, X_4\}$ ,  $\{X_3, X_5\}$ , and  $\{X_2, X_5, X_6\}$ .

We first calculate the probability  $p(x_1, \bar{x}_6)$ . To simplify the presentation we drop the subscript in the  $\psi_{X_C}(x_C)$  notation, relying on the argument to the function to make it clear which potential function is being referred to. Also we again make use of the notation  $m_i(x_{S_i})$  to denote the

intermediate factor that results from the summation over  $x_i$ . We have:

$$\begin{aligned}
p(x_1, \bar{x}_6) &= \frac{1}{Z} \sum_{x_2} \sum_{x_3} \sum_{x_4} \sum_{x_5} \sum_{x_6} \psi(x_1, x_2) \psi(x_1, x_3) \psi(x_2, x_4) \psi(x_3, x_5) \psi(x_2, x_5, x_6) \delta(x_6, \bar{x}_6) \\
&= \frac{1}{Z} \sum_{x_2} \psi(x_1, x_2) \sum_{x_3} \psi(x_1, x_3) \sum_{x_4} \psi(x_2, x_4) \sum_{x_5} \psi(x_3, x_5) \sum_{x_6} \psi(x_2, x_5, x_6) \delta(x_6, \bar{x}_6) \\
&= \frac{1}{Z} \sum_{x_2} \psi(x_1, x_2) \sum_{x_3} \psi(x_1, x_3) \sum_{x_4} \psi(x_2, x_4) \sum_{x_5} \psi(x_3, x_5) m_6(x_2, x_5) \\
&= \frac{1}{Z} \sum_{x_2} \psi(x_1, x_2) \sum_{x_3} \psi(x_1, x_3) m_5(x_2, x_3) \sum_{x_4} \psi(x_2, x_4) \\
&= \frac{1}{Z} \sum_{x_2} \psi(x_1, x_2) m_4(x_2) \sum_{x_3} \psi(x_1, x_3) m_5(x_2, x_3) \\
&= \frac{1}{Z} \sum_{x_2} \psi(x_1, x_2) m_4(x_2) m_3(x_1, x_2) \\
&= \frac{1}{Z} m_2(x_1).
\end{aligned} \tag{3.25}$$

Marginalizing further over  $x_1$  yields:

$$p(\bar{x}_6) = \frac{1}{Z} \sum_{x_1} m_2(x_1), \tag{3.26}$$

and we calculate the desired conditional as:

$$p(x_1 | \bar{x}_6) = \frac{m_2(x_1)}{\sum_{x_1} m_2(x_1)}, \tag{3.27}$$

where the normalization factor  $Z$  cancels.

Note that the calculation in the example is formally identical to the corresponding calculation for directed graphs. Note, however, that the sum  $m_4(x_2)$ , which earlier could be omitted, no longer necessarily sums to one and must be explicitly carried along in the calculation.

Finally, a remark on the computation of marginal probabilities  $p(x_i)$ . For a marginal probability the normalization factor  $Z$  does not cancel, and must be calculated explicitly. Just as in the other calculations in this section, however, the calculation of  $Z$  is a summation over the unnormalized representation of the joint probability, and indeed it is simply a summation over *all* of the variables. To obtain the marginal  $p(x_i)$ , we would define an elimination ordering in which  $x_i$  is the final variable, and then normalize the result to calculate  $Z$  and obtain the marginal.

In the directed case, a variable that is parentless has its marginal represented explicitly in the parameterization of the graphical model and no calculation is needed. In general, nodes that are downstream from a target node can simply be deleted, and marginalization involves an inference calculation involving the ancestors of the node. The worst case is a leaf node. In the undirected case, there is no notion of “ancestor,” and essentially all nodes are worst case. On the other hand, once  $Z$  is calculated from a particular elimination ordering, it can be used to normalize other marginal probabilities.

```

UNDIRECTEDGRAPHELIMINATE( $\mathcal{G}, I$ )
  for each node  $X_i$  in  $I$ 
    connect all of the remaining neighbors of  $X_i$ 
    remove  $X_i$  from the graph
  end

```

Figure 3.5: A simple greedy algorithm for eliminating nodes in an undirected graph  $\mathcal{G}$ .

## 3.2 Graph elimination

The simple ELIMINATE algorithm captures the key algorithmic operation underlying probabilistic inference—that of taking a sum over a product of potential functions. What can we say about the overall computational complexity of the algorithm? In particular, how can we control the “size” of the summands that appear in the sequence of summation operations?

In this section, we show that questions regarding the computational complexity of the ELIMINATE algorithm can be reduced to purely graph-theoretic considerations. This graphical interpretation will also provide hints about how to design improved inference algorithms that overcome the limitations of ELIMINATE.

### 3.2.1 A graph elimination algorithm

Let us put aside marginalization and probabilistic inference for a moment, and concentrate solely on graph-theoretic manipulations. We describe a simple procedure that eliminates nodes in a graph. As will become clear, this procedure captures the graph-theoretic operations underlying ELIMINATE.

We begin by describing a node-elimination algorithm for undirected graphs, making the link to directed graphs shortly.

Assume that we are given an undirected graph  $\mathcal{G} = (\mathcal{V}, \mathcal{E})$  and an elimination ordering  $I$ . We describe a simple graph-theoretic algorithm that successively eliminates the nodes of  $\mathcal{G}$ . In particular, at each step, the algorithm eliminates the next node in the ordering  $I$ , where “eliminate” means removing the node from the graph and connecting the (remaining) neighbors of the node. The algorithm, which we refer to as UNDIRECTEDGRAPHELIMINATE, is presented in Figure 3.5.

We will be interested in the *reconstituted graph*; the graph  $\tilde{\mathcal{G}} = (\mathcal{V}, \tilde{\mathcal{E}})$ , whose edge set  $\tilde{\mathcal{E}}$  is a superset of  $\mathcal{E}$ , incorporating all of the original edges  $\mathcal{E}$ , as well as any new edges created during a run of UNDIRECTEDGRAPHELIMINATE.

Consider in particular the graph in Figure 3.6(a) and the elimination ordering  $(6, 5, 4, 3, 2, 1)$ . Let us run through the graphical elimination procedure. Starting with node  $X_6$  we first connect its neighbors, adding an edge between  $X_2$  and  $X_5$ , as shown in Figure 3.6(b). We then remove  $X_6$ , which yields Figure 3.6(c). Moving to  $X_5$ , we connect its neighbors,  $X_2$  and  $X_3$ , and remove  $X_5$ , which yields Figure 3.6(d). The procedure continues in Figure 3.6(e)–(g), culminating in a graph with the single node  $X_1$ , which is then removed yielding the empty graph.

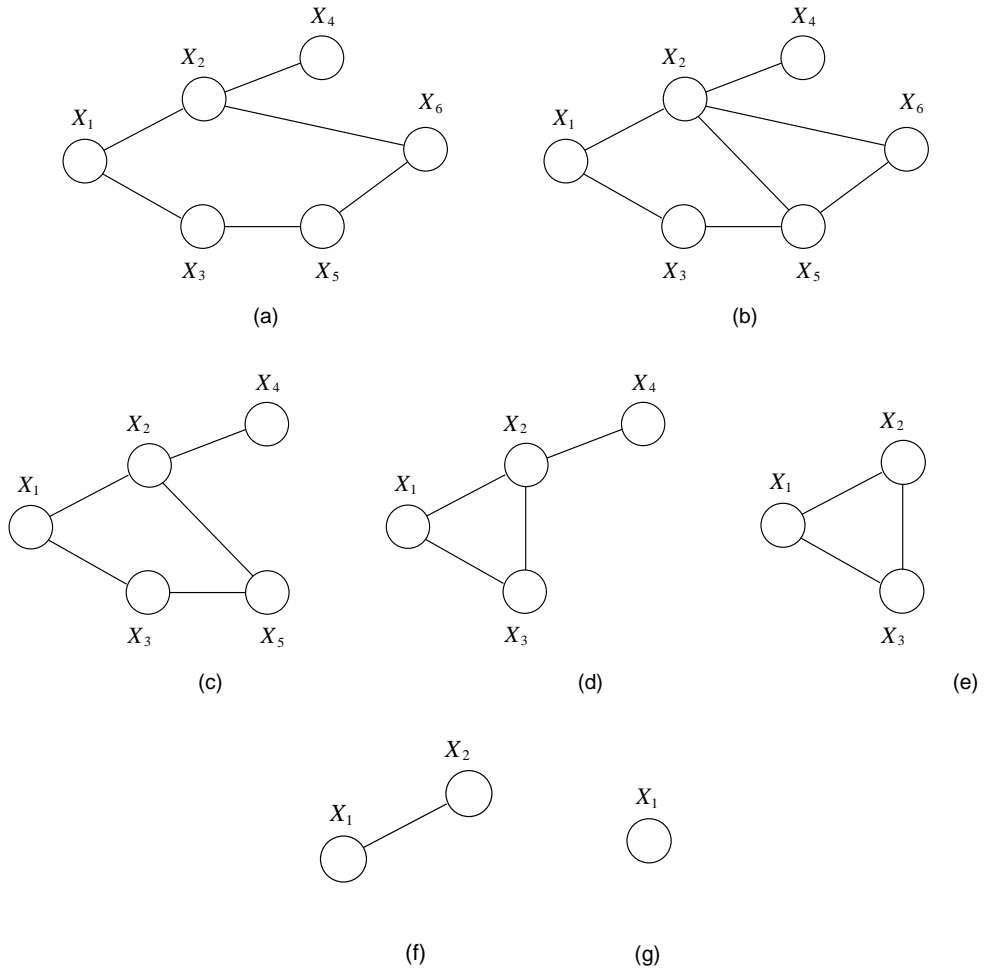


Figure 3.6: A run of the elimination algorithm under the elimination ordering  $(6, 5, 4, 3, 2, 1)$ . The original graph is shown in (a).

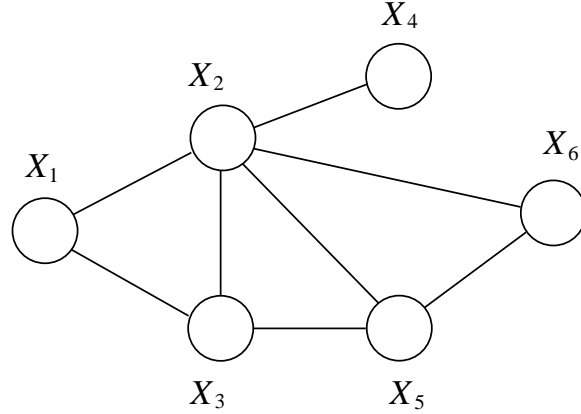


Figure 3.7: The reconstituted graph, showing the edges that were added during the elimination process.

Figure 3.7 shows the reconstituted graph, where we have retained the edges that were created during the elimination procedure (in particular, the edges between  $X_2$  and  $X_3$  and between  $X_2$  and  $X_5$ ). This graph turns out to have some important graph-theoretic properties, properties which underly the comprehensive theory of inference that will be the subject of Chapter 17.<sup>4</sup> For current purposes, however, the relevant properties of the graph can be captured by recording the *elimination cliques* of the graph. In particular, each time we remove a node  $X_i$  in the second step of the algorithm, let us record the collection of nodes that are the neighbors of  $X_i$  at that moment, including  $X_i$  itself. These nodes form a fully-connected subset of nodes by virtue of the first step of the algorithm; that is, they form a clique. We denote the set of indices of the nodes in this clique as  $T_i$ . Thus, in our example,  $T_6 = \{2, 5, 6\}$  and  $T_5 = \{2, 3, 5\}$ . (Note that index 6 does not appear in  $T_5$  because  $X_6$  has already been eliminated when we process node  $X_5$ ).

### 3.2.2 Graph elimination and marginalization

When we perform a marginalization operation, removing a random variable from a joint distribution, we perform a sum over the product of all factors that depend on that random variable. This couples together all of the other random variables that appear in those factors. Thus, for example, summing the product  $\psi(x_3, x_5)m_6(x_2, x_5)$  with respect to  $x_5$  creates an intermediate factor that involves  $x_2$  and  $x_3$ . This new factor does not in general factorize with respect to  $x_2$  and  $x_3$ ; thus, we have an *induced dependency* between  $x_2$  and  $x_3$ . Subsequent operations will have to treat  $x_2$  and  $x_3$  together. `UNDIRECTEDGRAPHELIMINATE` makes this coupling explicit, by linking the neighbors of the node being summed over.

In general, as we now show, the elimination cliques in `UNDIRECTEDGRAPHELIMINATE` are the graph-theoretic counterparts of the sets of variables on which summations operate in probabilistic

---

<sup>4</sup>For readers who cannot bear the wait, the key property of the reconstituted graph is that it is a *triangulated graph*; indeed, our elimination procedure is a simple algorithm for triangulating a graph.

inference using `ELIMINATE`.

Consider the argument  $x_{T_i}$  to the function  $\phi_i(x_{T_i})$  in `ELIMINATE`, the function which is the summand for the operator  $\sum_{x_i}$ . As our notation suggests, the variables referenced by  $\phi_i$  are exactly those in the elimination clique created by `UNDIRECTEDGRAPHELIMINATE` upon elimination of  $X_i$ . To see this, note that any potential removed from the active list by `ELIMINATE` (when summing over  $x_i$ ) must reference  $x_i$ . Now consider any other variable  $x_j$  referenced by  $\phi_i(x_{T_i})$ . We want to show that  $X_i$  and  $X_j$  must be neighbors in the graph constructed by `UNDIRECTEDGRAPHELIMINATE`. There are two cases to consider, corresponding to the two kinds of potentials that can link variables: (1) If the potential is one of the original potentials  $\psi_C(x_C)$ , then  $X_j$  is necessarily linked to  $X_i$ , because  $C$  is a clique (by definition). (2) If  $x_i$  and  $x_j$  appear together in an intermediate factor  $m_k(x_{S_k})$ , then this term was created by the elimination of an earlier node  $X_k$ . At the moment of eliminating  $X_k$ , `UNDIRECTEDGRAPHELIMINATE` must have linked the nodes  $X_i$  and  $X_j$ . Thus, in either case,  $X_j$  is a neighbor of  $X_i$ , and these nodes must appear together in the elimination clique  $X_{T_i}$ .

### 3.2.3 Computational complexity

Let us now consider the computational complexity of `ELIMINATE`. At each step we must sum over a variable  $x_i$  for all configurations of the variables in the summand  $\phi_i(x_{T_i})$ . Assuming that there is no special algebraic structure in this summand that can be exploited, the time and space complexities are exponential in the number of variables in the subset  $T_i$ . That is, the overall complexity of the algorithm is determined by the number of variables in the largest elimination clique. Thus, the question of the computational complexity of `ELIMINATE` can be reduced to the purely graph-theoretic question of the size of the largest elimination clique created by `UNDIRECTEDGRAPHELIMINATE`.

The problem of obtaining a largest elimination clique that is as small as possible, under all possible elimination orderings, is a well-studied problem in graph theory. The problem is generally expressed in terms of a parameter  $k$  known as the *treewidth*, which is one less than the smallest achievable value of the cardinality of the largest elimination clique, where we range over all possible elimination orderings.

Consider for example, the star graph on  $n$  nodes shown in Figure 3.8(a). If we were to eliminate the central node first, we would immediately link all other nodes, creating an elimination clique of size  $n$ . On the other hand, if we eliminate all of the leaf nodes first we never create a clique of cardinality greater than two. Indeed, the treewidth of this graph is equal to one.

Figure 3.8(b) shows a second example, in which it can be verified that it is possible to eliminate the nodes in such a way that the largest clique created is of size three. The treewidth is thus equal to two.

The general problem of finding the best elimination ordering of a graph—an elimination ordering that achieves the treewidth—turns out to be NP-hard. We discuss this hardness result, and its consequences for probabilistic inference, in more detail in Chapter 17. Indeed, in that chapter we discuss an inference algorithm (the junction tree algorithm) that generalizes `ELIMINATE` and necessitates a deeper discussion of the treewidth problem and methods for tackling it. As we will show, there are a number of useful heuristics for finding good elimination orders, and these can provide viable solutions in practical problems.

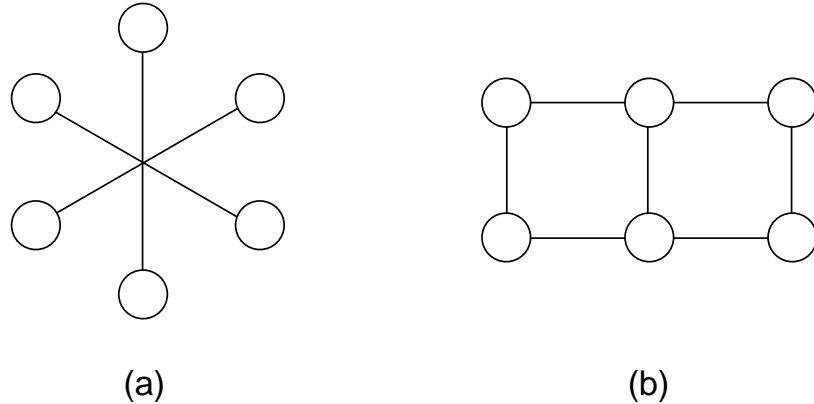


Figure 3.8: (a) A graph whose treewidth is equal to one. (b) A graph whose treewidth is equal to two.

In the meantime, all of the graphs that we study in intervening chapters will turn out to involve graphs that have “obvious” optimal elimination orderings.

The NP-hardness result should be taken as injecting a cautionary note into our study of elimination methods, suggesting that we should not expect `ELIMINATE` to provide a computationally-efficient solution to the general problem of probabilistic inference. On the other hand, we clearly should never have expected any such general solution from `ELIMINATE`. The fully-connected graph, for example, yields a single clique containing all of the nodes, under all possible elimination orderings, and thus has no graph-theoretic structure that `ELIMINATE` can exploit. To have any hope for efficient probabilistic inference in such a graph, we need to hope that other structural features of probability theory can be brought to bear.<sup>5</sup>

We can also take the NP-hardness result as providing a crisp statement of the computational bottleneck that arises in `ELIMINATE`. Indeed, note that `UNDIRECTEDGRAPHELIMINATE` provides a practically useful tool for assessing the severity of this bottleneck. For a given elimination ordering, we can obtain a cheap assessment of the predicted running time of `ELIMINATE` by running `UNDIRECTEDGRAPHELIMINATE`. If `UNDIRECTEDGRAPHELIMINATE` yields elimination cliques of reasonably small cardinality, then we know that it is viable to run `ELIMINATE`.

### 3.2.4 Graph elimination and directed graphs

All of the considerations of the previous three sections also apply to directed graphs. There is, however, a minor idiosyncracy of directed graphical models that must be addressed if we are to use the concept of “elimination clique” to analyze the directed version of `ELIMINATE`.

The functions that are used to initialize the active list in the directed case are conditional probabilities,  $p(x_i | x_{\pi_i})$ . Note that a pair of variables  $X_j$  and  $X_k$  that are parents of  $X_i$  are linked

---

<sup>5</sup>That is, there may be special algebraic structure in the potentials, or symmetries, or simplifications brought about by laws of large numbers. These issues will return in our consideration of approximate inference algorithms, in Chapter 20 and Chapter 21.

```

DIRECTEDGRAPHELIMINATE( $G, I$ )
 $G^m = \text{MORALIZE}(G)$ 
UNDIRECTEDGRAPHELIMINATE( $G^m, I$ )

MORALIZE( $G$ )
for each node  $X_i$  in  $I$ 
    connect all of the parents of  $X_i$ 
end
drop the orientation of all edges
return  $G$ 

```

Figure 3.9: An algorithm for eliminating nodes in an directed graph  $G$ .

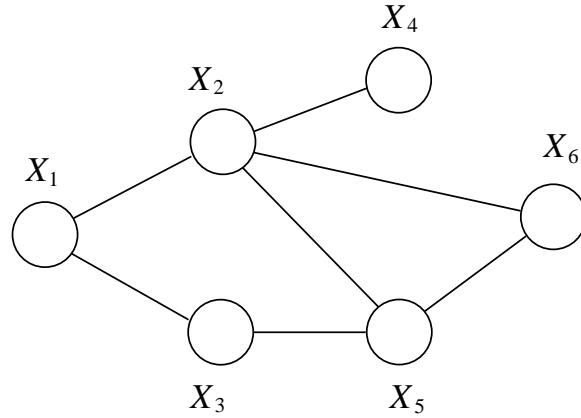


Figure 3.10: The moral graph corresponding to the directed graph in Figure 2.1.

functionally by their presence in the function  $p(x_i | x_{\pi_i})$ , but they are not necessarily neighbors in the graph  $\mathcal{G}$  (e.g.,  $X_2$  and  $X_5$  are not linked in Figure 3.1). This breaks the relationship between elimination cliques and sets of arguments that we established in the previous section for undirected graphs.

There is a simple fix. To define the elimination cliques for a directed graph, first connect all of the parents of each node—this captures the basic fact that factors involving all variables  $X_{\pi_i}$  will necessarily appear in our calculations. Then drop the orientation of all of the edges in the graph, converting the graph to an undirected graph. This procedure, of “marrying” the parents of the nodes in a directed graph and converting to an undirected graph, is referred to as *moralization*. The resulting graph is referred to as a *moral graph*. We use moralization as a subroutine in the algorithm, DIRECTEDGRAPHELIMINATE, for eliminating directed graphs (see Figure 3.9).

The graph in Figure 3.10 is the moral graph corresponding to the directed graph in Figure 2.1.

Note that (in the elimination order that we have been using in our example)  $X_6$  is eliminated before its parents  $X_2$  and  $X_5$ , and the elimination step already adds a link between these two nodes. That is, in this case, we do not need to moralize; elimination does it for us. On the other hand, if a parent of  $X_6$  appears before  $X_6$  in the elimination order, we need to moralize explicitly. Consider in particular an elimination ordering in which  $X_5$  is eliminated first. The other parent,  $X_2$ , is not a neighbor of  $X_5$  when the latter node is eliminated, and thus is not included within the elimination clique of  $X_5$ . This fails to capture the fact that summing over  $X_5$  creates an intermediate factor that refers to  $X_2$  and the other neighbors of  $X_5$ . In general we need to moralize in the directed graphical setting if we want the elimination cliques to capture all such dependencies.

The considerations in this section may help to explain the important role that undirected graphical models play in designing and analyzing inference algorithms, a role that we will see again in later chapters, even when the original graphical model is directed. In a directed model, the basic factors that appear in the joint probability are *conditional* probabilities. There is of course a great difference between the appearance of a variable on the left-hand or right-hand side of a conditional probability. From the point of view of ELIMINATE, however, this difference is irrelevant. When we sum over  $x_k$ , the factor  $p(x_i | x_j, x_k)$  and the factor  $p(x_j | x_i, x_k)$  both create an intermediate factor linking  $x_i$  and  $x_j$ . Thus, to understand the computational complexity of inference, we need to ignore the directionality associated with a conditional probability. The undirected graphical formalism, which treats such a probability as a general potential,  $\psi(x_i, x_j, x_k)$ , does this automatically.

### 3.3 Discussion

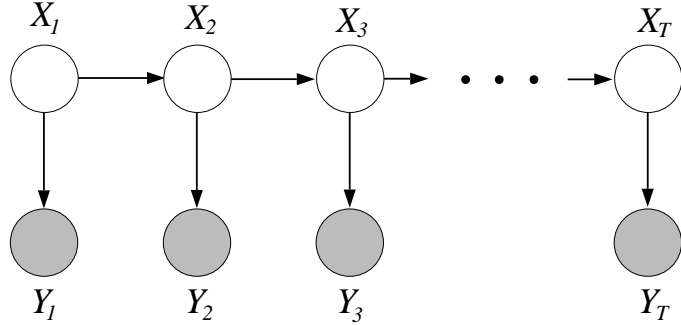
Our presentation of the elimination algorithm for probabilistic inference raises a number of questions:

- Can we prove that it works?
- What are its limitations?
- Can it be generalized?

Detailed answers to these questions will emerge in later chapters, but let us try to provide some short answers here.

It is not difficult to prove that the algorithm that we have presented is correct. Indeed, we ask the reader to provide a proof by induction in Exercise ??, and we present a proof by induction of the correctness of a closely-related algorithm (the SUM-PRODUCT algorithm) in Chapter 4. Moreover, in Chapter 17 we prove the correctness of the general junction tree algorithm, an algorithm that generalizes both ELIMINATE and SUM-PRODUCT.

The ELIMINATE algorithm has a number of limitations, some which are easily corrected and others which are not. In particular, taking ELIMINATE seriously as an algorithm to be implemented on a computer reveals a number of inefficiencies. Most importantly, the use of a single “active list” as a data structure requires an inefficient traversal of the entire list every time the algorithm eliminates a node. This can be fixed by maintaining a separate list, or “bucket,” for each node. Whenever the algorithm creates a new intermediate factor,  $m_i(x_{S_i})$ , it scans the elimination ordering  $I$ , and



combining intermediate factors. Rather than focusing on elimination orderings, the junction tree algorithm focuses on the relationships between intermediate factors, or “messages.” The same idea is present in simpler form in the SUM-PRODUCT algorithm, to which we now turn.

### 3.4 Historical remarks and bibliography

# An Introduction to Probabilistic Graphical Models

Michael I. Jordan  
*University of California, Berkeley*

June 30, 2003



## Chapter 4

# Probability Propagation and Factor Graphs

In this chapter we describe an algorithm for probabilistic inference known as the *sum-product*, or *belief propagation*, algorithm. The algorithm is closely related to the elimination algorithm, and indeed we will derive it from the perspective of elimination. The algorithm goes significantly beyond the elimination algorithm, however, in that it can compute all single-node marginals (for certain classes of graphs) rather than only a single marginal.

It is important to be clear that we are also taking a step backward in this chapter—while the elimination algorithm is applicable to arbitrary graphs, the sum-product algorithm is designed to work only in trees (or in the various “tree-like” graphs that we discuss in this chapter). Despite this step backward, there are at least three reasons why the sum-product algorithm overall represents significant progress: (1) Trees are important graphs. Indeed, a significant fraction of the classical literature on graphical models was entirely restricted to trees, and many of these classical applications require the ability to compute all singleton marginals. Examples include the hidden Markov model of Chapter 12 and the state-space model of Chapter 15. (2) The sum-product algorithm provides new insights into the inference problem, insights which will eventually allow us to provide a general solution to the exact inference problem (the *junction tree algorithm* of Chapter 17). The sum-product algorithm essentially involves an efficient “calculus of intermediate factors,” which recognizes that many of the same intermediate factors are used in different elimination orderings. The junction tree algorithm extends this calculus to general graphs, by essentially combining the key ideas of the sum-product algorithm and the elimination algorithm. (3) While our focus in the current chapter is exact inference, the sum-product algorithm also provides the basis of a class of *approximate* inference algorithms for general graphs, as we discuss in Chapter 20.

Another goal of the current chapter is to introduce *factor graphs*, an alternative graphical representation of probabilities that is of particular value in the context of the sum-product algorithm. In particular, we will show that the factor graph approach provides an elegant way to handle various general “tree-like” graphs, including “polytrees,” a class of directed graphical models in which nodes have multiple parents.

Finally, we also broaden our agenda in the current chapter, moving beyond the problem of com-

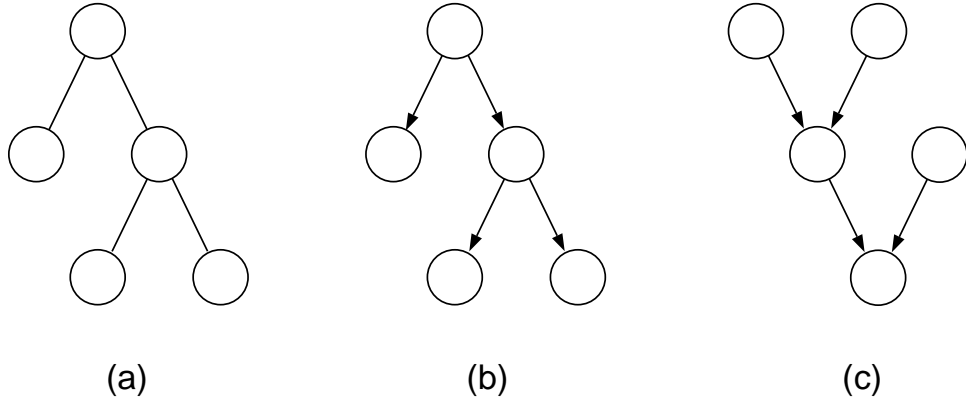


Figure 4.1: (a) An undirected tree. (b) A directed tree. (c) A polytree.

puting marginal and conditional probabilities to the problem of computing *maximum a posteriori probabilities*. We show that this problem can be solved via an algorithm that is closely related to the sum-product algorithm.

The chapter is organized as follows. In Section 4.1 we begin with a discussion of probabilistic inference on trees, treating both the directed case and the undirected case. Section ?? introduces *factor graphs*, discusses the relationships with directed and undirected graphs, and develops the sum-product algorithm for factor graphs. We discuss polytrees in Section 4.2.4, and discuss algorithms for computing maximum a posteriori probabilities in Section 4.3.

## 4.1 Probabilistic inference on trees

In this section we describe an inference algorithm for trees. Let us first clarify exactly what is meant by a “tree.” In the undirected case, a tree is an undirected graph in which there is one and only one path between any pair of nodes. An example of an undirected tree is shown in Figure 4.1(a).<sup>1</sup> In the directed case, we define a tree to be any graph whose moralized graph is an undirected tree. Figure 4.1(b) shows a directed tree. Note that directed trees have a single node that has no parent—the *root node*—and that all other nodes have exactly one parent. Finally, note that the graph in Figure 4.1(c) is not a directed tree; it has nodes with multiple parents, and the resulting moralized graph has loops.

Any undirected tree can be converted into a directed tree by choosing a root node and orienting all edges to point away from the root.

From the point of view of graphical model representation and inference there is little significant difference between directed trees and undirected trees. A directed tree and the corresponding undirected tree (the tree obtained by dropping the directionality of the edges) make exactly the same set of conditional independence assertions. Moreover, as we show below, the parameterizations

<sup>1</sup>Note that throughout the chapter we assume implicitly that our graphs are connected, and thus we have a single tree rather than a forest. This is done without loss of generality—in the case of a forest we have a collection of probabilistically independent trees, and it suffices to run an inference algorithm separately on each tree.

are essentially the same, with the undirected parameterization being slightly more flexible by not requiring potentials to be normalized (but, see Exercise ??, any undirected representation can be readily converted to a directed one).

### 4.1.1 Parameterization and conditioning

Let us first consider the parameterization of probability distributions on undirected trees. The cliques are single nodes and pairs of nodes, and thus the joint probability can be parameterized via potential functions  $\{\psi(x_i)\}$  and  $\{\psi(x_i, x_j)\}$ . In particular, we have:

$$p(x) = \frac{1}{Z} \left( \prod_{i \in \mathcal{V}} \psi(x_i) \prod_{(i,j) \in \mathcal{E}} \psi(x_i, x_j) \right), \quad (4.1)$$

for a tree  $\mathcal{T}(\mathcal{V}, \mathcal{E})$  with nodes  $\mathcal{V}$  and edges  $\mathcal{E}$ .

For directed trees, the joint probability is formed by taking a product over a marginal probability,  $p(x_r)$ , at the root node  $r$ , and conditional probabilities,  $\{p(x_j | x_i)\}$ , at all other nodes:

$$p(x) = p(x_r) \prod_{(i,j) \in \mathcal{E}} p(x_j | x_i), \quad (4.2)$$

where  $(i, j)$  is a directed edge such that  $i$  is the (unique) parent of  $j$  (i.e.,  $\{i\} = \pi_j$ ). We can treat such a parameterization as a special case of Eq. (4.1), and indeed it will be convenient to do so throughout this chapter. We define:

$$\psi(x_r) = p(x_r) \quad (4.3)$$

$$\psi(x_i, x_j) = p(x_j | x_i), \quad (4.4)$$

for  $i$  the parent of  $j$ , and define all other singleton potentials,  $\psi(x_i)$ , for  $i \neq r$ , to be equal to one. We thereby express the joint probability for a directed tree in the undirected form in Eq. (4.1), with  $Z = 1$ .

Recall that we use ‘‘evidence potentials’’ to capture conditioning. Thus, if we are interested in the conditional probability  $p(x_F | \bar{x}_E)$ , for some subset  $E$ , we define evidence potentials  $\delta(x_i, \bar{x}_i)$ , for  $i \in E$ , and multiply the joint probability by the product of these potentials. This simply reduces to multiplying  $\psi(x_i)$  by  $\delta(x_i, \bar{x}_i)$ , for  $i \in E$ . In particular, we define:

$$\psi_i^E(x_i) \triangleq \begin{cases} \psi_i(x_i) \delta(x_i, \bar{x}_i) & i \in E \\ \psi_i(x_i) & i \notin E, \end{cases} \quad (4.5)$$

and substitute in Eq. (4.1) to obtain:

$$p(x | \bar{x}_E) = \frac{1}{Z^E} \left( \prod_{i \in V} \psi_i^E(x_i) \prod_{(i,j) \in \mathcal{E}} \psi(x_i, x_j) \right), \quad (4.6)$$

where  $Z^E = \sum_x \left( \prod_{i \in V} \psi^E(x_i) \prod_{(i,j) \in \mathcal{E}} \psi(x_i, x_j) \right)$ . Note that the original  $Z$  vanishes.

In summary, the parameterization of unconditional distributions and conditional distributions on trees is formally identical, involving a product of potential functions associated with each node and each edge in the graph. We can thus proceed without making any special distinction between the unconditional case and the conditional case.

Are there any special features of directed trees that we lose in working exclusively with the undirected formalism? One feature of the parameterization for directed trees is that any summation of the form  $\sum_{x_j} p(x_j | x_i)$  is necessarily equal to one, and does not need to be performed explicitly. Indeed, in the unconditional case, we can arrange things such that all sums are of this form, by choosing an elimination ordering that begins at the leaves and proceeds backward to the root. (This shows that the normalization factor  $Z$  is necessarily equal to one in the unconditional case). When we condition, however, the resulting product of potentials is unnormalized (the normalization factor  $Z^E$  is no longer one), and we are brought closer to the general undirected case. It is still the case that we can “prune” any subtree that contains only variables that are not conditioned on, by again eliminating backwards. We view this as an implementation detail, however, assuming that any implementation of an inference algorithm will be smart enough to prune such subtrees at the outset. We then find ourselves in a situation in which the leaves of the tree are evidence nodes, and all of the sums have to be performed explicitly. In this case, there is no essential difference between the directed case and the undirected case, and in developing the general algorithm for inference on trees, it is convenient to focus exclusively on the latter.

#### 4.1.2 From elimination to message-passing

In this section and the following section, we derive the SUM-PRODUCT algorithm, a general algorithm for probabilistic inference on trees. The algorithm involves a simple mathematical update equation—a sum over a product of potentials—applied once for each outgoing edge at each node. We derive this update equation from the point of view of the ELIMINATE algorithm. We subsequently prove that a more general algorithm based on this update equation finds all (singleton) marginals simultaneously.

Let us begin by returning to ELIMINATE, but specializing to the case of a tree. Recall the basic structure of ELIMINATE: (1) Choose an elimination ordering  $I$  in which the query node  $f$  is the final node; (2) Place all potentials on an active list; (3) Eliminate a node  $i$  by removing all potentials referencing the node from the active list, taking the product, summing over  $x_i$ , and placing the resulting intermediate factor back on the active list. What are the special features of this procedure when the graph is a tree?

To take advantage of the recursive structure of a tree, we need to specify an elimination ordering  $I$  that respects this structure. In particular, we consider elimination orderings that arise from a *depth-first traversal* of the tree. Treat  $f$  as a root and view the tree as a directed tree by directing all edges of the tree to point away from  $f$ . We now consider any elimination ordering in which a node is eliminated only after all of its children in the directed version of the tree are eliminated. It can be easily verified that such an elimination ordering proceeds inward from the leaves, and generates elimination cliques of size at most two (showing that the tree-width of a tree is equal to

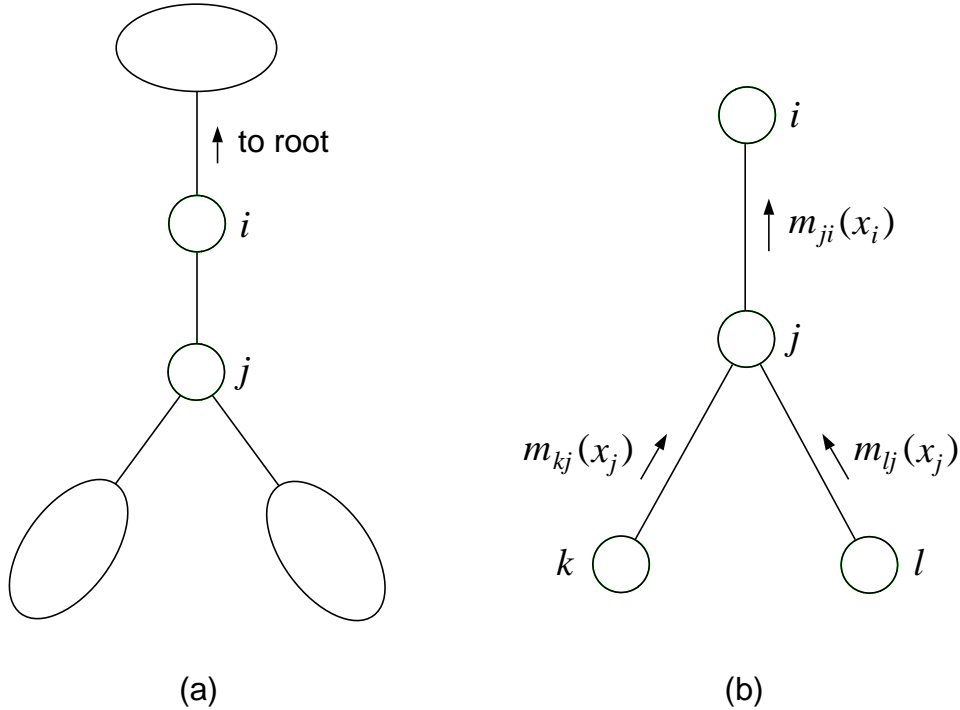


Figure 4.2: (a) A fragment of an undirected graph. Nodes *i* and *j* are neighbors, with *i* nearer to the root than *j*. (b) The messages that are created when nodes *k*, *l* and *j* are eliminated.

one).

Let us now consider the elimination step. Consider nodes *i* and *j* that are neighbors in the tree, where *i* is closer to the root than *j* (see Figure 4.2(a)). We are interested in the intermediate factor that is created when *j* is eliminated. This intermediate factor is a sum over a product of certain potentials. Which potentials are these? Clearly  $\psi(x_i, x_j)$  is one of these potentials, given that it references  $x_j$  and given that *i* has yet to be eliminated. Also,  $\psi^E(x_j)$  will appear. We can also exclude a number of possibilities. In particular, none of the potentials in the product can reference any variable in the subtree below *j*, given that all of these variables have already been eliminated. Moreover, none of these potentials can reference any other variable outside the subtree, due to the assumption that the graph is a tree. That is, for a node *k* in the subtree and a node *l* outside of the subtree, there can be no potential  $\psi(x_k, x_l)$  in the probability model. Thus, when eliminating nodes in the subtree, we can never introduce any variable outside of the subtree into a summand and thus into an intermediate factor.

We have shown that the intermediate factor created by the sum over  $x_j$  is a function solely of  $x_i$ . Let us introduce the notation " $m_{ji}(x_i)$ " to denote this term, where the first subscript denotes the variable being eliminated and the second subscript denotes the (sole) remaining neighbor of the variable (the "bucket" in the language of Section ??). Note that the latter index is superfluous in the context of ELIMINATE—it is determined by the graph structure and the elimination ordering—but

it will be needed in the context of the more general SUM-PRODUCT algorithm.

We refer to the intermediate factor  $m_{ji}(x_i)$  as a “message” that  $j$  sends to  $i$ . As suggested by Figure 4.2(b), we can think of this message as “flowing” along the edge linking  $j$  to  $i$ .

Let us now consider the mathematical operation that creates the message  $m_{ji}(x_i)$  in more detail. In particular, consider the potentials that are selected from the active list when we eliminate node  $j$ —the potentials that reference  $x_j$ . As we mentioned earlier, the potentials  $\psi(x_i, x_j)$  and  $\psi^E(x_j)$  are among the potentials selected. The other potentials that are selected are those created in earlier elimination steps in which the neighbors of node  $j$  (other than  $i$ ) are eliminated. As shown in Figure 4.2(b), these steps can be viewed as creating messages  $m_{kj}(x_j)$ , messages that flow from each neighbor  $k$ —where  $k \in \mathcal{N}(j) \setminus i$ —to  $j$ .

Thus, following the protocol of the ELIMINATE algorithm, to eliminate  $x_j$  we take the product over all potentials that reference  $x_j$  and sum over  $x_j$ :

$$m_{ji}(x_i) = \sum_{x_j} \left( \psi^E(x_j) \psi(x_i, x_j) \prod_{k \in \mathcal{N}(j) \setminus i} m_{kj}(x_j) \right). \quad (4.7)$$

This is the intermediate factor (“message”) that  $j$  sends to  $i$ .

Finally, let us consider the final node  $f$  in the elimination ordering  $I$ . All other nodes have been eliminated when we arrive at  $f$ , and thus messages  $m_{ef}(x_f)$  have been computed for each of the neighbors  $e \in \mathcal{N}(f)$ . These messages, and the potential  $\psi^E(x_f)$ , are the only terms on the active list at this point. Thus, again following the protocol of ELIMINATE, we write the marginal of  $x_f$  as the following product:

$$p(x_f | \bar{x}_E) \propto \psi^E(x_f) \prod_{e \in \mathcal{N}(f)} m_{ef}(x_f), \quad (4.8)$$

where the proportionality constant is obtained by summing the right-hand side with respect to  $x_f$ .

Eqs. (4.7) and (4.8) provide a concise mathematical summary of the ELIMINATE algorithm, for the special case of a tree. Leaving behind the algorithmic details of ELIMINATE, we see that probabilistic inference essentially involves solving a coupled system of equations in the variables  $m_{ji}(x_i)$ . To compute  $p(x_f)$ , we solve these equations in an order that corresponds to a depth-first traversal of a directed tree in which  $f$  is the root.

#### 4.1.3 The SUM-PRODUCT algorithm

In this section we show that Eqs. (4.7) and (4.8) suffice for obtaining not only a single marginal, but also for obtaining *all* of the marginals in the tree. The (somewhat magical) fact is that we can obtain all marginals by simply doubling the amount of work required to compute a single marginal. In particular, as we will show, after having passed messages inward from the leaves of the tree to an (arbitrary) root, we simply pass messages from the root back out to the leaves, again using Eq. (4.7) at each step. The net effect is that a single message will flow in both directions along each edge. Once all such messages have been computed, we invoke Eq. (4.8) independently at each node; this yields the desired marginals.

One way to understand why this algorithm works is to consider the naive approach of computing all marginals by using a different elimination ordering for each marginal. Consider in particular the tree fragment shown in Figure 4.3(a). To compute the marginal of  $X_1$  using elimination, we eliminate  $X_4$  and  $X_3$ , which, as we have seen, involves computing messages  $m_{42}(x_2)$  and  $m_{32}(x_2)$  that are sent to  $X_2$ . We subsequently eliminate  $X_2$ , which creates a message  $m_{21}(x_1)$  that is sent from  $X_2$  to  $X_1$ .

Now suppose that we wish to compute the marginal at  $X_2$  using elimination. As shown in Figure 4.3(b), we eliminate  $X_4$ ,  $X_3$ , and  $X_1$ , passing messages  $m_{42}(x_2)$ ,  $m_{32}(x_2)$  and  $m_{12}(x_2)$  to  $X_2$ . The message  $m_{12}(x_2)$  is new, but (crucially)  $m_{42}(x_2)$  and  $m_{32}(x_2)$  are the same messages as computed earlier. Similarly, if we wish to compute the marginal at  $X_4$ , as shown in Figure 4.3(c), we need a new message  $m_{24}(x_4)$ , but we can reuse the messages  $m_{32}(x_2)$  and  $m_{12}(x_2)$ . In general, if we compute a message for each direction along each edge in the tree, as shown in Figure 4.3(d), we can obtain all singleton marginals.

The idea that messages can be “reused” is important. In effect we can achieve the effect of computing over all possible elimination orderings (a huge number) by computing all possible messages (a small number). This is the key insight behind the SUM-PRODUCT algorithm.

The SUM-PRODUCT algorithm is based on Eqs. (4.7), (4.8), and a “protocol” that determines when any one of these equations can be invoked. The protocol is given as follows:

**Message-Passing Protocol.** *A node can send a message to a neighboring node when (and only when) it has received messages from all of its other neighbors.*

There are two principal ways to implement algorithms that respect this protocol. The first (and most direct) way is to interpret the protocol as the specification of a parallel algorithm. In particular, let us view each node as a processor, and assume that the node can repeatedly poll its incoming edges for the presence of messages. For a node of degree  $d$ , whenever messages have arrived on any subset of  $d - 1$  edges, the node computes a message for the remaining edge and delivers the message along that edge.

An example is shown in Figure 4.4. We assume a synchronous parallel algorithm, and at each step show the messages that are delivered along the edges. Note that messages start to flow in from the leaves. Note also that when the algorithm terminates, it is the case that a pair of messages have been computed for each edge, one for each direction. Finally, note that all incoming messages are eventually computed for each node, and that Eq. (4.8) can therefore be invoked at each node to compute the node marginal.

For this algorithm to be meaningful in general, we need to insure that all messages will eventually be computed and delivered; that is, that the algorithm will never “block.” We provide a proof that the protocol is non-blocking in Corollary ?? below.

We can also consider sequential implementations of the SUM-PRODUCT algorithm, in which messages are computed according to a particular “schedule.” One such schedule (a schedule that is widely used in practice) is a two-phase schedule based on depth-first traversal from an arbitrary root node.<sup>2</sup> In the first phase, messages flow inward from the leaves toward the root (as in Section 4.1.2).

---

<sup>2</sup>The original graph may have been a directed tree, with a corresponding root node. The “root” that is designated for the purposes of the SUM-PRODUCT algorithm is unrelated to this root node.

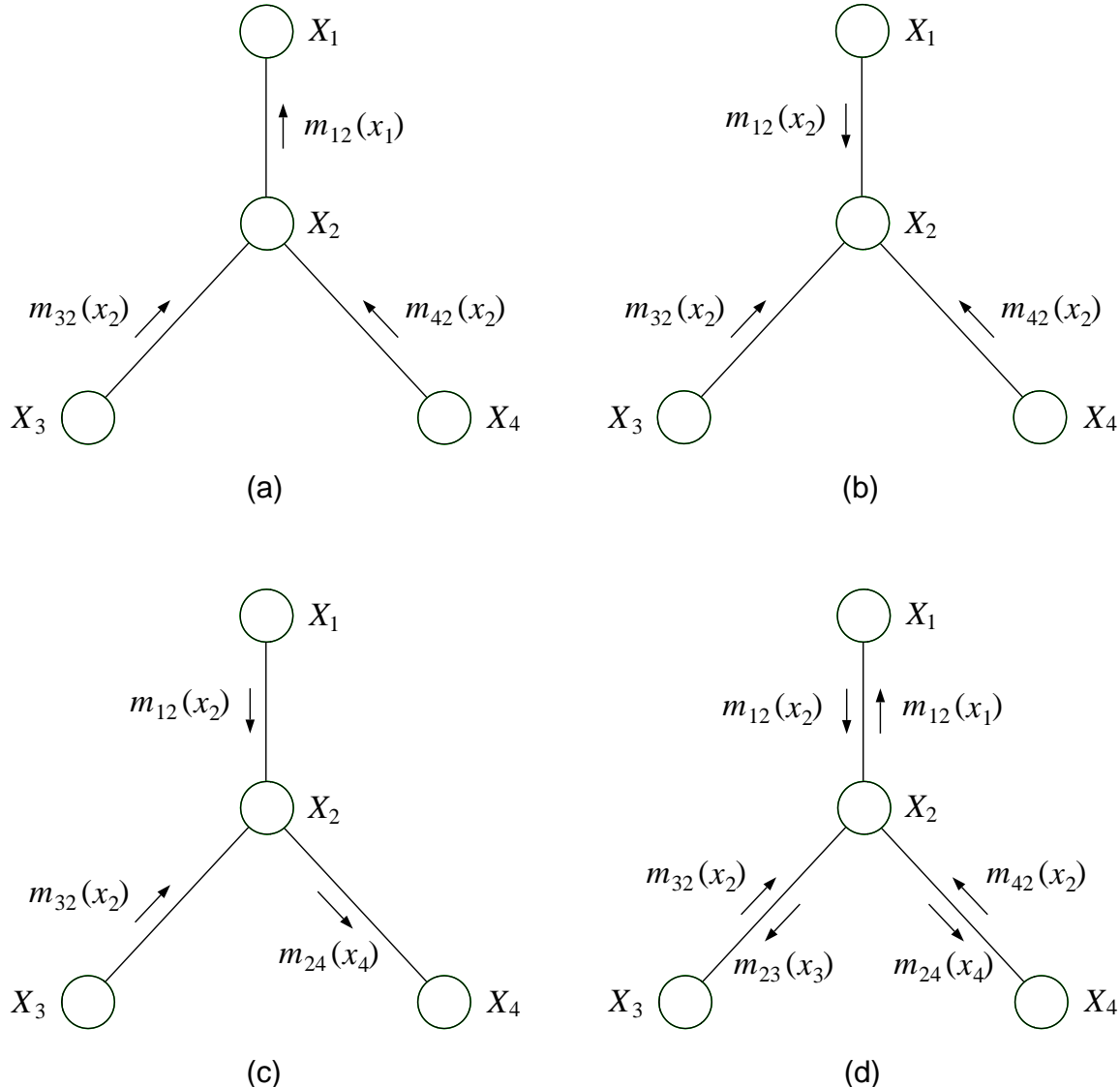


Figure 4.3: (a) The messages formed when computing the marginal of  $X_1$ . (b) The messages formed when computing the marginal of  $X_2$ . (c) The messages formed when computing the marginal of  $X_4$ . (d) All of the messages needed to compute all singleton marginals.

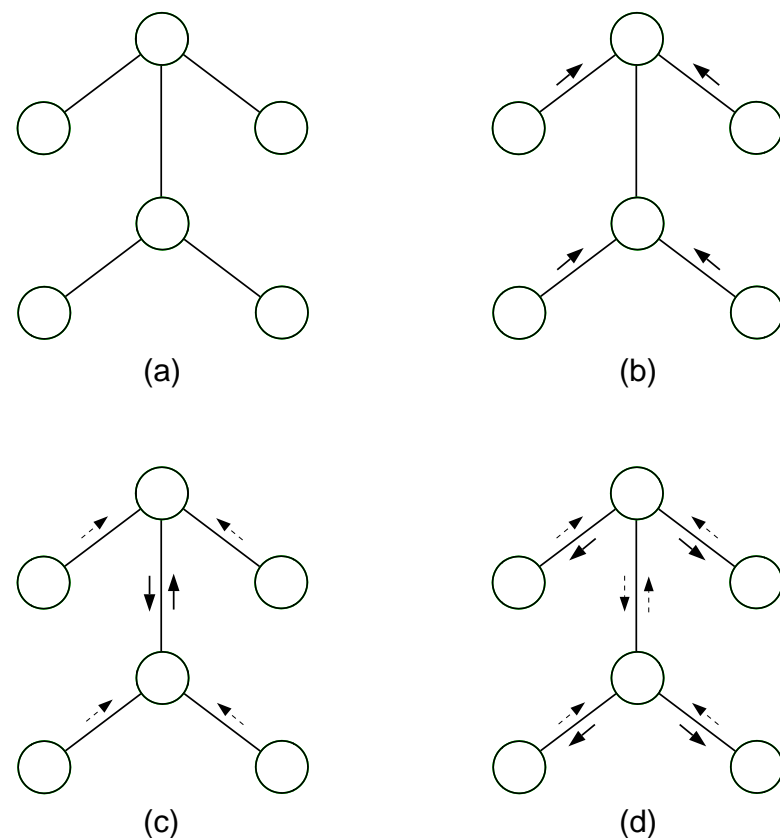


Figure 4.4: Message-passing under a synchronous parallel algorithm. The solid arrows are the messages passed at a given time step, and the dashed arrows are those passed on earlier time steps.

```

SUM-PRODUCT( $\mathcal{T}$ ,  $E$ )
  EVIDENCE( $E$ )
   $f = \text{CHOSEROOT}(\mathcal{V})$ 
  for  $e \in \mathcal{N}(f)$ 
    COLLECT( $f, e$ )
  for  $e \in \mathcal{N}(f)$ 
    DISTRIBUTE( $f, e$ )
  for  $i \in \mathcal{V}$ 
    COMPUTEMARGINAL( $i$ )

EVIDENCE( $E$ )
  for  $i \in E$ 
     $\psi^E(x_i) = \psi(x_i)\delta(x_i, \bar{x}_i)$ 
  for  $i \notin E$ 
     $\psi^E(x_i) = \psi(x_i)$ 

COLLECT( $i, j$ )
  for  $k \in \mathcal{N}(j) \setminus i$ 
    COLLECT( $j, k$ )
  SENDMESSAGE( $j, i$ )

DISTRIBUTE( $i, j$ )
  SENDMESSAGE( $i, j$ )
  for  $k \in \mathcal{N}(j) \setminus i$ 
    DISTRIBUTE( $j, k$ )

SENDMESSAGE( $j, i$ )
 $m_{ji}(x_i) = \sum_{x_j} (\psi^E(x_j) \psi(x_i, x_j) \prod_{k \in \mathcal{N}(j) \setminus i} m_{kj}(x_j))$ 

COMPUTEMARGINAL( $i$ )
 $p(x_i) \propto \psi^E(x_i) \prod_{j \in \mathcal{N}(i)} m_{ji}(x_i)$ 

```

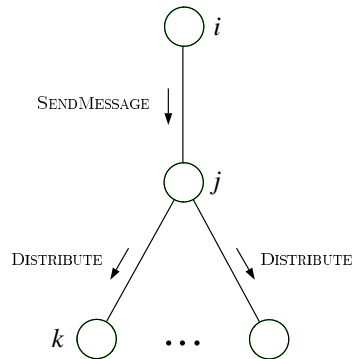
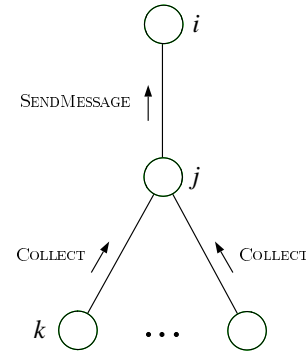


Figure 4.5: A sequential implementation of the SUM-PRODUCT algorithm for a tree  $\mathcal{T}(\mathcal{V}, \mathcal{E})$ . The algorithm works for any choice of root node, and thus we have left CHOSEROOT unspecified. A call to COLLECT causes messages to flow inward from the leaves to the root. A subsequent call to DISTRIBUTE causes messages to flow outward from the root to the leaves. After these calls have returned, the singleton marginals can be computed locally at each node.

In the second phase—which is initiated once all incoming messages have been received by the root node—messages flow outward from the root toward the leaves. In Figure 4.5, we show how such a schedule can be implemented via a pair of recursive function calls. In Exercise ??, we ask the reader to show that this schedule respects the Message-Passing Protocol, and to show that the overall effect of the schedule is that a single message flows in each direction along each and every edge.

#### 4.1.4 Proof of correctness of the SUM-PRODUCT algorithm<sup>3</sup>

[Section not yet written].

## 4.2 Factor graphs and the SUM-PRODUCT algorithm

The graphical model representations that we have discussed thus far—directed and undirected graphical models—aim at characterizing probability distributions in terms of conditional independence statements. *Factor graphs*, an alternative graphical representation of probability distributions, aim at capturing factorizations. As we have discussed (see Section ??), while closely related, conditional independence and factorization are not exactly the same concepts. Recall in particular our discussion of the parameterization of the complete graph on three nodes. This graph makes no conditional independence assertions, and the corresponding parameterization is simply the arbitrary potential  $\psi(x_1, x_2, x_3)$ . However, we may be interested in endowing the potentials with algebraic structure, for example:

$$\psi(x_1, x_2, x_3) = f_a(x_1, x_2)f_b(x_2, x_3)f_c(x_1, x_3), \quad (4.9)$$

for given functions  $f_a$ ,  $f_b$  and  $f_c$ . Such a factorized potential defines a proper subset of the family of probability distributions associated with the complete graph, a subset which has no interpretation in terms of conditional independence. Factor graphs provide a convenient way to represent subsets of this kind.

In the following section, we introduce the general factor graph representation, and discuss its relationships to directed and undirected graphs. We then focus on the special case of *factor trees* (factor graphs that are trees), and describe the variant of the SUM-PRODUCT algorithm that is geared to factor trees.

### 4.2.1 Factor graphs

Given a set of variables  $\{x_1, x_2, \dots, x_n\}$ , we let  $\mathcal{C}$  denote a set of subsets of  $\{1, 2, \dots, n\}$ . Thus, for example, given variables  $\{x_1, x_2, x_3, x_4, x_5\}$ , we might have  $\mathcal{C} = \{\{1, 3\}, \{3, 4\}, \{2, 4, 5\}, \{1, 3\}\}$ . Note that  $\mathcal{C}$  is a *multiset*—we allow the same subset of indices to appear multiple times. To avoid ambiguity, we therefore index the members of  $\mathcal{C}$  using an *index set*  $\mathcal{F}$ ; thus,  $\mathcal{C} = \{C_s : s \in \mathcal{F}\}$ .

---

<sup>3</sup>This section can be skipped without loss of continuity.

To each index  $s \in \mathcal{F}$ , we associate a *factor*  $f_s(x_{C_s})$ , a function on the subset of variables indexed by  $C_s$ . In our example, letting  $\mathcal{F} = \{a, b, c, d\}$  denote the indices, the factors are  $f_a(x_1, x_3)$ ,  $f_b(x_3, x_4)$ ,  $f_c(x_2, x_4, x_5)$  and  $f_d(x_1, x_3)$ .

Note also that there is no assumption that the subsets  $\mathcal{C}$  correspond to cliques of an underlying graph. Indeed, at this point we do not have any graph structure in mind— $\mathcal{C}$  is just an arbitrary collection of subsets of indices.

Given a collection of subsets and the associated factors, we define a multivariate function on the variables  $\{x_1, x_2, \dots, x_n\}$  by taking the product:

$$f(x_1, x_2, \dots, x_n) \triangleq \prod_{s=1}^S f_s(x_{C_s}). \quad (4.10)$$

Our goal will be to define a graphical representation of this function that will permit the efficient evaluation of *marginal functions*—functions of a single variable obtained by summing over all other variables.

Factorized functions in the form of Eq. (4.11) occur in many areas of mathematics, and the methods that we describe in this section has numerous applications outside of probability theory. Our interest, however, will be focused on factorized representations of probability distributions, and indeed the factorized probability distributions associated with directed and undirected graphical models provide examples of the general product-of-factors in Eq. (4.11).<sup>4</sup>

We now introduce a graphical representation of Eq. (4.11). This graphical representation—the *factor graph*—differs from directed and undirected graphical models in that it includes explicit nodes for the factors as well as the variables. We use round nodes to represent the variables and square nodes to represent the factors.

Formally, a factor graph is a bipartite graph  $\mathcal{G}(\mathcal{V}, \mathcal{F}, \mathcal{E})$ , where the vertices  $\mathcal{V}$  index the variables and the vertices  $\mathcal{F}$  index the factors. The edges  $\mathcal{E}$  are obtained as follows: each factor node  $s \in \mathcal{F}$  is linked to all variable nodes in the subset  $C_s$ . These are the only edges in the graph.

An example of a factor graph is shown in Figure 4.6. This graph represents the factorized function:

$$f(x_1, x_2, x_3, x_4, x_5) = f_a(x_1, x_3)f_b(x_3, x_4)f_c(x_2, x_4, x_5)f_d(x_1, x_3). \quad (4.11)$$

Note that  $f_a(x_1, x_3)$  and  $f_d(x_1, x_3)$  refer to the same set of variables. In an undirected graphical model these factors would be collapsed into a single potential function,  $\psi(x_1, x_3)$ . In a factor graph these functions are allowed to maintain a separate identity.

It will prove useful to define neighborhood functions on the nodes of a factor graph. In particular, let  $\mathcal{N}(s) \subset \mathcal{V}$  denote the set of neighbors of a factor node  $s \in \mathcal{F}$ , and let  $\mathcal{N}(i) \subset \mathcal{F}$  denote the set of neighbors of a variable node  $i \in \mathcal{V}$ . Note that  $\mathcal{N}(s)$  refers to the indices of all variables referenced by the factor  $f_s$ , and is identical to the subset  $C_s$  introduced earlier. On the other hand, the neighborhood set  $\mathcal{N}(i)$ , for a variable node  $i$ , is the set of all factors that reference the variable  $x_i$ .

Directed and undirected graphical models can be readily converted to factor graphs. For example, the directed graphical model shown in Figure 4.7(a) can be represented as a factor graph

---

<sup>4</sup>The normalization factor  $Z$  in the parameterization of undirected graphical models can be treated as a factor

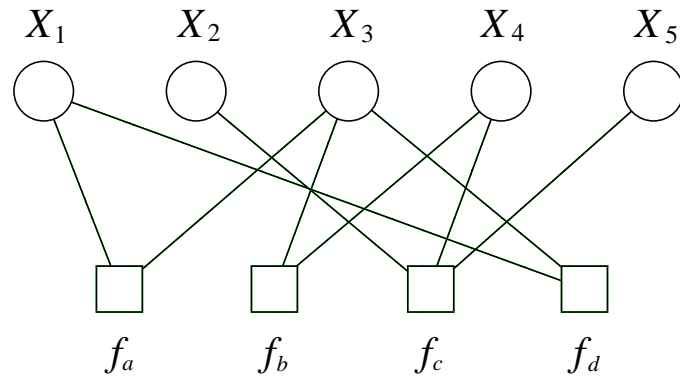


Figure 4.6: An example of a factor graph.

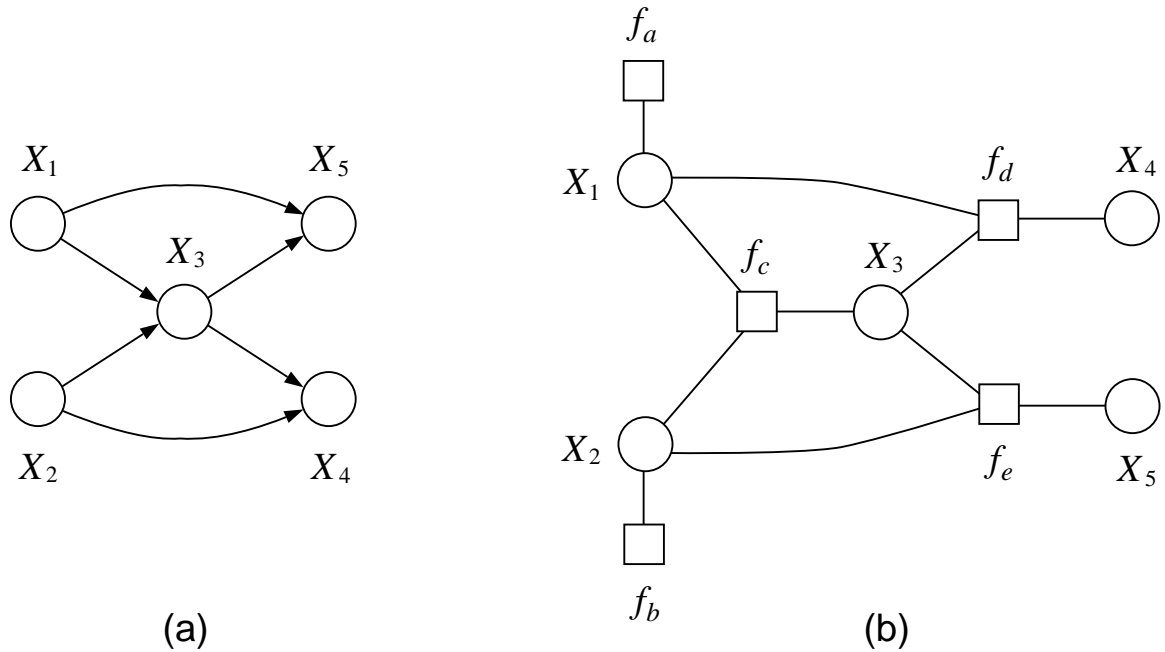


Figure 4.7: (a) A directed graphical model. (b) The corresponding factor graph. Note that there are six factor nodes, one for each local conditional probability in the directed graph.

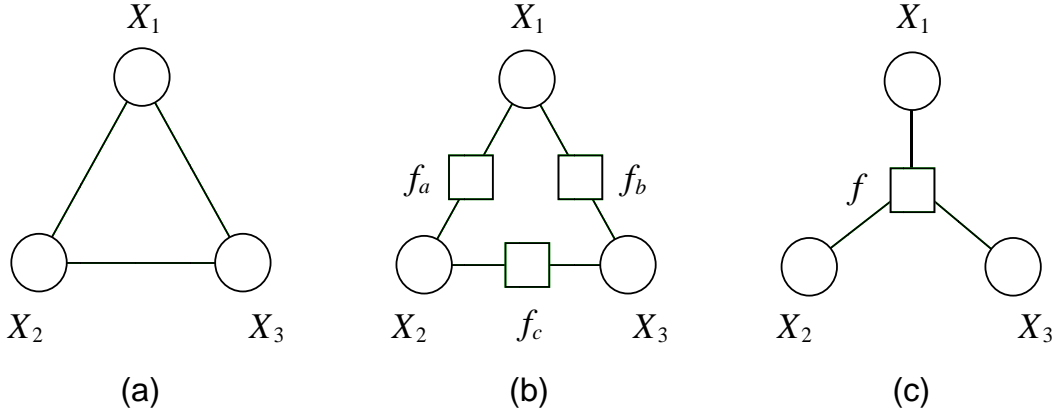


Figure 4.8: (a) An undirected graphical model provides no information about possible factorizations of the potential function associated with a given clique. (b) The factor graph corresponding to the factorized potential  $\psi(x_1, x_2, x_3) = f_a(x_1, x_2)f_b(x_2, x_3)f_c(x_1, x_3)$ . (c) The factor graph corresponding to the non-factorized potential  $\psi(x_1, x_2, x_3) = f(x_1, x_2, x_3)$ .

as shown in Figure 4.7(b).<sup>5</sup>

By representing each factor as a node in the graph, factor graphs provide a more fine-grained representation of probability distributions than is provided by directed and undirected graphical models. In particular, returning to the complete graph on three nodes shown in Figure 4.8(a), factor graphs make it possible to display fine-grained assumptions about the parameterization: Figure 4.8(b) shows the factor graph corresponding to the general potential  $\psi(x_1, x_2, x_3)$ , while Figure 4.8(c) shows the factor graph corresponding to the factorized potential in Eq. (4.9).

It is worth noting that it is always possible to mimic the fine-grained representation of factor graphs within the directed and undirected formalisms, so that formally factor graphs provide no additional representational power. For example, in Figure 4.9(a) we show an undirected graph that can represent the factorization in Eq. (4.9). In this graph, we have introduced three new random variables,  $Z_1$ ,  $Z_2$ , and  $Z_3$ . These variables are indicator variables picking out particular combinations of the underlying variables  $X_1$ ,  $X_2$  and  $X_3$ . Thus, for example, for binary  $X_1$  and  $X_2$ ,  $Z_1$  would take on four possible values, one for each pair of values of  $X_1$  and  $X_2$ , and the potential function  $\psi(z_1)$  would be set equal to the corresponding value of  $f_a(x_1, x_2)$ . (We ask the reader to fill in the details of this construction in Exercise ??).

Similarly, in Figure 4.9(b), we show a directed graph that mimics the factorization in Eq. (4.9). In this graph, the three new variables,  $W_1$ ,  $W_2$ , and  $W_3$ , are binary variables that are always set equal to one. We set  $p(W_1 = 1 | x_1, x_2)$  to the corresponding value of  $f_a(x_1, x_2)$ . (We again ask the reader to supply the details in Exercise ??).

---

associated with the empty set—which is appropriate given that it is a constant.

<sup>5</sup>In general, in the directed case each factor is a local conditional probability, and the subsets  $C_s$  correspond to “families” consisting of a node and its parents. Given that we do not assume that the subsets  $C_s$  correspond to cliques of an underlying graph, we do not need to “moralize” in the factor graph formalism. This is consistent with the fact that the factor graph does not attempt to represent conditional independencies.

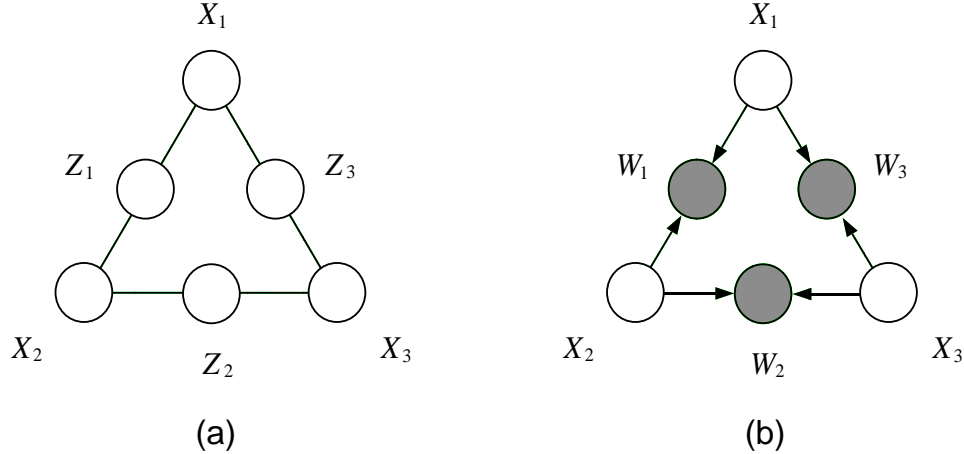


Figure 4.9: (a) An undirected graph that mimics the factorization shown in Figure 4.8(b) for appropriate choices of the indicator variables  $Z_i$ . (b) A directed graph that mimics the factorization shown in Figure 4.8(b) for appropriate choices of the indicator variables  $W_i$ .

In general, by introducing additional variables in a directed or undirected graph, we can mimic the factorization that is made explicit in the factor graph. However, this procedure is arguably rather artificial, and the factor graph representation provides a natural complement to undirected or directed graphs for situations in which a fine-grained representation of potentials is desired.

#### 4.2.2 The SUM-PRODUCT algorithm for factor trees

We now turn to the inference problem for factor graphs. As before, our goal is to compute all singleton marginal probabilities under the factorized representation of the joint probability. In this section we show how to do this for factor graphs that are trees.

A factor graph is defined to be a *factor tree* if the undirected graph obtained by ignoring the distinction between variable nodes and factor nodes is an undirected tree. Restricting ourselves to trees, we define a variant of the SUM-PRODUCT algorithm that provides all singleton marginal probabilities for factor trees.

As in the earlier SUM-PRODUCT algorithm, we define messages that flow along the edges of the graph. In the case of factor trees, there are *two* kinds of messages: messages  $\nu$  that flow from variable nodes to factor nodes, and messages  $\mu$  that flow from factor nodes to variable nodes.

These messages take the following form. We first consider the messages that flow from variable nodes to factor nodes. As depicted in Figure 4.10(a), the message  $\nu_{is}(x_i)$  that flows between the variable node  $i$  and the factor node  $s$  is computed as follows:

$$\nu_{is}(x_i) = \prod_{t \in \mathcal{N}(i) \setminus s} \mu_{ti}(x_i), \quad (4.12)$$

where the product is taken over all incoming messages to variable node  $i$ , other than the message from the factor node  $s$  that is the recipient of the message.

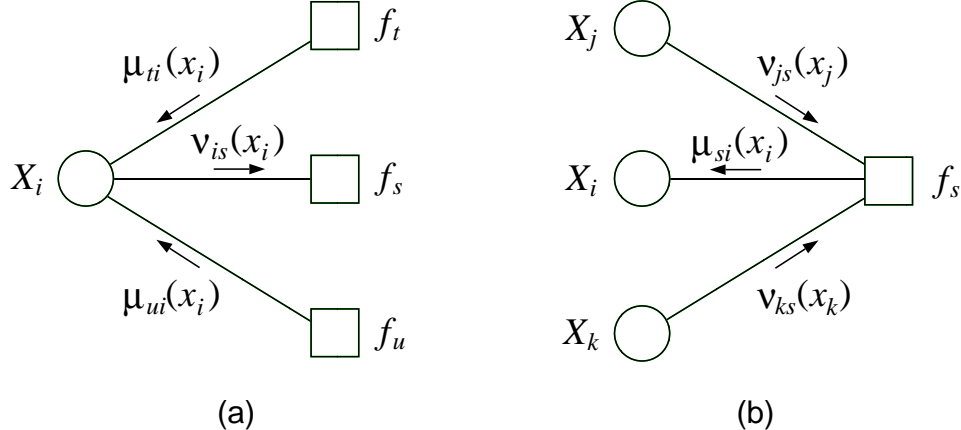


Figure 4.10: (a) The computation of the message  $\nu_{is}(x_i)$  that flows from factor node  $s$  to variable node  $i$ . (b) The computation of the message  $\mu_{si}(x_i)$  that flows from variable node  $i$  to factor node  $s$ .

Similarly, as shown in Figure 4.10(b), a message  $\mu_{si}(x_i)$  flows between the factor node  $s$  and the variable node  $i$ . This message is computed as follows:

$$\mu_{si}(x_i) = \sum_{x_{\mathcal{N}(s) \setminus i}} \left( f_s(x_{\mathcal{N}(s)}) \prod_{j \in \mathcal{N}(s) \setminus i} \nu_{js}(x_j) \right). \quad (4.13)$$

Note that the product is taken over all incoming messages to factor node  $s$ , other than the message from the variable node  $i$  that is the recipient of the message.

Thus we have a coupled set of equations for a set of messages. As in our earlier SUM-PRODUCT algorithm, a full specification of the algorithm requires a determination of when a given equation can be invoked. The protocol turns out to be exactly the same as the earlier protocol:

**Message-Passing Protocol.** *A node can send a message to a neighboring node when (and only when) it has received messages from all of its other neighbors.*

In the factor tree case, the protocol applies to both variable nodes and factor nodes.

Finally, once a message has arrived at each node from all of its neighbors, the marginal probability of a node is obtained as follows:

$$p(x_i) \propto \prod_{s \in \mathcal{N}(i)} \mu_{si}(x_i). \quad (4.14)$$

Given the definition of  $\nu_{is}(x_i)$  in Eq. (4.12), this can also be written as follows:

$$p(x_i) \propto \nu_{is}(x_i) \mu_{si}(x_i), \quad (4.15)$$

for any  $s \in \mathcal{N}(i)$ . That is, the marginal probability of node  $i$  can be obtained by taking the product of the pair of messages flowing along any edge incident on node  $i$ .

A sequential implementation of the SUM-PRODUCT algorithm for factor trees is provided in Figure 4.11.

Consider the example shown in Figure 4.6(a). The factor tree representation of this model is shown in Figure 4.12(b). Let us run through the steps of the SUM-PRODUCT algorithm. In the first step, shown in Figure 4.12(c), the only nodes that are able to send messages are the leaf nodes. These leaf nodes are factor nodes, and the product in Eq. (4.13) is a vacuous product, which by convention we set equal to one. Moreover, the sum in Eq. (4.13) is a vacuous sum. Thus, the message that flows in from a leaf node is simply the factor associated with that node:  $\mu_{si}(x_i) = \psi^E(x_i)$ , for  $i \in \mathcal{V}$ .

The second stage in the process is also rather uninteresting. As shown in Figure 4.12(d), the variable nodes  $X_1$  and  $X_3$  are able to send messages in this stage. For each node, the product in Eq. (4.12) is composed of only a single factor, and thus this factor is simply passed along the chain.

Now consider the third stage, shown in Figure 4.12(e). At the factor nodes along the backbone of the chain, a sum is taken over the product of the incoming message and the factor residing at that node. In the case of the message  $\mu_{d2}(x_2)$ , this yields  $\mu_{d2}(x_2) = \sum_{x_1} \psi^E(x_1) \psi(x_1, x_2)$ , and, similarly,  $\mu_{e2}(x_2) = \sum_{x_3} \psi^E(x_3) \psi(x_2, x_3)$ . Note that these messages are the same as the corresponding messages that would pass in a run of the SUM-PRODUCT algorithm for the undirected graph in Figure 4.12(a). That is, we have:  $\mu_{d2}(x_2) = m_{12}(x_2)$ , and  $\mu_{e2}(x_2) = m_{32}(x_2)$ .

Finally, in Figure 4.12(f), Figure 4.12(g), and Figure 4.12(h), we show the remaining steps of the algorithm. The reader can again verify a correspondence with the messages that would be computed in Figure 4.12(a):  $\mu_{d1}(x_1) = m_{21}(x_1)$  and  $\mu_{e3}(x_3) = m_{23}(x_3)$ . By the end of the algorithm, a message has passed in both directions along every edge.

In general, if we start with a graph that is an undirected tree and convert to a factor graph, then we find that there is a direct relationship between the “ $m$  messages” of the SUM-PRODUCT algorithm for the undirected graph and the “ $\mu$  messages” of the SUM-PRODUCT algorithm for the factor graph. Consider the graph fragment shown in Figure 4.13(a) and the corresponding factor graph representation in Figure 4.13(b). We claim that  $m_{ji}(x_i)$  in the undirected graph is equal to  $\mu_{si}(x_i)$  in the factor graph. Indeed, we have:

$$\mu_{si}(x_i) = \sum_{x_{\mathcal{N}(s) \setminus i}} \left( f_s(x_{\mathcal{N}(s)}) \prod_{j \in \mathcal{N}(s) \setminus i} \nu_{js}(x_j) \right) \quad (4.16)$$

$$= \sum_{x_j} \psi(x_i, x_j) \nu_{js}(x_j) \quad (4.17)$$

$$= \sum_{x_j} \psi(x_i, x_j) \prod_{t \in \mathcal{N}(j) \setminus s} \mu_{tj}(x_j) \quad (4.18)$$

$$= \sum_{x_j} \left( \psi^E(x_j) \psi(x_i, x_j) \prod_{t \in \mathcal{N}'(j) \setminus s} \mu_{tj}(x_j) \right), \quad (4.19)$$

where  $\mathcal{N}'(j)$  denotes the neighborhood of  $j$ , omitting the singleton factor node associated with  $\psi^E(x_j)$ . We see that the expression for  $\mu_{si}(x_i)$  is formally identical to the update equation for  $m_{ji}(x_i)$  in Eq. (4.7).

```

SUM-PRODUCT( $\mathcal{T}$ ,  $E$ )
  EVIDENCE( $E$ )
   $f = \text{CHOSEROOT}(\mathcal{V})$ 
  for  $s \in \mathcal{N}(f)$ 
     $\mu\text{-COLLECT}(f, s)$ 
    for  $s \in \mathcal{N}(f)$ 
       $\nu\text{-DISTRIBUTE}(f, s)$ 
    for  $i \in \mathcal{V}$ 
      COMPUTEMARGINAL( $i$ )

 $\mu\text{-COLLECT}(i, s)$ 
  for  $j \in \mathcal{N}(s) \setminus i$ 
     $\nu\text{-COLLECT}(s, j)$ 
     $\mu\text{-SENDMESSAGE}(s, i)$ 

 $\nu\text{-COLLECT}(s, i)$ 
  for  $t \in \mathcal{N}(i) \setminus s$ 
     $\mu\text{-COLLECT}(i, t)$ 
     $\nu\text{-SENDMESSAGE}(i, s)$ 

 $\mu\text{-DISTRIBUTE}(s, i)$ 
   $\mu\text{-SENDMESSAGE}(s, i)$ 
  for  $t \in \mathcal{N}(i) \setminus s$ 
     $\nu\text{-DISTRIBUTE}(i, t)$ 

 $\nu\text{-DISTRIBUTE}(i, s)$ 
   $\nu\text{-SENDMESSAGE}(i, s)$ 
  for  $j \in \mathcal{N}(s) \setminus i$ 
     $\mu\text{-DISTRIBUTE}(s, j)$ 

 $\mu\text{-SENDMESSAGE}(s, i)$ 
   $\mu_{si}(x_i) = \sum_{x_{\mathcal{N}(s) \setminus i}} (f_s(x_{\mathcal{N}(s)}) \prod_{j \in \mathcal{N}(s) \setminus i} \nu_{js}(x_j))$ 

 $\nu\text{-SENDMESSAGE}(i, s)$ 
   $\nu_{is}(x_i) = \prod_{t \in \mathcal{N}(i) \setminus s} \mu_{ti}(x_i)$ 

COMPUTEMARGINAL( $i$ )
   $p(x_i) \propto \nu_{is}(x_i) \mu_{si}(x_i)$ 

```

Figure 4.11: A sequential implementation of the SUM-PRODUCT algorithm for a factor tree  $\mathcal{T}(\mathcal{V}, \mathcal{F}, \mathcal{E})$ . The algorithm works for any choice of root node, and thus we have left CHOSEROOT unspecified. The subroutine EVIDENCE( $E$ ) is presented in Figure 4.5.

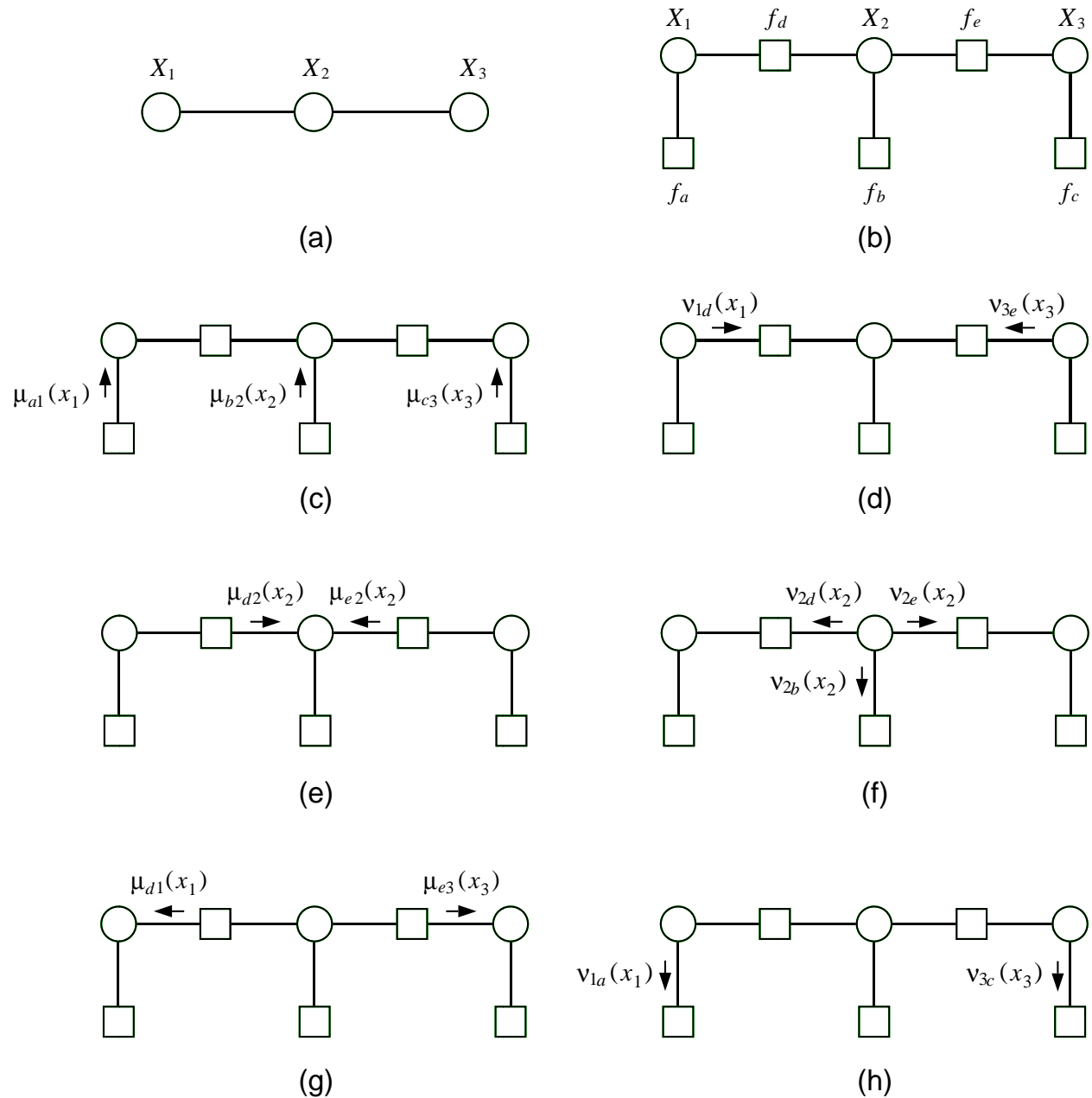


Figure 4.12: (a) A three-node undirected graphical model. (b) The factor tree representation. (c)-(h) A run of the SUM-PRODUCT algorithm on the factor tree.

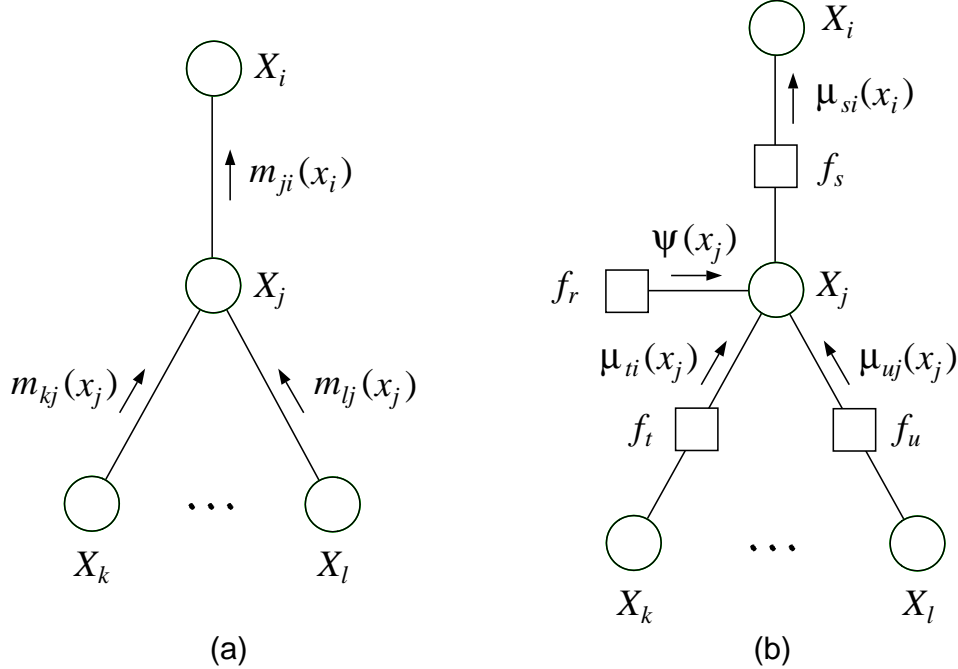


Figure 4.13: (a) A fragment of an undirected tree. (b) The corresponding fragment of a factor tree.

From this observation and an induction argument, it is not difficult to prove that the SUM-PRODUCT algorithm for factor trees is correct for factor trees that are obtained from undirected trees, by simply translating between the two versions of the SUM-PRODUCT algorithm. We leave this as an exercise (Exercise ??). It is also straightforward to develop a standalone proof by induction that the general SUM-PRODUCT algorithm for factor trees is correct, which we again leave as an exercise.

If a graph is originally a tree (undirected or directed), there is little to be gained by translating to the factor graph framework. The payoff for factor graphs arises when we consider various “tree-like” graphs, to which we now turn.

### 4.2.3 Tree-like graphs

Consider the graph shown in Figure 4.14(a). Assuming that the three-node cluster in the center of the graph is parameterized by a general non-factorized potential function, the probability distribution associated with the graph is given by:

$$p(x) \propto \psi(x_1, x_2)\psi(x_3, x_5)\psi(x_4, x_6)\psi(x_2, x_3, x_4), \quad (4.20)$$

where for simplicity we have neglected the singleton potentials. Although this graph is not a tree, it is “nearly” a tree. In particular, we could replace the three variables  $X_2$ ,  $X_3$ , and  $X_4$  with a new “super-variable”  $Z$ , whose range is the Cartesian product of the ranges of the three individual

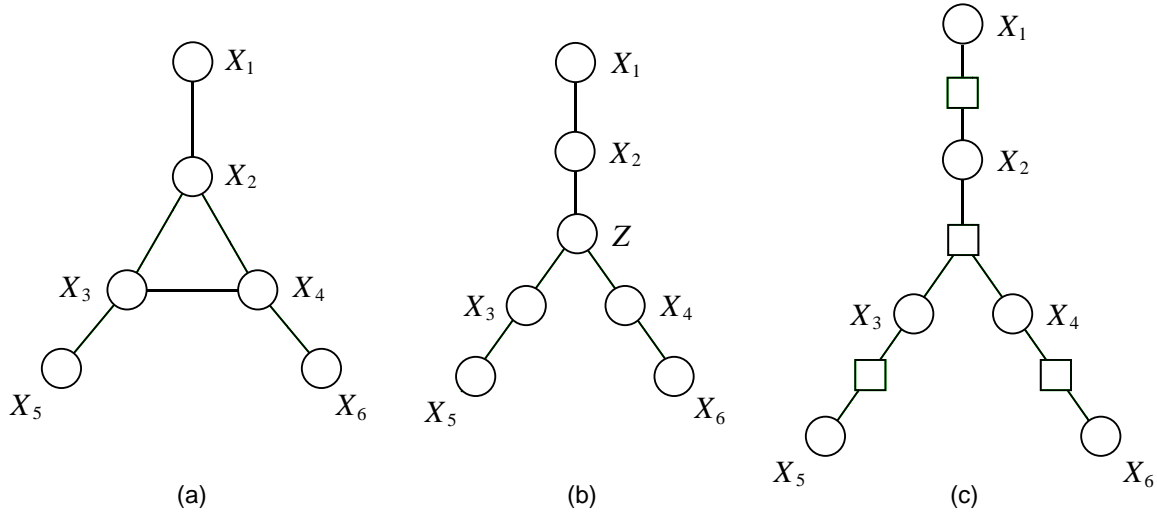


Figure 4.14: (a) An undirected graphical model in which the center cluster of nodes is assumed to be parameterized as a non-factorized potential,  $\psi(x_2, x_3, x_4)$ . (b) An equivalent undirected model based on the “super-variable”  $Z$ . (c) An equivalent factor graph.

variables. By creating new potential functions,  $\psi(x_1, z)$ ,  $\psi(x_5, z)$ ,  $\psi(x_6, z)$ , and  $\psi(z)$ , we can mimic the factorization in Eq. (4.20). Moreover, the corresponding undirected graphical model, shown in Figure 4.14(b), is a tree.

We can also capture the probability distribution in Eq. (4.20) using a factor graph. In particular, the graph translates directly to the factor graph shown in Figure 4.14(c). Note that the factor node at the center of the graph has three neighbors—representing the dependency structure of the potential  $\psi(x_2, x_3, x_4)$ . Note also that the factor graph is a factor tree.

We see that the distribution represented by the tree-like undirected graph in Figure 4.14(a) translates directly to a tree in the factor graph framework. There is no need to invent new variables and new potential functions.

Finally, of most significance is that the SUM-PRODUCT algorithm for factor trees applies directly to the graph in Figure 4.14(c). The fact that the original graph is not a tree is irrelevant—the factor graph *is* a tree, and the algorithm is correct for general factor trees.

In general, if the variables in an undirected graphical model can be clustered into non-overlapping cliques, and the parameterization of each clique is a general, non-factorized potential, then the corresponding factor graph is a tree, and the SUM-PRODUCT applies directly.

#### 4.2.4 Polytrees

A polytree is a tree-like graph that is important enough to merit its own section. In this section we discuss the SUM-PRODUCT algorithm for polytrees, again exploiting the factor graph framework.

As we have discussed, directed trees are essentially equivalent to undirected trees, providing no additional representational capability and no new issues for inference. On the other hand, the

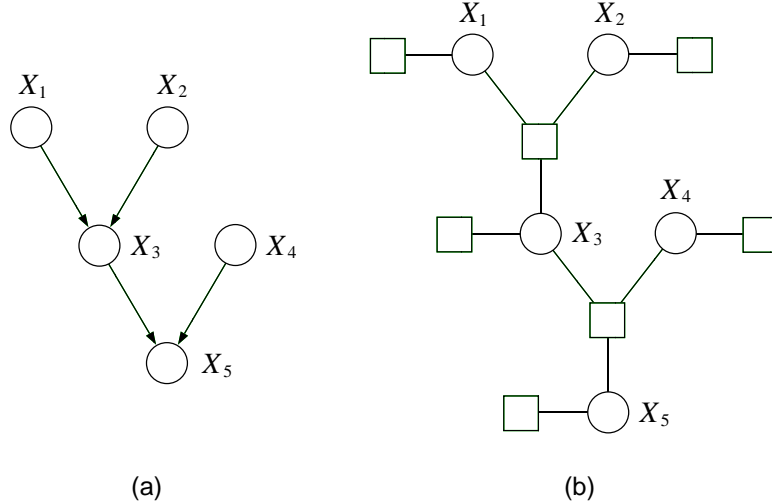


Figure 4.15: (a) A polytree. (b) The factor graph representation of the polytree in (a). Note that the factor graph is a factor tree.

directed graph shown in Figure 4.15(a) is a tree-like graph that does present new capabilities and new issues. As we saw in Chapter 2, the presence of nodes with multiple parents in a directed graph implies a conditional independence semantics that is not available in undirected graphs, including the “explaining-away” semantics that we studied in Chapter 2. Not surprisingly, this semantics has implications for inference, concretely via the conditional probability  $p(x_i | x_{\pi_i})$  that links a node with its parents.

A *polytree* is a directed graph that reduces to an undirected tree if we convert each directed edge to an undirected edge. Thus, polytrees have no loops in their underlying undirected graph.

One way to treat polytrees is via the “super-variable” approach. That is, we create a new variable for each combination of a node and its parents (each family) and link the super-variables (with undirected edges). It is easy to see that the resulting graph is a tree. This approach, however, suffers from the inelegance alluded to in the previous section.

Alternatively, we can use factor graphs. In Figure 4.15(b), we show the factor graph corresponding to the polytree in Figure 4.15(a). We see that the factor graph is a tree. Moreover, there is a factor corresponding to each family, representing the conditional probability  $p(x_i | x_{\pi_i})$ .

The fact that the factor graph corresponding to a polytree is a tree implies that the SUM-PRODUCT algorithm for factor graphs applies directly to polytrees.

Historically, polytrees were an important step along the way in the development of general exact inference algorithms for graphical models. In 1983, Kim and Pearl described a general sum-product-like algorithm for polytrees. As in the case of the SUM-PRODUCT algorithm for factor graphs, this algorithm also involves two kinds of messages—“ $\lambda$  messages” flowing from children to parents, and “ $\pi$  messages” flowing from parents to children. The algorithm can be derived readily from the SUM-PRODUCT algorithm for the corresponding factor graph. We present the algorithm in Exercise ??, and ask the reader to provide the derivation.

### 4.3 Maximum a posteriori probabilities

In this section we discuss a new problem—that of computing *maximum a posteriori probabilities*. Whereas the marginalization problem that we have addressed up until now involves summing over all configurations of sets of random variables, the maximum a posteriori (MAP) problem involves maximizing over such configurations. The problem has two aspects—that of finding the maximal probability and that of finding a configuration that achieves the maximal probability. We begin by focusing on the former problem.<sup>6</sup>

Given a probability distribution  $p(x)$ , where  $x = (x_1, x_2, \dots, x_n)$ , given a partition  $(E, F)$  of the indices, and given a fixed configuration  $\bar{x}_E$ , we wish to compute the maximum a posteriori probability  $\max_{x_F} p(x_F | \bar{x}_E)$ . Although we use the language of “maximum a posteriori probability” to describe this problem, the conditioning turns out to play little significant role in the problem. Indeed:

$$\max_{x_F} p(x_F | \bar{x}_E) = \max_{x_F} p(x_F, \bar{x}_E) \quad (4.21)$$

$$= \max_x p(x) \delta(x_E, \bar{x}_E) \quad (4.22)$$

$$\triangleq \max_x p^E(x), \quad (4.23)$$

where  $p^E(x)$  is the unnormalized representation of conditional probability introduced in Section 3.1.1. We see that without loss of generality we can study the unconditional case. That is, we treat the general problem of maximizing a nonnegative, factorized function of  $n$  variables; this includes as a special case the problem of maximizing such a function when some of the variables are held fixed.

It is important to be clear that the MAP problem is quite distinct from the marginalization problem. Naively, one might think that one could solve the MAP problem by first computing the marginal probability for each variable, and then computing the assignment of each variable that maximizes its individual marginal, but this is incorrect. Consider the pair of variables shown in Figure 4.16. The marginal probability of  $X$  is maximized by choosing  $X = 1$ , and the marginal probability of  $Y$  is maximized by choosing  $Y = 1$ . However, the joint probability of the configuration  $(X = 1, Y = 1)$  is equal to zero! The maximizing assignment is  $(X = 1, Y = 2)$ , which has probability 0.36.

Although the MAP problem is distinct from the marginalization problem, its algorithmic solution is quite similar. To see this, let us return to the example shown in Figure 4.17, a directed graphical model with the following factorization:

$$p(x) = p(x_1)p(x_2 | x_1)p(x_3 | x_1)p(x_4 | x_2)p(x_5 | x_3)p(x_6 | x_2, x_5). \quad (4.24)$$

To solve the MAP problem we expand the maximization into component-wise maximizations, and compute:

$$\max_x p(x) = \max_{x_1} \max_{x_2} \max_{x_3} \max_{x_4} \max_{x_5} \max_{x_6} p(x_1)p(x_2 | x_1)p(x_3 | x_1)p(x_4 | x_2)p(x_5 | x_3)p(x_6 | x_2, x_5)$$

---

<sup>6</sup>There are generalizations of the MAP problem that involve finding a small set of configurations that have high probability, and finding multiple configurations that have maximal probability when the maximum is not unique. In the current section, we restrict ourselves to the simpler problem of finding a single maximum.

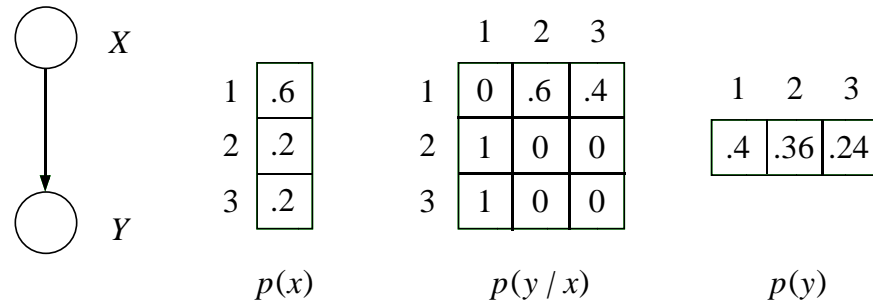


Figure 4.16: The marginal and conditional probabilities for a pair of variables  $(X, Y)$ . The maximizing values of the individual marginals are  $X = 1$  and  $Y = 1$ , but the configuration  $(X = 1, Y = 1)$  has zero probability.

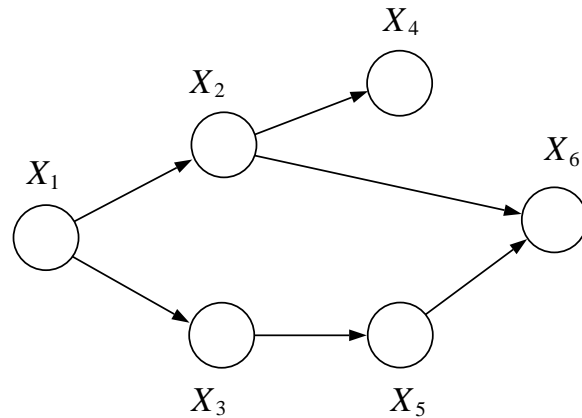


Figure 4.17: A directed graphical model.

```

MAP-ELIMINATE( $\mathcal{G}, E$ )
  INITIALIZE( $\mathcal{G}$ )
  EVIDENCE( $E$ )
  UPDATE( $\mathcal{G}$ )
  MAXIMUM

INITIALIZE( $\mathcal{G}$ )
  choose an ordering  $I$ 
  for each node  $X_i$  in  $\mathcal{V}$ 
    place  $p(x_i | x_{\pi_i})$  on the active list

EVIDENCE( $E$ )
  for each  $i$  in  $E$ 
    place  $\delta(x_i, \bar{x}_i)$  on the active list

UPDATE( $\mathcal{G}$ )
  for each  $i$  in  $I$ 
    find all potentials from the active list that reference  $x_i$  and remove them from the active list
    let  $\phi_i^{\max}(x_{T_i})$  denote the product of these potentials
    let  $m_i^{\max}(x_{S_i}) = \max_{x_i} \phi_i^{\max}(x_{T_i})$ 
    place  $m_i^{\max}(x_{S_i})$  on the active list

MAXIMUM
   $\max_x p^E(x) =$  the scalar value on the active list

```

Figure 4.18: The MAP-ELIMINATE algorithm for solving the maximum a posteriori problem. Note that after the final node has been eliminated in UPDATE, the active list contains a single scalar value, which is the value returned as the maximum by the algorithm.

$$= \max_{x_1} p(x_1) \max_{x_2} p(x_2 | x_1) \max_{x_3} p(x_3 | x_1) \max_{x_4} p(x_4 | x_2) \max_{x_5} p(x_5 | x_3) \max_{x_6} p(x_6 | x_2, x_5).$$

These steps should look familiar from our earlier example of marginalization in this graph. Continuing the computation, we perform the maximization with respect to  $x_6$ , thereby defining an “intermediate factor” that is a function of  $x_2$  and  $x_5$ . Subsequent steps are identical to those of a marginalization computation, with the “sum” operator replaced by the “max” operator.

More generally, all of the derivations that we have presented in this chapter and the previous chapter go through if the “sum” operator is replaced everywhere by the “max” operator. In particular, by making this substitution in ELIMINATE, we obtain a MAP version of ELIMINATE, which we present in Figure 4.18.

The reason that the derivations go through when “sum” is replaced by “max” is that both the “sum-product” pair and the “max-product” pair are examples of an algebraic structure known as a *commutative semiring*. A commutative semiring is a set endowed with two operations—generically

referred to as “addition” and “multiplication”—that obey certain laws. In particular, addition and multiplication are both required to be *associative* and *commutative*. Moreover, multiplication is *distributive* over addition:

$$a \cdot b + a \cdot c = a \cdot (b + c). \quad (4.25)$$

This distributive law played a key role in our derivation of ELIMINATE, in which the “sum” operator repeatedly migrates across the “product” operator. Also, the ability to group and reorder intermediate factors was required in the derivation of the ELIMINATE algorithm. In fact, it can be verified that the associative, commutative and distributive laws are all that are needed to derive the ELIMINATE algorithm and the SUM-PRODUCT algorithm. (Note in particular that we do not require division, an operation that is available in the more restrictive algebraic object known as a *ring*.)

If we let the “max” operator play the role of addition, the fact that “max” distributes over “product”:

$$\max(a \cdot b, a \cdot c) = a \cdot \max(b, c) \quad (4.26)$$

shows that “max-product” is a semiring (given the easy verification that “max” is associative and commutative), and justifies the MAP-ELIMINATE algorithm in Figure 4.18.

A practical problem with the MAP-ELIMINATE algorithm shown in Figure 4.18 is that the products of probabilities tend to underflow. This can be handled by transforming to the log scale, making use of the fact that:

$$\max_x p^E(x) = \max_x \log p^E(x), \quad (4.27)$$

which holds because the logarithm is a monotone function. Given that the logarithm of a product becomes a sum of logarithms, we see that such an implementation essentially involves working with a “max-sum” pair instead of a “max-product” pair. Fortunately, “max-sum” is also a semiring, in which “max” plays the role of addition and “sum” plays the role of multiplication. Indeed, the distributive law is easily verified:

$$\max(a + b, a + c) = a + \max(b, c), \quad (4.28)$$

as are the associative and commutative laws. Thus we can implement MAP-ELIMINATE algorithm by working with logarithms of potentials, and replacing “product” with “sum.”

There are many other commutative semirings, including semirings on polynomials and distributive lattices. We explore some of these commutative semirings in the exercises. The generic ELIMINATE algorithm can be easily adapted to each of these commutative semirings.

In Section ?? we showed that in the case of trees, the ELIMINATE algorithm can be equivalently expressed in terms of a coupled set of equations, or “messages,” a line of argument that led to the SUM-PRODUCT algorithm for inference on trees. The same arguments apply to arbitrary commutative semirings, and in particular we can obtain a “MAX-PRODUCT” version of the algorithm as follows:

$$m_{ji}^{\max}(x_i) = \max_{x_j} \left( \psi^E(x_j) \psi(x_i, x_j) \prod_{k \in \mathcal{N}(j) \setminus i} m_{kj}^{\max}(x_j) \right) \quad (4.29)$$

$$\max_x p^E(x) = \max_{x_i} \left( \psi^E(x_i) \prod_{j \in \mathcal{N}(i)} m_{ji}^{\max}(x_i) \right). \quad (4.30)$$

Implementing a depth-first traversal of the tree, thereby passing messages from the leaves toward an arbitrarily-defined root, we invoke Eq. (4.30) at the root and obtain the MAP solution.

Is there any value in considering a full message-passing algorithm in which we also send messages from the root back toward the leaves? If the problem is simply that of finding the maximal value of the MAP probability,  $\max_x p^E(x)$ , then the answer is no. Invoking Eq. (4.30) at multiple nodes in the graph, we obtain exactly the same solution—in all cases we have maximized over all nodes in the graph. However, if our goal is also that of obtaining a maximizing configuration—a configuration  $x^*$  such that  $x^* \in \arg \max_x p^E(x)$ —then we can make use of an appropriately defined outward phase. We explore this issue in the following section.

### 4.3.1 Maximum a posteriori configurations

Let us now consider the problem of finding a configuration  $x^*$  such that  $x^* \in \arg \max_x p^E(x)$ . This problem can be solved by keeping track of the maximizing values of variables in the inward pass of the MAX-PRODUCT algorithm, and using these values as indices in an outward pass.

Throughout this section we assume that an arbitrary root node  $f$  has been chosen, and refer to an “inward pass” in which messages flow from the leaves toward the root, and an “outward pass” in which messages flow from the root toward the leaves.

Note that when the MAX-PRODUCT algorithm arrives at the root node at the end of the inward pass, the final maximization in Eq. (4.30) provides us with a value of the root node that belongs to a maximizing configuration. Thus, letting  $f$  denote the root, we compute:

$$x_f^* \in \arg \max_{x_f} \left( \psi^E(x_f) \prod_{e \in \mathcal{N}(f)} m_{ef}^{\max}(x_f) \right), \quad (4.31)$$

and thereby obtain a value  $x_f^*$  that necessarily belongs to a maximizing configuration. Moreover, in principle we could perform an outward pass in which we evaluate Eq. (4.29) for each node from the root to the leaves, and subsequently perform the maximization in Eq. (4.30) at each node. This would yield values  $x_i^*$  that belong to maximizing configurations. Unfortunately, however, there is no guarantee that these values all belong to the *same* maximizing configuration. To find a single maximizing configuration we have to work a bit harder.

Suppose that during the inward pass we maintain a record of the maximizing values of nodes when we compute the messages  $m_{ji}^{\max}(x_i)$ . That is, whenever we send a message  $m_{ji}^{\max}(x_i)$  from node  $j$  to its parent node  $i$ , we also record the maximizing values in a table  $\delta_{ji}(x_i)$ :

$$\delta_{ji}(x_i) \in \arg \max_{x_j} \left( \psi^E(x_j) \psi(x_i, x_j) \prod_{k \in \mathcal{N}(j) \setminus i} m_{kj}^{\max}(x_j) \right). \quad (4.32)$$

Thus, for each  $x_i$ , the function  $\delta_{ji}(x_i)$  picks out a value of  $x_j$  (there may be several) that achieves the maximum.

Having defined the function  $\delta_{ji}(x_i)$  during the inward pass, we use  $\delta_{ji}(x_i)$  to define a consistent maximizing configuration during an outward pass. Thus, starting at the root  $f$ , we choose a maximizing value  $x_f^*$ . Given this value, which we pass to the children of  $f$ , we set  $x_e^* = \delta_{ef}(x_f^*)$  for each  $e \in \mathcal{N}(f)$ . This procedure continues outward to the leaves.

The resulting algorithm is summarized in Figure 4.19. Note that the computation of the  $m_{ji}^{\max}(x_i)$  messages in the inward pass of this algorithm is identical to the MAP-ELIMINATE algorithm (for undirected trees).

## 4.4 Conclusions

In this chapter we have presented a basic treatment of algorithms for computing probabilities on graphs. Restricting ourselves to trees, we presented the SUM-PRODUCT algorithm, an algorithm for computing all singleton marginal probabilities. We also presented a SUM-PRODUCT algorithm for factor trees, and showed how this algorithm allows us to compute marginal probabilities for various tree-like graphs, including polytrees. Finally, we showed that the algebra underlying the SUM-PRODUCT algorithm can be abstracted, yielding a general family of propagation algorithms based on commutative semirings. In particular, we presented the MAX-PRODUCT algorithm, an algorithm for computing maximum a posteriori probabilities.

Henceforth we will refer to all such propagation algorithms as *probability propagation algorithms*. While we have restricted ourselves to trees in the current chapter, we will be considering probability propagation algorithms on more general graphs in later chapters.

Thus far we have focused on the problems of representation and inference in graphical models. We return to these problems in Chapters 16 and 17, providing a more general and more formal treatment of topics such as conditional independence and probability propagation. In the intervening chapters, however, we shift to a different line of inquiry. In particular, we now begin to address the problem of interfacing graphical models to data, and we begin to develop methods for evaluating and improving models on the basis of such data. We thus take up the statistical side of the story.

## 4.5 Historical remarks and bibliography

```

MAX-PRODUCT( $\mathcal{T}$ ,  $E$ )
  EVIDENCE( $E$ )
   $f = \text{CHOSEROOT}(\mathcal{V})$ 
  for  $e \in \mathcal{N}(f)$ 
    COLLECT( $f, e$ )
     $MAP = \max_{x_f} (\psi^E(x_f) \prod_{e \in \mathcal{N}(f)} m_{ef}^{\max}(x_f))$ 
     $x_f^* = \arg \max_{x_f} (\psi^E(x_f) \prod_{e \in \mathcal{N}(f)} m_{ef}^{\max}(x_f))$ 
    for  $e \in \mathcal{N}(f)$ 
      DISTRIBUTE( $f, e$ )

COLLECT( $i, j$ )
  for  $k \in \mathcal{N}(j) \setminus i$ 
    COLLECT( $j, k$ )
    SENDMESSAGE( $j, i$ )

DISTRIBUTE( $i, j$ )
  SETVALUE( $i, j$ )
  for  $k \in \mathcal{N}(j) \setminus i$ 
    DISTRIBUTE( $j, k$ )

SENDMESSAGE( $j, i$ )
   $m_{ji}^{\max}(x_i) = \max_{x_j} (\psi^E(x_j) \psi(x_i, x_j) \prod_{k \in \mathcal{N}(j) \setminus i} m_{kj}^{\max}(x_j))$ 
   $\delta_{ji}(x_i) \in \arg \max_{x_j} (\psi^E(x_j) \psi(x_i, x_j) \prod_{k \in \mathcal{N}(j) \setminus i} m_{kj}^{\max}(x_j))$ 

SETVALUE( $i, j$ )
   $x_j^* = \delta_{ji}(x_i^*)$ 

```

Figure 4.19: A sequential implementation of the MAX-PRODUCT algorithm for a tree  $\mathcal{T}(\mathcal{V}, \mathcal{E})$ . The algorithm works for any choice of root node, and thus we have left CHOSEROOT unspecified. The subroutine EVIDENCE( $E$ ) is presented in Figure 4.5.

# An Introduction to Probabilistic Graphical Models

Michael I. Jordan  
*University of California, Berkeley*

June 30, 2003



## Chapter 5

# Statistical Concepts

It is useful to attempt to distinguish the activities of the probability theorist and the statistician. Our perspective in the previous chapters has been mainly that of the former—we have built graphical models involving sets of random variables and shown how to compute the probabilities of certain events associated with these random variables. Given a particular choice of graphical model, consisting of a graph and a set of local conditional probabilities or potentials, we have seen how to infer the probabilities of various events of interest, such as the marginal or conditional probability that a particular random variable takes on a particular value.

Statistics is in a certain sense the inverse of probability theory. In a statistical setting the random variables in our domain have been *observed* and are therefore no longer unknown, rather it is the model that is unknown. We wish to infer the model from the data rather than the data from the model.

The problem of “inferring the model from the data” is a deep one, raising fundamental questions regarding the nature of knowledge, reasoning, learning, and scientific inquiry. In statistics, the study of these fundamental questions has often come down to a distinction between two major schools of thought—the *Bayesian* and the *frequentist*. In the following section we briefly outline the key distinctions between these two schools. It is worth noting that our discussion here will be incomplete and that we will be returning to these distinctions at various junctures in the book as our development of graphical models begins to bring the distinctions into clearer relief. But an equally important point to make is that many of the problems—particularly the computational problems—faced in these frameworks are closely related, even identical. A great deal of important work can be done within the graphical models formalism that is equally useful to Bayesian and frequentist statistics.

Beyond our discussion of foundational issues, we will also introduce several classes of statistical problems in this chapter, in particular the core problems of *density estimation*, *regression* and *classification*. As in earlier chapters our goal is to present enough in the way of concrete details to make the discussion understandable, but to emphasize broad themes that will serve as landmarks for our more detailed presentation in later chapters.

## 5.1 Bayesian and frequentist statistics

Bayesian statistics is in essence an attempt to deny any fundamental distinction between probability theory and statistics. Probability theory itself provides the capability for inverting relationships between uncertain quantities—this is the essence of *Bayes rule*—and Bayesian statistics represents an attempt to treat all statistical inference as probabilistic inference.

Let us consider a problem in which we have already decided upon the model *structure* for a given problem domain—for example, we have chosen a particular graphical model including a particular pattern of connectivity—but we have not yet chosen the values of the model *parameters*—the numerical values of the local conditional probabilities or potentials. We wish to choose these parameter values on the basis of observed data. (In general we might also want to choose the model structure on the basis of observed data, but let us postpone that problem—see Section 5.3).

For every choice of parameter values we obtain a different numerical specification for the joint distribution of the random variables  $X$ . We will henceforth write this probability distribution as  $p(x|\theta)$  to reflect this dependence. Putting on our hats as probability theorists, we view the model  $p(x|\theta)$  as a conditional probability distribution; intuitively it is an assignment of probability mass to unknown values of  $X$ , given a fixed value of  $\theta$ . Thus,  $\theta$  is known and  $X$  is unknown. As statisticians, however, we view  $X$  as known—we have observed its realization  $x$ —and  $\theta$  as unknown. We thus in some sense need to invert the relationship between  $x$  and  $\theta$ . The Bayesian point of view implements this notion of “inversion” using Bayes rule:

$$p(\theta|x) = \frac{p(x|\theta)p(\theta)}{p(x)}. \quad (5.1)$$

The assumptions allowing us to write this equation are noteworthy. First, in order to interpret the left-hand side of the equation we must view  $\theta$  as a random variable. This is characteristic of the Bayesian approach—all unknown quantities are treated as random variables. Second, we view the data  $x$  as a quantity to be conditioned on—our inference is conditional on the event  $\{X = x\}$ . Third, in order to calculate  $p(\theta|x)$  we see (from the right-hand side of Eq. (5.1)) that we must have in hand the probability distribution  $p(\theta)$ —the *prior probability* of the parameters. Given that we are viewing  $\theta$  as a random variable, it is formally reasonable to assign a (marginal) probability to it, but one needs to think about what such a prior probability means in terms of the problem we are studying. Finally, note that Bayes rule yields a distribution over  $\theta$ —the *posterior probability* of  $\theta$  given  $x$ , not a single estimate of  $\theta$ . If we wish to obtain a single value, we must (and will) invoke additional principles, but it is worth noting at the outset that the Bayesian approach tends to resist collapsing distributions to points.

The frequentist approach wishes to avoid the use of prior probabilities in statistics, and thus avoids the use of Bayes rule for the purpose of assigning probabilities to parameters. The goal of frequentist methodology is to develop an “objective” statistical theory, in which two statisticians employing the methodology must necessarily draw the same conclusions from a particular set of data.

Consider in particular a coin-tossing experiment, where  $X \in \{0, 1\}$  is a binary variable representing the outcome of the coin toss, and  $\theta \in (0, 1)$  is a real-valued parameter denoting the probability of heads. Thus the model is the Bernoulli distribution,  $p(x|\theta) = \theta^x(1-\theta)^{1-x}$ . Approaching the

problem from a Bayesian perspective requires us to assign a prior probability to  $\theta$  before observing the outcome of the coin toss. Two different Bayesian statisticians may assign different priors to  $\theta$  and thus obtain different conclusions from the experiment. The frequentist statistician wishes to avoid such “subjectivity.” From another point of view, a frequentist may claim that  $\theta$  is a fixed property of the coin, and that it makes no sense to assign probability to it. A Bayesian may agree with the former statement, but would argue that  $p(\theta)$  need not represent anything about the physics of the situation, but rather represents the *statistician’s uncertainty* about the value of  $\theta$ . Tossing the coin reduces the statistician’s uncertainty, and changes the prior probability into the posterior probability  $p(\theta | x)$ . Bayesian statistics views the posterior probability and the prior probability alike as (possibly) subjective.

There are situations in which frequentist statistics and Bayesian statistics agree that parameters can be endowed with probability distributions. Suppose that we consider a factory that makes coins in batches, where each batch is characterized by a smelting process that affects the fairness of the resulting coins. A coin from a given batch has a different probability of heads than a coin from a different batch, and ranging over batches we obtain a distribution on the probability of heads  $\theta$ . A frequentist is in general happy to assign prior probabilities to parameters, as long as those probabilities refer to objective frequencies of observing values of the parameters in repeated experiments.

From the point of view of frequentist statistics, there is no single preferred methodology for inverting the relationship between parameters and data. Rather, the basic idea is to consider various *estimators* of  $\theta$ , where an estimator is some function of the observed data  $x$  (we will discuss a particular example below). One establishes various general criteria for evaluating the quality of various estimators, and chooses the estimator that is “best” according to these criteria. (Examples of such criteria include the *bias* and *variance* of estimators; these criteria will be discussed in Chapter 26). An important feature of this evaluation process is that it generally requires that the data  $x$  be viewed as the result of a random experiment that can be repeated and in which other possible values of  $x$  could have been obtained. This is of course consistent with the general frequentist philosophy, in which probabilities correspond to objective frequencies.

There is one particular estimator that is widely used in frequentist statistics, namely the *maximum likelihood* estimator. This estimator is popular for a number of reasons, in particular because it often yields “natural estimators” (e.g., sample proportions and sample means) in simple settings and also because of its favorable asymptotic properties.

To understand the maximum likelihood estimator, we must understand the notion of “likelihood” from which it derives. Recall that the probability model  $p(x | \theta)$  has the intuitive interpretation of assigning probability to  $X$  for each fixed value of  $\theta$ . In the Bayesian approach this intuition is formalized by treating  $p(x | \theta)$  as a conditional probability distribution. In the frequentist approach, however, such a formal interpretation is suspect, because it suggests that  $\theta$  is a random variable that can be conditioned on. The frequentist instead treats the model  $p(x | \theta)$  as a family of probability distributions indexed by  $\theta$ , with no implication that we are conditioning on  $\theta$ .<sup>1</sup> Moreover, to implement a notion of “inversion” between  $x$  and  $\theta$ , we simply change our point

---

<sup>1</sup>To acknowledge this interpretation, frequentist treatments often adopt the notation  $p_\theta(x)$  in place of  $p(x | \theta)$ . We will stick with  $p(x | \theta)$ , hoping that the frequentist-minded reader will forgive us this abuse of notation. It will

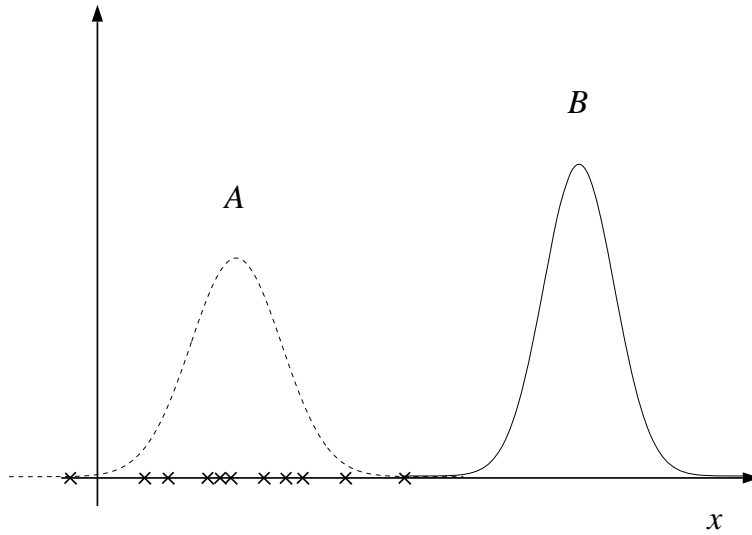


Figure 5.1: A univariate density estimation problem. (See Section 5.2.1 for a discussion of density estimation). The data  $\{x_1, x_2, \dots, x_N\}$  are given as X's along the abscissa. The parameter vector  $\theta$  is the mean  $\mu$  and variance  $\sigma^2$  of a Gaussian density. Two candidate densities, involving different values of  $\theta$ , are shown in the figure. Density A assigns higher probability to the observed data than density B, and thus would be preferred according to the principle of maximum likelihood.

of view—we treat  $p(x | \theta)$  as a function of  $\theta$  for fixed  $x$ . When interpreted in this way,  $p(x | \theta)$  is referred to as the *likelihood function* and it provides the basis for maximum likelihood estimation.

As suggested in Figure 5.1, the likelihood function can be used to evaluate particular choices of  $\theta$ . In particular, if for a given value of  $\theta$  we find that the observed value of  $x$  is assigned low probability, then this is perhaps a poor choice of  $\theta$ . A value of  $\theta$  that assigns higher probability to  $x$  is preferred. Ranging over all possible choices of  $\theta$ , we pick that value of  $\theta$  that assigns maximal probability to  $x$ , and treat this value as an estimate of the true  $\theta$ :

$$\hat{\theta}_{ML} = \operatorname{argmax}_\theta p(x | \theta). \quad (5.2)$$

Thus the maximum likelihood estimate is that value of  $\theta$  that maximizes the likelihood function.

Regardless of whether one agrees that this justification of the maximum likelihood estimate is a natural one, it is certainly true that we have an estimator—a function of  $x$ —and we can evaluate the properties of this estimator under various frequentist criteria. It turns out that maximum likelihood is a good estimator under a variety of measures of quality, particularly in settings of large sample sizes when asymptotic analyses are meaningful (indeed, maximum likelihood estimates can be shown to be “optimal” in such settings). In other settings, particularly in cases of small sample sizes, maximum likelihood plays an important role as the starting point for the development of more complex estimators.

---

simplify our presentation throughout the rest of the book, liberating us from having to make distinctions between Bayesian and frequentist interpretations where none are needed or implied.

Another appealing feature of likelihood-based estimation is that it provides a link between Bayesian methods and frequentist methods. In particular, note that the distribution  $p(x|\theta)$  appears in our basic Bayesian equation Eq. (5.1). Note moreover that Bayesian statisticians refer to this probability as a “likelihood” as do frequentist statisticians, even though the interpretation is different. Symbolically, we can interpret Eq. (5.1) as follows:

$$\text{posterior} \propto \text{likelihood} \times \text{prior}, \quad (5.3)$$

where we see that in the Bayesian approach the likelihood can be viewed as a data-dependent operator that transforms between the prior probability and the posterior probability. At a bare minimum, Bayesian approaches and likelihood-based frequentist approaches have in common the need to calculate the likelihood for various values of  $\theta$ . This is not a trivial fact—indeed a major focus of this book is the set of complex statistical models in which the computation of the likelihood is itself a daunting computational task. In working out effective computational procedures to deal with such models we are contributing to both Bayesian and frequentist statistics.

Let us explore this connection between Bayesian and frequentist approaches a bit further. Suppose in particular that we force the Bayesian to choose a particular value of  $\theta$ ; that is, to collapse the posterior distribution  $p(\theta|x)$  to a point estimate. Various possibilities present themselves; in particular one could choose the mean of the posterior distribution or perhaps the mode. The mean of the posterior is often referred to as a *Bayes estimate*:

$$\hat{\theta}_{\text{Bayes}} = \int \theta p(\theta|x)d\theta, \quad (5.4)$$

and it is possible and worthwhile to study the frequentist properties of Bayes estimates. The mode of the posterior is often referred to as the *maximum a posteriori (MAP)* estimate:

$$\hat{\theta}_{\text{MAP}} = \operatorname{argmax}_{\theta} p(\theta|x) \quad (5.5)$$

$$= \operatorname{argmax}_{\theta} p(x|\theta)p(\theta), \quad (5.6)$$

where in the second equation we have utilized the fact that the factor  $p(x)$  in the denominator of Bayes rule is independent of  $\theta$ . In a setting in which the prior probability is taken to be uniform on  $\theta$ , the MAP estimate reduces to the maximum likelihood estimate. When the prior is not taken to be uniform, one can still view Eq. (5.6) as the maximization of a *penalized likelihood*. To see this, note that one generally works with logarithms when maximizing over probability distributions (the fact that the logarithm is a monotonic function implies that it does not alter the optimizing value). Thus one has:

$$\hat{\theta}_{\text{MAP}} = \operatorname{argmax}_{\theta} \{ \log p(x|\theta) + \log p(\theta) \}, \quad (5.7)$$

as an alternative expression for the MAP estimate. Here the “penalty” is the additive term  $\log p(\theta)$ . Penalized log likelihoods are widely used in frequentist statistics to improve on maximum likelihood estimates in small sample settings (as we will see in Chapter 26).

It is important to emphasize, however, that MAP estimation involves a rather un-Bayesian use of the Bayesian formalism, and it would be wrong to understand the distinction between Bayesian and frequentist statistics as merely a matter of how to interpret a penalized log likelihood. To clarify,

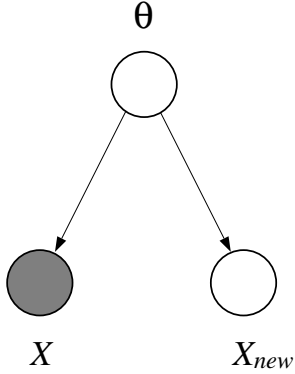


Figure 5.2: A graphical representation of the problem of prediction from a Bayesian point of view.

let us consider a somewhat broader problem in which the difference between MAP estimation and a fuller Bayesian approach is more salient. Let us consider the problem of *prediction*, where we are not interested in the value of  $\theta$  per se, but are interested in using a model based on  $\theta$  to predict future values of the random variable  $X$ . Let us suppose in particular that we have two random variables,  $X$  and  $X_{new}$ , which are characterized by the same distribution, and that we wish to use an observation of  $X$  to make a prediction regarding likely values of  $X_{new}$ . For simplicity, let us assume that  $X$  and  $X_{new}$  are independent; more precisely, we assume that they are conditionally independent given  $\theta$ . We write:

$$p(x_{new} | x) = \int p(x_{new}, \theta | x) d\theta \quad (5.8)$$

$$= \int p(x_{new} | \theta, x) p(\theta | x) d\theta \quad (5.9)$$

$$= \int p(x_{new} | \theta) p(\theta | x) d\theta. \quad (5.10)$$

From the latter equation we see that the Bayesian prediction is based on combining the predictions across all values of  $\theta$ , with the posterior distribution serving as a “weighting function.” That is, interpreting the conditional probability  $p(x_{new} | \theta)$  as the prediction of  $X_{new}$  given  $\theta$ , we weight this prediction by the posterior probability  $p(\theta | x)$ , and integrate over all such weighted predictions. Note in particular that this calculation requires the entire posterior probability, not merely its value at a single point.

Within a frequentist approach, we are not allowed to treat  $\theta$  as a random variable, and thus we do not attribute meaning to the integral in Eq. (5.10). Rather, we would consider various “estimates” of  $x_{new}$ ; a natural choice might be the “plug-in estimate”  $p(x_{new} | \hat{\theta}_{ML})$ . Here we see that the difference between the frequentist approach and the Bayesian approach has become more significant; in the latter case we have to perform an integral in order to obtain a prediction. We can relate the two approaches if we approximate the posterior distribution by collapsing it to a delta function at  $\hat{\theta}_{MAP}$ , in which case the integral in Eq. (5.10) reduces to the plug-in estimate

$p(x_{new} | \hat{\theta}_{MAP})$ . But in general this collapse would not satisfy the Bayesian (who views the integral as providing a better predictor than any predictor based on a point estimate) nor the frequentist (who wants to be free to consider a wider class of estimates than the plug-in estimate).

As a final note, consider the graphical model shown in Figure 5.2. This model captures the Bayesian point of view on the prediction problem that we have just discussed. The parameter  $\theta$  is depicted as a node in the model; this is of course consistent with the Bayesian approach of treating parameters as random variables. Moreover, the conditional independence of  $X$  and  $X_{new}$  given  $\theta$  is reflected as a Markov property in the graph. Finally, as we invite the reader to verify in Exercise ??, applying the elimination algorithm to the graph yields exactly the calculation in Eq. (5.10). This is a reflection of a general fact—graphical models provide a nice way to visualize and organize Bayesian calculations. We will return to this point in later chapters. But let us emphasize here that this linkage, appealing as it is, does not reflect any special affinity between graphical models and Bayesian methods, but rather is a reflection of the more general link between Bayesian methods and probabilistic inference.

## 5.2 Statistical problems

Let us now descend from the somewhat ethereal considerations of statistical foundations to a rather more concrete consideration of problems in statistical estimation. In this section we will discuss three major classes of statistical problems—*density estimation*, *regression*, and *classification*. Not all statistical problems fall into one of these three classes, nor is it always possible to unambiguously characterize a given problem in terms of these classes, but there are certain core aspects of these three problem categories that are worth isolating and studying in a purified form.

We have two main goals in this section. The first is to introduce the graphical approach to representing statistical modeling problems, in particular emphasizing how the graphical representation helps makes modeling assumptions explicit. Second, we wish to begin to work with specific probability distributions, in particular the Gaussian and multinomial distributions. We will use this introductory section to illustrate some of the calculations that arise when using these distributions.

### 5.2.1 Density estimation

Suppose that we have in hand a set of observations on a random variable  $X$ —in general a vector-valued random variable—and we wish to use these observations to induce a probability density (probability mass function for discrete variables) for  $X$ . This problem—which we refer to generically as the problem of density estimation—is a very general statistical problem. Obtaining a model of the density of  $X$  allows us to assess whether a particular observation of  $X$  is “typical,” an assessment that is required in many practical problems including *fault detection*, *outlier detection* and *clustering*. Density estimation also underlies many *dimensionality reduction* algorithms, where a joint density is projected onto a subspace or manifold, hopefully reducing the dimensionality of a data set while retaining its salient features. A related application is *compression*, where Shannon’s fundamental relationship between code length and the negative logarithm of the density can be used to design a source code. Finally, noting that a joint density on  $X$  can be used to infer conditional

densities among components of  $X$ , we can also use density estimates to solve problems in prediction.

To delimit the scope of the problem somewhat, note that in regression and classification the focus is on the relationship between a pair of variables,  $X$  and  $Y$ . That is, regression and classification problems differ from density estimation in that their focus is on a conditional density,  $p(y | x)$ , with the marginal  $p(x)$  and the corresponding joint density of less interest, and perhaps not modeled at all. We develop methods that are specific to conditional densities in Sections 5.2.2 and 5.2.3.

Density estimation arises in many ways in the setting of graphical models. In particular we may be interested in inferring the density of a parentless node in a directed graphical model, or the density of a set of nodes in a larger model (in which case the density of interest is a marginal density), or the joint density of all of the nodes of our model.

Let us begin with an example. Our example will be one of the most classical of all statistical problems—that of estimating the mean and variance of a univariate Gaussian distribution.

### Univariate Gaussian density estimation

Let us assume that  $X$  is a univariate random variable with a Gaussian distribution, that is:

$$p(x | \theta) = \frac{1}{(2\pi\sigma^2)^{1/2}} \exp\left\{-\frac{1}{2\sigma^2}(x - \mu)^2\right\}, \quad (5.11)$$

where  $\mu$  and  $\sigma^2$  are the mean and variance, respectively, and  $\theta \triangleq (\mu, \sigma^2)$ .<sup>2</sup> We wish to estimate  $\theta$  based on observations of  $X$ . Here we are assuming that we know the parametric form of the density of  $X$ , and what is unknown are the numerical values of the parameters (cf. Figure 5.1). Plugging estimates of the parameters back into Eq. (5.11) provides an estimate of the density function.

Clearly a single observation of  $X$  provides no information about the variance and relatively poor information about the mean. Thus we need to consider multiple observations. What do we mean by “multiple observations”? Let us interpret this to mean that we have a *set of random variables*,  $\{X_1, X_2, \dots, X_N\}$ , and that these random variables are *identically distributed*. Thus each of the variables  $X_n$  is characterized by a Gaussian distribution  $p(x_n | \theta)$ , with the same  $\theta$  for each  $X_n$ .

In graphical model terms, we have a model with  $N$  nodes, one for each random variable. Which graphical model should we use? What connectivity pattern should we use? Let us suppose that the variables are not only identically distributed but that they are also *independent*. Thus we have the graphical model shown in Figure 5.3. It should be emphasized that these assumptions are by no means necessary; they are simply one possible set of assumptions, corresponding to a particular choice of graphical model. (We will be seeing significantly more complex graphical models on  $N$  Gaussian nodes; see, e.g., the Kalman filter in Chapter 15).

The nodes in Figure 5.3 are shaded, reflecting the fact that they are *observed data*. In general, “data” are designated by the shading of nodes in our models. In the context of the Bayesian approach to estimation, this use of shading is the same convention as we used in Chapter 2—in the Bayesian approach we *condition on the data* in order to compute probabilities for the parameters. In the context of frequentist approaches, where we no longer view ourselves as conditioning on the

---

<sup>2</sup>We will often denote this density as  $\mathcal{N}(\mu, \sigma^2)$ .

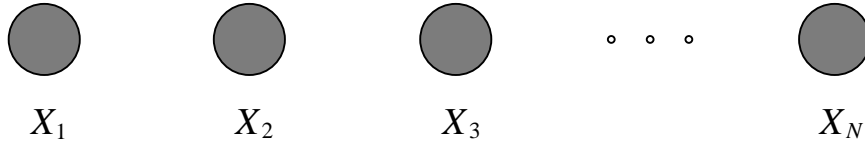


Figure 5.3: A graphical model representing the density estimation problem under an IID sampling model. The assumption that the data are sampled independently is reflected by the absence of links between the nodes. Each node is characterized by the same density.

data, we simply treat shading as a diagrammatic convention to indicate which nodes correspond to the observed data.

Letting  $X$  refer to the set of random variables  $(X_1, X_2, \dots, X_N)$ , and letting  $x$  refer to the observations  $(x_1, x_2, \dots, x_N)$ , we write the joint probability  $p(x | \theta)$  as the product of local probabilities, one for each node in Figure 5.3:

$$p(x | \theta) = \prod_{n=1}^N \frac{1}{(2\pi\sigma^2)^{1/2}} \exp\left\{-\frac{1}{2\sigma^2}(x_n - \mu)^2\right\} \quad (5.12)$$

$$= \frac{1}{(2\pi\sigma^2)^{N/2}} \exp\left\{-\frac{1}{2\sigma^2} \sum_{n=1}^N (x_n - \mu)^2\right\}, \quad (5.13)$$

or alternatively, given that this particular graph can be interpreted as either a directed graph or an undirected graph, we can view this joint probability as a product of potential functions on the cliques of the graph (which are singleton nodes in this case).

Let us proceed to calculating parameter estimates. In particular let us calculate the maximum likelihood estimates of  $\mu$  and  $\sigma^2$ . To do so we must maximize the likelihood  $p(x | \theta)$  with respect to  $\theta$ . We find it more convenient to maximize the logarithm of the likelihood, which, given that the logarithm is a monotonic function, will not change the results. Thus, let us define the *log likelihood*, denoted  $l(\theta; x)$ , as:

$$l(\theta; x) = \log p(x | \theta), \quad (5.14)$$

where we have reordered the variables on the left-hand side to emphasize that  $\theta$  is to be viewed as the variable and  $x$  is to be viewed as a fixed constant. We now take the derivative of the log likelihood with respect to  $\mu$ :

$$\frac{\partial l(\theta; x)}{\partial \mu} = \frac{\partial}{\partial \mu} \left( -\frac{N}{2} \log(2\pi) - \frac{N}{2} \log \sigma^2 - \frac{1}{2\sigma^2} \sum_{n=1}^N (x_n - \mu)^2 \right) \quad (5.15)$$

$$= \frac{1}{\sigma^2} \sum_{n=1}^N (x_n - \mu). \quad (5.16)$$

Setting equal to zero and solving, we obtain:

$$\hat{\mu}_{ML} = \frac{1}{N} \sum_{n=1}^N x_n. \quad (5.17)$$

Thus we see that the maximum likelihood estimate of the mean of a Gaussian distribution is the sample mean.

Similarly let us take the derivative of the log likelihood with respect to  $\sigma^2$ :

$$\frac{\partial l(\theta; x)}{\partial \sigma^2} = \frac{\partial}{\partial \sigma^2} \left( -\frac{N}{2} \log(2\pi) - \frac{N}{2} \log \sigma^2 - \frac{1}{2\sigma^2} \sum_{n=1}^N (x_n - \mu)^2 \right) \quad (5.18)$$

$$= -\frac{N}{2\sigma^2} + \frac{1}{2\sigma^4} \sum_{n=1}^N (x_n - \mu)^2. \quad (5.19)$$

Setting equal to zero and solving, we obtain:

$$\hat{\sigma}_{ML}^2 = \frac{1}{N} \sum_{n=1}^N (x_n - \hat{\mu}_{ML})^2, \quad (5.20)$$

and we see that the maximum likelihood estimate of the variance is the sample variance. (Note that we are finding the joint estimates of  $\mu$  and  $\sigma^2$  by setting both partial derivatives equal to zero and solving simultaneously; this explains the presence of  $\hat{\mu}_{ML}$  in the equation for  $\hat{\sigma}_{ML}^2$ ).

### Bayesian univariate Gaussian density estimation

In the Bayesian approach to density estimation the goal is to form a posterior density  $p(\theta | x)$ . Let us consider a simple version of this problem in which we take the variance  $\sigma^2$  to be a known constant and restrict our attention to the mean  $\mu$ . Thus we wish to obtain the posterior density  $p(\mu | x)$ , based on the prior density  $p(\mu)$  and the Gaussian likelihood  $p(x | \mu)$ .

What prior distribution should we take for  $\mu$ ? This is a modeling decision, as was the decision to utilize a Gaussian for the probability of the data  $x$  in the first place. As we will see, it is mathematically convenient to take  $p(\mu)$  to also be a Gaussian distribution. We will make this assumption in this section, but let us emphasize at the outset that mathematical convenience should not, and need not, dictate all of our modeling decisions. Indeed, a major thrust of this book is the development of methods for treating complex models, pushing back the frontier of what is “mathematically convenient” and, in the Bayesian setting, permitting a wide and expressive range of prior distributions.

If we take  $p(\mu)$  to be a Gaussian distribution, then we face another problem: what should we take as the mean and variance of this distribution? To be consistent with the general Bayesian philosophy, we should treat these parameters as random variables and endow them with a prior distribution. This is indeed the approach of *hierarchical Bayesian modeling*, where we endow parameters with distributions characterized by “hyperparameters,” which themselves can in turn

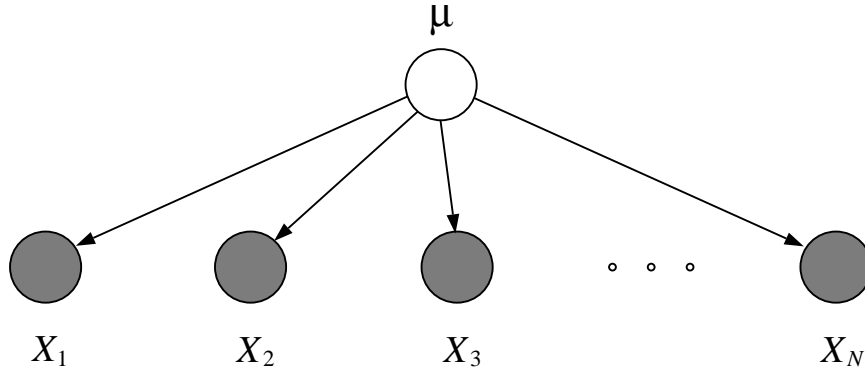


Figure 5.4: The graphical model for the Bayesian density estimation problem.

be endowed with distributions. While an infinite regress looms, in practice it is rare to take the hierarchical Bayesian approach to more than two or three levels, largely because there of diminishing returns—additional levels make little difference to the marginal probability of the data and thus to the expressiveness of our model.

Let us take the mean of  $p(\mu)$  to be a fixed constant  $\mu_0$  and take the variance to be a fixed constant  $\tau^2$ , while recognizing that in general we might endow these parameters with distributions.

The graphical model characterizing our problem is shown in Figure 5.4. The graph has been augmented with a node for the unknown mean  $\mu$ . Note that there is a single such node and that its children are the data  $\{X_n\}$ . Thus this graph provides more information than the graph of Figure 5.3; in particular the independence assumption is elaborated—the data are assumed to be *conditionally independent given the parameters*.

The likelihood is identical in form to the frequentist likelihood in Eq. (5.13). To obtain the posterior we therefore need only multiply by the prior:

$$p(\mu) = \frac{1}{(2\pi\tau^2)^{1/2}} \exp \left\{ -\frac{1}{2\tau^2} (\mu - \mu_0)^2 \right\} \quad (5.21)$$

to obtain the joint probability:

$$p(x, \mu) = \frac{1}{(2\pi\sigma^2)^{N/2}} \exp \left\{ -\frac{1}{2\sigma^2} \sum_{n=1}^N (x_n - \mu)^2 \right\} \frac{1}{(2\pi\tau^2)^{1/2}} \exp \left\{ -\frac{1}{2\tau^2} (\mu - \mu_0)^2 \right\}, \quad (5.22)$$

which when normalized yields the posterior  $p(\mu | x)$ . Multiplying the two exponentials together yields an exponent which is quadratic in the variable  $\mu$ ; thus, normalization involves “completing the square.” Appendix A presents the algebra (and in Chapter 13 we present a general matrix-based approach to completing the square—an operation that crops up often when working with Gaussian random variables). The result takes the following form:

$$p(\mu | x) = \frac{1}{(2\pi\tilde{\sigma}^2)^{1/2}} \exp \left\{ -\frac{1}{2\tilde{\sigma}^2} (\mu - \tilde{\mu})^2 \right\}, \quad (5.23)$$

where

$$\tilde{\mu} = \frac{N/\sigma^2}{N/\sigma^2 + 1/\tau^2} \bar{x} + \frac{1/\tau^2}{N/\sigma^2 + 1/\tau^2} \mu_0, \quad (5.24)$$

where  $\bar{x}$  is the sample mean, and where

$$\tilde{\sigma}^2 = \left( \frac{N}{\sigma^2} + \frac{1}{\tau^2} \right)^{-1}. \quad (5.25)$$

We see that the posterior probability is a Gaussian, with mean  $\tilde{\mu}$  and variance  $\tilde{\sigma}^2$ .

Both the posterior variance and the posterior mean have an intuitive interpretation. Note first that  $\sigma^2/N$  is the variance of a sum of  $N$  independent random variables with variance  $\sigma^2$ , thus  $\sigma^2/N$  is the variance associated with the data. Eq. (5.25) says that we add the inverse of this variance to the inverse of the prior variance to obtain the inverse of the posterior variance. Thus, inverse variances add. From Eq. (5.24) we see that the posterior mean is obtained as a linear combination of the sample mean and the prior mean. The weights in this combination can be interpreted as the fraction of the posterior variance accounted for by the variance from the data term and the prior variance respectively. These weights sum to one; thus, the combination in Eq. (5.24) is a *convex combination*.

As the number of data points  $N$  becomes large, the weight associated with  $\bar{x}$  goes to one and the weight associated with  $\mu_0$  approaches zero. Thus in the limit of large data sets, the Bayes estimate of  $\mu$  approaches the maximum likelihood estimate of  $\mu$ .

## Plates

Let us take a quick detour to discuss a notational device that we will find useful. Graphical models representing independent, identically distributed (IID) sampling have a repetitive structure that can be captured with a formal device known as a *plate*. Plates allow repeated motifs to be represented in a simple way. In particular, the simple IID model shown in Figure 5.5(a) can be represented more succinctly using the plate shown in Figure 5.5(b).

For the Bayesian model in Figure 5.6(a) we obtain the representation in Figure 5.6(b). Note that the parameter  $\mu$  appears *outside* the plate; this captures the fact that there is a single parameter value that is shared among the distributions for each of the  $X_n$ .

Formally, a plate is simply a graphical model “macro.” That is, to interpret Figure 5.5(b) or Figure 5.6(b) we copy the graphical object in the plate  $N$  times, where the number  $N$  is recorded in the lower right-hand corner of the box, and apply the usual graphical model semantics to the result.

## Density estimation for discrete data

Let us now consider the case in which the variables  $X_n$  are discrete variables, each taking on one of a finite number of possible values. We wish to study the density estimation problem in this setting, recalling that “probability density” means “probability mass function” in the discrete case.

As before, we will make the assumption that the data are IID, thus the modeling problem is represented by the plate shown in Figure 5.5(b). Each of the variables  $X_n$  can take on one of  $M$

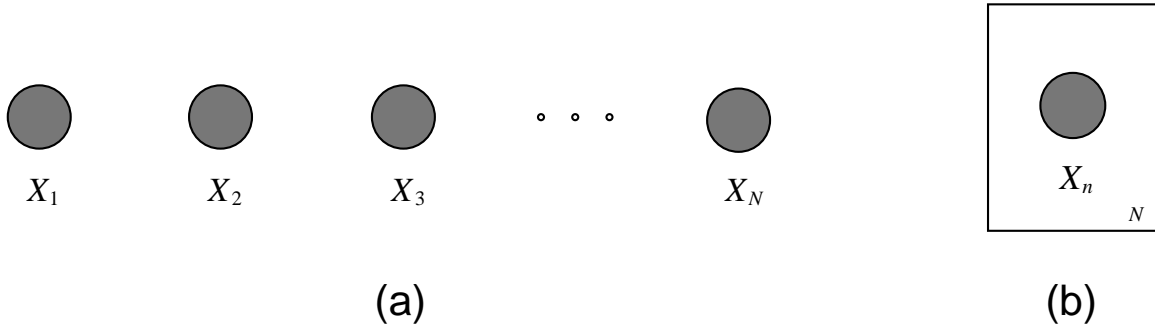


Figure 5.5: Repeated graphical motifs can be represented using plates. The IID sampling model for density estimation shown in (a) is represented using a plate in (b). The plate is interpreted by copying the graphical object within the box  $N$  times; thus the graph in (b) is a shorthand for the graph in (a).

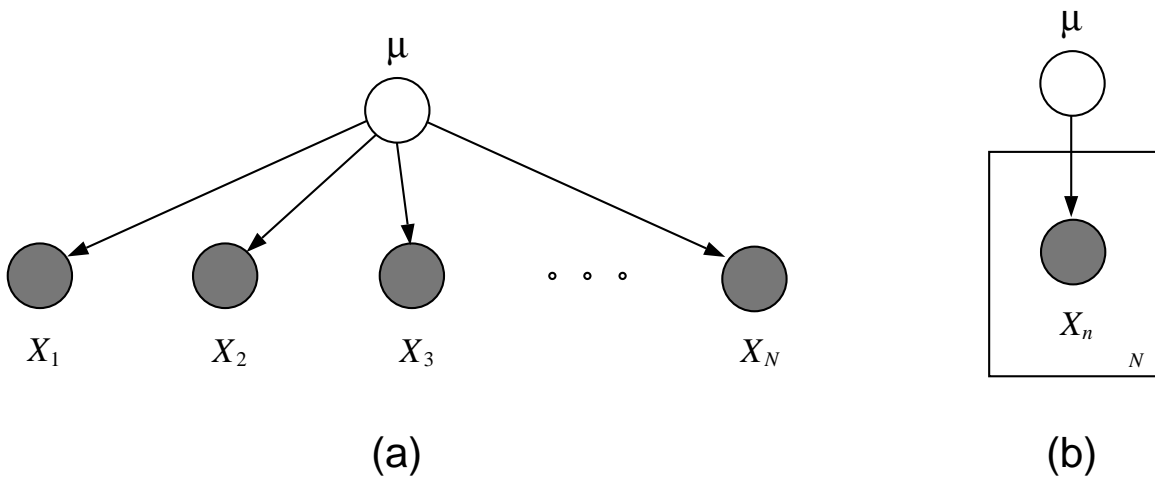


Figure 5.6: The Bayesian density estimation model shown in (a) is represented using a plate in (b). Again, the graph in (b) is to be interpreted as a shorthand for the graph in (a).

values. To represent this set of  $M$  values we will find it convenient to use a vector representation. In particular, let the range of  $X_n$  be the set of binary  $M$ -component vectors with one component equal to one and the other components equal to zero. Thus for a variable  $X_n$  taking on three values, we have:

$$X_n \in \left\{ \begin{bmatrix} 1 \\ 0 \\ 0 \end{bmatrix}, \begin{bmatrix} 0 \\ 1 \\ 0 \end{bmatrix}, \begin{bmatrix} 0 \\ 0 \\ 1 \end{bmatrix} \right\}. \quad (5.26)$$

We use superscripts to refer to the components of these vectors, thus  $X_n^k$  refers to the  $k$ th component of the variable  $X_n$ . We have  $X_n^k = 1$  if and only if the variable  $X_n$  takes on its  $k$ th value. Note that  $\sum_k X_n^k = 1$  by definition.

Using this representation, we can write the probability distribution for  $X_n$  in a convenient general form. In particular, letting  $\theta_k$  represent the probability that  $X_n$  takes on its  $k$ th value, i.e.,  $\theta_k \triangleq p(X_n^k = 1)$ , we have:

$$p(x_n | \theta) = \theta_1^{x_n^1} \theta_2^{x_n^2} \cdots \theta_M^{x_n^M}. \quad (5.27)$$

This is the *multinomial* probability distribution,  $\text{Mult}(1, \theta)$ , with parameter vector  $\theta = (\theta_1, \theta_2, \dots, \theta_M)$ . To calculate the probability of the observation  $x$ , we take the product over the individual multinomial probabilities:

$$p(x | \theta) = \prod_{n=1}^N \theta_1^{x_n^1} \theta_2^{x_n^2} \cdots \theta_M^{x_n^M} \quad (5.28)$$

$$= \theta_1^{\sum_{n=1}^N x_n^1} \theta_2^{\sum_{n=1}^N x_n^2} \cdots \theta_M^{\sum_{n=1}^N x_n^M}, \quad (5.29)$$

where the exponent  $\sum_{n=1}^N x_n^k$  is the count of the number of times the  $k$ th value of the multinomial variable is observed across the  $N$  observations.

To calculate the maximum likelihood estimates of the multinomial parameters we take the logarithm of Eq. (5.29) to obtain the log likelihood:

$$l(\theta; x) = \sum_{n=1}^N \sum_{k=1}^M x_n^k \log \theta_k, \quad (5.30)$$

and it is this expression that we must maximize with respect to  $\theta$ .

This is a constrained optimization problem for which we use Lagrange multipliers. Thus we form the Lagrangian:

$$\tilde{l}(\theta; x) = \sum_{n=1}^N \sum_{k=1}^M x_n^k \log \theta_k + \lambda \left( 1 - \sum_{k=1}^M \theta_k \right), \quad (5.31)$$

take derivatives with respect to  $\theta_k$ :

$$\frac{\partial \tilde{l}(\theta; x)}{\partial \theta_k} = \frac{\sum_{n=1}^N x_n^k}{\theta_k} - \lambda \quad (5.32)$$

and set equal to zero:

$$\frac{\sum_{n=1}^N x_n^k}{\hat{\theta}_{k,ML}} = \lambda. \quad (5.33)$$

Multiplying through by  $\hat{\theta}_{k,ML}$  and summing over  $k$  yields:

$$\lambda = \sum_{k=1}^M \sum_{n=1}^N x_n^k \quad (5.34)$$

$$= \sum_{n=1}^N \sum_{k=1}^M x_n^k \quad (5.35)$$

$$= N. \quad (5.36)$$

Finally, substituting Eq. (5.36) back into Eq. (5.33) we obtain:

$$\hat{\theta}_{k,ML} = \frac{1}{N} \sum_{n=1}^N x_n^k. \quad (5.37)$$

Noting again that  $\sum_{n=1}^N x_n^k$  is the count of the number of times that the  $k$ th value is observed, we see that the maximum likelihood estimate of  $\theta_k$  is a sample proportion.

### Bayesian density estimation for discrete data

In this section we discuss a Bayesian approach to density estimation for discrete data. As in the Gaussian setting, we specify a prior using a parameterized distribution and show how to compute the corresponding posterior.

An appealing feature of the solution to the Gaussian problem was that the prior and the posterior have the same distribution—both are Gaussian distributions. Among other virtues, this implies that Eq. (5.24) and Eq. (5.25) can be used *recursively*—the posterior based on earlier observations can serve as the prior for additional observations. At each step the posterior distribution remains in the Gaussian family.

To achieve a similar closure property in the discrete problem we must find a prior distribution which when multiplied by the multinomial distribution yields a posterior distribution in the same family. Clearly, this can be achieved by a prior distribution of the form:

$$p(\theta) = C(\alpha)\theta_1^{\alpha_1-1}\theta_2^{\alpha_2-1}\cdots\theta_M^{\alpha_M-1}, \quad (5.38)$$

for  $\sum_i \theta_i = 1$ , where  $\alpha = (\alpha_1, \dots, \alpha_M)$  are hyperparameters and  $C(\alpha)$  is a normalizing constant.<sup>3</sup> This distribution, known as the *Dirichlet distribution*, has the same functional form as the multinomial, but the  $\theta_i$  are random variables in the Dirichlet distribution and parameters in the multinomial distribution. The constant  $C(\alpha)$  is obtained via a bit of calculus (see Appendix B):

$$C(\alpha) = \frac{\Gamma(\sum_{i=1}^M \alpha_i)}{\prod_{i=1}^M \Gamma(\alpha_i)}, \quad (5.39)$$

---

<sup>3</sup>The negative one in the exponent is a convention; we could redefine the  $\alpha_i$  to remove it.

where  $\Gamma(\cdot)$  is the gamma function. In the rest of this section we will not bother with calculating the normalization; once we have a distribution in the Dirichlet form we can substitute into Eq. (5.39) to find the normalization factor.

We now calculate the posterior probability:

$$p(\theta | x) \propto \theta_1^{\sum_{n=1}^N x_n^1} \theta_2^{\sum_{n=1}^N x_n^2} \dots \theta_M^{\sum_{n=1}^N x_n^M} \theta_1^{\alpha_1-1} \theta_2^{\alpha_2-1} \dots \theta_M^{\alpha_M-1} \quad (5.40)$$

$$= \theta_1^{\sum_{n=1}^N x_n^1 + \alpha_1 - 1} \theta_2^{\sum_{n=1}^N x_n^2 + \alpha_2 - 1} \dots \theta_M^{\sum_{n=1}^N x_n^M + \alpha_M - 1}. \quad (5.41)$$

This is a Dirichlet density, with parameters  $\sum_{n=1}^N x_n^k + \alpha_k$ . We see that to update the prior into a posterior we simply add the count  $\sum_{n=1}^N x_n^k$  to the prior parameter  $\alpha_k$ .

It is worthwhile to consider the special case of the multinomial distribution when  $M = 2$ . In this setting,  $X_n$  is best treated as a binary variable rather than a vector; thus:  $x_n \in \{0, 1\}$ . The multinomial distribution reduces to:

$$p(x_n | \theta) = \theta^{x_n} (1 - \theta)^{1-x_n}; \quad (5.42)$$

the *Bernoulli distribution*. The parameter  $\theta$  encodes the probability that  $X_n$  takes the value one.

In the case  $M = 2$ , the Dirichlet distribution specializes to the *beta distribution*:

$$p(\theta) = C(\alpha) \theta^{\alpha_1-1} (1 - \theta)^{\alpha_2-1}, \quad (5.43)$$

where  $\alpha = (\alpha_1, \alpha_2)$  is the hyperparameter. The beta distribution has its support on the interval  $[0, 1]$ . Plots of the beta distribution are shown in Figure 5.7 for various values of  $\alpha_1$  and  $\alpha_2$ . Note that the *uniform distribution* is the special case of the beta distribution when  $\alpha_1 = 1$  and  $\alpha_2 = 1$ .

As the number of data points  $N$  becomes large, the sums  $\sum_{n=1}^N x_n^k$  dominate the prior terms  $\alpha_k$  in the posterior probability. In this limit, the posterior approaches the log likelihood in Eq. (5.30) and the Bayes estimate of  $\theta$  approaches the maximum likelihood estimate of  $\theta$ .

## Mixture models

It is important to recognize that the Gaussian and multinomial densities are by no means the universally best choices of density model. Suppose, for example, if the data are continuous data restricted to the half-infinite interval  $[0, \infty)$ . The Gaussian, which assigns density to the entire real line, is unnatural here, and densities such as the gamma or lognormal, whose support is  $[0, \infty)$ , may be preferred. Similarly, the multinomial distribution treats discrete data as an unordered, finite set of values. In problems involving ordered sets, and/or infinite ranges, probability distributions such as the Poisson or geometric may be more appropriate. Maximum likelihood and Bayesian estimates are available for these distributions, and indeed there is a general family known as the *exponential family*—which includes all of the distributions listed above and many more—in which explicit formulas can be obtained. (We will discuss the exponential family in Chapter 8).

This larger family of distributions is still, however, restrictive. Consider the probability density shown in Figure 5.8. This density is bimodal and we are unable to represent it within the family of Gaussian, gamma or lognormal densities. Given a data set  $\{x_n\}$  sampled from this density, we

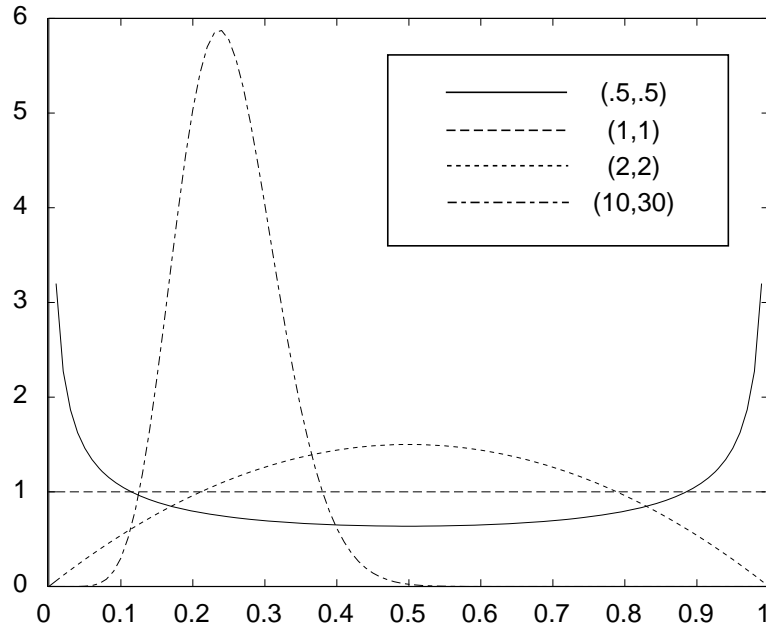


Figure 5.7: The beta( $\alpha_1, \alpha_2$ ) distribution for various values of the parameters  $\alpha_1$  and  $\alpha_2$ .

can naively fit a Gaussian density, but the likelihood that we achieve will in general be significantly smaller than the likelihood of the data under the true density, and the resulting density estimate will bear little relationship to the truth.

Multimodal densities often reflect the presence of *subpopulations* or *clusters* in the population from which we are sampling. Thus, for example, we would expect the density of heights of trees in a forest to be multimodal, reflecting the different distributions of heights of different species. It may be that for a particular species the heights are unimodal and reasonably well modeled by a simple density, such as a density in the exponential family. If so, this suggests a “divide-and-conquer” strategy in which the overall density estimation is broken down into a set of smaller density estimation problems that we know how to handle. Let us proceed to develop such a strategy.

Let  $f_k(x | \theta_k)$  be the density for the  $k$ th subpopulation, where  $\theta_k$  is a parameter vector. We define a *mixture density* for a random variable  $X$  by taking the convex sum over the component densities  $f_k(x | \theta_k)$ :

$$p(x | \theta) = \sum_{k=1}^K \alpha_k f_k(x | \theta_k), \quad (5.44)$$

where the  $\alpha_k$  are nonnegative constants that sum to one:

$$\sum_{k=1}^K \alpha_k = 1. \quad (5.45)$$

The densities  $f_k(x | \theta_k)$  are referred to in this setting as *mixture components* and the parameters  $\alpha_k$

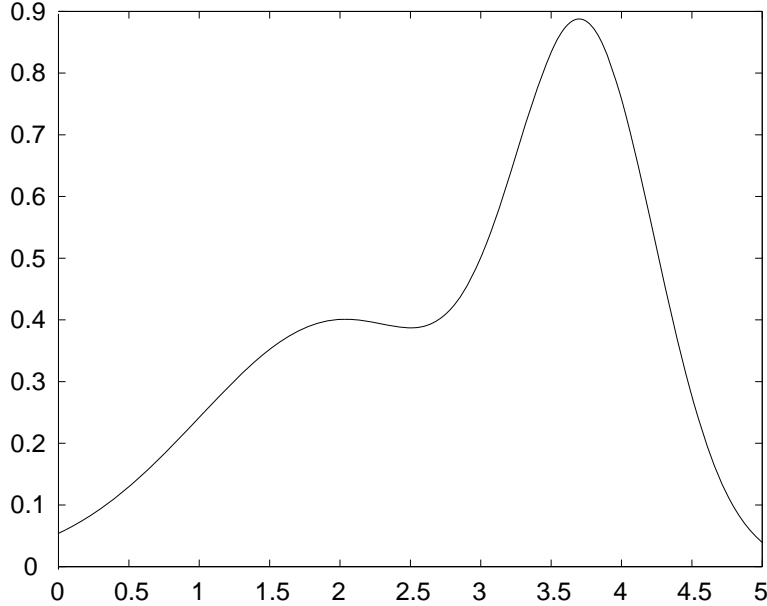


Figure 5.8: A bimodal probability density.

are referred to as *mixing proportions*. The parameter vector  $\theta$  is the collection of all of the parameters, including the mixing proportions:  $\theta \triangleq (\alpha_1, \dots, \alpha_K, \theta_1, \dots, \theta_K)$ . That the function  $p(x|\theta)$  that we have defined is in fact a density follows from the constraint that the mixing proportions sum to one.

The example shown in Figure 5.8 is a mixture density with  $K = 2$ :

$$p(x|\theta) = \alpha_1 \mathcal{N}(x|\mu_1, \sigma_1^2) + \alpha_2 \mathcal{N}(x|\mu_2, \sigma_2^2), \quad (5.46)$$

where the mixture components are Gaussian distributions with means  $\mu_k$  and variances  $\sigma_k^2$ . Gaussian mixtures are a popular form of mixture model, particular in multivariate settings (see Chapter 10).

It is illuminating to express the mixture density in Eq. (5.44) in a way that makes explicit its interpretation in terms of subpopulations. Let us do this using the machinery of graphical models. As shown in Figure 5.9, we introduce a multinomial random variable  $Z$  into our model. We also introduce an edge from  $Z$  to  $X$ . Following the recipe from Chapter 2 we endow this graph with a joint probability distribution by assigning a marginal probability to  $Z$  and a conditional probability to  $X$ . Let  $\alpha_k$  be the probability that  $Z$  takes on its  $k$ th value; thus,  $\alpha_k \triangleq p(z^k = 1)$ . Moreover, conditional on  $Z$  taking on its  $k$ th value, let the conditional probability of  $X$ ,  $p(x|z^k = 1)$ , be given by  $f_k(x|\theta_k)$ . The joint probability is therefore given by:

$$p(x, z^k = 1 | \theta) = p(x | z^k = 1, \theta)p(z^k = 1 | \theta) \quad (5.47)$$

$$= \alpha_k f_k(x | \theta_k), \quad (5.48)$$



Figure 5.9: A mixture model represented as a graphical model. The latent variable  $Z$  is a multinomial node taking on one of  $K$  values.

where  $\theta \triangleq (\alpha_1, \dots, \alpha_K, \theta_1, \dots, \theta_K)$ . To obtain the marginal probability of  $X$  we sum over  $k$ :

$$p(x | \theta) = \sum_{k=1}^K p(x, z^k = 1 | \theta) \quad (5.49)$$

$$= \sum_{k=1}^K \alpha_k f_k(x | \theta_k), \quad (5.50)$$

which is the mixture model in Eq. (5.44).

This model gives us our first opportunity to invoke our discussion of probabilistic inference from Chapter 3. In particular, given an observation  $x$ , we can use Bayes rule to invert the arrow in Figure 5.9 and calculate the conditional probability of  $Z$ :

$$p(z^k = 1 | x, \theta) = \frac{p(x | z^k = 1, \theta_k)p(z^k = 1)}{\sum_j p(x | z^j = 1, \theta_j)p(z^j = 1)} \quad (5.51)$$

$$= \frac{\alpha_k f_k(x | \theta_k)}{\sum_j \alpha_j f_j(x | \theta_j)}. \quad (5.52)$$

This calculation allows us to use the mixture model to *classify* or *categorize* the observation  $x$  into one of the subpopulations or clusters that we assume to underly the model. In particular we might classify  $x$  into the class  $k$  that maximizes  $p(z^k = 1 | x, \theta)$ .

Let us turn to the problem of estimating the parameters of the mixture model from data. We again assume for simplicity a sampling model in which we have  $N$  IID observations  $\{x_n; n = 1, \dots, N\}$ , while again noting that we will move beyond the IID setting in later chapters. The IID assumption corresponds to replicating our basic graphical model  $N$  times, yielding the plate shown in Figure 5.10. Note again that the variables  $Z_n$  are unshaded—they are *unobserved* or *latent* variables. We have introduced them into our model in order to make explicit the structural assumptions that lie behind the mixture density that we are using, but we need not assume that these variables are observed.

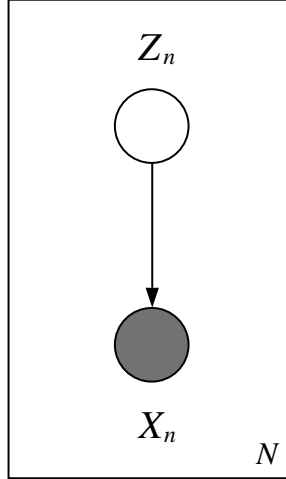


Figure 5.10: The mixture model under an IID sampling assumption.

The log likelihood is given by taking the logarithm of the joint probability associated with the model, which in the IID case becomes a sum of log probabilities. Again letting  $x = (x_1, \dots, x_N)$ , we have:

$$l(\theta; x) = \sum_{n=1}^N \log \sum_{k=1}^K \alpha_k f_k(x_n | \theta_k). \quad (5.53)$$

To obtain maximum likelihood estimates we take derivatives with respect to  $\theta$  and set to zero. The resulting equations are, however, nonlinear and do not admit a closed-form solution; solving these equations requires iterative methods. While any of a variety of numerical methods can be used, there is a particular iterative method—the *Expectation-Maximization (EM) algorithm*—that is natural not only for mixture models but also for more general graphical models. The EM algorithm involves an alternating pair of steps, the *E step* and the *M step*. The E step involves running an inference algorithm—for example the elimination algorithm that we discussed in Chapter 3—to essentially “fill in” the values of the unobserved nodes given the observed nodes. In the case of mixture models, this reduces to the invocation of Bayes rule in Eq. (5.52). The M step treats the “filled-in” graph as if all of the filled-in values had been observed, and updates the parameters to obtain improved values. In the mixture model setting this essentially reduces to finding separate density estimates for the separate subpopulations. We will present the EM algorithm formally in Chapter 11, and present its application to mixture models in Chapter 10.

### Nonparametric density estimation

In many cases data may come from a complex mechanism about which we have little or no prior knowledge. The density underlying the data may not fall into one of the “standard” forms. The density may be multimodal, but we may have no reason to suspect underlying subpopulations and may have no reason to attribute any particular meaning to the modes. When we find ourselves in

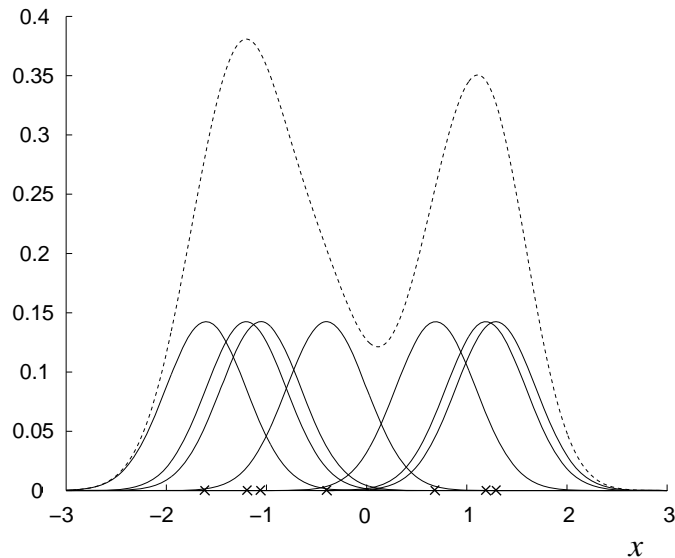


Figure 5.11: An example of kernel density estimation. The kernel functions are Gaussians centered at the data points  $x_n$  (shown as crosses on the abscissa). Each Gaussian has a standard deviation  $\lambda = 0.35$ . The Gaussians have been scaled by dividing by the number of data points ( $N = 8$ ). The density estimate (shown as a dotted curve) is the sum of these scaled kernels.

such a situation—by no means uncommon—what do we do?

*Nonparametric density estimation* provides a general class of methods for dealing with such knowledge-poor cases. In this section we introduce this approach via a simple, intuitive nonparametric method known as a *kernel density estimator*. We return to a fuller discussion of nonparametric methods in Chapter 25.

The basic intuition behind kernel density estimation is that each data point  $x_n$  provides evidence for non-zero probability density at that point. A simple way to harness this intuition is to place an “atom” of mass at that point (see Figure 5.11). Moreover, making the assumption that the underlying probability density is smooth, we let the atoms have a non-zero “width.” Superimposing  $N$  such atoms, one per data point, we obtain a density estimate.

More formally, let  $k(x, x_n, \lambda)$  be a *kernel function*—a nonnegative function integrating to one (with respect to  $x$ ). The argument  $x_n$  determines the location of the kernel function; kernels are generally symmetric about  $x_n$ . The parameter  $\lambda$  is a general “smoothing” parameter that determines the width of the kernel functions and thus the smoothness of the resulting density estimate. Superimposing  $N$  such kernel functions, and dividing by  $N$ , we obtain a probability density:

$$\hat{p}(x) = \frac{1}{N} \sum_{n=1}^N k(x, x_n, \lambda). \quad (5.54)$$

This density is the kernel density estimate of the underlying density  $p(x)$ .

A variety of different kernel functions are used in practice. Simple (e.g., piecewise polynomial)

functions are often preferred, partly for computational reasons (calculating the density at a given point  $x$  requires  $N$  function evaluations). Gaussian functions are sometimes used, in which case  $x_n$  plays the role of the mean and  $\lambda$  plays the role of the standard deviation.

While the kernel function is often chosen a priori, the value of  $\lambda$  is generally chosen based on the data. This is a nontrivial estimation problem for which classical estimation methods are often of little help. In particular, it is important to understand that maximum likelihood is *not* appropriate for solving this problem. Suppose that we interpret the density in Eq. (5.54) as a likelihood function, with  $\lambda$  as the parameter. For most reasonable kernels, this “likelihood” increases monotonically as  $\lambda$  goes to zero, because the kernel assigns more probability density to the points  $x_n$  for smaller values of  $\lambda$ . Indeed, in the limit of  $\lambda = 0$ , the kernel generally approaches a delta function, giving infinite likelihood to the data. A sum of delta functions is obviously a poor density estimate.

We will discuss methods for choosing smoothing parameters in Chapter 25. As we will see, most practical methods involve some form of *cross-validation*, in which a fraction of the data are held out and used to evaluate various choices of  $\lambda$ . Both overly small and overly large values of  $\lambda$  will tend to assign small probability density to the held-out data, and this provides a rational approach to choosing  $\lambda$ .

The problem here is a general one, motivating a distinction between *parametric models* and *nonparametric models* and suggesting the need for distinct methods for their estimation. Understanding the distinction requires us to consider how a given model would change if the number of data points  $N$  were to increase. For parametric models the basic structure of the model remains fixed as  $N$  increases. In particular, for the Gaussian estimation problem treated in Section 5.2.1, the class of densities that are possible fits to the data remains the same whatever the value of  $N$ ; for each  $N$  we obtain a Gaussian density with estimated parameters  $\hat{\mu}$  and  $\hat{\sigma}^2$ . Increasing the number of data points increases the precision of these estimates, but it does not increase the class of densities that we are considering. In the nonparametric case, on the other hand, the class of densities increases as  $N$  increases. In particular, with  $N + 1$  data points it is possible to obtain densities with  $N + 1$  modes; this is not possible with  $N$  data points.

An alternative perspective is to view the locations of the kernels as “parameters”; the number of such “parameters” increases with the number of data points. In effect, we can view nonparametric models as parametric, but with an unbounded, data-dependent, number of parameters. Indeed, in an alternative language that is often used, parametric models are referred to as “finite-dimensional models,” and nonparametric models are referred to as “infinite-dimensional models.”

It is worthwhile to compare the kernel density estimator in Eq. (5.54) to the mixture model in Eq. (5.44). Consider in particular the case in which Gaussian mixture components are used in Eq. (5.44) and Gaussian kernel functions are used in Eq. (5.54). In this case the kernel estimator can be viewed as a mixture model in which the means are fixed to the data point locations, the variances are set to  $\lambda^2$ , and the mixing proportions are set to  $1/N$ . In what sense are the two different approaches to density estimation really different?

Again, the key difference between the two approaches is revealed when we let the number of data points  $N$  grow. The mixture model is generally viewed as a parametric model, in which case the number of mixture components,  $K$ , does not increase as the number of data points grows. This is consistent with our interpretation of a mixture model in terms of a set of  $K$  underly-

ing subpopulations—if we believe that these subpopulations exist, then we do not vary  $K$  as  $N$  increases. In the kernel estimation approach, on the other hand, we have no commitment to underlying subpopulations, and we accord no special treatment to the number of kernels. As the number of data points grows, we allow the number of kernels to grow. Moreover we generally expect that  $\lambda$  will shrink as  $N$  grows to allow an increasingly close fit to the details of the true density.

There are several caveats to this discussion. First, in the mixture model setting, we may not know the number  $K$  of mixture components in practice and we may wish to estimate  $K$  from the data. This is a model selection problem (see Section 5.3). Solutions to model selection problems generally involve allowing  $K$  to increase as the number of data points increases, based on the fact that more data points are generally needed to provide more compelling evidence for multiple modes. Second, mixture models can also be used nonparametrically. In particular, a *mixture sieve* is a mixture model in which the number of components is allowed to grow with the number of data points. This differs from kernel density estimation in that the location of the mixture components are treated as free parameters rather than being fixed at the data points; moreover, each mixture component generally has its own (free) scale parameter. Also, the growth rate of the number of “parameters” in mixture sieves is slower than that of kernel density estimation (e.g.,  $\log N$  vs.  $N$ ). As this discussion begins to suggest, however, it becomes difficult to enforce a clear boundary between parametric and nonparametric methods. A given approach can be treated in one way or the other, depending on a modeler’s goals and assumptions.

There is a general tradeoff between flexibility and statistical efficiency that is relevant to this discussion. If the underlying “true” density is a Gaussian, then we probably want to estimate this density using a parametric approach, we can also use a kernel density estimate. The latter estimate will eventually converge to the true density, but it may require very many data points. A parametric estimator will converge more rapidly. Of course, if the true density is not a Gaussian, then the parametric estimate would still converge, but to the wrong density, whereas the nonparametric estimate would eventually converge to the true density. In sum, if we are willing to make more assumptions then we get faster convergence, but with the possibility of poor performance if reality does not match our assumptions. Nonparametric estimators allow us to get away with fewer assumptions, while requiring more data points for comparable levels of performance.

There is also a general point to be made with respect to the representation of densities in graphical models. As suggested in Figure 5.12, there are two ways to represent a multi-modal density as a graphical model. As shown in Figure 5.12(a), we can allow the class of densities  $p(x)$  at node  $X$  to include multi-modal densities, such as mixtures or kernel density estimates. Alternatively, we can use the “structured” model depicted in Figure 5.12(b), where we obtain a mixture distribution for  $X_n$  by marginalizing over the latent variable  $Z_n$ . Although it may seem natural to reserve the latter representation for parametric modeling, in particular for the setting in which we attribute a “meaning” to the latent variable, such a step is in general unwarranted. The mixture sieve exemplifies a situation in which we may wish to use graphical machinery to represent the structure of a nonparametric model explicitly. In general, the choices of how to use and how to interpret graphical structure are modeling decisions. While we may wish to use graphical representations to express domain-specific structural knowledge, we may also be guided by other factors, including mathematical convenience and the availability of computational tools.

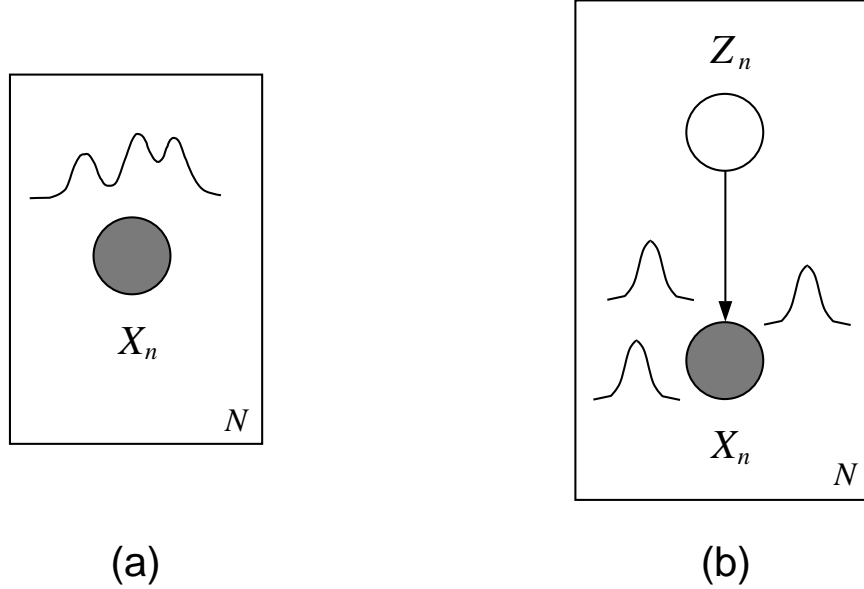


Figure 5.12: Two ways to represent a multi-modal density within the graphical model formalism. (a) The local probability model at each node is a mixture or a kernel density estimate. (b) A latent variable is used to represent mixture components explicitly; marginalizing over the latent variable yields a mixture model for the observable  $X_n$ .

There is nothing inappropriate about letting such factors be a guide, but in doing so we must be cautious about any interpretation or meaning that we attach to the model.

### Summary of density estimation

Our goal in this section has not been to provide a full treatment of density estimation; indeed we have only scratched the surface of what is an extensive literature in statistics. We do hope, however, to have introduced a few key ideas—the calculation of maximum likelihood and Bayesian parameter estimates for Gaussian and multinomial densities, the use of mixture models to obtain a richer class of density models, and the distinction between parametric and nonparametric density estimation. Each of these ideas will be picked up and pursued in numerous contexts throughout the book.

#### 5.2.2 Regression

In a *regression model* the goal is to model the dependence of a *response* or *output* variable  $Y$  on a *covariate* or *input* variable  $X$ . We capture this dependence via a conditional probability distribution  $p(y|x)$ . In graphical model terms, we have a two-node model in which  $X$  is the parent and  $Y$  is the child (see Figure 5.13).

One way to treat regression problems is to estimate the joint density of  $X$  and  $Y$  and to calculate



Figure 5.13: A regression model.

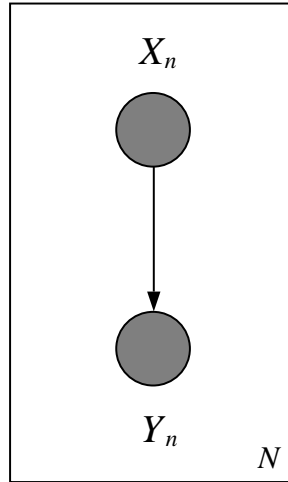


Figure 5.14: The IID regression model represented graphically.

the conditional  $p(y|x)$  from the estimated joint. This approach forces us to model  $X$ , however, which may not be desired. Indeed, in many applications of regression,  $X$  is high-dimensional and hard to model. Moreover, the observations of  $X$  are often fixed by experimental design or another form of non-random process, and it is problematic to treat them via a simple sampling model, such as the IID model. In summary, it is necessary to develop methods appropriate to conditional densities.

Our discussion here will be brief, with a focus on basic representational issues.

We assume that we have a set of pairs of observed data,  $\{(x_n, y_n); n = 1, \dots, N\}$ , where  $x_n$  is an observation of the input variable and  $y_n$  is a corresponding observation of the output variable. We again assume an independent, identical distributed (IID) sampling model for simplicity. The graphical representation of the IID regression model is shown as a plate in Figure 5.14.

Let us now consider some of the possible choices for the conditional probability model  $p(y_n | x_n)$ .

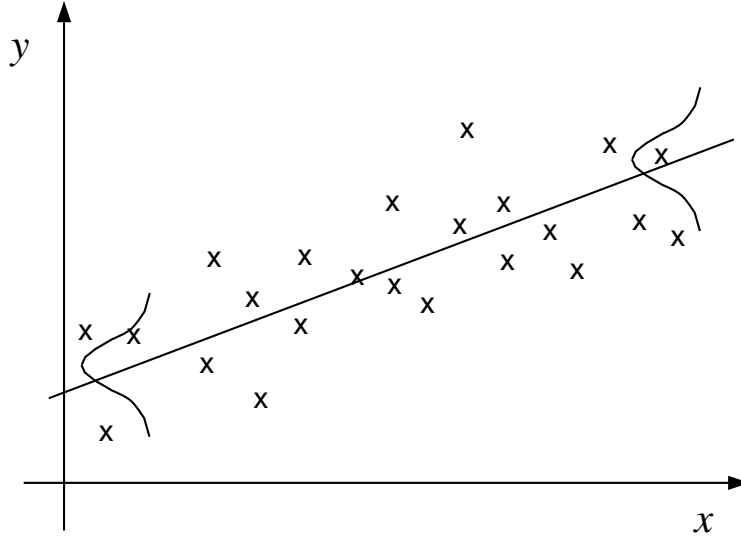


Figure 5.15: The linear regression model expresses the response variable  $Y$  in terms of the conditional mean function—the line in the figure—and input-independent random variation around the conditional mean.

As in the case of density estimation, we have a wide spectrum of possibilities, including parametric models, mixture models, and nonparametric models. We will discuss these models in detail in Chapters 6, 10, and 25, respectively, but let us sketch some of the possibilities here.

A *linear regression* model expresses  $Y_n$  as the sum of (1) a purely deterministic component that depends parametrically on  $x_n$ , and (2) a purely random component that is functionally independent of  $x_n$ :

$$Y_n = \beta^T x_n + \epsilon_n, \quad (5.55)$$

where  $\beta$  is a parameter vector and  $\epsilon_n$  is a random variable having zero mean. Taking the conditional expectation of both sides of this equation yields  $E[Y_n | x_n] = \beta^T x_n$ . Thus the linear regression model expresses  $Y_n$  in terms of input-independent random variation  $\epsilon_n$  around the conditional mean  $\beta^T x_n$  (see Figure 5.15). The choice of the distribution of  $\epsilon_n$ , which completes the specification of the model, is analogous to the choice of a density model in density estimation, and depends on the nature of  $Y_n$ . “Linear regression” generally refers to the case in which  $Y_n$  is real-valued and the distribution is taken to be  $\mathcal{N}(0, \sigma^2)$ . (In Chapter 8 we will be discussing “generalized linear models,” which are regression models that are appropriate for other types of response variables). In the linear regression case, we have:

$$P(y_n | x_n, \theta) = \frac{1}{(2\pi\sigma^2)^{1/2}} \exp \left\{ -\frac{1}{2\sigma^2} (y_n - \beta^T x_n)^2 \right\}, \quad (5.56)$$

where for simplicity we have taken  $y_n$  to be univariate. The parameter vector  $\theta$  includes  $\beta$ , which determines the conditional mean, and  $\sigma^2$ , which is the variance of  $\epsilon_n$  and determines the scale of

the variation around the conditional mean.

Linear regression is in fact broader than it may appear at first sight, in that the function  $\beta^T x_n$  need only be linear in  $\beta$  and in particular may be nonlinear in  $x_n$ . Thus the model:

$$Y_n = \beta^T \phi(x_n) + \epsilon_n, \quad (5.57)$$

where  $\phi(\cdot)$  is a vector-valued function of  $x_n$ , is a linear regression model. This model is a parametric model in that  $\phi(\cdot)$  is fixed and our freedom in modeling the data comes only from the finite set of parameters  $\beta$ .

The problem of estimating the parameters of regression models is in principle no different from the corresponding estimation problem for density estimation. In the maximum likelihood approach, we form the log likelihood:

$$l(\theta; x) = \sum_{n=1}^N \log p(y_n | x_n, \theta), \quad (5.58)$$

take derivatives with respect to  $\theta$ , set to zero and (attempt to) solve. We will discuss the issues that arise in carrying out this calculation in later chapters.

### Conditional mixture models

Mixture models provide a way to move beyond the strictures of linear regression modeling. We can consider both a broader class of conditional mean functions as well as a broader class of density models for  $\epsilon_n$ . Consider in particular the graphical model shown in Figure 5.16(a). We have introduced a multinomial latent variable  $Z_n$  that depends on the input  $X_n$ ; moreover, the response  $Y_n$  depends on both  $X_n$  and  $Z_n$ . This graph corresponds to the following probabilistic model:

$$p(y_n | x_n, \theta) = \sum_{k=1}^K p(z_n^k = 1 | x_n, \theta) p(y_n | z_n^k = 1, x_n, \theta), \quad (5.59)$$

a *conditional mixture model*. Each mixture component  $p(y_n | z_n^k = 1, x_n)$  corresponds to a different regression model, one for each value of  $k$ . The mixing proportions  $p(z_n^k = 1 | x_n)$  “switch” among the regression models as a function of  $x_n$ . Thus, as suggested in Figure 5.16(a), the mixing proportions can be used to pick out regions of the input space where different regression functions are used. We can parameterize both the mixing proportions and the regression models and estimate both sets of parameters from data. This is a “divide-and-conquer” methodology in the regression domain. (We provide a fuller description of this model in Chapter 10).

The example in Figure 5.16(a) utilizes mixing proportions that are sharp, nearly binary functions of  $X_n$ , but it is also of interest to consider models in which these functions are smoother, allowing overlap in the component regression functions. Indeed, in the limiting case we obtain the model shown in Figure 5.16(b) in which the latent variable  $Z_n$  is independent of  $X_n$ . Here the presence of the latent variable serves only to induce multimodality in the conditional distribution  $p(y_n | x_n)$ . Much as in the case of density estimation, such a regression model may arise from a set of subpopulations, each characterized by a different “conditional mean.”

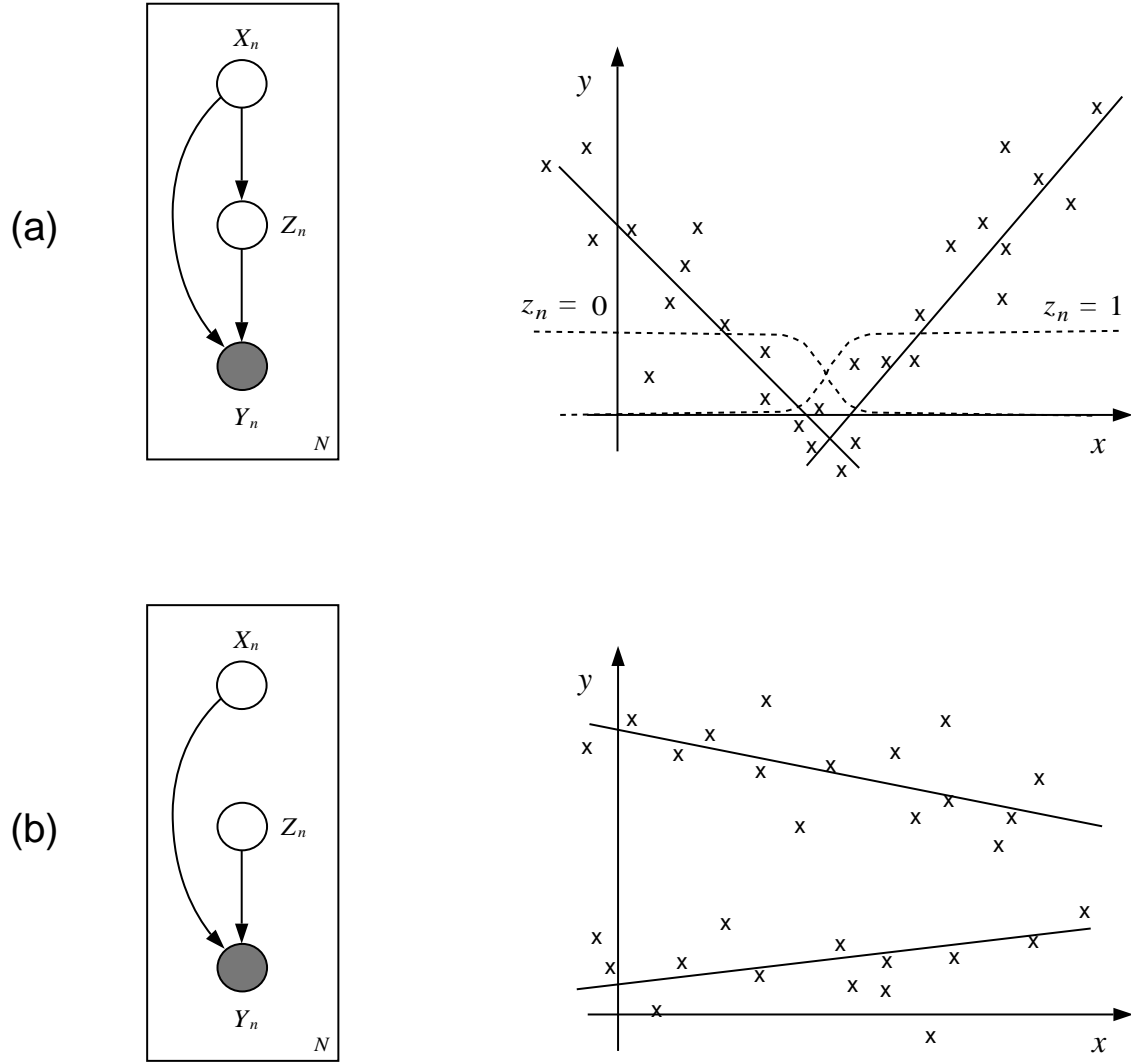


Figure 5.16: Two variants of conditional regression model. In (a), the latent variable  $Z_n$  is dependent on  $X_n$ . This corresponds to breaking up the input space into (partially overlapping) regions labeled by the values of  $Z_n$ . An example with binary  $Z_n$  is shown in the figure on the right, where the dashed line labeled by  $z_n = 1$  is the probability  $p(z_n = 1 | x_n)$ , and the dashed line labeled by  $z_n = 0$  is the probability  $p(z_n = 0 | x_n)$ . The two lines are the conditional means of the regressions,  $p(y_n | z_n, x_n)$ , for the two values of  $z_n$ , with the leftmost line corresponding to  $z_n = 0$  and the rightmost line corresponding to  $z_n = 1$ . In (b), the latent variable  $Z_n$  is independent of  $X_n$ . This corresponds to total overlap of the regions corresponding to the values of  $Z_n$  and yields an input-independent mixture density for each value of  $x_n$ .

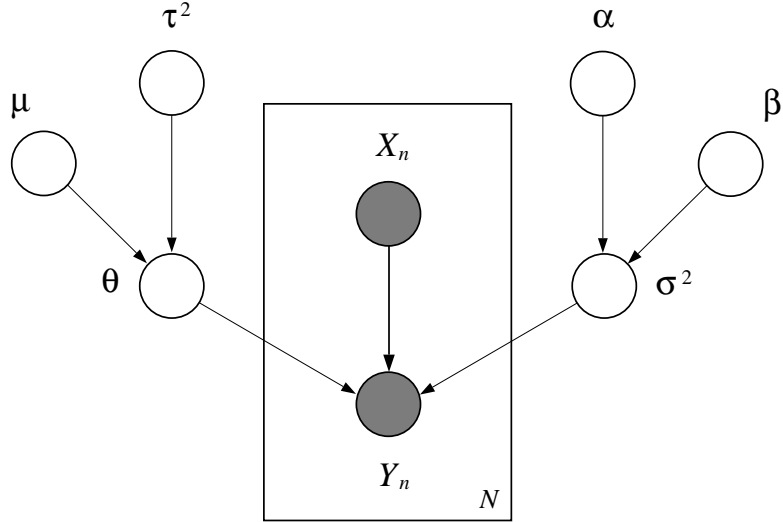


Figure 5.17: A Bayesian linear regression model. The parameter vector  $\theta$  is endowed with a Gaussian prior,  $\mathcal{N}(\mu, \tau^2)$ . The variance  $\sigma^2$  is endowed with an inverse gamma prior,  $IG(\alpha, \beta)$ .

The parameters of conditional mixture models can be estimated using the EM algorithm, as discussed in Chapter 10. Indeed, EM can be used quite generically for latent variable models such as those in Figure 5.16.

### Nonparametric regression

Let us briefly consider the nonparametric approach to regression. While it is possible to use nonparametric methods to expand the repertoire of probability models for  $\epsilon_n$ , a more common usage of nonparametric ideas involves allowing a wider class of conditional mean functions. The basic idea is to break up the input space into (possibly overlapping) regions, with one such region for each data point. Let us give an example from the class of methods known as *kernel regression*. As in kernel density estimation, let  $k(x, x_n, \lambda)$  be a *kernel function* centered around the data point  $x_n$ . Denoting the conditional mean function as  $f(x)$ , we form an estimate as follows:

$$\hat{f}(x) = \frac{\sum_{n=1}^N k(x, x_n, \lambda) y_n}{\sum_{m=1}^N k(x, x_m, \lambda)} \quad (5.60)$$

That is, we estimate the conditional mean at  $x$  as the convex sum of the observed values  $y_n$ , where the weights in the sum are given by the normalized values of the kernel functions, one for each  $x_n$ , evaluated at  $x$ . Given that kernel functions are generally chosen to be “local,” having most of their support near  $x_n$ , we see that the kernel regression estimate at  $x$  is a local average of the values  $y_n$  in the neighborhood of  $x$ .

We can once again forge a link between the mixture model approach and the nonparametric kernel regression approach. As we ask the reader to verify in Exercise ??, taking the conditional

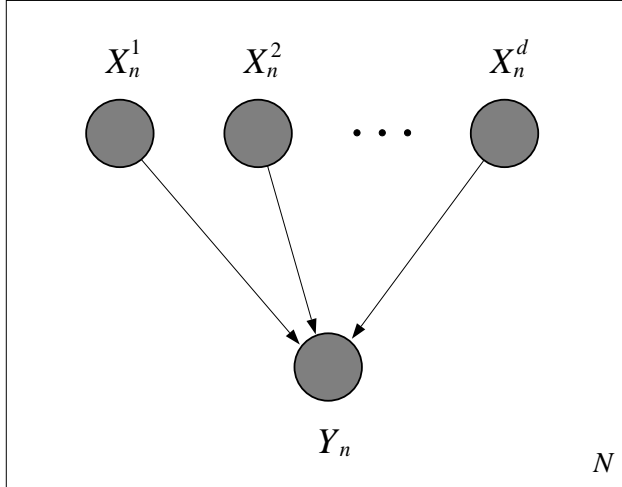


Figure 5.18: A graphical representation of the regression model in which the components of the input vector are treated as explicit nodes.

mean of Eq. (5.59) yields a weighted sum of conditional mean functions, one for each component  $k$ , where the weights are the mixing proportions  $p(z_n^k = 1 | x_n)$ . The kernel regression estimate in Eq. (5.60) can be viewed as an instance of this model, if we treat the normalized kernels  $k(x, x_n, \lambda) / \sum_{m=1}^N k(x, x_m, \lambda)$  as mixing proportions, and the values  $y_n$  as (constant) conditional means. The same comments apply to this reduction as to the analogous reduction in the case of density estimation. In particular, as  $N$  increases, the number of components  $K$  in a parametric conditional mixture model generally remain fixed, whereas the number of kernels in the kernel regression model grow. We can, however, consider *conditional mixture sieves*, and obtain a nonparametric variant of a mixture model.

### Bayesian approaches to regression

All of the models that we have considered in this section can be treated via Bayesian methods, where we endow the parameters (or entire conditional mean functions) with prior distributions. We then invoke Bayes rule to calculate posterior distributions. Figure 5.17 illustrates one such Bayesian regression model.

### Remarks

Let us make one final remark regarding the graphical representation of regression models. Note that in this section we have treated the input variables  $X_n$  as single nodes, not availing ourselves of the opportunity to represent the components of these vector-valued variables as separate nodes (see Figure 5.18). This is consistent with our treatment of  $X_n$  as fixed variables to be conditioned on; representing the components as separate nodes would imply marginal independence between the components, an assumption that we may or may not wish to make. It is important to note,

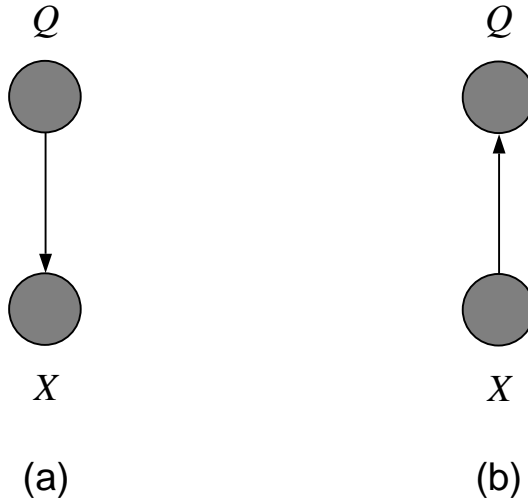


Figure 5.19: (a) The generative approach to classification represented as a graphical model. Fitting the model requires estimating the marginal probability  $p(q)$  and the conditional probability  $p(x|q)$ . (b) The discriminative approach to classification represented as a graphical model. Fitting the model requires estimating the conditional probability  $p(q|x)$ .

however, that regression methods are agnostic regarding modeling assumptions about the conditioning variables. Regression methods form an estimate of  $p(y|x)$  and this conditional density can be composed with an estimate of  $p(x)$  to obtain an estimate of the joint. This allows us to use regression models as components of larger models. In particular, in the context of a graphical model in which a node  $A$  has multiple parents  $B_1, B_2, \dots, B_k$ , we are free to use regression methods to represent  $p(A|B_1, B_2, \dots, B_k)$ , regardless of the modeling assumptions made regarding the nodes  $B_i$ . Indeed each of the  $B_i$  may themselves be modeled in terms of regressions on variables further “upstream.”

### 5.2.3 Classification

Classification problems are related to regression problems in that they involve pairs of variables. The distinguishing feature of classification problems is that the response variable ranges over a finite set, a seemingly minor issue that has important implications.

In classification we often refer to the covariate  $X$  as a *feature vector*, and the corresponding discrete response, which we denote by  $Q$ , as a *class label*. We typically view the feature vectors as descriptions of objects, and the goal is to label the objects, i.e., to classify the objects into one of a finite set of categories.

There are two basic approaches to classification problems, which can be interpreted graphically in terms of the direction of the edge between  $X$  and  $Q$ . The first approach, which we will refer to as *generative*, is based on the graphical model shown in Figure 5.19(a), in which there is an arrow from  $Q$  to  $X$ . This approach is closely related to density estimation—for each value of the discrete

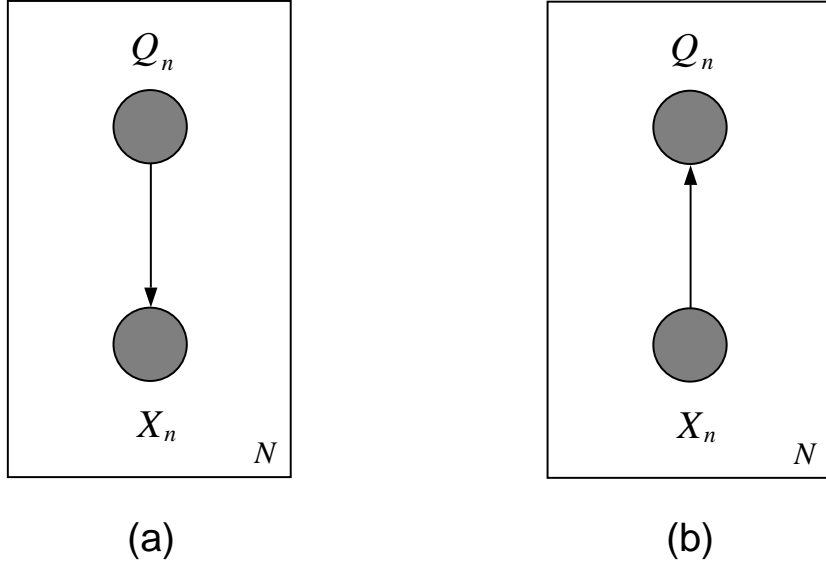


Figure 5.20: The IID classification models for the (a) generative approach and (b) discriminative approach.

variable  $Q$  we have a density,  $p(x|q)$ , which we refer to as a *class-conditional density*. We also require the marginal probability  $p(q)$ , which we refer to as the *prior probability* of the class  $Q$  (it is the probability of the class before a feature vector  $X$  is observed). This marginal probability is required if we are going to be able to “invert the arrow” and compute  $p(q|x)$ —the *posterior probability* of class  $Q$ .

The second approach to classification, which we refer to as *discriminative*, is closely related to regression. Here we represent the relationship between the feature vectors and the labels in terms of an arrow from  $X$  to  $Q$  (see Figure 5.19(b)). That is, we represent the relationship in terms of the conditional probability  $p(q|x)$ . When classifying an object we simply plug the corresponding feature vector  $x$  into the conditional probability and calculate  $p(q|x)$ . Performing this calculation, which tells us which class label has the highest probability, makes no reference to the marginal probability  $p(x)$  and, as in regression, we may wish to abstain from incorporating such a marginal into the model.

As in regression, we have a set of data pairs  $\{(x_n, q_n) : n = 1, \dots, N\}$ , assumed IID for simplicity. The representations of the classification problem as plates are shown in Figure 5.20.

Once again we postpone a general presentation of particular representations for the conditional probabilities in classification problems until later chapters. But let us briefly discuss a canonical example that will illustrate some typical representational choices, as well as illustrate some of the relationships between the generative and the discriminative approaches to classification. This example and several others will be developed in considerably greater detail in later chapters.

We specialize to two classes. Let us choose Gaussian class-conditional densities with equal covariance matrices for the two classes. An example of these densities (where we have assumed equal

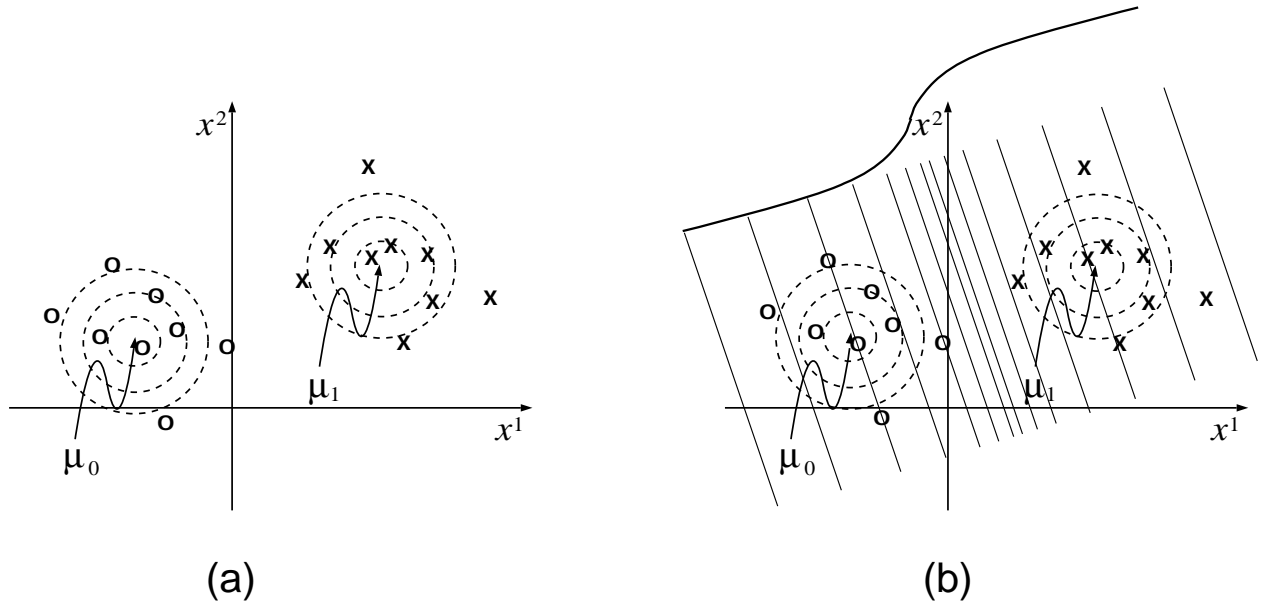


Figure 5.21: (a) Contour plots and samples from two Gaussian class-conditional densities for two-dimensional feature vectors  $x_n = (x_n^1, x_n^2)$ . The Gaussians have means  $\mu_0$  and  $\mu_1$  for class  $q_n = 0$  and  $q_n = 1$ , respectively, and equal covariance matrices. (b) The solid lines are the contours of the posterior probability,  $p(q_n = 1 | x_n)$ . In the direction orthogonal to the linear contours, the posterior probability is a monotonically increasing function given by (Eq. (5.61)). This function is sketched at the top of the figure.

class priors) is shown in Figure 5.21(a). We use Bayes rule to compute the posterior probability that a given feature vector  $x_n$  belongs to class  $q_n = 1$ . Intuitively, we expect to obtain a ramp-like function which is zero in the vicinity of the class  $q_n = 0$ , increases to one-half in the region between the two classes, and approaches one in the vicinity of the class  $q_n = 1$ . This posterior probability function is shown in Figure 5.21(b), where indeed we see the ramp-like shape.

Analytically, as we show in Chapter 7, for Gaussian class-conditional densities the ramp-like posterior probability turns out to be the *logistic function*:

$$p(q_n = 1 | x_n) = \frac{1}{1 + e^{-\theta^T x_n}}, \quad (5.61)$$

where  $\theta$  is a parameter vector that depends on the particular choices of means and covariances for the class-conditional densities, as well as the class priors. The inner product between  $\theta$  and  $x_n$  is a projection operation that is responsible for the linear contours that we see in Figure 5.21(b).

Given these parametric forms for the class-conditional densities (the Gaussian densities) and the posterior probability (the logistic function), we must specify how to estimate the parameters based on the data. It is here that the generative and discriminative approaches begin to diverge. From the generative point of view, the problem is that of estimating the means and covariances of the Gaussian class-conditional densities, as well as the class priors. These are density estimation

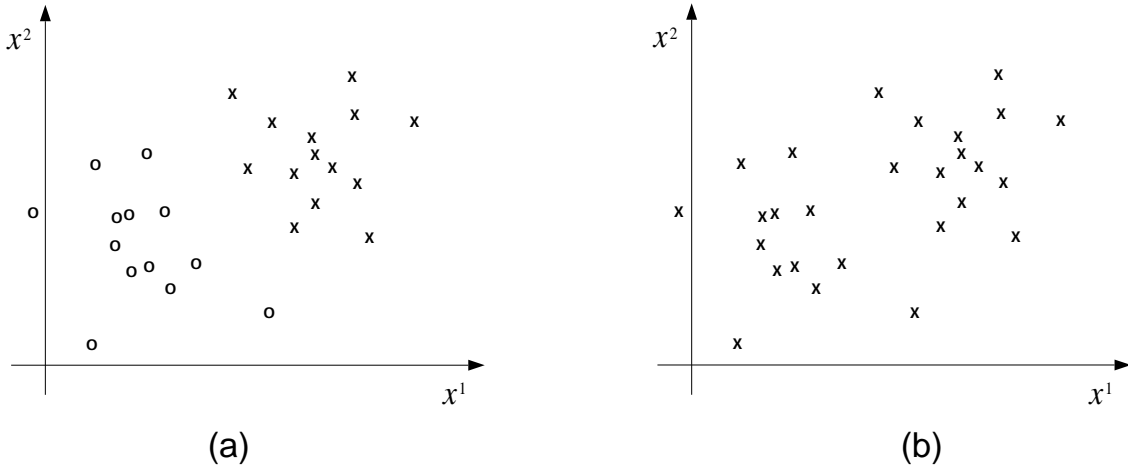


Figure 5.22: (a) A classification problem with the class  $q_n = 0$  labeled with a “0” and the class  $q_n = 1$  labeled with a “x”. (b) The same feature vectors  $x_n$  as in (a), but with the labels erased.

problems, and the machinery of Section 5.2.1 is invoked to solve them. With these density estimates in hand, we derive an estimate of  $\theta$  and thereby calculate an estimate of the posterior probability. Essentially, the goal is to model the classes, without any direct attempt to discriminate between the classes.

In the discriminative approach, on the other hand, the logistic function is the central object of analysis. Indeed, in Chapter 7, we describe a regression-like method for estimating  $\theta$  directly from data, without making reference to the means and covariances of an underlying generative model. Intuitively, this method can be viewed as an attempt to orient and position the ramp-like posterior probability in Figure 5.21(b) so as to assign a posterior probability that is near zero to the points  $x_n$  having label  $q_n = 0$ , and a posterior probability near one to the points  $x_n$  having label  $q_n = 1$ . Essentially, the goal is to discriminate between the classes, without any direct attempt to model the classes.

More generally, in a discriminative approach to classification we are not restricted to the logistic function, or to any other function that is derived from a generative model. Rather we can choose functions whose contours appear to provide a natural characterization of boundaries between classes. On the other hand, it may not always be apparent how to choose such functions, and in such cases we may prefer to take advantage of the generative approach, in which the boundaries arise implicitly via Bayes rule. In general, both the discriminative and the generative approaches are important tools to have in a modeling toolbox.

Mixture models revisited

Suppose we consider a classification problem in which none of the class labels are present. Is this a sensible problem to pose? What can one possibly learn from unlabeled data, particularly data that are completely unlabeled?

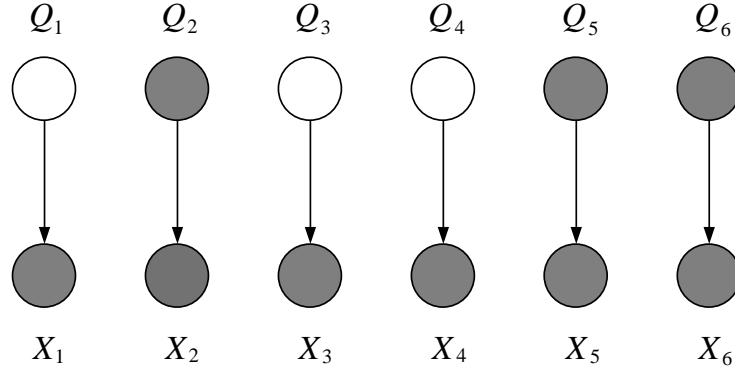


Figure 5.23: A model for partially labeled data in which the feature vectors  $x_2, x_5$  and  $x_6$  are labeled and the other feature vectors are unlabeled.

Consider Figure 5.22(a), where we have depicted a typical classification problem with two classes. Now consider Figure 5.22(b), where we have retained the feature vectors  $x_n$ , but erased the labels  $q_n$ . As this latter plot makes clear, although the labels are missing, there is still substantial statistical structure in the problem. Rather than solving a classification problem, we can solve a *clustering* problem, making explicit the fact that the data appear to fall into two clusters and assigning feature vectors to clusters.

In fact we have already solved this problem. The mixture model approach to density estimation discussed in Section 5.2.1 treats the density in terms of a set of underlying “subpopulations” labeled by a latent variable  $Z$ . The inferential calculation  $p(z_n | x_n)$  given in Eq. (5.52) explicitly calculates the probability that the feature vector  $x_n$  belongs to each of the subpopulations.

The relationship between classification and mixture models is also clarified by comparing the “generative” graphical model in Figure 5.19(b) and the mixture model in Figure 5.9(a). These are the same graphical model—the only difference is the shading, corresponding to the assumption that the labels  $Q_n$  are observed in classification whereas the latent variables  $Z_n$  are unobserved in mixture modeling. In the setting of unlabeled data the generative classification model becomes identical to a mixture model.

In a more general setting we may have a “partially labeled” case in which the labels  $Q_n$  are observed for some data points and unobserved for other data points. This situation is represented graphically in Figure 5.23. We will be able to treat the problem of estimation in this case using the EM algorithm; indeed this “partially labeled” case requires no additional machinery beyond that already required for the mixture model.

It is common to refer to classification and regression models as “supervised learning” models and to refer to density estimation models as “unsupervised learning” models. In the comparison between mixture models and classification models just discussed, the distinction refers to the observation of the labels  $Q_n$ ; one says that the labels in classification are provided by a “supervisor.” While this terminology can be useful in making broad distinctions between models, it is our view that the terminology does not reflect a fundamental underlying distinction and we will tend to avoid its use in this book. It is our feeling that many models are neither entirely “supervised” nor entirely

“unsupervised,” and invoking the distinction often forces us to group together methods that have little in common as well as to separate methods that are closely related. We feel that a better way to understand relationships between models is to make them explicit as graphs. Models can then be compared in terms of graphical features such as which variables are considered latent and which observed, the directionalities of arcs that are used to represent conditional relationships, and the presence or absence of particular structural motifs.

### Remarks

We have already indicated a relationship between mixture models and classification, but there are other roles for mixture models in the classification setting. In particular, we can use mixtures as class-conditional densities in the generative approach to classification, just as we used mixture models in the density estimation setting to extend the range of models that we considered. Also, in the context of the discriminative approach to classification, we can use conditional mixtures to represent the posterior probability  $p(q|x)$ , breaking this function into overlapping pieces, much as we did with the conditional mean in the case of regression.

Similarly, nonparametric methods have many roles to play in classification models. We can either extend the generative approach to allow nonparametric estimates of the class-conditional densities, or extend the discriminative approach to allow nonparametric estimates of the posterior probability.

Finally, there are once again Bayesian approaches in all of these cases. From a graphical point of view, these Bayesian approaches essentially involve making the parameters explicit as nodes, and using hyperparameters to express prior probability distributions on these nodes.

## 5.3 Model selection and model averaging

Thus far we have assumed that a specific model has been chosen in advance and we have focused on representing the model graphically and estimating its parameters. In some cases this assumption is reasonable—the model is determined by the problem and there is no need to consider data-driven approaches to choosing the model. More commonly, however, we wish to use the data to make informed choices regarding the model. We present a brief discussion of this problem—known as the *model selection* problem—in this section, anticipating our more detailed presentation in Chapter 26.

We consider a class  $\mathcal{M}$  of possible models, letting  $m \in \mathcal{M}$  denote a specific model in this family. We also augment our earlier notation to include explicit reference to the model; thus,  $p(x|\theta, m)$  refers to the probability model for the random variable  $X$ , given a specific model and a specific choice of parameters for that model.<sup>4</sup> Also, in the Bayesian approach,  $p(\theta|m)$  refers to the prior probability that we attach to the parameters  $\theta$ , and  $p(\theta|x, m)$  refers to the corresponding posterior. We wish to develop methods for choosing  $m$  based on the data  $x$ .

Let us begin with the Bayesian approach. Recall that unknowns are treated as random variables in the Bayesian approach; thus we introduce a random variable  $M$  to denote the model. The range

---

<sup>4</sup>For simplicity we use the same notation  $\theta$  to represent the parameters in each of the models; in general we could allow the parameterization to vary with  $m$ .

of  $M$  is  $\mathcal{M}$ , and  $m$  denotes a realization of  $M$ . The goal of Bayesian analysis is to calculate the posterior probability of  $M$ , conditioning on the data  $x$ :

$$p(m | x) = \frac{p(x | m)p(m)}{p(x)}. \quad (5.62)$$

Note two important features of this equation. First, as in the case of parameter estimation, we require a prior probability; in particular, we need to specify the prior probability  $p(m)$  of the model  $m$ . Second, note the absence of explicit mention of the parameter  $\theta$ . The probabilities needed for Bayesian model selection are *marginal* probabilities.

Let us consider this latter issue in more detail. The calculation of the posterior probability in Eq. (5.62) requires the probability  $p(x | m)$ , a conditional probability that is referred to as the *marginal likelihood*. We compute the marginal likelihood from the likelihood by integrating over the parameters:

$$p(x | m) = \int p(x, \theta | m) d\theta \quad (5.63)$$

$$= \int p(x | \theta, m)p(\theta | m) d\theta, \quad (5.64)$$

where the prior probability  $p(\theta | m)$  plays the role of a weighting function. Multiplying the marginal likelihood by the prior probability  $p(m)$  yields the desired posterior  $p(m | x)$ , up to the normalization factor  $p(x)$ .

If we wish to use the posterior to *select* a model, then we must collapse the posterior to a point. As in the case of parameter estimation, various possibilities present themselves; in particular, a popular approach is to pick the model that maximizes the posterior probability. An advantage of this approach is that it obviates the need to calculate the normalization constant  $p(x)$ .

More generally, however, the Bayesian approach aims to use the entire posterior. To illustrate the use of the model posterior, let us again consider the problem of prediction. Taking  $X_{new}$  to be conditionally independent of  $X$ , given  $\theta$  and  $m$ , we have:

$$p(x_{new} | x) = \int \int p(x_{new}, \theta, m | x) d\theta dm \quad (5.65)$$

$$= \int \int p(x_{new} | \theta, m)p(\theta, m | x) d\theta dm \quad (5.66)$$

$$= \int \int p(x_{new} | \theta, m)p(\theta | x, m)p(m | x) d\theta dm. \quad (5.67)$$

From this latter equation, we see that a full Bayesian approach to prediction requires two posterior probabilities: the model posterior  $p(m | x)$  from Eq. (5.62) and the parameter posterior  $p(\theta | x, m)$  from Eq. (5.1). These posteriors can be viewed as “weights” for the prediction  $p(x_{new} | \theta, m)$ ; the total prediction can be viewed as a “weighted prediction.” This approach to prediction is referred to as *model averaging*.

It should be acknowledged that it is a rare circumstance in which the integrals in Eq. (5.64) and Eq. (5.67) can be done exactly, and Bayesian model averaging and model selection generally involve making approximations. We will discuss some of these approximations in Chapter 26.

Frequentist approaches to model selection avoid the use of prior probabilities and Bayes rule. Rather, one considers various model selection *procedures*, and evaluates these procedures in terms of various frequentist criteria. For example, one could consider a scenario in which the true probability density is assumed to lie within the class  $\mathcal{M}$ , and ask that a model selection procedure pick the true model with high frequency. Alternatively, one could ask that the procedure select the “best” model in  $\mathcal{M}$ , where “best” is defined in terms of a measure such as the Kullback-Leibler divergence between a model and the true probability density.

It is important to understand that maximum likelihood itself cannot be used as a model selection procedure. Augmenting a model with additional parameters cannot decrease the likelihood, and thus maximum likelihood will prefer more complex models. More complex models may of course be better than simpler models, if they provide access to probability densities that are significantly closer to the true density, but at some point there are diminishing returns and more complex models principally provide access to additional poor models. The fact that we have to estimate parameters implies that with some probability we will select one of the poor models. Thus the “variance” introduced by the parameter estimation process can lead to poorer performance with a more complex model. Maximum likelihood is unable to address this “overfitting” phenomenon.

One approach to frequentist model selection is to “correct” maximum likelihood to account for the variance due to parameter estimation. The AIC method to be discussed in Chapter 26 exemplifies this approach. An alternative approach, also discussed in Chapter 26, is the *cross-validation* idea, in which the data are partitioned in subsets, with one subset used to fit parameters for various models, and another subset used to evaluate the resulting models.

## 5.4 Appendix A

In this section we calculate the posterior density of  $\mu$  in the univariate Gaussian density estimation problem. Recall that the joint probability of  $x$  and  $\mu$  is given by:

$$p(x, \mu) = \frac{1}{(2\pi\sigma^2)^{N/2}} \exp \left\{ -\frac{1}{2\sigma^2} \sum_{n=1}^N (x_n - \mu)^2 \right\} \frac{1}{(2\pi\tau^2)^{1/2}} \exp \left\{ -\frac{1}{2\tau^2} (\mu - \mu_0)^2 \right\}, \quad (5.68)$$

and the problem is to normalize this joint probability.

Let us focus on the terms involving  $\mu$ , treating all other terms as “constants” and dropping them throughout. We have:

$$p(x, \mu) \propto \exp \left\{ -\frac{1}{2\sigma^2} \sum_{n=1}^N (x_n^2 - 2x_n\mu + \mu^2) - \frac{1}{2\tau^2} (\mu^2 - 2\mu_0\mu + \mu_0^2) \right\} \quad (5.69)$$

$$= \exp \left\{ -\frac{1}{2} \sum_{n=1}^N \left[ \frac{1}{\sigma^2} (x_n^2 - 2x_n\mu + \mu^2) + \frac{1}{\tau^2} \left( \frac{\mu^2}{N} - 2\frac{\mu_0\mu}{N} + \frac{\mu_0^2}{N} \right) \right] \right\} \quad (5.70)$$

$$= \exp \left\{ -\frac{1}{2} \sum_{n=1}^N \left[ \left( \frac{1}{\sigma^2} + \frac{1}{N\tau^2} \right) \mu^2 - 2 \left( \frac{x_n}{\sigma^2} + \frac{\mu_0}{N\tau^2} \right) \mu + C \right] \right\} \quad (5.71)$$

$$\propto \exp \left\{ -\frac{1}{2} \left[ \left( \frac{N}{\sigma^2} + \frac{1}{\tau^2} \right) \mu^2 - 2 \left( \frac{N\bar{x}}{\sigma^2} + \frac{\mu_0}{\tau^2} \right) \mu \right] \right\} \quad (5.72)$$

$$\propto \exp \left\{ -\frac{1}{2} \left( \frac{N}{\sigma^2} + \frac{1}{\tau^2} \right) \left[ \mu^2 - 2 \left( \frac{N}{\sigma^2} + \frac{1}{\tau^2} \right)^{-1} \left( \frac{N\bar{x}}{\sigma^2} + \frac{\mu_0}{\tau^2} \right) \mu \right] \right\} \quad (5.73)$$

$$= \exp \left\{ -\frac{1}{2\tilde{\sigma}^2} [\mu^2 - 2\tilde{\mu}\mu] \right\}, \quad (5.74)$$

where

$$\tilde{\sigma}^2 = \left( \frac{N}{\sigma^2} + \frac{1}{\tau^2} \right)^{-1} \quad (5.75)$$

and

$$\tilde{\mu} = \frac{N/\sigma^2}{N/\sigma^2 + 1/\tau^2} \bar{x} + \frac{1/\tau^2}{N/\sigma^2 + 1/\tau^2} \mu_0, \quad (5.76)$$

This identifies the posterior as a Gaussian distribution with mean  $\tilde{\mu}$  and variance  $\tilde{\sigma}^2$ .

## 5.5 Historical remarks and bibliography

# An Introduction to Probabilistic Graphical Models

Michael I. Jordan  
*University of California, Berkeley*

June 30, 2003



## Chapter 6

# Linear Regression and the LMS algorithm

In the following chapters we discuss elementary building blocks for graphical models. We begin with the simple case of a single continuous-valued node whose mean is a linear function of the values of its parents. The parents can be discrete or continuous.

In specifying the linear regression model in Chapter 5, we made several assumptions in addition to the linearity assumption, in particular the assumption of IID sampling and the assumption of a Gaussian distribution for the variation around the conditional mean. These latter assumptions yielded a fully specified probabilistic model, enabling us to define a likelihood and thereby invoke frequentist or Bayesian statistical methods to estimate parameters. It might be useful, however, to step momentarily outside of the probabilistic framework and ask why we consider a parameter estimation problem to be well posed once we have defined a “fully specified probabilistic model.” In the current chapter, we address this foundational issue in a rather concrete way, taking advantage of the simplicity of the linear model to bring to the fore a different set of intuitions about parameter estimation. We begin by making the linearity assumption, but then let geometric rather than probabilistic intuitions be our guide. In particular, we view each data point as imposing a linear constraint on the parameters and treat parameter estimation as a (deterministic) constraint satisfaction problem. We focus on obtaining algorithms that solve this constraint satisfaction problem, exploiting the geometric framework to analyze the convergence of these algorithms.

The emphasis on constraint satisfaction algorithms in the current chapter has the advantage of focusing attention on some computational issues that are important in practice and were glossed over in our purely statistical discussion in Chapter 5. In particular, we will introduce the distinction between “batch” and “on-line” algorithms, a distinction which is of importance in real-time applications of statistical modeling and in situations involving large data sets.

At the end of the chapter, we return to the probabilistic perspective, showing that there is a natural correspondence between the (Euclidean) geometry underlying the constraint satisfaction formulation and the statistical assumptions alluded to above. Thus, we can view the excursion into geometry as providing support for the statistical perspective in Chapter 5; thus encouraged, we will be less bashful about bringing probabilistic machinery to bear at the outset in future chapters. At

the same time, we will continue to seek external support for probabilistic assumptions, particularly when they shed light on computational concerns.

## 6.1 Batch and on-line algorithms

Let us consider in some more detail how data points may be presented to the learner. We wish to distinguish two basic situations—the setting of “batch” presentation, in which data are available as a block, and the “on-line” setting in which data arrive sequentially. Both settings arise naturally in practice: In many problems it is necessary to respond in real time, and on-line methods are dictated; in other situations our only interest is in a final answer—the best answer that we can obtain given a certain data-gathering budget—and in such cases batch methods are natural.

On the other hand, we are often free to take either the batch or the on-line point of view on a learning problem—a sequential data stream can be stored for subsequent analysis as a block, and a block of data can be accessed sequentially. Moreover, a theoretical understanding of algorithms for parameter estimation is enhanced by approaching the problem from both points of view. We will see that the on-line point of view yields simple, intuitive algorithms, but a full analytical understand of on-line algorithms can be difficult, and we therefore turn to a related batch analysis to enhance understanding. On the other hand, batch methods are often usefully understood by taking an on-line point of view—in particular, large-scale batch problems generally require iterative algorithms that sweep repeatedly through the data. These sweeps can often be usefully analyzed as on-line algorithms.

A great deal of insight can be obtained by considering the elemental problem of updating the parameters of a linear model based on the presentation of a single data point. Let us begin with a discussion of the geometry underlying this problem, and show how simple geometric intuition leads us to an on-line algorithm known as the *LMS algorithm*. The acronym “LMS” refers to “least mean squares,” which, as we shall see, reflects the fact that the algorithm can be viewed as an optimization or constraint satisfaction procedure.

## 6.2 The LMS algorithm

Let us begin with a minimum of probabilistic pretension and consider the core of the linear model—the linear dependence of one variable on another. We consider the following question: Suppose that we have a pair of observed variables  $x_n$  and  $y_n$  that we assume are related linearly. What should a learning algorithm do when presented with a data point consisting of the pair  $(x_n, y_n)$ ? We shall be very naive and see if we can get any clues as to how to design a learning algorithm by considering the vector space geometry that characterizes the model.

We wish to express  $y_n$  as a linear function of  $x_n$ :

$$y_n = \theta^T x_n + \epsilon_n, \quad (6.1)$$

where  $\theta$  is a parameter vector. Let us view  $\epsilon_n$  as a deterministic “error term” whose presence in Eq. (6.1) is an admission that we don’t necessarily expect to be able to express  $y_n$  perfectly as a

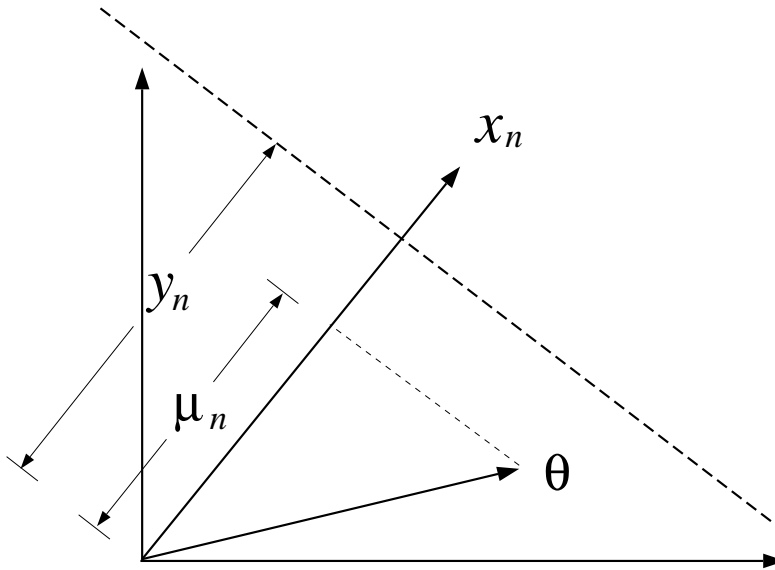


Figure 6.1: The geometry associated with the LMS algorithm. The figure shows the projection  $\mu_n$  of the parameter vector  $\theta$  on the input vector  $x_n$ . Also shown is the output value  $y_n$  as a distance along the  $x_n$  vector. The dashed line is the set of all vectors  $\theta$  that have a projection of  $y_n$  and thus are solutions. The error associated with  $\theta$  is the distance  $(y_n - \mu_n)$ . Changing  $\theta$  by the vector  $(y_n - \mu_n)x_n$  thus yields a solution vector.

linear function of  $x_n$ . In particular, let us forgo endowing  $\epsilon_n$  or any of the other terms in Eq. (6.1) with probability distributions.

Figure 6.1 displays the vectors  $x_n$  and  $\theta$  as well as the projection of  $\theta$  on  $x_n$ , whose value we denote by  $\mu_n$ . The projection  $\mu_n$  is the inner product  $\theta^T x_n$  divided by the norm of  $x_n$ .<sup>1</sup> Let us suppose for simplicity (temporarily) that  $x_n$  has norm one, so that the inner product  $\theta^T x_n$  is the same as the projection  $\mu_n$ . Now consider the problem of finding a vector  $\theta$  that maps  $x_n$  to  $y_n$  exactly; that is, a vector such that  $\epsilon_n$  is zero. Clearly we require a vector  $\theta$  whose projection onto  $x_n$  is equal to  $y_n$ , and as the figure shows, there is a line of possible solutions that is orthogonal to  $x_n$ . Any vector along this line projects to the desired value  $y_n$ . We can view the data point  $(x_n, y_n)$  as imposing a constraint upon the vector  $\theta$  that it lie along this line.

How might we design a learning algorithm to update the current value of the parameter vector

<sup>1</sup>Recall the fundamental relationship:

$$\cos \alpha = \frac{\theta^T x_n}{\|\theta\| \|x_n\|}, \quad (6.2)$$

where  $\alpha$  is the angle between  $\theta$  and  $x_n$ . From this relationship we obtain

$$\mu_n = \frac{\theta^T x_n}{\|x_n\|}. \quad (6.3)$$

for the projection  $\mu_n = \|\theta\| \cos \alpha$ .

$\theta$  such that the new value of  $\theta$  meets the constraint and lies on the solution line? Although there are an infinity of possible directions that we could move, note that there are two *natural* directions available to us: the direction associated with  $x_n$  and that associated with  $\theta$ . Let us be very naive and decide that we should choose one of these two directions as the direction in which to update  $\theta$ .

Although it is possible to figure out how far to move along the  $\theta$  direction so as to intersect the solution line, it is rather easier to figure out how far to move along the  $x_n$  direction, given the orthogonality of  $x_n$  and the solution line. Let us opt for simplicity and choose to follow  $x_n$ .

Given that  $x_n$  is a unit vector, and given that the error we incur using the current parameter vector is the difference  $(y_n - \theta^T x_n)$ , it is clear that we should move the parameter vector a distance  $(y_n - \theta^T x_n)$  in the  $x_n$  direction. Thus:

$$\theta^{(t+1)} = \theta^{(t)} + (y_n - \theta^{(t)T} x_n) x_n, \quad (6.4)$$

where  $\theta^{(t)}$  is the estimated value of  $\theta$  at the  $t$ th step of the algorithm. This algorithm jumps to the solution line.

If the vector  $x_n$  is not a unit vector, then we need to scale all of our distances by the norm of  $x_n$ . The projection is now  $\theta^T x_n / \|x_n\|$  and thus we need to choose a parameter vector whose projection onto  $x_n$  is  $y_n / \|x_n\|$ . This implies that the error we incur using  $\theta$  is given by  $(y_n - \theta^T x_n) / \|x_n\|$ , which is the amount we need to move in the direction of  $x_n$ . The unit vector in this direction is given by  $x_n / \|x_n\|$ ; thus we obtain the following learning algorithm:

$$\theta^{(t+1)} = \theta^{(t)} + \frac{1}{\|x_n\|^2} (y_n - \theta^{(t)T} x_n) x_n, \quad (6.5)$$

which again hops to the solution line in a single step.

More generally, we express our learning algorithm in the following form:

$$\theta^{(t+1)} = \theta^{(t)} + \rho (y_n - \theta^{(t)T} x_n) x_n, \quad (6.6)$$

where  $\rho$  is a free parameter known as the “step size.” Our analysis has shown that the choice  $\rho = 1 / \|x_n\|^2$  yields an algorithm that hops to the solution line in a single step. It is also easy to see that if  $0 < \rho < 2 / \|x_n\|^2$ , then on repeated presentations of  $x_n$  the algorithm will converge to the solution line asymptotically.

The algorithm in Equation 6.6 is the LMS algorithm.

### 6.2.1 Multiple data points

Let us now consider the case in which multiple data points are available. In particular we suppose that we have a “training set”  $\mathcal{X} = \{(x_n, y_n)\}_{n=1}^N$ , where  $N$ , the number of data points, is at least as large as  $k$ , the dimensionality of the parameter vector.

Let us begin by considering the simplest case, in which  $N = k$ ; let us also assume for simplicity that the vectors  $x_n$  are linearly independent. Under these conditions, the model given by Equation 6.1 imposes a set of  $k$  linearly independent equations on  $k$  unknowns. This implies the existence of a unique parameter vector  $\theta$  that achieves  $\epsilon_n = 0$  for each  $n$ . Will the LMS algorithm find this solution?

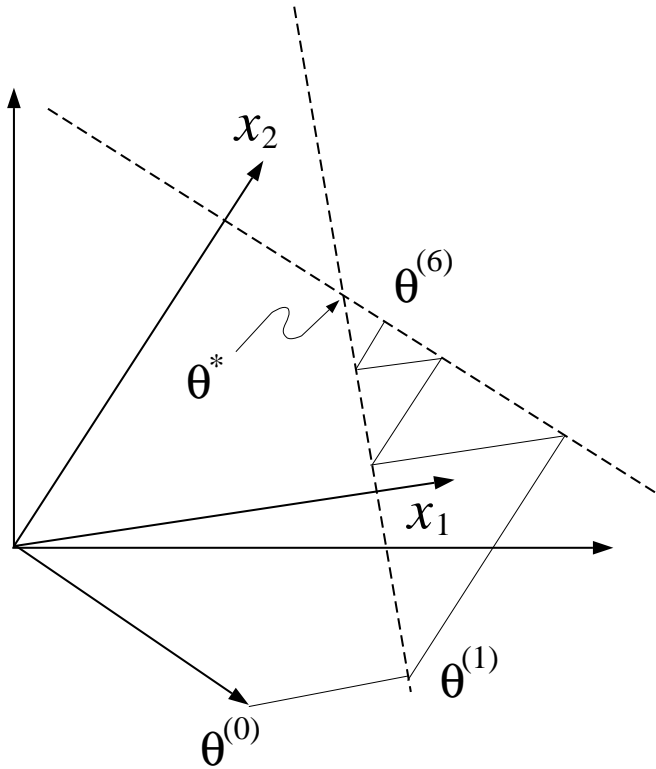


Figure 6.2: The geometry associated with the LMS algorithm in the case of two input vectors  $x_1$  and  $x_2$ . Associated with each vector is a line of solutions and the intersection of these lines is the vector  $\theta^*$  that solves the problem for both vectors. We show the path taken by the LMS algorithm upon repeated presentations of  $x_1$  and  $x_2$ .

Figure 6.2 presents an example for the case of  $N = 2$ . As shown in the figure, each of the directions determined by the vectors  $x_1$  and  $x_2$  is associated with a solution line of vectors  $\theta$  that map the given  $x_i$  to the corresponding  $y_i$ . The value  $\theta^*$  that maps both vectors  $x_n$  to their desired values lies at the intersection of these two lines. Assuming that the training regime alternates between the two data points, we see that the LMS algorithm takes a zigzag path, following first the  $x_1$  direction and then the  $x_2$  direction. It seems clear, and it is in fact true (as we will show), that there exists a maximum value of the step size for which the algorithm converges to the solution.

If we turn to the case of  $N > k$ , we expect to see a qualitatively similar behavior in which LMS takes a zigzag path through the parameter space. In this case, however, we have an overdetermined set of equations and the lines that achieve  $\epsilon_n$  for the various data points do not meet at a single point (see Figure 6.3). Given that LMS always moves from the current  $\theta$  towards the line of solutions corresponding to the current data point, we see that we cannot expect the algorithm to move to a single point and stay put. We do expect, however, that the LMS algorithm should “converge” towards a small region of the parameter space, given an appropriate choice of the step size. Making further progress on these issues requires us to characterize more formally the constraint satisfaction

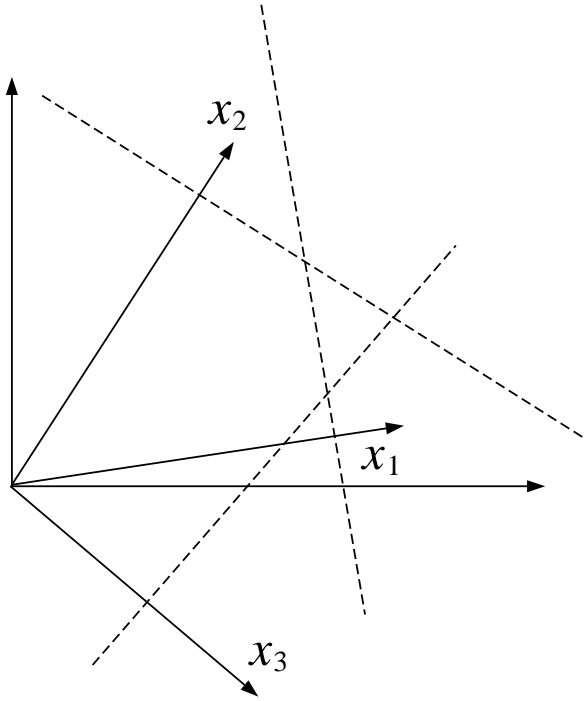


Figure 6.3: The geometry associated with the LMS algorithm in the case of three input vectors  $x_1$ ,  $x_2$  and  $x_3$ . Associated with each vector is a line of solutions. In general these lines do not intersect.

problem underlying the algorithm.

### 6.3 The sum of squares cost function and the normal equations

The approach that we pursue—which dates back to Gauss if not before—is to search for parameter vectors  $\theta$  that yield “small” values of  $\epsilon_n$ . We need to characterize what we mean by “small,” and decide how to combine the errors for different values of  $n$ . To make these decisions we again reason geometrically. We now work in a different geometry, however, namely an  $N$ -dimensional vector space, where  $N$  is the number of data points.

Let  $y$  denote a column vector with components  $y_n$  and let  $\hat{y}$  denote a column vector with components  $\hat{y}_n = \theta^T x_n$ . These are vectors in an  $N$ -dimensional vector space. We want to express the relationship between these vectors in a way that reveals more of the geometry behind the linear model. To do so, let  $X$  represent the matrix whose  $n$ th row is the row vector  $x_n^T$ . We write:

$$\hat{y} = X\theta, \quad (6.7)$$

showing that  $\hat{y}$  lies in the column space of the matrix  $X$ . Each column of  $X$  corresponds to a particular component of the vector  $x_n$ , and the set of columns of  $X$  can be viewed as spanning a vector subspace (see Figure 6.4). The vector  $\hat{y}$  lies in this vector subspace. The vector  $y$ , on the

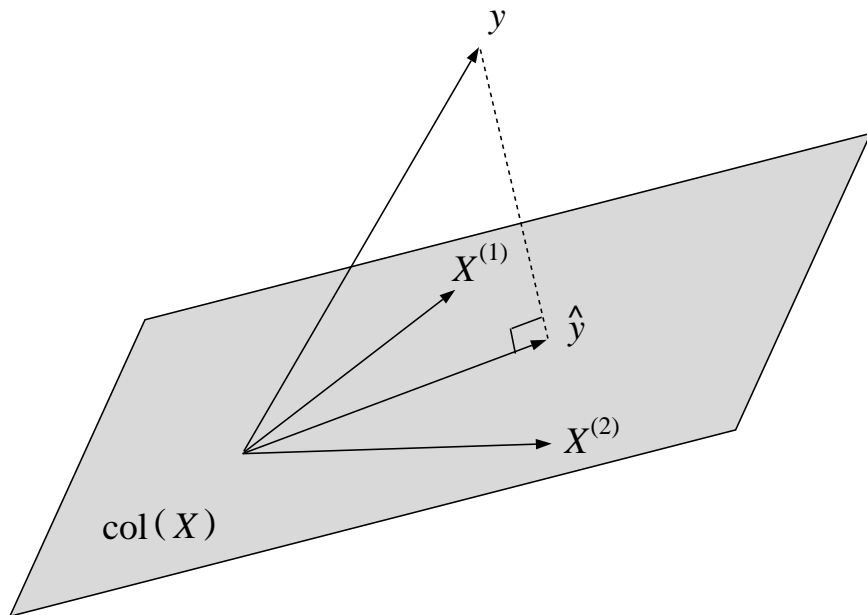


Figure 6.4: A geometric perspective on the linear regression problem for the case of the matrix  $X$  having two columns. Let  $X^{(1)}$  represent the first column of  $X$  and let  $X^{(2)}$  represent the second column. Denote the column space of  $X$  as  $\text{col}(X)$ . The approximating vector  $\hat{y}$  lies in this vector subspace, while the data vector  $y$  generally lies outside of this subspace. We wish to find a vector  $\hat{y}$  that is the orthogonal projection of  $y$  on  $\text{col}(X)$ .

other hand, generally lies outside of this vector subspace, reflecting the fact that in general the errors  $\epsilon_n$  cannot simultaneously be zero.

Our problem reduces to choosing a vector  $\hat{y}$  in a vector subspace that best represents a vector  $y$  outside of the subspace. A natural solution, from a geometric point of view, is to choose the *orthogonal projection* of  $y$  onto the subspace. We will solve the problem of finding a vector  $\theta^*$  that yields this projection in three different ways.

Our first solution appeals directly to the geometry in Figure 6.4. In particular, for  $\hat{y}$  to be the orthogonal projection of  $y$  on the column space of  $X$ , the difference vector  $\epsilon = y - \hat{y}$  must be orthogonal to this vector subspace. Thus  $y - \hat{y} = y - X\theta^*$  must be orthogonal to the columns of  $X$ , or, equivalently, orthogonal to the rows of  $X^T$ . This yields:

$$X^T(y - X\theta^*) = 0 \quad (6.8)$$

which implies

$$X^T X \theta^* = X^T y. \quad (6.9)$$

These equations, which characterize an optimizing vector  $\theta^*$ , are referred to as the *normal equations*.

There is an equivalent characterization of the orthogonal projection in terms of minimal Euclidean length; this characterization leads us to a calculus-based derivation of the normal equations. In particular, let us choose  $\hat{y}$  such that the error vector  $\epsilon = y - \hat{y}$  has minimal Euclidean length. Thus, working (equivalently) with the squared length, we wish to minimize the *least squares cost function*  $J(\theta)$ :

$$J(\theta) \triangleq \frac{1}{2} \sum_{n=1}^N \epsilon_n^2 = \frac{1}{2} \sum_{n=1}^N (y_n - \theta^T x_n)^2, \quad (6.10)$$

with respect to  $\theta$ .<sup>2</sup>

Differentiating  $J$  with respect to the  $i$ th component,  $\theta^i$ , of the vector  $\theta$ , we obtain:

$$\frac{\partial J}{\partial \theta^i} = - \sum_{n=1}^N (y_n - \theta^T x_n) x_n^i, \quad (6.11)$$

where  $x_n^i$  is the  $i$ th component of the vector  $x_n$ . Collecting these partial derivatives into a vector we obtain the following gradient:

$$\nabla_\theta J = - \sum_{n=1}^N (y_n - \theta^T x_n) x_n, \quad (6.12)$$

which we must set to zero to obtain conditions on the optimizing solution  $\theta^*$ .

To obtain an explicit solution it is useful to make use of the matrix  $X$  and write the gradient as a single matrix equation. Recalling that  $X$  has the vectors  $x_n$  on its rows, we can view Eq. (6.12) as a sum of the rows of  $X$ , weighted by the values  $(y_n - \theta^T x_n)$ . Equivalently this sum is the sum

---

<sup>2</sup>The factor of  $1/2$  is included for convenience; it cancels the factor arising from the exponent of 2 when we take derivatives.

of the columns of  $X^T$ . Recalling that the values  $\theta^T x_n$  are the components of the vector  $\hat{y} = X\theta$ , we have:

$$\nabla_{\theta} J = -X^T(y - X\theta). \quad (6.13)$$

Finally, setting to zero we obtain:

$$X^T(y - X\theta^*) = 0, \quad (6.14)$$

or equivalently:

$$X^T X \theta^* = X^T y, \quad (6.15)$$

which are the normal equations.

In Appendix XXX, we provide a short review of matrix and vector derivatives, which allows the reader to go directly from the cost function expressed in vector notation as:

$$J(\theta) = \frac{1}{2}(y - X\theta)^T(y - X\theta) \quad (6.16)$$

$$= \frac{1}{2}(y^T y - 2y^T X\theta + \theta^T X^T X\theta), \quad (6.17)$$

directly to the gradient:

$$\nabla_{\theta} J = -X^T(y - X\theta), \quad (6.18)$$

from which we again obtain the normal equations by setting to zero.

In most situations of practical interest, the number of data points  $N$  is larger than the dimensionality  $k$  of the input space and the matrix  $X$  has full column rank. If this condition holds, then it is easy to verify that  $X^T X$  is necessarily invertible and thus we can express  $\theta^*$  explicitly as follows:

$$\theta^* = (X^T X)^{-1} X^T y. \quad (6.19)$$

Moreover, if we take a second derivatives of  $J$  with respect to  $\theta$  we find that the Hessian matrix of  $J$  is given by  $X^T X$  (see Appendix XXX). The assumption that  $X^T X$  is invertible implies that  $X^T X$  is positive definite, and thus the critical point that we have found is a minimum. The solution to the normal equations provides the unique solution to the constraint satisfaction problem.

In Section ?? we discuss the case in which  $X$  has less than full column rank, and develop a *regularization* method to handle this case.

In the setting of “batch” presentation of data, in which data are available as a block, we can form the matrix  $X$  and the vector  $y$  and solve the normal equations. There are two major classes of methods for solving these equations: *direct methods* and *iterative methods*. The former class of methods, of which Gaussian elimination and QR decomposition are classical examples, converge in a finite number of steps. Iterative methods, which converge in a limiting sense, are of interest in the setting of particularly large problems, where direct approaches can be infeasible computationally.

Our next task is to try to understand the link between the two geometries that we have studied—the  $k$ -dimensional geometry of Figure 6.1 and the  $N$ -dimensional geometry of Figure 6.4. We also want to understand the relationship between the normal equations and the LMS algorithm. In the following section, we forge these links via the derivation of a steepest descent algorithm for solving the normal equations. This algorithm can be viewed as an example—one of many—of an iterative

method for the batch case. Our goal, however, is not to explore iterative solution methods for the batch case (indeed there are more sophisticated methods than steepest descent). Rather, we wish to use the normal equations and their solution via steepest descent as a point of departure for understanding the on-line case.

## 6.4 Steepest descent and the LMS algorithm

Following the negative of the gradient in Eq. (6.12) we obtain the following *steepest descent* algorithm:

$$\theta^{(t+1)} = \theta^{(t)} + \rho \sum_{n=1}^N (y_n - \theta^{(t)T} x_n) x_n, \quad (6.20)$$

where  $\theta^{(t)}$  is the parameter vector at the  $t$ th step of the iteration and where  $\rho$  is the step size. The algorithm is initialized at an arbitrary vector  $\theta^{(0)}$  and iterates until a convergence criterion is met.

The steepest descent algorithm involves a sum over all  $N$  input vectors, thus the algorithm is a batch algorithm. Note that this aspect of the algorithm can render it rather inefficient, and this inefficiency motivates us to consider on-line approaches. In particular, if  $N$  is large, say in the millions, then the algorithm can spend an inordinate amount of time passing through the training set in order to compute the gradient, at which point it takes a step in the parameter space. Given that one of the motivations for studying iterative algorithms is to be able to handle very large problems, this feature of steepest descent is disconcerting. Note moreover that if the data set is redundant—a common occurrence with large data sets—then it might not be necessary to sum all of the  $N$  terms in Eq. (6.20) to obtain an accurate estimate of the direction of the gradient (the magnitude of the gradient is irrelevant because it is being scaled by a constant  $\rho$  that is under our control). In such situations, algorithms that take a sum over a subset of the data—a “mini-batch”—can often be significantly more efficient than the full batch algorithm. Indeed, in the limiting case we can view a single term,  $-(y_n - \theta^{(t)T} x_n) x_n$ , as providing a rough estimate of the direction of the gradient. It may be advantageous to go ahead and follow this rough estimate and make progress in the parameter space rather than waiting to obtain a better estimate. This logic leads to the following algorithm, which adjusts the parameter vector according to the estimated gradient based on a single data point:

$$\theta^{(t+1)} = \theta^{(t)} + \rho(y_n - \theta^{(t)T} x_n) x_n. \quad (6.21)$$

This is of course the LMS algorithm. We see that the LMS algorithm can be viewed as an approximation to the steepest descent algorithm, where the approximation involves replacing the sum obtained in the batch algorithm with a single term. Such an approximation is referred to as a “stochastic gradient” algorithm, where “stochastic” refers to an assumption that the choice of data point  $(x_n, y_n)$  is made according to a stochastic process.

Let us emphasize that although LMS can be viewed as an approximation to steepest descent, it is often a much superior algorithm. Because it requires significantly less work per parameter update, it can converge significantly faster than steepest descent.

We are now in a position to learn something more about the convergence of the LMS algorithm. From the normal equations we have a characterization of the vector toward which we expect the LMS algorithm to tend, and from the steepest descent equations we have the possibility of characterizing the path that LMS will be expected to follow on average (under an appropriate stochastic analysis). In particular we may hope to learn something about the maximum possible value of  $\rho$ .

We present two analyses—one algebraic and one geometric—that yield the sought-after results. Both analyses involve analyzing the shape of the quadratic cost function  $J$  in the neighborhood of its minimum.

#### 6.4.1 An algebraic convergence analysis<sup>3</sup>

One way to understand the convergence of the steepest descent algorithm in Eq. (6.20) is to unfold the recursion and solve the resulting equation.

In particular, letting  $\theta^{(t)}$  represent the parameter vector at the  $t$ th iteration of the algorithm, we have:

$$\theta^{(t+1)} = \theta^{(t)} + \rho \sum_{n=1}^N (y_n - \theta^{(t)T} x_n) x_n \quad (6.22)$$

$$= \theta^{(t)} + \rho \sum_{n=1}^N x_n y_n - \rho \sum_{n=1}^N (x_n x_n^T) \theta^{(t)} \quad (6.23)$$

$$= \theta^{(t)} + \rho X^T y - \rho X^T X \theta^{(t)} \quad (6.24)$$

$$= (I - \rho X^T X) \theta^{(t)} + \rho X^T y. \quad (6.25)$$

Expanding the recursion, we have:

$$\theta^{(t+1)} = (I - \rho X^T X) \theta^{(t)} + \rho X^T y \quad (6.26)$$

$$= (I - \rho X^T X) [(I - \rho X^T X) \theta^{(t-1)} + \rho X^T y] + \rho X^T y \quad (6.27)$$

$$= (I - \rho X^T X)^{t+1} \theta^{(0)} + \rho \sum_{i=0}^t (I - \rho X^T X)^i X^T y. \quad (6.28)$$

We now let  $t$  go to infinity. Let us assume for now that the first term goes to zero as  $t$  goes to infinity—we will then return to this term and derive a condition that ensures that it goes to zero. Thus we have:

$$\theta^{(\infty)} = \rho \sum_{i=0}^{\infty} (I - \rho X^T X)^i X^T y \quad (6.29)$$

$$= \rho (\rho X^T X)^{-1} X^T y \quad (6.30)$$

$$= (X^T X)^{-1} X^T y, \quad (6.31)$$

---

<sup>3</sup>The material in this section is optional; it will not be needed in later chapters.

which are the normal equations. We have thus shown that the steepest descent algorithm converges to the minimum of the cost function, under the assumption that the first term in Eq. (6.28) converges to zero.

Let us now consider the matrix power  $(I - \rho X^T X)^{t+1}$  as  $t \rightarrow \infty$ . In general, to show that a matrix power converges to zero we need to show that its largest eigenvalue is less than one in absolute value. Now it is easy to verify that if  $\lambda$  is an eigenvalue of  $(I - B)$  for a matrix  $B$ , then  $1 - \lambda$  is an eigenvalue of  $B$ . Thus the absolute values of the eigenvalues of  $(I - B)$  are less than one if and only if the absolute values of the eigenvalues of  $B$  are between zero and two. Thus we have the condition:

$$0 < \lambda_{\max}[\rho X^T X] < 2, \quad (6.32)$$

where  $\lambda_{\max}$  represents the maximum eigenvalue of a matrix, or equivalently:

$$0 < \rho < 2/\lambda_{\max}[X^T X]. \quad (6.33)$$

This is the condition for convergence; the step size  $\rho$  can be no larger than two divided by the maximum eigenvalue of  $X^T X$ .

#### 6.4.2 A geometric convergence analysis<sup>4</sup>

To get a better understanding of the convergence condition that we have just derived, let us rederive it from a geometric point of view.

Our cost function is a quadratic function in the components  $\theta^i$  and can be plotted as a set of elliptical contours in the parameter space. In particular, for the example shown earlier in Figure 6.2, the corresponding contours are shown in Figure 6.5. Let us take a moment to understand how to obtain these contours.

We know that the minimum of the cost function is achieved by the vector  $\theta^*$  that solves the normal equations. Our analysis will be simplified if we choose this optimizing point as the origin of our coordinate system. We choose new coordinates  $\phi = \theta - \theta^*$  and express the cost function in these new coordinates:

$$\begin{aligned} J(\phi) &= \frac{1}{2} \sum_{n=1}^N (y_n - \theta^T x_n)^2 \\ &= \frac{1}{2} (y - X\theta)^T (y - X\theta) \\ &= \frac{1}{2} (y - X(\phi + \theta^*))^T (y - X(\phi + \theta^*)) \\ &= \frac{1}{2} (y^T y - \theta^{*T} X^T y + \phi^T X^T X \phi), \end{aligned}$$

where in passing from the third line to the fourth line we have expanded the quadratic expression and used the fact that  $\theta^*$  solves the normal equations. In the new coordinates we see that the cost function is expressed simply as:

$$J(\phi) = C + \frac{1}{2} \phi^T X^T X \phi, \quad (6.34)$$

---

<sup>4</sup>The material in this section is optional; it will not be needed in later chapters.

Figure 6.5: The contours of the cost function  $J(\theta)$  for the example in Figure 6.2.

where  $C = y^T y - \theta^{*T} X^T y$  is a constant.

We now rotate the coordinate system so that the axes point along the major and minor axes of the ellipse. This is achieved by making use of the eigenvectors of  $X^T X$ . In particular, let  $A$  be the matrix whose column vectors are the eigenvectors of  $X^T X$ . We have:

$$X^T X = A \Lambda A^T, \quad (6.35)$$

where  $\Lambda$  is a diagonal matrix whose elements are the eigenvalues  $\lambda_i$  of  $X^T X$ . Note also that the fact that  $X^T X$  is a symmetric matrix implies that  $A$  is orthogonal. Thus we have:

$$A^T X^T X A = \Lambda. \quad (6.36)$$

Now choose new coordinates  $\psi = A^T \phi$ . We obtain:

$$J(\psi) = C + \frac{1}{2} (A\psi)^T X^T X (A\psi) \quad (6.37)$$

$$= C + \frac{1}{2} \psi^T A^T X^T X A \psi \quad (6.38)$$

$$= C + \frac{1}{2} \psi^T \Lambda \psi. \quad (6.39)$$

This final equation is simply the weighted sum of squares of the components of  $\psi$ , with weights given by the eigenvalues  $\lambda_i$ . Setting  $J(\psi)$  equal to a constant yields the equation of an ellipsoid.

Let us now express the steepest descent equation in the new coordinates. We write the equation in matrix notation (cf. Eq. (6.24)) as:

$$\theta^{(t+1)} = \theta^{(t)} + \rho(X^T y - X^T X \theta^{(t)}) \quad (6.40)$$

Given that the  $\theta$  coordinates and the  $\psi$  coordinates are related via  $\theta = A\psi + \theta^*$ , we obtain:

$$A\psi^{(t+1)} = A\psi^{(t)} - \rho(X^T X A\psi^{(t)}), \quad (6.41)$$

where we have used the fact that  $\theta^*$  solves the normal equations. Premultiplying both sides of this equation by  $A^T$  (recalling that  $A$  is orthogonal), we obtain:

$$\psi^{(t+1)} = \psi^{(t)} - \rho(A^T X^T X A\psi^{(t)}) \quad (6.42)$$

$$= \psi^{(t)} - \rho\Lambda\psi^{(t)}. \quad (6.43)$$

This equation represents a decoupled set of equations in the components of the  $\psi$  vector:

$$\psi^{i(t+1)} = (1 - \rho\lambda_i)\psi^{i(t)}, \quad (6.44)$$

which converges if  $(1 - \rho\lambda_i)$  is less than one in absolute value. That is, we require:

$$\|1 - \rho\lambda_i\| < 1, \quad (6.45)$$

which is equivalent to:

$$0 < \rho < 2/\lambda_i. \quad (6.46)$$

Given that this must be true for all  $\lambda_i$  we have recovered the same condition for convergence as obtained in the previous section (Eq. (6.33)).

In the decoupled coordinate system, we see that convergence condition amounts to the condition that if the algorithm hops from one side of an axis of the ellipsoid to the other, it must end up no further away from the axis than when it started. The axis associated with the maximum eigenvalue puts the strongest constraint on the step size.

### 6.4.3 LMS and stochastic approximation

It is beyond the scope of the book to provide a detailed consideration of the sense in which the LMS algorithm (and related “on-line” algorithms) converges to a solution, and we will content ourselves with providing pointers to the literature on stochastic approximation where such issues are addressed.<sup>5</sup> To get some sense of the issues involved, however, note that the path taken by the LMS algorithm in the parameter space depends on the particular way in which the training set is ordered. There are many kinds of ordering that may arise practice; typical examples include: (1) the algorithm passes through the training set in a fixed order, (2) varying orderings are used for each pass through the training set, and (3) data points are selected randomly with replacement from the training set. Moreover, (4) in other cases there is no “training set”; rather, the data points arrive as a potentially infinite stream. Another set of issues arises when one considers the meaning of “convergence.” If the step size  $\rho$  remains fixed then the algorithm “converges” only in a stochastic sense, and there are several kinds of stochastic convergence that one can consider. It is also possible to consider variants of LMS in which the step size decreases to zero; under certain conditions (certain rates of decrease of the step size) the algorithm can be shown to converge to a point. As should be clear, a full analysis of LMS is a subtle business, and fairly sophisticated mathematical tools are required to do justice to the problem.

---

<sup>5</sup>See the section on “Historical remarks and bibliography” at the end of the chapter.

## 6.5 Weighted least squares

In later chapters we will need to solve a generalization of least squares, in which each data point is accompanied by a “weight”  $w_n$ . Intuitively, large weights correspond to data points that are “important,” and small weights correspond to data points that are “unimportant.” Let us set up this *weighted least squares* problem and display the corresponding normal equations.

Consider a set of weights  $w_n$  for each  $n = 1, \dots, N$ . Let us incorporate these weights into the cost function as follows:

$$J(\theta) = \frac{1}{2} \sum_{n=1}^N w_n (y_n - \theta^T x_n)^2, \quad (6.47)$$

We can write this cost function in matrix form by defining a diagonal matrix  $W \triangleq \text{diag}(w_1, w_2, \dots, w_N)$  and writing:

$$J(\theta) = \frac{1}{2} (y - X\theta)^T W (y - X\theta), \quad (6.48)$$

where we see that the weight matrix  $W$  can be viewed as defining a new metric with which to measure errors.

To obtain a solution  $\theta^*$ , we take the gradient of Eq. (6.48):

$$\nabla_{\theta} J = -X^T W y - X^T W X \theta. \quad (6.49)$$

and set to zero:

$$X^T W X \theta^* = X^T W y, \quad (6.50)$$

These equations are the normal equations for weighted least squares.

## 6.6 Probabilistic interpretation

Thus far we have avoided making any probabilistic interpretation of the linear model and the least squares cost function. Let us now return to the statistical framework of linear regression in Chapter 5 and endow the terms in the linear model with probability distributions.

In Chapter 5 we augmented the linearity assumption with the assumption that the errors  $\epsilon_n$  are Gaussian random variables having zero mean and variance  $\sigma^2$ . This assumption implies that the conditional probability of  $y_n$  given  $x_n$  is Gaussian with mean  $\theta^T x_n$ :

$$p(y_n|x_n, \theta) = \frac{1}{\sqrt{2\pi\sigma^2}} \exp \left\{ -\frac{1}{2\sigma^2} (y_n - \theta^T x_n)^2 \right\}. \quad (6.51)$$

We assumed moreover that the  $y_n$  are independent and identically distributed, conditional on  $x_n$ . Thus the joint conditional distribution of the data  $y$  is obtained by taking the product of the individual conditional probabilities:

$$p(y|x, \theta) = \frac{1}{(2\pi\sigma^2)^{N/2}} \exp \left\{ -\frac{1}{2\sigma^2} \sum_{n=1}^N (y_n - \theta^T x_n)^2 \right\}. \quad (6.52)$$

Taking the logarithm and dropping the terms that do not depend on the parameter  $\theta$ , we obtain the following expression for the log likelihood:

$$l(\theta; x, y) = -\frac{1}{2\sigma^2} \sum_{n=1}^N (y_n - \theta^T x_n)^2. \quad (6.53)$$

This log likelihood is equivalent to the least-squares cost function  $J(\theta)$  in Eq. (6.10). In particular, maximizing the log likelihood with respect to  $\theta$  is equivalent to minimizing the least-squares cost function.

What we have shown is that the assumptions of a Gaussian distribution and IID sampling imply—within a maximum likelihood framework—the minimization of the least-squares cost function. Moreover, the normal equations characterize the maximum likelihood solution to the linear regression problem.

We can view this result as providing support for the likelihood-based approach to parameter estimation. In particular, in imposing probabilistic assumptions on the linear model so as to obtain a likelihood function, we have imposed neither more nor less constraint on the problem than is required to obtain a well-posed deterministic problem in the constraint satisfaction formulation. In particular, in the latter formulation, we need to decide how to measure the magnitudes of the errors and how to combine these magnitudes. These decisions have correspondences in the probabilistic formulation, in particular the Gaussian assumption effectively determines the metric by which we measure the errors, and the IID assumption determines the way in which the errors are combined. Both formulations are useful. In particular the constraint satisfaction perspective has helped us to understand that the linear, IID, and Gaussian assumptions comprise a natural family, essentially reflecting a Euclidean geometry. The probabilistic perspective provides additional insight; in particular, a Gaussian distribution for the errors can be justified via the central limit theorem if it is the case that the error terms  $\epsilon_n$  are decomposable into sums of many small random terms.

It is also worth noting that in the frequentist approach to estimation we are not restricted to likelihood-based methods. In particular, we can view the least-squares cost function as providing an “estimator” that can be evaluated with the usual frequentist criteria. That is, we can define the least-squares estimator of a parameter as a value that minimizes the least-squares cost function, whether or not the underlying probability model involves a Gaussian assumption. If the underlying model is Gaussian then the least-squares approach and maximum likelihood coincide, but in general they can be viewed as competitors. The fact that least-squares estimates involve the solutions of systems of linear equations is a computational argument in their favor.

Although the geometric perspective provides significant insight in the case of the linear model, the probabilistic, likelihood-based perspective becomes increasingly powerful when we consider various generalizations of the linear model. For example, discrete variables are naturally handled by likelihood-based methods, as are hybrid models that involve combinations of discrete and continuous variables. Moreover, latent variables allow us to build more complex error models and Markov chains allow us to move beyond the IID assumption. Likelihood-based methods will be our focus throughout the remainder of the book.

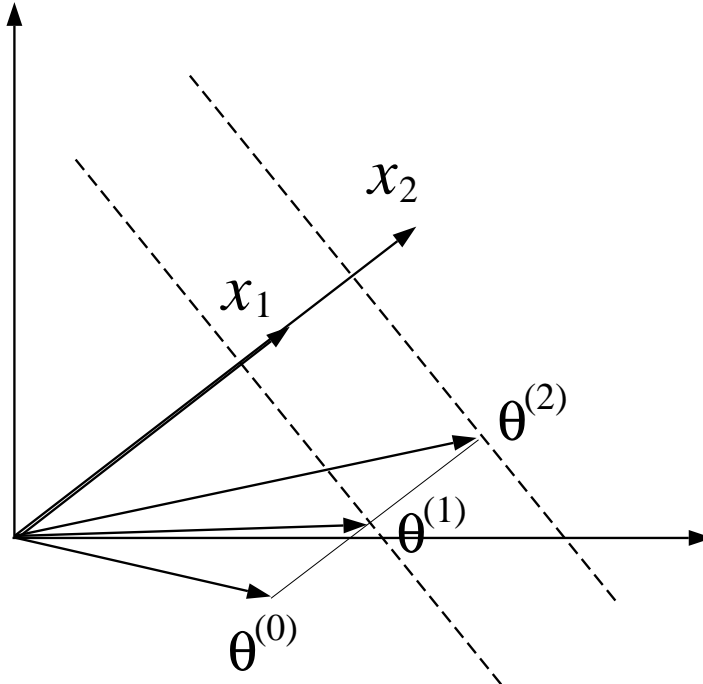


Figure 6.6: The geometry associated with the LMS algorithm in the case of two redundant input vectors  $x_1$  and  $x_2$ . The dashed lines represent lines of solutions corresponding to each of the input vectors. There is a line of least-squares solutions that lies halfway between these two lines. The component of the initial parameter vector  $\theta^{(0)}$  that is orthogonal to these lines does not vanish as the algorithm iterates.

## 6.7 Ridge regression

## 6.8 Sequential Bayesian methods

## 6.9 Historical remarks and bibliography

# An Introduction to Probabilistic Graphical Models

Michael I. Jordan  
*University of California, Berkeley*

June 30, 2003



# Chapter 7

## Linear classification

In this chapter we continue our discussion of elementary building blocks for graphical models, treating the case of a discrete node taking on a finite number of values. As in Chapter 6, our interest is in the conditional relationship between the node  $Y$  and a vector of explanatory variables  $X$ . We explore a number of possible representations for the conditional probability  $p(y | x)$ .

What form should our model of  $p(y | x)$  take in the case of discrete  $Y$ ? If  $X$  is also discrete, then we might consider models in which all possible combinations of  $X$  and  $Y$  are represented in a table. We will indeed consider such a model in this chapter; however, it is important to keep in mind that the size of such a table is exponential in the number of components of  $X$ , and we would like to develop models to handle the (commonplace) situation in which this number is large. Moreover, we wish to develop tools that allow for continuous-valued  $X$ . In either case a natural first step is to try and mimic what we did with regression, exploiting the simplicity and mathematical convenience of linearity assumptions. It is unclear, however, how to represent the conditional expectation of  $Y$ —a number between zero and one for Bernoulli and multinomial variables—within the framework of a linear model. Some sort of nonlinearity seems to be needed, but which nonlinearity? Does introducing such a nonlinearity leave us with any role for linearity?

One way to help organize our thinking on these issues is to recall that we have already seen problems involving discrete  $Y$  in Chapter 5. In particular, in our discussion of classification models in that chapter, we found it useful to explore the relationship between two kinds of models: *discriminative models*—in which  $Y$  is the child of  $X$ —and *generative models*—in which  $Y$  is the parent of  $X$ . While the former approach represents  $p(y | x)$  *explicitly*, the latter approach makes use of Bayes rule to represent the posterior probability  $p(y | x)$  *implicitly*, in terms of the class-conditional probability  $p(x | y)$  and the prior  $p(y)$ . Thus we can begin to get ideas for representations of  $p(y | x)$  by studying generative models in which  $Y$  is a parent of  $X$ , and using Bayes rule to invert the model and thereby calculate the corresponding posterior probability  $p(y | x)$ . This approach will allow us to achieve some of the goals that we alluded to above—it will suggest a certain basic mathematical structure in which linearity plays a role, and it will cope with both discrete-valued and continuous-valued  $X$ . Moreover, it will suggest a natural “upgrade path” to more complex models.

In this chapter we retain our assumption from the previous chapter that both  $X$  and  $Y$  are

observed in our data set. We cast our presentation within the context of classification, where as before we refer to  $Y$  and  $X$  as the “class label” and the “feature vector,” respectively. We will fill in some of the details that were glossed over in Chapter 5 regarding the parameterization and estimation of generative and discriminative approaches to the classification problem. We present maximum likelihood methods for parameter estimation in both frameworks.

While we place our activity in this chapter within the framework of classification, it is worth noting that there are aspects of classification problems that fall beyond the scope of our discussion. In particular, our goal in this chapter is that of obtaining a model of the conditional probability  $p(y|x)$ . While  $p(y|x)$  is a desirable quantity to model in a classification setting, it is also true that classification involves something more than evaluating a probability—in particular, classification involves making a *decision*. We can threshold the probability distribution  $p(y|x)$  to obtain a decision, but this is only one possible way to use this probability; perhaps there are others. Indeed, perhaps there are some decisions which are in some sense more costly than others; our thresholding scheme should be sensitive to such costs. Moreover, we can imagine classification algorithms that do not make use of posterior probability  $p(y|x)$  at all; rather they go directly from a data set to a decision rule. Evaluating these alternatives appropriately requires the mathematical framework of *decision theory*. In particular a decision-theoretic approach to classification allows us to specify costs associated with decisions and to evaluate alternative approaches to forming decision rules. We will return to these issues in Chapter 27, where we present a full treatment of decision theory in the graphical model setting. In that discussion we will in fact show that a reasonable first step in classification problems is to obtain a model of the conditional probability  $p(y|x)$ .

It is also worth noting that there is a flip side to this coin—there are problems other than classification problems for which the methods of this chapter are useful. In particular in Chapter 10 we discuss models that are structurally identical to the models in this chapter, but for which  $Y$  is no longer assumed to be observed; that is, for which  $Y$  is a latent variable. The results that we obtain here will play an important role in that chapter.

## 7.1 Linear regression and linear classification

A discrete-valued node can be viewed as a special case of a real-valued node, and this leads one to wonder why we need a separate treatment of discrete nodes. In particular, why not use the regression methods that we developed in Chapter 6 to solve classification problems?

To see some of the problems that arise if we pursue this approach, consider the simple case of a binary classification problem with a scalar-valued feature variable  $X$ . Let us represent the class label with a real-valued variable  $Y$ , with  $Y = 0$  and  $Y = 1$  representing the two classes. Figure 7.1 presents an example of such a problem, with the data pairs  $(x_n, y_n)$  represented as points in the plane. The linear regression fit to these data is also shown in the figure. Note that even though the data  $\{y_n\}$  are restricted to the values zero and one, the fitted line is not restricted to these values. How are we to interpret this line? In Chapter 6 we showed that the linear regression fit is a conditional mean—the expected value of  $Y$  conditioned on the observed value of  $X$ . For an indicator random variable  $Y$  the expected value is the same as the probability that the variable takes on the value 1. The fact that the fitted line in Figure 7.1 strays outside of the range  $(0, 1)$

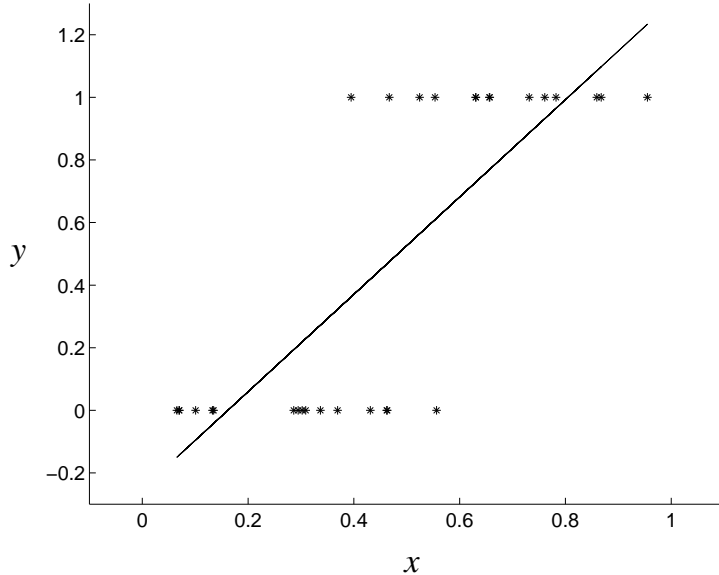


Figure 7.1: Data for a binary classification problem. The abscissa represents the one-dimensional feature vector  $x$ , and the ordinate represents the binary class label  $y$ , with 0 and 1 representing the two classes. Also shown is the least squares linear regression fit.

makes it difficult to sustain such an interpretation, however, in the setting of binary output data.

Even more serious problems arise when we consider in more detail how the regression fit depends on the data. Suppose in particular that we add the point  $(1.5, 1)$  to the data set (see Figure 7.2). The earlier fit (Figure 7.1) yields a fitted value of 2.01 at  $x = 1.5$ , suggesting, under any reasonable interpretation of this value (e.g., thresholding), that the predicted class label at  $x = 1.5$  should be 1. This correctly predicts the class of the new data point, suggesting that the parameters can already accommodate the new data point and need not be changed. Refitting the linear regression, however, changes the slope parameter from 1.55 to 1.23 and the intercept parameter from  $-0.32$  to  $-0.17$  (see Figure 7.2). Moreover, taking the value at which the fit equals 0.5 as the boundary between the two classes, this boundary changes significantly after the introduction of the new data point, leading to changes in the classification of some of the points near the boundary. If we add four additional data points at  $x = 1.5$  the boundary moves even further, as shown in Figure 7.2. Given that these new data points are predicted correctly by the original fit, and are far from the boundary, this behavior is disconcerting.

The assumptions underlying linear regression are clearly not met in the classification setting; in particular, the assumption that the variable  $Y$  is Gaussian is clearly false. This mismatch between the assumptions and the data is responsible for the problems that we have identified. Once we have made probabilistic assumptions that are appropriate for the classification setting—in particular once we have discarded the Gaussian assumption—we will obtain classification models in which the fitted values behave in an intuitively reasonable manner.

As in Chapter 6 we focus on linear models throughout the current chapter. The notion of

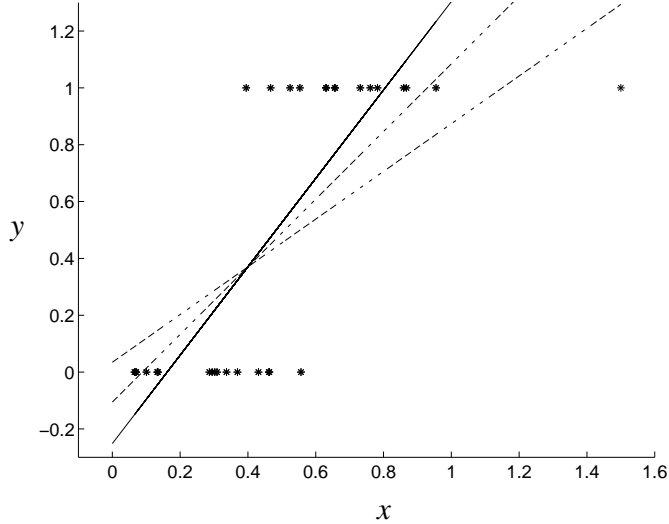


Figure 7.2: Three least squares regression fits. The solid line is the same fit as shown in Figure 7.1, the dash-dot line is the fit to the data with one additional point at  $(1.5, 1)$ , and the dashed line is the fit to the data with five additional points at  $(1.5, 1)$ .

“linearity” in the current chapter is, however, different from that in Chapter 6. We postpone the mathematical details until later sections, where in fact we will find that different classification models invoke the linearity assumption in somewhat different ways. All of the classification models that we study, however, can be viewed as providing a partitioning of the feature space into regions corresponding to the class labels. For linear models the boundaries between these regions are hyperplanes (see Figure 7.3).

## 7.2 Generative models

Figure 7.4 presents three graphical representations of generative classification models. In all three cases the class label node  $Y$  is the parent of the feature vector  $X = (X_1, X_2, \dots, X_m)$ . In Figure 7.4(a), the component features are treated as separate nodes; in this case, the children  $X_j$  are assumed to be conditionally independent given  $Y$ , as confirmed by the d-separation properties of the graph. This is a simplifying assumption that provides a starting point for our presentation and will be our focus through most of this section. In Figure 7.4(b), we have an alternative model in which the components of the feature vector are interdependent, with specific conditional independencies assumed to hold among specific sets of features. In this model general graphical model machinery must be invoked both to parameterize the class-conditional densities and to learn the values of the parameters. Accordingly we will not treat this model explicitly in this section but will return to it in later chapters once the appropriate machinery is in place. Finally, in Figure 7.4(c), we have a model in which no specific conditional independencies are assumed among the components of the

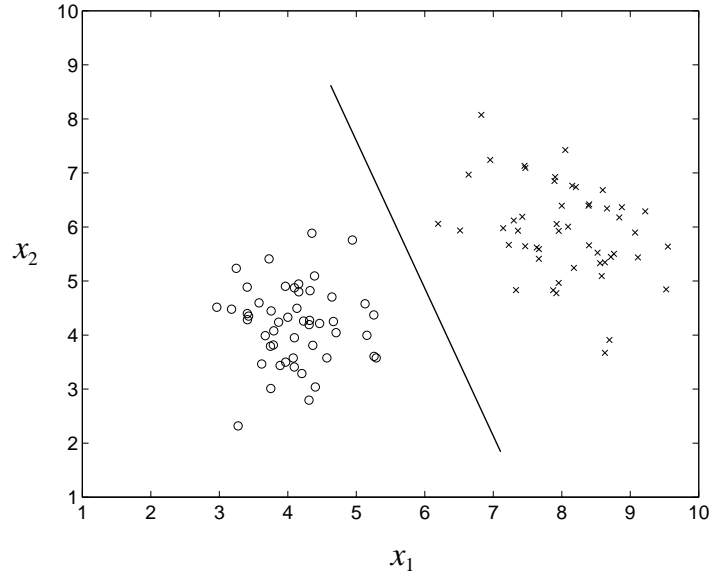


Figure 7.3: A binary classification problem in a two-dimensional feature space. The feature vectors in the training set are plotted as x's and o's for the two classes. Based on the training set, a classifier partitions the feature space into decision regions, one region for each class. In the case of a *linear classifier*, the boundaries between these regions are hyperplanes.

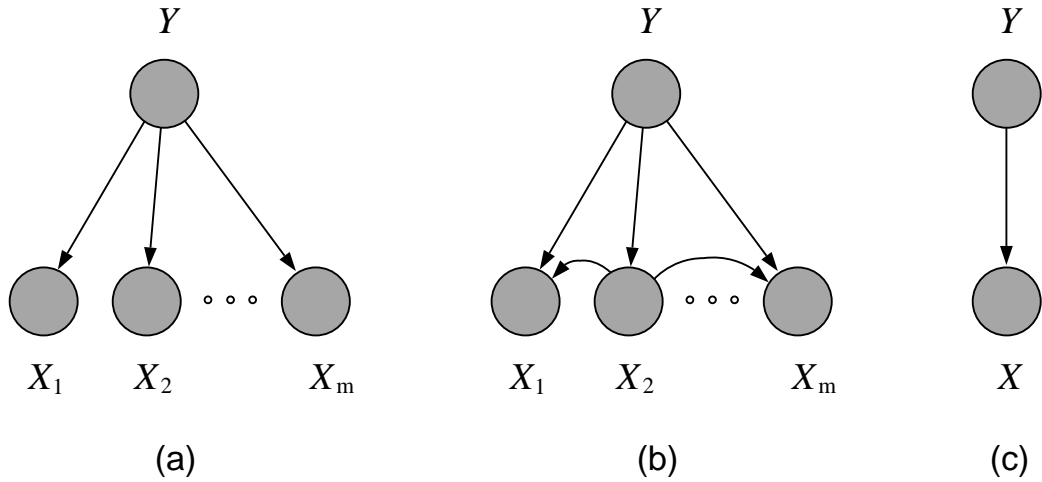


Figure 7.4: Three examples of generative classification models: (a) the case of conditionally independent features, (b) the case of dependent features with some conditional independence assumptions, and (c) the case of no conditional independence assumptions.

feature vector. In this case we represent the feature vector as a single node. This model, despite its simple graphical appearance, is the most general model of the three. We will discuss an example of this model in this section, where a Gaussian assumption for the class-conditional densities will allow us to obtain a simple model despite the absence of conditional independencies.

In all of the examples that we discuss, our goal is twofold: to describe the parametric representation of the posterior probability  $p(y | x)$  for particular models, and to present maximum likelihood methods for estimating the parameters of the model from data.

### 7.2.1 Gaussian class-conditional densities

We begin by discussing the model in Figure 7.4(a) in the setting in which the features are continuous and endowed with Gaussian distributions. We initially treat the case of *binary classification*, in which the class label  $Y$  can take on one of two values. The extension to multiple classes is discussed in Section 7.2.1.

The model in Figure 7.4(a) requires a marginal probability for  $Y$  and a conditional probability for  $X$  given  $Y$ . Let  $Y \in \{0, 1\}$  be a Bernoulli random variable with parameter  $\pi$ :

$$p(y | \pi) = \pi^y (1 - \pi)^{1-y}. \quad (7.1)$$

Given the conditional independence assumption expressed by the graph, the probability  $p(x | y)$  factors into a product over conditional probabilities  $p(x_j | y)$ . For  $Y = 0$ , let each  $X_j$  have a Gaussian distribution:

$$p(x_j | Y = 0, \theta_j) = \frac{1}{(2\pi\sigma_j^2)^{1/2}} \exp \left\{ -\frac{1}{2\sigma_j^2} (x_j - \mu_{0j})^2 \right\}, \quad (7.2)$$

where  $\mu_{0j}$  is the  $j$ th component of the mean vector for class  $Y = 0$ . For  $Y = 1$  we have:

$$p(x_j | Y = 1, \theta_j) = \frac{1}{(2\pi\sigma_j^2)^{1/2}} \exp \left\{ -\frac{1}{2\sigma_j^2} (x_j - \mu_{1j})^2 \right\}. \quad (7.3)$$

Note that we use  $\theta_j$  to denote all of the parameters for feature component  $x_j$ , including the means  $\mu_{0j}$  and  $\mu_{1j}$ , and the variance  $\sigma_j^2$ . Note also that the variances  $\sigma_j^2$  are allowed to vary across feature components  $x_j$ , but are assumed to be constant between the two classes.

Figure 7.5(a) presents an example of a contour plot of two Gaussians in a two-dimensional feature space for the case in which  $\sigma_0^2 = \sigma_1^2$ . An example in which the variances are unequal is shown in Figure 7.5(b).

The joint probability associated with the graph in Figure 7.4(a) is as follows:

$$p(x, y | \theta) = p(y | \pi) \prod_{j=1}^m p(x_j | y, \theta_j), \quad (7.4)$$

where  $\theta = (\pi, \theta_1, \theta_2, \dots, \theta_m)$ .

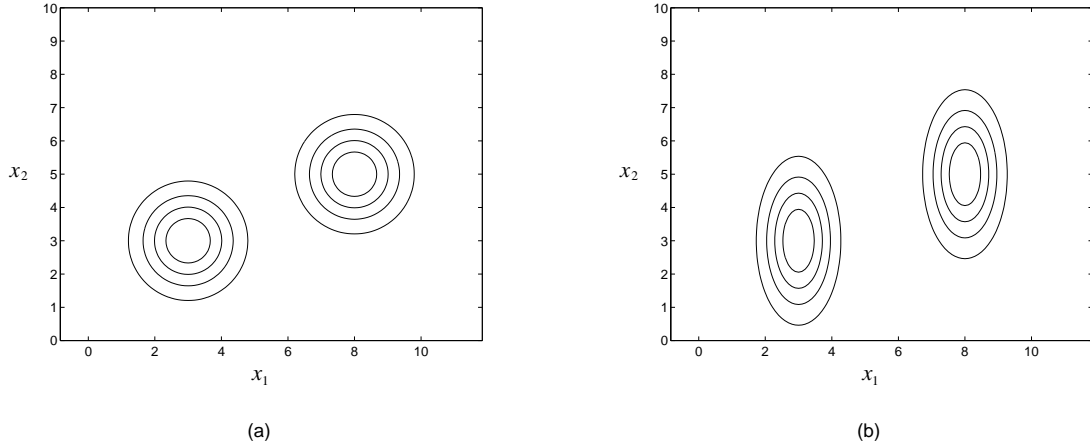


Figure 7.5: (a) A contour plot of Gaussian class-conditional densities for  $\sigma_1 = 1$  and  $\sigma_2 = 1$ . (b) A contour plot for Gaussian class-conditional densities when  $\sigma_1 = 0.5$  and  $\sigma_2 = 2.0$ .

### Posterior probability

Let us calculate the posterior probability  $p(Y = 1 | x, \theta)$ . The algebra is somewhat simplified if we work with matrix notation. Thus let:

$$p(x | y = k, \theta) = \frac{1}{(2\pi)^{1/2} |\Sigma|^{1/2}} \exp \left\{ -\frac{1}{2} (x - \mu_k)^T \Sigma^{-1} (x - \mu_k) \right\}, \quad (7.5)$$

for each of the two classes  $k \in \{0, 1\}$ , where  $\mu_k \triangleq (\mu_{k1}, \mu_{k2}, \dots, \mu_{km})^T$  is the vector of means for the  $k$ th Gaussian, and where  $\Sigma \triangleq \text{diag}(\sigma_1^2, \sigma_2^2, \dots, \sigma_m^2)$  is a diagonal covariance matrix. We have:

$$\begin{aligned} p(Y = 1 | x, \theta) &= \frac{p(x | Y = 1, \theta)p(Y = 1 | \pi)}{p(x | Y = 1, \theta)p(Y = 1 | \pi) + p(x | Y = 0, \theta)p(Y = 0 | \pi)} \\ &= \frac{\pi \exp\{-\frac{1}{2}(x - \mu_1)^T \Sigma^{-1} (x - \mu_1)\}}{\pi \exp\{-\frac{1}{2}(x - \mu_1)^T \Sigma^{-1} (x - \mu_1)\} + (1 - \pi) \exp\{-\frac{1}{2}(x - \mu_0)^T \Sigma^{-1} (x - \mu_0)\}} \\ &= \frac{1}{1 + \exp\{-\log \frac{\pi}{1-\pi} + \frac{1}{2}(x - \mu_1)^T \Sigma^{-1} (x - \mu_1) - \frac{1}{2}(x - \mu_0)^T \Sigma^{-1} (x - \mu_0)\}} \\ &= \frac{1}{1 + \exp\{-(\mu_1 - \mu_0)^T \Sigma^{-1} x + \frac{1}{2}(\mu_1 - \mu_0)^T \Sigma^{-1} (\mu_1 + \mu_0) - \log \frac{\pi}{1-\pi}\}} \end{aligned} \quad (7.6)$$

$$= \frac{1}{1 + \exp\{-\beta^T x - \gamma\}} \quad (7.7)$$

where the final equation defines parameters  $\beta$  and  $\gamma$ :

$$\beta \triangleq \Sigma^{-1}(\mu_1 - \mu_0) \quad \gamma \triangleq -\frac{1}{2}(\mu_1 - \mu_0)^T \Sigma^{-1}(\mu_1 + \mu_0) + \log \frac{\pi}{1 - \pi}. \quad (7.8)$$

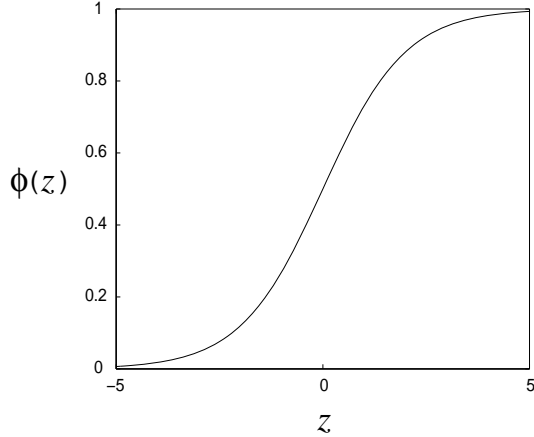


Figure 7.6: A plot of the logistic function.

We see that the posterior probability that  $Y = 1$  takes the form:

$$\phi(z) \triangleq \frac{1}{1 + e^{-z}}, \quad (7.9)$$

where  $z = \beta^T x + \gamma$  is an affine function of  $x$ . The function  $\phi(z)$  is a smooth, sigmoid-shaped function known as the *logistic function* (see Figure 7.6).

The fact that the feature vector  $x$  enters into the posterior probability via an affine function has an important geometric interpretation; in particular, this implies that the contours of equal posterior probability are lines in the feature space. That is, the term  $\beta^T x$  is proportional to the projection of  $x$  on  $\beta$ , and this projection is equal for all vectors  $x$  that lie along a line orthogonal to  $\beta$ . Consider in particular the case in which the variances  $\sigma_j^2$  are equal to one; thus let  $\Sigma = I$ . In this case  $\beta$  is equal to  $\mu_1 - \mu_0$ , and the contours of equal posterior probability are lines that are orthogonal to the difference vector between the means of the two classes (see Figure 7.7(a)).

We obtain equal values of posterior probability for the two classes when  $z = 0$  (because the logistic function in Eq. (7.9) evaluates to 0.5 when  $z = 0$ ). To interpret this result geometrically, consider first the case in which the prior probabilities  $\pi$  and  $1 - \pi$  are equal. In this case the term  $\log(\pi/(1 - \pi))$  vanishes and we can rewrite  $z$  as follows:

$$z = (\mu_1 - \mu_0)^T \left( x - \frac{(\mu_1 + \mu_0)}{2} \right). \quad (7.10)$$

This is equal to zero for vectors  $x$  whose projection on  $(\mu_1 - \mu_0)$  is equal to the arithmetic average of the two class means. Thus the posterior probabilities for the two classes are equal when  $x$  is equidistant from the two means. This corresponds to the solid line in Figure 7.7(a).

The prior probability  $\pi$  enters via the *log odds ratio*  $\log(\pi/(1 - \pi))$ . This effect of this term can be interpreted as a shift along the abscissa in Figure 7.6. For values of  $\pi$  larger than 0.5 we obtain a shift to the left, which, for a given point in the feature space, corresponds to a larger value of the

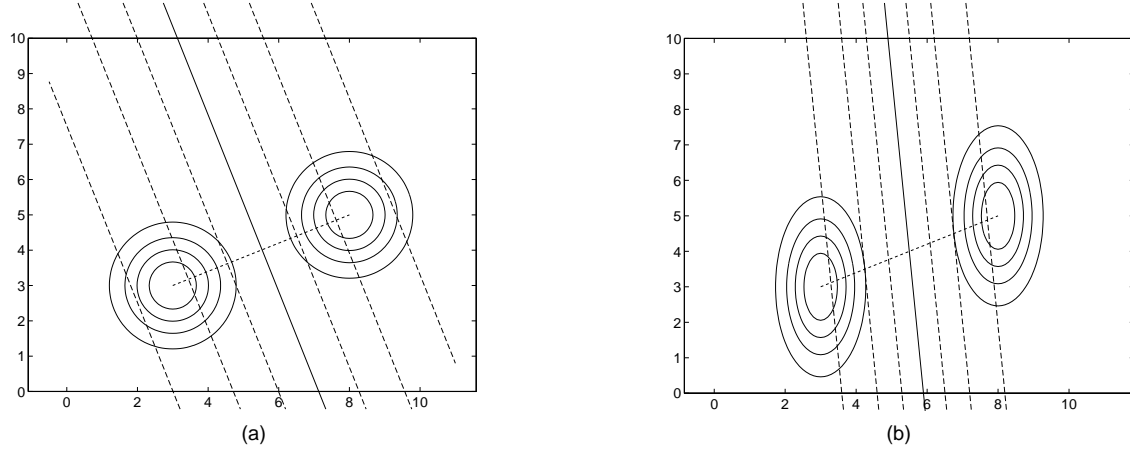


Figure 7.7: (a) The dashed lines and the solid line are contours of equal posterior probability. Note that they are orthogonal to the dotted line connecting the two mean vectors. (b) When  $\sigma_1 \neq \sigma_2$ , the contours of equal posterior probability are still lines, but they are no longer orthogonal to the difference between the mean vectors.

posterior for class  $Y = 1$  (see Figure 7.8(a)). We obtain a shift to the right for  $\pi$  smaller than 0.5 (see Figure 7.8(b)).

Finally, let us consider the case of a general matrix  $\Sigma$ . The contours of equal posterior probability are still lines in the feature space, but in general these lines are no longer orthogonal to the difference vector between the means. If we define new features  $w$  via the equation  $w \triangleq \Sigma^{-1}x$ , however, we obtain the orthogonal geometry of Figure 7.7(a) in the  $w$  feature space, which implies an affine geometry in the original feature space. Figure 7.7(b) is an example of this case. Note that the set of vectors that have equal posterior probability for the two classes—the solid line in the figure—are no longer equidistant from the two class means.<sup>1</sup>

As in Chapter 6 it is common to suppress the difference between linear and affine functions to simplify our notation. Thus we augment the vector  $x$  to include a first component that is equal to 1, and define the augmented parameter vector  $\theta \triangleq (\gamma - \log(\pi/(1-\pi)), \beta^T)^T$ . Using this notation, we can summarize the results of this section as follows: for Gaussian class-conditional densities, the posterior probability takes the form:

$$p(Y = 1 | x, \theta) = \frac{1}{1 + e^{-\theta^T x}} \quad (7.11)$$

where the parameter vector  $\theta$  is a function of the means  $\mu_k$ , the covariance matrix  $\Sigma$ , and the prior probability  $\pi$ .

In summary, we have found that the posterior probability for Gaussian class-conditional densities is the logistic function of a linear function of a feature vector  $x$ . We thus have obtained a

<sup>1</sup>We can redefine the distance metric, however, basing it on the matrix  $\Sigma^{-1}$ . In this case the points on the solid line are equidistant from the class means. This metric is known as *Mahalanobis distance*; see Exercise ?? for more details.

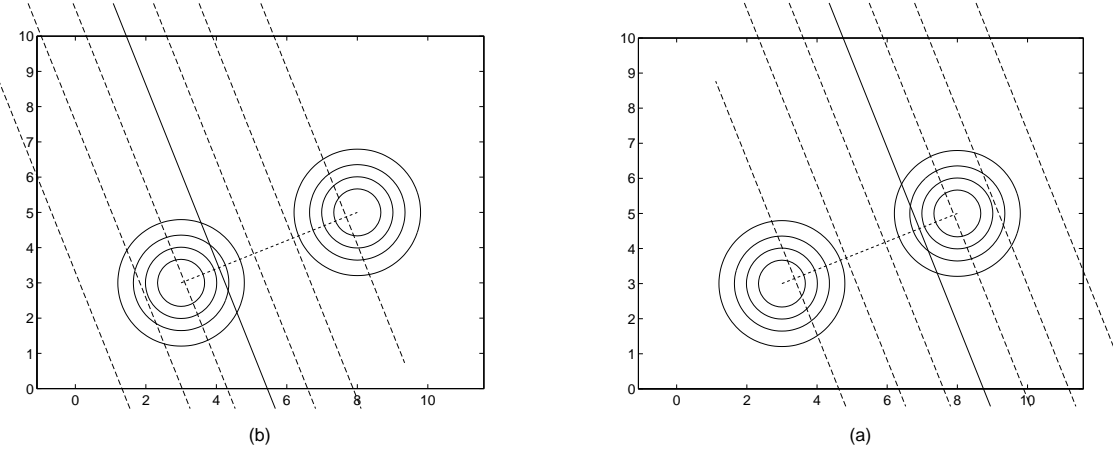


Figure 7.8: The class  $Y = 1$  is the upper rightmost of the two Gaussians. (a) When the prior  $\pi$  is greater than 0.5, the contours are shifted to the left, corresponding to a greater posterior probability of  $Y = 1$  for a given point in the feature space. (b) When the prior  $\pi$  is less than 0.5, the contours are shifted to the right.

*linear classifier*—contours of equal posterior probability are lines in the feature space. Inspecting the derivation that yielded this result, we see that the key assumption is that the covariance matrix is the same in the two classes; this leads to a cancellation of the quadratic  $x^T \Sigma^{-1} x$  term in the numerator and denominator of the posterior probability. If we retract this assumption and allow different covariance matrices for the two classes, we still obtain a logistic form for the posterior probability, but the argument to the logistic function is now quadratic in  $x$ . The corresponding classifier, which has quadratic contours of equal posterior probability, is referred to as a *quadratic classifier*.

### Maximum likelihood estimates

In this section we show how to obtain maximum likelihood parameter estimates based on a training set  $\mathcal{D}$  composed of  $N$  observations:  $\mathcal{D} = \{(x_n, y_n); n = 1, \dots, N\}$ . This problem has a straightforward solution that makes use of our work on density estimation in Chapter 5. Reasoning intuitively, suppose that we split the training data into two subsets, one in which  $y_n = 0$  and the other in which  $y_n = 1$ . To estimate  $\pi$  we calculate the proportion of the data in the subset corresponding to  $y_n = 1$ ; this is the maximum likelihood estimate of  $\pi$ . Moreover, we obtain separate maximum likelihood estimates of the Gaussian parameters for each of the two classes, pooling the estimates of the variances to take account of the fact that  $\sigma_j$  is the same in the two classes. This intuitively-defined solution is in fact the overall maximum likelihood solution, as we now verify.

We first form the log likelihood:

$$l(\theta | \mathcal{D}) = \log \left\{ \prod_{n=1}^N p(y_n | \pi) \prod_{j=1}^m p(x_{j,n} | y_n, \theta_j) \right\} \quad (7.12)$$

$$= \sum_{n=1}^N \log p(y_n | \pi) + \sum_{n=1}^N \sum_{j=1}^m \log p(x_{j,n} | y_n, \theta_j), \quad (7.13)$$

where we see that we obtain two separate terms, one for the marginal distribution of  $Y$  and the other for the conditional distribution of  $X_j$  given  $Y$ . Maximizing with respect to  $\pi$  involves only the former term, and for  $\pi$  we therefore obtain:

$$\hat{\pi}_{ML} = \arg \max_{\pi} \sum_{n=1}^N \log p(y_n | \pi) \quad (7.14)$$

$$= \arg \max_{\pi} \sum_{n=1}^N \{y_n \log \pi + (1 - y_n) \log(1 - \pi)\}, \quad (7.15)$$

where the latter equation uses Eq. (7.1). As we have seen in Chapter 5 (cf. Eq. (5.37)), the solution to this constrained optimization problem is the sample proportion:

$$\hat{\pi}_{ML} = \frac{\sum_{n=1}^N y_n}{N}, \quad (7.16)$$

where the numerator  $\sum_{n=1}^N y_n$  is the count of the number of times that the class  $Y = 1$  is observed.

Maximization with respect to the parameters  $\theta_j$  involves only the second term in Eq. (7.13), which we expand further as:

$$\begin{aligned} & \sum_{n=1}^N \sum_{j=1}^m \log p(x_{j,n} | y_n, \theta_j) \\ &= \sum_{n=1}^N \sum_{j=1}^m \log \{p(x_{j,n} | y_n = 1, \mu_{j1}, \sigma_j)^{y_n} p(x_{j,n} | y_n = 0, \mu_{j0}, \sigma_j)^{1-y_n}\} \end{aligned} \quad (7.17)$$

$$= \sum_{j=1}^m \left\{ \sum_{n=1}^N y_n \log p(x_{j,n} | y_n = 1, \mu_{j1}, \sigma_j) + \sum_{n=1}^N (1 - y_n) \log p(x_{j,n} | y_n = 0, \mu_{j0}, \sigma_j) \right\}. \quad (7.18)$$

Each term in the brackets depends on only one of the parameter vectors  $\theta_j = (\mu_{j0}, \mu_{j1}, \sigma_j)$ . Thus the problem decomposes into  $m$  separate optimization problems, one for each  $j$ .

Let us first consider the estimation of  $\mu_{j1}$ . Plugging in from Eq. (7.3) for  $p(x_{j,n} | y_n = 1, \mu_{j1}, \sigma_j)$ , and dropping constants, we have:

$$\hat{\mu}_{j1,ML} = \arg \max_{\mu_{j1}} \left\{ -\frac{1}{2} \sum_{n=1}^N y_n (x_{j,n} - \mu_{1j})^2 \right\}. \quad (7.19)$$

This is a weighted least-squares problem, where the “weights” are the binary values  $y_n$ . Taking the derivative and setting to zero, we obtain:

$$\hat{\mu}_{j1,ML} = \frac{\sum_{n=1}^N y_n x_{j,n}}{\sum_{n=1}^N y_n}. \quad (7.20)$$

Thus the maximum likelihood estimate is the sample average of the values  $x_{j,n}$  for those data points in class  $Y = 1$ . Similarly, for  $\hat{\mu}_{j0}$  we obtain:

$$\hat{\mu}_{j0,ML} = \frac{\sum_{n=1}^N (1 - y_n) x_{j,n}}{\sum_{n=1}^N (1 - y_n)}, \quad (7.21)$$

which is the average of the  $x_{j,n}$  for those data points in class  $Y = 0$ .

Finally, as we ask the reader to verify in Exercise ??, maximization with respect to the variance  $\sigma_j^2$  yields:

$$\hat{\sigma}_{j,ML}^2 = \frac{\sum_{n=1}^N y_n (x_{j,n} - \hat{\mu}_{j1,ML})^2 + \sum_{n=1}^N (1 - y_n) (x_{j,n} - \hat{\mu}_{j0,ML})^2}{N}; \quad (7.22)$$

a pooled estimate of the variance.

### Multiway classification

In this section we consider the generalization to multiway classification, in which the class label  $Y$  can take on one of  $K$  values.

Let  $Y$  be a multinomial random variable with components  $Y^k$  and parameter vector  $\pi$ . By definition we have:

$$\pi_k = p(Y^k = 1 | \pi). \quad (7.23)$$

For each of the  $K$  values of  $Y$ , define a Gaussian class-conditional density:

$$p(x | Y^k = 1, \theta) = \frac{1}{(2\pi)^{m/2} |\Sigma|^{1/2}} \exp \left\{ -\frac{1}{2} (x - \mu_k)^T \Sigma^{-1} (x - \mu_k) \right\}, \quad (7.24)$$

where  $\mu_k$  is the mean associated with the  $k$ th class and  $\Sigma$  is a covariance matrix, assumed constant across the  $K$  classes. If  $\Sigma$  is diagonal, then the components of  $X$  are conditionally independent given the class label  $Y$  and the appropriate graphical model is given by Figure 7.4(a). For general  $\Sigma$ , we represent our model as Figure 7.4(c).

The posterior probability of class  $k$  is obtained via Bayes rule:

$$p(Y^k = 1 | x, \theta) = \frac{p(x | Y^k = 1, \theta) p(Y^k = 1 | \pi)}{\sum_l p(x | Y^l = 1, \theta) p(Y^l = 1 | \pi)} \quad (7.25)$$

$$= \frac{\pi_k \exp\{-\frac{1}{2}(x - \mu_k)^T \Sigma^{-1} (x - \mu_k)\}}{\sum_l \pi_l \exp\{-\frac{1}{2}(x - \mu_l)^T \Sigma^{-1} (x - \mu_l)\}} \quad (7.26)$$

$$= \frac{\exp\{\mu_k^T \Sigma^{-1} x - \frac{1}{2} \mu_k^T \Sigma^{-1} \mu_k + \log \pi_k\}}{\sum_l \exp\{\mu_l^T \Sigma^{-1} x - \frac{1}{2} \mu_l^T \Sigma^{-1} \mu_l + \log \pi_l\}}, \quad (7.27)$$

where the cancellation of the quadratic  $x^T \Sigma^{-1} x$  terms again leaves us with exponents that are linear in  $x$ . Defining parameter vectors  $\beta_k$ :

$$\beta_k \triangleq \begin{bmatrix} -\mu_k^T \Sigma^{-1} \mu_k + \log \pi_k \\ \Sigma^{-1} \mu_k \end{bmatrix} \quad (7.28)$$

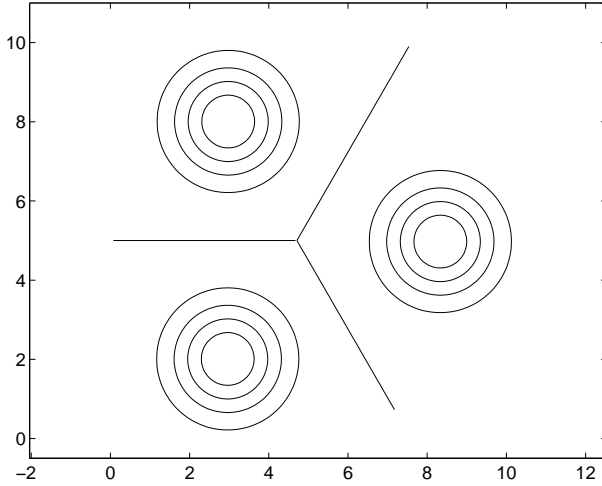


Figure 7.9: Contours of the softmax function. Each line is obtained by setting  $\phi_k(z) = \phi_l(z)$  for  $k \neq l$ . Such a line is a contour of equal posterior probability for classes  $k$  and  $l$ .

and again simplifying our result by augmenting the vector  $x$  to include a first component equal to one, we have:

$$p(Y^k = 1 | x, \theta) = \frac{e^{\beta_k^T x}}{\sum_l e^{\beta_l^T x}}. \quad (7.29)$$

The function  $\phi_k(z) \triangleq e^{z_k} / \sum_l e^{z_l}$  is a smooth function known as the *softmax function*.

The softmax function is a generalization of the logistic function and it has a similar geometric interpretation. Indeed we can transfer much of our earlier work to the multiway setting by considering the ratios of posterior probabilities between pairs of classes. In taking the ratio of  $p(Y^k = 1 | x, \theta)$  and  $p(Y^l = 1 | x, \theta)$ , for  $k \neq l$ , the denominator in the softmax function cancels and we obtain an exponential with exponent  $(\beta_k - \beta_l)^T x$ . This again involves a projection and thus contours of equal pairwise probability are again lines in the feature space (see Figure 7.9). Moreover, the prior probabilities  $\pi$  again take the form of log odds and act as additive constants in the exponential.

When  $\Sigma = \sigma I$ , we see from Eq. (7.28) that  $\beta_k$  is proportional to  $\mu_k$ , and thus the contours of equal probability are again orthogonal to the differences between the class means. For general  $\Sigma$  we obtain the same orthogonal geometry for the transformed coordinates  $w \triangleq \Sigma^{-1}x$ , which implies an affine geometry for the features  $x$ .

The calculation of maximum likelihood estimates for the multiway Gaussian classifier is straightforward and we ask the reader to carry out the calculation in Exercise ???. The results can be summarized as follows: We again divide the data into subsets corresponding to the different values of  $Y$ . Separate maximum likelihood estimates of the Gaussian parameters are obtained for each class, and the covariance estimates are pooled. Moreover, the maximum likelihood estimates of  $\pi$  are the proportions of data falling into the  $K$  classes.

The classifier that we have presented in this section is again a *linear classifier*. The linearity

again arises from the Gaussian assumption for the class-conditional densities, together with the assumption of a constant covariance matrix.

### 7.2.2 The naive Bayes classifier

We now turn to the setting of discrete features, in which each feature  $X_j$  can take on one of  $K$  values. In this setting the graphical model shown in Figure 7.4(a) is often referred to as the “naive Bayes classifier.” We discuss the naive Bayes classifier in this section, calculating the posterior probability and maximum likelihood parameter estimates.

Much of the work in the previous section carries over to the discrete setting. In particular, the joint probability remains the same as before:

$$p(x, y | \theta) = p(y | \pi) \prod_{j=1}^m p(x_j | y, \theta_j). \quad (7.30)$$

We again let  $Y$  be a multinomial random variable with components  $Y^k$ , defining the probability vector  $\pi$ , where:

$$\pi_k \triangleq p(Y^k = 1 | \pi). \quad (7.31)$$

Finally, treating the variables  $X_j$  as multinomial random variables with components  $X_j^k$ , where  $X_j^k = 1$  for one and only one value of  $k$ , we write the class-conditional densities as follows:

$$p(x_1, x_2, \dots, x_m | Y^i = 1, \eta) = \prod_j \prod_k \eta_{ijk}^{x_j^k}, \quad (7.32)$$

where  $\eta_{ijk} \triangleq p(x_j^k = 1 | Y^i = 1, \eta)$  is the probability that the  $j$ th feature  $X_j$  takes on its  $k$ th value, for the  $i$ th value of the class label  $Y$ . Note that the product over  $k$  in Eq. (7.32) arises from the definition of multinomial probabilities, and the product over  $j$  reflects the assumption that the features are conditionally independent.

### Posterior probability

Let us calculate the posterior probability for the naive Bayes classifier. We have:

$$p(Y^i = 1 | x, \eta) = \frac{\pi_i \prod_j \prod_k \eta_{ijk}^{x_j^k}}{\sum_l \pi_l \prod_j \prod_k \eta_{ljk}^{x_j^k}} \quad (7.33)$$

$$= \frac{\exp\{\log \pi_i + \sum_j \sum_k x_j^k \log \eta_{ijk}\}}{\sum_l \exp\{\log \pi_l + \sum_j \sum_k x_j^k \log \eta_{ljk}\}}. \quad (7.34)$$

As in the Gaussian case, this is again a softmax function of a linear combination of the features. We can express this result in the standardized form:

$$p(Y^i = 1 | x, \eta) = \frac{e^{\beta_i^T x}}{\sum_l e^{\beta_l^T x}}, \quad (7.35)$$

with a bit of creativity in the definitions of  $x$  and  $\beta$ . In particular, we redefine the vector  $x$  by stacking the multinomial vectors  $x_j$  vertically. Thus, the components of  $x$  are the values  $x_j^k$ , where the superscript  $k$  varies more rapidly than the subscript  $j$ . We also augment the resulting vector to have a first component of one. Similarly, we define  $\beta_i$  as a vector in which the doubly-indexed components  $\log \eta_{ijk}$  are arranged, with  $i$  fixed and  $k$  varying faster than  $j$ . We let the first component of  $\beta_i$  be equal to  $\log \pi_i$ . Given these definitions we obtain Eq. (7.35) as the posterior probability for the naive Bayes model.

Although the feature space is a discrete hypercube in the naive Bayes setting, it is interesting that the classifier is formally the same as the linear discriminant classifier, with log odds playing the role that difference vectors played in the Gaussian case.

In the case of binary classification, we can divide numerator and denominator by the numerator in Eq. (7.34) and obtain the logistic function of a linear function of the features:

$$p(Y = 1 | x, \theta) = \frac{1}{1 + \exp\{-\theta^T x\}} \quad (7.36)$$

for appropriate definitions of  $\theta$  and  $x$ .

### Maximum likelihood estimates

Finally, let us calculate the maximum likelihood estimates of the parameters for the naive Bayes classifier. We again assume that we have a training set  $\mathcal{D}$  composed of  $N$  observations:  $\mathcal{D} = \{(x_n, y_n); n = 1, \dots, N\}$ .

From Eq. (7.30) we obtain the log likelihood:

$$l(\theta | \mathcal{D}) = \sum_{n=1}^N \log p(y_n | \pi) + \sum_{n=1}^N \sum_{j=1}^m \log p(x_{j,n} | y_n, \eta), \quad (7.37)$$

where for the purposes of this section we define  $x$  and  $y$  to be the vectors of all observations  $x_{j,n}$  and  $y_n$ , respectively. The first term again decouples to yield separate maximum likelihood estimates of  $\pi$ . Focusing on the second term, and recalling that the sum over  $k$  of the parameters  $\eta_{ijk}$  must equal one, we introduce Lagrange multipliers  $\lambda_{ij}$  and maximize:

$$\tilde{l}(\eta | \mathcal{D}) \triangleq \sum_{n=1}^N \sum_i \sum_j \sum_k x_{j,n}^k y_n^i \log \eta_{ijk} + \sum_i \sum_j \lambda_{ij} \left(1 - \sum_k \eta_{ijk}\right). \quad (7.38)$$

This yields:

$$\frac{\partial \tilde{l}}{\partial \eta_{ijk}} = \frac{\sum_n x_{j,n}^k y_n^i}{\eta_{ijk}} - \lambda_{ij}. \quad (7.39)$$

Setting to zero and summing both sides with respect to  $k$ , we have:

$$\lambda_{ij} = \sum_k \sum_n x_{j,n}^k y_n^i \quad (7.40)$$

$$= \sum_n \sum_k x_{j,n}^k y_n^i \quad (7.41)$$

$$= \sum_n y_n^i. \quad (7.42)$$

Finally, substituting back into Eq. (7.39), we obtain:

$$\hat{\eta}_{ijk,ML} = \frac{\sum_n x_{j,n}^k y_n^i}{\sum_n y_n^i}, \quad (7.43)$$

in which the numerator is the number of observations in the  $i$ th class for which the  $j$ th feature takes on its  $k$ th value. The denominator normalizes this count by dividing by the number of observations in the  $i$ th class.

### 7.2.3 The exponential family

For all of the generative classification models studied thus far, the posterior probability takes a simple functional form—a logistic function for the binary problem and a softmax function in the multiway problem. Moreover, for multinomial and Gaussian class-conditional densities (in the latter case with equal, but otherwise arbitrary, class covariance matrices), the contours of equal posterior probability are hyperplanes in the feature space. In fact, as we see in this section, these results are not restricted to multinomial and Gaussian probabilities; but hold for a wide range of class-conditional densities.

The exponential family of probability distributions is a large family that includes the multinomial and Gaussian distributions, as well as a number of other classical distributions such as the binomial, the Poisson, the gamma and the Dirichlet. In Chapter 8 we provide a detailed discussion of the exponential family; here we simply present the functional form of this family, and consider using exponential family distributions as class-conditional densities for classification.

The exponential family is defined as follows:

$$p(x | \eta) = \exp\{\eta^T x - a(\eta)\}h(x), \quad (7.44)$$

where  $\eta$  is a parameter vector. It is a useful exercise to verify that the distributions listed above can all be put in this standard form, for appropriate definitions of the functions  $a(\eta)$  and  $h(x)$ . (We will carry out this exercise in Chapter 8).

Let us now consider a binary classification problem for a generic class-conditional density from the exponential family. We assume that the densities for the two classes are the same, up to the parameter vector  $\eta$ . That is, we let the density for class  $Y = 1$  be parameterized by  $\eta_1$  and let the density for class  $Y = 0$  be parameterized by  $\eta_0$ . Let the prior probabilities be equal for simplicity. We obtain the posterior probability from Bayes rule:

$$p(Y = 1 | x, \eta) = \frac{p(x | Y = 1, \eta)p(Y = 1 | \pi)}{p(x | Y = 1, \eta)p(Y = 1 | \pi) + p(x | Y = 0, \eta)p(Y = 0 | \pi)} \quad (7.45)$$

$$= \frac{\exp\{\eta_1^T x - a(\eta_1)\}h(x)}{\exp\{\eta_1^T x - a(\eta_1)\}h(x) + \exp\{\eta_0^T x - a(\eta_0)\}h(x)} \quad (7.46)$$

$$= \frac{1}{1 + \exp\{-(\eta_0 - \eta_1)^T x - a(\eta_0) + a(\eta_1)\}}. \quad (7.47)$$

Thus we find that the posterior probability is the logistic function of a linear function of  $x$ .

Similarly, for the multiway classification problem we have:

$$p(Y^k = 1 | x, \eta) = \frac{p(x | Y^k = 1, \eta_k)p(Y^k = 1 | \pi)}{\sum_l p(x | Y^l = 1, \eta_l)p(Y^l = 1 | \pi)} \quad (7.48)$$

$$= \frac{\exp\{\eta_k^T x - a(\eta_k)\}h(x)}{\sum_l \exp\{\eta_l^T x - a(\eta_l)\}h(x)} \quad (7.49)$$

$$= \frac{\exp\{\eta_k^T x - a(\eta_k)\}}{\sum_l \exp\{\eta_l^T x - a(\eta_l)\}}, \quad (7.50)$$

where again we have assumed equal class priors for simplicity. The result is the softmax function of a linear function of  $x$ .

### 7.3 Discriminative models

In Section 7.2.3 we have seen that a wide range of class-conditional densities all yield the same logistic-linear or softmax-linear form for the posterior probability. This invariance of the functional form of the posterior probability to the specific choice of class-conditional density is good news, because in practice it can be difficult to choose the class-conditional density. This problem is particularly difficult in the case of a high-dimensional feature vector. Consider the Gaussian case. The assumption of a diagonal covariance matrix—corresponding to conditional independence of the features—is often unrealistic. We can allow arbitrary covariance matrices, but this requires us to estimate  $O(m^2)$  parameters, which may be prohibitive for large  $m$ . Often we would like instead to consider families of covariance matrices that depend on more than  $m$  but fewer than  $m^2$  parameters. In some cases there is a natural ordering or grouping of the features (e.g., in the case of time series data or spatial data) that yield natural definitions of such structured covariance matrices. In many other cases, however, there is no obvious way to justify a particular form of structured covariance matrix, and we are left with a choice between the (highly-biased) case of a diagonal covariance matrix and the (highly-variable) case of a full covariance matrix. The fact, however, that all of these choices yield the same linear form for the posterior probability suggests that it may not be necessary to make such a choice. Moreover, the fact that densities other than the Gaussian density yield the same linear classifier suggests that we may not even need to specify the density.

In this section we discuss discriminative models. In discriminative modeling the posterior probability is modeled directly, quite apart from any considerations regarding class-conditional probabilities. Instead of assuming Gaussian or multinomial class-conditional densities and deriving the linearity of the classifier as a consequence, we instead assume linearity at the outset, by assuming that  $x$  enters into the model via a linear combination  $\theta^T x$ . To complete the model, we make an additional assumption regarding the (nonlinear) function that maps from  $\theta^T x$  to the posterior

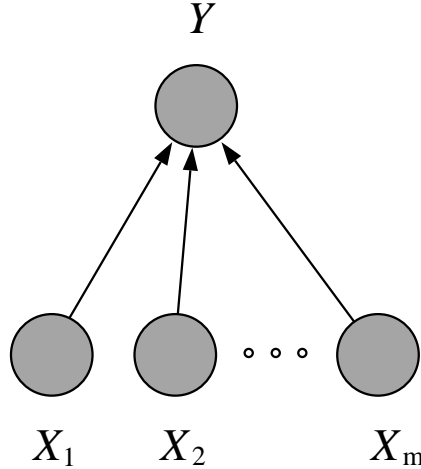


Figure 7.10: The graphical representation of a discriminative classification model.

probability. Taking a hint from the generative setting, we assume a logistic or softmax function at the outset, but we will also explore other possibilities.

The main problem will be that of estimating the parameters of the resulting classifier. Given that we no longer have underlying class-conditional densities, we cannot define the parameters of the classifier in terms of underlying means, covariances, log probabilities or the like. Instead we will have to find a way to estimate the parameters “directly.”

The graphical model that we study in this section is shown in Figure 7.10. Note that in this figure we have treated the components of the feature vector  $X$  as separate nodes:  $X_1, X_2, \dots, X_m$ . We have done this to emphasize the relationship—as well as the contrast—with the discussion of the generative approach in the previous section. Note in particular that we are not assuming nor implying conditional independence of the features. Indeed, in this section we make no assumptions regarding the marginal probability  $p(x)$ ; our goal is only to model the conditional probability  $p(y|x)$ . This is of course the same setting as that of regression, and indeed the methods that we discuss in this section are closely related to regression.

### 7.3.1 Logistic regression

We begin by considering the case of binary classification. The first model that we consider is *logistic regression*, in which the conditional probability  $p(y|x)$  is modeled as a function  $\phi(\theta^T x)$ , where  $\phi$  is the logistic function. This functional form is of course suggested by the generative models in Section 7.2.

The class label  $Y$  is a Bernoulli random variable, and the modeling problem is that of determining the probability that  $Y$  takes the value one for each input  $X$ . Note that this probability,  $p(Y = 1|x)$ , is the same as the conditional expectation:

$$E(y|x) = 1 \cdot p(Y = 1|x) + 0 \cdot p(Y = 0|x) \quad (7.51)$$

$$= p(Y = 1 | x). \quad (7.52)$$

Thus, as in the case of regression, the goal is that of modeling the conditional expectation of  $Y$  given  $X$ . In the regression case, we added a Gaussian error term  $\epsilon$  to the conditional expectation. This approach, however, is clearly inappropriate here given that  $Y$  can only take on the discrete values zero and one. Instead, we define  $\mu(x) \triangleq p(Y = 1 | x)$  and write the Bernoulli distribution in the following way:

$$p(y | x) = \mu(x)^y (1 - \mu(x))^{1-y}. \quad (7.53)$$

This is the usual definition of the Bernoulli distribution; however, we still need to specify the dependence of the Bernoulli parameter  $\mu(x)$  on  $x$ .

To complete the specification of the model, we assume that (1) the conditional expectation depends on  $x$  via the inner product  $\eta(x) \triangleq \theta^T x$ , where  $\theta$  is a parameter vector, and (2) the inner product  $\eta(x)$  is converted to a probability scale via the logistic function. Thus we have:

$$\mu(x) = \frac{1}{1 + e^{-\eta(x)}}. \quad (7.54)$$

as the probability model for the conditional expectation  $\mu(x) \triangleq p(Y = 1 | x, \theta)$ .

Recall that in the current section we simply treat these assumptions as axiomatic—as an attempt to model posterior probabilities in a simple parametric way independently of assumptions regarding class-conditional densities. Figure 7.11 shows an example that helps to suggest the reasonableness of this approach. In this figure it appears to be difficult to choose a model for the class-conditional densities; in particular, a Gaussian assumption does not seem reasonable. It seems significantly less problematic to choose a discriminative model in this case, and indeed the linear boundary implied by the logistic regression model appears to be reasonable. Such examples are by no means uncommon.

### Some properties of the logistic function

In this section we collect together several results regarding the logistic function that will be of use in the following section and in several later chapters.

Let us write the logistic function as a map from a variable  $\eta$  to a variable  $\mu$ :

$$\mu = \frac{1}{1 + e^{-\eta}} \quad (7.55)$$

The logistic function is invertible; thus we can also obtain a map from  $\mu$  to  $\eta$ :

$$\eta = \log \left( \frac{\mu}{1 - \mu} \right), \quad (7.56)$$

which has the form of a log odds.

This inverse form simplifies the calculation of derivatives. In particular, we have:

$$\frac{d\eta}{d\mu} = \frac{d}{d\mu} \log \left( \frac{\mu}{1 - \mu} \right) \quad (7.57)$$

$$= \frac{1}{\mu(1 - \mu)}, \quad (7.58)$$

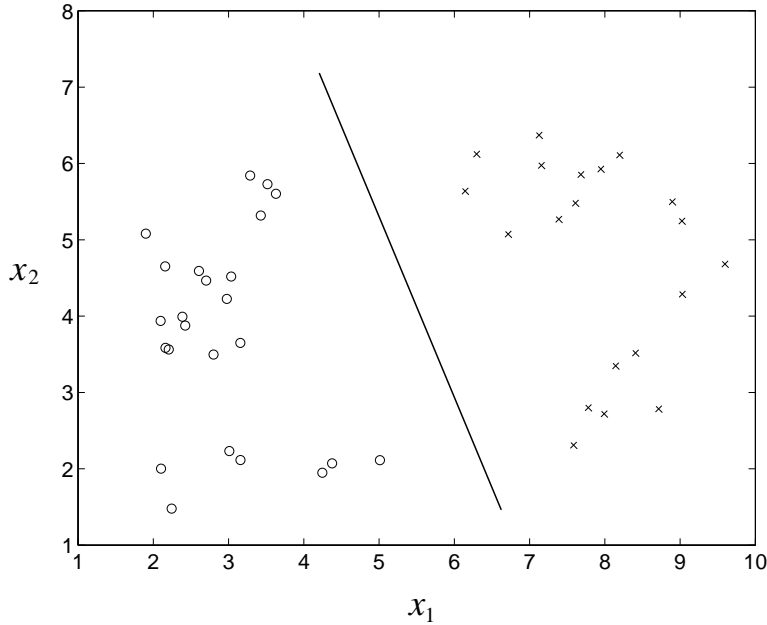


Figure 7.11: An example in which it is difficult to specify the class-conditional densities required for a generative model, but where a linear discriminative boundary between the classes seems reasonable.

from which we obtain:

$$\frac{d\mu}{d\eta} = \mu(1 - \mu). \quad (7.59)$$

This expresses the derivative of the logistic function as a function of  $\mu$ . We can also use Eq. (7.55) to obtain the derivative as a function of  $\eta$ , but the form in Eq. (7.59) will prove to be more useful.

### The likelihood

In this section we begin our discussion of maximum likelihood estimation of the parameters  $\theta$  based on a training set  $\mathcal{D} = \{(x_n, y_n); n = 1, \dots, N\}$ . As in our discussion of regression in Chapter 6, we consider batch and on-line methods for parameter estimation.

Let  $\eta_n = \theta^T x_n$  and let  $\mu_n = 1/(1 + e^{-\eta_n})$  denote the corresponding value of the logistic function, in accordance with our definitions in the previous section. Note that we have omitted the explicit dependence of  $\mu_n$  on  $x_n$  to simplify our notation. Moreover, let  $\eta$  and  $\mu$  denote the vectors of these values as we range across  $n$ ; thus:  $\eta = (\eta_1, \eta_2, \dots, \eta_N)$  and  $\mu = (\mu_1, \mu_2, \dots, \mu_N)$ .

To obtain the likelihood we take the product of  $N$  Bernoulli probabilities using Eq. (7.53):

$$p(y_1, \dots, y_N | x_1, \dots, x_N, \theta) = \prod_n \mu_n^{y_n} (1 - \mu_n)^{1-y_n}. \quad (7.60)$$

Taking logarithms yields:

$$l(\theta | \mathcal{D}) = \sum_n \{y_n \log \mu_n + (1 - y_n) \log(1 - \mu_n)\}, \quad (7.61)$$

and it is this expression that we must maximize with respect to  $\theta$ .<sup>2</sup> Recall that  $\mu_n$  is a function of  $\theta$  whereas  $y_n$  is not.

We calculate the gradient of the log likelihood:

$$\nabla_{\theta} l = \sum_n \left( \frac{y_n}{\mu_n} - \frac{1 - y_n}{1 - \mu_n} \right) \frac{d\mu_n}{d\eta_n} x_n \quad (7.62)$$

$$= \sum_n \frac{y_n - \mu_n}{\mu_n(1 - \mu_n)} \mu_n(1 - \mu_n) x_n \quad (7.63)$$

$$= \sum_n (y_n - \mu_n) x_n. \quad (7.64)$$

It is interesting to note that this gradient has the same form as the gradient of the log likelihood for linear regression (cf. Eq. (6.12)). In both cases we obtain a difference between  $y_n$  and the conditional expectation  $\mu_n$ , multiplied by the input  $x_n$ .

### An on-line estimation algorithm

An on-line estimation algorithm can be obtained by dropping the summation sign and following the stochastic gradient of the log likelihood. Let  $\theta^{(t)}$  denote the value of the parameter vector at the  $t$ th step of the algorithm. If  $(x_n, y_n)$  denotes the data point presented to the algorithm at the  $t$ th step, we write:

$$\theta^{(t+1)} = \theta^{(t)} + \rho(y_n - \mu_n^{(t)}) x_n, \quad (7.65)$$

where  $\mu_n^{(t)} \triangleq \phi(\theta^{(t)T} x_n)$  and where  $\rho$  is a step size.

Note that this on-line algorithm is identical in form to the LMS algorithm differing only in the definition of the conditional expectation. To understand the (important) implications of the difference, let us return to an issue that motivated our development of classification methods. Recall in particular Figure ??, where we considered the effect on linear regression of adding the point  $(1.5, 1)$  to the training set. The linear fit is altered significantly by the addition of this point. One way to see this is to note that the error,  $(y_n - \mu_n^{(t)})$ , in the LMS algorithm is large; thus the algorithm will make a large adjustment to the parameter vector  $\theta^{(t)}$ . For the on-line logistic regression algorithm in Eq. (7.65), however,  $\mu_n^{(t)}$  is near one, given that the logistic function is evaluated in its rightmost tail. As suggested in Figure 7.12, the error,  $(y_n - \mu_n^{(t)})$ , is therefore essentially zero. Thus, as we see from Eq. (7.65), there is little change in the parameters. In general, points that are already classified correctly do not affect the fit.

---

<sup>2</sup>The function in Eq. (7.61) is the *cross-entropy* function. See Appendix XXX for further discussion of the cross-entropy in the context of information theory.

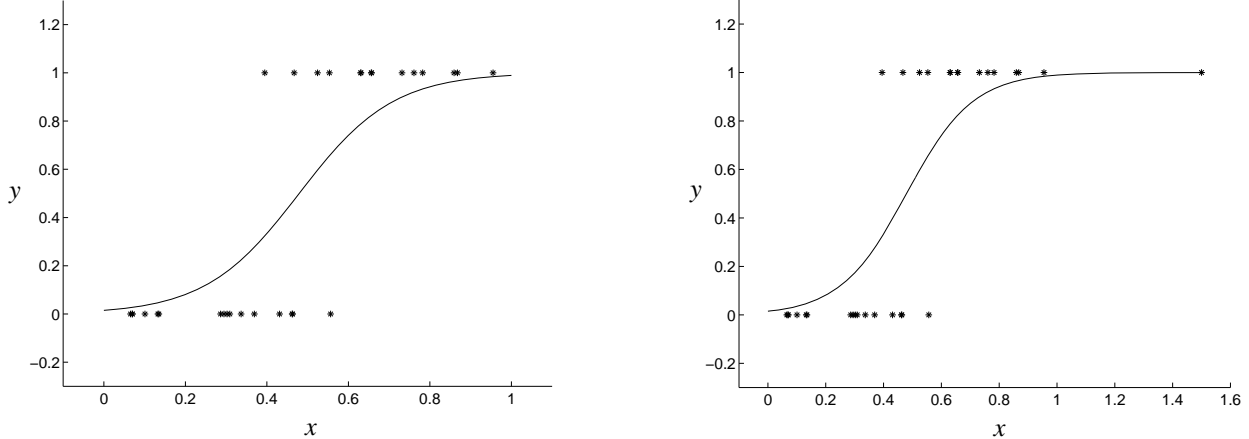


Figure 7.12: (a) The fit of a logistic regression model to the data in Figure 7.1. (b) Adding the point  $(1.5, 1)$  to the data set does not change the fit (cf. Figure 7.2).

### The iteratively reweighted least squares (IRLS) algorithm

To obtain a batch algorithm we could restore the summation sign in Eq. (7.64) and follow the steepest descent direction, but as in the linear regression case this algorithm has little to recommend it. We instead describe an algorithm, known as the *iteratively reweighted least squares (IRLS)* algorithm, that is closer in spirit to the direct solution of the normal equations.

The IRLS algorithm is a Newton-Raphson algorithm.<sup>3</sup> In preparation for deriving the algorithm, let us note that the normal equations can also be viewed, somewhat perversely, from the point of view of the Newton-Raphson algorithm.

Consider a function  $J(\theta)$  which is to be minimized with respect to  $\theta$ . Recall (see Appendix XXX) that the Newton-Raphson algorithm is an iterative algorithm that takes the following general form:

$$\theta^{(t+1)} = \theta^{(t)} - H^{-1} \nabla_{\theta} J, \quad (7.66)$$

where  $\nabla_{\theta} J$  and  $H$  are the gradient vector and Hessian matrix of  $J(\theta)$  respectively (and both are evaluated at  $\theta^{(t)}$ ).

In the case of linear regression, the cost function,  $J = \frac{1}{2}(y - X\theta)^T(y - X\theta)$ , is a quadratic function of  $\theta$ . We calculated the gradient of  $J$  in Chapter 6, finding:

$$\nabla_{\theta} J = -X^T(y - X\theta). \quad (7.67)$$

Taking another derivative we obtain the Hessian:

$$H = -X^T X. \quad (7.68)$$

---

<sup>3</sup>This statement is not entirely accurate, but it is accurate enough for current purposes. See Chapter 8 for further details.

Thus we can apply the Newton-Raphson algorithm to the problem of minimizing  $J$ , obtaining:

$$\theta^{(t+1)} = \theta^{(t)} + (X^T X)^{-1} X^T (y - X\theta^{(t)}) \quad (7.69)$$

$$= (X^T X)^{-1} X^T y, \quad (7.70)$$

where we see that the right-hand-side is the solution to the normal equations. Thus Newton-Raphson hops to the solution in a single step, not a surprise given that  $J$  is a quadratic function.

In the logistic regression problem, the function to be optimized is the log likelihood, and this function is not quadratic. Nonetheless it is “nearly” quadratic, and we should not be surprised to see that Newton-Raphson for logistic regression has similarities to the linear regression solution. Indeed, as we will see, the similarity is strong.

The function that we wish to optimize is the log likelihood shown in Eq. (7.61). We have already calculated the gradient of the log likelihood in Eq. (7.64). Writing this result in vector notation, we have:

$$\nabla_{\theta} l = \sum_n (y_n - \mu_n) x_n = X^T (y - \mu), \quad (7.71)$$

where we have defined  $\mu \triangleq (\mu_1, \mu_2, \dots, \mu_N)^T$ . Taking a second derivative, we have:

$$H = - \sum_n \frac{d\mu_n}{d\eta_n} x_n x_n^T \quad (7.72)$$

$$= - \sum_n \mu_n (1 - \mu_n) x_n x_n^T \quad (7.73)$$

$$= -X^T W X, \quad (7.74)$$

where we have defined the diagonal weight matrix:

$$W \triangleq \text{diag}\{\mu_1(1 - \mu_1), \mu_2(1 - \mu_2), \dots, \mu_N(1 - \mu_N)\}, \quad (7.75)$$

Note that the  $\mu_n$  values depend on the parameter vector  $\theta$ , thus the weight matrix  $W$  depends on  $\theta$ . We thus will use the notation  $W^{(t)}$  to denote the weight matrix at the  $t$ th iteration of the algorithm.

Substituting into Eq. (7.66), we obtain:

$$\theta^{(t+1)} = \theta^{(t)} + (X^T W^{(t)} X)^{-1} X^T (y - \mu^{(t)}) \quad (7.76)$$

$$= (X^T W^{(t)} X)^{-1} [X^T W^{(t)} X \theta^{(t)} + X^T (y - \mu^{(t)})] \quad (7.77)$$

$$= (X^T W^{(t)} X)^{-1} X^T W^{(t)} z^{(t)}, \quad (7.78)$$

where we define:

$$z^{(t)} = \eta + [W^{(t)}]^{-1} (y - \mu^{(t)}). \quad (7.79)$$

The algorithm in Eq. (7.78) is the IRLS algorithm.

Inspecting Eq. (7.78) makes it clear why the algorithm is known as the “iteratively reweighted least squares” algorithm. Each iteration of the algorithm involves solving a weighted least-squares

problem (recall Eq. (??)). Moreover, given that the weight matrix  $W$  changes at each iteration, the least-squares problem is “iteratively reweighted.”

We can obtain some more insight into the IRLS algorithm, and in particular understand the role played by  $z^{(t)}$ , if we view the Newton-Raphson algorithm as solving a sequence of linearized problems.

Consider the following (heuristic) argument. For a particular value  $\theta$ , and a particular vector  $x_n$ , let us linearize the logistic function around the “operating point,”  $\eta_n = \theta^T x_n$ . This linearization allows us to convert the value  $y_n$ , which is on a nonlinear scale, “backwards” to a value  $z_n$  on the linear scale defined by  $\eta_n$ . In particular, recall that the logistic function can be inverted (cf. Eq. (7.56)) to yield a map from  $\mu_n$  to  $\eta_n$ . Expanding this inverse function in a first-order Taylor series, we define:

$$z_n \triangleq \eta_n + \frac{d\eta_n}{d\mu_n} (y_n - \mu_n), \quad (7.80)$$

where the derivative is evaluated at  $\eta_n$ , and thus depends implicitly on the parameter vector  $\theta$ .

This argument suggests using  $z_n$  as a surrogate for  $y_n$ , in a linearized version of our logistic regression problem. We have another issue to deal with, however, if we wish to use linear regression methods to find parameter estimates: the Bernoulli random variables  $y_n$  do not have equal variance. In particular,  $y_n$  has variance  $\mu_n(1 - \mu_n)$ . To deal with this issue, we use weighted least squares. In particular, note that the elements of the weighting matrix  $W$  defined in Eq. (7.75) are exactly the Bernoulli variances. Thus we use  $W$  as our weight matrix.

We now solve a weighted least squares problem, with data  $z_n$  and weight matrix  $W$ . Writing the normal equations for this weighted least squares problem, and making the dependence on the iteration number  $t$  explicit, we obtain the IRLS iteration in Eq. (7.78).

The Newton-Raphson algorithm is a second-order algorithm and it generally converges rapidly. A small number of iterations of Eq. (7.78) are usually sufficient to obtain convergence of the parameter vector.

### 7.3.2 Multiway classification

In this section we discuss a generalization of logistic regression to the setting of multiway classification. Recall that in this case the class label  $Y$  can take on one of  $K$  values.

In Section 7.2.1 we derived the softmax-linear model:

$$p(Y^k = 1 | x, \theta) = \frac{e^{\theta_k^T x}}{\sum_l e^{\theta_l^T x}} \quad (7.81)$$

as the multiway generalization of the logistic-linear model. In that section, the softmax-linear form for the posterior probability was a consequence of our assumption of Gaussian (or more generally, exponential family) class-conditional probabilities. In the current section, however, we adopt a discriminative perspective in which the softmax-linear form is treated as an assumption, and we make no attempt to specify class-conditional probabilities. In this context, we refer to the model in Eq. (7.81) as a *softmax regression* model. As in the case of logistic regression, the main problem that we face is estimating the parameters  $\theta_k$  “directly,” without making use of an underlying class-conditional model.

We use the notation  $\mu_n^k$  to denote the posterior probability in Eq. (7.81). We also use  $\eta_n^k = \theta_k^T x_n$  to denote the linear component of the softmax-linear model.

### Some properties of the softmax function

The softmax function has several properties that are analogs of those of the logistic function that we discussed in Section 7.3.1.

The softmax function can be written as a map from a vector variable  $\eta$  to a vector variable  $\mu$ . Letting  $\eta^i$  represent the  $i$ th component of  $\eta$  and letting  $\mu^i$  represent the  $i$ th component of  $\mu$ , we write:

$$\mu^i = \frac{e^{\eta^i}}{\sum_k e^{\eta^k}}. \quad (7.82)$$

This function is invertible up to an additive constant. That is, if we add the constant  $C$  to each of the components  $\eta^i$ , then the factor  $e^C$  cancels in the numerator and denominator of Eq. (7.82), yielding the same value of  $\mu^i$ . Note in particular that if we take the logarithm of both sides of Eq. (7.82), we obtain the inverse:

$$\eta^i = \log \mu^i + D, \quad (7.83)$$

where  $D = \log \sum_k e^{\eta^k}$  is a constant. Any other constant (including zero) will yield an equivalent inverse of the softmax function.

We turn to the calculation of the softmax derivatives. A subtlety in this case is that the derivative of  $\mu_i$  with respect to  $\eta_j$  is non-zero for  $i \neq j$ , due to the denominator in Eq. (7.82). The calculation proceeds as follows:

$$\frac{\partial \mu_i}{\partial \eta_j} = \frac{(\sum_k e^{\eta_k}) e^{\eta_i} \delta_{ij} - e^{\eta_i} e^{\eta_j}}{(\sum_k e^{\eta_k})^2} \quad (7.84)$$

$$= \frac{e^{\eta_i}}{\sum_k e^{\eta_k}} \left( \delta_{ij} - \frac{e^{\eta_j}}{\sum_k e^{\eta_k}} \right) \quad (7.85)$$

$$= \mu_i (\delta_{ij} - \mu_j), \quad (7.86)$$

where  $\delta_{ij}$  is equal to one if  $i = j$  and zero otherwise.

### Maximum likelihood estimation

In the multiway classification problem the output  $Y$  is a multinomial random variable. Recalling that in softmax regression  $\mu_n^k$  denotes the posterior probability of the  $k$ th class for the  $n$ th data point, we can write the multinomial probability distribution in the following form:

$$p(y_n | x_n, \theta) = \prod_k \left( \mu_n^k \right)^{y_n^k} \quad (7.87)$$

where  $\theta \triangleq (\mu_n^1, \mu_n^2, \dots, \mu_n^K)^T$  is the multinomial parameter vector. The likelihood is the product of  $N$  such probabilities. Taking the logarithm, we obtain:

$$l(\theta | \mathcal{D}) = \sum_n \sum_k y_n^k \log \mu_n^k \quad (7.88)$$

as the log likelihood for the multiway classification problem. As in the binary case, this log likelihood has the form of a cross-entropy.

To calculate the gradient of the log likelihood with respect to the parameter vector  $\theta_i$ , we make use of the intermediate variable  $\eta_n^i = \theta_i^T x_n$ . Recalling that the derivative of  $\mu_n^k$  with respect to  $\eta_n^i$  is nonzero because of the shared denominator in the softmax function, we have:

$$\nabla_{\theta_i} l = \sum_n \sum_k \frac{\partial l}{\partial \mu_n^k} \frac{\partial \mu_n^k}{\partial \eta_n^i} \frac{d\eta_n^i}{d\theta_i} \quad (7.89)$$

$$= \sum_n \sum_k \frac{y_n^k}{\mu_n^k} \mu_n^k (\delta_{ik} - \mu_n^i) x_n \quad (7.90)$$

$$= \sum_n \sum_k y_n^k (\delta_{ik} - \mu_n^i) x_n \quad (7.91)$$

$$= \sum_n (y_n^i - \mu_n^i) x_n, \quad (7.92)$$

where we have used the fact that  $\sum_k y_n^k = 1$ .

The gradient that we have obtained has the same form as the gradient for logistic regression and linear regression! (Recall Eq. (7.64) and Eq. (6.21)). We will see in Chapter 8 that this result is not a coincidence, but reflects a general property of probability distributions in the exponential family.

As in the case of logistic regression and linear regression, we obtain an on-line parameter estimation algorithm by dropping the sum over  $n$  in Eq. (7.92). This algorithm is the analog of the LMS algorithm for multiway classification.

It is straightforward to generalize the IRLS algorithm and thereby obtain a batch algorithm for softmax regression. Rather than pursuing that generalization here, we return to the IRLS algorithm in Chapter 8, where we develop a generic IRLS algorithm for the family of generalized linear models, of which softmax regression and logistic regression are examples.

### 7.3.3 Probit regression

In this section and the remainder of the chapter, we return to binary classification and consider some alternatives to logistic regression.

Although the logistic regression model arises naturally from a generative perspective—as the posterior probability obtained from a wide class of class-conditional probabilities—there are other choices of class-conditional probabilities that do not yield the logistic-linear form for the posterior probability. Thus, even from a generative point of view there is some motivation for exploring alternative representations for the posterior probability. In this section we engage in such an exploration within the discriminative framework, motivating alternative models “directly,” without reference to class-conditional distributions. For simplicity we retain the linearity assumption, and motivate functions other than the logistic function for converting the linear combination  $\theta^T x$  to a probability scale.

One natural way to obtain a discriminative classification model is to consider “noisy threshold” models. In particular, we might suppose that a data pair  $(x, y)$  is obtained by a process in which some external agent converts the vector  $x$  to a scalar value  $\eta$ , defined as a linear combination  $\theta^T x$ , and compares the resulting value to a threshold. If the value exceeds the threshold, then the label 1 is assigned, otherwise the label 0 is assigned. A probabilistic version of this model can be obtained by assuming that the threshold is stochastic. Thus, let  $Z$  be a scalar random variable with a cumulative distribution function  $F(z)$ . We define:

$$p(Y = 1 | x) = p(Z \leq \eta) = F(\eta). \quad (7.93)$$

Making the further assumption that  $\eta$  is parameterized linearly, as  $\eta \triangleq \theta^T x$ , we obtain a discriminative classification model:

$$p(Y = 1 | x, \theta) = F(\theta^T x), \quad (7.94)$$

for a given distribution function  $F$ .

The logistic regression model can be interpreted as a special case of this model, given that the logistic function,  $1/(1 + \exp(-x))$ , is a distribution function. There is no particular reason to use a logistic random variable as the noisy threshold model, however. Indeed, given that many natural sources of “noise” have a Gaussian distribution, a common choice is to take  $Z$  to be a Gaussian random variable. This choice yields the *probit regression model*. Thus, in the probit model we have:

$$p(Y = 1 | x, \theta) = \Phi(\theta^T x), \quad (7.95)$$

where

$$\Phi(w) = \int_{-\infty}^w \frac{1}{(2\pi)^{1/2}} e^{-\frac{1}{2}\xi^2} d\xi \quad (7.96)$$

is the cumulative distribution function of a Gaussian random variable with zero mean and unit variance.<sup>4</sup>

Figure 7.13 shows a graphical model representation of the probit regression model. In this representation, the threshold variable  $Z$  is represented as an explicit latent variable. The graphical model requires a marginal distribution for  $Z$ , which in the probit model we take as  $\mathcal{N}(0, 1)$ , and a conditional distribution for  $Y$ , given  $X$  and  $Z$ . This conditional is a degenerate distribution:  $Y$  is equal to zero if  $\theta^T x$  is less than  $Z$ , and one otherwise.

Figure 7.14 shows a plot of the logistic function and the Gaussian cumulative distribution function. As this plot makes clear, there is not a large difference between the two functions, and indeed probit regression and logistic regression generally give rather similar results.

Probit regression is an instance of the family of generalized linear models that we describe in Chapter 8. Maximum likelihood estimates can be obtained via stochastic gradient descent or the general version of the IRLS algorithm that we present in that chapter.

---

<sup>4</sup>The assumption of zero mean and unit variance is without loss of generality, because any linear transformation of the features can be absorbed in the parameter vector  $\theta$ .

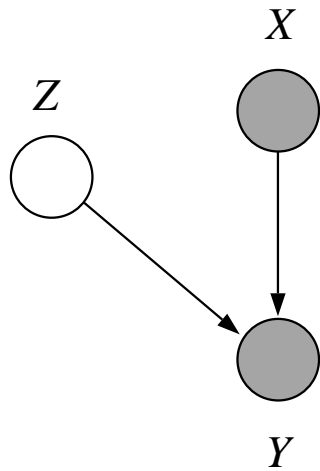


Figure 7.13: A graphical model representation of the probit regression model.

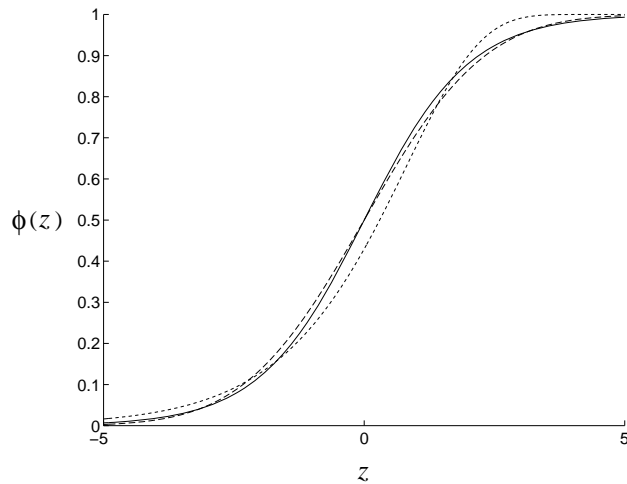


Figure 7.14: Link functions for binary classification. The solid curve is the logistic function (Eq. 7.55), the long-dashed curve is the cumulative Gaussian function (Eq. 7.96), and the small-dashed curve is the complementary log-log function (the inverse of Eq. 7.105).

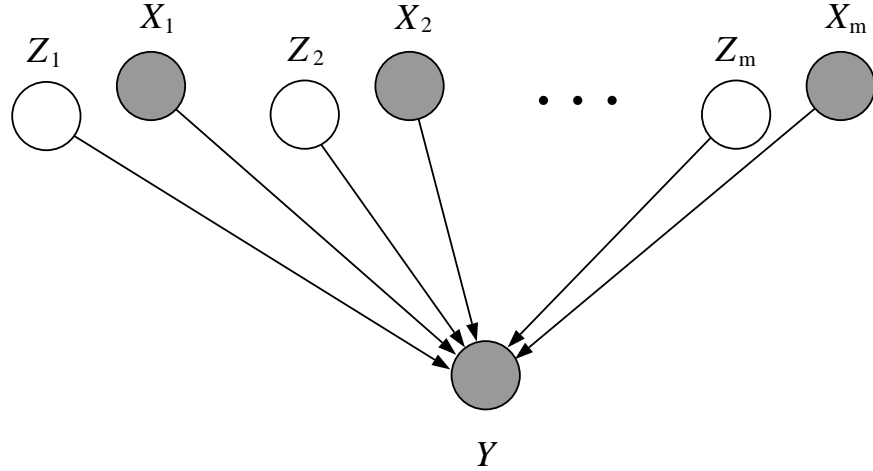


Figure 7.15: A graphical model representation of the noisy-OR model.

#### 7.3.4 The noisy-OR model

A wide range of models can be obtained as “noisy” versions of formulas from propositional logic, in the setting in which the features  $X_i$  are binary. In this section we describe an example of this class of models known as the *noisy-OR* model. As with the other models discussed in this chapter the noisy-OR model is a linear classifier.

Let us begin with the Boolean formula:

$$Y = X_1 \vee X_2 \vee \dots \vee X_m, \quad (7.97)$$

where  $X_i \in \{0, 1\}$ , for all  $i$ . To obtain a “noisy” version of the formula, let us view each variable  $X_i$  as encoding a binary “trigger” that can “cause”  $Y$  to occur. Eq. (7.97) states that the presence of any single trigger suffices to cause  $Y$  to occur. Suppose now that each trigger can “fail” with some probability  $\xi_i$ , in that the trigger can be present, but can fail to cause the occurrence of  $Y$ . Suppose moreover that the failure probabilities associated with the different triggers are independent. Thus, introducing independent binary random variables  $Z_i$  to represent the failure events, we have:

$$Y = \begin{cases} 1 & (X_1 \wedge \neg Z_1) \vee (X_2 \wedge \neg Z_2) \dots \vee (X_m \wedge \neg Z_m) \\ 0 & \text{otherwise.} \end{cases} \quad (7.98)$$

The graphical model representing this noisy version of the logical OR formula is shown in Figure 7.15.

If we let  $\xi_i \triangleq p(z_i = 1)$  denote the Bernoulli parameters associated with the  $Z_i$ , we obtain from Eq. (7.98):

$$p(Y = 0 | x, \xi) = \prod_{i=1}^m \{p(z_i = 1)\}^{x_i} = \prod_{i=1}^m \xi_i^{x_i}. \quad (7.99)$$

This formula can be interpreted as stating that the probability of  $Y$  *not* occurring is the product of the (independent) failure probabilities associated with those features  $x_i$  that are present in the input. That is, if all triggers fail, then  $Y$  doesn't occur.

To express the noisy-OR model in a linear form, let us rewrite Eq. (7.99):

$$p(Y = 0 \mid x, \xi) = \exp \left\{ \sum_{i=1}^m x_i \log \xi_i \right\}. \quad (7.100)$$

Letting  $\theta_i \triangleq -\log \xi_i$ , we obtain our final result:

$$p(Y = 1 \mid x, \theta) = 1 - e^{-\theta^T x} \quad (7.101)$$

for the posterior probability for the noisy-OR model.

### 7.3.5 Other exponential models

A number of useful classification models are based on the Poisson distribution. Recall that  $Z$  is a Poisson random variable with parameter  $\lambda$  if:

$$p(z \mid \lambda) = \frac{\lambda^z e^{-\lambda}}{z!}, \quad (7.102)$$

where  $z$  ranges over the nonnegative integers. Poisson variables arise in many contexts, in particular as models of counts of rarely occurring, independent events. For example, in a well-stirred solution that contains a small amount of a virus, the amount of virus in any sample might be a Poisson variable with parameter proportional to the volume of the sample. In such situations, it is often of interest to distinguish between the case in which  $Z$  takes on the value zero and the case in which  $Z$  takes on a non-zero value. (For example, a model of transmission of viral disease would want to distinguish the case that a sample of the solution contained no viral cells). Defining a binary variable  $Y$  that is equal to one in the latter case, we have:

$$p(Y = 1) = 1 - p(Z = 0) = 1 - e^{-\lambda}, \quad (7.103)$$

from Eq. (7.102). If we treat the parameter  $\lambda$  as a linear function of a set of input variables  $x$ , we obtain a classification model:

$$p(Y = 1 \mid x, \theta) = 1 - e^{-\theta^T x}. \quad (7.104)$$

This model is identical in form to the noisy-OR model, although the vector  $x$  is no longer restricted to be a binary vector.

An awkward aspect of the model in Eq. (7.104) is that the linear combination  $\theta^T x$  must be restricted to lie between zero and infinity if we are to obtain a posterior probability that lies between zero and one. To remove this restriction, it is convenient to reparameterize the model so that the argument  $\lambda$  is the exponential function of some underlying variable  $\eta$ . We obtain a linear classification model if we assume that the underlying variable  $\eta$  is linear in  $x$ :

$$p(Y = 1 \mid x, \theta) = 1 - e^{-e^{\theta^T x}}. \quad (7.105)$$

An appealing feature of this model is that there are no longer any restrictions on  $\theta$ . In fact, in situations involving Poisson variables it is often natural to measure the effect of the variables  $x$  on a logarithmic scale. In particular, in the example of the viral solution,  $x$  might measure the fraction of some diluting agent in the solution.

The model in Eq. (7.105) is referred to as the *complementary log-log model*. (The terminology refers to the inverse of the nonlinear function in Eq. (7.105)). Figure 7.14 includes a plot of the nonlinearity in this model. Note again the similarity to the logistic function.

## 7.4 Summary

We have presented a number of simple probabilistic models for discrete variables within the framework of binary and multiway classification problems. We discussed generative models, in which the discrete variable is a parent of the feature variables. We also discussed discriminative models, in which the discrete variable is a child of the feature variables. We also focused on some of the relationships between generative and discriminative models.

Maximum likelihood estimates are readily obtained in both cases. In the case of a generative model, maximum likelihood estimation essentially reduces to density estimation. That is, we find estimates of the class-conditional densities separately for each of the classes. In the discriminative setting, we model the class label as a Bernoulli or multinomial variable, which yields a cross entropy for the log likelihood. The IRLS algorithm can be used to maximize this log likelihood in the batch setting. We also presented a stochastic gradient algorithm for the on-line setting, noting the close relationship to the LMS algorithm.

All of the models that we have presented in this chapter are linear classifiers. That is, in all cases the input variable  $x$  enters into the model via a linear combination  $\eta = \theta^T x$ . In the generative setting this linear form was a consequence of the particular kinds of class-conditional densities that we assumed. In the discriminative setting we assumed the linear form at the outset.

Generative and discriminative models have complementary strengths and weaknesses. The generative approach allows knowledge about class-conditional densities to be exploited. If this knowledge is indeed reflective of the true data-generation process, then the generative approach can be more *efficient* than a corresponding discriminative model, in the sense that it will tend to require fewer data points. On the other hand, discriminative approaches tend to be more *robust* than generative approaches, making use of weaker assumptions regarding class-conditional densities. Note also that the discriminative framework presents a straightforward “upgrade path” toward the development of nonlinear classifiers—we can retain the logistic and softmax functions, but replace the linear combination  $\eta = \theta^T x$  with a nonlinear function (see Chapter 25).

## 7.5 Historical remarks and bibliography

# An Introduction to Probabilistic Graphical Models

Michael I. Jordan  
*University of California, Berkeley*

June 30, 2003



## Chapter 8

# The exponential family and generalized linear models

In this chapter we extend the scope of our modeling toolbox to accommodate a variety of additional data types, including counts, time intervals and rates. We introduce the exponential family of distributions, a family that includes the Gaussian, binomial, multinomial, Poisson, gamma, Rayleigh and beta distributions, as well as many others. We consider both unconditional and conditional models involving this family.

Much of our discussion is focused on the conditional setting, in which we have a directed model,  $X \rightarrow Y$ , with  $X$  and  $Y$  observed, and with  $Y$  having an exponential family distribution for each value of  $X$ . To parameterize this conditional distribution we introduce a class of models known as *generalized linear models (GLIM's)*. GLIM's are a general category of models that include linear regression and linear classification models as special cases. As in those models, GLIM's retain an important role for linearity, while introducing appropriate nonlinearities so as to cope with the idiosyncrasies of the particular exponential family distribution at hand. GLIM's have the dual virtue of systematizing the work that we have done thus far and showing how to extend that work to handle a wide range of additional data types.

At first blush this chapter may appear to involve a large dose of mathematical detail, but appearances shouldn't deceive—most of the detail involves working out examples that show how the exponential family and GLIM's relate to more familiar material. The real message of this chapter is the simplicity and elegance of exponential family and GLIM methods. Once the new ideas are mastered, it is often easier to work within the general exponential family and GLIM frameworks than with specific instances.

### 8.1 The exponential family

A probability density in the exponential family takes the following general form:

$$p(x | \eta) = h(x) \exp\{\eta^T T(x) - A(\eta)\} \quad (8.1)$$

for a parameter vector  $\eta$ , often referred to as the *natural parameter*, and for given functions  $T$ ,  $a$ , and  $h$ . The function  $T(X)$  is referred to as a *sufficient statistic*; the reasons for this nomenclature are discussed below. The form of the function  $h(x)$  is not of fundamental importance; it simply reflects the underlying measure with respect to which  $p(x | \eta)$  is a density. Of rather more importance is the function  $A(\eta)$ . Integrating Eq. (8.1) with respect to  $x$ , we have:

$$A(\eta) = \log \int h(x) \exp\{\eta^T T(x)\} dx \quad (8.2)$$

where we see that  $A(\eta)$  can be viewed as the logarithm of a normalization factor. The set of  $\eta$  for which this integral is finite is referred to as the *natural parameter space*.

It is also common to write the exponential family distribution in the following way:

$$p(x | \eta) = \frac{1}{Z(\eta)} h(x) \exp\{\eta^T T(x)\}, \quad (8.3)$$

which is equivalent to if we let  $A(\eta) = \log Z(\eta)$ . Although we focus on Eq. (8.1) throughout this chapter, we will also make use of Eq. (8.72) in later chapters.

### 8.1.1 Examples

#### The Bernoulli distribution

The probability mass function of a Bernoulli random variable  $X$  is given as follows:

$$p(x | \pi) = \pi^x (1 - \pi)^{1-x} \quad (8.4)$$

$$= \exp \left\{ \log \left( \frac{\pi}{1 - \pi} \right) x + \log(1 - \pi) \right\}. \quad (8.5)$$

where our trick, here and throughout the chapter, is to take the exponential of the logarithm of the original distribution. Thus we see that the Bernoulli distribution is an exponential family distribution with:

$$\eta = \frac{\pi}{1 - \pi} \quad (8.6)$$

$$T(x) = x \quad (8.7)$$

$$A(\eta) = -\log(1 - \pi) = \log(1 + e^\eta) \quad (8.8)$$

$$h(x) = 1. \quad (8.9)$$

Note moreover that the relationship between  $\eta$  and  $\pi$  is invertible. Solving Eq. (8.6) for  $\pi$ , we have:

$$\pi = \frac{1}{1 + e^{-\eta}}, \quad (8.10)$$

which is the logistic function.

### The Poisson distribution

The probability mass function of a Poisson random variable is given as follows:

$$p(x | \lambda) = \frac{\lambda^x e^{-\lambda}}{x!}. \quad (8.11)$$

Rewriting this expression we obtain:

$$p(x | \lambda) = \frac{1}{x!} \exp\{x \log \lambda - \lambda\}. \quad (8.12)$$

Thus the Poisson distribution is an exponential family distribution, with:

$$\eta = \log \lambda \quad (8.13)$$

$$T(x) = x \quad (8.14)$$

$$A(\eta) = \lambda = e^\eta \quad (8.15)$$

$$h(x) = \frac{1}{x!}. \quad (8.16)$$

Moreover, we can obviously invert the relationship between  $\eta$  and  $\lambda$ :

$$\lambda = e^\eta. \quad (8.17)$$

### The Gaussian distribution

The (univariate) Gaussian distribution can be written as follows:

$$p(x | \mu, \sigma^2) = \frac{1}{\sqrt{2\pi}\sigma} \exp\left\{-\frac{1}{2\sigma^2}(x - \mu)^2\right\} \quad (8.18)$$

$$= \frac{1}{\sqrt{2\pi}} \exp\left\{\frac{\mu}{\sigma^2}x - \frac{1}{2\sigma^2}x^2 - \frac{1}{2\sigma^2}\mu^2 - \ln \sigma\right\}. \quad (8.19)$$

This is in the exponential family form, with:

$$\eta = \begin{bmatrix} \mu/\sigma^2 \\ -1/2\sigma^2 \end{bmatrix} \quad (8.20)$$

$$T(x) = \begin{bmatrix} x \\ x^2 \end{bmatrix} \quad (8.21)$$

$$A(\eta) = \frac{\mu^2}{2\sigma^2} + \ln \sigma = -\frac{\eta_1^2}{4\eta_2} - \frac{1}{2} \ln(-2\eta_2) \quad (8.22)$$

$$h(x) = \frac{1}{\sqrt{2\pi}}. \quad (8.23)$$

Note in particular that the univariate Gaussian distribution is a two-parameter distribution and that its sufficient statistic is a vector.

The multivariate Gaussian distribution can also be written in the exponential family form; we leave the details to Exercise ?? and Chapter 13.

### The multinomial distribution

As a final example, let us consider the multinomial distribution. Let  $X = (X_1, X_2, \dots, X_m)$  be a collection of integer-valued random variables representing event counts, where  $X_i$  represents the count of the number of times the  $i$ th event occurs in a set of  $n$  independent trials. Let  $\pi_i$  represent the probability of the  $i$ th event occurring in any given trial. We have:

$$p(x | \pi) = \frac{n!}{x_1! x_2! \cdots x_m!} \pi_1^{x_1} \pi_2^{x_2} \cdots \pi_m^{x_m}, \quad (8.24)$$

as the probability mass function for such a collection.

Following the strategy of our previous examples, we rewrite the multinomial distribution as follows:

$$p(x | \pi) = \exp \left\{ \sum_{i=1}^m x_i \ln \pi_i \right\}. \quad (8.25)$$

While this shows that the multinomial distribution is in the exponential family, there are some troubling aspects to this expression. In particular it appears that the  $A(\eta)$  term is equal to zero. As we will be seeing (in Section 8.1.2), one of the principal virtues of the exponential family form is that moments can be calculated by taking derivatives of  $A(\eta)$ ; thus, the disappearance of this term is unsettling.

Our problem is caused by the fact that the parameters satisfy a linear constraint, namely:  $\sum_{i=1}^m \pi_i = 1$ . Let us define an exponential family to be of *full rank* if the parameters satisfy no such constraint—technically we assume that an  $m$ -dimensional parameter space contains an open rectangle of dimension  $m$ . (In the case of the multinomial the parameters lie on an  $m - 1$  dimensional simplex, and thus the parameter space does not contain a rectangle of dimension  $m$ ). To achieve a full rank representation for the multinomial, we parameterize the distribution using the first  $m - 1$  components of  $\pi$ :

$$p(x | \pi) = \exp \left\{ \sum_{i=1}^m x_i \ln \pi_i \right\} \quad (8.26)$$

$$= \exp \left\{ \sum_{i=1}^{m-1} x_i \ln \pi_i + \left( 1 - \sum_{i=1}^{m-1} x_i \right) \ln \left( 1 - \sum_{i=1}^{m-1} \pi_i \right) \right\} \quad (8.27)$$

$$= \exp \left\{ \sum_{i=1}^{m-1} \ln \left( \frac{\pi_i}{1 - \sum_{i=1}^{m-1} \pi_i} \right) x_i + \ln \left( 1 - \sum_{i=1}^{m-1} \pi_i \right) \right\}. \quad (8.28)$$

where we have used the fact that  $\pi_m = 1 - \sum_{i=1}^{m-1} \pi_i$ .

From this representation we obtain:

$$\eta_i = \ln \left( \frac{\pi_i}{1 - \sum_{i=1}^{m-1} \pi_i} \right) = \ln \left( \frac{\pi_i}{\pi_m} \right) \quad (8.29)$$

for  $i = 1, \dots, m - 1$ . For convenience we also can define  $\eta_m$ ; Eq. (8.29) implies that if we do so we must take  $\eta_m = 0$ .

As in the other examples of exponential family distributions, we can invert Eq. (8.29) to obtain a mapping that expresses  $\pi_i$  in terms of  $\eta_i$ . Taking the exponential of Eq. (8.29) and summing we obtain:

$$\pi_i = \frac{e^{\eta_i}}{\sum_{j=1}^m e^{\eta_j}}, \quad (8.30)$$

which is the softmax function.

Finally, from Eq. (8.28) we obtain:

$$A(\eta) = -\ln \left( 1 - \sum_{i=1}^{m-1} \pi_i \right) = \ln \left( \sum_{i=1}^m e^{\eta_i} \right) \quad (8.31)$$

as the log normalization factor for the multinomial.

### 8.1.2 Moments

An appealing feature of the exponential family representation is that we can obtain moments of the distribution by taking derivatives of the log normalization function  $A(\eta)$ . Before establishing this fact, let us consider an example.

Recall that in the case of the Bernoulli distribution we have  $A(\eta) = \log(1 + e^\eta)$ . Taking a first derivative yields:

$$\frac{dA}{d\eta} = \frac{e^\eta}{1 + e^\eta} \quad (8.32)$$

$$= \frac{1}{1 + e^{-\eta}} \quad (8.33)$$

$$= \mu, \quad (8.34)$$

which is the mean of a Bernoulli variable.

Taking a second derivative yields:

$$\frac{d^2a}{d\eta^2} = \frac{d\mu}{d\eta} \quad (8.35)$$

$$= \mu(1 - \mu), \quad (8.36)$$

which is the variance of a Bernoulli variable.

We now show that in general the first derivative of  $A(\eta)$  is equal to the mean of  $T(X)$ . We treat the case of scalar  $\eta$  for simplicity; the (straightforward) extension to vector  $\eta$  is considered in Exercise ???. Calculating the first derivative of  $A(\eta)$  yields:

$$\frac{dA}{d\eta} = \frac{d}{d\eta} \left\{ \log \int \exp\{\eta T(x)\} h(x) dx \right\} \quad (8.37)$$

$$= \frac{\int T(x) \exp\{\eta T(x)\} h(x) dx}{\int \exp\{\eta T(x)\} h(x) dx} \quad (8.38)$$

$$= \int T(x) \exp\{\eta^T T(x) - A(\eta)\} h(x) dx \quad (8.39)$$

$$= ET(X). \quad (8.40)$$

Thus we see that the first derivative of  $A(\eta)$  is equal to the mean of the sufficient statistic.

Let us now take a second derivative:

$$\frac{d^2 a}{d\eta^2} = \int T(x) \exp\{\eta T(x) - A(\eta)\}(T(x) - a'(\eta))h(x)dx \quad (8.41)$$

$$= \int T(x) \exp\{\eta T(x) - A(\eta)\}(T(x) - ET(X))h(x)dx \quad (8.42)$$

$$= \int T^2(x) \exp\{\eta T(x) - A(\eta)\}h(x)dx - ET(X) \int T(x) \exp\{\eta T(x) - A(\eta)\}h(x)dx \\ = ET^2(x) - (ET(X))^2 \quad (8.43)$$

$$= \text{Var}[T(x)], \quad (8.44)$$

and thus we see that the second derivative of  $A(\eta)$  is equal to the variance of the sufficient statistic.

### Example

Let us calculate the moments of the univariate Gaussian distribution. Recall the form taken by  $A(\eta)$ :

$$A(\eta) = -\frac{\eta_1^2}{4\eta_2} - \frac{1}{2} \ln(-2\eta_2), \quad (8.45)$$

where  $\eta_1 = \mu/\sigma^2$  and  $\eta_2 = -1/2\sigma^2$ .

Taking the derivative with respect to  $\eta_1$  yields:

$$\frac{\partial A}{\partial \eta_1} = \frac{\eta_1}{2\eta_2} \quad (8.46)$$

$$= \frac{\mu/\sigma^2}{1/\sigma^2} \quad (8.47)$$

$$= \mu, \quad (8.48)$$

which is the mean of  $X$ , the first component of the sufficient statistic.

Taking a second derivative with respect to  $\eta_1$  yields:

$$\frac{\partial^2 A}{\partial \eta_1^2} = -\frac{1}{2\eta_2} \quad (8.49)$$

$$= \sigma^2, \quad (8.50)$$

which is the variance of  $X$ .

Given that  $X^2$  is the second component of the sufficient statistic, we can also compute the variance by calculating the partial of  $a$  with respect to  $\eta_2$ . Moreover, we can calculate third moments by computing the mixed partial, and fourth moments by taking the second partial with respect to  $\eta_2$  (see Exercise ??).

### 8.1.3 The moment parameterization

In the previous section we have seen that it is possible to obtain the mean,  $\mu \triangleq ET(X)$ , as a function of the canonical parameter  $\eta$ :

$$\mu = \frac{dA}{d\eta}. \quad (8.51)$$

It turns out that this relationship is invertible.

To see this, note from Eq. (8.44) that the second derivative of  $A(\eta)$  is a variance and hence positive. This implies that  $A(\eta)$  is a convex function. For a convex function there is necessarily a one-to-one relationship between the argument to the function and the first derivative of the function. Hence the mapping from  $\eta$  to  $\mu$  is invertible.

We will represent the inverse mapping as  $\eta = \psi(\mu)$  in the remainder of the chapter.

This argument implies that a distribution in the exponential family can be parameterized not only by  $\eta$ —the canonical parameterization—but also by  $\mu$ —the *moment parameterization*. Many distributions are traditionally parameterized using the moment parameterization; indeed, in Section 8.1.1 our starting point was the moment parameterization for each of the examples. We subsequently reparameterized these distribution using the canonical parameterization. We also computed the mapping from  $\eta$  to  $\mu$  in each case, recovering some familiar functions, including the logistic function and the softmax function. We will return to this topic in Section 8.2 when we discuss generalized linear models.

### 8.1.4 Sufficiency

In this section we discuss the important concept of *sufficiency*. Sufficiency characterizes what is essential in a data set, or, alternatively, what is inessential and can therefore be thrown away. While the notion of sufficiency is broader than the exponential family, the ties to the exponential family are close, and it is natural to introduce the concept here.

A *statistic* is a function of a random variable. In particular, let  $X$  be a random variable and let  $T(X)$  be a statistic. Suppose that the distribution of  $X$  depends on a parameter  $\theta$ . The intuitive notion of sufficiency is that  $T(X)$  is sufficient for  $\theta$  if there is no information in  $X$  regarding  $\theta$  beyond that in  $T(X)$ . That is, having observed  $T(X)$ , we can throw away  $X$  for the purposes of inference with respect to  $\theta$ . Let us make this notion more precise.

Sufficiency is defined in somewhat different ways in the Bayesian and frequentist frameworks. Let us begin with the Bayesian approach, which is arguably more natural. In the Bayesian approach, we treat  $\theta$  as a random variable, and are therefore licensed to consider conditional independence relationships involving  $\theta$ . We say that  $T(X)$  is sufficient for  $\theta$  if the following conditional independence statement holds:

$$\theta \perp\!\!\!\perp X \mid T(X). \quad (8.52)$$

We can also write this in terms of probability distributions:

$$p(\theta \mid T(x), x) = p(\theta \mid T(x)). \quad (8.53)$$

Thus, as shown graphically in Figure 8.1(a), sufficiency means that  $\theta$  is independent of  $X$ , when

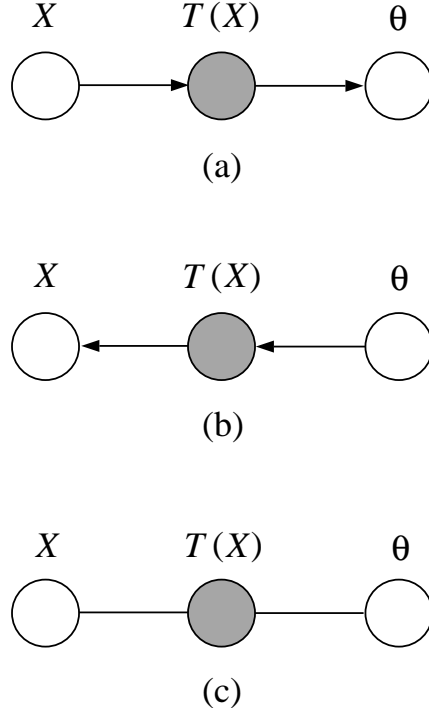


Figure 8.1: Graphical models whose conditional independence properties capture the notion of sufficiency in three equivalent ways.

we condition on  $T(X)$ . This captures the intuitive notion that  $T(X)$  contains all of the essential information in  $X$  regarding  $\theta$ .

To obtain a frequentist definition of sufficiency, let us consider the graphical model in Figure 8.1(b). This model expresses the same conditional independence semantics as Figure 8.1(a), asserting that  $\theta$  is independent of  $X$  conditional on  $T(X)$ , but the model is parameterized in a different way. From the factorized form of the joint probability we obtain:

$$p(x | T(x), \theta) = p(x | T(x)). \quad (8.54)$$

This expression suggests a frequentist definition of sufficiency. In particular, treating  $\theta$  as a label rather than a random variable, we define  $T(X)$  to be sufficient for  $\theta$  if the conditional distribution of  $X$  given  $T(X)$  is not a function of  $\theta$ .

Both the Bayesian and frequentist definitions of sufficiency imply a factorization of  $p(x | \theta)$ , and it is this factorization which is generally easiest to work with in practice. To obtain the factorization we use the undirected graphical model formalism. Note in particular that Figure 8.1(c) expresses the same conditional independence semantics as Figure 8.1(a) and Figure 8.1(b). Moreover, from Figure 8.1(c), we know that we can express the joint probability as a product of potential functions  $\psi_1$  and  $\psi_2$ :

$$p(x, T(x), \theta) = \psi_1(T(x), \theta)\psi_2(x, T(x)), \quad (8.55)$$

where we have absorbed the constant of proportionality  $Z$  in one of the potential functions. Now  $T(x)$  is a deterministic function of  $x$ , which implies that we can drop  $T(x)$  on the left-hand side of the equation. Dividing by  $p(\theta)$  we therefore obtain:

$$p(x | \theta) = g(T(x), \theta)h(x, T(x)), \quad (8.56)$$

for given functions  $g$  and  $h$ . Although we have motivated this result by using a Bayesian calculation, the result can be utilized within either the Bayesian or frequentist framework. Its equivalence to the frequentist definition of sufficiency is known as the Neyman factorization theorem.

### 8.1.5 Sufficiency and the exponential family

An important feature of the exponential family is that one can obtain sufficient statistics by inspection, once the distribution is expressed in the standard form. Recall the definition:

$$p(x | \eta) = h(x) \exp\{\eta^T T(x) - A(\eta)\}. \quad (8.57)$$

From Eq. (8.56) we see immediately that  $T(X)$  is a sufficient statistic for  $\eta$ .

### 8.1.6 IID sampling

The reduction obtainable by using a sufficient statistic is particularly notable in the case of IID sampling. Suppose that we have a collection of  $N$  independent random variables,  $X = (X_1, X_2, \dots, X_N)$ , characterized by the same exponential family density. Taking the product, we obtain the joint density:

$$p(x | \eta) = \prod_{n=1}^N h(x_n) \exp\{\eta^T T(x_n) - A(\eta)\} = \left( \prod_{n=1}^N h(x_n) \right) \exp \left\{ \eta^T \sum_{n=1}^N T(x_n) - NA(\eta) \right\}. \quad (8.58)$$

From this result we see that  $X$  is itself an exponential distribution, with sufficient statistic  $\sum_{n=1}^N T(x_n)$ .

For several of the examples we discussed earlier (in Section 8.1.1), including the Bernoulli, the Poisson, and the multinomial distributions, the sufficient statistic  $T(X)$  is equal to the random variable  $X$ . For a set of  $N$  IID observations from such distributions, the sufficient statistic is equal to  $\sum_{n=1}^N x_n$ . Thus in this case, it suffices to maintain a single value, the sum of the observations. The individual data points can be thrown away.

For the univariate Gaussian the sufficient statistic is the pair  $T(X) = (X, X^2)$ , and thus for  $N$  IID Gaussians it suffices to maintain the sum  $\sum_{n=1}^N x_n$ , and the sum of squares  $\sum_{n=1}^N x_n^2$ .

### 8.1.7 Maximum likelihood estimates

In this section we show how to obtain maximum likelihood estimates in exponential family distributions. We obtain a generic formula which generalizes our earlier work on density estimation in Chapter 5.

Consider an IID data set,  $\mathcal{D} = (x_1, x_2, \dots, x_N)$ . From Eq. (8.58) we obtain the following log likelihood:

$$l(\eta | \mathcal{D}) = \log \left( \prod_{n=1}^N h(x_n) \right) + \eta^T \left( \sum_{n=1}^N T(x_n) \right) - NA(\eta). \quad (8.59)$$

Taking the gradient with respect to  $\eta$  yields:

$$\nabla_\eta l = \sum_{n=1}^N T(x_n) - N \nabla_\eta A(\eta), \quad (8.60)$$

and setting to zero gives:

$$\nabla_\eta A(\hat{\eta}) = \frac{1}{N} \sum_{n=1}^N T(x_n). \quad (8.61)$$

Finally, defining  $\mu \triangleq E[T(x)]$ , and recalling Eq. (8.40), we obtain:

$$\hat{\mu}_{ML} = \frac{1}{N} \sum_{n=1}^N T(x_n) \quad (8.62)$$

as the general formula for maximum likelihood estimation in the exponential family.

It should not be surprising that our formula involves the data only via the sufficient statistic  $\sum_{n=1}^N T(X_n)$ . This gives operational meaning to sufficiency—for the purpose of estimating parameters we retain only the sufficient statistic.

For distributions in which  $T(X) = X$ , which include the Bernoulli distribution, the Poisson distribution, and the multinomial distribution, our result shows that the sample mean is the maximum likelihood estimate of the mean.

For the univariate Gaussian distribution, we see that the sample mean is the maximum likelihood estimate of the mean and the sample variance is the maximum likelihood estimate of the variance. For the multivariate Gaussian we obtain the same result, where by “variance” we mean the covariance matrix.

### 8.1.8 Maximum likelihood and the Kullback-Leibler divergence

In this section we point out a simple relationship between the maximum likelihood problem and the Kullback-Leibler (KL) divergence. This relationship is general; it has nothing to do specifically with the exponential family. We discuss it in the current chapter, however, because we have a hidden agenda. Our agenda, to be gradually revealed in Chapters 9, 11 and 19, involves building a number of very interesting and important relationships between the exponential family and the Kullback-Leibler (KL) divergence. By introducing a statistical interpretation of the KL divergence in the current chapter, we hope to hint subliminally at deeper connections to come.

To link the KL divergence and maximum likelihood, let us first define the *empirical distribution*,  $\tilde{p}(x)$ . This is a distribution which places a point mass at each data point  $x_n$  in our data set  $\mathcal{D}$ . We

have:

$$\tilde{p}(x) \triangleq \frac{1}{N} \sum_{n=1}^N \delta(x, x_n), \quad (8.63)$$

where  $\delta(x, x_n)$  is a Kronecker delta function in the continuous case. In the discrete case,  $\delta(x, x_n)$  is simply a function that is equal to one if its arguments agree and equal to zero otherwise.

If we integrate (in the continuous case) or sum (in the discrete case)  $\tilde{p}(x)$  against a function of  $x$ , we evaluate that function at each point  $x_n$ . In particular, the log likelihood can be written this way. In the discrete case we have:

$$\sum_x \tilde{p}(x) \log p(x | \theta) = \sum_x \frac{1}{N} \sum_{n=1}^N \delta(x, x_n) \log p(x | \theta) \quad (8.64)$$

$$= \frac{1}{N} \sum_{n=1}^N \sum_x \delta(x, x_n) \log p(x | \theta) \quad (8.65)$$

$$= \frac{1}{N} \sum_{n=1}^N \log p(x_n | \theta) \quad (8.66)$$

$$= \frac{1}{N} l(\theta | \mathcal{D}). \quad (8.67)$$

Thus by computing a cross-entropy between the empirical distribution and the model, we obtain the log likelihood, scaled by the constant  $1/N$ . We obtain an identical result in the continuous case by integrating.

Let us now calculate the KL divergence between the empirical distribution and the model  $p(x | \theta)$ . We have:

$$D(\tilde{p}(x) \| p(x | \theta)) = \sum_x \tilde{p}(x) \log \frac{\tilde{p}(x)}{p(x | \theta)} \quad (8.68)$$

$$= \sum_x \tilde{p}(x) \log \tilde{p}(x) - \sum_x \tilde{p}(x) \log p(x | \theta) \quad (8.69)$$

$$= + \sum_x \tilde{p}(x) \log \tilde{p}(x) - \frac{1}{N} l(\theta | \mathcal{D}). \quad (8.70)$$

The first term,  $\sum_x \tilde{p}(x) \log \tilde{p}(x)$ , is independent of  $\theta$ . Thus, the minimizing value of  $\theta$  on the left-hand side is equal to the maximizing value of  $\theta$  on the right-hand side.

In other words: *minimizing the KL divergence to the empirical distribution is equivalent to maximizing the likelihood*. This simple result will prove to be very useful in our later work.

### 8.1.9 Conjugacy and Bayesian estimates

[Section not yet written].

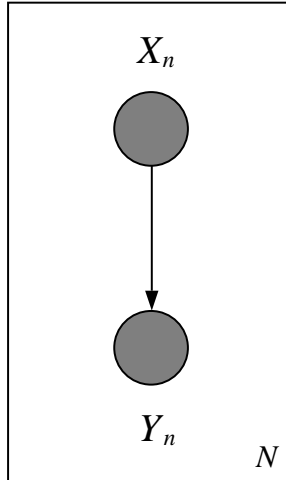


Figure 8.2: The graphical model representation of a generalized linear model.

## 8.2 Generalized linear models

We now turn to problems involving a pair of variables,  $X$  and  $Y$ , where both  $X$  and  $Y$  are assumed to be observed (see Figure 8.2). As in the linear regression and (discriminative) linear classification models that we discussed in Chapters 6 and 7, we focus on the conditional relationship between  $X$  and  $Y$ .

A common feature of both the linear regression and discriminative linear classification models is a particular choice of representation for the conditional expectation of  $Y$ . Letting  $\mu$  denote the modeled value of the conditional expectation, we can summarize the structural component of both types of models by writing:

$$\mu = f(\theta^T x). \quad (8.71)$$

In the case of linear regression the function  $f(\cdot)$  is the identity function. For the linear classification models, we studied a variety of possible choices for  $f(\cdot)$ , including the logistic function (for logistic regression) and the cumulative Gaussian (for probit regression).

To complete the model specification, we endow  $Y$  with a particular conditional probability distribution, having  $\mu$  as a parameter. For linear regression, this distribution is Gaussian, whereas for the linear classification models, this distribution is Bernoulli (for the binary case) or multinomial (for the multiway case).

The *generalized linear model (GLIM)* framework extends these ideas beyond the Gaussian, Bernoulli and multinomial settings to the more general exponential family. A GLIM makes three assumptions regarding the form of the conditional probability distribution  $p(y | x)$ :

- The observed input  $x$  is assumed to enter into the model via a linear combination  $\xi = \theta^T x$ ,
- The conditional mean  $\mu$  is represented as a function  $f(\xi)$  of the linear combination  $\xi$ , where  $f$  is known as the *response function*,

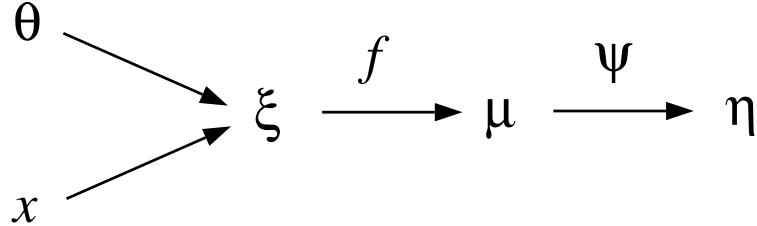


Figure 8.3: A diagram summarizing the relationships between the variables in a GLIM model.

- The observed output  $y$  is assumed to be characterized by an exponential family distribution with conditional mean  $\mu$ .

These assumptions are summarized diagrammatically in Figure 8.3. Note that the diagram includes the mapping from  $\mu$  to  $\eta$ , which we denote as  $\eta = \psi(\mu)$ . This mapping allows us to use the canonical parameterization to represent the exponential family distribution for  $Y$ .

Within the GLIM framework, it is convenient to work with a slight variation on the exponential family theme. In particular, in the GLIM framework we assume that the conditional distribution of  $Y$  takes the following form:

$$p(x | \eta, \phi) = h(x, \phi) \exp \left\{ \frac{\eta^T x - A(\eta)}{\phi} \right\}, \quad (8.72)$$

where we have augmented the representation in Eq. (8.1) to include an explicit *scale parameter*  $\phi$ . Many exponential family distributions, including the Gaussian and the gamma, are naturally expressed in this form. In particular, we can write the Gaussian distribution as follows:

$$p(x | \mu, \sigma^2) = \frac{1}{\sqrt{2\pi}\sigma} \exp \left\{ -\frac{1}{2\sigma^2}(x - \mu)^2 \right\} \quad (8.73)$$

$$= \left( \frac{1}{\sqrt{2\pi}\sigma^2} \exp \left\{ -\frac{x^2}{2\sigma^2} \right\} \right) \exp \left\{ \frac{\mu x - \mu^2/2}{\sigma^2} \right\}. \quad (8.74)$$

As we have seen, we can equivalently bundle the parameters  $\mu$  and  $\sigma^2$  into a single parameter vector, and express the Gaussian as a two-parameter exponential family distribution. The scale-parameter form is, however, often more natural. Note, moreover, that although the Gaussian yields a two-parameter exponential family when we bundle the canonical parameter and the scale parameter, in general we do not require that  $p(x | \eta, \phi)$  is expressible as a two-parameter exponential family. This gives some useful flexibility.

Note also that for the purposes of GLIM modeling we drop the  $T(\cdot)$  function in the exponential family representation. Thus we focus on distributions for which the observable  $Y$  is itself a sufficient statistic.

There are two principal choice points in the specification of a GLIM: (1) the choice of exponential family distribution, and (2) the choice of the response function  $f(\cdot)$ .

The choice of exponential family distribution is generally rather strongly constrained by the nature of the data  $Y$ . Thus, class labels are naturally represented by Bernoulli or multinomial distributions, counts by the Poisson distribution, intervals by the exponential or gamma distributions, etc.

This leaves us with the choice of the response function as the principal degree of freedom in the specification of a GLIM. There are constraints that we generally want to impose on this function, reflecting constraints on the conditional expectation. For example, in the case of the Bernoulli and multinomial distributions, the conditional expectation must lie between 0 and 1, and this suggests that we should choose a response function whose range is  $(0, 1)$ . Similarly, for a gamma distribution, the random variable is nonnegative, and we should presumably choose a response function whose range is  $(0, \infty)$ . Such constraints only give rough guidance, however, and in general for any given distribution there are many possible choices of response function. There is, however, a particular response function—the *canonical response function*—that is uniquely associated with a given exponential family distribution and has some appealing mathematical properties. In particular, if we assume that  $\xi = \eta$ , or equivalently that  $f(\cdot) = \psi^{-1}(\cdot)$ , we obtain the canonical response function. Note that the function  $\psi(\cdot)$  is determined once we have chosen a particular exponential family density. Thus if we decide to use the canonical response function the choice of the exponential family density completely determines the GLIM.

We will explore some of the properties of the canonical response function in the remainder of this chapter. It should be emphasized, however, that the canonical response function is by no means the universally best choice for all problems. Indeed, as we have already seen in the case of the classification models, different choices of response function can be appropriate in different situations, reflecting different underlying assumptions about the way that the data are generated. We might view the canonical response function as a reasonable default.

The first point to note about the canonical response function is that it automatically passes a sanity check with regards to the constraints on its range. That is, the modeled values  $\mu = f(\eta)$  are guaranteed to be possible values of the conditional expectation. To see this, note that:

$$f(\eta) = \psi^{-1}(\eta) = a'(\eta) = E[Y | \eta]. \quad (8.75)$$

Thus, for any value  $\eta$  such that  $a'(\eta)$  exists, we see that  $f(\eta)$  is equal to the conditional mean of an exponential family distribution in which  $\eta$  is the canonical parameter.

Some examples of canonical response functions are provided in the following table; these have been collected from the examples in Section 8.1 and from the exercises.

### 8.2.1 Maximum likelihood estimation

In this section we write down the likelihood for generalized linear models and present on-line and batch methods for maximizing the likelihood. We restrict ourselves to scalar  $Y$  in order to simplify the presentation; the results go through for vector  $Y$  with straightforward notational alterations (see Exercise ??).

Consider an IID data set,  $\mathcal{D} = \{(x_n, y_n); n = 1, \dots, N\}$ . Taking the logarithm of a product of  $N$  copies of the exponential family distribution in Eq. (8.72), we obtain the following log likelihood

tb

Model	Canonical response function
Gaussian	$\mu = \eta$
Bernoulli	$\mu = 1/(1 + e^{-\eta})$
multinomial	$\mu_i = \eta_i / \sum_j e^{\eta_j}$
Poisson	$\mu = e^\eta$
gamma	$\mu = -\eta^{-1}$

Figure 8.4: The canonical response functions for several exponential family distributions.

for GLIM models:

$$l(\theta | \mathcal{D}) = \log \left( \prod_{n=1}^N h(y_n) \exp\{\eta_n y_n - A(\eta_n)\} \right) \quad (8.76)$$

$$= \sum_{n=1}^N \log h(y_n) + \sum_{n=1}^N (\eta_n y_n - A(\eta_n)), \quad (8.77)$$

where  $\eta_n = \psi(\mu_n)$ ,  $\mu_n = f(\xi_n)$  and  $\xi_n = \theta^T x_n$ .

In the case of the canonical response function, for which  $\eta_n = \theta^T x_n$ , the log likelihood simplifies:

$$l(\theta | \mathcal{D}) = \sum_{n=1}^N \log h(y_n) + \sum_{n=1}^N (\theta^T x_n y_n - A(\eta_n)) \quad (8.78)$$

$$= \sum_{n=1}^N \log h(y_n) + \theta^T \sum_{n=1}^N x_n y_n - \sum_{n=1}^N A(\eta_n). \quad (8.79)$$

From this expression we can draw an important conclusion—*the sum  $\sum_{n=1}^N x_n y_n$  is a sufficient statistic for  $\theta$* . This sum has a fixed, finite dimension (the dimension of the vector  $x_n$ ), for any value of  $N$ . This has the very practical consequence that we can allocate a fixed amount of storage for collecting the information needed to estimate  $\theta$ , whatever the sample size  $N$ . This is an important motivation for considering canonical response functions.

Let us now calculate the gradient of the log likelihood:

$$\nabla_\theta l = \sum_{n=1}^N \frac{dl}{d\eta_n} \nabla_\theta \eta_n \quad (8.80)$$

$$= \sum_{n=1}^N (y_n - a'(\eta_n)) \nabla_\theta \eta_n \quad (8.81)$$

$$= \sum_{n=1}^N (y_n - \mu_n) \frac{d\eta_n}{d\mu_n} \frac{d\mu_n}{d\xi_n} x_n. \quad (8.82)$$

For the canonical response function, we have  $\eta_n = \xi_n$ , and thus the derivatives cancel, leaving us with the following simple expression for the log likelihood:

$$\nabla_{\theta} l = \sum_{n=1}^N (y_n - \mu_n) x_n. \quad (8.83)$$

This expression has the appealing feature that the parameter vector  $\theta$  and the “error”  $(y_n - \mu_n)$  are on the same scale.

### An on-line algorithm

A general on-line estimation algorithm can be obtained by following the stochastic gradient of the log likelihood function. Consider first the case of the canonical response function. Given an estimate  $\theta^{(t)}$  at the  $t$ th iteration of the algorithm, we obtain:

$$\theta^{(t+1)} = \theta^{(t)} + \rho(y_n - \mu_n^{(t)}) x_n, \quad (8.84)$$

where  $\mu_n^{(t)} = f(\theta^{(t)T} x_n)$  and where  $\rho$  is a step size.

We have obtained an algorithm that is formally identical to the LMS algorithm. Moreover, the geometry of the LMS algorithm that we discussed in Chapter 6 carries over to this more general setting. That is, as in Chapter 6, the on-line algorithm steps in the direction of the input vector  $x_n$ , weighted by the prediction error  $(y_n - \mu_n^{(t)})$ . The specific GLIM model makes its appearance only through the definition of the conditional expectation  $\mu_n$ .

If we do not use the canonical response function, then the gradient also includes the derivatives of  $f(\cdot)$  and  $\psi(\cdot)$ . These can be viewed as scaling coefficients that alter the step size  $\rho$ , but otherwise leave the general LMS form intact. Thus we have obtained a result worth remembering—the LMS-like algorithm in Eq. (8.84) is the generic stochastic gradient algorithm for models throughout the GLIM family.

### A batch algorithm

In our discussion of logistic regression (Section 7.3.1) we introduced the *iteratively reweighted least squares (IRLS) algorithm*—a Newton-Raphson algorithm for batch estimation of parameters. The algorithm goes through with essentially no change to the general GLIM setting. For completeness we present the algorithm and its derivation here.

We will assume the canonical response function, and indicate the changes that are needed to accommodate noncanonical response functions at the end of the section.

We begin by writing the gradient in vector notation:

$$\nabla_{\theta} l = \frac{1}{\phi} \sum_n (y_n - \mu_n) x_n = \frac{1}{\phi} X^T (y - \mu), \quad (8.85)$$

where  $X$  is the design matrix whose rows are the vector  $x_n^T$ ,  $y$  is defined as the  $N \times 1$  vector whose components are the values  $y_n$ , and similarly  $\mu$  is the  $N \times 1$  vector whose components are the values  $\mu_n$ .

Taking a second derivative, we calculate the Hessian matrix:

$$H = -\frac{1}{\phi} \sum_n \frac{d\mu_n}{d\eta_n} x_n x_n^T \quad (8.86)$$

$$= -\frac{1}{\phi} X^T W X, \quad (8.87)$$

where we have defined the diagonal weight matrix:

$$W \triangleq \text{diag} \left\{ \frac{d\mu_1}{d\eta_1}, \frac{d\mu_1}{d\eta_2}, \dots, \frac{d\mu_1}{d\eta_N} \right\}, \quad (8.88)$$

where  $d\mu_n/d\eta_n$  can be computed by calculating the second derivative of  $A(\eta_n)$ .

Note that the weights depend on the parameter vector  $\theta$ , and thus the weight matrix  $W$  depends on  $\theta$ . We use the notation  $W^{(t)}$  to denote the weight matrix at the  $t$ th iteration of the algorithm. Similarly, we use the notation  $\mu^{(t)}$  to denote the value of  $\mu$  at the  $t$ th iteration.

The Newton-Raphson algorithm is obtained by multiplying the gradient by the inverse Hessian matrix and subtracting the result from the current parameter vector:

$$\theta^{(t+1)} = \theta^{(t)} + (X^T W^{(t)} X)^{-1} X^T (y - \mu^{(t)}) \quad (8.89)$$

$$= (X^T W^{(t)} X)^{-1} \left[ X^T W^{(t)} X \theta^{(t)} + X^T (y - \mu^{(t)}) \right] \quad (8.90)$$

$$= (X^T W^{(t)} X)^{-1} X^T W^{(t)} z^{(t)}, \quad (8.91)$$

where we define:

$$z^{(t)} = \eta + [W^{(t)}]^{-1} (y - \mu^{(t)}). \quad (8.92)$$

The algorithm in Eq. (8.91) is the IRLS algorithm.

If we extend the derivation to handle noncanonical response functions, we find that the Hessian matrix has another term (see Exercise ??). Including this term yields the Newton-Raphson algorithm for noncanonical response functions. There is, however, an alternative approach. If we use the *expected Hessian* in place of the Hessian in the Newton-Raphson update formula, we obtain an alternative algorithm known as the *Fisher scoring method*.<sup>1</sup> This algorithm is a simplification in the case of noncanonical response functions—the extra term that appears in the Hessian contains the factor  $(y - \mu)$ , and this term therefore vanishes when we take expectations (see Exercise ??). Thus, the Fisher scoring method takes the form shown in Eq. (8.91) in all cases. It is generally the preferred way to implement the IRLS algorithm.

### 8.3 Historical remarks and bibliography

---

<sup>1</sup>Note that the expectation of the Hessian matrix is the Fisher information matrix.

# An Introduction to Probabilistic Graphical Models

Michael I. Jordan  
*University of California, Berkeley*

June 30, 2003



## Chapter 9

# Completely Observed Graphical Models

The models that we have discussed until now have, for the most part, involved a single node or a single node and its parents. We have seen how to find maximum likelihood estimates for a variety of models of this form.

In the current chapter, we learn that the techniques that we have developed extend with essentially no additional labor to the entire class of directed graphical models, under the assumption of *complete observations*. Thus, if we assume that our data set assigns values to all of the random variables in the model—i.e., that there are no *latent variables*—then we can find maximum likelihood estimates of parameters in a straightforward way, essentially by solving the problem separately at each node. The parameter estimation problem “decouples.” The underlying reason for this appealing result is the product form of the joint probability distribution.

We also discuss the problem of maximum likelihood parameter estimation for undirected graphical models. In this case the parameter estimation problem decouples only for a special class of graphical models, known as *decomposable models*. For general undirected models the parameter estimation problem does not decouple, the essential reason being the presence of the global normalization factor  $Z$ . Nonetheless, we will show that there is a local characterization of maximum likelihood estimates for general undirected models, and we present algorithms for finding these estimates.

In Section 9.4, we discuss the problems that arise when we remove the restriction to completely observed models. The material in this section sets the stage for our treatment of latent variable models in Chapters 10 through 15.

Our focus in this chapter is on the likelihood function and maximum likelihood estimation. We do, however, provide a short discussion of Bayesian estimation in the completely observed setting in Section ??.

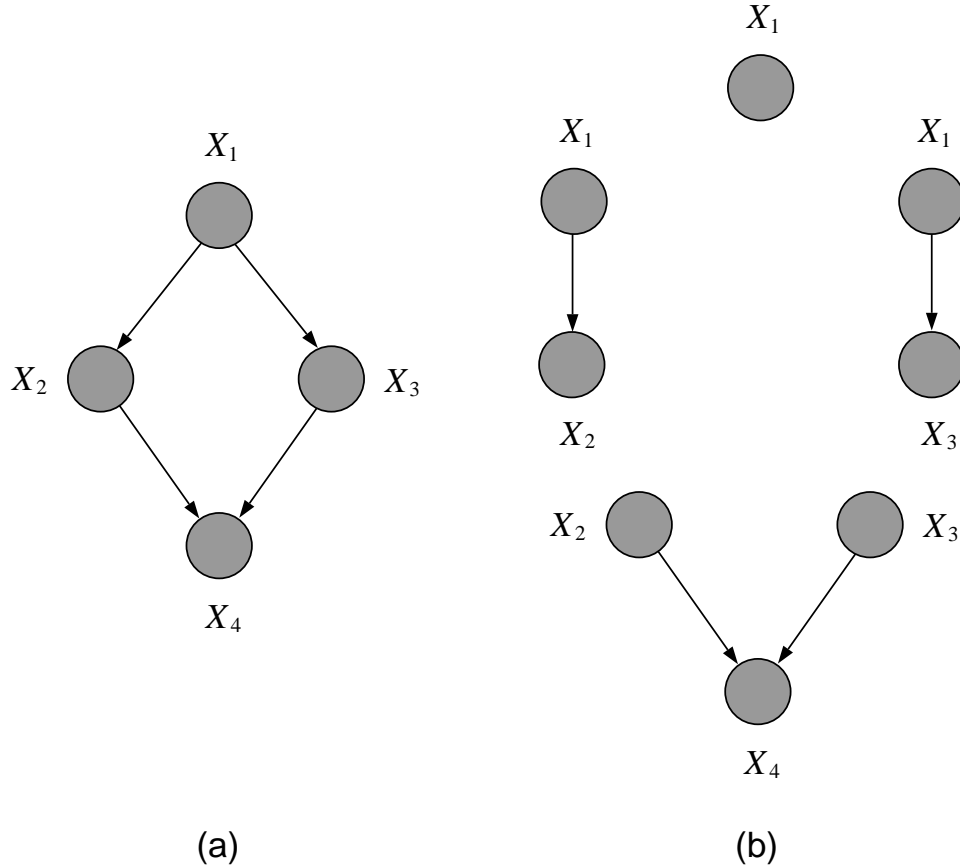


Figure 9.1: (a) A directed graphical model. (b) Solving the maximum likelihood problem in (a) is equivalent to solving separate maximum likelihood problems for each node conditioned on its parents.

## 9.1 The basic idea

Before jumping into the details, let us consider a simple example. The graphical model shown in Figure 9.1(a) has the following joint probability distribution:

$$p(x | \theta) = p(x_1 | \theta_1)p(x_2 | x_1, \theta_2)p(x_3 | x_1, \theta_3)p(x_4 | x_2, x_3, \theta_4). \quad (9.1)$$

Taking the logarithm of this distribution we have:

$$\log p(x|\theta) = \log p(x_1|\theta_1) + \log p(x_2|x_1, \theta_2) + \log p(x_3|x_1, \theta_3) + \log p(x_4|x_2, x_3, \theta_4). \quad (9.2)$$

From this expression, we see that the parameters,  $\theta_i$ , appear in different terms, and thus the maximization of the log probability with respect to a given  $\theta_i$  can be carried out independently of the other maximizations.

Figure 9.1(b) provides a graphical depiction of this fact. The problem of finding the maximum likelihood parameters for the model in Figure 9.1(a) breaks into separate maximum likelihood problems, one for each node in the graph. As suggested in Figure 9.1(b), if we solve these separate maximum likelihood problems, we have solved the overall maximum likelihood problem.

## 9.2 Directed models

This chapter marks our first attempt to treat rather general families of graphical models. Although our results are rather straightforward, we will need to be a bit fussier with regards to notation than we have been in earlier chapters. This will allow us to state our results in a simple and general way, and will prepare the ground for later chapters.

Let  $\mathcal{G}$  be a directed graph, where  $\mathcal{V}$  is the set of nodes and  $\mathcal{E}$  the set of edges of the graph. We associate a random vector  $X$  with the graph, where the components of the vector are indexed by the nodes in the graph. Thus,  $X_u$  denotes the random variable associated with node  $u \in \mathcal{V}$ , and  $x_u$  denotes a realization of this random variable.

Recall that we also allow subsets of  $\mathcal{V}$  to serve as indices; thus,  $X_C$  refers to the set of components indexed by a subset  $C \subseteq \mathcal{V}$ . The vector  $X$  will itself sometimes be written  $X_{\mathcal{V}}$ .

We define a probability model for a directed graph via a set of local conditional probability distributions. Thus, to each node  $u \in \mathcal{V}$  we associate a local conditional probability distribution  $p(x_u | x_{\pi_u}, \theta_u)$ , where  $\pi_u$  denotes the set of indices of the parents of  $u$  and where  $\theta_u$  is a parameter vector. The overall probability associated with the graph  $\mathcal{G}$  is a product of these local conditional probabilities:

$$p(x_{\mathcal{V}} | \theta) = \prod_{u \in \mathcal{V}} p(x_u | x_{\pi_u}, \theta_u), \quad (9.3)$$

where  $\theta = (\theta_1, \theta_2, \dots, \theta_m)$ .

We treat the case of complete observations in this chapter. A *complete observation* is an assignment of values to all of the random variables  $X_{\mathcal{V}}$  in the model.

In many problems the data are assumed to consist of a set of  $N$  independent, identically distributed (IID) observations. Such an assumption requires no special treatment within the graphical model formalism—we simply replicate a basic graphical structure  $N$  times. The result is itself a graphical model. It is important, however, to be able to continue to refer to the probability model associated with a single observable vector  $X_{\mathcal{V}}$ , apart from any considerations of the sampling mechanism, and also to be able to refer to the overall model that assigns probability to the IID replicates of  $X_{\mathcal{V}}$ . Let us continue to use the notation  $\mathcal{G}(\mathcal{V}, \mathcal{E})$  and  $p(x_{\mathcal{V}} | \theta)$  to refer to the probability model associated with a single observable vector  $X_{\mathcal{V}}$ . We also construct an augmented graphical model,  $\mathcal{G}^{(N)} = (\mathcal{V}^{(N)}, \mathcal{E}^{(N)})$ , that incorporates the IID sampling assumption—this graph consists of  $N$  disconnected replicates of  $\mathcal{G}$ . The nodes  $\mathcal{V}^{(N)}$  in this augmented graph are indexed using a pair of labels,  $(u, n)$ , where  $u \in \mathcal{V}$  designates a node in the underlying graphical model  $\mathcal{G}$ , and where  $n \in \{1, 2, \dots, N\}$  designates the replication number (see Figure 9.2).

We again allow subsets of indices to be used wherever single indexes are used. Thus,  $(C, n)$  denotes the  $n$ th replicate of the set  $C$ , for  $C \subseteq \mathcal{V}$ . In particular,  $(\mathcal{V}, n)$  denotes the  $n$ th replicate of

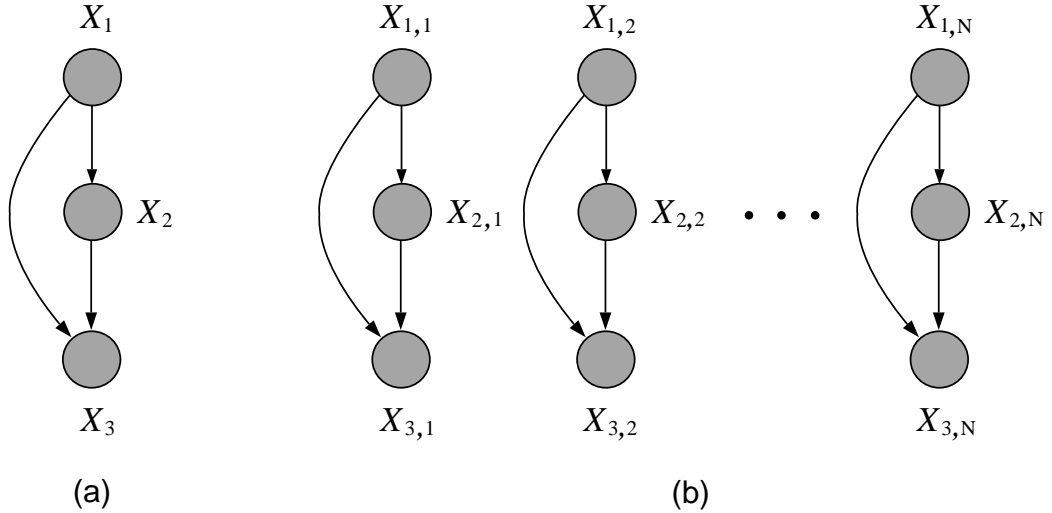


Figure 9.2: (a) An example of a graphical model  $\mathcal{G}$ , where  $\mathcal{V} = \{1, 2, 3\}$ . The set of random variables in the model is represented as  $X_{\mathcal{V}} = (X_1, X_2, X_3)$ , and  $x_{\mathcal{V}} = (x_1, x_2, x_3)$  represents a realization of these variables. (b) An example of the graph  $\mathcal{G}^{(N)}$ , obtained by making  $N$  replicates of  $\mathcal{G}$ . Each random variable in this graph is indexed with two indices,  $(u, n)$ , the first denoting the underlying node in  $\mathcal{G}$ , and the second denoting the replication number. The  $n$ th complete observation is an assignment of values to all of the nodes in the  $n$ th replicate, and is denoted  $x_{\mathcal{V},n} = (x_{1,n}, x_{2,n}, x_{3,n})$ .

the entire set of observable nodes  $\mathcal{V}$ . This notation allows us to write:

$$\mathcal{D} = (x_{\mathcal{V},1}, x_{\mathcal{V},2}, \dots, x_{\mathcal{V},N}) \quad (9.4)$$

as our representation for the entire set of *observed data* in the completely observed setting.

The local conditional probability associated with a node  $(u, n)$  in  $\mathcal{G}^{(N)}$  is defined to be the local conditional probability associated with the index  $u$  in the underlying graphical model  $\mathcal{G}$ . We thus obtain the following probability model for the graph  $\mathcal{G}^{(N)}$ :

$$p(\mathcal{D} \mid \theta) = \prod_n p(x_{\mathcal{V},n} \mid \theta) \quad (9.5)$$

$$= \prod_n \prod_u p(x_{u,n} \mid x_{\pi_u, n}, \theta_u), \quad (9.6)$$

where Eq. (9.5) is just the independence assumption, but it is also worth noting that it follows from the usual construction of the joint probability of a graph as a product over local conditional probabilities; here the graph is formed from a disconnected set of subgraphs indexed by  $n$ .

Taking the logarithm of Eq. (9.6) we obtain the log likelihood:

$$l(\theta; \mathcal{D}) = \sum_n \sum_u \log p(x_{u,n} | x_{\pi_u, n}, \theta_u); \quad (9.7)$$

Note that the log likelihood is a sum of a number of terms, each of which refers to only one of the parameter vectors  $\theta_u$ . In estimating  $\theta_u$  we can ignore all terms that involve  $\theta_{u'}$ , for  $u' \neq u$ . Note, moreover, that those terms involving  $\theta_u$  refer only to  $x_u$  and  $x_{\pi_u}$ , which are observations of node  $u$  and its parents  $\pi_u$ . Thus, for the purposes of estimating the parameter vector  $\theta_u$ , we need only focus on the data associated with the node  $u$  and its parents—we can ignore the data associated with the other nodes in the graph. In other words, the local subset of observations  $\{x_{u,n}, x_{\pi_u,n}\}_{n=1}^N$  associated with these nodes is *sufficient* for  $\theta_u$ .

We can often say more. In particular, if the observations  $\{x_{u,n}, x_{\pi_u,n}\}_{n=1}^N$  can themselves be summarized by finite-dimensional sufficient statistics, as they can if each local conditional probability model,  $p(x_u | x_{\pi_u}, \theta_u)$ , is an exponential family distribution, then the entire estimation problem can be reduced to a collection of finite-dimensional sufficient statistics. In essence, we can reduce our problem from observations associated with the graph  $\mathcal{G}^{(N)}$  to statistics associated with the graph  $\mathcal{G}$ , and from there to statistics associated with single nodes and their parents. In the next section we illustrate this reduction in the context of discrete graphical models.

### 9.2.1 Discrete models

Let us work out the sufficient statistics for a general graphical model in which all nodes are discrete. In doing so, we exemplify the general results that we have just discussed and also introduce a few “tricks of the trade” that will be useful in the following section as well as in later chapters.

#### Counts and marginal counts

We begin by introducing a notation for counts, which are the sufficient statistics for multinomial random variables. For a given configuration  $x_{\mathcal{V}}$ , let  $m(x_{\mathcal{V}})$  denote the number of times that  $x_{\mathcal{V}}$  is observed among the observations in the dataset  $\mathcal{D}$ . (There are only a finite number of possible configurations  $x_{\mathcal{V}}$ , and each data point  $x_{\mathcal{V},n}$  must be one of these configurations). We can represent this count as a sum:

$$m(x_{\mathcal{V}}) \triangleq \sum_n \delta(x_{\mathcal{V}}, x_{\mathcal{V},n}), \quad (9.8)$$

where  $\delta(x_{\mathcal{V}}, x_{\mathcal{V},n})$  is one if its arguments are equal and zero otherwise.

We can also define “marginal counts”—the counts associated with subsets of nodes. For any given subset  $C$ , let  $m(x_C)$  denote the number of times that configuration  $x_C$  is observed in the data set. This is obtained by computing:

$$m(x_C) \triangleq \sum_{x_{\mathcal{V} \setminus C}} m(x_{\mathcal{V}}), \quad (9.9)$$

which can be viewed as a “marginalization” operation.

As an example, suppose that  $\mathcal{V} = \{1, 2, 3\}$ . In this case,  $m(x_{\mathcal{V}})$  can be represented as a three-dimensional table. Suppose that the parent of  $X_2$  is  $X_1$ . To compute the marginal count  $m(x_1, x_2)$ , we sum over  $x_3$ :

$$m(x_1, x_2) = \sum_{x_3} m(x_1, x_2, x_3), \quad (9.10)$$

which is a two-dimensional table. To compute the marginal count  $m(x_1)$ , a one-dimensional table, we sum over  $x_2$  and  $x_3$ :

$$m(x_1) = \sum_{x_2, x_3} m(x_1, x_2, x_3) = \sum_{x_2} m(x_1, x_2). \quad (9.11)$$

Note also that if we sum over all three variables we obtain the scalar  $N$ , the total number of observations.

A particular subset of interest is the subset consisting of a node  $u$  and its parents  $\pi_u$ —the *family* associated with node  $u$ . Letting  $\phi_u \triangleq \{u\} \cup \pi_u$  denote this family, we have:

$$m(x_{\phi_u}) \triangleq \sum_{x_{\mathcal{V} \setminus \phi_u}} m(x_{\mathcal{V}}). \quad (9.12)$$

That is,  $m(x_{\phi_u})$  is the count of the number of times a node  $u$  takes on a specific value and its parents  $\pi_u$  take on a specific configuration. Study the expression under the summation sign carefully. We are taking the sum over all nodes in  $\mathcal{V}$  other than  $u$  and its parents  $\pi_u$ .

### The joint probability

Let us turn to the representation of the joint probability distribution in the discrete case. We begin by discussing the tabular case, in which a separate parameter is associated with each possible joint configuration of a node and its parents. In particular, we define the parameter vector  $\theta_v(x_{\phi_v})$  to be a nonnegative, multidimensional table indexed by the joint configuration of  $v$  and  $\pi_v$ . The normalization condition requires:

$$\sum_{x_v} \theta_v(x_{\phi_v}) = \sum_{x_v} \theta_v(x_v, x_{\pi_v}) = 1, \quad (9.13)$$

where we recall that  $\phi_v \triangleq \{v\} \cup \pi_v$  is the family associated with node  $v$ .

Given such a normalized table we define:

$$p(x_v | x_{\pi(v)}, \theta_v) \triangleq \theta_v(x_{\phi_v}) \quad (9.14)$$

as the local conditional probability of node  $v$ . This is a generic tabular representation that places no constraints on the local conditional probabilities beyond the normalization constraint.

Taking the product over  $v$ , we obtain the joint probability distribution:

$$p(x_{\mathcal{V}} | \theta) = \prod_v p(x_v | x_{\pi_v}, \theta_v) \quad (9.15)$$

$$= \prod_v \theta_v(x_{\phi_v}), \quad (9.16)$$

as a product of (normalized) potentials.

We take a further product over  $n$  to obtain the total probability of an IID data set  $\mathcal{D} = (x_{\mathcal{V},1}, x_{\mathcal{V},2}, \dots, x_{\mathcal{V},N})$ . At this point, however, we can make our results look neater if we recognize

that some of the observations have the same value. These observations necessarily have the same probability, and thus it is helpful to group them explicitly. To do this, we make use of a trick that should be familiar from our earlier work with the multinomial distribution:

$$p(x_{\mathcal{V},n} | \theta) = \prod_{x_{\mathcal{V}}} p(x_{\mathcal{V}} | \theta)^{\delta(x_{\mathcal{V}}, x_{\mathcal{V},n})}. \quad (9.17)$$

Here the dummy variable  $x_{\mathcal{V}}$  ranges across configurations of the nodes rather than across data points. Using this representation we write the joint probability as follows, working in the log domain for convenience:

$$\log p(\mathcal{D} | \theta) = \log \left( \prod_n p(x_{\mathcal{V},n} | \theta) \right) \quad (9.18)$$

$$= \sum_n \log \left( \prod_{x_{\mathcal{V}}} p(x_{\mathcal{V}} | \theta)^{\delta(x_{\mathcal{V}}, x_{\mathcal{V},n})} \right) \quad (9.19)$$

$$= \sum_n \sum_{x_{\mathcal{V}}} \delta(x_{\mathcal{V}}, x_{\mathcal{V},n}) \log p(x_{\mathcal{V}} | \theta) \quad (9.20)$$

$$= \sum_{x_{\mathcal{V}}} m(x_{\mathcal{V}}) \log p(x_{\mathcal{V}} | \theta). \quad (9.21)$$

Note that the sum over  $n$  has disappeared; we have in essence reduced our representation of joint probability from a function on the graph  $\mathcal{G}^{(N)}$  to a function on the graph  $\mathcal{G}$ . Continuing the derivation, we have:

$$\log p(\mathcal{D} | \theta) = \sum_{x_{\mathcal{V}}} m(x_{\mathcal{V}}) \log p(x_{\mathcal{V}} | \theta) \quad (9.22)$$

$$= \sum_{x_{\mathcal{V}}} m(x_{\mathcal{V}}) \log \left( \prod_v \theta_v(x_{\phi_v}) \right) \quad (9.23)$$

$$= \sum_{x_{\mathcal{V}}} m(x_{\mathcal{V}}) \sum_v \log \theta_v(x_{\phi_v}) \quad (9.24)$$

$$= \sum_v \sum_{x_{\phi_v}} \sum_{x_{\mathcal{V} \setminus \phi_v}} m(x_{\mathcal{V}}) \log \theta_v(x_{\phi_v}) \quad (9.25)$$

$$= \sum_v \sum_{x_{\phi_v}} \left( \sum_{x_{\mathcal{V} \setminus \phi_v}} m(x_{\mathcal{V}}) \right) \log \theta_v(x_{\phi_v}) \quad (9.26)$$

$$= \sum_v \sum_{x_{\phi_v}} m(x_{\phi_v}) \log \theta_v(x_{\phi_v}). \quad (9.27)$$

This result expresses the logarithm of the joint probability as a sum of terms defined on the families  $\{\phi_v\}$ .

Taking the exponential of both sides of Eq. (9.27), we see that we have an exponential family distribution for  $\mathcal{D}$ , with  $m(x_{\phi_v})$  as the sufficient statistics and  $\log \theta_v(x_{\phi_v})$  as the natural parameters.

Note also the decoupling discussed earlier. The parameters  $\theta_v(x_{\phi_v})$  appear in separate terms which can be optimized independently of each other. In particular, to estimate  $\theta_v(x_{\phi_v})$ , we maximize  $m(x_{\phi_v}) \log \theta_v(x_{\phi_v})$  with respect to  $\theta_v(x_{\phi_v})$ . Adding a Lagrangian term to handle the normalization constraint in Eq. (9.13), we obtain (see Exercise ??):

$$\hat{\theta}_{v,ML}(x_{\phi_v}) = \frac{m(x_{\phi_v})}{m(x_{\pi_v})} = \frac{m(x_v, x_{\pi_v})}{m(x_{\pi_v})}. \quad (9.28)$$

The result has an intuitively-appealing form—the maximum likelihood estimate is the ratio of the count of the number of times a node and its parents are jointly in a specific configuration to the count of the number of times its parents are in that configuration. These estimates are formed independently at each of the nodes in the graph.

Tabular representations are useful for graphs with small families, but quickly become unwieldy when the number of parents grows (the size of a table is exponential in the number of parents). For large families we generally wish to constrain  $p(x_v | x_{\pi_v}, \theta_v)$  in some way. The generalized linear models (GLIMs) studied in Chapter 8 provide one example of such a constrained representation. Moreover, for GLIMs we have an efficient algorithm—the IRLS algorithm—for obtaining parameter estimates. The decoupling of the log likelihood implies that if each local conditional model is a GLIM model, then we solve the maximum likelihood problem for the graph as a whole by running the IRLS algorithm separately at each node.

In general, in the case of completely observed data, any solution to the problem of estimating parameters at a single node (conditional on its parents) applies immediately to general directed graphs.

### 9.3 Undirected models

Undirected models are in certain respects more flexible than their directed counterparts. Whereas in directed models the potentials are restricted to conditional distributions that model the dependence of a variable on its parents, potentials in undirected models are unnormalized functions defined on arbitrary subsets of nodes. In domains such as vision and information retrieval, which involve large collections of variables that do not necessarily have a natural ordering, undirected models are often the preferred choice.

Such flexibility comes at a cost, however. In particular, undirected graphical models require an explicit global normalization factor—the  $1/Z$  factor in the definition of the joint probability. This global normalization factor couples the parameters and complicates the parameter estimation problem. There is, however, a special class of undirected models—the decomposable models—for which the parameter estimation problem decouples, despite the presence of the global normalization factor. For general undirected models the problem does not decouple, but, nonetheless, effective parameter estimation algorithms that exploit the structure of the graph are available. We describe some of the basic alternatives in this section, and treat the topic of parameter estimation for undirected models in more detail in Chapter 19.

Much of the notation for undirected models transfers over without change from the directed setting. Let  $\mathcal{G}(\mathcal{V}, \mathcal{E})$  be an undirected graph, where  $\mathcal{V}$  is the set of nodes and  $\mathcal{E}$  the set of edges of

the graph. We again associate a random vector  $X_{\mathcal{V}}$  with the graph and refer to random vectors associated with subsets of the nodes using the notation  $X_C$ , for  $C \subseteq \mathcal{V}$ . When the observed data are IID replicates, we again use a second index for the replicates. Thus  $X_{C,n}$  denotes the  $n$ th replicate of the subset  $C$ , and the observed data are denoted:

$$\mathcal{D} = (x_{\mathcal{V},1}, x_{\mathcal{V},2}, \dots, x_{\mathcal{V},N}), \quad (9.29)$$

where the index  $\mathcal{V}$  reflects our focus on complete data.

We parameterize an undirected graphical model via a set of clique potentials  $\psi_C(x_C)$ , for  $C \in \mathcal{C}$ , where  $\mathcal{C}$  is a set of cliques. Note that we do not necessarily assume that  $\mathcal{C}$  contains all of the cliques in the graph, nor that the cliques in  $\mathcal{C}$  are maximal. Given such a set of clique potentials, we define the joint probability,  $p(x_{\mathcal{V}} | \theta)$ , as follows:

$$p(x_{\mathcal{V}} | \theta) = \frac{1}{Z} \prod_C \psi_C(x_C), \quad (9.30)$$

where  $\theta = \{\psi_C(x_C), C \in \mathcal{C}\}$  is the collection of parameters, and where  $Z$  is the normalization factor:

$$Z = \sum_{x_{\mathcal{V}}} \prod_C \psi_C(x_C), \quad (9.31)$$

obtained by summing (or integrating in the continuous case) over all configurations  $x_{\mathcal{V}}$ .

### 9.3.1 Discrete models

In order to simplify our discussion we specialize to discrete random variables for the remainder of this section (see Chapter 19 for a discussion of continuous-valued undirected models).

Recall our notation for counts. The number of times that configuration  $x_{\mathcal{V}}$  is observed in a dataset  $\mathcal{D}$  is represented as follows:

$$m(x_{\mathcal{V}}) \triangleq \sum_n \delta(x_{\mathcal{V}}, x_{\mathcal{V},n}), \quad (9.32)$$

and

$$m(x_C) \triangleq \sum_{x_{\mathcal{V} \setminus C}} m(x_{\mathcal{V}}) \quad (9.33)$$

is the marginal count for clique  $C$ . Note in particular that

$$N = \sum_{x_{\mathcal{V}}} m(x_{\mathcal{V}}) \quad (9.34)$$

is the total number of observations.

To express the log likelihood in terms of counts (the sufficient statistics for discrete models) we proceed as in the directed case, introducing the dummy variable  $x_{\mathcal{V}}$ :

$$p(x_{\mathcal{V},n} | \theta) = \prod_{x_{\mathcal{V}}} p(x_{\mathcal{V}} | \theta)^{\delta(x_{\mathcal{V}}, x_{\mathcal{V},n})}, \quad (9.35)$$

and writing the probability of the observed data as follows:

$$p(\mathcal{D} | \theta) = \prod_n p(x_{\mathcal{V},n} | \theta) \quad (9.36)$$

$$= \prod_n \prod_{x_{\mathcal{V}}} p(x_{\mathcal{V}} | \theta)^{\delta(x_{\mathcal{V}}, x_{\mathcal{V},n})}. \quad (9.37)$$

This trick allows us to write the log likelihood in terms of the marginal counts:

$$l(\theta; \mathcal{D}) = \log p(\mathcal{D} | \theta) \quad (9.38)$$

$$= \sum_n \sum_{x_{\mathcal{V}}} \delta(x_{\mathcal{V}}, x_{\mathcal{V},n}) \log p(x_{\mathcal{V}} | \theta) \quad (9.39)$$

$$= \sum_{x_{\mathcal{V}}} m(x_{\mathcal{V}}) \log p(x_{\mathcal{V}} | \theta) \quad (9.40)$$

$$= \sum_{x_{\mathcal{V}}} m(x_{\mathcal{V}}) \log \left( \frac{1}{Z} \prod_C \psi_C(x_C) \right) \quad (9.41)$$

$$= \sum_{x_{\mathcal{V}}} m(x_{\mathcal{V}}) \sum_C \log \psi_C(x_C) - \sum_{x_{\mathcal{V}}} m(x_{\mathcal{V}}) \log Z \quad (9.42)$$

$$= \sum_C \sum_{x_C} m(x_C) \log \psi_C(x_C) - N \log Z \quad (9.43)$$

We see that the marginal counts  $m(x_C)$ , for  $C \in \mathcal{C}$ , are the sufficient statistics for our model. This is reminiscent of the directed case, where the cliques  $\mathcal{C}$  were the families  $\{\phi_v\}$ . Note, however, an important difference between the undirected log likelihood and its directed counterpart—the appearance of the term  $N \log Z$ .

### 9.3.2 Maximum likelihood estimation

To find maximum likelihood estimates we take derivatives of the log likelihood and set to zero. Unfortunately, due to the  $N \log Z$  term, such a calculation yields a coupled, nonlinear set of equations in which the parameters appear implicitly. It is not obvious how (in general) to solve these equations to obtain explicit estimates for the parameters. All is not lost, however; the implicit equations do reveal an interesting local property of the maximum likelihood estimates. Moreover, as we discuss in Section 9.3.4, this property provides the inspiration for an iterative algorithm for finding the parameter estimates.

Let us thus proceed to calculating the derivatives. In these calculations note that  $\psi_C(x_C)$  is the independent variable, where both the clique  $C$  and the configuration  $x_C$  have been fixed (in the discrete case, this picks out the cell indexed by  $x_C$  in the table representing the potential function on clique  $C$ ).

The derivative of the first term in the log likelihood, Eq. (9.43), with respect to  $\psi_C(x_C)$  is obtained immediately; it is equal to  $m(x_C)/\psi_C(x_C)$ . We turn to  $\log Z$ :

$$\frac{\partial \log Z}{\partial \psi_C(x_C)} = \frac{1}{Z} \frac{\partial}{\partial \psi_C(x_C)} \left( \sum_{\tilde{x}} \prod_D \psi_D(\tilde{x}_D) \right) \quad (9.44)$$

$$= \frac{1}{Z} \sum_{\tilde{x}} \delta(\tilde{x}_C, x_C) \frac{\partial}{\partial \psi_C(x_C)} \left( \prod_D \psi_D(\tilde{x}_D) \right) \quad (9.45)$$

$$= \frac{1}{Z} \sum_{\tilde{x}} \delta(\tilde{x}_C, x_C) \prod_{D \neq C} \psi_D(\tilde{x}_D) \quad (9.46)$$

$$= \sum_{\tilde{x}} \delta(\tilde{x}_C, x_C) \frac{1}{\psi_C(\tilde{x}_C)} \frac{1}{Z} \prod_D \psi_D(\tilde{x}_D) \quad (9.47)$$

$$= \frac{1}{\psi_C(x_C)} \sum_{\tilde{x}} \delta(\tilde{x}_C, x_C) p(\tilde{x}) \quad (9.48)$$

$$= \frac{p(x_C)}{\psi_C(x_C)}, \quad (9.49)$$

where we have dropped the explicit reference to  $\theta$  in our notation. With this result in hand, we obtain the derivative of the log likelihood:

$$\frac{\partial l}{\partial \psi_C(x_C)} = \frac{m(x_C)}{\psi_C(x_C)} - N \frac{p(x_C)}{\psi_C(x_C)}, \quad (9.50)$$

where we can assume without loss of generality that  $\psi_C(x_C) > 0$  (see Exercise ??).

Setting Eq. (9.50) equal to zero, we obtain:

$$\hat{p}_{ML}(x_C) = \frac{1}{N} m(x_C). \quad (9.51)$$

Defining the *empirical distribution*  $\tilde{p}(x) \triangleq m(x)/N$ , so that  $\tilde{p}(x_C) \triangleq m(x_C)/N$  is a marginal under the empirical distribution, we can rewrite the result as:

$$\hat{p}_{ML}(x_C) = \tilde{p}(x_C). \quad (9.52)$$

Thus we have the following important characterization of maximum likelihood estimates—for each clique  $C \in \mathcal{C}$ , the model marginals must be equal to the empirical marginals.

While this result constrains maximum likelihood models, it leaves us somewhat short of our goal. How do we find maximum likelihood estimates of the *parameters*? Eq. (9.52) provides us with a system of equations (by ranging over all  $C \in \mathcal{C}$ ) that constrains the maximum likelihood estimates, but the parameters  $\psi_C(x_C)$  themselves appear implicitly in these equations.

It turns out that for some graphs, in particular for a special class of graphs known as *decomposable graphs*, the situation is rather benign. Indeed, for these graphs, the maximum likelihood estimation problem decouples, and we can write down maximum likelihood estimates by inspection.

### 9.3.3 Decomposable models

Consider the example shown in Figure 9.3, a Markov chain on  $\{X_1, X_2, X_3\}$ . The probability model can be written as:

$$p(x_V) = \frac{1}{Z} \psi_{12}(x_1, x_2) \psi_{23}(x_2, x_3) \quad (9.53)$$

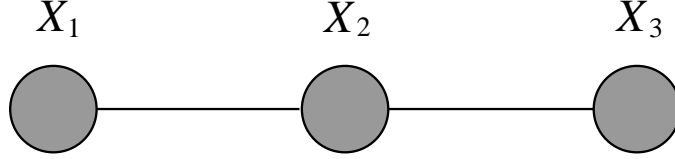


Figure 9.3: A Markov chain.

and the sufficient statistics under IID sampling are the empirical marginals  $\tilde{p}(x_1, x_2)$  and  $\tilde{p}(x_2, x_3)$ .

For a model to be a maximum likelihood model, we require the marginals to equal the empirical marginals. How do we set the parameters so as to achieve this result?

Let us make the following guess:

$$\hat{p}_{ML}(x_1, x_2, x_3) = \frac{\tilde{p}(x_1, x_2)\tilde{p}(x_2, x_3)}{\tilde{p}(x_2)}, \quad (9.54)$$

where  $\tilde{p}(x_2) = \sum_{x_1} \tilde{p}(x_1, x_2) = \sum_{x_3} \tilde{p}(x_2, x_3)$ . That this is a good guess is readily verified:

$$\hat{p}_{ML}(x_1, x_2) = \sum_{x_3} \hat{p}_{ML}(x_1, x_2, x_3) = \tilde{p}(x_1, x_2) \quad (9.55)$$

$$\hat{p}_{ML}(x_2, x_3) = \sum_{x_1} \hat{p}_{ML}(x_1, x_2, x_3) = \tilde{p}(x_2, x_3), \quad (9.56)$$

and we see that the model marginals are indeed equal to the empirical marginals on the cliques  $\mathcal{C}$ .

Moreover, we can also easily match the terms in the guessed distribution to the parameters. For example, we can let:

$$\hat{\psi}_{12,ML}(x_1, x_2) = \tilde{p}(x_1, x_2) \quad (9.57)$$

and

$$\hat{\psi}_{23,ML}(x_2, x_3) = \frac{\tilde{p}(x_2, x_3)}{\tilde{p}(x_2)}, \quad (9.58)$$

which together imply that  $Z = 1$ . There are obviously many other sets of parameter estimates that yield the same joint distribution; these are all maximum likelihood estimates.

That this approach cannot work in general, however, is shown by the graph in Figure 9.4(a). As we invite the reader to verify in Exercise ??, the analogous ratio of the empirical marginals does not yield a maximum likelihood distribution in this case.

The problem is not simply due to an inability to handle graphs with loops. This can be seen by considering Figure 9.4(b). Here the reader can verify that the guess:

$$\hat{p}_{ML}(x_1, x_2, x_3, x_4) = \frac{\tilde{p}(x_1, x_2, x_3)\tilde{p}(x_2, x_3, x_4)}{\tilde{p}(x_2, x_3)} \quad (9.59)$$

fits the empirical marginals correctly.

There is a subtlety in this latter case, however. To recover parameter estimates from the factored form in Eq. (9.59) we need to have potentials that have the appropriate arguments. That

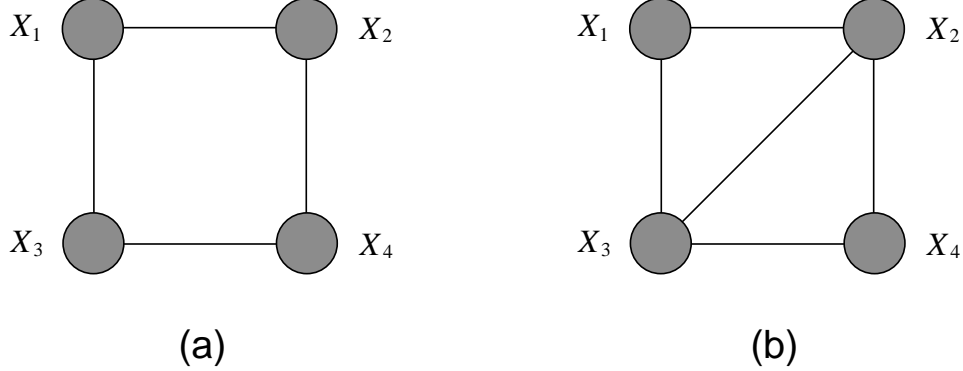


Figure 9.4: (a) A non-decomposable graph. (b) A decomposable graph.

is, in the case of Figure 9.4(b) we require that the model contain potentials  $\psi_{123}(x_1, x_2, x_3)$  and  $\psi_{234}(x_2, x_3, x_4)$ . If the graph is parameterized with potentials that only refer to proper subsets of the maximal cliques, for example, pairwise potentials, then the guess in Eq. (9.59) is not in fact a maximum likelihood distribution because it is not in our model family.

In the remainder of this section, we briefly discuss the underlying concept that makes it possible to write maximum likelihood estimates by inspection in some cases but not in others. We will be brief because an understanding of this concept—that of a decomposable graph—requires additional machinery that we will not have in hand until Chapter 17. For completeness, however, let us define decomposability, and provide a recipe for constructing maximum likelihood estimates for decomposable graphs.

A graph is said to be *decomposable* if it can be recursively subdivided into disjoint sets  $A$ ,  $B$  and  $S$ , where  $S$  separates  $A$  and  $B$ , and where  $S$  is complete.

The graph in Figure 9.3 is decomposable with  $A = X_1$ ,  $B = X_3$  and  $S = X_2$ . Similarly, the graph in Figure 9.4(b) is decomposable with  $A = X_1$ ,  $B = X_4$  and  $S = \{X_2, X_3\}$ . The reader can verify that the Figure 9.4(a) is not decomposable.

We can find maximum likelihood estimates for decomposable graphs by inspection, but only if the potentials are defined on maximal cliques. That is, our parameterization must be such that the set  $\mathcal{C}$  ranges over the maximal cliques in the graph. Given this constraint, the recipe is the following:

- for every clique  $C$ , set the clique potential to the empirical marginal for that clique,
- for every non-empty intersection between cliques, associate an empirical marginal with that intersection, and divide that empirical marginal into the potential of one of the two cliques that form the intersection.

For example, for the graph in Figure 9.3, this recipe leads immediately to the estimates given in Eq. (9.57) and Eq. (9.58).

We have barely scratched the surface of the decomposability concept, but we hope to have piqued the reader's interest. To get a further hint of what is to come (in Chapter 17), note that

there is another way to describe the differences between the graphs in Figures 9.3, 9.4(a), and 9.4(b): Only for Figure 9.4(a) is it impossible to eliminate the nodes in the graph without adding extra edges to the graph. This suggests a relationship between decomposability and graph elimination, and suggests (rightly) that decomposability lies with elimination at the core of the relationship between graphs and probabilities.

We now turn to an alternative algorithm for finding maximum likelihood estimates in all undirected graphs, whether decomposable and nondecomposable. In the decomposable case the algorithm turns out to converge in a finite number of iterations, updating each potential once. Indeed, in this case, the algorithm essentially implements the recipe for decomposable graphs that we described above. Thus the algorithm can be viewed as a general solution to the maximum likelihood estimation problem that takes advantage of the decomposable structure in the problem if it is present.

### 9.3.4 Iterative proportional fitting

A common strategy for solving systems of implicit equations is to “iterate,” hoping that the iterations converge to a “fixed point”—a set of values that solve the original implicit equations. *Iterative proportional fitting (IPF)*, an algorithm for maximum likelihood estimation in undirected models, can be viewed as an example of such a strategy. However, it is also possible to say something stronger about IPF. In general, the iteration of fixed-point equations does not necessarily yield a convergent algorithm; moreover, even if the iteration converges, it is not necessarily the case that the algorithm behaves well in the sense of ascending an objective function at each step. IPF, however, *does* converge, and *does* behave well—the log likelihood is guaranteed to increase or remain the same after each IPF update. The facts about IPF follow from the fact that it is not only a fixed-point algorithm, but that it is also a *coordinate ascent algorithm*.

We begin with a simple, heuristic justification of IPF in terms of fixed-point iteration, and present the more satisfying justification in terms of coordinate ascent later in this section.

To develop an iterative approach to maximum likelihood estimation for undirected models, let us return to the gradient of the log likelihood, but retain the  $\psi_C(x_C)$  factors. From Eq. (9.50) we have:

$$\frac{\tilde{p}(x_C)}{\psi_C(x_C)} = \frac{p(x_C)}{\psi_C(x_C)}, \quad (9.60)$$

where  $\tilde{p}(x_C) \triangleq m(x_C)/N$  is the empirical marginal. Note that the parameter  $\psi_C(x_C)$  appears explicitly in this equation in two places, but also appears implicitly in the marginal  $p(x_C)$ . We can obtain an iterative algorithm by holding the values of  $\psi_C(x_C)$  fixed on the right-hand side of the equation, both in the numerator and the denominator, and solving for the free parameter  $\psi_C(x_C)$  on the left-hand side.

In particular, let us denote the set of parameter estimates at iteration  $t$  by  $\psi_C^{(t)}(x_C)$ . Let  $p^{(t)}(x)$  denote the joint probability distribution based on these parameter estimates. Rearranging Eq. (9.60), we define the following update for  $\psi_C(x_C)$ :

$$\psi_C^{(t+1)}(x_C) = \psi_C^{(t)}(x_C) \frac{\tilde{p}(x_C)}{p^{(t)}(x_C)}, \quad (9.61)$$

which is the IPF algorithm. The IPF algorithm cycles through all of the cliques  $C \in \mathcal{C}$ , applying Eq. (9.61) to each clique in turn; such a cycle constitutes a single iteration of the algorithm.

Before providing an interpretation of IPF in terms of coordinate ascent, let us explore some of the properties of the algorithm.

### Properties of the IPF update equation

The IPF update equation in Eq. (9.61) has two interesting properties: (1) the marginal  $p^{(t+1)}(x_C)$  is equal to the empirical marginal  $\tilde{p}(x_C)$ , and (2) the normalization factor  $Z$  remains constant across IPF updates.

To establish these properties, let us calculate the marginal probability of  $x_C$  for the updated distribution:

$$p^{(t+1)}(x_C) = \sum_{x_{\mathcal{V} \setminus C}} p^{(t+1)}(x) \quad (9.62)$$

$$= \sum_{x_{\mathcal{V} \setminus C}} \frac{1}{Z^{(t+1)}} \prod_D \psi_D^{(t+1)}(x_D) \quad (9.63)$$

$$= \frac{1}{Z^{(t+1)}} \sum_{x_{\mathcal{V} \setminus C}} \psi_C^{(t+1)}(x_C) \prod_{D \neq C} \psi_D^{(t)}(x_D) \quad (9.64)$$

$$= \frac{1}{Z^{(t+1)}} \sum_{x_{\mathcal{V} \setminus C}} \psi_C^{(t)}(x_C) \frac{\tilde{p}(x_C)}{p^{(t)}(x_C)} \prod_{D \neq C} \psi_D^{(t)}(x_D) \quad (9.65)$$

$$= \frac{Z^{(t)}}{Z^{(t+1)}} \frac{\tilde{p}(x_C)}{p^{(t)}(x_C)} \sum_{x_{\mathcal{V} \setminus C}} \frac{1}{Z^{(t)}} \prod_D \psi_D^{(t)}(x_D) \quad (9.66)$$

$$= \frac{Z^{(t)}}{Z^{(t+1)}} \frac{\tilde{p}(x_C)}{p^{(t)}(x_C)} \sum_{x_{\mathcal{V} \setminus C}} p^{(t)}(x) \quad (9.67)$$

$$= \frac{Z^{(t)}}{Z^{(t+1)}} \frac{\tilde{p}(x_C)}{p^{(t)}(x_C)} p^{(t)}(x_C) \quad (9.68)$$

$$= \frac{Z^{(t)}}{Z^{(t+1)}} \tilde{p}(x_C). \quad (9.69)$$

Note that  $\tilde{p}(x_C)$  is a proportion and is therefore normalized, and  $p^{(t+1)}(x_C)$  is normalized because we have divided explicitly by  $Z^{(t+1)}$ . Thus, summing both sides of our result with respect to  $x_C$ , we have:

$$Z^{(t+1)} = Z^{(t)}. \quad (9.70)$$

We see that the normalization factor  $Z$  indeed remains constant across IPF updates. Moreover, now that we know that the factor  $Z^{(t)}/Z^{(t+1)}$  is equal to one, we see that we have also derived property (1):

$$p^{(t+1)}(x_C) = \tilde{p}(x_C). \quad (9.71)$$

That is, IPF finds a distribution such that the marginal with respect to the variables  $x_C$  is equal to the empirical marginal  $\tilde{p}(x_C)$ .

This interpretation of IPF accords well with the characterization of the maximum likelihood estimates that we gave in Section 9.3.2. We saw that for the maximum likelihood model, the model marginals are equal to the empirical marginals, for all  $C \in \mathcal{C}$ . IPF works toward the goal of equal model and empirical marginals, by equating a single model marginal and empirical marginal at a time.

The fact that the normalization factor  $Z$  stays constant across IPF iterations has another interesting consequence. As we ask the reader to verify (Exercise ??), the constancy of  $Z$  implies that we can write IPF in terms of joint probabilities:

$$p^{(t+1)}(x_{\mathcal{V}}) = p^{(t)}(x_{\mathcal{V}}) \frac{\tilde{p}(x_C)}{p^{(t)}(x_C)}, \quad (9.72)$$

and indeed this is how IPF is often defined.<sup>1</sup> From this equation, we immediately obtain:

$$p^{(t+1)}(x_{\mathcal{V}}) = p^{(t)}(x_{\mathcal{V} \setminus C} | x_C) \tilde{p}(x_C), \quad (9.73)$$

which provides an interpretation of an IPF iteration as retaining the “old” conditional probability  $p^{(t)}(x_{\mathcal{V} \setminus C} | x_C)$ , while replacing the “old” marginal probability  $p^{(t)}(x_C)$  with the “new” marginal  $\tilde{p}(x_C)$ .

### IPF as coordinate ascent

Let us now derive IPF as a coordinate ascent algorithm. A “coordinate” in this setting is a potential function.

To derive a coordinate ascent algorithm, we take the derivative of the log likelihood with respect to the “coordinate”  $\psi_C(x_C)$ , for fixed  $C$  and varying  $x_C$ , and solve for the maximizing values of these parameters while holding the remaining potentials fixed. To carry out this calculation, let us return to the calculation of the gradient in Section 9.3.2, pausing the derivation in midstream. From Eq. (9.46) we have:

$$\frac{\partial l}{\partial \psi_C(x_C)} = \frac{m(x_C)}{\psi_C(x_C)} - \frac{N}{Z} \sum_{\tilde{x}} \delta(\tilde{x}_C, x_C) \prod_{D \neq C} \psi_D(\tilde{x}_D). \quad (9.74)$$

Let us take some care here—the parameter  $\psi_C(x_C)$  on the right-hand side of this equation is a *variable* whose maximizing value we wish to solve for, where the remaining parameters  $\psi_D(\tilde{x}_D)$  are being held fixed. Adding superscripts to the latter to reflect the fact that they are being held fixed at iteration  $t$  of our algorithm, the gradient of the log likelihood becomes:

$$\frac{\partial l}{\partial \psi_C(x_C)} = \frac{m(x_C)}{\psi_C(x_C)} - \frac{N}{Z} \sum_{\tilde{x}} \delta(\tilde{x}_C, x_C) \prod_{D \neq C} \psi_D^{(t)}(\tilde{x}_D). \quad (9.75)$$

---

<sup>1</sup>Treating Eq. (9.72) as a definition of the IPF algorithm leaves open the actual implementation of an IPF step in terms of the structural components of the model, and we view Eq. (9.61) as the better definition.

If we were to multiply and divide the second term by the “old” parameter value  $\psi_C^{(t)}(\tilde{x}_C)$ , the sum would appear to reduce to the marginal  $p^{(t)}(x_C)$  much as in our earlier derivation. Setting to zero would yield the IPF update. However, we must not forget that  $Z$  also depends on  $\psi_C(x_C)$ . As  $\psi_C(x_C)$  varies,  $Z$  varies, and in general the varying value of  $Z$  is *not* the correct normalization for the *old* values of the parameters.

We have seen, however, that for a particular value of  $\psi_C(x_C)$ , namely  $\psi_C^{(t+1)}(x_C)$  as defined by the IPF update, we have  $Z^{(t+1)} = Z^{(t)}$ , which *is* the correct normalization for the old values of the parameters. Taking advantage of this fact, we obtain the following value of the derivative of log likelihood, where we now evaluate the derivative at  $\psi_C^{(t+1)}(x_C)$ :

$$\frac{\partial l}{\partial \psi_C(x_C)} = \frac{m(x_C)}{\psi_C^{(t+1)}(x_C)} - \frac{N}{Z^{(t+1)}} \sum_{\tilde{x}} \delta(\tilde{x}_C, x_C) \prod_{D \neq C} \psi_D^{(t)}(\tilde{x}_D) \quad (9.76)$$

$$= \frac{m(x_C)}{\psi_C^{(t+1)}(x_C)} - \frac{N}{Z^{(t)}} \sum_{\tilde{x}} \delta(\tilde{x}_C, x_C) \prod_{D \neq C} \psi_D^{(t)}(\tilde{x}_D) \quad (9.77)$$

$$= \frac{m(x_C)}{\psi_C^{(t+1)}(x_C)} - \frac{N}{\psi^{(t)}(x_C)} \sum_{\tilde{x}} \delta(\tilde{x}_C, x_C) \frac{1}{Z^{(t)}} \prod_D \psi_D^{(t)}(\tilde{x}_D) \quad (9.78)$$

$$= \frac{m(x_C)}{\psi_C^{(t+1)}(x_C)} - \frac{N}{\psi^{(t)}(x_C)} p^{(t)}(x_C), \quad (9.79)$$

and we see that the IPF update equation:

$$\psi_C^{(t+1)}(x_C) = \psi^{(t)}(x_C) \frac{\tilde{p}(x_C)}{p^{(t)}(x_C)} \quad (9.80)$$

does indeed set the gradient of the log likelihood to zero, and thus is a coordinate ascent step.

### View from the KL divergence

We have shown that the IPF algorithm is coordinate ascent in the log likelihood. A somewhat more elegant derivation of this result can be obtained via the KL divergence.

The KL divergence has a useful decomposition that reflects the decomposition of a joint distribution into the product of a marginal and a conditional. In particular, writing  $p(x_A, x_B) = p(x_B | x_A)p(x_A)$ , and  $q(x_A, x_B) = q(x_B | x_A)q(x_A)$ , we have:

$$D(p(x_A, x_B) \| q(x_A, x_B)) = D(p(x_A) \| q(x_A)) + \sum_{x_A} p(x_A) D(p(x_B | x_A) \| q(x_B | x_A)). \quad (9.81)$$

(This result is derived in Appendix XXX).

Recall that the problem of maximizing the likelihood is equivalent to that of minimizing the following KL divergence:

$$D(\tilde{p}(x) \| p(x | \theta)) = \sum_x \tilde{p}(x) \log \frac{\tilde{p}(x)}{p(x | \theta)}, \quad (9.82)$$

where  $\tilde{p}(x)$  is the empirical distribution. (The reason that these problems are equivalent is because the (negative) log likelihood and the KL divergence differ by the term  $\sum_x \tilde{p}(x) \log \tilde{p}(x)$ , which is independent of  $\theta$ ).

Thus we wish to perform coordinate descent in  $D(\tilde{p}(x) \parallel p(x | \theta))$ . That is, we pick a clique  $C$  and adjust the clique potential  $\psi_C(x_C)$  so as to minimize the KL divergence. Applying Eq. (9.81), we have:

$$D(\tilde{p}(x) \parallel p(x | \theta)) = D(\tilde{p}(x_C) \parallel p(x_C | \theta)) + \sum_{x_C} \tilde{p}(x_C) D(\tilde{p}(x_{\mathcal{V} \setminus C} | x_C) \parallel p(x_{\mathcal{V} \setminus C} | x_C, \theta)). \quad (9.83)$$

Changes to the clique potential  $\psi_C(x_C)$  have no effect on the conditional distribution  $p(x_{\mathcal{V} \setminus C} | x_C, \theta)$ .<sup>2</sup> Thus, the second term in Eq. (9.83) is unaltered by changes to  $\psi_C(x_C)$ , and minimizing the KL divergence reduces to minimizing the first term. This term is minimized by setting the marginal  $p(x_C | \theta)$  equal to the empirical marginal  $\tilde{p}(x_C)$ . But this is exactly what an IPF update achieves. Thus IPF is coordinate descent in  $D(\tilde{p}(x) \parallel p(x | \theta))$  or, equivalently, coordinate ascent in the log likelihood.

### 9.3.5 Gradient ascent

An alternative to IPF is to perform gradient ascent on the log likelihood. In this case, given that the gradient is evaluated only at the current value of the parameters, no subtleties arise.

Evaluating the gradient at  $\psi_C^{(t)}(x_C)$ , we have:

$$\frac{\partial l}{\partial \psi_C(x_C)} = \frac{m(x_C)}{\psi_C^{(t)}(x_C)} - \frac{N}{\psi^{(t)}(x_C)} p^{(t)}(x_C), \quad (9.84)$$

which leads to the following gradient ascent algorithm:

$$\psi_C^{(t+1)}(x_C) = \psi_C^{(t)}(x_C) + \frac{\rho}{\psi_C^{(t)}(x_C)} \left( \tilde{p}(x_C) - p^{(t)}(x_C) \right), \quad (9.85)$$

where  $\rho$  is a step size. We see that the difference between the empirical marginals and the model marginals drives the algorithm.

Gradient ascent has the advantage compared to IPF that all of the parameters can be adjusted simultaneously, although we will present a variant of IPF in Chapter 19 that also allows parameters to be adjusted simultaneously, so this advantage is somewhat diminished. Disadvantages of the gradient ascent approach include the need to choose a step size, and, even more seriously, the fact that the normalization factor  $Z$  does not remain constant, but must be recalculated anew after each iteration.

---

<sup>2</sup>This is proved by simply writing out the conditional distribution and noting that  $\psi_C(x_C)$  cancels in the numerator and denominator; see Exercise ?? for details.

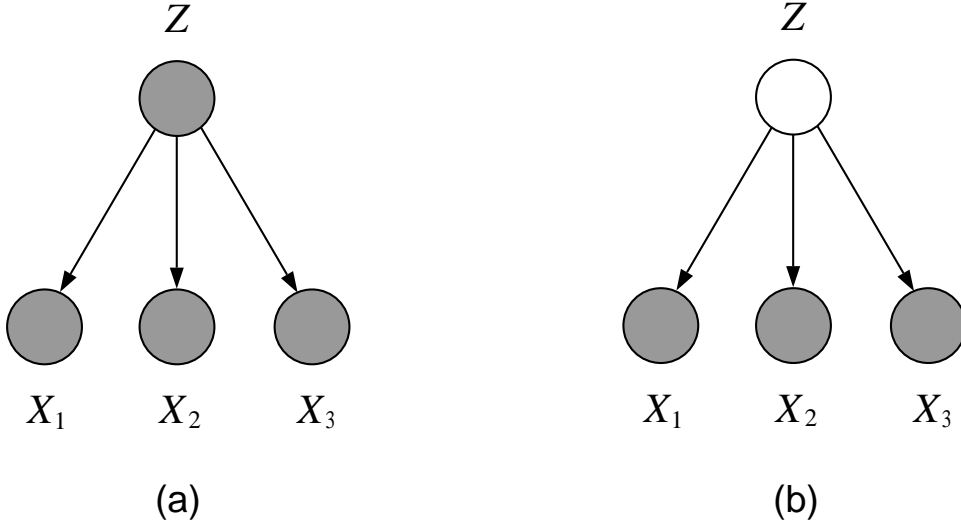


Figure 9.5: (a) The nodes  $X_i$  are conditionally independent given  $Z$ . (b) When  $Z$  is latent the variables  $X_i$  are no longer independent and this implies that the parameters are coupled in the log likelihood.

## 9.4 Latent variables

The algorithms that we have presented in this chapter all rely on the assumption of complete data. In the setting of complete data the likelihood is a product and the log likelihood is therefore a sum, where each of the parameters appear in different terms. This leads to a decoupling of the parameter estimation problem.

When some of the variables are unobserved, that is, when we have *latent variables*, this happy situation breaks down. When there are latent variables, the likelihood is a marginal probability, obtained by summing or integrating over the latent variables. The log likelihood is the logarithm of this sum, and the logarithm is prevented from moving past the sum to act on the product of potentials. The parameter estimation problem does not decouple.

Consider the graphical model shown in Figure 9.5(a). Here the nodes  $X_i$  are conditionally independent given  $Z$ ; thus, when  $Z$  is observed the log likelihood decouples:

$$l(\theta; x, z) = \log p(x, z | \theta) \quad (9.86)$$

$$= \log [p(z | \theta_z) p(x_1 | z, \theta_1) p(x_2 | z, \theta_2) p(x_3 | z, \theta_3)] \quad (9.87)$$

$$= \log p(z | \theta_z) + \log p(x_1 | z, \theta_1) + \log p(x_2 | z, \theta_2) + \log p(x_3 | z, \theta_3). \quad (9.88)$$

If, on the other hand,  $Z$  is latent, as shown in Figure 9.5(b), the log likelihood does not decouple:

$$l(\theta; x) = \log \sum_z p(x, z | \theta) \quad (9.89)$$

$$= \log \sum_z [p(z | \theta_z) p(x_1 | z, \theta_1) p(x_2 | z, \theta_2) p(x_3 | z, \theta_3)]. \quad (9.90)$$

Adjusting one parameter, say  $\theta_1$ , has an effect on all of the other parameters. This makes good sense probabilistically—our uncertainty about  $Z$  should be reflected in a probabilistic dependence among the variables  $X_i$  and hence among the estimates of the parameters  $\theta_i$ . This coupling is unfortunate from a computational point of view, however, in that it complicates the task of parameter estimation.

In Chapter 11 we present a general procedure for dealing with latent variable problems known as the *Expectation-Maximization (EM)* algorithm. The EM algorithm in essence allows us to treat latent variable problems with complete data tools. In particular, the EM algorithm allows us to solve the maximum likelihood problem for the graph in Figure 9.5(b) by solving a sequence of maximum likelihood problems based on the graph in Figure 9.5(a).

To give the briefest hint of what is involved in the EM algorithm, essentially EM makes use of convexity to move the logarithm past the sum in coupled log likelihoods such as Eq. (9.90). This decouples the problem and allows the complete data tools of the current chapter to be brought into play. Exactly how this is done in general is the story for Chapter 11. In the meantime, in the following chapter we work through a specific example of a latent variable problem, developing a special case of the EM algorithm that is particularly simple and intuitive.

## 9.5 Summary

In the current chapter we have discussed parameter estimation in completely observed graphical models, treating both directed graphs and undirected graphs.

For directed graphs, we saw that the log likelihood decouples into separate terms, one for each parameter, and that the problem of parameter estimation therefore also decouples. Essentially, one collects the sufficient statistics associated with each node and its parents and estimates the parameter vector at that node using those sufficient statistics. This is done independently at each node in the graph. In particular, if the probability model at each node is a generalized linear model, then we can run the IRLS algorithm independently at each node. This is a Newton algorithm on the graph as a whole.

For undirected graphs, we distinguish between decomposable models and nondecomposable models. Decomposable models are the easy case; for decomposable models we can solve for maximum likelihood estimates analytically. We have only briefly outlined the reasons for this in the current chapter; in Chapter 17, we provide a deeper discussion of decomposability, revealing the important relationship between decomposability and the general approach to inference known as the junction tree algorithm. We then return to the problem of parameter estimation in Chapter 20 and nail down the results that we have only sketched here.

For nondecomposable models, we discussed the iterative proportional fitting (IPF) approach to parameter estimation. IPF takes the form of a simple scaling algorithm in which the potentials are multiplied by a ratio of marginal probabilities. We showed that IPF can be viewed as a fixed point algorithm and also as a coordinate ascent algorithm. These themes—iterative algorithms, multiplicative updates of potentials, and coordinate ascent—will appear in several guises in the following chapters, and we will see several IPF-like algorithms as we proceed.

## **9.6 Historical remarks and bibliography**

# An Introduction to Probabilistic Graphical Models

Michael I. Jordan  
*University of California, Berkeley*

June 30, 2003



# Chapter 11

## The EM algorithm

The expectation-maximization (EM) algorithm provides a general approach to the problem of maximum likelihood parameter estimation in statistical models with latent variables. We have already seen two examples of the EM approach at work in the previous chapter. While these examples are revealing ones, it is important to understand that EM applies much more widely. Indeed, the EM approach goes hand-in-glove with general graphical model machinery, taking advantage of the conditional independence structure of graphical models in a systematic way. As such it occupies a central place in the book.

While in principle one can treat ML parameter estimation as a simple matter of passing a likelihood function to a black-box numerical optimization routine, in practice one would like to take advantage of the structure embodied in the model to break the optimization problem into more manageable pieces. EM provides a systematic way to implement such a divide-and-conquer strategy. As we will see, in this chapter and in later chapters, this approach leads to conceptual clarity and simplicity of algorithmic implementation. It also provides a guide to dealing with models in which issues of computational complexity begin to arise. Indeed, EM will provide a guide to dealing with problems in which the mere calculation of the likelihood or its derivatives appear to be intractable computational challenges.

The main goal of this short chapter is to present a general formulation of the EM algorithm. We show that EM is a rather simple optimization algorithm—it is *coordinate ascent* on an appropriately defined function. Thus, both the E step and the M step can be viewed as maximizations in an abstract space. We show how the *expected complete log likelihood* emerges from this perspective; in particular, we show how the maximization operation that defines the E step can also be viewed as an expectation. We also take the coordinate ascent story a bit further, showing that EM can be viewed as an *alternating minimization algorithm*—a special form of coordinate descent in a Kullback-Leibler divergence.

Finally, we sketch how the EM algorithm applies in the general setting of graphical models. Subsequent chapters will provide many examples of applications to graphical models and will fill in the various details appropriate to these special cases.

## 11.1 Latent variables and parameter estimation

Recall that latent or hidden variables are generally introduced into a model in order to simplify the model in some way. We may observe a complex pattern of dependency among a set of variables  $x = (x_1, \dots, x_m)$ . Rather than modeling this dependency directly, via edges linking these variables, we may find it simpler to account for their dependency via “top-down” dependency on a latent variable  $z$ . In the simplest case, we may find it possible to assume that the  $x_i$  are conditionally independent given  $z$ , and thus restrict our model to edges between the node  $z$  and the nodes  $x_i$ .

If the latent variables in the model could be observed, then generally the parameter estimation problem would be simplified as well. Indeed, this is one way of characterizing what we mean by the simplification achieved by introducing latent variables into a model. For example, in the case of the mixture of Gaussians model, if we could observe a class label corresponding to each data point, then we would break the data into classes and estimate the mean and covariance matrix separately for each class. The estimation problem would decouple.

But the latent variables are not observed, and this implies that the likelihood function is a marginal probability, obtained by summing or integrating over the latent variables. Marginalization couples the parameters and tends to obscure the underlying structure in the likelihood function.

The EM algorithm essentially allows us to treat latent variable problems using complete data tools, skirting the fact that the likelihood is a marginal probability and exploiting to the fullest the underlying structure induced by the latent variables. EM is an iterative algorithm, consisting of a linked pair of steps. In the *expectation step (E step)*, the values of the unobserved latent variables are essentially “filled in,” where the filling-in is achieved by calculating the probability of the latent variables, given the observed variables and the current values of the parameters.<sup>1</sup> In the *maximization step (M step)*, the parameters are adjusted based on the filled-in variables, a problem which is essentially no more complex than it would be if the latent variables had been observed.

## 11.2 The general setting

Let  $X$  denote the observable variables, and let  $Z$  denote the latent variables. Often,  $X$  and  $Z$  decompose into sets of independent, identically-distributed (IID) pairs, in particular  $X$  can often be written as  $X = (X_1, X_2, \dots, X_N)$ , where the  $X_i$  are IID variables and the observed data,  $x = (x_1, x_2, \dots, x_N)$ , are the observed values of  $X$ . We do not need to make this assumption, however, and indeed we will see many non-IID examples in later chapters. Thus,  $X$  represents the totality of observable variables and  $x$  is the entire observed dataset. Similarly  $Z$  represents the set of all latent variables. The probability model is  $p(x, z | \theta)$ .

If  $Z$  could be observed, then the ML estimation problem would amount to maximizing the quantity:

$$l_c(\theta; x, z) \triangleq \log p(x, z | \theta), \quad (11.1)$$

---

<sup>1</sup>We will see that a better way to express this is that in the E step we compute certain expected sufficient statistics, which in the case of multinomial variables reduces to computing the probability of the latent variables. But let us stick with the intuitive and picturesque language of “filling-in” for now.

which is referred to in the context of the EM algorithm as the *complete log likelihood*. If the probability  $p(x, z | \theta)$  factors in some way, such that separate components of  $\theta$  occur in separate factors, then the operation of the logarithm has the effect of separating the likelihood into terms that can be maximized independently. As we discussed in Chapter 9, this is what we generally mean by “decoupling” the estimation problem.

Given that  $Z$  is not in fact observed, the probability of the data  $x$  is a marginal probability, and the log likelihood (referred to in this context as the *incomplete log likelihood*) takes the following form:

$$l(\theta; x) = \log p(x | \theta) = \log \sum_z p(x, z | \theta), \quad (11.2)$$

where here as in the rest of the chapter we utilize summation to stand for marginalization—the derivation goes through without change if we integrate over continuous  $z$ . The logarithm on the right-hand side is separated from  $p(x, z | \theta)$  by the summation sign, and the problem does not decouple. It is not clear how to exploit the conditional independence structure that may be present in the probability model.

Let us not give up the hope of working with the complete log likelihood. Given that  $Z$  is not observed, the complete log likelihood is a random quantity, and cannot be maximized directly. But suppose we average over  $z$  to remove the randomness, using an “averaging distribution”  $q(z | x)$ . That is, let us define the *expected complete log likelihood*:

$$\langle l_c(\theta; x, z) \rangle_q \triangleq \sum_z q(z | x, \theta) \log p(x, z | \theta), \quad (11.3)$$

a quantity that is a deterministic function of  $\theta$ . Note that the expected complete log likelihood is linear in the complete log likelihood and thus should inherit its favorable computational properties. Moreover, if  $q$  is chosen well, then perhaps the expected complete log likelihood will not be too far from the log likelihood and can serve as an effective surrogate for the log likelihood. While we cannot hope that maximizing this surrogate will yield a value of  $\theta$  that maximizes the likelihood, perhaps it will represent an improvement from an initial value of  $\theta$ . If so then we can iterate the process and hill-climb. This is the basic idea behind the EM algorithm.

We begin the derivation of the EM algorithm by showing that an averaging distribution  $q(z | x)$  can be used to provide a lower bound on the log likelihood. Consider the following line of argument:

$$l(\theta; x) = \log p(x | \theta) \quad (11.4)$$

$$= \log \sum_z p(x, z | \theta) \quad (11.5)$$

$$= \log \sum_z q(z | x) \frac{p(x, z | \theta)}{q(z | x)} \quad (11.6)$$

$$\geq \sum_z q(z | x) \log \frac{p(x, z | \theta)}{q(z | x)} \quad (11.7)$$

$$\triangleq \mathcal{L}(q, \theta), \quad (11.8)$$

where the last line defines the function  $\mathcal{L}(q, \theta)$ , a function that we will refer to as an *auxiliary function*.<sup>2</sup> In Eq. 11.7 we have used Jensen’s inequality, a simple consequence of the concavity of the logarithm function (see Appendix XXX). What we have shown is that—for an arbitrary distribution  $q(z|x)$ —the auxiliary function  $\mathcal{L}(q, \theta)$  is a lower bound for the log likelihood.

The EM algorithm is a coordinate ascent algorithm on the function  $\mathcal{L}(q, \theta)$ . At the  $(t+1)$ st iteration, we first maximize  $\mathcal{L}(q, \theta^{(t)})$  with respect to  $q$ . For this optimizing choice of averaging distribution  $q^{(t+1)}$ , we then maximize  $\mathcal{L}(q^{(t+1)}, \theta)$  with respect to  $\theta$ , which yields the updated value  $\theta^{(t+1)}$ . Giving these steps their traditional names, we have:

$$\text{(E step)} \quad q^{(t+1)} = \arg \max_q \mathcal{L}(q, \theta^{(t)}) \quad (11.9)$$

$$\text{(M step)} \quad \theta^{(t+1)} = \arg \max_{\theta} \mathcal{L}(q^{(t+1)}, \theta). \quad (11.10)$$

We will soon explain why the first step can be referred to as an “expectation step.” We will also explain how a procedure based on maximizing a lower bound on the likelihood  $l(\theta; x)$  can maximize the likelihood itself.

The first important point to note is that the M step is equivalently viewed as the maximization of the expected complete log likelihood. To see this, note that the lower bound  $\mathcal{L}(q, \theta)$  breaks into two terms:

$$\mathcal{L}(q, \theta) = \sum_z q(z|x) \log \frac{p(x, z|\theta)}{q(z|x)} \quad (11.11)$$

$$= \sum_z q(z|x) \log p(x, z|\theta) - \sum_z q(z|x) \log q(z|x) \quad (11.12)$$

$$= \langle l_c(\theta; x, z) \rangle_q - \sum_z q(z|x) \log q(z|x), \quad (11.13)$$

and that the second term is independent of  $\theta$ . Thus, maximizing  $\mathcal{L}(q, \theta)$  with respect to  $\theta$  is equivalent to maximizing  $\langle l_c(\theta; x, z) \rangle_q$  with respect to  $\theta$ .

Let us now consider the E step, the maximization of  $\mathcal{L}(q, \theta^{(t)})$  with respect to the averaging distribution  $q$ . This maximization problem can be solved once and for all; indeed, we can verify that the choice  $q^{(t+1)}(z|x) = p(z|x, \theta^{(t)})$  yields the maximum. To see this, evaluate  $\mathcal{L}(q, \theta^{(t)})$  for this choice of  $q$ :

$$\mathcal{L}(p(z|x, \theta^{(t)}), \theta^{(t)}) = \sum_z p(z|x, \theta^{(t)}) \log \frac{p(x, z|\theta)}{p(z|x, \theta^{(t)})} \quad (11.14)$$

$$= \sum_z p(z|x, \theta^{(t)}) \log p(x|\theta^{(t)}) \quad (11.15)$$

$$= \log p(x|\theta^{(t)}) \quad (11.16)$$

$$= l(\theta^{(t)}; x). \quad (11.17)$$

Given that  $l(\theta; x)$  is an upper bound for  $\mathcal{L}(q, \theta^{(t)})$ , this shows that  $\mathcal{L}(q, \theta^{(t)})$  is maximized by setting  $q(z|x)$  equal to  $p(z|x, \theta^{(t)})$ .

---

<sup>2</sup>Note that  $\mathcal{L}(q, \theta)$  is a function of  $x$  as well. We omit this dependence, however, to lighten the notation.

There is slightly different way to show this result. We first show that the difference between  $l(\theta; x)$  and  $\mathcal{L}(q, \theta)$  is a Kullback-Leibler (KL) divergence:

$$l(\theta; x) - \mathcal{L}(q, \theta) = l(\theta; x) - \sum_z q(z|x) \log \frac{p(x, z|\theta)}{q(z|x)} \quad (11.18)$$

$$= \sum_z q(z|x) \log p(x|\theta) - \sum_z q(z|x) \log \frac{p(x, z|\theta)}{q(z|x)} \quad (11.19)$$

$$= \sum_z q(z|x) \log p(x|\theta) - \log \frac{q(z|x)}{p(z|x, \theta)} \quad (11.20)$$

$$= D(q(z|x) \| p(z|x, \theta)). \quad (11.21)$$

In Appendix XXX we show that the KL divergence is nonnegative (a simple consequence of Jensen's inequality), and that the KL divergence is uniquely minimized by letting  $q(z|x)$  equal  $p(z|x, \theta^{(t)})$ . Since minimizing the difference between  $l(\theta; x)$  and  $\mathcal{L}(q, \theta)$  is equivalent to maximizing  $\mathcal{L}(q, \theta)$ , we again have our result.

The conditional distribution  $p(z|x, \theta^{(t)})$  is an intuitively appealing choice of averaging distribution. Given the model  $p(x, z|\theta^{(t)})$ , a link between the observed data and the latent variables, the conditional  $p(z|x, \theta^{(t)})$  is our "best guess" as to the values of the latent variables, conditioned on the data  $x$ . What the EM algorithm does is to use this "best guess" distribution to calculate an expectation of the complete log likelihood. The M step then maximizes this expected complete log likelihood with respect to the parameters to yield new values  $\theta^{(t+1)}$ . We then presumably have an improved model, and we can now make a "better guess"  $p(z|x, \theta^{(t+1)})$ , which is used as the averaging distribution in a subsequent EM iteration.

What is the effect of an EM iteration on the log likelihood  $l(\theta; x)$ ? In the M step, we choose the parameters so as to increase a lower bound on the likelihood. Increasing a lower bound on a function does not necessarily increase the function itself, if there is a gap between the function and the bound. In the E step, however, we have closed the gap by an appropriate choice of the  $q$  distribution. That is, we have:

$$l(\theta^{(t)}; x) = \mathcal{L}(q^{(t+1)}, \theta^{(t)}), \quad (11.22)$$

by Eq. 11.17, and thus an M-step increase in  $\mathcal{L}(q^{(t+1)}, \theta)$  will also increase  $l(\theta; x)$ .

In summary, we have shown that the EM algorithm is a hill-climbing algorithm in the log likelihood  $l(\theta; x)$ . The algorithm achieves this hill-climbing behavior indirectly, by coordinate ascent in the auxiliary function  $\mathcal{L}(q, \theta)$ . The advantage of working with the latter function is that it involves maximization of the expected complete log likelihood rather than the log likelihood itself, and, as we have seen in examples, this is often a substantial simplification.

### 11.3 EM and alternating minimization

We can put our results in a slightly more elegant form by working with KL divergences rather than likelihoods.

Recall that in Chapter 8 we noted a simple equivalence between maximization of the likelihood and minimization of the KL divergence between the empirical distribution and the model. Let us return to that equivalence, and bound the KL divergence rather than the log likelihood. We have:

$$D(\tilde{p}(x) \parallel p(x|\theta)) = -\sum_x \tilde{p}(x) \log p(x|\theta) + \sum_x \tilde{p}(x) \log \tilde{p}(x) \quad (11.23)$$

$$\leq -\sum_x \tilde{p}(x) \mathcal{L}(q, \theta) + \sum_x \tilde{p}(x) \log \tilde{p}(x) \quad (11.24)$$

$$= -\sum_x \tilde{p}(x) \sum_z q(z|x) \log \frac{p(x, z|\theta)}{q(z|x)} + \sum_x \tilde{p}(x) \log \tilde{p}(x) \quad (11.25)$$

$$= \sum_x \tilde{p}(x) \sum_z q(z|x) \log \frac{\tilde{p}(x)q(z|x)}{p(x, z|\theta)} \quad (11.26)$$

$$= D(\tilde{p}(x)q(z|x) \parallel p(x, z|\theta)). \quad (11.27)$$

We see that the KL divergence between the empirical distribution and the model—the quantity that we wish to minimize—is upper bounded by a “complete KL divergence,” a KL divergence between joint distributions on  $(x, z)$ .

The term  $\sum_x \tilde{p}(x) \log \tilde{p}(x)$  is independent of  $q$  and  $\theta$  and its inclusion in the problem therefore does not change any of our previous results. In particular, minimizing the complete KL divergence with respect to  $q$  and  $\theta$  is equivalent to maximizing the auxiliary function  $\mathcal{L}(q, \theta)$  with respect to these variables. We can therefore reformulate the EM algorithm in terms of the KL divergence. Defining  $D(q \parallel \theta) \triangleq D(\tilde{p}(x)q(z|x) \parallel p(x, z|\theta))$  as a convenient shorthand, we have:

$$(\text{E step}) \quad q^{(t+1)}(z|x) = \arg \min_q D(q \parallel \theta^{(t)}) \quad (11.28)$$

$$(\text{M step}) \quad \theta^{(t+1)} = \arg \min_{\theta} D(q^{(t+1)} \parallel \theta) \quad (11.29)$$

We see that EM is a special kind of coordinate descent algorithm—an *alternating minimization* algorithm. We alternate between minimizing over the arguments of a KL divergence.

The alternating minimization perspective and the auxiliary function perspective are essentially the same, and the choice between the two is largely a matter of taste. We will see, however, in Chapter 19, that the alternating minimization view allows us to provide a geometric interpretation of EM as a sequence of projections between manifolds—a perspective reminiscent of our presentation of the LMS algorithm in Chapter 6.

## 11.4 EM, sufficient statistics and graphical models

[Section not yet written.]

## 11.5 Historical remarks and bibliography

# An Introduction to Probabilistic Graphical Models

Michael I. Jordan  
*University of California, Berkeley*

June 30, 2003



## Chapter 10

# Mixtures and conditional mixtures

In this chapter we begin the study of models with *latent* or *hidden* variables. Latent variables are simply random variables whose values are not specified in the observed data—in the graphical model formalism these variables are the unshaded nodes. Our focus in the current chapter is the simple case of latent variables that can take one of a finite set of values.

Let us take a moment to pose the question of why would one include a node in a model if the value of that node cannot be observed in the data. Shouldn’t we include variables in our model only if their values can be observed? One answer to this question is philosophical—surely much human knowledge involves explaining observed data in terms of unobserved concepts.<sup>1</sup> For example, we often introduce *distinctions* into our reasoning in order to simplify relationships between observables. Thus a doctor may group patients into those with a certain “syndrome” and those without, and this grouping may make it easier to understand the relationships between observed symptoms. A biologist may wish to group animals into distinct species, because it may be easier to explain behavioral or physiological patterns within each species than to explain such patterns without the help of the distinction. Although such distinctions may exist only in the mind of the doctor or biologist, at least at the outset, their utility for modeling the data may provide the motivation for further study in which one tries to uncover a “real” physical or biological interpretation of the distinction.

Viewing a “distinction” as a discrete random variable ranging over a finite, unordered set of values leads to the mixture models studied in the current chapter.

In Chapter ?? we study continuous latent variable models in which the latent variable parameterizes a  $k$ -dimensional subspace of the  $d$ -dimensional input space; here the latent variable achieves a “dimensionality reduction.” Chapter 12 and Chapter 15 discuss models in which latent variables are used in the time series setting to summarize past data; that is, the latent variables are “state variables.” In all of these cases, and in others that we will meet, the general idea is the same—models with latent variables can often be simpler than models without latent variables. In statistical terms we often find that we can get by with fewer parameters using a latent variable model, or we can avail ourselves of simple parametric distributions that have advantageous com-

---

<sup>1</sup>One should not, however, expect the philosophers to have agreed on this. Indeed, the philosophical school of *logical positivism* explicitly denied the meaningfulness of using unobservable concepts in scientific reasoning.

putational or analytical properties. We will not attempt to define “simplicity” more rigorously for now—that is the task of Chapter 26. Instead we proceed by example, describing latent variable models that have been shown to be useful in practice.

In this chapter we discuss two kinds of models based on discrete latent variables—*unconditional mixture models* and *conditional mixture models*. Roughly speaking, unconditional mixture models are used to solve density estimation problems, whereas conditional mixture models are used to solve regression and classification problems. One useful perspective to take on the latent variable methodology in both of these kinds of problems is that it allows us to break problems into subproblems. Thus, in unconditional mixture modeling, for each value of the latent variable we obtain a (presumably simpler) density estimation subproblem. In conditional mixture modeling, for each value of the latent variable we obtain a (presumably simpler) regression or classification subproblem. In general, mixture modeling can be viewed as a “divide-and-conquer” approach to statistical modeling.

## 10.1 Unconditional mixture models

We begin by discussing unconditional mixture models. While regression and classification models require the observation of  $(X, Y)$  pairs, unconditional mixture models make do with observations of  $X$  alone.

As we discussed in Chapter 5, mixture models can be used to solve density estimation problems, allowing us to answer questions about whether query vectors are “typical” or “untypical.” This has many applications, including the detection of outliers and the design of algorithms for data compression. Note that in such applications we are not necessarily interested in identifying or interpreting the structure of the probability distribution generating the data; rather we are simply interested in a flexible model that allows us to obtain a good estimate of the probability density.

In other problems, however, we may have a more “structural” interest in the mixture model. In particular, as we discussed in Chapter 5, we may wish to take the point of view that there are “subpopulations” underlying the data. In this setting, mixture modeling is closely linked to classification, in particular to the generative classification models discussed in Chapter 7. Indeed, treating the class label of a generative classification model as a latent variable converts the model into a mixture model. Reserving the term *classification* for the setting in which the labels are in fact observed, we use the term *clustering* for the problem of inferring the labels of data points when such labels are absent in the data. Mixture models provide a popular and widely used methodology for clustering.

In Chapter 5 we presented the following general formulation of an unconditional mixture model (see Figure 10.1). Let  $Z$  represent a multinomial random variable with components  $Z^i$ . We have:

$$p(x | \theta) = \sum_i p(Z^i = 1 | \pi_i) p(x | Z^i = 1, \theta_i) \quad (10.1)$$

$$= \sum_i \pi_i p(x | Z^i = 1, \theta_i). \quad (10.2)$$

where  $\theta = (\pi_1, \dots, \pi_K, \theta_1, \dots, \theta_K)$  and where the  $\pi_i$  are constrained to sum to one. Recall the



Figure 10.1: A mixture model represented as a graphical model. The latent variable  $Z$  is a multinomial node taking on one of  $K$  values.

terminology—the parameters  $\pi_i$  are referred to as *mixing proportions* and the densities  $p(x | Z^i = 1, \theta_i)$  are referred to as *mixture components*.

### 10.1.1 Gaussian mixture models

Let us begin by discussing the important special case of the Gaussian mixture model. In this model the mixture components are Gaussian distributions with parameters  $\theta_i \triangleq (\mu_i, \Sigma_i)$ . Note that we allow the covariance to vary across the mixture components. One can also consider models in which the covariance matrices are constrained to be equal.

From Eq. (10.2) we obtain the following probability model for a Gaussian mixture:

$$p(x | \theta) = \sum_i \pi_i \frac{1}{(2\pi)^{m/2} |\Sigma_i|^{1/2}} \exp \left\{ -\frac{1}{2} (x - \mu_i)^T \Sigma_i^{-1} (x - \mu_i) \right\}. \quad (10.3)$$

We will also write this as:

$$p(x | \theta) = \sum_i \pi_i \mathcal{N}(x | \mu_i, \Sigma_i) \quad (10.4)$$

to simplify notation.

Figure 10.2 shows a simple illustration of a Gaussian mixture model, together with a sample from the marginal distribution.

Let us calculate the probability of the latent variable  $Z$  conditioned on the observed variable  $X$ . This calculation is of obvious interest if we wish to use the mixture model in the clustering setting—the conditional probability of  $Z$  can be used to assign  $X$  to one of the clusters. We will also find that this conditional probability plays an important role in parameter estimation.

We let  $\tau^i$  denote the conditional probability that the  $i$ th component of  $Z$  is equal to one. From Bayes rule we have:

$$\tau^i \triangleq p(Z^i = 1 | x, \theta) \quad (10.5)$$

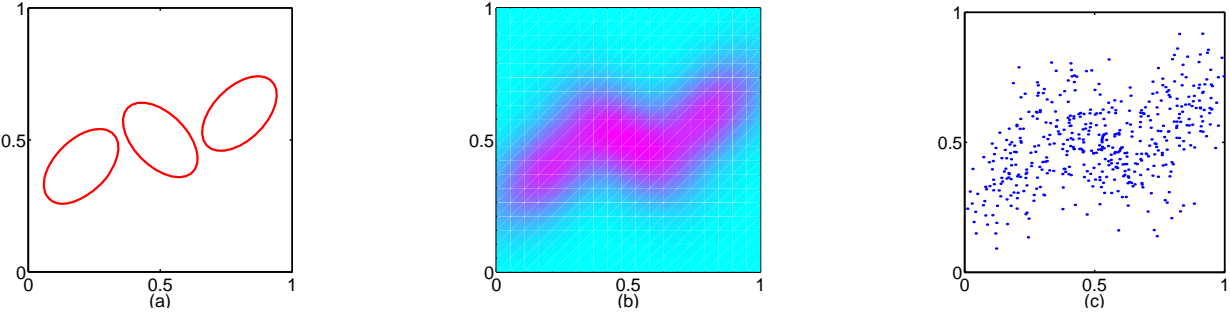


Figure 10.2: Illustration of a mixture of 3 Gaussians in a two-dimensional space showing (a) contours representing one standard deviation for each of the mixture components, (b) the marginal probability density of the mixture distribution, and (c) a sample of 500 points drawn from the marginal distribution.

$$= \frac{p(x | Z^i = 1, \theta_i)p(Z^i = 1 | \pi_i)}{p(x | \theta)} \quad (10.6)$$

$$= \frac{\pi_i \mathcal{N}(x, \mu_i | \Sigma_i)}{\sum_j \pi_j \mathcal{N}(x, \mu_j | \Sigma_j)} \quad (10.7)$$

Note the relationship to the generative classification models of Section 7.2. In particular, if we let the  $\Sigma_k$  be equal, then the quadratic terms cancel and we obtain the linear-softmax function as in that section.

It is common to refer to  $\pi_i$  as a “prior probability” and  $\tau^i$  as a “posterior probability.” This is a convenient terminology that reflects the fact that these probabilities are linked via Bayes rule. Please note, however, that the use of this terminology is unrelated to whether or not we use Bayesian methods to estimate the parameters  $\theta$ . Indeed, in this chapter our focus will be maximum likelihood estimation.

Let us now consider the problem of estimating  $\theta$  from an IID set of observations  $\mathcal{D} = \{x_n : n = 1, \dots, N\}$ . The model is shown in Figure 10.3, where we see that each data point  $x_n$  is accompanied by a multinomial latent variable  $Z_n$  that represents the “assignment” of  $x_n$  to one of the mixture components. We form the log likelihood:

$$l(\theta | \mathcal{D}) = \sum_n \log p(x_n | \theta) \quad (10.8)$$

$$= \sum_n \log \sum_i \pi_i \mathcal{N}(x_n | \mu_i, \Sigma_i) \quad (10.9)$$

by taking the log of the product of  $N$  copies of the probability model in Eq. (10.3). Note the disconcerting fact that the logarithm stops in front of the sum. In all of the models that we have considered up until now, the logarithm acted directly on the basic probability distributions in our model, which, given the exponential family distributions that we have worked with, yielded simple expressions such as squared error or cross entropy. Here the likelihood is a marginal probability.

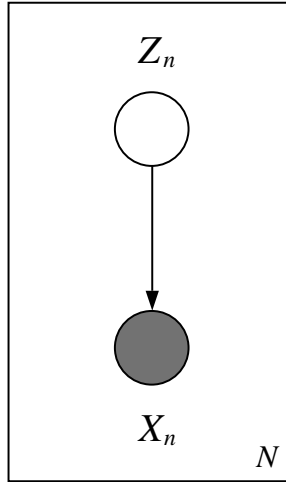


Figure 10.3: The mixture model under an IID sampling assumption.

This prevents the logarithm from acting directly on the component probability distributions and leaves us with a tangled nonlinear function to maximize.

One approach to maximizing this likelihood is to hand Eq. (10.9) to a nonlinear optimization algorithm such as conjugate gradient or Newton-Raphson. In Appendix XXX we provide some details regarding this approach. Our main focus, however, will be on an alternative approach to maximizing the likelihood known as the Expectation-Maximization (EM) algorithm. This algorithm is applicable far beyond the Gaussian mixture setting; indeed, it is applicable to arbitrary graphical models with latent variables. Its important virtue in the graphical model setting is that it allows us to take full advantage of the graphical structure underlying the likelihood; in particular, we will be able to exploit the inference algorithms discussed in Chapter 3 and Chapter 17. By relating the problem of parameter estimation and the problem of efficient inference, the EM algorithm brings together two of our major themes. It will play an important role throughout the book.

In this chapter we provide a heuristic introduction to the EM algorithm for Gaussian mixture models. Chapter 11 provides a rigorous derivation of EM, not only for Gaussian mixture models, but for the general case.

### 10.1.2 The K-means algorithm

To motivate the EM algorithm for Gaussian mixtures, it is useful to step briefly outside of the Gaussian mixture framework to consider an even simpler approach to clustering.

Recall that we have a set of observations  $\mathcal{D} = \{x_n : n = 1, \dots, N\}$ . Our goal is to group the data points into a set of  $K$  clusters, where we suppose that the value of  $K$  is given.

The *K-means algorithm* represents each cluster with a single vector, which we refer to as a “cluster mean.” The basic idea is to assign data points to clusters by finding the nearest cluster mean and assigning the data point to that cluster.

Note that we do not have a probabilistic model in mind, so “cluster mean” is perhaps a poor

terminology. “Cluster centroid” is better; the idea is that if we knew which data points were assigned to the  $i$ th cluster, then the cluster mean would be the centroid (the sample average) of those data points.

We are faced with a “chicken-and-egg” problem—if we knew the assignments we could find the means, or if we knew the means we could find the assignments. The basic idea of the  $K$ -means algorithm is to make an initial guess for one of these quantities (the means) and iterate back and forth.

The algorithm maintains two kinds of variables—means and assignments. Let  $\mu_i$  denote the cluster mean for the  $i$ th cluster. For each data point  $x_n$  let  $z_n$  be an indicator vector that represents the assignment of  $x_n$  to one of the clusters. Thus, if the  $x_n$  is assigned to the  $i$ th cluster, we set the component  $z_n^i$  equal to one, and all other components of  $z_n$  equal to zero.

The  $K$ -means algorithm begins by making some initial assignments for the  $\mu_i$ , for example taking the  $\mu_i$  to be given by a subset of the data vectors themselves. The algorithm then alternates between two phases. In the first phase, values for the indicator variables  $z_n^i$  are evaluated by assigning each data point  $x_n$  to the closest mean  $\mu_i$  (where distance is typically measured using a simple Euclidean metric) so that, for each  $n$ ,

$$z_n^i = \begin{cases} 1 & \text{if } i = \arg \min_j \|x_n - \mu_j\|^2 \\ 0 & \text{otherwise.} \end{cases} \quad (10.10)$$

In the second phase, the values of the means are recomputed by taking  $\mu_i$  to be equal to the sample mean of those vectors  $x_n$  which have been assigned to the  $i^{\text{th}}$  cluster:

$$\mu_i = \frac{\sum_n z_n^i x_n}{\sum_n z_n^i}. \quad (10.11)$$

The two phases of re-assigning data points to clusters and re-computing the cluster means are repeated in turn until there is no further change in the assignments (or until some maximum number of iterations is exceeded). It is easily seen that the  $K$ -means algorithm must converge after a finite number of iterations, since there are only a finite number of possible assignments for the set of discrete variables  $z_n^i$  and for each such assignment there is a unique value for the  $\{\mu_i\}$ .

Although we have motivated the  $K$ -means algorithm heuristically, the algorithm can also be motivated as the solution to an optimization problem. In particular, it turns out that the algorithm can be viewed as minimizing the *distortion measure* given by:

$$J = \sum_{n=1}^N \sum_{i=1}^K z_n^i \|x_n - \mu_i\|^2. \quad (10.12)$$

As we ask the reader to show in Exercise ??, Eq. (10.10) is obtained by minimizing  $J$  with respect to  $z_n^i$  while keeping  $\mu_i$  fixed, while Eq. (10.11) is obtained by minimizing  $J$  with respect to  $\mu_i$  while keeping  $z_n^i$  fixed. Thus  $K$ -means can be viewed as a *coordinate descent* algorithm.

The  $K$ -means algorithm is illustrated using a simple example in Figure 10.4. The data set, shown in plot (a), consists of 40 data points in two dimensions. We now apply the  $K$ -means algorithm, with  $K = 2$ , using the initial mean vectors shown as the red and blue crosses in plot (b).

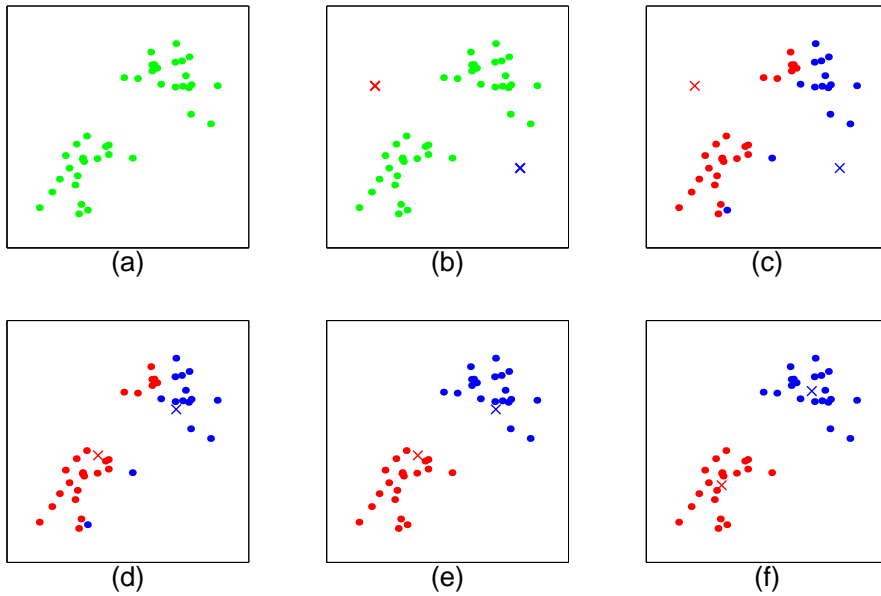


Figure 10.4: Illustration of the  $K$ -means algorithm. See the text for a full discussion.

Note that this is in fact a particularly poor initialization and has been chosen in order to provide a clear illustration of the operation of the algorithm. A better initialization would involve selecting random data points as the initial means, and would typically give faster convergence. The first stage of the algorithm involves assigning each data point to one of the two clusters according to its distance to each of the means. This results in the partitioning of the data set shown in plot (c), in which each data point has been colored according to the cluster (red or blue) to which it is assigned. Next we re-compute the mean vectors using the current partitioning, so that the blue mean is reassigned to the mean of the blue-colored data points, and similarly for the red mean, giving the new estimates for the means shown in plot (d). The two phases of the algorithm continue alternately, with repartitioning shown in plot (e), re-assignment in plot (f). On the next re-partitioning the assignment of data points does not change and hence the algorithm has converged.

### 10.1.3 The EM algorithm

Let us return to the probabilistic framework of mixture models. Adopting the language of the  $K$ -means algorithm, let us view the latent variables  $Z_n$  as “assignment variables.” These are random variables in the mixture model setting, reflecting our uncertainty about the cluster assignments.

If the  $Z_n$  were observed we would have a classification problem in which each data point  $X_n$  is assigned a “class label.” The estimate of the mean of the  $i$ th Gaussian would simply be the sample mean for the data points in the  $i$ th class (cf. Eq. (7.20)):

$$\hat{\mu}_i = \frac{\sum_n z_n^i x_n}{\sum_n z_n^i}. \quad (10.13)$$

This is identical to the  $K$ -means update formula, but here we are interpreting the variables  $z_n^i$  not as quantities to be manipulated by our algorithm, but rather as observed values of random variables.

Of course, we do not know the values of the  $Z_n$  variables. Our approach will be to replace these values with their conditional expectations, conditioning on the data (the  $x_n$  values). Recall that we use the notation  $\tau_n^i$  for these conditional expectations.<sup>2</sup> We try the following idea—let us replace  $z_n^i$  by  $\tau_n^i$  in Eq. (10.13):

$$\hat{\mu}_i = \frac{\sum_n \tau_n^i x_n}{\sum_n \tau_n^i}. \quad (10.14)$$

Thus, we have replaced a sample mean with a weighted sample mean. Each data point  $x_n$  contributes to the estimate of the  $i$ th mean in proportion to its posterior probability  $\tau_n^i$ . The quantity  $\tau_n^i$  is often referred to as a “soft assignment,” a natural terminology both from the point of view of Eq. (10.14) and the definition of  $\tau_n^i$  in Eq. (10.7).

We still have a chicken-and-egg problem, however. As seen in Eq. (10.7), the posterior probabilities  $\tau_n^i$  depend on the parameter estimates, which, according to Eq. (10.14), depend on the posterior probabilities.

Once again, the way out of this chicken-and-egg problem is to start with an initial guess (for the parameters) and to iterate. Given a set of parameters we calculate the posterior probabilities. Given a set of posterior probabilities, we compute new parameter estimates. This is the basic structure of the EM algorithm for Gaussian mixtures.

To clarify, let us augment our notation for  $\tau_n^i$  to include reference to the iteration number  $t$ :

$$\tau_n^{i(t)} = \frac{\pi_i^{(t)} \mathcal{N}(x_n | \mu_i^{(t)}, \Sigma_i^{(t)})}{\sum_j \pi_j^{(t)} \mathcal{N}(x_n | \mu_j^{(t)}, \Sigma_j^{(t)})}, \quad (10.15)$$

where we have also indexed the parameter estimates with a superscript to indicate the iteration number. We now define update equations for all of the parameters—the mixing proportions, the means and the covariance matrices. Motivated by the  $K$ -means algorithm we have the following formula for the means:

$$\mu_i^{(t+1)} = \frac{\sum_n \tau_n^{i(t)} x_n}{\sum_n \tau_n^{i(t)}}. \quad (10.16)$$

For the covariance matrices we use an analogous formula:

$$\Sigma_i^{(t+1)} = \frac{\sum_n \tau_n^{i(t)} (x_n - \mu_i^{(t+1)}) (x_n - \mu_i^{(t+1)})^T}{\sum_n \tau_n^{i(t)}}. \quad (10.17)$$

defining the update as a weighted sample covariance, with the posterior probabilities again serving as weights. Finally, viewing  $\tau_n^{i(t)}$  as a “soft assignment” of data point  $x_n$  to cluster  $i$ , it is natural to

---

<sup>2</sup>We use the elementary fact that conditional expectations and conditional probabilities are the same for binary-valued variables:  $E[Z_n^i | x_n] = p(Z_n^i = 1 | x_n)$ .

estimate  $\pi_i$  as the sum of these assignments across the data, divided by the number of data points:

$$\pi_i^{(t+1)} = \frac{1}{N} \sum_n \tau_n^{i(t)}. \quad (10.18)$$

Note that if we sum these estimates  $\pi_i^{(t+1)}$  with respect to  $i$  we obtain one; thus our “soft counting” has not undercounted or overcounted.

Equations 10.15, 10.18, 10.16, and 10.17 define the EM algorithm for Gaussian mixtures.

The first phase of the algorithm—the calculation of the posterior probability in Eq. (10.15)—is generally referred to as the “Expectation step,” or “E step.” The second phase of the algorithm—the parameter updates in Equations 10.18, 10.16, and 10.17—is generally referred to as the “Maximization step,” or “M step.” The explanation for this choice of terminology will be provided in Chapter 11.

In Figure 10.5 we illustrate the EM algorithm applied to a mixture of Gaussians using the same data set, shown in plot (a), as used to illustrate the  $K$ -means algorithm in Figure 10.4. Here a mixture of 2 Gaussians is used, with centers initialized using the same values as for the  $K$ -means algorithm, and with covariance matrices initialized to be proportional to the unit matrix. Contours of 1 standard deviation for each of the Gaussian components are shown in plot (b). In plot (c) we show the result of applying the initial E-step, in which points have been colored according to the posterior probabilities for the two components, such that the color ranges from blue to red as the probability  $P(\text{blue}|x_n)$  ranges from 1 to 0. We see in plot (c) that some points have a significant probability for belonging to either cluster and so appear purple. Plot (d) shows the result of the first M-step. We see that the mean of, say, the blue Gaussian is moved to the mean of the data set, weighted by the probabilities of each data point belonging to the blue cluster, in other words it moves to the mean of the blue ink. Similarly the covariance of the blue Gaussian becomes the sample covariance of the blue ink, with analogous results for the red component. Subsequent plots show the situation after various numbers  $L$  of complete EM cycles. In plot (i) the model is close to the final, converged state. Note that the EM algorithm takes many more iterations to reach (approximate) convergence compared with the  $K$ -means algorithm, and that each cycle requires significantly more computation. It is therefore common to run the  $K$ -means algorithm in order to find a suitable initialization for a Gaussian mixture model which is subsequently adapted using EM. The covariance matrices can conveniently be initialized to the sample covariances of the clusters found by the  $K$ -means algorithm, and the mixing proportions can be set to the fractions of data points assigned to the respective clusters.

#### 10.1.4 Necessary conditions

Although we have defined a simple, intuitively appealing algorithm, it is not yet clear what relationship this algorithm has to the quantity that we are trying to maximize, the log likelihood in Eq. (10.9). In this section and the following section, we take initial steps toward working out this relationship, and in so doing providing a more rigorous justification of the EM algorithm. The full justification will appear in Chapter 11, where we show that the EM algorithm—like the  $K$ -means algorithm—is a form of coordinate ascent.

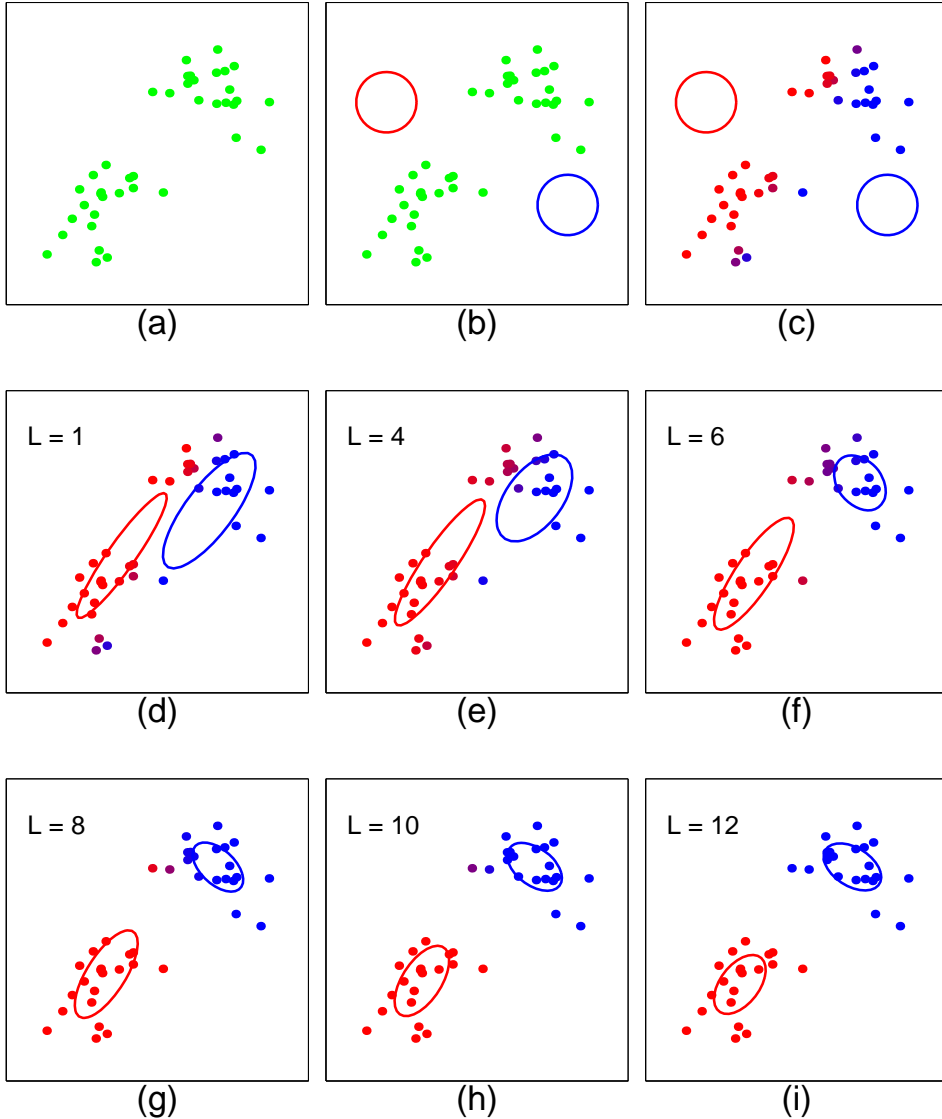


Figure 10.5: Illustration of the EM algorithm using the same data set as used for the illustration of the  $K$ -means algorithm in Figure 10.4. The value of  $L$  denotes the number of complete EM cycles. See the text for a full discussion.

In this section we write down a set of equations characterizing the stationary points of the log likelihood function. We show that the stationary points can be viewed as fixed points of the EM iteration.

We need to obtain the derivatives of  $l$  with respect to the parameters. Let us first take the

derivative with respect to  $\mu_i$ :

$$\frac{\partial l}{\partial \mu_i} = \frac{\partial}{\partial \mu_i} \left\{ \sum_n \log \sum_i \pi_i \mathcal{N}(x_n | \mu_i, \Sigma_i) \right\} \quad (10.19)$$

$$= \sum_n \frac{\pi_i \mathcal{N}(x_n | \mu_i, \Sigma_i)}{\sum_j \pi_j \mathcal{N}(x_n | \mu_j, \Sigma_j)} \frac{\partial}{\partial \mu_i} \log \mathcal{N}(x_n | \mu_i, \Sigma_i) \quad (10.20)$$

$$= \sum_n \tau_n^i \frac{\partial}{\partial \mu_i} \log \mathcal{N}(x_n | \mu_i, \Sigma_i) \quad (10.21)$$

$$= \sum_n \tau_n^i \Sigma_i^{-1} (x_n - \mu_i). \quad (10.22)$$

Setting to zero yields

$$\mu_i = \frac{\sum_{n=1}^N \tau_n^i x_n}{\sum_{n=1}^N \tau_n^i} \quad (10.23)$$

at a stationary point of the log likelihood.

A very similar calculation yields the following conditions for the covariance matrices:

$$\Sigma_i = \frac{\sum_{n=1}^N \tau_n^i (x_n - \mu_i)(x_n - \mu_i)^T}{\sum_{n=1}^N \tau_n^i} \quad (10.24)$$

and the mixing proportions:

$$\pi_i = \frac{1}{N} \sum_{n=1}^N \tau_n^i, \quad (10.25)$$

where in the latter case we use Lagrange multipliers.

These equations do not of course constitute an explicit solution since the posterior probabilities are themselves functions of the parameters, and so Equations 10.25, 10.23 and 10.24 represent a system of coupled, nonlinear equations. We can, however, attempt to solve these equations iteratively. In particular, given a parameter vector  $\theta^{(t)}$ , we plug into the right-hand side of Equations 10.25, 10.23 and 10.24 and obtain an updated parameter vector, which we define to be  $\theta^{(t+1)}$ .

Comparing to Equations 10.16, 10.17, and 10.18, we see that we have derived the EM update equations.

While this derivation of the EM iterations is perhaps preferable to our earlier heuristic arguments, it is still rather heuristic, leaving us with a number of questions regarding convergence. Moreover, the derivation provides us with little insight—the key quantity, the posterior probability  $\tau_n^i$ , emerges somewhat mysteriously from the algebra. To develop a deeper understanding and to apply the EM algorithm to more general graphical models, we will need some new concepts.

### 10.1.5 The expected complete log likelihood

In this section we derive the EM equations for the Gaussian mixture model simply and systematically, by introducing a key player in the EM story—the *expected complete log likelihood*. The full

treatment of the role played by the expected complete log likelihood in the EM algorithm will have to wait for Chapter 11, but we provide some initial intuition in this section, paving the way for the general presentation in Chapter 11.

To introduce the key idea, let us pretend for a moment that we are able to observe the latent variables  $Z_n$ . This is a pretense, but it will turn out to be a useful pretense. In particular, let us define a (fictional) data set  $\mathcal{D}_c = \{(x_n, z_n) : n = 1, \dots, N\}$  that we refer to as the *complete data*.

If we were to actually have such a data set, we would define the following likelihood, which we refer to as the *complete log likelihood*:

$$l_c(\theta | \mathcal{D}_c) = \sum_n \log p(x_n, z_n | \theta) \quad (10.26)$$

$$= \sum_n \log \prod_i [\pi_i \mathcal{N}(x_n | \mu_i, \Sigma_i)]^{z_n^i} \quad (10.27)$$

$$= \sum_n \sum_i z_n^i \log [\pi_i \mathcal{N}(x_n | \mu_i, \Sigma_i)] \quad (10.28)$$

Note the difference between this log likelihood and the original log likelihood for our problem, which we repeat here for convenience:

$$l(\theta | \mathcal{D}) = \sum_n \log \sum_i \pi_i \mathcal{N}(x_n | \mu_i, \Sigma_i). \quad (10.29)$$

In the latter log likelihood, the logarithm is outside of the summation over  $i$ , which, as we have remarked before, reflects the fact that the likelihood is a marginal probability. The complete log likelihood, on the other hand, is not a marginal probability, and thus the logarithm is inside the sum. This logarithm acts on the probabilities  $\pi_i$  and  $\mathcal{N}(x_n | \mu_i, \Sigma_i)$ , leading to the simple maximum likelihood formulas for generative classification that we studied in Chapter 7.

Of course the  $Z_n$  variables are not observed. The next step is the key one—as in our earlier discussion let us treat the values  $z_n$  in the complete log likelihood as random variables  $Z_n$  and take expectations. In calculating these expectations we condition on the observed data  $x_n$ , also fixing a particular parameter vector  $\theta^{(t)}$ . Using the operator notation  $\langle \cdot \rangle_{\theta^{(t)}}$  to denote these conditional expectations, we define an important quantity known as the *expected complete log likelihood*:

$$\langle l_c(\theta | \mathcal{D}_c) \rangle_{\theta^{(t)}} = \left\langle \sum_n \sum_i Z_n^i \log [\pi_i \mathcal{N}(x_n | \mu_i, \Sigma_i)] \right\rangle_{\theta^{(t)}} \quad (10.30)$$

$$= \sum_n \sum_i \langle Z_n^i \rangle_{\theta^{(t)}} \log \{\pi_i \mathcal{N}(x_n | \mu_i, \Sigma_i)\} \quad (10.31)$$

$$= \sum_n \sum_i \tau_n^{i(t)} \log \{\pi_i \mathcal{N}(x_n | \mu_i, \Sigma_i)\} \quad (10.32)$$

Comparing Eq. (10.28) and Eq. (10.32), we see that the expected complete log likelihood is obtained from the complete log likelihood by replacing the fictional “observations”  $z_n^i$  with the posterior probabilities  $\tau_n^i$ , where the latter are evaluated using the parameter vector  $\theta^{(t)}$ .

In general we define the E step of the EM algorithm to be the “calculation of the expected complete log likelihood.” In the Gaussian mixture problem this simply reduces to calculating the posterior probabilities  $\tau_n^i$ , and it may not be clear why we need the fancier language. In problems with multiple latent variables, however, there are generally interactions to account for, and the preferred method for defining the E step in the general setting is to calculate the expected complete log likelihood.

Moreover, the preferred method for obtaining the M step of an EM algorithm is to maximize the expected complete log likelihood with respect to the parameters. We will explain why this is the case in Chapter 11, but in the meantime let us treat it as a recipe and verify that we obtain the M step updates in Equations 10.18, 10.16, and 10.17 from the expected complete log likelihood in Eq. (10.32).

Let us first consider the update for the means. Collecting together the terms in Eq. (10.32) that depend on  $\mu_i$ , and denoting the result as  $J(\mu_i)$ , we obtain:

$$J(\mu_i) = -\frac{1}{2} \sum_n \tau_n^{i(t)} (x_n - \mu_i)^T \Sigma_i^{-1} (x_n - \mu_i). \quad (10.33)$$

We see that we have a weighted least-squares problem. Calculating the derivative of  $J(\mu_i)$  with respect to  $\mu_i$  and setting to zero yields:

$$\mu_i^{(t+1)} = \frac{\sum_n \tau_n^{i(t)} x_n}{\sum_n \tau_n^{i(t)}}, \quad (10.34)$$

which is Eq. (10.16).

Similarly, collecting together the terms that reference the covariance matrix  $\Sigma_i$ , we have:

$$J(\Sigma_i) = -\frac{1}{2} \sum_n \tau_n^{i(t)} \left\{ \log |\Sigma_i| + (x_n - \mu_i)^T \Sigma_i^{-1} (x_n - \mu_i) \right\}. \quad (10.35)$$

This is a weighted variant of the problem of estimating the covariance matrix of a Gaussian. Taking the derivative with respect to  $\Sigma_i$  and setting to zero yields:

$$\Sigma_i^{(t+1)} = \frac{\sum_n \tau_n^{i(t)} (x_n - \mu_i^{(t+1)}) (x_n - \mu_i^{(t+1)})^T}{\sum_n \tau_n^{i(t)}}. \quad (10.36)$$

which is Eq. (10.17).

Finally, the terms in the expected complete log likelihood that reference  $\pi$  are:

$$J(\pi) = \sum_n \sum_i \tau_n^{i(t)} \log \pi_i. \quad (10.37)$$

Adding a Lagrangian term to account for the constraint that the  $\pi_i$  sum to one, taking derivatives and setting to zero yields:

$$\pi_i^{(t+1)} = \frac{1}{N} \sum_n \tau_n^{i(t)}, \quad (10.38)$$

Figure 10.6:

Figure 10.7:

which is Eq. (10.18).

Although this derivation of the EM equations is no more intuitive than our earlier work, it has the virtue of yielding a simple algebraic recipe, both for the E step and the M step. It is also more general than our earlier work; indeed, the derivation that we have carried out here will extend readily to arbitrary graphical models. The key concepts that underly the usefulness of this approach are: (1) the decoupled form of the complete log likelihood, and (2) the linearity of the expectation operator.

This brief discussion suggests an important role for the “expected complete log likelihood,” particularly in providing a simple method for deriving EM update equations, but it still leaves us with a number of questions. How does the maximization of the expected complete log likelihood relate to the maximization of the actual log likelihood, which is after all our goal? We have claimed that the EM algorithm is a coordinate ascent algorithm—how does the expected complete log likelihood emerge in this picture? How general is the algorithm? Will the algorithm converge? These are the topics of Chapter 11. Before turning to these general considerations, however, let us consider another application of mixture model ideas.

## 10.2 Conditional mixture models

The “divide-and-conquer” approach to statistical modeling applies equally well in the regression and classification domains. In this section we study conditional mixture models, which are the analogs for regression and classification of the unconditional mixture models studied thus far.<sup>3</sup>

Consider the data set shown in Figure 17.16, where we clearly have a nonlinearity in the mapping from  $X$  to  $Y$ . We might utilize a rich set of basis functions to allow us to capture this nonlinearity, but it may be difficult to capture the sharp kink in the middle of the figure without requiring an overly large number of basis functions to the left and right of the kink, where the function would seem to be well modeled as a simple linear function.

An alternative way to model these data is to utilize a conditional mixture. Within the conditional mixture framework, we in essence split the problem into two subproblems, each of which can be treated as a simple linear regression. We must find the parameters of these regressions, and we must also decide where to split. Assuming that we can model the splitting decision using a simple parametric model, we may be able to model the overall nonlinear dependence of  $Y$  on  $X$  using a small number of parameters.

The conditional mixture model is shown as a graphical model in Figure 17.16. The model includes nodes for the observed variables  $X$  and  $Y$  and also incorporates a node for a multinomial

---

<sup>3</sup>Conditional mixture models are also referred to as “mixture of experts” models; where the term “expert” is used to designate a regression, classification, or other generalized regression model.

latent variable  $Z$ . The response variable  $Y$  is conditioned not only on  $X$  but also on the latent variable  $Z$ . This latent variable indexes the set of possible regressions of  $Y$  on  $X$ —for each value of  $Z$ , we obtain a possibly different parameterized regression. Note moreover that there is a link from  $X$  to  $Z$ . It is this dependency that allows us to obtain different regressions in different regions of the input space.

Let us consider how to parameterize each of the nodes in the model.  $Z$  is a multinomial variable, and its parent is the input variable  $X$ . The fact that the edge between these nodes points from  $X$  to  $Z$  suggests using the ideas that we discussed in the section on discriminative classification (Section ??) to parameterize the dependency. For example, we may use a softmax regression:

$$p(Z^i = 1 | x, \xi) = \frac{e^{\xi_i^T x}}{\sum_j e^{\xi_j^T x}}, \quad (10.39)$$

where  $\xi = (\xi_1, \xi_2, \dots, \xi_M)$  is a parameter vector.

The node  $Y$  has  $X$  and  $Z$  as parents, and thus we have a conditional probability  $p(Y | X, Z^i = 1, \theta_i)$ . The mathematical form of this conditional probability depends on the nature of the data  $Y$ . Let us not specify a particular model at this point, but assume that we will bring to bear the machinery of generalized linear models (GLIM's). For example we could consider a binary classification model in which  $p(Y | X, Z^i = 1, \theta_i)$  is a logistic regression model. Note that we have one such model for each value of  $Z$ .

As is usual in the regression or discriminative classification setting we treat the observations of  $X$  as fixed constants. Thus we do not incorporate a marginal probability for  $X$  into our model.

Putting together the pieces, we obtain the following model for the conditional probability of  $Y$  given  $X$ :

$$p(y | x, \theta) = \sum_i p(Z^i = 1 | x, \xi) p(y | Z^i = 1, x, \theta_i), \quad (10.40)$$

where  $\theta = (\xi_1, \dots, \xi_M, \theta_1, \dots, \theta_M)$ . This is a conditional mixture model, where both the *mixing proportions*,  $p(Z^i = 1 | x, \xi)$ , and the *mixture components*,  $p(y | Z^i = 1, x, \theta_i)$ , are conditional probabilities—both are conditioned on  $\{X = x\}$ .

As in the unconditional mixtures, a key quantity in conditional mixture modeling is the posterior probability of the latent variable  $Z$ . Here the notions of “prior” and “posterior” are relative to the observation of  $Y$ ; the variable  $X$  is taken to be always observed. Thus, let us define  $\pi_i(x, \xi) \triangleq p(Z^i = 1 | x, \xi)$  as the *prior probability* of the  $i$ th mixture component, conditioned solely on  $X$ . We now define the *posterior probability*  $\tau^i(x, y, \theta)$ :

$$\tau^i(x, y, \theta) \triangleq p(Z^i = 1 | x, y, \xi) \quad (10.41)$$

$$= \frac{p(Z^i = 1 | x, \xi) p(y | Z^i = 1, x, \theta_i)}{\sum_j p(Z^j = 1 | x, \xi) p(y | Z^j = 1, x, \theta_j)} \quad (10.42)$$

$$= \frac{\pi_i(x, \xi) p(y | Z^i = 1, x, \theta_i)}{\sum_j \pi_j(x, \xi) p(y | Z^j = 1, x, \theta_j)} \quad (10.43)$$

where we see that the prior probability of the  $i$ th class is updated by how probable the observation  $\{Y = y\}$  is under the  $i$ th model.

Figure 10.8:

### 10.2.1 Examples

Let us consider some specific choices for the mixture components  $p(y | Z^i = 1, x, \theta_i)$ .

#### Mixtures of linear regressions

For continuous variables  $Y$  it is natural to consider a mixture of linear regressions:

$$p(y | x, \theta) = \sum_i \pi_i(x, \xi) \mathcal{N}(y | \beta_i^T x, \sigma_i^2), \quad (10.44)$$

where we have allowed each linear regression to have a possibly different error variance  $\sigma_i^2$ .

Figure 17.16 shows a depiction of this model in the case of two mixture components. In this case the variable  $Z$  can be taken to be a binary variable and the mixing proportion  $\pi(x, \xi) \triangleq p(Z = 1 | x, \xi)$  can be modeled using logistic regression. The logistic curve shown in the figure thus models the input-dependent probability associated with the two mixture components. For negative values of  $X$ , the logistic curve assigns small probability to  $Z = 1$ , thus essentially choosing the regression curve labeled  $Z = 0$ . For positive values of  $X$ , the logistic curve assigns large probability to  $Z = 1$ , thus essentially choosing the regression curve labeled  $Z = 1$ . The point at which the logistic function is equal to 0.5 can be viewed as the “split” point.

Let us now consider the geometric interpretation of the posterior probability. As shown in Figure 17.16, conditioning on a specific value of  $X$  leaves us with two possible conditional expectations of  $Y$ —the conditional expectations associated with each of the two regressions. We have Gaussian distributions around each of these conditional expectations, with variances  $\sigma_1^2$  and  $\sigma_0^2$ , respectively. Thus the conditional distribution of  $Y$  given  $X$  is bimodal—we have a mixture distribution in the output space for each point in the input space. Consider now the point  $(x, y')$  in the figure. For this value of  $x$ , the prior  $\pi(x, \xi)$  is large, corresponding to a choice of the regression curve labeled  $Z = 1$ . Moreover, the value  $y'$  has high probability under this regression model and the corresponding posterior  $\tau(x, y', \xi)$  is therefore large. Consider, on the other hand, the point  $(x, y'')$ . The prior for this point is the same as before. The value  $y''$ , however, has low probability under the regression model labeled  $Z = 1$  and high probability under the regression model labeled  $Z = 0$ . The posterior  $\tau(x, y'', \xi)$  is therefore small, corresponding to a posterior choice of the regression model labeled  $Z = 0$ .

We see that the posterior probability has much the same interpretation as in the unconditional mixture model setting. That is, we can interpret the posterior probability as a “soft assignment,” but here the assignment process reflects both the prior partitioning of the input space into regions, modeled by  $\pi_i(x, \xi)$ , and the ability of each of the component regressions to accommodate the observed output  $y$  at that given value of  $x$ , modeled by  $p(y | Z^i = 1, x, \theta_i)$ .

### Mixtures of logistic regressions

We can readily extend the model of the previous section to mixtures of generalized linear models, thereby accommodating a wide variety of data types. An example is the mixture of logistic regressions:

$$p(y | x, \theta) = \sum_i \pi_i(x, \xi) \mu(\theta_i^T x)^y (1 - \mu(\theta_i^T x))^{1-y}, \quad (10.45)$$

where  $\mu(\theta_i^T x)$  is the logistic function:  $\mu(\theta_i^T x) = 1/(1 + e^{-\theta_i^T x})$ . This model allows us to bring the divide-and-conquer approach to bear on classification problems.

The interpretation of the prior and posterior probabilities is identical in this model to the linear regression case, with the likelihood being a Bernoulli distribution rather than a Gaussian distribution.

#### 10.2.2 Parameter estimation via the EM algorithm

At this point we have parameterized the graphical model in Figure 17.16, and the problem of maximum likelihood parameter estimation can be handled straightforwardly using the tools that we have developed in Section 10.1.3 and Section 10.1.5. Indeed the model is a good exercise of our skills. In this section we write down the log likelihood, the expected complete log likelihood, and the EM algorithm for conditional mixtures.

We assume an IID data set  $\mathcal{D} = \{(x_n, y_n) : n = 1, \dots, N\}$ . The likelihood is obtained as the sum of the logarithm of the probability model in Eq. (10.40):

$$l(\theta | \mathcal{D}) = \sum_n \log \sum_i \pi_i(x_n, \xi) p(y_n | Z^i = 1, x_n, \theta_i). \quad (10.46)$$

Note the presence of the logarithm outside of the summation; as in the unconditional case, the likelihood is a marginal probability.

The “complete data” is the data set  $\mathcal{D}_c = \{(x_n, z_n, y_n) : n = 1, \dots, N\}$ , where as before we imagine that we can observe the latent variable  $Z$ . The likelihood for  $N$  complete observations of the model is:

$$l(\theta | \mathcal{D}_c) = \prod_n \prod_i [\pi_i(x_n, \xi) p(y_n | Z^i = 1, x_n, \theta_i)]^{z_n^i} \quad (10.47)$$

and taking the logarithm yields the complete log likelihood:

$$l_c(\theta | \mathcal{D}_c) = \sum_n \sum_i z_n^i \log [\pi_i(x_n, \xi) p(y_n | Z^i = 1, x_n, \theta_i)], \quad (10.48)$$

where we now see the logarithm inside the summation.

We take the expectation of the complete log likelihood, where we now treat the variables  $Z_n^i$  as random variables. The expectation is taken with respect to the conditional probability distribution  $p(z | x, y, \theta^{(t)})$ . Given that the complete log likelihood is linear in  $z_n^i$ , we see that we can obtain the expectation by simply computing:

$$\langle Z_n^i \rangle_{\theta^{(t)}} = p(Z_n^i = 1 | x_n, y_n, \theta^{(t)}) \quad (10.49)$$

$$= \tau^i(x_n, y_n, \theta^{(t)}). \quad (10.50)$$

Thus we see that the E step of the EM algorithm amounts to computing the posterior probabilities  $\tau^i(x_n, y_n, \theta^{(t)})$ . These can be viewed as our “best guess” of the values of the latent variables  $Z_n$ , conditioned on the observed values  $x_n$  and  $y_n$ , and evaluated at the current value of the parameter vector  $\theta^{(t)}$ .

To summarize, the expected complete log likelihood takes the following form:

$$l_c(\theta | \mathcal{D}) = \sum_n \sum_i \tau_n^i(t) \log [\pi_i(x_n, \xi) p(y_n | Z^i = 1, x_n, \theta_i)], \quad (10.51)$$

where we write  $\tau_n^{i(t)}$  for the posterior probability  $\tau^i(x_n, y_n, \theta^{(t)})$ , in order to simplify notation.

With the expected complete log likelihood in hand, we can now turn to the M step. Let us first consider maximizing  $l_c$  with respect to the parameters  $\xi$ . Collecting together the terms that depend on  $\xi$ , and referring to the result as  $J(\xi)$ , we have:

$$J(\xi) = \sum_n \sum_i \tau_n^i(t) \log \pi_i(x_n, \xi). \quad (10.52)$$

This is identical to the log likelihood for the discriminative classification problem (cf. Eq. (??)), where the role of the class labels in that problem (the  $z_n^i$ ) is now played by the posterior probabilities (the  $\tau_n^{i(t)}$ ). The interpretation is that we “fill in” the values of the latent variables  $Z_n^i$  with our “best guess.” Based on these filled-in values we treat the problem of estimating the parameters of the conditional probability  $p(Z | x, \xi)$  as a discriminative classification problem. In particular we can use the IRLS algorithm to update these parameters.

It is also straightforward to derive an M step for the parameters  $\theta_i$ . Collecting together the terms in the expected complete log likelihood that depend on  $\theta_i$ , and referring to the result as  $J(\theta_i)$ , we obtain:

$$J(\theta_i) = \sum_n \tau_n^i(t) \log p(y_n | Z^i = 1, x_n, \theta_i). \quad (10.53)$$

For generalized linear models, the log probability in this expression is the logarithm of an exponential family distribution. Each data point,  $(x_n, y_n)$ , has an associated “weight,” the posterior probability  $\tau_n^i(t)$ . Thus we have a weighted maximum likelihood problem to solve. In essence, each data point is “assigned” to one of the mixture components, and the estimation of the parameters of each mixture component is carried out using the data points assigned to that component.

In the case of a mixture of linear regressions, we obtain a set of weighted least squares problems, one for each mixture component. For a mixture of logistic regressions, we have a set of weighted cross-entropies. In general we can treat all of these problems within the IRLS framework—recall our discussion of weighted IRLS in Section ??.

In summary, the EM algorithm for conditional mixtures takes the following form:

- (E step): Calculate the posterior probabilities  $\tau_n^{i(t)}$ .
- (M step): Use the IRLS algorithm to update the parameters  $\xi$ , based on data pairs  $(x_n, \tau_n^{i(t)})$ .
- (M step): Use the weighted IRLS algorithm to update the parameters  $\theta_i$ , based on data pairs  $(x_n, y_n)$ , with weights  $\tau_n^{i(t)}$ .

These steps iterate and, as we prove in Chapter 11, climb to a local maximum of the likelihood.

### 10.2.3 An on-line algorithm

We can obtain some additional insight into the conditional mixture model by developing an on-line estimation algorithm. As we discussed in Chapter 6, the problem here is to derive an update for the parameters based on a single data point.

To derive these updates we take the derivative of the log likelihood with respect to the parameters and delete the summation over  $n$ ; this yields the “stochastic gradient.” We omit the algebra, asking the reader to supply the details in Exercise ??.

In the equations below, we use the notation  $\mu_n^i(t)$  to denote the conditional expectation of  $Y$  given  $\{X = x\}$ , for the  $i$ th mixture component, the  $n$ th data point, and letting the parameter vector equal  $\theta^{(t)}$ . We assume that the canonical link function has been chosen.

Taking the derivative with respect to  $\theta_i$ , we obtain the following update equation:

$$\theta_i^{(t+1)} = \theta_i^{(t)} + \rho \tau_n^{i(t)} (y_n - \mu_n^i(t)) x_n, \quad (10.54)$$

where  $\rho$  is a step size. Similarly, taking the derivative with respect to  $\xi_i$ , we obtain:

$$\xi_i^{(t+1)} = \xi_i^{(t)} + \kappa (\tau_n^{i(t)} - \pi_i(x_n, \xi^{(t)})) x_n, \quad (10.55)$$

where  $\kappa$  is a step size.

Both of these equations have natural interpretations. The update of  $\theta_i$  in Eq. (10.54) has the form of the LMS algorithm, but with the additional feature that the step size is modulated by the posterior probability  $\tau_n^{i(t)}$ . Thus, if our current “best guess” is that the  $n$ th data point should be assigned to the  $i$ th mixture component, then we update the parameters in the normal way. If, on the other hand, we do not think that the  $n$ th data point should be assigned to the  $i$ th mixture component, then the step size is near zero and the parameters are not adjusted.

The update of  $\xi_i$  in Eq. (10.54) also has an appealing interpretation. The update again takes the form of the LMS algorithm, where the error is the difference between the posterior probability and the prior probability. In essence we have a classification problem in which the prior probability is a prediction of the class label associated with the mixture components, and the posterior probability is an improved estimate of that label.

Figure 17.16 shows a depiction of these update equations for the case of a mixture of linear regressions. In this case  $\mu_n^i(t) = \theta_i^{(tT)} x_n$ , and the error which drives the update of  $\theta_i$  is simply the difference  $(y_n - \theta_i^{(tT)} x_n)$ . This difference is shown in the figure for both of the regressions. Although the error is larger for the  $Z = 0$  regression, the posterior probability associated with this regression is vanishingly small (it is proportional to the exponential of the negative of the square of the error). Thus, as we show in Figure 17.16(b), the parameters associated with the upper ( $Z = 1$ ) curve change significantly, while the parameters associated with the lower ( $Z = 0$ ) curve change little.

Given that the posterior probability associated with the upper curve is near one, the error in Eq. (10.55) has the effect of shifting the logistic curve towards the left. As we show in Figure 17.16(b), this implies that on future presentations of this data point, the prior prediction will be closer to one.

### 10.2.4 Hierarchical conditional mixtures and decision trees

## 10.3 Appendix XXX

As an alternative to the EM algorithm, we can use standard nonlinear optimization algorithms such as conjugate gradients. In this appendix we discuss this approach for unconditional mixtures, focusing on the problem of implementing the probabilistic constraints on the parameters.

In evaluating the derivatives we must take account of the requirement for the mixing proportions to satisfy  $0 \leq \pi_i \leq 1$  and  $\sum_i \pi_i = 1$ . Similarly, the covariance matrices  $\Sigma_i$  must remain symmetric and positive-definite.

We can allow for the constraints on the mixing proportions  $\pi_i$  by expressing them as a nonlinear transformation of a corresponding set of unconstrained variables  $\eta_i$ . Specifically, we use the softmax transformation:

$$\pi_i = \frac{\exp(\eta_i)}{\sum_j \exp(\eta_j)}, \quad (10.56)$$

which has the property that the mixing proportions will automatically satisfy the required constraints.

In order to impose the required constraints on the covariance matrix we can represent the inverse<sup>4</sup> covariance matrix in terms of its Cholesky decomposition:

$$\Sigma^{-1} = A^T A \quad (10.57)$$

where  $A$  is an upper diagonal matrix, so that  $A_{ij} = 0$  if  $i < j$ . It is easily seen that there are  $d(d + 1)/2$  remaining independent elements in  $A$ , corresponding to the number of independent elements in  $\Sigma$ . In computing the expected complete-data log likelihood we need the inverse square root of the determinant of the covariance matrix, which is given by:

$$|\Sigma|^{-1/2} = \prod_{i=1}^d A_{ii}. \quad (10.58)$$

The covariance matrix will be positive definite provided the diagonal elements  $A_{ii}$  are positive, which can be ensured by writing them as the exponentials of real values  $A_{ii} = \exp(\alpha_i)$ .

In summary, if we treat the values of  $\eta_i$ ,  $A_{ij}$  (for  $j > i$ ),  $\alpha_i$  and the components of  $\mu_i$  as independent, unconstrained real values, the required constraints will be met. The required derivatives of the log likelihood with respect to these unconstrained variables are then easily obtained Exercise ??.

---

<sup>4</sup>The inverse of a positive definite symmetric matrix is also positive definite and symmetric.

# An Introduction to Probabilistic Graphical Models

Michael I. Jordan  
*University of California, Berkeley*

June 30, 2003



## Chapter 12

# Hidden Markov Models

In this chapter we finally relax the assumption of independent, identically distributed (IID) sampling that we have labored under until now. A hidden Markov model (HMM) is a graphical model that is appropriate for modeling sequential data; i.e., data sets in which successive samples are no longer assumed to be independent.

An HMM is a natural generalization of a mixture model; indeed, it is perhaps best viewed as a “dynamical” mixture model. To reflect this point of view, we adjust our terminology somewhat, referring to the “mixture components” of the mixture model as “states.” To see exactly what kind of generalization is involved, let us recall the process of generating IID data under a mixture model, using the new language (cf. Figure 12.1(a)):

- At each step, a state is selected according to the distribution  $p(z)$ . This selection is made independently of the choice of states at other steps.
- Given the state, a data vector is chosen from a distribution  $p(x|z)$ .

Within the HMM framework we no longer assume that the states are chosen independently at each step, but rather we assume that the choice of a state at a given step depends on the choice of the state at the previous step. Thus we augment the basic mixture model to include a matrix of *transition probabilities* linking the states at neighboring steps. If there are  $M$  states, then this is an  $M \times M$  matrix, whose  $(i, j)$ th entry represents the probability of transitioning from the  $i$ th state at a given step to the  $j$ th state at the following step. The process of generating data under the HMM is suggested in Figure 12.1(b), where we have drawn arrows between the probability distributions labeled by the states to suggest the transition probabilities. Other than the introduction of a state transition matrix, the HMM is the same as the simpler mixture model—in particular, given the state at a given step a data vector is generated from a distribution that depends only on that state.

As in any mixture model, the states underlying the data generation process are assumed to be “hidden” from the learner. We envision an HMM-based learning system observing the pattern of data in Figure 12.1(a)—one data point at a time—and interpreting the sequence in terms of the hypothesized states and state transitions of Figure 12.1(b). Just as in the simpler mixture model, the fact that the data form clusters is grist for the HMM mill, allowing the learner to differentiate the states. But while the clustering of the data is necessary for an HMM-based learner to be

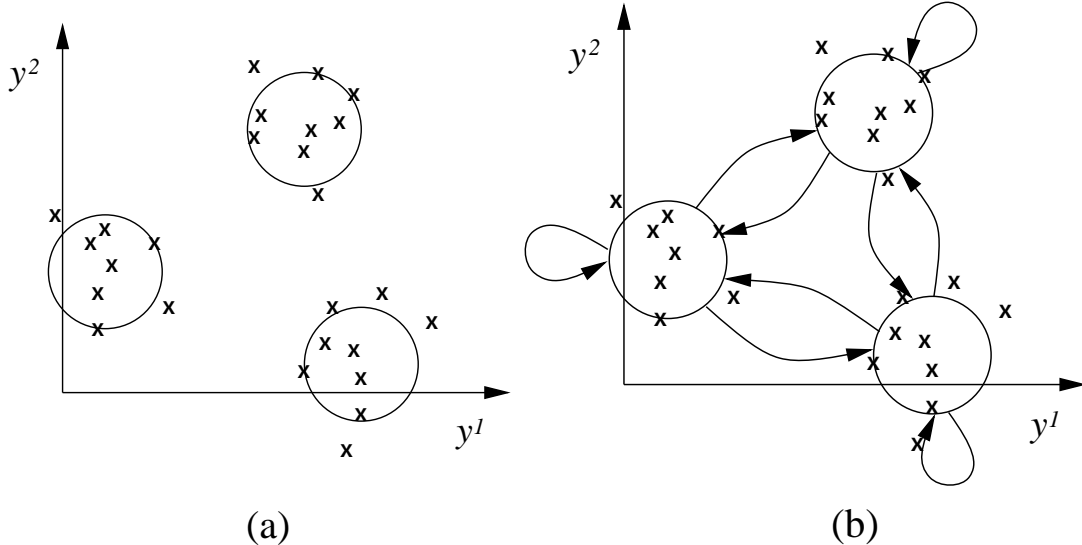


Figure 12.1: (a). A sample point is generated from a mixture model by first selecting a mixture component and then generating a data point from that mixture component. (b) An HMM generalizes the mixture model by allowing the choice of the mixture component at a given step to depend on the choice of the mixture component at the previous step. The arrows in the diagram represent these transitions between the mixture components.

justified in a given problem, it is not sufficient—there should also be regularities in the transitions between clusters.

The inference problem for HMMs involves taking as input the sequence of observed data and yielding as output a probability distribution on the underlying states. Given the dependence between the states, this problem is substantially more complex than the analogous inference problem for mixture models. Nonetheless, it is readily solved. Guided by Bayes rule, we will uncover a simple recursion that neatly computes the desired posterior probabilities. In fact, this algorithm marks an important milestone for us—it begins to suggest the general machinery for propagating probabilities on graphs that we will be our focus in much of the remainder of the book. With HMMs we begin our study of inference in graphical models in earnest.

## 12.1 The graphical model

The graphical model representation of an HMM is shown in Figure 12.2. As the diagram makes clear, the HMM can be viewed as a linked sequence of mixture models, with the linking occurring at the level of the mixture components, or “states.” We denote the state at time  $t$  as  $q_t$ , and let  $y_t$  represent the observable “output” at time  $t$ .<sup>1</sup>

<sup>1</sup>Throughout the chapter we refer to  $t$  as a temporal variable for concreteness; the HMM model is of course applicable to any kind of sequential data.

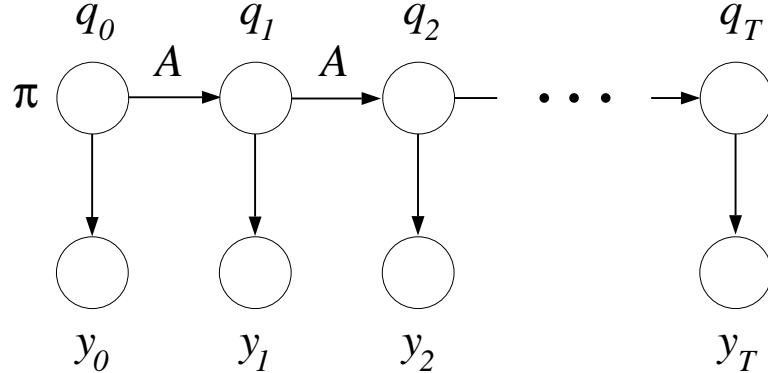


Figure 12.2: The representation of a HMM as a graphical model. Each vertical slice represents a time step. The top node in each slice represents the multinomial  $q_t$  variable and the bottom node in each slice represents the observable  $y_t$  variable.

We represent the state at time  $t$  as a multinomial random variable  $q_t$ , with components  $q_t^i$ , for  $i = 0, \dots, M$ . Thus  $q_t^i$  is equal to one for a particular value of  $i$  and is equal to zero for  $j \neq i$ . As for the output variables  $y_t$ , these variables are always observed in the HMM setting and thus they play a minimal role in the inference problem. We will accordingly leave their type undefined for now (the reader can think of them as multinomial or multivariate Gaussian for concreteness).

From the graphical model we can read off various conditional independencies. The main conditional independency of interest is that obtained by conditioning on a single state node. Conditioning on  $q_t$  renders  $q_{t-1}$  and  $q_{t+1}$  independent; moreover it renders  $q_s$  independent of  $q_u$ , for  $s < t$  and  $t < u$ . Thus, “the future is independent of the past, given the present.” This statement is also true for output nodes  $y_s$  and  $y_u$ , again conditioning on the state node  $q_t$ .

Note that conditioning on an output node, on the other hand, does not separate nodes in the graph and thus does not yield any conditional independencies. It is not true that the future is independent of the past, given the present, if by “present” we mean the current output.

Indeed, conditioning on *all* of the output nodes fails to separate any of the remaining nodes. That is, given the observable data, we cannot expect any independencies to be induced between the state nodes. Thus we should expect that our inference algorithm must take into account possible dependencies between states at arbitrary locations along the chain. In particular, learning something about the final state node in the chain,  $q_T$  (e.g., by observing  $y_T$ ), can change the posterior probability distribution for the first node in the chain,  $q_0$ . We expect that our inference algorithm will have to propagate information from one end of the chain to the other.

## 12.2 The parameterization

We now parameterize the HMM by assigning local conditional probabilities to each of the nodes. The first state node in the sequence has no parents; thus we endow this node with an unconditional distribution  $\pi^i \triangleq p(q_0^i = 1)$ . Each successive state node has the previous state node in the

chain as its (sole) parent; thus we need a  $M \times M$  matrix to specify its local conditional probability. We define a *state transition matrix*  $A$ , where the  $(i, j)$ th entry  $a_{ij}$  of  $A$  is defined to be the transition probability  $p(q_{t+1}^j = 1 | q_t^i = 1)$ . Note that we assume that this transition probability is independent of  $t$ ; that is, we assume a *homogeneous* HMM. (All of the algorithms that we describe are readily generalized to the case of a varying  $A$  matrix, however this case is less common in practice than the homogeneous case).

Each of the output nodes has a single state node as a parent, thus we require a probability distribution  $p(y_t | q_t)$ . We again assume this distribution to be independent of  $t$ . We make no further assumptions regarding the form of  $p(y_t | q_t)$  for now; for the purposes of developing the HMM inference algorithms we need only be able to evaluate  $p(y_t | q_t)$  for a fixed value of  $y_t$ .

The joint probability is obtained as always by taking the product over the local conditional probabilities. Thus, for a particular configuration  $(q, y) = (q_0, q_1, \dots, q_T, y_0, y_1, \dots, y_T)$ , we obtain the following joint probability:

$$p(q, y) = p(q_0) \prod_{t=0}^{T-1} p(q_{t+1} | q_t) \prod_{t=0}^T p(y_t | q_t). \quad (12.1)$$

To introduce the  $A$  and  $\pi$  parameters into this equation, we adopt a notation in which state variables can be used as indices. Thus, when  $q_t$  takes on its  $i$ th value and  $q_{t+1}$  takes on its  $j$ th value, we let  $a_{q_t, q_{t+1}}$  denote the  $(i, j)$ th entry of the matrix  $A$ . Formally, this interpretation is achieved via the following definition:

$$a_{q_t, q_{t+1}} \triangleq \prod_{i,j=1}^M [a_{ij}]^{q_t^i q_{t+1}^j}. \quad (12.2)$$

Recall that only one of the components of  $q_t$  is one, and thus only one factor in the product on the right-hand side is different from one; this picks out the appropriate entry in the matrix  $A$ . Similarly, we define  $\pi_{q_0}$  via:

$$\pi_{q_0} \triangleq \prod_{i=1}^M [\pi_i]^{q_0^i} \quad (12.3)$$

which has the effect of picking out the appropriate entry in the  $\pi$  vector. We use the simple shorthand forms  $a_{q_t, q_{t+1}}$  and  $\pi_{q_0}$  throughout the chapter, although the expanded forms in Eqs. 12.2 and 12.3 will also prove useful when we discuss parameter estimation.

Plugging the definitions into the joint probability, we have:

$$p(q, y) = \pi_{q_0} \prod_{t=0}^{T-1} a_{q_t, q_{t+1}} \prod_{t=0}^T p(y_t | q_t). \quad (12.4)$$

This is the parameterized probability distribution in which we wish to do inference.

### 12.3 The inference problem

There are quite a number of inference problems that are of interest in the setting of the HMM. The general inference problem involves computing the probability of a hidden state sequence  $q$  given an

observable output sequence  $y$ . Various marginal probabilities are also of interest, in particular the probability of a particular hidden state  $q_t$  given the output sequence.

It is also of interest to compute various probabilities conditioned on partial output sequences. In particular, consider the “on-line” problem in which a sequence of outputs  $y_t$  arrives and it is desired to compute the probability of the state at time  $t$  immediately, without waiting for future data. Computing this probability,  $p(q_t|y_0, \dots, y_t)$ , is generally called the *filtering problem*.<sup>2</sup> Another inference problem involves the calculation of  $p(q_t|y_0, \dots, y_s)$ , where  $t > s$ . This is referred to as the *prediction problem*. Finally, the problem of calculating a posterior probability based on data up to and including a future time, i.e.,  $p(q_t|y_0, \dots, y_u)$  for  $t < u$ , is referred to as the *smoothing problem*.

Let us consider the problem of computing the posterior probability  $p(q|y)$  where  $y = (y_0, \dots, y_T)$  is the entire observed output sequence at our disposal. Let  $q$  be an arbitrary fixed state sequence whose probability we wish to compute. By definition we have  $p(q|y) = p(q, y)/p(y)$ . The numerator is readily calculated by substituting  $q$  and  $y$  in Eq. 12.4. What about the denominator  $p(y)$ ?

Calculating the denominator involves taking a sum across all possible values of the hidden states:

$$p(y) = \sum_{q_0} \sum_{q_1} \cdots \sum_{q_T} \pi(q_0) \prod_{t=0}^{T-1} a_{q_t, q_{t+1}} \prod_{t=0}^T p(y_t|q_t, \eta). \quad (12.5)$$

This sum should give us pause. Each state node  $q_t$  can take on  $M$  values, and we have  $T$  state nodes. This implies that we must perform  $M^T$  sums, a wildly intractable number for reasonable values of  $M$  and  $T$ . Is it possible to perform inference efficiently for HMMs?

The way out of our seeming dilemma lies in the factorized form of the joint probability distribution (Eq. 12.4). Each factor involves only one or two of the state variables, and the factors form a neatly organized chain. This suggests that it ought to be possible to move these sums “inside” the product in a systematic way. Moving the sums as far as possible ought to reduce the computational burden significantly. Consider, for example, the sum over  $q_T$ . This sum can be brought inside until the end of the chain and applied to the two factors involving  $q_T$ . Once this sum is performed the result can be combined with the two factors involving  $q_{T-1}$  and the sum over  $q_{T-1}$  can be performed. We begin to hope that we can organize our calculation as a recursion.

## 12.4 Inference

To reveal the recursion behind the HMM inference problem as simply as possible, let us consider an inference problem that is seemingly easier than the full problem. Rather than calculating  $p(q|y)$  for the entire state sequence  $q$ , we focus on a particular state node  $q_t$  and ask to calculate its posterior probability, that is, we calculate  $p(q_t|y)$ . This posterior probability also has  $p(y)$  in its denominator,

---

<sup>2</sup>Why “filtering”? The terminology arises from the interpretation of the outputs  $y_t$  as providing “noisy” information about the underlying “signal”  $q_t$ . The inference problem is then one of “filtering” the noise from the signal. In the linear stochastic systems setting in which this terminology originally arose (cf. Chapter 15), the calculation of quantities such as  $p(q_t|y_0, \dots, y_t)$  often had a frequency domain interpretation in which some frequencies are passed and not others. In such a setting the terminology is rather natural. While recognizing the possible unnaturalness of the terminology outside of the linear systems setting, we bow to its wide usage and adopt it here.

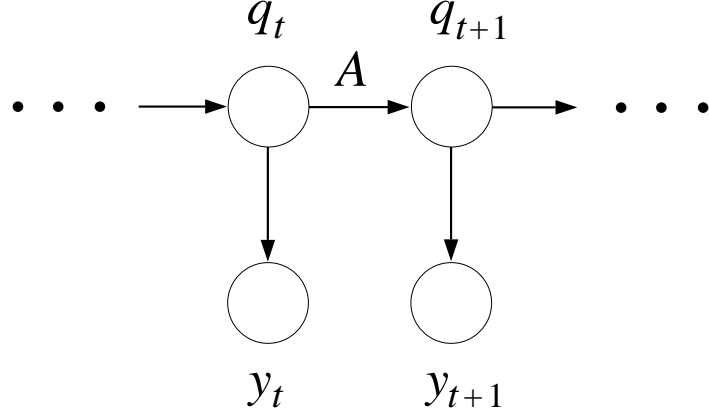


Figure 12.3: A fragment of the graphical model representation of an HMM.

and in fact we can easily adapt our algorithm for computing  $p(q_t|y)$  to compute  $p(q|y)$  or marginals over substrings of  $q$  (see Exercise ??).

We thus turn to the calculation of  $p(q_t|y)$ . To make progress, we need to take advantage of the conditional independencies in our graphical model, breaking the problem into pieces. To do so we condition on a state node (see Figure 12.3). We reverse the terms  $q_t$  and  $y$  via an application of Bayes rule, conditioning now on  $q_t$ , and use conditional independence:

$$p(q_t|y) = \frac{p(y|q_t)p(q_t)}{p(y)} \quad (12.6)$$

$$= \frac{p(y_0, \dots, y_t|q_t)p(y_{t+1}, \dots, y_T|q_t)p(q_t)}{p(y)}. \quad (12.7)$$

Finally, we regroup the terms and make a definition:

$$p(q_t|y) = \frac{p(y_0, \dots, y_t, q_t)p(y_{t+1}, \dots, y_T|q_t)}{p(y)} \quad (12.8)$$

$$= \frac{\alpha(q_t)\beta(q_t)}{p(y)}, \quad (12.9)$$

where

$$\alpha(q_t) \triangleq p(y_0, \dots, y_t, q_t) \quad (12.10)$$

is the probability of emitting a partial sequence of outputs  $y_0, \dots, y_t$  and ending up in state  $q_t$ , and

$$\beta(q_t) = p(y_{t+1}, \dots, y_T|q_t) \quad (12.11)$$

is the probability of emitting a partial sequence of outputs  $y_{t+1}, \dots, y_T$  given that the system starts in state  $q_t$ .

Given that the sum of  $p(q_t|y)$  over the possible values of  $q_t$  must equal one, we use Eq. 12.9 to obtain:

$$p(y) = \sum_{q_t} \alpha(q_t)\beta(q_t). \quad (12.12)$$

That is, we can obtain the likelihood  $p(y)$  by calculating  $\alpha(q_t)$  and  $\beta(q_t)$  for any  $t$  and summing their product.

We make one additional definition:  $\gamma(q_t)$  will denote the posterior probability  $p(q_t|y)$ . Thus:

$$\gamma(q_t) \triangleq \frac{\alpha(q_t)\beta(q_t)}{p(y)}, \quad (12.13)$$

where  $p(y)$  is computed once, as the normalization constant for a particular (arbitrary) choice of  $t$ .

We have reduced our problem to that of calculating the alphas and the betas. This is a useful reduction because, as we now see, these quantities can be computed recursively.

Let us first consider the alpha variables. Given that  $\alpha(q_t)$  depends only on quantities up to time  $t$ , and given the Markov properties of our model, we might hope to obtain a recursion between  $\alpha(q_t)$  and  $\alpha(q_{t+1})$ . Indeed, referring to Figure 12.3 to justify the conditional independencies we need, we obtain:

$$\alpha(q_{t+1}) = p(y_0, \dots, y_{t+1}, q_{t+1}) \quad (12.14)$$

$$= p(y_0, \dots, y_{t+1}|q_{t+1})p(q_{t+1}) \quad (12.15)$$

$$= p(y_0, \dots, y_t|q_{t+1})p(y_{t+1}|q_{t+1})p(q_{t+1}) \quad (12.16)$$

$$= p(y_0, \dots, y_t, q_{t+1})p(y_{t+1}|q_{t+1}) \quad (12.17)$$

$$= \sum_{q_t} p(y_0, \dots, y_t, q_t, q_{t+1})p(y_{t+1}|q_{t+1}) \quad (12.18)$$

$$= \sum_{q_t} p(y_0, \dots, y_t, q_{t+1}|q_t)p(q_t)p(y_{t+1}|q_{t+1}) \quad (12.19)$$

$$= \sum_{q_t} p(y_0, \dots, y_t|q_t)p(q_{t+1}|q_t)p(q_t)p(y_{t+1}|q_{t+1}) \quad (12.20)$$

$$= \sum_{q_t} p(y_0, \dots, y_t, q_t)p(q_{t+1}|q_t)p(y_{t+1}|q_{t+1}) \quad (12.21)$$

$$= \sum_{q_t} \alpha(q_t)a_{q_t, q_{t+1}}p(y_{t+1}|q_{t+1}). \quad (12.22)$$

Throughout this derivation the key idea is to condition on a state and then use the conditional independence properties of the model to decompose the equation. This is done in Eqs. 12.16 and 12.22, both of which can be verified via the graphical model fragment. The second key idea is to introduce a variable, in this case  $q_t$ , by marginalizing over it (cf. Eq. 12.18). Once  $q_t$  is introduced the recursion follows readily.

The computational complexity of each step of the alpha recursion is  $O(M^2)$ ; in particular, for each of the  $M$  values of  $q_{t+1}$ , we require  $M$  multiplications to compute the inner product of  $\alpha(q_t)$

with the appropriate column of the  $A$  matrix. To compute all of the alpha variables from  $t = 1$  to  $t = T$  thus requires time  $O(M^2T)$ .

Note that the algorithm proceeds “forward” in time. The definition of alpha at the first time step yields:

$$\alpha(q_0) = p(y_0, q_0) \quad (12.23)$$

$$= p(y_0|q_0)p(q_0) \quad (12.24)$$

$$= p(y_0|q_0)\pi_{q_0}. \quad (12.25)$$

and these values are used to initialize the recursion.

For the beta variables we obtain a “backward” recursion in which  $\beta(q_t)$  is expressed in terms of  $\beta(q_{t+1})$ , where once again the various steps are justified by making reference to the graphical model fragment in Figure 12.3:

$$\beta(q_t) = p(y_{t+1}, \dots, y_T|q_t) \quad (12.26)$$

$$= \sum_{q_{t+1}} p(y_{t+1}, \dots, y_T, q_{t+1}|q_t) \quad (12.27)$$

$$= \sum_{q_{t+1}} p(y_{t+1}, \dots, y_T|q_{t+1}, q_t)p(q_{t+1}|q_t) \quad (12.28)$$

$$= \sum_{q_{t+1}} p(y_{t+2}, \dots, y_T|q_{t+1})p(y_{t+1}|q_{t+1})p(q_{t+1}|q_t) \quad (12.29)$$

$$= \sum_{q_{t+1}} \beta(q_{t+1})a_{q_t, q_{t+1}}p(y_{t+1}|q_{t+1}). \quad (12.30)$$

Note that the beta recursion is a backwards recursion; that is, we start at the final time step  $T$  and proceed backwards to the initial time step.

As for the initialization of the beta recursion, the definition of  $\beta(q_T)$  is unhelpful, given that it makes reference to a non-existent  $y_{T+1}$ , but we see from applying the recursion once to compute  $\beta(q_{T-1})$  that this value will be calculated correctly if we define  $\beta(q_T)$  to be a vector of ones. Alternatively, computing  $p(y)$  at time  $T$ , we have:

$$p(y) = \sum_i \alpha(q_T^i)\beta(q_T^i) \quad (12.31)$$

$$= \sum_i \alpha(q_T^i) \quad (12.32)$$

$$= \sum_i p(y_0, \dots, y_T, q_T^i) \quad (12.33)$$

$$= p(y), \quad (12.34)$$

and we see that the definition makes sense.

If we need only the likelihood  $p(y)$ , Eq. 12.31 shows us that it is not necessary to compute the betas; a single forward pass for the alphas will suffice. Moreover, Eq. 12.12 tell us that any partial

forward pass up to time  $t$  to compute  $\alpha(q_t)$ , accompanied by a partial backward pass to compute  $\beta(q_t)$ , will also suffice. To compute the posterior probabilities for all of the states  $q_t$ , however, requires us to compute alphas and betas for each time step. Thus we require a forward pass and a backward pass for a complete solution to the inference problem.

## 12.5 An alternative inference algorithm

The alpha-beta algorithm is not the only way to compute the posterior probabilities of the states. In this section we describe an alternative approach in which the backward phase is a recursion defined directly on the  $\gamma(q_t)$  variables. An interesting feature of this algorithm is that the backward phase makes no use of the observations  $y_t$ ; only the forward phase uses the observed data. We can throw away the data as we filter.

The algorithm differs from the alpha-beta algorithm only in the backward phase. In the forward direction we run the alpha algorithm as before, calculating the filtered quantities  $\alpha(q_t) = p(y_0, \dots, y_t, q_t)$ .

To uncover a backward recursion linking the  $\gamma_t$  variables, we refer once again to the graphical model fragment in Figure 12.3. Our goal is to compute  $\gamma(q_t) = p(q_t | y_0, \dots, y_T)$ . As in our earlier calculations, our main tool for computing such quantities recursively is to condition on a state variable; such conditioning breaks the problem into two pieces. In particular, we condition on  $q_{t+1}$  and obtain:

$$p(q_t | q_{t+1}, y_0, \dots, y_T) = p(q_t | q_{t+1}, y_0, \dots, y_t). \quad (12.35)$$

This shows that we can get a conditional probability that depends on all of the data via a conditional probability that depends only on the partial sequence up to  $t$ . Moreover, the left-hand side can be readily converted into  $\gamma(q_t)$  by multiplying by  $p(q_{t+1} | y_0, \dots, y_T)$ —which is  $\gamma(q_{t+1})$  by definition—and summing over  $q_{t+1}$ . The details are as follows:

$$\gamma(q_t) = \sum_{q_{t+1}} p(q_t, q_{t+1} | y_0, \dots, y_T) \quad (12.36)$$

$$= \sum_{q_{t+1}} p(q_t | q_{t+1}, y_0, \dots, y_T) p(q_{t+1} | y_0, \dots, y_T) \quad (12.37)$$

$$= \sum_{q_{t+1}} p(q_t | q_{t+1}, y_0, \dots, y_t) p(q_{t+1} | y_0, \dots, y_T) \quad (12.38)$$

$$= \sum_{q_{t+1}} \frac{p(q_t, q_{t+1}, y_0, \dots, y_t)}{\sum_{q_t} p(q_t, q_{t+1}, y_0, \dots, y_t)} p(q_{t+1} | y_0, \dots, y_T) \quad (12.39)$$

$$= \sum_{q_{t+1}} \frac{p(q_t, y_0, \dots, y_t) p(q_{t+1} | q_t)}{\sum_{q_t} p(q_t, y_0, \dots, y_t) p(q_{t+1} | q_t)} p(q_{t+1} | y_0, \dots, y_T) \quad (12.40)$$

$$= \sum_{q_{t+1}} \frac{\alpha(q_t) a_{q_t, q_{t+1}}}{\sum_{q_t} \alpha(q_t) a_{q_t, q_{t+1}}} \gamma(q_{t+1}) \quad (12.41)$$

We see that this recursion makes use of the alpha variables, which therefore must be computed before the gamma recursion begins. The gamma recursion is initialized with  $\gamma(q_T) = \alpha(q_T)$ .

Note that the data  $y_t$  are not referenced in the gamma recursion; the alpha recursion has absorbed all of the necessary data likelihoods.

## 12.6 The $\xi(q_t, q_{t+1})$ variables

The alpha-beta or the alpha-gamma algorithm provide us with the posterior probability of the hidden states of the HMM. These quantities are the direct analogs of the posterior probabilities  $h_i$  that we studied in the simpler mixture setting. Moreover, they play the same role in estimating the parameters of the output distribution—as we will see in Section 12.8 they are the expected sufficient statistics for these parameters. To estimate the transition probability matrix  $A$ , however, we need something more. It is clear intuitively, and justified in Section 12.8, where we write out the complete log likelihood, that what is required is the matrix of cooccurrence probabilities  $p(q_t, q_{t+1}|y)$ . In this section we show how to calculate these posterior probabilities.

Let us define

$$\xi(q_t, q_{t+1}) \triangleq p(q_t, q_{t+1}|y). \quad (12.42)$$

There are several ways to calculate this quantity. One way is to return to first principles and develop recursions for the  $\xi(q_t, q_{t+1})$ , following much the same procedure as we followed for the singleton probabilities  $\gamma(q_t)$ . This is indeed a rather useful exercise (which we ask the reader to carry out in Exercise ??), not only because it reinforces the Markovian calculations that we have engaged in, but because it provides a stepping-stone to the general “junction tree algorithm” that we discuss in Chapter 17. That algorithm provides a general framework from which to derive all of the recursions that we describe in this chapter. Moreover, if we have an algorithm for calculating  $\xi(q_t, q_{t+1})$  in hand, we can also obtain the singleton probabilities via  $\gamma(q_t) = \sum_{q_{t+1}} \xi(q_t, q_{t+1})$ .

A second approach to calculating  $\xi(q_t, q_{t+1})$  is to build on the recursions already developed for the alphas and betas:

$$\xi(q_t, q_{t+1}) = p(q_t, q_{t+1}|y) \quad (12.43)$$

$$\begin{aligned} &= \frac{p(y|q_t, q_{t+1})p(q_{t+1}|q_t)p(q_t)}{p(y)} \\ &= \frac{p(y_0, \dots, y_t|q_t)p(y_{t+1}|q_{t+1})p(y_{t+2}, \dots, y_T|q_{t+1})p(q_{t+1}|q_t)p(q_t)}{p(y)} \\ &= \frac{\alpha(q_t)p(y_{t+1}|q_{t+1})\beta(q_{t+1})a_{q_t, q_{t+1}}}{p(y)}. \end{aligned} \quad (12.44)$$

This result can also be expressed in terms of alphas and gammas:

$$\xi(q_t, q_{t+1}) = \frac{\alpha(q_t)p(y_{t+1}|q_{t+1})\gamma(q_{t+1})a_{q_t, q_{t+1}}}{\alpha(q_{t+1})}. \quad (12.45)$$

In either case we see that we can readily calculate the  $\xi(q_t, q_{t+1})$  variables once we have finished the recursive calculation of the singleton probabilities  $\gamma(q_t)$ .

## 12.7 Numerical issues

To summarize, we have found that we can calculate all of the necessary posterior probabilities for the HMM recursively. Given an observed sequence  $y$ , we run the alpha recursion forward in time. If we require only the likelihood we simply sum the alphas at the final time step. If we also require the posterior probabilities of the states, we proceed to either the beta recursion or the gamma recursion.

Before these recursions are implemented on the computer, attention must be paid to numerical issues. In particular, the recursions involve repeated multiplications of small numbers and it is generally not long before the numbers underflow. To avoid underflow it suffices to normalize. We outline the basic ideas in Exercise ??, but in brief the procedure is as follows. The alpha variables,  $p(y_0, \dots, y_t, q_t)$ , can be viewed as unnormalized conditional probabilities. Indeed, normalizing means division by  $p(y_0, \dots, y_t)$ , which yields conditionals  $p(q_t|y_0, \dots, y_t)$ . Not only are these conditionals scaled in a numerically sensible manner, but they also have a sensible semantics—they are the filtered estimates of the states. In sum, one should always compute normalized alphas. In the backward direction, if one uses the gamma recursion one is already on safe ground—the gammas are conditional probabilities and hence sum to one. Moreover, it is easy to verify that normalized alphas can be used in Eq. 12.41 in place of the unnormalized alphas. Alternatively, if one uses the beta recursion, it turns out that a numerically sensible solution (although one that is devoid of probabilistic interpretation), is to use the normalization factors from the forward recursion to rescale the beta variables (these rescaled betas will not sum to one). It turns out that the rescaled variables are then used exactly as the original alphas and betas are used in the formulas for the posteriors  $\gamma(q_t)$  and  $\xi(q_t, q_{t+1})$  (i.e., the normalization factors cancel). See Exercise ?? for further discussion.

## 12.8 Parameter estimation

The parameters of an HMM are the transition matrix  $A$ , the initial probability distribution  $\pi$  and the parameters that are associated with the output probability distribution. In this section we discuss the problem of estimating these parameters from data.

Let  $\theta = (\pi, A, \eta)$  represent all of the parameters of the HMM model, where  $p(y_t|q_t, \eta)$  is the output distribution. The likelihood is given by  $p(y|\theta)$ , for a fixed observable sequence  $y$ . Taking the logarithm of Eq. 12.5 we have the following log likelihood:

$$p(y|\theta) = \log \sum_{q_0} \sum_{q_1} \cdots \sum_{q_T} \pi(q_0) \prod_{t=0}^{T-1} a_{q_t, q_{t+1}} \prod_{t=0}^T p(y_t|q_t, \eta). \quad (12.46)$$

Our goal is to maximize this expression with respect to  $\theta$ .

As with our earlier models, this is in principle just another optimization problem that can be solved via standard numerical optimization methods. In practice, however, the EM algorithm is generally used to estimate HMM parameters.

### 12.8.1 EM algorithm

The EM algorithm for the HMM presents no new difficulties to surmount and we will make relatively short work of the derivation. For concreteness we derive the algorithm for the case in which the outputs  $y_t$  are multinomial variables; it should be obvious how to change the derivation to accommodate other output types (cf. Exercise ??).

In the multinomial case,  $y_t$  is an  $N$ -component vector such that  $y_t^j$  is equal to one for a particular component and zero for all other components. We use the symbol  $\eta_{ij}$  to denote the probability that the  $j$ th component of  $y_t$  is one, given that the  $i$ th component of  $q_t$  is one; i.e.,  $\eta_{ij} \triangleq p(y_t^j = 1 | q_t^i = 1, \eta)$ . Using this notation we have:

$$p(y_t | q_t, \eta) = \prod_{i,j=1}^M [\eta_{ij}]^{q_t^i y_t^j} \quad (12.47)$$

as the general expression for the output distribution.

As usual we begin by writing down the complete log likelihood to discover the form of the M step estimates as well as the sufficient statistics that are needed for the E step. We have:

$$\log p(q, y) = \log \left\{ \pi_{q_0} \prod_{t=0}^{T-1} a_{q_t, q_{t+1}} \prod_{t=0}^T p(y_t | q_t, \eta) \right\} \quad (12.48)$$

$$= \log \left\{ \prod_{i=1}^M [\pi_i]^{q_0^i} \prod_{t=0}^{T-1} \prod_{i,j=1}^M [a_{ij}]^{q_t^i q_{t+1}^j} \prod_{t=0}^T \prod_{i,j=1}^M [\eta_{ij}]^{q_t^i y_t^j} \right\} \quad (12.49)$$

$$= \sum_{i=1}^M q_0^i \log \pi_i + \sum_{t=0}^{T-1} \sum_{i,j=1}^M q_t^i q_{t+1}^j \log a_{ij} + \sum_{t=0}^T \sum_{i,j=1}^M q_t^i y_t^j \log \eta_{ij}. \quad (12.50)$$

From this expression, we see that  $m_{ij} \triangleq \sum_{t=0}^{T-1} q_t^i q_{t+1}^j$  is the sufficient statistic for  $a_{ij}$ ,  $n_{ij} \triangleq \sum_{t=0}^T q_t^i y_t^j$  is the sufficient statistic for  $\eta_{ij}$ , and  $q_0^i$  is the sufficient statistic for  $\pi_i$ . The maximum likelihood estimates for the case of complete data are therefore given by:

$$\hat{a}_{ij} = \frac{m_{ij}}{\sum_{k=1}^M m_{ik}} \quad (12.51)$$

$$\hat{\eta}_{ij} = \frac{n_{ij}}{\sum_{k=1}^N n_{ik}} \quad (12.52)$$

$$\hat{\pi}_i = q_0^i. \quad (12.53)$$

All of these estimates have natural interpretations. Note that  $m_{ij}$  is the count of the number of times that the process is in state  $i$  and transitions to state  $j$ . Dividing by  $\sum_k m_{ik}$  yields the proportion of those transitions out of state  $i$  that go to state  $j$ —a natural estimate of  $a_{ij}$ . Similarly the estimate of  $\eta_{ij}$  is given by the proportion of times that the chain is in state  $i$  and produces the

$j$ th output value. Finally, for the estimate of  $\pi_i$ , we obtain a singular distribution that puts all of the probability mass at the observed initial state.<sup>3</sup>

We turn to the E step of the EM algorithm. Consider first the expectation of the sufficient statistic  $n_{ij} = \sum_{t=0}^T q_t^i y_t^j$ . We have:

$$E(n_{ij}|y, \theta^{(p)}) = \sum_{t=0}^T E(q_t^i|y, \theta^{(p)}) y_t^j \quad (12.54)$$

$$= \sum_{t=0}^T p(q_t^i = 1|y, \theta^{(p)}) y_t^j \quad (12.55)$$

$$\triangleq \sum_{t=0}^T \gamma_t^i y_t^j, \quad (12.56)$$

where we introduce the notation  $\gamma_t^i$  in the last line. By definition  $\gamma_t^i$  is equal to  $\gamma(q_t)$ , evaluated at that value of  $q_t$  such that  $q_t^i = 1$ . Note finally that the dependence of  $\gamma_t^i$  on  $\theta^{(p)}$  has been suppressed.

Similarly, for the sufficient statistic  $m_{ij}$ , we have:

$$E(m_{ij}|y, \theta^{(p)}) = \sum_{t=0}^{T-1} E(q_t^i q_{t+1}^j|y, \theta^{(p)}) \quad (12.57)$$

$$= \sum_{t=0}^{T-1} p(q_t^i q_{t+1}^j|y, \theta^{(p)}) \quad (12.58)$$

$$\triangleq \sum_{t=0}^{T-1} \xi_{t,t+1}^{ij}, \quad (12.59)$$

where we let  $\xi_{t,t+1}^{ij}$  denote  $\xi(q_t, q_{t+1})$  for  $(q_t, q_{t+1})$  such that  $q_t^i = 1$  and  $q_{t+1}^j = 1$ .

In summary, the sufficient statistics are calculated via the recursive forward-backward procedure from Section 12.4. We calculate the  $\gamma$  variables via either Eq.12.13 or Eq.12.41. The  $\xi$  variables are then calculated via Eq. 12.44 or Eq. 12.45.

With the estimated sufficient statistics in hand, we substitute into the maximum likelihood formulas (Eqs. 12.51, 12.52, and 12.53), to obtain the M step of the EM algorithm (also known, in the case of HMMs, as the “Baum-Welch updates”). We obtain:

$$\hat{\eta}_{ij}^{(p+1)} = \frac{\sum_{t=0}^T \gamma_t^i y_t^j}{\sum_{k=1}^N \sum_{t=0}^T \gamma_t^i y_t^k} = \frac{\sum_{t=0}^T \gamma_t^i y_t^j}{\sum_{t=0}^T \gamma_t^i}. \quad (12.60)$$

---

<sup>3</sup>In a more general setting, in which we have multiple repeated observations from a single HMM (i.e., data that are IID at the level of entire sequences), the estimate of  $\pi_i$  becomes the proportion of times that the chain starts in state  $i$ , and indeed the estimates in Eq. 12.51 and Eq. 12.52 also become averages over the multiple repetitions (cf. Exercise ??).

where we use the fact that  $\sum_{k=1}^N y_t^k = 1$ ,

$$\hat{a}_{ij}^{(p+1)} = \frac{\sum_{t=0}^{T-1} \xi_{t,t+1}^{i,j}}{\sum_{k=1}^M \sum_{t=0}^{T-1} \xi_{t,t+1}^{i,k}} = \frac{\sum_{t=0}^{T-1} \xi_{t,t+1}^{i,j}}{\sum_{t=0}^{T-1} \gamma_t^i}, \quad (12.61)$$

where by definition  $\sum_{k=1}^M \xi_{t,t+1}^{i,k} = \gamma_t^i$ , and:

$$\hat{\pi}_i^{(p+1)} = \gamma_0^i. \quad (12.62)$$

The EM algorithm iterates between performing these updates (the M step) and the forward-backward pass using the updated values (the E step).

## 12.9 Historical remarks and bibliography

# An Introduction to Probabilistic Graphical Models

Michael I. Jordan  
*University of California, Berkeley*

June 30, 2003



# Chapter 13

## The Multivariate Gaussian

In this chapter we present some basic facts regarding the multivariate Gaussian distribution. We discuss the two major parameterizations of the multivariate Gaussian—the *moment parameterization* and the *canonical parameterization*, and we show how the basic operations of marginalization and conditioning are carried out in these two parameterizations. We also discuss maximum likelihood estimation for the multivariate Gaussian.

### 13.1 Parameterizations

The multivariate Gaussian distribution is commonly expressed in terms of the parameters  $\mu$  and  $\Sigma$ , where  $\mu$  is an  $n \times 1$  vector and  $\Sigma$  is an  $n \times n$ , symmetric matrix. (We will assume for now that  $\Sigma$  is also positive definite, but later on we will have occasion to relax that constraint). We have the following form for the density function:

$$p(x|\mu, \Sigma) = \frac{1}{(2\pi)^{n/2} |\Sigma|^{1/2}} \exp \left\{ -\frac{1}{2}(x - \mu)^T \Sigma^{-1} (x - \mu) \right\}, \quad (13.1)$$

where  $x$  is a vector in  $\Re^n$ . The density can be integrated over volumes in  $\Re^n$  to assign probability mass to those volumes.

The geometry of the multivariate Gaussian is essentially that associated with the quadratic form  $f(x) = \frac{1}{2}(x - \mu)^T \Sigma^{-1} (x - \mu)$  in the exponent of the density. Recall our discussion in Chapter 6, where we showed that a quadratic form  $f(x)$  is a paraboloid with level surfaces, i.e., surfaces of the form  $f(x) = c$  for fixed  $c$ , being ellipsoids oriented along the eigenvectors of the matrix  $\Sigma$ . Now note that the exponential,  $\exp(\cdot)$ , is a scalar function that leaves the geometrical features of the quadratic form intact. That is, for any  $x$  lying on an ellipsoid  $f(x) = c$ , we obtain the value  $\exp\{-c\}$ . The maximum value of the exponential is 1, obtained at  $x = \mu$  where  $f(x) = 0$ . The paraboloid  $f(x)$  increases to infinity as we move away from  $x = \mu$ ; thus we obtain a “bump” in  $(n+1)$ -dimensional space centered at  $x = \mu$ . The level surfaces of the Gaussian bump are ellipsoids oriented along the eigenvectors of  $\Sigma$ .

The factor in front of the exponential in Eq. 13.1 is the normalization factor that ensures that the density integrates to one. To show that this factor is correct, we make use of the diagonalization

of  $\Sigma^{-1}$ . Diagonalization yields a product of  $n$  univariate Gaussians whose standard deviations are the eigenvalues of  $\Sigma$ . When we integrate, each of these univariate Gaussians contributes a factor  $\sqrt{2\pi}\lambda_i$  to the normalization, where  $\lambda_i$  is the  $i$ th eigenvalue of  $\Sigma$ . Recall that the determinant of a matrix is the product of its eigenvalues to obtain the result. (We ask the reader to fill in the details of this derivation in Exercise ??).

As in the univariate case, the parameters  $\mu$  and  $\Sigma$  have a probabilistic interpretation as the *moments* of the Gaussian distribution. In particular, we have the important result:

$$\mu = E(x) \tag{13.2}$$

$$\Sigma = E(x - \mu)(x - \mu)^T. \tag{13.3}$$

We will not bother to derive this standard result, but will provide a hint: diagonalize and appeal to the univariate case.

Although the moment parameterization of the Gaussian will play a principal role in our subsequent development, there is a second parameterization—the canonical parameterization—that will also be important. In particular, expanding the quadratic form in Eq. 13.1, and defining *canonical parameters*:

$$\Lambda = \Sigma^{-1} \tag{13.4}$$

$$\eta = \Sigma^{-1}\mu, \tag{13.5}$$

we obtain:

$$p(x|\eta, \Lambda) = \exp \left\{ a + \eta^T x - \frac{1}{2} x^T \Lambda x \right\}, \tag{13.6}$$

where  $a = -1/2(n \log(2\pi) - \log |\Lambda| + \eta^T \Lambda \eta)$  is the normalizing constant in this representation. The canonical parameterization is also sometimes referred to as the *information parameterization*.

We can also convert from canonical parameters to moment parameters:

$$\mu = \Lambda^{-1}\eta \tag{13.7}$$

$$\Sigma = \Lambda^{-1}. \tag{13.8}$$

Moment parameters and canonical parameters are useful in different circumstances. As we will see, different kinds of transformations are more readily carried out in one representation or the other.

## 13.2 Joint distributions

Suppose that we partition the  $n \times 1$  vector  $x$  into a  $p \times 1$  subvector  $x_1$  and a  $q \times 1$  subvector  $x_2$ , where  $n = p + q$ . Form corresponding partitions of the  $\mu$  and  $\Sigma$  parameters:

$$\mu = \begin{bmatrix} \mu_1 \\ \mu_2 \end{bmatrix} \quad \Sigma = \begin{bmatrix} \Sigma_{11} & \Sigma_{12} \\ \Sigma_{21} & \Sigma_{22} \end{bmatrix}, \tag{13.9}$$

We can write a joint Gaussian distribution for  $x_1$  and  $x_2$  using these partitioned parameters:

$$p(x|\mu, \Sigma) = \frac{1}{(2\pi)^{(p+q)/2} |\Sigma|^{1/2}} \exp \left\{ -\frac{1}{2} \begin{pmatrix} x_1 - \mu_1 \\ x_2 - \mu_2 \end{pmatrix}^T \begin{bmatrix} \Sigma_{11} & \Sigma_{12} \\ \Sigma_{21} & \Sigma_{22} \end{bmatrix}^{-1} \begin{pmatrix} x_1 - \mu_1 \\ x_2 - \mu_2 \end{pmatrix} \right\} \quad (13.10)$$

This partitioned form of the joint distribution raises a number of questions. In particular, we can equally well form partitioned versions of  $\eta$  and  $\Lambda$  and express the joint distribution in the canonical parameterization; is there any relationship between the partitioned form of these two representations? Also, what do the blocks in the partitioned forms have to do with the marginal and conditional probabilities of  $x_1$  and  $x_2$ ?

These questions all involve the manipulation of the quadratic forms in the exponents of the Gaussian densities; indeed, the underlying algebraic problem is that of “completing the square” of quadratic forms. In the next section, we discuss an algebra that provides a general solution to the problem of “completing the square.”

### 13.3 Partitioned matrices

Our first result in this section is to show how to block diagonalize a partitioned matrix. A number of useful results flow from this operation, including an explicit expression for the inverse of a partitioned matrix.

Consider a general partitioned matrix:

$$M = \begin{bmatrix} E & F \\ G & H \end{bmatrix}, \quad (13.11)$$

where we assume that both  $E$  and  $H$  are invertible. (Our results can be generalized beyond this setting). To invert this matrix, we follow a similar procedure to that of diagonalization. In particular, we wish to *block diagonalize* the matrix. We wish to put a block of zeros in place of  $G$  and a block of zeros in place of  $F$ .

To zero out the upper-right-hand corner of  $M$ , note that it suffices to *premultiply* the second block column of  $M$  by a “block row vector” having elements  $I$  and  $-FH^{-1}$ . Similarly, to zero out the lower-left-hand corner of  $M$ , it suffices to *postmultiply* the second row of  $M$  by a “block column vector” having elements  $I$  and  $-H^{-1}G$ . The magical fact is that these two operations do not interfere with each other; thus we can block diagonalize  $M$  by doing both operations. In particular, we have:

$$\begin{bmatrix} I & -FH^{-1} \\ 0 & I \end{bmatrix} \begin{bmatrix} E & F \\ G & H \end{bmatrix} \begin{bmatrix} I & 0 \\ -H^{-1}G & I \end{bmatrix} = \begin{bmatrix} E - FH^{-1}G & 0 \\ 0 & H \end{bmatrix}. \quad (13.12)$$

The correctness of this decomposition can be verified directly.

We define the *Schur complement* of the matrix  $M$  with respect to  $H$ , denoted  $M/H$ , as the term  $E - FH^{-1}G$  that appears in the block diagonal matrix. It is not difficult to show that  $M/H$  is invertible.

We now take the inverse of both sides of Eq. 13.12. Note that in a matrix expression of the form  $XYZ = W$  inverting both sides yields  $Y^{-1} = ZW^{-1}X$ ; this implies that we don't need to explicitly invert the block triangular matrices in Eq. 13.12 (although this is easily done). Note also that the inverse of a block diagonal matrix is the diagonal matrix of the inverse of its blocks. Thus we have:

$$\begin{bmatrix} E & F \\ G & H \end{bmatrix}^{-1} = \begin{bmatrix} I & 0 \\ -H^{-1}G & I \end{bmatrix} \begin{bmatrix} (M/H)^{-1} & 0 \\ 0 & H^{-1} \end{bmatrix} \begin{bmatrix} I & -FH^{-1} \\ 0 & I \end{bmatrix} \quad (13.13)$$

$$= \begin{bmatrix} (M/H)^{-1} & -(M/H)^{-1}FH^{-1} \\ -H^{-1}G(M/H)^{-1} & H^{-1} + H^{-1}G(M/H)^{-1}FH^{-1} \end{bmatrix}, \quad (13.14)$$

which expresses the inverse of a partitioned matrix in terms of its blocks.

We can also apply the determinant operator to both sides of Eq. 13.12. The block triangular matrices clearly have a determinant of one; thus we obtain another important result:

$$|M| = |M/H||H|. \quad (13.15)$$

(This result makes the choice of notation for the Schur complement seem quite natural!)

We are not yet finished. Note that we could alternatively have decomposed the matrix  $M$  in terms of  $E$  and  $M/E$ , yielding the following expression for the inverse:

$$\begin{bmatrix} E & F \\ G & H \end{bmatrix}^{-1} = \begin{bmatrix} E^{-1} + E^{-1}F(M/E)^{-1}GE^{-1} & -E^{-1}F(M/E)^{-1} \\ -(M/E)^{-1}GE^{-1} & (M/E)^{-1} \end{bmatrix}. \quad (13.16)$$

These two expressions for the inverse of  $M$  (Eq. 13.14 and Eq. 13.16) must be the same, thus we can set the corresponding blocks equal to each other. This yields:

$$(E - FH^{-1}G)^{-1} = E^{-1} + E^{-1}F(H - GE^{-1}F)^{-1}GE^{-1} \quad (13.17)$$

and

$$(E - FH^{-1}G)^{-1}FH^{-1} = E^{-1}F(H - GE^{-1}F)^{-1} \quad (13.18)$$

Both Eq. 13.17, which is generally referred to as the “matrix inversion lemma,” and Eq. 13.18 are quite useful in transformations involving Gaussian distributions. They allow expressions involving the inverse of  $E$  to be converted into expressions involving the inverse of  $H$  and vice versa.

## 13.4 Marginalization and conditioning

We now make use of our block diagonalization results to develop general formulas for the key operations of marginalization and conditioning in the multivariate Gaussian setting. We present results for both the moment parameterization and the canonical parameterization.

Our goal is to split the joint distribution Eq. 13.10 into a marginal probability for  $x_2$  and a conditional probability for  $x_1$  according to the factorization  $p(x_1, x_2) = p(x_1|x_2)p(x_2)$ . Focusing

first on the exponential factor, we make use of Eq. 13.12:

$$\begin{aligned}
& \exp \left\{ -\frac{1}{2} \begin{pmatrix} x_1 - \mu_1 \\ x_2 - \mu_2 \end{pmatrix}^T \begin{bmatrix} \Sigma_{11} & \Sigma_{12} \\ \Sigma_{21} & \Sigma_{22} \end{bmatrix}^{-1} \begin{pmatrix} x_1 - \mu_1 \\ x_2 - \mu_2 \end{pmatrix} \right\} \\
&= \exp \left\{ -\frac{1}{2} \begin{pmatrix} x_1 - \mu_1 \\ x_2 - \mu_2 \end{pmatrix}^T \begin{bmatrix} I & 0 \\ -\Sigma_{22}^{-1}\Sigma_{21} & I \end{bmatrix} \begin{bmatrix} (\Sigma/\Sigma_{22})^{-1} & 0 \\ 0 & \Sigma_{22}^{-1} \end{bmatrix} \begin{bmatrix} I & -\Sigma_{12}\Sigma_{22}^{-1} \\ 0 & I \end{bmatrix} \begin{pmatrix} x_1 - \mu_1 \\ x_2 - \mu_2 \end{pmatrix} \right\} \\
&= \exp \left\{ -\frac{1}{2}(x_1 - \mu_1 - \Sigma_{12}\Sigma_{22}^{-1}(x_2 - \mu_2))^T(\Sigma/\Sigma_{22})^{-1}(x_1 - \mu_1 - \Sigma_{12}\Sigma_{22}^{-1}(x_2 - \mu_2)) \right\} \\
&\quad \cdot \exp \left\{ -\frac{1}{2}(x_2 - \mu_2)^T\Sigma_{22}^{-1}(x_2 - \mu_2) \right\}. \tag{13.19}
\end{aligned}$$

We next exploit Eq. 13.15 to split the normalization into two factors:

$$\frac{1}{(2\pi)^{(p+q)/2}|\Sigma|^{1/2}} = \frac{1}{(2\pi)^{(p+q)/2}(|\Sigma/\Sigma_{22}| |\Sigma_{22}|)^{1/2}} \tag{13.20}$$

$$= \left( \frac{1}{(2\pi)^{p/2}|\Sigma/\Sigma_{22}|^{1/2}} \right) \left( \frac{1}{(2\pi)^{q/2}|\Sigma_{22}|^{1/2}} \right) \tag{13.21}$$

To see that we have achieved our goal of factorizing the joint distribution into the product of a marginal distribution and a conditional distribution, note that if we group the first factor in Eq. 13.19 with the first factor in Eq. 13.21 we obtain a normalized Gaussian in the variable  $x_1$ . Integrating with respect to  $x_1$ , these factors disappear and the remaining factors must therefore represent the marginal distribution of  $x_2$ :

$$p(x_2) = \frac{1}{(2\pi)^{q/2}|\Sigma/\Sigma_{22}|^{1/2}} \exp \left\{ -\frac{1}{2}(x_2 - \mu_2)^T\Sigma_{22}^{-1}(x_2 - \mu_2) \right\}. \tag{13.22}$$

Given this result, we are now licensed to interpret the factors that were integrated over as the conditional probability  $p(x_1|x_2)$ :

$$p(x_1|x_2) = \frac{1}{(2\pi)^{p/2}|\Sigma_{22}|^{1/2}} \exp \left\{ -\frac{1}{2}(x_1 - \mu_1 - \Sigma_{12}\Sigma_{22}^{-1}(x_2 - \mu_2))^T(\Sigma/\Sigma_{22})^{-1}(x_1 - \mu_1 - \Sigma_{12}\Sigma_{22}^{-1}(x_2 - \mu_2)) \right\} \tag{13.23}$$

To summarize our results, let  $(\mu_2^m, \Sigma_2^m)$  denote the moment parameters of the marginal distribution of  $x_2$ , and let  $(\mu_{1|2}^c, \Sigma_{1|2}^c)$  denote the moment parameters of the conditional distribution of  $x_1$  given  $x_2$ . Eq. 13.22 and Eq. 13.23 yield the following expressions for these parameters:

**Marginalization:**

$$\mu_2^m = \mu_2 \tag{13.24}$$

$$\Sigma_2^m = \Sigma_{22} \tag{13.25}$$

**Conditioning:**

$$\mu_{1|2}^c = \mu_1 + \Sigma_{12}\Sigma_{22}^{-1}(x_2 - \mu_2) \tag{13.26}$$

$$\Sigma_{1|2}^c = \Sigma_{11} - \Sigma_{12}\Sigma_{22}^{-1}\Sigma_{21} \tag{13.27}$$

We can also express the marginalization and conditioning operations in the canonical parameterization. The results can be obtained directly from the joint distribution, or indirectly by converting from the results for the moment parameterization. In any case, the results—which we ask the reader to derive in Exercise ??—are as follows:

### Marginalization:

$$\eta_2^m = \eta_2 - \Lambda_{21}\Lambda_{11}^{-1}\eta_1 \quad (13.28)$$

$$\Lambda_2^m = \Lambda_{22} - \Lambda_{21}\Lambda_{11}^{-1}\Lambda_{12} \quad (13.29)$$

### Conditioning:

$$\eta_{1|2}^c = \eta_1 - \Lambda_{12}x_2 \quad (13.30)$$

$$\Lambda_{1|2}^c = \Lambda_{11} \quad (13.31)$$

Note that the marginalization operation is simple in the moment parameterization and conditioning is complicated, whereas the opposite holds in the canonical parameterization.

## 13.5 Maximum likelihood estimation

Let us now suppose that we have an independently, identically distributed data set  $\mathcal{D} = \{x_1, x_2, \dots, x_N\}$  sampled from a multivariate Gaussian distribution. We want to estimate the parameters of the distribution via maximum likelihood.

We form the log likelihood function by taking the logarithm of the product of  $N$  Gaussians:

$$l(\mu, \Sigma | \mathcal{D}) = -\frac{N}{2} \log |\Sigma| - \frac{1}{2} \sum_{i=1}^N (x_i - \mu)^T \Sigma^{-1} (x_i - \mu). \quad (13.32)$$

Taking the derivative with respect to  $\mu$  is straightforward:

$$\frac{\partial l}{\partial \mu} = \sum_{i=1}^N (x_i - \mu)^T \Sigma^{-1}, \quad (13.33)$$

and setting to zero we obtain a pleasant result:

$$\hat{\mu} = \frac{1}{N} \sum_{i=1}^N x_i. \quad (13.34)$$

That is, the maximum likelihood estimate of the mean is the sample mean.

We now turn to the more challenging problem of computing the maximum likelihood estimate of the covariance matrix. Although the tools that we require to solve this problem are inevitably somewhat technical, they are important, and will reappear on several occasions later in the text.

Letting  $l(\Sigma | \mathcal{D})$  denote those terms in the log likelihood that are a function of  $\Sigma$ , we obtain:

$$l(\Sigma | \mathcal{D}) = -\frac{N}{2} \log |\Sigma| - \frac{1}{2} \sum_n (x_n - \mu)^T \Sigma^{-1} (x_n - \mu). \quad (13.35)$$

We need to take the derivative with respect to  $\Sigma$  and set to zero. To calculate this derivative we require a short detour.

### 13.5.1 Traces and derivatives

The trace of a square matrix  $A$  is defined to be the sum of the diagonal elements  $a_{ii}$  of  $A$ :

$$\text{tr}[A] \triangleq \sum_i a_{ii} \quad (13.36)$$

An important property possessed by the trace is its invariance under cyclical permutations of matrix products:

$$\text{tr}[ABC] = \text{tr}[CAB] = \text{tr}[BCA], \quad (13.37)$$

where  $A$ ,  $B$  and  $C$  are arbitrary matrices whose dimensions are conformal and are such that the product  $ABC$  (and therefore the other two products) is a square matrix. This result is easily established by writing out the matrix products explicitly.

Our interest in the trace is due to its usefulness in calculating derivatives of quadratic forms. In particular, we need to take the derivative of an expression of the form  $x^T Ax$  with respect to the matrix  $A$ . There is a “trick” involving the trace that makes such calculations easy. We write:

$$x^T Ax = \text{tr}[x^T Ax] = \text{tr}[xx^T A] \quad (13.38)$$

where the first equality follows from the fact that  $x^T Ax$  is a scalar. We see that we can calculate derivatives of quadratic forms by calculating derivatives of traces.

Let us calculate the derivative of  $\text{tr}[BA]$  with respect to  $A$ . We write out the matrix product explicitly and calculate the partial with respect to a matrix element  $a_{ij}$ :

$$\frac{\partial}{\partial a_{ij}} \text{tr}[AB] = \frac{\partial}{\partial a_{ij}} \sum_k \sum_l a_{kl} b_{lk} \quad (13.39)$$

$$= b_{ji}, \quad (13.40)$$

which shows that

$$\frac{\partial}{\partial A} \text{tr}[BA] = B^T. \quad (13.41)$$

We can now use this result to calculate the derivative of the quadratic form  $x^T Ax$ :

$$\frac{\partial}{\partial A} x^T Ax = \frac{\partial}{\partial A} \text{tr}[xx^T A] = [xx^T]^T = xx^T, \quad (13.42)$$

which is the outer product of the vector  $x$  with itself.

### 13.5.2 Determinants and derivatives

From Eq. (13.35) we see that we also need to take the derivative of the logarithm of a determinant. In this section we establish the following result:

$$\frac{\partial}{\partial A} \log |A| = A^{-T}, \quad (13.43)$$

which together with the result on traces will allow us to solve our estimation problem.

To establish the result, note that:

$$\frac{\partial}{\partial a_{ij}} \log |A| = \frac{1}{|A|} \frac{\partial}{\partial a_{ij}} |A| \quad (13.44)$$

and recall the formula for the matrix inverse:

$$A^{-1} = \frac{1}{|A|} \tilde{A}, \quad (13.45)$$

where  $\tilde{A}$  is the matrix of cofactors. This shows that we need only establish the following result:

$$\frac{\partial}{\partial a_{ij}} |A| = \tilde{A}. \quad (13.46)$$

The determinant of a square matrix  $A$  can be expanded as follows (this formula is often taken as the definition of the determinant):

$$|A| = \sum_j (-1)^{i+j} a_{ij} M_{ij} \quad (13.47)$$

where  $M_{ij}$  is the minor associated with matrix element  $a_{ij}$  (the determinant of the matrix obtained by removing the  $i$ th row and  $j$ th column of  $A$ ). Note that this formula holds for arbitrary  $i$ .

Given that  $a_{ij}$  does not appear in any of the minors in the sum, the derivative of  $|A|$  with respect to  $a_{ij}$  is just  $(-1)^{i+j} M_{ij}$ . But the matrix of these values is simply the transpose of the matrix of cofactors.

### 13.5.3 Maximum likelihood estimate of $\Sigma$

With these two results in hand, we return to the problem of calculating the maximum likelihood estimate of the covariance matrix  $\Sigma$ .

We use the trace trick to cope with the quadratic form:

$$l(\Sigma | \mathcal{D}) = -\frac{N}{2} \log |\Sigma| - \frac{1}{2} \sum_n (x_n - \mu)^T \Sigma^{-1} (x_n - \mu) \quad (13.48)$$

$$= \frac{N}{2} \log |\Sigma^{-1}| - \frac{1}{2} \sum_n \text{tr}[(x_n - \mu)^T \Sigma^{-1} (x_n - \mu)] \quad (13.49)$$

$$= \frac{N}{2} \log |\Sigma^{-1}| - \frac{1}{2} \sum_n \text{tr}[(x_n - \mu)(x_n - \mu)^T \Sigma^{-1}], \quad (13.50)$$

where we have also used the fact that the determinant of the inverse of a matrix is the inverse of the determinant.

We now take the derivative with respect to the matrix  $\Sigma^{-1}$ :

$$\frac{\partial l}{\partial \Sigma^{-1}} = \frac{N}{2} \Sigma - \frac{1}{2} \sum_n (x_n - \mu)(x_n - \mu)^T. \quad (13.51)$$

Finally, setting to zero yields the maximum likelihood estimator:

$$\hat{\Sigma}_{ML} = \frac{1}{N} \sum_n (x_n - \hat{\mu}_{ML})(x_n - \hat{\mu}_{ML})^T, \quad (13.52)$$

which is the expected result.

This result also allows us to obtain maximum likelihood estimates for the canonical parameters:

$$\hat{\Lambda} = \hat{\Sigma}_{ML}^{-1} \quad (13.53)$$

$$\hat{\eta} = \hat{\Sigma}_{ML}^{-1} \hat{\mu}_{ML}; \quad (13.54)$$

where we have used the fact that maximum likelihood estimates are invariant to changes in parameterization (see Exercise ??).

There is much more to say about maximum likelihood estimation for the multivariate Gaussian. In particular, it is significantly more interesting to obtain estimates of  $\Sigma$  when we have constraints on  $\Lambda$ , for example a constraint that requires that certain elements of  $\Lambda$  are zero. Indeed, as we will see in Chapter ??, this is a rather natural constraint in the world of graphical models.

## 13.6 Historical remarks and bibliography

[section yet to be written].

# An Introduction to Probabilistic Graphical Models

Michael I. Jordan  
*University of California, Berkeley*

June 30, 2003



## Chapter 14

# Factor Analysis

In this chapter we present a latent variable model in which the latent variable is a continuous random vector. The problem that we address is one of density estimation, although the ideas that we describe can be exploited in regression and classification settings well.

In many density estimation problems, the measured data vector may be high-dimensional, but we may have reason to believe that the data lie near a lower-dimensional manifold. In such a setting it may be useful to model the data generation process as a two-stage process, in which (1) a point in the manifold is generated according to a (simple) probability density, and (2) the observed data are generated conditionally from another (simple) density that is centered on the point. The coordinates of this point form the components of a latent random vector. Assuming that we wish to parameterize a continuous manifold, the latent variable is a continuous-valued random vector.

When we assume that the manifold is a linear subspace, we obtain a model known as *factor analysis*. Figure 14.3 shows the geometry underlying the factor analysis model. The observed data are assumed to lie near a  $p$ -dimensional subspace  $\mathcal{M}$  in  $\mathbb{R}^q$ , where  $p < q$ . Given a set of basis vectors  $\{\lambda_j\}$ , a point in  $\mathcal{M}$  can be represented as the product  $\Lambda x$ , where  $x$  is a coordinate vector and  $\Lambda$  is the matrix whose columns are the basis vectors  $\{\lambda_j\}$ . We treat the coordinate vectors as values of a continuous random vector  $X$ , endowing  $X$  with a probability density. Specifically, in the case of factor analysis, we assume that  $X$  is a Gaussian random vector. Finally, given a point in  $\mathcal{M}$ , the observed data  $Y$  are assumed to be generated according to a Gaussian distribution centered around that point. We can view the resulting density as the convolution of the Gaussian density on the manifold with a Gaussian distribution extending into  $\mathbb{R}^q$ , resulting in a “thick subspace” lying in  $\mathbb{R}^q$ .

From the point of view of generating the “thick subspace,” the basis vectors for  $\mathcal{M}$  are not unique. Indeed, as we will see in Section 14.1, any orthogonal transformation of the basis vectors leaves the likelihood invariant. Historically, factor analysis arose in a setting in which the goal was often that of recovering unique basis vectors—these are the “factors” that give the model its name. The lack of identifiability of the basis vectors is a problem from this point of view, and factor analysis has often been seen as “controversial.” From the point of view of density estimation, however, the interest is in the subspace and not any particular basis for describing the subspace. In this setting, factor analysis should not be viewed as any more “controversial” than any of the

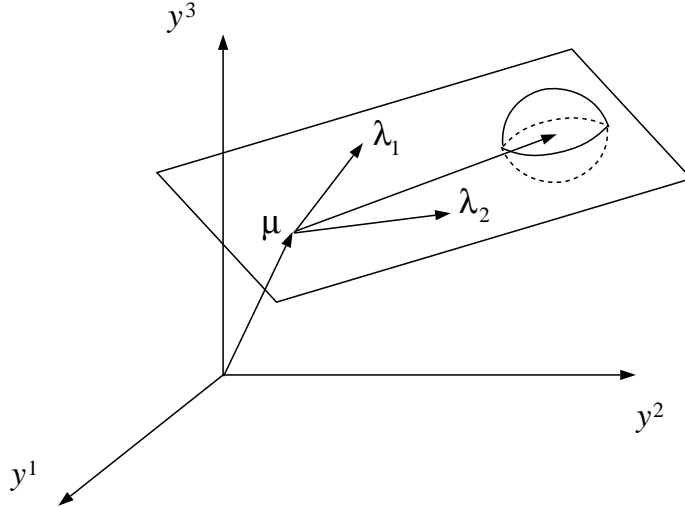


Figure 14.1: The geometry of the factor analysis model.

other models that we have described.

Factor analysis is closely related to *principal component analysis (PCA)*—another linear method for dimensionality reduction. Indeed, one can obtain PCA as a limiting case of factor analysis, much as one obtains the K-means algorithm as a limiting case of the Gaussian mixture model. We discuss PCA and some of the links between PCA and factor analysis in Section 14.4.

## 14.1 The model

The factor analysis model is shown as a graphical model in Figure 14.2. The model is comprised of a latent Gaussian variable  $X$  and an observable variable  $Y$ , where  $X$  is a  $p$ -dimensional random vector and  $Y$  a  $q$ -dimensional random vector, and where we assume  $p < q$ .

The model is parameterized as follows. Let  $X$  have a marginal Gaussian distribution:

$$X \sim \mathcal{N}(0, I), \quad (14.1)$$

with zero mean and an identity covariance matrix. Let the conditional distribution of  $Y$  be Gaussian, with mean  $\mu + \Lambda x$ :

$$Y \sim \mathcal{N}(\mu + \Lambda x, \Psi), \quad (14.2)$$

where  $\Psi$  is a diagonal covariance matrix.

The product of Gaussian distributions is Gaussian, and thus the joint distribution of  $X$  and  $Y$  is Gaussian, as are all marginals and conditionals computed under this joint. In particular, let us calculate the marginal of  $Y$  and the conditional distribution of  $X$  given  $Y$ .

We first calculate the marginal probability of  $Y$ , doing the calculation in two ways. The first approach is based on expressing  $Y$  as a sum:

$$Y = \mu + \Lambda x + W, \quad (14.3)$$

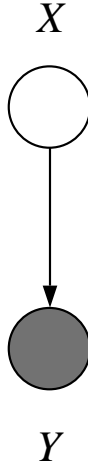


Figure 14.2: The factor analysis model as a graphical model.

where  $W$  is distributed as  $\mathcal{N}(0, \Psi)$ , and is independent of  $X$ . It is easy to verify that this representation yields the conditional distribution for  $Y$  in Eq. (14.2). We now make use of this representation to calculate the unconditional mean of  $Y$ :

$$E(Y) = E(\mu + \Lambda X + W) \quad (14.4)$$

$$= \mu + \Lambda EX + EW \quad (14.5)$$

$$= \mu, \quad (14.6)$$

and the unconditional covariance matrix of  $Y$ :

$$\text{Var}(Y) = E[(\mu + \Lambda X + W - \mu)(\mu + \Lambda X + W - \mu)^T] \quad (14.7)$$

$$= E[(\Lambda X + W)(\Lambda X + W)^T] \quad (14.8)$$

$$= \Lambda E(X X^T) \Lambda^T + E(W W^T) \quad (14.9)$$

$$= \Lambda \Lambda^T + \Psi. \quad (14.10)$$

Given that  $Y$  is Gaussian these two results determine the marginal distribution of  $Y$ .

There is another way to obtain these results that is based on the relationship between the conditional mean and covariance of a random vector  $Y$  and the unconditional mean and covariance. This approach will be particularly useful in Chapter 15. Recall that the conditional expectation,  $E(Y | X)$ , is a random variable, and thus it is meaningful to compute means and variances of  $E(Y | X)$ . In particular, in Appendix XXX we derive the following relationship:

$$E(Y) = E(E(Y | X)), \quad (14.11)$$

a result known as the *iterated expectation theorem*, and an analogous result for the variance:

$$\text{Var}(Y) = \text{Var}(E(Y | X)) + E(\text{Var}(Y | X)). \quad (14.12)$$

Let us now make use of these relationships to derive the unconditional distribution of  $Y$  for factor analysis. Using Eq. (14.11), we have:

$$E(Y) = E(\mu + \Lambda X) = \mu. \quad (14.13)$$

and from Eq. (14.12), we obtain:

$$\text{Var}(Y) = \text{Var}(\mu + \Lambda X) + E\Psi \quad (14.14)$$

$$= E[(\Lambda X)(\Lambda X)^T] + \Psi \quad (14.15)$$

$$= \Lambda\Lambda^T + \Psi; \quad (14.16)$$

the same results as before.

We also need to calculate the covariance of  $X$  and  $Y$ , which we can compute using Eq. (14.3):

$$\text{Cov}(X, Y) = E[X(\mu + \Lambda X + W - \mu)^T] \quad (14.17)$$

$$= E[X(\Lambda X + W)^T] \quad (14.18)$$

$$= \Lambda^T. \quad (14.19)$$

We can also obtain this expression using the following result from Appendix XXX:

$$\text{Cov}(X, Y) = \text{Cov}(X, E(Y | X)), \quad (14.20)$$

which yields:

$$\text{Cov}(X, Y) = \text{Cov}(X, \mu + \Lambda X) = \Lambda^T \quad (14.21)$$

as before.

Collecting together the results thus far, we have shown that the joint distribution of  $X$  and  $Y$  is a Gaussian with mean vector  $(0, \mu^T)^T$  and covariance matrix:

$$\Sigma = \begin{bmatrix} I & \Lambda^T \\ \Lambda & \Lambda\Lambda^T + \Psi \end{bmatrix}. \quad (14.22)$$

We can now calculate the conditional distribution of  $X$  given  $Y$ , using the results from Chapter 13. We begin by calculating the conditional mean of  $X$ :

$$E(X | y) = \Lambda^T(\Lambda\Lambda^T + \Psi)^{-1}(y - \mu). \quad (14.23)$$

Note that the matrix that must be inverted in this calculation is a  $(q \times q)$ -dimensional matrix. It is also possible to exploit Eq. (??) and invert a  $(p \times p)$ -dimensional matrix instead:

$$E(X | y) = (I + \Lambda^T\Psi^{-1}\Lambda)^{-1}\Lambda^T\Psi^{-1}(y - \mu). \quad (14.24)$$

In the context of factor analysis, in which  $p < q$ , Eq. (14.24) is the preferred way to compute the conditional expectation.

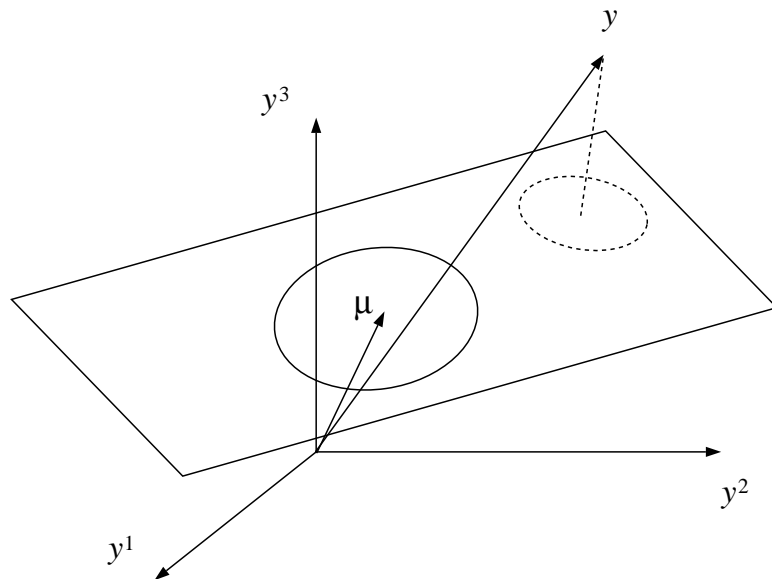


Figure 14.3: The solid ellipse corresponds to the Gaussian distribution of the latent variable  $X$  prior to the observation of  $Y$ . After  $Y = y$  is observed, the distribution of  $X$  is depicted as a dotted ellipse. The mean of the updated distribution given by Eq. (14.24) and the covariance is given by Eq. (14.26).

We also compute the conditional variance of  $X$ :

$$\text{Var}(X | y) = I - \Lambda^T(\Lambda\Lambda^T + \Psi)^{-1}\Lambda \quad (14.25)$$

$$= (I + \Lambda^T\Psi^{-1}\Lambda)^{-1}, \quad (14.26)$$

where we have used Eq. (??) in the second step. Again, for dimensionality reasons, we usually prefer to implement Eq. (14.26).

Figure ?? summarizes our results from a geometric point of view. Before observing  $Y$ , the distribution of  $X$  is a Gaussian centered around the origin of the latent variable subspace. After an observation  $Y = y$ , we obtain an updated distribution for  $X$ , where Eq. (14.24) determines the mean and Eq. (14.26) determines the updated covariance matrix of the updated distribution. We in essence “project”  $y$  onto the latent subspace, obtaining not only a point projection, but an estimate of uncertainty as well.

In summary, we have obtained the probability distribution of the latent variable given the observed variable—the analog of the calculation of the posterior probability  $\tau$  in Chapter ??.

## 14.2 Maximum likelihood estimation

We now turn to the problem of finding maximum likelihood estimates of the parameters of the factor analysis model.

### 14.2.1 The log likelihood

As in the case of the mixture model, the likelihood for the factor analysis model is a marginal probability. We have a seeming advantage in the case of the factor analysis, however, because the marginal probability can be calculated analytically. Indeed, as we have seen, the marginal probability of  $Y$  is a Gaussian with mean  $\mu$  and covariance matrix  $\Lambda\Lambda^T + \Psi$ . The log likelihood is therefore a Gaussian log likelihood:

$$l(\theta | D) = -\frac{N}{2} \log |\Lambda\Lambda^T + \Psi| - \frac{1}{2} \left\{ \sum_n (y_n - \mu)^T (\Lambda\Lambda^T + \Psi)^{-1} (y_n - \mu) \right\}, \quad (14.27)$$

where as usual we assume an IID data set  $D = \{y_n : n = 1, \dots, N\}$ .

We noted earlier that the likelihood remains invariant to orthogonal transformations of  $\Lambda$ . To show this, let  $R$  be an orthogonal matrix, and let  $\tilde{\Lambda} = \Lambda R$ . We have:

$$\tilde{\Lambda}\tilde{\Lambda}^T = \Lambda R(\Lambda R)^T = \Lambda R R^T \Lambda^T = \Lambda\Lambda^T. \quad (14.28)$$

Thus the likelihood, which depends on  $\Lambda$  only through the product  $\Lambda\Lambda^T$  is not changed if  $\Lambda$  is postmultiplied by  $R$ .

One useful consequence of Eq. (14.27) is an analytical formula for estimating the mean  $\mu$ . Indeed, from the point of view of estimating  $\mu$ , Eq. (14.27) is simply a Gaussian log likelihood, and we obtain the usual maximum likelihood estimate:

$$\hat{\mu}_{ML} = \frac{1}{N} \sum_n y_n, \quad (14.29)$$

by differentiating with respect to  $\mu$  and setting to zero.

In the remainder of this section, we will omit reference to the mean  $\mu$  in order to simplify our notation. In practice we estimate  $\mu$  according to Eq. (14.29) and then subtract the estimate from the data vectors. The resulting centered variables play the role of the data vectors  $y_n$  in the remainder of our discussion.

Unfortunately further progress in estimating the parameters is stymied—the parameters  $\Lambda$  and  $\Psi$  are coupled in Eq. (14.27), both by the determinant and the matrix inverse. There are no closed form expressions for the maxima of the log likelihood with respect to these parameters.

To decouple the parameters and obtain a simple algorithm for maximum likelihood estimation in factor analysis, we again make use of the EM algorithm.<sup>1</sup>

### 14.2.2 An EM algorithm

To derive an EM algorithm, we follow the recipe discussed in Chapter 11. In particular, we write down the complete log likelihood, take the expectation, and maximize the resulting expected complete log likelihood with respect to the parameters.

Before immersing ourselves in the algebra, however, let us step back and consider the results that we expect to obtain. Suppose in particular that we have “complete data”—pairs of observations of  $X$  and  $Y$ . Clearly the estimation of the distribution of  $X$  would reduce to a Gaussian density estimation problem in this case, although given our assumption that  $X$  has zero mean and identity covariance matrix, we have no parameters to estimate for the distribution of  $X$ . From Eq. (14.3) we see that  $Y$  is a linear function of  $x$ , with additive white Gaussian noise  $W$ . Thus, if both  $X$  and  $Y$  were observed, we would have a linear regression problem.

This argument suggests that if we can “fill in”  $X$  in the E step, we should find that the M step reduces to estimating  $\Lambda$  and  $\Psi$  using linear regression. This is in fact correct, but we need to take care in defining what we mean by “fill in.” In particular, it is not correct to simply replace  $X$  with its conditional expectation in the linear regression formulas. To obtain the correct result, we need to calculate the expected complete log likelihood and identify the expected sufficient statistics for our problem.

### 14.2.3 The E step

Given complete data,  $\mathcal{D}_c = \{(x_n, y_n) : n = 1, \dots, N\}$ , the complete likelihood is simply a product of Gaussian distributions. Taking the logarithm, we obtain:

$$l_c(\theta | \mathcal{D}_c) = -\frac{N}{2} \log |\Psi| - \frac{1}{2} \sum_n x_n^T x_n - \frac{1}{2} \sum_n (y_n - \Lambda x_n)^T \Psi^{-1} (y_n - \Lambda x_n). \quad (14.30)$$

Although this expression may appear daunting, it has the important property that  $\Lambda$  and  $\Psi$  are decoupled, although this fact may not yet be clear. It is in fact a much simpler expression to maximize than the log likelihood.

---

<sup>1</sup>An alternative approach is to use a nonlinear optimization algorithm such as conjugate gradients. See [?] for a presentation of this approach.

To make further progress we use the “trace trick.” Rewriting the quadratic forms, we have:

$$\begin{aligned} l_c(\theta | \mathcal{D}_c) &= -\frac{N}{2} \log |\Psi| - \frac{1}{2} \sum_n \text{tr}(x_n^T x_n) - \frac{1}{2} \sum_n \text{tr}[(y_n - \Lambda x_n)^T \Psi^{-1} (y_n - \Lambda x_n)] \\ &= -\frac{N}{2} \log |\Psi| - \frac{1}{2} \sum_n \text{tr}(x_n x_n^T) - \frac{1}{2} \sum_n \text{tr}[(y_n - \Lambda x_n)(y_n - \Lambda x_n)^T \Psi^{-1}] \\ &= -\frac{N}{2} \log |\Psi| - \frac{N}{2} \text{tr}(S \Psi^{-1}), \end{aligned} \quad (14.31)$$

where we have defined:

$$S \triangleq \frac{1}{N} \sum_n (y_n - \Lambda x_n)(y_n - \Lambda x_n)^T. \quad (14.32)$$

Note that this matrix has the form of a sample covariance matrix, although it depends on the unknown parameter  $\Lambda$ .

We now take the conditional expectation of the complete log likelihood, conditioning on the observed data  $y$  and the current parameter vector  $\theta^{(t)}$ . Using the operator notation  $\langle \cdot \rangle$  to denote this conditional expectation, we obtain:

$$Q(\theta | \theta^{(t)}) = -\frac{N}{2} \log |\Psi| - \frac{N}{2} \text{tr}(\langle S \rangle \Psi^{-1}), \quad (14.33)$$

We now calculate the conditional expectation  $\langle S \rangle$ —where we substitute the random variable  $X_n$  for  $x_n$  in the definition of  $S$  and treat  $S$  as a random quantity. We have:

$$\langle S \rangle = \frac{1}{N} \sum_n \langle y_n y_n^T - y_n X_n^T \Lambda^T - \Lambda X_n y_n^T + \Lambda X_n X_n^T \Lambda^T \rangle \quad (14.34)$$

$$= \frac{1}{N} \sum_n (y_n y_n^T - y_n \langle X_n^T \rangle \Lambda^T - \Lambda \langle X_n \rangle y_n^T + \Lambda \langle X_n X_n^T \rangle \Lambda^T), \quad (14.35)$$

where we see that we require the conditional expectations  $\langle X_n \rangle$  and  $\langle X_n X_n^T \rangle$ .

In summary, the expected sufficient statistics that we require for the E step are the conditional expectations  $\langle X_n \rangle$  and  $\langle X_n X_n^T \rangle$ . We have already obtained these expectations in Section 14.1. Thus:

$$\langle X_n \rangle = E(X_n | Y_n) \quad (14.36)$$

$$\langle X_n X_n^T \rangle = \text{Var}(X_n | y_n) + E(X_n | y_n)E(X_n | y_n)^T. \quad (14.37)$$

With these equations we “fill in” the conditional distribution of the latent variable  $X_n$ .

#### 14.2.4 The M step

We now turn to the M step. To calculate the necessary derivatives, let us recall from Section 13.5.2 how to take derivatives of log determinants:

$$\frac{\partial}{\partial A} \log |A| = A^{-T}, \quad (14.38)$$

and derivatives of traces:

$$\frac{\partial}{\partial A} \text{tr}[BA] = B^T. \quad (14.39)$$

In Appendix A we also derive a slight extension of the latter result:

$$\frac{\partial}{\partial A} \text{tr}[BA^TCA] = 2CAB, \quad (14.40)$$

when  $B$  and  $C$  are symmetric.

We compute the derivative of  $Q$  with respect to  $\Lambda$ . The relevant terms are:

$$Q(\Lambda | \theta^{(t)}) = -\frac{1}{2} \sum_n \text{tr} \left\{ (y_n y_n^T - y_n \langle X_n^T \rangle \Lambda^T - \Lambda \langle X_n \rangle y_n^T + \Lambda \langle X_n X_n^T \rangle \Lambda^T) \Psi^{-1} \right\}. \quad (14.41)$$

Taking the derivative, we obtain:

$$\frac{\partial Q}{\partial \Lambda} = \sum_n \Psi^{-1} y_n \langle X_n^T \rangle - \sum_n \Psi^{-1} \Lambda \langle X_n X_n^T \rangle, \quad (14.42)$$

where we have used the fact that  $\text{tr}[A] = \text{tr}[A^T]$  and the circulation property of the trace. Setting to zero, we obtain:

$$\Lambda^{(t+1)} = \left( \sum_n y_n \langle X_n^T \rangle \right) \left( \sum_n \langle X_n X_n^T \rangle \right)^{-1}. \quad (14.43)$$

This is the expected result—we have obtained the normal equations from linear regression.<sup>2</sup>

Finally we compute the derivative of  $Q$  with respect to  $\Psi$ . The terms in the expected complete log likelihood that depend on  $\Psi$  are:

$$Q(\Psi | \theta^{(t)}) = -\frac{N}{2} \log |\Psi| - \frac{N}{2} \text{tr}(\langle S \rangle \Psi^{-1}). \quad (14.44)$$

Recall that  $\Psi$  is a diagonal matrix. To calculate the derivative of  $Q$  with respect to  $\Psi$ , we take the usual matrix derivative but retain only the diagonal terms. Taking the derivative with respect to  $\Psi^{-1}$ , setting to zero and retaining only the diagonal terms yields:

$$\Psi^{(t+1)} = \text{diag}(\langle S \rangle). \quad (14.45)$$

Recall that  $S$  depends on the parameter  $\Lambda$ . Thus we must substitute  $\Lambda^{(t+1)}$  from Eq. (14.43) into the expression for  $\langle S \rangle$ . Carrying out this substitution, we find that we in fact obtain a simplification:

$$\langle S \rangle = \frac{1}{N} \sum_n \left( y_n y_n^T - y_n \langle X_n^T \rangle \Lambda^{(t+1)T} - \Lambda^{(t+1)} \langle X_n \rangle y_n^T + \Lambda^{(t+1)} \langle X_n X_n^T \rangle \Lambda^{(t+1)T} \right) \quad (14.46)$$

$$= \frac{1}{N} \left( \sum_n y_n y_n^T - \Lambda^{(t+1)} \langle X_n \rangle y_n^T \right), \quad (14.47)$$

---

<sup>2</sup>Note that in univariate regression the parameter vector enters into the regression model as a *row* vector. Writing the regression model using the notation of this chapter, we have:  $Y = \mu + \theta^T x + W$ , where  $Y$  is a scalar. In factor analysis each row of the matrix  $\Lambda$  corresponds to a parameter vector in univariate regression:  $Y = \mu + \Lambda x + W$ , where  $Y$  is a vector. Thus we should expect to obtain the transpose of the usual normal equations, and this is indeed what we obtain in Eq. (14.43).

and thus we have:

$$\Psi^{(t+1)} = \frac{1}{N} \text{diag} \left\{ \sum_n y_n y_n^T - \Lambda^{(t+1)} \sum_n \langle X_n \rangle y_n^T \right\}, \quad (14.48)$$

as the M step for  $\Psi$ .

### 14.3 Mixtures of factor analyzers

[Section not yet written].

### 14.4 Principal components analysis and factor analysis

[Section not yet written].

### 14.5 Appendix A

In this section we show how to calculate the derivative of the expression  $\text{tr}[BA^TCA]$  with respect to  $A$ . The calculation is based on the equation:

$$\frac{\partial}{\partial A} \text{tr}[BA] = B^T \quad (14.49)$$

that we established in Section 13.5.1.

We use the product rule, first holding  $A^T$  constant and then holding  $A$  constant. Placing a bar over a matrix to indicate that it is being treated as a constant, we have:

$$\frac{\partial}{\partial A} \text{tr}[BA^TCA] = \frac{\partial}{\partial A} \text{tr}[B\bar{A}^TCA] + \frac{\partial}{\partial A} \text{tr}[BA^TCA\bar{A}] \quad (14.50)$$

$$= (BA^T C)^T + \frac{\partial}{\partial A} \text{tr}[\bar{A}^T C^T AB^T] \quad (14.51)$$

$$= C^T AB^T + \frac{\partial}{\partial A} \text{tr}[B^T \bar{A}^T C^T A] \quad (14.52)$$

$$= C^T AB^T + (B^T A^T C^T)^T \quad (14.53)$$

$$= C^T AB^T + CAB. \quad (14.54)$$

A special case of this result is obtained when  $B$  and  $C$  are symmetric:

$$\frac{\partial}{\partial A} \text{tr}[BA^TCA] = 2CAB, \quad (14.55)$$

which is the result that we require in Section 14.2.4.

# An Introduction to Probabilistic Graphical Models

Michael I. Jordan  
*University of California, Berkeley*

June 30, 2003



## Chapter 15

# Kalman filtering and smoothing

Thus far we have presented two major categories of latent variable models: *mixture models*, which are based on a discrete latent variable, and *factor analysis models*, which are based on a continuous latent variable. The graphs underlying these models are identical—two-node graphs in which a single latent variable is connected to a single observable variable.

Chapter 12 presented a dynamical generalization of mixture models—the hidden Markov model (HMM). Graphically, the HMM was obtained by copying the two-node mixture model as a spatial array, connecting successive state nodes in the array. It is natural to wonder if a similar generalization of factor analysis might be worth considering. In fact the dynamical generalization of factor analysis is well worth considering—it yields an interesting and important methodology for time series analysis known as the *Kalman filter*. In fact, in an attempt to develop a consistent terminology, we reserve the term “Kalman filter” for the recursive inference algorithm that is the analog of the “alpha” algorithm in the HMM setting. The underlying model, which we refer to as the “state space model (SSM),” is structurally identical to the HMM; only the type of the nodes (real-valued vectors) and the probability model (linear-Gaussian) changes. The model has exactly the same Markov properties as the HMM, and its states are hidden in exactly the same way as in the HMM.

Historically, the HMM and the Kalman filtering methodology were developed in separate research communities and their close relationship has not always been widely appreciated. This is partly due to the fact that the general framework of graphical models came later than the HMM and the Kalman filter. Without the graphical framework, the algorithms underlying the inference calculation in the two cases look rather different (as we will see). This is, however, simply a reflection of the differences between the multinomial distribution and the Gaussian distribution, and it is imperative that we not let these details—important as they may be in practice—obscure the fundamental similarity between the two models.

We will develop the inference procedures for the SSM in some detail in this chapter. This is not only to acknowledge the historical importance of the Kalman filter, but also to provide an additional concrete example of the solution of the inference problem for a reasonably complex graphical model. Once we develop a general perspective on graphical models in Chapter 15, we will return to the SSM and the HMM, not only to provide concrete examples to ground our general theory, but also

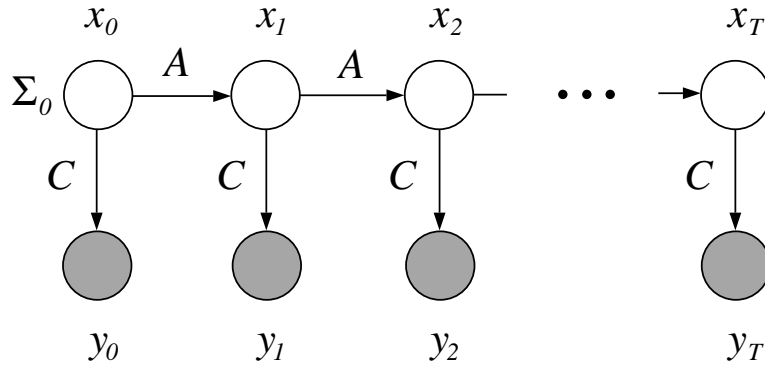


Figure 15.1: The SSM as a graphical model. Each vertical slice represents a time step. The top node in each slice represents the state variable  $x_t$  and the bottom node in each slice represents the observable output variable  $y_t$ .

to indicate that both are best viewed as jumping-off points for a much larger class of models.

## 15.1 The state space model

As we have already discussed, the model underlying Kalman filtering is a graphical model in the form of a chain (see Figure 15.1). We copy the two-node factor analysis model as an array and we link successive state nodes.

The independence relationships that characterize the SSM are identical to those that characterize the HMM. In particular, given the state at one moment in time, the states in the future are conditionally independent of those in the past. Moreover, the observation of the output nodes fails to separate any of the state nodes, and in general we expect for there to be a probabilistic relationship in the posterior distribution between all of the state nodes. As in the HMM, we hope that we can calculate these relationships recursively.

The state nodes in the factor analysis model are continuous, vector-valued nodes endowed with a Gaussian probability distribution. To develop a dynamical generalization of the factor analysis model we must represent the transition between the nodes at successive moments in time. Perhaps the simplest choice that we can make is to allow the mean of the state at time  $t+1$  to be a linear function of the state at time  $t$ . Thus we write:

$$x_{t+1} = Ax_t + Gw_t, \quad (15.1)$$

where  $w_t$  is a “noise” term—a Gaussian random variable that is independent of  $w_s$  for  $s < t$ , and thus independent of  $x_t$ . We assume that  $w_t$  has zero mean and covariance matrix  $Q$ . Given that the sum of Gaussian variables is Gaussian, we have that  $x_{t+1}$  is indeed Gaussian. Conditional on  $x_t$ , its mean is  $Ax_t$  and its covariance is  $GQG^T$ .

In the factor analysis model, the output is endowed with a Gaussian distribution having a mean

that is a linear function of the state. We continue to use this model for the output of the SSM:

$$y_t = Cx_t + v_t, \quad (15.2)$$

where  $v_t$  is a Gaussian random variable with zero mean and covariance matrix  $R$ . Conditional on  $x_t$ ,  $y_t$  is a Gaussian with mean  $Cx_t$  and covariance  $R$ .

Finally we endow the initial state,  $x_0$ , with a Gaussian distribution having mean 0 and covariance  $\Sigma_0$ . The assumption of zero mean is without loss of generality (a non-zero mean gives rise to a deterministic component that can be added to the probabilistic solution; see Exercise XXX for the details).

## 15.2 The unconditional distribution

Before beginning our investigation of the inference problem for the SSM, it is of interest to study the unconditional distribution of the states  $x_t$ .

The unconditional mean of  $x_t$  is clearly zero. This follows from the assumption that  $x_0$  has zero mean, and via the dynamical equation (Eq. 15.1) each successive state has zero mean.

Turning to the unconditional covariance, which we denote  $\Sigma_t$ , we have:

$$\Sigma_{t+1} \triangleq E[x_{t+1}x_{t+1}^T] \quad (15.3)$$

$$= E[(Ax_t + Gw_t)(Ax_t + Gw_t)^T] \quad (15.4)$$

$$= AE[x_t x_t^T]A^T + GE[w_t w_t^T]G^T \quad (15.5)$$

$$= A\Sigma_t A^T + GQG^T, \quad (15.6)$$

where we have made use of our independence assumptions. This equation, a dynamical equation for the evolution of the unconditional covariance, is referred to as the *Lyapunov equation*.

It can also be verified that the unconditional covariance between neighboring states  $x_t$  and  $x_{t+1}$  is given by  $\Sigma_t A^T$ .

## 15.3 Inference

The inference problem for the SSM is the same as it was for the HMM—that of calculating the posterior probability of the states given an output sequence. Based on our experience with the HMM, we hope to be able to calculate such posterior probabilities recursively.

In the case of the HMM, we were able to decompose the inference problem into a “forward” problem and a “backward” problem. In the forward problem the evidence consisted of a partial sequence of outputs—all those outputs up to time  $t$ . The backward problem also utilized a partial sequence—all those outputs after time  $t$ . We will find that this same decomposition will yield recursive algorithms for the SSM.

As in the case of the HMM we distinguish between “filtering” and “smoothing”—two classes of problems that arise in this graphical model when we introduce evidence. We develop algorithms for solving both problems.

## 15.4 Filtering

The problem is to calculate an estimate of the state  $x_t$  based on a partial output sequence  $y_0, \dots, y_t$ . That is, we wish to calculate  $P(x_t|y_0, \dots, y_t)$ .<sup>1</sup>

Sums of Gaussian variables are Gaussian, and thus, considering all of the variables in the SSM jointly, we have a (large) multivariate Gaussian distribution. Conditionals of Gaussians are Gaussian (see Chapter 13) and thus the probability distribution  $P(x_t|y_0, \dots, y_t)$  must be Gaussian. This implies that we need only calculate a mean vector and a covariance matrix (or the corresponding canonical parameters). As we will see, inference in the SSM involves finding a recursion linking these conditional means and conditional covariances at neighboring moments in time.

We use a simplified notation for the conditional means and conditional covariances that emphasizes the particular output sequence being conditioned on. We write  $\hat{x}_{t|t}$  to denote the mean of  $x_t$  conditioned on the partial sequence  $y_0, \dots, y_t$ . The covariance matrix of  $x_t$  conditioned on  $y_0, \dots, y_t$  is denoted  $P_{t|t}$ ; thus:

$$\hat{x}_{t|t} \triangleq E[x_t|y_0, \dots, y_t] \quad (15.7)$$

$$P_{t|t} \triangleq E[(x_t - \hat{x}_{t|t})(x_t - \hat{x}_{t|t})^T|y_0, \dots, y_t]. \quad (15.8)$$

In our derivation of the algorithm, we will find that it is useful as an intermediate step to compute the probability distribution of  $x_t$  conditioned on  $y_0, \dots, y_{t-1}$ . In our new notation, this distribution has mean  $\hat{x}_{t|t-1}$  and covariance matrix  $P_{t|t-1}$ .

To uncover the recursion behind the Kalman filter, let us refer to the graphical model fragments in Figure 15.2. In the fragment on the left, where we condition on the outputs  $y_0, \dots, y_t$ , we assume that we have already calculated  $P(x_t|y_0, \dots, y_t)$ ; that is, we have calculated  $\hat{x}_{t|t}$  and  $P_{t|t}$ . We wish to carry this distribution forward into the fragment on the right, where we condition on  $y_0, \dots, y_{t-1}$ . We decompose the transformation into two steps:

**time update:**  $P(x_t|y_0, \dots, y_t) \rightarrow P(x_{t+1}|y_0, \dots, y_t)$

**measurement update:**  $P(x_{t+1}|y_0, \dots, y_t) \rightarrow P(x_{t+1}|y_0, \dots, y_{t+1})$

Thus, in the *time update* step, we simply propagate the distribution forward one step in time, calculating the new mean and covariance based on the old mean and covariance, but based on no new measurements (i.e., no new outputs). In the *measurement update* step, we incorporate the new measurement  $y_{t+1}$  and update the probability distribution for  $x_{t+1}$ . The overall result is a transformation from  $\hat{x}_{t|t}$  and  $P_{t|t}$  to  $\hat{x}_{t+1|t+1}$  and  $P_{t+1|t+1}$ .

Let us first consider the time update step. Recall the dynamic equation (Eq. 15.1):

$$x_{t+1} = Ax_t + Gw_t. \quad (15.9)$$

---

<sup>1</sup>Note that this quantity is analogous to the normalized alpha variable from the HMM—the alpha variables themselves are *joint* probabilities:  $P(x_t, y_0, \dots, y_t)$ . The alphas and normalized alphas differ from each other, however, only by the normalization constant. In the Gaussian case we represent probability distributions by storing only the mean and covariance matrix (or the corresponding canonical parameters); the normalization factor is implicit. Thus there is no difference between “alphas” and “normalized alphas” in the SSM setting; all probabilities are implicitly normalized.

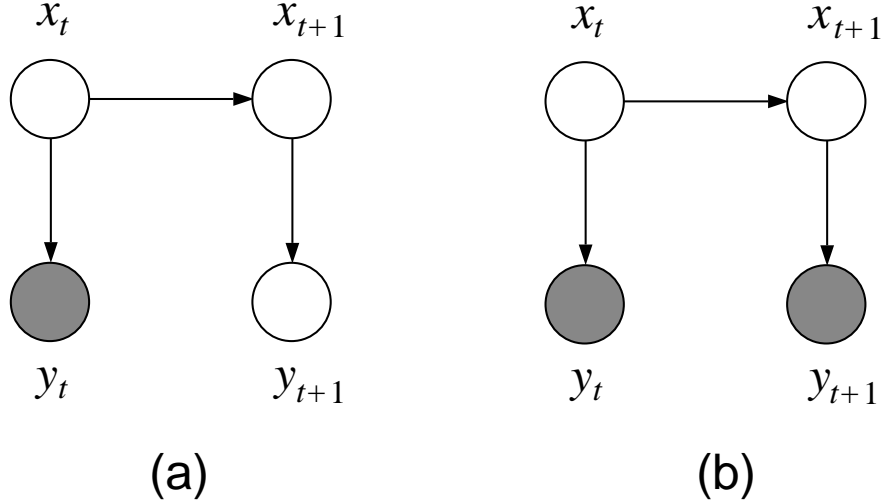


Figure 15.2: (a) A fragment of an SSM before a measurement update and (b) after a measurement update.

We take the conditional expectation on both sides of this equation. Given that  $w_t$  is independent of the conditioning variables  $y_0, \dots, y_t$ , the second term vanishes, and we have:

$$\hat{x}_{t+1|t} = A\hat{x}_{t|t}. \quad (15.10)$$

Similarly, taking the conditional covariance of both sides of the dynamic equation, we have:

$$P_{t+1|t} = E \left[ (x_{t+1} - \hat{x}_{t+1|t})(x_{t+1} - \hat{x}_{t+1|t})^T \mid y_0, \dots, y_t \right] \quad (15.11)$$

$$= E[(Ax_t + Gw_t - A\hat{x}_{t|t})(Ax_t + Gw_t - A\hat{x}_{t|t})^T | y_0, \dots, y_t] \quad (15.12)$$

$$= AP_{t|t}A^T + GQG^T, \quad (15.13)$$

where we have used the facts that  $\hat{x}_{t+1|t}$  is a constant in the conditional distribution,  $w_t$  has zero mean, and  $w_t$  and  $x_t$  are independent.

Now that we know the conditional distribution of  $x_{t+1}$  we proceed further in the graphical model fragment and calculate the conditional mean and covariance of  $y_{t+1}$ , as well as the conditional covariance of  $x_{t+1}$  and  $y_{t+1}$ . These calculations allow us to write down the joint conditional distribution of  $x_{t+1}$  and  $y_{t+1}$ , at which point the measurement update becomes a simple matter of “reversing the arrow”—calculating the conditional distribution of  $x_{t+1}$  given  $y_{t+1}$ .

The calculations are straightforward:

$$E[y_{t+1}|y_0, \dots, y_t] = E[Cx_{t+1} + v_{t+1}|y_0, \dots, y_t] \quad (15.14)$$

$$= C\hat{x}_{t+1|t} \quad (15.15)$$

$$E \left[ (y_{t+1} - \hat{y}_{t+1|t}) (y_{t+1} - \hat{y}_{t+1|t})^T | y_0, \dots, y_t \right]$$

$$= E[(Cx_{t+1} + v_{t+1} - C\hat{x}_{t+1|t})(Cx_{t+1} + v_{t+1} - C\hat{x}_{t+1|t})^T | y_0, \dots, y_t] \quad (15.16)$$

$$= CP_{t+1|t}C^T + R \quad (15.17)$$

and

$$E[(y_{t+1} - \hat{y}_{t+1|t})(x_{t+1} - \hat{x}_{t+1|t})^T | y_0, \dots, y_t]$$

$$= E[(Cx_{t+1} + v_{t+1} - \hat{y}_{t+1|t})(x_{t+1} - \hat{x}_{t+1|t})^T | y_0, \dots, y_t] \quad (15.18)$$

$$= CP_{t+1|t}, \quad (15.19)$$

where we have made use of the various independence assumptions.

We summarize these results as follows. Conditioned on the past outputs  $y_0, \dots, y_t$ , the variables  $x_{t+1}$  and  $y_{t+1}$  have a joint Gaussian distribution, with mean and covariance matrix:

$$\begin{bmatrix} \hat{x}_{t+1|t} \\ C\hat{x}_{t+1|t} \end{bmatrix} \quad \text{and} \quad \begin{bmatrix} P_{t+1|t} & P_{t+1|t}C^T \\ CP_{t+1|t} & CP_{t+1|t}C^T + R \end{bmatrix} \quad (15.20)$$

This leaves us in a situation which is familiar to us from factor analysis. Making reference to Figure 15.2(b), we have a Gaussian graphical model fragment in which we wish to reverse the arrow; that is, we wish to compute the conditional distribution of  $x_{t+1}$  given  $y_{t+1}$ , where  $x_{t+1}$  and  $y_{t+1}$  have a joint Gaussian distribution. The only difference in the current situation is that the joint distribution is itself a conditional distribution, conditioned on the past outputs  $y_0, \dots, y_t$ .

Utilizing Eq. 13.26 and 13.27 from Chapter 13, we obtain:

$$\hat{x}_{t+1|t+1} = \hat{x}_{t+1|t} + P_{t+1|t}C^T(CP_{t+1|t}C^T + R)^{-1}(y_{t+1} - C\hat{x}_{t+1|t}) \quad (15.21)$$

$$P_{t+1|t+1} = P_{t+1|t} - P_{t+1|t}C^T(CP_{t+1|t}C^T + R)^{-1}CP_{t+1|t}. \quad (15.22)$$

We summarize the filtering equations that we have obtained. At time  $t$  we assume that we have available the mean estimate  $\hat{x}_{t|t}$  and the covariance estimate  $P_{t|t}$ . Based on these estimates we calculate  $\hat{x}_{t+1|t+1}$  and  $P_{t+1|t+1}$  recursively as follows:

$$\hat{x}_{t+1|t} = A\hat{x}_{t|t} \quad (15.23)$$

$$P_{t+1|t} = AP_{t|t}A^T + GQG^T \quad (15.24)$$

$$\hat{x}_{t+1|t+1} = \hat{x}_{t+1|t} + P_{t+1|t}C^T(CP_{t+1|t}C^T + R)^{-1}(y_{t+1} - C\hat{x}_{t+1|t}) \quad (15.25)$$

$$P_{t+1|t+1} = P_{t+1|t} - P_{t+1|t}C^T(CP_{t+1|t}C^T + R)^{-1}CP_{t+1|t}. \quad (15.26)$$

These recursions constitute the Kalman filter. They are initialized with  $\hat{x}_{0|-1} = 0$  and  $P_{0|-1} = P_0$ .

The update in Eq. 15.25 is often summarized in more a compact form by defining the *Kalman gain matrix*:

$$K_{t+1} \triangleq P_{t+1|t}C^T(CP_{t+1|t}C^T + R)^{-1}. \quad (15.27)$$

Using this notation we have:

$$\hat{x}_{t+1|t+1} = \hat{x}_{t+1|t} + K_{t+1}(y_{t+1} - C\hat{x}_{t+1|t}). \quad (15.28)$$

Moreover, we can use the matrix inversion formulas to write the gain matrix in an alternative form. In particular, using Eq. 13.17 and Eq. 13.18, we obtain:

$$K_{t+1} = P_{t+1|t} C^T (C P_{t+1|t} C^T + R)^{-1} \quad (15.29)$$

$$= (P_{t+1|t}^{-1} + C^T R C)^{-1} C^T R^{-1} \quad (15.30)$$

$$= (P_{t+1|t} + P_{t+1|t} C^T (C P_{t+1|t} C^T + R)^{-1} C P_{t+1|t}) C^T R^{-1} \quad (15.31)$$

$$= P_{t+1|t+1} C^T R^{-1}, \quad (15.32)$$

which expresses the gain matrix in terms of the updated matrix  $P_{t+1|t+1}$ .

## 15.5 Interpretation and relationship to LMS

The Kalman filtering equations have an appealing interpretation as an error-correcting algorithm. Let us write a single equation for the update of the mean by combining Eq. 15.23 and Eq. 15.25:

$$\hat{x}_{t+1|t+1} = A\hat{x}_{t|t} + K_{t+1}(y_{t+1} - CA\hat{x}_{t|t}). \quad (15.33)$$

Eq. 15.33 describes an error-correcting algorithm for estimating the state  $x_{t+1}$ . In particular, at time  $t$ , our best estimate of the state  $x_t$  is  $\hat{x}_{t|t}$ . Imitating the dynamical equation we produce an estimate  $A\hat{x}_{t|t}$  of the state at time  $t+1$ . This estimate is then corrected based on the observation  $y_{t+1}$ ; in particular, we adjust our estimate by a term  $(y_{t+1} - CA\hat{x}_{t|t})$  that is proportional to the error between the observed output and our prediction of the output.

This error-correction procedure is reminiscent of the LMS algorithm. To clarify the relationship, consider a simplified situation in which the matrix  $A$  is the identity matrix and the noise term  $w_t$  is zero. In this case, the “dynamical equation”  $x_{t+1} = x_t + Gw_t$  reduces to the statement that the “state” is a constant. Let  $\theta$  denote this constant. Furthermore, let the matrix  $C$  in Eq. 15.2 be replaced by the (time-varying) vector  $x_t^T$  (as in Section XXX). In this case, Eq. 15.2 reduces to:

$$y_t = x_t^T \theta + v_t. \quad (15.34)$$

We are back in the world of linear regression, in which the outputs  $y_t$  are a sequence of iid observations that provide information about the parameter vector  $\theta$ . In this case the Kalman filtering equation becomes:

$$\hat{\theta}_{t+1} = \hat{\theta}_t + P_{t+1} R^{-1} (y_{t+1} - x_t^T \hat{\theta}) x_t, \quad (15.35)$$

where we have used the fact that  $R^{-1}$  is a scalar and have dropped the unnecessary second time subscript on the  $P$  matrix.

We have derived an equation which, when combined with the update for  $P_{t+1}$ , is referred to as the *recursive least squares (RLS) algorithm*. RLS is a special case of the Kalman filter and, as such, provides the optimal least-squares estimate of  $\theta$  based on data  $y_t$  up to and including time  $t$ .

If we proceed further and approximate the matrix  $P_{t+1} R^{-1}$  with a scalar multiplier  $\mu$ , Eq. 15.35 reduces to the LMS algorithm (Eq. 6.6). Thus LMS can be viewed as an approximation to the Kalman filter. We have gained in simplicity—no longer needing to carry forward a covariance

matrix—but we have lost in accuracy. The LMS algorithm requires multiple passes through a data set to converge to the least-squares estimate of the parameter; the Kalman filter converges in a single pass.

Although this connection between the Kalman filter and the LMS algorithm is a interesting and useful relationship to be aware of, the approximation of  $P_{t+1}R^{-1}$  by a scalar multiplier receives no particular justification within the theory of Kalman filtering. Rather it requires a different theoretical framework (that of stochastic approximation) for its justification.

## 15.6 Information filter

Recall that the multivariate Gaussian distribution can be described using either the moment parameterization or the canonical parameterization. Our derivation of the Kalman filter used the moment parameterization of the Gaussian, but it is also of interest to define a filtering algorithm in terms of the canonical parameterization. The result is an algorithm known as an *information filter*.

We can derive the information filter either from first principles or by transforming the equations that we have already obtained. We pursue the former approach in Chapter 18, where we reconsider the SSM from the perspective of the junction tree framework. In the current section we pursue the latter approach. This is essentially an exercise in the use of the matrix inversion lemmas (Eq. 13.17 and Eq. 13.18).

Recall from Chapter 13 that the canonical parameters of a Gaussian distribution can be obtained from the moment parameters by the following transformation (cf. Eq. 13.5):  $\Lambda = \Sigma^{-1}$  and  $\xi = \Sigma^{-1}\mu$ . Define  $\hat{\xi}_{t|t-1}$  and  $S_{t|t-1}$  to be the canonical parameters of the distribution of  $x_t$  conditioned on  $y_{1,\dots,t-1}$  and let  $\hat{\xi}_{t|t}$  and  $S_{t|t}$  to be the canonical parameters of the distribution of  $x_t$  conditioned on  $y_{1,\dots,t}$ . We obtain a set of recursions for these quantities by substituting from Eqs. 15.23 to 15.26.

Let us begin with the inverse covariance matrices. Defining  $H \triangleq GQG^T$  to simplify the notation, we have:

$$S_{t+1|t} = P_{t+1|t}^{-1} \quad (15.36)$$

$$= (AP_{t|t}A^T + H)^{-1} \quad (15.37)$$

$$= H^{-1} - H^{-1}A(P_{t|t}^{-1} + A^TH^{-1}A)^{-1}A^TH^{-1} \quad (15.38)$$

$$= H^{-1} - H^{-1}A(S_{t|t} + A^TH^{-1}A)^{-1}A^TH^{-1}. \quad (15.39)$$

A further application of the matrix inversion lemma yields:

$$S_{t+1|t+1} = P_{t+1|t+1}^{-1} \quad (15.40)$$

$$= (P_{t+1|t} - P_{t+1|t}C^T(CP_{t+1|t}C^T + R)^{-1}CP_{t+1|t})^{-1} \quad (15.41)$$

$$= P_{t+1|t}^{-1} + C^TR^{-1}C \quad (15.42)$$

$$= S_{t+1|t} + C^TR^{-1}C. \quad (15.43)$$

Turning now to the  $\xi$  parameters, we have:

$$\hat{\xi}_{t+1|t} = P_{t+1|t}^{-1} \hat{x}_{t+1|t} \quad (15.44)$$

$$= P_{t+1|t}^{-1} A \hat{x}_{t|t} \quad (15.45)$$

$$= P_{t+1|t}^{-1} A P_{t|t} \hat{\xi}_{t|t} \quad (15.46)$$

$$= (A P_{t|t} A^T + H)^{-1} A P_{t|t} \hat{\xi}_{t|t} \quad (15.47)$$

$$= H^{-1} A (P_{t|t}^{-1} + A^T H^{-1} A)^{-1} \hat{\xi}_{t|t} \quad (15.48)$$

$$= H^{-1} A (S_{t|t} + A^T H^{-1} A)^{-1} \hat{\xi}_{t|t}, \quad (15.49)$$

and

$$\hat{\xi}_{t+1|t+1} = P_{t+1|t+1}^{-1} \hat{x}_{t+1|t+1} \quad (15.50)$$

$$= P_{t+1|t+1}^{-1} (\hat{x}_{t+1|t} + P_{t+1|t+1} C^T R^{-1} (y_{t+1} - C \hat{x}_{t+1|t})) \quad (15.51)$$

$$= (P_{t+1|t+1}^{-1} - C^T R^{-1} C) P_{t+1|t}^{-1} \hat{\xi}_{t+1|t} + C^T R^{-1} y_{t+1} \quad (15.52)$$

$$= (P_{t+1|t}^{-1} + C^T R^{-1} C - C^T R^{-1} C) P_{t+1|t}^{-1} \hat{\xi}_{t+1|t} + C^T R^{-1} y_{t+1} \quad (15.53)$$

$$= \hat{\xi}_{t+1|t} + C^T R^{-1} y_{t+1}. \quad (15.54)$$

We summarize the information filter equations. At time  $t$  we assume that we have available  $\hat{\xi}_{t|t}$  and  $S_{t|t}$ . Based on these estimates we calculate  $\hat{\xi}_{t+1|t+1}$  and  $S_{t+1|t+1}$  recursively as follows:

$$\hat{\xi}_{t+1|t} = H^{-1} A (S_{t|t} + A^T H A)^{-1} \hat{\xi}_{t|t} \quad (15.55)$$

$$\hat{\xi}_{t+1|t+1} = \hat{\xi}_{t+1|t} + C^T R^{-1} y_{t+1} \quad (15.56)$$

$$S_{t+1|t} = H^{-1} - H^{-1} A (S_{t|t} + A^T H^{-1} A)^{-1} A^T H^{-1} \quad (15.57)$$

$$S_{t+1|t+1} = S_{t+1|t} + C^T R^{-1} C. \quad (15.58)$$

These recursions are initialized with  $\hat{\xi}_{0|-1} = \bar{\xi}_0$  and  $S_{0|-1} = S_0$ .

The Kalman filter and the information filter are mathematically equivalent; the major practical difference between them is essentially numerical. Recall that the condition number of a matrix is the reciprocal of the condition number of its inverse; this implies that poor conditioning for one set of recursions generally implies good conditioning for the other set. A related issue concerns the initial conditions. If we are quite certain about the initial state, then we would set  $P_0$  to zero, in which case  $S_0$  is undefined and we would be forced to use the Kalman filter. On the other hand, if we are quite uncertain about the initial state, we would set  $S_0$ , in which case  $P_0$  is undefined and we would be forced to use the information filter.

## 15.7 Smoothing

We now turn to the issue of obtaining estimates of the state at time  $t$  based on data up to and including a later time  $T$ . As in the case of the HMM, the calculation of this state estimate requires

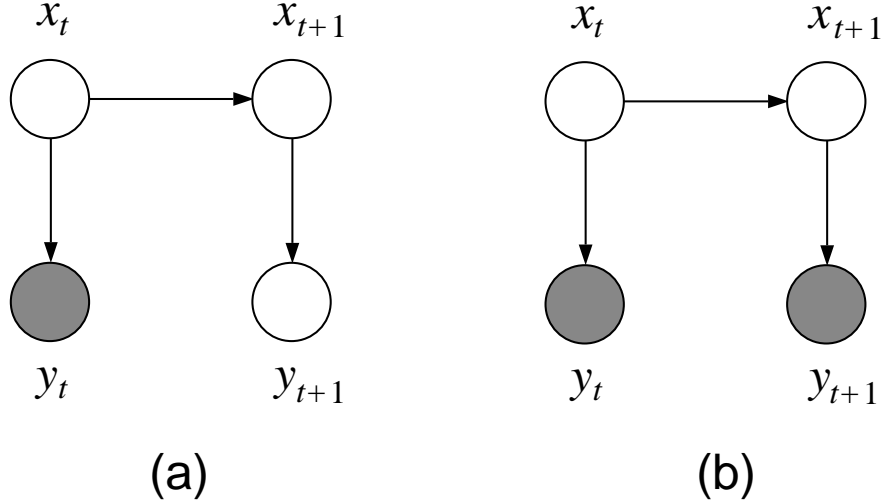


Figure 15.3: (a) A fragment of an SSM in which the observations up to and including  $y_t$  are available, and (b) the same fragment in which observations  $y_{t+1}$  to  $y_T$  are available.

us to combine a forward recursion with a backward recursion. Furthermore, we once again have the choice between an algorithm that computes backward-filtered estimates and combines them with the forward-filtered estimates (an “alpha-beta algorithm”), or an algorithm that recurses directly on the filtered-and-smoothed estimates (an “alpha-gamma algorithm”). Both kinds of algorithm are available in the literature on state-space models, but the latter approach appears to dominate (as opposed to the HMM literature, where the former approach dominates). In this section we begin with the “alpha-gamma” approach, deriving the the “Rauch-Tung-Striebel (RTS) smoothing algorithm,” and then turn to an alternative “alpha-beta” approach.

### 15.7.1 The Rauch-Tung-Striebel (RTS) smoother

Our approach to deriving the RTS smoothing algorithm will once again be based on the graphical model fragment shown in Figure 15.2, which we reproduce in Figure 15.3. We begin by writing down the joint distribution of  $x_t$  and  $x_{t+1}$ , conditional on  $y_0, \dots, y_t$ . Recall that  $\hat{x}_{t+1|t} = A\hat{x}_{t|t}$ , which implies:

$$E[(x_t - \hat{x}_{t|t})(x_{t+1} - \hat{x}_{t+1|t})^T | y_0, \dots, y_t] = P_{t|t}A^T. \quad (15.59)$$

Thus our distribution has the following mean and covariance matrix:

$$\begin{bmatrix} \hat{x}_{t|t} \\ \hat{x}_{t+1|t} \end{bmatrix} \quad \text{and} \quad \begin{bmatrix} P_{t|t} & P_{t|t}A^T \\ AP_{t|t} & P_{t+1|t} \end{bmatrix}, \quad (15.60)$$

where all of the quantities are available to us after a forward Kalman filtering pass.

We now introduce a “backwards” computation. In particular, we condition on  $x_{t+1}$  and calculate the probability of  $x_t$ , still conditioning on  $y_0, \dots, y_t$ . Using the by-now familiar Gaussian

conditioning rule (Eq. 13.26), we obtain:

$$E[x_t|x_{t+1}, y_0, \dots, y_t] = \hat{x}_{t|t} + P_{t|t} A^T P_{t+1|t}^{-1} (x_{t+1} - \hat{x}_{t+1|t}) \quad (15.61)$$

$$= \hat{x}_{t|t} + L_t (x_{t+1} - \hat{x}_{t+1|t}), \quad (15.62)$$

where we have introduced the notation  $L_t \triangleq P_{t|t} A^T P_{t+1|t}^{-1}$ , and

$$\text{Var}[x_t|x_{t+1}, y_0, \dots, y_t] = P_{t|t} - P_{t|t} A^T P_{t+1|t}^{-1} A P_{t|t} \quad (15.63)$$

$$= P_{t|t} - L_t P_{t+1|t} L_t^T. \quad (15.64)$$

The purpose of conditioning on  $x_{t+1}$  is to render  $x_t$  independent of the future observations  $y_{t+1}, \dots, y_T$ . That is, we can use conditional independence to write:

$$E[x_t|x_{t+1}, y_0, \dots, y_T] = E[x_t|x_{t+1}, y_0, \dots, y_t] \quad (15.65)$$

$$= \hat{x}_{t|t} + L_t (x_{t+1} - \hat{x}_{t+1|t}) \quad (15.66)$$

and

$$\text{Var}[x_t|x_{t+1}, y_0, \dots, y_T] = \text{Var}[x_t|x_{t+1}, y_0, \dots, y_t] \quad (15.67)$$

$$= P_{t|t} - L_t P_{t+1|t} L_t^T. \quad (15.68)$$

The quantities on the left-hand side of these equations are almost what we want; indeed, if we could drop  $x_{t+1}$  we would have the desired filtered-and-smoothed quantities.

The remainder of the derivation is an exercise in conditional expectation. Recall from Appendix XXX the following fundamental facts about conditional expectations:

$$E[X|Z] = E[E[X|Y, Z]|Z] \quad (15.69)$$

and

$$\text{Var}[X|Z] = \text{Var}[E[X|Y, Z]|Z] + E[\text{Var}[X|Y, Z]|Z] \quad (15.70)$$

which show us how to compute unconditional expectations using conditional expectations. We will substitute  $x_t$  for  $X$ ,  $x_{t+1}$  for  $Y$ , and  $y_0, \dots, y_T$  for  $Z$  in these equations.

Beginning with Eq. 15.66, we take the conditional expectation on both sides, conditioning with respect to  $y_0, \dots, y_T$ :

$$\hat{x}_{t|T} \triangleq E[x_t|y_0, \dots, y_T] \quad (15.71)$$

$$= E[E[x_t|x_{t+1}, y_0, \dots, y_T]|y_0, \dots, y_T] \quad (15.72)$$

$$= E[\hat{x}_{t|t} + L_t (x_{t+1} - \hat{x}_{t+1|t})|y_0, \dots, y_T] \quad (15.73)$$

$$= \hat{x}_{t|t} + L_t (x_{t+1|T} - \hat{x}_{t+1|t}), \quad (15.74)$$

where we have used the fact that all of the quantities in Eq. 15.74 other than  $x_{t+1}$  are constants when we condition on  $y_0, \dots, y_T$ .

Eq. 15.74 is the basic update equation in the RTS smoothing algorithm. We see that a estimate of  $x_t$  based on all of the data can be obtained by correcting the filtered estimate  $\hat{x}_{t|t}$  by an error term composed of a smoothed estimate of  $x_{t+1}$  and the filtered estimate  $\hat{x}_{t+1|t}$ . The gain matrix  $L_t$  is a quantity that depends only on matrices computed during the forward pass.

We now work on the conditional variance equation (Eq. 15.68). Using Eq. 15.70, we have:

$$P_{t|T} \triangleq \text{Var}[x_t|y_0, \dots, y_T] \quad (15.75)$$

$$= \text{Var}[E[x_t|x_{t+1}, y_0, \dots, y_T]|y_0, \dots, y_T] + E[\text{Var}[x_t|x_{t+1}, y_0, \dots, y_T]|y_0, \dots, y_T] \quad (15.76)$$

$$= \text{Var}[\hat{x}_{t|t} + L_t(x_{t+1} - \hat{x}_{t+1|t})|y_0, \dots, y_T] + E[P_{t|t} - L_t P_{t+1|t} L_t^T|y_0, \dots, y_T] \quad (15.77)$$

$$= L_t \text{Var}[(x_{t+1} - \hat{x}_{t+1|t})|y_0, \dots, y_T] L_t^T + P_{t|t} - L_t P_{t+1|t} L_t^T \quad (15.78)$$

$$= L_t \text{Var}[x_{t+1}|y_0, \dots, y_T] L_t^T + P_{t|t} - L_t P_{t+1|t} L_t^T \quad (15.79)$$

$$= L_t P_{t+1|T} L_t^T + P_{t|t} - L_t P_{t+1|t} L_t^T \quad (15.80)$$

$$= P_{t|t} + L_t(P_{t+1|T} - P_{t+1|t})L_t^T, \quad (15.81)$$

where at several junctures we have used the fact that expectations taken with respect to  $y_0, \dots, y_T$  are constant when conditioning with respect to the larger conditioning set  $y_0, \dots, y_T$ .

We summarize the RTS smoothing algorithm. Based on the quantities  $\hat{x}_{t+1|t}$ ,  $P_{t|t}$  and  $P_{t+1|t}^{-1}$  from the filtering algorithm, we compute:

$$\hat{x}_{t|T} = \hat{x}_{t|t} + L_t(x_{t+1|T} - \hat{x}_{t+1|t}), \quad (15.82)$$

$$P_{t|T} = P_{t|t} + L_t(P_{t+1|T} - P_{t+1|t})J_t^T, \quad (15.83)$$

where  $L_t \triangleq P_{t|t} A^T P_{t+1|t}^{-1}$ . The algorithm is initialized by using  $\hat{x}_{T|T}$  and  $P_{T|T}$  from the filtering pass.

### 15.7.2 The two-filter smoother

In this section we describe an alternative approach to smoothing in the SSM which is the analog of the alpha-beta algorithm for the HMM. In this approach, known as the “two-filter algorithm,” the idea is to combine the “forward” conditional probability  $P(x_t|y_0, \dots, y_t)$  with the “backward” conditional probability  $P(x_t|y_{t+1}, \dots, y_T)$ . Note that the latter quantity, like the former quantity, is a “filtered estimate”; that is, a conditional probability of the state given a (partial) output sequence. This differs from the traditional beta variable in the HMM, which is the conditional probability of the output sequence given the state. Clearly we can move from one to the other, however, by multiplying or dividing by the unconditional probability of the state,  $P(x_t)$ , which is available via the Lyapunov equation. Thus, the difference is minor and it is appropriate to think of the two-filter algorithm as the analog of the alpha-beta algorithm.

Given that we want filtered estimates in the backward direction, a simple approach to deriving the backward algorithm is to “invert the dynamics” and apply a forward filtering algorithm to the inverted dynamics. In graphical model terms, we invert the arrows in the graph. This is in itself a useful exercise.

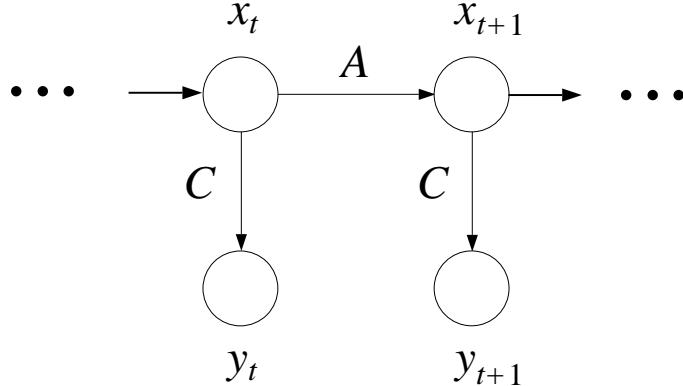


Figure 15.4: (a) A fragment of an SSM with no observations.

In this section we assume that the matrix  $A$  is invertible and make use of  $A^{-1}$  in our derivation of the algorithm. In fact this assumption is not necessary, and a lookahead at the algorithm that we derive shows that  $A^{-1}$  does not appear. (In Chapter 18 we present an alternative derivation of the algorithm from the point of view of the junction tree algorithm, and in that derivation we do not make use of  $A^{-1}$ ).

The naive approach to inverting the dynamical equation is to simply write:

$$x_t = A^{-1}x_{t+1} - A^{-1}Gw_t, \quad (15.84)$$

and let  $t$  run backwards in time. This approach is not viable, however, because  $w_t$  is not independent of the “past” values of the state; i.e.,  $x_{t+1}, \dots, x_T$ . Indeed, these states are all a function of  $w_t$ . Thus one of the assumptions that we used in deriving the Kalman filter is not valid and we cannot simply apply the Kalman filter to Eq. 15.84.

To obtain a more useful inverse of the dynamics, consider the graphical model fragment shown in Figure 15.4. The forward dynamics yields a joint probability distribution on  $(x_t, x_{t+1})$  characterized by the Lyapunov equation  $\Sigma_{t+1} = A\Sigma_t A^T + GQG^T$ . Indeed the covariance matrix of  $(x_t, x_{t+1})$  is given by:

$$\begin{bmatrix} \Sigma_t & \Sigma_t A^T \\ A\Sigma_t & A\Sigma_t A^T + GQG^T \end{bmatrix} \quad (15.85)$$

We can invert the relationship between  $x_t$  and  $x_{t+1}$  by solving for  $\Sigma_t$  in terms of  $\Sigma_{t+1}$  and rewriting the covariance matrix in terms of  $\Sigma_{t+1}$ . Thus:

$$\Sigma_t = A^{-1}\Sigma_{t+1}A^{-T} - A^{-1}GQG^TA^{-T}, \quad (15.86)$$

where we assume that  $A$  is invertible.<sup>2</sup> This equation also implies:

$$A\Sigma_t = \Sigma_{t+1}A^{-T} - GQG^TA^{-T}, \quad (15.87)$$

---

<sup>2</sup>In fact this assumption is not necessary, see Exercise XXX.

and we can rewrite the covariance matrix as follows:

$$\begin{bmatrix} A^{-1}\Sigma_{t+1}A^{-T} - A^{-1}GQG^TA^{-T} & A^{-1}\Sigma_{t+1} - A^{-1}GQG^T \\ \Sigma_{t+1}A^{-T} - GQG^TA^{-T} & \Sigma_{t+1} \end{bmatrix} \quad (15.88)$$

Noting that the upper-right-hand corner of this matrix can be written as  $A^{-1}(I - A^{-1}GQG^T\Sigma_{t+1}^{-1})\Sigma_{t+1}$ , we see that if we define:

$$\tilde{A} = A^{-1}(I - A^{-1}GQG^T\Sigma_{t+1}^{-1}) \quad (15.89)$$

then we obtain  $\tilde{A}\Sigma_{t+1}$  and  $\Sigma_{t+1}\tilde{A}^T$  in the corners of the matrix, and the matrix begins to take the form of a forward covariance matrix. This suggests that we define the inverse dynamics via:

$$x_t = \tilde{A}x_{t+1} + \tilde{G}\tilde{w}_{t+1}, \quad (15.90)$$

with  $\tilde{G}$  and  $\tilde{w}_t$  chosen appropriately so as to match the forward dynamics (Eq. 15.1). Indeed, choosing

$$\tilde{G} = -A^{-1}G \quad (15.91)$$

$$\tilde{w}_{t+1} = w_t - QG^T\Sigma_{t+1}^{-1}x_{t+1} \quad (15.92)$$

Eq. 15.90 matches Eq. 15.1. Moreover, we have:

$$\tilde{Q} \triangleq E[\tilde{w}_{t+1}\tilde{w}_{t+1}^T] = Q - QG^T\Sigma_{t+1}^{-1}GQ, \quad (15.93)$$

and substituting Eqs. 15.89, 15.92 and 15.93 in the backward Lyapunov equation:

$$\Sigma_t = \tilde{A}\Sigma_{t+1}\tilde{A}^T + \tilde{G}\tilde{Q}\tilde{G}^T \quad (15.94)$$

we recover the forward Lyapunov equation.

Finally, it can also be verified (see Exercise XXX) that  $\tilde{w}_{t+1}$  is independent of the “past” values of the state  $x_{t+1}, \dots, x_T$ .

We have therefore succeeded in obtaining a version of the inverse dynamics to which standard filtering algorithms can be applied. If we use the canonical parameterization (i.e., the information filter in Eqs. 15.39, 15.43, 15.49, and 15.54), utilizing the inverse dynamical equation and noting that the output equation  $y_t = Cx_t + v_t$  has not changed, we obtain:

$$S_{t|t+1} = A^T H A + \Sigma_t^{-1} - A^T H^{-1} (S_{t+1|t+1} + H^{-1} - \Sigma_{t+1}^{-1})^{-1} H^{-1} A \quad (15.95)$$

$$S_{t|t} = S_{t|t+1} + C^T R^{-1} C \quad (15.96)$$

$$\hat{\xi}_{t|t+1} = A^T H^{-1} (S_{t+1|t+1} + H^{-1} - \Sigma_{t+1}^{-1})^{-1} \hat{\xi}_{t+1|t+1} \quad (15.97)$$

$$\hat{\xi}_{t|t} = \hat{\xi}_{t|t+1} + C^T R^{-1} y_t, \quad (15.98)$$

where  $t$  and  $t + 1$  have been interchanged to reflect the fact that we are filtering backward in time. This filter calculates the canonical representation of  $P(x_t|y_{t+1}, \dots, y_T)$ . Thus, converting to the moment representation, we have  $\hat{x}_{t|t+1} = S_{t|t+1}^{-1} \hat{\xi}_{t|t+1}$  and  $P_{t|t+1} = S_{t|t+1}^{-1}$ .

The final issue that we must address involves the fusing of the probability distributions  $P(x_t|y_0, \dots, y_t)$  and  $P(x_t|y_{t+1}, \dots, y_T)$  to obtain the posterior probability  $P(x_t|y_0, \dots, y_T)$ . This problem is not unique to the filtering and smoothing domain, but arises in many other settings as well. It is therefore worth posing and solving the problem in full generality; this we do in the following section. Anticipating the result, we have the following fusion rule for  $\hat{x}_{t|T}$ , the estimate of  $x_t$  based on all of the data:

$$\hat{x}_{t|T} = P_{t|T}^{-1} (\hat{x}_{t|t} + P_{t|t+1}^{-1} \hat{x}_{t|t+1}), \quad (15.99)$$

where the covariance matrix  $P_{t|T}$  is computed as follows:

$$P_{t|T} = \left( P_{t|t}^{-1} + P_{t|t+1}^{-1} - \Sigma_t^{-1} \right)^{-1}. \quad (15.100)$$

The appearance of  $\Sigma_t^{-1}$  in the latter equation should not be a surprise. The filtering process and the smoothing process both make use of the prior statistics on  $x_t$ ; in the latter case this is because we have inverted the dynamics. When the covariance matrices of these two processes are combined we have included the prior covariance twice. To avoid double-counting  $\Sigma_t^{-1}$  must be subtracted in the combination rule.

### 15.7.3 Fusion of Gaussian posterior probabilities

Let us consider three sets of random variables:  $x$ ,  $z_1$  and  $z_2$ . Suppose that these variables are characterized by a multivariate Gaussian distribution and suppose moreover that  $z_1$  and  $z_2$  are conditionally independent given  $x$ . We wish to fuse the posteriors  $P(x|z_1)$  and  $P(x|z_2)$  into an overall posterior  $P(x|z_1, z_2)$ .

Let us assume, without loss of generality, that  $x$ ,  $z_1$ , and  $z_2$  have zero means. Non-zero means can be subtracted away and added back at the end of the analysis.

Under the conditional independence assumption, there are three ways to represent the distribution of  $x$ ,  $z_1$ , and  $z_2$  as a directed graphical model. The representation given in Figure 15.5(a) is particularly useful for our purposes. To parameterize the graph, we require the marginal  $P(x)$ , and conditionals  $P(z_1|x)$  and  $P(z_2|x)$ . For the marginal, we endow  $x$  with a zero mean and covariance  $\Sigma$ . For the conditionals, recall that Gaussian conditionals are linear functions of the conditioning variable (cf. Eq. ref{eq:Gaussian-conditional-mean}). Thus we can write:

$$z_1 = M_1 x + v_1 \quad (15.101)$$

$$z_2 = M_2 x + v_2, \quad (15.102)$$

for appropriately chosen matrices  $M_1$  and  $M_2$  and zero-mean Gaussian variables  $v_1$  and  $v_2$  having covariance matrices  $R_1$  and  $R_2$ . Note moreover that  $v_1$  and  $v_2$  are independent of  $x$  and are conditionally independent of each other given  $x$ .

Let us now consider a generic linear equation  $z = Mx + v$ , where  $v$  is independent of  $x$  and has covariance  $R$ . To calculate the conditional expectation of  $x$  given  $z$  we first obtain the covariance matrix of the pair  $(x, z)$ :

$$\begin{bmatrix} \Sigma & \Sigma M^T \\ M\Sigma & M\Sigma M^T + R \end{bmatrix}. \quad (15.103)$$

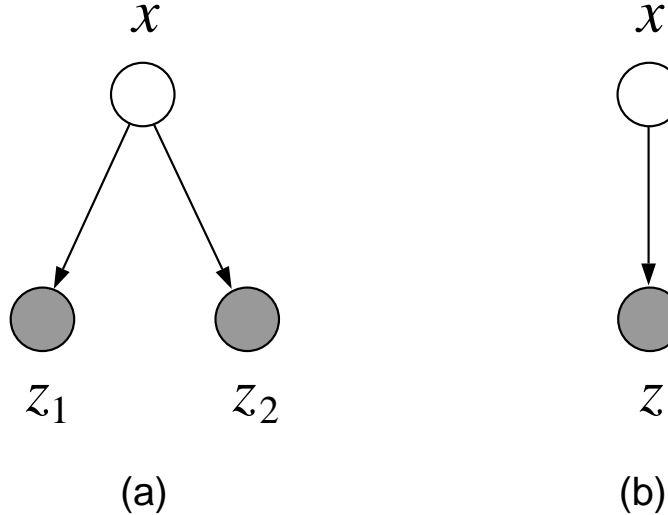


Figure 15.5: A graphical model representation of the fusion problem. (a) The observables  $z_1$  and  $z_2$  are assumed conditionally independent given  $x$ . The conditional probabilities of  $z_i$  are parameterized as linear functions of  $x$  with additive, independent noise terms. (b) Conjoining  $z_1$  and  $z_2$  into a single observable vector  $z$ .

We then apply the usual Gaussian conditioning formulas (Eqs. 13.26 and 13.27) to obtain the conditional distribution of  $x$  given  $z$ . Denoting the mean of this conditional distribution as  $\hat{x}$  and the covariance as  $P$ , we have:

$$\hat{x} = \Sigma M^T (M \Sigma M^T + R)^{-1} z \quad (15.104)$$

$$= (M^T R^{-1} M + \Sigma^{-1})^{-1} M^T R^{-1} z, \quad (15.105)$$

where we have used a matrix inversion identity (Eq. 13.18) in the second step, and:

$$P = \Sigma - \Sigma M^T (M \Sigma M^T + R)^{-1} M \Sigma \quad (15.106)$$

$$= (\Sigma^{-1} + M^T R^{-1} M)^{-1}, \quad (15.107)$$

where again we use a matrix inversion identity (Eq. 13.17) to simplify the result.

The individual conditionals of  $x$  given  $z_1$  and  $z_2$  are special cases of the foregoing equations. Defining  $\hat{x}_i \triangleq E(x|z_i)$  and letting  $P_i$  denote the corresponding conditional covariance, we have:

$$\hat{x}_1 = (M_1^T R_1^{-1} M_1 + \Sigma^{-1})^{-1} M_1^T R_1^{-1} z_1 \quad (15.108)$$

$$\hat{x}_2 = (M_2^T R_2^{-1} M_2 + \Sigma^{-1})^{-1} M_2^T R_2^{-1} z_2, \quad (15.109)$$

and

$$P_1 = (M_1^T R_1^{-1} M_1 + \Sigma^{-1})^{-1} \quad (15.110)$$

$$P_2 = (M_2^T R_2^{-1} M_2 + \Sigma^{-1})^{-1}. \quad (15.111)$$

Now let us consider the overall posterior of  $x$  given both  $z_1$  and  $z_2$ . Grouping  $z_1$  and  $z_2$  into a single variable  $z$  (cf. Figure 15.5(b)), we can apply Eqs. 15.105 and 15.107 where:

$$M \triangleq \begin{bmatrix} M_1 \\ M_2 \end{bmatrix} \quad \text{and} \quad R \triangleq \begin{bmatrix} R_1 & 0 \\ 0 & R_2 \end{bmatrix}. \quad (15.112)$$

From these definitions we obtain:

$$\hat{x} = \left( [M_1^T \ M_2^T] \begin{bmatrix} R_1^{-1} & 0 \\ 0 & R_2^{-1} \end{bmatrix} \begin{bmatrix} M_1 \\ M_2 \end{bmatrix} + \Sigma^{-1} \right)^{-1} [M_1^T \ M_2^T] \begin{bmatrix} R_1^{-1} & 0 \\ 0 & R_2^{-1} \end{bmatrix} \begin{bmatrix} z_1 \\ z_2 \end{bmatrix} \quad (15.113)$$

$$= (M_1^T R_1^{-1} M_1 + M_2^T R_2^{-1} M_2 + \Sigma^{-1})^{-1} (M_1^T R_1^{-1} z_1 + M_2^T R_2^{-1} z_2) \quad (15.114)$$

$$= (P_1^{-1} + P_2^{-1} - \Sigma^{-1})^{-1} (P_1^{-1} \hat{x}_1 + P_2^{-1} \hat{x}_2) \quad (15.114)$$

We can similarly expand Eq. 15.107 to obtain the overall conditional covariance  $P$ :

$$P = (P_1^{-1} + P_2^{-1} - \Sigma^{-1})^{-1}, \quad (15.115)$$

thus allowing us to rewrite Eq. 15.114 as:

$$\hat{x} = P(P_1^{-1} \hat{x}_1 + P_2^{-1} \hat{x}_2). \quad (15.116)$$

Eqs. 15.116 and 15.115 are our general solution to the Gaussian fusion problem.

Let us relate these results back to the two-filter smoothing problem. We collect the observations up to and including time  $t$  into a single “past” vector  $z_1 \triangleq (y_0, \dots, y_t)$ , and collect the “future” observations into a single vector  $z_2 \triangleq (y_{t+1}, \dots, y_T)$ . Let  $x \triangleq x_t$ . These definitions fit the problem specification of the current section; in particular  $(x, z_1, z_2)$  are characterized by a multivariate Gaussian distribution (a marginal of the larger Gaussian distribution that includes the other state variables), and moreover  $z_1$  and  $z_2$  are independent given  $x$ . The estimate  $\hat{x}_{t|t}$  is the conditional expectation of  $x$  given  $z_1$ , and must therefore have the form in Eq. 15.109, for matrices  $M_1$  and  $R_1$  that we do not bother to calculate. Similarly  $\hat{x}_{t|t+1}$  must be of the form in Eq. 15.109, and the conditional covariances  $P_{t|t}$  and  $P_{t|t+1}$  must have the form of Eqs. 15.111 and 15.111. Substituting into Eqs. 15.116 and 15.115 we obtain the fusion rules at the end of the previous section (Eqs. 15.99 and 15.100).

## 15.8 Parameter estimation

We follow the by now familiar recipe for developing an EM algorithm for parameter estimation for the SSM. We write out the expected complete log likelihood, identify the expected sufficient statistics, solve for maximum likelihood estimates in terms of these expected sufficient statistics. This latter problem is simply linear regression.

[Section not yet finished].

## 15.9 Historical remarks and bibliography

# Chapter 4

## Markov Properties

In Chapter ? we highlighted the central role played by conditional independence in probabilistic modelling. We also introduced the concept of a directed graph and related the *absence* of links in the graph to statements of conditional independence of a corresponding probability distribution. We shall refer to these conditional independence statements as Markov properties, since they can be viewed as a generalization of the conditional independence property of a Markov chain discussed in Chapter ?. In this chapter we undertake a more comprehensive and systematic study of conditional independence and its graphical representation.

In Section 4.1 we introduce and prove a number of useful results relating to conditional independence. Equipped with this foundation we then explore the conditional independence properties of directed graphs in Section 4.2. In particular we introduce the concept of *d-separation* which allows conditional independences to be read directly from the graph. Since all of the conditional independence properties implied by the graph can be found using d-separation, it captures the *global* Markov properties of the graph. We then demonstrate the equivalence of d-separation to the factorization property for directed graphs introduced in Chapter ?.

Next we introduce the concept of *undirected* graphs in Section 4.3. These have a different semantics from that of the directed acyclic graphs discussed so far in the book. As we shall see in Chapter ?, undirected graphs play a crucial role in solving inference and learning problems efficiently, even for models whose definition is based originally on a directed graph. We discuss the factorization property for undirected graphs and relate this to the graph's global Markov properties.

In Section 4.4 we return to directed graphs for a further exploration of

their conditional independence properties. We use the machinery of undirected graphs developed in Section 4.3 to develop an alternative formulation of the global Markov properties of directed graphs. Also we introduce *local* and *pairwise* Markov properties and investigate their relation to global Markov properties and to factorization.

In Section 4.5 we complete our discussion of the Markov properties of undirected graphs by introducing definitions of pairwise and local Markov, and relating these to global Markov properties and to factorization.

Finally, in Section 4.6 we outline some extensions of the graphical formalism, and discuss its limitations for representing conditional independencies.

Concepts from graph theory will be introduced in this chapter as they are needed. However, the key concepts are also summarized in Appendix A.

## 4.1 Conditional Independence

In discussing conditional independence properties, it is useful to follow Dawid's notation in which  $A \perp\!\!\!\perp B | C$  denotes that  $A$  is independent of  $B$  given  $C$ . Here  $A$ ,  $B$  and  $C$  represent variables, or more generally groups of variables, with some joint distribution  $P(A, B, C)$ . The conditional independence property  $A \perp\!\!\!\perp B | C$  is simply a statement that the conditional distribution  $P(A|B, C)$  satisfies

$$P(A|B, C) = P(A|C) \quad (4.1)$$

so that, once the value of  $C$  has been fixed, subsequently learning the value of  $B$  tells us nothing further about the distribution of  $A$ . It should be emphasized that the property (4.1) must hold for every possible instantiation of  $C$ .

If we multiply both sides of (4.1) by  $P(B|C)$  we obtain an equivalent statement for the distribution  $P(A, B|C)$  in the form

$$P(A, B|C) = P(A|C)P(B|C) \quad (4.2)$$

so that, once  $C$  is known, the joint conditional distribution of  $A$  and  $B$  factorizes into the product of the marginal conditional distributions.

A special case of conditional independence arises when there are no conditioning variables so that if, for example,  $A$  is marginally independent

of  $B$ , which we write as  $A \perp\!\!\!\perp B | \emptyset$ , then  $P(A|B) = P(A)$ , or equivalently  $P(A, B) = P(A)P(B)$ .

While some conditional independence relations hold universally, others apply only to a restricted class of distributions. An important such class consists of those distributions which are strictly positive, in other words where every possible instantiation of the variables has a non-zero probability. Distributions which have zeros, and hence are not strictly positive, can arise if there are logical relations between the variables. For instance if  $A = B$  then  $P(A \neq B) = 0$ .

Using the sum and product rules of probability we can easily prove the following four properties of conditional independence.

**Theorem 4.1 (Symmetry)** *If  $A$  is conditionally independent of  $B$  given  $C$ , then  $B$  is conditionally independent of  $A$  given  $C$ , so that*

$$A \perp\!\!\!\perp B | C \Leftrightarrow B \perp\!\!\!\perp A | C. \quad (4.3)$$

**Proof:** If  $A \perp\!\!\!\perp B | C$  then  $P(A|B, C) = P(A|C)$ . Hence

$$P(B|A, C) = \frac{P(A, B|C)}{P(A|C)} = \frac{P(A|B, C)P(B|C)}{P(A|C)} = P(B|C) \quad (4.4)$$

and so  $B \perp\!\!\!\perp A | C$ . □

**Theorem 4.2 (Decomposition)**

$$A \perp\!\!\!\perp (B \cup D) | C \Rightarrow A \perp\!\!\!\perp B | C \text{ and } A \perp\!\!\!\perp D | C. \quad (4.5)$$

**Proof:** Using  $A \perp\!\!\!\perp (B \cup D) | C$  we have  $P(A|B, C, D) = P(A|C)$ , and

hence

$$\begin{aligned}
 P(A|B, C, D) &= \sum_D P(A, D|B, C) \\
 &= \sum_D P(A|B, C, D)P(D|B, C) \\
 &= P(A|C) \sum_D P(D|B, C) \\
 &= P(A|C)
 \end{aligned} \tag{4.6}$$

□

and hence  $A \perp\!\!\!\perp B | C$ . Similarly we can show  $A \perp\!\!\!\perp D | C$ .

### Theorem 4.3 (Weak Union)

$$A \perp\!\!\!\perp (B \cup D) | C \Rightarrow A \perp\!\!\!\perp B | C \cup D \text{ and } A \perp\!\!\!\perp D | C \cup B. \tag{4.7}$$

**Proof:** From  $A \perp\!\!\!\perp (B \cup D) | C$  we have  $P(A|B, C, D) = P(A|C)$  and from the decomposition property Theorem 4.2 we have  $P(A|C, D) = P(A|C)$ . Thus  $P(A|B, C, D) = P(A|C, D)$  and hence  $A \perp\!\!\!\perp B | C \cup D$ . An analogous argument is used to show  $A \perp\!\!\!\perp D | C \cup B$ . □

### Theorem 4.4 (Contraction)

$$A \perp\!\!\!\perp B | (C \cup D) \text{ and } A \perp\!\!\!\perp D | C \Rightarrow A \perp\!\!\!\perp (B \cup D) | C. \tag{4.8}$$

**Proof:** From  $A \perp\!\!\!\perp B | (C \cup D)$  we have  $P(A|B, C, D) = P(A|C, D)$ . Similarly from  $A \perp\!\!\!\perp D | C$  we have  $P(A|C, D) = P(A|C)$ . Combining these we obtain  $P(A|B, C, D) = P(A|C)$ , and hence  $A \perp\!\!\!\perp (B \cup D) | C$ . □

The following property does not hold universally. It does hold, however, for distributions which are strictly positive.

**Theorem 4.5 (Intersection)** *For strictly positive distributions*

$$A \perp\!\!\!\perp B \mid (C \cup D) \quad \text{and} \quad A \perp\!\!\!\perp C \mid (B \cup D) \quad \Rightarrow \quad A \perp\!\!\!\perp (B \cup C) \mid D. \quad (4.9)$$

**Proof:** Using  $A \perp\!\!\!\perp B \mid (C \cup D)$  we have

$$P(A, B, C \mid D) = P(A \mid C, D)P(B, C \mid D). \quad (4.10)$$

Similarly using  $A \perp\!\!\!\perp C \mid (B \cup D)$  we have

$$P(A, B, C \mid D) = P(A \mid B, D)P(B, C \mid D). \quad (4.11)$$

Equating these two we obtain

$$P(A \mid C, D) = P(A \mid B, D) \quad (4.12)$$

where we have assumed  $P(B, C \mid D) \neq 0$ . From this it follows that the marginal distribution of  $A$  is given by

$$\begin{aligned} P(A \mid D) &= \sum_B P(A \mid B, D)P(B \mid D) \\ &= \sum_B P(A \mid C, D)P(B \mid D) \\ &= P(A \mid C, D). \end{aligned} \quad (4.13)$$

Using (4.10) we then have

$$P(A, B, C \mid D) = P(A \mid C, D)P(B, C \mid D) = P(A \mid D)P(B, C \mid D) \quad (4.14)$$

and hence  $A \perp\!\!\!\perp (B \cup C) \mid D$ . □

## 4.2 Directed Graphs

We begin our study of Markov properties by reviewing the factorization property for directed graphs, discussed already in Chapter ?. Next we introduce the concept of d-separation, which allows the conditional independence properties to be read directly from the graph. We then show the equivalence of d-separation and factorization, and also show the equivalence to the Bayes' Ball procedure of Chapter ?.

### 4.2.1 Directed Factorization

We have already observed in Chapter ? that, given some ordering of the variables, a general joint distribution can be factorized into a product of conditional distributions, one for each variable. For example, given  $M$  variables  $X_1, X_2, \dots, X_M$  we have

$$\begin{aligned} P(X_1, X_2, X_3, \dots, X_M) &= P(X_1)P(X_2|X_1) \\ &\quad P(X_3|X_1, X_2) \cdots P(X_M|X_1, X_2, \dots, X_{M-1}). \end{aligned} \tag{4.15}$$

We can represent this factorization graphically, as shown for the case of  $M = 4$  in Figure 4.1, in which each node has all lower-numbered nodes as its parent set.

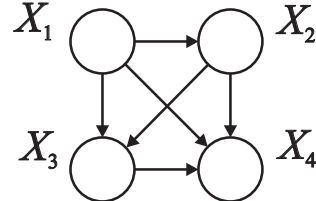


Figure 4.1: A fully connected directed graph comprising four nodes.

While this holds true for arbitrary distributions, we can define a restricted family of distributions by introducing a factorization with respect to a given directed acyclic graph in the form

$$P(S) = \prod_{i \in S} P(S_i|\text{pa}(S_i)) \tag{4.16}$$

where  $\text{pa}(S_i)$  denotes the set of parents of  $S_i$  in the graph. A directed graph is acyclic if (and only if) the nodes can be numbered such that for every node all the parents of that node have a lower number than the node itself. For example, given the graph in Figure 4.2 we have the following factorization

$$\begin{aligned} P(X_1, X_2, X_3, X_4, X_5) &= P(X_1)P(X_2)P(X_3|X_1, X_2) \\ &\quad P(X_4|X_2)P(X_5|X_3, X_4). \end{aligned} \quad (4.17)$$

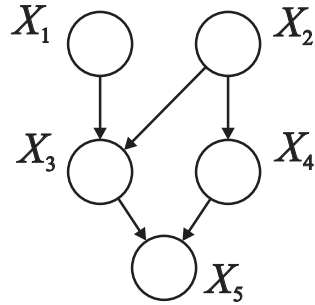


Figure 4.2: A directed graph comprising five nodes.

Comparing (4.15) with (4.17) we see that the latter has variables missing from some the conditioning sets of the conditional distributions, corresponding to missing links in the directed graph of Figure 4.2. This implies that any distribution which factorizes according to (4.17) will exhibit some conditional independence properties. A central goal in this section is to uncover these conditional independencies and to relate them quantitatively to the factorization property.

In discussing Markov properties it may be helpful to regard the directed acyclic graph as a filter. A graph with  $M$  nodes defines a particular factorization of the joint distribution according to (4.16). Any given distribution over  $M$  variables will only pass through the filter if it can be expressed in terms of the corresponding factorization. Thus the graph defines a family of distributions, namely the set of all distributions over  $M$  variables which can be expressed in the form (4.16). We denote this factorization property with respect to a directed graph by  $\mathcal{DF}$  (for ‘directed factorization’).

### 4.2.2 d-separation

In order to uncover the conditional independencies implied by a given graph we consider some simple 3-node graphs, of the kind already discussed in Chapter ?. First we define a *path* from a node  $a$  to a node  $b$  as a sequence of nodes starting with  $a$  and ending with  $b$  such that successive nodes are connected by a link. Note that a path may involve traversing directed links in either direction. We will use the notion of a path to introduce the concept of nodes which are *head-to-head*, *head-to-tail* or *tail-to-tail* with respect to a particular path through the graph. From this we obtain the framework of *d-separation* which allows all of the conditional independencies implied by the graph to be obtained from the graph itself.

We begin by considering the directed graph shown in Figure 4.3 which involves 3 nodes  $A$ ,  $B$ , and  $C$  in which we have conditioned on  $C$ . As we

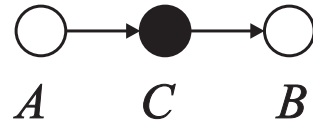


Figure 4.3: A directed graph of three nodes for which  $A \perp\!\!\!\perp B | C$ .

have already seen in Chapter ? that this graph satisfies the independence property  $A \perp\!\!\!\perp B | C$ . Conversely, in general  $A$  and  $B$  are not independent if  $C$  is not observed, so that  $A \not\perp\!\!\!\perp B | \emptyset$ . The node  $C$  is said to be *head-to-tail* with respect to the path  $A-C-B$  since the arrow on one of the links points towards node  $C$  while the arrow on the other link points away from  $C$ . Conditioning on the node  $C$  is said to *block* the path from  $A$  to  $B$ .

Similarly, consider the graph in Figure 4.4. As we discussed in Chap-

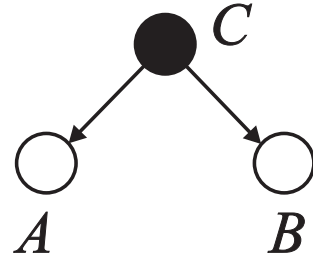


Figure 4.4: Another directed graph for which  $A \perp\!\!\!\perp B | C$ .

ter ?, the graph satisfies the conditional independence property  $A \perp\!\!\!\perp B | C$ . Similarly, as before,  $A \not\perp\!\!\!\perp B | \emptyset$ . The node  $C$  is called a *tail-to-tail* node with

respect to the path  $A-C-B$  since both arrows point away from  $C$ . Again, we have the notion that conditioning on  $C$  has blocked the path from  $A$  to  $B$ , and rendered  $A$  and  $B$  conditionally independent.

Finally we consider the graph of Figure 4.5. In this case we have quite

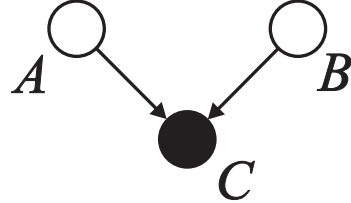


Figure 4.5: A directed graph which does not imply  $A \perp\!\!\!\perp B | C$ .

different conditional independence properties from the two previous examples since  $A \perp\!\!\!\perp B | \emptyset$  whereas  $A \not\perp\!\!\!\perp B | C$ . Node  $C$  is called *head-to-head* with respect to the path  $A-C-B$  since both arrows point towards the node. We see that a head-to-head node has the opposite behaviour from a head-to-tail or tail-to-tail node. The path is blocked if  $C$  is unobserved, so that  $A$  and  $B$  are marginally independent. However, the node becomes unblocked if we condition on  $C$ .

It should be emphasised that, in more complex graphs, a particular node can, for example, be tail-to-tail with respect to one path through the node and head-to-tail or head-to-head with respect to a different path.

Given the above observations we might suspect that more general conditional independent statements can be read directly from a graph by considering paths through the graph and observing whether the paths are blocked or not. This leads to the concept of *d-separation*.

We wish to ascertain whether a particular conditional independence statement  $A \perp\!\!\!\perp B | C$  is implied by a given directed acyclic graph, where  $A$ ,  $B$  and  $C$  are non-intersecting sets of nodes. A path is said to be *blocked* if it includes a node such that either

- (a) the arrows on the path do not meet head-to-head at the node, and the node is in the conditioning set, or
- (b) the arrows do meet head-to-head, and neither the node, nor any of its descendants, is in the conditioning set.

Given a set of conditioning nodes  $C$ , if every path from any node in a set  $A$  to any node in a set  $B$  is blocked, then  $A$  is said to be d-separated from  $B$  by

$C$ . As we will see, this implies that the distribution will satisfy  $A \perp\!\!\!\perp B | C$ . The concept of d-separation is illustrated in Figure 4.6.

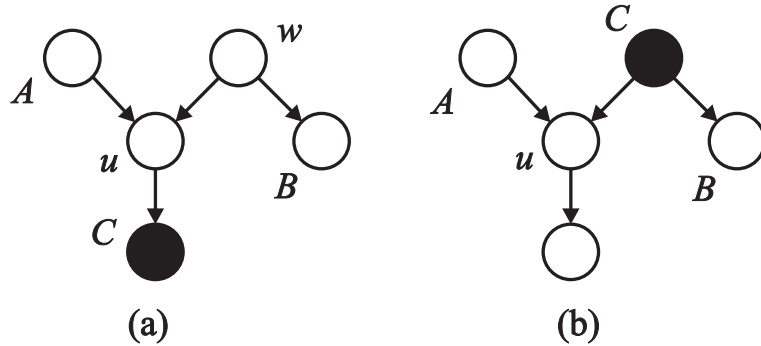


Figure 4.6: Illustration of d-separation. In graph (a) the path from  $A$  to  $B$  is not blocked by node  $w$  since it is not a head-to-head node and is not observed, nor is it blocked by node  $u$  since, although the latter is a head-to-head node, it has a descendent  $C$  which is in the conditioning set. Thus the conditional independence statement  $A \perp\!\!\!\perp B | C$  does not follow from this graph. In graph (b) the path from  $A$  to  $B$  is blocked by node  $C$  since this is a tail-to-tail node which is observed, and is also blocked by node  $u$  since  $u$  is a head-to-head node and neither it nor its descendants are in the conditioning set, and so  $A \perp\!\!\!\perp B | C$  will be satisfied by any distribution which factorizes according to this graph.

We can regard the d-separation property as a filter, so that, for a particular directed acyclic graph we can test whether any given joint distribution satisfies all of the conditional independence properties implied by the graph through d-separation. Clearly if the graph is fully connected (each node has all lower-numbered nodes in its parent set) then all possible joint distributions will pass the filter. Conversely if there are no links at all between nodes of the graph then only distributions which factorize completely into the product of the marginal distributions over each variable will pass the filter.

The three example graphs considered so far clearly have the property that their conditional independence properties can be determined by the d-separation criterion. We now show that this is a general result for arbitrary directed acyclic graphs, in other words if a distribution factorizes according to a particular graph, then any conditional independence property which follows from the graph will be satisfied by the distribution.

**Theorem 4.6** ( $\mathcal{DF} \Rightarrow d\text{-separation}$ ). *If a joint distribution factorizes according to a directed acyclic graph, and if  $A$ ,  $B$  and  $C$  are disjoint subsets of nodes such that  $C$  d-separates  $A$  from  $B$  in the graph, then the distribution satisfies  $A \perp\!\!\!\perp B | C$ .*

**Proof:** We prove this result by induction on the number  $N$  of nodes in the graph. First we observe that the result holds trivially for a graph with one node. Next we assume that it holds for all DAGs with  $N - 1$  nodes and then prove the result for DAGs with  $N$  nodes. Let the nodes in a DAG  $\mathcal{D}$  of size  $N$  be given a topological ordering and let the highest numbered node be  $\omega$  (hence  $\omega$  has no children). We denote by  $\mathcal{D}'$  the DAG  $\mathcal{D}$  with  $\omega$  removed, and observe that the distribution over the reduced set of variables also factorizes with respect to  $\mathcal{D}'$ . Now consider three disjoint subsets of nodes  $A$ ,  $B$  and  $C$  such that  $C$  d-separates  $A$  from  $B$ . The following three possibilities are exhaustive:

- (a) The final vertex  $\omega \notin A \cup B \cup C$ . Since all paths from  $A$  to  $B$  are, by assumption, blocked it must be true that  $C$  d-separates  $A$  from  $B$  in  $\mathcal{D}'$ , and hence  $A \perp\!\!\!\perp B | C$ .
- (b) The vertex  $\omega$  is a member of  $A$  (or equivalently  $B$ ). Denote  $A' = A \setminus \omega$ , and note that  $A'$  will be d-separated by  $C$  from  $B$  in  $\mathcal{D}'$ . Since there can be no direct links from  $A$  to  $B$  it follows that none of the parents of  $\omega$  are in  $B$ . Let  $P$  be the set of parents of  $\omega$  which are not in  $C$ . Then  $P$  is also d-separated from  $B$  by  $C$  in  $\mathcal{D}'$  since any path from  $P$  to  $B$  either goes through  $\omega$  (and hence is blocked since  $\omega$  must be a head-to-head node for such a path and  $\omega$  is not part of the conditioning set  $C$ ) or the path can be extended by one step to become a path from  $\omega$  to  $B$  (and such a path must be blocked by the assumption of d-separation in  $\mathcal{D}$  but it is not blocked at the parent of  $\omega$  in  $P$  since this is an unobserved node and is not head-to-head and so the path must be blocked elsewhere). Thus both  $A'$  and  $P$  are d-separated from  $B$  by  $C$  in  $\mathcal{D}'$  and hence  $A' \cup P$  is d-separated from  $B$  by  $C$  in  $\mathcal{D}'$  and so  $A' \cup P \perp\!\!\!\perp B | C$  in  $\mathcal{D}'$ . Since the addition of the blocking node  $\omega$  cannot create new unblocked paths it follows that  $A' \cup P \perp\!\!\!\perp B | C$  in  $\mathcal{D}$ . We also have  $\omega \perp\!\!\!\perp B | A' \cup C \cup P$  since the conditioning set includes all of the parents of  $\omega$ . Using the result (4.4) we then have  $A \cup P \perp\!\!\!\perp B | C$  and hence  $A \perp\!\!\!\perp B | C$ .
- (c) Finally, we consider  $\omega \in C$ . Note that no path can be blocked at  $\omega$ , and hence  $A$  and  $B$  must be d-separated by  $C' = C \setminus \omega$ . Also,  $\omega$  must be d-separated from  $A$  or  $B$  (or both) by  $C'$  otherwise there would be an unblocked path from  $A$  to  $B$  via  $\omega$ . Suppose this holds for  $B$  so

that  $A \cup \omega$  is d-separated from  $B$  by  $C'$ . Using the result from case **(b)** above we then have  $A \cup \omega \perp\!\!\!\perp B \mid C'$ . Using (4.3) we then have  $A \perp\!\!\!\perp B \mid C' \cup \omega$  and hence  $A \perp\!\!\!\perp B \mid C$ .

□

The converse of this theorem also holds, namely that if a joint distribution satisfies all of the conditional independence properties which can be read from a graph by d-separation then the distribution must also factorize according to that graph using (4.16). We give a formal proof of this result in Section 4.4.

Of course, not all conditional independencies present in the distribution can necessarily be determined from the graph by d-separation since there may be additional independencies arising from the specific numerical values associated with the conditional distributions. However, it is possible to construct an example model which is such that any conditional independencies which do not correspond to d-separation are not present in the distribution, showing that in general d-separation will find all of the conditional independencies which can be determined directly from the DAG.

[here we return to the Bayes' Ball algorithm introduced in Chapter ?, and demonstrate its equivalence to d-separation]

In some probability distributions there may be deterministic relationships between the variables. In this case there is probability one that the relationship occurs, and combinations of variable values which do not respect the relationship have probability zero. When the conditional distribution of a node conditioned on its parents depends deterministically on one of its parents, the corresponding edge in the directed acyclic graph is sometimes denoted by a double arrow ' $\Longrightarrow$ ' connecting the nodes.

Since Theorem 4.6 does not require positivity of the joint distribution, we can use d-separation to read off conditional independence properties even when deterministic relations are present. However, we can extract additional independencies using D-separation, which is simply an extension of d-separation in which, if a variable is observed, then all other variables which are deterministically related to that variable are also considered to be observed. An example is shown in Figure 4.7

### 4.3 Undirected Graphs

So far in this book we have discussed models based on directed acyclic graphs. However, to begin our discussion of Markov properties it is con-

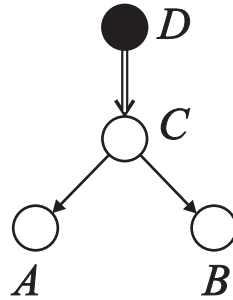


Figure 4.7: An illustration of D-separation showing a directed acyclic graph over four variables in which  $C$  depends deterministically on  $D$ . The conditional independence statement  $A \perp\!\!\!\perp B | D$  does not follow from the standard d-separation criterion. In the D-separation criterion, however, we also infer that  $C$  is an observed node and hence that  $A \perp\!\!\!\perp B | D$ .

venient to consider undirected graphs. Not only do they have simpler semantics than directed graphs, but they will prove useful in formulating and understanding the Markov properties of directed graphs.

We first introduce the concept of graph separation on an undirected graph as follows. Given three disjoint subsets  $A$ ,  $B$ , and  $C$  of nodes on the graph, we say that  $C$  separates  $A$  and  $B$  if every *path* on the graph from any node in  $A$  to any node in  $B$  passes through at least one node in  $C$ . This is illustrated in Figure 4.8.

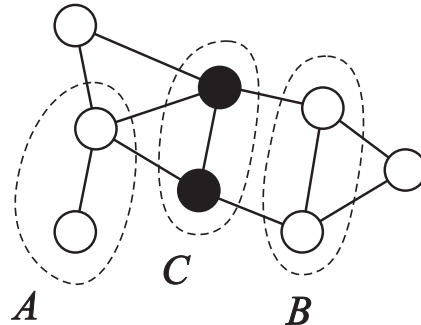


Figure 4.8: An illustration of the concept of graph separation in undirected graphs. The set  $C$  separates  $A$  from  $B$  since every path from a node in  $A$  to a node in  $B$  must pass through a node in  $C$ .

As for directed graphs we consider the global Markov properties for undirected graphs, and then relate these to a factorization property of the

joint distribution.

### 4.3.1 Global Markov

First we introduce the *global Markov* property for undirected graphs, which we denote by  $\mathcal{G}$ . A probability distribution is said to be global Markov with respect to a graph if, for any disjoint subsets of nodes  $A, B, C$  such that  $C$  separates  $A$  and  $B$  on the graph, the distribution satisfies  $A \perp\!\!\!\perp B | C$ .

Again, we can think of the graph as a kind of filter. Consider the set of all possible distributions over the variables corresponding to the nodes of the graph. We could test each distribution in the set to see if it exhibits the conditional independencies implied by the graph. Those probability distributions which pass the test form a family of distributions, every member of which is global Markov with respect to the given graph.

Note that any distribution which factorizes with respect to all of the variables will always be global Markov for any graph since any possible conditional independence statement will always be satisfied. Conversely, if we consider a graph which is fully connected then any distribution will be global Markov for this graph since the graph implies no conditional independence statements.

### 4.3.2 Factorization

We saw in Chapter ? how a probability distribution could be constructed from a product of conditional distributions defined with respect to a directed graph. Here we introduce the corresponding factorization property for undirected graphs, which we denote by  $\mathcal{F}$ . First we define a set of nodes to be *complete* if there is a link from each node to every other node in the set. A probability distribution is said to factorize with respect to a given undirected graph if it can be expressed as the product of functions over the complete sets of nodes of the graph

$$P(S) = \prod_{a \text{ complete}} \psi_a(S_a) \quad (4.18)$$

where the functions  $\psi_a(S_a)$  are known as potentials.

An alternative, equivalent formulation of undirected factorization can be obtained by introducing the notion of a *clique*, which is a complete set of nodes which is also maximal, so that inclusion of any other node in the

set would render it incomplete. The concept of a clique is illustrated in Figure 4.9.

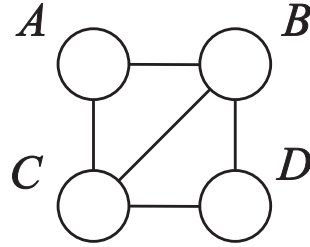


Figure 4.9: Illustration of the concept of a clique. In this graph there are two cliques comprising the sets  $\{A, B, C\}$  and  $\{B, C, D\}$ .

Suppose we define the potential function for each clique in the graph to be initially unity. Then we take each of the potential functions  $\psi_a(S_a)$  in (4.18) and multiply it into the corresponding clique potential. We then obtain a representation of the form

$$P(S) = \prod_C \psi_C(S_C) \quad (4.19)$$

where the product is over all cliques in the graph. Again, we can think of the graph as a filter in which only joint distributions which can be expressed in the form (4.19) will be accepted.

We next show that, for any graph and any distribution, the factorization property implies the global Markov property.

**Theorem 4.7** ( $\mathcal{F} \Rightarrow \mathcal{G}$ ) *For any undirected graph, any distribution which satisfies the factorization property with respect to the graph will also respect the global Markov properties of the graph.*

**Proof:** Consider three disjoint subsets of nodes  $A$ ,  $B$  and  $C$  such that  $C$  separates  $A$  from  $B$  in the graph. Let  $V$  denote the set of all nodes in the graph, and let  $\tilde{A}$  denote the set of all nodes in  $A$  together with all nodes in  $V \setminus S$  which are connected to  $A$ . By the separation assumption  $\tilde{A}$  will not contain any nodes from  $B$ . We then let  $\tilde{B} = (V \setminus S) \cup \tilde{A}$ , so that  $\tilde{A}$ ,  $\tilde{B}$  and  $S$  form disjoint sets such that  $V = \tilde{A} \cup \tilde{B} \cup S$ , and  $S$  separates  $\tilde{A}$  from  $\tilde{B}$ . It follows that any clique is composed either of nodes from  $S \cup \tilde{A}$  or of nodes

from  $S \cup \tilde{B}$ , and so by the factorization property

$$P(V) \equiv P(\tilde{A}, \tilde{B}, S) = f(\tilde{A}, S)g(\tilde{B}, S). \quad (4.20)$$

We therefore have

$$\begin{aligned} P(\tilde{A}, \tilde{B}|S) &= \frac{P(\tilde{A}, \tilde{B}, S)}{\sum_A \sum_B P(\tilde{A}, \tilde{B}, S)} \\ &= \frac{f(\tilde{A}, S)}{\sum_A f(\tilde{A}, S)} \frac{g(\tilde{B}, S)}{\sum_B g(\tilde{B}, S)} \\ &= P(\tilde{A}|S)P(\tilde{B}|S) \end{aligned} \quad (4.21)$$

and hence  $\tilde{A} \perp\!\!\!\perp \tilde{B} | S$ . By noting that  $A$  is a subset of  $\tilde{A}$ , and  $B$  is a subset of  $\tilde{B}$ , and then applying Theorem 4.2 twice we obtain  $A \perp\!\!\!\perp B | S$  as required.  $\square$

The converse of Theorem 4.7 does not hold for all distributions. However, the Hammersley-Clifford theorem states that, for strictly positive probability distributions, the global Markov property is equivalent to the factorization property. The proof of this theorem is postponed to Section 4.5.3 since it makes use of additional Markov properties discussed in Section 4.5.

In the next section we exploit the formalism of undirected graphs to gain further insights into the properties of directed graphs.

## 4.4 Directed Graphs Revisited

We now return to a discussion of directed graphs, and make use of the techniques of undirected graphs discussed in the previous section to develop an alternative formulation of the global Markov properties for directed graphs which in some respects is simpler than the d-separation criterion discussed so far. This will also motivate the graphical concept of *moralization* which will prove useful in discussing inference algorithms in Chapter ?. We will also complete our discussion of the Markov properties of directed graphs by introducing the concepts of local and pairwise Markov, and relate these to the global Markov properties and to factorization.

#### 4.4.1 Directed Global Markov

We have seen that the global Markov properties of an undirected graph can be obtained through simple graph separation, whereas in the case of directed graphs we have to employ the significantly more complex d-separation criterion. It is natural then to ask whether we can use the machinery of undirected graphs to obtain an alternative formulation of the global Markov properties of directed graphs.

As we shall see, simply dropping the arrows on the links of a directed graph, and then applying undirected graph separation does not yield the required conditional independencies. However, we will show that from the original directed graph we can extract an appropriate undirected graph which does exhibit the required independence properties. The specific undirected graph which is needed will depend upon the particular nodes which are included in the conditioning set.

To begin with consider the directed graph shown in Figure 4.10 involving 3 nodes  $A$ ,  $B$ , and  $C$  in which we have conditioned on  $C$ . We have al-

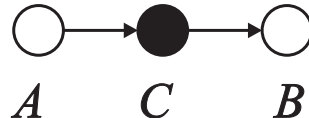


Figure 4.10: A directed graph of three nodes for which  $A \perp\!\!\!\perp B | C$ .

ready seen in Section 4.2.2 that this graph satisfies the independence property  $A \perp\!\!\!\perp B | C$ . Note that this property could have been read off from an undirected graph obtained simply by dropping the arrows on the links, as shown in Figure 4.11.

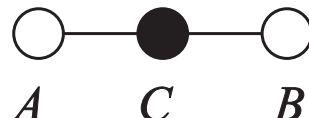


Figure 4.11: The undirected graph obtained from Figure 4.3 by dropping the arrows on the links. This graph also satisfies  $A \perp\!\!\!\perp B | C$ .

Similarly, consider the graph in Figure 4.12. Again, the conditional independence property  $A \perp\!\!\!\perp B | C$  can be read off by graph separation from the corresponding undirected graph, again given by Figure 4.12.

However, the situation is different for the ‘head-to-head’ node shown in Figure 4.13. The undirected graph in this case is again given by Fig-

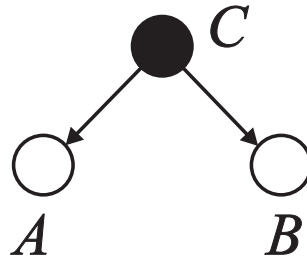


Figure 4.12: Another directed graph for which  $A \perp\!\!\!\perp B \mid C$ .

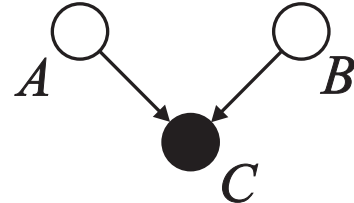


Figure 4.13: A directed graph for which  $A \not\perp\!\!\!\perp B \mid C$ .

ure 4.12, but this now does not give the correct conditional independence result since the undirected graph predicts  $A \perp\!\!\!\perp B \mid C$ , whereas this result does not follow from the original directed graph. We can avoid the introduction of this spurious conditional independence property by first introducing an extra link between the two parents of the conditioning node  $C$  and then dropping the arrows on the links to give the undirected graph of Figure 4.14. This separation properties of this graph now no longer imply

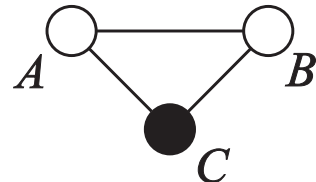


Figure 4.14: The undirected graph obtained by moralizing the directed graph of Figure 4.5.

an incorrect conditional independence statement.

The procedure of adding links to connect nodes with a common descendant is called *moralization*<sup>1</sup> and plays an important role in our discussion of

---

<sup>1</sup>This term originally arose from the idea of ‘marrying the parents’ of the node. We

graphical models. To construct the moral graph from an arbitrary directed acyclic graph we first add additional links between all pairs of nodes having a common child and then drop the arrows on the links. An example of a DAG and its moral graph is shown in Figure 4.15.

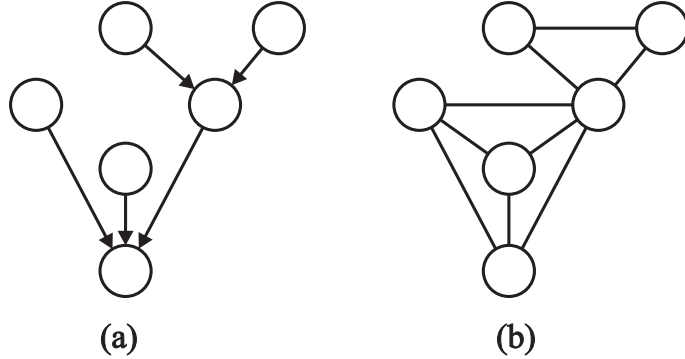


Figure 4.15: An example of a directed acyclic graph (a), together with the corresponding moral graph (b).

We now show that moralization is a sufficient condition to ensure that any conditional independence statement inferred by graph separation on the moral graph holds true also in the factorized distribution.

**Theorem 4.8** *If a probability distribution factorizes according to a directed acyclic graph then it respects the global Markov property of the corresponding moral graph.*

**Proof:** Each factor in the factorization (4.16) is a conditional distribution for a node conditioned on its parents. In the moral graph, this subgraph is complete, since all pairs of parents have been connected by a link. Thus we can take the undirected moral graph, and starting with all of the clique potentials set to unity, multiply each factor in (4.16) into the corresponding clique potential, yielding a factorized representation for the joint distribution of the form (4.19). Hence the directed factorization property  $\mathcal{DF}$  implies undirected factorization  $\mathcal{F}$  on the corresponding moral graph. We then invoke Theorem 4.7 which shows that factorization on the moral graph implies that the distribution is global Markov with respect to that graph.  $\square$

---

continue to use the term moralization throughout this book since it is now in widespread use.

We now ask whether the converse is true, that is whether every conditional independence statement implied by the directed graph holds on the moral graph. The answer is clearly that it does not, as illustrated in Figure 4.16. The problem in Figure 4.16 arises from the node  $W$ . Since this

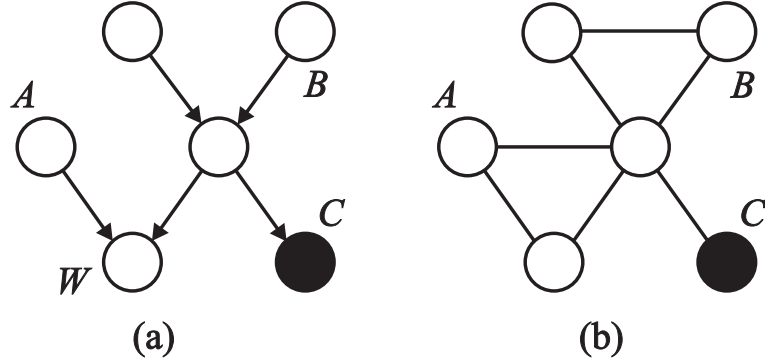


Figure 4.16: Example of a directed graph (a) which exhibits a conditional independence statement  $A \perp\!\!\!\perp B | C$ , which is not represented in the corresponding moral graph (b).

node is not part of the conditioning set it should really be removed from the graph before moralization to avoid the introduction of a spurious link.

We can see how to address this problem more generally by noting that the conditional independence statement  $A \perp\!\!\!\perp B | C$  is a property of the marginal distribution  $P(A, B, C)$  in which the remaining variables have been summed out. Any variables which are not part of  $A \cup B \cup C$  or their ancestors can trivially be removed from the distribution to leave a marginal distribution over the remaining variables simply by removing the corresponding conditional distributions from the product in (4.15).

This motivates the consideration of *ancestral sets*. A node  $A$  is said to be an *ancestor* of a node  $B$  if there is a directed link from  $A$  to  $B$ . Similarly  $B$  is then said to be a *descendent* of  $A$ . We say that a sub-set of nodes within a directed acyclic graph is an ancestral set if, for every node in the set all ancestors of that node are also in the set. Using this concept we can now introduce a new definition for the global Markov property of directed graphs, which provides an alternative to d-separation.

The global markov property for directed graphs, denoted by  $\mathcal{DG}$ , says that  $A \perp\!\!\!\perp B | C$  whenever  $C$  separates  $A$  from  $B$  in the moral graph of the smallest ancestral DAG containing  $A$ ,  $B$  and  $C$ . This is illustrated in Figure 4.17, using the example of Figure 4.16.

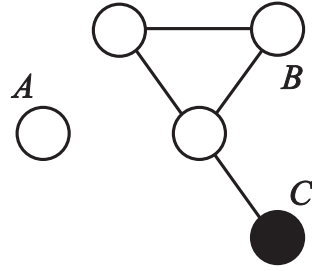


Figure 4.17: The moral graph of the smallest ancestral set from Figure 4.16(a) containing nodes  $A$ ,  $B$  and  $C$ . In this case the conditional independence property  $A \perp\!\!\!\perp B \mid C$  follows correctly from undirected graph separation.

We now show that any independence property which can be found by graph separation in the moral graph of the smallest ancestral set containing the relevant variables must hold also in the probability distribution.

**Theorem 4.9** ( $\mathcal{DF} \Rightarrow \mathcal{DG}$ ) *If a probability distribution factorizes according to a directed acyclic graph, then  $A \perp\!\!\!\perp B \mid C$  whenever  $A$  and  $B$  are separated by  $C$  in the moral graph of the smallest ancestral set containing  $A \cup B \cup C$ .*

**Proof:** If a probability distribution factorizes with respect to a particular directed graph, then the marginal distribution over a subset of nodes corresponding to an ancestral set will factorize with respect to the corresponding ancestral graph. This is easily seen by marginalizing the factored expression (4.16) over the remaining variables. Then, using Theorem 4.8 it follows that any independence obtained by graph separation in the moral graph of the smallest ancestral set containing  $A \cup B \cup C$  will hold also in the marginal distribution. Hence  $\mathcal{DF} \Rightarrow \mathcal{DG}$  as required.  $\square$

#### 4.4.2 Directed Local Markov

Next we describe the local Markov property for directed graphs, denoted by  $\mathcal{DL}$ , which is defined as follows. We define the descendants of a node  $\alpha$  to be the set of nodes which can be reached from  $\alpha$  by following links in the direction of the arrows. All of the remaining nodes, except  $\alpha$  itself, constitute the non-descendants of  $\alpha$ , denoted  $nd(\alpha)$ . A probability distribution satisfies the directed local Markov property for a given directed graph if every variable  $\alpha$  is conditionally independent of its non-descendants given

its parents

$$\alpha \perp\!\!\!\perp \text{nd}(\alpha) \mid \text{pa}(\alpha). \quad (4.22)$$

We next show that the directed global Markov property implies the directed local Markov property. If we think of these properties as filters, this says that any distribution which passes the  $\mathcal{DG}$  filter will also pass the  $\mathcal{DL}$  filter.

**Theorem 4.10** ( $\mathcal{DG} \Rightarrow \mathcal{DL}$ ) *If a probability distribution respects the directed global Markov property for a given directed acyclic graph then it also respects the directed local Markov property.*

**Proof:** We first note that  $\alpha \cup \text{nd}(\alpha)$  is an ancestral set. Next we observe that  $\text{pa}(\alpha)$  separates  $\alpha$  from  $\text{nd}(\alpha) \setminus \text{pa}(\alpha)$  within this ancestral set. The directed local Markov property then follows as a special case of the global directed Markov property.  $\square$

We now complete the loop by showing that the directed local Markov property implies directed factorization.

**Theorem 4.11** ( $\mathcal{DL} \Rightarrow \mathcal{DF}$ ) *For any directed graph, and any distribution, if the distribution satisfies the local Markov property with respect to the graph then it will also factorize according to the graph.*

**Proof:** The proof is based on induction in the number  $N$  of vertices in the graph. Suppose the result holds for an arbitrary directed acyclic graph with  $N$  nodes. Now add an additional node  $X_{N+1}$  which is a terminal node of the graph. For an arbitrary joint distribution over the  $N + 1$  variables we have

$$P(X_1, \dots, X_{N+1}) = P(X_1, \dots, X_N)P(X_{N+1}|X_1, \dots, X_N). \quad (4.23)$$

Using the directed local Markov property  $\mathcal{DL}$  we have  $P(X_{N+1}|X_1, \dots, X_N) = P(X_{N+1}|\text{pa}(X_{N+1}))$ . Also, by the inductive assumption  $P(X_1, \dots, X_N)$  factorizes according to  $\mathcal{DF}$ . Hence  $P(X_1, \dots, X_{N+1})$  factorizes according to  $\mathcal{DF}$ .  $\square$

We end this section by relating d-separation back to the directed local Markov property.

**Theorem 4.12** (d-separation  $\Rightarrow \mathcal{DL}$ ) *If a probability distribution satisfies the*

*conditional independencies implied by d-separation over a particular directed graph, then it will also satisfy the local Markov properties implied by that graph.*

**Proof:** For each node  $\alpha$  in the graph, suppose we have conditioned on the parents of  $\alpha$ , and consider all possible paths which start at  $\alpha$  and which end at a node in the set of non-descendents of  $\alpha$ . Any such path must either (i) pass through a parent of  $\alpha$  or (ii) pass through a child of  $\alpha$ . In case (i) the parent is clearly not a head-to-head node with respect to the path, and since the parent node is in the conditioning set such a path must be blocked. In case (ii) the path must at some point pass through a head-to-head node in order to reach a non-descendant and since neither that node nor any of its descendents is in the conditioning set the node must again block the path. Since all such paths are blocked, the d-separation criterion implies  $\alpha \perp\!\!\!\perp \text{nd}(\alpha) | \text{pa}(\alpha)$ .  $\square$

#### 4.4.3 Directed Pairwise Markov

Our last Markov property for directed graphs is directed pairwise Markov, denoted  $\mathcal{DP}$ . We say that a distribution obeys the directed pairwise Markov property in respect of a given directed acyclic graph if, for any two nodes  $\alpha$  and  $\beta$  such that  $\beta \in \text{nd}(\alpha)$

$$\alpha \perp\!\!\!\perp \beta | \text{nd}(\alpha) \setminus \beta. \quad (4.24)$$

This is illustrated in Figure 4.18.

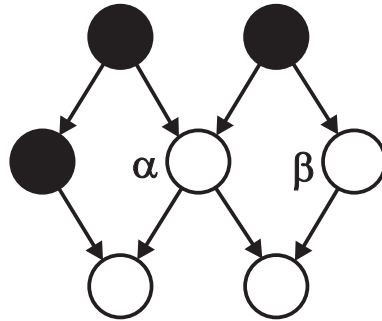


Figure 4.18: An illustration of the pairwise Markov property in which  $\alpha \perp\!\!\!\perp \beta | \text{nd}(\alpha) \setminus \beta$ .

We now show that the directed local Markov property implies the di-

rected pairwise Markov property for all graphs and for all distributions.

**Theorem 4.13** ( $\mathcal{DL} \Rightarrow \mathcal{DP}$ ) *If a distribution satisfies the directed local Markov property with respect to some directed graph, then it also satisfies the directed pairwise Markov property with respect to the same graph.*

**Proof:** From the definition (4.22) of the directed local Markov property we have

$$\alpha \perp\!\!\!\perp (\text{nd}(\alpha) \setminus \beta) \cup \beta \mid \text{pa}(\alpha) \quad (4.25)$$

where we have made use of  $\beta \in \text{nd}(\alpha)$ . From Theorem 4.3 we then have

$$\alpha \perp\!\!\!\perp \beta \mid (\text{nd}(\alpha) \setminus \beta) \cup \text{pa}(\alpha). \quad (4.26)$$

Finally, since  $\text{pa}(\alpha) \subseteq \text{nd}(\alpha)$ , and since  $\beta \notin \text{pa}(\alpha)$  we have  $\alpha \perp\!\!\!\perp \beta \mid \text{nd}(\alpha) \setminus \beta$ .  $\square$

Note that the converse of this theorem is not in general true. However, if we restrict attention to distributions which satisfy the intersection property (4.9), for example distributions which are strictly positive, then  $\mathcal{DP} \Rightarrow \mathcal{DL}$ .

**Theorem 4.14** ( $\mathcal{DP} \Rightarrow \mathcal{DL}$ ) *If a distribution satisfies the directed pairwise Markov property with respect to some directed graph, and respects the intersection property (4.9), then it also satisfies the directed local Markov property with respect to the same graph.*

**Proof:** We prove this result by induction as follows. Let the nodes in  $\text{nd}(\alpha)$  which are not members of  $\text{pa}(\alpha)$  be labelled  $\beta_1, \dots, \beta_N$ , and suppose

$$\alpha \perp\!\!\!\perp \beta_1 \cup \dots \cup \beta_m \mid \text{pa}(\alpha) \cup \beta_{m+1} \cup \dots \cup \beta_N. \quad (4.27)$$

This result clearly holds for  $m = 1$  from the pairwise Markov property. Also from the pairwise Markov property we have

$$\alpha \perp\!\!\!\perp \beta_{m+1} \mid \text{pa}(\alpha) \cup \beta_1 \cup \dots \cup \beta_m \cup \beta_{m+2} \cup \dots \cup \beta_N. \quad (4.28)$$

Now using Theorem 4.5 we have

$$\alpha \perp\!\!\!\perp \beta_1 \cup \dots \cup \beta_{m+1} \mid \text{pa}(\alpha) \cup \beta_{m+2} \cup \dots \cup \beta_N. \quad (4.29)$$

Continuing this inductive process we arrive at (4.29) with  $m + 1 = N$  which is the required result.  $\square$

#### 4.4.4 Summary of Markov properties for Directed Graphs

So far in this chapter we have shown that  $\mathcal{DF} \Rightarrow$  d-separation (Theorem 4.6),  $\mathcal{DF} \Rightarrow \mathcal{DG}$  (Theorem 4.9),  $\mathcal{DG} \Rightarrow \mathcal{DL}$  (Theorem 4.10),  $\mathcal{DL} \Rightarrow \mathcal{DF}$  (Theorem 4.11), and d-separation  $\Rightarrow \mathcal{DL}$  (Theorem 4.12). Hence, without restriction on the graph or the distribution, we have

$$\mathcal{DF} \Leftrightarrow \mathcal{DL} \Leftrightarrow \mathcal{DG} \Leftrightarrow \text{d-separation.} \quad (4.30)$$

Note that this confirms that the directed global Markov property defined through the moral graph of the smallest ancestral set is equivalent to the d-separation criterion. We have also shown that  $\mathcal{DL} \Rightarrow \mathcal{DP}$  (Theorem 4.13) and hence  $\mathcal{DF}, \mathcal{DL}, \mathcal{DG}$  and d-separation all imply  $\mathcal{DP}$ .

If we restrict attention to distributions satisfying the intersection property (4.9) then we have the further result  $\mathcal{DP} \Rightarrow \mathcal{DL}$  (Theorem 4.14) and hence, for such distributions, all of the Markov properties as well as d-separation and the factorization property are equivalent.

## 4.5 Undirected Graphs Revisited

In this section we complete our discussion of the Markov properties of undirected graphs by considering pairwise and local Markov and their relation to global Markov and to factorization. This material is included mainly for technical completeness and is not required in subsequent chapters.

### 4.5.1 Pairwise Markov

We first define the *pairwise Markov* property for undirected graphs, which we denote by  $\mathcal{P}$ . A distribution is pairwise Markov with respect to a given graph if, for any two nodes  $\alpha$  and  $\beta$  in the graph such that there is no direct link in the graph from  $\alpha$  to  $\beta$ , then  $\alpha$  is independent of  $\beta$  given the states of all of the remaining nodes, so that

$$\alpha \perp\!\!\!\perp \beta \mid S \setminus \{\alpha, \beta\} \quad (4.31)$$

where  $S$  denotes the set of all nodes in the graph.

If there is no direct link between the nodes then they are necessarily separated by the remaining nodes according to the graph separation criterion. Thus the pairwise Markov property is a special case of the global Markov property, so that  $\mathcal{G} \Rightarrow \mathcal{P}$ . In other words if a distribution is global Markov with respect to a particular graph then it is necessarily also pairwise Markov. However, the converse does not necessarily hold. A sufficient condition for equivalence of  $\mathcal{G}$  and  $\mathcal{P}$  is that the intersection property of Eq. (4.9) is satisfied, which will be the case, for example, if we restrict attention to distributions which are strictly positive. This leads to the following result.

**Theorem 4.15** ( $\mathcal{P} \Rightarrow \mathcal{G}$ ) *For any undirected graph, and for distributions which satisfy the intersection property (4.9), if a distribution satisfies the pairwise Markov property with respect to the graph then it will also satisfy the global Markov property.*

**Proof:** Consider three disjoint subsets  $A$ ,  $B$  and  $C$  of nodes, and suppose that  $C$  separates  $A$  from  $B$  on the graph. We also assume that the pairwise Markov property  $\mathcal{P}$  holds and that (4.9) is valid. Our goal is to prove that  $A \perp\!\!\!\perp B | C$ . We can do this by induction on the number  $|C|$  of nodes in the separating set  $C$ . Suppose  $|C| = |S| - 2$  where  $|S|$  is the total number of nodes. Then  $A$  and  $B$  each contain one node and the pairwise Markov property implies directly that  $A \perp\!\!\!\perp B | C$ . We then suppose that  $\mathcal{G}$  holds for all values of  $|C|$  greater than some value  $n$  and then show that it also holds for  $|C| = n$ . There are now two possibilities to consider. In the first, suppose that  $A \cup B \cup C = S$ . This implies that either  $A$  or  $B$ , or both, has more than one node. Suppose  $A$  has more than one node and that  $\alpha \in A$ , as illustrated in Figure 4.19. Since  $C$  separates  $A$  from  $B$  it follows that  $C \cup \alpha$

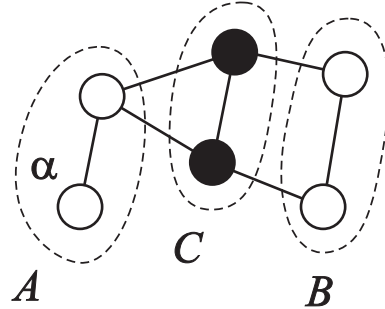


Figure 4.19: Example of a graph corresponding to case (i) in Theorem 4.15.

must separate  $A \setminus \alpha$  from  $B$ . Using the inductive assumption that separation implies independence for  $|C| > n$  we have  $A \setminus \alpha \perp\!\!\!\perp B | C$ . Similarly,  $C \cup A \setminus \alpha$  separates  $\alpha$  from  $B$  and so  $\alpha \perp\!\!\!\perp B | C \cup A \setminus \alpha$ . Using the intersection property (4.9) we then have  $A \perp\!\!\!\perp B | C$  as required. The second possibility is that  $A \cup B \cup C \subset S$  so that some nodes lie outside the sets  $A$ ,  $B$  and  $C$ , as illustrated in Figure 4.20. We then choose  $\alpha \in S \setminus (A \cup B \cup C)$ . Then  $S \cup \alpha$

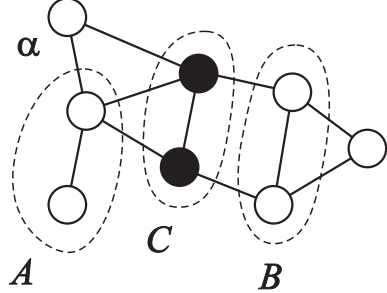


Figure 4.20: Example of a graph corresponding to case (ii) in Theorem 4.15.

separates  $A$  from  $B$  in the graph and so  $A \perp\!\!\!\perp B | C \cup \alpha$ , since adding a node to the conditioning set cannot revoke a separation property. There are now two sub-possibilities to consider. We can have  $A \cup C$  separates  $\alpha$  from  $B$  (as illustrated in Figure 4.20) in which case  $\alpha \perp\!\!\!\perp B | A \cup C$  from which, using (4.9) we obtain  $A \perp\!\!\!\perp B | C$  as required. Alternative we can have that  $B \cup C$  separates  $\alpha$  from  $A$  and hence  $\alpha \perp\!\!\!\perp A | B \cup C$  from which, using (4.9), we again obtain  $A \perp\!\!\!\perp B | C$ .  $\square$

### 4.5.2 Local Markov

Next we consider the *local Markov property*, denoted by  $\mathcal{L}$ , which says that the conditional distribution of a variable  $\alpha$  given the neighbours of  $\alpha$  in the graph is independent of the remaining nodes. We can express this more formally by introducing the concept of the *boundary* of  $\alpha$ , denoted  $bd(\alpha)$ , which comprises all of the nodes which have a direct link to  $\alpha$ . Similarly we define the *closure* of  $\alpha$ , denoted  $cl(\alpha)$ , to be the union of  $\alpha$  and its boundary,  $cl(\alpha) \equiv \alpha \cup bd(\alpha)$ . The local Markov property for undirected graphs can then be expressed as

$$\alpha \perp\!\!\!\perp S \setminus cl(\alpha) | bd(\alpha). \quad (4.32)$$

This is illustrated in Figure 4.21.

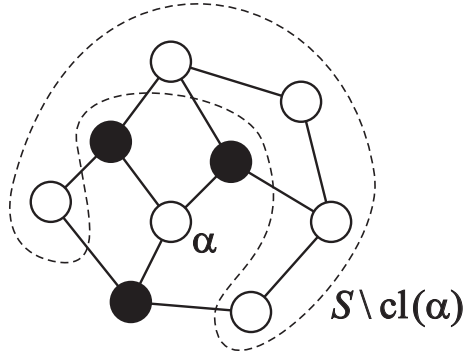


Figure 4.21: Illustration of the local Markov property (4.32) in which the black nodes represent the boundary of  $\alpha$ .

Clearly the local Markov property is a special case of the global Markov property, so  $\mathcal{G} \Rightarrow \mathcal{L}$ . We now prove that local Markov implies pairwise Markov.

**Theorem 4.16** ( $\mathcal{L} \Rightarrow \mathcal{P}$ ) *For any undirected graph and any distribution, if the distribution satisfies the local Markov property with respect to a graph then it will also satisfy the pairwise Markov property for that graph.*

**Proof:** Consider two nodes  $\alpha$  and  $\beta$ , let  $\text{bd}(\alpha)$  denote the boundary of  $\alpha$  and let  $B$  denote the remaining nodes including  $\beta$ , as illustrated in Figure 4.22. Then the local Markov property tells us that

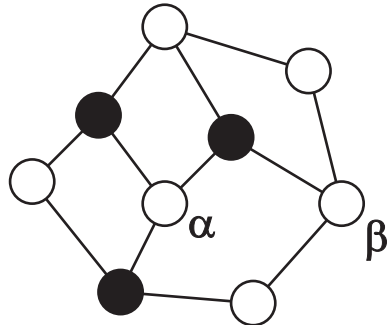


Figure 4.22: Example of an undirected graph in which the black nodes denote the boundary of a particular node  $\alpha$ . The remaining white nodes constitute the set  $B$  which includes a specific node  $\beta$ .

$$\alpha \perp\!\!\!\perp B \mid \text{bd}(\alpha). \quad (4.33)$$

Since  $\beta \in B$  we have  $B \equiv \beta \cup (B \setminus \beta)$ . We can then apply the weak union property (4.7) to obtain

$$\alpha \perp\!\!\!\perp \beta \mid \text{bd}(\alpha) \cup (B \setminus \beta) \quad (4.34)$$

and since the union of  $\text{bd}(\alpha)$  and  $(B \setminus \beta)$  represents the complete set  $S$  of nodes in the graph, less  $\alpha$  and  $\beta$  we have

$$\alpha \perp\!\!\!\perp \beta \mid S \setminus (\alpha \cup \beta) \quad (4.35)$$

which is the pairwise Markov property.  $\square$

### 4.5.3 Hammersley-Clifford Theorem

We now return to the Hammersley-Clifford theorem, and use the results derived earlier in this section to provide a formal proof. First we prove the Möbius inversion lemma.

**Lemma 4.1** *Consider a finite set  $V$  of elements  $a \in V$ , and let  $\Psi$  and  $\Phi$  be functions defined over all possible subsets of  $V$ . Then the statement*

$$\Psi(a) = \sum_{b:b \subseteq a} \Phi(b) \quad (4.36)$$

*is equivalent to the statement*

$$\Phi(a) = \sum_{b:b \subseteq a} (-1)^{|a \setminus b|} \Psi(b) \quad (4.37)$$

*where  $|a|$  denotes the cardinality of the subset  $a$ .*

**Proof:** We show that (4.37) implies (4.36), with the proof of the converse proceeding analogously. Consider

$$\begin{aligned} \sum_{b:b \subseteq a} \Phi(b) &= \sum_{b:b \subseteq a} \sum_{c:c \subseteq b} (-1)^{|b \setminus c|} \Psi(c) \\ &= \sum_{c:c \subseteq a} \left\{ \sum_{b:c \subseteq b \subseteq a} (-1)^{|b \setminus c|} \right\} \\ &= \sum_{c:c \subseteq a} \left\{ \sum_{h:h \subseteq a \setminus c} (-1)^{|h|} \right\}. \end{aligned}$$

The final sum on the right hand side is zero unless  $\subseteq a \setminus c = \emptyset$  (i.e.  $c = a$ ) since for any finite, non-empty set the number of subsets of even cardinality is the same as the number of subsets of odd cardinality (as is easily verified by induction).  $\square$

We now use Lemma 4.1 to prove the Hammersley-Clifford theorem.

**Theorem 4.17 (Hammersley-Clifford):**  $\mathcal{P} \Rightarrow \mathcal{F}$  For distributions which satisfy the intersection property (4.9), and for arbitrary undirected graphs, any distribution which satisfies the pairwise Markov property for a particular graph will factorize according to that graph.

**Proof:** Consider the joint distribution  $P(S)$  where  $S \equiv \{S_\alpha\}$  and the  $S_\alpha$  take values in some space  $\chi$ . Now choose a particular (arbitrary) value  $S^* \in \chi$ . For each possible subset  $a \subseteq S$  we define the function

$$H_a(S) = \ln P(\hat{S}a) \quad (4.38)$$

where  $\hat{S}_a$  has components  $\hat{S}^{a\alpha} = S_\alpha$  for  $\alpha \in a$  and  $\hat{S}_{a\alpha} = S^*$  for  $\alpha \notin a$ . Thus  $H_a(S)$  depends on  $S$  only through  $S_a$ . Now define the following set of functions for all  $a \subseteq S$

$$\phi_a(S) = \sum_{b:b \subseteq a} (-1)^{|a \setminus b|} H_b(S). \quad (4.39)$$

Again we see that  $\phi_a(S)$  depends on  $S$  only through  $S_a$ . Using Lemma 4.36 we obtain

$$H_S(S) = \sum_{a:a \subseteq S} \phi_a(S). \quad (4.40)$$

From the definition of  $H_A(S)$  we also have  $H_S(S) = \ln P(S)$ . Defining  $\psi_a(S_a) = \exp \phi_a(S_a)$  and taking the exponential of both sides of (4.40) we obtain

$$P(S) = \prod_{a:a \subseteq S} \phi_a(S) \quad (4.41)$$

which has the required form of a product over potential functions. The final step is to show that  $\phi_a(S)$  vanishes unless the subset  $a$  is complete. To do this we make use of the assumed pairwise Markov property. Let  $\alpha, \beta \in a$  be two nodes with no direct link between them, and let  $c = a \setminus \{\alpha, \beta\}$ . If we let  $H_a$  denote  $H_a(S)$  then

$$\phi_a(S) = \sum_{b:b \subseteq c} (-1)^{|c \setminus b|} \{ H_b - H_{b \cup \alpha} - H_{b \cup \beta} + H_{b \cup \{\alpha, \beta\}} \}. \quad (4.42)$$

If we define  $d = S \setminus \{\alpha, \beta\}$ , then by the pairwise Markov property  $\alpha \perp\!\!\!\perp \beta | d$  and hence

$$\begin{aligned}
 H_{b \cup \{\alpha, \beta\}} - H_{b \cup \alpha} &= \ln \frac{P(S_b, S_\alpha, S_\beta, S_{d \setminus b}^*)}{P(S_b, S_\alpha, S_\beta^*, S_{d \setminus b}^*)} \\
 &= \ln \frac{P(S_\alpha | S_b, S_{d \setminus b}^*) P(S_\beta, S_b, S_{d \setminus b}^*)}{P(S_\alpha | S_b, S_{d \setminus b}^*) P(S_\beta^*, S_b, S_{d \setminus b}^*)} \\
 &= \ln \frac{P(S_\alpha^* | S_b, S_{d \setminus b}^*) P(S_\beta, S_b, S_{d \setminus b}^*)}{P(S_\alpha^* | S_b, S_{d \setminus b}^*) P(S_\beta^*, S_b, S_{d \setminus b}^*)} \\
 &= \ln \frac{P(S_b, S_\alpha^*, S_\beta, S_{d \setminus b}^*)}{P(S_b, S_\alpha, S_\beta^*, S_{d \setminus b}^*)} \\
 &= H_{b \cup \beta} - H_b.
 \end{aligned}$$

Hence the sum of the terms in the brackets on the right hand side of (4.42) vanishes whenever we can find two nodes  $\alpha$  and  $\beta$  having no direct connection between them. Thus  $\phi_a(S)$  vanishes unless  $a$  is a complete set.  $\square$

#### 4.5.4 Summary of Markov Properties for Undirected Graphs

In this chapter we have proved the following results:  $\mathcal{F} \Rightarrow \mathcal{G}$  (Theorem 4.7) and  $\mathcal{L} \Rightarrow \mathcal{P}$  (Theorem 4.16). Since the local and pairwise Markov properties are special cases of the global Markov property, we also trivially have  $\mathcal{G} \Rightarrow \mathcal{L}$  and  $\mathcal{G} \Rightarrow \mathcal{P}$ . Thus for all distributions

$$\mathcal{F} \Rightarrow \mathcal{G} \Rightarrow \mathcal{P} \Leftrightarrow \mathcal{L}. \quad (4.43)$$

For distributions which satisfy the intersection property (4.9), for example strictly positive distributions, we have also shown that  $\mathcal{P} \Rightarrow \mathcal{G}$  (Theorem 4.15) and  $\mathcal{G} \Rightarrow \mathcal{F}$  (Theorem 4.17), and so for such distributions the three Markov properties, as well as the factorization property, are all equivalent.

In Chapter ? we introduce the idea of triangulation of an undirected graph. Essentially this involves the addition of extra links such that every

cycle of four or more nodes has a chord. It can be shown that the global Markov and the factorization properties are equivalent for all distributions (without restriction) if, and only if, the graph is triangulated.

## 4.6 Representational Limitations

We have considered three alternative ways in which to specify the conditional independence properties of a joint distribution: (i) write down an explicit list of conditional independence statements, (ii) specify an undirected graph, (iii) specify a directed graph. Here we consider the relationship between the corresponding families of distributions.

Earlier we considered a specific (directed or undirected) graph as being a filter, so that the set of all possible distributions over the given variables could be reduced to a sub-set which respect the conditional independencies implied by the graph. A graph is said to be a *D-map* (for ‘dependency map’) of a distribution if every conditional independence statement satisfied by the distribution is reflected in the graph. Thus a completely disconnected graph (no links) will be a trivial D-map for any distribution.

Alternatively, we can consider a specific distribution and ask which graphs have the appropriate conditional independence properties. If every conditional independence statement implied by a graph is satisfied by a specific distribution, then the graph is said to be an *I-map* (for ‘independence map’) of that distribution. Clearly a fully connected graph will be a trivial I-map for any distribution.

If it is the case that every conditional independence property of the distribution is reflected in graph separation, and vice versa, then the graph is said to be a *perfect map*. A perfect map is therefore both an I-map and a D-map for the distribution.

Consider the set of distributions such that for each distribution there exists a directed graph which is a perfect map. This set is distinct from the set of distributions such that for each distribution there exists an undirected graph which is a perfect map. In addition there are distributions for which neither directed nor undirected graphs offer a perfect map. This is illustrated as a Venn diagram in Figure 4.23.

Figure 4.24 shows an example of a directed graph which is a perfect map for a distribution satisfying the conditional independence properties  $A \perp\!\!\!\perp B | \emptyset$  and  $A \not\perp\!\!\!\perp B | C$ . There is no corresponding undirected graph over the same three variables which is a perfect map.

Conversely, consider the undirected graph over four variables show in

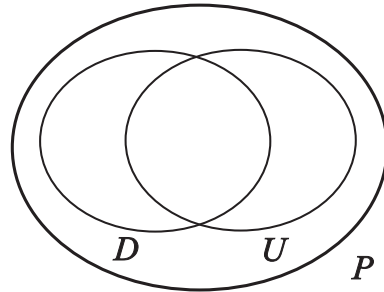


Figure 4.23: Venn diagram illustrating the set of all distributions  $P$  over a given set of variables, together the set of distributions  $D$  which can be represented as a perfect map using a directed graph, and the set  $U$  which can be represented as a perfect map using an undirected graph.

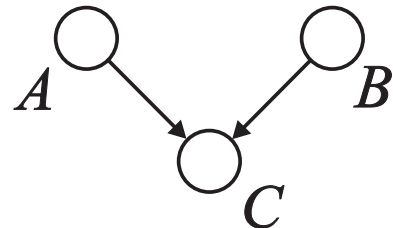


Figure 4.24: A directed graph whose conditional independence properties cannot be expressed using a directed graph over the same three variables.

Figure 4.25. This graph exhibits the properties  $A \not\perp\!\!\!\perp B \mid \emptyset$ ,  $C \perp\!\!\!\perp D \mid A \cup B$  and  $A \perp\!\!\!\perp B \mid C \cup D$ . There is no directed graph over four variables which implies the same set of conditional independence properties.

The graphical framework can be extended to graphs which include both directed and undirected edges and which contain the directed and undirected graphs considered so far as special cases. Such graphs are called *chain graphs*, and although they represent a broader class than either directed or undirected alone, there remain distributions for which even a chain graph cannot provide a perfect map. Chain graphs are not discussed further in this book.

#### 4.6.1 Markov Equivalent Graphs

For distributions whose conditional independence properties can be represented graphically, we might ask whether the graph is unique. Here we

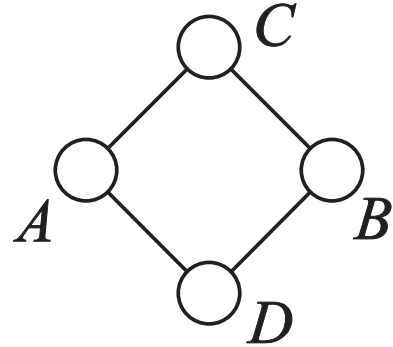


Figure 4.25: An undirected graph whose conditional independence properties cannot be expressed in terms of a directed graph over the same variables.

consider directed graphs, and discuss whether two different graphs can be Markov equivalent, that is whether they can imply the same list of conditional independence statements. [to be completed]

## 4.7 Historical Remarks and Bibliography

History of the Hammersley-Clifford theorem. Acknowledgement to Lauritzen's book for proofs. Castello's book. I-maps, D-maps and d-separation introduced by Pearl. The use of D-separation to determine global Markov properties for directed graphs with deterministic connections is discussed in Geiger and Pearl (1990). Geiger, Verma, and Pearl (1990) constructed an example model which is such that any conditional independencies which do not correspond to d-separation on a DAG are not present in the distribution, showing that in general d-separation will find all of the conditional independencies which can be determined directly from the DAG.

## Exercises

- 4.1 (\*)** Consider three binary variables  $A, B, C \in \{0, 1\}$  having the joint distribution given in Table 4.1. Show by direct evaluation that this distribution has the property that  $A$  and  $B$  are marginally dependent, so that  $P(A, B) \neq P(A)P(B)$ , but that they become independent when conditioned on  $C$ , so that  $P(A, B|C) = P(A|C)P(B|C)$  for both  $C = 0$  and  $C = 1$ .

$A$	$B$	$C$	$P(A, B, C)$
0	0	0	?
0	0	1	?
0	1	0	?
0	1	1	?
1	0	0	?
1	0	1	?
1	1	0	?
1	1	1	?

Table 4.1: The joint distribution over three binary variables.

**4.2 (\*)** Using the result of the Exercise 4.1 show that the joint distribution specified in Table 4.1 can be expressed in the form  $P(A, B, C) = P(A)P(C|A)P(B|C)$ . Draw the corresponding directed graph.

**4.3 (\*)** Show that there are  $2^{M(M-1)/2}$  distinct undirected graphs over  $M$  variables. Draw the 8 possibilities for the case of  $M = 3$ .

**4.4 (\*)** Consider the simple graph shown in Figure 4.26, together with the probability distribution over three binary variables  $X$ ,  $Y$  and  $Z$  such that  $P(X = 0) = P(X = 1) = 0.5$  and  $X = Y = Z$ . Show that for this graph and distribution the pairwise Markov property is satisfied, but not the local Markov property. Note that this distribution is not strictly positive since, for instance,  $P(X = 0, Y = 1, Z = 1) = 0$ .



Figure 4.26: A graph which provides a counter example to the claim  $\mathcal{P} \Rightarrow \mathcal{L}$ .

# An Introduction to Probabilistic Graphical Models

Michael I. Jordan  
*University of California, Berkeley*

June 30, 2003



## Chapter 17

# The Junction Tree Algorithm

In earlier chapters we have presented a number of examples of inferential calculations in graphical models. The general problem has been to calculate the conditional probability of a node or a set of nodes, given the observed values of another set of nodes. In the case of mixture models and factor analysis models the problem was to calculate the conditional probabilities of the latent variables given the observed data, and the solution was a rather straightforward application of Bayes rule. In the case of the HMM and the state-space model we saw a somewhat more complex inference problem involving dependencies between nodes arranged in a sequence. The solution was again an application of Bayes rule, but it was necessary to find recursions that allowed the inference problem to be solved efficiently. The Markov properties of the underlying graphical model provided the formal machinery to justify these recursions.

In the current chapter we present a general approach to inference that makes systematic use of the Markov properties of graphical models. All of the examples that we have treated until now emerge as special cases; moreover, the recursions that we worked out rather painstakingly in each individual case can now be derived more systematically. The general idea is to use the Markov properties of graphical models to find ways to decompose a general probabilistic calculation into a linked set of local computations. The key to this approach is an appropriate definition of “local.”

Chapter 3 presented a simple elimination algorithm (`ELIMINATION`) for inference on directed or undirected graphs. As `ELIMINATION` runs it creates dependencies between nodes, in effect redefining the “locality” relationships in the graph. To develop a deeper understanding of probabilistic inference, it proves helpful to abstract away from the specific process of elimination and to focus on this general notion of locality. In effect we shift our focus from the *process* of inference to the *data structures* that underly inference. We find that a particular data structure—the *junction tree*—emerges from these considerations. The junction tree makes explicit the important (and beautiful) relationship between graph-theoretic locality and efficient probabilistic inference.

Although we present specific algorithms for probabilistic inference in this chapter, it is important to emphasize at the outset that our goal is less that of providing specific recipes as it is of providing an understanding of the key general concepts that underly inference. Thus, while we will describe concrete algorithms (the “Hugin algorithm,” the “Shafer-Shenoy algorithm,” and the “Lauritzen-Spiegelhalter algorithm”), we view all of these algorithms as instances of a general algorithmic

framework that we will refer to generically as the *junction tree algorithm*. Understanding the general framework makes it easy to see how various specific algorithms arise and how they interrelate. Moreover, an important bonus of developing the general junction tree framework is the realization that probabilistic inference is itself an instance of a more general class of problems, all of which involve factorized potentials on graphs, and all of which can be solved using suitable variations on the junction tree theme. We discuss some instances of this more general class at the end of the chapter.

We begin by returning to the elimination algorithm from Chapter 3, stripping away some of its inessential details, and aiming to overcome some of its deficiencies.

## 17.1 From elimination to the junction tree

In Figure 17.1(a) we show the graph that served as a running example in Chapter 3. The factored form of the joint probability distribution for this graph is as follows:

$$p(x_1, x_2, \dots, x_6) = p(x_1)p(x_2 | x_1)p(x_3 | x_1)p(x_4 | x_2)p(x_5 | x_3)p(x_6 | x_2, x_5). \quad (17.1)$$

As in Chapter 3 we will use the elimination ordering  $(X_6, X_5, X_4, X_3, X_2, X_1)$  in our examples.

Each factor in Eq. (17.1) expresses a dependency among one or more variables. Forming summands during a run of the elimination algorithm creates additional dependencies—for example, summing over  $x_6$  creates an intermediate factor that is a function of  $x_2$  and  $x_5$ . The *elimination cliques* associated with an elimination ordering can be viewed as an explicit record of these dependencies. Recall that we can abstract away from probabilistic inference and view these elimination cliques as being formed by a purely graph-theoretic procedure (called `UNDIRECTED-GRAPHELIMINATE` in Chapter 3) in which we link all of the neighbors of a given node (thus forming a clique), and remove the node from the graph. In particular, for the elimination ordering  $(X_6, X_5, X_4, X_3, X_2, X_1)$ , the elimination cliques are as shown in Figure ??(b). While the elimination algorithm `ELIMINATION` does not explicitly form these cliques, the graph-theoretic operation of forming elimination cliques parallels the algebraic operation of marginalizing over a node, and neatly summarizes the graphical consequences of marginalization.

The elimination algorithm is “query-oriented.” That is, the algorithm yields the marginal or conditional probability of a given query node—the last node in the elimination ordering. Intermediate factors that are created along the way are discarded. While in some cases this is what we want, in many cases it is not. Consider in particular the chain-structured graphical model associated with the HMM or the state-space model. To calculate the posterior probability of any particular node we can eliminate forward and backward until we arrive at the node. In doing so we create a number of intermediate factors. Many of these same intermediate factors can be used in calculating the posterior probability of other nodes. Clearly we wish to avoid recomputing such factors, as we would do in a naive application of elimination. We also need to know which intermediate factors are needed for which posterior probabilities and how to combine factors—in essence we need a calculus for the intermediate factors. The elimination algorithm provides us with little help in this regard.

As a first step in moving beyond the elimination algorithm we need to allocate data structures—“permanent storage”—to the intermediate factors. Each such factor is associated with one of the

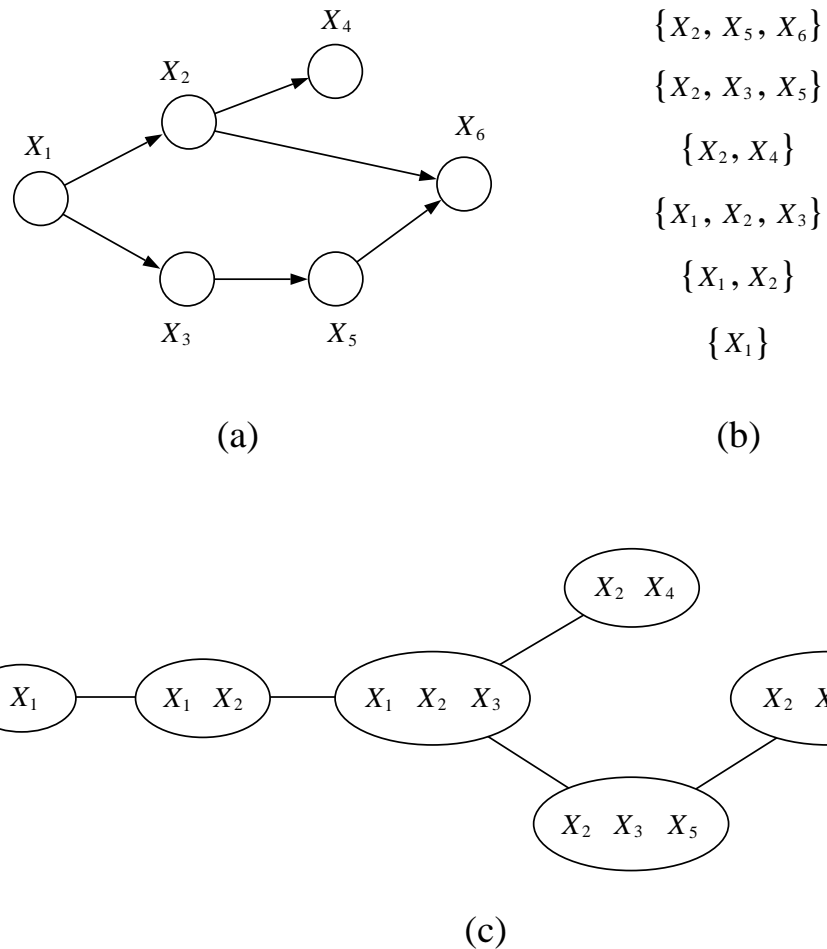


Figure 17.1: (a) The six-node example from Chapter 3. (b) The elimination clique created from a run of the elimination algorithm using the ordering  $(X_6, X_5, X_4, X_3, X_2, X_1)$ . (c) The elimination cliques arranged into a clique tree.

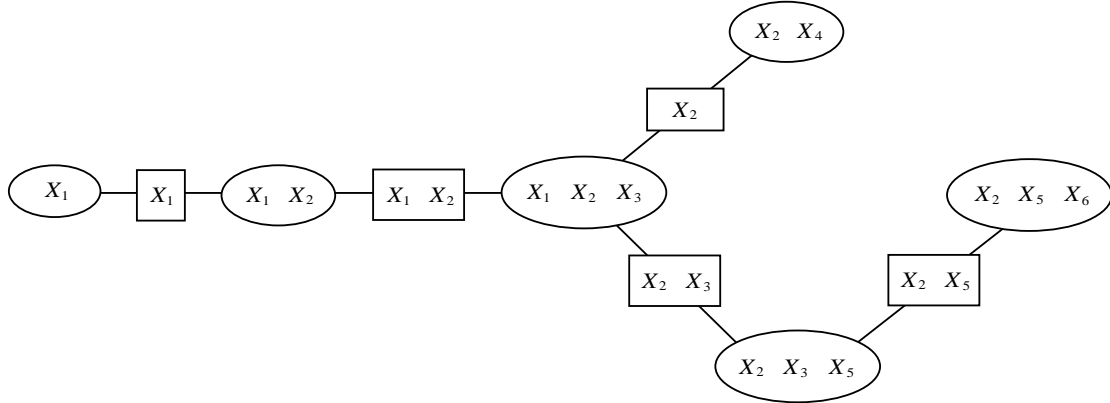


Figure 17.2: A clique tree annotated with separator sets.

elimination cliques in Figure 17.1(b). We can therefore view the nodes in this figure as representations of the storage that we need if we are to record the intermediate factors created during a run of the elimination algorithm.

While a list of the elimination cliques reveals some of the structure associated with the elimination algorithm, there is additional structure that is worth noting. In particular, as we have seen, summing over a variable produces an intermediate factor that subsequently appears in the summand associated with a later variable. For example, summing over  $x_5$  creates an intermediate factor that refers to  $x_3$  and thus appears in the summand when we subsequently sum over  $x_3$ . If we view the nodes in Figure 17.1(b) as storage sites, and if we view the operation of summing as operating on the data stored at these sites, then it is natural to try to represent the transfer of information between these sites. For example, the sum over  $x_3$  requires the factor created at the  $x_5$  site, and we therefore need to transfer this factor between the site corresponding to the elimination of  $x_5$ —the elimination clique  $\{X_2, X_3, X_5\}$ —and the site corresponding to the elimination of  $x_3$ —the elimination clique  $\{X_1, X_2, X_3\}$ . As shown in Figure 17.1(c), we can capture this flow of information by drawing an edge between these elimination cliques.

The graphical object in Figure 2.1(c) is a *clique tree*—a singly-connected graph in which the nodes are the cliques of an underlying graph. Every run of the elimination algorithm can be viewed as implicitly creating a clique tree—the clique tree can be viewed in essence as an “execution trace” of the algorithm. What we are groping towards, however, is an algorithm that goes beyond the elimination framework by explicitly representing a clique tree as a data structure. The nodes in such a clique tree will store intermediate factors, allowing these factors to be reused in multiple queries. Information will flow around the clique tree in multiple directions.

In Figure 17.2 we annotate the clique tree with some additional structure that will prove to be useful. Between each linked pair of cliques we introduce a *separator set*—the intersection of the corresponding cliques. The separator sets are themselves cliques, being the intersection of cliques. These sets provide an explicit representation of the variables referred to by the intermediate factors that pass between cliques. Consider, for example, the intermediate factor created at the clique  $\{X_2, X_3, X_5\}$ . Summing over  $x_5$  creates a factor that is a function of  $x_2$  and  $x_3$ , and this factor

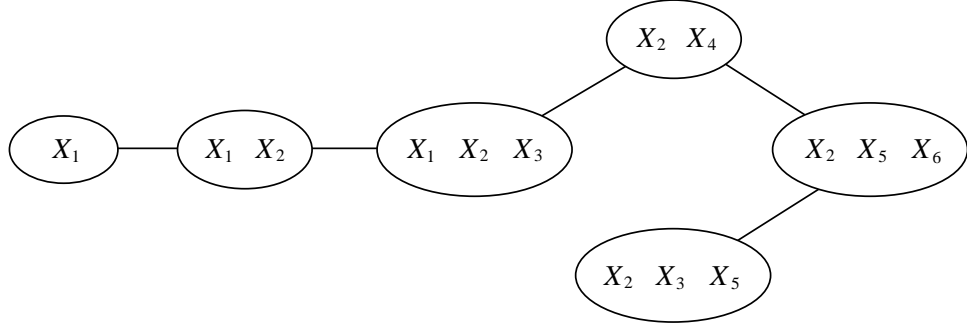


Figure 17.3: A clique tree that does not possess the junction tree property. Note in particular that the cliques containing the node  $X_3$  do not form a connected subtree.

is sent to the clique  $\{X_1, X_2, X_3\}$ , where we subsequently sum over  $x_3$ . The separator set on the link between these cliques contains the nodes  $\{X_2, X_3\}$ , and thus explicitly represents the domain of the intermediate factor transferred between the cliques.

Not all clique trees are created equal. In particular, the clique tree in Figure 2.1(c) has some special properties. Note that the index “2” appears in five different nodes in the figure, and that these five nodes are connected—they form a *connected subtree*. Moreover, this is true of all of the other node indices. This interesting and important property is known as the *junction tree property*. Not all clique trees possess the junction tree property; for example, the tree in Figure 17.3 does not possess the junction tree property. As we will see in the remainder of the chapter, understanding the junction tree property is the key to a general understanding of probabilistic inference.

## 17.2 Potentials

With the discussion in the previous section as background, we embark on a general discussion of the junction tree algorithm. We will be focusing on a particular variant of the general junction tree algorithm known as the “Hugin algorithm,” and will discuss other variations in later sections and in the exercises.

Let  $G = (V, E)$  denote a directed or undirected graph with vertices  $V$  and edges  $E$ . Let  $\mathcal{C}$  denote a set of *cliques* of  $G$ ; i.e.,  $\mathcal{C}$  is a set of completely connected subsets of  $V$ . We generally require these subsets to be maximal, so that no member of  $\mathcal{C}$  is a subset of another member of  $\mathcal{C}$ . However, at the cost of a bit of redundancy it is at times convenient to allow such proper subsets to appear in  $\mathcal{C}$ .

Let  $X$  be a random vector indexed by the vertices  $V$ . Recall that we allow subsets of the vertex set  $V$  to be used as indices; thus, corresponding to each clique  $C \in \mathcal{C}$ , we have a set of random variables  $X_C$ , with realizations  $x_C$ . The number of such realizations is the product of the number of realizations of each individual random variable  $X_u$ , for  $u \in C$ .

Associated with each  $C \in \mathcal{C}$  we define a *potential*  $\psi_C(x_C)$ , a nonnegative function on the realizations  $x_C$ . In general there are no constraints on the potential functions other than nonnegativity. Note in particular that the sets  $C$  can overlap, and we make no “consistency” requirements on the

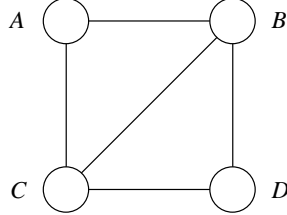


Figure 17.4: A four-node model which we assume is parameterized with pairwise potentials:  $\psi_{AB}$ ,  $\psi_{AC}$ ,  $\psi_{BC}$ ,  $\psi_{BD}$ , and  $\psi_{CD}$ .

overlap.

We now define a joint probability distribution on  $X$  as the normalized product of potential functions:

$$p(x) \triangleq \frac{1}{Z} \prod_{C \in \mathcal{C}} \psi_C(x_C). \quad (17.2)$$

This is of course the same definition as that used for undirected graphs. Note, however, a subtle but important change in focus—in the current section we view the set of subsets  $\mathcal{C}$  as an explicit data structure, with the underlying graph in the background. Technically, our data structure is a *hypergraph*—a set of subsets—with Eq. (17.2) defining the joint probability distribution associated with the hypergraph.

There are problems in which it is natural to pose the problem directly in terms of factored potentials on sets of subsets, without focusing on an underlying graph. Most commonly, however, the potentials on the hypergraph are *initialized* from those of an underlying graph. Let us consider how this initialization process works for both undirected and directed graphs.

Undirected graphs come endowed with potential functions on cliques, and if these cliques are the same as the set of subsets  $\mathcal{C}$ , then the initialization problem is vacuous; we simply define  $\psi_C(x_C)$  to be the corresponding potential from the underlying graph. In general, however, these sets are not the same. In particular, we generally include only the maximal cliques in the set  $\mathcal{C}$ . If the parameterization of the underlying undirected graph is restricted to cliques that are proper subsets of the maximal cliques of the graph, as is often the case, then we have a many-to-one mapping from parameterized cliques to  $\mathcal{C}$ . Consider, for example, the undirected graphical model in Figure 17.4, where we assume that the model is parameterized via pairwise potentials. The maximal cliques of the graph are, however, triplets of nodes. In such a situation, the potentials on maximal cliques in Eq. (17.2) are formed as the product of potentials from the underlying graph. Thus, in our example, we define  $\psi_{ABC}$  to be the product  $\psi_{AB}\psi_{AC}$ , while we define  $\psi_{BCD}$  to be the product  $\psi_{BC}\psi_{BD}\psi_{CD}$ . Note that  $\psi_{BC}$  can be associated with either triple; we have arbitrarily assigned it to  $\psi_{BCD}$ . In general each potential  $\psi_D$  on the underlying graph is assigned to one and only one  $\psi_C$  on the hypergraph, where  $D \subset C$ . If we assume that  $\mathcal{C}$  includes the maximal cliques, then this can always be done.

Having assigned each underlying potential to one and only one  $\psi_C$ , the product in Eq. (17.2) is a faithful representation of the joint probability from the underlying graph.

Similar issues arise when we initialize a set of clique potentials from an underlying directed

$\text{MORALIZE}(G)$

```

for each node  $X_i$  in  $I$ 
    connect all of the parents of  $X_i$ 
end drop the orientation of all edges
return  $G$ 

```

Figure 17.5: An algorithm to moralize a directed graph.

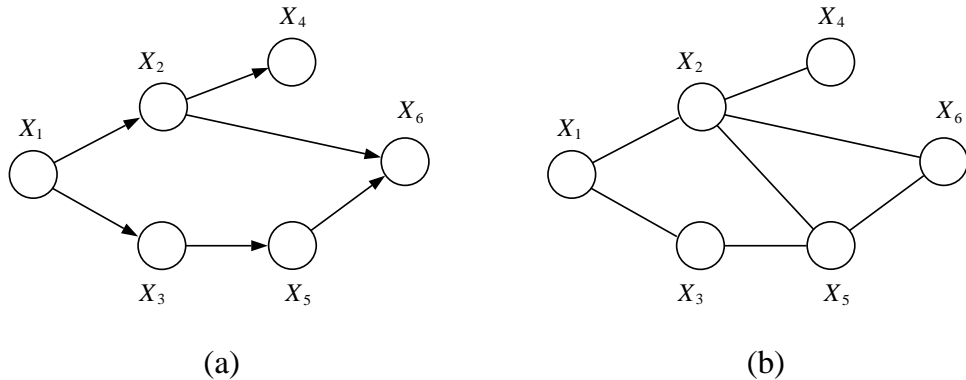


Figure 17.6: (a) A directed graph. Note that the conditional probability  $p(x_6 | x_2, x_5)$  has as arguments a subset of nodes that are not contained in any clique in the graph. In the moral graph in (b), an edge has been added between  $X_2$  and  $X_5$ , and now the arguments in the potential  $p(x_6 | x_2, x_5)$  are contained with the clique  $\{X_2, X_5, X_6\}$ .

graph, with the additional complication that the original potentials—the local conditional probabilities from the directed graph—need not be defined on cliques. In particular, if the parents of node  $X_i$  are not linked, then  $p(x_i | x_{\pi_i})$  is not a function on a clique. To handle this situation, and thereby allow a uniform treatment of directed and undirected graphs, we *moralize* the directed graph. Recall from Chapter 3 that the moral graph  $G^m$  corresponding to a directed graph  $G$  is obtained by linking the parents of each node and dropping the directionality of the edges. We define the moralization procedure more formally in Figure 17.2. On a moral graph, the local conditional probabilities are potential functions on cliques. We associate each such probability with one and only one potential  $\psi_C(x_C)$ , again assuming that  $C$  includes the maximal cliques. Taking the product over these potentials is then equivalent to taking the product  $\prod_i p(x_i | x_{\pi_i})$ , and faithfully represents the joint probability from the underlying directed graph.

Note that for directed graphs the potentials are already normalized; in other words, the normalization factor  $Z$  is automatically one.

Figure 17.2 shows an example for a directed graph.

Note that the moralization procedure adds edges to a directed graph. How does this procedure

square with the semantic distinctions between directed graphs and undirected graphs presented in the previous chapter? Recall that a given graph—directed or undirected—is associated with a family of probability distributions. This family can be specified by writing down the list of conditional independence statements associated with the graph. Any distribution that respects all of the conditional independence statements in the list belongs to the family. Clearly, if we make *fewer* statements we make the family *larger*. Now note that a moral graph necessarily makes fewer conditional independence statements than its corresponding directed graph. In particular, a directed graph asserts all of the conditional independencies that characterize the moral graph, as well as additional independencies between the parents of a given node in the marginal distribution in which the node is eliminated. Thus the set of probability distributions associated with the directed graph is a subset of the set of probability distributions associated with the moral graph. If we solve the inference problem for the family of probability distributions associated with the undirected moral graph, we solve it for the family of probability distributions associated with the directed graph as well.

Moralization is not merely a convenience, but is also a necessary component of any inference algorithm. Marginalization or conditioning couples the parents of a node, creating an intermediate factor that is in general a non-trivial function of the parents.<sup>1</sup> Intuitively, moralization is necessary to capture dependencies such as “explaining-away” that arise whenever a node is an evidence node or has descendants that are evidence nodes.

To summarize, our procedure will be to identify the maximal cliques of an undirected or (moralized) directed graph.<sup>2</sup> We initialize the potential functions associated with these cliques from the potentials and local conditional probabilities on the underlying graph.

### 17.3 Introducing evidence

We now consider the problem of conditioning, or “introducing evidence.” We suppose that the nodes are partitioned into subsets  $H$  and  $E$ , and that the random vector  $X_E$  is observed to take on a specific value. The problem that we discuss in this section is that of representing the conditional probability  $p(x_H | x_E)$ . Once we have decided on such a representation, the inferential problem of computing marginals under this probability—the conditional probabilities of subsets of the nodes  $X_H$ —will be no different in principle from the calculation of marginal probabilities under the overall joint  $p(x)$ .

Our general approach will be to represent conditionals via taking “slices” of the potentials defining the joint probability. Suppose in particular that we have represented the joint probability as a product over cliques as in Eq. (17.2). For each clique  $C$ , consider the intersection  $C \cap E$ . The nodes in this intersection have been fixed to specific values, and the potential in effect now ranges

---

<sup>1</sup>If a node is not an evidence node or has no descendants that are evidence nodes, summing over the values of the node yields the trivial value of one.

<sup>2</sup>Some readers may wonder how we can achieve this—finding maximal cliques is an NP-hard problem! In fact, we will not be finding the maximal cliques of arbitrary graphs, but only of a special class—the *triangulated graphs*. Maximal cliques of triangulated graphs can be found easily. Let us postpone our discussion of triangulation, however, at the cost of a bit of naiveté with regards to identifying maximal cliques.

over the complement (in  $C$ ) of this set of nodes, i.e.,  $C \cap H$ . where  $C = (C \cap H) \cup (C \cap E)$  by the assumption that  $H$  and  $E$  partition  $V$ . Thus, for a particular fixed configuration  $\bar{x}_E$ , we have:

$$p(x_H, \bar{x}_E) = \frac{1}{Z} \prod_{C \in \mathcal{C}} \psi_C(x_{C \cap H}, \bar{x}_{C \cap E}). \quad (17.3)$$

This is a product of “slices” of potential functions.

A slice of a potential function is itself a potential function. Thus we can also view Eq. (17.3) as a product of potential functions on subsets  $\{X_{C \cap H}$  of the nodes  $X_H$ , suppressing reference to the nodes  $X_E$ . That is, writing  $\tilde{\psi}_{C \cap H}(x_{C \cap H}) \triangleq \psi_C(x_{C \cap H}, \bar{x}_{C \cap E})$  to suppress the explicit reference to the fixed configuration  $\bar{x}_E$ , we have:

$$p(x_H, \bar{x}_E) = \frac{1}{Z} \prod_{C \in \mathcal{C}} \tilde{\psi}_{C \cap H}(x_{C \cap H}) \quad (17.4)$$

as a product of potential functions over  $X_H$ .

There is an oddity to Eq. (17.4), however, in that the normalization factor  $Z$  is obtained by summing over both  $X_H$  and  $X_E$ , whereas the product is defined only over  $X_H$ . It should be no surprise that  $Z$  is not in fact the normalization factor for the product of potentials  $\tilde{\psi}_{C \cap H}$ ; indeed, this product is not normalized. Let us compute the normalization factor. Summing over  $H$ , and denoting the sum as  $\tilde{Z}$ , we compute:

$$\tilde{Z} \triangleq \sum_H p(x_H, \bar{x}_E) \quad (17.5)$$

$$= \sum_H \frac{1}{Z} \prod_{C \in \mathcal{C}} \tilde{\psi}_{C \cap H}(x_{C \cap H}). \quad (17.6)$$

We also know, however, that  $\sum_H p(x_H, \bar{x}_E) = p(\bar{x}_E)$ , by definition. Putting these facts together, we have:

$$\frac{p(x_H, \bar{x}_E)}{p(\bar{x}_E)} = \frac{\prod_{C \in \mathcal{C}} \tilde{\psi}_{C \cap H}(x_{C \cap H})}{\sum_H \prod_{C \in \mathcal{C}} \tilde{\psi}_{C \cap H}(x_{C \cap H})}. \quad (17.7)$$

That is, the slices  $\tilde{\psi}_{C \cap H}(x_{C \cap H})$  provide a potential function representation of the *conditional* probability  $p(x_H | \bar{x}_E)$ . The normalization factor for this representation is the marginal probability  $\tilde{Z} = p(\bar{x}_E)$ . Note that the original normalization constant,  $Z$ , cancels when we form the ratio on the right-hand-side of Eq. (17.7). Thus, for the purpose of calculating conditional probabilities, we have no need of knowing the normalization constant associated with the original set of potentials; it suffices to compute the normalization constant of the sliced potentials.

Let us see how this works for a particularly simple case. In Figure 17.7. we show a directed graph and the corresponding moralized graph for two binary nodes  $X$  and  $Y$ . Given the three probabilities  $p(X = 1) = .8$ ,  $p(Y = 1 | X = 1) = .7$  and  $p(Y = 1 | X = 0) = .4$ , we can construct a joint probability distribution. Converting to a set of cliques, we have a single clique  $\{X, Y\}$ , with clique potential given by the product  $p(x)p(y | x)$ :

$$\psi_{\{X, Y\}} = \begin{bmatrix} .12 & .08 \\ .24 & .56 \end{bmatrix} \quad (17.8)$$



Figure 17.7: A two-node graphical model with its moralized graph.

Given that this potential arises from a directed graph, it is no surprise that the clique potential is normalized. Suppose that we now observe evidence  $Y = 1$ . We obtain the slice:

$$\tilde{\psi}_{\{X\}} = \begin{bmatrix} .08 \\ .56 \end{bmatrix}, \quad (17.9)$$

which is a function only of  $X$ . Note that this new clique potential is unnormalized. Normalizing yields the number  $\tilde{Z} = .64$ , which we recognize as the probability  $p(Y = 1)$ . Moreover, the normalized potential is given by dividing  $\tilde{\psi}_{\{X\}}$  by  $\tilde{Z} = .64$ :

$$\frac{1}{\tilde{Z}} \tilde{\psi}_{\{X\}} = \begin{bmatrix} .125 \\ .875 \end{bmatrix}, \quad (17.10)$$

which is the conditional distribution  $p(x | Y = 1)$ .

To summarize, our general representation of a probability distribution is a (possibly) unnormalized set of potentials on a set of cliques. Conditioning is handled by restricting attention to subsets of the original set of cliques, and by defining potentials on these subsets that are slices of the original potentials. In general we make no fundamental representational distinction between conditional and joint distributions.

This perspective also helps to reveal more of the unity in undirected and directed representations of probabilities. In the directed case, the set of potentials is normalized at the outset:  $Z = 1$ . But as soon as we observe evidence, the resulting set of slices is no longer normalized, and the conditional distribution is represented as an unnormalized product of potential functions, as in the undirected case.

An equivalent approach to representing conditional probability distributions involves introducing “evidence potentials.” An evidence potential is a delta function,  $\delta(x_E, \bar{x}_E)$ , i.e., a function which is equal to one if its arguments are equal and zero otherwise. We used evidence potentials in our presentation of the elimination algorithm in Chapter 3. Multiplying the original product of potentials by the evidence potential yields an unnormalized product on the set  $(X_H, X_E)$ . Summing over  $x_E$  has the effect of setting  $p(x_H, x_E)$  equal to  $p(x_H, \bar{x}_E)$ . Thus we obtain the same representation as that considered in this section, once we “marginalize” and restrict attention to  $X_H$ . The approach based on evidence potentials is elegant because it treats slices as formally equivalent to marginalization; indeed that was the reason that we introduced it in Chapter 3. In practice, however, using evidence potentials involves introducing zeros and then summing over those zeros. As an algorithmic matter it is more efficient to simply take slices.

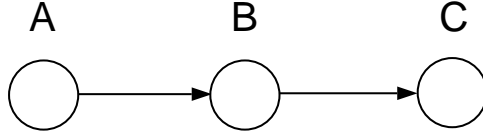


Figure 17.8: A three-node Markov chain.

## 17.4 Clique trees

We now begin to address the crux of the problem, which is that of computing *marginal probabilities*. Thus, we wish to compute the marginal  $p(x_F | x_E)$ , where  $(F, G)$  is a partition of  $H$  and where  $F$  ranges over a set of subsets of interest. In particular, we may wish to compute all probabilities  $p(x_F | x_E)$ , where  $F$  ranges over all singleton nodes. More generally, we will address the problem of computing  $p(x_F | x_E)$ , where  $F$  ranges over all cliques in  $\mathcal{C}$ , and over all subsets of these cliques.

A still more general problem is that of computing  $p(x_F | x_E)$  for arbitrary  $F$ , and while we will address this problem in Section ??, it is worth noting that in most applications it suffices to compute marginal probabilities for the cliques. In particular, the cliques are sufficient statistics for distributions that factor according to Eq. (17.2); thus, for computing expected sufficient statistics in the context of an EM algorithm it suffices to obtain clique marginals.

We define a *clique tree* as a singly-connected graph whose nodes represent members of the clique set  $\mathcal{C}$ . Edges in this graph will allow us to define information flows between cliques. The junction tree algorithm can be understood as an algorithm that uses these information flows to manipulate the clique potentials so as to yield marginal probabilities. In particular, after the algorithm runs, the potential  $\psi_C$  will be equal to the marginal probability  $p(x_C, \bar{x}_E)$ . This probability is an un-normalized version of the conditional  $p(x_C | \bar{x}_E)$ , where the normalization constant is obtained by summing or integrating  $\psi_C$  over  $x_C$ . Thus, we can obtain the desired marginal probabilities via a local operation. The goal of the remainder of the chapter is to explain how this is achieved.

In the previous two sections, we showed how to initialize the clique potentials so as obtain a representation of the joint or conditional probability. This is a global representation; the individual potentials do not necessarily correspond to local probabilities. Consider in particular the Markov chain shown in Figure 17.8. The cliques of this graph are  $\{A, B\}$  and  $\{B, C\}$ . The joint probability is  $p(x_A, x_B, x_C) = p(x_A)p(x_B | x_A)p(x_C | x_B)$ , and while  $p(x_A)$  and  $p(x_B | x_A)$  can be grouped to initialize the potential  $\psi_{AB}$  to the marginal  $p(x_A, x_B)$ , the remaining factor  $\psi_{BC} = p(x_C | x_B)$  is not a marginal. To convert this potential into a marginal, we marginalize  $\psi_{BC}$  to obtain  $p(x_B)$ , and multiply  $\psi_{BC}$  by this factor. The transfer of the probability  $p(x_B)$  is an instance of the information flow that we referred to above.

After adjusting  $\psi_{BC}$  we have achieved the goal of obtaining marginal probabilities for both of the cliques, but we have also lost something. In particular, the joint probability on  $(x_A, x_B, x_C)$  is not equal to the product of marginals  $p(A, B)$  and  $p(B, C)$ , and thus the product of the clique potentials is no longer a representation of the joint probability.

The junction tree approach in essence allows us to have our cake and eat it too, retaining a representation of the joint probability while also manipulating the clique potentials so as to convert

them into marginal probabilities. This is done by utilizing an extended representation of joint probabilities that makes use of the separator sets discussed in Section ???. The remainder of this section introduces this important generalized representation.

On each edge of a clique tree we associate a *separator set* which contains the intersection of the cliques that it links. For example, in Figure 17.16, the separator is the singleton  $X_B$ . For a general clique tree on  $N$  nodes, we have  $N - 1$  separators.

We now augment our potential-based representation of joint probabilities to include potential functions on the separators as well as the cliques. Thus, letting  $\mathcal{S}$  denote the set of all separators, we introduce a potential function  $\phi_S(x_S)$  for each  $S \in \mathcal{S}$ . Given a clique tree with cliques  $\mathcal{C}$  and separators  $\mathcal{S}$  we define the joint probability as follows:

$$p(x) = \frac{\prod_C \psi_C(x_C)}{\prod_S \phi_S(x_S)}. \quad (17.11)$$

Note that we have omitted explicit reference to a normalizing constant  $Z$ . We adopt a convention of including the empty set as one of the separators and letting the “potential” on this empty set be the normalizing constant  $Z$ .

We have several questions to answer regarding this extended representation, but let us first return to our example and show what the representation achieves for us.

Expanding the joint probability associated with Figure 17.8, we have:

$$p(x_A, x_B, x_C) = p(x_A, x_B)p(x_C | x_B) \quad (17.12)$$

$$= \frac{p(x_A, x_B)p(x_B, x_C)}{p(x_B)}. \quad (17.13)$$

This has the form of the extended representation shown in Eq. (17.11), where we define  $\psi_{AB} = p(x_A, x_B)$ ,  $\psi_{BC} = p(x_B, x_C)$ , and  $\phi_B = p(x_B)$ . Thus, making use of the flexibility offered by the separator potentials, we are able to achieve a representation that is a product of marginals, and yet is also a representation of the joint probability. It turns out that we can always find this kind of representation for a given probability distribution. The proof of this fact will emerge during our development of the junction tree algorithm.

In our discussion of the Hammersley-Clifford theorem in Chapter 16, we showed that the representation of joint probability in Eq. (17.2) is general, in the sense that it allows us to capture all of the joint probability distributions that respect the conditional independence statements asserted by a graph. Clearly the extended representation includes all such joint probability distributions (set the separator potentials to unity). Does it include any others? The answer is no. This is seen by noting that the separators are (by definition) subsets of one or more cliques. Associating each separator with one such clique, and dividing that clique potential by the separator potential, we obtain a new set of clique potentials that represent the same joint, but without the separators. Thus the separator potentials do not enlarge the set of joint probability distributions that we can represent. They are essentially a convenience—they allow us to represent the set of joint probability distributions associated with a graphical model in a more flexible way.

An additional issue that we need to consider is the possibility of division by zero. We allow division by zero but only in a constrained set of circumstances. In particular, we define a separator

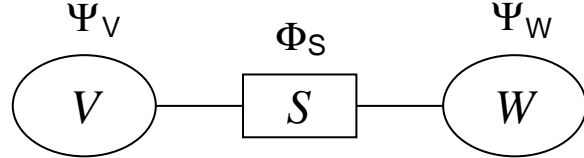


Figure 17.9: The basic data structures underlying the flow of information between cliques  $V$  and  $W$ .

potential to be *supportive* if whenever a configuration yields a value of zero for the separator potential, the clique potentials at both ends of the edge containing that separator also evaluate to zero. Thus we can never divide by zero in Eq. (17.11) unless the numerator is also zero. In this case we define the ratio to be zero. This makes sense—if a clique potential is zero for a configuration then the probability of that configuration should also be zero.

Each step of the junction tree algorithm is guaranteed to maintain supportiveness (see Exercise ??). Thus, if we have supportive separator potentials at the outset then we maintain supportiveness as the algorithm runs.

We initialize the separator potentials to unity. Thus, at the outset, once we have introduced evidence, the set of clique potentials and separator potentials are (as before) a global representation of the joint conditional probability  $p(x_H | x_E)$ . The new capability that the extended representation has provided is the ability (in principle) to obtain a local representation of marginal probabilities, while maintaining an overall representation of the joint. We now show how this is achieved in practice.

## 17.5 Local consistency

Note that cliques can overlap, so the same node can appear in multiple cliques. Clearly, if the potentials are to represent marginal probabilities, it is necessary that they be consistent with each other; that is, they must give the same marginals for nodes that they have in common. This seemingly innocuous observation is the germ of the junction tree algorithm. We will find that consistency is not only a necessary condition, but it is also a sufficient condition for a probabilistic inference algorithm. Moreover, it turns out not to be necessary to compare all pairs of cliques that intersect; it will suffice to arrange the cliques into a special clique tree—a “junction tree”—and require only that cliques that are neighbors in the junction tree agree on the nodes that they have in common.

Let us postpone the general junction tree construction, and instead focus on the elemental problem of achieving consistency between a pair of cliques. Suppose that we have two cliques  $V$  and  $W$  and suppose that  $V$  and  $W$  have a non-empty intersection  $S$  (see Figure 17.9). The cliques  $V$  and  $W$  have potentials  $\psi_V$  and  $\psi_W$ , and we also endow  $S$  with a potential  $\phi_S$  that we initialize to unity. The basic operation of the junction tree algorithm is an exchange of information between  $V$  and  $W$ , with  $S$  serving as a conduit for the flow of information. We first update  $W$  based on  $V$ ,

where the asterisk means “updated value of”:

$$\phi_S^* = \sum_{V \setminus S} \psi_V \quad (17.14)$$

$$\psi_W^* = \frac{\phi_S^*}{\phi_S} \psi_W. \quad (17.15)$$

The first equation *marginalizes* the potential  $\psi_V$  with respect to  $S$ , storing the result in the separator potential. The second equation *rescales* the potential on  $W$  by multiplying by an “update factor” that is the ratio of the new separator potential to its old value.

This update has an important invariant: the joint distribution  $p(x_H, \bar{x}_E)$ . Note that  $\psi_V$  is unchanged during the update. Defining  $\psi_V^* = \psi_V$ , we have:

$$\frac{\psi_V^* \psi_W^*}{\phi_S^*} = \frac{\psi_V \psi_W \phi_S^*}{\phi_S \phi_S^*} \quad (17.16)$$

$$= \frac{\psi_V \psi_W}{\phi_S}, \quad (17.17)$$

and thus the joint distribution as defined in Eq. ?? is unchanged. Whether or not we have achieved anything useful with the update is as yet unclear; but at least the joint probability has not been altered.

We now pass information from  $W$  back to  $V$ , using the same update rule. In particular:

$$\phi_S^{**} = \sum_{W \setminus S} \psi_W^* \quad (17.18)$$

$$\psi_V^{**} = \frac{\phi_S^{**}}{\phi_S^*} \psi_V^*. \quad (17.19)$$

(Noting that  $\psi_W^*$  is unchanged during this update, we define  $\psi_W^{**} = \psi_W^*$ ).

Note that once again the joint probability  $p(x_H, \bar{x}_E)$  remains unaltered by the update.

There is another important property that characterizes the pair of updates. In particular, the potentials  $\psi_V^{**}$  and  $\psi_W^{**}$  are consistent with respect to their intersection  $S$ ; that is, they have the same marginals. This is easily verified:

$$\sum_{V \setminus S} \psi_V^{**} = \sum_{V \setminus S} \frac{\phi_S^{**}}{\phi_S^*} \psi_V^* \quad (17.20)$$

$$= \frac{\phi_S^{**}}{\phi_S^*} \sum_{V \setminus S} \psi_V^* \quad (17.21)$$

$$= \frac{\phi_S^{**}}{\phi_S^*} \phi_S^* \quad (17.22)$$

$$= \phi_S^{**} \quad (17.23)$$

$$= \sum_{W \setminus S} \psi_W^{**}. \quad (17.24)$$

Inspecting this derivation, we see that the key steps for achieving consistency are Eqs. 17.14 and 17.19. In the forward pass, from  $V$  to  $W$ , the algorithm stores the marginal of the  $V$  potential in the separator potential. In the backward pass, from  $W$  to  $V$ , the algorithm divides the  $V$  potential by its stored marginal and multiplies the result by the new marginal  $\phi_S^{**}$ . This latter marginal is the marginal of the  $W$  potential. The rescaling equation essentially substitutes one marginal for another, thus making the two clique potentials consistent. This is achieved in the context of a symmetric algorithm that passes information in both directions, and leaves the joint probability distribution invariant.

Consider for example the Markov chain in Figure 17.8. Initially, the clique potential on  $\{X, Y\}$  is  $p(x, y)$ , and the clique potential on  $\{Y, Z\}$  is  $p(z | y)$ . The first pair of update equations results in the following update:

$$\phi_Y^* = \sum_x p(x, y) = p(y) \quad (17.25)$$

$$\psi_{YZ}^* = \frac{p(y)}{1} p(z | y) = p(y, z), \quad (17.26)$$

and we see that the clique potentials have become marginal probabilities. The backward phase in this case is vacuous; marginalizing over  $p(y, z)$  yields  $p(y)$  again for the separator marginal and the update factor is unity.

Now consider the chain in the case in which evidence is observed. Suppose for simplicity that all nodes are binary, and the evidence is  $X = 1$ . Incorporating the evidence means taking the slice of the potential on  $\{X, Y\}$  in which  $X = 1$ ; i.e., taking the second row of the potential table. The marginalization operation is now a vacuous operation, and we have:

$$\phi_Y^* = p(X = 1, y). \quad (17.27)$$

Performing the update of the  $\{Y, Z\}$  potential yields:

$$\psi_{YZ}^* = p(X = 1, y)p(z | y) = p(X = 1, y, z). \quad (17.28)$$

Thus our potentials are as follows:

$$\psi_{XY}^* = p(X = 1, y) \quad (17.29)$$

$$\phi_Y^* = p(X = 1, y) \quad (17.30)$$

$$\psi_{YZ}^* = p(X = 1, y, z), \quad (17.31)$$

and we see that we have obtained marginals as before, but these are unnormalized marginals. Normalizing (a local operation), we can readily read off the conditionals  $p(y | X = 1)$ ,  $p(y | X = 1)$ , and  $p(y, z | X = 1)$ . Note that once again the backward pass is vacuous.

The reader may wish to try the cases in which evidence  $Z = 1$  is available and when both  $X = 1$  and  $Z = 1$  are observed.

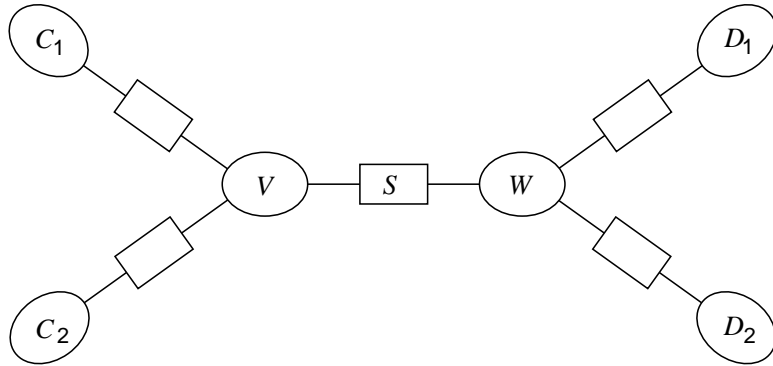


Figure 17.10: A clique tree with explicit representation of the separators. The separators are the intersection of the pair of cliques at the ends of the edge. Thus, for example,  $S = V \cap W$ .

## 17.6 Propagation in a clique tree

We now turn to the issue of how to perform local updates when we have multiple overlapping cliques.

In Figure 17.10 we show a clique tree. Each edge in this tree is associated with a separator. Cliques that are neighbors in this tree are subject to the updating procedure described in the previous section.

There are two issues that we must address—how to construct an appropriate clique tree and how to perform the updates so that local consistency obtained between a clique and its neighbor is not ruined by subsequent updates between the clique and other neighbors. In this section we focus on the second issue, returning to the problem of constructing the tree in Section 17.10.

How do we maintain local consistency in a clique tree? Consider again the clique tree shown in Figure 17.10. Suppose that we were to achieve local consistency between  $V$  and  $W$  using the pair of updates discussed in the previous section, and subsequently we update  $W$  based on its other neighbors. The latter updates would generally ruin the consistency that has been achieved between  $V$  and  $W$ . To ensure that this does not happen, we develop a protocol that constrains the order in which updates are performed.<sup>3</sup>

Let us refer to the update of one clique based on another as a “message-passing” operation. That is, we “pass a message” from  $V$  to  $W$  by evaluating Eqs. 17.14 and 17.15. In general, as we saw in the previous section, we require a message in both directions in order to render a pair of cliques consistent with each other.

Our problem is to decide when a given clique is allowed to pass a message to one of its neighbors. This problem is solved by the following protocol:

**Message-Passing Protocol.** *A clique can send a message to a neighboring clique only when it has received messages from all of its other neighbors.*

---

<sup>3</sup>In fact the protocol is not needed if we are willing to perform redundant steps. If each node is updated repeatedly (for example in parallel), consistency-ruining steps will eventually be corrected (see Exercise ??).

For example, in Figure 17.10, we can send a message from  $W$  to  $V$  only when  $W$  has received messages from its other neighbors  $D_1$  and  $D_2$ .

An easy argument establishes the correctness of the protocol. Consider the moment in time at which  $W$  has received all of the messages from its other neighbors, and is sending a message to  $V$ . There are two cases to consider: either  $V$  has not yet sent its message to  $W$ , or  $V$  has already sent its message to  $W$ . In the latter case, we know that  $V$  has already received messages from all of its other neighbors. The message from  $W$  to  $V$  renders the cliques consistent. Neither clique receives any additional messages, thus consistency is maintained. In the former case,  $W$  sends a message to  $V$ , storing its marginal on  $S$ , and waits. At some later time,  $V$  will have received all of the messages from its other neighbors and will send a message to  $W$ . This message will utilize the stored marginal and render  $W$  consistent with  $V$ . Neither clique will undergo any additional updates and consistency is maintained.

Although our protocol is correct, is it realizable? Are there message-passing algorithms that realize the protocol and ensure that a message is passed in both directions between every pair of cliques?

There are in fact many message-passing algorithms that realize the protocol; their existence is a simple consequence of the recursive definition of a tree. One way to obtain such algorithms is based on designating one clique in the tree as the root. Once a root of the clique tree is designated, the tree becomes an oriented tree with each leaf having a unique path to the root. Clearly each leaf can send a message inward at any time. Interior nodes send a message toward the root once they have received messages from all of their children. Once all messages have arrived at the root, we propagate messages outward to the leaves.

More formally, we define the following pair of recursive procedures:

```

COLLECTEVIDENCE( node )
begin
    for each child of node
        begin
            UPDATE( node, COLLECTEVIDENCE( child ) )
        end
    return( node )
end

DISTRIBUTEVIDENCE( node )
begin
    for each child of node
        begin
            UPDATE( child, node )
            DISTRIBUTEVIDENCE( child )
        end
    end
end

```

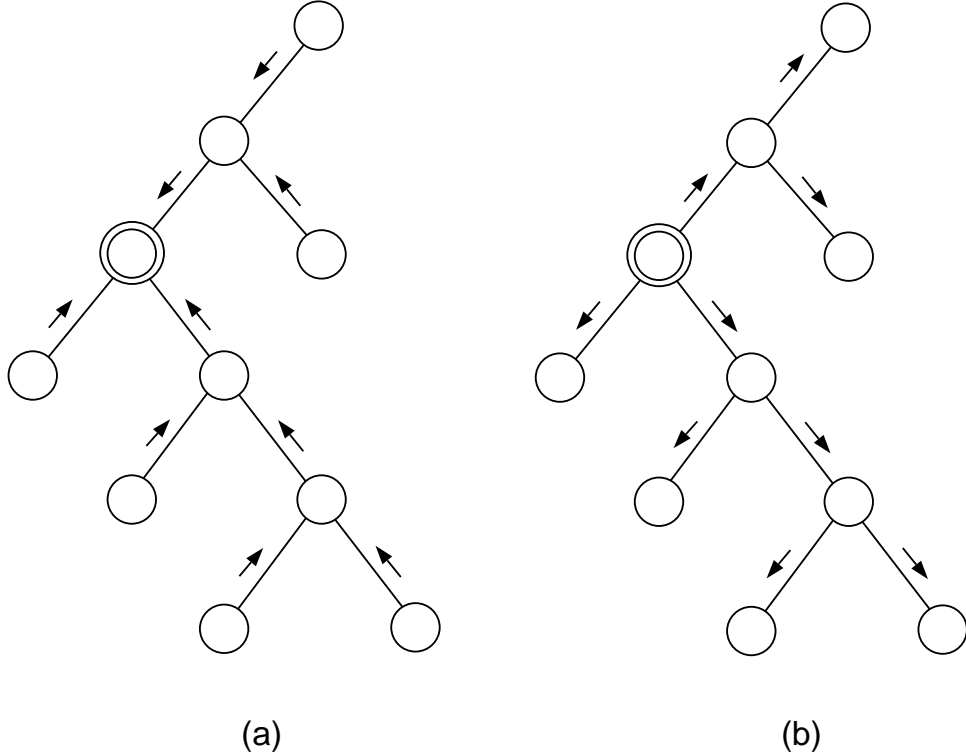


Figure 17.11: (a) The message-passing resulting from a call of `COLLECTEVIDENCE` at the root node (the doubly-circled node). (b) The message-passing resulting from a call of `DISTRIBUTEEVIDENCE` at the root node.

where  $\text{UPDATE}(V, W)$  is a routine that invokes the pair of equations Eq. 17.14 and 17.15. Calling `COLLECTEVIDENCE(root)` followed by `DISTRIBUTEEVIDENCE(root)` causes messages to propagate inward to the root and outward to the leaves.

**Theorem 1** *The `COLLECTEVIDENCE` and `DISTRIBUTEEVIDENCE` recursions respect the Message-Passing Protocol.*

**Proof.** When `COLLECTEVIDENCE` is called at a node, the node calls all of its other neighbors and waits on return messages from those nodes before returning a message back to its caller. Thus `COLLECTEVIDENCE` obeys the protocol.

After `COLLECTEVIDENCE` has run, each node has received a message from all of its neighbors except its parent. Once it receives a message from its parent it is free to send messages to any other node. `DISTRIBUTEEVIDENCE` sends a message from a parent to its child before calling itself on that child. Thus `DISTRIBUTEEVIDENCE` respects the protocol.  $\square$

Consider the example shown in Figure 17.11, where the doubly-circled node is designated as

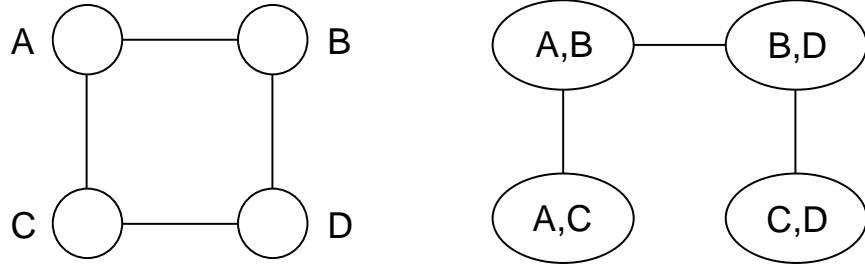


Figure 17.12: An undirected graphical model and a corresponding clique tree.

the root node. A call of `COLLECTEVIDENCE` results in messages proceeding inward as shown in Figure 17.11, and a call of `DISTRIBUTEVIDENCE` results in the outward-going messages shown in Figure 17.11. Note that it is clear that one and only one message is passed in both directions between every pair of cliques.

## 17.7 The junction tree property

At this point we have developed most of the machinery associated with the junction tree algorithm, and we are in the position to describe recursive inference algorithms for some non-trivial graphical models. In fact the machinery discussed thus far is sufficient to handle all of the models that we considered in Part I. In particular, an impatient reader could jump to Chapter 18 to see how the algorithm specializes to the case of the HMM and the state-space model. Both of those cases involve a rather obvious choice for the tree of cliques, and given a particular choice of root node, the recursive algorithms that we developed in earlier chapters fall out naturally from `COLLECTEVIDENCE` and `DISTRIBUTEVIDENCE`.

Despite this heady success, we have as yet no theoretical guarantee that the algorithm is correct for general graphical models. In fact it turns out that the algorithm as developed thus far is *not* correct for general graphical models. In this section we identify the (last) problem that must be addressed. We should emphasize at the outset that the problem is essentially a data structure problem involving the construction of the clique tree. There is in fact no problem with our marginalizing and rescaling equations, nor with our Message-Passing Protocol. It suffices to get the data structure right.

To see that our labor is not yet finished, consider the undirected graphical model shown in Figure 17.12. There are four cliques in this graph. A particular choice of clique tree is shown in Figure 17.12. Note that this clique tree has a problematic feature. In particular, the node  $C$  appears in two different cliques in the tree and these cliques are not neighbors. Given that our algorithm only enforces local consistency, there is no guarantee that the two cliques containing  $C$  will be consistent. Indeed, if the leftmost clique that contains  $C$  is changed (e.g., by the introduction of evidence), there is no mechanism to insure that this information will flow to the rightmost clique that contains  $C$ . In general, local consistency does not imply global consistency.

Note that the lack of global consistency does not imply that we have an incorrect representation

of the joint probability distribution. Indeed, as we saw earlier, the junction tree algorithm does not alter the joint probability, and thus we maintain a correct representation of the joint throughout. What we fail to achieve in Figure 17.12 is locality—the clique potentials correctly represent the joint probability, but they are not local marginal probabilities.

The reader can verify that there is no alternative clique tree that avoids the problem. All clique trees have a pair of nodes that lie in non-neighboring cliques.

A clue to understanding the problem comes from observing that the elimination algorithm would unavoidably create new links in the graph in Figure 17.12; e.g., eliminating  $C$  would connect  $A$  and  $B$ . Another way to put the problem is that there is no way to choose an elimination ordering such that the elimination cliques are contained within the cliques of the original graph.

While this argument based on elimination provides insight, we prefer to restate the problem directly in terms of properties of clique trees. To do so, we articulate a property that rules out the problematic configurations of the kind that we saw in Figure 17.12. The relevant property is known as the *junction tree property*:

**The junction tree property.** A clique tree possesses the *junction tree property* if for every pair of cliques  $V$  and  $W$ , all cliques on the (unique) path between  $V$  and  $W$  contain  $V \cap W$ .

A clique tree that possesses the junction tree property is referred to as a *junction tree*.

The consequences of the junction tree property for inference are as follows. If a node  $A$  appears in two cliques in a junction tree, then  $A$  is contained in every clique along the path between these two cliques. If the cliques along the path are *pairwise* consistent with respect to  $A$  then they will be *jointly* consistent with respect to  $A$ . *In a junction tree, local consistency implies global consistency.*

This argument implies that if we are fortunate enough to have a clique tree that is a junction tree, and if we run the message-passing procedure as described in the previous section, we achieve not only local consistency but also global consistency. We can get the same answer for any node  $A$  by consulting any potential that contains  $A$ .

Recall however that our goal is to obtain a set of potentials that are not only consistent, but are also marginals—that is, each potential represents the marginal probability of the nodes in its clique. It is conceivable that the junction tree could be consistent, but the potentials would not be marginals. In fact, somewhat surprisingly, this cannot be the case. In a junction tree, the junction tree algorithm not only achieves global consistency, but it yields the sought-after clique marginals as well. To prove this important result we require the following lemma.

**Lemma 1** *Let  $C$  be a leaf in a junction tree for a graph with vertex set  $V$ . Let  $S$  be the associated separator (see Figure 17.13). Let  $R = C \setminus S$  be the set of nodes in  $C$  but not in the separator, and let  $U = V \setminus C$  be the set of nodes in  $V$  but not in  $C$ . Then:*

$$R \perp\!\!\!\perp U \mid S \tag{17.32}$$

**Proof.** Suppose, by way of contradiction, that  $A \in R$  has a neighbor  $N \in U$ . Consider the maximal complete subset containing both  $A$  and  $N$ . This clique is not  $C$  because  $N \notin C$ . However,  $A$  cannot be contained in any clique other than  $C$  because  $A$  would have to belong to  $S$  as well, by

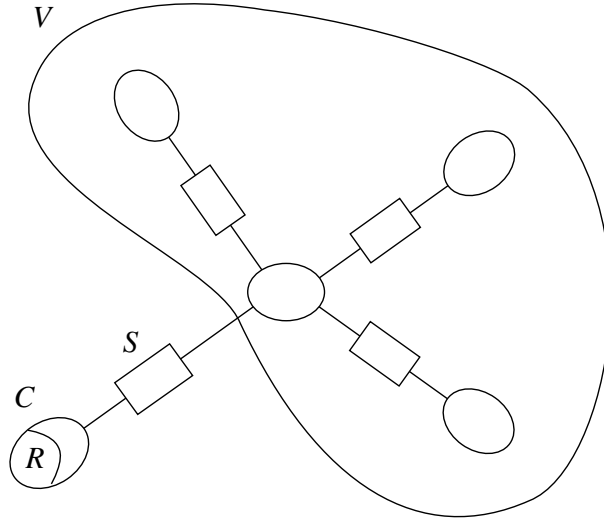


Figure 17.13: The “residual” set  $R = C \setminus S$  is the set of nodes in  $C$  that are not in  $S$ , and, by the junction tree property, also not in  $U$ .

the junction tree property, and nodes in  $R$  are not in  $S$  by definition. Thus no such  $N$  exists and  $S$  must therefore separate  $A$  from  $U$ . Since  $A$  is arbitrary,  $S$  separates  $R$  from  $T$ .  $\square$

We now state and prove our main result.

**Theorem 2** *Let the probability  $p(x_H, \bar{x}_E)$  be represented by the clique potentials  $\psi_C$  and separator potentials  $\phi_S$  of a junction tree. When the junction tree algorithm terminates, the clique potentials and separator potentials are proportional to local marginal probabilities. In particular:*

$$\psi_C = p(x_C, \bar{x}_E) \quad (17.33)$$

$$\phi_S = p(x_S, \bar{x}_E) \quad (17.34)$$

**Proof.** The separators are subsets of the cliques. That the separator potentials are proportional to marginals therefore follows from the fact that they are consistent with the clique potentials. Thus we need only prove the result for the clique potentials.

The proof is a proof by induction. The result holds for the base case of a single clique by definition. Let us suppose that the result holds for junction trees of  $N$  or fewer cliques, and consider a junction tree with  $N + 1$  cliques.

We choose a clique  $\tilde{C}$  that is a leaf in the junction tree. Let  $\tilde{S}$  be the corresponding separator, let  $\tilde{R} = \tilde{C} \setminus \tilde{S}$  and let  $\tilde{T} = V \setminus \tilde{C}$ . We also define analogous quantities in which the evidence variables are omitted. In particular, let  $C = \tilde{C} \setminus E$ ,  $R = \tilde{R} \setminus E$  and  $T = \tilde{T} \setminus E$ . By Lemma 1 we have:

$$p(x_H, \bar{x}_E) = p(x_R, x_S, x_T, \bar{x}_E) = p(x_R | x_S, \bar{x}_E)p(x_S, x_T, \bar{x}_E). \quad (17.35)$$

Summing both sides over  $R$ , we obtain:

$$p(x_S, x_T, \bar{x}_E) = \sum_R p(H, \bar{x}_E) \quad (17.36)$$

$$= \sum_R \frac{\prod_C \psi_C(x_C)}{\prod_S \phi_S(x_S)} \quad (17.37)$$

$$= \sum_R \frac{\psi_C}{\phi_S} \frac{\prod_{C' \neq C} \psi_{C'}(C')}{\prod_{S \neq S'} \phi_{S'}(x'_S)} \quad (17.38)$$

$$= \frac{\sum_R \psi_C}{\phi_S} \frac{\prod_{C' \neq C} \psi_{C'}(C')}{\prod_{S \neq S'} \phi_{S'}(x'_S)} \quad (17.39)$$

$$= \frac{\prod_{C' \neq C} \psi_{C'}(C')}{\prod_{S \neq S'} \phi_{S'}(x'_S)} \quad (17.40)$$

where Eq. 17.40 follows from the fact that  $C$  and  $S$  are consistent and thus  $\sum_R \psi_C = \phi_S$ .

Eq. 17.40 shows that  $p(x_S, x_T, \bar{x}_E)$  is represented by the clique potentials and separator potentials on the junction tree over  $S \cup T$ . By the induction hypothesis, after a full round of message passing the clique potentials on this junction tree are equal to marginals.

It remains to show that the clique potential on  $C$  is a marginal. Let  $D$  be the neighbor of  $C$  in the junction tree. By consistency we have  $\phi_S(x_S) = \sum_{D \setminus S} \psi_D(x_D)$ . We have  $\psi_D = p(x_D, \bar{x}_E)$  and thus  $\psi_S(x_S) = p(x_S, \bar{x}_E)$ . Thus:

$$p(x_R | x_S, \bar{x}_E) = \frac{\psi_C(x_C)}{\phi_S(x_S)} \quad (17.41)$$

$$= \frac{\psi_C(x_C)}{p(x_S, \bar{x}_E)} \quad (17.42)$$

which implies  $\psi_C(x_C) = p(x_C, \bar{x}_E)$ .  $\square$

## 17.8 Triangulated graph $\Rightarrow$ Junction tree

The junction tree property provides a sufficient condition for the correctness of the junction tree algorithm. What class of graphs have a junction tree? How do we handle graphs that do not have a junction tree?

In this section we present a sufficient condition for a graph to have a junction tree—the condition is that the graph must be *triangulated*. It turns out that triangulation is also a necessary condition for a graph to have a junction tree. In the current section, however, we restrict ourselves to the proof of sufficiency, proving necessity in Appendix A. The Appendix also demonstrates that triangulation is equivalent to *decomposability*; a characterization of graphs that we discussed in Section ??.

We begin by defining a triangulated graph and then proceed to the proof of sufficiency. The reader willing to accept the proof on faith can read the definition of triangulation in the next paragraph and then skip to the following section without loss of continuity.

Consider a cycle in an undirected graph. A cycle is *chordless* if there are no edges between nodes that are not successors in the cycle. For example, the cycle  $A - B - D - C - A$  in Figure 17.12 is chordless because there is no edge between  $A$  and  $C$  or between  $B$  and  $D$ . A graph is said to be *triangulated* if there are no chordless cycles in the graph.

Our first stop in the proof of sufficiency is a simple lemma that shows that triangulated graphs can be decomposed into three subsets with special properties.

**Lemma 2** *Let  $\mathcal{G} = (V, E)$  be a noncomplete triangulated graph with at least three nodes. Then there exists a decomposition of  $V$  into disjoint sets  $A$ ,  $B$  and  $S$  such that  $S$  separates  $A$  and  $B$  and  $S$  is complete.*

**Proof.** Choose a pair of nonadjacent nodes  $\alpha$  and  $\beta$ . Let  $S$  be the minimal set of nodes such that any path from  $\alpha$  to  $\beta$  passes through  $S$ . Let  $A$  be the set of nodes reachable from  $\alpha$  when  $S$  is removed and similarly let  $B$  be the set of nodes reachable from  $\beta$  when  $S$  is removed. Clearly these two sets are separated by  $S$ . We need only establish that  $S$  is complete.

Let  $C$  and  $D$  be nodes in  $S$ . Since  $S$  is minimal, there is a path from  $\alpha$  to  $C$  and from  $\alpha$  to  $D$ ; thus there is a path from  $C$  to  $D$  in  $A \cup S$ . Take the shortest such path. Similarly take the shortest path joining  $C$  to  $D$  in  $B \cup S$ . Link these paths to obtain a cycle. This cycle must have a chord. This chord must be an edge between  $C$  and  $D$ , by our choice of shortest paths. Thus  $C$  and  $D$  are neighbors.  $\square$

We also require the notion of a simplicial node. A node is *simplicial* if all of its neighbors are connected. The following lemma guarantees the existence of simplicial nodes in triangulated graphs.

**Lemma 3** *Every triangulated graph that contains at least two nodes has at least two simplicial nodes. If the graph is not complete, then these nodes can be chosen to be nonadjacent.*

**Proof.** We again use induction and again the base case is trivial. Consider a triangulated graph  $\mathcal{G}$  with  $N + 1$  nodes. If the graph is complete then all nodes are simplicial. Otherwise we use Lemma 2 to decompose the graph into disjoint sets  $A$ ,  $B$  and  $S$ . The subgraphs  $A \cup S$  and  $B \cup S$  cannot contain any chordless cycles (because any such cycles would also be chordless in  $\mathcal{G}$ ), and thus they are both triangulated. The induction hypothesis implies the existence of two simplicial nodes in  $A \cup S$ . If  $A \cup S$  is not complete these can be taken to be nonadjacent, and, given that  $S$  is complete, one of the two nodes can be taken to be in  $A$ . Otherwise, pick any node in  $A$ . Similarly, the induction hypothesis implies the existence of two simplicial nodes in  $B \cup S$ , and one of these can be taken in  $B$ . Given that  $A$  and  $B$  are separated by  $S$ , the two nodes that we have selected are simplicial in  $\mathcal{G}$  and they are also nonadjacent.  $\square$

We now demonstrate that triangulation implies the existence of a clique tree with the junction tree property.

**Theorem 3** *All triangulated graphs have a junction tree.*

**Proof.** We once again use induction and once again the base case is trivial. Consider a graph  $\mathcal{G}$  with  $N + 1$  nodes. By Lemma 3, the graph has at least one simplicial node  $\alpha$ .

Removing a simplicial node from a triangulated graph yields a triangulated graph, because no chordless cycles can be created. Thus by the induction hypothesis, the graph with  $\alpha$  removed has a junction tree  $T$ . We construct a junction tree for  $\mathcal{G}$  from  $T$ .

Let  $C$  denote the clique formed by  $\alpha$  and its neighbors. If  $C \setminus \alpha$  is a clique in  $T$ , then simply add  $\alpha$  to that clique;  $T$  with the augmented clique is a junction tree for  $\mathcal{G}$ .

If  $C \setminus \alpha$  is not a clique  $D$  in  $T$ , then it is a subset of a clique  $D$  in  $T$ . Add  $C$  as a new leaf node for  $T$ , with a link to  $D$  and a separator set  $S = C \setminus \alpha$ . The result is a junction tree. This is established by noting that (1)  $\alpha$  is contained only in  $C$  and therefore cannot violate the junction tree property; and (2) all other nodes in  $C$  are in  $S$  and in  $D$  and therefore cannot violate the junction tree property.  $\square$

## 17.9 Elimination $\Rightarrow$ Triangulation

In this section we show that `UNDIRECTEDGRAPHELIMINATE` can be viewed as a procedure for creating a triangulated graph. This result will show us how to deal with nontriangulated graphs within the junction tree framework. It also allows us to demonstrate that the elimination algorithm is a special case of the junction tree algorithm.

Recall that `UNDIRECTEDGRAPHELIMINATE` is a simple iterative algorithm that successively eliminates the nodes in a graph by (1) connecting the (remaining) neighbors of the node and (2) removing the node and its edges from the graph. The input to the algorithm is a graph and an elimination ordering.

**Theorem 4** `UNDIRECTEDGRAPHELIMINATE` yields a triangulated graph.

**Proof.** We prove the theorem by induction. The base case is a graph with a single node, which is obviously triangulated. Suppose now that the hypothesis holds for graphs with  $N$  or fewer nodes and consider a graph with  $N + 1$  nodes. Eliminating a node results in a graph with  $N$  nodes, which cannot contain a chordless cycle by the induction hypothesis. Moreover, it is not possible to form a chordless cycle involving the eliminated node, because the elimination step connects all of the neighbors of the node.  $\square$

Thus the edges added by the `UNDIRECTEDGRAPHELIMINATE` algorithm are exactly those that turn a nontriangulated graph into a triangulated graph.

This result suggests the following general approach to dealing with nontriangulated graphs. Given an initial undirected graph (possibly obtained by moralizing a directed graph), we first triangulate the graph using `UNDIRECTEDGRAPHELIMINATE`. We are not constrained in our choice of elimination ordering and can use any of a variety of heuristics to choose a “good” elimination ordering; e.g., one that introduces as few extra edges as possible (see Appendix A). Given a triangulation, we construct a junction tree from the triangulated graph and run the message-passing procedure. The algorithm calculates marginal probabilities for all of the cliques of the triangulated graph. Marginals for subsets of these cliques (e.g., individual nodes) can be obtained by further marginalization and normalization of individual potentials.

The correctness of this approach follows from an argument similar to that used to justify moralization. Adding edges to a graph can only decrease the set of conditional independencies

associated with the graph and thus expand the set of probability distributions associated with the graph. This implies that the set of probability distributions associated with the triangulation of a graph includes the set of probability distributions associated with the original graph. Solving the inference problem for the triangulated graph solves it for the original graph as well.

Our argument also suggests (correctly) that the elimination algorithm is a special case of the junction tree algorithm. As we ask the reader to show in Exercise ??, applying the junction tree algorithm to the cliques of the triangulated graph resulting from a given elimination ordering we recover exactly the probabilistic calculations of the elimination algorithm.

It is possible to prove a converse to Theorem 4 showing that for any triangulated graph there exists an ordering such that elimination using that ordering introduces no new edges.<sup>4</sup> Thus, elimination and triangulation are essentially equivalent notions. This does not imply, however, that practical algorithms for triangulation are necessarily best viewed as elimination algorithms. Rather, treating triangulation as a combinatorial optimization problem provides a broader perspective on the problem. In Appendix A, we return to these issues and describe practical algorithms for graph triangulation.

If our goal is to obtain the marginal probabilities of all of the non-evidence nodes in the graph, then the naive elimination algorithm would require us to choose different elimination orderings in which the target node is the final node in the ordering. These different elimination orderings would in general produce incommensurate elimination cliques, and make it difficult, if not impossible, to share the intermediate potentials. The junction tree framework, on the other hand, calculates a single triangulation, in effect using a single elimination ordering. While this ordering may not be optimal for calculating any given individual marginal, the choice of a single ordering makes it possible to share intermediate potentials, and thus supports the efficient calculation of marginals for all cliques in the graph.

## 17.10 Constructing the junction tree

The results of Section 17.8 show that every triangulated graph has a junction tree. This proof—an existence proof—leaves us just short of our goal. How do we construct a junction tree from a triangulated graph?

It is certainly not the case that every clique tree obtained from a triangulated graph is a junction tree. Consider the triangulated graph shown in Figure 17.14(a). The clique tree in Figure 17.14(b) is not a junction tree (consider node B). A junction tree for this graph is shown in Figure 17.14(c).

The separators in Figure 17.14(b) are  $\{C, D\}$  and  $\{D\}$ , whereas in Figure 17.14(c) the separators are  $\{B, D\}$  and  $\{C, D\}$ . The total cardinality of the separator sets is larger in the latter figure. Intuitively this fact would seem to have something to do with the fact that Figure 17.14(c) possesses the junction tree property while Figure 17.14(b) does not.

To each clique tree  $T$  associated with a triangulated graph we can assign a *weight*  $w(T)$  given by the sum of the cardinalities of the separator sets in the tree. We show in this section that a clique tree is a junction tree if and only if it has maximal weight, ranging over all possible trees of cliques. There may be several such trees.

---

<sup>4</sup>See, e.g., Jensen, (1996).

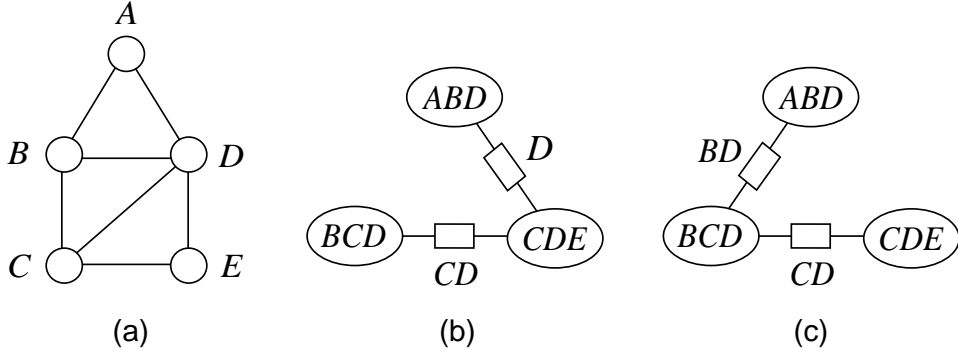


Figure 17.14: (a) A triangulated graph. (b) A clique tree based on (a) that does not have the junction tree property. (c) A clique tree based on (a) that does have the junction tree property.

Our problem is an instance of the classical “maximal spanning tree problem.” The problem is readily solved via one of a number of simple greedy algorithms. One solution is given by Kruskal’s algorithm: Begin with no edges between the cliques. At each step add an edge that has maximal separator cardinality, ensuring that the resulting graph has no cycles. Once the graph is fully connected (there is a path between any pair of cliques), we have a maximal spanning tree.<sup>5</sup>

Consider a node  $X_k$  and a clique tree  $T$  with cliques  $C_i$  and separators  $S_j$ . Consider further the count of the number of times that  $X_k$  appears as an element in one the cliques  $C_i$ , as well as the count of the number of times that  $X_k$  appears as an element in one of the  $S_j$ . Clearly these counts are related, and in particular the fact that  $T$  is a tree implies that the latter count is no more than the former count less one:

$$\sum_{j=1}^{M-1} \mathbb{1}(X_k \in S_j) \leq \sum_{i=1}^M \mathbb{1}(X_k \in C_i) - 1, \quad (17.43)$$

where  $\mathbb{1}(\cdot)$  is the indicator function and where  $M$  is the number of cliques. Moreover, this inequality becomes an equality when the subgraph of  $T$  induced by  $X_k$  is a tree.

As we have noted earlier, the statement that the subgraph of  $T$  induced by a node  $X_k$  is a tree is nothing more than a restatement of the junction tree property. Thus we have in Eq. 17.43 an inequality which is indicative of the junction tree property, at least with respect to a single node  $X_k$ .

We are now ready to state the theorem linking junction trees and maximal spanning trees.

**Theorem 5** *A clique tree  $T$  is a junction tree if and only if it is a maximal spanning tree.*

**Proof.** The total weight of a clique tree is equal to the sum of the cardinalities of its separators.

---

<sup>5</sup>See Cormen, Leiserson, and Rivest (1990) for a proof of this result. Another approach is given by Prim’s algorithm, which maintains a partial tree at each step and iteratively adds nodes to this tree.

Thus we have:

$$w(T) = \sum_{j=1}^{M-1} |S_j| \quad (17.44)$$

$$= \sum_{j=1}^{M-1} \sum_{k=1}^N 1(X_k \in S_j) \quad (17.45)$$

$$= \sum_{k=1}^N \sum_{j=1}^{M-1} 1(X_k \in S_j) \quad (17.46)$$

$$\leq \sum_{k=1}^N \left[ \sum_{i=1}^M 1(X_k \in C_i) - 1 \right] \quad (17.47)$$

$$= \sum_{i=1}^M \sum_{k=1}^N 1(X_k \in C_i) - M \quad (17.48)$$

$$= \sum_{i=1}^M |C_i| - M. \quad (17.49)$$

Noting that the right-hand side is independent of  $T$ , and that the inequality in Eq. 17.47 is an equality if and only if  $T$  is a junction tree, we obtain the result.  $\square$

## 17.11 The Hugin algorithm

The algorithm that we have developed in previous sections is known as the “Hugin algorithm,” an instance of the general junction tree framework. We summarize the algorithm here. There are five principal steps to the algorithm, the first of which applies only to directed graphs.

- **Moralization.** The moralization step converts a directed graph into an undirected graph. Nodes that have a common child are linked, and directed edges are converted to undirected edges. The local conditional probability of each node is multiplied onto the potential of a clique that contains the node and its parents.
- **Introduction of evidence.** Evidence is introduced by taking slices of the potentials.
- **Triangulation.** The graph is triangulated, using one of several possible algorithms. The potential of each clique of the original graph is multiplied onto the potential of a clique that contains the clique.
- **Construction of junction tree.** A junction tree is constructed by forming a maximal spanning tree from the cliques of the triangulated graph. Separators are introduced and their potentials are initialized to unity.

- **Propagation of probabilities.** Computation proceeds in the junction tree via the following update equations:

$$\phi_S^* = \sum_{V \setminus S} \psi_V \quad (17.50)$$

$$\psi_W^* = \frac{\phi_S^*}{\phi_S} \psi_W. \quad (17.51)$$

The updates must respect the Message-Passing Protocol. This can be achieved by designating a root node and calling `COLLECTEVIDENCE` and `DISTRIBUTEEVIDENCE` from the root. Once the algorithm terminates, the clique potentials and separator potentials are proportional to marginal probabilities. Further marginalization can be performed to obtain the probabilities of singleton nodes or other subsets.

## 17.12 The Shafer-Shenoy algorithm

There are a number of variations on the junction tree theme. All of these variations have at their core the notion of a triangulated graph and the junction tree property, but the way that propagation proceeds on the junction tree can be different. Some of these variations can provide additional insights into exact inference and provide different pathways for generalizations to approximate inference. Moreover, different variations on junction tree propagation can have different numerical properties or time/space properties. In this section we discuss one such variation—the Shafer-Shenoy algorithm.

The Shafer-Shenoy algorithm can be viewed as a variation on the junction tree framework in which no use is made of separator potentials. While the separator potentials have been useful in providing a simple mechanism for achieving consistency between neighboring cliques, and while we will encounter architectural examples in which separator potentials are particularly useful (cf. Section 18.2.4), there is a sense in which separator potentials are redundant (they are simply marginals of the clique potentials) and perhaps they can be disposed with.

Rather than focusing on separator potentials, let us instead focus on the ratios of separator potentials; the quantities that we referred to as “update factors” in our earlier presentation. Recall that in the second step of the message-passing calculation (Eq. 17.15), the clique potential is multiplied by the update factor. What we will show is that a propagation procedure can be based solely on the update factors.

Consider the pair of cliques  $C_i$  and  $C_j$  in Figure 17.15, with separator  $S_{ij} = C_i \cap C_j$ . We wish to exchange messages between these cliques so as to implement a junction tree algorithm, and we wish to do so without making use of a potential on the separator  $S_{ij}$ . To do so, define  $\mu_{ij}(S_{ij})$  as the message sent from  $C_i$  to  $C_j$ .<sup>6</sup> The Shafer-Shenoy algorithm tells us how to calculate  $\mu_{ij}(S_{ij})$  based on the messages arriving at clique  $C_i$  from all cliques other than clique  $C_j$ :

$$\mu_{ij}(S_{ij}) = \sum_{C_i \setminus S_{ij}} \psi_{C_i} \prod_{k \neq i} \mu_{ki}(S_{ki}) \quad (17.52)$$

---

<sup>6</sup>Note that we are using the term “message” in a slightly more specific manner than before; for the Shafer-Shenoy algorithm, we equate “message” with the values  $\mu_{ij}(S_{ij})$ .

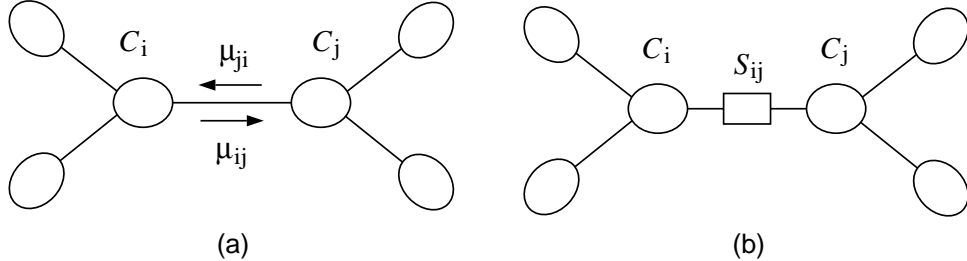


Figure 17.15: (a) A junction tree showing the messages  $\mu_{ij}$  and  $\mu_{ji}$  that are passed between cliques  $C_i$  and  $C_j$ . Note that both messages are functions of the separator  $S_{ij}$ . (b) A junction tree showing the separator explicitly.

Once clique  $C_i$  has received messages from all of its neighbors, we compute the marginal probability for  $C_i$  as follows:

$$p(C_i) \propto \psi_{C_i} \prod_k \mu_{ki}(S_{ki}). \quad (17.53)$$

Equations 17.52 and 17.53 constitute the Shafer-Shenoy algorithm. We now derive this algorithm from the point of view of our earlier junction tree algorithm, thereby proving the correctness of the implicit assertion in Eq. 17.53—that we do in fact obtain the marginal probabilities via this algorithm.

Consider now the pair of cliques  $C_i$  and  $C_j$  in Figure 17.15(b) with the explicit separator  $S_{ij}$ . The connection between the new algorithm and the earlier algorithm is made as follows. Define  $\mu_{ij}(S_{ij})$  to be the update factor associated with the update of the link in the direction from  $C_i$  to  $C_j$ . That is, if the first update of this link proceeds in the  $i$ -to- $j$  direction, let:

$$\mu_{ij}(S_{ij}) \triangleq \frac{\phi_{S_{ij}}^*}{\phi_{S_{ij}}^{**}}; \quad (17.54)$$

otherwise, let:

$$\mu_{ij}(S_{ij}) \triangleq \frac{\phi_{S_{ij}}^{**}}{\phi_{S_{ij}}^*}. \quad (17.55)$$

In either case,  $\mu_{ij}(S_{ij})$  is the update factor arriving at clique  $C_j$  from clique  $C_i$ . Now note that the final potential at a given clique is the product of its initial potential and all of the update factors arriving from its neighbors. This immediately shows that Eq. 17.53 has the correct form. We have reduced our problem to that of establishing the correctness of Eq. 17.52.

We consider two cases. Suppose first that the initial update of the link between  $C_i$  and  $C_j$  occurs in the  $i$ -to- $j$  direction. For this update to occur it must be the case that  $C_i$  has already received updates from all of its other neighbors (the Message-Passing Protocol). Thus at the moment when the update occurs, the value of the potential on  $C_i$  must be the product of its initial potential and the update factors from its neighbors  $C_k$ , for  $k \neq j$ . Let us assume (as an inductive hypothesis) that these update factors are correctly given by  $\mu_{ki}(S_{ki})$ , and consider the update factor that  $C_i$

sends to  $C_j$ . From Eq. 17.14 we have:

$$\phi_{S_{ij}}^* = \sum_{C_i \setminus S_{ij}} \psi_{C_i} \prod_{k \neq i} \mu_{ki}(S_{ki}). \quad (17.56)$$

Comparing this with Eq. 17.52, we see that  $\mu_{ij}(S_{ij}) = \phi_{S_{ij}}^*$  and, recalling that the initial value of the separator potential,  $\phi_{S_{ij}}$ , is unity, we have  $\mu_{ij}(S_{ij}) = \phi_{S_{ij}}^* \phi_{S_{ij}}$  as required.

Now consider the case in which an earlier update has already occurred in the  $j$ -to- $i$  direction. In this case, at the moment of the update from  $C_i$  to  $C_j$ , the potential on  $C_i$  must be the product of its initial potential and the update factors from *all* of its neighbors, including  $C_j$ . Thus, from Eq. 17.14 we have:

$$\phi_{S_{ij}}^{**} = \sum_{C_i \setminus S_{ij}} \psi_{C_i} \prod_k \mu_{ki}(S_{ki}) \quad (17.57)$$

$$= \sum_{C_i \setminus S_{ij}} \psi_{C_i} \mu_{ji}(S_{ji}) \prod_{k \neq j} \mu_{ki}(S_{ki}) \quad (17.58)$$

$$= \sum_{C_i \setminus S_{ij}} \psi_{C_i} \frac{\phi_{S_{ij}}^*}{\phi_{S_{ij}}} \prod_{k \neq j} \mu_{ki}(S_{ki}) \quad (17.59)$$

$$(17.60)$$

and this yields:

$$\frac{\phi_{S_{ij}}^{**}}{\phi_{S_{ij}}^*} = \sum_{C_i \setminus S_{ij}} \prod_{k \neq j} \mu_{ki}(S_{ki}), \quad (17.61)$$

where we again use the fact that  $\phi_{S_{ij}} \equiv 1$ . Comparing this result with Eq. 17.52, we see that  $\mu_{ij}(S_{ij}) = \phi_{S_{ij}}^{**}/\phi_{S_{ij}}^*$  as required.

### 17.13 Computational complexity

In this section we discuss the computational complexity of the junction tree algorithm. For concreteness we focus on the Hugin algorithm and consider the computational complexity of the Shafer-Shenoy algorithm in the exercises.

It is important to distinguish between two phases of the junction tree algorithm. The first phase, which we will refer to as the *compilation phase*, involves moralization, triangulation and the maximal spanning tree algorithm. The second phase, the *propagation phase*, involves the introduction of evidence and message-passing on the junction tree.

The compilation phase is an “off-line” phase, occurring once for a given graphical model. The algorithms in the propagation phase are “on-line,” running each time a new set of conditional probabilities is desired.

Moralization is clearly a computationally tractable procedure. Letting  $N$  denote the number of nodes in the graph, and  $M$  the number of edges, moralization runs in time  $O(N + M)$ .

Moreover, the maximal spanning tree problem is computationally tractable. This is a well-studied problem and the computational complexity results are classical. In particular, the run time of Kruskal's algorithm is  $O(N^2)$  and the run time of Prim's algorithm is  $O(N^2)$ .<sup>7</sup>

Let us turn to the triangulation problem. If we are not concerned with optimality (e.g., finding a junction tree with the smallest maximal clique, or the smallest number of edges), then finding a triangulation is computationally tractable. In particular, the run time of `UNDIRECTEDGRAPHELIMINATE` is easily seen to be  $O(XXX)$ . The problem of finding an optimal junction tree, however, is an NP-hard problem, under any of a number of definitions of optimality. We discuss this intractability result in more detail in Appendix A.

The fact that triangulation is an off-line phase of the junction tree algorithm tempers some of the concern that accompanies the NP-hardness result. Moreover, as we discuss in Appendix A, there are heuristic algorithms available for triangulation that perform reasonably well in empirical experiments. One may be willing to pay the cost of allowing one of these algorithms to run for a substantial time to obtain a good triangulation. Finally, it is important to be aware that for many graphical models the initial graph is sufficiently dense that even the optimal triangulation, if it could be found, would have a large number of edges or a large maximal clique size. It is the size of these cliques, which impacts the second phase of the junction tree algorithm, which is generally the key practical limitation in using the algorithm.

The second phase of the algorithm involves conditioning and message-passing. Conditioning is a straightforward procedure that simply annotates each clique with the indices that are to be held fixed in the slice corresponding to the conditioning variables. We therefore turn to the message-passing procedure.

Each step of the message-passing procedure involves the marginalization and rescaling of clique potentials. Let us suppose that these potentials are represented nonparametrically, as tables. This is a worst-case assumption, and specific parametric representations of the clique potentials may give more favorable complexity results. Marginalizing a table requires us to access each entry in the table, and thus the number of operations scales as the number of entries in the table. The number of such entries is exponential in the number of variables in the corresponding clique. This exponentiality is the key determinant of the computational complexity of the junction tree algorithm.

Rescaling a potential again involves accessing each entry in the affected clique potential, and thus is again exponential in the number of variables in the clique.

The number of cliques in a junction tree is no more than  $N$ , the number of nodes in the underlying graph (assuming that we use maximal cliques). Thus the number of separators is bounded above by  $N - 1$ , and we have at most  $2N - 1$  messages flowing in a run of the Hugin algorithm. Each message involves two operations on clique potentials—a marginalization operation and a rescaling operation. In summary, a complete run of the Hugin algorithm involves at most  $4N - 2$  such operations. Given that the size of a clique can be as large as the number of nodes  $N$ , the exponentiality of an individual marginalization or rescaling operation dominates the computational complexity.

It is of interest to compare the number of operations needed to obtain the marginal probabilities

---

<sup>7</sup>See, e.g., Cormen Leisherson, and Rivest (1990).

Figure 17.16: XXX

of all of the nodes in the graph—obtained via the junction tree algorithm—to the number of operations needed to obtain the marginal probabilities of a single node in the graph—obtained via the elimination algorithm. The latter algorithm is special case; just run `CollectEvidence`. Touches each potential once.

## 17.14 Generalized marginalization

One of the virtues of the junction tree framework is its clear distinction between the graph-theoretic and the algebraic machinery involved in probabilistic inference. The algebraic machinery that we utilized in deriving the algorithm was elementary—our proofs reposed on the associative, commutative and distributive laws of arithmetic. As we discuss in this section, if we replace the specific algebraic operators that we used with other operators that obey these same laws, we find that the junction tree framework extends readily to a wide class of other problems involving factorized algebraic expressions, of which probabilistic inference is a special case.

### 17.14.1 Maximum probability configurations

In Section ?? we discussed the Viterbi algorithm for hidden Markov models. Given an observation sequence, this algorithm returns a single configuration of the hidden states that has maximal probability. In this section we describe a “generalized Viterbi algorithm” that computes most probable configurations for arbitrary graphical models.

That we need to do essentially no additional work to derive such an algorithm is suggested by returning to the example in Figure 17.16. Let us find a set of values of the nodes—a *configuration*—that maximizes the joint probability  $p(x_1, x_2, \dots, x_6)$ .

The first few steps of the calculation are as follows:

$$\begin{aligned} \max_x p(x) &= \max_{x_1} \max_{x_2} \max_{x_3} \max_{x_4} \max_{x_5} \max_{x_6} p(x_1)p(x_2 | x_1)p(x_3 | x_1)p(x_4 | x_2)p(x_5 | x_3)p(x_6 | x_2, x_5) \\ &= \max_{x_1} p(x_1) \max_{x_2} p(x_2 | x_1) \max_{x_3} p(x_3 | x_1) \max_{x_4} p(x_4 | x_2) \max_{x_5} p(x_5 | x_3) \max_{x_6} p(x_6 | x_2, x_5). \end{aligned}$$

Computing the maximum of  $p(x_6 | x_2, x_5)$  with respect to  $x_6$  yields an intermediate factor that is a function of  $x_2$  and  $x_5$ . This factor is then retained until needed in a subsequent maximization, in this case the maximization over  $x_5$ .

The sequence of steps continue in an identical manner to those that we carried out in our development of the elimination algorithm in Chapter 3. Clearly, from a symbolic point of view, the computation is the same. In particular, the graphical consequences of the maximization operator are identical to those of our earlier calculations with the summation operator.

In the light of this example, let us consider replacing “sum” with “max” in the junction tree algorithm. The only step in the algorithm that specifically refers to summation is the marginalization

step in Eq. (17.14). Changing this step to maximization, we have:

$$\phi_S^* = \max_{V \setminus S} \psi_V \quad (17.62)$$

$$\psi_W^* = \frac{\phi_S^*}{\phi_S} \psi_W, \quad (17.63)$$

where the rescaling step is unchanged.

In essence we now obtain an inference algorithm based on a generalized notion of marginalization. All of the steps that we took in deriving the junction tree algorithm go through as before, given that the maximization operator has the same commutativity and associativity properties as summation, and given that maximization distributes over multiplication just as summation distributes over multiplication.

What do we obtain from this algorithm? Recall that our key result is that contained in Theorem 2, where we showed that at the end of the junction tree procedure, each clique potential is equal to its marginal probability. Here “marginal” means that the random variables not contained in the clique have been “summed out.” If we replace summation by maximization, we obtain the same result, but now “marginal” means that the random variables not contained in the clique have been “maximized out.” Thus, we must have

$$\psi_C(x_C) = \max_{V \setminus C} p(x). \quad (17.64)$$

We interpret the resulting entries in the clique potential as containing the values of the maximal probability attainable for each possible configuration of the random variables  $X_C$ . Maximizing over these values, we obtain the actual configuration

We could also take one or more of the variables to be evidence variables and maximize the conditional probability distribution of the remaining variables; this would simply involve holding the evidence variables fixed.

### 17.14.2 Appendix A. Decomposable $\equiv$ Triangulated $\equiv$ Junction tree

In Section 17.8 we showed that all triangulated graphs possess a junction tree. For the purpose of devising an inference algorithm, this result suffices, focusing our attention on the problem of finding a triangulation of a graph. It is of interest to know, however, that in a certain sense triangulation is not merely a means to an end, but rather triangulation is forced on us if we wish to avail ourselves of the junction tree property. In particular, in this Appendix we strengthen our earlier result and show that a graph has a junction tree if and only if the graph is triangulated.

We also show that these two properties are equivalent to a third property—*decomposability*. Recall from Section ?? that a graph is *decomposable* if it can be recursively subdivided into sets  $A$ ,  $B$  and  $S$ , where  $S$  separates  $A$  and  $B$ , and where  $S$  is complete. The equivalence of decomposability and the junction tree property provides an appealing interpretation of the junction tree algorithm as a divide-and-conquer algorithm.

**Theorem 6** *All decomposable graphs are triangulated.*

**Proof.** We prove the result by induction. The base case of a single node is trivial. We assume that the result holds for  $N$  or fewer nodes and consider a graph with  $N + 1$  nodes.

If the graph is complete then it is obviously triangulated. Otherwise, the definition of decomposability implies a decomposition of the graph into sets  $A$ ,  $B$ , and  $S$  such that  $S$  is complete and  $S$  separates  $A$  and  $B$ . Also, both  $A \cup S$  and  $B \cup S$  are decomposable. By the induction hypothesis there are no chordless cycles in either  $A \cup S$  or  $B \cup S$ . The only possible chordless cycles must therefore include one or more nodes in both  $A$  and  $B$ . But such cycles must pass twice through  $S$ , and the completeness of  $S$  implies that they have a chord.  $\square$

Theorem 6 and Theorem 3 together show that all decomposable graphs have a junction tree. We have proved the correctness of the junction tree algorithm for the class of decomposable graphs.

We now show a stronger result, namely that decomposability, triangulation and the junction tree property are equivalent. This implies that the junction tree algorithm is correct *only* for the class of decomposable graphs.

**Theorem 7** *The following are equivalent characterizations of an undirected graph  $\mathcal{G}$ :*

- (D)  $\mathcal{G}$  is decomposable.
- (T)  $\mathcal{G}$  is triangulated.
- (J)  $\mathcal{G}$  has a junction tree.

**Proof.** We have already shown that (D) implies (T) implies (J). Thus we can prove the theorem by showing that (J) implies (D).

The proof is a proof by induction. In the base case  $\mathcal{G}$  has a single clique and is decomposable by definition. Suppose that the theorem holds for junction trees with  $N$  or fewer cliques and consider a junction tree  $T$  for  $\mathcal{G} = (X, E)$  with  $N + 1$  cliques.

Let  $C$  be a leaf node in  $T$  with separator  $S$ . Define  $R = C \setminus S$  (recall Figure 17.13). Consider the disjoint sets  $R$ ,  $X \setminus C$  and  $S$ . We show that these sets are a decomposition of  $\mathcal{G}$ .

Lemma 1 implies that  $S$  separates  $R$  and  $X \setminus C$ . That  $S$  is complete follows from the fact that  $S$  is the intersection of a pair of cliques.

To show that  $\mathcal{G}$  is decomposable it remains to show that  $C = R \cup S$  and  $X \setminus R = (X \setminus C) \cup S$  are decomposable. We show that both subsets have junction trees and conclude by the induction hypothesis that they are decomposable.

That  $C$  has a junction tree follows immediately because it is a single clique.

Consider the effect on the junction tree  $T$  of the removal of nodes in  $R$ . Each node in  $R$  is contained only in  $C$  and its neighbors are therefore fully connected (i.e., nodes in  $R$  are simplicial). Removing any such node therefore leaves the remaining nodes in  $C$  fully connected, and thus  $C$  remains a clique and the junction tree  $T$  is unaltered. When all nodes in  $R$  have been removed, all that remains of  $C$  is the separator  $S$ , which is a subset of the neighboring clique in  $T$ . By simply pruning the  $C$  clique and its separator  $S$  from  $T$  we therefore obtain a junction tree for  $X \setminus R$ .  $\square$

## 17.15 Historical remarks and bibliography

# An Introduction to Probabilistic Graphical Models

Michael I. Jordan  
*University of California, Berkeley*

June 30, 2003



## Chapter 18

# The HMM and State Space Model Revisited

In this chapter we revisit the Hidden Markov model and the Linear Gaussian model from the more general point of view of the previous two chapters. It is illuminating to see the relationship between the recursive algorithms that we developed in Chapters 12 and 15 and the general junction tree constructions in Chapter 17.

### 18.1 Hidden Markov models

Recall that the Hidden Markov model (HMM) can be represented as the chain-structured graphical model shown in Figure 18.1(a). The multinomial *state variables*  $q_t$  form the backbone of the model; from this backbone hang the observable *output variables*  $y_t$ .

We parameterize the model by endowing the first node with an *initial probability*  $\pi$ , where  $\pi_i \triangleq P(q_1^i = 1)$ , and each subsequent state node with a *transition matrix*  $A$ , where  $a_{ij} \triangleq P(q_{t+1}^j = 1 | q_t^i = 1)$ . The output nodes are assigned the local conditional probability  $P(y_t | q_t)$ . For concreteness

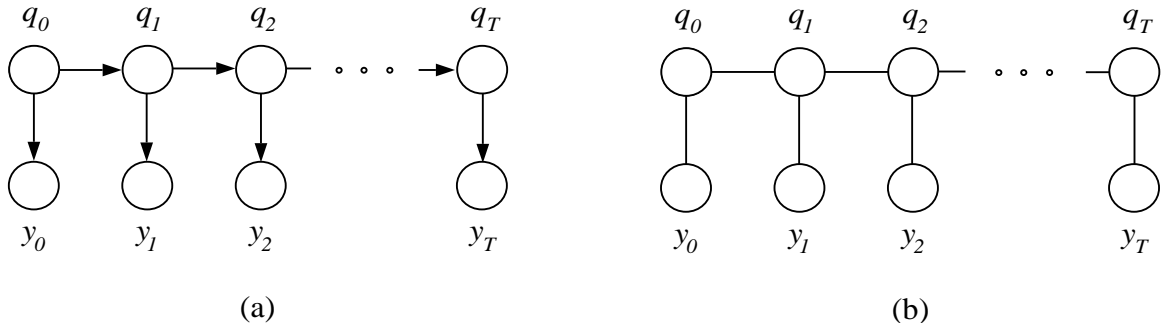


Figure 18.1: (a) The representation of a HMM as a graphical model. (b) The moralized, triangulated HMM graph.

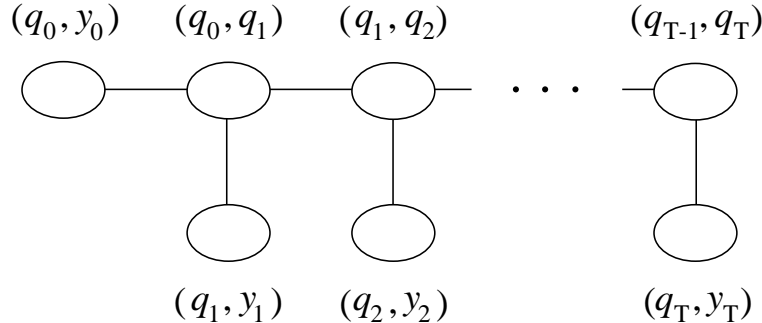


Figure 18.2: A maximal spanning tree on the cliques of the HMM graph.

we will assume that  $y_t$  is a multinomial node, so that  $P(y_t|q_t)$  can be viewed as a matrix  $B$ , where  $b_{ij} \triangleq P(y_t^j = 1|q_t^i = 1)$ . However, given that  $y_t$  is always observed, this assumption will play no critical role in our discussion.

To convert the HMM into a junction tree, we proceed as outlined in the previous chapter. The moralization step is vacuous in this case, given that each node has at most a single parent. Moreover, the triangulation step is also vacuous, given that the graph has no cycles. We are left with the moralized, triangulated graph shown in Figure 18.1(b).

The cliques in the graph in Figure 18.1(b). are given by the pairs  $(q_t, q_{t+1})$  and  $(q_t, y_t)$ . There are several ways to connect these pairs so as to obtain a maximal spanning tree; with a bit of foresight we choose the maximal spanning tree shown in Figure 18.2.<sup>1</sup> This then is our junction tree.

Figure 18.3 shows the junction tree in which the separator sets have been made explicit and the potentials have been labeled. We make the following choice for the assignment of local conditional probabilities to potentials. The initial probability  $P(q_0)$  as well as the conditional prob-

---

<sup>1</sup>In Exercise XXX we ask the reader to explore some of the alternative inference algorithms generated by the alternative choices of maximal spanning tree.

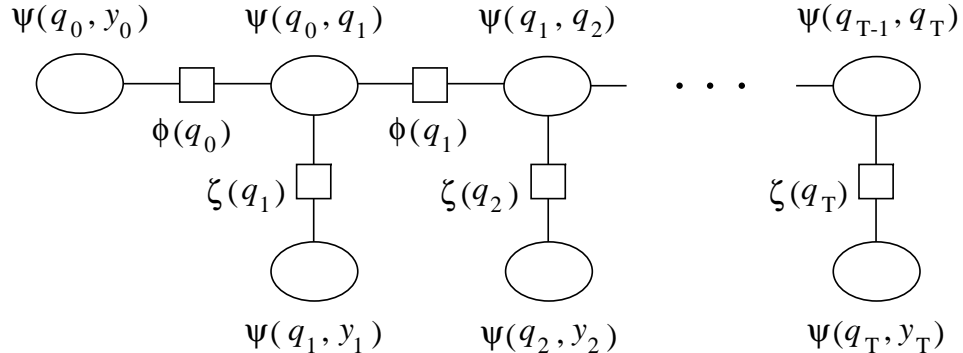


Figure 18.3: A junction tree for the HMM with the potentials labeled.

ability  $P(y_0|q_0)$  is assigned to the potential  $\psi(q_0, y_0)$ . Note that this implies that this potential is initially set to the marginal  $P(q_0, y_0)$ . The state-to-state potentials are given the assignment  $\psi(q_t, q_{t+1}) = P(q_{t+1}|q_t)$ ; note that these are conditional probabilities rather than marginals. Finally, the remaining output probabilities  $P(y_t|q_t)$  are assigned to the potentials  $\psi(q_t, y_t)$  and all separator potentials are initialized to one.

### 18.1.1 Unconditional inference

It is instructive to consider running the junction tree inference algorithm before any evidence has been observed. Suppose that we designate the node  $(q_{T-1}, q_T)$  as the root and collect to the root.

Consider first the operation of passing a message upward from a clique  $(q_t, y_t)$  to its neighbor  $(q_{t-1}, q_t)$ , for  $t > 1$ . The marginalization operation in this case yields  $\sum_{y_t} \psi(q_t, y_t) = \sum_{y_t} P(y_t|q_t) = 1$ ; thus the separator potential  $\zeta^*(q_t)$  remains set at one. This implies that the update factor  $\zeta^*(q_t)\zeta(q_t)$  is one, and thus the potential  $\psi(q_{t-1}, q_t)$  remains unchanged. In general, the messages that are passed upward from the leaves  $(q_t, y_t)$  have no effect when no evidence is observed.

Now consider the message from  $(q_0, y_0)$  to  $(q_0, q_1)$  (see Figure 18.3). We have:

$$\phi^*(q_0) = \sum_{y_0} \psi(q_0, y_0) = \sum_{y_0} P(q_0, y_0) = P(q_0) \quad (18.1)$$

$$\psi^*(q_0, q_1) = \psi(q_0, q_1)\phi^*(q_0) = P(q_1|q_0)P(q_0) = P(q_0, q_1). \quad (18.2)$$

This transformation propagates forward along the chain, changing the separator potentials on  $q_t$  into the marginals  $P(q_t)$  and the clique potentials on  $(q_t, q_{t+1})$  into the marginals  $P(q_t, q_{t+1})$ . Thus, all potentials along the backbone of the chain become marginals.

A subsequent pass of DistributeEvidence will have no effect on the potentials along the backbone of the chain (as the reader can verify), but it will convert the potentials  $\zeta(q_t)$  into marginals  $P(q_t)$  and the potentials  $\psi(q_t, y_t)$  into marginals  $P(q_t, y_t)$ . Thus all potentials throughout the junction tree become marginal probabilities. This result is not surprising, given that it is an easy special case of Theorem 2, but it is reassuring.

Our result also helps to clarify the representation of the joint probability as the product of the clique potentials divided by the product of the separator potentials (cf. Eq. 17.11). While we would not expect to be able to represent the joint in general as the product of marginals such as  $P(q_t, q_{t+1})$ , we do get this representation if we divide by the separator potentials and those separator potentials are also marginals. Thus, for example, each pairing of a clique potential and a separator potential along the backbone contributes a factor  $P(q_t, q_{t+1})/P(q_t)$  to the joint, which is nothing but the original local conditional  $P(q_{t+1}|P(q_t))$ .

### 18.1.2 Introducing evidence

We now suppose that the outputs  $y$  are observed. We wish to calculate the likelihood  $P(y)$  as well as marginal posterior probabilities such as  $P(q_t|y)$  and  $P(q_t, q_{t+1}|y)$ . We return to the original junction tree in which the separator potentials are initialized to unity.

The first step is to alter the potentials to reflect the introduction of the evidence. In the case that  $y_t$  is a multinomial node, recall that the potential  $\psi(q_t, y_t)$  can be viewed as a matrix  $B$ ,

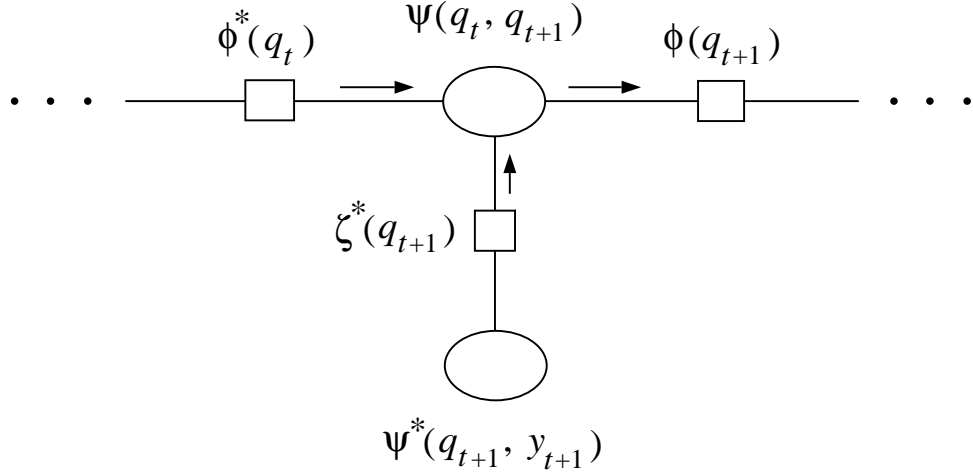


Figure 18.4: A fragment of the junction tree for the HMM.

with columns labeled by the possible values of  $y_t$ . Conceptually, observing  $y_t$  to be in its  $i$ th state corresponds to setting all other columns to zero, so that a subsequent marginalization over  $y_t$  simply picks out the  $i$ th column of the matrix. In practice we would simply set the separator potential to the desired column. Thus, we have:

$$\zeta^*(q_t) = P(y_t|q_t), \quad (18.3)$$

where  $y_t$  is viewed as a fixed constant.

### 18.1.3 Collecting to the root

We designate the clique  $(q_{T-1}, q_T)$  as the root of the junction tree and collect to the root.

Consider the update of clique  $(q_t, q_{t+1})$ , as shown in Figure 18.4. We suppose that the preceding separator potential  $\phi^*(q_t)$  has already been updated and consider the computation of  $\psi^*(q_t, q_{t+1})$  and  $\phi^*(q_{t+1})$ . Combining the update of clique  $(q_t, q_{t+1})$  based on both of its neighbors  $(q_{t-1}, q_t)$  and  $(q_{t+1}, y_{t+1})$ , we have:

$$\psi^*(q_t, q_{t+1}) = \psi(q_t, q_{t+1})\phi^*(q_t)\zeta^*(q_{t+1}) \quad (18.4)$$

$$= a_{q_t, q_{t+1}}\phi^*(q_t)P(y_{t+1}|q_{t+1}), \quad (18.5)$$

where, as in Chapter 12, we utilize the shorthand  $a_{q_t, q_{t+1}} \triangleq P(q_{t+1}|q_t)$ . Proceeding forward along the chain, we obtain:

$$\phi^*(q_{t+1}) = \sum_{q_t} \psi^*(q_t, q_{t+1}) \quad (18.6)$$

$$= \sum_{q_t} a_{q_t, q_{t+1}}\phi^*(q_t)P(y_{t+1}|q_{t+1}). \quad (18.7)$$

Defining  $\alpha(q_t) \triangleq \phi^*(q_t)$ , we see that we have recovered exactly the alpha algorithm from Chapter 12 (cf. Eq. 12.22).

Although this definition of  $\phi^*(q_t)$  achieves a formal equivalence of the update formulas, is it a reasonable definition? Is  $\phi^*(q_t)$  equal to  $P(y_0, \dots, y_t, q_t)$ ? Indeed, we have  $\phi^*(q_0) = P(y_0, q_0)$  by definition, and recursively:

$$\phi^*(q_{t+1}) = \sum_{q_t} a_{q_t, q_{t+1}} \phi^*(q_t) P(y_{t+1} | q_{t+1}) \quad (18.8)$$

$$= \sum_{q_t} P(q_{t+1} | q_t) P(y_0, \dots, y_t, q_t) P(y_{t+1} | q_{t+1}) \quad (18.9)$$

$$= \sum_{q_t} P(y_0, \dots, y_t, y_{t+1}, q_t, q_{t+1}) \quad (18.10)$$

$$= P(y_0, \dots, y_t, y_{t+1}, q_{t+1}), \quad (18.11)$$

so the definition is justified.

It is also possible to develop an alternative approach to the forward inference problem by specifying a recurrence on the  $(q_t, q_{t+1})$  clique potentials. In fact, given that  $\phi^*(q_t) = \sum_{q_{t-1}} \psi^*(q_{t-1}, q_t)$ , substitution in Eq. 18.5 yields:

$$\psi^*(q_t, q_{t+1}) = a_{q_t, q_{t+1}} \sum_{q_{t-1}} \psi^*(q_{t-1}, q_t) P(y_{t+1} | q_{t+1}), \quad (18.12)$$

The reader can verify that  $\psi^*(q_t, q_{t+1}) = P(y_0, \dots, y_{t+1}, q_t, q_{t+1})$ . Thus, defining the variable  $\rho(q_t, q_{t+1}) \triangleq P(y_0, \dots, y_{t+1}, q_t, q_{t+1})$ , we have established the recurrence relation:

$$\rho(q_t, q_{t+1}) = a_{q_t, q_{t+1}} \sum_{q_{t-1}} \rho(q_{t-1}, q_t) P(y_{t+1} | q_{t+1}), \quad (18.13)$$

which is an alternative to the traditional alpha algorithm. Indeed, in Section 18.1.5 we will establish a backward recurrence involving the cliques  $(q_t, q_{t+1})$  which, together with Eq. 18.13 will yield an alternative approach to HMM inference that produces the “xi” variables directly and the “alpha/gamma” variables indirectly.

The collect phase of the algorithm terminates with the update of  $\psi(q_{T-1}, q_T)$ . The updated potential will equal  $P(y_0, \dots, y_T, q_t, q_{t+1})$ , and thus by marginalization:

$$P(y) = \sum_{q_{T-1}, q_T} \psi^*(q_{T-1}, q_T) \quad (18.14)$$

we obtain the likelihood  $P(y)$ .

#### 18.1.4 An alternative root

Suppose that instead of designating clique  $(q_{T-1}, q_T)$  as the root node of the junction tree, we instead utilize  $(q_0, q_1)$  as the root. Exercise XXX studies this case, showing that the result is the

beta algorithm. Thus, we find that  $\phi^*(q_t) = P(y_{t+1}, \dots, y_T | q_t)$  and, moreover, the junction tree recursion linking  $\phi^*(q_t)$  and  $\phi^*(q_{t+1})$  is exactly the beta recursion of Eq. 12.30.

It is not necessary, however, to change the root of the junction tree to derive the beta algorithm. As we show in Section 18.1.5, the beta algorithm arises during the DistributeEvidence pass when utilizing clique  $(q_{T-1}, q_T)$  as the root. This is the preferred way to map the traditional HMM inference algorithms onto the junction tree machinery.

A final comment regarding the forward/backward algorithms and the notion of *filtering*; that of obtaining the conditional expectation of a state given a partial observation sequence. Note that the beta variables are conditionals  $P(y_{t+1}, \dots, y_T | q_t)$ , involving the probability of a partial evidence sequence given the state. The alpha variables, on the other hand, are marginals  $P(y_0, \dots, y_t, q_t)$ , involving the probability of a partial evidence sequence *and* the state at time  $t$ . Converting the latter variables to filtered quantities of the form  $P(q_t | y_0, \dots, y_t)$  is straightforward; one simply normalizes. Converting the beta variables to (backward) filtered quantities of the form  $P(q_t | y_{t+1}, \dots, y_T)$ , on the other hand, is not so straightforward. Obtaining this conditional requires us to know  $P(q_t)$ , which is not available in the junction tree.

Suppose, however, that we consider a pre-initialized junction tree in which the inference algorithm has been performed without evidence. We saw in Section 18.1.1 that this procedure converts the potentials throughout the tree, including the separator potentials, into marginal probabilities. Thus, a marginal such as  $P(q_t)$  is available in this tree, and we might expect to obtain a marginal version of the beta algorithm if we subsequently collect to the root. Indeed, in Exercise XXX we verify that this procedure yields  $\phi^*(q_t) = P(y_{t+1}, \dots, y_T, q_t)$ . This quantity is readily converted to the filtered estimate  $P(q_t | y_{t+1}, \dots, y_T)$  by normalization.

### 18.1.5 Distributing from the root

We now return to our main thread, and consider running the DistributeEvidence algorithm from the root  $(q_{T-1}, q_T)$ . We assume that we have already collected to this root, and thus the potentials at the outset of the DistributeEvidence are those discussed in Section 18.1.3.

The DistributeEvidence phase proceeds backward along the backbone of the state-to-state cliques as well as downward into the state-to-output cliques. Given that we have already obtained the likelihood, which is the only information regarding the probability of the outputs that is generally of interest, we restrict our attention to the updates along the backbone.

Referring to Figure 18.5, we suppose that the preceding separator potential  $\phi^{**}(q_{t+1})$  has already been updated and consider the update of  $\psi^{**}(q_t, q_{t+1})$  and  $\phi^{**}(q_t)$ . We have:

$$\psi^{**}(q_t, q_{t+1}) = \psi^*(q_t, q_{t+1}) \frac{\phi^{**}(q_{t+1})}{\phi^*(q_{t+1})}, \quad (18.15)$$

and proceeding backward a further step:

$$\begin{aligned} \phi^{**}(q_t) &= \sum_{q_{t+1}} \frac{\psi^*(q_t, q_{t+1})}{\phi^*(q_{t+1})} \phi^{**}(q_{t+1}) \\ &= \sum_{q_{t+1}} \frac{\psi^*(q_t, q_{t+1})}{\sum_{q_t} \psi^*(q_t, q_{t+1})} \phi^{**}(q_{t+1}). \end{aligned} \quad (18.16)$$

$$(18.17)$$

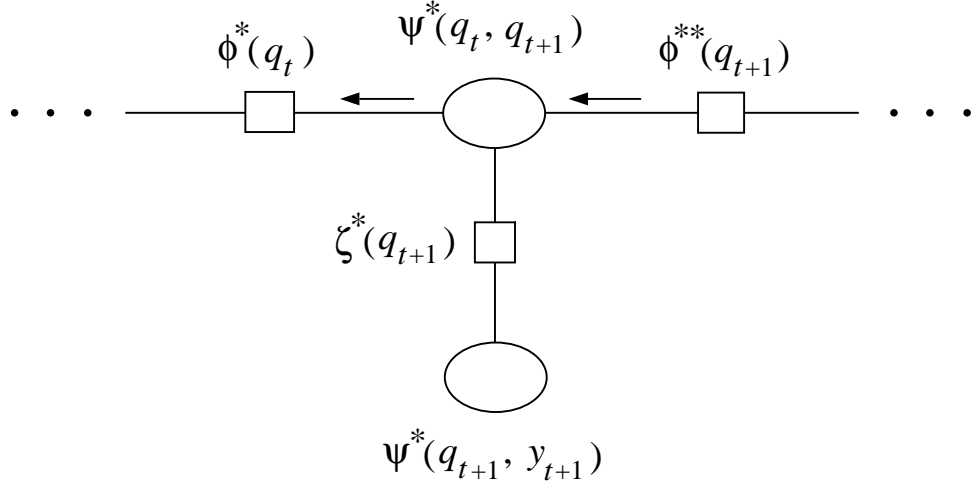


Figure 18.5: A fragment of the junction tree for the HMM with backward-going messages.

Substituting from Eq. 18.5 we have:

$$\phi^{**}(q_t) = \sum_{q_{t+1}} \frac{a_{q_t, q_{t+1}} \phi^*(q_t)}{\sum_{q_t} a_{q_t, q_{t+1}} \phi^*(q_t)} \phi^{**}(q_{t+1}) \quad (18.18)$$

$$= \sum_{q_{t+1}} \frac{a_{q_t, q_{t+1}} \alpha(q_t)}{\sum_{q_t} a_{q_t, q_{t+1}} \alpha(q_t)} \phi^{**}(q_{t+1}). \quad (18.19)$$

Defining  $\gamma(q_t)$  as equal to  $\phi^{**}(q_t)$ , up to a constant of proportionality, we see that we have recovered the gamma recursion from Chapter 12 (cf. Eq. 12.41).

Once again we can reassure ourselves that  $\gamma(q_t)$  defined this way is indeed proportional to the posterior probability  $P(q_t | y_0, \dots, y_T)$ . This can be done by direct calculation (cf. Exercise XXX). Alternatively, we can trust the general theory of Chapter 17, which assures us that the potentials produced by the junction tree algorithm must be proportional to the posterior probabilities. Indeed, it is easy to verify that  $\phi^{**}(q_t) = P(y_0, \dots, y_T, q_t)$  and thus the proportionality constant is the likelihood  $P(y)$ . Once the junction tree algorithm has run, we can obtain the likelihood by normalizing any of the potentials.

In summary, we have identified the alpha and the gamma variables in the junction tree algorithm, and have derived the “alpha-gamma” recursion discussed in Chapter 12. We can also derive the “alpha-beta” recursion via the junction tree algorithm. Consider in particular the update factor  $\phi^{**}(q_t)/\phi^*(q_t)$ :

$$\frac{\phi^{**}(q_t)}{\phi^*(q_t)} = \frac{\sum_{q_{t+1}} \psi^{**}(q_t, q_{t+1})}{\phi^*(q_t)} \quad (18.20)$$

$$= \sum_{q_{t+1}} \frac{\psi^*(q_t, q_{t+1})}{\phi^*(q_t)} \frac{\phi^{**}(q_{t+1})}{\phi^*(q_{t+1})} \quad (18.21)$$

$$= \sum_{q_{t+1}} \frac{a_{q_t, q_{t+1}} \phi^*(q_t) P(y_{t+1} | q_{t+1})}{\phi^*(q_t)} \frac{\phi^{**}(q_{t+1})}{\phi^*(q_{t+1})} \quad (18.22)$$

$$= \sum_{q_{t+1}} a_{q_t, q_{t+1}} P(y_{t+1} | q_{t+1}) \frac{\phi^{**}(q_{t+1})}{\phi^*(q_{t+1})}. \quad (18.23)$$

where we have used Eq. 18.5 in the third equality. Defining  $\beta(q_t) \triangleq \phi^{**}(q_t)/\phi^*(q_t)$ , we have recovered the beta recursion from Chapter 12 (cf. Eq. 12.30). Moreover, putting together our definitions, we have:

$$\alpha(q_t) \beta(q_t) = \phi^*(q_t) \frac{\phi^{**}(q_t)}{\phi^*(q_t)} = \phi^{**}(q_t) \propto \gamma(q_t) \quad (18.24)$$

and thus we have also recovered the original definition of  $\gamma(q_t)$  in Eq. 12.13.

Finally, it is also of interest to note that the junction tree algorithm gives us an explicit recursion in the variables  $\xi(q_t, q_{t+1})$  (cf. Eq. 12.42). Starting from Eq. 18.15, we have:

$$\psi^{**}(q_{t-1}, q_t) = \psi^*(q_{t-1}, q_t) \frac{\phi^{**}(q_t)}{\phi^*(q_t)} \quad (18.25)$$

$$= \frac{\psi^*(q_{t-1}, q_t)}{\phi^*(q_t)} \sum_{q_{t+1}} \psi^{**}(q_t, q_{t+1}) \quad (18.26)$$

$$= \frac{\rho(q_{t-1}, q_t)}{\sum_{q_{t-1}} \rho(q_{t-1}, q_t)} \sum_{q_{t+1}} \psi^{**}(q_t, q_{t+1}). \quad (18.27)$$

Defining  $\xi(q_t, q_{t+1})$  to be equal to  $\psi^{**}(q_t, q_{t+1})$ , again up to a constant of proportionality which turns out to be the likelihood, we have obtained an explicit recursion for the  $\xi(q_t, q_{t+1})$  variables:

$$\xi(q_{t-1}, q_t) = \frac{\rho(q_{t-1}, q_t)}{\sum_{q_{t-1}} \rho(q_{t-1}, q_t)} \sum_{q_{t+1}} \xi(q_t, q_{t+1}). \quad (18.28)$$

This “rho-xi algorithm” is the analog of the “alpha-gamma algorithm.”

Once the rho-xi algorithm has run,  $\alpha(q_t)$  and  $\gamma(q_t)$  can be obtained via:

$$\alpha(q_t) = \sum_{q_{t-1}} \rho(q_{t-1}, q_t) \quad (18.29)$$

$$\gamma(q_t) = \sum_{q_{t-1}} \xi(q_{t-1}, q_t), \quad (18.30)$$

which are verified by plugging in the corresponding junction tree definitions.

## 18.2 Linear Gaussian models

We now turn to the linear Gaussian model (the “LG-HMM”). We rederive two of the LG-HMM inference algorithms—a forward (filtering) algorithm and a backward (smoothing) algorithm—from Chapter 15 in order to exemplify the relationships between the junction tree and the earlier material.

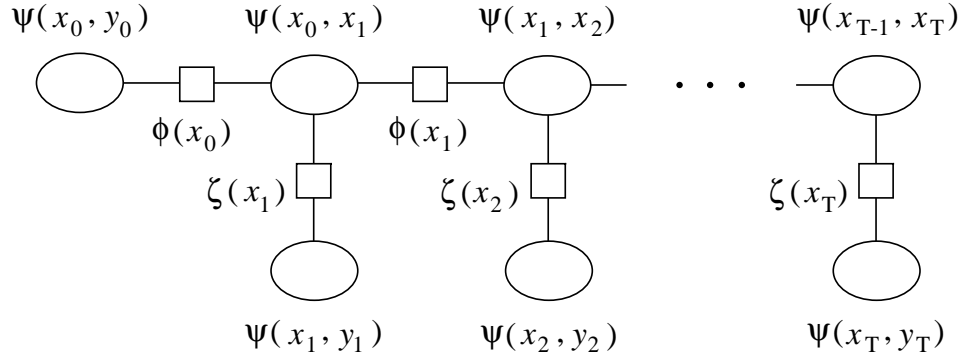


Figure 18.6: A junction tree for the LG-HMM with the potentials labeled.

Recall from Chapter 15 that the LG-HMM has the same graphical structure as the HMM, the difference being the node types and the parameterization. Thus, as before, Figure 18.1(a) is the graphical model for the LG-HMM (substituting “ $x$ ” for “ $q$ ”) and Figure 18.1(b) is the moralized, triangulated graph. Also, the junction tree for the LG-HMM, shown in Figure 18.6, is identical to that for the HMM.<sup>2</sup> Figure 18.6

The potentials in the junction tree are Gaussian potentials on pairs of nodes (the cliques) or singletons (the separators). We set up an assignment of local conditional probabilities to clique potentials that parallels that of the HMM. In particular, clique  $(x_0, y_0)$  is assigned the initial state probability  $P(x_0)$  and the conditional  $P(y_0|x_0)$ , and thus  $\psi(x_0, y_0)$  is initialized to the marginal  $P(x_0, y_0)$ . All of the other clique potentials are conditionals; in particular the state-to-state clique potential  $\psi(x_t, x_{t+1})$  is set equal to  $P(x_{t+1}|x_t)$  and the state-to-output potential  $\psi(x_t, y_t)$  is set equal to  $P(y_t|x_t)$ .

Consider first the potential  $\psi(x_t, x_{t+1})$ . Given the dynamical equation:

$$x_{t+1} = Ax_t + Gw_t, \quad (18.31)$$

the conditional probability  $P(x_{t+1}|x_t)$  is a multivariate Gaussian with mean  $Ax_t$  and covariance matrix  $GQG^T$ , where  $Q$  is the covariance matrix of  $w_t$ . Letting  $H \triangleq GQG^T$ , we have:

$$P(x_{t+1}|x_t) \propto \exp \left\{ -\frac{1}{2}(x_{t+1} - Ax_t)^T H^{-1}(x_{t+1} - Ax_t) \right\}. \quad (18.32)$$

Expressing the quadratic form as a function of two variables, we obtain:

$$\psi(x_{t+1}|x_t) = \exp \left\{ -\frac{1}{2} \begin{pmatrix} x_t \\ x_{t+1} \end{pmatrix}^T \begin{bmatrix} A^T H^{-1} A & -A^T H^{-1} \\ H^{-1} A & H^{-1} \end{bmatrix} \begin{pmatrix} x_t \\ x_{t+1} \end{pmatrix} \right\} \quad (18.33)$$

Note that in this representation, and in all subsequent potential function representations of Gaussians, we carry along only the exponential factor and ignore the Gaussian normalization factor.

---

<sup>2</sup>As in the case of the HMM, it is a worthwhile exercise to investigate the algorithms that arise from alternative choices for the junction tree.

The reason for this is as follows. At the end of the junction tree algorithm we are guaranteed that the potentials are equal to marginal probabilities, up to a normalization factor. Now, all of the potentials in the LG-HMM are Gaussian, both before and after the running of the inference algorithm. This implies that we can simply read off the normalization factors from the final form of the potentials; we are not required to explicitly normalize before or during the inference procedure.

From the output equation of the LG-HMM:

$$y_t = Cx_t + v_t, \quad (18.34)$$

we have that  $P(y_t|x_t)$  is a multivariate Gaussian with mean  $Cx_t$  and covariance matrix  $R$ , where  $R$  is the covariance matrix of  $v_t$ . This yields:

$$P(y_t|x_t) \propto \exp \left\{ -\frac{1}{2}(y_t - Cx_t)^T R^{-1} (y_t - Cx_t) \right\}. \quad (18.35)$$

We can proceed as before and convert this to a bivariate representation for  $\psi(x_t, y_t)$ . Note, however, that  $y_t$  is an observed constant in applications of the LG-HMM. This implies that the marginalization step that yields  $\zeta^*(x_t)$  simply reproduces Eq. 18.35 for that observed value of  $y_t$  (i.e., we integrate  $\psi(x_t, y_t)$  against a delta function). We thus leave Eq. 18.35 unexpanded in anticipation of its later role as  $\zeta^*(x_t)$ .

Multivariate Gaussian potentials can be represented in terms of either moments  $(\mu, \Sigma)$ , or canonical parameters  $(\xi, \Lambda)$ . In Chapter 13 we derived the formulas for marginalization and conditioning in both representations. In the context of the junction tree algorithm we also need to multiply potentials. This is significantly easier in the canonical parameterization. Thus, if we have potentials  $\psi_1(x) = \exp \xi_1^T x - 1/2x^T K_1 x$  and  $\psi_2(x) = \exp \xi_2^T x - 1/2x^T K_2 x$ , the product is a potential  $\psi(x) = \exp \xi^T x - 1/2x^T K x$ , where:

$$K = K_1 + K_2 \quad (18.36)$$

$$\xi = \xi_1 + \xi_2. \quad (18.37)$$

Expressing this operation in terms of moments requires an application of the inverse matrix lemma. On the other hand, if our interest is in obtaining filtered or smoothed estimates of the states—i.e., moments—then we if we develop an algorithm in terms of canonical parameters we will require an application of the inverse matrix lemma at the end. The situation is “pay now or pay later.”

Moreover, in the context of linear Gaussian systems, moments behave particularly nicely and calculations on moments can save substantial labor. If we take the junction tree algorithm literally and require ourselves to multiply the Gaussian potentials then we miss out on this opportunity. Indeed, in doing the necessary inverse matrix operations we are essentially rederiving the fact that the parameters  $\mu$  and  $\Sigma$  are moments of the Gaussian distribution. It is also possible to replace the multiplication step of the junction tree algorithm with a step that calculates the moments of the product directly, utilizing the probabilistic interpretation of the potentials. For example, suppose that we know that  $\phi(x)$  is proportional to the marginal of  $x$  and we have that  $\psi(x, y)$  is proportional to the conditional of  $y$  given  $x$ . Moreover, let  $y = Cx + v$ . In this case we can directly compute  $E[y]$ ,  $\text{Var}[y]$  and  $\text{Cov}[x, y]$  in terms of the moment parameterization of  $\phi(x)$ , thereby obtaining the moment parameterization of  $\psi^*(x, y) = \psi(x, y)\phi(x)$ .

In this chapter we generally take the more literal interpretation of the junction tree algorithm and work in the canonical representation (with the notable exception of the following section, where we exploit moment calculations). Exercise XXX asks the reader to develop the moment-based approach more generally, in particular relating this approach to the derivation of the Kalman filter that we presented in Chapter 15.

### 18.2.1 Unconditional inference

As in the HMM case it is useful to consider running the junction tree inference algorithm before any evidence has been observed. Suppose that we designate the node  $(x_{T-1}, x_T)$  as the root and collect to the root.

The derivation that we carried out in Section 18.1.1 for the HMM was entirely generic, and (replacing the sums with integrals) we obtain the same results for the LG-HMM. In particular, once again the operation of passing a message upward from the leaves  $(x_t, y_t)$  to the cliques  $(x_t, x_{t+1})$ , for  $t > 1$ , has no effect. The operation of passing messages from  $(x_0, y_0)$  to  $(x_0, x_1)$  and subsequently along the backbone of cliques  $(x_t, x_{t+1})$  has the effect of changing all of those clique potentials, as well as the separator potentials, to marginal probabilities.

The form that these marginal probabilities take is readily obtained via moment calculations. Let  $(\mu_t, \Sigma_t)$  denote the mean and covariance matrix of  $x_t$ . Given the dynamical equation  $x_{t+1} = Ax_t + Gw_t$ , and given our assumption that the initial state has mean zero, we see that  $\mu_t = 0$  for all  $t$ . As for the covariance matrix, we obtain:

$$\Sigma_{t+1} = A\Sigma_t A^T + H, \quad (18.38)$$

which is the *Lyapunov equation* of Chapter 15 (cf. Eq. 15.6). Thus after the CollectEvidence phase, the separator potentials can be represented by  $(0, \Sigma_t)$ , or by  $(0, \Sigma_t^{-1})$  in canonical parameters. The clique potential  $\psi(x_t, x_{t+1})$  is represented in moment parameters by:

$$\begin{bmatrix} 0 \\ 0 \end{bmatrix}, \quad \begin{bmatrix} \Sigma_t & -\Sigma_t A \\ -A^T \Sigma_t & A\Sigma_t A^T + H \end{bmatrix} \quad (18.39)$$

The representation in terms of canonical parameters can be obtained by inverting the covariance matrix (using the partitioned matrix inverse theorem, Eq. 13.16):

$$\begin{bmatrix} 0 \\ 0 \end{bmatrix}, \quad \begin{bmatrix} A^T H^{-1} A + \Sigma_t^{-1} & -A^T H^{-1} \\ -H^{-1} A & H^{-1} \end{bmatrix} \quad (18.40)$$

### 18.2.2 Introducing evidence

We return to the original junction tree in which the separator potentials are initialized to unity and now suppose that the outputs  $y$  are observed.

As in the case of the HMM we are not interested in the potential on  $(x_t, y_t)$  beyond its effect on the separator potential  $\zeta^*(x_t)$ . Moreover,  $\zeta^*(x_t)$  is obtained by simply evaluating  $P(y_t|x_t)$  at the observed value  $y_t$ :

$$\zeta^*(x_t) = \exp \left\{ -\frac{1}{2} (y_t - Cx_t)^T R^{-1} (y_t - Cx_t) \right\}. \quad (18.41)$$

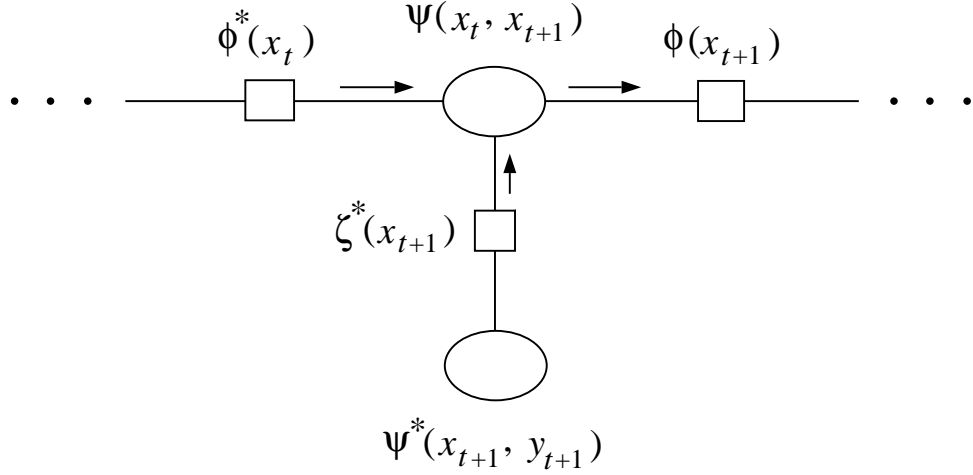


Figure 18.7: A fragment of the junction tree for the LG-HMM.

In canonical parameters this potential can be represented as:  $(-C^T y_t, C^T R^{-1} C)$ .

### 18.2.3 A forward algorithm

We designate the clique  $(x_{T-1}, x_T)$  as the root of the junction tree and collect to the root.

Let  $(\hat{\xi}_{t|t}, S_{t|t})$  be the canonical parameters of the distribution of  $x_t$  conditioned on  $(y_0, \dots, y_t)$ . Similarly, let  $(\hat{\xi}_{t+1|t}, S_{t+1|t})$  be the canonical parameters of the distribution of  $x_t$  conditioned on  $(y_0, \dots, y_{t+1})$ . Our goal is to establish recursions for these quantities.

Consider the junction tree fragment shown in Figure 18.7. We suppose that the preceding separator potential Suppose that we have already obtained an updated  $\phi^*(x_t)$  and wish to update  $\psi(x_t, x_{t+1})$ . We know from our general theory and (our experience with the HMM) that  $\phi^*(x_t)$  must be proportional to  $P(x_t | y_0, \dots, y_t)$ ; thus, we immediately identify the canonical parameters of  $\phi^*(x_t)$  with  $(\hat{\xi}_{t|t}, S_{t|t})$ . Using Eq. 18.33 we now update  $\psi(x_t, x_{t+1})$  by multiplying by  $\phi^*(x_t)$ . This yields the following canonical parameters for the updated potential:

$$\begin{bmatrix} \hat{\xi}_{t|t} \\ 0 \end{bmatrix}, \quad \begin{bmatrix} S_{t|t} + A^T H^{-1} A & -A^T H^{-1} \\ H^{-1} A & H^{-1} \end{bmatrix}. \quad (18.42)$$

If we now marginalize this potential with respect to  $x_t$ , we should expect to obtain a representation for  $P(x_{t+1} | y_0, \dots, y_t)$ . Indeed, applying Eq. 13.29 and Eq. 13.29, we obtain:

$$\hat{\xi}_{t+1|t} = H^{-1} A (S_{t|t} + A^T H^{-1} A)^{-1} \hat{\xi}_{t|t} \quad (18.43)$$

$$S_{t+1|t} = H^{-1} - H^{-1} A (S_{t|t} + A^T H^{-1} A)^{-1} A^T H^{-1}. \quad (18.44)$$

These two equations are identical to the time updates for the information filter in Chapter 15 (cf. Eq. 15.49 and Eq. 15.39).

The next step is to incorporate the evidence  $y_{t+1}$  by multiplying the updated clique potential on  $(x_t, x_{t+1})$  by  $\zeta^*(x_{t+1})$ . This yields the following canonical parameterization for  $(x_t, x_{t+1})$ :

$$\begin{bmatrix} \hat{\xi}_{t|t} \\ C^T R^{-1} y_{t+1} \end{bmatrix}, \quad \begin{bmatrix} S_{t|t} + A^T H^{-1} A & -A^T H^{-1} \\ H^{-1} A & H^{-1} + C^T R^{-1} C \end{bmatrix}. \quad (18.45)$$

Once again we marginalize this potential with respect to  $x_t$ . The result is the canonical parameterization of  $\phi^*(x_{t+1})$ :

$$\hat{\xi}_{t+1|t+1} = C^T R^{-1} y_{t+1} + H^{-1} A (S_{t|t-1} + A^T H^{-1} A)^{-1} \hat{\xi}_{t|t} \quad (18.46)$$

$$= \hat{\xi}_{t+1|t} + C^T R^{-1} y_{t+1} \quad (18.47)$$

$$S_{t+1|t+1} = H^{-1} + C^T R^{-1} C - H^{-1} A (S_{t|t} + A^T H^{-1} A)^{-1} A^T H^{-1} \quad (18.48)$$

$$= S_{t+1|t} + C^T R^{-1} C. \quad (18.49)$$

These results are identical to the measurement updates for the information filter in Chapter 15 (cf. Eq. 15.54 and Eq. 15.43).

#### 18.2.4 A backward algorithm

In Section 15.7.2 we derived a backward algorithm for the LG-HMM by explicitly inverting the dynamics of the linear-Gaussian model and applying the information filter to the inverted dynamics. Recall that this approach yielded filtered estimates, i.e., conditional probabilities  $P(x_t|y_{t+1}, \dots, y_T)$ , rather than the usual “beta variables”  $P(y_{t+1}, \dots, y_T|x_t)$ .

In this section we see that this algorithm emerges in a straightforward way from the junction tree algorithm. In particular, suppose that we pre-initialize the junction tree by running a forward pass without evidence. From Section 18.2.1 we know that this pre-initialization pass leaves marginal probabilities on both the clique and the separator potentials. We would expect that a subsequent backward pass in the pre-initialized tree should yield filtered estimates  $P(x_t|y_{t+1}, \dots, y_T)$ .

Note in particular that whereas in Section 15.7.2 we had to invert the dynamics explicitly, this is not necessary in the current approach. The junction tree algorithm effectively inverts the dynamics for us. (In particular the derivation does not assume that  $A$  is an invertible matrix).

The derivation of the algorithm is similar to that of the previous section; the main difference being that we must remember to divide by the pre-initialized separator potentials. These potentials have the canonical representation  $(0, \Sigma_t^{-1})$ . Recall also that the initial values of the clique potentials are given by Eq. 18.40.

To obtain a two-step procedure in the backwards direction, it is useful to utilize an alternative junction tree in which the clique  $(x_t, y_t)$  is attached to the clique  $(x_t, x_{t+1})$  rather than  $(x_{t-1}, x_t)$ . This junction tree is shown in Figure 18.8 where we see that it is the final clique and not the initial clique that has two state-to-output neighbors. Note that in this junction tree the evidence node  $(x_t, y_t)$  is to the left of the separator  $(x_{t+1})$ , just as the evidence node  $(x_{t+1}, y_{t+1})$  was to the right of the separator  $(x_t)$  in the earlier junction tree (Figure 18.2). As we will see, this allows us to obtain the usual two-step time and measurement updates from the junction tree.

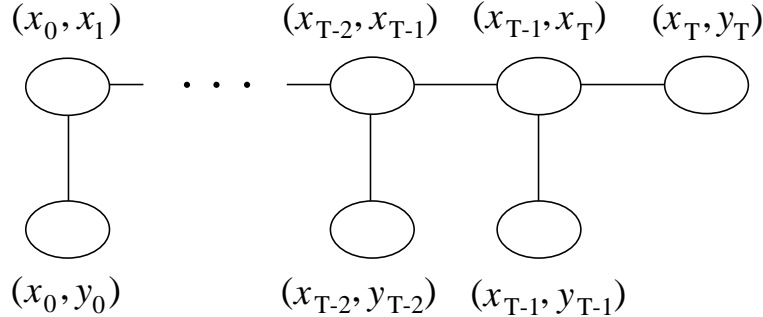


Figure 18.8: An alternative maximal spanning tree for the LG-HMM.

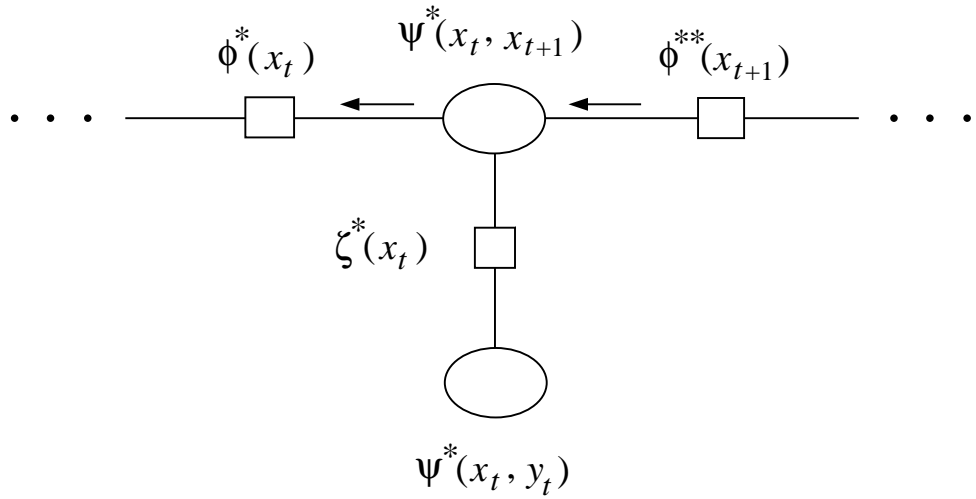


Figure 18.9: A fragment of the alternative junction tree for the LG-HMM.

We initially set the potentials of all cliques and separators to be proportional to the corresponding (unconditional) marginal probabilities. In particular, the potential  $\psi(x_T, y_T)$  at the end of the chain is set proportional to  $P(x_T, y_T) = P(y_T|x_T)P(x_T)$ . We can conceptually view this assignment of potentials as resulting from a forward pass in the unconditioned graph (cf. Section 18.2.1).

Let us denote the canonical parameters of  $\phi^*(x_{t+1})$  by  $(\hat{\xi}_{t+1|t+1}, S_{t+1|t+1})$ ; note that this potential reflects the evidence from  $y_{t+1}$  onward. We now update  $\psi(x_t, x_{t+1})$  by multiplying by  $\phi^*(x_{t+1})$  and dividing by  $\phi(x_{t+1})$ , where the latter refers to the potential that was obtained unconditionally (see Figure 18.9). The parameters of the updated potential are:

$$\begin{bmatrix} 0 \\ \hat{\xi}_{t+1|t+1} \end{bmatrix}, \quad \begin{bmatrix} A^T H^{-1} A + \Sigma_t^{-1} & -A^T H^{-1} \\ H^{-1} A & S_{t+1|t+1} + H^{-1} - \Sigma_{t+1}^{-1} \end{bmatrix}, \quad (18.50)$$

where the  $S_{t+1|t+1}$  in the lower-right-hand corner is due to multiplication by  $\psi(x_t, x_{t+1})$  and the  $\Sigma_{t+1}^{-1}$  is due to division by  $\phi(x_{t+1})$ .

We now marginalize with respect to  $x_{t+1}$  to obtain the canonical representation of  $P(x_t|y_{t+1}, \dots, y_T)$ :

$$\hat{\xi}_{t|t+1} = A^T H^{-1} (S_{t+1|t+1} + H^{-1} - \Sigma_{t+1}^{-1})^{-1} \hat{\xi}_{t+1|t+1} \quad (18.51)$$

$$S_{t|t+1} = A^T H^{-1} (S_{t+1|t+1} + H^{-1} - \Sigma_{t+1}^{-1})^{-1} H^{-1} A. \quad (18.52)$$

These updates are identical to Eq. 15.98 and Eq. 15.96.

We now update the clique potential on  $(x_t, x_{t+1})$  to reflect the evidence  $y_t$ . This amounts to adding the term  $C^T R^{-1} C$  to the inverse covariance matrix and  $C^T R^{-1} y_t$  to the linear term:

$$\begin{bmatrix} C^T R^{-1} y_t \\ \hat{\xi}_{t+1|t+1} \end{bmatrix}, \quad \begin{bmatrix} A^T H^{-1} A + \Sigma_t^{-1} + C^T R^{-1} C & -A^T H^{-1} \\ H^{-1} A & S_{t+1|t+1} + H^{-1} - \Sigma_{t+1}^{-1} \end{bmatrix}. \quad (18.53)$$

Marginalizing with respect to  $x_{t+1}$  yields the canonical representation of  $P(x_t|y_t, \dots, y_T)$ :

$$\hat{\xi}_{t|t} = \hat{\xi}_{t|t+1} + C^T R^{-1} y_t \quad (18.54)$$

$$S_{t|t+1} = S_{t|t+1} + C^T R^{-1} C, \quad (18.55)$$

which are identical to Eq. 15.98 and Eq. 15.97.

## 18.3 Summary

In this chapter we have shown how to derive many of the classical algorithms associated with the HMM and the LG-HMM from the point of view of the junction tree framework. Although we have not derived all possible algorithms, we have provided a representative sampling that shows several of the tricks of the trade.

A virtue of the junction tree formalism is that it displays all of relevant dependencies and their interrelationships; in particular, the pairwise clique potentials in the case of HMMs and LG-HMMs. This is a useful display for deriving algorithms, whether or not one uses the junction tree update formulas literally as we have done in this chapter, or uses the junction tree structure to derive alternative update formulas (e.g., based on moments).

## 18.4 Historical remarks and bibliography

# An Introduction to Probabilistic Graphical Models

Michael I. Jordan  
*University of California, Berkeley*

June 30, 2003



## Chapter 19

# Features, maximum entropy, and duality

Chapter 16 and Chapter 17 have presented aspects of the general theory of graphical models. As we have seen, this theory is based on associating potential functions with the cliques in the graph, focusing in particular on the maximal cliques of the graph. By ranging over all possible potentials on the maximal cliques of a graph, we obtain all of the probability distributions that respect the Markov properties of the graph. Moreover, by forming junction trees that include all of the maximal cliques of a triangulated graph, we obtain a general inference algorithm that fully exploits these Markov properties.

While the focus on maximal cliques is necessary for the theory to take its simplest and most general form, in practical applications of graphical models one does not necessarily want to work with families of probability distributions that range over arbitrary potentials on maximal cliques. Large, fully-parameterized cliques are problematic both for computational reasons (inference is exponential in the clique sizes) and for statistical reasons (the estimation of large numbers of parameters requires large amounts of data). One generally wants to work with reduced parameterizations that range over proper subsets of the set of all possible potential functions on maximal cliques.

Consider, for example, the applied problem of building a graphical that assigns high probability to strings that respect the orthographic rules of English and low probability to strings that do not. Let us use a very simple model of strings of letters in which, for a given string length, each position in the string is represented by a multinomial random variable that takes on one of 26 values. Thus, for strings of length five we have five nodes and a sample space of size  $26^5$ . One fact about English is that strings ending in *ing* have relatively high probability, and we would like to incorporate this fact into our model. Assigning high probability to *ing*, above and beyond the probabilities that we assign to singletons *i*, *n* and *g*, and the pairs *in* and *ng*, requires that we include a third-order term in our model—a potential function on three nodes. A table on three nodes has  $26^3$  entries, however, and such a large parameter count gives us pause. It would be unfortunate if we were required to assign values to all of these entries just so that we can assign a value to a particular cell, the *ing* cell. Clearly the way out of this dilemma is to consider reduced parameterizations of the clique potential. In particular, we might construct a parameterized “feature” that varies on the

ing cell and is uniform on all other cells.

Another example of a reduced parameterization arises when we build a potential function on a maximal clique from potential functions on non-maximal cliques. For example, we may want to parameterize the clique potential on three nodes,  $\psi_{123}(x_1, x_2, x_3)$ , in terms of pairwise potentials  $\psi_{12}(x_1, x_2)$ ,  $\psi_{13}(x_1, x_3)$ , and  $\psi_{23}(x_2, x_3)$ . We have:

$$\psi_{123}(x_1, x_2, x_3) = \psi_{12}(x_1, x_2)\psi_{13}(x_1, x_3)\psi_{23}(x_2, x_3). \quad (19.1)$$

Letting the pairwise potentials range over all possible values, the product  $\psi_{123}(x_1, x_2, x_3)$  ranges over a proper subset of the set of possible potentials on three nodes.

In this chapter we discuss parameterizations of graphical models, focusing on representational issues. We have already touched on some of this material before, in particular in Chapter 8 and Chapter 9. In the current chapter we present a broader and more systematic treatment of this material.

We begin by discussing “features,” and their relationship to exponential family representations. We then step back and provide a general motivation for using exponential family representations, introducing the variational principle of *maximum entropy*. Finally, we explore the relationships between maximum entropy and maximum likelihood, showing that they are dual optimization methods, and providing a geometrical interpretation of their duality.

## 19.1 Features

The goal is to find useful parameterizations of clique potentials, and to be able to estimate parameters from data.

One way to conceptualize this problem is to try to represent potential functions in terms of *features*—elementary functions on subsets of nodes. We put the features together to construct clique potentials. By using a relatively small number of features we obtain a reduced parameterization with relatively few independent degrees of freedom.

For example, to represent the high probability associated with the substring *ing*, we might use a binary feature  $f_{\text{ing}}(x)$  that is equal to one if the three nodes in question are in the states *i*, *n* and *g*, respectively, and is equal to zero otherwise. Thus we have an indicator function that picks out a particular cell among the  $26^3$  cells that form the domain of a potential function on three nodes. We associate with this function, and thus with this cell, a parameter  $\theta_{\text{ing}}$  that represents the numerical strength of the feature. In particular, we will be working with exponential representations in this chapter, so let us define a potential which is equal to one in all cells except the *ing* cell where it is equal to  $e^{\theta_{\text{ing}}}$ . We achieve this by defining a base potential  $h(x)$  that is equal to one in all  $26^3$  of the cells, and multiplying this base potential by the factor  $e^{\theta_{\text{ing}} f_{\text{ing}}(x)}$ .

We can also define additional features, corresponding to other cells. For example, *ate* and *ion* also appear with high probability at the end of English words. Each such substring corresponds to a different cell, which we can represent with indicator features  $f_{\text{ate}}(x)$  and  $f_{\text{ion}}(x)$ . Multiplying the potential by the factors  $e^{\theta_{\text{ate}} f_{\text{ate}}(x)}$  and  $e^{\theta_{\text{ion}} f_{\text{ion}}(x)}$  parameterizes the *ate* and *ion* cells, while leaving the potential unchanged in the other cells. The resulting potential,  $h(x)e^{\theta_{\text{ing}} f_{\text{ing}}(x) + \theta_{\text{ate}} f_{\text{ate}}(x) + \theta_{\text{ion}} f_{\text{ion}}(x)}$ , has independently varying parameters in three cells, and is equal to one in all other cells. In the

limiting case, if we utilize one binary feature for each cell in the table, we obtain a full parameterization of the potential function in which all cells in the table have an independently adjustable parameter. See Figure 19.1 for a simple example of this construction.

There is no reason, however, for us to be required to use fully parameterized potentials; we may wish to allow only a few of the cells to vary. Moreover, we are not required to utilize features that are indicators of single cells—features that pick out subsets of cells may be of interest. Also, we need not be restricted to binary-valued features or to discrete variables. In particular, for continuous-valued random variables, the notion of “cell” loses its meaning, and it is natural to consider “features” as arbitrary functions on subsets of nodes.

Generalized linear models (GLIMs) can be thought of in terms of features. By taking a linear combination of the parents of a given node, we are considering a subset of all possible probability distributions (all configurations of parents that yield the same value of the linear combination must have the same probability). Here the setting is a directed graph, and the clique of interest is a clique in the moral graph (it is the subset of nodes consisting of a node and its parents). The linear combination used in the GLIM parameterization is a feature on this clique.

Let us formalize these ideas. In the general case, we parameterize a clique  $C$  as follows. Define a set of features  $f_i(x_{C_i})$ , where  $C_i \subseteq C$  is the subset of variables that feature  $f_i$  references. The subsets  $C_i$  are unconstrained, overlapping subsets; in fact, the same subset can appear multiple times. (Indeed, this occurs in Figure 19.1 and in any example in which we represent the cells in a potential table using binary features). Associated with each feature there is a scalar parameter  $\theta_i$ . Given the features and the parameters we define the clique potential  $\psi_C(x_C)$  as follows:

$$\psi_C(x_C) \triangleq \prod_{i \in \mathcal{I}_C} \exp\{\theta_i f_i(x_{C_i})\} \quad (19.2)$$

$$= \exp \left\{ \sum_{i \in \mathcal{I}_C} \theta_i f_i(x_{C_i}) \right\}, \quad (19.3)$$

where  $\mathcal{I}_C$  is a set of indices for the features associated with clique  $C$ . If the functions  $f_i$  are linearly independent, we obtain a representation of the clique potential that has  $|\mathcal{I}_C|$  degrees of freedom.

Taking the product over clique potentials and normalizing, we obtain the usual joint probability distribution associated with the graph:

$$p(x | \theta) = \frac{1}{Z(\theta)} \prod_{C \in \mathcal{C}} \psi_C(x_C) \quad (19.4)$$

$$= \frac{1}{Z(\theta)} \prod_{C \in \mathcal{C}} \exp \left\{ \sum_{i \in \mathcal{I}_C} \theta_i f_i(x_{C_i}) \right\} \quad (19.5)$$

$$= \frac{1}{Z(\theta)} \exp \left\{ \sum_{C \in \mathcal{C}} \sum_{i \in \mathcal{I}_C} \theta_i f_i(x_{C_i}) \right\}. \quad (19.6)$$

This representation makes explicit the association of features to maximal cliques. In many cases, however, we may not need to make this association explicit, and we can simplify our representation

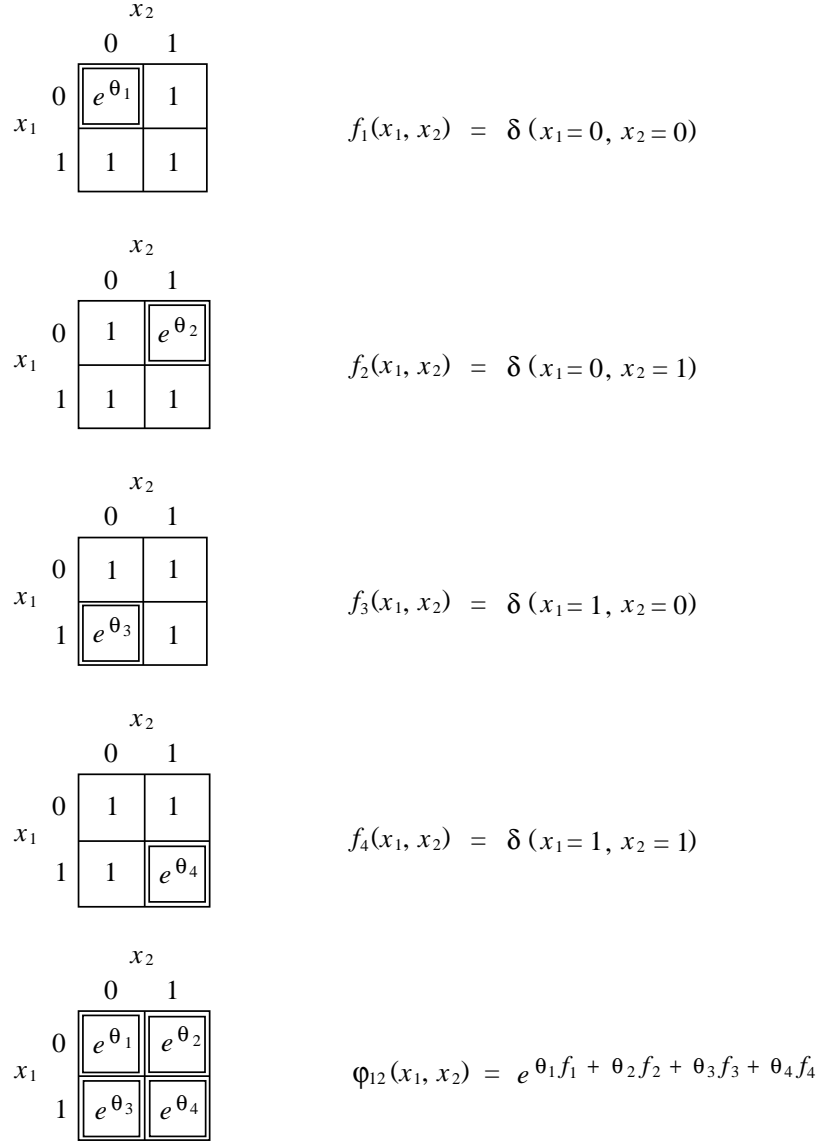


Figure 19.1: The representation of a clique potential using binary “indicator” features. The first four diagrams show potentials with a single degree of freedom corresponding to a single cell. The potential in each case is defined as  $e^{\theta_i f_i}$ . The final diagram shows a fully parameterized clique potential formed by the product of the four one-degree-of-freedom potentials.

by simply summing over all features associated with a given graph, irrespective of their association with maximal cliques. Thus, consider a set of features  $\{f_i(x_{C_i})\}$ , for  $i$  in an index set  $\mathcal{I}$ , where  $C_i$  is the set of nodes referred to by feature  $f_i$ . We have:

$$p(x | \theta) = \frac{1}{Z(\theta)} \exp \left\{ \sum_{i \in \mathcal{I}} \theta_i f_i(x_{C_i}) \right\}. \quad (19.7)$$

We see that the featural representation is nothing but the exponential family representation from Chapter 8. The “features” are the sufficient statistics in the exponential family representation. Thus, in working with “features,” as we do in this chapter, we are back on familiar terrain.

### 19.1.1 Graph first or features first?

Thus far we have assumed that a graph has been specified and our task is that of finding a parameterization for that graph. This reduces to finding a parameterization for the maximal cliques in the graph, which, as we have shown, can be achieved using a featural representation.

On the other hand, one might approach a modeling problem with a given set of features and Eq. (19.7) in mind, quite apart from any explicit graphical representation. Indeed, in the literature on exponential family models (also known as *loglinear models*), this is quite commonly done.

Given a set of features and an exponential family model, one can of course always construct a graphical representation. In particular, given features  $f_i(x_{C_i})$ , construct a graph by linking any pair of nodes that appear together in a subset  $C_i$  for some feature  $i$ . Let  $C \in \mathcal{C}$  range over the maximal cliques of the resulting graph. Each subset  $C_i$  is contained in (at least) one such maximal clique by construction; pick one such clique  $C$  and associate  $C_i$  to that  $C$ . Define the potential  $\psi_C(x_C)$  to be the product of the factors  $\exp\{\theta_i f_i(x_{C_i})\}$ , for all  $C_i$  associated with  $C$ . Given that each feature appears only once, the usual definition of the joint probability for an undirected graph:

$$p(x | \theta) = \frac{1}{Z(\theta)} \prod_{C \in \mathcal{C}} \psi_C(x_C) \quad (19.8)$$

is equivalent to Eq. (19.7).

This reduction to a graphical model is useful for a number of purposes, including defining junction-tree-based exact inference algorithms for an exponential family model. Yet it also involves a loss of information. Let us return to our orthography example. The presence of an `ing` feature implies a dependence between the three corresponding nodes in the model. Our graph-construction procedure would accordingly add links between these three nodes. We obtain a clique on three nodes, and we have no way of distinguishing this model from an alternative model in which all  $26^3$  configurations in this clique are independently parameterized—the featural representation has disappeared.

Indeed, for short strings of letters we are very likely to want to use a few features that span all of the letters in the string. Any such features lead to all nodes being connected, a rather uninformative graphical model.

[Something on the alternative, “factor graph” representation of features.]

## 19.2 Maximum entropy and maximum likelihood

In Chapter 8 we introduced the exponential family of distributions, motivating the family as a natural generalization of the Bernoulli, Gaussian, and Poisson distributions. In this section we provide a stronger justification for referring to this as a “natural generalization.” We show that the exponential family can be motivated as the expression of a variational principle—the principle of *maximum entropy*.

The maximum entropy formalism also provides us with new insights into the problem of fitting a model to data. From the maximum entropy point of view this problem is treated as a constrained optimization problem, in which we place constraints on expectations of a set of “features,” but otherwise make no specific parametric assumptions regarding the form of the model. It is a *consequence* of the variational principle that we obtain a specific parametric form, in particular the exponential family form. The parameters in the exponential family representation are Lagrange multipliers that enforce the constraints.

Although the insights afforded by the maximum entropy point of view are interesting and important, it is also important to understand that the resulting procedure is the same as the procedure that we obtain from the maximum likelihood point of view. Maximum entropy and maximum likelihood are *dual problems*, yielding the same optimum (there is no “duality gap”). Maximum entropy simply provides an alternative, dual point of view on the problem of maximum likelihood estimation in the exponential family.

In this section, we develop these ideas in detail, beginning by recalling the maximum likelihood problem and its solution, then stating and solving the maximum entropy problem, and finally proceeding to the identification of the maximum likelihood and maximum entropy as dual problems. We work with discrete variables throughout for simplicity, but all of our results also go through for continuous variables.

### 19.2.1 Maximum likelihood

In Chapter 8 we presented the general solution to the maximum likelihood problem for exponential family models. The reader can turn back to that chapter to retrieve the result, but it is just as easy to rederive it. From Eq. (19.7) we have the following log likelihood:

$$l(\theta; \mathcal{D}) = \sum_x m(x) \log p(x | \theta) \quad (19.9)$$

$$= \sum_x m(x) \left( \sum_i \theta_i f_i(x) - \log Z(\theta) \right) \quad (19.10)$$

$$= \sum_x m(x) \sum_i \theta_i f_i(x) - N \log Z(\theta), \quad (19.11)$$

where  $m(x)$  is the number of occurrences of configuration  $x$  in the data set  $\mathcal{D}$ , and where we have lightened our notation somewhat by suppressing the dependence of the sufficient statistics on the subsets  $C_i$ .

Recalling that the derivatives of  $\log Z(\theta)$  with respect to  $\theta_i$  are the expectations of the corresponding sufficient statistics, we obtain:

$$\frac{\partial l}{\partial \theta_i} = \sum_x m(x) f_i(x) - N \frac{\partial}{\partial \theta_i} \log Z(\theta) \quad (19.12)$$

$$= \sum_x m(x) f_i(x) - N \sum_x p(x | \theta) f_i(x). \quad (19.13)$$

This yields the following characterization of maximum likelihood estimates:

$$\sum_x p(x | \theta) f_i(x) = \sum_x \tilde{p}(x) f_i(x), \quad (19.14)$$

where  $\tilde{p}(x) \triangleq m(x)/N$  is the empirical distribution. We see that the marginals of the sufficient statistics (the “features”) must be equal to the empirical marginals. This provides an implicit set of equations for the parameters  $\theta_i$ .

As an aside, recall that in Chapter 9 we discussed the problem of finding maximum likelihood estimates in the setting of general undirected graphical models. The characterization of maximum likelihood estimates in that setting was the following—for each maximal clique in the graph, the marginals of the random variables in the clique must be equal to the empirical marginals. We now see that this result is, unsurprisingly, a consequence of the more general result in Eq. (19.14). Marginal probabilities can be viewed as expectations of indicator variables. If we use features that are indicator variables that pick out the cells in the maximal cliques, as in Figure 19.1, then Eq. (19.14) implies that the clique marginals must equal the empirical marginals.

### 19.2.2 Maximum entropy

Let us now consider the maximum entropy formulation. We begin with a random vector  $X$  and with a set of “features”  $f_i(x)$ , where  $i \in \mathcal{I}$  for an index set  $\mathcal{I}$ . Rather than assuming a specific functional form for the distribution of  $X$ , we instead specify a probability distribution for  $X$  indirectly, by specifying constraints that such a distribution must satisfy. In particular, we require that the expectations of the features  $f_i$  be equal to particular given constants  $\alpha_i$ :

$$\sum_x p(x) f_i(x) = \alpha_i, \quad (19.15)$$

The unknowns here are the probabilities  $p(x)$ . Note that the constraints are linear in the unknowns.

We ask that a distribution satisfy all of these constraints. In general, of course, it is not clear that such a distribution exists, but for now we skirt that problem by assuming the existence of at least one such distribution. In essence, we assume that our constraints are consistent. We return to the problem of consistency later in this section.

There may be many distributions that satisfy the constraints, and thus we make an additional requirement—among those distributions that satisfy the constraints we choose the distribution that has maximum entropy. Actually, we will generalize somewhat and ask for a distribution that has minimum Kullback-Leibler divergence with respect to a given reference distribution  $h(x)$ . (If  $h(x)$

is the uniform distribution we obtain the maximum entropy problem). We thus have the following constrained optimization problem:

$$\min \quad D(p \parallel h) \triangleq \sum_x p(x) \log \frac{p(x)}{h(x)} \quad (19.16)$$

$$\text{subject to} \quad \sum_x p(x) f_i(x) = \alpha_i \quad (19.17)$$

$$\sum_x p(x) = 1, \quad (19.18)$$

where the final constraint embodies our desire to obtain a probability distribution.

To solve this problem, we form the Lagrangian:

$$\mathcal{L} = \sum_x p(x) \log \frac{p(x)}{h(x)} - \sum_i \theta_i \left( \sum_x p(x) f_i(x) - \alpha_i \right) - \mu \left( \sum_x p(x) - 1 \right), \quad (19.19)$$

and take the derivative of  $\mathcal{L}$  with respect to the unknowns  $p(x)$ :

$$\frac{\partial \mathcal{L}}{\partial p(x)} = 1 + \log p(x) - \log h(x) - \sum_i \theta_i f_i(x) - \mu. \quad (19.20)$$

Setting to zero and rearranging yields:

$$p(x) = e^{\mu-1} h(x) \exp \left\{ \sum_i \theta_i f_i(x) \right\}. \quad (19.21)$$

Summing over  $x$  must yield one, and thus:

$$e^{-(\mu-1)} = \sum_x h(x) \exp \left\{ \sum_i \theta_i f_i(x) \right\} \quad (19.22)$$

is the normalization factor. Letting  $Z(\theta) \triangleq e^{-(\mu-1)}$  denote this normalization factor, we obtain:

$$p(x \mid \theta) = \frac{1}{Z(\theta)} h(x) \exp \left\{ \sum_i \theta_i f_i(x) \right\}. \quad (19.23)$$

This is of course the exponential family distribution. We have derived the exponential family distribution as an expression of the maximum entropy principle. The features  $f_i(x)$  are the sufficient statistics, and the Lagrange multipliers  $\theta_i$  are the canonical parameters.

Where do the values  $\alpha_i$  come from? The variational principle itself does not specify any particular source of the  $\alpha_i$ , and indeed there are applications of maximum entropy in optimization theory in which the  $\alpha_i$  are simply boundary conditions that come from prior knowledge. In our application, however—a statistical application—we need to make the  $\alpha_i$  depend in some way on

the data. Noting that Eq. (19.15) sets the expectations of the features equal to  $\alpha_i$ , it is natural to choose the  $\alpha_i$  to be equal to the empirical expectations of the features. This is the “method of moments,” an estimation method that is motivated by the law of large numbers. Given this assumption we have:

$$\alpha_i = \sum_x \tilde{p}(x) f_i(x), \quad (19.24)$$

and thus our optimization problem becomes:

$$\min \quad D(p \parallel h) \triangleq \sum_x p(x) \log \frac{p(x)}{h(x)} \quad (19.25)$$

$$\text{subject to} \quad \sum_x p(x) f_i(x) = \sum_x \tilde{p}(x) f_i(x) \quad (19.26)$$

$$\sum_x p(x) = 1; \quad (19.27)$$

a convex minimization problem under linear constraints.

With this form of the constraints we have also solved our consistency problem. There clearly is at least one distribution  $p(x)$  that is consistent with the constraints—the empirical distribution  $\tilde{p}(x)$ . Thus there must exist a solution to the maximum entropy problem.

Moreover, that solution must be unique. As we ask the reader to show in Exercise ??, the KL divergence is strictly convex in the variables  $p(x)$ . The problem of minimizing a strictly convex function with respect to linear constraints has at most a single solution.

### 19.2.3 Duality

The results in the previous two sections suggest that the maximum likelihood problem and the maximum entropy problem are very closely related. In one case (maximum likelihood) we assume the exponential family distribution and show that the model expectations must equal the empirical expectations. In the other case (maximum entropy) we assume that the model expectations must equal the empirical expectations and show that we must use an exponential family distribution.

The relationship turns out to be one of *duality*—the maximum likelihood problem and the maximum entropy problem are Lagrangian duals. We prove this fact in this section and also provide a geometric interpretation of the result.

A dual function is obtained by solving for the primal variables  $p(x)$  and substituting the solution back into the Lagrangian  $\mathcal{L}$ . (See Appendix XXX for a review of Lagrangian duality). This yields a function  $g(\theta)$  that we must maximize.

Returning to Eq. (19.19), we plug Eq. (19.23) into the Lagrangian. We drop the term involving  $\mu$ ; given that Eq. (19.23) is explicitly normalized this term must be zero. We have:

$$\begin{aligned} g(\theta) &= \sum_x p(x|\theta) \log \frac{p(x|\theta)}{h(x)} - \sum_i \theta_i \left( \sum_x p(x|\theta) (f_i(x) - \sum_x \tilde{p}(x) f_i(x)) \right) \\ &= \sum_x p(x|\theta) \left( \sum_i \theta_i f_i(x) - \log Z(\theta) \right) - \sum_i \theta_i \sum_x p(x|\theta) f_i(x) + \sum_i \theta_i \sum_x \tilde{p}(x) f_i(x) \end{aligned}$$

$$= \sum_x \bar{p}(x) \sum_i \theta_i f_i(x) - \log Z(\theta). \quad (19.28)$$

Up to a scaling factor  $N$ , this expression is simply the log likelihood (cf. Eq. 19.11). Thus we see that maximum likelihood is dual to maximum entropy.

For convex problems it is a fact of optimization theory that there is no duality gap between the primal and dual problems (see Appendix XXX). Actually there is a technicality here, which is discussed in the Appendix—we require a regularity condition such as the Slater condition). That is, the primal problem and the dual problem must yield the same value of the objective. Indeed, we have already seen, in Eq. (19.14), that maximum likelihood sets the parameters  $\theta_i$  such that the expectations of the features are equal to the empirical expectations. This is the same constraint that defines the maximum entropy problem, and both problems therefore pick out the same exponential family distribution.

### Geometric interpretation

We now show that the duality result can be given an appealing geometric interpretation.

Let us define two subsets of the simplex of probability distributions  $\{p(x)\}$ . The first will be the subset  $\mathcal{E}$  of all exponential family distributions based on a given set of features  $\{f_i(x)\}$  and a given base measure  $h(x)$ :

$$\mathcal{E} = \left\{ p(x) : p(x) = \frac{1}{Z(\theta)} h(x) \exp \left\{ \sum_i \theta_i f_i(x) \right\} \right\}. \quad (19.29)$$

Note that any two distributions in this family are related by a multiplicative factor. That is, given a distribution  $p(x|\theta_M)$  and a distribution  $p(x|\theta)$ , we have:

$$p(x|\theta) = \frac{Z(\theta_M)}{Z(\theta)} \exp \left\{ \sum_i \Delta \theta_i f_i(x) \right\} p(x|\theta_M), \quad (19.30)$$

where  $\Delta \theta \triangleq \theta - \theta_M$ .<sup>1</sup>

The second subset that we define is the set  $\mathcal{M}$  of all distributions that meet the moment constraints:

$$\mathcal{M} = \left\{ p(x) : \sum_x p(x) f_i(x) = \sum_x \bar{p}(x) f_i(x) \right\}. \quad (19.31)$$

Note that in general the distributions in  $\mathcal{M}$  are not exponential family distributions. Indeed, our results in the previous section have shown that there is a single distribution that is in  $\mathcal{M}$  and is also in  $\mathcal{E}$ . We denote this distribution, the maximum entropy or maximum likelihood distribution, as  $p(x|\theta_M)$ , or  $p_M$  for short.

We thus have the geometry suggested in Figure 19.2; subsets  $\mathcal{M}$  and  $\mathcal{E}$  that meet at the single point  $p_M$ .

---

<sup>1</sup>Taking logarithms, it is interesting to note that this can be viewed as an affine transformation on a log scale, where  $f_i$  are the “coordinates.”

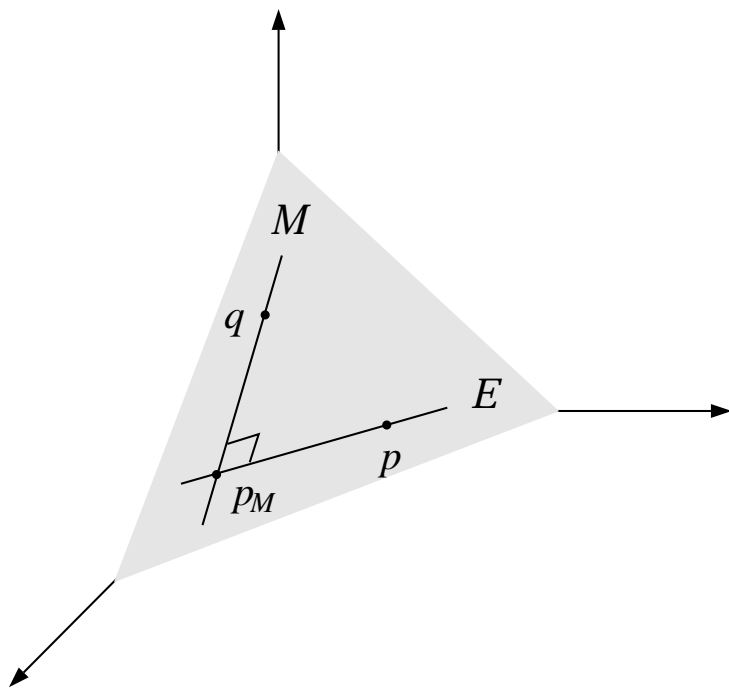


Figure 19.2: The set  $\mathcal{E}$  of exponential family distributions and the set  $\mathcal{M}$  of distributions that meet the moment constraints lie in a probability simplex and intersect at the point  $p_M$ , the maximum likelihood or maximum entropy point. A generalized Pythagorean theorem for the KL divergence holds among the points  $p$ ,  $q$ , and  $p_M$ .

Moreover, there is an interesting “orthogonality” relationship between these subsets. Let  $p$  be any other point in  $\mathcal{E}$  (an exponential family distribution with parameters  $\theta$ ), and let  $q$  be any other point in  $\mathcal{M}$ . We now prove the following fact:

$$D(q \parallel p) = D(q \parallel p_M) + D(p_M \parallel p), \quad (19.32)$$

which can be viewed as a generalized “Pythagorean theorem.”

To prove this theorem, we compute the difference between the left-hand side and the right-hand sides of Eq. (19.32):

$$\begin{aligned} & D(q \parallel p) - D(q \parallel p_M) - D(p_M \parallel p) \\ &= \sum_x q(x) \log \frac{q(x)}{p(x)} - \sum_x q(x) \log \frac{q(x)}{p_M(x)} - \sum_x p_M(x) \log \frac{p_M(x)}{p(x)} \end{aligned} \quad (19.33)$$

$$= \sum_x p_M(x) \log \frac{p(x)}{p_M(x)} - \sum_x q(x) \log \frac{p(x)}{p_M(x)} \quad (19.34)$$

$$= \sum_x p_M(x) \left( \sum_i \Delta\theta_i f_i(x) - \log \frac{Z(\theta_M)}{Z(\theta)} \right) - \sum_x q(x) \left( \sum_i \Delta\theta_i f_i(x) - \log \frac{Z(\theta_M)}{Z(\theta)} \right) \quad (19.35)$$

$$= \sum_i \Delta\theta_i \left( \sum_x p_M(x) f_i(x) - \sum_x q(x) f_i(x) \right) \quad (19.36)$$

$$= 0, \quad (19.37)$$

by the definition of  $\mathcal{M}$ .

We have derived a Pythagorean theorem by making use of our duality results, but we can also turn the argument around. Let us assume Eq. (19.32), and assume the existence of a point  $p_M$  in  $\mathcal{E} \cap \mathcal{M}$ . Write the maximum entropy problem as follows:

$$\min \quad D(q \parallel h) \quad (19.38)$$

$$\text{subject to} \quad q \in \mathcal{M}. \quad (19.39)$$

From Eq. (19.32) we have:

$$D(q \parallel h) = D(q \parallel p_M) + D(p_M \parallel h). \quad (19.40)$$

The second term is independent of  $q$  and can be ignored. Given that the KL divergence—and  $D(q \parallel p_M)$  in particular—is greater than or equal to zero, we see immediately that  $p_M$  minimizes  $D(q \parallel h)$  for  $q \in \mathcal{M}$ .

Moreover, we can write the maximum likelihood problem succinctly as follows:

$$\min \quad D(\tilde{p} \parallel p) \quad (19.41)$$

$$\text{subject to} \quad p \in \mathcal{E}. \quad (19.42)$$

From Eq. (19.32) we have:

$$D(\tilde{p} \parallel p) = D(\tilde{p} \parallel p_M) + D(p_M \parallel p). \quad (19.43)$$

The first term is independent of  $p$  and can be ignored. The second term is minimized by choosing  $p$  equal to  $p_M$ , which is therefore the maximum likelihood distribution.

Finally, let us introduce a bit of terminology to summarize our results. Given a subset of probability distributions  $\mathcal{M}$  defined by moment constraints, and given a fixed reference distribution  $h$ , let us refer to the distribution  $q \in \mathcal{M}$  that minimizes  $D(q \parallel h)$  as the *I-projection* of  $h$  on  $\mathcal{M}$ . Thus the Pythagorean theorem holds for an arbitrary point in  $\mathcal{M}$ , an arbitrary point  $h$  and the I-projection of  $h$  on  $\mathcal{M}$ .

### 19.3 Summary

In this chapter we have focused on the parameterization of graphical models, emphasizing discrete, undirected graphical models. We have seen how to represent potential functions in terms of collections of “features.” In particular, we have shown how indicator features can be used to pick out the cells in potential tables and associate independently-varying parameters with each of these cells. In general, however, we are not restricted to indicator features—we can define a potential in terms of arbitrary collections of features.

The relationship between exponential family models and graphical models is a very close one. If we use an exponential representation for the contribution of each individual feature, then the product of potential functions leads to an exponential family representation for the joint distribution associated with the graphical model. Alternatively, we can also represent an arbitrary exponential family model as a graphical model by connecting nodes that appear together as arguments to the features.

In the final section of the chapter, we showed that the exponential family distribution can be viewed as the expression of a variational principle, namely that of maximum entropy. We also showed that the maximum entropy principle leads to a perspective on parameter estimation that is dual to maximum likelihood.

In the following chapter, we continue our exploration of exponential family parameterizations of graphical models. In particular, we will discuss the problem of parameter estimation in general exponential families, presenting algorithms that exploit graphical structure, and exploring some of the relationships between these algorithms and the inference algorithms discussed in earlier chapters.

### 19.4 Historical remarks and bibliography

# An Introduction to Probabilistic Graphical Models

Michael I. Jordan  
*University of California, Berkeley*

June 30, 2003



# Chapter 20

## Iterative scaling algorithms

In this chapter we turn our attention to algorithms for maximum likelihood estimation in general graphical models. We revisit the iterative proportional fitting (IPF) algorithm for estimating the clique potentials of undirected graphical models from Chapter 9, as well as the special case of decomposable models. With the junction tree algorithm in hand, we are in a position to understand these methods more deeply. Also, now that we understand that a clique potential can be viewed as a special case of collections of parameterized features, it is natural to ask if the IPF algorithm generalizes to general collections of features. We will see that the answer is yes, and will present the *generalized iterative scaling algorithm*, emphasizing the connections to IPF. Finally, we consider parameter estimation for general graphical family models with latent variables, relating the material in this chapter to the material in Chapter 11 on the EM algorithm.

We focus for the most part on discrete random variables, in order to provide a simple presentation that emphasizes the connections between the various methods that we present. In Section ??, however, we discuss the case of general Gaussian models.

### 20.1 Complete observations

We begin by considering the case of completely observed data, returning to the material on decomposable models and general undirected models from Chapter 9.

Recall the necessary condition for obtaining maximum likelihood estimates—the expectations of the sufficient statistics (“features”) must be equal to their empirical expectations. In the case of indicator features, this is equivalent to asking for the marginals of the model to be equal to the empirical marginals. The algorithms that we discuss in this section and in the following sections all aim to satisfy this condition.

#### 20.1.1 Decomposable models

Decomposable graphical models can be treated either within the directed formalism or the undirected formalism; indeed, the decomposable models are precisely the intersection of directed model and undirected models. We begin by discussing the undirected case. Thus, our setting is the

parameterization:

$$p(x) = \frac{1}{Z(\psi)} \prod_{C \in \mathcal{C}} \psi_C(x_C), \quad (20.1)$$

where  $\mathcal{C}$  ranges over maximal cliques, and where the potential functions  $\psi_C(x_C)$  are “fully parameterized”—that is, each configuration  $x_C$  is associated with an independently-varying parameter. In this setting—that of a decomposable graph, fully-parameterized potentials and maximal cliques—we are able to write down maximum likelihood estimates analytically.

Recall from our work in Chapter 17 that a graph is decomposable if and only if it is triangulated. Moreover, either of these conditions is equivalent to the existence of a junction tree on the maximal cliques of the graph. Let  $\mathcal{T}$  be such a junction tree, and let  $\mathcal{S}$  range over the separator sets in this junction tree. Define the following potentials for the junction tree:

$$\psi_C(x_C) = \tilde{p}(x_C) = \frac{1}{N} m(x_C) \quad (20.2)$$

$$\phi_S(x_S) = \tilde{p}(x_S) = \frac{1}{N} m(x_S). \quad (20.3)$$

That is, we let the potentials equal the empirical marginals.

With this choice of potentials, it is easy to see that the junction tree is globally consistent. In particular, consider passing a message from a clique  $V$  to a clique  $W$  via the separator  $S$ . We have:

$$\phi_S^*(x_S) = \sum_{V \setminus S} \psi_V(x_V) \quad (20.4)$$

$$= \sum_{V \setminus S} \tilde{p}(x_V) \quad (20.5)$$

$$= \tilde{p}(x_S), \quad (20.6)$$

which is the same as the initial value  $\phi_S(x_S)$ . Thus the update factor is one, and the message transmitted to  $W$  is vacuous. The junction tree is therefore globally consistent.

From our work on the junction tree algorithm, we know that if a junction tree is globally consistent, then the clique potentials must be proportional to the clique marginals. Thus, we have:

$$p(x_C) \propto \psi_C(x_C). \quad (20.7)$$

But we also have  $\psi_C(x_C) = \tilde{p}(x_C)$ , by definition, which implies that  $\psi_C(x_C)$  is normalized and that the proportionality must in fact be an equality. We have:

$$p(x_C) = \tilde{p}(x_C), \quad (20.8)$$

for all  $C$ . But this is the necessary condition for the maximum likelihood estimate. Thus, it must be the case that the product:

$$\hat{p}_{ML}(x) = \frac{\prod_{C \in \mathcal{C}} \psi_C(x_C)}{\prod_{S \in \mathcal{S}} \psi_S(x_S)} = \frac{\prod_{C \in \mathcal{C}} \tilde{p}(x_C)}{\prod_{S \in \mathcal{S}} \tilde{p}(x_S)} \quad (20.9)$$

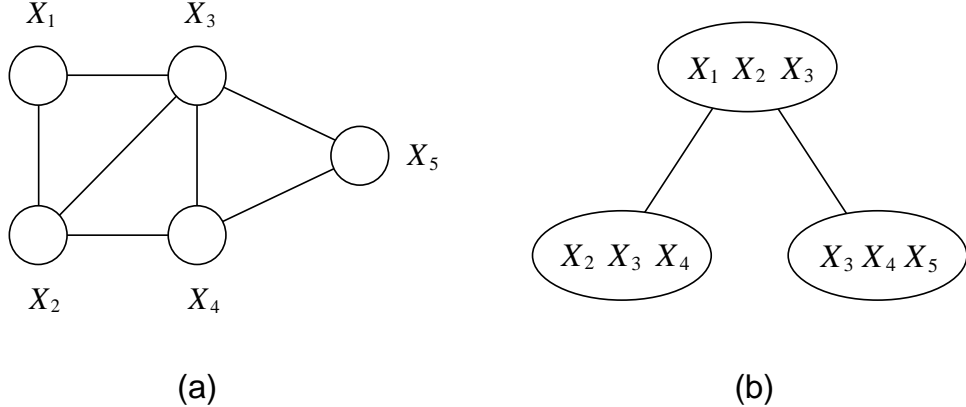


Figure 20.1: (a) A decomposable graph. (b) A junction tree for the graph in (a).

is a representation of the maximum likelihood estimate of the joint probability distribution.

We can readily turn this representation into an estimate of the parameters  $\psi$ . We simply need to divide the denominator factors in Eq. (20.9) into appropriate factors in the numerator so as to be able to write the equation as a simple product over clique potentials (i.e., rather than a ratio). For each  $S \in \mathcal{S}$ , there is a clique  $C$  such that  $S \subseteq C$ . We divide  $\phi_S(x_S)$  into  $\psi_C(x_C)$ , redefining  $\psi_C(x_C)$  and setting  $\phi_S(x_S)$  equal to unity. These transformations leave Eq. (20.9) invariant, and thus we still have a representation of the maximum likelihood estimate of the joint probability distribution. Moreover, given our assumption of fully-parameterized clique potentials, dividing  $\phi_S(x_S)$  into  $\psi_C(x_C)$  leaves us in the same model family.

It therefore suffices to associate  $S$  with a neighboring clique  $C$ . One way to achieve this is to orient the junction tree, and associate each separator  $S \in \mathcal{S}$  with the clique  $C \in \mathcal{C}$  that is on the path to the root. Letting  $\xi(C)$  denote the set of separators associated with clique  $C$ , we define:

$$\hat{\psi}_{C,ML}(x_C) = \frac{\tilde{p}(x_C)}{\prod_{S \in \xi(C)} \tilde{p}(x_S)} \quad (20.10)$$

as a maximum likelihood estimate of the parameters. Taking a product of such estimates over all  $C$  accounts for all of the factors in Eq. (20.9), and thus the normalization factor  $Z(\hat{\psi}_{ML})$  must be one.

Consider the example shown in Figure 20.1(a). Orienting the junction tree as shown in Figure 20.1(b), we obtain:

$$\hat{\psi}_{123,ML}(x_1, x_2, x_3) = \tilde{p}(x_1, x_2, x_3) \quad (20.11)$$

$$\hat{\psi}_{234,ML}(x_2, x_3, x_4) = \frac{\tilde{p}(x_2, x_3, x_4)}{\tilde{p}(x_2, x_3)} \quad (20.12)$$

$$\hat{\psi}_{345,ML}(x_3, x_4, x_5) = \frac{\tilde{p}(x_3, x_4, x_5)}{\tilde{p}(x_3, x_4)}. \quad (20.13)$$

Note that the latter two potentials can be rewritten as conditionals under the empirical distribution.

If the original graph is a directed graph, then we can orient the junction tree so as to respect the ordering among the nodes in the original graph (see Exercise ??). In this case, the parameter estimates are conditional probabilities, as they must be in the directed case.

### 20.1.2 Iterative proportional fitting

The iterative proportional fitting (IPF) algorithm is a general algorithm for finding maximum likelihood estimates in graphical models, decomposable or not (see Chapter 9). To apply IPF we still require the clique potentials to be fully parameterized, but we no longer require the parameterized cliques to be maximal cliques.

Recall from our previous discussion that IPF is a coordinate ascent algorithm. The parameters are the clique potentials, and a single “coordinate” ascent step adjusts all of the parameters in a single clique potential simultaneously. Such a step has the following form:

$$\psi_C^{(t+1)}(x_C) = \psi_C^{(t)}(x_C) \frac{\tilde{p}(x_C)}{p^{(t)}(x_C)}, \quad (20.14)$$

where the old potential is multiplied by an “update factor” consisting of the empirical marginal divided by the current model marginal. Recall that in Chapter 9 we also saw that IPF can be written in terms of the joint probability:

$$p^{(t+1)}(x_U) = p^{(t)}(x_U) \frac{\tilde{p}(x_C)}{p^{(t)}(x_C)}, \quad (20.15)$$

and this equation implies:

$$p^{(t+1)}(x_U) = p^{(t)}(x_{U \setminus C} | x_C) \tilde{p}(x_C). \quad (20.16)$$

Note that while these latter two versions of the IPF update provide insight into the nature of the algorithm, the implementation of the algorithm is based on Eq. (20.14).

We have two goals in this section. The first is to provide a geometrical interpretation of the algorithm, showing that it can be understood in terms of I-projections. The second is to delve more deeply into the implementation of the algorithm, in particular discussing the interaction between IPF and the junction tree algorithm.

#### IPF as a sequence of I-projections

IPF is an algorithm for finding maximum likelihood estimates. Our duality results, however, also allow us to view IPF as an algorithm for finding maximum entropy distributions. In this section we exploit this duality to uncover some of the geometry underlying the IPF algorithm.

The overall geometry is that shown earlier in Figure 19.2. IPF converges to the solution  $p_M$  which is at the intersection of the set  $\mathcal{E}$  and the set  $\mathcal{M}$ . We can view the procedure as finding the member of the exponential family which has the correct marginals, or as finding the member of the set of distributions with the correct marginals that has maximum entropy. In the latter case, we minimize  $D(p \parallel h)$  for  $p \in \mathcal{M}$ . That is, we find the I-projection of  $h$  on  $\mathcal{M}$ .

But we can also say more. In particular we can characterize each step of the IPF algorithm as an I-projection. To see this, consider the following maximum entropy problem:

$$\min D(p(x) \parallel p^{(t)}(x)) \quad (20.17)$$

$$\text{subject to } p(x_C) = \tilde{p}(x_C), \quad (20.18)$$

where  $C$  is a particular fixed clique. (Thus, Eq. (20.18) is a set of constraints for all configurations  $x_C$  in the clique  $C$ ). From the dual point of view, we must find maximum likelihood estimates in a particular exponential family, namely one that has a single fully-parameterized clique  $C$ . Moreover, the base density (which is denoted  $h(x)$  in the general case) is  $p^{(t)}(x)$ . We can thus write this exponential family as follows:

$$p(x) = \frac{1}{Z} p^{(t)}(x) \exp\{\phi_C(x_C)\}, \quad (20.19)$$

where  $\phi_C(x_C)$  is a clique potential for the clique  $C$ . This problem is readily solved analytically. Summing both sides of Eq. (20.19) over  $U \setminus C$ , and using  $p(x_C) = \tilde{p}(x_C)$ , we obtain:

$$\exp\{\phi(x_C)\} = \frac{\tilde{p}(x_C)}{p^{(t)}(x_C)} \quad (20.20)$$

and  $Z = 1$ . Substituting these results back into Eq. (20.19), we obtain the IPF update.

Thus, the distribution  $p^{(t+1)}(x)$  in Eq. (20.15) solves our maximum likelihood problem and therefore must also be the solution to the maximum entropy problem in Eq. (20.18). An IPF step is an I-projection of  $p^{(t)}(x)$  on the set defined by a single marginal constraint.

Let  $\mathcal{M}_C$  denote the set corresponding to the marginal constraint  $p(x_C) = \tilde{p}(x_C)$ . The overall solution  $p_M$  is a distribution in the set of distributions which satisfy all of these marginal constraints. We can write this set as an intersection:

$$\mathcal{M} = \cap_{C \in \mathcal{C}} \mathcal{M}_C. \quad (20.21)$$

The resulting geometry is shown in Figure 20.2. The basic setting is the exponential family  $\mathcal{E}$ ; all IPF iterates lie in this set. Each of the sets  $\mathcal{M}_C$  has an intersection with this family—these are the lines shown in the figure (the sets  $\mathcal{M}_C$  should be envisaged as planes extending out of the paper in a third dimension). The intersection of the planes  $\mathcal{M}_C$  is a line  $\mathcal{M}$ , again extending out of the paper, and the intersection of  $\mathcal{E}$  with this line is the point  $p_M$ .

As shown in the figure, at each step IPF projects onto one of the subsets  $\mathcal{M}_C$ . Each of these projections is an I-projection. This sequence of projections converges to  $p_M$  in the limit. Moreover, each step of the algorithm draws nearer to the empirical distribution  $\tilde{p}$ , a point which lies in the set  $\mathcal{M}$  but not (in general) in the set  $\mathcal{E}$ .

Thus we obtain a geometric picture of IPF that is very reminiscent of the picture of the LMS algorithm as a sequence of projections in Chapter 6—recall Figure 6.2. The projections in the case of LMS were Euclidean projections, and the orthogonality that served as the basis of much of our analysis was Euclidean orthogonality. Here the projections are I-projections, and the projections are “orthogonal” in the sense of Eq. (19.32). But the overall picture and much of the analysis is the same.

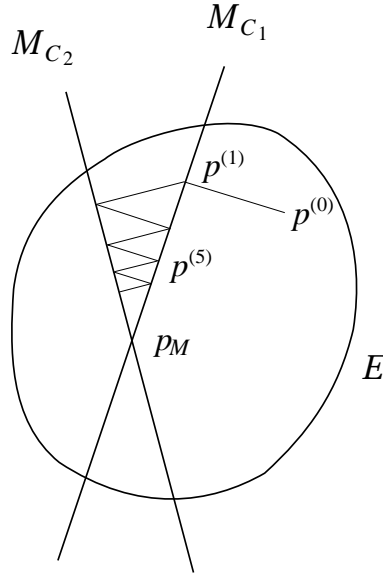


Figure 20.2: The geometry underlying the IPF algorithm. Each step of IPF is an I-projection onto a manifold which has the correct marginals for one of the cliques. All iterates lie in the exponential family  $\mathcal{E}$ , and the algorithm converges to the single point that is at the intersection of  $\mathcal{E}$  and all of the manifolds  $\mathcal{M}_\mathcal{C}$ .

### Efficient IPF

[section not yet written].

#### 20.1.3 Iterative scaling

We now turn to the general case in which the clique potentials are parameterized by arbitrary collections of features. As in Section 19.1, we drop the association of features to cliques in our notation, and simply consider a general exponential family model:

$$p(x | \theta) = \frac{1}{Z(\theta)} \exp \left\{ \sum_i \theta_i f_i(x) \right\} \quad (20.22)$$

with features  $f_i(x)$ , where  $Z(\theta)$  is the normalization factor:

$$Z(\theta) = \sum_x \exp \left\{ \sum_i \theta_i f_i(x) \right\}. \quad (20.23)$$

The goal is to estimate the parameters  $\theta_i$  from data  $\mathcal{D}$ .

We will work with the scaled likelihood function:

$$\tilde{l}(\theta | \mathcal{D}) = \sum_x \tilde{p}(x) \log p(x), \quad (20.24)$$

where  $\tilde{l}(\theta | \mathcal{D}) = l(\theta | \mathcal{D})/N$  and  $\tilde{p}(x)$  is the empirical distribution.

The *generalized iterative scaling (GIS)* algorithm is an iterative algorithm for finding maximum likelihood parameter estimates. GIS applies to arbitrary collections of features, subject to two constraints: the features must be nonnegative and they must sum to one. That is,

$$f_i(x) \geq 0, \quad \sum_i f_i(x) = 1, \quad (20.25)$$

for each  $x$ . We will see later in this section how to maneuver around these constraints, but let us impose them for now.

The GIS algorithm forms a sequence of (unnormalized) distributions  $p^{(t)}(x)$ . The algorithm, which we derive later in this section, takes the following general form:

$$p^{(t+1)}(x) = p^{(t)}(x) \prod_i \left( \frac{\sum_x \tilde{p}(x) f_i(x)}{\sum_x p^{(t)}(x) f_i(x)} \right)^{f_i(x)}. \quad (20.26)$$

As in case of the IPF algorithm, GIS involves a ratio of expectations, in which the numerators are expectations with respect to the empirical distribution and the denominators are expectations with respect to the current model. These ratios are “update factors” that multiply the current distribution. Note an important difference between GIS and IPF, however: GIS is a fully “parallel” algorithm—the product in the algorithm is a product over all features.

Let us consider the relationship between IPF and GIS in somewhat more detail. Recall that the IPF algorithm is parallel at the level of a single clique, where we parameterize the clique potential  $\psi_C(x_C)$  using a set of indicator features  $f_i(x_C)$ . For any given  $x$ , only one of these features are equal to one and the others are equal to zero. Thus we meet the constraints imposed in Eq. (20.25) and can apply GIS to this set of features. Moreover, the expectation of an indicator,  $\sum_x p(x) f_i(x_C)$ , is equal to the marginal probability,  $p(x_C)$ . From this it can easily be seen that Eq. (20.26) reduces to the IPF update Eq. (20.14). Thus, each step of IPF—which is parallel across the features corresponding to a single clique—is a GIS update. On the other hand, a sequence of IPF iterations corresponds to a sequence of GIS iterations with a changing set of features at each iteration.

Is it possible to obtain a fully parallel version of IPF, in which all of the features throughout the graph are updated in parallel? A problem arises here, which is that the sum across features,  $\sum_i f_i(x)$ , is no longer one in such a setting. (It is equal to the number of cliques, and hence is a constant, but not equal to one). As we mentioned above, however, it will be possible to maneuver around the sum-to-one constraint, and obtain a fully parallel IPF.

We return to the GIS algorithm. Although we have written the algorithm in terms of (unnormalized) joint probabilities, it is also possible to view the algorithm in terms of updates to individual parameters. Let the estimate of the parameter  $\theta_i$  at iteration  $t$  be denoted  $\theta_i^{(t)}$ . Consider the following update:

$$\theta_i^{(t+1)} = \theta_i^{(t)} + \log \left( \frac{\sum_x \tilde{p}(x) f_i(x)}{\sum_x p^{(t)}(x) f_i(x)} \right). \quad (20.27)$$

Multiplying both sides by  $f_i(x)$ , and taking the exponential, we obtain:

$$\exp \left\{ (\theta_i^{(t+1)} - \theta_i^{(t)}) f_i(x) \right\} = \left( \frac{\sum_x \tilde{p}(x) f_i(x)}{\sum_x p^{(t)}(x) f_i(x)} \right)^{f_i(x)}. \quad (20.28)$$

If we multiply an exponential family distribution by the left-hand side of this equation, we change  $\theta_i^{(t+1)}$  to  $\theta_i^{(t)}$ . Thus the right-hand side is the “update factor” for parameter  $\theta_i$ . Multiplying by the update factors for all of the parameters, we recover the GIS algorithm.

What about normalization? In general the sequence of GIS iterates  $p^{(t)}(x)$  are *not* normalized. This might seem problematic, in that we need to take expectations in the denominator of Eq. (20.26). But if we explicitly normalize both occurrences of  $p^{(t)}(x)$  on the right-hand side of Eq. (20.26), it is easily verified that the normalization factors cancel (we carry out the calculation below). Thus we obtain the same result whether or not we use normalized distributions. Critical to this argument is the fact that  $\sum_i f_i(x) = 1$ .

In fact, even though the sequence of iterates are not normalized, the limiting distribution  $p^\infty(x)$  *is* normalized. We prove this fact below.

Let us turn to a derivation of the GIS algorithm. Our derivation is in the spirit of our derivation of the EM algorithm in Chapter 11. In particular we make use of convexity to obtain an *auxiliary function*—a lower bound for the log likelihood. This bound is tight at the current values of the parameters, and thus by increasing the lower bound, we increase the log likelihood.

We begin by writing out the log likelihood:

$$\tilde{l}(\theta | \mathcal{D}) = \sum_x \tilde{p}(x) \log p(x) \quad (20.29)$$

$$= \sum_x \tilde{p}(x) \sum_i \theta_i f_i(x) - \log Z(\theta) \quad (20.30)$$

$$= \sum_i \theta_i \sum_x \tilde{p}(x) f_i(x) - \log Z(\theta). \quad (20.31)$$

As in the EM derivation, we must bound the log of a sum, but here the logarithm appears with a negative sign. To obtain a lower bound, we upper bound the logarithm using the elementary convexity result (see Figure 20.3), which yields:

$$\log Z(\theta) \leq \mu Z(\theta) - \log \mu - 1. \quad (20.32)$$

This bound holds for all  $\mu$ , and in particular it holds for  $\mu = Z^{-1}(\theta^{(t)})$ . Thus we have:

$$\tilde{l}(\theta | \mathcal{D}) \geq \sum_x \tilde{p}(x) \sum_i \theta_i f_i(x) - \frac{Z(\theta)}{Z(\theta^{(t)})} - \log Z(\theta^{(t)}) + 1. \quad (20.33)$$

Note that the inequality is an equality at  $Z(\theta^{(t)})$ , which is verified by simple substitution. Moreover, given the smoothness of the logarithm we expect the bound to be reasonably tight in the neighborhood of  $Z(\theta^{(t)})$ .

Define  $\Delta\theta_i^{(t)} \triangleq \theta_i - \theta_i^{(t)}$ . Continuing the derivation, we have:

$$\begin{aligned} \tilde{l}(\theta | \mathcal{D}) &= \sum_x \tilde{p}(x) \sum_i \theta_i f_i(x) - \frac{1}{Z(\theta^{(t)})} \sum_x \exp \left( \sum_i \theta_i f_i(x) \right) - \log Z(\theta^{(t)}) + 1 \\ &= \sum_i \theta_i \sum_x \tilde{p}(x) f_i(x) - \frac{1}{Z(\theta^{(t)})} \sum_x \exp \left( \sum_i \theta_i^{(t)} f_i(x) \right) \exp \left( \sum_i \Delta\theta_i^{(t)} f_i(x) \right) - \log Z(\theta^{(t)}) + 1 \end{aligned}$$

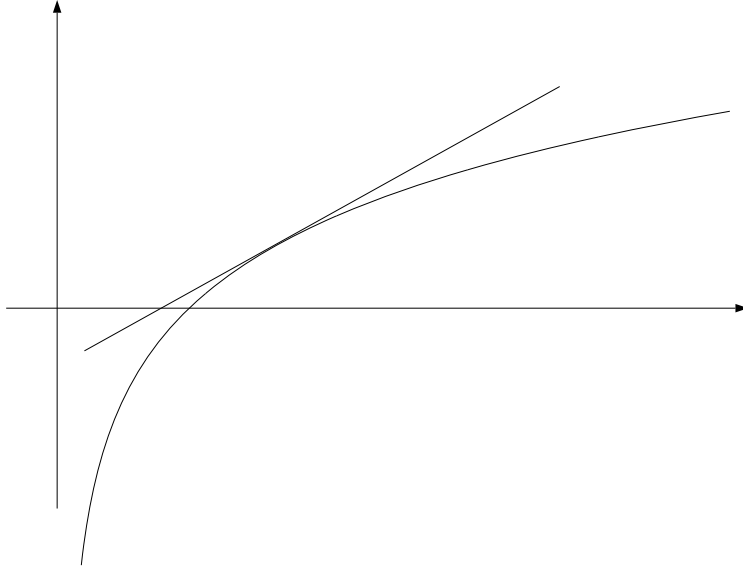


Figure 20.3: The convexity of the logarithm implies that we can upper bound the logarithm with a line:  $\log x \leq \mu x - \log \mu - 1$ . Moreover, the upper bound is tight at the point  $x$  when the slope  $\mu$  matches the derivative of the logarithm at that point:  $\mu = 1/x$ .

$$= \sum_i \theta_i \sum_x \tilde{p}(x) f_i(x) - \sum_x p(x | \theta^{(t)}) \exp \left( \sum_i \Delta \theta_i^{(t)} f_i(x) \right) - \log Z(\theta^{(t)}) + 1. \quad (20.34)$$

We have a lower bound that has begun to take on the form of the difference between expectations. The exponential couples the parameters, however, and taking the derivative of this lower bound would not give the simple product form of the GIS update. To decouple the parameters, we need to invoke convexity a second time. In particular, we use Jensen's inequality:

$$\exp \left( \sum_i \pi_i x_i \right) \leq \sum_i \pi_i \exp (x_i), \quad (20.35)$$

for  $\sum_i \pi = 1$ . The  $f_i(x)$  are positive and sum to one, and therefore can play the role of the  $\pi_i$ . We obtain:

$$\begin{aligned} \tilde{l}(\theta | \mathcal{D}) &\geq \sum_i \theta_i \sum_x \tilde{p}(x) f_i(x) - \sum_x p(x | \theta^{(t)}) \sum_i f_i(x) \exp(\Delta \theta_i^{(t)}) - \log Z(\theta^{(t)}) + 1 \\ &\triangleq \Lambda(\theta), \end{aligned} \quad (20.36)$$

a lower bound in which the parameters are decoupled. Note, moreover, that the bound continues to be exact at  $\theta^{(t)}$ .

Taking the derivative with respect to  $\theta_i$ , we obtain:

$$\frac{\partial \Lambda}{\partial \theta_i} = \sum_x \tilde{p}(x) f_i(x) - e^{\Delta \theta_i^{(t)}} \sum_x p(x | \theta^{(t)}) f_i(x) \quad (20.37)$$

and setting to zero:

$$e^{\Delta \theta_i^{(t)}} = \frac{\sum_x \tilde{p}(x) f_i(x)}{\sum_x p(x | \theta^{(t)}) f_i(x)} = \frac{\sum_x \tilde{p}(x) f_i(x)}{\sum_x p^{(t)}(x) f_i(x)} Z(\theta^{(t)}) \quad (20.38)$$

where the second equation defines  $p^{(t)}(x)$  as the unnormalized version of  $p(x | \theta^{(t)})$ .

To update the parameters from  $\theta^{(t)}$  to  $\theta^{(t+1)}$ , we simply multiply  $p(x | \theta^{(t)})$  by  $e^{\Delta \theta_i^{(t)} f_i(x)}$  for all  $i$ . We obtain:

$$p^{(t+1)}(x) = \frac{p^{(t)}(x)}{Z(\theta^{(t)})} \prod_i \left( \frac{\sum_x \tilde{p}(x) f_i(x)}{\sum_x p^{(t)}(x) f_i(x)} Z(\theta^{(t)}) \right)^{f_i(x)} \quad (20.39)$$

$$= \frac{p^{(t)}(x)}{Z(\theta^{(t)})} \prod_i \left( \frac{\sum_x \tilde{p}(x) f_i(x)}{\sum_x p^{(t)}(x) f_i(x)} \right)^{f_i(x)} \prod_i \left( Z(\theta^{(t)}) \right)^{f_i(x)} \quad (20.40)$$

$$= p^{(t)}(x) \prod_i \left( \frac{\sum_x \tilde{p}(x) f_i(x)}{\sum_x p^{(t)}(x) f_i(x)} \right)^{f_i(x)}, \quad (20.41)$$

which is the GIS algorithm.

#### 20.1.4 IPF for Gaussian models

[Section not yet written. An alternation between setting cliques of  $\Sigma$  to the empirical covariances and setting entries of  $\Sigma^{-1}$  to zero.]

## 20.2 Latent variables

In this final section, we turn to the problem of parameter estimation when there are latent variables. Solving such problems involves making use of the EM algorithm, with the junction tree algorithm (or some other inference algorithm) providing the E step, and the generalized iterative scaling algorithm (or some other estimation algorithm) providing the M step. In this section we bring all of these ideas together.

We begin by discussing the EM algorithm in the context of general exponential family models with latent variables, showing how the the M step can be implemented via the GIS algorithm. We then turn to the special case of directed graphical models, parameterized with generalized linear models at each node, where the IRLS algorithm provides the preferred method for implementing the M step. Finally we discuss some of the geometry associated with the EM algorithm.

### 20.2.1 Exponential family models

Let  $X_E$  represent the totality of observed variables in the problem and let  $X_H$  represent the unobserved or latent variables. Our goal is to estimate the parameters  $\theta_i$  in a general exponential family model that includes both  $X_E$  and  $X_H$ :

$$p(x_E, x_H | \theta) = \frac{1}{Z(\theta)} \exp \left\{ \sum_i \theta_i f_i(x_E, x_H) \right\}. \quad (20.42)$$

This is the *complete data model*. We assume that only  $X_E$  is observed and that  $X_H$  is latent. Thus we wish to estimate the parameters by maximizing the *incomplete log likelihood*:

$$\tilde{l}(\theta | \mathcal{D}) = \sum_{x_E} \tilde{p}(x_E) \log p(x_E | \theta), \quad (20.43)$$

where  $\mathcal{D}$  is the observed data  $x_E$ , and where  $p(x_E | \theta)$  is the marginal probability obtained from summing the complete data probability model over  $x_H$ .

The features  $f_i(x_E, x_H)$  depend in general on subsets of the variables  $x_E$  and  $x_H$ . Although we have not specified these subsets in our notation, it is of course critically important to identify them and to exploit them in implementing an inference algorithm, a point that we return to in our discussion of the E step of EM.

Let us briefly review the EM framework from Chapter 11. Recall that we define the following KL divergence:

$$D(q \| \theta) \triangleq D(\tilde{p}(x_E)q(x_H | x_E) \| p(x_E, x_H | \theta)), \quad (20.44)$$

where  $q(x_H | x_E)$  is an arbitrary conditional probability distribution. The EM algorithm is an alternating minimization algorithm composed of two steps:

$$\text{(E step)} \quad q^{(t+1)} = \arg \min_q D(q \| \theta^{(t)}) \quad (20.45)$$

$$\text{(M step)} \quad \theta^{(t+1)} = \arg \min_{\theta} D(q^{(t+1)} \| \theta). \quad (20.46)$$

In the remainder of this section we discuss how to implement the EM algorithm using the general tools for inference and estimation that we now have at our disposal.

The E step of the EM algorithm involves computing the optimal averaging distribution  $q(x_H | x_E)$ . As we saw in Chapter 11, this problem can be solved—at an abstract level—once and for all. The conditional probability that minimizes the KL divergence is simply:

$$q^{(t+1)}(x_H | x_E) = p(x_H | x_E, \theta^{(t)}), \quad (20.47)$$

the conditional under the current complete data model. Note, however, we do not need to obtain this conditional in any explicit sense; rather, we need to be able to use this conditional to compute averages. To understand more clearly what is involved in implementing the E step, it is first useful to understand what averages we need to compute, and for this we turn to the M step.

Only one of the terms in the KL divergence involves the parameters  $\theta$ , and thus the M step can be written equivalently as follows:

$$\theta^{(t+1)} = \arg \max_{\theta} D(q^{(t+1)} \parallel \theta) \quad (20.48)$$

$$= \arg \max_{\theta} \sum_{x_E} \sum_{x_H} \tilde{p}(x_E) p(x_H | x_E, \theta^{(t)}) \log p(x_E, x_H | \theta) \quad (20.49)$$

$$= \arg \max_{\theta} \sum_{x_E} \sum_{x_H} \tilde{p}(x_E) p(x_H | x_E, \theta^{(t)}) \sum_i \theta_i f_i(x_E, x_H) - \log Z(\theta) \quad (20.50)$$

$$= \arg \max_{\theta} \sum_i \theta_i \sum_{x_E} \sum_{x_H} \tilde{p}(x_E) p(x_H | x_E, \theta^{(t)}) f_i(x_E, x_H) - \log Z(\theta). \quad (20.51)$$

We see that we obtain an expression that is formally identical to the log likelihood that we obtained earlier for the complete data setting (cf. Eq. (20.31)). Whereas the earlier log likelihood involved the average of the features with respect to the empirical distribution  $\tilde{p}(x)$ , the current log likelihood involves the average of the features with respect to the joint distribution  $\tilde{p}(x_E) p(x_H | x_E, \theta^{(t)})$ . In the earlier case the features were denoted  $f_i(x)$ , and depended only on the observed variables  $x$ , whereas in the current setting the features are denoted  $f_i(x_E, x_H)$ , and depend on both the observed variables  $x_E$  and the latent variables  $x_H$ . In either case, however, we compute averages of the feature values; that is, we compute *expected sufficient statistics*. Once these averages are computed, we are left with the same function of the parameters  $\theta_i$  to minimize.

This line of argument shows that the algorithms that we have developed in this chapter for complete data apply immediately to the general latent variable problem as the M step in the EM algorithm. In particular, we can use the GIS algorithm as an M step simply by replacing the expectations  $\sum_x \tilde{p}(x) f_i(x)$  in the numerator of the GIS update in Eq. (20.26) by the expectations  $\sum_{x_E} \sum_{x_H} \tilde{p}(x_E) p(x_H | x_E, \theta^{(t)}) f_i(x_E, x_H)$ . That is, each GIS iteration takes the form:

$$p^{(t+1)}(x_E, x_H) = p^{(t)}(x_E, x_H) \prod_i \left( \frac{\sum_{x_E} \tilde{p}(x_E) p(x_H | x_E, \theta^{(t)}) f_i(x_E, x_H)}{\sum_{x_E} p^{(t)}(x_E, x_H) f_i(x_E, x_H)} \right)^{f_i(x_E, x_H)}. \quad (20.52)$$

Note, moreover, that each step of GIS increases the expected complete log likelihood. Overall we obtain an alternating minimization algorithm composed of an outer loop (the alternation between E and M steps) and an inner loop (the GIS iterations that implement the M step). Both the E step and the inner loop M steps decrease the objective function  $D(q \parallel \theta)$  at each and every step.

If the features are indicator features of fully-parameterized clique potentials, then we can use the IPF algorithm to implement the inner loop. Each IPF step again decreases the objective function. Moreover, in this case we can view the overall algorithm as coordinate descent in the joint set of variables  $q(x_H | x_E)$  and  $\theta_i$ .

Let us now return to the E step. We have seen that the job of the E step is to compute the expected sufficient statistics. Thus we do not need  $p(x_H | x_E, \theta^{(t)})$  explicitly, but we do need to be able to compute the expectations  $\sum_{x_H} p(x_H | x_E, \theta^{(t)}) f_i(x_E, x_H)$ .

There are two ways to implement the E step, corresponding to the two ways of constructing a graphical model to perform inference for an exponential family model (see Section ??). On the

one hand, we can construct a graphical model by linking all nodes that appear together as the arguments for any feature  $f_i(x_E, x_H)$ . We then construct a junction tree based on this graphical model. A given feature  $f_i(x_E, x_H)$  will then have its support contained entirely in one of the cliques of the junction tree. To compute the expectation of the feature it suffices to multiply the initial clique potential by  $f_i(x_E, x_H)$  and to run CollectEvidence with that clique as root. If we wish to compute the expectations of all features in parallel, we run a full pass of CollectEvidence and DistributeEvidence, abbreviating the latter algorithm to pass messages only into branches of the junction tree that contain features to be evaluated.

### 20.2.2 Geometry of the EM algorithm

[Section not yet written. We define two manifolds:

$$\mathcal{V} = \{p(x_E, x_H) : p(x_E) = \tilde{p}(x_E)\}. \quad (20.53)$$

and

$$\mathcal{E} = \left\{ p(x_E, x_H) : p(x_E, x_H | \theta) = \frac{1}{Z(\theta)} h(x_E, x_H) \exp \left\{ \sum_i \theta_i f_i(x_E, x_H) \right\} \right\}. \quad (20.54)$$

which are nonintersecting, except in the uninteresting case that  $p(x_E, x_H | \theta)$  is such that the variables  $X$  form a clique (in which case there's no need for the latent variables). EM alternates between these manifolds. Moreover, we can display an IPF inner loop as a sequence of I-projections on manifolds that intersect  $\mathcal{E}$  and are successively redefined by the E step.]

## 20.3 Historical remarks and bibliography

# Chapter 1

## Sampling Methods

There are many probabilistic models of practical interest for which exact inference is intractable. One important class of inference algorithms is based on deterministic approximation schemes and includes methods such as variational methods. Here we consider an alternative very general and widely used framework for approximate inference based on numerical sampling, also known as the Monte Carlo technique.

Although for some applications of graphical models the posterior distribution over unobserved variables will be of direct interest in itself, for most situations the posterior distribution is required primarily for the purpose of evaluating expectations, for example in order to make predictions.

The fundamental problem which we therefore wish to address in this chapter involves finding the expectation of some function  $f(x)$  with respect to a probability distribution  $p(x)$ . Here, the components of  $x$  might comprise discrete or continuous variables, or some combination of the two. Thus in the case of continuous variables we wish to evaluate the expectation

$$\langle f \rangle = \int f(x)p(x) dx. \quad (1.1)$$

This is illustrated schematically for a 1-dimensional distribution in Figure ???. We shall suppose

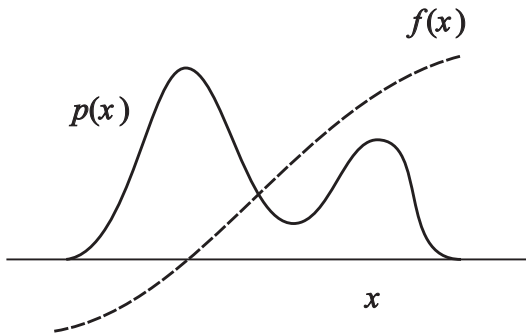


Figure 1.1: Schematic illustration of a function  $f(x)$  whose expectation is to be evaluated with respect to a distribution  $p(x)$ .

that such expectations are too complex to be evaluated exactly using analytical techniques. In some cases an expectation can be evaluated by first finding an analytic approximation to the posterior distribution. One approach to finding an approximate posterior distribution is to use variational

methods, as discussed at length in Chapter ???. The Laplace approximation framework, described in Chapter ???, has also been applied to this problem.

The general idea behind sampling methods is to obtain a set of samples  $x^{(l)}$  (where  $m = 1, \dots, M$ ) drawn from the distribution  $p(x)$ . This allows the expectation (??) to be approximated by a finite sum

$$\hat{f} = \frac{1}{M} \sum_{m=1}^M f(x^{(m)}). \quad (1.2)$$

The accuracy of such an approximation will depend on a variety of factors, some of which will be discussed in greater detail later in this chapter. Here we note that as long as the samples  $x^{(m)}$  are drawn from the distribution  $p(x)$  then  $\langle \hat{f} \rangle = \langle f \rangle$  and so the estimator has the correct mean. The variance of the estimator is easily seen to be  $\sigma^2/M$ , where

$$\sigma^2 = \langle (f - \langle f \rangle)^2 \rangle \quad (1.3)$$

is the variance of the function  $f(x)$  under the distribution  $p(x)$ . It is worth emphasizing that the accuracy of the estimator therefore does not depend on the dimensionality of  $x$ , and that, potentially, high accuracy may be achievable with a relatively small number of samples  $x^{(m)}$ . Furthermore, the variance of the estimator will decrease with increasing number  $M$  of samples.

One potential difficulty, however, is that the samples  $\{x^{(m)}\}$  might not be independent, and so the effective sample size might be much smaller than the apparent sample size. Also, referring back to Figure ??, we note that if  $f(x)$  is small in regions where  $p(x)$  is large, and vice versa, then the expectation may be dominated by regions of small probability, implying that relatively large sample sizes will be required to achieve sufficient accuracy.

While sampling methods have wide applicability, we shall of course be primarily interested in the case in which the distribution  $p(x)$  is specified in terms of a graphical model. In the case of a directed graph with no observed variables it is straightforward to sample from the joint distribution (assuming that it is possible to sample from the conditional distributions at each node) using the following *ancestral sampling* approach. The joint distribution is specified by

$$p(x) = \prod_{i=1}^d p(x_i | x_{\pi(i)}) \quad (1.4)$$

where  $x_{\pi(i)}$  denotes the set of variables associated with the parents of  $x_i$ . To obtain a sample from the joint distribution we make one pass through the set of variables in the order  $x_1, \dots, x_d$  sampling from the conditional distributions  $p(x_i | x_{\pi(i)})$ . This is always possible since at each step all of the parent values will have been instantiated. After one pass through the graph we will have obtained a sample from the joint distribution.

Now consider the case of a directed graph in which some of the nodes are instantiated with observed values. We can in principle extend the above procedure, at least in the case of nodes representing discrete variables, to give the following *logic sampling* approach, which can be seen as a special case of ‘importance sampling’ discussed in Section ???. At each step, when a sampled value is obtained for a variable  $x_i$  whose value is observed, the sampled value is compared to the observed value and if they agree then again the sample value is retained and the algorithm proceeds to next variable in turn. However, if the sampled value and the observed value disagree, then the whole sample so far is discarded and the algorithm starts again with the first node in the graph. This algorithm samples correctly from the posterior distribution since it corresponds

simply to drawing samples from the joint distribution of hidden variables and data variables and then discarding those samples which disagree with the observed data (with the slight saving of not continuing with the sampling from the joint distribution as soon as one contradictory value is observed). However, the overall probability of accepting a sample from the posterior decreases rapidly as the number of observed variables, and the number of states which those variables can take, increases.

In the case of probability distributions defined by an undirected graph there is no one-pass sampling strategy which will sample even from the prior distribution with no observed variables. Instead, computationally more expensive techniques must be employed, such as Gibbs sampling which is discussed in Section ??.

As well as sampling from conditional distributions we may also require samples from a marginal distribution. If we already have a strategy for sampling from a joint distribution  $p(x, y)$  then it is straightforward to obtain samples from the marginal distribution  $p(x)$  simply by ignoring the values for  $y$  in each sample.

### 1.0.1 Sampling and the EM Algorithm

In addition to providing a mechanism for direct implementation of the Bayesian framework, Monte Carlo methods can also play a role in the frequentist paradigm, for example to find maximum likelihood solutions. In particular, sampling methods can be used to approximate the E-step of the EM algorithm for models in which the E-step cannot be performed analytically. Consider a model with hidden variables  $x_H$ , visible (observed) variables  $x_V$  and parameters  $\theta$ . The function which is optimized with respect to  $\theta$  in the M-step is the expected complete-data log likelihood, given by

$$Q(\theta, \theta_{\text{old}}) = \int p(x_H|x_V, \theta_{\text{old}}) \ln p(x_H, x_V|\theta) dx_H. \quad (1.5)$$

We can use sampling methods to approximate this integral by a finite sum over samples  $\{x_H^{(l)}\}$  drawn from the current estimate for the posterior distribution  $p(x_H|x_V, \theta_{\text{old}})$ , so that

$$Q(\theta, \theta_{\text{old}}) \simeq \frac{1}{M} \sum_{m=1}^M \ln p(x_H^{(m)}, x_V|\theta). \quad (1.6)$$

The  $Q$  function is then optimized in the usual way in the M-step. This procedure is called the *Monte Carlo EM algorithm*.

It is straightforward to extend this to the problem of finding the mode of the posterior distribution over  $\theta$  (the MAP estimate) when a prior distribution  $p(\theta)$  has been defined, simply by adding  $\ln p(\theta)$  to the function  $Q(\theta, \theta_{\text{old}})$  before performing the M-step.

A particular instance of the Monte Carlo EM algorithm, called *stochastic EM*, arises if we consider a finite mixture model, and draw just one sample at each E-step. Suppose the  $L$ -dimensional binary latent variable  $x_z$  characterizes which of the  $L$  components of the mixture is responsible for generating each data point. In particular there is one vector-valued element of  $x_z$  for each data point in the data set, and each such vector has all of its  $L$  elements equal to zero except for the particular element representing the corresponding component of the mixture. In the E-step a sample of  $x_z$  is taken from the posterior distribution  $p(x_z|x_V, \theta_{\text{old}})$  where  $x_V$  is the data set. This effectively makes a hard assignment of each data point to one of the components in the mixture. In the M-step, this sampled approximation to the posterior distribution is used to update the model parameters in the usual way.

Now suppose we move from a maximum likelihood approach to a full Bayesian treatment in

which we wish to sample from the posterior distribution over  $\theta$ . In principle we would like to draw samples from the joint posterior  $p(\theta, x_H | x_V)$ , but we shall suppose that this is computationally difficult. Suppose further that it is relatively straightforward to sample from the complete-data parameter posterior  $p(\theta | x_H, x_V)$ . This inspires the *data augmentation* algorithm, which alternates between two steps known as the I-step (imputation step, analogous to an E-step) and the P-step (posterior step, analogous to an M-step).

**I-step.** We wish to sample from  $p(x_H | x_V)$  but we cannot do this directly. We therefore note the relation

$$p(x_H | x_V) = \int p(x_H | \theta, x_V) p(\theta | x_V) d\theta \quad (1.7)$$

and hence for  $m = 1, \dots, M$  we first draw a sample  $\theta^{(m)}$  from the current estimate for  $p(\theta | x_V)$ , and then use this to draw a sample  $x_H^{(m)}$  from  $p(x_H | \theta^{(m)}, x_V)$ .

**P-step.** Given the relation

$$p(\theta | x_V) = \int p(\theta | x_H, x_V) p(x_H | x_V) dx_H \quad (1.8)$$

we use the samples  $\{x_H^{(m)}\}$  obtained from the I-step to compute a revised estimate of the posterior distribution over  $\theta$  given by

$$p(\theta | x_V) \simeq \frac{1}{M} \sum_{m=1}^M p(\theta | x_H^{(m)}, x_V). \quad (1.9)$$

By assumption, it will be feasible to sample from this approximation in the I-step.

Note that we are making a (somewhat artificial) distinction between parameters  $\theta$  and hidden variables  $x_H$ . From now on we blur this distinction and focus simply on the problem of drawing samples from a given joint posterior distribution.

## 1.1 Basic Sampling Algorithms

In this section we consider the problem of sampling from some standard distributions defined over a single, continuous variable  $x \in \mathbb{R}$ . Since the samples will be generated by a computer algorithm they will in fact be *pseudo-random* numbers, that is, they will be deterministically calculated, but must nevertheless pass appropriate tests for randomness. We begin by looking at the problem of generating pseudo-random numbers with a uniform distribution over  $(0, 1)$ , as this forms the basis for generating numbers having other, non-uniform, distributions.

### 1.1.1 Standard Distributions

Pseudo-random number generators are typically based on successive applications of a transformation function  $D(\cdot)$ , so that a sequence  $(x^{(1)}, \dots, x^{(N)})$  is obtained using  $x^{(n)} = D(x^{(n-1)})$ . The particular sequence of numbers obtained is determined by the initial value  $x^{(1)}$ , known as the *seed*.

It might appear that the use of one of the standard chaotic functions for  $D(\cdot)$  might be appropriate. A chaotic function would have the property that the resulting sequence is highly sensitive

to the initial value  $x^{(1)}$ , so that changes in subsequent values due to a small change in  $x^{(1)}$  would grow exponentially as the sequence progresses. However, it turns out that a chaotic  $D(\cdot)$  need not give rise to a practically acceptable random number generator, even when the limiting distribution is correct. For example, the finite precision used to represent continuous variables in a digital computer can result in some functions leading to sequences which converge to a fixed value.

Instead we seek choices for  $D(\cdot)$  which take account of the finite representations of digital computers. It is often convenient to consider integer representations for random numbers, so that the output of the random number generator is an integer  $x$  from the set  $\{0, \dots, N\}$ , where  $N$  is the largest integer which can be stored by the computer. Corresponding continuous numbers from  $[0, 1)$  can subsequently be obtained using  $x/(N + 1)$  which is interpreted as a floating point operation. First we define the *period* of a random number generator to be the smallest integer  $T$  such that  $x^{(n+T)} = x^{(n)}$  for all  $n$ , in other words such that  $D(\cdot)^T$  is the identity operator. Clearly the largest value which the period of a simple generator of the form  $x^{(n)} = D(x^{(n-1)})$  can take is  $M + 1$ , but carelessness over the design of the random number generator can easily lead to significantly smaller values. Longer periods can be obtained using extensions of the transformation approach, such as using functions of  $x^{(n)}$  and  $x^{(n-1)}$ .

Many common random number generators are based on the *linear congruential* method which defines

$$D(x) = (ax + b) \mod (M + 1). \quad (1.10)$$

Considerable care must be exercised in the choice of the constants  $a$  and  $b$  in order to ensure a generator with acceptable properties. One obviously desirable property is that the sequence have its maximum period of  $M + 1$ .

We next consider how to generate random numbers from non-uniform distributions, assuming that we already have available a source of uniformly distributed random numbers. Suppose that  $x$  is uniformly distributed over the interval  $(0, 1)$ , and suppose that we transform the values of  $x$  using some function  $f(\cdot)$  so that  $y = f(x)$ . The distribution of  $y$  will be governed by

$$p(y) = p(x) \left| \frac{dx}{dy} \right| \quad (1.11)$$

where, in this case,  $p(x) = 1$ . Our goal is to choose the function  $f(x)$  such that the resulting values of  $y$  have some specific desired distribution  $p(y)$ . Integrating (??) we obtain  $x = h(y) \equiv \int_{-\infty}^y p(y') dy'$  which is the indefinite integral of  $p(y)$ . Thus,  $y = h^{-1}(x)$ , and so we have to transform the uniformly distributed random numbers using a function which is the inverse of the indefinite integral of the desired distribution. This is illustrated in Figure ??.

Consider for example the exponential distribution

$$p(y) = \lambda \exp(-\lambda y). \quad (1.12)$$

In this case  $h(y) = 1 - \exp(-\lambda y)$  and so if we transform our uniformly distributed variable  $x$  using  $y = -\lambda^{-1} \ln(1 - x)$  then  $y$  will have an exponential distribution.

Another example of a distribution to which the transformation method can be applied is given by the Cauchy distribution

$$p(y) = \frac{1}{\pi} \frac{1}{1 + y^2}. \quad (1.13)$$

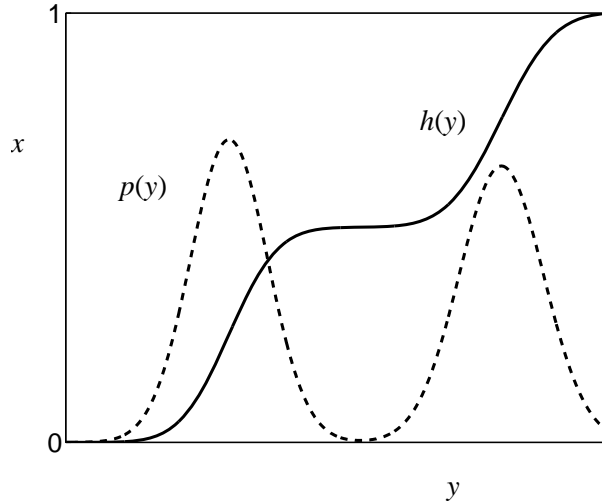


Figure 1.2: Geometrical interpretation of the transformation method for generating non-uniformly distributed random numbers.  $h(y)$  is the indefinite integral of the desired distribution  $p(y)$ . If a uniformly distributed random variable  $x$  is transformed using  $y = h^{-1}(x)$  then  $y$  will be distributed according to  $p(y)$ .

In this case the inverse of the indefinite integral is the ‘tan’ function.

The generalization to multiple variables is straightforward and involves the Jacobian of the change of variables, so that

$$p(y_1, \dots, y_d) = p(x_1, \dots, x_d) \left| \frac{\partial(y_1, \dots, y_d)}{\partial(x_1, \dots, x_d)} \right|. \quad (1.14)$$

As a final example of the transformation method we consider the Box-Muller method for generating samples from a Gaussian distribution. Suppose we generate pairs of uniformly distributed random numbers  $x_1, x_2 \in (-1, 1)$  (which we can do by transforming a variable distributed uniformly over  $(0, 1)$  using  $x \rightarrow 2x - 1$ ). Next we discard each pair unless it satisfies  $x_1^2 + x_2^2 \leq 1$ . This leads to a uniform distribution of points inside the unit circle with  $p(x_1, x_2) = 1/\pi$ , as illustrated in Figure ???. Then, for each pair  $x_1, x_2$  we evaluate the quantities

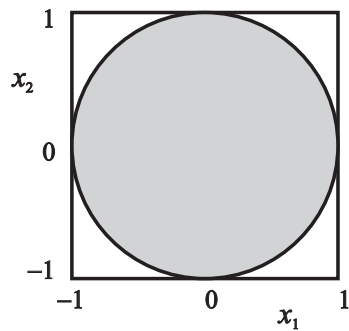


Figure 1.3: The Box-Muller method for generating normally distributed random numbers involves generating samples from a uniform distribution inside the unit circle.

$$y_1 = x_1 \left( \frac{-2 \ln x_1}{r^2} \right)^{1/2} \quad (1.15)$$

$$y_2 = x_2 \left( \frac{-2 \ln x_2}{r^2} \right)^{1/2} \quad (1.16)$$

where  $r^2 = x_1^2 + x_2^2$ . Then the joint distribution of  $y_1$  and  $y_2$  is given by

$$p(y_1, y_2) = p(x_1, Xx_2) \left| \frac{\partial(y_1, y_2)}{\partial(x_1, x_2)} \right| \quad (1.17)$$

$$= \left[ \frac{1}{\sqrt{2\pi}} \exp(-y_1^2/2) \right] \left[ \frac{1}{\sqrt{2\pi}} \exp(-y_2^2/2) \right] \quad (1.18)$$

and so  $y_1$  and  $y_2$  are independent and each has a normal distribution with zero mean and unit variance.

Clearly the transformation  $y \rightarrow \sigma y + \mu$  can be used to generate normally distributed random numbers with mean  $\mu$  and variance  $\sigma^2$ .

To generate vector-valued variables having a multi-variate normal distribution with mean  $\mu$  and covariance  $\Sigma$  we can employ the eigenvector/eigenvalue decomposition of the covariance matrix

$$\Sigma u_i = \lambda_i u_i. \quad (1.19)$$

It is then easily verified that, if  $x_i$  are univariate and normally distributed, then the variable

$$y = \mu + \sum_i \lambda_i^{1/2} x_i u_i \quad (1.20)$$

has the required multi-variate distribution. This is illustrated geometrically in Figure ???. In practice it is computationally more efficient, and also more robust, to use a Cholesky decomposition of the form  $\Sigma = LL^T$ . Then, if  $x$  is a vector valued random variable whose components are independent and normally distributed with zero mean and unit variance, then  $y = \mu + Lx$  will have mean  $\mu$  and covariance  $\Sigma$ .

Obviously the transformation technique depends for its success on the ability to calculate and then invert the indefinite integral of the required distribution. Such operations will only be feasible for a limited number of very simple distributions, and so we must turn to alternative approaches in search of a more general strategy. Here we consider two techniques called *rejection sampling* and *importance sampling*. Although mainly limited to univariate distributions and thus not directly applicable to complex problems in many dimensions, they do form important components in more general strategies.

## 1.1.2 Rejection Sampling

The rejection sampling framework allows us to sample from relatively complex distributions, subject to certain constraints. We begin by considering univariate distributions and discuss the extension to multiple dimensions subsequently.

Suppose we wish to samples from a distribution  $p(x)$  which is not one of the simple, standard

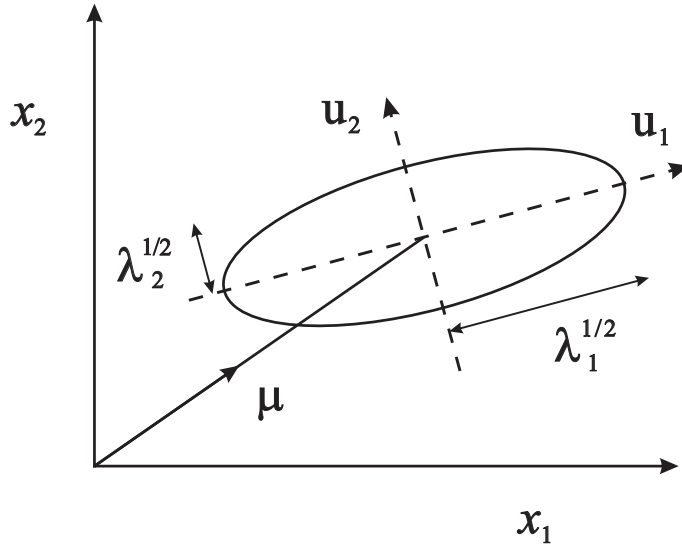


Figure 1.4: Geometrical view of a procedure for generating samples from a multi-variate normal distribution, given a source of univariate normally-distributed random numbers. The ellipse represents the one standard deviation contour of a Gaussian distribution with mean  $\mu$  whose covariance matrix has eigenvectors  $u_i$  with corresponding eigenvalues  $\lambda_i$ . A sample from the multivariate Gaussian distribution can be obtained using a linear combination of the eigenvectors with coefficients given by suitably scaled univariate Gaussian distributed random variables.

distributions considered so far, and that sampling directly from  $p(x)$  is difficult. Furthermore suppose, as is often the case, that we are easily able to evaluate  $p(x)$  for any given value of  $x$ , up to some normalizing constant  $Z$ , so that

$$p(x) = \frac{1}{Z}\tilde{p}(x) \quad (1.21)$$

where  $\tilde{p}(x)$  can readily be evaluated, but  $Z$  is unknown.

In order to apply rejection sampling we need some simpler distribution  $q(x)$ , sometimes called a proposal distribution, from which we can readily draw samples. We next introduce a constant  $k$  whose value is chosen such that  $kq(x) \geq \tilde{p}(x)$  for all values of  $x$ . The function  $kq(x)$  is called the comparison function, and is illustrated in Figure ???. Each step of the rejection sampler involves generating two random numbers. First, we generate a number  $x_0$  from the distribution  $q(x)$ . Next, we generate a number  $u_0$  from the uniform distribution over  $[0, kq(x_0)]$ . This pair of random numbers has uniform distribution under the curve of the function  $kq(x)$ . Finally, if  $u_0 > \tilde{p}(x_0)$  then the sample is rejected, otherwise  $u_0$  is retained. Thus the pair is rejected if it lies in the grey shaded region in Figure ???. The remaining pairs then have uniform distribution under the curve of  $\tilde{p}(X)$ , and hence the corresponding  $X$  values are distributed according to  $p(x)$ , as desired.

We can see more formally that the rejection sampling procedure samples from the correct distribution as follows. The original values of  $x$  are generated with distribution  $q(x)$  and these samples are then accepted with probability  $\tilde{p}(x)/kq(x)$  and so the resulting distribution of  $x$  is given by

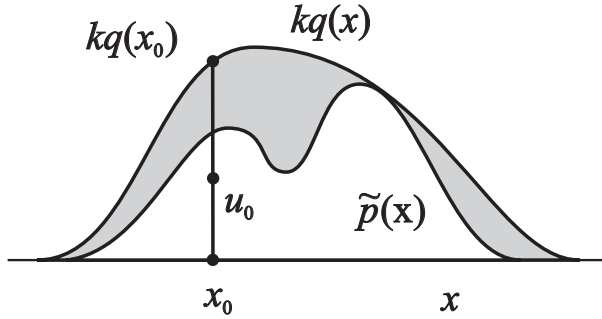


Figure 1.5: In the rejection sampling method, samples are drawn from a simple distribution  $q(x)$  and rejected if they fall in the grey area shown. The resulting samples are distributed according to  $p(x)$ , which is the normalized version of  $\tilde{p}(x)$ .

normalization as

$$\frac{[\tilde{p}(x)/kq(x)]q(x)}{\int [\tilde{p}(x)/kq(x)]q(x) dx} = \frac{\tilde{p}(x)}{\int \tilde{p}(x) dx} = p(x). \quad (1.22)$$

The probability that a sample will be accepted is given by

$$\begin{aligned} p(\text{accept}) &= \int [\tilde{p}(x)/kq(x)]q(x) dx \\ &= \frac{1}{k} \int \tilde{p}(x) dx. \end{aligned} \quad (1.23)$$

Thus the fraction of points which are rejected by this method depends on the ratio of the area under the unnormalized distribution  $\tilde{p}(x)$  to the area under the curve  $kq(x)$ . We therefore see that the constant  $k$  should be as small as possible subject to the limitation that  $kq(x)$  must be nowhere less than  $\tilde{p}(x)$ .

As an illustration of the use of rejection sampling, consider the task of sampling from the Gamma distribution

$$\text{Gam}(x|a) = \frac{x^{a-1} \exp(-ax)}{\Gamma(a)}. \quad (1.24)$$

where  $a > 0$ . This has, for  $a > 1$ , a bell-shaped form, as shown in Figure ???. A suitable proposal distribution is therefore the Cauchy (??) since this too is bell-shaped and since we can use the transformation method, discussed earlier, to sample from it. We need to generalize the Cauchy slightly to ensure that it nowhere has a smaller value than the Gamma distribution. This can be achieved by transforming a uniform random variable  $z$  using  $x = b \tan z + c$ , which gives random numbers distributed according to

$$q(x) = \frac{k}{1 + (x - c)^2/b^2}. \quad (1.25)$$

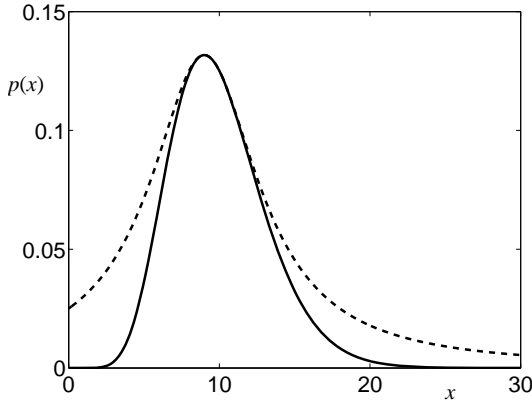


Figure 1.6: Plot showing the Gamma distribution given by (??) as the solid curve, with a scaled Cauchy proposal distribution given by the dashed curve. Samples from the Gamma distribution can be obtained by sampling from the Cauchy and then applying the rejection sampling criterion.

The minimum reject rate is obtained by setting  $c = a - 1$ ,  $b^2 = 2a - 1$  and choosing the constant  $k$  to be as small as possible while still satisfying the requirement  $kq(x) \geq \tilde{p}(x)$ . The resulting comparison function is shown, together with the Gamma distribution, in Figure ??.

### 1.1.3 Adaptive Rejection Sampling

In many instances where we might wish to apply rejection sampling it proves difficult to determine a suitable analytic form for the envelope distribution  $q(x)$ . An alternative approach is to construct the envelope function on the fly based on measured values of the distribution  $p(x)$ . We consider only the univariate case since it is only here that the algorithm is of significant practical value. Construction of an envelope function is particularly straightforward for cases in which  $p(x)$  is log concave, in other words when  $\ln p(x)$  has derivatives which are non-increasing functions of  $x$ . The construction of a suitable envelope function is illustrated graphically in Figure ??.

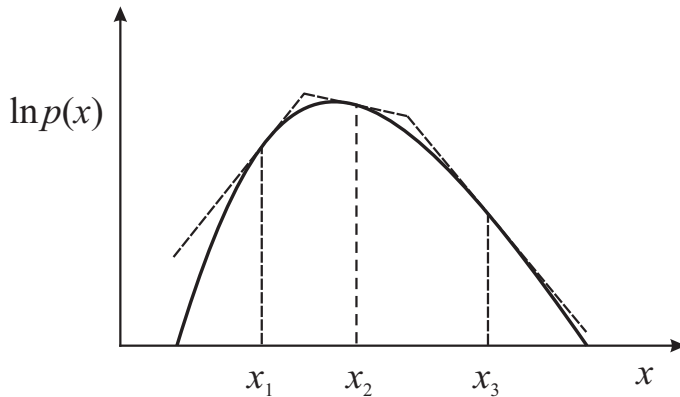


Figure 1.7: In the case of distributions which are log concave, an envelope function for use in rejection sampling can be constructed using the tangent lines computed at a set of grid points. If a sample point is rejected it is added to the set of grid points and used to refine the envelope distribution.

The function  $\ln p(x)$  and its gradient are evaluated at some initial set of grid points, and the intersections of resulting tangent lines are used to construct the envelope function. Next a sample value is drawn from the envelope distribution. This is straightforward (Exercise ??) since the log of the envelope distribution is a succession of linear functions, and hence the envelope distribution itself comprises a piecewise exponential distribution of the form

$$q(x) = k_i \lambda_i \exp \{-\lambda_i(x - x_{i-1})\} \quad x \in (x_{i-1}, x_i]. \quad (1.26)$$

Once a sample has been drawn the usual rejection criterion can be applied. If the sample is accepted then it will be a draw from the desired distribution. If, however, the sample is rejected, then it is incorporated into the set of grid points, a new tangent line is computed and the envelope function is thereby refined. As the number of grid points increases, so the envelope function becomes a better approximation of the desired distribution  $p(x)$  and the probability of rejection decreases.

A variant of the algorithm exists which avoids the evaluation of derivatives. The adaptive rejection sampling framework can also be extended to distributions which are not log concave, simply by following each rejection sampling step with a Metropolis-Hastings step, giving rise to *adaptive rejection Metropolis* sampling.

Clearly for rejection sampling to be of practical value we require that the comparison function be close to the required distribution so that the rate of rejection is kept to a minimum. Now let us examine what happens when we try to use rejection sampling in spaces of high dimensionality. Consider, for the sake of illustration, a somewhat artificial problem in which we wish to sample from a zero-mean multi-variate normal distribution with covariance  $\sigma_P^2 I$ , where  $I$  is the unit matrix, by rejection sampling from a proposal distribution which is itself a zero-mean normal distribution having covariance  $\sigma_Q^2 I$ . Obviously we must have  $\sigma_Q^2 > \sigma_P^2$  in order that there exists a  $k$  such that  $kq(x) \geq p(x)$ . In  $d$ -dimensions the optimum value of  $k$  is given by  $k = (\sigma_q/\sigma_p)^d$ , as illustrated for  $d = 1$  in Figure ??.

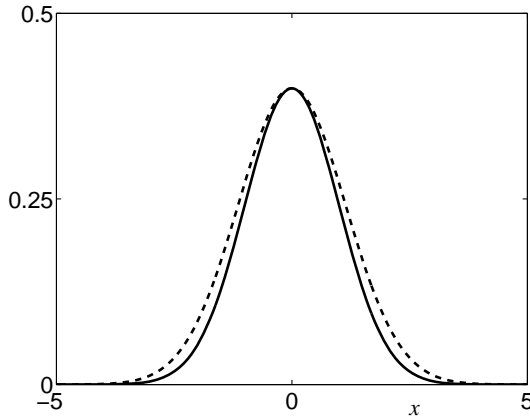


Figure 1.8: Illustrative example of rejection sampling involving sampling from a normal distribution  $p(x)$  shown by the solid curve, by using rejection sampling from a proposal distribution  $q(x)$ , shown by the dashed curve, which is also normal.

$p(x)$  and  $kq(x)$  which, since both distributions are normalized, is just  $1/k$ . Thus the acceptance rate diminishes exponentially with dimensionality. Even if  $\sigma_q$  exceeds  $\sigma_p$  by just one percent, for  $d = 1000$  the acceptance ratio will be approximately  $1/20,000$ . In this illustrative example the comparison function is close to the required distribution. For more practical examples, where the desired distribution may be multi-modal and sharply peaked, it will be extremely difficult to find

a good proposal distribution and comparison function. Furthermore, the exponential decrease of acceptance rate with dimensionality is a generic feature of rejection sampling. Although rejection can be a useful technique in one or two dimensions it is unsuited to problems of high dimensionality. It can, however, play a role as a sub-routine in more sophisticated algorithms for sampling in high dimensional spaces.

### 1.1.4 Importance Sampling

One of the principal reasons for wishing to sample from complicated probability distributions is to be able to evaluate expectations of the form (??). Importance sampling provides a framework for approximating expectations, but does not itself provide a mechanism for drawing samples from distribution  $p(x)$ .

The finite sum approximation to the expectation, given by (??), depends on being able to draw samples from the distribution  $p(x)$ . Suppose, however, that it is impractical to sample directly from  $p(x)$  by that we can evaluate  $p(x)$  easily for any given value of  $x$ . As we discussed at the start of this chapter, one strategy for evaluating expectations would be to discretize the  $x$ -space into a uniform grid and to evaluate the integrand as a sum of the form

$$\langle f \rangle \simeq \sum_{m=1}^M p(x^{(m)}) f(x^{(m)}). \quad (1.27)$$

An obvious problem with this approach is that the number of terms in the summation grows exponentially with the dimensionality of  $x$ . Furthermore, as we have already noted, the kinds of probability distributions of interest will often have much of their mass confined to relatively small regions of  $x$  space and so uniform sampling will be very inefficient since in high dimensional problems only a very small proportion of the samples will make a significant contribution to the sum. We would really like to choose the sample points to fall in regions where  $p(x)$  is large (or more precisely where the product  $p(x)f(x)$  is large).

As in the case of rejection sampling, importance sampling is based on the use of a distribution  $q(x)$  from which it is easy to draw samples. This is illustrated in Figure ?? We can then express the

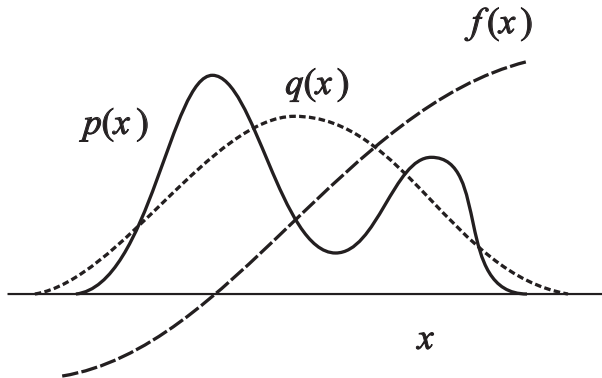


Figure 1.9: Importance sampling addresses the problem of evaluating the expectation of a function  $f(x)$  with respect to a distribution  $p(x)$  from which it is difficult to draw samples directly. Instead, samples  $\{x^{(m)}\}$  are drawn from a simpler distribution  $q(x)$  and the corresponding terms in the summation are weighted by the ratios  $p(x^{(m)})/q(x^{(m)})$ .

expectation in the form of a finite sum over samples  $\{x^{(m)}\}$  drawn from  $q(x)$

$$\begin{aligned}\langle f \rangle &= \int f(x)p(x) dx \\ &= \int f(x) \frac{p(x)}{q(x)} q(x) dx \\ &\simeq \frac{1}{M} \sum_{m=1}^M \frac{p(x^{(m)})}{q(x^{(m)})} f(x^{(m)}).\end{aligned}\tag{1.28}$$

The quantities  $r_m = p(x^{(m)})/q(x^{(m)})$  are known as importance weights, and they correct the bias introduced by sampling from the wrong distribution. Note that, unlike rejection sampling, all of the samples generated are retained.

It will often be the case that the distribution  $p(x)$  can only be evaluated up to a normalization constant, so that  $p(x) = \tilde{p}(x)/Z_p$  where  $\tilde{p}(x)$  can be evaluated easily, whereas  $Z_p$  is unknown. Similarly, we may wish to use an importance sampling distribution  $q(x) = \tilde{q}(x)/Z_q$  which has the same property. We then have

$$\begin{aligned}\langle f \rangle &= \int f(x)p(x) dx \\ &= \frac{Z_q}{Z_p} \int f(x) \frac{\tilde{p}(x)}{\tilde{q}(x)} q(x) dx \\ &\simeq \frac{Z_q}{Z_p} \frac{1}{M} \sum_{m=1}^M r_m f(x^{(m)}).\end{aligned}\tag{1.29}$$

where  $r_m = \tilde{p}(x^{(m)})/\tilde{q}(x^{(m)})$ . We can use the same sample set to evaluate the ratio  $Z_p/Z_q$  with the result

$$\begin{aligned}\frac{Z_p}{Z_q} &= \frac{1}{Z_q} \int \tilde{p}(x) dx \\ &= \int p(x) \frac{q(x)}{\tilde{q}(x)} dx \\ &\simeq \frac{1}{L} \sum_{m=1}^L r_m\end{aligned}\tag{1.30}$$

and hence

$$\langle f \rangle \simeq \frac{\sum_m r_m f(x^{(m)})}{\sum_m r_m}.\tag{1.31}$$

As with rejection sampling, the success of the importance sampling approach depends crucially

on how well the sampling distribution  $q(x)$  matches the desired distribution  $p(x)$ . If, as is often the case,  $p(x)f(x)$  is strongly varying and has a significant proportion of its mass concentrated over relatively small regions of  $x$  space, then the set of importance weights  $\{r_m\}$  may be dominated by a few weights having large values, with the remaining weights being relatively insignificant. Thus the effective sample size can be much smaller than the apparent sample size  $M$ . The problem is even more severe if none of the samples fall in the regions where  $p(x)f(x)$  is large. In that case the apparent variances of  $r_m$  and  $r_m f(x_m)$  may be small even though the estimate of the expectation may be severely wrong. Hence a major drawback of the importance sampling method is the potential to produce results which are arbitrarily in error and with no diagnostic indication. This also highlights a key requirement for the sampling distribution  $q(x)$ , namely that it should not be small or zero in regions where  $p(x)$  may be significant. In practice for continuous densities this implies the requirement to use distributions  $q(x)$  which are heavy tailed.

We can apply the importance sampling technique to distributions defined by graphical models in various ways. For discrete variables a very simple approach is called *uniform sampling*. The joint distribution for a directed graph is defined by (??). Each sample from the joint distribution is obtained by first setting those variables  $x_i$  which are in the evidence set equal to their observed values. Each of the remaining variables is then sampled independently from a uniform distribution over the space of possible instantiations. To determine the corresponding weight associated with a sample  $x^{(m)}$  we note that the sampling distribution  $\tilde{q}(x)$  is uniform over the possible choices for  $x$ , and that  $\tilde{p}(x|e) = \tilde{p}(x)$ , where  $e$  denotes the evidence associated with instantiated variables, and the equality follows from the fact that every sample  $x$  which is generated is necessarily consistent with the evidence. Thus the weights  $r_m$  are simply proportional to  $p(x)$ . Note that the variables can be sampled in any order. This approach can again yield poor results if the posterior distribution is far from uniform.

An improvement on this approach is called *likelihood weighted sampling* and is based on ancestral sampling of the variables. For each variable  $x_i$  in turn, if that variable is in the evidence set then it is just set to its instantiated value. If it is not in the evidence set then it is sampled from the conditional distribution  $p(x_i|x_{\pi(i)})$  in which the conditioning variables are set to their currently sampled values. The weighting associated with the resulting sample  $x$  is given by

$$r(x) = \prod_{i \notin e} \frac{p(x_i|x_{\pi(i)})}{p(x_i|x_{\pi(i)})} \prod_{i \in e} \frac{p(x_i|x_{\pi(i)})}{1} = \prod_{i \in e} p(x_i|x_{\pi(i)}). \quad (1.32)$$

This method can be further extended using *self-importance sampling* in which the importance sampling distribution is continually updated to reflect the current estimated posterior distribution. A further refinement called *Markov blanket scoring* distributes fractions of samples to the states of a node in proportion to the probability of these values conditioned on the Markov blanket of a node.

### 1.1.5 Sampling-Importance-Resampling

The rejection sampling method discussed in Section ?? depends in part for its success on the determination of a suitable value for the constant  $k$ . For many examples of distributions  $p(x)$  and  $q(x)$  it will be impractical to determine a suitable value for  $k$  in that any value which is sufficiently large to guarantee a bound on the desired distribution will lead to impractically small acceptance rates.

As in the case of rejection sampling, the *sampling-importance-resampling* (SIR) approach also makes use of a sampling distribution  $q(x)$ , but avoids having to determine the constant  $k$ . There are two stages to the scheme. In the first stage  $N$  samples  $x^{(1)}, \dots, x^{(N)}$  are drawn from  $q(x)$ . Then

in the second stage weights  $w^{(1)}, \dots, w^{(N)}$  are constructed using

$$w^{(n)} = \frac{\tilde{p}(x^{(n)})/q(x^{(n)})}{\sum_{n=1}^N \tilde{p}(x^{(n)})/q(x^{(n)})}. \quad (1.33)$$

A second set of  $M$  samples is drawn from the discrete distribution  $(x^{(1)}, \dots, x^{(N)})$  with probabilities given by the weights  $(w^{(1)}, \dots, w^{(N)})$ .

The resulting  $M$  samples are only approximately distributed according to  $p(x)$ , but the distribution becomes correct in the limit  $N \rightarrow \infty$ . To see this we note that the cumulative distribution of the resampled values is given by

$$\begin{aligned} \Pr(x \leq a) &= \sum_{n:x_n \leq a} w^{(n)} \\ &= \frac{\sum_{n=1}^N I(x_n \leq a) \tilde{p}(x_n)/q(x_n)}{\sum_{n=1}^N \tilde{p}(x_n)/q(x_n)} \end{aligned} \quad (1.34)$$

where  $I(\cdot)$  is the indicator function (which equals 1 if its argument is true and 0 otherwise). Taking the limit  $N \rightarrow \infty$ , and assuming suitable regularity of the distributions, we can replace the sums by integrals weighted according to the original sampling distribution  $q(x)$

$$\begin{aligned} \Pr(x \leq a) &= \frac{\int I(x \leq a) [\tilde{p}(x)/q(x)] q(x) dx}{\int [\tilde{p}(x)/q(x)] q(x) dx} \\ &= \frac{\int I(x \leq a) \tilde{p}(x) dx}{\int \tilde{p}(x) dx} \\ &= \int I(x \leq a) p(x) dx \end{aligned} \quad (1.35)$$

which is the cumulative distribution function of  $p(x)$ . Again we see that the normalization of  $p(x)$  is not required.

For a finite value of  $N$ , and a given initial sample set, the resampled values will only approximately be drawn from the desired distribution. As with rejection sampling, the approximation improves as the sampling distribution  $q(x)$  gets closer to the desired distribution  $p(x)$ . When  $q(x) = p(x)$  the initial samples  $(x^{(1)}, \dots, x^{(N)})$  have the desired distribution, and the weights  $w_n = 1/N$  so that the resampled values also have the desired distribution.

If moments with respect to the distribution  $p(x)$  are required, then they can be evaluated di-

rectly using the original samples together with the weights, since

$$\begin{aligned}
 \langle F(x) \rangle &= \int F(x)p(x) dx \\
 &= \frac{\int F(x)[\tilde{p}(x)/q(x)]q(x) dx}{\int [\tilde{p}(x)/q(x)]q(x) dx} \\
 &\simeq \sum_{n=1}^N F(x_n)w_n.
 \end{aligned} \tag{1.36}$$

### 1.1.6 Particle Filters

We can apply the re-sampling formalism of Section ?? to obtain a sequential Monte Carlo algorithm known as the particle filter. Consider the class of distributions represented by the graphical model in Figure ???. In many applications the observed data  $y_t$  arrive sequentially and we wish

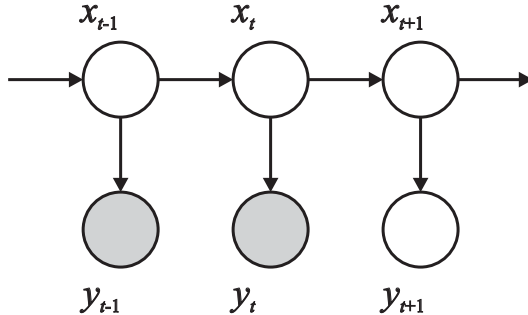


Figure 1.10: Directed graphical model in which a sequence of observations  $y_1, \dots, y_t, \dots$  is explained in terms of a hidden Markov chain of latent variables  $x_1, \dots, x_t, \dots$ . Sampling from the posterior distribution of the hidden variables can be performed sequentially using the particle filter algorithm.

to update the posterior distribution of the hidden variables in the light of each new observation. The probabilistic model is specified in terms of the transition probability  $p(x_t|x_{t-1})$  and the observation model  $p(y_t|x_t)$ . This class of models includes the hidden Markov model (Chapter ??) and the Kalman filter (Chapter ??) as special cases. The standard hidden Markov model uses discrete distributions while the simplest form of the Kalman filter is based on linear-Gaussian distributions, and so both models are amenable to exact solution, as discussed already.

There is, however, considerable interest in extending such models to more complex choices for the conditional probability distributions, particularly for the observation model  $p(y_t|x_t)$ . This can lead to highly complex posterior distributions over the hidden variables  $x_t$  which are no longer analytically tractable. We therefore consider the application of sampling methods. In particular, suppose we are given the observed values  $y_{(t)} = (y_1, \dots, y_t)$  and we wish to draw  $M$  samples from the posterior distribution  $p(x_t|y_{(t)})$ , in order to evaluate the expectation of some function  $f(x)$  with

respect to this distribution. Using Bayes' theorem we have

$$\begin{aligned}
\langle f(x_t) \rangle &= \int f(x_t) p(x_t | y_{(t)}) dx_t \\
&= \int f(x_t) p(x_t | y_t, y_{(t-1)}) dx_t \\
&= \frac{\int f(x_t) p(y_t | x_t) p(x_t | y_{(t-1)}) dx_t}{\int p(y_t | x_t) p(x_t | y_{(t-1)}) dx_t} \\
&\simeq \sum_{m=1}^M w_t^{(m)} f(x_t^{(m)}) \tag{1.37}
\end{aligned}$$

where  $\{x_t^{(m)}\}$  is a set of samples drawn from  $p(x_t | y_{(t-1)})$ , and we have made use of the conditional independence property  $p(y_t | x_t, y_{(t-1)}) = p(y_t | x_t)$  which follows from the graph in Figure ???. The sampling weights  $\{w_t^{(m)}\}$  are defined by

$$w_t^{(m)} = \frac{p(y_t | x_t^{(m)})}{\sum_{m=1}^M p(y_t | x_t^{(m)})}. \tag{1.38}$$

Thus the posterior distribution  $p(x_t | y_t)$  is represented by the set of samples  $\{x_t^{(m)}\}$  together with the corresponding weights  $\{w_t^{(m)}\}$ . Note that these weights satisfy  $0 \leq w_t^{(m)} \leq 1$  and  $\sum_m w_t^{(m)} = 1$ .

Since we wish to find a sequential sampling scheme we suppose that a set of samples and weights have been obtained at time step  $t$  and that we have subsequently observed the value of  $y_{t+1}$  and we wish to find the weights and samples at time step  $t + 1$ . We first sample from the distribution  $p(x_{t+1} | y_{(t)})$ . This is straightforward since, again using Bayes' theorem

$$\begin{aligned}
p(x_{t+1} | y_{(t)}) &= \int p(x_{t+1} | x_t, y_{(t)}) p(x_t | y_{(t)}) dx_t \\
&= \int p(x_{t+1} | x_t) p(x_t | y_{(t)}) dx_t \\
&= \int p(x_{t+1} | x_t) p(x_t | y_t, y_{(t-1)}) dx_t \\
&= \frac{\int p(x_{t+1} | x_t) p(y_t | x_t) p(x_t | y_{(t-1)}) dx_t}{\int p(y_t | x_t) p(x_t | y_{(t-1)}) dx_t} \\
&= \sum_m w_t^{(m)} p(x_{t+1} | x_t^{(m)}) \tag{1.39}
\end{aligned}$$

where we have made use of the conditional independence properties  $p(x_{t+1}|x_t, y_{(t)}) = p(x_{t+1}|x_t)$  and  $p(y_t|x_t, y_{(t-1)}) = p(y_t|x_t)$  which follow from the application of the d-separation criterion to the graph in Figure ???. The distribution given by (??) is a mixture distribution, and samples can be drawn by choosing a component  $m$  with probability given by the mixing coefficients  $w^{(m)}$  and then drawing a sample from the corresponding component.

In summary, we can view each step of the particle filter algorithm as comprising two stages. At time step  $t$  we have a sample representation of the posterior distribution  $p(x_t|y_{(t)})$  expressed as samples  $\{x_t^{(m)}\}$  with corresponding weights  $\{w_t^{(m)}\}$ . This can be viewed as a mixture representation of the form (??). To obtain the corresponding representation for the next time step, we first draw  $M$  samples from the mixture distribution (??), and then for each sample we use the new observation  $y_{t+1}$  to evaluate the corresponding weights  $w_{t+1}^m \propto p(y_{t+1}|x_{t+1}^{(m)})$ . This is illustrated schematically in Figure ??.

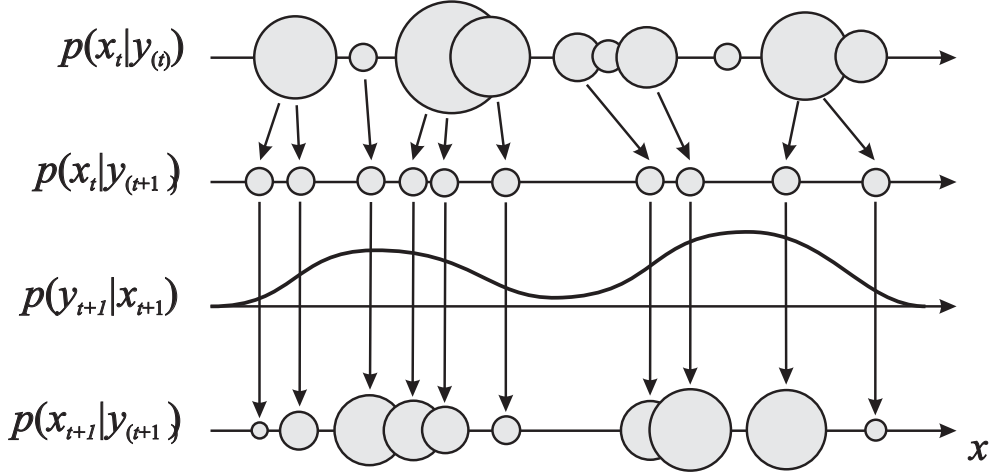


Figure 1.11: Schematic illustration of the operation of the particle filter. At time step  $t$  the posterior  $p(x_t|y_t^{(m)})$  is represented as a mixture distribution, shown schematically as circles whose sizes are proportional to the weights  $w_t^m$ . A set of  $M$  samples is then drawn from this distribution, and the new weights  $w_{t+1}^m$  evaluated using  $p(y_{t+1}|x_{t+1}^{(m)})$ .

## 1.2 Markov Chain Monte Carlo

In the previous section we discussed the rejection sampling and importance sampling strategies for evaluating expectations of functions, and we saw that they suffer from severe limitations particularly in spaces of high dimensionality. We turn in this section to a very general and powerful framework called Markov chain Monte Carlo (MCMC) which allows sampling from a large class of distributions, and which scales well with the dimensionality of the sample space.

As with rejection and importance sampling we again sample from a distribution  $q(x)$ , known as a *proposal distribution*, which differs from the desired distribution  $p(x)$ . This time, however, we maintain a record of the current state  $x^{(t)}$ , and the proposal distribution  $q(x|x^{(t)})$  depends on this current state, and so the sequence of samples forms a Markov chain. Again, if we write  $p(x) = \tilde{p}(x)/Z$ , we assume that  $\tilde{p}(x)$  can readily be evaluated for any given value of  $x$ , although the value of  $Z$  may be unknown. The proposal distribution itself is chosen to be sufficiently simple that it is straightforward to draw samples from it directly. At each cycle of the algorithm we generate a

candidate sample  $x^*$  from the proposal distribution and then accept the sample according to an appropriate criterion. In the basic *Metropolis* algorithm we assume that the proposal distribution is symmetric, that is  $q(x_1|x_2) = q(x_2|x_1)$  for all values of  $x_1$  and  $x_2$ . The candidate sample is then accepted with probability

$$A(x^*, x^{(t)}) = \min \left( 1, \frac{\tilde{p}(x^*)}{\tilde{p}(x^{(t)})} \right). \quad (1.40)$$

This can be achieved by choosing a random number  $u$  with uniform distribution over the unit interval  $(0, 1)$  and then accepting the sample if  $A(x^*, x^{(t)}) > u$ . Note that if the step from  $x^{(t)}$  to  $x^*$  causes an increase in the value of  $p(x)$  then the candidate point is certain to be kept.

If the candidate sample is accepted then  $x^{(t+1)} = x^*$ , otherwise the candidate point  $x^*$  is discarded,  $x^{(t+1)}$  is set to  $x^{(t)}$ , and another candidate sample drawn from the distribution  $Q(x; x^{(t)})$ . This is in contrast to rejection sampling, where rejected samples are simple discarded. In the Metropolis algorithm when a candidate point is rejected, the previous sample is included instead in the final list of samples, leaded to multiple copies of samples<sup>1</sup>. As we shall see, as long as  $q(x_1, x_2)$  is positive for any values of  $x_1$  and  $x_2$  (this is a sufficient but not necessary condition) the distribution of  $x^{(t)}$  tends to  $p(x)$  as  $t \rightarrow \infty$ . It should be emphasized, however, that the sequence  $x_1, x_2, \dots$  is not a set of independent samples from  $p(x)$  since successive samples are highly correlated. If we wish to obtain independent samples then we can discard most of the sequence and just retain every  $N^{\text{th}}$  sample. For  $N$  sufficiently large the retained samples will for all practical purposes be independent.

Figure ?? shows a simple illustrative example of sampling from two-dimensional normal distribution using the Metropolis algorithm in which the proposal distribution is an isotropic Gaussian.

Further insight into the nature of Markov chain Monte Carlo algorithms can be gleaned by looking at the properties of a specific example namely a simple random walk. Consider a state space consisting of the integers, with probabilities

$$\begin{aligned} p(x_{n+1} = x_n) &= 0.5 \\ p(x_{n+1} = x_n + 1) &= 0.25 \\ p(x_{n+1} = x_n - 1) &= 0.25 \end{aligned} \quad (1.41)$$

where  $x_n$  denotes the state at step  $n$ . If the initial state is  $x_1 = 0$  then by symmetry the expected state at time  $n$  will also be zero  $\langle x_n \rangle = 0$ , and similarly it is easily seen that  $\langle x_n^2 \rangle = n/2$ . Thus after  $n$  steps the random walk has only travelled a distance which on average is proportional to the square root of  $n$ . This square root dependence is typical of random walk behaviour and shows that random walks are very inefficient in exploring the state space. As we shall see, a central goal in designing Markov chain Monte Carlo methods is to avoid random walk behaviour.

### 1.2.1 Markov Chains

Before discussing Markov chain Monte Carlo methods in more detail, it is useful to study some general properties of Markov chains in more detail. In particular we ask under what circumstances will a Markov chain converge to the desired distribution. A first-order Markov chain is defined

---

<sup>1</sup>In a practical implementation only a single copy of each retained sample would be kept, along with an integer weighting factor recording how many times that state was retained.

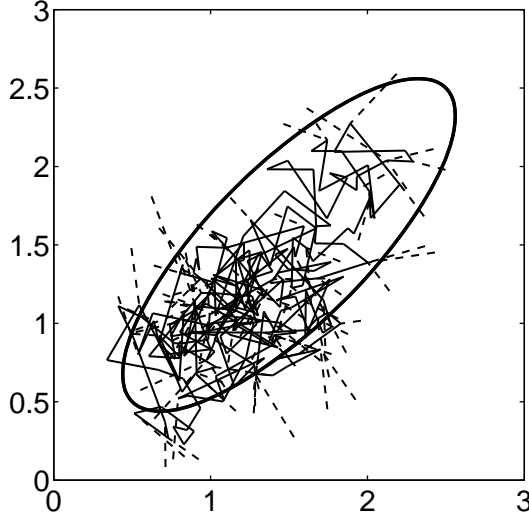


Figure 1.12: A simple illustration using Metropolis algorithm to sample from a normal distribution whose one standard deviation contour is shown by the ellipse. The proposal distribution is an isotropic normal distribution whose standard deviation is 0.2. Steps which are accepted are shown as solid lines, while rejected steps are shown dashed. A total of 300 candidate samples are generated, which include 85 rejections.

to be a series of random variables  $x_1, \dots, x_M$  such that the following conditional independence property holds for  $m \in \{1, \dots, M - 1\}$

$$p(x_{m+1} | x_1, \dots, x_m) = p(x_{m+1} | x_m). \quad (1.42)$$

This of course can be represented as a directed graph in the form of a chain. We can then specify the Markov chain by giving the probability distribution for the initial variable  $p_0(x)$  together with the conditional probabilities for subsequent variables in the form of *transition probabilities*  $T_m(x_m, x_{m+1}) \equiv p(x_{m+1} | x_m)$ . A Markov chain is called *homogeneous* if the transition probabilities are the same for all  $m$ . Initially we will restrict attention to finite, discrete state spaces for the variables, and discuss the extension to countably infinite and continuous state spaces later.

The marginal probability for a particular variable can be expressed in terms of the marginal probability for the previous variable in the chain in the form

$$p(x_{m+1}) = \sum_{x_m} p(x_{m+1} | x_m) p(x_m). \quad (1.43)$$

A distribution is said to be invariant, or stationary, with respect to a Markov chain if each step in the chain leaves that distribution invariant. Thus, for a homogeneous Markov chain with transition probabilities  $T(x, x')$ , the distribution  $p^*(x)$  is invariant if

$$p^*(x) = \sum_{x'} T(x', x) p^*(x'). \quad (1.44)$$

Note that a given Markov chain may have more than one invariant distribution. For instance, if

the transition probabilities are given by the identity transformation, then any distribution will be invariant.

A sufficient (but not necessary) condition for ensuring that the required distribution  $p(x)$  is invariant, is to choose the transition probabilities to satisfy the property of *detailed balance*, defined by

$$p^*(x)T(x, x') = p^*(x')T(x', x) \quad (1.45)$$

for the particular distribution  $p^*(x)$ . It is easily seen that a transition probability which satisfies detailed balance with respect to a particular distribution will leave that distribution invariant, since

$$\sum_{x'} p^*(x')T(x', x) = \sum_{x'} p^*(x)T(x, x') = p^*(x) \sum_{x'} p(x'|x) = p^*(x). \quad (1.46)$$

A Markov chain which respects detailed balance is said to be *reversible*.

Our goal is to use Markov chains to sample from a given distribution. We can achieve this if we set up a Markov chain such that the desired distribution is invariant. However, we must also require that for,  $m \rightarrow \infty$ , the distribution  $p_m(x)$  converges to the required invariant distribution  $p^*(x)$ , irrespective of the choice of initial distribution  $p_0(x)$ . This property is called *ergodicity*, and the invariant distribution is then called the *equilibrium* distribution. Clearly an ergodic Markov chain can have only one equilibrium distribution.

In Appendix ?? we show that a homogeneous Markov chain will be ergodic, subject only to weak restrictions on the invariant distribution and the transition probabilities.

In practice we often construct the transition probabilities from a set of ‘base’ transitions  $B_1, \dots, B_n$ . This can be achieved through a mixture distribution of the form

$$T(x, x') = \sum_{k=1}^n \alpha_k B_k(x, x') \quad (1.47)$$

for some set of mixing coefficients  $\alpha_1, \dots, \alpha_n$  satisfying  $\alpha_k \geq 0$  and  $\sum_k \alpha_k = 1$ . Alternatively, the base transitions may be combined through successive application, so that

$$T(x, x') = \sum_{x_1} \dots \sum_{x_{n-1}} B_1(x, x_1) \dots B_{n-1}(x_{n-2}, x_{n-1}) B_n(x_{n-1}, x'). \quad (1.48)$$

If a distribution is invariant with respect to each of the base transitions, then obviously it will also be invariant with respect to either of the  $T(x, x')$  given by (??) or (??). For the case of the mixture (??), if each of the base transitions satisfies detailed balance, then the mixture transition  $T$  will also satisfy detailed balance. This does not hold for the transition probability constructed using (??), although by symmetrizing the order of application of the base transitions, in the form  $B_1, B_2, \dots, B_n, B_n, \dots, B_2, B_1$ , detailed balance can be restored.

A common example of the use of composite transition probabilities is where each base transition changes only a subset of the variables. Clearly each base transition itself will not be ergodic. However, the composite probability will be ergodic, as long as condition (??) is satisfied.

## 1.2.2 The Metropolis-Hastings Algorithm

Earlier we introduced the basic Metropolis algorithm, without actually demonstrating that it samples from the required distribution. Before giving a proof we first discuss a generalization, known as the *Metropolis-Hastings* algorithm, to the case where the proposal distribution is no longer a symmetric function of its arguments. In particular at step  $n$  of the algorithm, in which the current state is  $x_n$ , we draw a sample  $x^*$  from the distribution  $q_k(x, x_n)$  and then accept it with probability  $A_k(x^*, x_n)$  where

$$A_k(x', x) = \min \left( 1, \frac{p(x')q_k(x', x)}{p(x)q_k(x, x')} \right). \quad (1.49)$$

Here  $k$  labels the members of the set of possible transitions being considered. This is generally referred to as the Metropolis-Hastings algorithm. Obviously for a symmetric proposal distribution this reduces to the standard Metropolis criterion given by (??).

We can show that  $p(x)$  is an invariant distribution of the Markov chain defined by the Metropolis-Hastings algorithm by showing that detailed balance, defined by (??), is satisfied. Using (??) we have

$$\begin{aligned} p(x)q_k(x, x')A_k(x', x) &= \min(p(x)q_k(x, x'), p(x')q_k(x', x)) \\ &= \min(p(x')q_k(x', x), p(x)q_k(x, x')) \\ &= p(x')q_k(x', x)A_k(x, x') \end{aligned} \quad (1.50)$$

as required.

It is worth noting that the evaluation of the acceptance criterion (??) does not require knowledge of the normalizing constant  $Z$  in the probability distribution  $p(x) = \tilde{p}(x)/Z$ .

The specific choice of proposal distribution can have a marked effect on the performance of the algorithm. For continuous state spaces a common choice is a Gaussian centered on the current state, leading to an important trade-off in determining the width parameter of this distribution. If the width is small then the proportion of accepted transitions will be high, but progress through the state space takes the form of a slow random walk leading to very long correlation times. However, if the width parameter is large then the rejection rate will be high since, in the kind of complex problems we are considering, many of the proposed steps will be to states for which the probability  $p(x)$  is low. Consider a multi-variate distribution  $p(x)$  having strong correlations between the components of  $x$ , as illustrated in Figure ???. The scale  $\rho$  of the proposal distribution should be as large as possible without incurring high rejection rates. This suggests that  $\rho$  should be of the same order as the smallest length scale  $\sigma_{\min}$ . The system then explores the distribution along the more extended direction by means of a random walk, and so the number of steps to arrive at a state which is more or less independent of the original state is of order  $(\sigma_{\max}/\sigma_{\min})^2$ . In fact in two dimensions the increase in rejection rate as  $\rho$  increases is offset by the larger steps sizes of those transitions which are accepted, and more generally for a multivariate Gaussian the number of steps required to obtain independent samples scales like  $(\sigma_{\max}/\sigma_2)^2$  where  $\sigma_2$  is the second smallest standard deviation. These details aside, it remains the case that if the length scales over which the distributions varies are very different in different directions then the Metropolis Hastings algorithm can lead to very slow convergence.

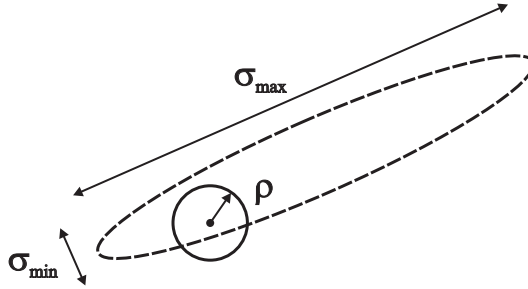


Figure 1.13: Schematic illustration of the use of an isotropic Gaussian proposal distribution (circle) to sample from a correlated multivariate Gaussian distribution (dashed ellipse) having very different standard deviations in different directions, using the Metropolis-Hastings algorithm. In order to keep the rejection rate low the scale  $\rho$  of the proposal distribution should be of the order of the smallest standard deviation  $\sigma_{\min}$ , which leads to random walk behaviour in which independent states are separated by roughly  $(\sigma_{\max}/\sigma_{\min})^2$  steps where  $\sigma_{\max}$  is the largest standard deviation.

### 1.3 Gibbs Sampling

Gibbs sampling is a simple and widely applicable Markov chain Monte Carlo algorithm, which has been used extensively in the context of probabilistic graphical models. As we shall see, Gibbs sampling can be seen as a special case of the Metropolis-Hastings algorithm.

Consider the distribution  $p(x) = p(x_1, \dots, x_d)$  from which we wish to sample, and suppose that we have chosen some initial state for the Markov chain. Each step of the Gibbs sampling procedure involves replacing the value of one of the variables by a value drawn from the distribution of that variable conditioned on the values of the remaining variables. Thus we replace  $x_i$  by a value drawn from the distribution  $p(x_i | \{x_j \neq i\})$ , where  $x_i$  denotes the  $i$ th component of  $x$ . This procedure is repeated either by cycling through the variables in some particular order, or by choosing the variable to be updated at each step at random from some distribution.

For example, suppose we have a distribution  $p(x_1, x_2, x_3)$  over three variables, and at step  $\tau$  of the algorithm we have selected values  $x_1^{(\tau)}, x_2^{(\tau)}$  and  $x_3^{(\tau)}$ . We first replace  $x_1^{(\tau)}$  by a new value  $x_1^{(\tau+1)}$  obtained by sampling from the conditional distribution

$$p(x_1 | x_2^{(\tau)}, x_3^{(\tau)}). \quad (1.51)$$

Next we replace  $x_2^{(\tau)}$  by a value  $x_2^{(\tau+1)}$  obtained by sampling from the conditional distribution

$$p(x_2 | x_1^{(\tau+1)}, x_3^{(\tau)}) \quad (1.52)$$

so that the new value for  $x_1$  is used straight away in subsequent sampling steps. Then we update  $x_3$  with a sample  $x_3^{(\tau+1)}$  drawn from

$$p(x_3 | x_1^{(\tau+1)}, x_2^{(\tau+1)}) \quad (1.53)$$

and so on, cycling through the three variables in turn. The basic Gibbs sampling algorithm is summarized in Figure ??.

To show that this procedure samples from the required distribution we first of all note that

```

1. Initialize  $\{x_i : i = 1, \dots, n\}$ 
2. For  $\tau = 1, \dots, T$ .
   - Sample  $x_1^{(\tau+1)} \sim p(x_1 | x_2^{(\tau)}, x_3^{(\tau)}, \dots, x_n^{(\tau)})$ .
   - Sample  $x_2^{(\tau+1)} \sim p(x_2 | x_1^{(\tau+1)}, x_3^{(\tau)}, \dots, x_n^{(\tau)})$ .
   :
   - Sample  $x_j^{(\tau+1)} \sim p(x_j | x_1^{(\tau+1)}, \dots, x_{j-1}^{(\tau+1)}, x_{j+1}^{(\tau)}, \dots, x_n^{(\tau)})$ .
   :
   - Sample  $x_n^{(\tau+1)} \sim p(x_n | x_1^{(\tau+1)}, x_2^{(\tau+1)}, \dots, x_{n-1}^{(\tau+1)})$ .

```

Figure 1.14: Psuedo-code for the Gibbs sampling algorithm.

the distribution  $p(x)$  is an invariant of each the Gibbs sampling steps individually, and hence of the whole Markov chain. This follows from the fact that when we sample from  $p(x_i | \{x_{j \neq i}\})$  the marginal distribution  $p(\{x_{j \neq i}\})$  is clearly invariant since the values of the  $\{x_{j \neq i}\}$  are unchanged. Also, each step by definition samples from the correct conditional distribution  $p(x_i | \{x_{j \neq i}\})$ . Since these conditional and marginal distributions together specify the joint distribution, we see that the joint distribution is itself invariant.

The second requirement to be satisfied in order that the Gibbs sampling procedure samples from the correct distribution is that it be ergodic. A sufficient condition for ergodicity is that none of the conditional distributions be anywhere zero. If this is the case then any point in  $x$  space can be reached from any other point in a finite number of steps involving one update of each of the component variables. If this requirement is not satisfied, so that some of the conditional distributions have zeros, then ergodicity, if it applies, must be proven explicitly.

The distribution of initial states must also be specified in order to complete the algorithm, although samples drawn after many iterations should become independent of this distribution. Of course successive samples from the Markov chain will be highly correlated, and so to obtain samples which are nearly independent it will be necessary to sub-sample the sequence.

Where appropriate we can generalize the Gibbs procedure slightly to sample from sets of variables, conditioned on the remaining variables, at each step. Note that these sets do not need to be disjoint.

We can obtain the Gibbs sampling procedure as a particular instance of the Metropolis-Hastings algorithm as follows. Consider a Metropolis-Hastings sampling step involving the group of variable  $x_k$  in which the remaining variables  $x_{-k}$  remain fixed, and for which the transition probability  $q_k(x, x')$  is given by  $p(x'_k | x_{-k})$ . We note that  $x'_{-k} = x_{-k}$  since these components are unchanged by the sampling step. Also,  $p(x) = p(x_k | x_{-k})p(x_{-k})$ . Thus the factor which determines the acceptance probability in the Metropolis-Hastings (??) is given by

$$\frac{p(x')q_k(x', x)}{p(x)q_k(x, x')} = \frac{p(x'_k | x'_{-k})p(x'_{-k})p(x_k | x'_{-k})}{p(x_k | x_{-k})p(x_{-k})p(x'_k | x_{-k})} = 1. \quad (1.54)$$

Thus the Metropolis-Hastings steps are always accepted, and therefore this choice of proposal distribution corresponds to the Gibbs sampling algorithm.

The practical applicability of Gibbs sampling depends on the ease with which samples can be

drawn from conditional distributions  $p(x_k | x_{-k})$ . In the case of graphical models, the conditional distributions for individual nodes depend only on the variables in the corresponding Markov blankets, as illustrated in Figure ???. For directed graphs, a very broad choice of conditional distribu-

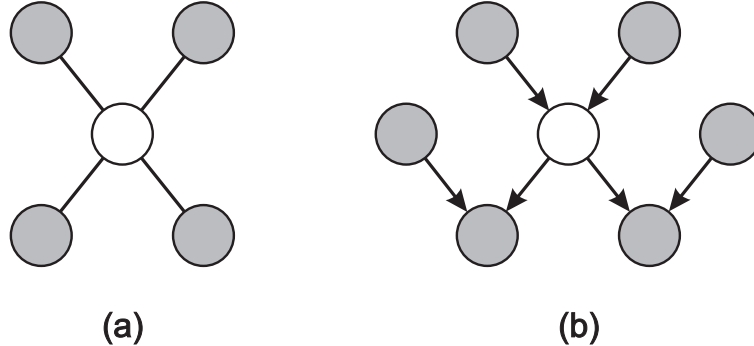


Figure 1.15: The Gibbs sampling requires samples to be drawn from the conditional distribution of a variable conditioned on the remaining variables. For graphical models, this conditional distribution is a function only of the states of the nodes in the Markov blanket. In the case of an undirected graph (a) this comprises the set of neighbours while for a directed graph (b) the Markov blanket comprises the parents, the children and the co-parents.

tions for the individual nodes conditioned on their parents will lead to conditional distributions for Gibbs sampling which are log concave. The adaptive rejection sampling methods discussed in Section ?? therefore provide a framework for Monte Carlo sampling from directed graphs with broad applicability.

As with the Metropolis algorithm, we can gain some insight into the behaviour of Gibbs sampling by investigating its application to a Gaussian distribution. Consider a correlated Gaussian in two variables, as illustrated in Figure ??, having a conditional distribution of width  $l$  and a marginal distribution of width  $L$ . The typical step size is governed by the conditional distributions and will be of order  $l$ . Since the state evolves according to a random walk, the number of steps needed to obtain independent samples from the distribution will be of order  $(L/l)^2$ . Of course if the Gaussian distribution were uncorrelated then the Gibbs sampling procedure would be optimally efficient. For this simple problem we could rotate the coordinate system in order to decorrelate the variable, however, in practical applications it will generally be infeasible to find such transformations.

One approach to reducing random walk behaviour in Gibbs sampling is called *over-relaxation*. In its original form this applies to problems for which the conditional distributions are Gaussian. This represents a more general class of distributions than the multi-variate Gaussian, since for example the non-Gaussian distribution  $p(x, y) \propto \exp(-x^2 y^2)$  has Gaussian conditional distributions. At each step of the Gibbs sampling algorithm the conditional distribution for a particular component  $x_i$  has some mean  $\mu_i$  and some variance  $\sigma_i^2$ . In the over-relaxation framework the value of  $x_i$  is replaced with

$$x'_i = \mu_i + \alpha(x_i - \mu_i) + \sigma_i(1 - \alpha^2)^{1/2}\nu \quad (1.55)$$

where  $\nu$  is a Gaussian random variate with zero mean and unit variance, and  $\alpha$  is a parameter such that  $-1 < \alpha < 1$ . For  $\alpha = 0$  the method is equivalent to standard Gibbs sampling. When  $\alpha$  is negative the step is biased to the opposite side of the mean. It is easily seen that this step leaves the desired distribution invariant since if  $x_i$  has mean  $\mu_i$  and variance  $\sigma_i^2$ , then so too does  $x'_i$ . Also it is clear that if the original Gibbs sampling is ergodic, then the over-relaxed version will be ergodic

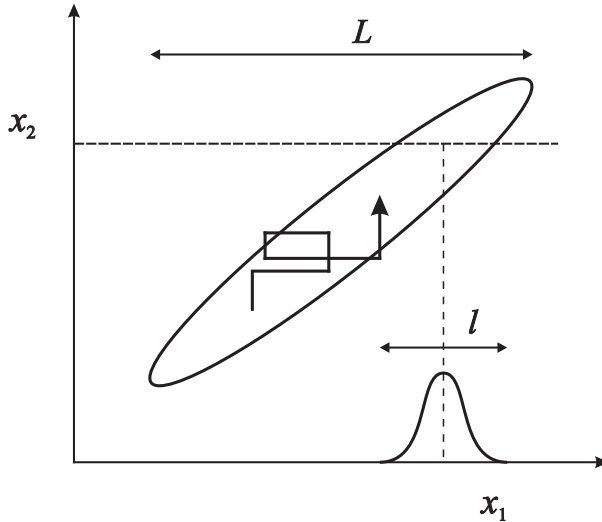


Figure 1.16: Illustration of Gibbs sampling by alternate updates of two variables whose distribution is a correlated Gaussian. The step size is governed by standard deviation of the conditional distribution, and is  $O(l)$ , leading to slow progress in the direction of elongation of the distribution. The number of steps needed to obtain an independent sample from the distribution is  $O((L/l)^2)$ .

also. Thus the effect of over-relaxation is to tend to produce directed motion through state space when the variables are highly correlated. The framework of *ordered over-relaxation* generalizes this approach to non-Gaussian distributions.

The simplicity of Gibbs sampling allows it to be applied to a broad range of models. In fact it has been used as the basis for a general purpose software package BUGS ('Bayesian inference Using Gibbs Sampling') for sampling from models specified as directed acyclic graphs. The conditional distribution for each node is dependent only on the states of nodes in the corresponding Markov blanket. If the graph is constructed using distributions from the exponential family, and if the parent-child relationships preserve conjugacy, then the full conditional distributions arising in Gibbs sampling will take the same form as the original conditional distributions (conditioned on the parents) defining each node, and so standard sampling techniques can be employed. In general the full conditional distributions will be of a complex form that does not permit the use of standard sampling algorithms. However, these conditionals will be log concave and sampling can be done efficiently using adaptive rejection sampling (assuming the corresponding variable is a scalar).

Because the basic Gibbs sampling technique considers one variable at a time, there are strong dependencies between successive samples. At the opposite extreme, if we could draw samples directly from the joint distribution (an operation that we are supposing is intractable) then successive samples would be independent. We can hope to improve on the simple Gibbs sampler by sampling successively from groups of variables rather than individual variables. This is achieved in the *blocking Gibbs* sampling algorithm by choosing blocks of variables, not necessarily disjoint, and then sampling jointly from the variables in each block in turn, conditioned on the remaining variables. This can be done in a way that preserves tractability while leading to a large block by starting with the junction tree for the full graph in which the block comprises the complete set of variables, and then removing variables from the block until a tractable structure is obtained.

## 1.4 Slice Sampling

We have seen that one of the difficulties with the Metropolis algorithm is the sensitivity to step size. If this is too small the result is slow decorrelation due to random walk behaviour while if it is too large the result is inefficiency due to a high rejection rate. The technique of *slice sampling* provides an adaptive step size which is automatically adjusted to match the characteristics of the distribution. Again it requires that we be able to evaluate the unnormalized distribution  $\tilde{p}(x)$ .

Slice sampling involves augmenting  $x$  with an additional variable  $u$  and then drawing samples from the joint  $(x, u)$  space. We shall see another example of this approach when we discuss hybrid Monte Carlo in Section ???. As with rejection sampling, the goal is to sample uniformly from the volume under the surface defined by  $\tilde{p}(x, u)$ , in other words to sample from the distribution given by

$$\hat{p}(x, u) = \begin{cases} 1/Z & \text{if } 0 \leq u \leq p(x) \\ 0 & \text{otherwise} \end{cases}$$

where  $Z = \int \tilde{p}(x) dx$ . The marginal distribution over  $x$  is given by

$$\int \hat{p}(x, u) du = \int_0^{\tilde{p}(x)} \frac{1}{Z} du = \frac{\tilde{p}(x)}{Z} = p(x)$$

and so we can sample from  $p(x)$  by sampling from  $\hat{p}(x, u)$  and then ignoring the  $u$  values. This can be achieved by alternately sampling  $x$  and  $u$ . Given the value of  $x$  we evaluate  $\tilde{p}(x)$  and then sample  $u$  uniformly in the range  $0 \leq u \leq \tilde{p}(x)$ , which is straightforward. Then we fix  $u$  and sample  $x$  uniformly from the ‘slice’ through the distribution defined by  $\{x : \tilde{p}(x) > u\}$ . This is illustrated in Figure ??(a).

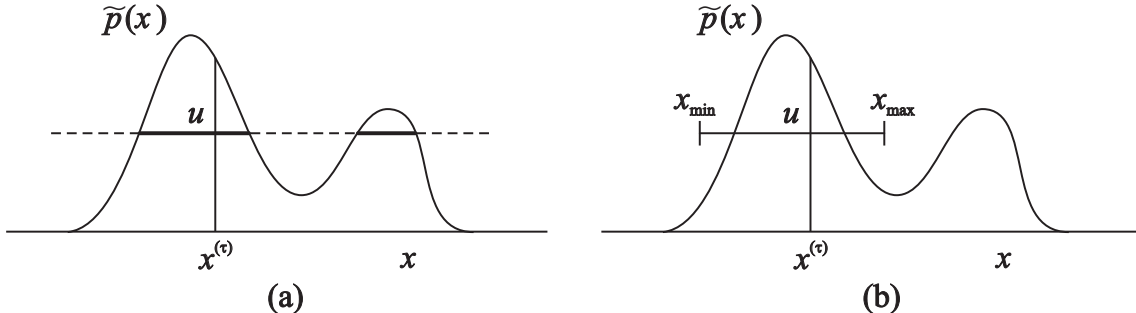


Figure 1.17: Illustration of slice sampling. (a) For a given value  $x^{(\tau)}$ , a value of  $u$  is chosen uniformly in the region  $0 \leq u \leq \tilde{p}(x^{(\tau)})$ , which defines a ‘slice’ through the distribution, shown by the solid horizontal lines. (b) Since sampling directly from a slice is infeasible, a new sample of  $x$  is drawn from a region  $x_{\min} \leq x \leq x_{\max}$  which contains the previous value  $x^{(\tau)}$ .

In practice it can be difficult to sample directly from a slice through the distribution and so instead we define a sampling scheme which leaves the uniform distribution under  $\hat{p}(x, u)$  invariant, which can be achieved by ensuring that detailed balance is satisfied. Here we consider the case of a univariate  $x$ .

Suppose the current value of  $x$  is denoted  $x^{(\tau)}$  and that we have obtained a corresponding sample  $u$ . The next value of  $x$  is sampled uniformly from a region  $x_{\min} \leq x \leq x_{\max}$  which contains

$x^{(\tau)}$ . If the sample chosen lies within the slice, in other words if  $\tilde{p}(x) > u$ , then the sample is retained and forms  $x^{(\tau+1)}$ .

It is in the choice of the region  $x_{\min} \leq x \leq x_{\max}$  that the adaptation to the characteristic length scales of the distribution takes place. We want the region to encompass as much of the slice as possible so as to allow large moves in  $x$  space, while having as little as possible of this region lying outside the slice, since this makes the sampling less efficient.

One approach to the choice of region involves starting with a region containing  $x^{(\tau)}$  having some width  $w$  and then testing each of the end points to see if they lie within the slice. If either end point does not then the region is extended in that direction by increments of value  $w$  until the endpoint lies outside the region. A candidate value  $x'$  is then chosen uniformly from this region and if it lies within the slice then it forms  $x^{(\tau+1)}$ . If it lies outside the slice then the region is shrunk such that  $x'$  forms an end point and such that the region still contains  $x^{(\tau)}$ . Then another candidate point is drawn uniformly from this reduced region and so on, until a value of  $x$  is found which lies within the slice.

Slice sampling can be applied to multivariate distributions by repeatedly sampling each variable in turn, in the manner of Gibbs sampling. This requires that we are able to compute, for each component  $x_i$ , a function which is proportional to  $p(x_i | \{x_j\}_{j \neq i})$ .

## 1.5 The Hybrid Monte Carlo Algorithm

As we have already noted, one of the major limitations of the Metropolis algorithm is that it can exhibit random walk behaviour whereby the distance traversed through the state space grows only as the square root of the number of steps. The problem cannot be resolved simply by taking bigger steps as this leads to a high rejection rate.

In this section we introduce a more sophisticated class of transitions based on an analogy with physical systems and which has the property of being able to make large changes to the system state while keeping the rejection probability small. It is applicable to distributions over continuous variables for which we can readily evaluate the gradient of the log probability with respect to the state variables. We discuss the dynamical systems framework in Section ??, and then in Section ?? we explain how this may be combined with the Metropolis algorithm to yield the powerful hybrid Monte Carlo algorithm.

### 1.5.1 Dynamical Systems

The dynamical approach to stochastic sampling has its origins in algorithms for simulating the behaviour of physical systems evolving under Hamiltonian dynamics. In a Markov chain Monte Carlo simulation the goal is to sample from a given probability distribution  $p(x)$ . The framework of Hamiltonian dynamics is exploited by casting the probabilistic simulation in the form of a Hamiltonian system. In order to remain in keeping with the literature in this area we make use of the relevant dynamical systems terminology where appropriate. This will be defined as we go along, and no background knowledge of the physical basis for this formalism is required.

The dynamics which we consider corresponds to the evolution of the state variable  $x = \{x_i\}$  under continuous time, which we denote by  $\tau$ . Classical dynamics is described by second order differential equations over time (acceleration is proportional to the applied force). We can decompose a second order equation into two coupled first order equations by introducing intermediate *momentum* variables  $r$  corresponding to the rate of change of the state variables  $x$ . Thus

$$r_i = \frac{dx_i}{d\tau} \tag{1.56}$$

where the  $x_i$  can be regarded as *position* variables in this dynamics perspective. Thus for each position variable there is a corresponding momentum variable, and the joint space of position and momentum variables is called *phase space*.

Without loss of generality we can write the probability distribution  $p(x)$  in the form

$$p(x) = \frac{1}{Z} \exp(-E(x)) \quad (1.57)$$

where  $E(x)$  is interpreted as the *potential energy* of the system when in state  $x$ . The system acceleration is the rate of change of momentum and is given by the applied *force* which itself is the negative gradient of the potential energy

$$\frac{dR_i}{d\tau} = -\frac{\partial E(x)}{\partial x_i}. \quad (1.58)$$

It is convenient to reformulate this dynamical system using the Hamiltonian framework. To do this, we first define the *kinetic energy* by

$$K(r) = \frac{1}{2} \|r\|^2 = \frac{1}{2} \sum_i r_i^2. \quad (1.59)$$

The total energy of the system is then the sum of its potential and kinetic energies

$$H(x, r) = E(x) + K(r) \quad (1.60)$$

which is called the *Hamiltonian* function. Using (??), (??), (??) and (??) we can now express the dynamics of the system in terms of the Hamiltonian equations given by

$$\frac{dx_i}{d\tau} = \frac{\partial H}{\partial r_i} \quad (1.61)$$

$$\frac{dr_i}{d\tau} = -\frac{\partial H}{\partial x_i}. \quad (1.62)$$

$$(1.63)$$

During the evolution of this dynamical system, the value of the Hamiltonian  $H$  is constant, as is easily seen by differentiation

$$\begin{aligned} \frac{dH}{d\tau} &= \sum_i \left\{ \frac{\partial H}{\partial x_i} \frac{dx_i}{d\tau} + \frac{\partial H}{\partial r_i} \frac{dr_i}{d\tau} \right\} \\ &= \sum_i \left\{ \frac{\partial H}{\partial x_i} \frac{\partial H}{\partial r_i} - \frac{\partial H}{\partial r_i} \frac{\partial H}{\partial x_i} \right\} = 0. \end{aligned} \quad (1.64)$$

A second important property of Hamiltonian dynamical systems, known as *Liouville's Theorem*, is that they preserve volume in phase space. This can be seen by noting that the flow field (rate of

change of location in phase space) is given by

$$V = \left( \frac{dx}{d\tau}, \frac{dr}{d\tau} \right) \quad (1.65)$$

and that the divergence of this field vanishes

$$\operatorname{div} V = \sum_i \left\{ \frac{\partial}{\partial x_i} \frac{\partial H}{\partial x_i} + \frac{\partial}{\partial r_i} \frac{\partial H}{\partial r_i} \right\} = \sum_i \left\{ \frac{\partial^2 H}{\partial x_i \partial r_i} - \frac{\partial^2 H}{\partial r_i \partial x_i} \right\} = 0. \quad (1.66)$$

Now consider the joint distribution over phase space whose total energy is the Hamiltonian, i.e. the distribution given by

$$p(x, r) = \frac{1}{Z_H} \exp(-H(x, r)). \quad (1.67)$$

Using the two results of conservation of volume and conservation of  $H$  it follows that the Hamiltonian dynamics will leave  $p(x, r)$  invariant. This can be seen by considering a small region of phase space over which  $H$  is approximately constant. If we follow the evolution of the Hamiltonian equations for a finite time, then the volume of this region will remain unchanged as will the value of  $H$  in this region, and hence the probability density, which is a function only of  $H$ , will also be unchanged.

Although  $H$  is invariant, the values of  $x$  and  $r$  will vary, and so by integrating the Hamiltonian dynamics over a finite time duration it becomes possible to make large changes to  $x$  in a systematic way which avoids random walk behaviour.

Evolution under the Hamiltonian dynamics will not, however, sample ergodically from  $p(x, r)$  since the value of  $H$  is constant. In order to make arrive at an ergodic sampling scheme we can introduce additional moves in phase space which change the value of  $H$  while also leaving the distribution  $p(x, r)$  invariant. The simplest way to achieve this is to replace the value of  $r$  with one drawn from its distribution conditioned on  $x$ . This can be regarded as a Gibbs sampling step, and hence from Section ?? we see that this leaves the desired distribution invariant. Noting that  $x$  and  $r$  are independent in the distribution  $p(x, r)$  we see that the conditional distribution of  $r$  is a Gaussian from which it is straightforward to sample.

In a practical application of this approach we have to address the problem of performing a numerical integration of the Hamiltonian equations. This will necessarily introduce numerical errors and so we should devise a scheme which minimizes the impact of such errors. In fact it turns out that integration schemes can be devised for which Liouville's theorem still holds exactly. This property will be important in the hybrid Monte Carlo algorithm which is discussed in Section ???. One scheme for achieving this is called the *leapfrog* discretization and involves alternately updating discrete-time approximations  $\hat{x}$  and  $\hat{r}$  to the position and momentum variables using

$$\hat{r}_i(\tau + \epsilon/2) = \hat{r}_i(\tau) - \frac{\epsilon}{2} \frac{\partial E}{\partial x_i}(\hat{x}(\tau)) \quad (1.68)$$

$$\hat{x}_i(\tau + \epsilon) = \hat{x}_i(\tau) + \epsilon \hat{r}_i(\tau + \epsilon/2) \quad (1.69)$$

$$\hat{r}_i(\tau + \epsilon) = \hat{r}_i(\tau + \epsilon/2) - \frac{\epsilon}{2} \frac{\partial E}{\partial x_i}(\hat{x}(\tau + \epsilon)). \quad (1.70)$$

We see that this takes the form of a half-step update of the momentum variables with step size  $\epsilon/2$ , followed by a full-step update of the position variables with step size  $\epsilon$ , followed by a second half-step update of the momentum variables. If several leapfrog steps are applied in succession, it can be seen that half-step updates to the momentum variables can be combined into full-step updates with step size  $\epsilon$ . The successive updates to position and momentum variables then leapfrog over each other. In order to advance the dynamics by a time interval  $\tau$  we need to take  $\tau/\epsilon$  steps. The error involved in the discretized approximation to the continuous time dynamics will go to zero, assuming a smooth function  $E(x)$ , in the limit  $\epsilon \rightarrow 0$ . However, for a non-zero  $\epsilon$  as used in practice, some residual error will remain. We shall see in Section ?? how the effects of such errors can be eliminated in the hybrid Monte Carlo algorithm.

In summary then, the Hamiltonian dynamical approach involves alternating between a series of leapfrog updates and a re-sampling of the momentum variables from their marginal distribution.

Note that the Hamiltonian dynamics method, unlike the basic Metropolis algorithm, is able to make use of information about the gradient of the log probability distribution as well as about the distribution itself. An analogous situation is familiar from the domain of function optimization. In most cases where gradient information is available it is highly advantageous to make use of it. Informally, this follows from the fact that in a space of dimension  $d$  the additional computational cost of evaluating a gradient compared to evaluating the function itself will typically be a fixed factor independent of  $d$ , whereas the gradient vector conveys  $d$  pieces of information compared to the one piece of information given by the function itself.

### 1.5.2 Hybrid Monte Carlo

As we discussed in the previous section, for a non-zero step size  $\epsilon$  the discretization of the leapfrog algorithm will introduce errors into the integration of the Hamiltonian dynamical equations. Hybrid Monte Carlo combines Hamiltonian dynamics with the Metropolis algorithm and thereby removes any bias associated with the discretization.

Specifically, the algorithm uses a Markov chain consisting of alternate stochastic updates of the momentum variables  $r$  and Hamiltonian dynamical updates using the leapfrog algorithm. After each application of the leapfrog algorithm the resulting candidate state is accepted or rejected according to the Metropolis criterion based on the value of the Hamiltonian  $H$ . Thus if  $(x, r)$  is the initial state and  $(x^*, r^*)$  is the state after the leapfrog integration, then this candidate state is accepted with probability

$$\min(1, \exp\{H(x, r) - H(x^*, r^*)\}). \quad (1.71)$$

If the leapfrog integration were to simulate the Hamiltonian dynamics perfectly, then every such candidate step would automatically be accepted since the value of  $H$  would be unchanged. Due to numerical errors, the value of  $H$  may sometimes decrease, and we would like the Metropolis criterion to remove any bias due to this effect and ensure that the resulting samples are indeed drawn from the required distribution. In order for this to be the case, we need to ensure that the update equations corresponding to the leapfrog integration satisfy detailed balance (??). This is easily achieved by modifying the leapfrog scheme as follows. Before the start of each leapfrog integration sequence we choose at random, with equal probability, whether to integrate forwards in time (using step size  $\epsilon$ ) or backwards in time (using step size  $-\epsilon$ ). We first note that the leapfrog integration scheme (??)-(??) is time-reversible, so that integration for  $L$  steps using stepsize  $-\epsilon$  will exactly undo the effect of integration for  $L$  steps using stepsize  $\epsilon$ .

Next we show that the leapfrog integration preserves phase space volume exactly. This follows from the fact that each step in the leapfrog scheme updates either the  $x_i$  variable or the  $r_i$  variable by an amount which is a function only of the other variable. As shown in Figure ?? this has the

effect of shearing a region of phase space while not altering its volume.

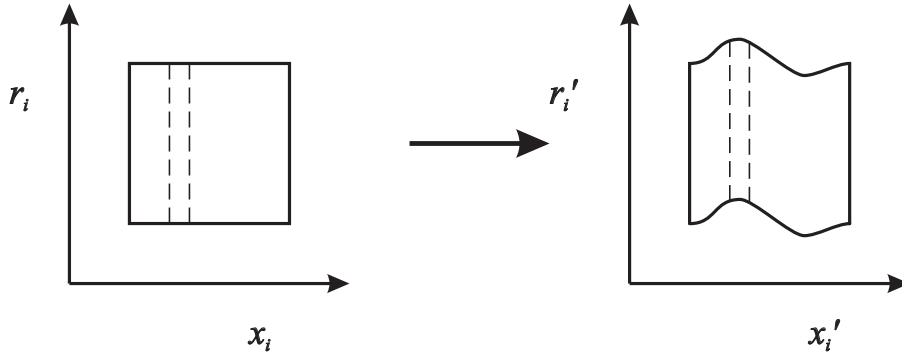


Figure 1.18: Each step of the leapfrog algorithm (??)–(??) modifies either a position variable  $x_i$  or a momentum variable  $r_i$ . Since the change to one variable is a function only of the other, any region in phase space will be sheared without change of volume.

Finally, we use these results to show that detailed balance holds. Consider a small region  $\mathcal{R}$  of phase space which, under a sequence of  $L$  leapfrog iterations of step size  $\epsilon$ , maps to a region  $\mathcal{R}'$ . Using conservation of volume under the leapfrog iteration we see that if  $\mathcal{R}$  has volume  $\delta V$  then so too will  $\mathcal{R}'$ . If we choose an initial point from the distribution (??) and then update using  $L$  leapfrog interactions, the probability of the transition going from  $\mathcal{R}$  to  $\mathcal{R}'$  is given by

$$\frac{1}{Z_H} \exp(-H(\mathcal{R})) \delta V \frac{1}{2} \min \{1, \exp(-H(\mathcal{R}) + H(\mathcal{R}'))\}. \quad (1.72)$$

where the factor of  $1/2$  arises from the probability of choosing to integrate with a positive step size rather than a negative one. Similarly, the probability of starting in region  $\mathcal{R}'$  and integrating backwards in time to end up in region  $\mathcal{R}$  is given by

$$\frac{1}{Z_H} \exp(-H(\mathcal{R}')) \delta V \frac{1}{2} \min \{1, \exp(-H(\mathcal{R}') + H(\mathcal{R}))\}. \quad (1.73)$$

It is easily seen that the two probabilities (??) and (??) are equal, and hence detailed balance holds<sup>2</sup>.

It is not difficult to construct examples for which the leapfrog algorithm returns to its starting position after a particular number of iterations. In such cases the random replacement of the momentum values before each leapfrog integration will not be sufficient to ensure ergodicity since the position variables will never be updated. Such phenomena are easily avoided by choosing the magnitude of the step size at random from some small interval, before each leapfrog integration.

We can gain some insight into the behaviour of the hybrid Monte Carlo algorithm by considering its application to a multivariate Gaussian. For convenience consider a Gaussian distribution  $p(x)$  with independent components, for which the Hamiltonian is given by

$$H(x, r) = \frac{1}{2} \sum_i \frac{1}{\sigma_i^2} x_i^2 + \frac{1}{2} \sum_i r_i^2. \quad (1.74)$$

Our conclusions will be equally valid for a Gaussian distribution having correlated components

---

<sup>2</sup>This proof ignores any overlap between the regions  $\mathcal{R}$  and  $\mathcal{R}'$ , but is easily generalized to allow for such overlap.

since the hybrid Monte Carlo algorithm exhibits rotational isotropy. During the leapfrog integration each pair of phase space variables  $x_i, r_i$  evolves independently. However, the acceptance or rejection of the candidate point is based on the value of  $H$  which depends on the values of all of the variables. Thus, a significant integration error in any one of the variables could lead to a high probability of rejection. In order that the discrete leapfrog integration be a reasonably good approximation to the true continuous-time dynamics it is necessary for the leapfrog integration scale  $\epsilon$  to be smaller than the shortest length-scale over which the potential is varying significantly. This is governed by the smallest value of  $\sigma_i$  which we denote by  $\sigma_{\min}$ . Recall that the goal of the leapfrog integration in hybrid Monte Carlo is move to a substantial distance through phase space to a new state which is relatively independent of the initial state and still achieve a high probability of acceptance. In order to achieve this the leapfrog integration must be continued for a number of iterations of order  $\sigma_{\max} / \sigma_{\min}$ .

By contrast, consider the behaviour of a simple Metropolis algorithm with an isotropic Gaussian proposal distribution of variance  $s^2$ . In order to avoid high rejection rates the value of  $s$  must be of order  $\sigma_{\min}$ . The exploration of state space then proceeds by a random walk, and takes of order  $(\sigma_{\max} / \sigma_{\min})^2$  steps to arrive at a roughly independent state.

## 1.6 Estimating the Partition Function

As we have seen, most of the sampling algorithms considered in this chapter require only the functional form of the probability distribution up to a multiplicative constant. Thus if we write

$$p_E(x) = \frac{1}{Z_E} \exp(-E(x)) \quad (1.75)$$

then the value of the partition function  $Z$  is not needed in order to draw samples from  $p(x)$ . However, knowledge of the value of  $Z$  can be useful for Bayesian model comparison, and so it is of interest to consider how its value might be obtained. We assume that direct evaluation by summing, or integrating, the function  $\exp(-E(x))$  over the state space of  $x$  is intractable.

For model comparison it is actually the ratio of the partition functions for two models which is required. Multiplication of this ratio by the ratio of prior probabilities gives the ratio of posterior probabilities, which can then be used for model selection or model averaging.

One way to estimate a ratio of partition functions is to use importance sampling from a distribution with energy function  $G(x)$

$$\begin{aligned} \frac{Z_E}{Z_G} &= \frac{\sum_x \exp(-E(x))}{\sum_x \exp(-G(x))} \\ &= \frac{\sum_x \exp(-E(x) + G(x)) \exp(-G(x))}{\sum_x \exp(-G(x))} \\ &= \langle \exp(-E + G) \rangle_G \\ &\simeq \sum_i \exp(-E(x_i) + G(x_i)) \end{aligned} \quad (1.76)$$

where  $\{x_i\}$  are samples drawn from the distribution defined by  $p_G(x)$ . If the distribution  $p_G$  is one for which the partition function can be evaluated analytically, for example a Gaussian, then the

absolute value of  $Z_E$  can be obtained.

This approach will only yield accurate results if the importance sampling distribution  $p_G$  is closely matched to the distribution  $p_E$ , so that the ratio  $E(x)/G(x)$  does not have wide variations. In practice suitable analytically specified importance sampling distributions cannot readily be found for the kinds of complex models considered in this book.

An alternative approach is therefore to use the samples obtained from a Markov chain to define the importance sampling distribution. If the transition probability for the Markov chain is given by  $T(x, x')$ , and the sample set is given by  $x_1, \dots, x_N$ , then the sampling distribution can be written as

$$\frac{1}{Z_G} \exp(-G) = \sum_{n=1}^N T(x_n, x) \quad (1.77)$$

which can be used directly in (??).

Methods for estimating the ratio of two partition functions require for their success that the two corresponding distributions be reasonably closely matched. This is especially problematic if we wish to find the absolute value of the partition function for a complex distribution since it is only for relatively simple distributions that the partition function can be evaluated directly, and so attempting to estimate the ratio of partition functions directly is unlikely to be successful. This problem can be tackled using a technique known as *chaining* which involved introducing a succession of intermediate distributions  $P_2, \dots, P_{M-1}$  which interpolate between a simple distribution  $P_1(x)$  for which we can evaluate the normalization  $Z_1$ , and the desired complex distribution  $P_M(x)$ . We then have

$$\frac{Z_M}{Z_1} = \frac{Z_2}{Z_1} \frac{Z_3}{Z_2} \dots \frac{Z_M}{Z_{M-1}} \quad (1.78)$$

in which the intermediate ratios can be determined using Monte Carlo methods as discussed above. One way to construct such a sequence of intermediate systems is to use an energy function containing a continuous parameter  $0 \leq \alpha \leq 1$  which interpolates between the two distributions

$$E_\alpha(x) = (1 - \alpha)E_1(x) + \alpha E_M(x). \quad (1.79)$$

If the intermediate ratios in (??) are to be found using Monte Carlo, it may be more efficient to use a single Markov chain run than to restart the Markov chain for each ratio. In this case the Markov chain is run initially for the system  $P_1$  and then after some suitable number of steps moves on to the next distribution in the sequence. Note, however, that the system must remain close to the equilibrium distribution at each stage.

## 1.7 Simulated Annealing

In order to apply sampling methods to inference tasks involving graphical models, a variety of matters must be addressed. Our goal here is not to provide an extensive practitioners manual, but rather to highlight some of the more significant issues.

Since a Markov chain takes some time to reach its equilibrium distribution it is common to discard the values obtained from the early part of the chain (called the ‘burn in’ period). This highlights an important trade-off in running Markov chain samplers with limited computational resources. For the same computational expense it will be possible to run one long Markov chain,

or alternatively several short ones. With a single chain there is only one burn in period. However, such a chain may become stuck exploring a relatively isolated region of the distribution while failing to discover other regions of significant probability.

An important concern in practice is the speed of convergence of a Markov chain to its equilibrium distribution, as well as the decorrelation time between independent samples. This can become particularly problematic in situations where the distribution has relatively isolated regions of high probability such that transitions from one region to another are infrequent. One technique for addressing this problem is called *simulated annealing*. Consider the problem of sampling from a distribution of the form

$$p(x) = \frac{1}{Z} \exp(-E(x)). \quad (1.80)$$

We first modify the distribution by introduction of a *temperature* parameter  $T$  to give

$$p(x) = \frac{1}{Z(T)} \exp(-E(x)/T) \quad (1.81)$$

so that the original distribution corresponds to  $T = 1$ . The effect of using values of  $T > 1$  is to deemphasize the dynamic range between regions of high and low probability and hence increase the probability of transition from one high probability region to another through an intervening region of low probability. During the course of the simulation the value of  $T$  is gradually reduced from a high value down to  $T = 1$ . Note that this procedure no longer samples from the correct distribution, but it may be used to locate a region of high probability, after which the simulation is continued using  $T = 1$  to allow samples from the correct distribution to be obtained. The method can also be used as an optimization technique in which  $T$  is gradually reduced to zero, so that the samples converge onto a (local) minimum of the function  $E(x)$ .

A variant of the simulated annealing approach involves decomposing the energy function  $E(x)$  into the sum of a term  $E_0(x)$  which has nice properties (for example it may be separable or it may be a convex function) and a term  $E_1(x)$  which represents the difference between  $E_0(x)$  and the true energy  $E(x)$ . Samples are then drawn from the distribution

$$p(x) = \frac{1}{Z(T)} \exp(-E_0(x) + E_1(x)/T) \quad (1.82)$$

with initially  $T \gg 1$ , and again  $T$  is gradually reduced to 1. For example  $E_0(x)$  may correspond to the prior, and  $E_1(x)$  may represent the contribution from the likelihood function.

An important consideration in the use of simulated annealing is the choice of annealing schedule for the reduction in  $T$ . In the simplest case this is pre-defined, for example a geometric reduction in  $T$  obtained by multiplying  $T$  by a fixed constant  $0 < \alpha < 1$  after each iteration, although in more sophisticated approaches the reduction in  $T$  may be governed by the observed sequence of sampled values.

Although simulated annealing does not quite sample from the correct distribution, the related technique of *simulated tempering* avoids this problem. It involves the introduction of a fixed set of temperature values of which  $T = 1$  is the lowest. The state of the temperature becomes a stochastic variable and is itself sampled as part of the Markov chain, and a modification to the energy function encourages the system to spend roughly equal times at the different temperatures. At higher temperature values the system can move more freely from one region of state space to another, whereas when the system has temperature  $T = 1$  the state space samples are drawn from the required distribution.

## 1.8 Historical Remarks and Bibliography

Markov chain Monte Carlo methods have their origins in physics, and it was only towards the end of the 1980s that they started to have significant impact in the field of statistics. The first published paper to describe the Monte Carlo methods was ?), and the Metropolis algorithm was introduced by ?). An important contribution by ?) showed that the Metropolis algorithm, and its generalization the Metropolis-Hastings algorithm, are members of a large family of possible algorithms.

The logic sampling method for directed graphs with evidence was introduced by ?). Likelihood weighted sampling was proposed by ?), and also by ?) who also proposed the ‘self-importance’ sampling and ‘Markov blanket scoring’ extensions.

Adaptive rejection sampling was developed by ?) and extended to the derivative-free case by ?). The adaptive rejection Metropolis sampling technique for non log-concave distributions is described in ?).

The particle filtering, or sequential Monte Carlo, approach has appeared in the literature under various names including the *bootstrap filter* (?), *survival of the fittest* (?) and *condensation* (?). It has been applied to Markov decision processes by ?).

Gibbs sampling was popularized by the work of ?), and the BUGS software, which builds heavily on the Gibbs sampling framework, is described in ?). The technique of blocking Gibbs was proposed by ?).

Slice sampling was introduced by ?), who also provides a proof that it samples from the desired distribution. The hybrid Monte Carlo algorithm was introduced originally in the physics literature by ?), and later applied to Bayesian inference for neural networks by ?).

Diagnostic tests for convergence of Markov chain Monte Carlo algorithms are summarized in Chapter 8 of ?).

There are numerous texts dealing with Monte Carlo methods. Those of particular interest from the statistical inference perspective include ?, ?, ?, ?, ?, ?, ?, ?) and ?). Also there are review articles by ?, ?, ?, ?, ?, ?, ?, ?) and ?) which provide additional information on sampling methods for statistical inference.

## Exercises

- 1.1(\*) Show that the finite sample estimator (??) has mean  $\langle f \rangle$  and variance  $\sigma^2/L$  where  $\sigma^2$  is defined by (??).
- 1.2(\*) Let  $x$  be a  $d$ -dimensional random variable having a Gaussian distribution with zero mean and unit covariance matrix, and suppose that the positive definite symmetric matrix  $\Sigma$  has the Cholesky decomposition  $\Sigma L L^T$ . Show that the variable  $y = \mu + Lx$  has a Gaussian distribution with mean  $\mu$  and covariance  $\Sigma$ . This provides a technique for generating samples from a general multivariate Gaussian using samples from a univariate Gaussian having zero mean and unit variance.
- 1.3(\*) Suppose that  $z$  has a uniform distribution over the interval  $[0, 1]$ . Show that the variable  $x = b \tan z + c$  has a Cauchy distribution given by (??).
- 1.4(\*\*) Determine expressions for the coefficients  $k_i$  in the envelope distribution (??) for adaptive rejection sampling using the properties of continuity and normalization. Hence determine a scheme for sampling from this distribution.
- 1.5(\*) Use the sum and product rules of probability to verify directly the conditional independence properties  $p(x_{t+1}|x_t, y_{(t)}) = p(x_{t+1}|x_t)$  and  $p(y_t|x_t, y_{(t-1)}) = p(y_t|x_t)$  for the graph in Figure ??.

**1.6(\*)** Show that the simple random walk over the integers defined by (??) has the property that  $\langle x_n^2 \rangle = \langle x_{n-1}^2 \rangle + 1/2$  and hence by induction that  $\langle x_n^2 \rangle = n/2$ .

**1.7(\*\*)** Show that the Gibbs sampling algorithm, discussed in Section ??, satisfies detailed balance as defined by (??).

**1.8(\*\*)** Consider the simple 3-node graph shown in Figure ?? in which the observed node  $x$  is given by a Gaussian distribution  $\mathcal{N}(x|\mu, \tau)$  with mean  $\mu$  and precision  $\tau$ . Suppose that the

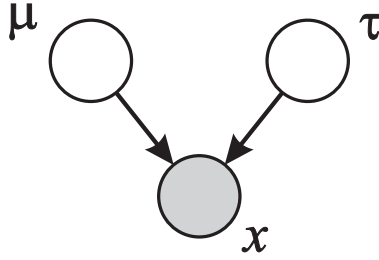


Figure 1.19: A graph involving an observed Gaussian variable  $x$  with prior distributions over its mean  $\mu$  and precision  $\tau$ .

marginal distributions over the mean and precision are given by  $\mathcal{N}(\mu|\mu_0, s_0)$  and  $\text{Gam}(\tau|a, b)$ , where  $\text{Gam}(\cdot|a, b)$  denotes a Gamma distribution. Write down expressions for the conditional distributions  $p(\mu|x, \tau)$  and  $p(\tau|x, \mu)$  which would be required in order to apply Gibbs sampling from the posterior distribution  $p(\mu, \tau|x)$ .

**1.9(\*)** Verify that the over relaxation update (??), in which  $x_i$  has mean  $\mu_i$  and variance  $\sigma_i$ , and where  $\nu$  has zero mean and unit variance, gives a value  $x'_i$  with mean  $\mu_i$  and variance  $\sigma_i^2$ .

## 1 Ergodicity of Markov Chains

In this appendix we show that a homogeneous Markov chain will be ergodic, subject only to a weak restriction on the invariant distribution and the transition probabilities.

**Theorem .1** Consider a transition probability  $T(x', x)$  defining the relation between the marginal probabilities of  $x$  at subsequent steps of a Markov chain

$$p_{m+1}(x) = \sum_{x'} T(x', x)p_m(x'). \quad (83)$$

together with a particular distribution  $p^*(x)$  which is an invariant distribution of  $T(x', x)$  and which is such that

$$\nu = \min_x \min_{\{x' : p^*(x') > 0\}} \frac{T(x, x')}{p^*(x)} > 0. \quad (84)$$

The corresponding Markov chain will be ergodic, so that for any choice of initial distribution  $p_0(x)$

$$\lim_{m \rightarrow \infty} p_m(x) = p^*(x). \quad (85)$$

**Proof:** The proof uses induction to show that the distribution at step  $m$  can be written as a mixture of the invariant distribution and some other distribution. At each step the proportion of the invariant component cannot decrease, while the condition (??) ensures that the remaining component will generate some contribution to the invariant component.

We suppose that at step  $m$  the following holds

$$p_m(x) = [1 - (1 - \nu)^m]p^*(x) + (1 - \nu)^m r_m(x) \quad (86)$$

where  $r_m(x)$  is an arbitrary non-negative and normalized function, which can represent a valid probability distribution. Since we cannot have  $p^*(x' \text{ prime}) < T(x', x)$  for all  $x'$ , we must have  $\nu < 1$ , and so  $p_m(x)$  is a convex combination of two distributions and hence is also a valid probability distribution. The result (??) clearly holds for  $m = 0$ , with  $r_0(x) = p_0(x)$ . We now show that the equivalent result must hold at step  $m + 1$ . Using (??) we have

$$\begin{aligned} p_{m+1}(x) &= \sum_{x'} p_m(x')T(x', x) \\ &= [1 - (1 - \nu)^m] \sum_{x'} p^*(x')T(x', x) + (1 - \nu)^m \sum_{x'} r_m(x')T(x', x) \\ &= [1 - (1 - \nu)^m]p^*(x) + (1 - \nu)^m \sum_{x'} r_m(x') \{T(x', x) - \nu p^*(x) + \nu p^*(x)\} \\ &= [1 - (1 - \nu)^{m+1}]p^*(x) + (1 - \nu)^{m+1} \sum_{x'} r_m(x') \frac{T(x', x) - \nu p^*(x)}{1 - \nu} \\ &= [1 - (1 - \nu)^{m+1}]p^*(x) + (1 - \nu)^{m+1}r_{m+1}(x) \end{aligned} \quad (87)$$

where we have defined

$$r_{m+1}(x) = \sum_{x'} r_m(x') \frac{T(x', x) - \nu p^*(x)}{1 - \nu}. \quad (88)$$

Clearly  $\sum_x r_{m+1}(x) = 1$ , and from (??) we have  $r_{m+1}(x) \geq 0$ , so that  $r_{m+1}(x)$  therefore represents a probability distribution.  $\square$

This theorem easily generalizes to Markov chains over continuous state spaces.

# Graphical models, exponential families, and variational inference

Martin J. Wainwright  
Department of Electrical Engineering  
and Computer Science  
University of California, Berkeley  
`martinw@eecs.berkeley.edu`

Michael I. Jordan  
Division of Computer Science  
Department of Statistics  
University of California, Berkeley  
`jordan@stat.berkeley.edu`

July 29, 2003

## 1 Introduction

Graphical models bring together graph theory and probability theory in a powerful formalism for multivariate statistical modeling. In applied fields such as bioinformatics, speech processing, image processing and control theory, statistical models have long been formulated in terms of graphs, and algorithms for computing basic statistical quantities such as likelihoods and score functions have often been expressed in terms of recursions operating on these graphs—examples include phylogenies, pedigrees, hidden Markov models, Markov random fields, and Kalman filters. These ideas can be understood, unified and generalized within the formalism of graphical models. Indeed, the graphical model formalism provides a natural tool for formulating variations on these classical architectures, and for exploring entirely new families of statistical models. In fields that involve the study of large numbers of interacting variables, graphical models are increasingly in evidence.

Graph theory plays an important role in many computationally-oriented fields, including combinatorial optimization, statistical physics and economics. Beyond its role as a language for formulating models, graph theory also plays a fundamental role in these fields in helping to reveal what is computationally feasible and what is not. In particular, the running times of algorithms or the magnitude of an error bound can often be characterized in terms of structural properties of a graph. This is also true in the graphical model formalism. As we will show, the computational complexity of a basic algorithm known as the *junction tree algorithm*—an algorithm which generalizes many of the probabilistic recursions on graphs cited above—can be characterized in terms of a natural graph-theoretic measure of interaction among variables. For suitably sparse graphs, the junction tree algorithm provides a systematic solution to the problem of computing likelihoods and other marginal probabilities on graphs.

Unfortunately, many graphical models of practical interest are not “suitably sparse,” and the junction tree algorithm does not provide a viable computational framework for these models. One popular source of methods for attempting to cope with such cases is the *Markov chain Monte Carlo* (MCMC) framework, and indeed there is a significant literature on the application of MCMC methods to graphical models [11, ?]. Our focus in the current paper, however, is different—we present an alternative approach to statistical inference that is based on *variational methods*. Variational methods provide a general class of alternatives to MCMC, and have applications outside of the graphical model framework. As we will see, however, they are particularly natural in their application to graphical models, due to their relationships with the structural properties of graphs.

The phrase “variational” is an umbrella term that refers to mathematical tools for formulating problems as optimization problems, as well as associated techniques for their solution. The general idea is to express a quantity of interest as the solution of an optimization problem. We then “relax” the optimization problem in various ways, either by approximating the function to be optimized or by approximating the set over which the optimization takes place. Such relaxations are a fertile source for approximation methods.

Both MCMC methods and variational methods have their roots in physics, in particular in statistical physics, and indeed their successful deployment in statistical physics motivated and predated their entry into statistics. The development of specifically-statistical MCMC methodology has, however, played an important role in sparking widespread application of such methods in statistics [43]. A similar development in the case of variational methodology would be of significant interest. In our view, the most promising way to achieve such a specifically-statistical variational methodology is to build on existing links between variational analysis and the exponential family of distributions [5, 18, 36]. Indeed, notions of convexity that are at the heart of the statistical theory of the exponential family have immediate implications for the design of variational relaxations. Moreover, these variational relaxations have particularly interesting algorithmic consequences in the setting of graphical models, where they again lead to recursions on graphs.

Thus we present a story with three interrelated themes. We begin by discussing graphical models, providing an overview of the general mathematical framework in Section 2 and presenting several examples. All of these examples, as well as the majority of current applications of graphical models, involve distributions in the exponential family. Thus in Section 3 we turn to a discussion of exponential families, focusing on the mathematical links to convex analysis, and thus anticipating our development of variational methods. In particular, the principal object of interest in our exposition is a certain conjugate dual function associated with exponential families. Building on the foundation of conjugate duality, we develop a general variational representation for marginal probabilities in exponential families in Section 4. Most of the remainder of the paper—Sections 5 through 9—is devoted to the exploration of various relaxations of this variational representation, relaxations which yield various algorithms for computing approximations to marginal probabilities. In more detail, we discuss *mean field theory* in Section 5, the *Bethe approximation* in Section 6, and general *cluster variational methods* based on hypertrees, including the *Kikuchi method*, in Section 7. All of these methods are non-convex relaxations. In Sections 8 and 9 we turn to convex relaxations of the variational principle. Finally, in Section 10, we develop a variational formulation of the problem of computing modes of distributions, and again describe various relaxations of this exact variational principle.

We have a limited focus in this paper—we are concerned with the problem of computing marginal probabilities (including likelihoods), and the problem of computing modes of distributions, for distributions represented as graphical models. We refer to such problems as problems of “probabilistic inference,” or “inference” for short. As with presentations of MCMC methods, such a limited focus may appear to aim most directly at applications in Bayesian statistics. While Bayesian statistics is indeed a natural terrain for deploying many of the methods that we present here, we see these methods as having applications throughout statistics, within both the frequentist and Bayesian paradigms, and we will attempt to indicate some of these applications at various junctures in the paper.

## 2 Background

### 2.1 Graphical models

A graphical model consists of a collection of probability distributions<sup>1</sup> that factorize according to the structure of an underlying graph. A graph  $G = (V, E)$  is formed by a collection of vertices  $V$ , and a collection of edges  $E$ . An edge consists of a pair of vertices, and may either be directed or undirected. Associated with each vertex  $s \in V$  is a random variable  $x_s$  taking values in some set  $\mathcal{X}_s$ , which may either be continuous (e.g.,  $\mathcal{X}_s = \mathbb{R}$ ) or discrete (e.g.,  $\mathcal{X}_s = \{0, 1, \dots, m - 1\}$ ). For any subset  $A$  of the vertex set  $V$ , we define  $x_A := \{x_s \mid s \in A\}$ .

**Directed graphical models:** In the directed case, each edge is directed from parent to child. We let  $\pi(s)$  denote the set of all parents of given node  $s \in V$ . (If  $s$  has no parents, then the set  $\pi(s)$  should be understood to be empty). With this notation, a *directed graphical model* consists of a collection of probability distributions that factorize in the following way:

$$p(\mathbf{x}) = \prod_{s \in V} p(x_s \mid x_{\pi(s)}). \quad (1)$$

Note that our use of notation is consistent, in that  $p(x_s \mid x_{\pi(s)})$  is, in fact, the conditional distribution for the global distribution  $p(\mathbf{x})$  thus defined.

**Undirected graphical models:** In the undirected case, the probability distribution factorizes according to functions defined on the *cliques* of the graph (i.e., fully-connected subsets of  $V$ ). In particular, associated with each clique  $C$  is a *compatibility function*  $\psi_C : \mathcal{X}^n \rightarrow \mathbb{R}_+$  that depends *only* on  $x_C$ . With this notation, an *undirected graphical model* (also known as a *Markov random field*) consists of a collection of distributions that factorize as follows:

$$p(\mathbf{x}) = \frac{1}{Z} \prod_C \psi_C(x_C), \quad (2)$$

where the product is taken over all cliques of the graph. The quantity  $Z$  is a constant chosen to ensure that the distribution is normalized. In contrast to the directed case (1), in general the compatibility functions  $\psi_C$  need not have any obvious or direct relation to local marginal distributions.

### 2.2 Conditional independence

Families of probability distributions as defined as in (1) or (2) also have a characterization in terms of conditional independencies among subsets of random variables. We briefly mention this characterization here but do not elaborate, as it is not needed in the remainder of the paper. See [61] for a full treatment.

Consider first the case of undirected graphical models. For all disjoint subsets of vertices  $A$ ,  $B$  and  $C$ , we assert that  $x_A$  is independent of  $x_B$  given  $x_C$ , if there is no path from a vertex in  $A$  to a vertex in  $B$  when we remove the vertices  $C$  from the graph. Thus we associate conditional independence with a graph-theoretic notion of *reachability*.

---

<sup>1</sup>Here we are using the terminology “distribution” loosely; our notation  $p(\cdot)$  should be understood as a mass function (density with respect to counting measure) in the discrete case, and a density with respect to Lebesgue measure in the continuous case.

Ranging over all possible choices of subsets  $A$ ,  $B$  and  $C$ , we obtain a list of conditional independence assertions. It is possible to show that this list is consistent (i.e., there exist probability distributions that satisfy all of these assertions), and that indeed the set of probability distributions that satisfy all assertions on the list is exactly the set of probability distributions defined by (2) (where we range over all possible choices of compatibility functions).

Thus there are two equivalent characterizations of the family of probability distributions associated with an undirected graph. This is a fundamental mathematical result, linking an algebraic concept (factorization) and a graph-theoretic concept (reachability). The result also has algorithmic consequences, in that it reduces the problem of assessing conditional independence to the problem of assessing reachability on a graph, a problem that is readily solved using simple breadth-first search algorithms [23].

An analogous result holds in the case of directed graphical models, with the only alteration being a different notion of reachability [61]. Once again it is possible to establish the equivalence between two characterizations of families of probability distributions—that given by (1) and one given in terms of a set of conditional independence assertions.

### 2.3 Inference problems and exact algorithms

Given a probability distribution  $p(\cdot)$  defined by a graphical model, our focus will be solving one or more of the following *inference problems*:

- (a) computing the likelihood of observed data.
- (b) computing the marginal distribution  $p(x_A)$  over a particular subset  $A \subset V$  of nodes.
- (c) computing the conditional distribution  $p(x_A | x_B)$ , for disjoint subsets  $A$  and  $B$ , where  $A \cup B$  is in general a proper subset of  $V$ .
- (d) computing a mode of the density (i.e.,  $\hat{\mathbf{x}} \in \arg \max_{\mathbf{x} \in \mathcal{X}^n} p(\mathbf{x})$ ).

From a computational perspective, problems (a) and (b) are essentially equivalent, since they both involve summing or integrating over a subset of random variables. Moreover, the computation of a conditional probability in (c) also involves marginalization, requiring marginalization to obtain the numerator  $p(x_A, x_B)$ , and a further marginalization to obtain the denominator  $p(x_B)$ . Thus the computational complexity is that associated with obtaining the marginal probability in the denominator. In contrast, the problem of computing modes stated in (d) is fundamentally different, since it entails maximization rather than integration. Nonetheless, our variational development in the sequel will highlight some important connections between the problem of computing marginals and that of computing modes.

To understand the challenges inherent in these inference problems, consider the case of a discrete random vector  $\mathbf{x} \in \mathcal{X}^n$ , where  $\mathcal{X}_s = \{0, 1, \dots, m - 1\}$  for each vertex  $s \in V$ . A naive approach to computing a marginal at a single node—say  $p(x_s)$ —entails summing over all configurations of the form  $\{\mathbf{x}' \mid x'_s = x_s\}$ . Since this set has  $m^{n-1}$  elements, it is clear that a brute force approach will rapidly become intractable. Even with binary variables ( $m = 2$ ) and a graph with  $n \approx 400$  nodes (a modest size for many applications), this summation involves more terms than atoms in the visible universe. Similarly, in this discrete case, computing a mode entails solving an integer programming problem over an exponential number of configurations. For continuous random vectors, the problems are no easier<sup>2</sup> and typically harder, since they require computing a large number of integrals.

---

<sup>2</sup>The Gaussian case is an important exception to this statement.

For graphs without cycles—also known as *trees*—these inference problems can be solved exactly by recursive “message-passing” algorithms of a dynamic programming nature, with a computational complexity that scales only linearly in the number of nodes. In particular, for the case of computing marginals, the dynamic programming solution takes the form of a general algorithm known as the *sum-product algorithm*, whereas for the problem of computing modes it takes the form of an analogous algorithm known as the *max-product algorithm*. We describe these algorithms in Section 2.5.1. More generally, as we discuss in Section 2.5.2, the *junction tree algorithm* provides a solution to inference problems for arbitrary graphs. The junction tree algorithm has a computational complexity that is exponential in a quantity known as the *treewidth* of the graph.

Before turning to these algorithmic issues, however, we present some examples of applications of graphical models.

## 2.4 Applications

This section illustrates the use of graphical models in various application areas, including the general area of Bayesian hierarchical modeling, as well as specific applications in bioinformatics, speech and language processing, image processing and error-correcting coding.

### 2.4.1 Bioinformatics and language

Many classical models in the fields of bioinformatics and language processing are instances of graphical models, and the graphical model formalism is also often invoked in the design of new models in these fields. In this section we briefly review some instances of graphical models in bioinformatics and language processing, both classical and recent.

Sequential data obviously play a central role in bioinformatics and language, and the workhorse underlying the modeling of sequential data is the same in both domains—the *hidden Markov model* (HMM) shown in Figure 1(a). The HMM is in essence a dynamical version of a finite mixture

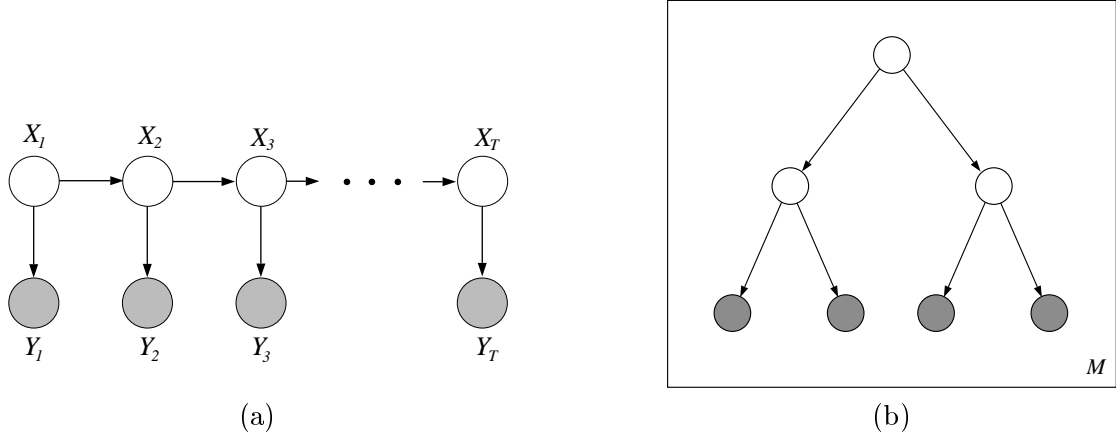


**Figure 1.** (a) The graphical model representation of a generic hidden Markov model. The shaded nodes are the observations and the unshaded nodes are the hidden state variables. The latter form a Markov chain, in which  $X_s$  is independent of  $X_u$  conditional on  $X_t$ , where  $s < t < u$ . (b) The graphical model representation of a phylogeny on four extant organisms and  $M$  sites. The tree encodes the assumption that there is a first speciation event and then two further speciation events that lead to the four extant organisms. The box around the tree (a “plate”) is a graphical model representation of replication; here representing the assumption that the  $M$  sites evolve independently.

model, in which observations are generated conditionally on a underlying latent (“hidden”) state

variable. The state variables, which are generally taken to be multinomial random variables,<sup>3</sup> form a Markov chain.

Applying the junction tree formalism to the HMM yields an algorithm that passes messages in both directions along the chain of state variables, and computes the marginal probabilities  $p(x_t, x_{t+1} | y)$  and  $p(x_t | y)$ . In the HMM context, this algorithm is often referred to as the *forward-backward algorithm*. These marginal probabilities are often of interest in and of themselves, but are also important in their role as expected sufficient statistics in an expectation-maximization (EM) algorithm for estimating the parameters of the HMM. Similarly, the maximum a posteriori state sequence can also be computed by the junction tree algorithm (with summation replaced by maximization)—in the HMM context the resulting algorithm is generally referred to as the *Viterbi algorithm*.

Gene-finding provides an important example of the application of the HMM [34]. To a first order of approximation, the genomic sequence of an organism can be segmented into regions containing genes, as well as intergenic regions separating the genes, with a gene being defined as a sequence of nucleotides that can be further segmented into meaningful intragenic structures (exons and introns). The boundaries between these segments are highly stochastic and difficult to find reliably. HMMs are currently the methodology of choice for attacking this problem, with designers choosing states and state transitions to reflect biological knowledge concerning gene structure [19].

HMMs are also widely used to model aspects of protein structure. For example, membrane proteins are specific kinds of proteins that embed themselves in the membranes of cells and play important roles in the transmission of signals in and out of the cell. These proteins loop in and out of the membrane many times, alternating between hydrophilic amino acids (which prefer the environment of the membrane) and hydrophobic amino acids (which prefer the environment inside or outside the membrane). These and other biological facts are used to design the states and state transition matrix of the *transmembrane hidden Markov model*, an HMM for modeling membrane proteins [56].

In language problems, HMMs also play a fundamental role. An example is the *part-of-speech* problem, in which words in sentences are to be labeled as to their part of speech (noun, verb, adjective, etc). Here the state variables are the parts of speech, and the transition matrix is estimated from a corpus via the EM algorithm [66]. The result of running the Viterbi algorithm on a new sentence is a tagging of the sentence according to the hypothesized parts of speech of the words in the sentence.

Essentially all modern speech recognition systems are built on the foundation of HMMs [51]. In this case the observations are generally a sequence of short-range speech spectra, and the states correspond to longer-range units of speech such as phonemes or pairs of phonemes. Large-scale systems are built by composing elementary HMMs into larger graphical models.

Trees also play an important role in bioinformatics and language processing. For example, phylogenetic trees can be treated as graphical models. As shown in Figure 1(b), a phylogenetic tree is a tree-structured graphical model in which a set of observed nucleotides (or other biological characters) are assumed to have evolved from an underlying set of ancestral species. The conditional probabilities in the tree are obtained from evolutionary substitution models, and the computation of likelihoods are achieved by a recursion on the tree known as “pruning” [39]. This recursion is a special case of the junction tree algorithm.

Finally, we turn to some examples of more complex graphical models that are currently being

---

<sup>3</sup>The graphical model in Figure 1(a) is also a representation of the state-space model underlying Kalman filtering and smoothing, where the state variable is a Gaussian vector. These models thus also have a right to be referred to as “hidden Markov models,” but the terminology is most commonly used to refer to models in which the state variables are discrete.

explored in bioinformatics and language processing. Figure 2(a) shows a *hidden Markov phylogeny*, an HMM in which the observations are sets of nucleotides related by a phylogenetic tree [67, 76, 86]. This model has been used by [67] for gene-finding in the human genome based on data for multiple primate species. The graphical model shown in Figure 2(b) is a *coupled HMM*, in which two chains of state variables are coupled via links between the chains; this model is appropriate for fusing pairs of data streams such as audio and lip-reading data in speech recognition [82].

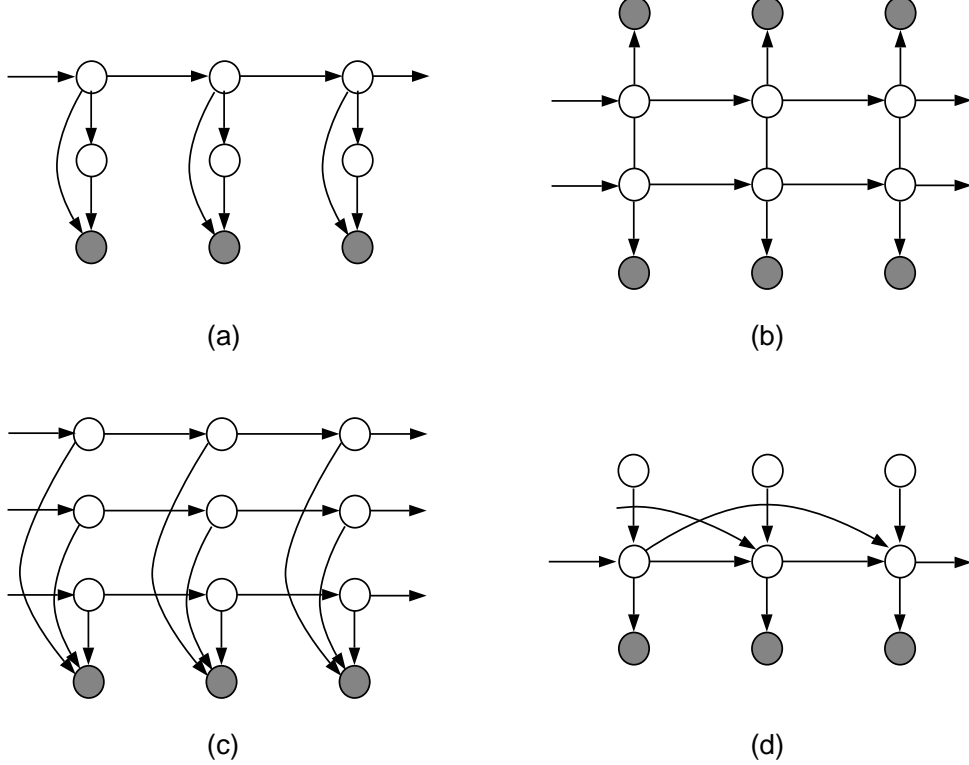


**Figure 2:** Variations on the HMM theme. [[Figure needs revision.]]

Figure 2(c) shows a *factorial HMM*, in which multiple chains are coupled by their links to a common set of observed variables [45]. This model captures the problem of *multi-locus linkage analysis* in genetics, where the state variables correspond to phase (maternal or paternal) along the chromosomes in meiosis [90]. Finally, in Figure 2(d) we show a variation of the HMM in which the state-dependent observation distribution is a finite mixture model. This variant is widely used in speech recognition systems [51].

#### 2.4.2 Image processing

For several decades, undirected graphical models (also known as Markov random fields) have played an important role in image processing [e.g., 100, 48, 25, 10], as well as in spatial statistics more generally. The simplest use of a Markov random field model is in the pixel domain, where each pixel in the image is associated with a node in an underlying graph. More structured models are based on feature vectors at each spatial location, where each feature could be a linear multiscale filter (e.g., a wavelet), or a more complicated nonlinear operator.

For image modeling, one very natural choice of graphical structure is a 2D lattice, such as the 4-nearest neighbor variety shown in Figure 3(a). The potential functions on the edges between

adjacent pixels (or more generally, features) are typically chosen to enforce local smoothness conditions. Various tasks in image processing, including denoising, segmentation, and super-resolution, require solving an inference problem on such a Markov random field. However, exact inference

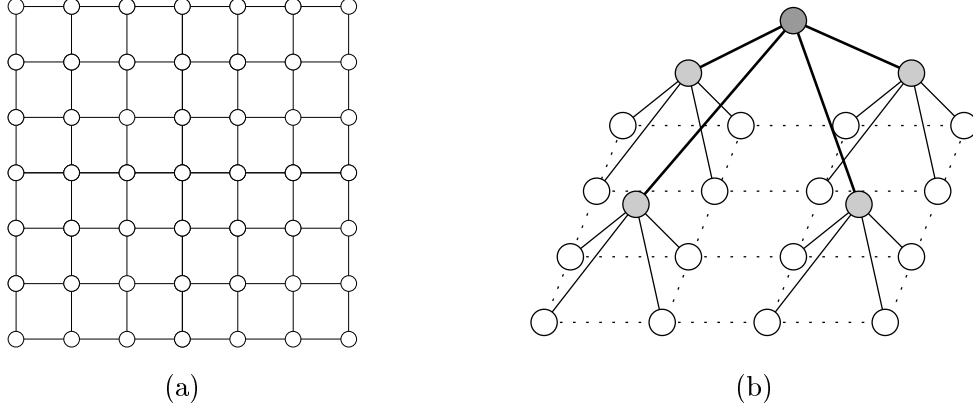


**Figure 3.** (a) The 4-nearest neighbor lattice model in 2D is often used for image modeling. (b) A multiscale quadtree approximation to a 2D lattice model. Nodes in the original lattice (drawn in white) lie at the finest scale of the tree. The middle and top scales of the tree consist of auxiliary nodes (drawn in gray), introduced to model the fine scale behavior.

for large-scale lattice models is intractable, which necessitates the use of approximate methods. Markov chain Monte Carlo methods (e.g., Gibbs sampling [44]) are often used, but they are too slow and computationally intensive for many applications. More recently, the sum-product algorithm has become popular as an approximate inference method for image processing and computer vision problems [e.g., 40].

An alternative strategy is to sidestep the intractability of the lattice model by replacing it with a simpler—albeit approximate—model. For instance, multiscale quad trees, such as that illustrated in Figure 3(b), can be used to approximate lattice models [65]. The advantage of such a multiscale model is in permitting the application of efficient tree algorithms to perform exact inference. The trade-off is that the model is imperfect, and can introduce artifacts into image reconstructions.

#### 2.4.3 Error-correcting coding

A central problem in communication theory is that of transmitting information, represented as a sequence of bits, from one point to another. Examples include transmission from a personal computer over a network, or from a satellite to a ground position. If the communication channel is noisy, then some of the transmitted bits may be corrupted. In order to combat this noisiness, a natural strategy is to add redundancy to the transmitted bits, thereby defining codewords. In principle, this coding strategy allows the transmission to be decoded perfectly even in the presence of some number of errors.

Many of the best codes in use today, including turbo codes and low-density parity check codes [e.g., 42, 68], are based on graphical models. To illustrate, we consider a toy low-density parity check (LDPC) code of length  $n = 6$  (i.e., codewords are binary sequences of length six). For two bits  $x_1$  and  $x_2$ , let  $x_1 \oplus x_2$  denote binary addition in modulo two arithmetic. We define codewords to be those binary sequences that satisfy the parity check relation  $x_s \oplus x_t \oplus x_u = 0$ , where the index set  $\mathcal{I} := \{s, t, u, v\}$  ranges over  $\{1, 3, 4\}$ ,  $\{2, 5, 6\}$ ,  $\{1, 3, 5\}$ , and  $\{2, 4, 6\}$ . For instance, the sequence (101000) is a valid codeword, whereas (111000) is invalid. Figure 4 provides a graphical

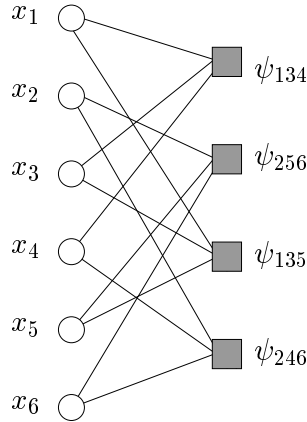


**Figure 4.** A factor graph representation of a LDPC code of length  $n = 6$ . Open circles represent bits in the code, whereas gray squares represent the compatibility functions that define the parity checks. This particular code is a  $(2,3)$  code, since each bit is connected to two parity checks, and each parity check involves three bits.

representation of this code as an undirected graphical model. The particular representation given here is a factor graph [57], in that open circles correspond to bits in the code, whereas the gray squares are auxiliary nodes that serve as placeholders to represent the local compatibility functions or parity checks (also known as factors).

The decoding problem entails estimating which codeword was transmitted on the basis of a noisy observation  $\mathbf{y}$ . With the specification of a model for channel noise, this decoding problem can be cast as an inference problem. Depending on the loss function, optimal decoding is based either on computing the marginal probability  $p(x_s = 1|\mathbf{y})$  at each node, or computing the most likely codeword (i.e., the mode of the posterior). For the simple Hamming code of Figure 4, optimal decoding is easily achievable via the junction tree algorithm. Of interest in many applications, however, are much larger codes in which the number of bits is easily several thousand. Moreover, the graphs underlying these codes are not of low treewidth, so that the junction tree algorithm is not viable.

For many graphical codes, the most successful decoder is based on applying the sum-product updates (7). As the factor graphs defining good codes invariably have cycles, the sum-product algorithm is longer guaranteed to compute the correct marginals, nor even to converge. Nonetheless, the behavior of this approximate decoding algorithm is remarkably good for a large class of codes. The behavior of sum-product algorithm is well-understood in the asymptotic limit (as the code length  $n$  goes to infinity), where martingale arguments can be used to prove concentration results [77, 64]. In contrast, its behavior is not as well-understood for intermediate code lengths.

## 2.5 Exact inference algorithms

In this section, we turn to a description of the basic exact inference algorithms for graphical models. In computing a marginal probability, we must sum or integrate the joint probability distribution over one or more variables. We can perform this computation as a sequence of operations by choosing a specific ordering of the variables (and making an appeal to Fubini's theorem in the continuous case). Recall that for either directed or undirected graphical models the joint probability is a

factored expression over subsets of the variables. Thus we can make use of the distributive law to move individual sums or integrals across factors that do not involve the variables being summed or integrated over. “Exact inference” refers to the (essentially symbolic) problem of organizing this sequential computation, including managing the intermediate factors that arise. Assuming that each individual sum or integral is performed exactly, then the overall algorithm yields an exact numerical result.

To obtain the marginal probability of a single variable,  $p(x_s)$ , it suffices to choose a specific ordering of the remaining variables and to “eliminate” (sum or integrate) variables according to that order. Although we could repeat this operation for each individual variable to obtain marginals of all variables, this is wasteful—there are intermediate terms in these computations that can be shared. The sum-product and junction tree algorithms are essentially dynamic programming algorithms that provide a calculus for sharing intermediate terms. The algorithms involve “message-passing” operations on graphs—where the messages are exactly these shared intermediate terms. After the algorithms run, we obtain marginal probabilities for all cliques of the original graph.

Both directed and undirected graphical models involve factorized expressions for joint probabilities, and it should come as no surprise that exact inference algorithms treat them essentially identically. Indeed, to permit a simple unified treatment of inference algorithms, it is convenient to convert directed models to undirected models and to work exclusively within the undirected formalism. We do this by observing that the factors in (1) are not necessarily defined on cliques (the parents of a given vertex are not necessarily connected). We thus transform a directed graph to an undirected *moral graph*, in which all parents of each child are linked, and all edges are converted to undirected edges. On the moral graph, the factors in (1) are all defined on cliques, and (1) is a special case of the undirected representation in (2). Throughout the rest of the paper we will assume that this transformation has been carried out.

### 2.5.1 Message-passing on trees

We now turn to a description of message-passing algorithms for exact inference on trees. Our treatment is brief; further details can be found in various sources [1, 30, 57, 53, 62]. We begin by observing that the cliques of a tree-structured graph  $T = (V, E(T))$  are simply the individual nodes and edges. As a consequence, any tree-structured graphical model has the following factorization:

$$p(\mathbf{x}) = \frac{1}{Z} \prod_{s \in V} \psi_s(x_s) \prod_{(s,t) \in E(T)} \psi_{st}(x_s, x_t). \quad (3)$$

Here we describe how the sum-product algorithm computes the marginal distribution

$$\mu_s(x_s) := \sum_{\{\mathbf{x}' \mid x'_s = x_s\}} p(\mathbf{x}) \quad (4)$$

for every node of a tree-structured graph. We will focus on detail on the case of discrete random variables, with the understanding that the computations carry over (at least in principle) to the continuous case by replacing sums with integrals.

**Sum-product algorithm:** The sum-product algorithm is a form of non-serial dynamic programming (DP). It represents a generalization to arbitrary tree-structured graphs of the serial form of deterministic dynamic programming [e.g., 7]. The essential principle underlying DP is that of divide and conquer: we solve a large problem by breaking it down into a sequence of simpler problems. In the context of graphical models, the tree itself provides a natural way to break down the problem.

For an arbitrary  $s \in V$ , consider the set of its neighbors  $\mathcal{N}(s) = \{u \in V \mid (s, u) \in E\}$ . For each  $u \in \mathcal{N}(s)$ , let  $T_u = (V_u, E_u)$  be the subgraph formed by the set of nodes (and edges joining them) that can be reached from  $u$  by paths that *do not* pass through node  $s$ . The key property of a tree is that each such subgraph  $T_u$  is again a tree, and  $T_u$  and  $T_v$  are disjoint for  $u \neq v$ . In this way, each vertex  $u \in \mathcal{N}(s)$  can be viewed as the root of a subtree  $T_u$ , as illustrated in Figure 5.

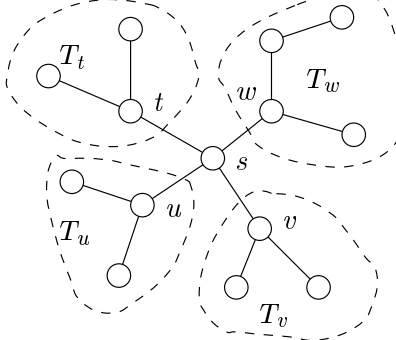


**Figure 5.** Decomposition of a tree, rooted at node  $s$ , into subtrees. Each neighbor (e.g.,  $u$ ) of node  $s$  is the root of a subtree (e.g.,  $T_u$ ). Subtrees  $T_u$  and  $T_v$ , for  $t \neq u$ , are disconnected when node  $s$  is removed from the graph.

For each subtree  $T_t$ , we define  $x_{V_t} := \{x_u \mid u \in V_t\}$ . Now consider the collection of terms in equation (3) associated with vertices or edges in  $T_t$ . We collect all of these terms into the following product:

$$p(x_{V_t}; T_t) \propto \prod_{u \in V_t} \psi_u(x_u) \prod_{(u,v) \in E_t} \psi_{uv}(x_u, x_v). \quad (5)$$

With this notation, the conditional independence properties of a tree allow the computation of the marginal at node  $\mu_s$  to be broken down into a product of subproblems, one for each of the subtrees in the set  $\{T_t, t \in \mathcal{N}(s)\}$ , in the following way:

$$\mu_s(x_s) = \kappa \psi_s(x_s) \prod_{t \in \mathcal{N}(s)} M_{ts}^*(x_s) \quad (6a)$$

$$M_{ts}^*(x_s) := \sum_{\{\mathbf{x}'_{T_t} \mid x'_s = x_s\}} \psi_{st}(x_s, x'_t) p(\mathbf{x}'_{T_t}; T_t) \quad (6b)$$

Here  $\kappa$  denotes a positive constant chosen to ensure that  $\mu_s$  normalizes properly. For fixed  $x_s$ , the subproblem defining  $M_{ts}^*(x_s)$  is again a tree-structured summation, albeit involving a subtree  $T_t$  *smaller* than the original tree  $T$ . Therefore, it too can be broken down recursively in a similar fashion. In this way, the marginal at node  $s$  can be computed by a series of recursive updates.

Rather than applying the procedure described above to each node separately, the *sum-product algorithm* computes the marginals for all nodes simultaneously and in parallel. At each iteration, each node  $t$  passes a “message” to each of its neighbors  $u \in \mathcal{N}(t)$ . This message, which we denote by  $M_{tu}(x_u)$ , is a function of the possible states  $x_u \in \mathcal{X}_u$  (i.e., a vector of length  $|\mathcal{X}_u|$  for discrete random variables). On the full graph, there are a total of  $2|E|$  messages, one for each direction of each edge. This full collection of messages is updated, typically in parallel, according to the following recursion:

$$M_{ts}(x_s) \leftarrow \kappa \sum_{x'_t} \left\{ \psi_{st}(x_s, x'_t) \psi_t(x'_t) \prod_{u \in \mathcal{N}(t)/s} M_{ut}(x'_t) \right\}. \quad (7)$$

It can be shown [75] that for tree-structured graphs, iterates generated by the update (7) will converge to a unique fixed point  $M^* = \{M_{st}^*, M_{ts}^*, (s, t) \in E\}$  after a finite number of iterations. Moreover, component  $M_{ts}^*$  of this fixed point is precisely equal, up to a normalization constant, to the subproblem defined in equation (6b), which justifies our abuse of notation post hoc. Since the fixed point  $M^*$  specifies the solution to all of the subproblems, the marginal  $\mu_s$  at every node  $s \in V$  can be computed easily via equation (6a).

**Max-product algorithm:** Suppose that the summation in the update (7) is replaced by a maximization. The resulting *max-product* algorithm solves the problem of finding a mode of a tree-structured distribution  $p(\mathbf{x})$ . In particular, the max-product updates will converge to another unique fixed point  $M^*$ —distinct, of course, from the sum-product fixed point. This fixed point can be used to compute the *max-marginal*  $\nu_s(x_s) := \max_{\{\mathbf{x}' \mid x'_s = x_s\}} p(\mathbf{x}')$  at each node of the graph, via the analog of equation (5). Given these max-marginals, it is straightforward to compute a mode  $\hat{\mathbf{x}} \in \arg \max_{\mathbf{x}} p(\mathbf{x})$  of the distribution; see the papers [30, 95] for further details. More generally, updates of this form apply to arbitrary *commutative semirings* on tree-structured graphs [93, 84, 30, 1]. The pairs “sum-product” and “max-product” are two particular examples of such an algebraic structure.

### 2.5.2 Junction tree representation

We have seen that inference problems on trees can be solved exactly by recursive message-passing algorithms. Given a graph with cycles, a natural idea is to cluster its nodes so as to form a *clique tree*—that is, an acyclic graph whose nodes are formed by cliques of  $G$ . Having done so, it is tempting to simply apply a standard algorithm for inference on trees. However, the clique tree must satisfy an additional restriction so as to ensure consistency of these computations. In particular, since a given vertex  $s \in V$  may appear in multiple cliques (say  $C_1$  and  $C_2$ ), what is required is a mechanism for enforcing consistency among the different appearances of the random variable  $x_s$ . It turns out that the following property is necessary and sufficient to enforce such consistency:

**Definition 1.** A clique tree has the *running intersection property* if for any two clique nodes  $C_1$  and  $C_2$ , all nodes on the unique path joining them contain the intersection  $C_1 \cap C_2$ . A clique tree with this property is known as a *junction tree*.

For what type of graphs can one build junction trees? An important result in graph theory establishes that a graph  $G$  has a junction tree if and only if it is *triangulated*, meaning that every cycle of length four or longer has a chord. (See Lauritzen [61] for a proof.) This result underlies the *junction tree algorithm* [62] for exact inference on arbitrary graphs:

1. Given a graph with cycles  $G$ , triangulate it by adding edges as necessary.
2. Form a junction tree associated with the triangulated graph  $\tilde{G}$ .
3. Run a tree inference algorithm on the junction tree.

**Example 1.** To illustrate the junction tree construction, consider the  $3 \times 3$  grid shown in Figure 6(a). The first step is to form a triangulated version  $\tilde{G}$ , as shown in Figure 6(b). Note that the graph would not be triangulated if the additional edge joining nodes 2 and 8 were not present. Without this edge, the 4-cycle  $(2 - 4 - 8 - 6 - 2)$  would lack a chord. As a result of this additional edge, the junction tree has two 4-cliques in the middle, as shown in Figure 6(c). These cliques only grow larger as the grid size is increased. ◇

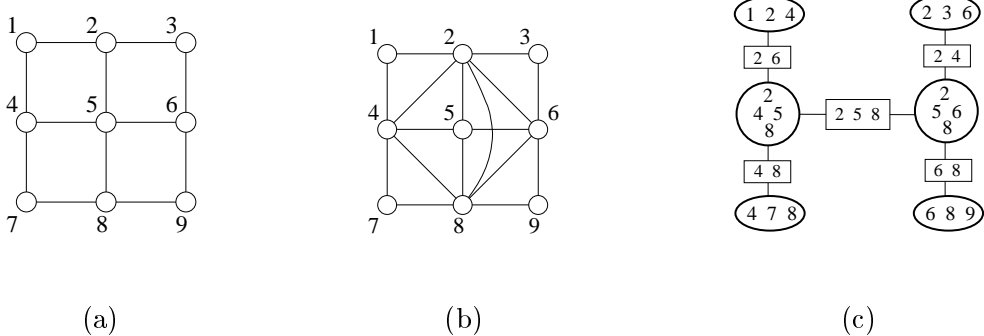


**Figure 6.** Illustration of junction tree construction. (a) Original graph is a  $3 \times 3$  grid. (b) Triangulated version of original graph. Note the two 4-cliques in the middle. (c) Corresponding junction tree for triangulated graph in (b), with maximal cliques depicted within ellipses, and separator sets within rectangles.

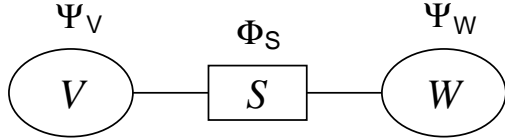


**Figure 7:** A message-passing operation between cliques  $V$  and  $W$ .

Let us expand on the third step in the junction tree algorithm—that of running an inference algorithm on the junction tree. There is an elegant way to express the basic algebraic operations in such an algorithm that involves introducing potential functions not only on the cliques in the junction tree, but also on the *separators* in the junction tree—the intersections of cliques that are adjacent in the junction tree (the rectangles in Figure 6). Thus, let  $\phi_C(x_C)$  denote a potential on a clique  $C$ , and let  $\phi_S(x_S)$  denote a potential on a separator  $S$ . We initialize the clique potentials by assigning each compatibility function in the original graph to (exactly) one clique potential and taking the product over these compatibility functions. The separator potentials are initialized to unity. Given this setup, the basic message-passing step of the junction tree algorithm can be written in the following form:

$$\phi_S^*(x_S) = \sum_{x_{V \setminus S}} \phi_V(x_V) \quad (8a)$$

$$\phi_W^*(x_W) = \frac{\phi_S^*(x_S)}{\phi_S(x_S)} \phi_W(x_W), \quad (8b)$$

where in the continuous case the summation is replaced by a suitable integral. We refer to this pair of operations as “passing a message from clique  $V$  to clique  $W$ ” (see Figure 7). It can be verified that if a message is passed from  $V$  to  $W$ , and subsequently from  $W$  to  $V$ , then the resulting clique potentials are consistent with each other; that is, they agree with respect to the vertices  $S$ .

After a round of message passing on the junction tree, it can be shown that the clique potentials are proportional to marginal probabilities throughout the junction tree. That is, letting  $\mu_C(x_C)$  denote the marginal probability of  $x_C$ , we have  $\mu_C(x_C) \propto \phi_C(x_C)$  for all cliques  $C$ . A proof of this fact can be obtained by a suitable generalization of the proof of correctness of the sum-product algorithm presented in the previous section [61].

Note that achieving local consistency between pairs of cliques is obviously a necessary condition if the clique potentials are to be proportional to marginal probabilities. Moreover, the key role of the running intersection property is now apparent—it ensures that local consistency implies global consistency.

An important by-product of the junction tree algorithm is an alternative representation of a distribution  $p(\cdot)$ . Let  $\mathcal{C}$  denote the set of all maximal cliques in  $\tilde{G}$  (i.e., nodes in the junction tree), and let  $\mathcal{S}$  represent the set of all separator sets (i.e., intersections between cliques that are adjacent in the junction tree). For each separator set  $S \in \mathcal{S}$ , let  $d(S)$  denote the number of maximal cliques to which it is adjacent. The junction tree framework guarantees that the distribution  $p(\cdot)$  factorizes in the form

$$p(\mathbf{x}) = \frac{\prod_{C \in \mathcal{C}} \mu_C(x_C)}{\prod_{S \in \mathcal{S}} [\mu_S(x_S)]^{d(S)-1}}, \quad (9)$$

where  $\mu_C$  and  $\mu_S$  are the marginal distributions over the cliques and separator sets respectively. Unlike the representation of equation (2), the decomposition of equation (9) is directly in terms of marginal distributions, and does not require a normalization constant.

**Example 2 (Markov chain).** Consider the Markov chain  $p(x_1, x_2, x_3) = p(x_1) p(x_2 | x_1) p(x_3 | x_2)$ . The cliques in a graphical model representation are  $\{1, 2\}$  and  $\{2, 3\}$ , with separator  $\{2\}$ . Clearly the distribution cannot be written as the product of marginals over clique potentials. It can, however, be written in terms of marginals if we include the separator:

$$p(x_1, x_2, x_3) = \frac{p(x_1, x_2)p(x_2, x_3)}{p(x_2)}.$$

Moreover, it can be easily verified that these marginals result from a single application of equation (8), given the initialization  $\phi_{\{1, 2\}}(x_1, x_2) = p(x_1)p(x_2 | x_1)$  and  $\phi_{\{2, 3\}}(x_2, x_3) = p(x_3 | x_2)$ .

To anticipate part of our development in the sequel, it is helpful to consider the following “inverse” perspective on this junction tree representation. Suppose that we are given a set of functions  $\tau_C(x_C)$  and  $\tau_S(x_S)$  associated with the cliques and separator sets in the junction tree. What conditions are necessary to ensure that these functions are valid marginals for some distribution? Suppose that the functions  $\{\tau_S, \tau_C\}$  are *locally consistent* in the following sense:

$$\sum_{x_S} \tau_S(x_S) = 1 \quad \text{normalization} \quad (10a)$$

$$\sum_{\{\mathbf{x}'_C \mid \mathbf{x}'_S = x_S\}} \tau_C(\mathbf{x}'_C) = \tau_S(x_S) \quad \text{marginalization} \quad (10b)$$

The essence of the junction tree results that we have cited above is that such local consistency is both necessary and sufficient to ensure that these functions are valid marginals for some distribution. For the sake of future reference, we state this result in the following:

**Proposition 1.** *A candidate set of local marginals  $\{\tau_S, \tau_C\}$  on the separator sets and cliques of a junction tree is globally consistent if and only if it is locally consistent in the sense of equation (10). Moreover, a locally consistent set of potentials are marginals of the joint probability defined by equation (9).*

This consequence of the junction tree representation will play a fundamental role in our development in the sequel.

Finally, let us turn to the key issue of the computational complexity of the junction tree algorithm. Inspecting equation (8), we see that the computational costs grow exponentially in the size of the maximal clique in the junction tree. Clearly it is of interest to control the size of this clique. The size of the maximal clique over all possible triangulations of a graph is an important graph-theoretic quantity known as the *treewidth* of the graph.<sup>4</sup> Thus the junction tree algorithm is exponential in the treewidth.

For certain classes of graphs, including chains and trees, the treewidth is small and the junction tree algorithm provides an effective solution to the inference problem. This includes many classical graphical model architectures, and indeed the junction tree algorithm subsumes many classical recursions on graphs, including the pruning and peeling algorithms from computational genetics, the forward-backward algorithms for hidden Markov models, and the Kalman filtering-smoothing algorithms for state-space models. On the other hand, there are many graphical models, including several of the examples treated in Section 2.4, for which the treewidth is infeasibly large. To attempt to cope with such models, we must leave the junction tree framework behind and turn to approximate inference algorithms.

## 2.6 Message-passing algorithms for approximate inference

It is the goal of the remainder of the paper to develop a general theoretical framework for understanding a class of approximate inference algorithms known as *variational inference algorithms*. Developing this framework will require the mathematical background on convex analysis and exponential families that we provide starting in Section 3. Historically, however, many of these algorithms have been developed without this background, but instead proceeding via analogy to exact or Monte Carlo algorithms, or simply via intuition. In this section, we present two simple variational inference algorithms, emphasizing their simple, intuitive nature, and suggesting the kinds of algorithms that we want our mathematical framework to generate.

The first variational algorithm that we consider is the so-called “loopy” form of the sum-product algorithm (also referred to as the *belief propagation* algorithm). Recall that the sum-product algorithm is an exact inference algorithm for trees. From an algorithmic point of view, however, there is nothing that prevents us from running the procedure on a graph with loops. That is, the message updates (7) can be applied at a given node while ignoring the presence of cycles—essentially we pretend that any given node is embedded in a tree. Intuitively, such an algorithm might be expected to work if the graph is sparse, such that messages are suitably diminished in magnitude once they return around a cycle, or if suitable symmetries are present. As discussed in Section 2.4, this algorithm is in fact successfully used in various applications. Also, an analogous loopy version of the max-product algorithm is used for computing approximate modes in graphical models with cycles.

A second variational algorithm is the so-called *naive mean field* algorithm. For concreteness, we focus on the application of the naive mean field algorithm to the Ising model of statistical physics. The Ising model is a Markov random field involving a binary random vector  $\mathbf{x} \in \{0, 1\}^n$ , in which pairs of adjacent nodes are coupled with a weight  $\theta_{st}$ , and each node has an observation weight  $\theta_s$ . (We describe it in more detail in Example 3 of Section 3.2). Consider now the Gibbs sampler for such a model. The basic step of a Gibbs sampler is to choose a node and to update its state according to the probability of the node conditioned on the states of its neighbors. Considering a node  $s \in V$ , denoting the neighbors of  $s$  as  $\mathcal{N}(s)$ , and letting  $x_{\mathcal{N}(s)}^{(p)}$  denote the state of the neighbors

---

<sup>4</sup>To be more accurate, the treewidth is one less than the size of this largest clique [see 13].

of  $s$  at iteration  $p$ , it is easy to see that the Gibbs update for node  $s$  has the following form:

$$x_s^{(p+1)} = \begin{cases} 1 & \text{if } u \leq \{1 + \exp[-(\theta_s + \sum_{t \in \mathcal{N}(s)} \theta_{st} x_t^{(p)})]\}^{-1} \\ 0 & \text{otherwise} \end{cases}, \quad (11)$$

where  $u$  is a sample from a uniform distribution  $\mathcal{U}(0, 1)$ .

In a dense graph, such that the cardinality of  $\mathcal{N}(s)$  is large, we might attempt to invoke a law of large numbers or some other concentration result for  $\sum_{t \in \mathcal{N}(s)} \theta_{st} x_t^{(p)}$ . To the extent that such sums are concentrated, it might make sense to replace sample values with expectations. That is, letting  $\mu_s$  denote an estimate of the marginal probability  $p(x_s = 1)$  at each vertex  $s \in V$ , we might consider the following averaged version of equation (11):

$$\mu_s \leftarrow \left\{ 1 + \exp \left[ -(\theta_s + \sum_{t \in \mathcal{N}(s)} \theta_{st} \mu_t) \right] \right\}^{-1}. \quad (12)$$

Thus, rather than flipping the random variable  $x_s$  with a probability that depends on the state of its neighbors, we update a parameter  $\mu_s$  deterministically that depends on the corresponding parameters at its neighbors. This equation defines the naive mean field algorithm for the Ising model. As in the case of the sum-product algorithm, the mean field algorithm can be viewed as a message-passing algorithm, in which the right-hand-side of (12) is the “message” arriving at vertex  $s$ .

Message-passing algorithms of this nature might seem rather mysterious, and do raise some questions. Do the updates have fixed points? Do the updates converge? What is the relation between the fixed points and the exact quantities? The goal of the remainder of this paper is to shed some light on such issues. Ultimately, we will see that a broad class of message-passing algorithms, including the mean field updates, the sum-product and max-product algorithms, as well as various extensions of these methods can all be understood as solving either exact or approximate versions of variational problems. Exponential families and convex analysis, which are the subject of the following section, provide the appropriate framework in which to develop these variational principles in an unified manner.

### 3 Exponential families and convex analysis

In this section, we introduce exponential families of distributions, focusing on the links with convex analysis and specifically with the theory of conjugate duality. Further details on exponential families and their properties can be found in various sources [4, 5, 18, 36]. For further background on convex analysis, we refer the reader to [15, 49, 79].

#### 3.1 Basics of exponential families

For the sake of readability, we begin by restating our basic notation for random vectors and sample spaces, originally given in Section 2.1. For each  $s = 1, \dots, n$ , let  $x_s$  be a random variable taking values in some sample space  $\mathcal{X}_s$ , which may be continuous (e.g.,  $\mathcal{X}_s = \mathbb{R}$ ), or a discrete alphabet (e.g.,  $\mathcal{X}_s = \{0, 1, \dots, m-1\}$ ). The random vector  $\mathbf{x} = \{x_s \mid s = 1, \dots, n\}$  then takes values in the Cartesian product space  $\mathcal{X}_1 \times \mathcal{X}_2 \times \dots \times \mathcal{X}_n$ , which we denote by  $\mathcal{X}^n$ . Given some arbitrary function<sup>5</sup>  $h : \mathcal{X}^n \rightarrow \mathbb{R}_+$ , we endow  $\mathcal{X}^n$  with the measure  $\nu$  defined via  $d\nu = h(\mathbf{x}) d\mathbf{x}$ , where component

---

<sup>5</sup>Here  $\mathbb{R}_+ = \{y \in \mathbb{R} \mid y \geq 0\}$ .

$dx_s$  in the product  $d\mathbf{x} = \prod_{s=1}^n dx_s$  is usually (a suitably restricted version of) Lebesgue measure when  $\mathcal{X}_s$  is a continuous space, or the counting measure when  $\mathcal{X}_s$  is discrete.

An exponential family consists of a particular class of densities taken with respect to the dominating measure  $\nu$ . Let  $\phi = \{\phi_\alpha \mid \alpha \in \mathcal{I}\}$  be a collection of Borel measurable functions  $\phi_\alpha : \mathcal{X}^n \rightarrow \mathbb{R}$ . These functions are known either as *potentials* or *sufficient statistics*. Here  $\mathcal{I}$  is an index set with  $d = |\mathcal{I}|$  elements to be specified, so that  $\phi$  itself can be viewed as a vector-valued mapping from  $\mathcal{X}^n$  to  $\mathbb{R}^d$ . Associated with  $\phi$  is a vector  $\theta = \{\theta_\alpha \mid \alpha \in \mathcal{I}\}$  of *exponential* or *canonical* parameters. For each fixed  $\mathbf{x} \in \mathcal{X}^n$ , we use  $\langle \theta, \phi(\mathbf{x}) \rangle$  to denote the (Euclidean) inner product in  $\mathbb{R}^d$  of the two vectors  $\theta$  and  $\phi(\mathbf{x})$ . With this notation, the *exponential family* associated with  $\phi$  consists of the following parameterized collection of density functions (taken with respect to  $d\nu$ ):

$$p(\mathbf{x}; \theta) = \exp \{ \langle \theta, \phi(\mathbf{x}) \rangle - A(\theta) \}. \quad (13)$$

The quantity  $A$ , known as the *log partition function*, is defined by the integral:

$$A(\theta) = \log \int_{\mathcal{X}^n} \exp \langle \theta, \phi(\mathbf{x}) \rangle \nu(d\mathbf{x}). \quad (14)$$

Presuming that the integral is finite, this definition ensures that  $p(\mathbf{x}; \theta)$  is properly normalized (i.e.,  $\int_{\mathcal{X}^n} p(\mathbf{x}; \theta) \nu(d\mathbf{x}) = 1$ ).

With the set of potentials  $\phi$  is fixed, each parameter vector  $\theta$  indexes a particular member  $p(\mathbf{x}; \theta)$  of the family. The exponential parameters  $\theta$  of interest belong to the set

$$\Theta := \{ \theta \in \mathbb{R}^d \mid A(\theta) < \infty \}. \quad (15)$$

We will see shortly that  $A$  is a convex function of  $\theta$ , which in turn implies that  $\Theta$  must be a convex set. The log partition  $A$  plays a prominent role in this paper.

The following notions will be important in subsequent development:

**Regular families:** An exponential family for which the domain  $\Theta$  of equation (15) is an open set is known as a *regular* family. Although there do exist exponential families for which  $\Theta$  is closed [see, e.g., 18], herein we restrict our attention to regular exponential families.

**Minimal:** It is typical to define an exponential family with a collection of functions  $\phi = \{\phi_\alpha\}$  for which there is no linear combination  $\langle a, \phi(\mathbf{x}) \rangle = \sum_{\alpha \in \mathcal{I}} a_\alpha \phi_\alpha(\mathbf{x})$  equal to a constant ( $\nu$ -a.e.). This condition gives rise to a so-called *minimal representation*, in which there is a unique parameter vector  $\theta$  associated with each distribution.

**Overcomplete:** Instead of a minimal representation, it can be convenient to use an *overcomplete representation*, which is non-minimal (so that some linear combination of  $\phi$  is equal to a constant  $\nu$ -a.e.). In this case, there exists an entire affine subset of parameter vectors  $\theta$ , each associated with the same distribution.

**Remark:** The reader might question the utility of an overcomplete representation. Indeed, it seems highly undesirable in a statistical setting because identifiability of the parameter vector  $\theta$  is lost. However, this notion of overcompleteness will play a key role in our later analysis of the sum-product algorithm and its generalizations (Sections 6 and 7).

Table 1 provides some examples of well-known scalar exponential families. Observe that all of these families are both regular (since  $\Theta$  is open), and minimal (since the collection of sufficient statistics  $\phi$  do not satisfy any linear relations).

Family	$\mathcal{X}$	$\nu$	$\log p(\mathbf{x}; \theta)$	$A(\theta)$	$\Theta$
Bernoulli	$\{0, 1\}$	Counting	$\theta x - A(\theta)$	$\log[1 + \exp(\theta)]$	$\mathbb{R}$
Gaussian	$\mathbb{R}$	Lebesgue	$\theta_1 x + \theta_2 x^2 - A(\theta)$	$\frac{1}{2}[\theta_1 + \log \frac{2\pi e}{-\theta_2}]$	$\{\theta \in \mathbb{R}^2 \mid \theta_2 < 0\}$
Exponential	$(0, +\infty)$	Lebesgue	$\theta(-x) - A(\theta)$	$-\log \theta$	$(0, +\infty)$
Poisson	$\{0, 1, 2, \dots\}$	Counting $h(x) = 1/x!$	$\theta x - A(\theta)$	$\exp(\theta)$	$\mathbb{R}$
Beta	$(0, 1)$	Lebesgue	$\theta_1 \log x + \theta_2 \log(1-x)$ $-A(\theta)$	$\sum_{i=1}^2 \log \Gamma(\theta_i + 1)$ $-\log \Gamma(\sum_{i=1}^2 (\theta_i + 1))$	$(-1, +\infty)^2$

**Table 1.** Several well-known classes of scalar random variables as exponential families. In all cases, the base measure  $\nu$  is either Lebesgue or counting measure, suitably restricted to the sample space  $\mathcal{X}$ . All of these examples are both minimal and regular.

### 3.2 Graphical models and exponential families

The scalar examples in Table 1 serve as building blocks for the construction of more complex exponential families for which graphical structure does play a role. Earlier, we described graphical models in terms of products of functions, as in equations (1) and (2). In the context of exponential families, these products become additive decompositions within the exponent.

**Example 3 (Ising model).** We begin with the *Ising model* from statistical physics [6, 21, 73], which is a particular kind of Markov random field. Consider a graph  $G = (V, E)$  and suppose that the random variable  $x_s$  associated with node  $s \in V$  is Bernoulli. Components  $x_s$  and  $x_t$  of the full random vector  $\mathbf{x}$  are allowed to interact directly only if  $s$  and  $t$  are joined by an edge in the graph. This set-up leads to an exponential family of the form

$$p(\mathbf{x}; \theta) = \exp \left\{ \sum_{s \in V} \theta_s x_s + \sum_{(s,t) \in E} \theta_{st} x_s x_t - A(\theta) \right\}, \quad (16)$$

taken with respect to counting measure restricted to  $\{0, 1\}^n$ . Here  $\theta_{st}$  is the strength of edge  $(s, t)$ , and  $\theta_s$  is the node parameter for node  $s$ . (Strictly speaking, this model is more general than the classical Ising model, in which  $\theta_{st}$  is constant for all edges.) The index set  $\mathcal{I}$  consists of the union  $V \cup E$ , and the dimension of the family is  $d = n + |E|$ . The domain  $\Theta$  is the full space  $\mathbb{R}^d$ , since the sum that defines the log partition function  $A(\theta)$  is finite for all  $\theta \in \mathbb{R}^d$ . Hence, the family is regular. Moreover, it is a minimal representation, since there is no linear combination of the potentials equal to a constant  $\nu$ -a.e.  $\diamond$

The standard Ising model can be generalized in a number of different ways. First of all, although equation (16) includes only pairwise interactions, higher-order interactions among the random variables can also be included. For example, in order to include coupling within the 3-clique  $\{s, t, u\}$ , we add a monomial of the form  $x_s x_t x_u$ , with corresponding exponential parameter  $\theta_{stu}$ , to equation (16). More generally, to incorporate coupling in  $k$ -cliques, we can add monomials up to order  $k$ . At the upper extreme, taking  $k = n$  amounts to connecting all nodes in the graphical model, which allows one to represent any distribution over a binary random vector  $\mathbf{x} \in \{0, 1\}^n$ . It is also straightforward to extend these models to the multinomial case, in which each  $x_s$  belongs to the

space  $\mathcal{X}_s = \{0, 1, \dots, m - 1\}$ .

We now turn to another important class of graphical models:

**Example 4 (Gaussian MRF).** A Gaussian Markov random field [e.g., 87] consists of a multivariate Gaussian random vector that respects the Markov properties of a graph  $G = (V, E)$ . It can be represented in exponential form using the potentials  $\{x_s, x_s^2 \mid s \in V\} \cup \{x_s x_t \mid (s, t) \in E\}$ , with associated parameters  $\{\theta_s, s \in V\} \cup \{\theta_{st} \mid (s, t) \in E\}$ . Note that there are a total of  $d = 2n + |E|$  potential functions. It is convenient to represent the potentials and parameters compactly as  $(n + 1) \times (n + 1)$  symmetric matrices:

$$\mathbf{X} := \begin{bmatrix} 1 \\ \mathbf{x} \end{bmatrix} [1 \quad \mathbf{x}], \quad U(\theta) := \begin{bmatrix} 0 & \theta_1 & \theta_2 & \dots & \theta_n \\ \theta_1 & \theta_{11} & \theta_{12} & \dots & \theta_{1n} \\ \theta_2 & \theta_{21} & \theta_{22} & \dots & \theta_{2n} \\ \vdots & \vdots & \vdots & \vdots & \vdots \\ \theta_n & \theta_{n1} & \theta_{n2} & \dots & \theta_{nn} \end{bmatrix} = \begin{bmatrix} 0 & z^T(\theta) \\ z(\theta) & Z(\theta) \end{bmatrix} \quad (17)$$

Here  $z(\theta)$  denotes the  $n$ -vector  $[\theta_1 \dots \theta_n]^T$ , while  $Z(\theta)$  denotes the  $n \times n$  matrix of the  $\{\theta_{st}\}$ . It should be understood that  $\theta_{st} = 0$  whenever  $(s, t) \notin E$ , which reflects the Markov structure of the underlying graph. For any two symmetric matrices  $C$  and  $D$ , we let  $\langle\langle C, D \rangle\rangle$  denote the inner product defined by  $\text{trace}(C D)$ . Using this notation, a Gaussian MRF can be represented as an exponential family of the form

$$p(\mathbf{x}; \theta) = \exp \{ \langle\langle U(\theta), \mathbf{X} \rangle\rangle - A(\theta) \}. \quad (18)$$

The integral defining  $A(\theta)$  is finite only if  $Z(\theta) \prec 0$ , so that  $\Theta = \{\theta \in \mathbb{R}^d \mid Z(\theta) \prec 0\}$ .  $\diamond$

Graphical models are not limited to cases in which the random variables at each node belong to the same exponential family. More generally, we can consider heterogeneous combinations of exponential family members, as illustrated in the following example.

**Example 5 (LDA).** The *Latent Dirichlet allocation* model [12], shown as a graphical model in Figure 8, involves three different types of random variables: “words”  $w$ , “documents”  $z$ , and Dirichlet variables  $u$ . The vector of exponential parameters  $\theta$  can be partitioned as  $\theta = (\alpha, \gamma)$ . The quantity  $\alpha$  is an exponential parameter for the Dirichlet variable  $u$ , which has a density

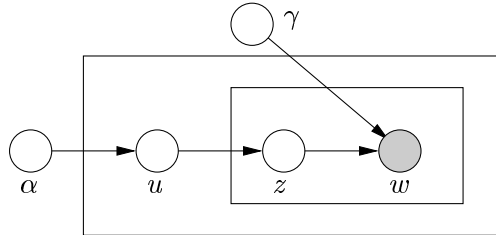


**Figure 8.** Graphical illustration of the Latent Dirichlet allocation (LDA) model. The variable  $u$ , which is distributed as Dirichlet with parameter  $\alpha$ , specifies the parameter for the multinomial  $z$ . Finally,  $w$  is also multinomial conditioned on  $z$ , with  $\gamma$  specifying the transition probabilities. The rectangles, known as plates, denote replication of the random variables.

with respect to Lebesgue measure of the form  $p(u; \alpha) \propto \exp\{\sum_{i=1}^n \alpha_i \log u_i\}$ . The Dirichlet variable  $u$ , in turn, serves as the parameter for the multinomial variable  $z \in \{1, 2, \dots, k\}$ , so that

$p(z; u) = \exp \left\{ \sum_{i=1}^k \mathbb{I}_i[z] \log u_i \right\}$ , where  $\mathbb{I}_i[z]$  is the indicator for the event  $\{z = i\}$ . Finally, the conditional distribution of  $w$  given  $z$  is parameterized by  $\gamma$  as follows:

$$p(w = j | z = i, \gamma) = \exp(\gamma_{ij}), \quad \forall i = 1, \dots, k, \quad j = 1, \dots, l.$$

This set of equations can be written more compactly as  $p(w | z, \gamma) = \exp \left\{ \sum_{i=1}^k \sum_{j=1}^l \gamma_{ij} \mathbb{I}_i[z] \mathbb{I}_j[w] \right\}$ .

Overall then, for a single triplet  $\mathbf{x} := (u, z, w)$ , the LDA model is an exponential family with parameter vector  $\theta := (\alpha, \gamma)$ , with a density of the following form:

$$p(u; \alpha) p(z; u) p(w | z, \gamma) \propto \exp \left\{ \sum_{i=1}^n \alpha_i \log u_i + \sum_{i=1}^k \mathbb{I}_i[z] \log u_i + \sum_{i=1}^k \sum_{j=1}^l \gamma_{ij} \mathbb{I}_i[z] \mathbb{I}_j[w] \right\}. \quad (19)$$

The sufficient statistics  $\phi$  consist of the collections  $\{\log u_i, i = 1, \dots, k\}$ ,  $\{\mathbb{I}_i[z] \log u_i, i = 1, \dots, k\}$ , and  $\{\mathbb{I}_i[z] \mathbb{I}_j[w], i = 1, \dots, k, j = 1, \dots, l\}$ . As illustrated in Figure 8, the full LDA model entails replicating these types of local structures many times.  $\diamond$

### 3.3 Properties of $A$

In this section, we first develop some basic properties of the log partition function, which we then build on by drawing connections to convex analysis. Of particular importance is the idea that the expectations of  $\phi(\mathbf{x})$  under  $p(\mathbf{x}; \theta)$  define an alternative parameterization of the exponential family, known as the *mean parameterization*.

#### 3.3.1 Derivatives and convexity

We begin by establishing that the log partition function is both smooth and convex in terms of  $\theta$ .

**Proposition 2.** *The log partition function is lower semi-continuous on  $\mathbb{R}^d$ , and  $C^\infty$  on  $\Theta$ . Its derivatives are the cumulants of the random vector  $\phi(\mathbf{x})$ —in particular:*

$$\frac{\partial A}{\partial \theta_\alpha}(\theta) = \mathbb{E}_\theta[\phi_\alpha(\mathbf{x})] := \int \phi_\alpha(\mathbf{x}) p(\mathbf{x}; \theta) \nu(d\mathbf{x}). \quad (20a)$$

$$\frac{\partial^2 A}{\partial \theta_\alpha \partial \theta_\beta}(\theta) = \mathbb{E}_\theta[\phi_\alpha(\mathbf{x}) \phi_\beta(\mathbf{x})] - \mathbb{E}_\theta[\phi_\alpha(\mathbf{x})] \mathbb{E}_\theta[\phi_\beta(\mathbf{x})]. \quad (20b)$$

Moreover,  $\|\nabla A(\theta^t)\| \rightarrow +\infty$  for any sequence  $\{\theta^t\} \subset \Theta$  approaching the boundary.

The conditions in Proposition 2 ensure that  $A$  is *essentially smooth* [79], also referred to as *steep* in statistical settings [18]. This property plays an important role in subsequent development. Moreover, Proposition 2 identifies  $A$  as the *cumulant generating function* of the random vector  $\phi(\mathbf{x})$ . In particular, equation (20b) shows that the Hessian  $\nabla^2 A(\theta)$  can be interpreted as a particular type of Gram matrix, which leads to the following:

**Corollary 1.** *The log partition function  $A$  is a convex function of  $\theta$ , and strictly so if the representation is minimal.*

### 3.3.2 Mapping to mean parameters

Given a potential function vector  $\phi : \mathcal{X}^n \rightarrow \mathbb{R}^d$ , it is of interest to consider the set of vectors  $\mu \in \mathbb{R}^d$  that are formed by taking expectations of  $\phi$  under an arbitrary distribution that is absolutely continuous with respect to  $\nu$ . Accordingly, we define the following set:

$$\mathcal{M} := \left\{ \mu \in \mathbb{R}^d \mid \exists p(\cdot) \text{ s. t. } \int \phi(\mathbf{x}) p(\mathbf{x}) \nu(d\mathbf{x}) = \mu \right\}. \quad (21)$$

Note that  $\mathcal{M}$  is a convex set.

Given an arbitrary member of the exponential family defined by  $\phi$ , we can define a mapping  $\Lambda : \Theta \rightarrow \mathcal{M}$  as follows:

$$\Lambda(\theta) := \mathbb{E}_\theta [\phi(\mathbf{x})] = \int_{\mathcal{X}^n} \phi(\mathbf{x}) p(\mathbf{x}; \theta) \nu(d\mathbf{x}). \quad (22)$$

Note that  $\Lambda$  is a particular case of a gradient mapping, since  $\Lambda(\theta) = \nabla A(\theta)$  by equation (20a). The mapping  $\Lambda$  associates to each  $\theta \in \Theta$  a vector of *mean parameters*  $\mu := \Lambda(\theta)$  belonging to the set  $\mathcal{M}$ . The goal of this section is to obtain a precise characterization of the nature of this correspondence between  $\theta$  and  $\mu$ . Of particular interest are the following two issues:

1. determining when  $\Lambda$  is one-to-one and hence invertible on its image, and
2. characterizing the image of  $\Theta$  under the mapping  $\Lambda$ .

The answer to the first question turns out to be straightforward, hinging essentially on the minimality of the representation. Although the answer to the second question is also straightforward—namely,  $\Lambda$  is onto the (relative) interior of  $\mathcal{M}$ —the proof is more involved. To be clear, this question is not trivial, because the definition (21) allows the density  $p(\cdot)$  to be arbitrary, whereas the mapping  $\Lambda$  uses only members of the exponential family. We begin with a result addressing the first question:

**Proposition 3.** *The mapping  $\Lambda$  is one-to-one if and only if the exponential representation is minimal.*

Proposition 3 asserts that the mean parameter mapping is not invertible for an overcomplete representation. More specifically, the inverse image  $\Lambda^{-1}(\mu) := \{\theta \in \Theta \mid \Lambda(\theta) = \mu\}$ —rather than being a singleton (as it would be for an invertible mapping)—is a (non-trivial) affine subset of  $\Theta$ .

**Example 6.** To illustrate, consider a Bernoulli random variable  $x \in \{0, 1\}$ . Suppose that we use the overcomplete exponential representation  $p(x; \theta) \propto \exp\{\theta_0(1 - x) + \theta_1x\}$ , so that  $\Theta = \mathbb{R}^2$ . In this case, the mean parameters  $(\mu_0, \mu_1)$  are simply marginal probabilities—viz.  $\mu_i = p(x = i)$  for  $i = 0, 1$ . The set  $\mathcal{M}$  of realizable mean parameters is the simplex  $\{\mu \geq 0 \mid \mu_0 + \mu_1 = 1\}$ . For a fixed mean parameter  $\mu > 0$  in the simplex, it is easy to show that the inverse image consists of the affine set  $\Lambda^{-1}(\mu) := \{(\theta_0, \theta_1) \in \mathbb{R}^2 \mid \theta_1 - \theta_0 = \log \frac{\mu_1}{\mu_0}\}$ .  $\diamond$

In general, although there is no longer a bijection between  $\Theta$  and  $\Lambda(\Theta)$  in an overcomplete representation, there is still a bijection between each element of  $\Lambda(\Theta)$  and an affine subset of  $\Theta$ . For either a minimal or an overcomplete representation, we say that a pair  $(\theta, \mu)$  is *dually coupled* if  $\mu = \Lambda(\theta)$ , and hence  $\theta \in \Lambda^{-1}(\mu)$ . This notion of dual coupling plays an important role in the sequel.

We now turn to the second question regarding the range of  $\Lambda$ .

**Theorem 1.** *The mean parameter mapping  $\Lambda$  is onto the (relative) interior of  $\mathcal{M}$  (i.e.,  $\Lambda(\Theta) = \text{ri } \mathcal{M}$ ).*

**Remark:** The relative interior of a convex set is the interior taken with respect to its affine hull. A key fact is that any non-empty convex set is guaranteed to have a non-empty relative interior. See Appendix B for more details.

**Remarks:** Typically, the exponential family  $\{p(\mathbf{x}; \theta) \mid \theta \in \Theta\}$  describes only a strict subset of all possible densities. Observe that the definition (21) of  $\mathcal{M}$  allows the density  $p(\cdot)$  to be arbitrary. The significance of Theorem 5, then, lies in the fact that for any mean parameter  $\mu \in \text{ri } \mathcal{M}$ , it suffices to restrict the expectations in definition (21) to members of the exponential family. Moreover, for a minimal exponential family, Proposition 3 guarantees that there is a *unique* exponential parameter  $\theta(\mu)$  such that  $\Lambda(\theta(\mu)) = \mu$ . However, if the exponential family describes a strict subset of all densities, then there exists at least some other density  $p(\cdot)$ —albeit not a member of the exponential family—that also realizes  $\mu$  (i.e., for which  $\int \phi(\mathbf{x})p(\mathbf{x})\nu(d\mathbf{x}) = \mu$ ). As discussed in the following section, the distinguishing property of  $p(\mathbf{x}; \theta(\mu))$  lies in the notion of maximum entropy.

### 3.3.3 Fenchel-Legendre conjugate

We now turn to consideration of the Fenchel-Legendre conjugate of the log partition function  $A$ . In particular, this conjugate dual function, which we denote by  $A^*$ , is defined as follows:

$$A^*(\mu) := \sup_{\theta \in \Theta} \{\langle \mu, \theta \rangle - A(\theta)\}. \quad (23)$$

Here  $\mu \in \mathbb{R}^d$  is a vector of so-called dual variables of the same dimension as  $\theta$ . Our choice of notation—i.e., using  $\mu$  again—is deliberately suggestive, in that these dual variables turn out to have a natural interpretation as mean parameters.

The (Boltzmann-Shannon) entropy of the density  $p(\mathbf{x}; \theta)$  with respect to  $\nu$  is defined as follows:

$$H(p(\mathbf{x}; \theta)) = - \int_{\mathcal{X}^n} p(\mathbf{x}; \theta) \log [p(\mathbf{x}; \theta)] \nu(d\mathbf{x}) = -\mathbb{E}_\theta [\log p(\mathbf{x}; \theta)]. \quad (24)$$

The main result of Theorem 2 is that when  $\mu \in \text{ri } \mathcal{M}$ , then the value of the dual function  $A^*(\mu)$  is precisely the negative entropy of  $p(\mathbf{x}; \theta(\mu))$ , where  $\theta(\mu)$  is an element of the inverse image  $\Lambda^{-1}(\mu)$ . Of course, it is also important to consider  $\mu \notin \text{ri } \mathcal{M}$ , in which case  $\Lambda^{-1}(\mu)$  is empty. In this case, the behavior of the supremum defining  $A^*(\mu)$  requires a more delicate analysis. As we show in the following theorem, it turns out that when  $\mu \notin \text{cl } \mathcal{M}$ , then  $A^*(\mu) = +\infty$ .

More formally, we state the following:

**Theorem 2.**

(a) For any  $\mu \in \text{ri } \mathcal{M}$ , let  $\theta(\mu)$  denote a member of  $\Lambda^{-1}(\mu)$ . The Fenchel-Legendre dual of  $A$  has the following form:

$$A^*(\mu) = \begin{cases} -H(p(\mathbf{x}; \theta(\mu))) & \text{if } \mu \in \text{ri } \mathcal{M} \\ +\infty & \text{if } \mu \notin \text{cl } \mathcal{M}. \end{cases} \quad (25)$$

For any boundary point  $\mu \in \text{bd } \mathcal{M} := \text{cl } \mathcal{M} \setminus \text{ri } \mathcal{M}$ , we have  $A^*(\mu) = \lim_{n \rightarrow +\infty} [-H(p(\mathbf{x}; \theta(\mu^n)))]$ , taken over a sequence  $\{\mu^n\} \subset \text{ri } \mathcal{M}$  converging to  $\mu$ .

(b) In terms of this dual, the log partition function has the following variational representation:

$$A(\theta) = \sup_{\mu \in \mathcal{M}} \{\langle \theta, \mu \rangle - A^*(\mu)\}. \quad (26)$$

The fact that  $A^*(\mu) = +\infty$  for  $\mu \notin \text{cl } \mathcal{M}$  is essential for our approach to variational inference. In particular, it implies that the variational representation of the log partition function reduces to an optimization over  $\mathcal{M}$ , as we see in equation (26). Thus  $\mathcal{M}$  is the domain over which our key optimization problem takes place, and we will be interested in various approximations of this set.

Table 2 provides the conjugate dual pair  $(A, A^*)$  for several well-known exponential families of scalar random variables. For each family, the table also lists  $\Theta \equiv \text{dom } A$ , as well as the set  $\mathcal{M}$ , which contains the effective domain of  $A^*$  (by Theorem 2(a)).

Family	$\Theta$	$A(\theta)$	$\mathcal{M}$	$A^*(\mu)$
Bernoulli	$\mathbb{R}$	$\log[1 + \exp(\theta)]$	$[0, 1]$	$\mu \log \mu + (1 - \mu) \log(1 - \mu)$
Gaussian	$\{(\theta_1, \theta_2) \mid \theta_2 < 0\}$	$\frac{1}{2}[\theta_1 + \log \frac{2\pi e}{-\theta_2}]$	$\{(\mu_1, \mu_2) \mid \mu_2 - (\mu_1)^2 > 0\}$	$-\frac{1}{2} \log[2\pi e(\mu_2 - \mu_1^2)]$
Exponential	$(0, +\infty)$	$-\log \theta$	$(-\infty, 0)$	$-1 - \log(-\mu)$
Poisson	$\mathbb{R}$	$\exp(\theta)$	$(0, +\infty)$	$\mu \log \mu - \mu$

**Table 2.** Conjugate dual relations of Theorem 2 for several well-known exponential families of scalar variables.

On the basis of these examples, it can be seen that the specific behavior of  $A^*$  on the boundary  $\text{bd } \mathcal{M} := \text{cl } \mathcal{M} \setminus \text{ri } \mathcal{M}$  varies depending on the exponential family. For example, for the Bernoulli family, the boundary of  $\mathcal{M} = [0, 1]$  consists of the points 0 and 1. As  $\mu$  approaches either of these points, the dual function  $A^*(\mu) = \mu \log \mu + (1 - \mu) \log(1 - \mu)$  tends to zero. This limiting behavior corresponds to the fact that the underlying distribution  $p(\mathbf{x}; \theta(\mu))$  is tending to a delta function, which has a discrete entropy of zero. Therefore, we conclude that  $\text{dom } A^* = [0, 1] \equiv \mathcal{M}$  in the Bernoulli case. This type of reasoning can be generalized to the multinomial case.

On the other hand, in the scalar Gaussian case, the set  $\mathcal{M}$  is defined by the quadratic constraint  $\mu_2 - (\mu_1)^2 > 0$ , corresponding to the fact that the variance of a (non-degenerate) Gaussian must be (strictly) positive. Note that  $(0, 0)$  is a boundary point of  $\mathcal{M}$ . We can compute the value of  $A^*(0, 0)$  by taking the limit  $A^*(\mu^n)$  for a sequence  $\{\mu^n\} \rightarrow (0, 0)$  contained within  $\text{int } \mathcal{M} \equiv \mathcal{M}$ . Considering, in particular, the sequence  $\mu^n = (0, 1/n)$  and using the form of  $A^*$  given in Table 2, we obtain  $\lim_{n \rightarrow +\infty} A^*(\mu^n) = +\infty$ . This result is consistent with the limiting behavior of (differential) entropy for densities with a delta component.

### 3.3.4 Kullback-Leibler divergence

The conjugate duality between  $A$  and  $A^*$ , as characterized in Theorem 2, leads to several alternative forms of the Kullback-Leibler (KL) divergence for exponential family members, which we summarize

here for the sake of subsequent developments. The standard definition [24] of the KL divergence between two distributions with densities  $q$  and  $p$  with respect to  $\nu$  is as follows:

$$D(q \parallel p) := \int_{\mathcal{X}^n} q(\mathbf{x}) \log \frac{q(\mathbf{x})}{p(\mathbf{x})} \nu(d\mathbf{x}). \quad (27)$$

The key result that underlies alternative representations for exponential families is *Fenchel's inequality* which, as applied to  $(A, A^*)$ , asserts that for *any* pair  $(\theta, \mu) \in \mathbb{R}^d \times \mathbb{R}^d$ :

$$A(\theta) + A^*(\mu) \geq \langle \mu, \theta \rangle. \quad (28)$$

Moreover, equality holds in this equation if and only if  $\theta$  and  $\mu$  are dually coupled, meaning that  $\mu = \Lambda(\theta)$  and  $\theta \in \Lambda^{-1}(\mu)$ .

Consider two exponential parameter vectors  $\theta^1, \theta^2 \in \Theta$ ; with a slight abuse of notation, we use  $D(\theta^1 \parallel \theta^2)$  to refer to the KL divergence between  $p(\mathbf{x}; \theta^1)$  and  $p(\mathbf{x}; \theta^2)$ . We use  $\mu^1$  and  $\mu^2$  to denote the respective mean parameters (i.e.,  $\mu^i = \Lambda(\theta^i)$  for  $i = 1, 2$ ). A first alternative form of the KL divergence is obtained by substituting the exponential representations of  $p(\mathbf{x}; \theta^i)$  into equation (27) and then expanding and simplifying as follows:

$$D(\theta^1 \parallel \theta^2) = \mathbb{E}_{\theta^1} \left[ \log \frac{p(\mathbf{x}; \theta^1)}{p(\mathbf{x}; \theta^2)} \right] = A(\theta^2) - A(\theta^1) - \langle \mu^1, \theta^2 - \theta^1 \rangle. \quad (29)$$

We refer to this representation as the *primal form* of the KL divergence. As illustrated in Figure 9,

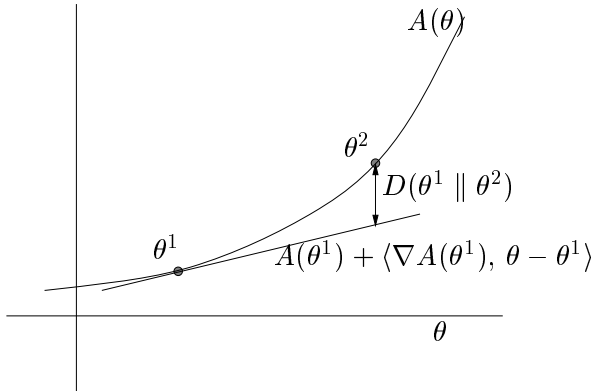


**Figure 9.** The hyperplane  $A(\theta^1) + \langle \nabla A(\theta^1), \theta - \theta^1 \rangle$  supports the epigraph of  $A$  at  $\theta^1$ . The Kullback-Leibler divergence  $D(\theta \parallel \theta^2)$  is equal to the difference between  $A(\theta^2)$  and this hyperplane.

this form of the KL divergence can be interpreted as the difference between  $A(\theta^2)$  and the hyperplane tangent to  $A$  at  $\theta^1$  with normal  $\nabla A(\theta^1) = \mu^1$ . This interpretation shows that the KL divergence is a particular example of a Bregman distance [17, 20].

A second form of the KL divergence can be obtained by using the fact that Fenchel's inequality (28) holds with equality for the dually coupled pair  $(\theta^1, \mu^1)$ . In this way, we can transform equation (29) into the following *mixed form* of the KL divergence:

$$D(\theta^1 \parallel \theta^2) \equiv D(\mu^1 \parallel \theta^2) = A(\theta^2) + A^*(\mu^1) - \langle \mu^1, \theta^2 \rangle. \quad (30)$$

Note that this mixed form of the divergence corresponds to the slack in Fenchel's inequality (28). It also provides an alternative view of the variational representation given in Theorem 2(b). In particular, equation (26) can be rewritten as follows:

$$\inf_{\mu \in \mathcal{M}} \{A(\theta) + A^*(\mu) - \langle \theta, \mu \rangle\} = 0$$

Using equation (30), the variational representation in Theorem 2(b) is seen to be equivalent to the assertion that  $\inf_{\mu \in \mathcal{M}} D(\mu \| \theta) = 0$ .

Finally, by applying equation (28) as an equality once again, this time for the coupled pair  $(\theta^2, \mu^2)$ , the mixed form (30) can be transformed into a purely *dual form* of the KL divergence:

$$D(\theta^1 \| \theta^2) \equiv D(\mu^1 \| \mu^2) = A^*(\mu^1) - A^*(\mu^2) - \langle \theta^2, \mu^1 - \mu^2 \rangle. \quad (31)$$

Note the symmetry between representations (29) and (31). In particular, to move from one to the other, we simply exchange the log partition function  $A$  for the negative entropy  $A^*$ , and we interchange the roles of  $\theta^1$  and  $\theta^2$  (as well as  $\mu^1$  and  $\mu^2$ ). This form of the KL divergence has an interpretation analogous to that of Figure 9, but with  $A$  replaced by the dual  $A^*$ .

## 4 Variational methods for computing mean parameters

For the next several sections, we focus on the first two inference problems described in Section 2.3. Restated in the language of exponential families, these problems correspond to computing the log partition function  $A(\theta)$ , and the mean parameters  $\mu = \mathbb{E}_\theta[\phi(\mathbf{x})]$  for a given distribution  $p(\mathbf{x}; \theta)$ . The current section is devoted to consideration of the ingredients in the variational approach.

Of central importance to the computation of the log partition function and the mean parameters is Theorem 2(b), which we restate here for convenient reference:

$$A(\theta) = \sup_{\mu \in \mathcal{M}} \{ \langle \theta, \mu \rangle - A^*(\mu) \}. \quad (32)$$

It should be emphasized that equation (32) is a variational representation in two senses. First of all, it specifies  $A(\theta)$  as the solution of a particular optimization problem in which  $\theta$  plays the role of a parameter. Secondly, equation (32) provides a variational procedure for computing mean parameters, as stated formally in the following:

**Proposition 4.** *For all  $\theta \in \Theta$ , the supremum in equation (32) is attained uniquely at the vector  $\mu \in \text{ri } \mathcal{M}$  specified by:*

$$\mu = \mathbb{E}_\theta[\phi(\mathbf{x})] = \int_{\mathcal{X}^n} \phi(\mathbf{x}) p(\mathbf{x}; \theta) \nu(d\mathbf{x}).$$

The essence of Proposition 4 is the following: an additional by-product of solving problem (32), apart from computing the log partition function, is the set of the mean parameters  $\mu = \mathbb{E}_\theta[\phi(\mathbf{x})]$  associated with  $p(\mathbf{x}; \theta)$ . It is tempting, then, to assert that the problem of computing mean parameters is now solved, since we have “reduced” it to a convex optimization problem. In this context, the simple scalar examples of Table 2, for which problem (32) had an explicit form and could be solved easily, are very misleading. For general multivariate exponential families, in contrast, there are two primary challenges associated with the variational representation:

- (a) in many cases, the constraint set  $\mathcal{M}$  of realizable mean parameters is extremely difficult to characterize in an explicit manner.
- (b) the negative entropy function  $A^*$  is defined indirectly—in a variational manner—so that it too typically lacks an explicit form.

These difficulties motivate the use of approximations to  $\mathcal{M}$  and  $A^*$ . Indeed, as shown in later sections, a broad class of methods for approximate inference are based on this strategy. The

remainder of this section is devoted a more in-depth consideration of the nature of the set  $\mathcal{M}$  of realizable mean parameters, as well as the dual function  $A^*$ . We also investigate particular large-scale exponential families for which the variational principle (32) is tractable; such cases provide building blocks for our later development of approximate variational principles.

## 4.1 Sets of realizable mean parameters

Recall that for a given set of sufficient statistics  $\phi$ , the set  $\mathcal{M}$  consists of all mean parameters  $\mu$  that are realizable—viz:

$$\mathcal{M} := \{ \mu \in \mathbb{R}^d \mid \exists p(\cdot) \text{ s.t. } \int \phi(\mathbf{x}) p(\mathbf{x}) \nu(d\mathbf{x}) = \mu \}. \quad (33)$$

Despite the apparent simplicity of this representation of  $\mathcal{M}$ , even assessing whether a single  $\mu$  belongs to  $\mathcal{M}$  poses a serious challenge. The difficulty stems from the fact that there can exist global—and often rather subtle—dependencies among the mean parameters associated with the vector of sufficient statistics  $\phi$ .

We begin by discussing some general properties of the sets  $\mathcal{M}$ . We then discuss two important classes of exponential families for which  $\mathcal{M}$  is straightforward to characterize—namely, arbitrary Gaussian distributions, and multinomial distributions on junction trees. Before proceeding, a remark on notation: since much of our discussion involves graphs, it is convenient to introduce the notation  $\mathcal{M}(G)$ , which indicates explicitly that  $\mathcal{M}$  arises from a vector of sufficient statistics  $\phi$  associated with a graph  $G$ .

### 4.1.1 General properties of $\mathcal{M}$

From its definition, it is clear that  $\mathcal{M}$  is always a convex set. Other more specific properties of  $\mathcal{M}$  turn out to be determined by the properties of the exponential family. A convex set  $\mathcal{M} \subseteq \mathbb{R}^d$  is *full-dimensional* if its affine hull is equal to  $\mathbb{R}^d$ . With this notion, we have the following:

**Proposition 5.** *The set  $\mathcal{M}$  has the following properties:*

- (a)  $\mathcal{M}$  is full-dimensional if and only if the exponential family is minimal.
- (b)  $\mathcal{M}$  is bounded if and only if  $\Theta = \mathbb{R}^d$  and  $A$  is globally Lipschitz on  $\mathbb{R}^d$ .

**Remark:** With reference to Proposition 5(b), the necessity of the condition  $\Theta = \mathbb{R}^d$  for  $\mathcal{M}$  to be bounded is clear from the boundary behavior of  $\nabla A$  given in Proposition 2. However, the additional global Lipschitz condition is also necessary, as demonstrated by the Poisson family (see Table 2). In this case, we have  $\Theta = \mathbb{R}$  yet the set of mean parameters  $\mathcal{M} = (0, +\infty)$  is unbounded. This unboundedness occurs because the function  $A(\theta) = \exp(\theta)$ , while finite on  $\mathbb{R}$ , is not globally Lipschitz.

We now turn to some specific cases for which we can give explicit characterizations of  $\mathcal{M}$ .

### 4.1.2 Gaussian distributions

The exponential parameterization of a Gaussian Markov random field was described in Example 4. In this example, we consider the structure of  $\mathcal{M}$  for such a model, focusing for simplicity on the case where  $G = K_n$ , the complete graph on  $n$  nodes. The case with arbitrary  $G$  can be dealt with by considering suitable projections of the set  $\mathcal{M}_{\text{Gauss}} \equiv \mathcal{M}_{\text{Gauss}}(K_n)$  characterized here.

Associated with the exponential parameterization (17) of a multivariate Gaussian is a mean parameter vector  $\mu \in \mathbb{R}^d$ . It is convenient to represent  $\mu$  in terms of  $(n+1) \times (n+1)$  matrix, denoted by  $W(\mu)$ , defined in the following way:

$$W(\mu) := \mathbb{E}_\theta \left\{ \begin{bmatrix} 1 \\ \mathbf{x} \end{bmatrix} \begin{bmatrix} 1 & \mathbf{x} \end{bmatrix} \right\} = \begin{bmatrix} 1 & z^T(\mu) \\ z(\mu) & Z(\mu) \end{bmatrix}. \quad (34)$$

In this definition,  $z(\mu) := \mathbb{E}_\theta[\mathbf{x}]$  is a column vector of means, whereas  $Z(\mu) := \mathbb{E}_\theta[\mathbf{x}\mathbf{x}^T]$  is the  $n \times n$  matrix of second order moments.

An attractive feature of the Gaussian case is that the validity of the mean parameter vector  $\mu = \{\mu_s, \mu_{st} \mid s, t = 1, \dots, n\}$  can be assessed very easily:

**Proposition 6.** *In the Gaussian case, the set  $\mathcal{M}$  has the form*

$$\mathcal{M}_{Gauss} = \{\mu \in \mathbb{R}^d \mid W(\mu) \succ 0\}. \quad (35)$$

The geometry of the set  $\mathcal{M}_{Gauss}$  can be understood as follows. Let  $\mathcal{S}_+^{n+1}$  denote the cone of symmetric positive definite matrices. Then  $\mathcal{M}_{Gauss}$  is the intersection of  $\mathcal{S}_+^{n+1}$  with a single hyperplane, corresponding to the constraint  $[W(\mu)]_{11} = 1$ . As a consequence,  $\mathcal{M}_{Gauss}$  is not itself a cone. For instance, in the scalar case  $n = 1$ , it is a parabolic set of the form  $\{\mu \in \mathbb{R}^2 \mid \mu_{11} - \mu_1^2 > 0\}$ .

#### 4.1.3 Multinomial distributions

Now suppose that  $\mathcal{X}^n = \mathcal{X}_1 \times \mathcal{X}_2 \times \dots \times \mathcal{X}_n$  is a Cartesian product of finite discrete sets (i.e.,  $\mathcal{X}_s = \{0, 1, \dots, m_s\}$  for each  $s = 1, \dots, n$ ), so that  $\mathbf{x} \in \mathcal{X}^n$  is a multinomial random vector. In this case, the boundary of  $\mathcal{M}$  is no longer curved, but rather formed of straight lines.

**Proposition 7.** *In the multinomial case, the set  $\mathcal{M}$  is a polytope, meaning that it has a representation of the form*

$$\mathcal{M} = \{\mu \in \mathbb{R}^d \mid \langle a_j, \mu \rangle \leq b_j \quad \forall j \in \mathcal{J}\}, \quad (36)$$

where the index set  $\mathcal{J}$  is finite. Moreover, any extreme point is of the form  $\mu_e := \phi(e)$ .

**Remark:** Since any convex set can be represented as the intersection of half-spaces containing it [79], the crucial part of Proposition 7, then, is that the index set  $\mathcal{J}$  in equation (36) has *finite cardinality*.

Motivated by Proposition 7, we use  $\text{MARG}(G)$  to denote the *marginal polytope* associated with the graph  $G$ . Figure 10 provides a geometrical illustration of such an object. The extreme points (i.e., those that cannot be expressed as convex combinations of other points) are all of the form  $\mu_e := \phi(e)$ . Such a point is realized by the distribution  $\delta_e(\mathbf{x})$ , which is equal to one if  $\mathbf{x} = e$  and 0 otherwise. The faces of the marginal polytope are specified by hyperplane constraints of the form  $\langle a_j, \mu \rangle \leq b_j$ . The maximal faces (i.e., those that are not contained in any other face) are known as *facets*.

As one might expect, it turns out that the nature of a marginal polytope depends crucially on the underlying graph structure. Although the number of constraints  $|\mathcal{J}|$  defining  $\text{MARG}(G)$  is always finite, the number can grow very quickly with increasing graph size. In this sense, Figure 10 is not at all faithful, since marginal polytopes may have an exceedingly large number of facets. The book by Deza and Laurent [33] provides a wealth of information on the binary case; as a concrete example, for a binary random vector on the complete graph with  $n = 7$  nodes, the associated

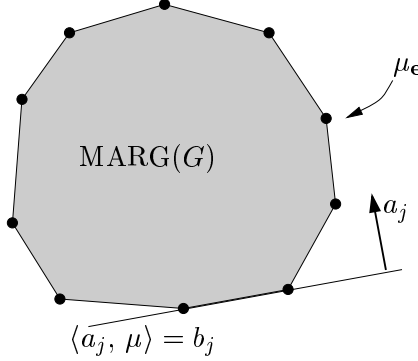


**Figure 10.** Geometrical illustration of a marginal polytope. Each vertex corresponds to the mean parameter  $\mu_e := \phi(e)$  realized by the distribution  $\delta_e(\mathbf{x})$  that puts all of its mass on the configuration  $e \in \mathcal{X}^n$ . The faces of the marginal polytope are specified by hyperplane constraints  $\langle a_j, \mu \rangle \leq b_j$ .

marginal polytope is known to have in excess of  $2 \times 10^8$  facets! In contrast, tree-structured graphs are dramatically different: the growth is only linear in the number of nodes  $n$ , as shown via the following example.

**Example 7 (Minimal representation of tree marginal polytope).** The case of a binary random vector  $\mathbf{x} \in \{0, 1\}^n$  suffices to illustrate the nature of the marginal polytope  $MARG(T)$  for a tree-structured graph  $T = (V, E)$ . We use the minimal (Ising) representation of Example 3, with the singleton  $x_s$  for each  $s \in V$ , and the pairwise product  $x_s x_t$  for each edge  $(s, t) \in E$ . The relevant mean parameters in this representation, then, are as follows:

$$\mu_s = \mathbb{E}_\theta[x_s] = p(x_s = 1; \theta), \quad \mu_{st} = \mathbb{E}_\theta[x_s x_t] = p(x_s = 1, x_t = 1; \theta).$$

(The fact that these mean parameters are equal to particular values of marginal probabilities justifies our terminology). For each edge  $(s, t)$ , the triplet  $\{\mu_s, \mu_t, \mu_{st}\}$  uniquely determines a joint marginal  $p(x_s, x_t; \mu)$  as follows:

$$p(x_s, x_t; \mu) = \begin{bmatrix} (1 + \mu_{st} - \mu_s - \mu_t) & (\mu_t - \mu_{st}) \\ (\mu_s - \mu_{st}) & \mu_{st} \end{bmatrix}.$$

Note that for any choice of  $\{\mu_s, \mu_t, \mu_{st}\}$ , this joint marginal satisfies the normalization constraint  $\sum_{x_s, x_t} p(x_s, x_t; \mu) = 1$ . Therefore, to ensure that it is a joint marginal, it is necessary and sufficient to impose non-negativity constraints on all four entries, as follows:

$$1 + \mu_{st} - \mu_s - \mu_t \geq 0 \tag{37a}$$

$$\mu_{st} \geq 0 \tag{37b}$$

$$\mu_v - \mu_{st} \geq 0 \quad \text{for } v = s, t \tag{37c}$$

We are now set up to apply the junction tree theorem; in particular, by Proposition 1, the full collection  $\mu = \{\mu_s, s \in V\} \cup \{\mu_{st}, (s, t) \in E\}$  determines a globally-consistent distribution if and only if the four inequalities (37) are satisfied for every edge. Since any tree on  $n$  nodes has  $n - 1$  edges, the marginal polytope for a tree-structured graph in the binary case can be characterized by  $4(n - 1)$  constraints.  $\diamond$

**Remarks:** (a) Example 7 can be extended to minimal exponential families for multinomials (i.e.,  $\mathcal{X}_s = \{0, 1, \dots, m - 1\}$ ) as well. In particular, given a minimal representation, we simply determine the inequality constraints that guarantee the existence of a pairwise marginal, and then invoke Proposition 1.

(b) Similarly, this development can be extended to junction tree models, of which ordinary trees are a particular case. See Section 2.5.2 for a description of junction trees.

**Canonical overcomplete representation:** One unpleasant feature of describing marginal polytopes in minimal representations is that the interpretation of constraints can be far from transparent. Consider, for instance, equation (37a): with a bit of thought and an application of the inclusion-exclusion principle, one can see that  $(1 + \mu_{st} - \mu_s - \mu_t)$  is equal to the marginal probability  $p(x_s = 0, x_t = 0)$ , from which the non-negativity constraint follows. This interpretation, however, may not be obvious at a glance. This lack of transparency only becomes worse in the general case, where individual mean parameters need not correspond to individual marginal values.

In contrast, a judicious choice of an overcomplete exponential representation leads to easily interpretable constraints. Here we describe a particular overcomplete representation, applicable to the multinomial space  $\mathcal{X}_s = \{0, 1, \dots, m_s - 1\}$ , that plays an important role in the sequel. For each  $j \in \mathcal{X}_s$ , let  $\mathbb{I}_j(x_s)$  be an indicator function for the event  $\{x_s = j\}$ . Similarly, for each pair  $(j, k) \in \mathcal{X}_s \times \mathcal{X}_t$ , let  $\mathbb{I}_{jk}(x_s, x_t)$  be an indicator for the event  $\{(x_s, x_t) = (j, k)\}$ . These indicator functions define the statistics for the following overcomplete representation:

$$\mathbb{I}_j(x_s) \quad \text{for } s = 1, \dots, n, \quad j \in \mathcal{X}_s \quad (38a)$$

$$\mathbb{I}_{jk}(x_s, x_t) \quad \text{for } (s, t) \in E, \quad (j, k) \in \mathcal{X}_s \times \mathcal{X}_t. \quad (38b)$$

The overcompleteness is clear in various linear relations satisfied by the indicator functions (e.g.,  $\sum_{j \in \mathcal{X}_s} \mathbb{I}_j(x_s) = 1$ ). More generally, we can define indicators on higher order cliques; for instance, to treat a graph with a 3-clique  $\{s, t, u\}$ , we incorporate a term of the form  $\mathbb{I}_{stu}(x_s, x_t, x_u)$ . We refer to the representation defined by (38a) and (38b) as the *canonical overcomplete representation* for multinomial distributions.

An attractive feature of this representation is that mean parameters are simply local marginal probabilities—viz.:

$$\mu_{s;j} := p(x_s = j; \theta) \quad \forall s \in V, \quad \mu_{st;jk} := p((x_s, x_t) = (j, k); \theta) \quad \forall (s, t) \in E \quad (39)$$

For calculations in the sequel, it is convenient to use these marginals to define functional forms of the single node and joint marginal parameters as follows:

$$\mu_s(x_s) := \sum_{j \in \mathcal{X}_s} \mu_{s;j} \mathbb{I}_j(x_s), \quad \mu_{st}(x_s, x_t) := \sum_{(j, k) \in \mathcal{X}_s \times \mathcal{X}_t} \mu_{st;jk} \mathbb{I}_{jk}(x_s, x_t) \quad (40)$$

More generally, marginal functions over higher-order cliques are defined in an analogous manner.

**Example 8 (Tree marginals in overcomplete form).** To illustrate the use of the canonical overcomplete representation, we show that the tree-structured MARG( $T$ ) has a simple and easily interpretable characterization. Consider the single node  $\mu_s$  and joint pairwise marginal functions  $\mu_{st}$ . As marginal distributions, they must of course be non-negative. In addition, they must satisfy normalization conditions (i.e.,  $\sum_{x_s} \mu_s(x_s) = 1$ ), and the pairwise marginalization conditions (i.e.,  $\sum_{x_t} \mu_{st}(x_s, x_t) = \mu_s(x_s)$ ). Accordingly, we define for an *arbitrary* graph  $G$  the following constraint set:

$$\text{LOCAL}(G) := \{ \mu \geq 0 \mid \sum_{x_s} \mu_s(x_s) = 1, \quad \sum_{x_t} \mu_{st}(x_s, x_t) = \mu_s(x_s) \}, \quad (41)$$

for  $(s, t) \in E$ . Note that the normalization of the single node marginal, in conjunction with the marginalization constraint, imply that each joint marginal  $\mu_{st}$  is also properly normalized. Since any set of local marginals (regardless of the underlying graph structure) must satisfy these local consistency constraints, we are guaranteed that  $\text{MARG}(G) \subseteq \text{LOCAL}(G)$  for *any* graph  $G$ . When the graph is actually tree-structured, then the junction tree theorem, in the form of Proposition 1, guarantees that the local consistency constraints in equation (41) imply global consistency, so that in fact  $\text{MARG}(T) = \text{LOCAL}(T)$ .  $\diamond$

**Remark:** It is worthwhile understanding the link between the tree marginal polytope  $\text{MARG}(T)$  in the canonical overcomplete representation, and its analogue in a minimal representation. In the overcomplete representation,<sup>6</sup> there are a total of  $d' = mn + m^2|E|$  mean parameters; therefore, the marginal polytope lies in  $\mathbb{R}^{d'}$ . However, the presence of equality constraints in equation (41) indicates the polytope actually lies strictly within an affine subset of  $\mathbb{R}^{d'}$ . Therefore, consistent with Proposition 5(a), it is not a full-dimensional set. Eliminating the equality constraints leads a reduced but equivalent description in a lower-dimensional space  $\mathbb{R}^d$ , wherein all of the constraints are one-sided inequalities. It is not difficult to show that the dimension of the reduced representation is  $d = (m - 1)n + (m - 1)^2|E|$ . In the binary case ( $m = 2$ ), Example 7 provides an explicit representation of this reduced representation.

## 4.2 Nature of the dual function

We now turn to a more in-depth consideration of the nature of the dual function  $A^*$ . Its variational definition in equation (23) is both a blessing and a curse. On one hand, it guarantees that  $A^*$  is a convex and well-behaved function; however, the absence of a closed form expression for  $A^*$  presents substantial computational challenges. As with our earlier discussion of  $\mathcal{M}$ , important exceptions include the Gaussian and tree-structured cases.

### 4.2.1 General properties of $A^*$

As noted earlier, the examples given in Table 2, in which the dual  $A^*$  had a closed form, are the exception rather than the rule. In general, the dual function is defined implicitly via the composition of two functions: (i) first compute an exponential parameter  $\theta(\mu)$  in the inverse image  $\Lambda^{-1}(\mu)$ ; and then (ii) compute the negative entropy of the distribution  $p(\mathbf{x}; \theta(\mu))$ . The block diagram in Figure 11 illustrates this decomposition of the function  $A^*$ .

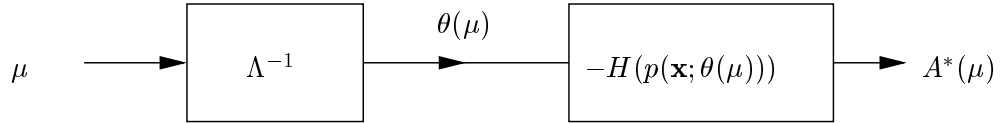


**Figure 11.** A block diagram decomposition of  $A^*$  as the composition of two functions. Given a marginal vector  $\mu$ , first compute an exponential parameter  $\theta(\mu)$  in the inverse image  $\Lambda^{-1}$ , then compute the negative entropy of  $p(\mathbf{x}; \theta(\mu))$ .

Despite the fact that  $A^*$  is not given in closed form, a number of properties can be inferred from its variational definition (23). For instance, an immediate consequence is that  $A^*$  is always convex. More specific properties of  $A^*$  depend on the nature of the exponential family, as summarized in the following:

---

<sup>6</sup>For simplicity, we are assuming that  $m_s = m$  for all nodes.

**Proposition 8.** *The dual function  $A^*$  is always convex and lower semi-continuous. Moreover, in a minimal representation:*

- (a)  *$A^*$  is differentiable on  $\text{int } \mathcal{M}$ , and  $\nabla A^*(\mu) = \Lambda^{-1}(\mu)$ .*
- (b)  *$A^*$  is strictly convex.*
- (c) *For any sequence  $\{\mu^n\}$  contained in  $\text{int } \mathcal{M}$  and approaching the boundary  $\text{bd } \mathcal{M}$ , we have  $\lim_{n \rightarrow +\infty} \|\nabla A^*(\mu^n)\| = +\infty$ .*

**Remarks:** The essential smoothness can be verified explicitly for the examples shown in Table 2, for which we have closed form expressions for  $A^*$ . For instance, in the Bernoulli case, we have  $\mathcal{M} = [0, 1]$  and  $|\nabla A^*(\mu)| = |\log[(1 - \mu)/\mu]|$ , which tends to infinity as  $\mu \rightarrow 0^+$  or  $\mu \rightarrow 1^-$ . Similarly, in the Poisson case, we have  $\mathcal{M} = (0, +\infty)$  and  $|\nabla A^*(\mu)| = |\log \mu|$ , which tends to infinity as  $\mu$  tends to the boundary point 0.

Despite the desirable properties guaranteed by Proposition 8, the function  $A^*$  presents substantial computational challenges. Indeed, both operations in the decomposition of  $A^*$  given in Figure 11 are troublesome. First of all, the inverse image  $\Lambda^{-1}(\mu)$  of the mean parameter mapping, while well-defined mathematically, does not usually have a closed form expression. It is typically necessary to resort to iterative methods, such as iterative proportional fitting or generalized iterative scaling [e.g., 29, 28], in order to compute this mapping. In any case, these algorithms presuppose that it is possible to perform exact inference, which is the problem that we are trying to solve in the first place. Second, even if we were able to compute a parameter  $\theta(\mu) \in \Lambda^{-1}(\mu)$ , there remains the task of computing the entropy  $H(p(\mathbf{x}; \theta(\mu)))$ , which is not possible in general for a large problem.

To parallel our earlier discussion of  $\mathcal{M}$ , we now turn to two important cases where  $A^*$  can be characterized in closed form, even for large problems.

#### 4.2.2 Gaussian distributions

Consider the case of a multivariate Gaussian random vector  $\mathbf{x}$ , discussed previously in Section 4.1.2. It is well-known [24] that the Gaussian entropy is  $\frac{1}{2} \log \det \text{cov}(\mathbf{x}) + \frac{n}{2} \log 2\pi e$ , where  $\text{cov}(\mathbf{x})$  is the  $n \times n$  covariance matrix of  $\mathbf{x}$ . As originally defined in equation (34), let  $W(\mu)$  be the matrix of mean parameters associated with  $\mathbf{x}$ :

$$W(\mu) = \begin{bmatrix} 1 & z^T(\mu) \\ z(\mu) & Z(\mu) \end{bmatrix}. \quad (42)$$

Applying the Schur complement formula [50] yields  $\det W(\mu) = \det[Z(\mu) - z(\mu)z^T(\mu)] = \det(\text{cov}(\mathbf{x}))$ , from which we conclude that

$$A_{Gauss}^*(\mu) = -\frac{1}{2} \log \det W(\mu) - \frac{n}{2} \log 2\pi e, \quad (43)$$

valid for all  $\mu \in \mathcal{M}_{Gauss}$ . (To understand the negative signs, recall from Theorem 2 that  $A^*$  is equal to negative entropy for  $\mu \in \mathcal{M}_{Gauss}$ .) Combining this exact expression for  $A_{Gauss}^*$  with our characterization of  $\mathcal{M}_{Gauss}$  from Proposition 6 leads to

$$A_{Gauss}(\theta) = \sup_{W(\mu) \succ 0, [W(\mu)]_{11}=1} \{ \langle\langle U(\theta), W(\mu) \rangle\rangle + \frac{1}{2} \log \det W(\mu) + \frac{1}{2} \log 2\pi e \}, \quad (44)$$

which corresponds to the variational principle (32) specialized to the Gaussian case.

If  $W(\mu) \succ 0$  were the only constraint, then, using the fact that  $\nabla \log \det W = W^{-1}$  for any symmetric positive matrix  $W$ , the optimal solution to problem (44) would simply be  $W(\mu) = -2[U(\theta)]^{-1}$ . Accordingly, if we enforce the constraint  $[W(\mu)]_{11} = 1$  using a Lagrange multiplier  $\lambda$ , then it follows from the Karush-Kuhn-Tucker conditions [8] that the optimal solution will assume the form  $W(\mu) = -2[U(\theta) + \lambda^* E_{11}]^{-1}$ , where  $\lambda^*$  is the optimal setting of the Lagrange multiplier and  $E_{11}$  is an  $(n+1) \times (n+1)$  matrix with a one in the upper left hand corner, and zero in all other entries. Finally, using the standard formula for the inverse of a block-partitioned matrix [50], it is straightforward to verify that the blocks in the optimal  $W(\mu)$  are related to the blocks of  $U(\theta)$  by the relations:

$$Z(\mu) - z(\mu)z^T(\mu) = -2[Z(\theta)]^{-1} \quad (45a)$$

$$z(\mu) = -[Z(\theta)]^{-1} z(\theta) \quad (45b)$$

(The multiplier  $\lambda^*$  turns out not to be involved in these particular blocks). In order to interpret these relations, it is helpful to return to the definition of  $U(\theta)$  given in equation (17), and the Gaussian density of equation (18). In this way, we see that equation (45a) corresponds to the fact<sup>7</sup> that the covariance matrix is the inverse of the precision matrix, whereas equation (45b) corresponds to the normal equations for the mean  $z(\mu)$  of a Gaussian. Thus, as a special case of the general variational principle (32), we have re-derived the familiar equations for Gaussian inference.

#### 4.2.3 Tree-structured problems

We now return to the case of tree-structured multinomial distributions, discussed previously in Section 4.1.3. Another consequence of the junction tree representation is that  $A^*$  has a closed-form expression for any distribution defined by a junction tree. The case of an ordinary tree  $T = (V, E(T))$  suffices to illustrate. In the canonical overcomplete representation of equation (38), the mean parameters  $\mu = \{\mu_s, \mu_{st}\}$  correspond to local marginals associated with single nodes and edges. In particular, we make use of the local marginal functions  $\mu_s(x_s)$  and  $\mu_{st}(x_s, x_t)$  defined in equation (40).

By a special case of the junction tree decomposition (9), any tree-structured distribution factorizes in terms of the local marginal distributions as follows:

$$p(\mathbf{x}) = \prod_{s \in V} \mu_s(x_s) \prod_{(s,t) \in E(T)} \frac{\mu_{st}(x_s, x_t)}{\mu_s(x_s) \mu_t(x_t)}. \quad (46)$$

Using the definition of Boltzmann-Shannon entropy (24) and Theorem 2(a), this factorization leads immediately to an explicit form for the dual function, valid for all  $\mu \in \text{ri MARG}(T)$ :

$$A_{tree}^*(\mu) = - \sum_{s \in V} H_s(\mu_s) + \sum_{(s,t) \in E(T)} I_{st}(\mu_{st}). \quad (47)$$

Here  $H_s$  and  $I_{st}$  are, respectively, single node entropy and mutual information terms:

$$H_s(\mu_s) := - \sum_{x_s} \mu_s(x_s) \log \mu_s(x_s), \quad I_{st}(\mu_{st}) := \sum_{x_s, x_t} \mu_{st}(x_s, x_t) \log \frac{\mu_{st}(x_s, x_t)}{\mu_s(x_s) \mu_t(x_t)}. \quad (48)$$

---

<sup>7</sup>The factor of negative two in equation (45a) arises due to the exponential parameterization of the multivariate Gaussian used in equation (18).

Again, it is worth combining this expression with our characterization of the marginal polytope  $\text{MARG}(T)$  from Example 8. In this way, we obtain the following tree-structured form of the general variational principle (32):

$$\max_{\mu \in \text{MARG}(T)} \left\{ \langle \theta, \mu \rangle + \sum_{s \in V} H_s(\mu_s) - \sum_{(s,t) \in E(T)} I_{st}(\mu_{st}) \right\}. \quad (49)$$

Note that this problem has a simple structure: the cost function is concave and differentiable, and the constraint set  $\text{MARG}(T)$  is a polytope specified by a small ( $\mathcal{O}(n)$ ) number of constraints. In fact, we will establish, as a corollary of our analysis of the Bethe approximation in Section 6, that the sum-product updates (7) are a Lagrangian-based method for solving problem (49).

In overview, we have seen how the general variational principle (32) takes explicit and simple forms for multivariate Gaussians on arbitrary graphs, and discrete random vectors on tree-structured graphs. The perspective given here clarifies that inference in such models is relatively easy because the underlying variational problem has simple structure. In the following sections, we demonstrate how the Gaussian and tree-structured characterizations of  $\mathcal{M}$  and  $A^*$ , though presented as exact representations in the preceding sections, also play an important role in approximate inference.

## 5 Mean field theory

This section is devoted to a discussion of mean field methods, which are classical techniques in statistical physics [e.g., 73, 6, 21]. From the perspective of this paper, mean field theory is based on the variational principle of equation (32), but entails imposing limitations on the optimization. More specifically, as discussed in Section 4, there are two fundamental difficulties associated with the variational principle (32): the nature of the constraint set  $\mathcal{M}$ , and the lack of an explicit form for the dual function  $A^*$ . Mean field theory entails limiting the optimization to a subset of distributions for which  $A^*$  is relatively easy to characterize. Throughout this section, we will refer to a distribution with this property as a *tractable* distribution.

### 5.1 Tractable families

Let  $H$  represent a subgraph of  $G$  over which it feasible to perform exact calculations, for example a graph with small treewidth. We refer to  $H$  as a *tractable subgraph*. In an exponential formulation, the set of all distributions that respect the structure of  $H$  can be represented by a linear subspace of exponential parameters. More specifically, letting  $\mathcal{I}(H)$  be the subset of indices associated with cliques in  $H$ , the set of exponential parameters corresponding to distributions structured according to  $H$  is given by:

$$\mathcal{E}(H) := \{\theta \in \Theta \mid \theta_\alpha = 0 \quad \forall \alpha \in \mathcal{I} \setminus \mathcal{I}(H)\}. \quad (50)$$

We consider some examples to illustrate:

**Example 9 (Tractable subgraphs).** The simplest (non-trivial) instance of a tractable subgraph is the completely disconnected graph  $H_0 = (V, \emptyset)$ . Permissible parameters belong to the subspace  $\mathcal{E}(H_0) := \{\theta \in \Theta \mid \theta_{st} = 0 \quad \forall (s, t) \in E\}$ , where  $\theta_{st}$  refers to the collection of exponential parameters associated with edge  $(s, t)$ . The associated distributions are of the product form  $p(\mathbf{x}; \theta) = \prod_{s \in V} p(x_s; \theta_s)$ , where  $\theta_s$  refers to the collection of exponential parameters associated with vertex  $s$ .

To obtain a more structured approximation, one could choose a spanning tree  $T = (V, E(T))$ . In this case, we are free to choose the exponential parameters corresponding to vertices and edges in  $T$ , but we must set to zero any exponential parameters corresponding to edges not in the tree. Accordingly, the subspace of tree-structured distributions is given by  $\mathcal{E}(T) = \{\theta \mid \theta_{st} = 0 \ \forall (s, t) \notin E(T)\}$ .  $\diamond$

For a given subgraph  $H$ , consider the set of all possible mean parameters that are realizable by tractable distributions:

$$\mathcal{M}_{\text{tract}}(G; H) := \{\mu \in \mathbb{R}^d \mid \mu = \mathbb{E}_\theta[\phi(\mathbf{x})] \text{ for some } \theta \in \mathcal{E}(H)\}. \quad (51)$$

The notation  $\mathcal{M}_{\text{tract}}(G; H)$  indicates that mean parameters in this set correspond to potentials on the graph  $G$ , but that they must be realizable by a tractable distribution—i.e., one that respects the structure of  $H$ . Since any  $\mu$  that arises from a tractable distribution is certainly a valid mean parameter, the inclusion  $\mathcal{M}_{\text{tract}}(G; H) \subseteq \mathcal{M}(G)$  always holds. In this sense,  $\mathcal{M}_{\text{tract}}$  is an *inner approximation* to the set  $\mathcal{M}$  of realizable mean parameters.

## 5.2 Optimization and lower bounds

We now have the necessary ingredients to develop the mean field approach to approximate inference. Let  $p(\mathbf{x}; \theta)$  denote the *target distribution* that we are interested in approximating. The basis of the mean field method is the following fact: any valid mean parameter specifies a lower bound on the log partition function.

**Proposition 9 (Mean field lower bound).** *For any  $\mu \in \text{ri } \mathcal{M}$ , we have the following lower bound:*

$$A(\theta) \geq \langle \theta, \mu \rangle - A^*(\mu). \quad (52)$$

*Proof.* In the context of our exposition, the validity of this lower bound is an immediate consequence of the variational principle (32). Alternatively, it can be established via Jensen's inequality. For any mean parameter  $\mu \in \text{ri } \mathcal{M}$ , Theorem 5 guarantees the existence of some  $\theta(\mu) \in \Lambda^{-1}(\mu)$ . Using the distribution  $p(\mathbf{x}; \theta(\mu))$ , we write:

$$\begin{aligned} A(\theta) &= \log \int_{\mathcal{X}^n} p(\mathbf{x}; \theta(\mu)) \frac{\exp\{\langle \theta, \phi(\mathbf{x}) \rangle\}}{p(\mathbf{x}; \theta(\mu))} \nu(d\mathbf{x}) \\ &\stackrel{(a)}{\geq} \int_{\mathcal{X}^n} p(\mathbf{x}; \theta(\mu)) [\langle \theta, \phi(\mathbf{x}) \rangle - \log p(\mathbf{x}; \theta(\mu))] \nu(d\mathbf{x}) \\ &\stackrel{(b)}{=} \langle \theta, \mu \rangle - A^*(\mu). \end{aligned}$$

In this argument, step (a) follows from Jensen's inequality [e.g., 49], whereas step (b) follows from the relations  $\mathbb{E}_{\theta(\mu)}[\phi(\mathbf{x})] = \mu$ , and  $A^*(\mu) = -H(p(\mathbf{x}; \theta(\mu)))$  from Theorem 2(a).  $\square$

Since the dual function  $A^*$  typically lacks an explicit form, it is not possible, at least in general, to compute the lower bound (52). The mean field approach circumvents this difficulty by restricting the choice of  $\mu$  to a tractable subset  $\mathcal{M}_{\text{tract}}(G; H)$ , for which the dual function has an explicit form  $A_H^*$ . As long as  $\mu$  belongs to  $\mathcal{M}_{\text{tract}}(G; H)$ , then the lower bound (52) will be computable.

Of course, for a non-trivial class of tractable distributions, there are many such bounds. The goal of the mean field method is the natural one: find the best approximation  $\mu^{\text{MF}}$ , as measured

in terms of the tightness of the bound. This optimal approximation is specified as the solution of the optimization problem

$$\sup_{\mu \in \mathcal{M}_{\text{tract}}(G; H)} \{ \langle \mu, \theta \rangle - A_H^*(\mu) \}. \quad (53)$$

The optimal value specifies a lower bound on  $A(\theta)$ , and it is (by definition) the best one that can be obtained by using a distribution from the tractable class.

An important alternative interpretation of the mean field solution (53) is as minimizing the Kullback-Leibler divergence between the approximating (tractable) distribution and the target distribution. In particular, for a given mean parameter  $\mu \in \mathcal{M}_{\text{tract}}(G; H)$ , the difference between the log partition function  $A(\theta)$  and the quantity  $\langle \mu, \theta \rangle - A_H^*(\mu)$  to be maximized is equivalent to

$$D(\mu \| \theta) = A(\theta) + A_H^*(\mu) - \langle \mu, \theta \rangle,$$

corresponding to the mixed form of the Kullback-Leibler divergence defined in equation (30). On the basis of this relation, it can be seen that solving the variational problem (53) is equivalent to minimizing the KL divergence  $D(\mu \| \theta)$  subject to the constraint that  $\mu \in \mathcal{M}_{\text{tract}}(G; H)$ . Note that this problem entails a minimization over mean parameters with respect to the *first* argument of the Kullback-Leibler divergence. As a consequence, the mean field procedure is an operation that differs in fundamental ways from the I-projection with KL divergences [3, 27].

### 5.2.1 Naive mean field updates

The *naive mean field* approach corresponds to choosing a fully factorized or product distribution in order to approximate the original distribution. The naive mean field updates are a particular set of recursions for finding a stationary point of the resulting optimization problem.

**Example 10.** As an illustration, we derive the naive mean field updates for the Ising model introduced in Example 3. Letting  $H_0$  denote the fully disconnected graph (i.e., no edges), the tractable set  $\mathcal{M}_{\text{tract}}(G; H_0)$  consists of all mean parameters  $\{\mu_s, \mu_{st}\}$  that arise from a product distribution. Explicitly, in this binary case, we have

$$\mathcal{M}_{\text{tract}}(G; H_0) := \{(\mu_s, \mu_{st}) \mid 0 \leq \mu_s \leq 1, \mu_{st} = \mu_s \mu_t\}.$$

Moreover, the negative entropy of a product distribution over binary random variables decomposes into the sum  $A_{H_0}^*(\mu) = \sum_{s \in V} [\mu_s \log \mu_s + (1 - \mu_s) \log(1 - \mu_s)]$ . Accordingly, the associated naive mean field problem takes the form  $\max_{\mu \in \mathcal{M}_{\text{tract}}(G; H_0)} \{ \langle \mu, \theta \rangle - A_{H_0}^*(\mu) \}$ . In this particular case, it is straightforward to eliminate  $\mu_{st}$  by replacing it by the product  $\mu_s \mu_t$ . Doing so leads to a reduced form of the problem:

$$\max_{\{\mu_s\} \in [0, 1]^n} \left\{ \sum_{s \in V} \theta_s \mu_s + \sum_{(s, t) \in E} \theta_{st} \mu_s \mu_t - \sum_{s \in V} [\mu_s \log \mu_s + (1 - \mu_s) \log(1 - \mu_s)] \right\} \quad (54)$$

Let  $F$  denote the function of  $\mu$  within curly braces in equation (54). It can be seen that for any  $s \in V$ , it is strictly concave in  $\mu_s$  when all the other coordinates are held fixed. Therefore, the maximum over  $\mu_s$  with  $\mu_t, t \neq s$  fixed is attained in the interior  $(0, 1)$ , and can be found by taking the gradient and setting it equal to zero. Doing so yields the following update for  $\mu_s$ :

$$\mu_s \leftarrow \sigma(\theta_s + \sum_{t \in \mathcal{N}(s)} \theta_{st} \mu_t), \quad (55)$$

where  $\sigma(z) := [1 + \exp(-z)]^{-1}$  is the logistic function. Applying equation (55) iteratively to each node in succession amounts to performing coordinate ascent of the mean field variational problem (54). We have derived the update equation presented earlier in equation (12).  $\diamond$

Similarly, it is straightforward to apply the naive mean field approximation to other types of graphical models, as we illustrate for a multivariate Gaussian.

**Example 11 (Gaussian mean field).** The mean parameters for a multivariate Gaussian are of the form  $\mu_s = \mathbb{E}[x_s]$ ,  $\mu_{ss} = \mathbb{E}[x_s^2]$  and  $\mu_{st} = \mathbb{E}[x_s x_t]$  for  $s \neq t$ . Using only Gaussians in product form, the set of tractable mean parameters takes the form

$$\mathcal{M}_{\text{tract}}(G; H_0) = \{\mu \in \mathbb{R}^d \mid \mu_{st} = \mu_s \mu_t \forall s \neq t, \mu_{ss} - \mu_s^2 > 0\}.$$

As with naive mean field on the Ising model, the constraints  $\mu_{st} = \mu_s \mu_t$  for  $s \neq t$  can be imposed directly, thereby leaving only the inequality  $\mu_{ss} - \mu_s^2 > 0$  for each node. The negative entropy of a Gaussian in product form can be written as  $A_{\text{Gauss}}^*(\mu) = -\sum_{s=1}^n \frac{1}{2} \log(\mu_{ss} - \mu_s^2) - \frac{n}{2} \log 2\pi e$ . Combining  $A_{\text{Gauss}}^*$  with the constraints leads to the naive MF problem for a multivariate Gaussian:

$$\sup_{\{(\mu_s, \mu_{ss}) \mid \mu_{ss} - \mu_s^2 > 0\}} \{\langle\langle U(\theta), W(\mu) \rangle\rangle + \sum_{s=1}^n \frac{1}{2} \log(\mu_{ss} - \mu_s^2) + \frac{n}{2} \log 2\pi e\}.$$

Here it should be understood that any terms  $\mu_{st}, s \neq t$  contained in  $W(\mu)$  are replaced with the product  $\mu_s \mu_t$ .

Taking derivatives with respect to  $\mu_{ss}$  and  $\mu_s$  and re-arranging yields the stationary conditions  $\frac{1}{2(\mu_{ss} - \mu_s^2)} = -\theta_{ss}$  and  $\frac{\mu_s}{2(\mu_{ss} - \mu_s^2)} = \theta_s + \sum_{t \in \mathcal{N}(s)} \theta_{st} \mu_t$ . Since  $\theta_{ss} < 0$ , we can combine both equations into the update  $\mu_s \leftarrow -\frac{1}{\theta_{ss}} \{\theta_s + \sum_{t \in \mathcal{N}(s)} \theta_{st} \mu_t\}$ . The resulting algorithm is equivalent, in fact, to the Gauss-Jacobi method for solving the quadratic system associated with the Gaussian problem. Therefore, under suitable conditions [31], the updates will converge, and compute the correct mean vector  $[\mu_1 \dots \mu_n]$ .  $\diamond$

### 5.2.2 Structured mean field

Of course, the essential principles underlying the mean field approach are not limited to fully factorized distributions. More generally, we can consider classes of tractable distributions that incorporate additional structure. This *structured mean field approach* was first proposed by Saul and Jordan [81], and further developed by various researchers [e.g., 99].

Here we discuss a general form of the updates for an approximation based on an arbitrary subgraph  $H$  of the original graph  $G$ . We make no claims as to the practical advantages of these updates; our main goal here is the conceptual one of understanding the structure of the solution. Depending on the particular context, other types of updates [e.g., 99] or techniques from nonlinear programming may be more suitable for solving the mean field problem (53).

Let  $\mathcal{I}(H)$  be the subset of indices corresponding to sufficient statistics associated with  $H$ , and let  $\mu(H) := \{\mu_\alpha \mid \alpha \in \mathcal{I}(H)\}$  be the associated set of mean parameters. The mean field problem has the following key properties:

- (a) the subvector  $\mu(H)$  can be an arbitrary member of  $\mathcal{M}(H)$ , the set of realizable mean parameters defined by the subgraph  $H$ .
- (b) the dual function  $A_H^*$  actually depends only on  $\mu(H)$ , and *not* on mean parameters  $\mu_\beta$  for indices  $\beta$  in the complement  $\mathcal{I}^c(H) := \mathcal{I}(G) \setminus \mathcal{I}(H)$ .

Of course, mean parameters  $\mu_\beta$  with  $\beta \in \mathcal{I}^c(H)$  do play a role in the problem; in particular, they arise within the linear term  $\langle \mu, \theta \rangle$ . Moreover, each mean parameter  $\mu_\beta$  is constrained in a nonlinear way by the choice of  $\mu(H)$ . Accordingly, for each  $\beta \in \mathcal{I}^c(H)$ , we write  $\mu_\beta = g_\beta(\mu(H))$  for some

nonlinear function  $g_\beta$ , of which particular examples are given below. Based on these observations, the optimization problem (53) can be rewritten in the form

$$\begin{aligned} \sup_{\mu \in \mathcal{M}_{tract}(G; H)} \{ \langle \theta, \mu \rangle - A_H^*(\mu) \} = \\ \sup_{\mu(H) \in \mathcal{M}(H)} \left\{ \sum_{\alpha \in \mathcal{I}(H)} \theta_\alpha \mu_\alpha + \sum_{\alpha \in \mathcal{I}^c(H)} \theta_\alpha g_\alpha(\mu(H)) - A_H^*(\mu(H)) \right\}. \end{aligned} \quad (56)$$

On the LHS, the optimization takes place over vector  $\mu \in \mathcal{M}_{tract}(G; H)$ , which is of the same dimension as  $\theta \in \Theta \subseteq \mathbb{R}^d$ . The optimization on the RHS, in contrast, takes place over a lower-dimensional vector  $\mu(H) \in \mathcal{M}(H)$ .

To illustrate this transformation, consider the case of naive mean field for the Ising model, where  $H \equiv H_0$  is the completely disconnected graph. In this case, each edge  $(s, t) \in E$  corresponds to an index in the set  $\mathcal{I}^c(H_0)$ ; moreover, for any such edge, we have  $g_{st}(\mu(H_0)) = \mu_s \mu_t$ . Since  $H_0$  is the completely disconnected graph,  $\mathcal{M}(H_0)$  is simply the hypercube  $[0, 1]^n$ . Therefore, for this particular example, the RHS of equation (56) is equivalent to equation (54).

Letting  $F(\mu(H))$  denote the cost function on the RHS of equation (56), we take derivatives with respect to some  $\mu_\beta$  with  $\beta \in \mathcal{I}(H)$ :

$$\frac{\partial F}{\partial \mu_\beta} = \theta_\beta + \sum_{\alpha \in \mathcal{I}(G) \setminus \mathcal{I}(H)} \theta_\alpha \frac{\partial g_\alpha}{\partial \mu_\beta} - \frac{\partial A_H^*}{\partial \mu_\beta}. \quad (57)$$

From Proposition 8, the derivative  $\frac{\partial A_H^*}{\partial \mu_\beta}$  defines the inverse moment mapping, so that it is equal to the exponential parameter associated with  $\mu_\beta(H)$ , which we denote by  $\gamma_\beta(H)$ . Consequently, setting  $\frac{\partial F}{\partial \mu_\beta}$  to zero and re-arranging yields a generalized MF update:

$$\gamma_\beta(H) \leftarrow \bar{\theta}_\beta + \sum_{\alpha \in \mathcal{I}(G) \setminus \mathcal{I}(H)} \bar{\theta}_\alpha \frac{\partial g_\alpha}{\partial \mu_\beta}. \quad (58)$$

After any such update, it is then necessary to adjust all of the mean parameters  $\mu_\delta(H)$  that depend on  $\theta_\beta(H)$  (e.g., via junction tree updates), so that global consistency is maintained.

Let us check that equation (58) reduces appropriately to the naive mean field updates (55). In particular, for product distributions on the Ising model, we have  $g_{st}(\mu(H_0)) = \mu_s \mu_t$  for all edges  $(s, t)$ , so that

$$\frac{\partial g_{st}}{\partial \mu_\alpha} = \begin{cases} \mu_t & \text{if } \alpha = s \\ \mu_s & \text{if } \alpha = t \\ 0 & \text{otherwise.} \end{cases}$$

Thus, equation (58) is equivalent to  $\theta_s \leftarrow \theta_s + \sum_{t \in \mathcal{N}(s)} \theta_{st} \mu_t$ . In a product distribution, only  $\mu_s$  depends on  $\theta_s$ , so that we can update  $\mu_s$  by applying the logistic function  $\sigma(\cdot)$ , thereby recovering equation (55).

**Example 12 (Structured MF for factorial HMMs).** To provide a more interesting example of the updates (58), consider a factorial hidden Markov model, as described in Ghahramani and Jordan [45]. Figure 12(a) shows the original model, which consists of a set of  $M$  Markov chains ( $M = 3$  in this diagram), which share at each time a common observation (shaded nodes). Although the separate chains are a priori independent, the common observation induces an effective coupling between all nodes at each time. Thus, an equivalent model is shown in panel (b), where the dotted

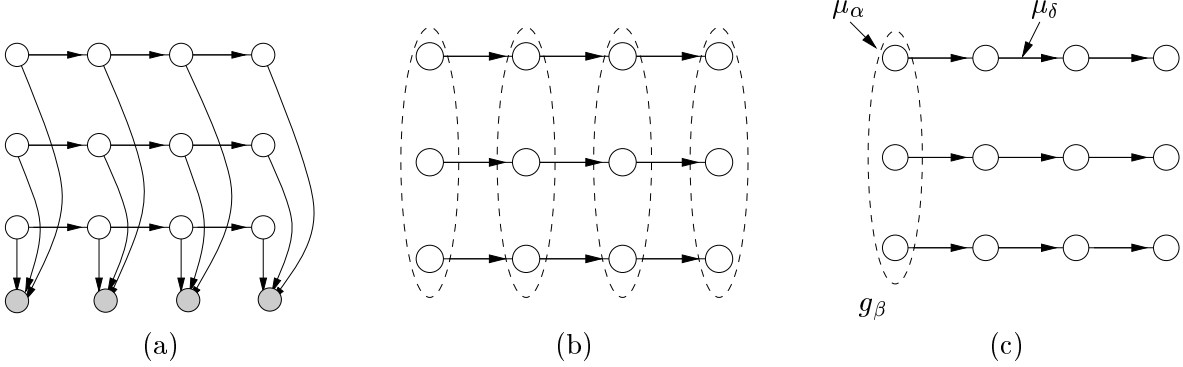


**Figure 12.** Structured mean field approximation for a factorial HMM. (a) Original model consists of a set of hidden Markov models (defined on chains), coupled at each time by a common observation. (b) An equivalent model, where the ellipses represent interactions among all nodes at a fixed time, induced by the common observation. (c) Approximating distribution formed by a product of chain-structured models. Here  $\mu_\alpha$  and  $\mu_\delta$  are the sets of mean parameters associated with the indicated vertex and edge respectively.

ellipses represent the induced coupling of each observation. A natural choice of approximating distribution in this case is based on the decoupled set of  $M$  chains, as illustrated in panel (c).

Now consider the nature of the quantities  $g_\beta(\mu)$ , which arise in the cost function (56). In this case, any function  $g_\beta$  will be defined on some subset of  $M$  nodes that are coupled at a given time slice (e.g., see ellipse in panel (c)). Note that this subset of nodes is independent with respect to the approximating distribution. Therefore, the function  $g_\beta(\mu)$  will decouple into a product of terms of the form  $f_i(\{\mu_i\})$ , where each  $f_i$  is some function of the mean parameters  $\{\mu_i\}$  associated with node  $i = 1, \dots, M$  in the relevant cluster. For instance, if the factorial HMM involved binary variables and  $M = 3$  and  $\beta = (stu)$ , then  $g_{stu}(\mu) = \mu_s \mu_t \mu_u$ .

The decoupled nature of the approximation yields valuable savings on the computational side. In particular, all intermediate quantities necessary for the updates can be calculated by applying the forward-backward algorithm (i.e., the sum-product updates as an exact method) to each chain separately. This decoupling also has important consequences for the structure of any mean field fixed point. In particular, it can be seen that no term  $g_\beta(\mu)$  will ever depend on mean parameters associated with edges in any of the chains (e.g.,  $\mu_\delta$  in panel (c)). Otherwise stated, the partial derivative  $\frac{\partial g_\beta}{\partial \mu_\delta}$  is equal to 0 for all  $\beta \in \mathcal{I}(G) \setminus \mathcal{I}(H)$ , whence MF  $\theta_\delta = \theta_\delta$  for all iterations of the updates (58). Any intermediate junction tree steps to maintain consistency will not affect  $\theta_\delta$  either. We conclude that it is, in fact, optimal to simply copy the original edge potentials  $\theta_\delta$  onto each of the edges. In this particular form of structured mean field, only the single node potentials will be altered from their original setting. This conclusion is sensible, since the structured approximation (c) is a factorized approximation on a set of  $M$  clusters. Each cluster consists of an entire chain, the internal structure of which is fully preserved in the approximation.  $\diamond$

### 5.3 Parameter estimation and variational EM

In this section we consider the problem of parameter estimation, focusing specifically on the setting in which some variables are observed and others are unobserved (“latent” or “hidden”). This is the setting in which the expectation-maximization (EM) algorithm provides a general approach to maximum likelihood parameter estimation [32]. While the EM algorithm is often presented as an alternation between an expectation step (E step) and a maximization step (M step), it is also

possible to take a variational perspective on EM and view both steps as maximization steps [26, 70]. This perspective makes it possible to understand how variational inference algorithms can be used in place of exact inference algorithms in the E step within the EM framework, and also shows how the mean field approach is particularly appropriate for this task.

The brief outline of our presentation in this section is as follows. In the exponential family setting, the E step reduces to the computation of expected sufficient statistics—i.e., mean parameters. As we have seen, the variational framework provides a general class of methods for computing approximations of mean parameters. This suggests a general class of *variational EM algorithms*, in which the approximation provided by a variational inference algorithm is substituted for the mean parameters in the E step. In general one loses the guarantees that are associated with the EM algorithm in making such a substitution. In the specific case of mean field algorithms, however, one does retain a convergence guarantee; in particular, the algorithm will converge to a stationary point of a lower bound for the likelihood function.

Let us partition the set of random variables into *observed* variables  $\mathbf{x}$  and *unobserved* variables  $\mathbf{z}$ . The probability model is a joint exponential family distribution for  $(\mathbf{x}, \mathbf{z})$ :

$$p(\mathbf{x}, \mathbf{z}; \theta) = \exp \{ \langle \theta, \phi(\mathbf{x}, \mathbf{z}) \rangle - A(\theta) \}. \quad (59)$$

Given an observation  $\mathbf{x}$ , we can also form the conditional distribution

$$p(\mathbf{z} | \mathbf{x}; \theta) = \frac{\exp \{ \langle \theta, \phi(\mathbf{x}, \mathbf{z}) \rangle \}}{\int_{\mathcal{X}^n} \exp \{ \langle \theta, \phi(\mathbf{x}, \mathbf{z}) \rangle \} \nu(d\mathbf{z})} \quad (60)$$

$$:= \exp \{ \langle \theta, \phi(\mathbf{x}, \mathbf{z}) \rangle - A_x(\theta) \}, \quad (61)$$

where the second equation defines the log partition function associated with the conditional.

We see that the conditional is also an exponential family distribution. We thus have the variational representation:

$$A_x(\theta) = \sup_{\mu \in \mathcal{M}_x} \{ \langle \theta, \mu \rangle - A_x^*(\mu) \}, \quad (62)$$

where the conjugate dual is also defined variationally:

$$A_x^*(\mu) := \sup_{\theta \in \Theta} \{ \langle \mu, \theta \rangle - A_x(\theta) \}, \quad (63)$$

and where  $\mathcal{M}_x$  is defined as the set of possible expectations of  $\phi(\mathbf{x}, \mathbf{z})$ , where  $\mathbf{z}$  is random and  $\mathbf{x}$  is held fixed.

The *incomplete log likelihood* is the log probability of the observed data  $\mathbf{x}$ . It is easy to verify that this log likelihood can be written as a difference of log partition functions:

$$\log p(\mathbf{x}; \theta) = A_x(\theta) - A(\theta). \quad (64)$$

We now appeal to the Fenchel inequality to obtain a lower bound for  $A_x(\theta)$ :

$$A_x(\theta) \geq \langle \mu, \theta \rangle - A_x^*(\mu), \quad (65)$$

where  $\mu \in \mathcal{M}_x$ , and hence a lower bound for the incomplete log likelihood:

$$\log p(\mathbf{x}; \theta) \geq \langle \mu, \theta \rangle - A_x^*(\mu) - A(\theta) \quad (66)$$

$$:= \mathcal{L}(\mu, \theta), \quad (67)$$

where the final line defines  $\mathcal{L}(\mu, \theta)$ .

The EM algorithm is coordinate ascent in  $\mathcal{L}$ :

$$(\mathbf{E} \text{ step}) \quad \mu^{(t+1)} = \operatorname{argmax}_{\mu \in \mathcal{M}_x} \mathcal{L}(\mu, \theta^{(t)}) \quad (68)$$

$$(\mathbf{M} \text{ step}) \quad \theta^{(t+1)} = \operatorname{argmax}_{\theta \in \Theta} \mathcal{L}(\mu^{(t+1)}, \theta). \quad (69)$$

To see the correspondence with the traditional presentation of the EM algorithm, note first that the maximization underlying the E step reduces to

$$\max_{\mu \in \mathcal{M}_x} \{\langle \mu, \theta^{(t)} \rangle - A_x^*(\mu)\}, \quad (70)$$

which by (62) is equal to  $A_x(\theta^{(t)})$ , with the maximizing argument equal to the mean parameter that is dually coupled with  $\theta^{(t)}$ . Thus the vector  $\mu^{(t+1)}$  that is computed in the E step is exactly the expectation of the sufficient statistics given the current parameter value  $\theta^{(t)}$ , a computation that is traditionally referred to as the E step. Moreover, the maximization underlying the M step reduces to

$$\max_{\theta \in \Theta} \{\langle \mu^{(t+1)}, \theta \rangle - A(\theta)\}, \quad (71)$$

which is simply a maximum likelihood problem based on the expected sufficient statistics  $\mu^{(t+1)}$ —traditionally referred to as the M step.

Moreover, given that the value achieved by the E step on the right-hand-side of (70) is equal to  $A_x(\theta^{(t)})$ , the inequality in (66) becomes an equality by (64). Thus, after the E step, the lower bound  $\mathcal{L}(\mu, \theta^{(t)})$  is actually equal to the incomplete log likelihood  $\log p(\mathbf{x}; \theta^{(t)})$ , and the subsequent maximization of  $\mathcal{L}$  with respect to  $\theta$  in the M step is guaranteed to increase the log likelihood as well.

What if it is infeasible to compute the expected sufficient statistics? One possible response to this problem is to make use of a variational relaxation for the E step. In particular, we compute

$$(\mathbf{Variational E step}) \quad \mu^{(t+1)} = \operatorname{argmax}_{\mu \in \mathcal{M}_{tract}(G; H)} \mathcal{L}(\mu, \theta^{(t)}), \quad (72)$$

where  $\mathcal{M}_{tract}(G; H)$  is the set of dual parameters associated with a tractable subgraph. The variational E step thus reduces to

$$\max_{\mu \in \mathcal{M}_{tract}(G; H)} \{\langle \mu, \theta^{(t)} \rangle - A_{x,H}^*(\mu)\}, \quad (73)$$

which is exactly the mean field approximation. The variational E step thus involves replacing expected sufficient statistics with the approximate expected sufficient statistics obtained by a mean field algorithm. The resulting variational EM algorithm is still coordinate ascent in  $\mathcal{L}$ . However, given that the E step no longer closes the gap between  $\mathcal{L}$  and the incomplete log likelihood, it is no longer the case that the algorithm necessarily goes uphill in the latter quantity.

We will present a number of variational relaxations in the remainder of the paper. It is tempting, and common in practice, to substitute the approximate expected sufficient statistics obtained from these relaxations in the place of the expected sufficient statistics in defining a “variational EM algorithm.” This is particularly tempting given that these methods can yield better approximations to mean parameters than the mean field approach. Care must be taken in working with these algorithms, however, because the underlying relaxations do not generally involve lower bounds on the log partition function. The connection to EM is thus less clear than in the mean field case, and the algorithm is not guaranteed to converge.

## 5.4 Non-convexity of mean field

An important fact about the mean field approach is that the variational problem (53) may be non-convex, so that there may be local minima, and the mean field updates can have multiple solutions. Here we explore the source of the non-convexity, which can be understood in several different ways.

Consider first the representation of the mean field problem on the RHS of equation (56). The constraint set in this formulation—namely,  $\mathcal{M}(H)$ —is certainly convex. The cost function consists of a (concave) entropy term  $-A_H^*(\mu)$  and a set of terms  $\sum_{\alpha \in \mathcal{I}(H)} \theta_\alpha \mu_\alpha$  that are linear in  $\mu$ . In contrast, the terms  $\sum_{\alpha \notin \mathcal{I}(H)} \theta_\alpha g_\alpha(\mu)$  involve the *nonlinear* functions  $g_\alpha$ , so that they may introduce non-convexity. For example, in the case of naive mean field on the Ising model, these functions are monomials of the form  $\mu_s \mu_t$ . Consequently, the overall cost function in equation (54) includes a quadratic form in  $\{\mu_v\}$ , so that it need not be convex in general.

In these simple cases, it can be seen explicitly how the nonlinear functions  $g_\alpha(\mu)$  lead to non-convexity in the MF problem. In order to gain a more general and geometric understanding of this non-convexity, let us return to the form of mean field variational problem given in equation (53). In this formulation, observe that the function to be maximized—namely,  $\langle \mu, \theta \rangle - A_H^*(\mu)$ —is always a concave function of  $\mu$ . Consequently, the source of any non-convexity must lie in the nature of the constraint set  $\mathcal{M}_{tract}(G; H)$ . To provide some geometric intuition for this set, let us return again to naive mean field on the Ising model.

**Example 13 (Non-convexity of  $\mathcal{M}_{tract}$ ).** Consider a pair of binary variables on the (trivial) graph  $G$  consisting of a single edge. In the standard minimal representation, there are three mean parameters— $\mu_1$ ,  $\mu_2$  and  $\mu_{12}$ . From the development of Example 7, the marginal polytope  $\mathcal{M}(G) \equiv \text{MARG}(G)$  is fully characterized by the four inequalities  $1 + \mu_{12} - \mu_1 - \mu_2 \geq 0$ ,  $\mu_{12} \geq 0$ , and  $\mu_s - \mu_{12} \geq 0$  for  $s = 1, 2$ . So as to facilitate visualization, consider a particular projection of this polytope—namely, that corresponding to intersection with the hyperplane  $\mu_1 = \mu_2$ . In this case, the four inequalities reduce to three simpler ones—namely:

$$\mu_{12} \geq 2\mu_1 - 1, \quad \mu_{12} \geq 0, \quad \mu_1 \geq \mu_{12}. \quad (74)$$

Figure 13 shows the resulting two-dimensional polytope, shaded in gray. Let us now consider the

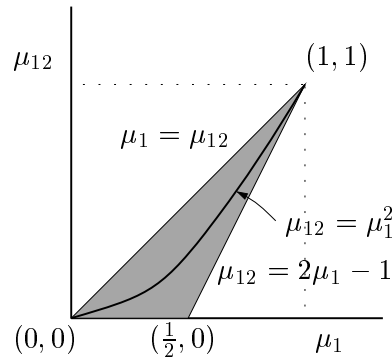


**Figure 13.** Non-convexity of the set of fully factorized marginals for a pair of binary variables. The gray area shows the polytope defined by equation (74), corresponding to the intersection of  $\mathcal{M}(G)$  with the hyperplane  $\mu_1 = \mu_2$ . The (non-convex) quadratic curve  $\mu_{12} = \mu_1^2$  corresponds to the intersection of  $\mu_1 = \mu_2$  with the set  $\mathcal{M}_{tract}(G; H_0)$  of fully factorized marginals.

intersection between  $\mu_1 = \mu_2$  and the set of factorized marginals  $\mathcal{M}_{tract}(G; H_0)$ . It is easy to see that this intersection is given by the equation  $\mu_{12} = \mu_1^2$ . This quadratic curve lies within the

two-dimensional polytope described by the equations (74), as illustrated in Figure 13. Since this quadratic set is not convex, this establishes that  $\mathcal{M}_{tract}$  is not convex either. (If  $\mathcal{M}_{tract}$  were convex, then its intersection with any hyperplane would also be convex.)  $\diamond$

Equipped with intuition from this example, we can formulate a result that characterizes the non-convexity of mean field approximations more generally:

**Proposition 10 (Non-convexity).** *Suppose that  $\text{cl } \mathcal{M}(G)$  contains no full lines. Consider a set of tractable mean parameters  $\text{cl } \mathcal{M}_{tract}(G; H) \subsetneq \text{cl } \mathcal{M}(G)$  that contains all extreme points and directions of  $\text{cl } \mathcal{M}(G)$ . Then  $\mathcal{M}_{tract}(G; H)$  is a non-convex set.*

*Proof.* The assumption that  $\text{cl } \mathcal{M}(G)$  contains no full lines guarantees that it can be represented as the convex hull of its extreme points and directions (Thm. 18.5, [79]). Since  $\text{cl } \mathcal{M}_{tract}(G; H)$  contains these extreme points and directions by assumption, its convex hull must be equal to  $\text{cl } \mathcal{M}(G)$ . Therefore,  $\text{cl } \mathcal{M}_{tract}(G; H)$  cannot be convex, since it is properly contained within  $\text{cl } \mathcal{M}(G)$ . (If it were convex, then  $\text{cl } \mathcal{M}_{tract}(G; H) = \text{conv cl } \mathcal{M}_{tract}(G; H) = \text{cl } \mathcal{M}(G)$ , which is a contradiction).  $\square$

The assumptions underlying Proposition 10 hold in most applications of mean field. Certainly, the set of tractable mean parameters is invariably a subset of  $\text{cl } \mathcal{M}(G)$ , since we are trying to approximate a model assumed to be intractable. Moreover, the set  $\text{cl } \mathcal{M}_{tract}(G; H)$  typically contains the extreme points and directions of  $\text{cl } \mathcal{M}(G)$ . Let us consider some examples to illustrate:

**Multinomial:** In this case, Proposition 7 ensures that  $\text{cl } \mathcal{M}(G) = \text{cl MARG}(G)$  is bounded, and so contains no full lines or extreme directions. Its extreme points are simply the vertices  $\mu_e$ , as illustrated below in Figure 14. Whether  $\text{cl } \mathcal{M}(G; H)$  is realized by product distributions (as in

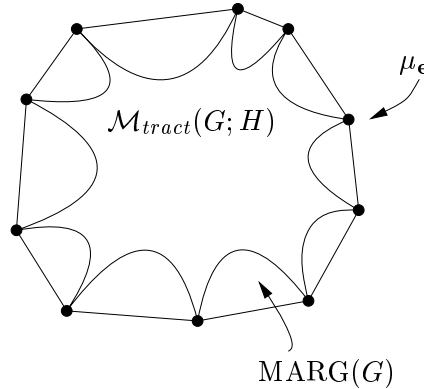


**Figure 14.** The set  $\mathcal{M}_{tract}(G; H)$  of mean parameters that arise from tractable distributions is a non-convex inner bound on  $\mathcal{M}(G)$ . Illustrated here is the multinomial case where  $\mathcal{M}(G) \equiv \text{MARG}(G)$  is a polytope. The circles correspond to mean parameters that arise from delta distributions, and belong to both  $\mathcal{M}(G)$  and  $\mathcal{M}_{tract}(G; H)$ .

naive mean field) or by more structured distributions, it will contain these vertices (since delta distributions are certainly product distributions). Therefore, the set  $\mathcal{M}_{tract}(G; H)$  is a *non-convex inner approximation* to the polytope  $\text{MARG}(G)$ .

**Gaussian case:** In this case, it is clear that  $\text{cl } \mathcal{M}_{Gauss}$  contains no full lines (since, e.g.,  $\mu_{ss} = \mathbb{E}[x_s^2]$  is always non-negative). It can also be verified that although  $\text{cl } \mathcal{M}_{Gauss}$  contains half-lines, none of them are extreme directions. Lastly, it can be shown that the extreme points of  $\text{cl } \mathcal{M}_{Gauss}$  correspond to the mean parameters  $\mu_{\mathbf{e}}$  such that the matrix  $W(\mu_{\mathbf{e}})$  is rank one. Such mean parameters are realized by delta distributions (i.e., the limit of a Gaussian as the covariance shrinks to zero), so that they will also be realized by typical sets of tractable distributions.

The non-convexity of the mean field approximation has important consequences. First of all, there are often multiple local minima, so that in practical terms, the result of applying mean field updates can be sensitive to the initial conditions. Secondly, the mean field method can exhibit “spontaneous symmetry breaking”, wherein the mean field approximation is asymmetric even though the original problem is perfectly symmetric; see Jaakkola [52] for an illustration of this phenomenon.

## 6 Bethe entropy approximation and sum-product algorithm

In this section, we turn to another important message-passing algorithm for approximate inference, known either as *belief propagation*, or the *sum-product algorithm*. In Section 2.5.1, we described the use of the sum-product algorithm for trees, in which context it is guaranteed to converge and perform exact inference. When applied to graphs with cycles, there are no such guarantees, but it is nonetheless widely used to compute approximate marginals. In this section, we will describe the variational interpretation of the sum-product updates, first elucidated by Yedidia, Freeman and Weiss [101]. While mean field and sum-product are similar as message-passing algorithms, their respective variational interpretations are fundamentally different. In particular, whereas the essence of mean field is to *restrict* optimization to a limited class of distributions for which the negative entropy and mean parameters can be characterized *exactly*, the the sum-product algorithm, in contrast, is based on *enlarging* the constraint set and *approximating* the entropy function.

### 6.1 Basic ingredients

The Bethe approximation applies to an undirected graphical model with potential functions involving at most pairs of variables; we refer to any such model as a *pairwise Markov random field*. In principle, by selectively introducing auxiliary variables, any undirected graphical model can be converted<sup>8</sup> to an equivalent pairwise form to which the Bethe approximation can be applied. It can also be useful to treat higher order interactions directly, which can be done using the approximations discussed in Section 7.

For the current section, let us assume that the given model is a pairwise Markov random field defined by a graph  $G = (V, E)$ . Although the Bethe approximation can be developed more generally, we also limit our discussion to multinomial random vectors, for which each  $x_s$  takes values in the space  $\mathcal{X}_s = \{0, 1, \dots, m_s - 1\}$ . In this section, we will use the canonical overcomplete representation which, as previously described in equation (38), is based on the indicator functions  $\{\mathbb{I}_j(x_s), j \in \mathcal{X}_s\}$  for  $s \in V$  and  $\{\mathbb{I}_{jk}(x_s, x_t), (j, k) \in \mathcal{X}_s \times \mathcal{X}_t\}$  for  $(s, t) \in E$ . In this representation, any pairwise Markov random field has the form:

$$p(\mathbf{x}; \theta) \propto \exp \left\{ \sum_{s \in V} \theta_s(x_s) + \sum_{(s,t) \in E} \theta_{st}(x_s, x_t) \right\}, \quad (75)$$

---

<sup>8</sup>See Freeman and Weiss [41] for a detailed description of this procedure.

where we have used the convenient shorthand

$$\theta_s(x_s) := \sum_{j \in \mathcal{X}_s} \theta_{s;j} \mathbb{I}_j(x_s), \quad \theta_{st}(x_s, x_t) := \sum_{(j,k) \in \mathcal{X}_s \times \mathcal{X}_t} \theta_{st;jk} \mathbb{I}_{jk}(x_s, x_t). \quad (76)$$

The associated marginal functions  $\mu_s(x_s)$  and  $\mu_{st}(x_s, x_t)$  are defined analogously to  $\theta_s(x_s)$  and  $\theta_{st}(x_s, x_t)$ , as in equation (40). Finally, we denote the marginal polytope associated with this exponential representation by  $\text{MARG}(G)$ .

### 6.1.1 Bethe entropy approximation

As discussed at length in Section (40), the negative entropy  $A^*$ , as a function of only the mean parameters  $\mu$ , typically lacks a closed form expression. We observed, moreover, that junction tree theorem provides an important class of exceptions to this general rule. As a special case, for tree-structured distributions, the function  $A^*$  has a closed-form expression that is straightforward to compute (see Section 4.2.3).

In the tree case, the negative entropy  $A^*$  decomposes into a sum of single node entropy and edgewise mutual information terms, defined as follows:

$$H_s(\mu_s) := - \sum_{x_s} \mu_s(x_s) \log \mu_s(x_s), \quad (77a)$$

$$I_{st}(\mu_{st}) := \sum_{x_s, x_t} \mu_{st}(x_s, x_t) \log \frac{\mu_{st}(x_s, x_t)}{\mu_s(x_s) \mu_t(x_t)} = H_s(\mu_s) + H_t(\mu_t) - H_{st}(\mu_{st}). \quad (77b)$$

Of course, the entropy of a distribution defined by a graph with cycles will not, in general, decompose additively like a tree. Nonetheless, one can imagine using the sum of local terms as an approximation to the entropy. Doing so yields the following *Bethe approximation* to the entropy on a graph with cycles:

$$H_{\text{Bethe}}(\mu) := \sum_{s \in V} H_s(\mu_s) - \sum_{(s,t) \in E} I_{st}(\mu_{st}). \quad (78)$$

To be clear,  $H_{\text{Bethe}}(\mu)$  is an approximation to  $-A^*(\mu)$ . From our development in Section 4.2.3, we know if that if the graph is tree-structured, then  $H_{\text{Bethe}}(\mu) = -A^*(\mu)$ , so that the approximation is exact.

**Remark:** An alternative form of the Bethe entropy approximation can be derived by using the relation between mutual information and entropy given in equation (77b). In particular, expanding the mutual information terms in this way, and then collecting all the single node entropy terms yields  $H_{\text{Bethe}}(\mu) = \sum_{s \in V} (1 - d_s) H_s(\mu_s) + \sum_{(s,t) \in E} H_{st}(\mu_{st})$ , where  $d_s$  denotes the number of neighbors of node  $s$ . This representation is the form of the Bethe entropy introduced by Yedidia et al. [101]; the form in equation (78) turns out to be more convenient for our purposes.

### 6.1.2 Tree-based outer bound

Note that the Bethe entropy approximation  $H_{\text{Bethe}}$  is well-defined for any  $\mu \in \text{MARG}(G)$ . However, as discussed in Section 4.1.3, characterizing this polytope of realizable marginals is a very challenging problem. Accordingly, a natural approach is to specify a subset of necessary constraints, which leads to an outer bound on  $\text{MARG}(G)$ .

Let  $\tau_s(x_s)$  and  $\tau_{st}(x_s, x_t)$  be a set of candidate marginal distributions. In Example 8, we considered the following constraint set:

$$\text{LOCAL}(G) = \{ \tau \geq 0 \mid \sum_{x_s} \tau_s(x_s) = 1, \sum_{x_s} \tau_{st}(x_s, x_t) = \tau_t(x_t) \}.$$

Although  $\text{LOCAL}(G)$  is an exact description of the marginal polytope for a tree-structured graph, it is only an outer bound for graphs with cycles. (See Example 14 for a vector  $\tau \in \text{LOCAL}(G)$  that does *not* belong to  $\text{MARG}(G)$ ). For this reason, our change in notation—i.e., from  $\mu$  to  $\tau$ —is quite deliberate, with the goal of emphasizing that members  $\tau$  of  $\text{LOCAL}(G)$  need not be realizable. We refer to members of  $\text{LOCAL}(G)$  as *pseudomarginals*.

Figure 15 provides an idealized illustration of the constraint set  $\text{LOCAL}(G)$ , and its relation to the exact marginal polytope  $\text{MARG}(G)$ . By construction,  $\text{LOCAL}(G)$  is another polytope that

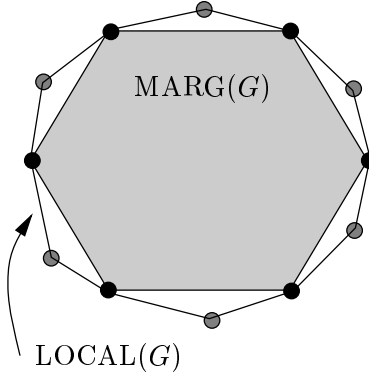


**Figure 15.** An idealized illustration of the tree-based constraint set  $\text{LOCAL}(G)$  as an outer bound on the marginal polytope  $\text{MARG}(G)$ .

is a *convex outer approximation* to  $\text{MARG}(G)$ . It is worthwhile contrasting with the *non-convex inner approximation* used by a mean field approximation, as illustrated in Figure 14.

## 6.2 Bethe variational problem and sum-product

Combining the entropy approximation  $H_{\text{Bethe}}$  with the tree-based constraint set  $\text{LOCAL}(G)$  leads to the *Bethe variational problem*:

$$\max_{\tau \in \text{LOCAL}(G)} \{ \langle \theta, \tau \rangle + \sum_{s \in V} H_s(\tau_s) - \sum_{(s,t) \in E} I_{st}(\tau_{st}) \}. \quad (79)$$

Although ostensibly similar to a (structured) mean field approach, the Bethe variational problem (BVP) is fundamentally different in a number of ways. As discussed in Section 5, a mean field method is based on an exact representation of the entropy, albeit over a limited class of distributions. In contrast, with the exception of tree-structured graphs, the Bethe entropy is a bona fide *approximation* to the entropy. For instance, it is not difficult to see that it can be negative, which of course can never happen for an exact entropy. Secondly, the mean field approach entails optimizing over an *inner bound* on the marginal polytope, which ensures that any mean field solution is always globally consistent with respect to at least one distribution, and that it yields a lower bound on the log partition function. In contrast, since  $\text{LOCAL}(G)$  is a strict outer bound on the set of realizable marginals  $\text{MARG}(G)$ , the optimizing pseudomarginals  $\tau^*$  of the BVP may not be globally consistent with any distribution.

### 6.2.1 Solving the Bethe variational problem

We now consider methods for solving the BVP. Observe that the set  $\text{LOCAL}(G)$  is a polytope defined by  $\mathcal{O}(n + |E|)$  constraints. A natural approach to solving the BVP, then, is to attach Lagrange multipliers to these constraints, and find stationary points of the Lagrangian. The key insight of Yedidia et al. [101] is that the sum-product updates (7) are a particular technique for trying to find such Lagrangian stationary points.

**Proposition 11 (Message-passing).** *For each  $x_s \in \mathcal{X}_s$ , let  $\lambda_{st}(x_s)$  be a Lagrange multiplier associated with the constraint  $C_{ts}(x_s) = 0$ , where  $C_{ts}(x_s) := \tau_s(x_s) - \sum_{x_t} \tau_{st}(x_s, x_t)$ . Consider the partial Lagrangian corresponding to the Bethe variational problem (79):*

$$\mathcal{L}(\tau; \lambda) := \langle \theta, \tau \rangle + \sum_{s \in V} H_s(\tau_s) - \sum_{(s,t) \in E} I_{st}(\tau_{st}) + \sum_{(s,t) \in E} \left[ \sum_{x_s} \lambda_{ts}(x_s) C_{ts}(x_s) + \sum_{x_t} \lambda_{st}(x_t) C_{st}(x_t) \right].$$

Then any fixed point of the sum-product updates specifies a pair  $(\tau^*, \lambda^*)$  such that:

$$\nabla_\tau \mathcal{L}(\tau^*; \lambda^*) = 0, \quad \nabla_\lambda \mathcal{L}(\tau^*; \lambda^*) = 0 \quad (80)$$

*Proof.* Note that this Lagrangian formulation is a partial one, because it assigns Lagrange multipliers to the constraints  $C_{ts}(x_s) = 0$ , and deals with the normalization and non-negativity constraints explicitly. Computing  $\nabla_\tau \mathcal{L}(\tau; \lambda)$  and setting it to zero yields the relations:

$$\log \tau_s(x_s) = c + \theta_s(x_s) + \sum_{t \in \mathcal{N}(s)} \lambda_{ts}(x_s) \quad (81a)$$

$$\log \frac{\tau_{st}(x_s, x_t)}{\left[ \sum_{x_s} \tau_{st}(x_s, x_t) \right] \left[ \sum_{x_t} \tau_{st}(x_s, x_t) \right]} = c' + \theta_{st}(x_s, x_t) - \lambda_{ts}(x_s) - \lambda_{st}(x_t). \quad (81b)$$

Here  $c, c'$  are constants that we are free to adjust in order to satisfy normalization conditions.<sup>9</sup>

The condition  $\nabla_\lambda \mathcal{L}(\tau; \lambda)$  is equivalent to  $C_{ts}(x_s) = 0$ . Using this consistency condition and equation (81a), we can re-arrange equation (81b) to obtain:

$$\log \tau_{st}(x_s, x_t) = c + \theta_{st}(x_s, x_t) + \theta_s(x_s) + \theta_t(x_t) + \sum_{u \in \mathcal{N}(s) \setminus t} \lambda_{us}(x_s) + \sum_{u \in \mathcal{N}(t) \setminus s} \lambda_{ut}(x_t). \quad (82)$$

So as to make explicit the connection to the sum-product algorithm, we define messages in terms of the Lagrange multipliers via  $M_{ts}(x_s) = \exp(\lambda_{ts}(x_s))$ . With this notation, we can then write equivalent forms of equations (81a) and (82):

$$\tau_s(x_s) = \kappa \exp(\theta_s(x_s)) \prod_{t \in \mathcal{N}(s)} M_{ts}(x_s) \quad (83a)$$

$$\tau_{st}(x_s, x_t) = \kappa' \exp(\theta_{st}(x_s, x_t) + \theta_s(x_s) + \theta_t(x_t)) \prod_{u \in \mathcal{N}(s) \setminus t} M_{us}(x_s) \prod_{u \in \mathcal{N}(t) \setminus s} M_{ut}(x_t) \quad (83b)$$

Here  $\kappa, \kappa'$  are positive constants chosen so that the pseudomarginals satisfy normalization conditions. Note that  $\tau_s$  and  $\tau_{st}$  so defined are clearly non-negative.

To conclude, we need to adjust the Lagrange multipliers or messages so that the constraint  $\sum_{x_s} \tau_{st}(x_s, x_t) = \tau_s(x_s)$  is satisfied for every edge. Using equations (83a) and (83b) and performing some algebra, the end result is

$$M_{ts}(x_s) = \kappa \sum_{x_t} \exp \{ \theta_{st}(x_s, x_t) + \theta_t(x_t) \} \prod_{u \in \mathcal{N}(t) \setminus s} M_{ut}(x_t), \quad (84)$$

---

<sup>9</sup>The value of arbitrary constants like  $c$  can change from line to line.

which is equivalent to the familiar sum-product update (7). By construction, any fixed point  $M^*$  of these updates specifies a pair  $(\tau^*, \lambda^*)$  that satisfies the stationary conditions (80).  $\square$

**Remarks:** (a) An important consequence of Proposition 11 is to guarantee the existence of sum-product fixed points. Observe that the cost function in the Bethe variational problem (79) is continuous and bounded above, and the constraint set  $\text{LOCAL}(G)$  is non-empty and compact; therefore, at least some (possibly local) maximum is attained. Moreover, since the constraints are linear, there will always be a set of Lagrange multipliers associated with any local maximum [8]. These Lagrange multipliers can be used to construct a fixed point of the sum-product updates, as in the proof of Proposition 11.

(b) For graphs with cycles, Proposition 11 provides no guarantees on the convergence of the sum-product updates; indeed, whether or not the algorithm converges depends both on the potential strengths and the topology of the graph. In the standard scheduling of the messages, each node applies equation (84) in parallel. Other more global schemes for message-passing are possible, and commonly used in certain applications like turbo-decoding [e.g., 68]. Tatikonda and Jordan [89] have shown that the convergence of parallel updates is related to the structure of Gibbs measures on the computation tree. Other researchers [e.g., 103, 98] have proposed alternatives to sum-product that are guaranteed to converge, albeit at the price of increased computational cost.

(c) With the exception of trees and other special cases [72, 69], the BVP is usually a non-convex problem, in that  $H_{\text{Bethe}}$  fails to be concave. As a consequence, there may be multiple local optima to the BVP, and there are no guarantees that sum-product (or other iterative algorithms) will find a global optimum.

### 6.2.2 Nature of fixed points

This section explores an alternative characterization of sum-product fixed points [96], one which makes connections to the junction tree algorithm for exact inference described in Section 2.5.2. One view of the junction tree algorithm is as follows: taking as input a set of potential functions on the cliques of some graph, it returns as output an *alternative factorization* of the same distribution in terms of local marginal distributions on the cliques and separator sets of a junction tree. In the special case of an ordinary tree, the alternative factorization is a product of local marginals at single nodes and edges of the tree, as in equation (46). Indeed, the sum-product algorithm for trees can be understood as an efficient method for computing this alternative parameterization.

The following result shows that the sum-product algorithm, when applied to a graph with cycles, can still be interpreted as performing a type of reparameterization:

**Proposition 12.** *Any fixed point  $\tau^* = \{\tau_s^*, \tau_{st}^*\}$  of the sum-product algorithm, and more generally any local optimum of the Bethe variational problem, specifies a reparameterization of the form:*

$$p(\mathbf{x}; \theta) \propto \prod_{s \in V} \tau_s^*(x_s) \prod_{(s,t) \in E} \frac{\tau_{st}^*(x_s, x_t)}{\tau_s^*(x_s) \tau_t^*(x_t)}. \quad (85)$$

*Proof.* By remark (a) following Proposition 11, any local optimum of the BVP can be associated with a sum-product fixed point. By definition of the pseudomarginals in equations (83a) and (83b), we have the equivalence  $\tau_{st}^*(x_s, x_t)/[\tau_s^*(x_s) \tau_t^*(x_t)] \propto \exp\{\theta_{st}(x_s, x_t)\} [M_{st}^*(x_t) M_{ts}^*(x_s)]$ . Using this relation, we rewrite the product on the RHS of equation (85) as follows:

$$\prod_{s \in V} \tau_s^*(x_s) \prod_{(s,t) \in E} \frac{\tau_{st}^*(x_s, x_t)}{\tau_s^*(x_s) \tau_t^*(x_t)} = \kappa \prod_{s \in V} [\exp\{\theta_s(x_s)\} \prod_{u \in \mathcal{N}(s)} M_{us}^*(x_s)] \prod_{(s,t) \in E} \frac{\exp(\theta_{st}(x_s, x_t))}{M_{st}^*(x_t) M_{ts}^*(x_s)}.$$

Consider a particular message  $M_{vw}^*$  associated with the edge in the direction  $v$  to  $w$ . Observe that it appears once in the numerator (in the term for node  $w$  in the product over vertices) and once in the denominator (in the term for edge  $(v, w)$  in the product over edges). Consequently, all the messages cancel out in the full product, thereby establishing that

$$\prod_{s \in V} \tau_s^*(x_s) \prod_{(s,t) \in E} \frac{\tau_{st}^*(x_s, x_t)}{\tau_s^*(x_s) \tau_t^*(x_t)} \propto \exp \left\{ \sum_{s \in V} \theta_s(x_s) + \sum_{(s,t) \in E} \theta_{st}(x_s, x_t) \right\},$$

which is the reparameterization claim.  $\square$

**Remarks:** (a) This result provides some insight into the geometry of the BVP and the nature of its local optima [see 96]. Note that the reparameterization statement (85) is possible only because the BVP is formulated in an overcomplete representation. Due to this overcompleteness, the target parameter  $\theta$  is associated with an affine subset  $\mathcal{C}(\theta)$ , such that  $p(\mathbf{x}; \gamma) = p(\mathbf{x}; \theta)$  for all  $\gamma \in \mathcal{C}(\theta)$ . Equation (85) can be restated in the following way: given any local optimum  $\tau^* \in \text{ri LOCAL}(G)$  of the BVP, the parameter  $\gamma^*$  with components

$$\gamma_s^*(x_s) := \begin{cases} \log \tau_s^*(x_s) & \text{for } s \in V, x_s \in \mathcal{X}_s \\ \log[\tau_{st}^*(x_s, x_t)/\tau_s^*(x_s) \tau_t^*(x_t)] & \text{for } (s, t) \in E, (x_s, x_t) \in \mathcal{X}_s \times \mathcal{X}_t \end{cases}$$

is a member of  $\mathcal{C}(\theta)$ . The proof of Proposition 12 shows that the sum-product algorithm has a stronger property—namely, that all its iterates are confined to  $\mathcal{C}(\theta)$ . Although alternative algorithms [e.g., 103, 98] for solving the BVP may evolve outside of this affine set, they must eventually converge to it.

(b) Proposition 12 provides insight into the nature of the *approximation error*: that is, the difference between the exact marginals  $\mu_s$  of  $p(\mathbf{x}; \theta)$  and the approximations  $\tau_s^*$  computed by the sum-product algorithm. Given any tree  $T = (V(T), E(T))$  contained within  $G$ , let  $\tau^*(T)$  denote the pseudomarginals associated with nodes and edges in  $T$ . This reduced set of pseudomarginals defines a tree-structured distribution as follows:

$$p(\mathbf{x}; \tau^*(T)) := \prod_{s \in V} \tau_s^*(x_s) \prod_{(s,t) \in E(T)} \frac{\tau_{st}^*(x_s, x_t)}{\tau_s^*(x_s) \tau_t^*(x_t)}. \quad (86)$$

The junction tree theorem (see Proposition 1) ensures that  $\tau^*(T)$  are the *exact marginals* for the tree-structured distribution  $p(\mathbf{x}; \tau^*(T))$ , and moreover that no additional normalization constant is required. Therefore, each  $\tau_s^*$  is the exact marginal distribution for every tree of the graph. Consequently, the error in the BVP approximation—i.e., the difference between  $\tau_s^*$  and  $\mu_s$ —stems from the perturbation of removing edges and potentials  $\theta_{st}(x_s, x_t)$  from  $p(\mathbf{x}; \theta)$  so as to obtain a tree-structured problem. On this basis, it is possible to derive computable bounds on the approximation error, as described in more detail in Wainwright et al. [96].

As illustrated in Figure 15, the constraint set  $\text{LOCAL}(G)$  of the Bethe variational problem is a strict outer bound on  $\text{MARG}(G)$ , in which the exact marginals of  $p(\mathbf{x}; \theta)$  must lie. A natural question, then, is whether solutions to the Bethe variational problem ever fall into the region  $\text{LOCAL}(G) \setminus \text{MARG}(G)$ . Proposition 12 provides a straightforward answer to this question: it enables us to specify, for *any* pseudomarginal  $\tau \in \text{ri LOCAL}(G)$ , a distribution  $p(\mathbf{x}; \theta)$  for which  $\tau$  is a fixed point of the sum-product algorithm. The following example illustrates this construction.

**Example 14 (Globally inconsistent fixed point).** We illustrate using a binary random vector on the simplest possible graph for which sum-product is not exact—namely, a single cycle with

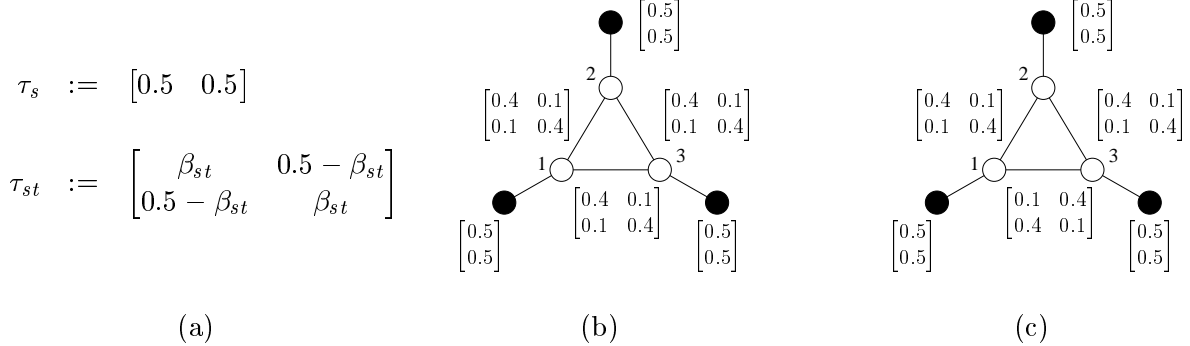


**Figure 16.** Illustration of the marginal polytope for a single cycle graph on three nodes. (a) Form of single node and joint pairwise marginals. The parameter  $\beta_{st}$  takes values in  $[0, 0.5]$ . (b) Setting  $\beta_{st} = 0.4$  for all three edges gives a globally consistent set of marginals. (c) With  $\beta_{13}$  perturbed to 0.1, the marginals (though locally consistent) are no longer globally so.

three nodes. Consider candidate marginal distributions  $\{\tau_s, \tau_{st}\}$  of the form illustrated in Figure 16(a), where  $\beta_{st} \in [0, 0.5]$  is a parameter to be specified independently for each edge  $(s, t)$ . It is straightforward to verify that  $\{\tau_s, \tau_{st}\}$  belong to  $\text{LOCAL}(G)$  for any choice of  $\beta_{st} \in [0, 0.5]$ .

First, consider the setting  $\beta_{st} = 0.4$  for all edges  $(s, t)$ , as illustrated in panel (b). It is not difficult to show that the resulting marginals thus defined are realizable; in fact, they can be obtained from the distribution that places probability 0.35 on each of the configurations  $[0 \ 0 \ 0]$  and  $[1 \ 1 \ 1]$ , and probability 0.05 on each of the remaining six configurations. Now suppose that we perturb one of the pairwise marginals—say  $\tau_{13}$ —by setting  $\beta_{13} = 0.1$ . The resulting problem is illustrated in panel (c). Observe that there are now strong (positive) dependencies between the pairs of variables  $(x_1, x_2)$  and  $(x_2, x_3)$ : both pairs are quite likely to agree (with probability 0.8). In contrast, the pair  $(x_1, x_3)$  can only share the same value relatively infrequently (with probability 0.2). This arrangement should provoke some doubt. Indeed, it can be shown that  $\tau \notin \text{MARG}(G)$  by attempting but failing to construct a distribution that realizes  $\tau$ . See Example 24 of Section 9 for a quick proof using semidefinite constraints.

We now wish to construct a problem  $p(\mathbf{x}; \theta)$  for which the pseudomarginals  $\tau$  are a fixed point of the sum-product algorithm. Proposition 12 enables us to do so easily. In particular, suppose that we define  $\theta_s(x_s) = \log \tau_s(x_s)$  and  $\theta_{st}(x_s, x_t) = \log \tau_{st}(x_s, x_t)/[\tau_s(x_s)\tau_t(x_t)]$ . Now consider the sum-product algorithm updates of equation (84) with the messages  $M_{st}$  initialized to all ones. With these uniform messages and  $\theta = \{\theta_s, \theta_{st}\}$  defined as above, we have:

$$\kappa \sum_{x_t} \exp \{ \theta_{st}(x_s, x_t) + \theta_t(x_t) \} \prod_{u \in \mathcal{N}(t) \setminus s} M_{ut}(x_t) = \kappa \sum_{x_t} \frac{\tau_{st}(x_s, x_t)}{\tau_s(x_s)} = 1$$

Thus, the vector  $\tau \in \text{LOCAL}(G) \setminus \text{MARG}(G)$  is a fixed point of sum-product as applied to the constructed  $p(\mathbf{x}; \theta)$ . More generally, this construction applies to an arbitrary member of  $\text{riLOCAL}(G)$ .  $\diamond$

## 7 Hypertree-based approximations and generalized sum-product

From our development in the previous section, it is clear that there are two *distinct* components to the Bethe variational principle: (a) the entropy approximation  $H_{\text{Bethe}}$ , and (b) the approxi-

mation  $\text{LOCAL}(G)$  to the set of realizable marginal parameters. In principle, the BVP could be strengthened by improving either one, or both, of these components.

In this section, we discuss a natural generalization of the BVP, pioneered by Yedidia et al. [102], that improves both components simultaneously. The approximations in the Bethe approach are based on trees, which represent a special case of the junction trees. A natural strategy, then, is to strengthen the approximations by exploiting more complex junction trees. These approximations are most easily understood in terms of hypertrees, which represent an alternative way in which to describe junction trees. Accordingly, we begin with some necessary background on hypergraphs and hypertrees.

## 7.1 Hypergraphs

A hypergraph  $G = (V, E)$  is a natural generalization of a graph; in particular, it consists of a vertex set  $V = \{1, \dots, n\}$ , and a set of hyperedges  $E$ , where each *hyperedge*  $h$  is a particular subset of  $V$  (i.e., an element of the power set of  $V$ ). The set of hyperedges can be viewed naturally as a partially-ordered set [88], where the partial ordering is specified by inclusion. Given two hyperedges  $g$  and  $h$ , one of three possibilities can hold: (a) the hyperedge  $g$  is contained within  $h$ , in which case we write  $g < h$ ; (b) if  $h$  is contained within  $g$ , then we write  $h < g$ ; and (c) finally, if neither containment relation holds, then  $g$  and  $h$  are incomparable. With these definitions, we see that an ordinary graph is a special case of a hypergraph, in which each maximal hyperedge consists of a pair of vertices (i.e., an ordinary edge of the graph). Note the minor inconsistency in our definition of the hypertree edge set  $E$ ; for hypergraphs (unlike graphs), the set of hyperedges can include (a subset of the) individual vertices.

### 7.1.1 Poset diagrams

A convenient graphical representation of a hypergraph is in terms of a diagram of its hyperedges, with (directed) edges representing the inclusion relations. We refer to such representations as *poset diagrams*; they are also known as Hasse diagrams. Figure 17 provides some simple graphical

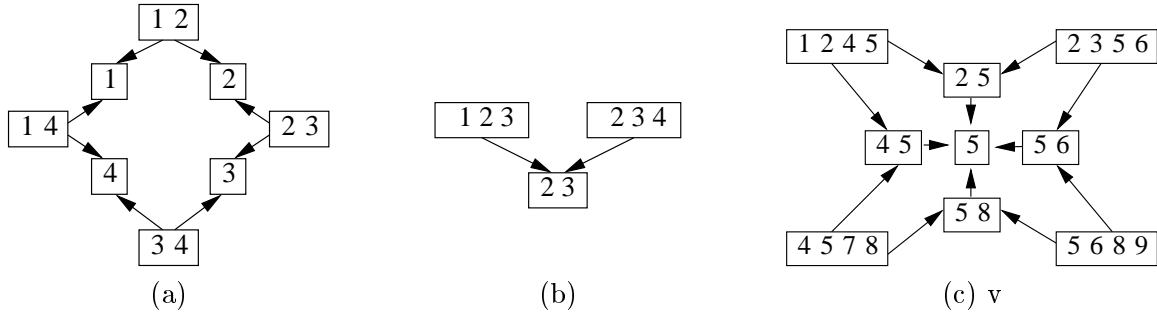


**Figure 17.** Graphical representations of hypergraphs. Subsets of nodes corresponding to hyperedges are shown in rectangles, whereas the arrows represent inclusion relations among hyperedges. (a) An ordinary single cycle graph represented as a hypergraph. (b) A simple hypergraph. (c) A more complex hypergraph.

illustrations of hypergraphs. Any ordinary graph, as a special case of a hypergraph, can be drawn as a hypergraph; in particular, panel (a) shows the hypergraph representation of a single cycle on four nodes. Panel (b) shows a hypergraph that is not equivalent to an ordinary graph, consisting of two hyperedges of size three joined by their intersection of size two. Shown in panel (c) is a more complex hypergraph, to which we will return in the sequel.

Given any hyperedge  $h$ , we define the sets of its *descendants* and *ancestors* in the following way:

$$\mathcal{D}(h) := \{g \in E \mid g < h\}, \quad \mathcal{A}(h) := \{g \in E \mid g > h\}. \quad (87)$$

For example, given the hyperedge  $h = (1245)$  in the hypergraph in Figure 17(c), we have  $\mathcal{A}(h) = \emptyset$  and  $\mathcal{D}(h) = \{(25), (45), (5)\}$ . We use the notation  $\mathcal{D}^+(h)$  and  $\mathcal{A}^+(h)$  as shorthand for the sets  $\mathcal{D}(h) \cup h$  and  $\mathcal{A}(h) \cup h$  respectively.

### 7.1.2 Hypertrees

Hypertrees or acyclic hypergraphs provide an alternative way to describe the concept of junction trees, as originally described in Section 2.5.2. In particular, a hypergraph is *acyclic* if it is possible to specify a junction tree using its maximal hyperedges and their intersections. The *width* of an acyclic hypergraph is the size of the largest hyperedge minus one; we use the term  $k$ -hypertree to mean a singly-connected acyclic hypergraph of width  $k$ . Thus, for example, a spanning tree of an ordinary graph is a 1-hypertree, because its maximal hyperedges (i.e., ordinary edges) all have size two. As a second example, consider the hypergraph shown in Figure 18(a). It is clear that this hypergraph is equivalent to the junction tree with maximal cliques  $\{(1245), (4578), (2356)\}$  and separator sets  $\{(25), (45)\}$ . Therefore, it is a hypertree with width three, since the maximal hyperedges have size four.

It should be noted that there is *not* a one-to-one correspondence between poset diagrams without cycles, and acyclic hypergraphs. In particular, a poset diagram may have cycles, but nonetheless correspond to a hypertree. This possibility is exemplified by Figure 18(b), which shows a set of hyperedges for which the poset diagram involves cycles. Nonetheless, it can be seen that this

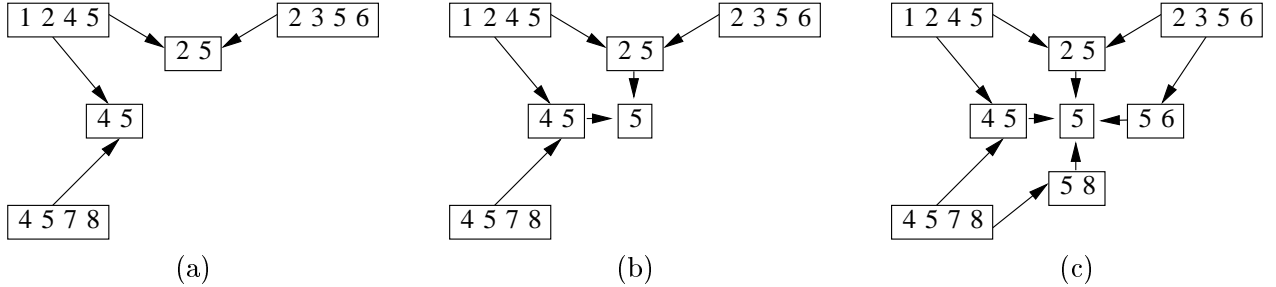


**Figure 18.** Three different graphical representations of the same underlying hypertree. (a) This diagram clearly corresponds to an acyclic hypergraph. (b) This representation seems different, but in fact corresponds to the same hypertree. (c) Another representation of the same hypertree. Hence hypertrees cannot be identified simply by the absence (or presence) of cycles in poset diagrams.

hypergraph is acyclic. A similar statement holds for the hypergraph in (c), which has even more cycles in its poset diagram. In fact, the junction tree corresponding to the hypertree in Figure 18(a) also constitutes a junction tree for the hypergraphs in Figures 18(b) and (c).

### 7.2 Hypertree factorization and entropy

In this section, we develop an alternative form of the junction tree factorization (9), and show how it leads to a local decomposition of the entropy. Associated with any poset is a Möbius function  $\omega : E \times E \rightarrow \mathbb{Z}$ ; see Stanley [88] and Appendix C for more details. We use the Möbius function

to define a correspondence between the collection of marginals  $\mu := \{\mu_h\}$  associated with the hyperedges of a hypergraph, and a new set of functions  $\varphi := \{\varphi_h\}$ , as follows:

$$\log \mu_h(x_h) = \sum_{g \in \mathcal{D}^+(h)} \log \varphi_g(x_g), \quad \log \varphi_h(x_h) = \sum_{g \in \mathcal{D}^+(h)} \omega(g, h) \log \mu_g(x_g). \quad (88)$$

For a hypertree with an edge set containing all intersections between maximal hyperedges, the underlying distribution is guaranteed to factorize as follows:

$$p(\mathbf{x}) = \prod_{h \in E} \varphi_h(x_h). \quad (89)$$

Equation (89) is an alternative formulation of the well-known junction tree decomposition (9), for which some examples provide intuition.

**Example 15.** (a) First suppose that the hypertree is an ordinary tree, in which case the hyperedge set consists of the union of the vertex set with the (ordinary) edge set. For any vertex  $s$ , we have  $\varphi_s(x_s) = \mu_s(x_s)$ , whereas for any edge  $(s, t)$  we have  $\varphi_{st}(x_s, x_t) = \mu_{st}(x_s, x_t)/[\mu_s(x_s) \mu_t(x_t)]$ . In this special case, equation (89) reduces to the tree factorization in equation (46).

(b) Now consider the acyclic hypergraph specified by  $\{(1245), (2356), (4578), (25), (45), (56), (58), (5)\}$ , as illustrated in Figure 18(c). Omitting explicit dependence on  $\mathbf{x}$  for notational simplicity, we first calculate  $\varphi_{1245} = \frac{\mu_{1245}}{\varphi_{25}\varphi_{45}\varphi_5} = \frac{\mu_{1245}}{[\mu_{25}/\mu_5][\mu_{45}/\mu_5]\mu_5}$ , with analogous expressions for  $\varphi_{2356}$  and  $\varphi_{4578}$ . We also have  $\varphi_{25} = \mu_{25}/\mu_5$ , with analogous expressions for the other pairwise terms. Putting the pieces together yields

$$p = \frac{\mu_{1245}}{\frac{\mu_{25}}{\mu_5} \frac{\mu_{45}}{\mu_5} \mu_5} \frac{\mu_{2356}}{\frac{\mu_{25}}{\mu_5} \frac{\mu_{56}}{\mu_5} \mu_5} \frac{\mu_{4578}}{\frac{\mu_{45}}{\mu_5} \frac{\mu_{58}}{\mu_5} \mu_5} \frac{\mu_{25}}{\mu_5} \frac{\mu_{45}}{\mu_5} \frac{\mu_{56}}{\mu_5} \frac{\mu_{58}}{\mu_5} \mu_5 = \frac{\mu_{1245} \mu_{2356} \mu_{4578}}{\mu_{25} \mu_{45}},$$

which agrees with the expression from the junction tree formula (9).  $\diamond$

An immediate but important consequence of the factorization (89) is a local decomposition of the entropy.

**Proposition 13 (Hypertree entropy).** *The entropy of a hypertree-structured distribution decomposes as*

$$H_{\text{hyper}}(\mu) \stackrel{(a)}{=} - \sum_{h \in E} I_h(\mu_h) \stackrel{(b)}{=} \sum_{h \in E} c(h) H_h(\mu_h), \quad (90)$$

where  $I_h(\mu_h) := \sum_{\mathbf{x}} \mu_h(x_h) \log \varphi_h(x_h)$  is a multi-information,  $H_h(\mu_h) := -\sum_{\mathbf{x}} \mu_h(x_h) \log \mu_h(x_h)$  is the entropy associated with hyperedge  $h \in E$ , and  $c(f) := \sum_{e \in \mathcal{A}^+(f)} \omega(f, e)$  are overcounting numbers.

*Proof.* Equality (a) follows immediately from the hypertree factorization (89) and the definition of  $I_h$ . Equality (b) follows by applying the Möbius inversion relation (88) between  $\log \varphi_h(\mathbf{x})$  and  $\log \mu_h(x_h)$ , expanding, and simplifying.  $\square$

We illustrate by continuing with Example 15:

**Example 16.** (a) For an ordinary tree, there are two types of multi-information: for an edge  $(s, t)$ ,  $I_{st}$  is equivalent to the ordinary mutual information, whereas for any vertex  $s \in V$ , the term  $I_s$  is equal to the negative entropy  $-H_s$ . Consequently, in this special case, equation (90) is equivalent to the tree entropy given in equation (47). The overcounting numbers for a tree are  $c((s, t)) = 1$  for any edge  $(s, t)$ , and  $c(s) = 1 - \deg(s)$  for any vertex  $s$ , where  $\deg(s)$  denotes its degree.

(b) Consider again the hypertree in Figure 18(c). On the basis of our previous calculations in Example 15(c), we calculate  $I_{1245} = -[H_{1245} - H_{25} - H_{45} + H_5]$ . The expressions for the other two maximal hyperedges (i.e.,  $I_{2356}$  and  $I_{4578}$ ) are analogous. Similarly, we can compute  $I_{25} = H_5 - H_{25}$ , with analogous expressions for the other hyperedges of size two. Finally, we have  $I_5 = -H_5$ . Putting the pieces together and doing some algebra yields  $H_{\text{hyper}} = H_{1245} + H_{2356} + H_{4578} - H_{25} - H_{45}$ .  $\diamond$

### 7.3 Hypertree-based approximations

Recall that the core of the Bethe approach of Section 6 consists of two components: (a) a particular tree-based (Bethe) approximation to entropy; and (b) a tree-based outer bound on the marginal polytope. In this section, we show how to use hypertrees to form approximations to marginal polytopes and entropies.

Our starting point is a Markov random field (MRF) defined by some (non-acyclic) hypergraph  $G' = (V, E')$ , meaning that  $p(\cdot)$  has a factorization of the form:

$$p(\mathbf{x}) \propto \exp \left\{ \sum_{h \in E'} \theta_h(x_h) \right\}. \quad (91)$$

Note that this equation reduces to our earlier representation (75) of a pairwise MRF when the hypergraph is an ordinary graph.

One strategy is to develop techniques for approximate inference based directly on the structure of  $G'$ . The Bethe approximation is of this form, corresponding to the case when  $G'$  is an ordinary graph. Rather than basing approximations on the structure of  $G'$ , it can be beneficial to build them based on an *augmented hypergraph*. A natural way in which to construct such augmented hypergraphs is by clustering nodes so as to define new hyperedges; different techniques of this nature are discussed in various sources [e.g., 102, 72, 69].

For the purposes of this discussion, we focus on a subclass of augmented hypergraphs. In particular, we require that the original hypergraph  $G'$  is *covered* by the augmented hypergraph, meaning that  $E' \subseteq E$ . A desirable feature of this requirement is that any Markov random field defined by  $G'$  can also be viewed as an MRF on a covering hypergraph  $G$ , simply by setting  $\theta_h = 0$  for all  $h \in E \setminus E'$ .

**Example 17 (Covering hypergraph).** To illustrate, suppose that the original hypergraph  $G'$  is simply an ordinary graph—namely, the  $3 \times 3$  grid shown in Figure 19(a). As illustrated in panel (b), we cluster the nodes into groups of four, which is known as Kikuchi 4-plaque clustering in statistical physics [102]. We then form the augmented hypergraph  $G$  shown in panel (c), with hyperedge set  $E := E' \cup \{(1245), (2356), (4578), (5689)\}$ . The darkness of the boxes in this diagram reflects the depth of the hyperedges in the poset diagram.  $\diamond$

As emphasized by Yedidia et al. [102], it turns out to be important to ensure that every hyperedge in the original hypergraph  $G'$  is counted exactly once in the augmented hypergraph  $G$ . More specifically, for a given hyperedge  $h' \in E'$ , consider the set  $\mathcal{C}(h') := \{f \in E \mid f > h'\}$  of hyperedges in  $E$  that contain  $f$ . For ease of reference, we restate the definition of the overcounting numbers

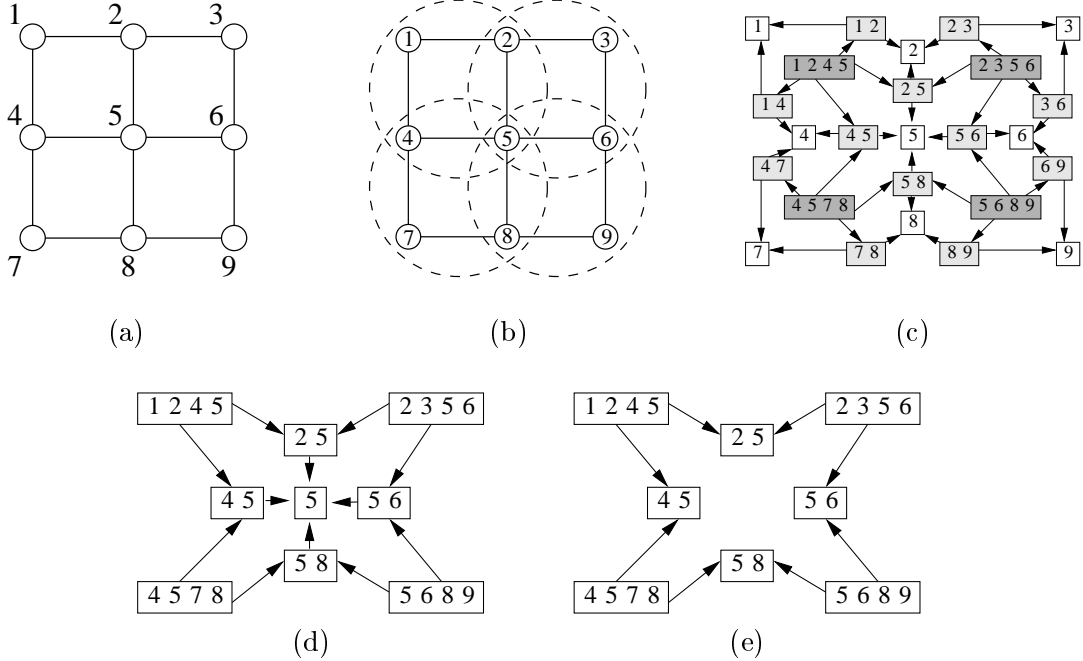


**Figure 19.** Constructing new hypergraphs via clustering and the single counting criterion. (a) Original (hyper)graph  $G'$  is a  $3 \times 3$  grid. Its hyperedge set  $E'$  consists of the union of the vertex set with the (ordinary) edge set. (b) Nodes are clustered into groups of four. (c) A covering hypergraph  $G$  formed by adjoining these 4-clusters to the original hyperedge set  $E'$ . Darkness of the boxes indicates depth of the hyperedges in the poset representation. (d) An augmented hypergraph constructed by the Kikuchi method. (e) A third augmented hypergraph that fails the single counting criterion for (5).

$c(\cdot)$  associated with the hypergraph  $G$ , originally defined in Proposition 13. In particular, these overcounting numbers are defined in terms of the Möbius function associated with  $G$ , viewed as a poset, in the following way:

$$c(f) := \sum_{e \in \mathcal{A}^+(f)} \omega(f, e). \quad (92)$$

The *single counting criterion* requires that for all  $h' \in E'$ , there holds

$$\sum_{f \in \mathcal{C}(h')} c(f) = 1. \quad (93)$$

**Example 18 (Single counting).** To illustrate the single counting criterion, we consider two additional hypergraphs that can be constructed from the  $3 \times 3$  grid of Figure 19(a). The vertex set and edge set of the grid form the original hyperedge set  $E'$ . The hypergraph in panel (d) is constructed by the Kikuchi method described by Yedidia et al. [102]. In this construction, we include the four clusters, all of their pairwise intersections, and all the intersections of intersections (only (5) in this case). The hypergraph in panel (e) includes only the hyperedges of size four and two; that is, it omits the hyperedge (5).

Let us focus first on the hypergraph (e), and understand why it violates the single counting criterion for hyperedge (5). Viewed as a poset, all of the maximal hyperedges (of size four) in this

hypergraph have a counting number of  $c(h) = \omega(h, h) = 1$ . Any hyperedge  $f$  of size two has two parents, each with an overcounting number of 1, so that  $c(f) = 1 - (1 + 1) = -1$ . The hyperedge (5) is a member of the original hyperedge set  $E'$  (of the  $3 \times 3$  grid), but not of the augmented hypergraph. It is included in all the hyperedges, so that  $\mathcal{C}(5) = E$  and  $\sum_{h \in \mathcal{C}(5)} c(h) = 0$ . Thus, the single criterion condition fails to hold for hypergraph (e). In contrast, it can be verified that for the hypergraphs in panels (c) and (d), the single counting condition holds for all hyperedges  $h' \in E'$ .

There is another interesting fact about hypergraphs (c) and (d). If we eliminate from hypergraph (c) all hyperedges that have zero overcounting numbers, the result is hypergraph (d). To understand this reduction, consider for instance the hyperedge (14) which appears in (c) but not in (d). Since it has only one parent (which is a maximal hyperedge), we have  $c(14) = 0$ . In a similar fashion, we see that  $c(12) = 0$ . These two equalities together imply that  $c(1) = 0$ , so that we can eliminate hyperedges (12), (14) and (1) from hypergraph (c). By applying a similar argument to the remaining hyperedges, we can fully reduce hypergraph (c) to hypergraph (d).  $\diamond$

It turns out that if the augmented hypergraph  $G$  covers the original hypergraph  $G'$  (i.e.,  $E \supseteq E'$ ), then the single counting criterion is always satisfied. The proof is quite straightforward: we begin by observing that under the covering condition, the set  $\mathcal{C}(h)$  is equal to  $\mathcal{A}^+(h)$  in the augmented hypergraph  $G$ . We then invoke the following result:

**Lemma 1 (Single counting).** *For any  $h \in E$ , the associated overcounting numbers satisfy the identity  $\sum_{e \in \mathcal{A}^+(h)} c(e) = 1$ , which can be written equivalently as  $c(h) = 1 - \sum_{e \in \mathcal{A}(h)} c(e)$ .*

*Proof.* From the definition of  $c(h)$ , we have the identity:

$$\sum_{h \in \mathcal{A}^+(g)} c(h) = \sum_{h \in \mathcal{A}^+(g)} \sum_{f \in \mathcal{A}^+(h)} \omega(h, f). \quad (94)$$

Considering the double sum on the RHS, we see that for a fixed  $d \in \mathcal{A}^+(g)$ , there is a term  $\omega(d, e)$  for each  $e$  such that  $g \leq e \leq d$ . Using this observation, we can write

$$\sum_{h \in \mathcal{A}^+(g)} \sum_{f \in \mathcal{A}^+(h)} \omega(h, f) = \sum_{d \in \mathcal{A}^+(g)} \sum_{\{e \mid g \leq e \leq d\}} \omega(e, d) \stackrel{(a)}{=} \sum_{d \in \mathcal{A}^+(g)} \delta(d, g) \stackrel{(b)}{=} 1.$$

Here equality (a) follows from the definition of the Möbius function (see Appendix C), and  $\delta(d, g)$  is the Kronecker delta function, from which equality (b) follows.  $\square$

Thus, the construction that we have described, in which the original hypergraph  $G'$  is covered by  $G$  (i.e.,  $E' \subseteq E$ ) and the partial ordering is set inclusion, ensures that the single counting criterion is always satisfied. Other valid constructions are possible; see Yedidia et al. [102] for details. For all of the analysis to follow, we assume that the augmented hypergraph satisfies the single counting criterion.

## 7.4 Hypertree-based approximations

We now have the necessary ingredients to specify hypertree-based approximations to the exact variational principle of Theorem 2.

### 7.4.1 Approximate variational principle

Given an augmented hypergraph  $G$ , let  $\tau = \{\tau_h\}$  be a collection of local marginals associated with the hyperedges  $h \in E$ . Of course, any such quantity must satisfy the obvious normalization condition  $\sum_{\mathbf{x}'_h} \tau_h(\mathbf{x}'_h) = 1$ . Similarly, these local marginals must be consistent with one another wherever they overlap; more precisely, for any pair of hyperedges  $g < h$ , the following *marginalization* condition must hold:

$$\sum_{\{\mathbf{x}'_h \mid \mathbf{x}'_g = x_g\}} \tau_h(\mathbf{x}'_h) = \tau_g(x_g).$$

Imposing these normalization and marginalization conditions leads to the following constraint set:

$$\text{LOCAL}(G) = \left\{ \tau \geq 0 \mid \sum_{\mathbf{x}'_h} \tau_h(\mathbf{x}'_h) = 1 \quad \forall h \in E, \quad \sum_{\{\mathbf{x}'_h \mid \mathbf{x}'_g = x_g\}} \tau_h(\mathbf{x}'_h) = \tau_g(x_g) \quad \forall g < h \right\}. \quad (95)$$

Note that this constraint set is a natural generalization of the tree-based constraint set defined in equation (41). In particular, definition (95) coincides with definition (41) when the hypergraph  $G$  is simply an ordinary graph. As before, we refer to members  $\text{LOCAL}(G)$  as *pseudomarginals*. By the junction tree conditions in Proposition 1, the local constraints defining  $\text{LOCAL}(G)$  are sufficient to guarantee global consistency whenever  $G$  is a hypertree.

In analogy to the Bethe entropy approximation, Proposition 13 motivates the following hypertree-based approximation to the entropy:

$$H_{app}(\tau) = \sum_{g \in E} c(g) H_g(\tau_g). \quad (96)$$

Here  $c(g) = \sum_{f \in \mathcal{A}^+(g)} \omega(g, f)$  are the overcounting numbers defined in equation (92). This entropy approximation and the outer bound  $\text{LOCAL}(G)$  on the marginal polytope, in conjunction, lead to the following hypertree-based approximation to the exact variational principle:

$$\max_{\tau \in \text{LOCAL}(G)} \left\{ \langle \theta, \tau \rangle + H_{app}(\tau) \right\}. \quad (97)$$

This problem is the hypertree-based generalization of the Bethe variational problem (79).

**Example 19 (Kikuchi method).** To illustrate the approximate variational principle (97), consider the augmented hypergraph in Figure 19(d). To determine the form of the entropy approximation  $H_{app}$ , we first calculate the overcounting numbers  $c(\cdot)$ . By definition,  $c(h) = 1$  for each of the four maximal hyperedges (e.g.,  $h = (1245)$ ). Since each of the 2-hyperedges has two parents, Lemma 1 yields that  $c(g) = -1$  in this case. Applying Lemma 1 once more yields that  $c(5) = 1$ . Overall, the entropy approximation takes the form

$$H_{app} = [H_{1245} + H_{2356} + H_{4578} + H_{5689}] - [H_{25} + H_{45} + H_{56} + H_{58}] + H_5. \quad (98)$$

◊

### 7.4.2 Generalized sum-product

In principle, the variational problem (97) could be solved by a number of methods. Here we describe an algorithm, referred to as *parent-to-child message-passing* by Yedidia et al. [102], that is a natural

generalization of the ordinary sum-product updates for the Bethe approximation. Throughout this section, it is convenient to use the notation  $\psi_h(x_h) := \exp\{\theta_h(x_h)\}$ .

As indicated by its name, the defining feature of this scheme is that the only messages passed are from parents to children—i.e., along directed edges in the poset representation of a hypergraph. For any hyperedge  $h \in E$ , the associated pseudomarginal  $\tau_h$  includes a compatibility function  $\psi_g$  for each hyperedge  $g$  in  $\mathcal{D}^+(h) := \mathcal{D}(h) \cup h$ . It also collects a message from each hyperedge  $f \notin \mathcal{D}^+(h)$  that is a parent of some hyperedge  $g \in \mathcal{D}^+(h)$ . The motivation is to collect all necessary information from hyperedges that lie outside the region  $\mathcal{D}^+(h)$ . These considerations lead to the following equation for the pseudomarginal  $\tau_h$ :

$$\tau_h(x_h) = \kappa \left[ \prod_{g \in \mathcal{D}^+(h)} \psi_g(x_g) \right] \left[ \prod_{g \in \mathcal{D}^+(h)} \prod_{f \in \text{Par}(g) \setminus \mathcal{D}^+(h)} M_{f \rightarrow g}(x_g) \right]. \quad (99)$$

We illustrate this construction with an example:

**Example 20 (Parent-to-child for Kikuchi).** In order to illustrate the parent-to-child message-passing, consider the Kikuchi approximation for a  $3 \times 3$  grid, illustrated in Figure 19(d) and discussed in Example 19. Focusing first on the hyperedge (1245), we take a product of compatibility functions  $\psi_g$  as  $g$  ranges over  $\mathcal{D}^+(1245)$ . Since this approximation was based on a grid, there is no compatibility function  $\psi_{1245}$  for the cluster (1245), meaning that it can be taken as constant.

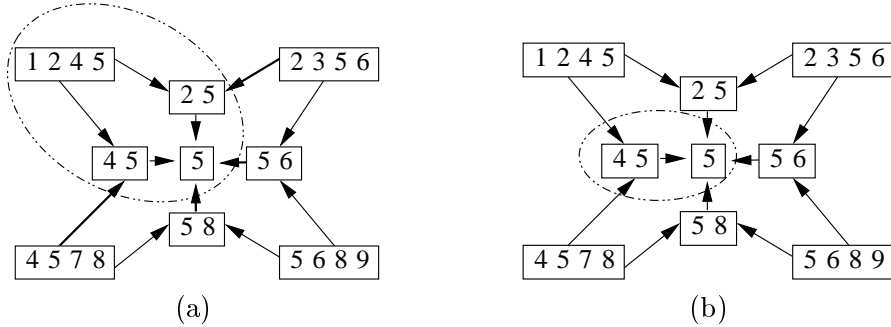


**Figure 20.** Illustration of relevant regions for parent-to-child message-passing in a Kikuchi approximation. (a) Message-passing for hyperedge (1245). Set of descendants  $\mathcal{D}^+\{(1245)\}$  is shown within a dotted ellipse. Relevant parents for  $\tau_{1245}$  consists of the set  $\{(2356), (4578), (56), (58)\}$ . (b) Message-passing for hyperedge (45). Dotted ellipse shows descendant set  $\mathcal{D}^+\{(45)\}$ . In this case, relevant parent hyperedges are  $\{(1245), (4578), (25), (56), (58)\}$ .

The first product in equation (99) picks up compatibility functions from the edges (12), (14), (25) and (45), along with the four vertices. We then take the product over messages from hyperedges that are parents of hyperedges in  $\mathcal{D}\{(1245)\}$ , excluding hyperedges in  $\mathcal{D}\{(1245)\}$  itself. Figure 20(a) provides an illustration; the set  $\mathcal{D}^+\{(1245)\}$  is given by the hyperedges within the dotted ellipses. In this case, the set  $\bigcup_g \text{Par}(g) \setminus \mathcal{D}^+(h)$  is given by (2356) and (4578), corresponding to the parents of (25) and (45) respectively, combined with hyperedges (56) and (58), which are both parents of hyperedge (5). The overall result is an expression of the following form:

$$\tau_{1245} = \kappa \psi_{12} \psi_{14} \psi_{25} \psi_{45} \psi_1 \psi_2 \psi_4 \psi_5 M_{(2356) \rightarrow (25)} M_{(4578) \rightarrow (45)} M_{(56) \rightarrow 5} M_{(58) \rightarrow 5}.$$

By symmetry, the expressions for the pseudomarginals on the other 4-hyperedges are analogous. By similar arguments, it is straightforward to compute the following expression for  $\tau_{45}$  and  $\tau_5$ :

$$\begin{aligned} \tau_{45} &= \kappa \psi_{45} \psi_4 \psi_5 M_{(1245) \rightarrow (25)} M_{(4578) \rightarrow (45)} M_{(25) \rightarrow 5} M_{(56) \rightarrow 5} M_{(58) \rightarrow 5} \\ \tau_5 &= \kappa \psi_5 M_{(45) \rightarrow 5} M_{(25) \rightarrow 5} M_{(56) \rightarrow 5} M_{(58) \rightarrow 5}. \end{aligned}$$

◊

As in the proof of Proposition 11, it can be shown that the messages in equation (99) can be interpreted as (the exponentials of) Lagrange multipliers associated with a Lagrangian formulation of the variational problem (97). Generalized forms of the sum-product updates follow by updating the messages so as to enforce the marginalization constraints defining membership in  $\text{LOCAL}(G)$ . Fixed points of these updates satisfy the necessary stationary conditions of the Lagrangian formulation. Further details can be found in Yedidia et al. [102]. Similarly, there is an analog to Proposition 12: any fixed point of such message-passing updates defines a hypertree-consistent reparameterization of the original distribution [96]. In analogy to the Bethe case, the error stems from the potentials that must be removed from the full hypergraph  $G$  so as to obtain a hypertree-structured distribution.

## 8 Upper bounds via convex relaxations

Up to this point, we have considered two broad classes of variational methods: mean field methods (Section 5) and Bethe-type approaches (Sections 6 and 7). Mean field methods provide not only approximate mean parameters but also lower bounds on the log partition function. In contrast, the Bethe-type approaches lead to *neither* upper or lower bounds on this important quantity. Bounds on the log partition function are useful in a variety of contexts, including parameter estimation and large deviations bounds. A feature common to both mean field and Bethe methods is that the underlying variational methods are usually not convex. As we have discussed, this lack of convexity can lead to local minima, and causes substantial algorithmic difficulties.

The motivation of this section, then, is to describe variational principles that are both convex, and also provide upper bounds on the log partition function. The basic strategy is straightforward: so as to obtain upper bounds, we *relax* the variational representation of  $A$  in equation (32) by modifying it in the following two ways:

- (a) by using a convex *outer bound* on the marginal polytope  $\text{MARG}(G)$ .
- (b) by replacing the negative dual function  $-A^*$  with a concave *upper bound*.

From the variational principle of Theorem 2, it is clear that the solution of the modified variational problem so obtained will yield an upper bound on the log partition function. In addition, requiring a concave upper bound ensures that the modified variational problem has a unique (global) optimum.

The convex relaxation procedure summarized by steps (a) and (b) can be applied quite generally to obtain upper bounds on  $A$  in arbitrary exponential families. In this section, we illustrate this procedure by developing a class of convex relaxations for multinomial problems that are closely related to the Bethe-type approximations discussed in Sections 6 and 7.

### 8.1 Combinations of trees

As in Section 6, let us consider again the case of a pairwise Markov random field, and use the standard overcomplete representation based on indicator functions at single nodes and edges. Suppose that  $\mu = \{\mu_s, \mu_{st}\} \in \text{MARG}(G)$  is a valid set of single node and joint pairwise marginals. We begin by describing how to upper bound the entropy  $-A^*(\mu) = H(p(\mathbf{x}; \theta(\mu)))$  using tree-structured distributions.

Given an arbitrary spanning tree  $T = (V, E(T))$  of the graph, we let  $\mu(T)$  represent the set of all mean parameters associated with vertices  $s \in V$ , and edges  $(s, t) \in E(T)$ . The vector  $\mu(T)$

defines a tree-structured distribution of the following form:

$$p(\mathbf{x}; \mu(T)) = \prod_{s \in V} \mu_s(x_s) \prod_{(s,t) \in E(T)} \frac{\mu_{st}(x_s, x_t)}{\mu_s(x_s) \mu_t(x_t)}.$$

By construction, the value of the dual function  $A^*(\mu(T))$  is simply the negative entropy of  $p(\mathbf{x}; \mu(T))$ .

We now claim that the tree-structured entropy  $-A^*(\mu(T))$  provides an upper bound on the original entropy  $-A^*(\mu)$ . The intuition is based on the maximum entropy characterization of graphical models. In particular, the presence of an edge in a graph-structured distribution corresponds to some constraint that is active in the associated maximum entropy problem. Removing edges, then, corresponds to dropping constraints from the maximum entropy problem, so that the entropy of the tree-structured distribution with matched mean parameters must be larger than the entropy of the original distribution. More formally, we state and prove the following result:

**Lemma 2 (Trees as maximum entropy).** *For any  $\mu \in \text{ri MARG}(G)$ , and for any spanning tree  $T = (V, E(T))$ , we have  $-A^*(\mu) \leq -A^*(\mu(T))$ .*

*Proof.* Since  $T$  is a subgraph of  $G$ , we have  $\text{MARG}(G) \subset \mathbb{R}^{d+}$  and  $\text{MARG}(T) \subset \mathbb{R}^d$ , where  $d < d^+$ . We use  $\mu(T) \in \mathbb{R}^d$  to construct an exponential parameter  $\theta^+(T) \in \mathbb{R}^{d^+}$  as follows:

$$\theta^+(T)_\alpha := \begin{cases} \log \mu_{s;j} & \text{if } \alpha = (s; j) \text{ for } s \in V \\ \log [\mu_{st;jk}/(\mu_{s;j} \mu_{t;k})] & \text{if } \alpha = (st; jk) \text{ for } (s, t) \in E(T) \\ 0 & \text{otherwise.} \end{cases}$$

The constraint  $\mu \in \text{ri MARG}(G)$  ensures that  $\mu_\alpha > 0$  for all indices  $\alpha$ , so that the logarithms are well-defined. Let  $\theta(T)$  denote the lower-dimensional vector in  $\mathbb{R}^d$ , obtained by removing the zeroed-out coordinates in  $\theta^+(T)$ . Observe that by construction,  $\mu(T)$  and  $\theta(T)$  are dually coupled with respect to  $T$  (i.e.,  $\mu(T) = \Lambda(\theta(T))$ ). We can then write:

$$\begin{aligned} A^*(\mu) &\stackrel{(a)}{=} \sup_{\theta \in \Theta} \{ \langle \theta, \mu \rangle - A(\theta) \} \\ &\geq \langle \theta^+(T), \mu \rangle - A(\theta^+(T)) \\ &\stackrel{(b)}{=} A^*(\mu(T)), \end{aligned}$$

where equality (a) follows from the variational representation of Theorem 2(a), and equality (b) follows because  $\mu(T)$  and  $\theta(T)$  are dually coupled by construction.  $\square$

Since the upper bound of Lemma 2 holds for each spanning tree of the graph, it will also hold for any convex combination of spanning trees. In particular, let us consider a probability distribution  $\rho$  over spanning trees:

$$\rho = \{ \rho(T) \mid \sum_T \rho(T) = 1, \rho(T) \geq 0 \} \quad (100)$$

In the sequel, it will be necessary to study the probability  $\rho_{st} := \Pr_{\rho}\{(s, t) \in T\}$  that a given edge  $(s, t)$  belongs to a tree chosen randomly under  $\rho$ . By definition, the vector  $\rho_e = \{\rho_e \mid e \in E\}$  of edge appearance probabilities must belong to the so-called *spanning tree polytope* associated with  $G$ , which we denote by  $\mathbb{S}(G)$ . Let  $\mathbb{I}[e \in T]$  denote an indicator function for the event that edge

$e$  belongs to spanning tree  $T$ . The spanning tree polytope is defined as the convex hull of these indicator functions:

$$\mathbb{S}(G) = \{\boldsymbol{\rho}_e \in \mathbb{R}^{|E|} \mid \forall e \in E \quad \rho_e = \mathbb{E}_{\boldsymbol{\rho}}\{\mathbb{I}[e \in T]\} \quad \text{for some } \boldsymbol{\rho}\}. \quad (101)$$

A simple example should help to provide intuition.

**Example 21 (Edge appearance probabilities).** Figure 21(a) shows a graph, and panels (b) through (d) show three of its spanning trees  $\{T^1, T^2, T^3\}$ . Suppose that we form a uniform dis-

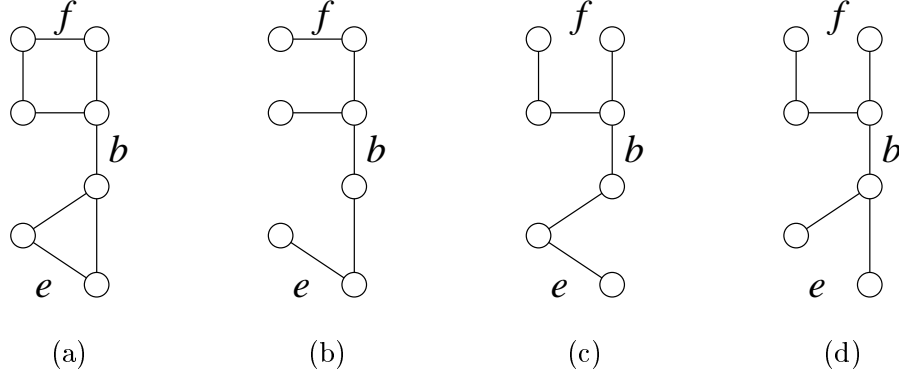


**Figure 21.** Illustration of valid edge appearance probabilities. Original graph is shown in panel (a). Probability 1/3 is assigned to each of the three spanning trees  $\{T_i \mid i = 1, 2, 3\}$  shown in panels (b)–(d). Edge  $b$  appears in all three trees so that  $\rho_b = 1$ . Edges  $e$  and  $f$  appear in two and one of the spanning trees respectively, which gives rise to edge appearance probabilities  $\rho_e = 2/3$  and  $\rho_f = 1/3$ .

tribution  $\boldsymbol{\rho}$  over these trees by assigning probability  $\rho(T^i) = 1/3$  to each  $T^i$ ,  $i = 1, 2, 3$ . Consider the edge with label  $f$ ; notice that it appears in  $T^1$ , but in neither of  $T^2$  and  $T^3$ . Therefore, under the uniform distribution  $\boldsymbol{\rho}$ , the associated edge appearance probability is  $\rho_f = 1/3$ . Since edge  $e$  appears in two of the three spanning trees, similar reasoning establishes that  $\rho_e = 2/3$ . Finally, observe that edge  $b$  appears in any spanning tree (i.e., it is a bridge), so that it must have edge appearance probability  $\rho_b = 1$ .  $\diamond$

As defined in equation (101), the spanning tree polytope is the convex hull of a finite—albeit large—number of vectors. Therefore, by the Minkowski-Weyl theorem [79], it has an equivalent characterization in terms of linear inequalities. The linear inequality description of  $\mathbb{S}(G)$  is well-known from combinatorial optimization and matroid theory [e.g., 35, 22]. We begin with some definitions: given a subset  $F \subseteq E$ , let  $G(F)$  denote the induced subgraph. Let  $v(F)$  be the number of vertices in  $G(F)$ , and let  $c(F)$  be the number of connected components in  $G(F)$ . The *rank* of  $F$  is defined as  $r(F) = v(F) - c(F)$ . When  $G(F)$  is connected so that  $c(F) = 1$ , then the rank function  $r(F)$  corresponds simply to the number of edges in the largest acyclic subgraph of  $G(F)$ . For example, when  $F = E$ , then the largest acyclic subgraph is a spanning tree. Since any spanning tree has  $n - 1$  edges, we have  $r(E) = n - 1$ .

The following lemma, based on a result of Edmonds [35], provides a characterization of  $\mathbb{S}(G)$ :

**Lemma 3 (Spanning tree polytope).** *The spanning tree polytope  $\mathbb{S}(G)$  is characterized com-*

pletely by the non-negativity condition  $\rho_e \geq 0$  combined with the constraints:

$$\sum_{e \in F} \rho_e \leq r(F) \quad \forall F \subseteq E, \quad (102a)$$

$$\sum_{e \in E} \rho_e = n - 1. \quad (102b)$$

In order to gain some intuition for the constraints in equation (102), we consider some particular cases. The necessity of the non-negativity constraints  $\rho_e \geq 0$  is clear, since each  $\rho_e$  corresponds to an edge appearance probability. The corresponding upper bounds  $\rho_e \leq 1$  are obtained by applying equation (102a) to the singleton edge set  $F = \{e\}$ . In this case, we have  $v(F) = 2$  and  $c(F) = 1$ , so that  $r(F) = 1$  and equation (102a) reduces to  $\rho_e \leq 1$ . Equation (102b) can be established via the following argument. Letting  $\boldsymbol{\rho} = \{\rho(T)\}$  be the distribution giving rise to the edge appearance probabilities  $\rho$ , we have the sequence of equalities:

$$\sum_{e \in E} \rho_e = \sum_{e \in E} \sum_{T \in \mathfrak{T}} \rho(T) \mathbb{I}[e \in T] = \sum_{T \in \mathfrak{T}} \rho(T) \sum_{e \in E} \mathbb{I}[e \in T] \stackrel{(a)}{=} n - 1.$$

The final equality (a) follows from the fact that any spanning tree  $T$  on  $n$  nodes has  $n - 1$  edges, and hence  $\sum_{e \in E} \mathbb{I}[e \in T] = n - 1$ .

## 8.2 Tree-based upper bound

We now have the necessary ingredients to state and prove an upper bound on  $A$  based on a convex combination of trees. Not surprisingly, the resulting variational problem turns out to be closely related to the Bethe variational problem.

**Proposition 14 (Tree-based upper bounds).** *For any choice of edge appearance vector  $\boldsymbol{\rho}_e$  in the spanning tree polytope  $\mathbb{S}(G)$ , the log partition function is upper bounded by the solution of the following variational problem:*

$$A(\theta) \leq \max_{\tau \in \text{LOCAL}(G)} \left\{ \langle \tau, \theta \rangle + \sum_{s \in V} H_s(\tau_s) - \sum_{(s,t) \in E} \rho_{st} I_{st}(\tau_{st}) \right\}. \quad (103)$$

For any  $\boldsymbol{\rho}_e \in \mathbb{S}(G)$ , this problem is convex, and strictly so if  $\rho_e > 0$  for all edges  $e$ .

**Remark:** Observe that equation (103) is closely related to the Bethe variational problem of equation (79). In particular, if we set  $\rho_{st} = 1$  for all edges  $(s, t) \in E$ , then the two formulations are equivalent. Note that  $\rho_{st} = 1$  implies that every edge appears in every spanning tree of the graph with probability one, which can happen if and only if the graph is actually tree-structured. (See, in particular, constraint (102b) in the definition of the spanning tree polytope). In the context of Proposition 14, then, the ordinary Bethe choice  $\boldsymbol{\rho}_e = \mathbf{1}$  is valid only for tree-structured graphs.

*Proof:* By definition, for any  $\boldsymbol{\rho}_e \in \mathbb{S}(G)$ , there is an underlying distribution  $\boldsymbol{\rho} = \{\rho(T)\}$  such that  $\mathbb{E}_{\boldsymbol{\rho}}[\mathbb{I}[e \in T]] = \rho_e$  for all  $e \in E$ . By Lemma 2, for any tree  $T$ , we have the upper bound  $-A^*(\mu) \leq -A^*(\mu(T))$ . Taking averages with respect to  $\boldsymbol{\rho}$  yields

$$-A^*(\mu) \leq -\mathbb{E}_{\boldsymbol{\rho}}[A^*(\mu(T))] = -\mathbb{E}_{\boldsymbol{\rho}} \left[ \sum_{s \in V} H_s(\mu_s) - \sum_{(s,t) \in E} I_{st}(\mu_{st}) \right], \quad (104)$$

where we have used the standard decomposition of tree entropy from equation (47). We now expand the expectation over  $\rho$  by linearity. Since the trees are all spanning, each entropy term  $H_s$  for node  $s \in V$  receives a weight of one. On the other hand, the edge  $(s, t)$  receives exactly weight  $\rho_{st} = \mathbb{E}_\rho(\mathbb{I}[e \in T])$ . Overall, we obtain the following upper bound on the exact entropy:

$$-A^*(\mu) \leq \sum_{s \in V} H_s(\mu_s) - \sum_{(s,t) \in E} \rho_{st} I_{st}(\mu_{st}).$$

Applying this upper bound to the variational formulation of equation (32) yields

$$A(\theta) \leq \max_{\mu \in \text{MARG}(G)} \left\{ \langle \mu, \theta \rangle + \sum_{s \in V} H_s(\tau_s) - \sum_{(s,t) \in E} \rho_{st} I_{st}(\tau_{st}) \right\}. \quad (105)$$

Finally, using the fact that  $\text{LOCAL}(G)$  is an outer bound on the marginal polytope leads to the upper bound (103).

To establish convexity of the variational problem, observe that  $\text{LOCAL}(G)$  is linear and hence convex. The cost function consists of a linear term  $\langle \theta, \mu \rangle$  and a convex combination  $-\mathbb{E}_\rho[A^*(\mu(T))]$  of tree entropies, and hence is concave. To establish strict concavity, it suffices to show that the function  $\mathbb{E}_\rho[A^*(\mu(T))]$  is strictly convex on  $\text{ri LOCAL}(G)$  when  $\rho_e > 0$  for all  $e \in E$ . This function is a convex combination of functions of the form  $A^*(\mu(T))$ , each of which is strictly convex in the (non-zero) components of  $\mu(T)$ , but independent of the other components in the full vector  $\mu$ . For any vector  $\lambda \in \mathbb{R}^d$ , define  $\Pi^T(\lambda)_\alpha = \lambda_\alpha$  if  $\alpha \in \mathcal{I}(T)$ , and  $\Pi^T(\lambda)_\alpha = 0$  otherwise. We then have

$$\langle \lambda, \nabla^2 A^*(\mu(T)) \lambda \rangle = \langle \Pi^T(\lambda), \nabla^2 A^*(\mu(T)) \Pi^T(\lambda) \rangle \geq 0,$$

with strict inequality unless  $\Pi^T(\lambda) = 0$ . Now the condition  $\rho_e > 0$  for all  $e \in E$  ensures that  $\lambda \neq 0$  implies that  $\Pi^T(\lambda)$  must be distinct from zero for at least one tree  $T'$ . Therefore, for any  $\lambda \neq 0$ , we have

$$\langle \lambda, \mathbb{E}_\rho[\nabla^2 A^*(\mu(T))] \lambda \rangle \geq \langle \Pi^{T'}(\lambda), \nabla^2 A^*(\mu(T')) \Pi^{T'}(\lambda) \rangle > 0,$$

which establishes the assertion of strict convexity.  $\square$

### 8.3 Tree-reweighted sum-product

Recall that Proposition 11 established that the sum-product algorithm can be understood as an iterative algorithm for attempting to solve the Bethe variational problem (79). Given the close link between the variational formulation of Proposition 14 and the Bethe problem, it is natural to suspect that the sum-product algorithm could be appropriately modified so as to apply to the tree-reweighted case. Indeed this intuition is correct; moreover, whenever  $\rho_e \in \mathbb{S}(G)$ , the tree-reweighted form is guaranteed to converge (under a suitable scheduling of messages). We first state the form of the reweighted updates, and then prove that they solve the variational problem (103).

Like the ordinary sum-product updates, the algorithm involves passing messages  $M_{ts}(x_s)$  from node at node. These messages are initialized with arbitrary positive numbers, and then updated according to the following recursion:

$$M_{ts}^{n+1}(x_s) = \kappa \sum_{x'_t \in \mathcal{X}_t} \exp\left(\frac{1}{\rho_{st}} \theta_{st}(x_s, x'_t) + \theta_t(x'_t)\right) \left\{ \frac{\prod_{v \in \mathcal{N}(t) \setminus s} [M_{vt}^n(x'_t)]^{\rho_{vt}}}{[M_{st}^n(x'_t)]^{(1-\rho_{ts})}} \right\}. \quad (106)$$

Note that the update equation (106) reduces to the ordinary sum-product update under the choice  $\rho_e = 1$ . In general, however, equation (106) differs from the usual updates in three ways.

First of all, the messages passed along edge  $(s, t)$  are reweighted by  $\rho_{st}$ . Secondly, the potential function on edge  $(s, t)$  is reweighted by  $1/\rho_{st}$ . Thirdly, in sharp contrast to ordinary sum-product, the update for message  $M_{ts}$  from node  $t$  to node  $s$  depends on the message  $M_{st}$  running in the *reverse direction* on the same edge.

**Proposition 15 (Tree-reweighted sum-product).** *For any  $\rho_e \in \mathbb{S}(G)$  with  $\rho_e > 0$ , any fixed point  $M^*$  of the updates (106) specifies an optimizing solution of variational problem (103) as follows:*

$$\tau_s(x_s) = \kappa \exp\{\theta_s(x_s)\} \prod_{v \in \mathcal{N}(s)} [M_{vs}(x_s)]^{\rho_{vs}} \quad (107a)$$

$$\tau_{st}(x_s, x_t) = \kappa \varphi_{st}(x_s, x_t; \theta) \frac{\prod_{v \in \mathcal{N}(s) \setminus t} [M_{vs}(x_s)]^{\rho_{vs}}}{[M_{ts}(x_s)]^{(1-\rho_{st})}} \frac{\prod_{v \in \mathcal{N}(t) \setminus s} [M_{vt}(x_t)]^{\rho_{vt}}}{[M_{st}(x_t)]^{(1-\rho_{ts})}}, \quad (107b)$$

where  $\varphi_{st}(x_s, x_t; \theta) := \exp\{\frac{1}{\rho_{st}}\theta_{st}(x_s, x_t) + \theta_s(x_s) + \theta_t(x_t)\}$ .

Moreover, if the pair of messages crossing each edge are updated (with all other messages fixed) until equation (106) is satisfied, then the algorithm is guaranteed to converge.

*Proof.* As in the proof of Proposition 11, we enforce the non-negativity constraints (i.e.,  $\tau_s(x_s) \geq 0$  and  $\tau_{st}(x_s, x_t) \geq 0$ ), as well as the normalization constraints (i.e.,  $\sum_{x_s} \tau_s(x_s) = 1$ ) explicitly, without Lagrange multipliers. Assigning a Lagrange multiplier  $\lambda_{ts}(x_s)$  to each marginalization constraint of the form  $C_{ts}(x_s) := \tau_s(x_s) - \sum_{x_t} \tau_{st}(x_s, x_t)$ ,  $\lambda_s(x_s)$ , we then consider the associated Lagrangian:

$$\mathcal{L}(\tau; \lambda) := \langle \theta, \tau \rangle + \sum_{s \in V} H_s(\tau_s) - \sum_{(s, t) \in E} \rho_{st} I_{st}(\tau_{st}) + \sum_{(s, t) \in E} [\lambda_{ts}(x_s) C_{ts}(x_s) + \lambda_s(x_s) \tau_s(x_s)]. \quad (108)$$

For a fixed set of multipliers  $\lambda$ , maximizing the Lagrangian over non-negative and normalized  $\tau$  defines the dual function  $\mathcal{Q}(\lambda) := \max_{\tau \geq 0} \mathcal{L}(\tau; \lambda)$ . By Proposition 14, the original problem is convex and  $\text{LOCAL}(G)$  is polyhedral, so that strong duality holds [8]. Therefore, it is equivalent to perform an unconstrained minimization of  $\mathcal{Q}$ .

For each fixed  $\lambda$ , calculations entirely analogous to the proof of Proposition 11 show that the (unique) optimum  $\tau(\lambda) = \arg \max_{\tau \geq 0} \mathcal{L}(\tau; \lambda)$  that defines  $\mathcal{Q}(\lambda)$  is specified by equations (107a) and (107b). Since this optimum is uniquely attained, the function  $\mathcal{Q}$  is differentiable, with partial derivatives given by

$$\frac{\partial \mathcal{Q}}{\partial \lambda_{st}}(\lambda) = \left\{ \sum_{x_t} \tau_{st}(x_s, x_t) - \tau_s(x_s) \right\} \Big|_{\tau(\lambda)}. \quad (109)$$

In this equation,  $\tau(\lambda)$  denotes the optimizing  $\tau$  defined by equation (107). Setting this partial derivative to zero and simplifying yields the message update equation (106).

If, in particular, we update each edge individually in an asynchronous fashion, then the algorithm performs a (block) coordinate descent of the dual function  $\mathcal{Q}$ . Since  $\mathcal{Q}$  is strictly jointly convex, this coordinate descent algorithm is guaranteed to converge to the global optimum [8].  $\square$

## 8.4 Convex combinations of hypertrees

In analogy to the hypertree-based extensions of the Bethe variational problem described in Section 7, the definitions and analysis leading up to Propositions 14 and 15 can be extended to hypertrees as well. In this section, we sketch out this extension, and provide a simple example to illustrate.

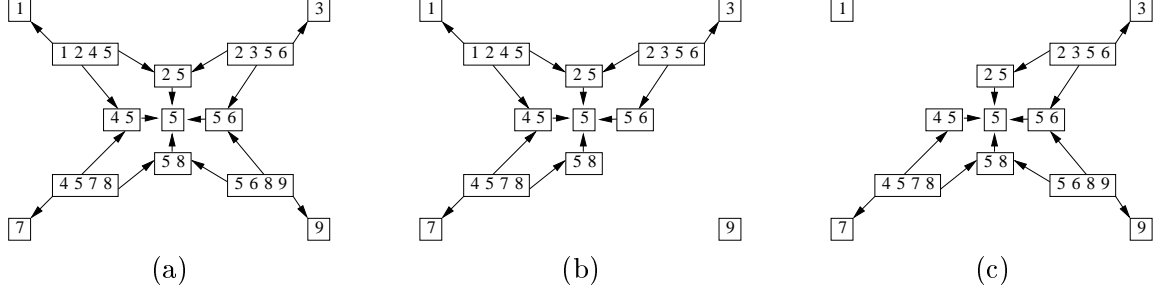


**Figure 22.** Hyperforests embedded within augmented hypergraphs. (a) An augmented hypergraph for the  $3 \times 3$  grid with maximal hyperedges of size 4 that satisfies the single counting criterion. (b) One hyperforest of width three embedded within (a). (c) A second hyperforest of width three.

For a given treewidth  $t$ , consider the set of all hypertrees of width less than or equal to  $t$ . The intrinsic assumption is that  $t$  is sufficiently small that performing exact computations on hypertrees of this width is feasible. It is clear that Lemma 2 generalizes naturally: for any hypertree  $T$ , the exact entropy  $-A^*(\mu)$  is upper bounded by  $-A^*(\mu(T))$  of a hypertree-structured distribution with matched mean parameters. As before, we consider a convex combination of such upper bounds, where the combination is based on a probability distribution use  $\rho = \{\rho(T)\}$  over the set of all hypertrees of width at most  $t$ . Overall, we obtain an upper bound on the entropy of the form

$$A^*(\mu) \leq -\mathbb{E}_\rho[A^*(\mu(T))] = -\sum_T \rho(T) A^*(\mu(T)). \quad (110)$$

For a fixed  $\rho$ , our strategy is to optimize the RHS of this upper bound over all pseudomarginals that are consistent on each hypertree. The resulting constraint set is precisely the polytope  $\text{LOCAL}(G)$  defined in equation (95).

With this set-up, the hypertree analog of Proposition 14 asserts that the log partition function  $A$  is upper bounded as follows:

$$A(\theta) \leq \max_{\tau \in \text{LOCAL}(G)} \{\langle \tau, \theta \rangle - \mathbb{E}_\rho[A^*(\mu(T))]\}. \quad (111)$$

Moreover, the cost function in this variational problem is concave for all choices of distributions  $\rho$  over the hypertrees. Equation (111) is the hypertree analog of equation (103); in fact, it reduces to the latter equation in the special case  $t = 1$ .

**Example 22 (Convex combinations of hypertrees).** Let us derive an explicit form of equation (111) for a particular hypergraph and choice of hypertrees. The original graph is the  $3 \times 3$  grid, as illustrated in the earlier Figure 19(a). Based on this grid, we construct the augmented hypergraph shown in Figure 22(a), which has the hyperedge set

$$E := \{(1245), (2356), (4578), (5689), (25), (45), (56), (58), (5), (1), (3), (7), (9)\}. \quad (112)$$

It is straightforward to verify that it satisfies the single counting criterion.

Now consider a convex combination of four hypertrees, each obtained by removing one of the 4-hyperedges from the edge set. For instance, shown in Figure 22(b) is one particular acyclic substructure  $T^1$  with hyperedge set

$$E(T^1) = \{(1245), (2356), (4578), (25), (45), (56), (58), (5), (1), (3), (7), (9)\},$$

obtained by removing (5689) from the full hyperedge set  $E$ . To be precise, the structure  $T^1$  so defined is a spanning hyperforest, since it consists of two connected components (namely, the isolated hyperedge (9) along with the larger hypertree). This choice, as opposed to a spanning hypertree, turns out to be simplify the development to follow. Figure 22(c) shows the analogous spanning hyperforest  $T^2$  obtained by removing hyperedge (1245); the final two hyperforests  $T^3$  and  $T^4$  are defined analogously.

To specify the associated hypertree factorization, we first compute the form of  $\varphi_h$  for the maximal hyperedges (i.e., of size four). For instance, looking at the  $h = (1245)$ , we see that hyperedges (25), (45), (5), and (1) are contained within it. Thus, using the definition in equation (??), we write (suppressing the functional dependence on  $\mathbf{x}$ ):

$$\varphi_{1245} = \frac{\tau_{1245}}{\varphi_{25} \varphi_{45} \varphi_5 \varphi_1} = \frac{\tau_{1245}}{\frac{\tau_{25}}{\tau_5} \frac{\tau_{45}}{\tau_5} \tau_5 \tau_1} = \frac{\tau_{1245} \tau_5}{\tau_{25} \tau_{45} \tau_1}.$$

Having calculated all the functions  $\varphi_h$ , we can combine them, using the hypertree equation (89), in order to obtain the following factorization for a distribution on  $T^1$ :

$$p(\mathbf{x}; \tau(T^1)) = \left[ \frac{\tau_{1245} \tau_5}{\tau_{25} \tau_{45} \tau_1} \right] \left[ \frac{\tau_{2356} \tau_5}{\tau_{25} \tau_{56} \tau_3} \right] \left[ \frac{\tau_{4578} \tau_5}{\tau_{45} \tau_{58} \tau_7} \right] \left[ \frac{\tau_{25}}{\tau_5} \right] \left[ \frac{\tau_{45}}{\tau_5} \right] \left[ \frac{\tau_{56}}{\tau_5} \right] \left[ \frac{\tau_{58}}{\tau_5} \right] [\tau_1] [\tau_3] [\tau_5] [\tau_7] [\tau_9]. \quad (113)$$

Here each term within square brackets corresponds to  $\varphi_h$  for some hyperedge  $h \in E(T^1)$ ; for instance, the first three terms correspond to the three maximal 4-hyperedges in  $T^1$ . Although this factorization could be simplified, leaving it in its current form makes the connection to Kikuchi approximations more explicit. As in Proposition 13, the factorization (113) leads immediately to a decomposition of the entropy.

In an analogous manner, it is straightforward to derive factorizations and entropy decompositions for the remaining three hyperforests  $\{T^i, i = 2, 3, 4\}$ . Let  $E_4 = \{(1245), (2356), (5689), (4578)\}$  denote the set of all 4-hyperedges. We then form the convex combination of the four (negative) entropies with uniform weight 1/4 on each  $T^i$ :

$$\begin{aligned} \sum_{i=1}^4 \frac{1}{4} A^*(\tau(T^i)) &= \frac{3}{4} \sum_{h \in E_4} \sum_{x_h} \tau_h(x_h) \log \varphi_h(x_h) + \sum_{s \in \{2, 4, 6, 8\}} \sum_{x_{s5}} \tau_{s5}(x_{s5}) \log \frac{\tau_{s5}(x_{s5})}{\tau_5(x_5)} \\ &\quad + \sum_{s \in \{1, 3, 5, 7, 9\}} \sum_{x_s} \tau_s(x_s) \log \tau_s(x_s). \end{aligned} \quad (114)$$

The weight 3/4 arises because each of the maximal hyperedges  $h \in E_4$  appears in three of the four hypertrees. All of the (non-maximal) hyperedge terms receive a weight of one, because they appear in all four hypertrees. Overall, then, these weights represent hyperedge appearance probabilities for this particular example, in analogy to ordinary edge appearance probabilities in the tree case. We now simplify the expression in equation (114) by expanding and collecting terms; doing so yields that  $-\sum_{i=1}^4 \frac{1}{4} A^*(\tau(T^i))$  is equal to the following weighted combination of entropies:

$$\begin{aligned} \frac{3}{4} [H_{1245} + H_{2356} + H_{5689} + H_{4578}] - \frac{1}{2} [H_{25} + H_{45} + H_{56} + H_{58}] \\ + \frac{1}{4} [H_1 + H_3 + H_7 + H_9]. \end{aligned} \quad (115)$$

If, on the other hand, starting from equation (114) again, suppose that we included each maximal hyperedge with a weight of 1, instead of 3/4. Then, after some simplification, we would find that

the (negative of) equation (114) is equal to the following combination of local entropies:

$$\left[ H_{1245} + H_{2356} + H_{5689} + H_{4578} \right] - \left[ H_{25} + H_{45} + H_{56} + H_{58} \right] + H_5,$$

which is equivalent to the Kikuchi approximation derived in Example 19. However, the choice of all ones for the hyperedge appearance probabilities is *invalid*—that is, it could never arise from taking a convex combination of hypertree entropies.  $\diamond$

More generally, any entropy approximation formed by taking such convex combinations of hypertree entropies will necessarily be convex. In contrast, with the exception of certain special cases [72, 69], Kikuchi and other hypergraph-based entropy approximations are typically not convex.

## 9 Semidefinite relaxations for inference

Semidefinite constraints have arisen at several points in the preceding sections, particularly in the context of Gaussian problems. This section is devoted to a more in-depth development of semidefinite constraints for expressing constraints on mean parameters. The use of semidefinite constraints for this purpose has a rich history [e.g., 2, 54], particularly in the context of scalar random variables. The basis of our presentation is more recent work [e.g., 58, 59, 60, 74] that applies to multivariate moment problems. Much of this work is based on results from real algebraic geometry, which we do not discuss here. In lieu, we take the statistical perspective of imposing positive semidefiniteness on covariance and other moment matrices. We also establish some new results relating the tightness of semidefinite constraints to the underlying graph structure.

We begin with some background on linear matrix inequalities, and then describe how such constraints can be applied to moment matrices. Although semidefinite constraints are more generally applicable, much of our development focuses on the multinomial case. More specifically, we describe a nested sequence of semidefinite outer bounds on the marginal polytopes, the last of which provides an exact characterization for any graph. We also address the role of graphical structure in semidefinite constraints, proving in particular that treewidth determines tightness of semidefinite outer bounds. We compare these sequences of semidefinite outer bounds to the hypertree-based outer bounds discussed in Section 7. Finally, to illustrate the use of semidefinite constraints, we combine semidefinite constraints with a Gaussian-based entropy approximation to form a log-determinant relaxation for approximate inference [97].

### 9.1 Moment matrices and semidefinite constraints

We use  $\mathcal{S}_+^n$  to denote the cone of  $n \times n$  symmetric positive semidefinite matrices. For two symmetric matrices  $A$  and  $B$ , we define the inner product  $\langle\langle A, B \rangle\rangle := \text{trace}(AB)$ . Given a vector  $\mu \in \mathbb{R}^d$ , consider a linear matrix-valued function  $F(\mu) = F_0 + \sum_{i=1}^d \mu_i F_i$ , where the matrices  $F_i, i = 0, \dots, d$  are  $n \times n$  and symmetric. Requiring that  $F(\mu)$  be positive semidefinite, which we denote by  $F(\mu) \succeq 0$ , is a *linear matrix inequality* (LMI). The class of constraints that can be expressed in this manner is fairly broad, including as special cases both linear and quadratic constraints [see 91]. For instance, the linear constraint  $A\mu \geq b$  is equivalent to the LMI  $\text{diag}\{A\mu - b\} \succeq 0$ , where the diag operator places the elements of a vector on the diagonal of a matrix. In general, the constraint set carved out by a linear matrix inequality has a mixture of polyhedral (i.e., linear) and curved faces.

Given a random vector  $\mathbf{y}$  with  $n$  components, let  $\lambda_{st} = \mathbb{E}[y_s y_t]$  denote its second-order moments.

Using these moments, we can form the following symmetric  $n \times n$  matrix:

$$M[\lambda] = \mathbb{E}[\mathbf{y}\mathbf{y}^T] = \begin{bmatrix} \lambda_{11} & \lambda_{12} & \cdots & \lambda_{1n} \\ \lambda_{21} & \lambda_{22} & \cdots & \lambda_{2n} \\ \vdots & \vdots & \cdots & \vdots \\ \lambda_{n1} & \lambda_{n2} & \cdots & \lambda_{nn} \end{bmatrix} \quad (116)$$

At first sight, this definition might seem limiting, because the matrix involves only second-order moments. However, given some random vector  $\mathbf{x}$  of interest, we can expose any of its moments by defining  $\mathbf{y} = f(\mathbf{x})$  for a suitable choice of function  $f$ , and then considering the associated second-order moment matrix (116) for  $\mathbf{y}$ . For instance, by setting  $\mathbf{y} = [1 \ \mathbf{x}]$ , the moment matrix (116) will include both first and second-order moments of  $\mathbf{x}$ . Similarly, by including terms of the form  $x_s x_t$  in the definition of  $\mathbf{y}$ , we can expose third moments of  $\mathbf{x}$ .

The significance of the moment matrix (116) lies in the following simple result:

**Lemma 4 (Moment matrices).** *Any valid moment matrix  $M[\lambda]$  is positive semidefinite.*

*Proof.* We must show that  $a^T M[\lambda] a \geq 0$  for an arbitrary vector  $a \in \mathbb{R}^n$ . If  $\lambda$  is a valid moment vector, then it arises by taking expectations under some distribution  $p$ . Accordingly, we can write  $a^T M[\lambda] a = \mathbb{E}_p[a^T \mathbf{y} \mathbf{y}^T a] = \mathbb{E}_p[\|a^T \mathbf{y}\|^2]$ , which is clearly non-negative.  $\square$

**Remarks:** Lemma 4 provides a *necessary* condition for a collection  $\{\lambda_{st}\}$  to be a valid set of second-order moments. Such a condition is both necessary and sufficient for certain classical moment problems involving scalar random variables [e.g., 54, 50]. This condition is of course also necessary and sufficient for a Gaussian random vector, as stated in Proposition 6.

## 9.2 Semidefinite outer bounds on marginal polytopes

We now turn to the use of semidefinite constraints in providing outer bounds on marginal polytopes associated with multinomial random vectors.

### 9.2.1 Multi-index notation

Recall the exponential representation of the Ising model in Example 3, which was based on sufficient statistics of the form  $x_s$  and  $x_s x_t$ . The natural generalization of this representation to non-binary discrete variables is based on monomials of the form  $\mathbf{x}^\alpha := \prod_{s=1}^n x_s^{\alpha_s}$ , where  $\alpha := (\alpha_1, \alpha_2, \dots, \alpha_n)$  is a vector of non-negative indices  $\alpha_s$ . We refer to  $\alpha$  as a *multi-index*. Our convention for the all-zeros multi-index 0 is that  $\mathbf{x}^0 = 1$ . Given two multi-indices  $\alpha$  and  $\beta$ , it will be useful to specify their component-wise sum  $\alpha + \beta = (\alpha_1 + \beta_1, \dots, \alpha_n + \beta_n)$ .

Consider a multinomial random vector  $\mathbf{x}$ , where each  $x_s$  takes values in  $\mathcal{X} := \{0, 1, \dots, m-1\}$ . (A bit more generally, we could allow the cardinality of  $\mathcal{X}_s$  to vary for each vertex). A convenient exponential representation, based on the monomials  $\mathbf{x}^\alpha$ , is as follows:

$$p(\mathbf{x}; \theta) = \exp \left\{ \sum_{\alpha} \theta_{\alpha} \mathbf{x}^{\alpha} - A(\theta) \right\}. \quad (117)$$

Without loss of generality, the range of the sum over  $\alpha$  in equation (117) can be restricted. In particular, observe that for any multinomial variable  $x \in \mathcal{X} = \{0, 1, \dots, m-1\}$ , there always holds

$$\prod_{j=0}^{m-1} (x-j) = 0. \quad (118)$$

A minor re-arrangement of this relation yields an expression for  $x^m$  as a polynomial of degree  $m - 1$ , which implies that any monomial  $x^i$  with  $i \geq m$  can be expressed as a linear combination of lower-order monomials. Therefore, we can always assume without loss of generality that the sum is taken only over multi-indices for which the maximum degree  $\|\alpha\|_\infty := \max_s \alpha_s$  is less than or equal to  $m - 1$ . Herein all multi-indices should be understood to satisfy this restriction.

Particular classes of models are obtained by imposing constraints on the set of  $\alpha$ ; for instance, restricting  $\alpha$  to be non-zero in at most two positions corresponds to a pairwise Markov random field. We can write this constraint compactly using the  $\ell_0$  norm  $\|\alpha\|_0 := \#\{s \mid \alpha_s > 0\}$ , which counts the number of non-zero entries. With this notation, the set of monomials  $\mathbf{x}^\alpha$  associated with a pairwise Markov random field are those with multi-indices in the set  $\mathcal{I}_2 = \{\alpha \mid \|\alpha\|_0 \leq 2\}$ . More generally, for each integer  $k = 1, \dots, n$ , we define the multi-index set  $\mathcal{I}_k = \{\alpha \mid \|\alpha\|_0 \leq k\}$ . This nested set of multi-index sets describes a hierarchy of Markov random field models, defined on hypergraphs with increasing sizes of hyperedges.

To calculate the cardinality of  $\mathcal{I}_k$ , observe that for each  $i = 0, \dots, k$ , there are  $\binom{n}{i}$  possible subsets of size  $i$ . Moreover, for each member of each such subset, there are  $(m - 1)$  possible choices of the index value, so that  $\mathcal{I}_k$  has  $\sum_{i=0}^k \binom{n}{i} (m - 1)^i$  elements in total. The total number of all possible multi-indices (with  $\|\alpha\|_\infty \leq m - 1$ ) is given by  $|\mathcal{I}_n| = \sum_{i=0}^n \binom{n}{i} (m - 1)^i = m^n$ .

### 9.2.2 First-order semidefinite outer bound

For any multi-index  $\alpha$ , let  $\mu_\alpha = \mathbb{E}[\mathbf{x}^\alpha]$  denote the associated mean parameter or moment. For each  $k = 1, \dots, n$ , let us introduce  $K_{k,n}$  to denote the hypergraph that includes *all* hyperedges of size up to  $k$  on a set of  $n$  nodes. For instance,  $K_{1,n}$  is simply a disconnected graph, whereas  $K_{2,n} \equiv K_n$  is the usual complete graph on  $n$  nodes. We can then consider the associated marginal polytope

$$\text{MARG}(K_{k,n}) := \{\mu_\alpha \in \mathbb{R}^{|\mathcal{I}_k|} \mid \alpha \in \mathcal{I}_k\}, \quad (119)$$

which corresponds to all valid moments  $\mu_\alpha$  of order  $\|\alpha\|_0 \leq k$ . More generally, for any hypergraph  $G$ , we use  $\text{MARG}(G)$  to denote the associated marginal polytope.

We now show how to use moment matrices to develop semidefinite outer bounds on marginal polytopes. For concreteness, we focus on a pairwise Markov random field, so that the relevant singleton and pairwise moments belong to the set  $\text{MARG}(K_{2,n}) \equiv \text{MARG}(K_n)$ . Given a random vector, we denote by  $M_1[\mu]$  the moment matrix corresponding to the choice  $\mathbf{y} = \{\mathbf{x}^\alpha \mid \alpha \in \mathcal{I}_1\}$  in equation (116). Explicitly, the rows and columns of  $M_1[\mu]$  are indexed by multi-indices  $\alpha, \beta \in \mathcal{I}_1$ , where entry  $(\alpha, \beta)$  is given by

$$(M_1[\mu])_{\alpha\beta} = \mu_{\alpha+\beta}. \quad (120)$$

Since  $\|\alpha\|_0 \leq 1$  for each  $\alpha \in \mathcal{I}_1$ , there always holds  $\|\alpha + \beta\|_0 \leq 2$ .

**Example 23 (Binary case).** We illustrate  $M_1[\mu]$  explicitly for the binary case  $\mathbf{x} \in \{0, 1\}^n$ , for which  $\{\mathbf{x}^\alpha \mid \alpha \in \mathcal{I}_1\} = (1, x_1, \dots, x_n)$ . On this basis, we calculate:

$$M_1[\mu] := \begin{bmatrix} 1 & \mu_1 & \mu_2 & \cdots & \mu_{n-1} & \mu_n \\ \mu_1 & \mu_1 & \mu_{12} & \cdots & \cdots & \mu_{1n} \\ \mu_2 & \mu_{12} & \mu_2 & \cdots & \cdots & \mu_{2n} \\ \vdots & \vdots & \vdots & \vdots & \vdots & \vdots \\ \mu_{n-1} & \vdots & \vdots & \vdots & \vdots & \mu_{(n-1),n} \\ \mu_n & \mu_{n1} & \mu_{n2} & \cdots & \mu_{(n-1),n} & \mu_n \end{bmatrix}. \quad (121)$$

An important point to note is that in forming  $M_1[\mu]$ , we use the fact that  $x_s^2 = x_s$  for any  $x_s \in \{0, 1\}$  in order to simplify the moment calculations. In particular, for each of the diagonal terms (other than the 1 in the  $(1, 1)$  entry), we use the fact that  $\mathbb{E}[x_s^2] = \mathbb{E}[x_s] = \mu_s$ . In the general multinomial case, similar simplifications follow from equation (118).  $\diamond$

We now use the matrix  $M_1[\mu]$  to define the following semidefinite constraint set:

$$\text{SDEF}_1 := \{\mu_\alpha, \alpha \in \mathcal{I}_2 \mid M_1[\mu] \succeq 0\}. \quad (122)$$

The definition of  $M_1[\mu]$  and Lemma 4 guarantee the following inclusion:

**Lemma 5 (First-order outer bound).** *The marginal polytope  $\text{MARG}(K_n)$  is contained within the semidefinite constraint set  $\text{SDEF}_1$ .*

**Example 24.** To illustrate Lemma 5, recall the (hitherto unproven) claim of Example 14: for the fully connected graph  $K_3$  on three nodes, the following pseudomarginal  $\tau$  lies outside  $\text{MARG}(K_3)$ :

$$\tau_s = 0.5 \text{ for } s = 1, 2, 3, \quad \tau_{12} = \tau_{23} = 0.4, \quad \tau_{13} = 0.1.$$

(Note that we have translated the overcomplete canonical representation of Example 14 to a minimal representation.) We now construct the matrix  $M_1$  for this trial set of mean parameters:

$$M_1[\tau] = \begin{bmatrix} 1 & 0.5 & 0.5 & 0.5 \\ 0.5 & 0.5 & 0.4 & 0.1 \\ 0.5 & 0.4 & 0.5 & 0.4 \\ 0.5 & 0.1 & 0.4 & 0.5 \end{bmatrix}.$$

A simple calculation shows that it is not positive definite, whence  $\tau \notin \text{SDEF}_1$ . Applying Lemma 5 yields that  $\tau \notin \text{MARG}(K_3)$ .  $\diamond$

### 9.2.3 Projections and exactness

Lemma 5 shows that the semidefinite constraint set  $\text{SDEF}_1$  provides an outer bound on the set  $\text{MARG}(K_n)$  of valid second-order marginals. This same constraint set also induces an outer bound on  $\text{MARG}(G)$ , where  $G$  is any subgraph of the complete graph  $K_n$ , in the following way. Let  $\mathcal{I}(G) \subset \mathcal{I}(K_n)$  be the multi-index sets associated with  $G$  and  $K_n$  respectively. Given any outer bound  $\text{OUT}(K_n)$  on  $\text{MARG}(K_n)$ , we define its *projection* onto the coordinates of  $\mathcal{I}(G)$  as follows:

$$\Pi_G(\text{OUT}(K_n)) = \{\mu_\alpha, \alpha \in \mathcal{I}(G) \mid \mu_\alpha = \eta_\alpha \text{ for some } \eta \in \text{OUT}(K_n)\}. \quad (123)$$

With this definition, an immediate corollary of Lemma 5 is that  $\Pi_G(\text{SDEF}_1)$  is an outer bound on  $\text{MARG}(G)$  for any graph.

We now turn to a natural question: in which cases does  $\text{SDEF}_1$  (or a suitable projection thereof) provide an exact description of a marginal polytope? To gain intuition, let us return to the binary case of Example 23. It can be seen that for any moment  $\mu_s$ , the matrix  $M_1[\mu]$  of equation (120) contains a  $2 \times 2$  principal submatrix of the form

$$\begin{bmatrix} 1 & \mu_s \\ \mu_s & \mu_s \end{bmatrix}.$$

The positive semidefiniteness of this submatrix enforces the constraint  $\mu_s(1 - \mu_s) \geq 0$ , which is equivalent to the interval constraint  $\mu_s \in [0, 1]$ . Note that the marginal polytope  $\text{MARG}(K_{1,n})$ ,

which consists only of the first-order moments  $\mu_s$ , is completely characterized by these interval constraints. Therefore, we conclude that  $\Pi_{K_{1,n}}(\text{SDEF}_1) = \text{MARG}(K_{1,n})$ . This equivalence can be extended easily to the general multinomial case (i.e.,  $m > 2$ ).

This exactness breaks down for more interesting examples. For instance,  $\text{SDEF}_1$  is a *strict* outer bound on the marginal polytope  $\text{MARG}(K_{2,n}) \equiv \text{MARG}(K_n)$ , as illustrated in the following example.

**Example 25 (Strict inclusion for binary pair).** Let us demonstrate the strict inclusion  $\text{SDEF}_1 \supset \text{MARG}(K_n)$  for a pair  $(x_1, x_2)$  of binary random variables (i.e.,  $n = 2$ ). In this case,  $\text{MARG}(K_2)$  consists of three moments  $\{\mu_1, \mu_2, \mu_{12}\}$ . So as to facilitate visualization, we focus on the intersection of both the marginal polytope and the constraint set  $\text{SDEF}_1$  with the hyperplane  $\mu_1 = \mu_2$ . The semidefinite constraint set is defined by the LMI constraint:

$$M_1[\mu] = \begin{bmatrix} 1 & \mu_1 & \mu_2 \\ \mu_1 & \mu_1 & \mu_{12} \\ \mu_2 & \mu_{12} & \mu_2 \end{bmatrix} \succeq 0. \quad (124)$$

In order to deduce the implied constraints, we apply Sylvester's criterion, making the substitution  $\mu_1 = \mu_2$  throughout. Positivity of the  $(1, 1)$  subminor is trivial ( $1 > 0$ ), and the  $(1, 2)$  subminor yields the interval constraint  $\mu_1 \in [0, 1]$ . After some simplification, non-negativity of the full determinant leads to the constraint  $\mu_{12}^2 - (2\mu_1^2)\mu_{12} + (2\mu_1^3 - \mu_1^2) \leq 0$ . Viewing the LHS as a quadratic in  $\mu_{12}$ , we can factor it into the product  $[\mu_{12} - \mu_1][\mu_{12} - \mu_1(2\mu_1 - 1)]$ . For  $\mu_1 \in [0, 1]$ , this quadratic inequality is equivalent to the pair of constraints

$$\mu_{12} \leq \mu_1, \quad \mu_{12} \geq \mu_1(2\mu_1 - 1). \quad (125)$$

The gray area in Figure 23 shows the intersection of the marginal polytope  $\text{MARG}(K_2)$  with

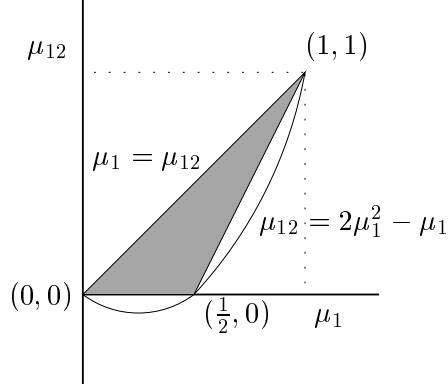


**Figure 23.** Nature of the semidefinite outer bound  $\text{SDEF}_1$  on the marginal polytope  $\text{MARG}(K_2)$  for a pair  $(x_1, x_2) \in \{0, 1\}^2$ . The gray area shows the cross-section of the binary marginal polytope  $\text{MARG}(K_2)$  corresponding to intersection with the hyperplane  $\mu_1 = \mu_2$ . The intersection of  $\text{SDEF}_1$  with this same hyperplane is defined by the inclusion  $\mu_1 \in [0, 1]$ , the linear constraint  $\mu_{12} \leq \mu_1$ , and the quadratic constraint  $\mu_{12} \geq 2\mu_1^2 - \mu_1$ . Consequently, there are points belonging to  $\text{SDEF}_1$  that lie strictly outside  $\text{MARG}(K_2)$ .

the hyperplane  $\mu_1 = \mu_2$ . The intersection of the semidefinite constraint set  $\text{SDEF}_1$  with this same hyperplane is characterized by the interval inclusion  $\mu_1 \in [0, 1]$  and the two inequalities in equation (125). Note that the semidefinite constraint set is an outer bound on  $\text{MARG}(K_2)$ , but

that it includes points that are clearly not valid marginals. For instance, it can be verified that  $(\mu_1, \mu_2, \mu_{12}) = (\frac{1}{4}, \frac{1}{4}, -\frac{1}{8})$  corresponds to a positive semidefinite  $M_1[\mu]$ , but this vector certainly does not belong to  $\text{MARG}(K_2)$ .  $\diamond$

#### 9.2.4 Higher-order semidefinite constraints

The previous construction of  $M_1[\mu]$  was based only on first and second-order moments of the random vector  $\mathbf{x}$ . Of course, we can also consider moments  $\mu_\alpha$  for higher-order multi-indices  $\alpha$  as well; doing so leads to what is known as the Lasserre sequence of relaxations [59, 58].

If the given model has higher than pairwise interactions, then considering such higher-order moments is absolutely necessary. However, it may also be useful even when considering a pairwise Markov random field on an ordinary graph  $G$  (i.e., for which  $\text{MARG}(G)$  involves only pairwise moments). Indeed, suppose that we have an outer bound on  $\text{MARG}(K_{k,n})$  for some  $k \geq 3$ . For any graph  $G$ , this outer bound can be projected, as in equation (123), to obtain an outer bound on  $\text{MARG}(G)$ .

Accordingly, for each  $t = 2, \dots, n$ , we form an  $|\mathcal{I}_t| \times |\mathcal{I}_t|$  matrix  $M_t[\mu]$  where each row and column is associated with some multi-index  $\alpha \in \mathcal{I}_t$ . The entries of  $M_t[\mu]$  are specified as follows:

$$(M_t[\mu])_{\alpha\beta} = \mu_{\alpha+\beta}. \quad (126)$$

When  $t = 1$ , this definition reduces to our previous definition of  $M_1[\mu]$  in equation (120). Note any moment  $\mu_{\alpha+\beta}$  involved in  $M_t[\mu]$  has order  $\|\alpha + \beta\|_0 \leq \min\{2t, n\}$ .

**Example 26 (Higher-order semidefinite constraint).** To provide a simple illustration, consider a triplet  $(x_1, x_2, x_3)$  of binary variables, so that

$$\{\mathbf{x}^\alpha \mid \alpha \in \mathcal{I}_2\} = \{1, x_1, x_2, x_3, x_1x_2, x_1x_3, x_2x_3\}$$

In this case, the matrix  $M_2[\mu]$  is  $7 \times 7$ , and takes the following form:

$$M_2[\mu] = \begin{bmatrix} 1 & \mu_1 & \mu_2 & \mu_3 & \mu_{12} & \mu_{13} & \mu_{23} \\ \mu_1 & \mu_1 & \mu_{12} & \mu_{13} & \mu_{12} & \mu_{13} & \mu_{123} \\ \mu_2 & \mu_{12} & \mu_2 & \mu_{23} & \mu_{12} & \mu_{123} & \mu_{23} \\ \mu_3 & \mu_{13} & \mu_{23} & \mu_3 & \mu_{123} & \mu_{13} & \mu_{23} \\ \mu_{12} & \mu_{12} & \mu_{12} & \mu_{123} & \mu_{12} & \mu_{123} & \mu_{123} \\ \mu_{13} & \mu_{13} & \mu_{123} & \mu_{13} & \mu_{123} & \mu_{13} & \mu_{123} \\ \mu_{23} & \mu_{123} & \mu_{23} & \mu_{23} & \mu_{123} & \mu_{123} & \mu_{23} \end{bmatrix} \quad (127)$$

In calculating the form of  $M_2[\mu]$ , we use the fact that  $x_s^2 = x_s$  whenever  $x_s \in \{0, 1\}$  in order to simplify the moment calculations. For example, in calculating the (5, 7) entry, we use the reduction  $\mathbb{E}[(x_1 x_2)(x_2 x_3)] = \mathbb{E}[x_1 x_2 x_3] = \mu_{123}$ .  $\diamond$

As with the argument preceding Lemma 5, for each  $t = 1, \dots, n$ , the matrix  $M_t[\mu]$  can be used to specify an outer bound<sup>10</sup> on the marginal polytope  $\text{MARG}(K_{2t,n})$ . In particular, we use  $M_t[\mu]$  to define the following semidefinite constraint set:

$$\text{SDEF}_t := \{\mu_\alpha, \alpha \in \mathcal{I}_{2t} \mid M_t[\mu] \succeq 0\}. \quad (128)$$

Note that when  $t = 1$ , definition (128) is equivalent to the earlier definition of  $\text{SDEF}_1$  in equation (122). In analogy to Lemma 5, these semidefinite constraints generate outer bounds on marginal polytopes:

---

<sup>10</sup>Strictly speaking, it defines an outer bound on  $\text{MARG}(K_{r(t),n})$  where  $r(t) := \min\{2t, n\}$ , but we suppress the subtlety in the interests of readability.

**Lemma 6.** For each  $t = 1, \dots, n$ , the set  $\text{SDEF}_t$  is an outer bound on  $\text{MARG}(K_{2t,n})$ . Moreover, for any hypergraph  $G$  contained within  $K_{2t,n}$ , the projection  $\Pi_G(\text{SDEF}_t)$  is an outer bound on  $\text{MARG}(G)$ .

An important property of this sequence of outer bounds is that they are *nested*. Considering in particular  $\text{MARG}(K_n) \equiv \text{MARG}(K_{2,n})$ , we have the set of inclusions

$$\text{SDEF}_1 = \Pi_{K_n}(\text{SDEF}_1) \supseteq \Pi_{K_n}(\text{SDEF}_2) \supseteq \dots \supseteq \Pi_{K_n}(\text{SDEF}_n). \quad (129)$$

This nesting relation holds because for  $t' < t$ , the matrix  $M_{t'}[\mu]$  is a principal subminor of the larger matrix  $M_t[\mu]$ . For instance, observe that for the binary case, the matrix  $M_1[\mu]$  of equation (124) is equivalent to the top  $3 \times 3$  block of  $M_2[\mu]$  defined in equation (127).

We have terminated the nested sequence in equation (129) at  $\text{SDEF}_n$ . The validity of this finite termination was proved by Lasserre [58], and also by Laurent [60] using more direct methods in the binary case. Here we provide an alternative proof of finite termination for the general multinomial case:

**Proposition 16 (Tightness of semidefinite constraints).** For any multinomial random vector  $\mathbf{x} \in \{0, 1, \dots, m-1\}^n$ , the semidefinite constraint set  $\text{SDEF}_n$  and its projections provide an exact characterization of the marginal polytope  $\text{MARG}(G)$  for any hypergraph  $G$ .

*Proof.* For each  $J = (j_1, \dots, j_n) \in \mathcal{X}^n$ , define the indicator function  $\mathbb{I}_J(\mathbf{x}) := \prod_{s=1}^n \mathbb{I}_{j_s}(x_s)$ . First consider the following identities between the scalar indicator functions  $\mathbb{I}_j(u)$  and monomials  $u^j$ :

$$\mathbb{I}_j(u) = \prod_{k \neq j} \frac{u - k}{j - k}, \quad u^j = \sum_{k=0}^{m-1} k^j \mathbb{I}_k(u). \quad (130)$$

For each  $\alpha \in \mathcal{I}_n$ , the monomial  $\mathbf{x}^\alpha$  decomposes as the product  $\prod_{s=1}^n x_s^{\alpha_s}$ , so that it is a linear combination of the indicators  $\mathbb{I}_J(\mathbf{x}) := \prod_{s=1}^n \mathbb{I}_{j_s}(x_s)$ . Conversely, for each  $J \in \mathcal{X}^n$ , the indicator function  $\mathbb{I}_J(\mathbf{x})$  is also equal to a linear combination of the monomials  $\{\mathbf{x}^\alpha, \alpha \in \mathcal{I}_n\}$ . Thus, there is an invertible linear transformation (with matrix  $B$ ) between the indicator functions  $\{\mathbb{I}_J(\mathbf{x}), J \in \mathcal{X}^n\}$  and the monomials  $\{\mathbf{x}^\alpha, \alpha \in \mathcal{I}_n\}$ .

Consider the  $m^n \times m^n$  moment matrix defined by the functions  $\{\mathbb{I}_J(\mathbf{x}), J \in \mathcal{X}^n\}$ . Its form is very simple: since the product  $\mathbb{I}_J(\mathbf{x})\mathbb{I}_{J'}(\mathbf{x})$  vanishes for all  $J \neq J'$ , it is a diagonal matrix  $D = \text{diag}(\mu_J)$ , where  $\mu_J$  is the probability of the configuration  $J \in \mathcal{X}^n$ . Given the constraint  $\sum_J \mathbb{I}_J(\mathbf{x}) = 1$ , the positive semidefinite constraint  $D \succeq 0$  is necessary and sufficient to ensure that  $\{\mu_J, J \in \mathcal{X}^n\}$  specifies a valid probability distribution. Moreover, by the linear bijection established above, we have  $M_n[\mu] = B D B^T$  with  $B$  invertible, so that  $D \succeq 0$  if and only if  $M_n[\mu] \succeq 0$ .  $\square$

**Remarks:** This result shows that imposing a semidefinite constraint on the largest possible moment matrix  $M_n[\mu]$  is sufficient to fully characterize all marginal polytopes. From a practical point of view, however, the consequences of this result are limited, because  $M_n[\mu]$  is a  $|\mathcal{I}_n| \times |\mathcal{I}_n|$  matrix, where  $|\mathcal{I}_n| = |\mathcal{X}^n| = m^n$  is exponentially large.

To illustrate Proposition 16, we consider a very simple example.

**Example 27.** Consider the marginal polytope  $\text{MARG}(K_2)$  for a binary pair  $(x_1, x_2) \in \{0, 1\}^2$ . In this case, the full moment matrix  $M_2[\mu]$  is  $4 \times 4$ , corresponding to the set  $\{1, x_1, x_2, x_1 x_2\}$ . It takes

the form

$$M_2[\mu] = \begin{bmatrix} 1 & \mu_1 & \mu_2 & \mu_{12} \\ \mu_1 & \mu_1 & \mu_{12} & \mu_{12} \\ \mu_2 & \mu_{12} & \mu_2 & \mu_{12} \\ \mu_{12} & \mu_{12} & \mu_{12} & \mu_{12} \end{bmatrix}. \quad (131)$$

Positivity of the diagonal element  $(4, 4)$  gives the constraint  $\mu_{12} \geq 0$ . Positivity of the  $(3, 4)$  subminor, combined with the constraint  $\mu_{12} \geq 0$ , leads to  $\mu_2 - \mu_{12} \geq 0$ . By symmetry, the  $(2, 4)$  subminor gives  $\mu_1 - \mu_{12} \geq 0$ . Finally, the determinant of  $M_2[\mu]$  can be calculated

$$\det M_2[\mu] = \mu_{12} [\mu_1 - \mu_{12}] [\mu_1 - \mu_{12}] [1 + \mu_{12} - \mu_1 - \mu_2]. \quad (132)$$

The constraint  $\det M_2[\mu] \geq 0$ , in conjunction with the previous constraints, implies the inequality  $1 + \mu_{12} - \mu_1 - \mu_2 \geq 0$ . (In fact, the quantities  $\{\mu_{12}, \mu_1 - \mu_{12}, \mu_2 - \mu_{12}, 1 + \mu_{12} - \mu_1 - \mu_2\}$  are the eigenvalues of  $M_2[\mu]$ , so positive semidefiniteness of  $M_2[\mu]$  is equivalent to non-negativity of these four quantities.) These four inequalities provide a complete description of the marginal polytope in this simple case, as can be seen by comparison to Example 7. It is also worthwhile comparing to Example 25, where we showed that positive semidefiniteness of the  $3 \times 3$  moment matrix  $M_1[\mu]$ , which is simply the  $(1, 2, 3)$  principal submatrix of  $M_2[\mu]$ , provides only a partial characterization of  $\text{MARG}(K_2)$ .

◇

### 9.3 Link to graphical structure

Recall from our discussion in Section 4.1.3 that the complexity of a given marginal polytope  $\text{MARG}(G)$  depends very strongly on the structure of the (hyper)graph  $G$ . We now turn to a more detailed consideration of the role of graphical structure in semidefinite constraints. One consequence of the junction tree theorem, as stated in Proposition 1, is that marginal polytopes associated with hypertrees are straightforward to characterize. This simplicity is also apparent in the context of semidefinite characterizations.

#### 9.3.1 Notation for graph-structured semidefinite constraints

Before turning to results, we require some additional notation. Given a hypergraph  $H$ , let  $\mathcal{I}(H)$  be the set of multi-indices associated with all possible monomials  $\mathbf{x}^\alpha$  defined on its hyperedges. For example, if  $H$  is simply the complete graph  $K_n$ , then the set  $\mathcal{I}(K_n)$  consists of all multi-indices satisfying  $\|\alpha\|_0 \leq 2$ . Let  $M_H[\mu]$  be the  $|\mathcal{I}(H)| \times |\mathcal{I}(H)|$  moment matrix defined by  $\{\mathbf{x}^\alpha, \alpha \in \mathcal{I}(H)\}$ . Note that  $M_H[\mu]$  generalizes the previously defined moment matrix  $M_t[\mu] \equiv M_{K_{t,n}}[\mu]$ , where  $K_{t,n}$  is the complete hypergraph including all hyperedges of size less than or equal to  $t$ .

Using these moment matrices, we define the semidefinite constraint sets

$$\text{SDEF}_H := \Pi_H \left[ \{\mu \mid M_H[\mu] \succeq 0\} \right]. \quad (133)$$

Observe that the set  $\text{SDEF}_H$  is a generalization of the semidefinite constraint sets  $\text{SDEF}_t$  defined in equation (128); more specifically,  $\text{SDEF}_t$  is equivalent to  $\text{SDEF}_{K_{t,n}}$ . Finally, for any pair of graphs  $H$  and  $G$ , we define the projection

$$\text{SDEF}_H(G) := \Pi_G [\text{SDEF}_H] \quad (134)$$

of  $\text{SDEF}_H$  onto the set of mean parameters  $\{\mu_\alpha, \alpha \in \mathcal{I}(G)\}$ . When  $H = G$ , we use  $\text{SDEF}(G)$  as short-hand for set  $\text{SDEF}_G$ .

### 9.3.2 Semidefinite characterization of hypertrees

When the hypergraph  $G$  is a hypertree, then its marginal polytope is characterized by a relatively small set of semidefinite constraints:

**Proposition 17 (Hypertrees).** *For any hypertree  $G$ , there holds*

$$\text{SDEF}(G) = \text{MARG}(G). \quad (135)$$

*Proof.* For any hyperedge  $h$  of  $G$ , let  $\mathcal{I}(h)$  denote the associated multi-indices (including  $\alpha = \mathbf{0}$  for the empty subset), and define  $k := |\mathcal{I}(h)|$ . By definition, for every hyperedge  $h$  of the hypertree  $G$ , the moment matrix  $M_G[\mu]$  includes an  $k \times k$  principal submatrix, corresponding to all of moments of the form  $\mu_{\alpha+\beta}$  for pairs  $\alpha, \beta \in \mathcal{I}(h)$ . For the subset of random variables  $x_h := \{x_s \mid s \in h\}$ , this principal submatrix is equivalent to the matrix  $M_{K_{k,k}}[\mu]$ . By Sylvester's criterion [50], the positive semidefiniteness of  $M_G[\mu]$  implies that all principal submatrices must be positive semidefinite. By Proposition 16, the positive semidefiniteness of  $M_{K_{k,k}}[\mu]$  implies that the mean parameters  $\{\mu_\alpha \mid \alpha \in \mathcal{I}(h)\}$  are locally consistent over the hyperedge  $h$ . The junction tree characterization of Proposition 1 then guarantees global consistency.  $\square$

**Remarks:** (a) This result is of an analogous nature to the junction tree sufficiency condition of Proposition 1. It is worthwhile contrasting with the earlier Proposition 16, which guarantees tightness of semidefinite constraints involving the *full* moment matrix (of size  $m^n$ ). The essence of Proposition 17 is that if, in addition,  $G$  is a hypertree, a much lower order of semidefinite constraints provides a complete characterization of the marginal polytope. In particular, for a hypergraph  $G$  with maximal hyperedges of size  $t+1$ , the moment matrix  $M_G[\mu]$  is only of size  $\mathcal{O}(m^{t+1}|E|)$ .  
(b) As a particular example, consider the case of an ordinary tree  $T$ , which has treewidth  $t=1$ . Proposition 17 then asserts that  $\text{SDEF}(T)$ , which is defined by a moment matrix with only  $\mathcal{O}(m^2n)$  elements, is an exact characterization of the tree marginal polytope  $\text{MARG}(T)$ .

### 9.3.3 Comparison to junction tree

In Section 7, we described outer bounds on the marginal polytope of an arbitrary hypergraph based on hypertree consistency. It is worthwhile understanding the connection between such outer bounds  $\text{LOCAL}(G)$ , as defined in equation (95), and the constraint sets  $\text{SDEF}(G)$  defined in the previous section.

First of all, whenever  $G$  is a hypertree, there holds

$$\text{LOCAL}(G) \stackrel{(a)}{=} \text{MARG}(G) \stackrel{(b)}{=} \text{SDEF}(G), \quad (136)$$

where equality (a) is a consequence of Proposition 1, and equality (b) is the assertion of Proposition 17. More generally, the following relation holds:

**Proposition 18.** *For any hypergraph  $G$ , we have  $\text{SDEF}(G) \subseteq \text{LOCAL}(G)$ .*

*Proof.* The proof is similar to the proof of Proposition 17. In particular, for any hyperedge  $h$  in the hypergraph, set  $k := |\mathcal{I}(h)|$ , and observe that the moment matrix  $M_G[\mu]$  contains a principal submatrix of the form  $M_{K_{k,k}}[\mu]$ . The positive semidefiniteness of this principal submatrix enforces the constraint that  $\{\mu_\alpha, \alpha \in \mathcal{I}(h)\}$  defines a valid local marginal. Therefore, the constraints defining  $\text{SDEF}(G)$  imply those defining  $\text{LOCAL}(G)$ , thereby establishing containment.  $\square$

**Remarks:** (a) Laurent [60] proved this result for binary variables, where the sequences  $\text{SDEF}(K_{t,n})$  and  $\text{LOCAL}(K_{t,n})$  for  $t = 1, \dots, n$  defined by the complete hypergraphs  $K_{t,n}$  are known as the Lasserre [58] and Sherali-Adams [85] relaxations respectively.

(b) An interesting by-product of Proposition 18, or rather of its proof, is showing that the linear constraint set  $\text{LOCAL}(G)$  can be viewed as an intersection of locally-defined semidefinite constraint sets. In particular, for any hyperedge  $g$  of  $E$ , let  $H_g$  be the subhypergraph induced by  $g$ . More explicitly,  $H_g$  is simply a hypergraph with vertex set  $g$  and a single hyperedge  $\{g\}$ . The semidefinite constraint set  $\text{SDEF}(H_g)$  is defined by the moment matrix  $M_{K_{k,k}}[\mu]$ , where  $k = |\mathcal{I}(g)|$ . With this notation, we have the following equivalence:

$$\text{LOCAL}(G) = \bigcap_{g \in E} \text{SDEF}(H_g), \quad (137)$$

where  $g$  ranges over the hyperedge set of  $G$ . (In fact, it suffices to restrict  $g$  to maximal hyperedges.)

**Example 28.** Consider the case of a pairwise Markov random field, so that  $\text{LOCAL}(G)$  corresponds to the constraint set used in the Bethe variational problem. In this case, the maximal hyperedges of  $G$  are simply pairs  $(st)$  of nodes connected by edges. Each subhypergraph  $H_{st}$  consists of the nodes  $s$  and  $t$  joined by an edge. The semidefinite constraint set  $\text{SDEF}(H_{st})$  enforces the pairwise consistency of the mean parameters associated with  $(x_s, x_t)$ . For instance, in the binary case, this semidefinite constraint set is enforced by a  $4 \times 4$  matrix, defined in equation (131) of Example 27. The intersection of all of these constraint sets, one for each edge  $(s, t)$ , is equivalent to  $\text{LOCAL}(G)$ .  $\diamond$

## 9.4 Log-determinant relaxation

In this section, we illustrate one possible use of semidefinite constraints in approximate inference. Recall from Section 8 that a convex relaxation of the exact variational principle requires both a convex outer bound on the set of realizable mean parameters, and a concave upper bound on the entropy. Combining a semidefinite outer bound with a Gaussian-based entropy approximation leads to a log-determinant relaxation of the exact variational principle.

Although the techniques described in this section can be applied more generally, for concreteness we focus on the case of a binary random vector  $\mathbf{x} \in \{0, 1\}^n$ , with a distribution in the Ising form

$$p(\mathbf{x}; \theta) = \exp \left\{ \sum_{s \in V} \theta_s x_s + \sum_{(s,t)} \theta_{st} x_s x_t - A(\theta) \right\}. \quad (138)$$

Without loss of generality, we assume that the underlying graph is the complete graph  $K_n$ , so that the marginal polytope of interest is  $\text{MARG}(K_n)$ . Of course, a problem defined on an arbitrary  $G = (V, E)$  can be embedded into the complete graph by setting  $\theta_{st} = 0$  for all  $(s, t) \notin E$ .

### 9.4.1 Gaussian entropy bound

In order to upper bound the entropy, we return to the familiar interpretation of the Gaussian as the maximum entropy distribution subject to covariance constraints [see 24]. In particular, the differential entropy  $h(\tilde{\mathbf{x}})$  of any continuous random vector  $\tilde{\mathbf{x}}$  is upper bounded by the entropy of a Gaussian with matched covariance, or in analytical terms

$$h(\tilde{\mathbf{x}}) \leq \frac{1}{2} \log \det \text{cov}(\tilde{\mathbf{x}}) + \frac{n}{2} \log(2\pi e), \quad (139)$$

where  $\text{cov}(\tilde{\mathbf{x}})$  is the covariance matrix of  $\tilde{\mathbf{x}}$ .

The upper bound (139) is not directly applicable to a random vector taking values in a discrete space (since differential entropy in this case diverges to minus infinity). Therefore, in order to exploit this bound for the random vector  $\mathbf{x} \in \{0, 1\}^n$ , it is necessary to construct a suitably matched continuous version of  $\mathbf{x}$ . One method to do so is by the addition of an independent random vector  $\mathbf{u}$ , such that the delta functions in the density of  $\mathbf{x}$  are smoothed out.

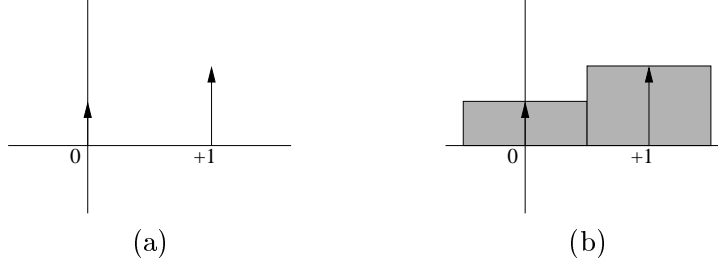


**Figure 24.** Illustration of the smoothing procedure. (a) Original probability mass function with impulses at  $\{0, 1\}$ . (b) Transformed version, where the impulses are spread out with a uniform random variable on  $[-\frac{1}{2}, \frac{1}{2}]$ . By construction, the (differential) entropy of the continuous random variable in (b) is equivalent to the discrete entropy of the original one in (a).

In order to do so, we use  $\mathbf{x}$  to define a continuous random vector  $\tilde{\mathbf{x}} := \mathbf{x} + \mathbf{u}$ , where  $\mathbf{u}$  is independent of  $\mathbf{x}$ , with independent components distributed uniformly as  $u_s \sim \mathcal{U}[-\frac{1}{2}, \frac{1}{2}]$ . This construction is illustrated for the scalar case in Figure 24. A key property of this construction is that it matches the discrete entropy of  $\mathbf{x}$  with the differential entropy of  $\tilde{\mathbf{x}}$ .

**Lemma 7.** *Let  $h$  and  $H$  denote the differential and discrete entropies of  $\tilde{\mathbf{x}}$  and  $\mathbf{x}$  respectively. Then  $h(\tilde{\mathbf{x}}) = H(\mathbf{x})$ .*

*Proof.* Let  $p(\cdot)$  denote the density of  $\tilde{\mathbf{x}}$  (with respect to Lebesgue measure), and let  $P(\cdot)$  denote the mass function of  $\mathbf{x}$  (i.e., density with respect to counting measure on  $\{0, 1\}^n$ ). Letting  $\mathcal{D} := \{\tilde{\mathbf{x}} \in \mathbb{R}^n \mid p(\tilde{\mathbf{x}}) > 0\}$  denote the support of  $p$ , the differential entropy is given by  $h(\tilde{\mathbf{x}}) = -\int_{\mathcal{D}} p(\tilde{\mathbf{x}}) \log p(\tilde{\mathbf{x}}) d\tilde{\mathbf{x}}$ . By construction,  $\mathcal{D}$  can be decomposed into a disjoint union of hyperboxes  $\cup_{\mathbf{e}} B(\mathbf{e})$  of unit volume, one for each configuration  $\mathbf{e} \in \{0, 1\}^n$ . Using this decomposition,  $h$  can be decomposed as

$$h(\tilde{\mathbf{x}}) = - \sum_{\mathbf{e} \in \{0, 1\}^n} \int_{B(\mathbf{e})} p(\tilde{\mathbf{x}}) \log p(\tilde{\mathbf{x}}) d\tilde{\mathbf{x}} \stackrel{(a)}{=} - \sum_{\mathbf{e} \in \{0, 1\}^n} P(\mathbf{e}) \log P(\mathbf{e}),$$

where equality (a) follows from the fact that  $p(\tilde{\mathbf{x}}) \log p(\tilde{\mathbf{x}})$  is equal to the constant  $P(\mathbf{e}) \log P(\mathbf{e})$  over each hyperbox.  $\square$

#### 9.4.2 Log-determinant relaxation

Equipped with these building blocks, we are now ready to state a log-determinant relaxation for the log partition function. Recall the definition of SDEF<sub>1</sub> from equation (122).

**Theorem 3.** *Let  $\mathbf{x} \in \{0, 1\}^n$ , and let OUT( $K_n$ ) be any convex outer bound on MARG( $K_n$ ) that is contained within SDEF<sub>1</sub>  $\equiv$  SDEF<sub>1</sub>( $K_n$ ). Then the log partition function  $A(\theta)$  is upper bounded as follows:*

$$A(\theta) \leq \max_{\mu \in \text{OUT}(K_n)} \left\{ \langle \theta, \mu \rangle + \frac{1}{2} \log \det \left[ M_1(\mu) + \frac{1}{12} \text{blkdiag}[0, I_n] \right] \right\} + \frac{n}{2} \log(2\pi e) \quad (140)$$

where  $\text{blkdiag}[0, I_n]$  is a  $(n+1) \times (n+1)$  block-diagonal matrix.

**Remarks:** The inclusion  $\text{OUT}(K_n) \subseteq \text{SDEF}_1(K_n)$  guarantees that the matrix  $M_1(\mu)$  (and hence  $M_1(\mu) + \frac{1}{12} \text{blkdiag}[0, I_n]$ ) will always be positive semidefinite. Importantly, the optimization problem in equation (140) is a determinant maximization problem, for which efficient interior point methods have been developed [e.g., 92].

*Proof of Theorem 3:*

The proof is based on the variational representation of  $A$  from equation (26) of Theorem 2(b). By Theorem 5, any vector  $\mu \in \text{ri MARG}(K_n)$  is realized by some distribution  $p(\mathbf{x}; \theta(\mu))$ . Let  $\mathbf{x} \in \{0, 1\}^n$  be distributed according to  $p(\mathbf{x}; \theta(\mu))$ . Consider the continuous-valued random vector  $\tilde{\mathbf{x}} = \mathbf{x} + \mathbf{u}$ . From Lemma 7, we have  $H(\mathbf{x}) = h(\tilde{\mathbf{x}})$ ; combining this equality with equation (139) yields the upper bound

$$-A^*(\mu) = H(\mathbf{x}) \leq \frac{1}{2} \log \det \text{cov}(\tilde{\mathbf{x}}) + \frac{n}{2} \log(2\pi e). \quad (141)$$

Using the independence of  $\mathbf{x}$  and  $\mathbf{u}$ , we can write  $\text{cov}(\tilde{\mathbf{x}}) = \text{cov}(\mathbf{x}) + \text{cov}(\mathbf{u}) = \text{cov}(\mathbf{x}) + \frac{1}{12} I_n$ , where we have used the fact that  $\text{cov}(\mathbf{u}) = \frac{1}{12} I_n$  for the IID uniform random vector  $\mathbf{u}$  on  $[-1/2, 1/2]^n$ . Combining this decomposition with equation (141) yields the upper bound

$$\begin{aligned} -A^*(\mu) &\leq \frac{1}{2} \log \det [\text{cov}(\mathbf{x}) + \frac{1}{12} I_n] + \frac{n}{2} \log(2\pi e) \\ &= \frac{1}{2} \log \det [M_1[\mu] + \frac{1}{12} \text{blkdiag}(0, I_n)] + \frac{n}{2} \log(2\pi e), \end{aligned} \quad (142)$$

where the final equality follows by the Schur complement formula [50]. Finally, substituting the upper bound (142) into equation (26) yields

$$\begin{aligned} A(\theta) &\leq \max_{\mu \in \text{MARG}(K_n)} \left\{ \langle \theta, \mu \rangle + \frac{1}{2} \log \det [M_1(\mu) + \frac{1}{12} \text{blkdiag}[0, I_n]] + \frac{n}{2} \log(2\pi e) \right\} \\ &\leq \max_{\mu \in \text{OUT}(K_n)} \left\{ \langle \theta, \mu \rangle + \frac{1}{2} \log \det [M_1(\mu) + \frac{1}{12} \text{blkdiag}[0, I_n]] \right\} + \frac{n}{2} \log(2\pi e), \end{aligned}$$

where the final inequality follows because  $\text{OUT}(K_n)$  is an outer bound on the marginal polytope by assumption.  $\square$

**Remark:** Just as the Bethe variational principle (79) is a tree-based approximation, the log-determinant relaxation (140) is a Gaussian-based approximation. In particular, it is worthwhile comparing the structure of the log-determinant relaxation (140) of Theorem 3 to the exact variational principle for a multivariate Gaussian, as described in Section 4.2.2. More details on the log-determinant relaxation and its performance for approximate inference can be found in [97].

## 10 Approximate computation of modes

The preceding sections have focused exclusively on variational methods for approximate computation of the log partition function  $A(\theta)$  and mean parameters  $\mu = \mathbb{E}_\theta[\phi(\mathbf{x})]$  associated with a given density  $p(\mathbf{x}; \theta)$ . In this section, we turn our attention to a related but distinct problem—namely, that of computing a mode of  $p(\mathbf{x}; \theta)$ . It turns out that the mode problem has a variational formulation in which the set  $\mathcal{M}$  once again plays a central role.

## 10.1 Variational formulation of computing modes

The problem of mode computation corresponds to finding a configuration  $\mathbf{x}^* \in \mathcal{X}^n$  that maximizes  $p(\mathbf{x}; \theta)$ . Note that we are assuming that at least one mode exists, so that the maximum is attained. Given the exponential form of  $p(\mathbf{x}; \theta)$  and the fact that the log partition function  $A(\theta)$  does not depend on  $\mathbf{x}$ , it is equivalent to find a configuration  $\mathbf{x}^* \in \arg \max_{\mathbf{x}} \langle \theta, \phi(\mathbf{x}) \rangle$ .

We begin by providing intuition for the more formal result to follow. Recall that the log partition function is defined by

$$A(\theta) := \log \int \exp \{ \langle \theta, \phi(\mathbf{x}) \rangle \} \nu(d\mathbf{x}), \quad (143)$$

presuming that the integral exists (i.e.,  $\theta \in \Theta$ ). Now suppose that we rescale the exponential parameter  $\theta$  by some scalar  $\beta > 0$ . For the sake of this heuristic argument, let us assume that  $\beta\theta \in \Theta$  for all  $\beta > 0$ . Such a rescaling will put more weight, in a relative sense, on regions of the sample space  $\mathcal{X}^n$  for which  $\langle \theta, \phi(\mathbf{x}) \rangle$  is large. Ultimately, as  $\beta \rightarrow +\infty$ , probability mass should remain only on configurations  $\mathbf{x}^*$  in the set  $\arg \max_{\mathbf{x}} \langle \theta, \phi(\mathbf{x}) \rangle$ . This type of rescaling is equivalent to the so-called “zero-temperature limit” of statistical physics.

This intuition suggests that the behavior of the function  $A(\beta\theta)$  should have a close connection to the problem of computing  $\max_{\mathbf{x}} \langle \theta, \phi(\mathbf{x}) \rangle$ . Since  $A(\beta\theta)$  may diverge as  $\beta \rightarrow +\infty$ , it is most natural to consider the limiting behavior of the scaled quantity  $A(\beta\theta)/\beta$ . More formally, we state and prove the following:

**Theorem 4.** *For all  $\theta \in \Theta$ , the problem of mode computation has the following alternative representations:*

$$\max_{\mathbf{x} \in \mathcal{X}^n} \langle \theta, \phi(\mathbf{x}) \rangle \stackrel{(a)}{=} \sup_{\mu \in \text{cl } \mathcal{M}} \langle \theta, \mu \rangle \stackrel{(b)}{=} \lim_{\beta \rightarrow +\infty} \frac{A(\beta\theta)}{\beta}. \quad (144)$$

Moreover, if  $\mathcal{M}$  contains no lines, then the supremum is attained at an extreme point of  $\mathcal{M}$ .

*Proof.* As pointed out earlier, the problem  $\max_{\mathbf{x} \in \mathcal{X}^n} \langle \theta, \phi(\mathbf{x}) \rangle$  is equivalent to computing a mode for the exponential family member  $p(\mathbf{x}; \theta)$ .

Equality (a): Let  $\mathcal{P}$  be the space of all densities  $p(\cdot)$ , taken with respect to  $\nu$ . On one hand, for any  $p \in \mathcal{P}$ , we have  $\int \langle \theta, \phi(\mathbf{x}) \rangle p(\mathbf{x}) \nu(d\mathbf{x}) \leq \max_{\mathbf{x} \in \mathcal{X}^n} \langle \theta, \phi(\mathbf{x}) \rangle$ , whence

$$\sup_{p \in \mathcal{P}} \int \langle \theta, \phi(\mathbf{x}) \rangle p(\mathbf{x}) \nu(d\mathbf{x}) \leq \max_{\mathbf{x} \in \mathcal{X}^n} \langle \theta, \phi(\mathbf{x}) \rangle. \quad (145)$$

Since the support of  $\nu$  is  $\mathcal{X}^n$ , equality is achieved in (145) by taking a sequence  $p^n$  converging to a delta function  $\mathbb{I}_{\mathbf{x}^*}$ , where  $\mathbf{x}^* \in \arg \max_{\mathbf{x}} \langle \theta, \phi(\mathbf{x}) \rangle$ . Finally, by linearity of expectation and the definition of  $\mathcal{M}$ , we have  $\sup_{p \in \mathcal{P}} \int \langle \theta, \phi(\mathbf{x}) \rangle p(\mathbf{x}) \nu(d\mathbf{x}) = \sup_{\mu \in \mathcal{M}} \langle \theta, \mu \rangle$ .

Equality (b): By Proposition 2, the function  $A$  is lower semi-continuous. Therefore, for all  $\theta \in \Theta$ , the quantity  $\lim_{\beta \rightarrow +\infty} A(\beta\theta)/\beta$  is equivalent to the recession function of  $A$ , which we denote by  $A_\infty$  (Corollary 8.5.2, [79]). Hence, it suffices to establish that  $A_\infty(\theta)$  is equal to  $\sup_{\mu \in \mathcal{M}} \langle \theta, \mu \rangle$ . Using the lower semi-continuity of  $A$  and Theorem 13.3 of Rockafellar [79], the recession function of  $A$  corresponds to the support function of the effective domain of its dual. By Theorem 2, we have  $\text{cl dom } A^* = \text{cl } \mathcal{M}$ , whence  $A_\infty(\theta) = \sup_{\mu \in \text{cl } \mathcal{M}} \langle \theta, \mu \rangle$ . Finally, the supremum is not affected by taking the closure.

To establish the last assertion, for a fixed  $\theta \neq 0$ , the function  $\langle \theta, \mu \rangle$  is non-constant, linear and (hence) convex in  $\mu$ . If the convex set  $\mathcal{M}$  contains no lines, then the supremum must be attained at an extreme point (Cor. 32.3.2, [79]).  $\square$

**Remarks:** (a) Theorem 4 shows that the problem of mode computation is equivalent to maximizing a linear function over the convex set  $\mathcal{M}$ . In fact, the function  $A_\infty(\theta) := \sup_{\mu \in \mathcal{M}} \langle \theta, \mu \rangle$  corresponds to the *support function* of  $\mathcal{M}$ . It is clear that  $A_\infty$  is convex; moreover, it can be verified that its subdifferential  $\partial A_\infty(\theta)$  has the form:

$$\mathcal{F}_\mathcal{M}(\theta) := \{\mu^* \in \text{cl } \mathcal{M} \mid \langle \theta, \mu^* \rangle = \sup_{\mu \in \mathcal{M}} \langle \theta, \mu \rangle\}. \quad (146)$$

This set corresponds to the face of  $\mathcal{M}$  that is exposed by the direction  $\theta$ .

(b) On the basis of Theorem 2, it is possible to gain additional insight into why  $\lim_{\beta \rightarrow +\infty} A(\beta\theta)/\beta$  is equivalent to the support function of  $\mathcal{M}$ . In particular, using Theorem 2, we write

$$\lim_{\beta \rightarrow +\infty} \frac{A(\beta\theta)}{\beta} = \lim_{\beta \rightarrow +\infty} \frac{1}{\beta} \sup_{\mu \in \mathcal{M}} \{\langle \beta\theta, \mu \rangle - A^*(\mu)\} = \lim_{\beta \rightarrow +\infty} \sup_{\mu \in \mathcal{M}} \{\langle \theta, \mu \rangle - \frac{1}{\beta} A^*(\mu)\}.$$

Equality (b) of Theorem 4 amounts to asserting that the order of the limit over  $\beta$  and the supremum over  $\mu$  can be exchanged. The convexity of  $A^*$ , as exploited in the proof, is crucial in permitting this exchange.

(c) In the particular case of discrete random vectors, the problem of finding a mode is an integer programming problem, and the set  $\mathcal{M}$  is a polytope by Proposition 7. Thus, as a special case of Theorem 4, the integer programming problem  $\max_{\mathbf{x}} \langle \theta, \phi(\mathbf{x}) \rangle$  is equivalent to a linear program over the marginal polytope. Since integer programming problems are NP-hard in general, this equivalence underscores the inherent complexity of  $\mathcal{M}$ . This type of transformation—i.e., from an integer program to the convex hull of its solutions—is a frequently used technique in integer programming and combinatorial optimization [e.g., 9, 47, 71, 83]. We return to this multinomial case in Section 10.2.2.

Theorem 4 is essentially a result concerning the *value* of any mode (i.e.,  $\max_{\mathbf{x}} \langle \theta, \phi(\mathbf{x}) \rangle$ ), and its link to rescaled forms of  $A$ . It is also of interest to investigate the limiting behavior of the mean parameters associated with  $p(\mathbf{x}; \beta\theta)$ , and their connection to the modes of  $p(\mathbf{x}; \theta)$ .

**Corollary 2.** *For any  $\beta > 0$ , let  $\mu(\beta) := \mathbb{E}_{\beta\theta}[\phi(\mathbf{x})]$  be the mean parameters associated with  $p(\mathbf{x}; \beta\theta)$ . If  $p(\mathbf{x}; \theta)$  has at least one mode for all  $\theta \in \Theta$ , then  $\mathcal{F}_\mathcal{M}(\theta)$  is non-empty for all  $\theta \in \Theta$ . Moreover, for all  $\epsilon > 0$ , there exists  $\beta_\epsilon$  such that for all  $\beta \geq \beta_\epsilon$ ,*

$$\mu(\beta) \in [\mathcal{F}_\mathcal{M}(\theta) + \mathcal{B}(0; \epsilon)], \quad (147)$$

where  $\mathcal{B}(0; \epsilon)$  is an  $\epsilon$ -ball around zero in  $\mathbb{R}^d$ . In the special case that  $p(\mathbf{x}; \theta)$  has a unique mode  $\mathbf{x}^*$ , then  $\mathcal{F}_\mathcal{M}(\theta) = \{\mu_{\mathbf{x}^*}\}$  where  $\mu_{\mathbf{x}^*} := \phi(\mathbf{x}^*)$ , and  $\lim_{\beta \rightarrow +\infty} \|\mu(\beta) - \mu_{\mathbf{x}^*}\| = 0$ .

*Proof.* For each  $\beta > 0$ , define the function  $A_\beta(\theta) := \frac{1}{\beta} A(\beta\theta)$ . From Theorem 4, the sequence of functions  $\{A_\beta\}$  converges to  $A_\infty$  pointwise on  $\Theta$ . By Proposition 2, for each fixed  $\beta < +\infty$ ,  $A_\beta$  is differentiable, and  $\nabla A_\beta(\theta) = \mathbb{E}_{\beta\theta}[\phi(\mathbf{x})]$  by the chain rule. By straightforward computations, the subdifferential of the support function  $A_\infty(\theta)$  is the set  $\mathcal{F}_\mathcal{M}(\theta)$ , so that equation (147) follows from Theorem 24.5 of Rockafellar [79].  $\square$

The interpretation of Corollary 2 is quite intuitive: it guarantees that for  $\beta > 0$  sufficiently large, the unique optimizer of the problem  $A_\beta(\theta) = \sup_{\mu \in \mathcal{M}} \{\langle \theta, \mu \rangle - \frac{1}{\beta} A^*(\mu)\}$  is close to the set of optimizers of the problem  $A_\infty(\theta) = \sup_{\mu \in \text{cl } \mathcal{M}} \langle \theta, \mu \rangle$ . In principle, then, one could imagine attempting to compute  $A_\infty(\theta)$  by computing  $A_\beta(\theta)$  for an increasing sequence of  $\beta$ . Such a strategy can be viewed as a deterministic analog of simulated annealing [78].

## 10.2 Exact mode computation by variational principle

In this section, we illustrate Theorem 4 with some examples where the support function can be computed, and modes can be found exactly. To parallel our discussion in Section 4, we focus in particular on the Gaussian case, and finite discrete spaces. As with the computation of mean parameters, these exact cases serve as building blocks for convex relaxations of the exact principle in more challenging cases.

### 10.2.1 Gaussian case

Recall our parameterization of a multivariate Gaussian random vector (of length  $n$ ) on the complete graph, as presented in Sections 4.1.2 and 4.2.2. There are a total of  $d = n + \binom{n}{2}$  exponential and mean parameters, one for each node and edge in the graph. It is convenient to represent the exponential and mean parameters by a pair of  $(n+1) \times (n+1)$  matrices, defined as follows:

$$U(\theta) := \begin{bmatrix} 0 & z^T(\theta) \\ z(\theta) & Z(\theta) \end{bmatrix}, \quad W(\mu) := \begin{bmatrix} 1 & z^T(\mu) \\ z(\mu) & Z(\mu) \end{bmatrix}. \quad (148)$$

Here  $z(\mu) := [\mu_1, \mu_2, \dots, \mu_n]^T$  is the  $n$ -vector of means, whereas  $Z(\mu) = [z_{st}]$  is the  $n \times n$  matrix of second-order moments. The analogous blocks of  $U(\theta)$  are filled with the corresponding exponential parameters. Recall from Example 4 that  $\Theta = \{\theta \in \mathbb{R}^d \mid Z(\theta) \prec 0\}$ , whereas from Proposition 6, the set of realizable mean parameters is given by  $\mathcal{M}_{Gauss} = \{\mu \in \mathbb{R}^d \mid W(\mu) \succ 0\}$ . For two symmetric matrices  $A$  and  $Y$ , let  $\langle\langle A, Y \rangle\rangle := \text{trace}(AY)$  be the Frobenius inner product.

Semidefinite programs [91] entail maximizing a linear function subject to linear matrix inequalities (see Section 9). In the Gaussian case, the support function representation of Theorem 2 turns out to be a semidefinite program. Using Proposition 6, the constraint set of  $\text{cl } \mathcal{M}_{Gauss}$  is characterized by the linear matrix inequality  $W(\mu) \succeq 0$ . By the Schur complement formula [50], the LMI constraint holds if and only if  $Z(\mu) - z(\mu)z^T(\mu) \succeq 0$ . The cost function  $\langle\langle U(\theta), W(\mu) \rangle\rangle$  is linear in  $\mu$ , so that the overall problem is a semidefinite program (SDP).

We claim that for all  $\theta \in \Theta$ , this SDP has the unique optimal solution

$$z(\mu^*) = -[Z(\theta)]^{-1}z(\theta), \quad Z(\mu^*) = z(\mu^*)z^T(\mu^*), \quad (149)$$

where  $z(\mu^*) \equiv \mathbf{x}^*$  for some  $\mathbf{x}^* \in \mathbb{R}^d$ . The interpretation is that  $\mu^*$  is realized by a Gaussian with zero covariance that places all its mass on the point  $\mathbf{x}^*$ . Note that the form of  $\mathbf{x}^* \equiv z(\mu^*)$  coincides with the familiar expression for the mode of a Gaussian. Moreover, the optimal solution lies at an extreme point of  $\mathcal{M}_{Gauss}$ , which is consistent with the last assertion in Theorem 4. Figure 25 provides a geometric illustration of the result in the case  $n = 1$ , for which the set  $\text{cl } \mathcal{M}_{Gauss}$  is a parabola.

To establish equation (149), we begin by noting that the cone of symmetric positive semidefinite matrices is self-dual [16]; hence,  $A \succeq 0$  if and only if  $\langle\langle A, B \rangle\rangle \geq 0$  for all  $B \succeq 0$ . Applying this fact with the choices  $A := Z(\mu) - z(\mu)z^T(\mu) \succeq 0$  and  $B := -Z(\theta) \succ 0$  yields that  $\langle\langle Z(\theta), Z(\mu) \rangle\rangle \leq \langle\langle Z(\theta), z(\mu)z^T(\mu) \rangle\rangle$ . Using this bound, we can write

$$\begin{aligned} \langle\langle U(\theta), W(\mu) \rangle\rangle &= 2\langle z(\theta), z(\mu) \rangle + \langle\langle Z(\theta), Z(\mu) \rangle\rangle \\ &\leq 2\langle z(\theta), z(\mu) \rangle + \langle\langle Z(\theta), z(\mu)z^T(\mu) \rangle\rangle. \end{aligned} \quad (150)$$

Observe that this upper bound (150) is simply a quadratic program in  $z(\mu)$ , with its maximum attained at  $z(\mu^*) := -[Z(\theta)]^{-1}z(\theta)$ . Thus, if we take the supremum over  $\mu \in \text{cl } \mathcal{M}_{Gauss}$ , the bound will be met with equality, and attained at a point  $W(\mu^*)$  of the form given in equation (149).

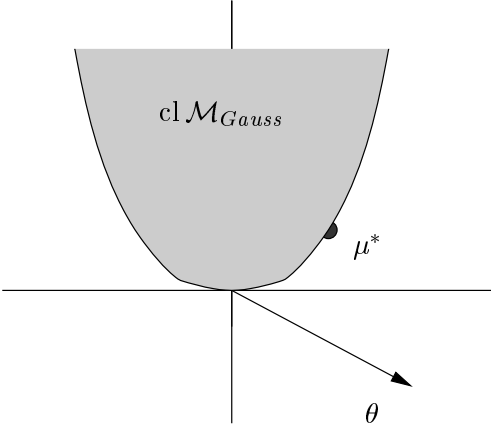


**Figure 25.** Illustration of the geometry of optimizing over the set  $\text{cl } \mathcal{M}_{\text{Gauss}}$ . For  $n = 1$ , the set  $\text{cl } \mathcal{M}_{\text{Gauss}} = \{(\mu_1, \mu_2) \mid \mu_2 - \mu_1^2 \geq 0\}$ . The optimum will always be attained at a boundary point of  $\text{cl } \mathcal{M}_{\text{Gauss}}$ , for which  $\mu_2 - \mu_1^2 = 0$ , corresponding to a Gaussian with zero variance concentrated on  $\mu_1$ .

In practice, of course, one would not compute the mode of a Gaussian problem via this semidefinite formulation. However, this formulation provides valuable perspective for semidefinite relaxations of integer programming problems, as discussed in Section 10.3.3.

### 10.2.2 Discrete case

Recall from Section 4.1.3 that in the finite discrete case, the set of realizable mean parameters  $\mathcal{M}$  is a polytope, meaning that it is bounded and can be characterized by a finite number of linear inequality constraints. Throughout this section, we use the canonical overcomplete representation (38), so that mean parameters correspond to particular values of marginal distributions. We use  $\text{MARG}(G)$  to denote the set of realizable marginals associated with potentials on the cliques of  $G$ , which we refer to as a marginal polytope.

Since  $\text{MARG}(G)$  is a polytope, the support function representation (144) for computing modes reduces to a linear program (LP). As such, it has a particular geometry, which provides more intuition into the variational representation of Theorem 4. Figure 26 illustrates the geometry of optimizing over a marginal polytope. Extreme points of the marginal polytope are all of the form  $\mu_e = \phi(e)$ , for some configuration  $e \in \mathcal{X}^n$ . The vector  $\theta$  specifies a direction in the space. In order to maximize  $\langle \theta, \mu \rangle$  over  $\text{MARG}(G)$ , we translate a hyperplane with normal  $\theta$  outwards until it is tangent to  $\text{MARG}(G)$ . An important result in linear programming [9] is that this tangency, while it may occur at multiple points, will always involve at least one vertex of the polytope  $\text{MARG}(G)$ . In Figure 26(a), the tangency occurs at a single vertex  $\mu_{e^*}$ , so that  $e^* \in \mathcal{X}^n$  is the unique MAP configuration for the problem. In panel (b), the tangency occurs along a higher-order face of the polytope, and any vertex in the face will be a MAP solution. In either case, the optimal solution to the LP will be attained at a vertex of  $\text{MARG}(G)$ .

**Tree-structured case:** As discussed in Section 4.1.3, the nature of  $\text{MARG}(G)$  depends strongly on the nature of the underlying graph  $G$ . To build on Example 8, we return to the case of a tree-structured graph  $T = (V, E(T))$ . Let  $\mu_s(x_s)$  and  $\mu_{st}(x_s, x_t)$  denote a set of marginal functions (see equation (40)) associated with the nodes and edges of  $T$ . Similarly, we also define functions of

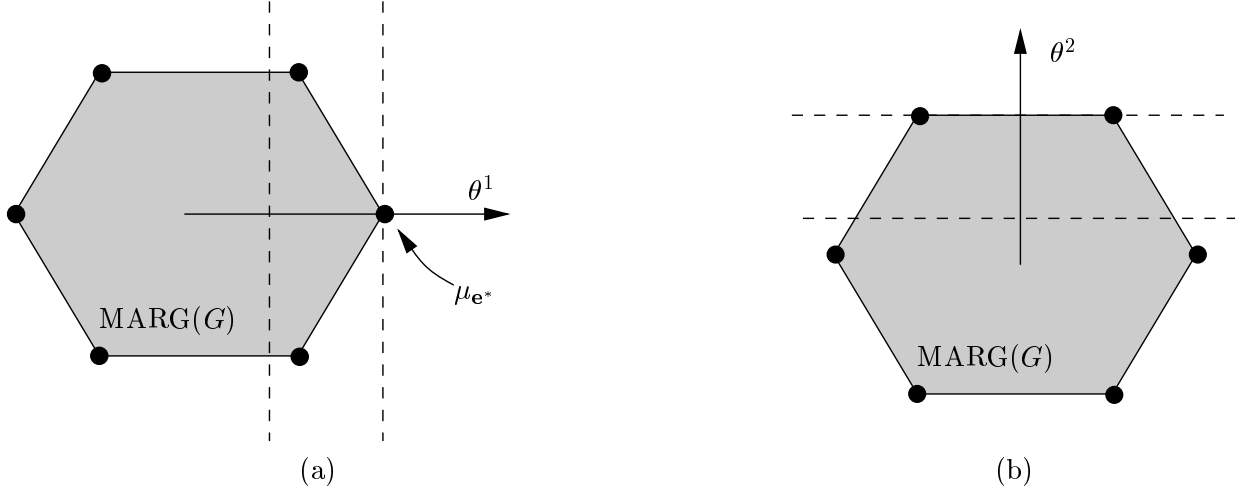


**Figure 26.** Geometry of optimizing over the marginal polytope  $\text{MARG}(G)$ . The vector  $\theta^i$  specifies the cost direction; the hyperplane with this normal is translated until it is tangent to  $\text{MARG}(G)$ . (a) For the cost direction  $\theta^1$ , the tangency occurs uniquely at the vertex  $\mu_{\mathbf{e}^*}$ , in which case  $\mathbf{e}^* \in \mathcal{X}^n$  is the unique global optimum. (b) For  $\theta^2$ , the tangency occurs along a higher-order face, in which case all vertices in the face are global optima.

the exponential parameters as follows:

$$\theta_s(x_s) := \sum_{j \in \mathcal{X}_s} \theta_{s;j} \mathbb{I}_j(x_s), \quad \theta_s(x_s) := \sum_{(j,k) \in \mathcal{X}_s \times \mathcal{X}_t} \theta_{st;jk} \mathbb{I}_{jk}(x_s, x_t).$$

In Example 8, we proved that the marginal polytope  $\text{MARG}(T)$  is characterized by the following set of local constraints:

$$\text{LOCAL}(T) := \{\mu \geq 0 \mid \sum_{x_s} \mu_s(x_s) = 1, \quad \sum_{x_t} \mu_{st}(x_s, x_t) = \mu_s(x_s)\}.$$

Applying Theorem 4, we conclude that finding the mode of a tree-structured problem is equivalent to solving the linear program:

$$\max_{\mu \in \text{LOCAL}(T)} \langle \mu, \theta \rangle = \max_{\mu \in \text{LOCAL}(T)} \left\{ \sum_{s \in V} \sum_{x_s} \mu_s(x_s) \theta_s(x_s) + \sum_{(s,t) \in E(T)} \sum_{x_s, x_t} \mu_{st}(x_s, x_t) \theta_{st}(x_s, x_t) \right\}. \quad (151)$$

Letting  $m$  denote  $\max_s |\mathcal{X}_s|$ , it can be seen that  $\text{LOCAL}(T)$  involves  $\mathcal{O}(mn + m^2|E|) = \mathcal{O}(m^2n)$  constraints. Presuming that  $m$  is not overly large, the LP of equation (151) is easily solvable by standard methods, including the simplex algorithm [9].

Of interest here is the connection between the variational problem (151) and the iterative max-product algorithm described in Section 2.5.1. Recall that the max-product algorithm is based on passing “messages”, denoted by  $M_{ts}(x_s)$ , between nodes in the tree. These messages are updated according to the following recursion:

$$M_{ts}(x_s) = \kappa \max_{x_t \in \mathcal{X}_t} \left[ \exp \left\{ \theta_{st}(x_s, x_t) + \theta_t(x_t) \right\} \prod_{u \in \mathcal{N}(t) \setminus s} M_{ut}(x_t) \right]. \quad (152)$$

Note that equation (152) is the analog of the sum-product update (84) given in the proof of Proposition 11, with the summation replaced by maximization.

To understand why such a connection should exist, recall that for tree-structured problems, the exact variational principle of Theorem 2 has a concrete and tractable formulation (49), one which involves  $\text{LOCAL}(T)$  as the constraint set (see Section 4.2.3). An immediate corollary of

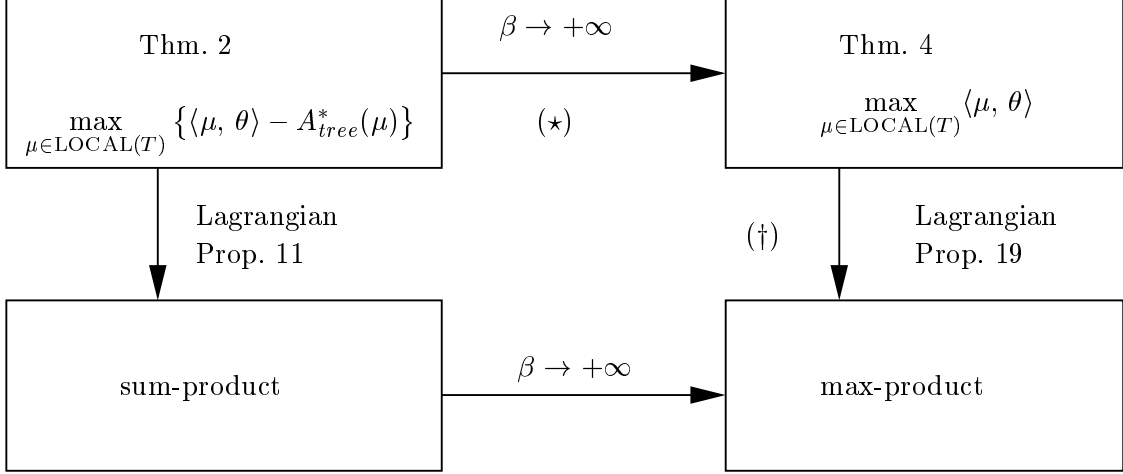


**Figure 27.** Block diagram of the relationships between variational principles and associated message-passing algorithms. In the tree-structured case, all the implications indicated by arrows are valid. For general graphs with cycles, both implications  $(\star)$  and  $(\dagger)$  break down.

Proposition 11 is that the sum-product algorithm on trees is an iterative method for solving a Lagrangian formulation of this problem. These results and their interconnection are shown in the two left-side boxes in the block diagram of Figure 27. Next, as a special case of Theorem 4, the tree-structured linear program (151) can be obtained by taking “zero-temperature limit” of the tree-structured variational principle (49). In particular, this limiting process is described in remark (c) following the proof of Theorem 4. This implication is denoted by  $(\star)$  in Figure 27.

Overall, this intuition suggests that the max-product algorithm on trees should be related to the tree-structured LP (151), which the following result makes precise:

**Proposition 19.** *For each  $x_s \in \mathcal{X}_s$ , let  $\lambda_{st}(x_s)$  be a Lagrange multiplier associated with the constraint  $C_{ts}(x_s) = 0$ , where  $C_{ts}(x_s) := \tau_s(x_s) - \sum_{x_t} \tau_{st}(x_s, x_t)$ . Let  $N$  be the set of  $\tau$  that are non-negative and appropriately normalized:*

$$N := \{\tau \geq 0 \mid \sum_{x_s} \tau_s(x_s) = 1, \sum_{x_s, x_t} \tau_{st}(x_s, x_t) = 1\}. \quad (153)$$

Consider the dual function  $\mathcal{Q}$  defined by the following partial Lagrangian formulation of the tree-structured LP (151):

$$\mathcal{Q}(\lambda) := \max_{\tau \in N} \mathcal{L}(\tau; \lambda), \quad (154a)$$

$$\mathcal{L}(\tau; \lambda) := \langle \theta, \tau \rangle + \sum_{(s,t) \in E(T)} \left[ \sum_{x_s} \lambda_{ts}(x_s) C_{ts}(x_s) + \sum_{x_t} \lambda_{st}(x_t) C_{st}(x_t) \right]. \quad (154b)$$

For any fixed point  $M^*$  of the max-product updates (152), the vector  $\lambda^* := \log M^*$  is an optimal solution of the dual problem  $\min_{\lambda} \mathcal{Q}(\lambda)$ .

*Proof.* We begin by converting to a directed tree by first designating some node  $r \in V$  as the root, and then directing all the edges from parent to child  $t \rightarrow s$ . With regard to this rooted tree, the

objective function  $\langle \theta, \tau \rangle$  has the alternative decomposition:

$$\sum_{x_r} \tau_r(x_r) \theta_r(x_r) + \sum_{t \rightarrow s} \sum_{x_t, x_s} \tau_{st}(x_s, x_t) [\theta_{st}(x_s, x_t) + \theta_s(x_s)].$$

With this form of the cost function, the dual function can be put into the form:

$$\mathcal{Q}(\lambda) := \max_{\tau \in N} \left\{ \sum_{x_r} \tau_r(x_r) \nu_s(x_s) + \sum_{t \rightarrow s} \sum_{x_t, x_s} \tau_{st}(x_s, x_t) [\nu_{st}(x_s, x_t) - \nu_t(x_t)] \right\}, \quad (155)$$

where the quantities  $\nu_s$  and  $\nu_{st}$  are defined in terms of  $\lambda$  and  $\theta$  as:

$$\nu_s(x_t) = \theta_t(x_t) + \sum_{u \in \mathcal{N}(t)} \lambda_{ut}(x_t) \quad (156a)$$

$$\nu_{st}(x_s, x_t) = \theta_{st}(x_s, x_t) + \theta_s(x_s) + \theta_t(x_t) + \sum_{u \in \mathcal{N}(s) \setminus t} \lambda_{us}(x_s) + \sum_{u \in \mathcal{N}(t) \setminus s} \lambda_{ut}(x_t). \quad (156b)$$

Taking the maximum over  $\tau \in N$  in equation (155) yields the explicit form for the dual function  $\mathcal{Q}(\lambda) = \max_{x_r} \nu_r(x_r) + \sum_{t \rightarrow s} \max_{x_s, x_t} [\nu_{st}(x_s, x_t) - \nu_t(x_t)]$ .

Any message  $M$  in the max-product algorithm defines a vector of Lagrange multipliers via  $\lambda = \log M$ . With a bit of algebra, it can be seen that a message vector  $M^*$  is a fixed point of the max-product updates (152) if and only if the associated  $\nu_s^*$  and  $\nu_{st}^*$ , as defined by  $\lambda^* := \log M^*$ , satisfy the *edgewise consistency* condition  $\max_{x_s} \nu_{st}^*(x_s, x_t) = \kappa \nu_t^*(x_t)$ , for some constant  $\kappa > 0$  independent of  $\mathbf{x}$ . We now show that any such  $\lambda^*$  is a dual optimal solution.

Under the edgewise consistency condition on a tree-structured graph, we can always find at least one configuration  $\mathbf{x}^*$  that satisfies

$$x_s^* \in \arg \max_{x_s} \nu_s^*(x_s) \quad \forall s \in V, \quad (x_s^*, x_t^*) \in \arg \max_{x_s, x_t} \nu_{st}^*(x_s, x_t) \quad \forall (s, t) \in E$$

The edgewise consistency condition also guarantees the following equalities:

$$\max_{x_s, x_t} [\nu_{st}^*(x_s, x_t) - \nu_t^*(x_t)] = \max_{x_s, x_t} [\nu_{st}^*(x_s, x_t)] - \max_{x_t} \nu_t^*(x_t) = \nu_{st}^*(x_s^*, x_t^*) - \nu_t^*(x_t^*).$$

Combining these two relations yields the following expression for the dual value at  $\lambda^*$ :

$$\mathcal{Q}(\lambda^*) = \nu_r^*(x_r^*) + \sum_{t \rightarrow s} [\nu_{st}^*(x_s^*, x_t^*) - \nu_t^*(x_t^*)] \stackrel{(a)}{=} \theta_r(x_r^*) + \sum_{t \rightarrow s} [\theta_{st}(x_s^*, x_t^*) + \theta_s(x_s^*)], \quad (157)$$

where equality (a) follows by applying the definition of  $\{\nu_s^*, \nu_{st}^*\}$  from equation (156) and simplifying.

Now consider the primal solution defined by  $\tau_s^*(x_s) := \mathbb{I}_{x_s^*}[x_s]$  and  $\tau_{st}^*(x_s, x_t) = \mathbb{I}_{x_s^*}[x_s] \mathbb{I}_{x_t^*}[x_t]$ , where  $\mathbb{I}_{x_s^*}[x_s]$  is an indicator function for the event  $\{x_s = x_s^*\}$ . It is clear that  $\tau^*$  is primal feasible; moreover, the primal cost is equal to

$$\sum_{x_r} \tau_r^*(x_r) \theta_r(x_r) + \sum_{t \rightarrow s} \sum_{x_t, x_s} \tau_{st}^*(x_s, x_t) [\theta_{st}(x_s, x_t) + \theta_s(x_s)] = \theta_r(x_r^*) + \sum_{t \rightarrow s} [\theta_{st}(x_s^*, x_t^*) + \theta_s(x_s^*)],$$

which is precisely equal to  $\mathcal{Q}(\lambda^*)$ . Therefore, by strong duality for linear programs [9], the pair  $(\tau^*, \lambda^*)$  is primal-dual optimal.  $\square$

**Remark:** A careful examination of the proof of Proposition 19 shows that several steps rely heavily on the fact that the underlying graph is a tree. In fact, the corresponding result for a graph with cycles *fails* to hold, as we will discuss in the following section.

### 10.3 Relaxations of the exact principle

We now consider relaxations of the exact variational principle of Theorem 4. The development of this section is specialized to the multinomial case, for which the set of realizable mean parameters is a marginal polytope  $\text{MARG}(G)$ .

#### 10.3.1 Relaxations from zero-temperature limits

In remark (b) following Theorem 4, we discussed how the support function representation of computing modes arises as a zero-temperature limit of the variational principle from Theorem 2(b). In analogy to this result, we begin by showing how taking the zero-temperature limit of any convex relaxation for inference leads to a corresponding relaxation for MAP estimation.

**Proposition 20.** *Consider a relaxation for computing approximate mean parameters based on the variational problem*

$$B(\theta) := \max_{\tau \in \text{OUT}(G)} \{\langle \theta, \tau \rangle - B^*(\tau)\}, \quad (158)$$

where  $\text{OUT}(G)$  is a compact and convex outer bound on  $\text{MARG}(G)$ , and  $B^*$  is a convex approximation to the dual function  $A^*$ . In the zero-temperature limit, we obtain the following relaxation for approximate mode computation:

$$\max_{\mu \in \text{MARG}(G)} \langle \theta, \mu \rangle = A_\infty(\theta) \leq B_\infty(\theta) := \max_{\tau \in \text{OUT}(G)} \langle \theta, \tau \rangle. \quad (159)$$

*Proof.* In the finite discrete case, we have  $\text{dom } A = \mathbb{R}^d$ ; moreover, by the compactness of  $\text{OUT}(G)$ , we also have  $\text{dom } B = \mathbb{R}^d$ . Consequently, the respective recession functions are defined for all  $\theta \in \mathbb{R}^d$  by the following limits:

$$A_\infty(\theta) := \lim_{\beta \rightarrow +\infty} \frac{A(\beta\theta)}{\beta}, \quad \text{and} \quad B_\infty(\theta) := \lim_{\beta \rightarrow +\infty} \frac{B(\beta\theta)}{\beta}.$$

By Theorem 4, we have  $A_\infty(\theta) = \sup_{\mu \in \text{MARG}(G)} \langle \theta, \mu \rangle$ . Secondly, observe that  $B$ , as defined in equation (158), can be interpreted as the conjugate dual to the extended real-valued function  $B^*$ , where  $B^*(\tau) := +\infty$  for  $\tau \notin \text{OUT}(G)$ . With this definition, the (effective) domain of  $B^*$  is simply the set  $\text{OUT}(G)$ . As a conjugate function,  $B$  is lower semi-continuous; therefore, by Theorem 13.3 of Rockafellar [79], the recession function of  $B$  is given by the support function of  $\text{dom } B^*$ ; in analytical terms, we have  $B_\infty(\theta) = \max_{\tau \in \text{OUT}(G)} \langle \theta, \tau \rangle$ . The bound  $A_\infty(\theta) \leq B_\infty(\theta)$  follows because  $\text{OUT}(G)$  is an outer bound on  $\text{MARG}(G)$  by assumption.  $\square$

**Remark:** Of course, the inequality  $\max_{\mu \in \text{MARG}(G)} \langle \theta, \mu \rangle \leq \max_{\tau \in \text{OUT}(G)} \langle \theta, \tau \rangle$  could be obtained more directly, simply by observing that  $\text{OUT}(G)$  is a convex outer bound on  $\text{MARG}(G)$ . Nonetheless, it is interesting to obtain it as a zero-temperature limit of a corresponding convex relaxation for computing mean parameters. It should also be noted that the proof of Proposition 20 relies on the convexity of  $A^*$ . For instance, it does not apply directly to the Bethe entropy approximation or any of its non-convex extensions.

Proposition 20 gives a straightforward way to transform any convex relaxation for computing approximate mean parameters into a corresponding relaxation for approximate mode computation. We illustrate in the following sections with a number of examples.

### 10.3.2 Linear programming relaxations

We begin by considering linear programming (LP) relaxations of the exact principle, wherein the exact marginal polytope  $\text{MARG}(G)$  is replaced by an outer bound formed entirely of linear constraints. For various classes of problems in combinatorial optimization, such LP relaxations have been studied extensively; see the books [47, 71] for further details.

The case of a pairwise Markov random field suffices to illustrate the basic notion of a generic LP relaxation. It is convenient to use the canonical overcomplete representation based on indicator functions, as defined in equation (38) of Section 4.1.3. The constraint set  $\text{LOCAL}(G)$ , first discussed in Example 8, constitutes an outer bound on  $\text{MARG}(G)$ . Recall from Example 14 that it is a strict outer bound on  $\text{MARG}(G)$ , unless  $G$  is actually tree-structured. The set  $\text{LOCAL}(G)$  specifies the following relaxation of mode computation for a multinomial distribution defined a pairwise Markov random field:

$$\max_{\mathbf{x} \in \mathcal{X}^n} \langle \theta, \phi(\mathbf{x}) \rangle = \max_{\mu \in \text{MARG}(G)} \langle \theta, \mu \rangle \leq \max_{\tau \in \text{LOCAL}(G)} \langle \theta, \mu \rangle. \quad (160)$$

Since the relaxed constraint set  $\text{LOCAL}(G)$  (like  $\text{MARG}(G)$ ) is a polytope, the relaxation on the RHS of equation (160) is a linear program. Consequently, by standard properties of linear programs [9], the relaxed optimum must be attained at a vertex (possibly more than one) of the polytope  $\text{LOCAL}(G)$ .

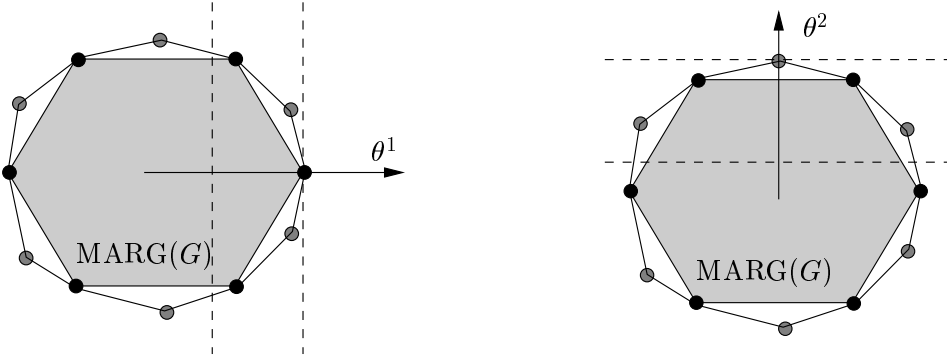


**Figure 28.** The constraint set  $\text{LOCAL}(G)$  is an outer bound on the exact marginal polytope. Its vertex set includes all the vertices of  $\text{MARG}(G)$ , which are in one-to-one correspondence with optimal solutions of the integer program. It also includes additional fractional vertices, which are *not* vertices of  $\text{MARG}(G)$ .

We say that a vertex of  $\text{LOCAL}(G)$  is *integral* if all of its components are zero or one, and *fractional* otherwise. The following result characterizes the vertices of  $\text{LOCAL}(G)$ :

**Proposition 21.** *All vertices of  $\text{MARG}(G)$  are also vertices of the relaxed polytope  $\text{LOCAL}(G)$ . In addition, when  $G$  is not tree-structured, then  $\text{LOCAL}(G)$  includes additional fractional vertices that lie outside of  $\text{MARG}(G)$ .*

*Proof.* In the canonical overcomplete representation of a multinomial ( $\mathcal{X} = \{0, 1, \dots, m - 1\}$ ) on a pairwise MRF, the polytope  $\text{LOCAL}(G)$  lies within  $\mathbb{R}^d$ , where  $d = mn + m^2|E|$ . The set  $\text{LOCAL}(G)$  is defined by the  $d$  inequality constraints  $\mu_\alpha \geq 0$  for all  $\alpha \in \mathcal{I}$ , and the normalization and marginalization equality constraints (see equation (41)). By Proposition 7, every vertex of  $\text{MARG}(G)$  is of the form  $\mu_J$  for some configuration  $J \in \mathcal{X}^n$ . This vector has components  $[\mu_J]_s(x_s) = \mathbb{I}_{j_s}(x_s)$ , and  $[\mu_J]_{st}(x_s, x_t) = \mathbb{I}_{j_s}(x_s)\mathbb{I}_{j_t}(x_t)$ . To show that  $\mu_J$  is also a vertex of  $\text{LOCAL}(G)$ , it

suffices [9] to show that there are  $d$  constraints of  $\text{LOCAL}(G)$  that are active at  $\mu_J$  and linearly independent. For any  $J \in \mathcal{X}^n$ , we have  $\mathbb{I}_k(x_s) = 0$  for all  $k \in \mathcal{X} \setminus \{j_s\}$ , and  $\mathbb{I}_k(x_s)\mathbb{I}_l(x_t) = 0$  for all  $(k, l) \in (\mathcal{X} \setminus \{j_s\}) \times (\mathcal{X} \setminus \{j_t\})$ . All of these active inequality constraints are linearly independent, and there are a total of  $d' = (m-1)n + (m^2 - 1)|E|$ . All of the normalization and marginalization constraints are also satisfied by  $\mu_J$ , but not all of them are linearly independent (when added to the active inequality constraints). However, we can add the normalization constraints for each  $s = 1, \dots, n$  and for each  $(s, t) \in E$ , while still preserving linear independence. Adding these  $n + |E|$  equality constraints to the  $d'$  inequality constraints yields a total of  $d$  linearly independent constraints of  $\text{LOCAL}(G)$  that are satisfied by  $\mu_J$ , so that it is a vertex. Note that each of these vertices has  $0 - 1$  components, and so is integral.

The set  $\text{LOCAL}(G)$  is a polytope, so that it is equal to the convex hull of its vertices [79]. Moreover, it is a strict outer bound on  $\text{MARG}(G)$ , so that it must contain additional vertices that are not members of  $\text{MARG}(G)$ . Any such vertex must be fractional; otherwise, it could be identified with a unique configuration  $J \in \mathcal{X}^n$ , and hence would belong to  $\text{MARG}(G)$  by Proposition 7.  $\square$

The distinction between fractional and integral vertices is crucial, because it determines whether or not the LP relaxation (160) specified by  $\text{LOCAL}(G)$  is tight. In particular, there are only two possible outcomes to solving the relaxation:

- (a) the optimum is attained at a vertex of  $\text{MARG}(G)$ , in which case the upper bound in equation (160) is tight, and a mode can be obtained.
- (b) the optimum is attained only at one or more fractional vertices of  $\text{LOCAL}(G)$ , which lie strictly outside  $\text{MARG}(G)$ . In this case, the upper bound of equation (160) is loose, and the relaxation does not output the optimal configuration.

Figure 28 illustrates both of these possibilities. The vector  $\theta^1$  corresponds to case (a), in which the optimum is attained at a vertex of  $\text{MARG}(G)$ . The vector  $\theta^2$  represents a less fortunate setting, in which the optimum is attained only at a fractional vertex of  $\text{LOCAL}(G)$ . In simple cases, one can explicitly demonstrate a fractional vertex of the polytope  $\text{LOCAL}(G)$ .

**Example 29.** Here we explicitly construct a fractional vertex for a binary problem  $\mathbf{x} \in \{0, 1\}^3$  on the complete graph  $K_3$ . Consider the exponential parameter  $\theta$  shown in matrix form in Figure 29(a).

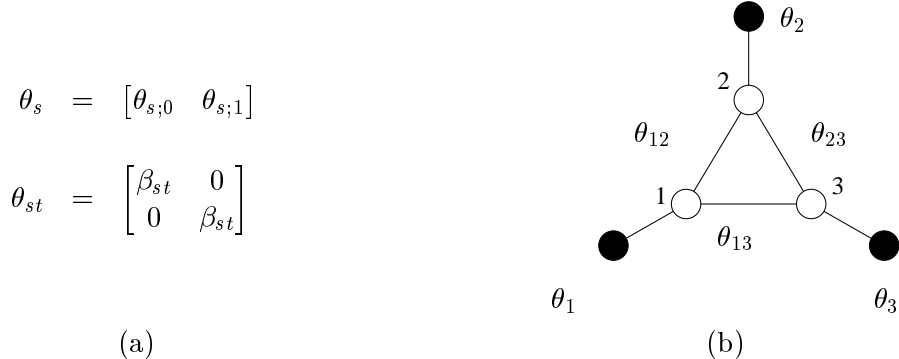


**Figure 29.** The smallest graph  $G = (V, E)$  on which the relaxation (160) can fail to be tight. For  $\beta_{st} \geq 0$  for all  $(s, t) \in E$ , the relaxation is tight for any choice of  $\theta_s, s \in V$ . On the other hand, if  $\beta_{st} < 0$  for all edges  $(s, t)$ , the relaxation will fail for certain choices of  $\theta_s, s \in V$ .

When  $\beta_{st} < 0$ , then configurations with  $x_s \neq x_t$  are favored, so that the interaction is repulsive. In

contrast, when  $\beta_{st} > 0$ , the interaction is attractive, because it favors configurations with  $x_s = x_t$ . When  $\beta_{st} > 0$  for all  $(s, t) \in E$ , it can be shown that the relaxation (160) is tight, regardless of the choice of  $\theta_s, s \in V$ . In contrast, when  $\beta_{st} < 0$  for all edges, then there are choices of  $\theta_s, s \in V$  for which the relaxation breaks down.

The following exponential parameter corresponds to a direction for which the relaxation (160) is *not* tight, and hence exposes a fractional vertex. First choose  $\theta_s^* = [0 \ 0]^T$  for  $s = 1, 2, 3$ , and then set  $\beta_{st} = \beta < 0$  for all edges  $(s, t)$  to define  $\theta_{st}^*$  via the construction in Figure 29(a). Observe that for any configuration  $\mathbf{x} \in \{0, 1\}^3$ , we must have  $x_s \neq x_t$  for at least one edge  $(s, t) \in E$ . Therefore, any  $\mu \in \text{MARG}(G)$  must place non-zero mass on at least one term of  $\theta^*$  involving  $\beta$ , whence  $A_\infty(\theta^*) = \max_{\mu \in \text{MARG}(G)} \langle \theta, \mu \rangle < 0$ . In fact, the optimal value  $A_\infty(\theta^*)$  is exactly equal to  $\beta < 0$ .

On the other, consider the pseudomarginal  $\tau^* \in \text{LOCAL}(G)$  defined as follows:

$$\tau_s^* := [0.5 \ 0.5]^T \quad \text{for } s \in V, \quad \tau_{st}^* := \begin{bmatrix} 0 & 0.5 \\ 0.5 & 0 \end{bmatrix} \quad \text{for } (s, t) \in E.$$

Observe that  $\langle \theta^*, \tau^* \rangle = 0$ . Since  $\theta_\alpha^* \leq 0$  for all elements  $\alpha$ , this value is the optimum of  $\langle \theta^*, \tau \rangle$  over  $\text{LOCAL}(G)$ . Since  $\max_{\mu \in \text{MARG}(G)} \langle \theta^*, \mu \rangle < 0$ , the relaxation (160) is not tight. Finally, to establish that  $\tau^*$  is a vertex of  $\text{LOCAL}(G)$ , we will show that  $\langle \theta^*, \tau \rangle < 0$  for all  $\tau \neq \tau^*$ . If  $\langle \theta^*, \tau \rangle = 0$ , then for all  $(s, t) \in E$  the pairwise pseudomarginals must be of the form

$$\tau_{st} := \begin{bmatrix} 0 & \alpha_{st} \\ 1 - \alpha_{st} & 0 \end{bmatrix}$$

for some  $\alpha_{st} \in [0, 1]$ . Enforcing the marginalization constraints on these pairwise pseudomarginals yields the constraints  $\alpha_{12} = \alpha_{13} = \alpha_{23}$  and  $1 - \alpha_{12} = \alpha_{23}$ , whence  $\alpha_{st} = 0.5$  is the only possibility. Therefore,  $\tau^*$  is a fractional vertex.  $\diamond$

**Remarks:** (a) The tree-based relaxation (160) can be extended to hypertrees of higher width, by using the hypertree-based constraint sets  $\text{LOCAL}_t(G)$  described in Section 7. This extension produces a sequence of progressively tighter LP relaxations. In the binary  $\{0, 1\}$  case, this sequence has been studied by various researchers [14, 85], although without the connections to the underlying graphical structure.

(b) Feldman et al. [38, 37] have applied the tree-based relaxation (160) to the task of decoding turbo and low-density parity check (LDPC) codes. This LP-based decoding method performs better than max-product (min-sum) decoding, and comparably to sum-product decoding. In this case, fractional vertices have a very specific interpretation as *pseudocodewords* of the underlying code.

(c) In analogy to Proposition 11, one might postulate that Proposition 19 could be extended to graphs with cycles—specifically, that the max-product algorithm solves the dual of the tree-based relaxation (160). This conjecture is false, since it is possible to construct problems (on graphs with cycles) for which the max-product algorithm will output a non-optimal configuration. (Any LP relaxation will either output a configuration with a guarantee of correctness, or a fractional vertex.) However, the tree-reweighted analog of the max-product algorithm, analogous to the tree-reweighted sum-product algorithm of Section 8.3, can be shown to find dual-optimal solutions of the tree-based relaxation (160) under certain conditions; see Wainwright et al. [94] for further details.

### 10.3.3 Semidefinite relaxations for mode computation

It is also possible to develop relaxations for computing modes based on semidefinite outer approximations to  $\text{MARG}(G)$ , as described in Section 9. The resulting optimization problem is a *semidefinite program* [91], since it entails optimizing a linear function subject to linear matrix inequalities. Such semidefinite relaxations are widely-used in combinatorial optimization [e.g., 47, 46, 63], as well as for programs involving semialgebraic constraints more generally [e.g., 59, 58, 74].

For the sake of brevity, we limit ourselves to describing a well-known semidefinite programming relaxation that applies to the Ising model, as described in Example 3. In particular, the problem of computing the mode of a model in Ising form is equivalent to solving the following binary integer program:

$$\max_{\mathbf{x} \in \{-1,1\}^n} \left\{ \sum_{s \in V} \theta_s x_s + \sum_{(s,t)} \theta_{st} x_s x_t \right\}. \quad (161)$$

Without loss of generality, we assume that the problem is formulated on the complete graph  $K_n$ , since a problem defined on an arbitrary graph can be put in this form by setting  $\theta_{st} = 0$  for all  $(s,t) \notin E$ . By applying Theorem 4, we conclude that the the binary quadratic program (161) is equivalent to a linear program over the marginal polytope  $\text{MARG}(K_n)$ . Since the marginal polytope is difficult to characterize, it is natural to replace it with the first-order semidefinite outer bound  $\text{SDEF}_1$ , as defined in equation (122). Doing so leads to the following semidefinite relaxation of the integer program:

$$\max_{\mu \in \text{MARG}(K_n)} \langle \theta, \mu \rangle \leq \max_{\mu \in \text{SDEF}_1} \langle \theta, \mu \rangle, \quad (162)$$

where the RHS corresponds to a semidefinite program (SDP). Recall from our discussion of the exact computation of Gaussian modes in Section 10.2.1 the  $n \times n$  matrices of exponential parameters  $U(\theta)$  and mean parameters  $W(\mu)$ . It is instructive to re-write the semidefinite program (SDP) in terms of these quantities as follows:

$$\max_{\mu \in \text{SDEF}_1} \langle \theta, \mu \rangle = \frac{1}{2} \max_{W(\mu) \succeq 0, \mu_{ss}=1} \langle\langle U(\theta), W(\mu) \rangle\rangle. \quad (163)$$

This formulation demonstrates that the relaxation is essentially Gaussian-based. Moreover, any optimal solution  $\mu^*$  can be associated with the moment matrix  $W(\mu^*)$  of a Gaussian (subject to the unit variance  $\mu_{ss} = 1$  constraint).

When the SDP relaxation (162) is applied to the MAX-CUT problem,<sup>11</sup> Goemans and Williamson [46] provided a random sampling scheme for generating solutions, and proved a remarkable guarantee on its expected performance. Although not originally described in these terms, their method can be understood as solving the SDP relaxation, thereby obtaining the moment matrix  $W(\mu^*)$  of the optimal Gaussian. The sampling scheme itself entails drawing random samples from the zero-mean Gaussian with covariance matrix specified by  $W(\mu^*)$ , and then taking their sign to generate an integral vector in  $\{-1, +1\}^n$ . Goemans and Williamsom showed that the expected value of a randomized solution generated in this way is *at worst* a factor  $\alpha \approx 0.878$  less than the optimal value. Subsequent work [e.g., 55] established that this approximation ratio is, in fact, sharp. Other researchers have developed similar approximation algorithms based on semidefinite constraints for a variety of other combinatorial optimization problems, including satisfiability problems and vertex coloring.

---

<sup>11</sup>The MAX-CUT problem is a particular case of the general binary quadratic program (161), in which  $\theta_s = 0$  for all  $s \in V$  and  $\theta_{st} \leq 0$  for all  $(s,t) \in E$ .

## 11 Discussion

[[not yet written]].

## A Proofs

**Proposition 22.** *The log partition function is lower semi-continuous on  $\mathbb{R}^d$ , and  $C^\infty$  on  $\Theta$ . Its derivatives are the cumulants of the random vector  $\phi(\mathbf{x})$ —in particular:*

$$\frac{\partial A}{\partial \theta_\alpha}(\theta) = \mathbb{E}_\theta[\phi_\alpha(\mathbf{x})] := \int \phi_\alpha(\mathbf{x}) p(\mathbf{x}; \theta) \nu(d\mathbf{x}). \quad (164a)$$

$$\frac{\partial^2 A}{\partial \theta_\alpha \partial \theta_\beta}(\theta) = \mathbb{E}_\theta[\phi_\alpha(\mathbf{x})\phi_\beta(\mathbf{x})] - \mathbb{E}_\theta[\phi_\alpha(\mathbf{x})]\mathbb{E}_\theta[\phi_\beta(\mathbf{x})]. \quad (164b)$$

Moreover,  $\|\nabla A(\theta^t)\| \rightarrow +\infty$  for any sequence  $\{\theta^t\} \subset \Theta$  approaching the boundary.

*Proof.* The proof of these results are straightforward; see, for example, Brown [18] for more details. Lower semi-continuity follows from Fatou’s lemma [80]. Interchanging the order of differentiation and integration can be justified via a standard argument using the dominated convergence theorem [80], from which derivatives can be calculated by chain rule. To establish the last claim, let  $\theta^b$  be a boundary point, and let  $\theta^0 \in \Theta$  be arbitrary. By the convexity and openness of  $\Theta$ , the line  $\theta^t := t\theta^b + (1-t)\theta^0$  is contained in  $\Theta$  for all  $t \in [0, 1)$  (see Thm. 6.1, [79]). Using the differentiability of  $A$  on  $\Theta$  and its convexity (Corollary 1), for any  $t < 1$ , we can write  $A(\theta^0) \geq A(\theta^t) + \langle \nabla A(\theta^t), \theta^0 - \theta^t \rangle$ . Re-arranging and applying the Cauchy-Schwartz inequality yields that  $A(\theta^t) - A(\theta^0) \leq \|\theta^t - \theta^0\| \|\nabla A(\theta^t)\|$ . Now as  $t \rightarrow 1^-$ , the LHS tends to infinity by the lower semi-continuity of  $A$ . Consequently, the RHS must also tend to infinity; since  $\|\theta^t - \theta^0\|$  is bounded, we conclude that  $\|\nabla A(\theta^t)\| \rightarrow +\infty$ , as claimed.  $\square$

**Corollary 3.** *The log partition function  $A$  is a convex function of  $\theta$ , and strictly so if the representation is minimal.*

*Proof.* From equation (20b), the Hessian  $\nabla^2 A(\theta)$  is a Gram matrix and hence must be positive semidefinite on the open set  $\Theta$ , which ensures convexity (Thm. 4.3.1, [49]). If the representation is minimal, there is no vector  $a \in \mathbb{R}^d$  and constant  $b \in \mathbb{R}$  such that  $\langle a, \phi(\mathbf{x}) \rangle = b$  holds  $\nu$ -almost-everywhere. This condition implies  $\text{var}_\theta[\langle a, \phi(\mathbf{x}) \rangle] = a^T \nabla^2 A(\theta) a > 0$  for all  $a \in \mathbb{R}^d$  and  $\theta \in \Theta$ ; this strict positive definiteness of the Hessian on the open set  $\Theta$  implies strict convexity [49].  $\square$

**Proposition 23.** *The mapping  $\Lambda$  is one-to-one if and only if the exponential representation is minimal.*

*Proof.* If the representation is not minimal, then there exists a distinct pair  $\theta^1 \neq \theta^2$  for which  $p(\mathbf{x}; \theta^1) = p(\mathbf{x}; \theta^2)$ . For this pair, we have  $\Lambda(\theta^1) = \Lambda(\theta^2)$ , so that  $\Lambda$  is not one-to-one. Conversely, if the representation is minimal, then  $A$  must be strictly convex by Corollary 1. For any strictly convex function, the inequality  $\langle \nabla A(\theta^1) - \nabla A(\theta^2), \theta^1 - \theta^2 \rangle > 0$  holds for all  $\theta^1 \neq \theta^2$ , which is equivalent to  $\Lambda$  being one-to-one.  $\square$

**Theorem 5.** *The mean parameter mapping  $\Lambda$  is onto the (relative) interior of  $\mathcal{M}$  (i.e.,  $\Lambda(\Theta) = \text{ri } \mathcal{M}$ ).*

**Remark:** The relative interior of a convex set is the interior taken with respect to its affine hull. A key fact is that any non-empty convex set is guaranteed to have a non-empty relative interior. See Appendix B for more details.

*Proof of Theorem 5:* We prove the result first for a minimal representation, and then discuss its extension to the overcomplete case. By definition, a convex subset of  $\mathbb{R}^d$  is *full-dimensional* if its affine hull is equal to  $\mathbb{R}^d$ . As shown in Proposition 5,  $\mathcal{M}$  is a full-dimensional convex set whenever

the representation is minimal. Consequently, we can deal with the interior (as opposed to relative interior). Our proof makes use of the following properties of a full-dimensional convex set [see 49, 79]: (a)  $\text{int } \mathcal{M}$  is non-empty, and  $\text{int}[\text{cl}(\mathcal{M})] = \text{int}(\mathcal{M})$ ; and (b) the vector  $0 \in \text{int}(\mathcal{M}) \iff$  for all non-zero  $\gamma \in \mathbb{R}^d$ , there exists some  $\mu \in \mathcal{M}$  with  $\langle \gamma, \mu \rangle > 0$ .

$\Lambda(\Theta) \subseteq \text{int } \mathcal{M}$ : By shifting the potential  $\phi$  by a constant vector if necessary, it suffices to consider the case  $0 \in \Lambda(\Theta)$ . Let  $\theta^0 \in \Theta$  be the associated exponential parameter satisfying  $\Lambda(\theta^0) = 0$ . We prove that for all non-zero directions  $\gamma \in \mathbb{R}^d$ , there is some  $\mu \in \mathcal{M}$  such that  $\langle \gamma, \mu \rangle > 0$ , which implies  $0 \in \text{int}(\mathcal{M})$  by property (b).

For any  $\gamma \in \mathbb{R}^d$ , the openness of  $\Theta$  ensures the existence of some  $\delta > 0$  such that  $(\theta^0 + \delta\gamma) \in \Theta$ . Using the strict convexity and differentiability of  $A$  on  $\Theta$  and the fact that  $\Lambda(\theta^0) = 0$  by assumption, there holds  $A(\theta^0 + \delta\gamma) > A(\theta^0) + \langle \Lambda(\theta^0), \delta\gamma \rangle = A(\theta^0)$ . Similarly, defining  $\mu^\delta := \Lambda(\theta^0 + \delta\gamma)$ , we can write  $A(\theta^0) > A(\theta^0 + \delta\gamma) + \langle \mu^\delta, -\delta\gamma \rangle$ . These two inequalities in conjunction imply that

$$\delta \langle \mu^\delta, \gamma \rangle > A(\theta^0 + \delta\gamma) - A(\theta^0) > 0.$$

Since  $\mu^\delta \in \Lambda(\Theta) \subseteq \mathcal{M}$  and  $\gamma \in \mathbb{R}^d$  was arbitrary, this establishes that  $0 \in \text{int}(\mathcal{M})$ .

$\text{int } \mathcal{M} \subseteq \Lambda(\Theta)$ : As in the preceding argument, we may take  $0 \in \text{int } \mathcal{M}$  without loss of generality. Then, we must establish the existence of  $\theta \in \Theta$  such that  $\Lambda(\theta) = \nabla A(\theta) = 0$ . By convexity, it is equivalent to show that  $\inf_{\theta \in \Theta} A(\theta)$  is attained. To establish the attainment of this infimum, we prove that  $A$  has no directions of recession, meaning that  $\lim_{n \rightarrow +\infty} A(\theta^n) = +\infty$  for all sequences  $\{\theta^n\}$  such that  $\|\theta^n\| \rightarrow +\infty$ .

For an arbitrary non-zero direction  $\gamma \in \mathbb{R}^d$  and  $\epsilon > 0$ , consider the half space  $H_{\gamma, \epsilon} := \{\mathbf{x} \in \mathcal{X}^n \mid \langle \gamma, \phi(\mathbf{x}) \rangle \geq \epsilon\}$ . Since  $0 \in \text{int } \mathcal{M}$ , this half-space must have positive measure under  $\nu$  for all sufficiently small  $\epsilon > 0$ . Otherwise, the inequality  $\langle \gamma, \phi(\mathbf{x}) \rangle \leq 0$  would hold  $\nu$ -a.e., which implies that  $\langle \gamma, \mu \rangle \leq 0$  for all  $\mu \in \text{cl}(\mathcal{M})$ . By the convexity of  $\mathcal{M}$ , this inequality would imply that  $0 \notin \text{int cl}(\mathcal{M}) = \text{int}(\mathcal{M})$ , which contradicts our starting assumption.

For an arbitrary  $\theta^0 \in \Theta$ , we now write

$$A(\theta^0 + t\gamma) \geq \log \int_{H_{\gamma, \epsilon}} \exp \{ \langle \theta^0 + t\gamma, \phi(\mathbf{x}) \rangle \} \nu(d\mathbf{x}) \geq t\epsilon + \underbrace{\log \int_{H_{\gamma, \epsilon}} \exp \{ \langle \theta^0, \phi(\mathbf{x}) \rangle \} \nu(d\mathbf{x})}_{C(\theta^0)}.$$

Note that we must have  $C(\theta^0) > -\infty$ , because  $\exp \{ \langle \theta^0, \phi(\mathbf{x}) \rangle \} > 0$  for all  $\mathbf{x} \in \mathcal{X}^n$ , and  $\nu(H_{\gamma, \epsilon}) > 0$ . Hence, we conclude that  $\lim_{t \rightarrow +\infty} A(\theta^0 + t\gamma) = +\infty$  for all directions  $\gamma \in \mathbb{R}^d$ , showing that  $A$  has no directions of recession.

Extension to overcomplete case: For any overcomplete representation  $\phi$ , let  $\varphi$  be a set of potential functions in an equivalent minimal representation. In particular, a collection  $\varphi$  can be specified by eliminating elements of  $\phi$  until no affine dependencies remain. Let  $\Lambda_\varphi$  and  $\Lambda_\phi$  be the respective mean parameter mappings associated with  $\varphi$  and  $\phi$ , with the sets  $\mathcal{M}_\varphi$  and  $\mathcal{M}_\phi$  similarly defined. By the result just established,  $\Lambda_\varphi$  is onto the interior of  $\mathcal{M}_\varphi$ . By construction of  $\varphi$ , each member in the relative interior of  $\mathcal{M}_\phi$  is associated with a unique element in the interior of  $\mathcal{M}_\varphi$ . We conclude that the mean parameter mapping  $\Lambda_\phi$  is onto the relative interior of  $\mathcal{M}_\phi$ .  $\square$

### Theorem 6.

(a) For any  $\mu \in \text{ri } \mathcal{M}$ , let  $\theta(\mu)$  denote a member of  $\Lambda^{-1}(\mu)$ . The Fenchel-Legendre dual of  $A$  has the following form:

$$A^*(\mu) = \begin{cases} -H(p(\mathbf{x}; \theta(\mu))) & \text{if } \mu \in \text{ri } \mathcal{M} \\ +\infty & \text{if } \mu \notin \text{cl } \mathcal{M}. \end{cases} \quad (165)$$

For any boundary point  $\mu \in \text{bd } \mathcal{M} := \text{cl } \mathcal{M} \setminus \text{ri } \mathcal{M}$ , we have  $A^*(\mu) = \lim_{n \rightarrow +\infty} [-H(p(\mathbf{x}; \theta(\mu^n)))]$ , taken over a sequence  $\{\mu^n\} \subset \text{ri } \mathcal{M}$  converging to  $\mu$ .

(b) In terms of this dual, the log partition function has the following variational representation:

$$A(\theta) = \sup_{\mu \in \mathcal{M}} \{\langle \theta, \mu \rangle - A^*(\mu)\}. \quad (166)$$

*Proof.* (a) Case (i)  $\mu \in \text{ri } \mathcal{M}$ : In this case, Theorem 5 guarantees that the inverse image  $\Lambda^{-1}(\mu)$  is non-empty. Any point in this inverse image attains the supremum in equation (23). In a minimal representation, there is only one optimizing point, whereas there is an affine subset for an overcomplete representation. Nonetheless, for any  $\theta(\mu) \in \Lambda^{-1}(\mu)$ , the value of the optimum is:  $A^*(\mu) = \langle \theta(\mu), \mu \rangle - A(\theta(\mu))$ . We conclude by observing that

$$-H(p(\mathbf{x}; \theta(\mu))) = \mathbb{E}_\theta [\langle \theta(\mu), \phi(\mathbf{x}) \rangle - A(\theta(\mu))] = \langle \theta(\mu), \mu \rangle - A(\theta(\mu)).$$

Case (ii)  $\mu \notin \text{cl } \mathcal{M}$ : Let  $\text{dom } A^* = \{\mu \in \mathbb{R}^d \mid A^*(\mu) < +\infty\}$  denote the effective domain of  $A^*$ . With this notation, we must prove that  $\text{cl } \mathcal{M} \supseteq \text{dom } A^*$ . From Proposition 2, the function  $A$  is essentially smooth and lower semi-continuous. From Theorem 5, we have  $\nabla A(\Theta) = \text{ri } \mathcal{M}$ . By Corollary 26.4.1 of Rockafellar [79], these conditions guarantee that  $\text{ri dom } A^* \subseteq \text{ri } \mathcal{M} \subseteq \text{dom } A^*$ . Since both  $\mathcal{M}$  and  $\text{dom } A^*$  are convex sets, taking closures in these inclusions yields that  $\text{cl dom } A^* = \text{cl ri } \mathcal{M} = \text{cl } \mathcal{M}$ , where the second equality follows by the convexity of  $\mathcal{M}$ . Therefore, by definition of the effective domain,  $A^*(\mu) = +\infty$  for any  $\mu \notin \text{cl } \mathcal{M}$ .

Case (iii)  $\mu \in \text{cl } \mathcal{M} \setminus \text{ri } \mathcal{M}$ : Since  $A^*$  is defined as a conjugate function, it is lower semi-continuous. Therefore, the value of  $A^*(\mu)$  for any boundary point  $\mu \in \text{cl } \mathcal{M} \setminus \text{ri } \mathcal{M}$  is determined by the limit over a sequence approaching  $\mu$  from inside  $\text{ri } \mathcal{M}$ , as claimed.

(b) From Proposition 2,  $A$  is lower semi-continuous, which ensures that  $(A^*)^* = A$  so that we can write  $A(\theta) = \sup_{\mu \in \text{cl dom } A^*} \{\langle \theta, \mu \rangle - A^*(\mu)\}$ . Part (a) shows that  $\text{cl dom } A^* = \text{cl } \mathcal{M}$ , so that equation (26) follows. Whether the supremum is taken over  $\mathcal{M}$  or over  $\text{cl } \mathcal{M}$  is inconsequential.  $\square$

**Proposition 24.** *For all  $\theta \in \Theta$ , the supremum in equation (32) is attained uniquely at the vector  $\mu \in \text{ri } \mathcal{M}$  specified by:*

$$\mu = \mathbb{E}_\theta [\phi(\mathbf{x})] = \int_{\mathcal{X}^n} \phi(\mathbf{x}) p(\mathbf{x}; \theta) \nu(d\mathbf{x}).$$

*Proof.* For a minimal representation, Proposition 3 and Theorem 5 guarantee that the gradient mapping  $\nabla A$  is a bijection between  $\Theta$  and  $\text{ri } \mathcal{M}$ . On this basis, it follows that the gradient mapping  $\nabla A^*$  also exists and is bijective [79], whence the supremum (32) is attained at a unique point whenever  $\theta \in \Theta$ . The analogous statement for an overcomplete representation can be proved via reduction to a minimal representation.  $\square$

**Proposition 25.** *The set  $\mathcal{M}$  has the following properties:*

- (a)  $\mathcal{M}$  is full-dimensional if and only if the exponential family is minimal.
- (b)  $\mathcal{M}$  is bounded if and only if  $\Theta = \mathbb{R}^d$  and  $A$  is globally Lipschitz on  $\mathbb{R}^d$ .

*Proof.* (a) The representation is *not* minimal if and only if there exists some vector  $a \in \mathbb{R}^d$  and constant  $b \in \mathbb{R}$  such that  $\langle a, \phi(\mathbf{x}) \rangle = b$  holds  $\nu$ -a.e. By definition of  $\mathcal{M}$ , this equality holds if and only if  $\langle a, \mu \rangle = b$  for all  $\mu \in \mathcal{M}$ , which is equivalent to  $\mathcal{M}$  not being full-dimensional.

(b) By Theorem 4 of Section 10, the recession function  $A_\infty$  is the support function  $\sup_{\mu \in \mathcal{M}} \langle \mu, \theta \rangle$ . Therefore, the set  $\mathcal{M}$  is bounded if and only if  $A_\infty(\theta)$  is finite for all  $\theta \in \mathbb{R}^d$ . The recession function  $A_\infty$  is finite-valued if and only if  $A$  is Lipschitz (hence finite) on all of  $\mathbb{R}^d$  (Prop. 3.2.7; [49]).  $\square$

**Proposition 26.** *In the Gaussian case, the set  $\mathcal{M}$  has the form*

$$\mathcal{M}_{Gauss} = \{\mu \in \mathbb{R}^d \mid W(\mu) \succ 0\}. \quad (167)$$

*Proof.* By the Schur complement formula [50], the  $(n+1) \times (n+1)$  matrix  $W(\mu)$  is positive definite if and only if the  $n \times n$  matrix  $Z(\mu) - z(\mu)z^T(\mu)$  is positive definite. But this latter matrix can be interpreted as the covariance of  $\mathbf{x}$ . Any Gaussian random vector gives rise to a positive definite covariance. Conversely, given a matrix  $W(\mu)$  that is positive definite, we can construct a Gaussian with mean  $z(\mu)$  and covariance  $Z(\mu) - z(\mu)z^T(\mu)$ .  $\square$

**Proposition 27.** *In the multinomial case, the set  $\mathcal{M}$  is a polytope, meaning that it has a representation of the form*

$$\mathcal{M} = \{\mu \in \mathbb{R}^d \mid \langle a_j, \mu \rangle \leq b_j \quad \forall j \in \mathcal{J}\}, \quad (168)$$

where the index set  $\mathcal{J}$  is finite. Moreover, any extreme point is of the form  $\mu_e := \phi(e)$ .

*Proof.* The definition (33) shows that  $\mathcal{M}$  is given by the convex hull of the vectors  $\{\phi(\mathbf{x}) \mid \mathbf{x} \in \mathcal{X}^n\}$ . Regardless of the specific choice of  $\phi$ , there are only a finite number of vectors  $\phi(\mathbf{x})$  in this convex hull. Therefore, the Minkowski-Weyl theorem [79, 49] guarantees that  $\mathcal{M}$  has a representation as in equation (36). By definition, any  $\mu \in \mathcal{M}$  has a representation of the form  $\mu = \sum_{\mathbf{x}} p(\mathbf{x})\phi(\mathbf{x})$ . If  $\mu$  is not of the form  $\mu_e = \phi(e)$ , then  $p(\mathbf{x}^i) > 0$  for at least two distinct  $\mathbf{x}^1, \mathbf{x}^2$ . Hence, it is not an extreme point.  $\square$

**Proposition 28.** *The dual function  $A^*$  is always convex and lower semi-continuous. Moreover, in a minimal representation:*

- (a)  $A^*$  is differentiable on  $\text{int } \mathcal{M}$ , and  $\nabla A^*(\mu) = \Lambda^{-1}(\mu)$ .
- (b)  $A^*$  is strictly convex.
- (c) For any sequence  $\{\mu^n\}$  contained in  $\text{int } \mathcal{M}$  and approaching the boundary  $\text{bd } \mathcal{M}$ , we have  $\lim_{n \rightarrow +\infty} \|\nabla A^*(\mu^n)\| = +\infty$ .

*Proof.* The convexity and lower semi-continuity (l.s.c.) follow because  $A^*$  is the supremum of collection of functions linear in  $\mu$ . Statements (a)–(c) are equivalent to the assertion that  $A^*$  is strictly convex and essentially smooth. Since both  $A$  and  $A^*$  are l.s.c.,  $A^*$  has these properties if and only if  $A$  is strictly convex and essentially smooth (Thm. 26.3; [79]). For a minimal representation,  $A$  is strictly convex by Corollary 1, and it is essentially smooth by Proposition 2, so that the result follows.  $\square$

## B Affine hulls and relative interior

The interior of a convex set  $C \subseteq \mathbb{R}^d$  consists of all vectors  $\mathbf{z} \in C$  for which there exists some  $\epsilon > 0$  such that the  $\epsilon$ -ball  $B_\epsilon(\mathbf{z}) := \{\mathbf{y} \in \mathbb{R}^d \mid \|\mathbf{y} - \mathbf{z}\| < \epsilon\}$  is contained within  $C$ . The relative interior is defined similarly, except that the interior is taken with respect to the affine hull of  $C$ , denoted  $\text{aff } C$ . More formally, the *relative interior* of  $C$ , denoted  $\text{ri } C$ , is the set of all points  $\mathbf{z}$  such that for some  $\epsilon > 0$ , the set  $B_\epsilon(\mathbf{z}) \cap \text{aff}(C)$  is contained within  $C$ . To illustrate the distinction, note that the interior of the convex set  $[0, 1]$ , when viewed as a subset of  $\mathbb{R}^2$ , is empty; the affine hull of  $[0, 1]$  is the real line, so that the relative interior is the open interval  $(0, 1)$ .

A key property of any convex set  $C$  is that its relative interior is always non-empty [79]. A convex set  $C \subseteq \mathbb{R}^d$  is *full-dimensional* if its affine hull  $\text{aff } C$  is equal to  $\mathbb{R}^d$ . In this case, the notion of interior and relative interior coincide.

## C Möbius inversion

This appendix provides a brief overview of the Möbius function associated with a partially-ordered set (poset); see Stanley [88] for a thorough treatment. The *zeta function*  $\zeta(g, h)$  of a poset is defined as:

$$\zeta(g, h) = \begin{cases} 1 & \text{if } g \leq h \\ 0 & \text{otherwise} \end{cases} \quad (169)$$

The Möbius function  $\omega$  arises as the multiplicative inverse of this zeta function. It is defined in a recursive fashion, by first specifying  $\omega(g, g) = 1$  for all  $g$ . Once  $\omega(g, f)$  has been defined for all  $f$  such that  $g \leq f < h$ , we then define:

$$\omega(g, h) = - \sum_{\{f \mid g \leq f < h\}} \omega(g, f) \quad (170)$$

With this definition, it can be seen that  $\omega$  and  $\zeta$  are multiplicative inverses, in the sense that

$$\sum_{\{f \mid g \leq f \leq h\}} \omega(g, f) \zeta(f, h) = \delta(g, h)$$

where  $\delta(g, h)$  is the Kronecker delta.

**Lemma 8 (Möbius inversion formula).** *Let  $\Upsilon(h)$  be a real-valued function defined for  $h$  in a poset. Define a new real-valued function  $\Omega$  via:*

$$\Omega(h) = \sum_{g \in \mathcal{D}^+(h)} \Upsilon(g) \quad (171)$$

where  $\mathcal{D}^+(h) := \{g \mid g \leq h\}$  is the set of descendants of  $h$ . Then we have the relation

$$\Upsilon(h) = \sum_{g \in \mathcal{D}^+(h)} \omega(g, h) \Omega(g) \quad (172)$$

where  $\omega$  is the associated Möbius function.

## References

- [1] S. Aji and R. McEliece. The generalized distributive law. *IEEE Trans. Info. Theory*, 46:325–343, March 2000.
- [2] N. I. Akhiezer. *The classical moment problem and some related questions in analysis*. Hafner Publishing Co., New York, NY, 1966.
- [3] S. Amari. Differential geometry of curved exponential families — curvatures and information loss. *Annals of Statistics*, 10(2):357–385, 1982.
- [4] S. Amari and H. Nagaoka. *Methods of information geometry*. American Mathematical Society, Providence, RI, 2000.
- [5] O. E. Barndorff-Nielson. *Information and exponential families*. Wiley, Chichester, 1978.
- [6] R. J. Baxter. *Exactly solved models in statistical mechanics*. Academic Press, New York, 1982.
- [7] D. Bertsekas. *Dynamic programming and stochastic control*, volume 1. Athena Scientific, Belmont, MA, 1995.
- [8] D. Bertsekas. *Nonlinear programming*. Athena Scientific, Belmont, MA, 1995.
- [9] D. Bertsimas and J. Tsitsiklis. *Introduction to linear optimization*. Athena Scientific, Belmont, MA, 1997.
- [10] J. Besag. On the statistical analysis of dirty pictures. *Journal of the Royal Statistical Society, Series B*, 48(3):259–279, 1986.
- [11] J. Besag and P. J. Green. Spatial statistics and Bayesian computation. *J. R. Stat. Soc. B*, 55(1):25–37, 1993.
- [12] D. M. Blei, A. Y. Ng, and M. I. Jordan. Latent Dirichlet Allocation. *Journal of Machine Learning Research*, 3:993–1022, 2003.
- [13] H. Bodlaender. A tourist guide through treewidth. *Acta Cybernetica*, 11:1–21, 1993.
- [14] E. Boros and P. L. Hammer. Pseudo-boolean optimization. Technical report, Rutgers Univ., 2001.
- [15] J. Borwein and A. Lewis. *Convex Analysis*. Springer-Verlag, New York, NY, 1999.
- [16] S. Boyd and L. Vandenberghe. *Convex optimization*. Courses notes; to be published. Stanford University, Palo Alto, CA, 2002.
- [17] L. M. Bregman. The relaxation method for finding the common point of convex sets and its application to the solution of problems in convex programming. *USSR Computational Mathematics and Mathematical Physics*, 7:191–204, 1967.
- [18] L. Brown. *Fundamentals of statistical exponential families*. Institute of Mathematical Statistics, Hayward, CA, 1986.
- [19] C. B. Burge and S. Karlin. Finding the genes in genomic dna. *Current Opinion in Structural Biology*, 8:346–354, 1998.
- [20] Y. Censor and S. A. Zenios. *Parallel Optimization: Theory, Algorithms, and Applications*. Numerical Mathematics and Scientific Computation. Oxford University Press, 1988.
- [21] D. Chandler. *Introduction to modern statistical mechanics*. Oxford University Press, Oxford, 1987.
- [22] S. Chopra. On the spanning tree polyhedron. *Operations Research Letters*, 8:25–29, 1989.
- [23] T. H. Cormen, C. E. Leiserson, and R. L. Rivest. *Introduction to Algorithms*. MIT Press, Cambridge, MA, 1990.
- [24] T. Cover and J. Thomas. *Elements of Information Theory*. John Wiley and Sons, New York, 1991.
- [25] G. Cross and A. Jain. Markov random field texture models. *IEEE Trans PAMI*, 5:25–39, 1983.
- [26] I. Csiszár and G. Tusnády. Information geometry and alternating minimization procedures. In E. J. D. et al., editor, *Recent results in estimation theory and related topics*. 1984.
- [27] I. Csiszár. I-divergence geometry of probability distributions and minimization problems. *Annals of Probability*, 3(1):146–158, Feb. 1975.
- [28] I. Csiszár. A geometric interpretation of Darroch and Ratcliff's generalized iterative scaling. *Annals of Statistics*, 17(3):1409–1413, Sep. 1989.
- [29] J. N. Darroch and D. Ratcliff. Generalized iterative scaling for log-linear models. *Annals of Mathematical Statistics*, 43:1470–1480, 1972.
- [30] A. P. Dawid. Applications of a general propagation algorithm for probabilistic expert systems. *Statistics and Computing*, 2:25–36, 1992.
- [31] J. Demmel. *Applied numerical linear algebra*. SIAM, Philadelphia, 1997.

- [32] A. P. Dempster, N. M. Laird, and D. B. Rubin. Maximum likelihood from incomplete data via the EM algorithm (with discussion). *J. Royal Stat. Soc. B*, 39:1–38, 1977.
- [33] M. Deza and M. Laurent. *Geometry of cuts and metric embeddings*. Springer-Verlag, New York, 1997.
- [34] R. Durbin, S. Eddy, A. Krogh, and G. Mitchison, editors. *Biological Sequence Analysis*. Cambridge University Press, Cambridge, 1998.
- [35] J. Edmonds. Matroids and the greedy algorithm. *Mathematical Programming*, 1:127–136, 1971.
- [36] B. Efron. The geometry of exponential families. *Annals of Statistics*, 6:362–376, 1978.
- [37] J. Feldman, D. R. Karger, and M. J. Wainwright. Linear programming-based decoding of turbo codes and its relation to iterative approaches. In *Proc. Allerton Conf. Communication, Control and Computing*, October 2002.
- [38] J. Feldman, D. R. Karger, and M. J. Wainwright. Using linear programming to decode ldpc codes. In *Conference on Information Science and Systems*, March 2003.
- [39] J. Felsenstein. Evolutionary trees from DNA sequences: a maximum likelihood approach. *Journal of Molecular Evolution*, 17:368–376, 1981.
- [40] W. T. Freeman, E. C. Pasztor, and O. T. Carmichael. Learning low-level vision. *Intl. J. Computer Vision*, 40(1):25–47, 2000.
- [41] W. T. Freeman and Y. Weiss. On the optimality of solutions of the max-product belief propagation algorithm in arbitrary graphs. *IEEE Trans. Info. Theory*, 47:736–744, 2001.
- [42] R. G. Gallager. *Low-density parity check codes*. MIT Press, Cambridge, MA, 1963.
- [43] A. E. Gelfand and A. F. M. Smith. Sampling-based approaches to calculating marginal densities. *Journal of the American Statistical Association*, 85:398–409, 1990.
- [44] S. Geman and D. Geman. Stochastic relaxation, Gibbs distributions, and the Bayesian restoration of images. *IEEE Pat. Anal. Mach. Intell.*, 6:721–741, 1984.
- [45] Z. Ghahramani and M. Jordan. Factorial hidden Markov models. *Machine Learning*, 29:245–273, 1997.
- [46] M. X. Goemans and D. P. Williamson. Improved approximation algorithms for maximum cut and satisfiability problems using semidefinite programming. *Journal of the ACM*, 42:1115–1145, 1995.
- [47] M. Grötschel, L. Lovász, and A. Schrijver. *Geometric algorithms and combinatorial optimization*. Springer-Verlag, Berlin, Germany, 1993.
- [48] M. Hassner and J. Sklansky. The use of Markov random fields as models of texture. *Comp. Graphics Image Proc.*, 12:357–370, 1980.
- [49] J. Hiriart-Urruty and C. Lemaréchal. *Convex analysis and minimization algorithms*, volume 1. Springer-Verlag, New York, 1993.
- [50] R. A. Horn and C. R. Johnson. *Matrix Analysis*. Cambridge University Press, Cambridge, 1985.
- [51] X. Huang, A. Acero, H.-W. Hon, and R. Reddy. *Spoken Language Processing*. Prentice Hall, New York, 2001.
- [52] T. S. Jaakkola. Tutorial on variational approximation methods. In *Advanced mean field methods*. MIT Press, 2001.
- [53] M. Jordan, Z. Ghahramani, T. S. Jaakkola, and L. Saul. An introduction to variational methods for graphical models. In *Learning in graphical models*, pages 105–161. MIT Press, 1999.
- [54] S. Karlin and W. Studden. *Tchebycheff systems, with applications in analysis and statistics*. Interscience Publishers, New York, NY, 1966.
- [55] H. Karloff. How good is the goemans-williamsom max-cut algorithm? *SIAM J. Computing*, 29:336–350, 1999.
- [56] A. Krogh, B. Larsson, G. von Heijne, and E. L. L. Sonnhammer. Predicting transmembrane protein topology with a hidden markov model: Application to complete genomes. *Journal of Molecular Biology*, 305(3):567–580, 2001.
- [57] F. Kschischang and B. Frey. Iterative decoding of compound codes by probability propagation in graphical models. *IEEE Sel. Areas Comm.*, 16(2):219–230, February 1998.
- [58] J. B. Lasserre. An explicit equivalent positive semidefinite program for nonlinear 0-1 programs. *SIAM Journal on Optimization*, 12:756–769, 2001.
- [59] J. B. Lasserre. Global optimization with polynomials and the problem of moments. *SIAM Journal on Optimization*, 11(3):796–817, 2001.
- [60] M. Laurent. A comparison of the Sherali-Adams, Lovász-Schrijver and Lasserre relaxations for 0-1 programming. *Mathematics of Operations Research*, To appear, 2002.

- [61] S. L. Lauritzen. *Graphical models*. Oxford University Press, Oxford, 1996.
- [62] S. L. Lauritzen and D. J. Spiegelhalter. Local computations with probabilities on graphical structures and their application to expert systems (with discussion). *Journal of the Royal Statistical Society B*, 50:155–224, January 1988.
- [63] L. Lovasz. On the Shannon capacity of a graph. *IEEE Trans. Information Theory*, IT-25:1–8, 1979.
- [64] M. Luby, M. Mitzenmacher, M. A. Shokrollahi, and D. Spielman. Improved low-density parity check codes using irregular graphs. *IEEE Trans. Info. Theory*, 47:585–598, February 2001.
- [65] M. Luettgen, W. Karl, A. Willsky, and R. Tenney. Multiscale representations of Markov random fields. *IEEE Transactions on Signal Processing*, 41(12):3377–3396, December 1993.
- [66] C. D. Manning and H. Schütze. *Foundations of Statistical Natural Language Processing*. MIT Press, Cambridge, MA, 1999.
- [67] J. McAuliffe, L. Pachter, and M. I. Jordan. Multiple-sequence functional annotation and the generalized hidden markov phylogeny. Technical report, Department of Statistics, University of California, 2003.
- [68] R. McEliece, D. McKay, and J. Cheng. Turbo decoding as an instance of Pearl’s belief propagation algorithm. *IEEE Jour. Sel. Communication*, 16(2):140–152, February 1998.
- [69] R. J. McEliece and M. Yildirim. Belief propagation on partially ordered sets. In D. Gilliam and J. Rosenthal, editors, *Mathematical Theory of Systems and Networks*. Institute for Mathematics and its Applications, 2002.
- [70] R. Neal and G. E. Hinton. A view of the em algorithm that justifies incremental, sparse, and other variants. In *Learning in Graphical Models*. MIT Press, Cambridge, MA, 1999.
- [71] G. L. Nemhauser and L. A. Wolsey. *Integer and combinatorial optimization*. Wiley-Interscience, New York, 1999.
- [72] P. Pakzad and V. Anantharam. Iterative algorithms and free energy minimization. In *CISS*, March 2002.
- [73] G. Parisi. *Statistical field theory*. Addison-Wesley, 1988.
- [74] P. Parrilo. Semidefinite programming relaxations for semialgebraic problems. *Mathematics of Operations Research*, To appear, 2002.
- [75] J. Pearl. *Probabilistic reasoning in intelligent systems*. Morgan Kaufman, San Mateo, 1988.
- [76] J. S. Pedersen and J. Hein. Gene finding with a hidden Markov model of genome structure and evolution. *Bioinformatics*, 19:219–227, 2003.
- [77] T. Richardson and R. Urbanke. The capacity of low-density parity check codes under message-passing decoding. *IEEE Trans. Info. Theory*, 47:599–618, February 2001.
- [78] C. P. Robert and G. Casella. *Monte Carlo statistical methods*. Springer texts in statistics. Springer-Verlag, New York, NY, 1999.
- [79] G. Rockafellar. *Convex Analysis*. Princeton University Press, Princeton, 1970.
- [80] H. Royden. *Real Analysis*. Prentice-Hall, New Jersey, 1988.
- [81] L. K. Saul and M. Jordan. Exploiting tractable substructures in intractable networks. In *NIPS 8*, pages 486–492. MIT Press, 1996.
- [82] L. K. Saul and M. I. Jordan. Boltzmann chains and hidden Markov models. In *Advances in Neural Information Processing Systems 7*. MIT Press, Cambridge, MA, 1995.
- [83] A. Schrijver. *Theory of linear and integer programming*. Wiley-Interscience Series in Discrete Mathematics, Wiley, NY, 1989.
- [84] G. R. Shafer and P. P. Shenoy. Probability propagation. *Annals of Mathematics and Artificial Intelligence*, 2:327–352, 1990.
- [85] H. D. Sherali and W. P. Adams. A hierarchy of relaxations between the continuous and convex hull representations for zero-one programming problems. *SIAM Journal on Discrete Mathematics*, 3:411–430, 1990.
- [86] A. Siepel and D. Haussler. Combining phylogenetic and hidden Markov models in biosequence analysis. In *Proceedings of the Seventh Annual International Conference on Computational Biology*, pages 277–286, 2003.
- [87] T. P. Speed and H. T. Kiiiveri. Gaussian Markov distributions over finite graphs. *Annals of Statistics*, 14(1):138–150, March 1986.
- [88] R. P. Stanley. *Enumerative combinatorics*, volume 1. Cambridge University Press, Cambridge, UK, 1997.

- [89] S. Tatikonda and M. I. Jordan. Loopy belief propagation and Gibbs measures. In *Proc. Uncertainty in Artificial Intelligence*, volume 18, pages 493–500, August 2002.
- [90] A. Thomas, A. Gutin, V. Abkevich, and A. Bansal. Multilocus linkage analysis by blocked Gibbs sampling. *Statistics and Computing*, 10:259–269, 2000.
- [91] L. Vandenberghe and S. Boyd. Semidefinite programming. *SIAM Review*, 38:49–95, 1996.
- [92] L. Vandenberghe, S. Boyd, and S. Wu. Determinant maximization with linear matrix inequality constraints. *SIAM Journal on Matrix Analysis and Applications*, 19:499–533, 1998.
- [93] S. Verdú and H. V. Poor. Abstract dynamic programming models under commutativity conditions. *SIAM J. Control and Optimization*, 25(4):990–1006, July 1987.
- [94] M. J. Wainwright, T. S. Jaakkola, and A. S. Willsky. MAP estimation via agreement on (hyper)trees: Message-passing and linear programming approaches. In *Proc. Allerton conference on Communication, Control and Computing*, October 2002.
- [95] M. J. Wainwright, T. S. Jaakkola, and A. S. Willsky. Tree consistency and bounds on the max-product algorithm and its generalizations. LIDS Tech. report, P-2554 MIT; Available online at <http://www.eecs.berkeley.edu/~martinw>, July 2002.
- [96] M. J. Wainwright, T. S. Jaakkola, and A. S. Willsky. Tree-based reparameterization framework for analysis of sum-product and related algorithms. *IEEE Trans. Info. Theory*, 49(5):1120–1146, May 2003.
- [97] M. J. Wainwright and M. I. Jordan. Semidefinite relaxations for approximate inference on graphs with cycles. Technical report, UC Berkeley, UCB/CSD-3-1226, January 2003.
- [98] M. Welling and Y. Teh. Belief optimization: A stable alternative to loopy belief propagation. In *Uncertainty in Artificial Intelligence*, July 2001.
- [99] W. Wiegerinck. Variational approximations between mean field theory and the junction tree algorithm. In *UAI 2000*, San Francisco, CA, 2000. Morgan Kaufmann Publishers.
- [100] J. Woods. Markov image modeling. *IEEE Transactions on Automatic Control*, 23:846–850, October 1978.
- [101] J. S. Yedidia, W. T. Freeman, and Y. Weiss. Generalized belief propagation. In *NIPS 13*, pages 689–695. MIT Press, 2001.
- [102] J. S. Yedidia, W. T. Freeman, and Y. Weiss. Understanding belief propagation and its generalizations. Technical Report TR2001-22, Mitsubishi Electric Research Labs, January 2002.
- [103] A. Yuille. CCCP algorithms to minimize the Bethe and Kikuchi free energies: Convergent alternatives to belief propagation. *Neural Computation*, 14:1691–1722, 2002.

# Probabilistic Graphical Models

Michael I. Jordan  
Christopher M. Bishop

January 29, 2001

# Chapter 1

## Decision Graphs

In earlier chapters of this book we have developed extensive graphical machinery for solving the inference problem, that is the task of evaluating conditional probabilities given evidence in the form of observed values for random variables. For practical applications, however, the role of the probabilities is an intermediate one in the task of making decisions, or equivalently taking actions. In order to make decisions which are optimal according to some criterion, we combine the inferred conditional probabilities with a utility (or cost) function. In the simplest case we have a single decision to take, and the optimal decision is generally defined to be that which maximizes the expected utility.

More complex decision scenarios involve multiple, sequential stages of decision making, in which new information is revealed after each decision is made. In this chapter we review the basic concepts of decision theory and then we demonstrate the role which graphical models can play in arriving at optimal decisions for complex problems involving multiple decision stages. In particular, we shall formulate the multi-stage decision problem in terms of directed acyclic graphs having both decision nodes and utility nodes in addition to the usual stochastic nodes describing random variables. We shall then develop an exact and efficient algorithm for finding the optimal set of decisions together with the corresponding maximum utility. Our approach is based on an extension of the elimination algorithm introduced in Chapter ???. We shall restrict attention in this chapter to problems in which the random variables as well as the decision variables are all discrete.

### 1.1 Decision Theory

#### 1.1.1 Single-step Decisions

As a simple example of a decision problem, suppose we have to decide whether to provide treatment for a patient who might potentially have cancer, in which the treatment itself has undesirable side effects. There is a single binary random variable  $X$  which describes whether or not the patient has cancer, and there is a single binary decision variable  $d$  corresponding to the decision to provide treatment or not. Finally there is a utility function which depends on both  $X$  and  $d$ , and which is therefore a  $2 \times 2$  matrix, an example of which is shown in Figure 1.1. In this example we see that there is negative utility associated with having cancer, but that this is diminished if treatment is provided. For a patient with no cancer there is a negative utility associated with receiving treatment due to side effects associated with the treatment itself.

At the time the decision must be taken, the state of the random variable  $X$  is unknown. Thus the actual utility arising from a particular decision will not be known when the decision is made. We can, however, calculate the expected utility by marginalizing over the random variable. This

$$\begin{pmatrix} 0 & -30 \\ -1000 & -200 \end{pmatrix} \quad (1.1)$$

Figure 1.1: An example of a utility matrix  $U(X, d)$  for the cancer treatment problem. The first and second rows correspond to the states of the random variable  $X = \text{'normal'}$  and  $X = \text{'cancer'}$ , while first and second columns correspond to the states of the decision variable  $d = \text{'no treatment'}$  and  $d = \text{'treatment'}$ .

allows us to choose the decision variable using the criterion of *maximum expected utility*. While such a criterion is intuitively appealing, it can also be justified more formally from a frequentist perspective as being the criterion which yields the greatest reward in a long run series of decisions (for example in a gambling scenario). An analogous argument can be made from a Bayesian perspective, in which case it applies also to the situation where there is only a single trial.

In order to find the expected utility for the cancer example, however, we need to know the probability that the patient has cancer. For example, suppose that

$$P(X = \text{'normal'}) = 0.9 \quad (1.2)$$

$$P(X = \text{'cancer'}) = 0.1. \quad (1.3)$$

The expected utilities associated with providing treatment or not providing treatment are then easily evaluated to give

$$\langle U(d = \text{'no treatment'}) \rangle = 0.9 \times 0 + 0.1 \times (-1000) = -100 \quad (1.4)$$

$$\langle U(d = \text{'treatment'}) \rangle = 0.9 \times (-30) + 0.1 \times (-200) = -47 \quad (1.5)$$

where  $\langle \cdot \rangle$  denotes an average over the random variable  $X$ . Thus the expected utility is maximized in this example by providing the cancer treatment, and the value of that expected utility is  $-47$ .

We can represent the random, decision and utility variables in this problem as a simple directed graph, as shown in Figure 1.2. The semantics of such graphs will be discussed more fully in Sec-

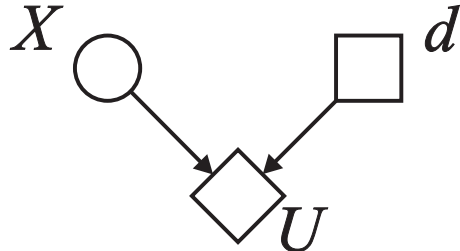


Figure 1.2: A simple decision graph corresponding to the cancer treatment problem described in the text. The circular node represents a random variable  $X$  describing whether or not the patient has cancer, the square node represents the decision variable describing whether or not the patient receives treatment, and the diamond node represents the utility function  $U$ . Arrows from the random and decision variables into the utility node indicate that the utility function depends on both  $X$  and  $d$ .

tion 1.2.1. We shall subsequently use such decision graphs as the basis for a graphical solution to the decision problem obtained by extending the elimination algorithm of Chapter ??.

Note that without loss of generality we can replace utility functions with cost (or loss) functions, in which the goal is to make decisions which minimize the expected cost. A cost function can always be defined as the negative of a utility, and so from now on we work exclusively with utilities.

### 1.1.2 Multiple Decisions

In the decision problem considered so far, there has been a single random variable  $X$  and a single decision variable  $d$ . We now turn to more general decision problems involving multiple stages of decision making which occur sequentially, together with multiple random variables. The states of some random variables may be known before the first decision is taken. After each decision the states of other random variables may be revealed and these may influence subsequent decisions. In this case there is a more complex interaction between inference and decision, and we shall see in Section 1.2 that the formalism of graphical models can be extended and exploited to provide a computationally efficient solution to the problem of making optimal decisions in such a scenario.

In order to introduce the concept of multi-stage decision problems we consider an extension of the cancer treatment example given in Section 1.1.1. We first introduce a random variable  $X_1$ , representing the presence or absence of symptoms in the patient which could be indicative of cancer. Initially the state of  $X_1$  is revealed to the decision maker. Subsequently a decision is made, described by a decision variable  $d_1$ , as to whether to conduct a test which will provide further information on whether the patient may have cancer. There is an associated utility  $U_1(d_1)$  which will have a negative value if the test is conducted corresponding to the cost of the test. After the test is conducted the state of a random variable  $X_2$  is revealed, where  $X_2$  represents the result of the test<sup>1</sup>. Subsequently a second decision is taken, represented by the decision variable  $d_2$ , as to whether to provide treatment to the patient. The final random variable  $X_3$  describes whether the patient actually has cancer or not, and the state of this variable will be unknown at the times that decisions  $d_1$  and  $d_2$  must be taken. There is a second utility  $U_2(X_3, d_2)$  whose value depends both on whether the patient actually has cancer and on whether treatment was administered (it might for example be given by the table in Figure 1.1). The total utility function is given by the sum  $U_1 + U_2$ . Note that there is a natural ordering of the random and decision variables in the form  $(X_1, d_1, X_2, d_2, X_3)$  such that when decision  $d_i$  is taken only the values of random variables  $X_i$  with  $i < d$  will be known. The decision graph corresponding to the extended cancer treatment example is shown in Figure 1.3.

### 1.1.3 The General Multi-Stage Decision Problem

We can formulate the general multi-stage decision problem as follows. Suppose we have a sequence of decision variables  $d_1, d_2, \dots, d_M$  such that decision  $d_i$  is taken before decision  $d_{i+1}$ . The random variables can be partitioned into corresponding groups  $X_i$  such that after decision  $d_i$  is taken the states of the variables in group  $X_{i+1}$  are revealed. Combining the random and decision variables we have an overall decision sequence of the form  $(X_1, d_1, X_2, d_2, \dots, d_M, X_{M+1})$ . Note that the decisions  $d_i$  can also comprise groups of variables, although for simplicity we shall limit attention to the case of a single variable  $d_i$  (the generalization to groups of decision variables is straightforward).

---

<sup>1</sup>Note that if the decision is made not to conduct the test, then the result of the test will of course not be revealed. We return to a discussion of this asymmetry in Section 1.2.6

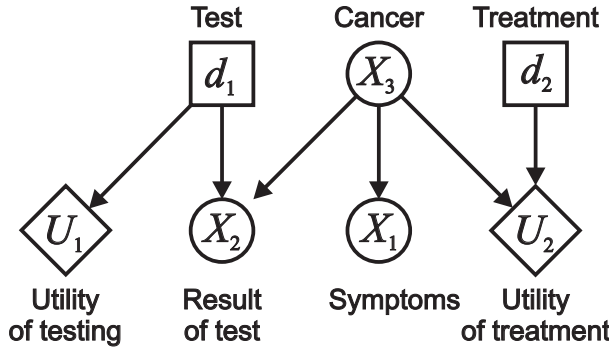


Figure 1.3: Decision graph corresponding to the extended cancer treatment example discussed in the text.

Without loss of generality we can exploit the ordering of the random variables to specify their joint distribution as a factorization in terms of conditional distributions of the form

$$P(X_{i+1}|X_1, \dots, X_i, d_1, \dots, d_M) \quad (1.6)$$

where  $i = 1, \dots, M$ .

However, we must also impose a constraint to reflect the causality requirement that the value of a decision variable cannot influence any of the random variables which appear earlier in the decision sequence. This is equivalent to a set of conditional independence statements of the form

$$P(X_{i+1}|X_1, \dots, X_i, d_1, \dots, d_M) = P(X_{i+1}|X_1, \dots, X_i, d_1, \dots, d_i). \quad (1.7)$$

Any consistent model of a multi-stage decision problem must respect these constraints.

Thus the probabilistic model is specified by defining the following set of conditional probabilities

$$P(X_1) \quad (1.8)$$

$$\begin{aligned} &P(X_2|X_1, d_1) \\ &\dots \end{aligned} \quad (1.9)$$

$$P(X_{M+1}|X_1, d_1, \dots, X_M, d_M). \quad (1.10)$$

Although these represent the most general situation, in any particular model there may be variables missing from the conditioning sets in (1.8) – (1.10) corresponding to additional conditional independence properties. When we develop the extended elimination algorithm for decision graphs in Section 1.2 we will seek to exploit these conditional independences in order to obtain efficient computation.

The decision problem specification is completed by defining the utility function, which in general can depend on all of the random and decision variables

$$U(X, d) = U(X_1, d_1, \dots, X_M, d_M, X_{M+1}). \quad (1.11)$$

This utility function often takes the form of the sum of a number of terms, each of which depends only on a subset of the variables. Again, we seek an algorithm which can exploit this additive structure to achieve efficient computation.

### 1.1.4 Solution of the Multi-stage Decision Problem

Now let us consider how to solve the multi-stage decision problem in the general case. The solution will take the form of a set of tables which specify the optimal decision  $\hat{d}_i$  for all possible settings of the previous decision variables (which may have been chosen suboptimally) and of the random variables whose values will be known at the time that  $d_i$  must be chosen. Thus we seek a set of tables, called a decision *mapping*, of the form

$$\hat{d}_1(X_1) \quad (1.12)$$

$$\hat{d}_2(X_1, d_1, X_2) \quad (1.13)$$

...

$$\hat{d}_M(X_1, d_1, X_2, \dots, d_{M-1}, X_M). \quad (1.14)$$

Given this set of tables any particular decision can be taken optimally since the required values of previous decision variables and random variables will be known at the time the decision must be taken.

The overall optimal decision is one in which the complete set of decision variables is chosen jointly to maximize the expected utility. To do this the first decision is made optimally using (1.12), and then this optimal decision  $\hat{d}_1$  is used to find the optimal value for the second decision variable using (1.13) and so on. Thus the overall optimum can be found from the decision mapping by substitution to give

$$\hat{d}_1(X_1) \quad (1.15)$$

$$\hat{d}_2(X_1, \hat{d}_1, X_2) \quad (1.16)$$

...

$$\hat{d}_M(X_1, \hat{d}_1, X_2, \dots, \hat{d}_{M-1}, X_M). \quad (1.17)$$

Now consider the problem of computing one of the tables  $\hat{d}_i(X_1, d_1, \dots, d_{i-1}, X_i)$  in the decision mapping (1.12) – (1.14). For each setting of the known variables  $(X_1, d_1, \dots, d_{i-1}, X_i)$  we must determine the setting of the decision variable  $d_i$  such that the overall expected utility is maximized. This expected utility will involve averages over the as yet unobserved random variables  $X_{i+1}, \dots, X_{M+1}$  but will also depend on the choices made for future decisions which themselves must be taken optimally. Thus to find  $\hat{d}_i(\dots)$  we must in general consider all possible combinations of settings of all of the decision variables, and indeed this turns out to be an NP-hard problem.

We can evaluate the decision mapping tables by a backwards induction process starting with the final decision. Thus we can first determine  $\hat{d}_M$  as a function of  $(X_1, d_1, \dots, X_M)$  by first

marginalizing the utility function over  $X_{M+1}$  to define an expected utility function given by

$$\overline{U}_M(X_1, d_1, \dots, X_M, d_M) = \sum_{X_{M+1}} P(X_{M+1}|X_1, d_1, \dots, X_M, d_M) U(X_1, d_1, \dots, X_M, d_M, X_{M+1}) \quad (1.18)$$

and then maximizing with respect to  $d_M$  for all possible choices of  $(X_1, d_1, \dots, d_{M-1}, X_M)$

$$\hat{d}_M(X_1, d_1, \dots, X_M) = \arg \max_{d_M} \overline{U}_M(X_1, d_1, \dots, X_M, d_M). \quad (1.19)$$

Substituting  $\hat{d}_M$  into the expected utility function  $\overline{U}_M$  yields a new utility function in which  $d_M$  and  $X_{M+1}$  have been eliminated

$$U_{M-1}(X_1, d_1, \dots, X_M) = \overline{U}_M(X_1, d_1, \dots, X_M, \hat{d}_M(X_1, d_1, \dots, X_M)) \quad (1.20)$$

and corresponds to a multi-stage decision problem over a reduced set of variables. Thus the above procedure can be applied recursively until the complete set of decision mapping tables has been evaluated.

The full solution to the decision problem to find the jointly optimal set of decisions is therefore given by

$$\sum_{X_1} \max_{d_1} \sum_{X_2} \cdots \max_{d_M} \sum_{X_{M+1}} P(X|d) U(X, d) \quad (1.21)$$

where we have defined

$$P(X|d) = P(X_{M+1}|X_1, \dots, d_M) \cdots P(X_2|X_1, d_1) P(X_1). \quad (1.22)$$

Note that the quantity  $P(X|d)$  can only be interpreted as the conditional distribution of  $X$  conditioned on  $d$  if the values of  $d$  are set externally. If the values of  $d$  are chosen to maximize expected utility then they will depend on the values of  $X$  and so in this case  $P(X|d)$  can no longer be viewed as the conditional distribution.

Our goal is to evaluate the successive summations and maximizations given by (1.21). The values which are assigned to the decision variables will then yield the decision mapping corresponding to (1.12) – (1.14), and the final value of the quantity in (1.21) gives the corresponding maximum value of the expected utility. Our approach will generalize the elimination algorithm of Chapter ?? and will be based on the idea of commuting the summation and maximization operations through the various factors in  $P(X|d)U(X, d)$  in order to achieve efficient computations which act on small groups of variables at a time. Before developing this framework, however, we consider a brute force approach, called *decision trees*, which emphasises the nature of the computations which must be performed.

### 1.1.5 Decision Trees

In this section we introduce a simple graphical technique, called *decision trees*, for setting out the solution to a multi-stage decision problem. Although for many complex problems decision trees can be computationally inefficient compared to the elimination algorithm developed shortly, they

serve a useful role in emphasising the underlying computations which must be performed.

Consider again the extended cancer treatment problem discussed in Section 1.1.2. The decision tree is simply a graphical representation of all possible combinations of choices for the decision variables and the random variables. In the cancer problem the first variable to be revealed is the random variable  $X_1$  corresponding to the presence or absence of symptoms. Subsequently a decision  $d_1$  is taken as to whether a test should be conducted. As a consequence the result  $X_2$  of the test is revealed and then a decision  $d_2$  can be made as to whether to provide treatment. The final random variable  $X_3$  describes whether the patient has cancer or not and is only known after both decisions have been taken. The full decision tree corresponding to this problem involves many possible paths through the states of these variables. Two such paths are shown in Figure 1.4. Note

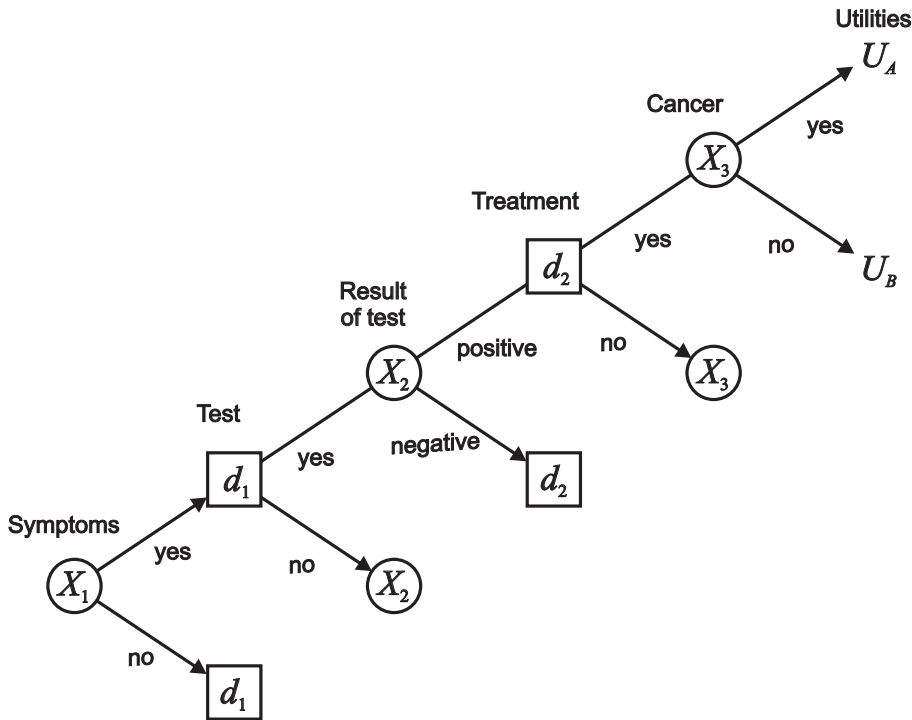


Figure 1.4: Decision tree for the extended cancer treatment example discussed in Section 1.1.2. For clarity only two of the possible paths from the root node to the utilities are shown.

that if decision  $d_1$  is set so that no test is conducted then there will be no test result to observe. This asymmetry, which is exploited efficiently in decision trees, is discussed further in Section 1.2.5.

By following each path in the decision tree from the root to a leaf we can evaluate the corresponding utility at the leaf. It is then a simple matter to find, for any given decision node in the tree, the decision which will give rise to the maximum expected utility. Consider for instance the decision node  $d_2$  in Figure 1.4 corresponding to the decision on whether to administer treatment in the case of a positive test result. The expected utility for the choice ‘yes’ for  $d_2$  is obtained by averaging the two utilities  $U_A$  and  $U_B$ , weighted by the appropriate conditional probabilities for the states of  $X_3$ . Thus the process of solving the decision problem using the decision tree framework involves a backwards recursion starting with the final state utilities. So in Figure 1.4, we first evaluate the marginal utilities at each of the ‘ $X_3$ ’ nodes by computing sums of utilities weighted by their corresponding probabilities (conditioned on the previous variables in the path). Next, for each decision node ‘ $d_2$ ’ we chose the maximum expected utility. These expected utilities are then

fed back to the  $X_2$  nodes where again they are summed with weights given by the corresponding conditional probabilities, to give an expected utility at each  $X_2$  node. The optimal decision for the  $d_1$  node is found by choosing the maximum of the expected utilities at the  $X_2$  nodes. Finally, the value of the maximum expected utility is obtained by summing over the  $X_1$  variable weighted by its marginal probability.

Note that the conditional probabilities required to evaluate this decision tree are given by

$$P(X_3|X_1, X_2, d_1, d_2)$$

$$P(X_2|X_1, d_1)$$

$$P(X_1)$$

whereas we see from Figure 1.3 that the original problem is formulated most naturally using conditional probabilities in the form

$$P(X_3)$$

$$P(X_1|X_3)$$

$$P(X_2|X_3, d_1).$$

In order to apply the decision tree technique to this problem we must therefore perform some initial pre-processing using the sum and product rules of probability in order to recast the conditional probabilities in the correct form. The requirement for such pre-processing is a general feature of decision trees. As we shall see, the required manipulations are performed automatically when we make use of the elimination algorithm, and so the need to pre-process the conditional probabilities is avoided.

The principal disadvantage of decision trees, however, is that they exhaustively enumerate every possible path and so fail to take advantage of conditional independencies which might exist in the model. This is resolved by moving to an elimination tree approach, discussed in Section 1.2.

## 1.2 Elimination Algorithm for Decision Graphs

We turn now to the development of a general framework for solving multi-stage decision problems in a computationally efficient manner. Our approach will be based on an extension of the elimination algorithm introduced in Chapter ???. Note that an alternative approach would be to extend the junction tree algorithm of Chapter ???. Although a junction tree approach may often be more efficient in terms of storage, as we discuss in Section 1.2.5, the algorithm itself is more complex as it requires additional book keeping. For simplicity we therefore limit attention to the elimination tree approach.

In Chapter ?? we viewed the elimination algorithm as an efficient procedure for evaluating conditional probabilities obtained by commuting summation (marginalization) operators with the factors comprising the joint probability distribution, so that the summations act only on small subsets of the variables. For the case of multi-stage decision problems our goal is the evaluation of the sequence of summations and maximizations defined by (1.21) in which the joint distribution  $P(X|d)$  is defined by (1.22). To achieve this efficiently we again seek to commute the factors in the joint distribution through the summation and maximization operators so that the operations are

performed over sets of low cardinality. The utility function itself may also comprise the sum of several terms each of which only depends on a subset of the random and decision variables, and again we wish to exploit such structure to achieve computational efficiency.

In the case of purely probabilistic models we were also able to choose an efficient order in which to marginalize, and therefore eliminate, the variables. However, a key point to emphasise in the case of decision problems is that the elimination ordering is restricted because it is not possible to permute a summation with a maximization. To see this consider the cancer example described in Section 1.1.1 whose utility function is shown in Figure 1.1. The value of the maximum expected utility was obtained by first averaging over the two states of the random variable  $X$  for each possible value of the decision variable  $d$  (in order to obtain the expected utility as a function of  $d$ ), and then subsequently choosing the value of  $d$  for which the expected utility was greater. This gave an expected utility of  $-47$ . Now suppose that instead we perform the maximization first, and then subsequently marginalize over  $X$ . For  $X = \text{'normal'}$  the maximum value of the utility  $U(X, d)$  occurs for  $d = \text{'no treatment'}$  and has the value  $0$ , while for  $X = \text{'cancer'}$  the maximum value of the utility occurs for  $d = \text{'treatment'}$  and has the value  $-200$ . Thus the expected value of this maximum utility is given by

$$\langle U \rangle = 0.9 \times 0 + 0.1 \times (-200) = -20. \quad (1.23)$$

Thus the value of the maximum expected utility is different in the two cases, and also in the second case the optimal decision on whether to provide treatment is dependent on the state of the variable  $X$ . Making the decision before averaging over  $X$  corresponds to the case where the state of health of the patient is known before the decision to treat is taken. This of course leads to a higher expected utility since the decision is better informed.

Thus we see that summations and maximizations cannot be commuted. We are still free to choose the elimination ordering of the variables within each group of random variables  $X_i$  (and similarly within each of the  $d_i$  if these comprise more than one decision variable) but we cannot interchange the groups.

### 1.2.1 Definition of Decision Graphs

In order to extend the elimination algorithm to the case of decision problems we first of all generalize the concept of a directed probabilistic graph to include decision variables and utility functions, and we shall refer to these as *decision graphs*. We have encountered two examples of such graphs already in Figures 1.2 and 1.3.

We can define a decision graph in general as follows. Consider first a problem involving only random variables. The joint distribution over these variables can be characterized by a directed acyclic graph, as discussed in Chapter ???. Now suppose that in addition we have some decision variables  $d_i$ . These enter as conditioning variables in the conditional probabilities (1.6). We therefore introduce an additional node (represented as a square) for each decision variable  $d_i$  and this will be a parent of every random variable node for which  $d_i$  appears in the conditioning set of the corresponding conditional distribution. Thus decision nodes themselves have no parents and have random nodes as their children.

Next we wish to represent the utility functions. For each utility term  $U_m(X, d)$  we introduce a corresponding node (represented as a diamond) whose parents are the set of random variables and decision variables on which that term depends. Thus utility nodes can have both random and decision variables as parents, but themselves have no children.

There is one final constraint on the structure of the graph, which arises from the causality requirement represented by the conditional independence conditions (1.7). Specifically we require that, ignoring the utility nodes, for each decision node, all random variables which are descen-

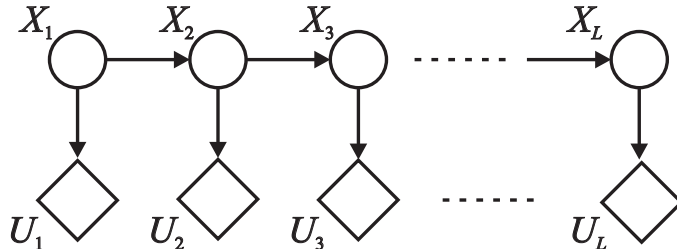
dents of that decision node must appear later in the decision sequence than that decision variable. To see that this implies the conditions (1.7) consider the joint distribution  $P(X|d)$  formed by taking the product of the individual conditionals given by (1.6). For any given decision variable  $d_m$  we can marginalize the joint distribution with respect to the descendants of  $d_m$ . Now from Chapter ?? we know that if we marginalize over a random node that has no descendants, the joint distribution of the remaining variables factorizes with respect to the graph obtained by removing that node. We can therefore work backwards from the leaf nodes and remove nodes one at a time from the graph. Once we have removed all of the descendants of  $d_m$ , the node corresponding to  $d_m$  will be isolated and so the joint distribution of the remaining variables will be independent of  $d_m$ . It is easy to see that this implies that all of the factors which comprise that joint distribution will also be independent of  $d_m$ , and so we have shown that the conditions (1.7) must hold.

Note that there is a closely related graphical representation of multi-stage decision problems called *influence diagrams*. They differ from the directed decision graphs discussed here through the addition of extra edges, called *information arcs*, leading into decision nodes which reflect the causal consistency constraint. Specifically, for any decision node, the ancestors of the node in the directed graph correspond to the variables (decision and random) whose values will be known at the time the decision is taken. The causality requirement then translates into a requirement that the directed graph be acyclic. Here we consider graphs without information arcs, but we must then maintain separately a record of the partial ordering of the variables in the problem.

## 1.2.2 Elimination for Decision Graphs

In order to construct the computational machinery needed to solve the decision problem, we will generalize the elimination algorithm introduced in Chapter ???. We will show how the sequential elimination of variables allows us to define a tree of eliminations sets satisfying the running intersection property, and we will then generalize the concept of the clique potentials, introduced in Chapter ???, to include utilities. As we shall see, it is appropriate to use potentials consisting of pairs of functions, with one member of each pair representing a probabilistic component and the other member representing a utility component.

In order to motivate the use of function pairs for potentials, consider the graph shown in Figure 1.5. This graph contains no decision nodes, only random and utility nodes, and the goal is to



Clearly a very bad way to solve this problem would be to evaluate the function

$$P(X_1)P(X_2|X_1)\dots P(X_L|X_{L-1})\{U_1(X_1) + U_2(X_2) + \dots + U_L(X_L)\} \quad (1.25)$$

for all combinations of variable values and then perform the  $L$  successive summations. If each of the random variables has  $K$  states then this would require evaluation and storage of a function of the joint space of all  $L$  variables, comprising  $K^L$  states, and subsequent summation over this number of states.

Another approach would be to expand out the bracket and solve  $L$  separate problems, one for each term of the utility function, and then add the results together. This again is inefficient since many of the summation operations would be common to the  $L$  sub-problems and hence there would be substantial replication of computation.

We can find a more efficient approach by exploiting the conditional independence properties of the probabilistic ‘backbone’ in the graph in Figure 1.5, together with the additive decomposition of the utility function. Here we consider how to set up such a computation in which we eliminate (i.e. sum over)  $X_1$  first<sup>2</sup>, then  $X_2$  and so on up to  $X_L$ . If we commute the conditional probabilities through the summations as far as we can we obtain the following expression for the expected utility

$$\sum_{X_L} \dots \sum_{X_2} P(X_3|X_2) \sum_{X_1} P(X_1)P(X_2|X_1) \{U_1(X_1) + U_2(X_2) + \dots + U_L(X_L)\}. \quad (1.26)$$

Now we exploit the additive structure of the utility function. Consider first the summation over  $X_1$ , and define the following quantities

$$\gamma_1^*(X_2) = \sum_{X_1} P(X_1)P(X_2|X_1) \quad (1.27)$$

$$\eta_1^*(X_2) = \sum_{X_1} P(X_1)P(X_2|X_1)U_1(X_1) \quad (1.28)$$

where the \* superscript denotes that a variable has been marginalized out. We shall interpret these quantities shortly as messages passed between cliques of the elimination tree. Using (1.27) and (1.28) we can write (1.26) in the form

$$\sum_{X_L} \dots \sum_{X_2} P(X_3|X_2) \{\eta_1^*(X_2) + \gamma_1^*(X_2) [U_2(X_2) + \dots + U_L(X_L)]\}. \quad (1.29)$$

We have therefore succeeded in eliminating the variable  $X_1$ . Note that this operation required the evaluation of *two* different summations over  $X_1$  given by (1.27) and (1.28). These quantities must be computed for all values of the variable  $X_2$ . However, because of the conditional independence property  $X_3 \perp\!\!\!\perp X_1 | X_2$ , corresponding to the absence of an edge from  $X_1$  to  $X_3$  in the graph in Figure 1.5, we do not need to involve the variable  $X_3$  (or indeed any of the remaining variables) at this stage, so the summations involve storage and computation only over the variables ( $X_1, X_2$ ).

For reasons which we shall discuss shortly, it is convenient to work with normalized expected

---

<sup>2</sup>Since this problem involves only random variables and no decision variables, we can consider any elimination order we wish. Other elimination orderings are considered in the exercises.

utilities. We therefore define a new quantity given by

$$\mu_1^*(X_2) = \frac{\eta_1^*(X_2)}{\gamma_1^*(X_2)}. \quad (1.30)$$

This allows us to pull out a common factor of  $\gamma_1^*(X_2)$  from the braces in (1.29) go give

$$\sum_{X_L} \dots \sum_{X_2} P(X_3|X_2) \gamma_1^*(X_2) \{ \mu_1^*(X_2) + U_2(X_2) + \dots + U_L(X_L) \}. \quad (1.31)$$

The key point to emphasize here is that we have to maintain separately two quantities resulting from summations over  $X_1$ . The first of these,  $\gamma_1^*(X_2)$ , involves only conditional probabilities, while the second,  $\mu_1^*(X_2)$ , takes the form of an expected utility.

When we come to eliminate variable  $X_2$  we can work in the joint space  $(X_2, X_3)$ . From (1.31) we see that this requires us to have access to the quantities  $\gamma_1^*(X_2)$  and  $\mu_1^*(X_2)$  separately, otherwise we would be forced to work in the larger joint space  $(X_1, X_2, X_3)$ .

We can continue eliminating the variables one at a time, working our way along the chain and exploiting its conditional independence properties. The elimination of the  $m$ th variable involves a summation given by

$$\sum_{X_L} \dots \sum_{X_m} P(X_{m+1}|X_m) \gamma_{m-1}^*(X_m) \{ \mu_{m-1}^*(X_m) + U_m(X_m) + \dots + U_L(X_L) \}. \quad (1.32)$$

We now define the quantities

$$\hat{\gamma}_m(X_{m+1}, X_m) = P(X_{m+1}|X_m) \gamma_{m-1}^*(X_m) \quad (1.33)$$

$$\hat{\mu}_m(X_m) = \mu_{m-1}^*(X_m) + U_m(X_m) \quad (1.34)$$

which we shall interpret in Section 1.2.4 as the two components of a clique potential, modified by absorption of the messages  $\gamma_{m-1}^*$  and  $\mu_{m-1}^*$ . The total expected utility, after summing out variables  $X_1$  to  $X_{m-1}$ , then becomes

$$\sum_{X_L} \dots \sum_{X_m} \hat{\gamma}_m(X_{m+1}, X_m) \{ \hat{\mu}_m(X_m) + U_{m+1}(X_{m+1}) + \dots + U_M(X_M) \}. \quad (1.35)$$

Again there are two distinct summations over  $X_m$  to be performed, giving rise to the two quantities

$$\gamma_m^*(X_{m+1}) = \sum_{X_m} \hat{\gamma}_m(X_{m+1}, X_m) \quad (1.36)$$

$$\mu_m^*(X_{m+1}) = \frac{\sum_{X_m} \hat{\mu}_m(X_m) \gamma_m(X_{m+1}, X_m)}{\gamma_m^*(X_{m+1})} \quad (1.37)$$

which, as we shall see in Section 1.2.5, are the messages transmitted to the next clique in the elimination tree when the variable  $X_m$  is eliminated. Thus we see that, in order to maintain computational efficiency, two types of quantities (and, as we shall see, only two) need to be maintained and

propagated.

Note that if there were only probability nodes and no utility (or decision) nodes, then we would only need to propagate  $\gamma$  variables, as we have seen in previous chapters. They are updated and marginalized using the standard elimination algorithm for probabilistic models as discussed in Chapter ???. The computational saving arising from the use of pairs of functions in the potentials stems from the additive nature of the utility function.

### 1.2.3 Elimination Trees

In Chapter ?? we gave an informal introduction to the elimination algorithm in the context of directed graphs of random nodes. Recall that when we eliminate a node from a graph we connect together all of the neighbours of that node. Here we revisit the elimination algorithm and show how it can be used to construct a particular form of junction tree called an *elimination tree*. We then extend this procedure to general decision graphs.

Consider first a graph consisting entirely of random nodes. As we have already seen in Chapter ?, the first step is to moralize the graph in order that each of the conditional probabilities can be associated with at least one of the cliques of the resulting elimination tree. After moralization the graph can be triangulated.

Here we define a particular algorithm for triangulation, called *one step look-ahead*, which is an alternative to the maximum cardinality search considered in Chapter ??, and we then use this to construct an elimination tree.

**Algorithm 1.1 (One step look-ahead triangulation)** Consider a (directed or undirected) graph  $\mathcal{G}$  with  $L$  vertices. Set the variable  $i = L$ , and let all the vertices initially be unnumbered. While there are still unnumbered vertices in the graph:

1. Choose an unnumbered vertex having the smallest number of unnumbered neighbours, and give it the label  $i$ .
2. Define the set  $C_i$  to consist of the vertex  $i$  together with all of its unnumbered neighbours.
3. Add edges to the graph as required such that the set  $C_i$  becomes fully connected.
4. Eliminate the vertex  $i$  from the graph and decrement  $i$  by 1.

At each step of this algorithm the variable to be eliminated is chosen so as to give rise to the smallest elimination set  $C_i$ . As we shall see, the corresponding computation involves the joint space of the variables in the clique and so it is here that the elimination approach for decision graphs achieves its computational efficiency. This is, however, a greedy algorithm so is not guaranteed to find the optimal triangulation (recall from Chapter ?? that triangulation is NP-hard).

Next we treat the sets  $C_i$  as nodes in a graph, and add edges between pairs of nodes so as to form a tree. This is achieved using the following procedure

**Algorithm 1.2 (Elimination tree construction)** For  $i = 1, \dots, L$ , if  $C_i$  contains more than one vertex, add an edge between  $C_i$  and  $C_j$ , where  $j$  is the largest index of the vertices in  $C_i$  (excluding vertex  $i$  itself). Finally, add an extra node, containing no vertices, and connect it to all nodes having a single vertex.

This procedure ensures that when we eliminate a variable, the remaining variables in that elimination set are connected to a node in which those variables also appear. A consequence of this is that the elimination tree will satisfy the running intersection property. To see this, note that for each variable there will be a particular node at which it is eliminated, and that it will not appear in any node which is nearer to the root than this node. If there is any other node in which the same variable appears then, since it will not be eliminated in that node, it must appear in the next node in the tree which is nearer the root. By induction the same variable must appear in every node

on the path which connects any two nodes in which the variable appears, and hence the tree has the running intersection property. This is therefore a junction tree of sets of nodes. Note, however, although the cliques will appear as nodes of the tree, there will in general also be other nodes comprising subsets of nodes in cliques. Thus the elimination is not a junction tree of cliques.

As an illustration of this procedure, consider the directed graph of Figure ?? in Chapter ??, reproduced for convenience in Figure 1.6. Applying the triangulation algorithm 1.1 followed by

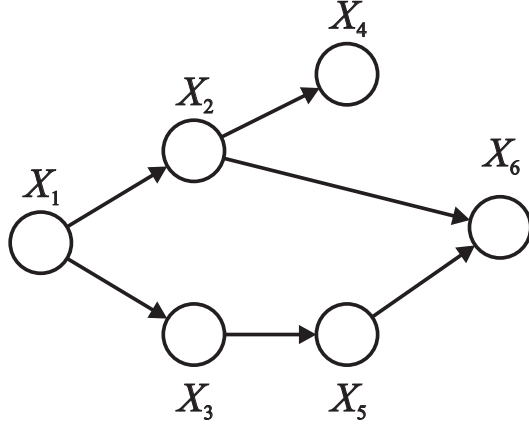


Figure 1.6: The graph introduced in Chapter ?? to illustrate the technique of elimination.

algorithm 1.2 we obtain the elimination tree shown in Figure 1.7. Note that are several possible

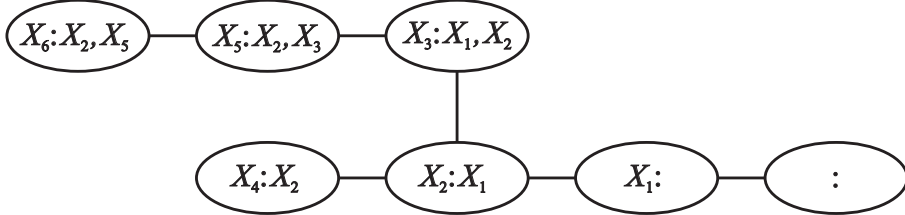


Figure 1.7: The elimination tree resulting from the application of the elimination algorithm 1.1 to the graph in Figure 1.6 followed by the tree construction procedure given by algorithm 1.2. The notation  $X : Y, \dots, Z$  associated with a node denotes that the variable  $X$  is eliminated in that node, and that the remaining variables in the node are  $Y, \dots, Z$ . It is easily seen that this tree satisfies the running intersection property.

elimination orderings which are consistent with the algorithm 1.1. We choose an ordering which is the same as that considered in Chapter ??.

In order to extend the construction of an elimination graph to the framework of decision graphs we need to take account of both utility nodes and decision nodes. Each utility node is associated with an additive term in the total utility function. Recall that utility nodes have only parents and no descendants. The moralization step will add links between all pairs of parents for each utility node. After the moralization step the utility nodes can be deleted from the graph and each term in the utility function can then be associated with the corresponding complete set of nodes on the moral graph. As we saw in Section 1.1.4, the presence of decision variables places restrictions on the order in which variables may be eliminated. This can be accommodated simply by altering the triangulation algorithm 1.1 so as to consider only those elimination orderings which are consistent

with the causality constraints of the particular problem being solved. More formally we have the following algorithm:

**Algorithm 1.3 (One step look-ahead triangulation for decision graphs)** Consider a moralized decision graph  $\mathcal{G}$  with the decision sequence  $(X_1, d_1, X_2, d_2, \dots, d_M, X_{M+1})$  having a total of  $L$  nodes after the utility nodes have been removed. Set the variable  $i = L$ , set  $j = M + 1$ , and let all the vertices initially be unnumbered. While there are still unnumbered vertices in the graph:

1. Choose an unnumbered vertex from the set  $X_j$  having the smallest number of unnumbered neighbours, and give it the label  $i$ . If there are no such vertices then select decision variable  $d_j$ , give it the label  $i$ , and decrement  $j$  by 1.
2. Define the set  $C_i$  to consist of the vertex  $i$  together with all of its unnumbered neighbours.
3. Add edges to the graph as required such that the set  $C_i$  becomes fully connected.
4. Eliminate the vertex  $i$  from the graph and decrement  $i$  by 1.

Again we use algorithm 1.2 to construct an elimination tree of cliques, with the empty clique designated as the root.

#### 1.2.4 Decision Potentials

We are now in a position to set up the formalism for solving decision problems through the use of elimination trees. This will involve defining decision potentials, initialization of the tree, and then message passing on the tree to determine the optimal decisions and the maximum value of the expected utility.

As we have already seen, the efficient solution of problems involving decision graphs requires that we keep separate track of two different quantities, one related to probabilities and the other to expected utilities. We therefore define a *decision potential*  $\phi$  to consist of a pair of variables  $(\gamma, \mu)$  where the first variable  $\gamma$  represents a probability and the second variable  $\mu$  represents an expected utility. For problems in which there are no decision or utility nodes, the formalism will reduce to an exact inference algorithm for probabilistic graphs.

We now define the three key operations on decision potentials:

**Multiplication** Given two potentials  $\phi_1 = (\gamma_1, \mu_1)$  and  $\phi_2 = (\gamma_2, \mu_2)$  we define their product to be the potential

$$\phi_1 \phi_2 = (\gamma_1 \gamma_2, \mu_1 + \mu_2) \quad (1.38)$$

so that the probability parts combine multiplicatively while the utility parts are additive.

**Sum-marginalization** We define the sum-marginalization over a random variable  $X$  as

$$\mathbf{S}_X \phi = \left( \sum_X \gamma, \frac{\sum_X \gamma \mu}{\sum_X \gamma} \right) \quad (1.39)$$

**Max-marginalization** We define the max marginalization over a decision variable  $d$  as

$$\mathbf{M}_d \phi = \left( \gamma(d = \hat{d}), \mu(d = \hat{d}) \right) \quad (1.40)$$

where

$$\hat{d} = \arg \max_d (\gamma \mu). \quad (1.41)$$

### 1.2.5 Initialization and Message Passing for the Elimination Tree

In order to construct an elimination tree for solving the decision problem we take the original directed decision graph and then moralize it by adding edges connecting parents of nodes and then dropping the directions on the edges. This ensures that there will exist a clique on the undirected graph corresponding to each of the conditional probabilities  $P(X_i|X_1, d_1, \dots)$  and similarly a clique for each utility function  $U_m$ . Once this has been done the nodes corresponding to utility functions can be removed.

We now initialize the elimination tree as follows. For every clique  $C_i$  we define a decision potential  $\phi_i = (\gamma_i, \mu_i)$ , with the probability term  $\gamma_i$  initialized to unity and the utility term  $\mu_i$  initialized to zero. Then, for each factor  $P(X_i|X_1, d_1, \dots)$  in the joint probability  $P(X|d)$  we identify a clique containing all of the variables in this factor and we multiply the probability term in that clique potential by  $P(X_i|X_1, d_1, \dots)$ . When this is done, the product over all decision potentials will have a probability term which is the joint probability  $P(X|d)$ .

Then for each utility function  $U_m$  we identify a clique containing the arguments of  $U_m$  and then add  $U_m$  to the utility term in that clique's decision potential. When this is done the sum of all the utility terms in all of the decision potentials will equal the total utility function. Thus, from the definition of the product of decision potentials, given by (1.38), the product of all the decision potentials, given by

$$\phi_V = \prod_i \phi_i \quad (1.42)$$

will have a utility term which is equal to the total utility function. Note that there is no need to introduce separator sets and separator potentials since, as we shall see, the solution to the decision problem involves only one-way message passing (equivalent to a 'CollectEvidence' operation, with no corresponding 'DistributeEvidence').

Next we define a message passing step whereby a variable is eliminated either by summation (probability variable) or maximization (decision variable). Suppose  $C$  is an elimination set of an elimination tree, and let  $C_1, \dots, C_M$  be the neighbours of  $C$  which are further from the root than  $C$  itself. Then the action of absorption consists of the evaluation of messages  $\phi_m^*$  for each of the sets  $C_m$  and the absorption of these messages by multiplication into the decision potential  $\phi_C$  for clique  $C$ . Specifically

$$\phi_m^* = \begin{cases} M_d \phi_m & \text{if } C_m \text{ is the elimination set of a decision variable } d \\ S_X \phi_m & \text{if } C_m \text{ is the elimination set of a random variable } X \end{cases} \quad (1.43)$$

and

$$\hat{\phi}_C = \phi_C \phi_1^* \dots \phi_M^*. \quad (1.44)$$

This absorption operation then forms the basic step of 'CollectEvidence' which is defined recursively. When CollectEvidence is called at a particular node it first calls CollectEvidence in any neighbours which are further from the root, and subsequently absorbs messages from them. The

solution of the decision problem then involves a call to CollectEvidence at the root node of the elimination tree. This leads to a sequence of absorptions starting at the leaves of the tree and working inwards towards the root. Once this has terminated the root clique potential will contain the maximum expected utility, and the optimal values for all of the decision variables will have been determined during the various max-marignalizations. We give a formal proof of this result in Section 1.2.6.

One issue which is worth exploring in more detail concerns the definition of sum marginalization given by (1.39) which involved normalization of the expected utilities, and hence which requires divisions to be performed. In the general formulation of the decision problem given by (1.21) there are no division operations, so it worth looking more closely at the motivation for this definition. To do this we consider the elimination tree shown in Figure 1.8, in which the elimination ordering is  $(X_1, \dots, X_L, Z)$ . This graph could be considered as part of a larger elimination tree.

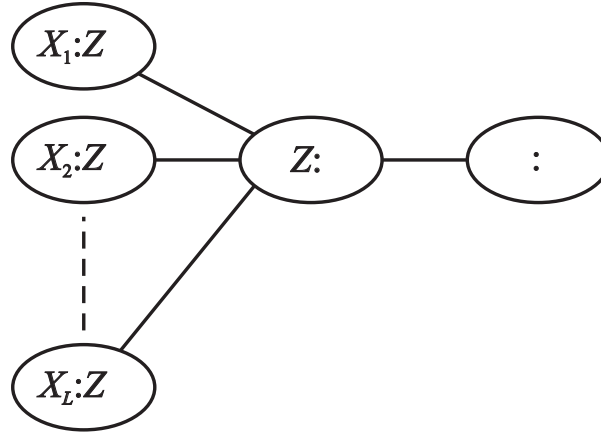


Figure 1.8: An elimination tree used to motivate the use of normalized expected utilities in the definition of message passing.

Note that in this instance there are only random variables and no decision variables. The key point is that several different messages are to be absorbed into the same node  $Z$ . Associated with each node of the tree we have initial potentials  $\phi_i(X_i, Z) = (\gamma_i(X_i, Z), \mu_i(X_i, Z))$  for  $i = 1, \dots, L$  and  $\phi_Z(Z) = (\gamma_Z(Z), \mu_Z(Z))$ . Marginalization over the random variables to yield the total expected utility corresponds to the following operations

$$\langle U \rangle = \sum_Z \sum_{X_1} \dots \sum_{X_L} \gamma_Z(Z) \gamma_1(X_1, Z) \dots \gamma_L(X_L, Z) \{ \mu_1(X_1, Z) + \dots + \mu_L(X_L, Z) + \mu_Z(X_Z) \}. \quad (1.45)$$

In the approach discussed here we seek a message passing scheme such that we can absorb from the nodes sequentially while preserving all the required information using only the two local potentials  $\gamma$  and  $\mu$  in each node of the elimination tree. To see how this is achieved, suppose we first eliminate variable  $X_L$  from (1.45). We require that the result of this be a similar elimination tree with the node  $(X_L : Z)$  removed and with suitably modified potentials  $\hat{\gamma}_Z(Z)$  and  $\hat{\mu}_Z(Z)$  in node  $Z$  so that

$$\langle U \rangle = \sum_Z \sum_{X_1} \dots \sum_{X_{L-1}} \hat{\gamma}_Z(Z) \gamma_1(X_1, Z) \dots \gamma_{L-1}(X_{L-1}, Z) \{ \mu_1(X_1, Z) + \dots + \mu_{L-1}(X_{L-1}, Z) + \hat{\mu}_Z(Z) \}. \quad (1.46)$$

By identifying corresponding terms in (1.45) and (1.46) we obtain

$$\hat{\gamma}_Z(Z) = \gamma_Z(Z) \sum_{X_L} \gamma_L(X_L, Z) \quad (1.47)$$

$$\hat{\mu}_Z(X_Z) = \mu_Z(Z) + \frac{\sum_{X_L} \gamma_L(X_L, Z) \mu_L(X_L, Z)}{\sum_{X_L} \gamma_L(X_L, Z)} \quad (1.48)$$

which corresponds to the definition of sum marginalization introduced in Section 1.2.

Note that we could avoid divisions by keeping track of all the incoming messages to a node, at the expense of extra storage. This would be analogous to the Shafer-Shenoy algorithm discussed in Chapter ??.

Because the elimination tree approach involves eliminating one variable at a time, the number of cliques in the tree (excluding the empty clique) will be equal to the total number of random and decision variables. Instead of using an elimination tree, we could instead have extended the junction tree framework of Chapter ?? to allow for decision variables and utility nodes. Although this can be more efficient in terms of storage, it requires additional book keeping since to construct the message from a given clique it may have to marginalize out several random and decision variables and hence must keep track of the ordering of those variables. Note that the junction tree approach would require only a ‘CollectEvidence’ step. Since no ‘DistributeEvidence’ is needed, the separator potentials play no role and can be omitted.

We saw in the case of the extended cancer example of Section 1.1.2 that there was an asymmetry in that if a decision  $d_1$  was made not to carry out the test, then the random variable representing the result  $X_2$  of the test would remain unobserved. Such issues can easily be handled within the elimination algorithm framework by simply expanding the state space of  $X_2$  to include a ‘no result’ state. The disadvantage, however, is that the expanded state space leads to additional computation, a problem which is avoided in the decision tree approach.

## 1.2.6 Summary and Proof of Elimination Algorithm

So far in this chapter we have assembled and motivated all of the ingredients needed for the formulation of an elimination algorithm to solve the multi-stage decision problem. We now summarize the steps of the algorithm, and then we give a formal proof that it does indeed generate the correct solution.

### Algorithm 1.4 (Elimination Algorithm for Multi-stage Decision Problems)

*Consider a multi-stage decision problem represented by the decision sequence*

$$(X_1, d_1, X_2, d_2, \dots, d_M, X_{M+1}) \quad (1.49)$$

*with corresponding sets of conditional probabilities*

$$P(X_i | X_1, \dots, X_{i-1}, d_1, \dots, d_{i-1}). \quad (1.50)$$

*The algorithm consists of the following steps:*

1. Construct the decision graph using the formulation described in Section 1.2.1.
2. Moralize the decision graph and remove utility nodes.

3. Triangulate the graph using Algorithm 1.3 and then construct elimination tree using Algorithm 1.2.
4. Initialize the decision potentials on the nodes of the elimination tree as described in Section 1.2.5.
5. Call CollectEvidence recursively starting from the root node of the elimination tree.
6. Read off the decision mapping and the maximum expected utility.

We now prove that this algorithm does indeed lead to the correct solution to the decision problem. To do this we first introduce some notation. First of all we expand out the decision sequence so that each of the probabilistic variables is represented individually

$$(X_1^1, \dots, X_1^{k_1}, d_1, X_2^1, \dots, X_2^{k_2}, d_2, \dots, X_{M+1}^{k_{M+1}}) \quad (1.51)$$

such that the variables are eliminated in the reverse order to that given. Next we define

$$(C_1^1, \dots, C_1^{k_1}, C_{d_1}, C_2^1, \dots, C_2^{k_2}, C_{d_2}, \dots, C_{M+1}^{k_{M+1}}) \quad (1.52)$$

to be the corresponding sequence of elimination sets obtained by running algorithm 1.3. We also define the subsets

$$T_i^j = \{C_1^1, \dots, C_1^{k_1}, C_{d_1}, C_2^1, \dots, C_2^{k_2}, d_2, \dots, C_i^j\} \quad j > 0 \quad (1.53)$$

$$T_i^0 = \{C_1^1, \dots, C_1^{k_1}, C_{d_1}, C_2^1, \dots, C_2^{k_2}, d_2, \dots, d_{i-1}\}. \quad (1.54)$$

We shall also use  $\Phi[T_i^j]$  to denote the product of all the decision potentials in the subset  $T_i^j$ . Finally we denote

$$P_i^j = \sum_{X_i^{j+1}} \dots \sum_{X_{M+1}^{k_{M+1}}} P(X|d) \quad (1.55)$$

$$V_i^j = \sum_{X_i^{j+1}} \dots \max_{d_i} \dots \sum_{X_{M+1}^{k_{M+1}}} P(X|d) U(X, d) \quad (1.56)$$

so that  $P_i^j$  involves only the subsequence of sum marginalizations and represents a conditional probability, whereas  $V_i^j$  involves the complete sequence of sum and max marginalizations and represents a partially maximized expected utility. Armed with this notation, we are now ready to proceed with the proof.

The key idea is to show that, after each elimination of a (probability or decision) variable, the product of the decision potentials over the remaining cliques (corresponding to variables that have yet to be eliminated) takes the form

$$\Phi[T_i^j] = (P_i^j, V_i^j / P_i^j). \quad (1.57)$$

Note that  $P_1^0 = 1$  since, from (1.55) this is just the sum over all probability variables of the conditional distribution  $P(X|d)$ , and that  $V_1^0$  is the globally maximum expected utility. Thus (1.57) implies that, once all of the variables are eliminated, the decision potential for the null clique in the

elimination tree (the root) will be  $(P_1^0, V_1^0/P_1^0)$  and so will contain the maximum expected utility. Furthermore, we shall show that each of the max marginalizations is equivalent to the corresponding max marginalization occurring in the general formulation (1.21) and so each of the decision variables will be set to its optimal value.

We now prove by induction that (1.57) holds after each variable is eliminated. When the elimination tree is initialized, before any variables have been eliminated, we have

$$\Phi[T_{M+1}^{k_{M+1}}] = (P_{M+1}^{k_{M+1}}, V_{M+1}^{k_{M+1}}/P_{M+1}^{k_{M+1}}) \quad (1.58)$$

where  $P_{M+1}^{k_{M+1}} = P(X|d)$  and  $V_{M+1}^{k_{M+1}} = P(X|d)U(X, d)$ , and so this provides a starting point for the inductive proof.

Now suppose that (1.57) holds for some particular values of  $i$  and  $j$ , and that the next variable to be eliminated is a probabilistic variable,  $X_i^j$ . By definition we have

$$\Phi[T_i^j] = \Phi[T_i^{j-1}] \phi_{C_i^j}. \quad (1.59)$$

We now operate on both sides of this equation with the sum-marginalization operator for variable  $X_i^j$ . On the left hand side of (1.59) we have

$$\mathbf{S}_{X_i^j} \Phi[T_i^j] = \left( \sum_{X_i^j} P_i^j, \frac{\sum_{X_i^j} P_i^j (V_i^j/P_i^j)}{\sum_{X_i^j} P_i^j} \right) \quad (1.60)$$

$$= (P_i^{j-1}, V_i^{j-1}/P_i^{j-1}). \quad (1.61)$$

Now consider the sum marginalization operator acting on the right hand side of (1.59). We can temporarily de-clutter the notation by writing  $X \equiv X_i^j$ ,  $\Phi \equiv \Phi[T_i^{j-1}]$  and  $\phi \equiv \phi_{C_i^j}$ . Noting that  $\Phi$  does not depend on  $X$  we then have

$$\begin{aligned} \mathbf{S}_{X_i^j}(\Phi\phi) &= \left( \sum_X \gamma_\Phi \gamma_\phi, \frac{\sum_X \gamma_\Phi \gamma_\phi (\mu_\Phi + \mu_\phi)}{\sum_X \gamma_\Phi \gamma_\phi} \right) \\ &= \left( \gamma_\Phi \sum_X \gamma_\phi, \frac{\gamma_\Phi \mu_\Phi \sum_X \gamma_\phi + \gamma_\Phi \sum_X \gamma_\phi \mu_\phi}{\gamma_\Phi \sum_X \gamma_\phi} \right) \\ &= \left( \gamma_\Phi \sum_X \gamma_\phi, \mu_\Phi + \frac{\sum_X \gamma_\phi \mu_\phi}{\sum_X \gamma_\phi} \right) \\ &= \Phi \mathbf{S}_{X_i^j} \phi. \end{aligned} \quad (1.62)$$

Thus from (1.59), (1.61) and (1.62) we have

$$\Phi[T_i^{j-1}] \mathbf{S}_{X_i^j} \phi_{C_i^j} = (P_i^{j-1}, V_i^{j-1}/P_i^{j-1}). \quad (1.63)$$

The left hand side of (1.63) represents the computation of a message in the clique  $C_i^j$  and the absorption of that message in the neighbouring clique nearer the root. From (1.63) we see that the resulting product of decision potentials over the remaining cliques indeed has the form (1.57). This completes the inductive step over  $i$  for a given value of  $j$  in the case where we absorb a random variable. For a given value of  $i$  we can apply this result repeatedly until we have eliminated all of the random variables in the group  $X_i$ . At this stage we have the result

$$\Phi[T_i^0] = (P_i^0, V_i^0 / P_i^0) \quad (1.64)$$

Next we come to the elimination of the decision variable  $d_{i-1}$ . By definition we have

$$\Phi[T_i^0] = \Phi[T_{i-1}^{k_{i-1}}] \phi_{C_{d_{i-1}}}. \quad (1.65)$$

We now operate on both sides of this equation with the max-marginalization operator for the decision variable  $d_{i-1}$ . On the left hand side of (1.65) we can use the definition of the max marginalization operator, together with (1.55) and (1.56), to obtain

$$\mathbf{M}_{d_{i-1}} \Phi[T_i^0] = (P_{i-1}^{k_{i-1}}, V_{i-1}^{k_{i-1}} / P_{i-1}^{k_{i-1}}) \quad (1.66)$$

where we have used the causal consistency requirement which implies that  $P_i^0$  is independent of  $d_{i-1}$  and hence that  $P_{i-1}^{k_{i-1}} = P_i^0$ . To see this note that  $P_i^0$  is the product of conditional probabilities of the form

$$P_i^0 = P(X_1^1 | \dots) \dots P(X_{i-1}^{k_{i-1}} | \dots) \quad (1.67)$$

and then make use of (1.7).

For the max-marginalization operator acting on the right hand side of (1.65) we note that  $\Phi[T_{i-1}^{k_{i-1}}]$  is independent of  $d_{i-1}$  since it involves the product of clique potentials over variables later in the elimination sequence. Furthermore, the probability term  $\gamma$  in  $\phi_{C_{d_{i-1}}}$  is also independent of  $d_{i-1}$  since it involves products of conditional distributions only up to

$$P(X_{i-1} | X_1, \dots, X_{i-2}, d_1, \dots, d_{i-2}) \quad (1.68)$$

which, from the conditional independence properties (1.7) implied by the causal consistency requirement, is independent of  $d_{i-1}$ . Again we can temporarily de-clutter the notation by writing  $\Phi \equiv \Phi[T_{i-1}^{k_{i-1}}]$  and  $\phi \equiv \phi_{C_{d_{i-1}}}$ . We then have

$$\begin{aligned} \mathbf{M}_{d_{i-1}}(\Phi\phi) &= \mathbf{M}_{d_{i-1}}(\gamma_\Phi\gamma_\phi, \mu_\Phi + \mu_\phi) \\ &= (\gamma_\Phi\gamma_\phi, \mu_\Phi + \hat{\mu}_\phi) \\ &= (\gamma_\Phi, \mu_\Phi)(\gamma_\phi, \hat{\mu}_\phi) \\ &= (\gamma_\Phi, \mu_\Phi) \mathbf{M}_{d_{i-1}}(\gamma_\phi, \mu_\phi) \\ &= \Phi \mathbf{M}_{d_{i-1}}\phi \end{aligned} \quad (1.69)$$

where  $\hat{\mu}_\phi = \mu_\phi(d_{i-1} = \hat{d}_{i-1})$  and  $\hat{d}_{i-1} = \arg \max_{d_{i-1}} (\gamma_\phi \mu_\phi)$ . Combining (1.65), (1.66) and (1.69) we have

$$\Phi[T_{i-1}^{k_{i-1}}] \mathbf{M}_{d_{i-1}} \phi_{C_{d_{i-1}}} = (P_{i-1}^{k_{i-1}}, V_{i-1}^{k_{i-1}} / P_{i-1}^{k_{i-1}}). \quad (1.70)$$

The operation on the left hand side of (1.70) represents the evaluation of the message resulting from the elimination of the decision variable  $d_{i-1}$  and the absorption of that message into the decision potential of the next clique in the elimination tree. Again we see that this takes the general form (1.57).

Thus we have reduced the index  $i$  by 1, and so this completes the inductive step over  $i$ , and hence the result (1.57) is proved for all permissible values of  $i$  and  $j$ .

## 1.3 Reinforcement Learning

## 1.4 Historical Remarks and Bibliography

### Exercises

- 1.1 (\*\*)** Apply the general elimination framework summarized in Section 1.2.6 to the graph of Figure 1.5. Do this by considering an elimination ordering  $(X_m, X_{m+1}, \dots, X_L, X_{m-1}, X_{m-2}, \dots, X_1)$  which starts at some node  $X_m$  part way along the chain. Show that after the call to `CollectEvidence` the root node of the elimination tree contains the expected utility in the utility part of its decision potential.
- 1.2 (\*)** Consider the application of the elimination algorithm to the two-stage cancer problem represented by the graph in Figure 1.3. Show that the restriction on the elimination ordering arising from causality means that no computational saving compared to brute force evaluation is possible for this problem.
- 1.3 (\*\*\*)** Show that the elimination algorithm 1.1 adds edges to the original graph  $\mathcal{G}$  such as to triangulate the graph.
- 1.4 (\*\*)** Show that the elimination algorithm 1.1 generates a graph whose cliques are contained within the elimination sets  $C_i$ .
- 1.5 (\*)** Set out a formal proof of the running intersection property for the elimination algorithm 1.2 as set out in Section 1.2.3.
- 1.6 (\*)** Verify that when multiple messages are absorbed into a clique of an elimination tree, the order in which the messages are received is unimportant.
- 1.7 (\*)** Apply the elimination algorithm summarized in Section 1.2.6 to the graph given in Figure 1.5. First of all write down a suitable elimination tree for this problem. Then show that, after absorption of all the messages, the utility part of the potential in the final node contains the total expected utility.